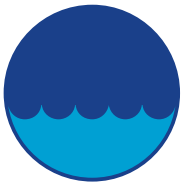

MIDDLE POMERANIAN SCIENTIFIC SOCIETY
OF THE ENVIRONMENT PROTECTION

ŚRODKOWO-POMORSKIE TOWARZYSTWO NAUKOWE
OCHRONY ŚRODOWISKA

Annual Set
The Environment Protection
Volume 19. Year 2017

Rocznik
Ochrona Środowiska
Tom 19. Rok 2017

Koszalin, Poland 2017

MIDDLE POMERANIAN SCIENTIFIC SOCIETY
OF THE ENVIRONMENT PROTECTION

Annual Set
The Environment Protection
Volume 19. Year 2017

Koszalin 2017

ISSN 1506-218X

Annual Set The Environment Protection is covered by:
Polish Ministry of Science and Higher Education – Part A, no. 9867
Journal Rankings of Environmental Science
Master Journal List, Thomson Reuters

Publication of Middle Pomeranian Scientific Society
of The Environment Protection
Koszalin phone +48 94 3410542, +48 94 3478524 or 609800439

Edition 200 copies, 42 publishing sheets, format B-5
Printed by: INTRO-DRUK, Koszalin

Reviewers

Stanisław Biedugnis, *Warsaw University of Technology*
Tomasz Błaszczyński, *Poznan University of Technology*
Tomasz Boczar, *Opole University of Technology*
Tadeusz Bohdal, *Koszalin University of Technology*
Dorota Burchart-Korol, *Central Mining Institute, Katowice*
Andrzej Butarewicz, *Bialystok University of Technology*
Czesław Cempel, *Central Institute for Labour Protection – National Research Institute, Warszawa*
Maria J. Chmiel, *University of Agriculture, Kraków*
Lidia Dąbrowska, *Czestochowa University of Technology*
Wojciech Dąbrowski, *Bialystok University of Technology*
Sławczo Denczew, *The Main School of Fire Service, Warszawa*
Józef Domagała, *University of Szczecin*
Mariusz Dudziak, *Silesian University of Technology, Gliwice*
Julita Dunalska, *University of Warmia and Mazury in Olsztyn*
Ewa Dzika, *University of Warmia and Mazury in Olsztyn*
Urszula Filipkowska, *University of Warmia and Mazury in Olsztyn*
Magdalena Gajewska, *Gdańsk University of Technology*
Marek Gaworski, *Warsaw University of Life Sciences – SGGW*
Jerzy Grabiński, *Institute of Soil Science and Plant Cultivation – National Research Institute, Puławy*
Andrzej Heim, *State University of Applied Sciences, Kalisz*
Katarzyna Ignatowicz, *Bialystok University of Technology*
Wojciech Janczukowicz, *University of Warmia and Mazury in Olsztyn*
Janusz Jeżowiecki, *Wrocław University of Science and Technology*
Krzysztof Jóźwiakowski, *University of Life Sciences, Lublin*
Katarzyna Juda-Rezler, *Warsaw University of Technology*
Jolanta Kanclerz, *Poznań University of Life Sciences*
Włodzimierz Kanownik, *University of Agriculture, Kraków*
Ewa Karwowska, *Warsaw University of Technology*
Vytatuas Kesminas, *Laboratory of Ecology and Physiology of Hydrobionts, Nature Research Centre, Vilnius, Lithuania*
Marta Kosior-Kazberuk, *Bialystok University of Technology*
Piotr Koszelnik, *Rzeszow University of Technology*
Marek Kowalik, *University of Technology and Humanities in Radom*
Anna Kryszak, *Poznań University of Life Sciences*
Renata Krzyżyńska, *Wrocław University of Science and Technology*
Joanna Lach, *Czestochowa University of Technology*
Eugeniusz Mokrzycki, *Mineral and Energy Economy Research Institute PAoS, Kraków*
Sadżide Murat-Błażejewska, *Poznań University of Life Sciences*
Przemysław Niedzielski, *Adam Mickiewicz University in Poznań*
Krzysztof Nowacki, *Silesian University of Technology, Katowice*

ŚRODKOWO-POMORSKIE TOWARZYSTWO NAUKOWE
OCHRONY ŚRODOWISKA

Rocznik
Ochrona Środowiska
Tom 19. Rok 2017

Koszalin 2017

ISSN 1506-218X

Rocznik Ochrona Środowiska znajduje się w wykazie czasopism:
Ministerstwa Nauki i Szkolnictwa Wyższego – Część A, poz. 9867
Journal Rankings of Environmental Science
Master Journal List, Thomson Reuters

Wydawnictwo Środkowo-Pomorskiego Towarzystwa
Naukowego Ochrony Środowiska
Koszalin tel. +48 94 3410542, +48 94 3478524 lub tel. kom. 609800439

Nakład 200 egzemplarzy, ark. wyd. 42, format B-5
Druk: INTRO-DRUK, Koszalin

Recenzenci

Stanisław Biedugnis, *Politechnika Warszawska*
Tomasz Błaszczyński, *Politechnika Poznańska*
Tomasz Boczar, *Politechnika Opolska*
Tadeusz Bohdal, *Politechnika Koszalińska*
Dorota Burchart-Korol, *Główny Instytut Górnictwa, Katowice*
Andrzej Butarewicz, *Politechnika Białostocka*
Czesław Cempel, *Centralny Instytut Ochrony Pracy – Państwowy Instytut Badawczy –, Warszawa*
Maria J. Chmiel, *Uniwersytet Rolniczy im. Hugona Kołłątaja, Kraków*
Lidia Dąbrowska, *Politechnika Częstochowska*
Wojciech Dąbrowski, *Politechnika Białostocka*
Sławczo Denczew, *Szkoła Główna Służby Pożarniczej, Warszawa*
Józef Domagała, *Uniwersytet Szczeciński*
Mariusz Dudziak, *Politechnika Śląska, Gliwice*
Julita Dunalska, *Uniwersytet Warmińsko-Mazurski, Olsztyn*
Ewa Dzika, *Uniwersytet Warmińsko-Mazurski, Olsztyn*
Urszula Filipkowska, *Uniwersytet Warmińsko-Mazurski, Olsztyn*
Magdalena Gajewska, *Politechnika Gdańska*
Marek Gaworski, *Szkoła Główna Gospodarstwa Wiejskiego, Warszawa*
Jerzy Grabiński, *Instytut Uprawy Nawożenia i Gleboznawstwa – Państwowy Instytut Badawczy, Puławy*
Andrzej Heim, *Państwowa Wyższa Szkoła Zawodowa im. Prezydenta Stanisława Wojciechowskiego, Kalisz*
Katarzyna Ignatowicz, *Politechnika Białostocka*
Wojciech Janczukowicz, *Uniwersytet Warmińsko-Mazurski, Olsztyn*
Janusz Jeżowiecki, *Politechnika Wrocławska*
Krzysztof Jóźwiakowski, *Uniwersytet Przyrodniczy, Lublin*
Katarzyna Juda-Rezler, *Politechnika Warszawska*
Jolanta Kanclerz, *Uniwersytet Przyrodniczy, Poznań*
Włodzimierz Kanownik, *Uniwersytet Rolniczy im. Hugona Kołłątaja, Kraków*
Ewa Karwowska, *Politechnika Warszawska*
Vytatuas Kesminas, *Laboratory of Ecology and Physiology of Hydrobionts, Nature Research Centre, Vilnius, Lithuania*
Marta Kosior-Kazberuk, *Politechnika Białostocka*
Piotr Koszelnik, *Politechnika Rzeszowska*
Marek Kowalik, *Uniwersytet Technologiczno-Humanistyczny, Radom*
Anna Kryszak, *Uniwersytet Przyrodniczy, Poznań*
Renata Krzyżyńska, *Politechnika Wrocławska*
Joanna Lach, *Politechnika Częstochowska*
Eugeniusz Mokrzycki, *Instytut Gospodarki Surowcami Mineralnymi i Energią PAN, Kraków*
Sadżide Murat-Błażejewska, *Uniwersytet Przyrodniczy, Poznań*
Przemysław Niedzielski, *Uniwersytet im. Adama Mickiewicza, Poznań*

Table of Contents

Spis treści

MIDDLE POMERANIAN SCIENTIFIC SOCIETY OF THE ENVIRONMENT PROTECTION
ŚRODKOWO-POMORSKIE TOWARZYSTWO NAUKOWE OCHRONY ŚRODOWISKA

Annual Set The Environment Protection
Rocznik Ochrona Środowiska

Volume/Tom 19. Year/Rok 2017 ISSN 1506-218X 17-35

Water Quality Trends of the Tisa River Along its Flow Through Serbia

Jasmina Josimov Dundjerski, Radovan Savic, Jasna Grabic, Bosko Blagojevic
University of Novi Sad, Serbia

1. Introduction

The Tisa River is the longest tributary of the Danube River. It originates by joining two watercourses, the White and the Black Tisa. It is an international river which flows through Ukraine, Romania, Slovakia, Hungary and its lower part is in Serbia. A small part of its basin is located in Serbia, only about 6%. The total catchment area is 157220 km^2, of which 24% is in mountainous region, 32% in hilly and 34% is in lowland (ICPDR 2016). Since the lowland part of Hungary has been often flooded, in the nineteenth century extensive river regulation works were performed reducing its length from 1419 km to 966 km. After accomplishing the works 589 km of riverbed remained cut off from the river and 136 km of new riverbed has been excavated (Pavic et al. 2009). However, even after a large number of cuts of accented river bends, the Tisa River still represents one of the most uniform meandering watercourses in the world (Czaya 1998). Since 1972 the lower part of the Tisa River is exposed to the effects of backwater from the dam Djerdap on the Danube and from 1977 the section upstream from Novi Becej is exposed to the effects of backwater from the dam near Novi Becej, built at 65 river-km. Due to this causes flow regime of the Tisa has changed compared to earlier natural condition (Skoric 2014).

The Tisa River runs through Serbia along its downstream section 164 km in length. It confluences the Danube opposite to Stari Slankamen

(Gavrilovic & Dukic 2002). The river has a character of meandering, slow flowing watercourse which speed has additionally been slow down along a section upstream of the dam near Novi Becej. In the average the Tisa is the richest with water during the spring, with maximal flow rates and water level in April, while during autumn months in September and October flow rates and water levels are minimal (Pavic & Mesaros 2006, Pavic et al. 2009). The average flow rate of the Tisa is about 830 $m^3 s^{-1}$, which represent 5.6% of the total runoff of the Danube basin (Savic et al. 2014).

The largest number of tributaries, including the most powerful, such as the Moris and the Samos, the Tisa receives upstream, along its flow trough Hungary. In Serbia, the only larger tributary is the Begej River. Besides, it receives waters after joining with the Keres, canalized Zlatica, the Adjanska bara, the Cik, canal Hs DTD Novi Becej – Bezdan and the Jegricka. Baring in mind that the most of the Tisa's basin is located outside Serbia this river enters Serbia already polluted (Skoric 2014).

The Tisa is one of the most important watercourses in Serbia and has great significance for water management of the region, especially since it has become a central part of the Hydrosystem Danube-Tisa-Danube (Hs DTD). Together with the Danube it represents the source of water supply for the Hs DTD and is also a recipient of excess and waste water (Skoric 2014). The area of Vojvodina (the northern part of Serbia), through which the Tisa River flows, is dominated by flatland with about 85% of agricultural land and 75% of arable land. However, it was concluded that concentrated pollutants originating from settlements and industries still have more significant impact on the quality of surface waters in comparison to agriculture (Becelic-Tomin et al. 2015, Besermenji et al. 2011, Savic et al. 2017, Vujovic et al. 2013). Used water degrade ecosystem of the canal system, especially during the summer months. Water quality is of crucial importance for the public water supply, agriculture, industry, the development of forestry, fishing, nautical tourism and recreation (Andjelkovic et al. 2014, Cramer & Kistinger 2003, Csatho et al. 2007, Rodic et al. 2003).

It should be noted that the natural boundaries of the Tisa River basin, within this area have been disturbed after construction of the Hs DTD. The system of sluices and other hydrotechnical facilities has established an artificial water regime and enabling water redirection within the canal network between the Tisa and the Danube River.

The paper presents comparative analysis of indicators of the quality of the water body Tisa along its flow through Serbia and their trends. The examination of trends was confined to the trends over time, the period from 2004 to 2014. The quantification of trends was performed and their significance was demonstrated.

2. Materials and Methods

The scope of this analyses are water quality data of the Tisa River for period 2004-2014, obtained from monitoring points located along its flow through Serbia: Martonos, Novi Becej and Titel. Data sources for water quality parameters, used in this paper, were the Republic Hydrometeorological Service of Serbia and the Agency for Environmental Protection of the Republic of Serbia. Water quality parameters, chosen for this analysis, were those physical-chemical parameters used for assessment of water bodies, i.e. for classification and are sampled monthly in average:

- Conductivity (EC) $\mu S\ cm^{-1}$,
- Dissolved oxygen (DO) $mg\ dm^{-3}$,
- Biochemical oxygen demand (BOD_5) $mg\ dm^{-3}$,
- Chemical oxygen demand (COD) $mg\ dm^{-3}$,
- Nitrates (NO_3) $mg\ dm^{-3}$ and
- Total phosphorus (Tot. P) $mg\ dm^{-3}$.

This water quality analyses encompassed 2376 data in total.

On the basis of a set of measurements of parameters, from the measuring points, samples were formed. Numerical characteristics of the samples were obtained using the average annual values, which were further exploited for analysis and interpretation of results. Applied methods:

- Basic statistical data processing

Mean annual values were obtained by calculating the arithmetic mean of the measured parameter values during the year.

- Linear regression for determining trend

Linear regression for obtaining regression lines is a common procedure for calculation based on a data set containing pairs of observations (Xi, Yi) in order to obtain an inclination that best fits the data. In the case of temporal data, value Xi represents the time, while Yi represents a value of parameters of the studied phenomena. Assessment of the trend is

obtained from the slope of the regression line, as a measure of the severity of the trend. Trends of the analyzed parameters were obtained from the sign of the coefficients of direction of regression lines, determined by linear regression. Statistical analysis of linear regression, of mean annual values of the parameters analyzed, has been performed by the application of statistical functions executed in Microsoft Office Excel 2007.

- Mann-Kendall non-parametric test for assessing the significance of the trend together with Sen's method for assessing slope (US EPA 2006, Veljkovic & Jovicic 2009, Zelenakova et al. 2015).

Mann-Kendall test enables quantifying the trend, slope evaluation and proof that the trend assessment is statistically different from zero. Sen's method, used for the evaluation of slope, was applied for calculating slope of all pairs of temporal points. Furthermore, the average of all slopes is used as the score of the total slope. If there are n temporal points and Yi denotes the data value for the i-th temporal point, if there are no missing data, then there will be $n(n-1)/2$ possible pairs of temporal points (i, j), where $i < j$. The slope of this pair of points represents the change in the value of the time interval and is expressed by the formula:

$$Q = (Yj - Yi)/(j - i) \quad (1)$$

where:
Q – the slope between the data Yi and Yj,
Yi – temporal data i,
Yj – temporal data j,
j – any time after time i.

Moreover, statistic S (Mann-Kendall S) is calculated, which represents the difference between the number of positive and negative values of Q by the formula:

$$S = \sum Q(+) - \sum Q(-) \quad (2)$$

If there is no trend, then the number of positive and negative slopes will be about the same, and S will be close to zero. In the case where the number of positive slopes prevails ($S \gg 0$), an ascending trend can be expected and vice versa, if the negative slopes are prevalent ($S \ll 0$), a descending trend can be expected. After determining the slope of all Q, obtained Q values are ranked in ascending sequence. Finally, the median of the Q' is determined, which represents the score of the slope.

Sen's estimate determines median Q' of the series according to formula (3) or (4) which represents score of the slope:

$$Q' = Q[(N' + 1)/2] \quad \text{if N' is odd} \tag{3}$$

$$Q' = (Q[(N'/2] + Q[(N' + 2)/2] \quad \text{if N' is even} \tag{4}$$

where:
N' – number of calculated slopes.

This method is used for determining if obtained median is statistically different from zero. Interval of trust of the median is determined by estimating the level of upper and lower bounds of the trust interval using slopes of appropriate rank. For two-sided confidence interval around the median of the slope, at the first place z is determined for certain confidence, i.e. two-sided 95% $z_{(1-0,05/2)} = z_{0.975} = 1.96$. Furthermore, estimate of the variance is calculated using Mann-Kendall statistics S, developed by Kendall, 1975 (US EPA 2006, Veljkovic & Jovicic 2009, Zelenakova et al. 2015), according to the formula:

$$\mathrm{VAR(S)} = \frac{1}{18}\left[n(n-1)(2n+5) - \sum_{p=1}^{q} tp(tp-1)(2tp+5)\right] \tag{5}$$

where:
n – number of data of the examined sample,
q – number of different Q data which are repeating,
tp – number of repeating of each of the Q data which is repeating.

Then statistics z_0 is calculated by formula:

$$z_0 = \frac{S - \mathrm{sign(S)}}{\sqrt{\mathrm{VAR(S)}}} \tag{6}$$

where:
S – Mann-Kendall statistics S,

$$\mathrm{sign(S)} \begin{cases} 1 \text{ if } S > 0 \\ 0 \text{ if } S = 0 \\ -1 \text{ if } S < 0 \end{cases}$$

To determine the extent of rank for required confidence interval, C_α value is determined by the formula:

$$C_\alpha = z_{(1-\alpha/2)} \sqrt{\mathrm{VAR(S)}} \tag{7}$$

where:

$z_{(1-\alpha/2)}$ – critical values for the selected threshold of significance after the Normal distribution.

Using values C_α the rank of the lower (M_1) and upper (M_2+1) bounds of the confidence interval are determined by the formula (8) and (9):

$$M_1 = (N' - C_\alpha)/2 \quad (8)$$

$$M_2 = (N' + C_\alpha)/2 \quad (9)$$

Values (M_1) and (M_2+1) are representing serial numbers of the slope Q in the regulated growing sequence. If zero (change of sign) does not lie between the upper and lower bounds of the confidence interval, then it can be concluded that the median of the slope is statistically significant for the required level of significance.

- Assessment of the Tisa River water quality

The assessment of water quality has been carried out on the basis of multi-year average annual values of parameters obtained by calculating the arithmetic mean of average annual value, in a similar manner as in a study of (Kanownik & Policht-Latawiec 2015, Sojka & Murat-Blazejewska 2009, Veljkovic & Jovicic 2009, Zelenakova et al. 2015).

Table 1. National water quality classification of surface waters bodies, Velike nizijske reke (Official Gazette RS 74/2011, 50/2012)
Tabela 1. Krajowa klasyfikacja jakości wód powierzchniowych, Velike nizijske reke (Official Gazette RS 74/2011, 50/2012)

Parameters	Limit values for classes				
	I	**II**	**III**	**IV**	**V**
EC (μS cm^{-1})	<1000	<1000	1000-1500	1500-3000	>3000
DO (mg dm^{-3})	>8.5	8.5-7	7-5	5-4	<4
BOD_5 (mg dm^{-3})	<2	2-5	5-8	8-20	>20
COD (mg dm^{-3})	<5	5-10	10-20	20-50	>50
NO_3 (mg dm^{-3})	<1	1-3	3-6	6-15	>15
Tot. P (mg dm^{-3})	<0.05	0.05-0.2	0.2-0.4	0.4-1	>1

Comprehensive revision of water policy is present in the EU member countries, where among others the rules of Water Framework Directive (WFD) were introduced and implemented (Mrozik et al. 2015). In Serbia

current classification and criteria for water quality were used for the assessment in the paper (Table 1), (Official Gazette RS 74/2011, 50/2012), all harmonized with the Water Framework Directive (Directive 2000/60/EC).

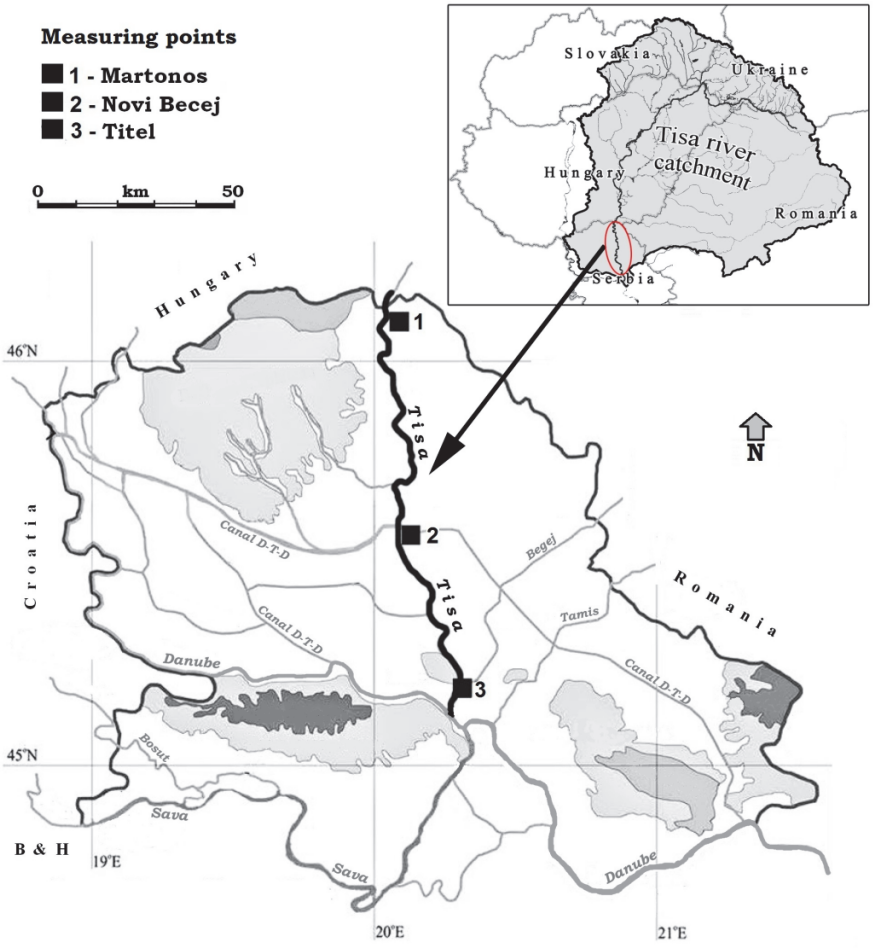

Fig. 1. Location of the measuring points on the Tisa River in Serbia
Rys. 1. Lokalizacja punktów pomiarowych na rzece Tisa w Serbii

Figure 1 shows position of the measuring points along the Tisa River in Serbia, which water quality monitoring data were used in this analyses, while Table 2 presents detailed description of the measuring

points, as well as the hydrological characteristics (Distance: the distance in km from the mouth of the Tisa River; Catchment: the area in square km, from which water drains towards the measuring point; Sampling location in profile: L – Left bank, M – Middle of the river, R – Right bank).

Table 2. List of measuring points on the Tisa River in Serbia
Tabela 2. Lista punktów pomiarowych na rzece Tisa w Serbii

Location name/ Measuring point	Latitude d. m. s.	Longitude d. m. s.	Distance (river-km)	Catchment (km^2)	Profile location
Martonos	46 06 52	20 05 13	155.0	135130	R
Novi Becej	45 35 06	20 08 30	65.0	145415	L
Titel	45 11 52	20 19 07	8.7	157174	M

3. Results and Discussion

Table 3 and Figures 2, 3 and 4 are showing the average annual and multiannual values of the analyzed water quality parameters of the Tisa River (EC, DO, BOD_5, COD, NO_3 and Tot. P), for the period 2004-2014. Water quality at all measuring points (Martonos, Novi Becej and Titel) is assessed according to the contemporary regulations (Official Gazette RS 74/2011, 50/2012), prescribed criteria and reference values. All average annual values belong to I and II classes. Therefore, it can be concluded that, the ecological status of the Tisa River is excellent to good that is also in line with the requirements of the WFD (Directive 2000/60/EC).

However, when index of degradation quality (IDQ) was applied (Savic et al 2014), which is defined by the quotient value of the parameters on the downstream and upstream measuring point, quality degradation processes are present in the section Matonos – Novi Becej (parameters: dissolved oxygen IDQ=0.88, BOD_5 IDQ=1.16 and COD IDQ=1.04). The reason is most probably due to backwater from the dam near Novi Becej. On the downstream section Novi Becej – Titel quality degradation processes are not significantly expressed. Lescesen et al. (2014) draw similar conclusions reached by the application of water quality index (WQI) on the Tisa for the period 2003-2012 at measuring points: Martonos, Novi Becej and Titel.

Table 3. Water quality assessment of the Tisa River in Serbia, average values and classes of ecological status for the period 2004-2014
Tabela 3. Ocena jakości wody rzeki Tisa w Serbii, wartości średnie i klasy stanu ekologicznego w latach 2004-2014

Measuring points	**EC** ($\mu S\ cm^{-1}$)	**DO** ($mg\ dm^{-3}$)	**BOD_5** ($mg\ dm^{-3}$)	**COD** ($mg\ dm^{-3}$)	**NO_3** ($mg\ dm^{-3}$)	**Tot. P** ($mg\ dm^{-3}$)
Martonos	excellent class I 438.44	excellent class I 10.09	excellent class I 1.89	good class II 5.09	good class II 1.06	good class II 0.148
Novi Becej	excellent class I 439.19	excellent class I 8.86	good class II 2.19	good class II 5.27	good class II 1.05	good class II 0.147
Titel	excellent class I 438.81	excellent class I 8.91	good class II 2.01	good class II 5.16	good class II 1.02	good class II 0.145

According to the results of water quality analysis overall conclusion is that the Tisa and the catchment area that belongs to Serbia is under pressure from pollution directly from polluters situated along its course, as well as from canals of the Hs DTD. Due to the small decline, which in the lower reaches of the Tisa is only 4.5 cm km^{-1}, self-purification is slower. The biggest share of pollution originates from the canal network. On some sections of the Hs DTD in Backa degradation of water quality is constantly present (Grabic et al. 2016, Milanovic et al. 2011, Pantelic et al. 2012).

Degradation of canal water quality is accelerated after joining of the Krivaja River, which is one of the most polluted rivers in Serbia (Savic et al. 2014). Furthermore, the greatest danger threatening the Tisa is from hasardous pollution. Last such accident happened in the spring of 2000, when from the Samos River, Romanian tributary of the Tisa, large amounts of cyanide and heavy metals reached the Tisa. Contamination has been so great that the use of water and fish from the Tisa and the Danube in Serbia was prohibited during four months (Pavic et al. 2010).

Changes in the quality of the water bodies of the Tisa River at measuring points in the period 2004-2014 are presented with regression lines, trends lines for analyzed parameters, at Figures 2-4. In the Figures 2, 3 and 4 and in Table 4, in the equations of regression lines, the value x represents the ordinal number of years for which the parameter values are given (x = 1, 2, ..., 11).

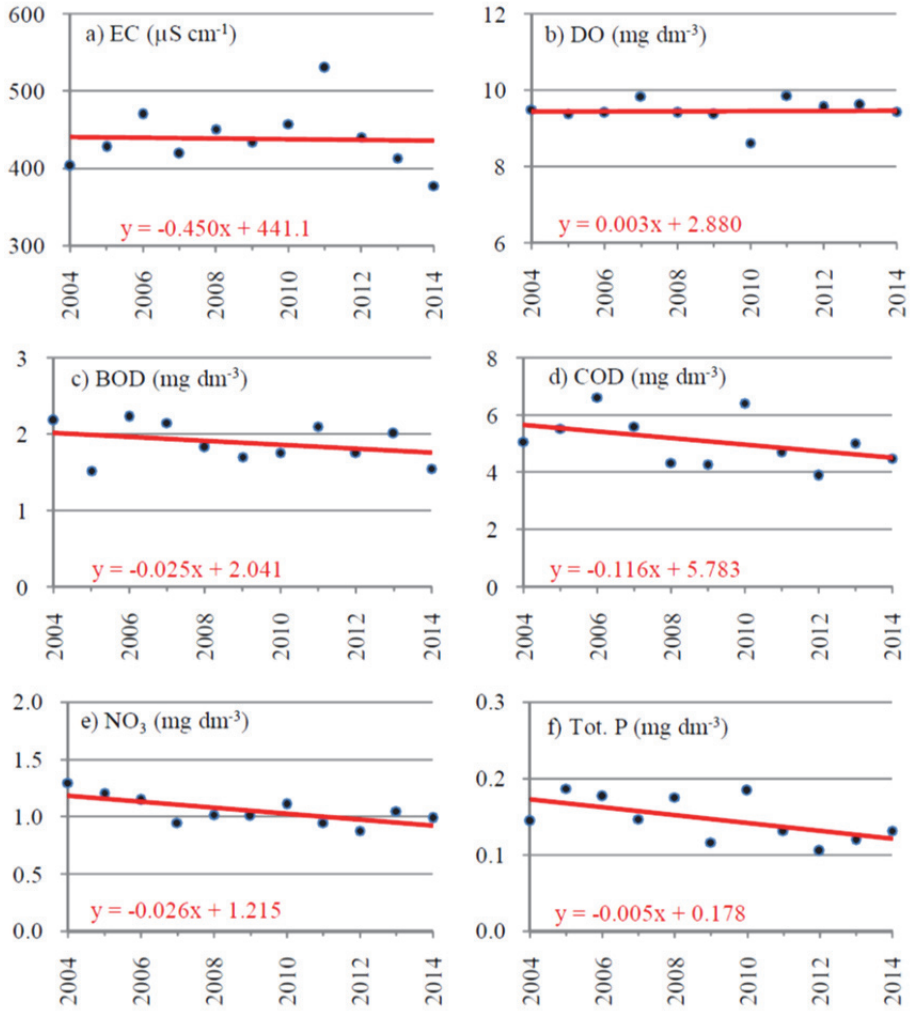

Fig. 2. The Tisa River, measuring point Martonos, average annual values of water quality parameters and regression lines; (x – ordinal number of years, x = 1, 2, ..., 11)

Rys. 2. Rzeka Tisa, punkt pomiarowy Martonos, średnie roczne wartości parametrów jakości wody i linie regresji; (x – liczba porządkowa lat, x = 1, 2, ..., 11)

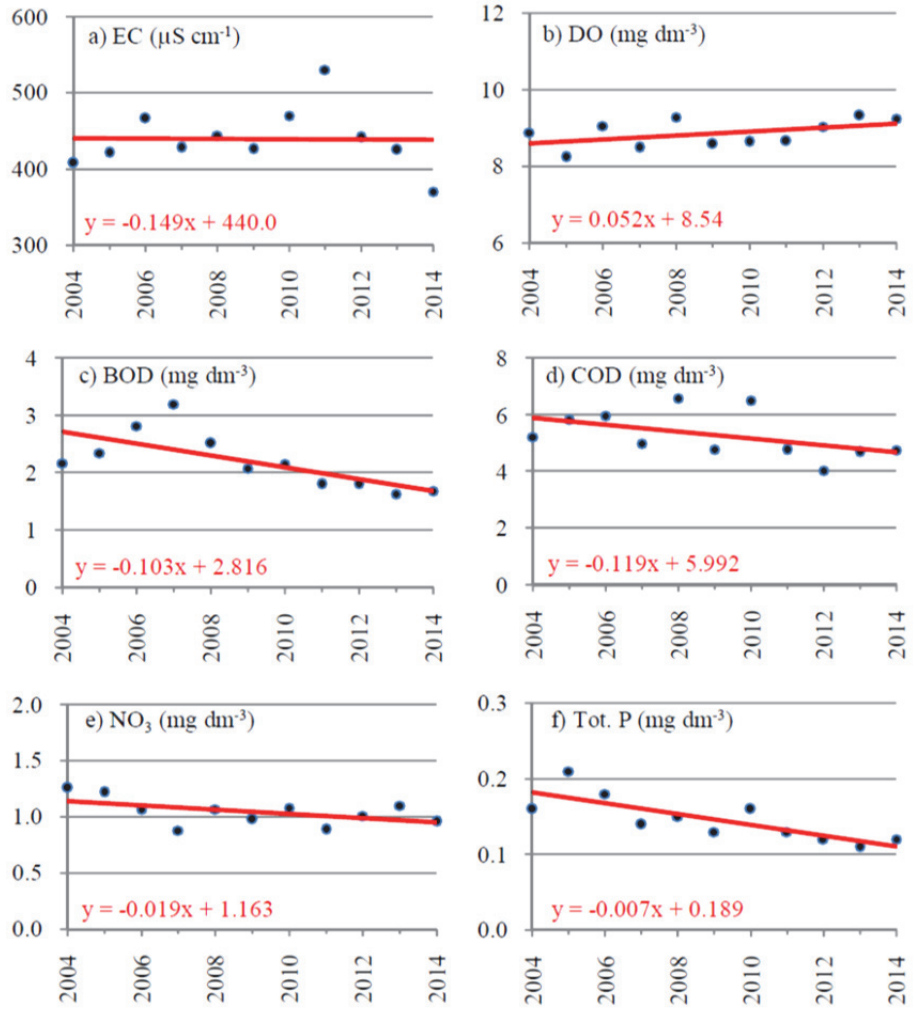

Fig. 3. The Tisa River, measuring point Novi Becej, average annual values of water quality parameters and regression lines (x – ordinal number of years, x = 1, 2, ..., 11).

Rys. 3. Rzeka Tisa, punkt pomiarowy Novi Becej, średnie roczne wartości parametrów jakości wody i linie regresji; (x – liczba porządkowa lat, x = 1, 2, ..., 11)

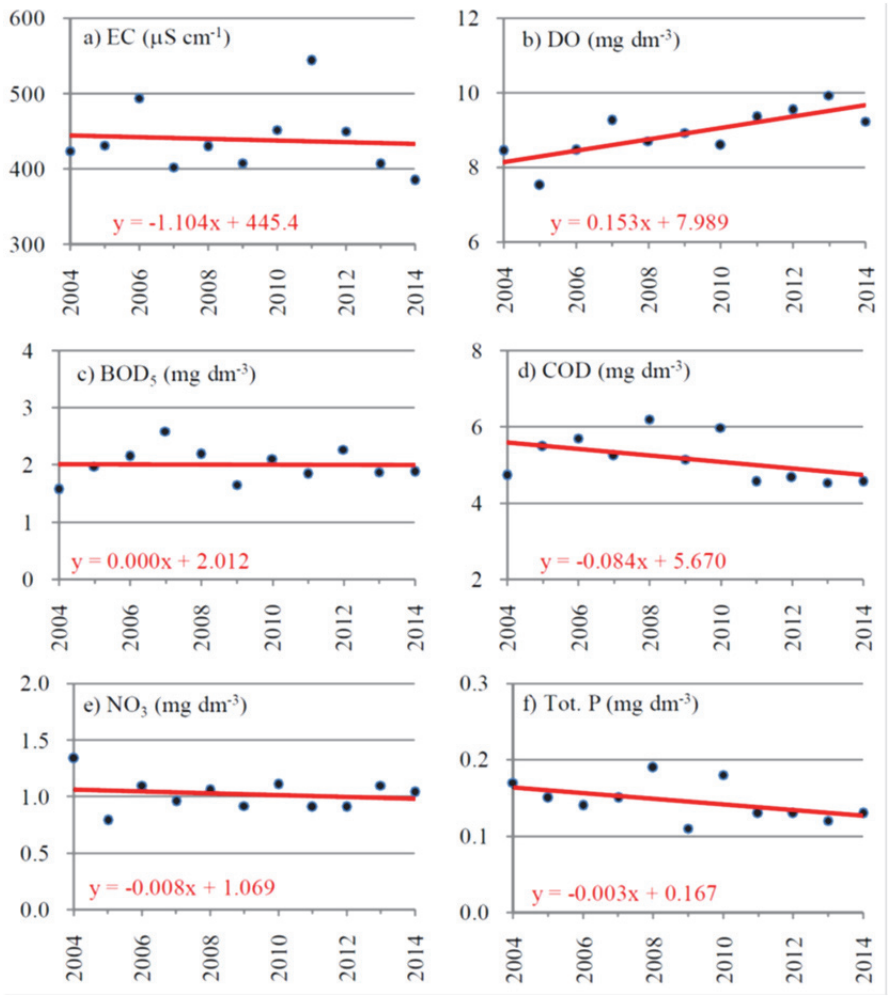

Fig. 4. The Tisa River, measuring point Titel, average annual values of water quality parameters and regression lines (x – ordinal number of years, x = 1, 2, ..., 11)
Rys. 4. Rzeka Tisa, punkt pomiarowy Titel, średnie roczne wartości parametrów jakości wody i linie regresji; (x – liczba porządkowa lat, x = 1, 2, ..., 11)

Applied Mann-Kendall test enabled the quantification of the trend, rating of slope and proving that the assessment of the trend is statistically different from zero at a significance level of α=0.05. The results of the analysis of the significance of the trend are shown in Table 4. For

the parameters analyzed from the measuring point: Martonos, Novi Becej and Titel, regression lines are given, as well as statistics S which sign represents the direction of the trend, calculated estimates of variance Var(S) of the statistics S, statistics z_0 and the probability p determined by finding the probability p ($Z > |z_0|$) to test the existence of a trend.

Table 4. Trend analysis of water quality parameters at the measuring points using the Mann-Kendall test
Tabela 4. Analiza trendów parametrów jakości wody w punktach pomiarowych przy użyciu testu Mann-Kendall

Param.	Linear regression	Mann-Kendall statistic (S)	Var(S)	Z_0	p	Increasing/ Decreasing trend (↗/↘)
Martonos						
EC	y = -0.450x + 441.1	-1	165.00	0.00	0.5000	no trend
DO	y = 0.003x + 2.880	6	165.00	0.39	0.3485	no trend
BOD_5	y = -0.025x + 2.041	-16	151.33	-1.22	0.1112	no trend
COD	y = -0.116x + 5.783	-17	163.00	-1.25	0.1056	no trend
NO_3	y = -0.026x + 1.215	-28	132.00	-2.35	0.0094	**Decreasing↘**
Tot. P	y = -0.005x + 0.178	-22	155.00	-1.69	0.0455	no trend
Novi Becej						
EC	y = -0.149x + 440.0	3	165.00	0.16	0.4364	no trend
DO	y = 0.052x + 8.540	23	157.00	1.76	0.0392	no trend
BOD_5	y = -0.103x + 2.816	-34	146.00	-2.73	0.0032	**Decreasing↘**
COD	y = -0.119x + 5.992	-25	159.00	-1.90	0.0287	no trend
NO_3	y = -0.019x + 1.163	-16	134.67	-1.29	0.0985	no trend
Tot. P	y = -0.007x + 0.189	-39	152.33	-3.08	0.0010	**Decreasing↘**
Titel						
EC	y = -1.104x + 445.4	-7	165.00	-0.47	0.3192	no trend
DO	y = 0.153x + 7.989	35	162.00	2.67	0.0038	**Increasing↗**
BOD_5	y = 0.000x + 2.012	3	150.67	0.16	0.4364	no trend
COD	y = -0.084x + 5.670	-22	159.00	-1.67	0.0475	no trend
NO_3	y = -0.008x + 1.069	-7	139.33	-0.51	0.3050	no trend
Tot. P	y = -0.003x + 0.167	-21	152.33	-1.62	0.0526	no trend

According to the normal distribution, at the threshold of significance α=0.05, for two-sided test, the critical value of $z_{(1-\alpha/2)}$ for the normal distribution is $z_{(1-0,05/2)} = z_{0.975} = 1.96$. The results showed existence of trends along the analyzed section: decreasing at measuring points Martonos and Novi Becej, and increasing at measuring point Titel. For most of the parameters, although the trend line shows the growth or de-

cline (e.g. in Figures 2f, 3b and 4d), applied methodology has not confirmed their significance.

In Table 5 median estimates of trends by Sen's method are given. At the level of significance of α=0.05, for the two-sided confidence interval of 95%, values (M_1) and (M_2+1) determine the rank of the lower and upper bounds of the confidence interval and are representing number of the growing series of slopes, while (Q_{M1}) and (Q_{M2+1}) of the slope value.

Table 5. Estimate of the median slope of water quality parameters using Sen's method

Tabela 5. Szacowanie średniego nachylenia parametrów jakości wody przy użyciu metody Sen

Parameter	Median of slope Q′	M_1	M_2+1	Q_{M1}	Q_{M2+1}	Significance of the slope
Martonos						
EC	-6.05	14.91	41.10	-36.7300	30.6100	no significance
DO	0.03	14.91	41.10	-0.1840	0.2100	no significance
BOD_5	-0.13	15.45	40.56	-0.3900	0.1260	no significance
COD	-0.53	14.99	41.02	-1.2403	0.3810	no significance
NO_3	-0.10	16.23	39.77	-0.2000	-0.0223	**Significant**
Tot. P	-0.03	15.30	40.70	-0.0506	0.0027	no significance
Novi Becej						
EC	4.13	14.91	41.10	-38.5429	33.8770	no significance
DO	0.23	15.22	40.78	-0.0356	0.5202	no significance
BOD_5	-0.39	15.66	40.34	-0.7100	-0.1530	**Significant**
COD	-0.45	15.14	40.86	-1.1886	0.0588	no significance
NO_3	-0.09	16.13	39.78	-0.1800	0.0178	no significance
Tot. P	-0.03	15.41	40.61	-0.0448	-0.0102	**Significant**
Titel						
EC	-15.65	14.91	41.10	-43.2463	2.7570	no significance
DO	0.63	15.03	40.98	0.1815	0.9990	**Significant**
BOD_5	0.03	15.48	40.53	-0.3100	0.2512	no significance
COD	-0.34	15.14	40.86	-0.9200	0.0988	no significance
NO_3	-0.01	15.94	40.07	-0.1518	0.1207	no significance
Tot. P	-0.02	15.41	40.61	-0.0366	0.0052	no significance

Based on presented results, in most (14) cases there is no significant trend, but it is confirmed that there are also significant trends: for nitrates at the measureing point Martonos; BOD_5 and total phosphorus at the measuring point Novi Becej and for dissolved oxygen at the measuring point Titel. The signs of these significant trends speak in favor of future improvements in the quality of a the water body Tisa in Serbia.

4. Conclusion

The Tisa River is one of the most important watercourses in Serbia. The river has significant water importance for water management, especially since it has become a central hydrological junction of the Hs DTD. Together with the Danube it represents the source of the water supply for the Hs DTD and at the same time it receives excess and waste water. According to the results of the analysis of water quality overall conclusion is that the water body Tisa, within basin belonging to Serbia, is under pressure from pollution originating, either directly from polluterse located along its course and from tributaries – rivers and the canal Hs DTD. Assessment of quality of the water body was carried out using the current classification criteria of the Republic of Serbia, harmonized with WFD. Reference conditions for achieving excellent ecological status, i.e. class I, are achieved for conductivity and dissolved oxygen observed along the flow (measuring points: Martonos, Novi Becej and Titel) and BOD_5 at measuring point Martonos. Downstream at measuring points Novi Becej and Titel, for BOD_5, water quality belongs to class II. According to the concentration of the parameters COD, nitrates and total phosphorus water quality belongs exclusively to class II.

Trend analysis of water quality using the Mann-Kendall test in most (14/18) cases, i.e. in 78%, confirmed the non-existence of a significant trend. Therefore, it can be concluded that water quality during the past decade is stable. A statisticaly significant trend was confirmed in 4 cases: nitrates (measuring point Martonos, descending trend), BOD_5 and total phosphorus (measuring point Novi Becej, descending trend), and dissolved oxygen (measuring point Titel, increasing trend).

The signs of these statsiticaly significant trends are speaking in favor of future improvements in the quality of the water body Tisa in Serbia. Esentially, all values of these parameters are belonging to excellent or good ecological status, i.e. I or II water quality class, which attainment is required by the Water Framework Directive.

References

Andjelkovic, A., Djekovic, V., Milosevic, N. (2014). Quality control of the water and sludge in Palic lake. [In Serbian]. *Forestry, 1-2*, 113-129.

Becelic-Tomin, M., Dalmacija, B., Stanojevic, D., Pesic, V., Krcmar, D., Kerkez, D., Tomasevic, D. (2015). Current and planned activities in the field of water management in Serbia. *International Journal of Sanitary Engineering Research, 9(1)*, 14-20.

Besermenji, S., Kosi, K., Vujacic, M. (2011). Pollution of water resources in vojvodina. *Geographica Timisiensis, 20(2)*, 5-12.

Cramer, T. & Kistinger, S. (2003). Risk and water resource management in the Tisa River basin. *Wasser und Boden, 55(5)*, 33-37.

Csatho, P., Sisak, I., Radimszky, L., Lushaj, S., Spiegel, H., Nikolova, M.T., Nikolov, N., Cermak, P., Klir, J., Astover, A., Karklins, A., Lazauskas, S., Kopinski, J., Hera, C., Dumitru, E., Manojlovic, M., Bogdanovic, D., Torma, S., Leskosek, M., Khristenko A. (2007). Agriculture as a source of phosphorus causing eutrophication in Central and Eastern Europe. *Soil Use and Management, 23(1)*, 36-56.

Czaya, E. (1998). *The rivers of the Earth*. Budapest: Gondolat.

Directive 2000/60/EC of the European Parliament and the Council of 23 October 2000 establishing a framework for Community action in the field of water policy (L 327/1 of 22.12.2000).

Gavrilovic, LJ. & Dukic, D. (2002). *Rivers of Serbia*. [In Serbian]. Belgrade: Zavod za udzbenike i nastavna sredstva.

Grabic, J., Bezdan, A., Benka, P., Josimov Dundjerski, J., Salvai, A. (2016). Water quality management for preserving fish populations within Hydrosystem Danube-Tisa-Danube, Serbia. *Carpathian Journal of Earth and Environmental Sciences, 11,* 235-243.

ICPDR – International Commission for the Protection of the Danube River, Tisza Basin, Last visited: 6th of December, 2016. (https://www.icpdr.org/main/danube-basin/tisza-basin)

Kanownik, W. & Policht-Latawiec, A. (2015). Changeability of oxygen and biogenic indices in waters flowing through the areas under various anthropopressure. *Polish Journal of Environmental Studies, 24(4)*, 1633-1640.

Lescesen, I., Pantelic, M., Dolinaj, D., Lukic, T. (2014). Assessment of water quality of the Tisa river (Vojvodina, North Serbia) for ten year period using Serbian Water Quality Index (SWQI). *Geographica Pannonica, 18,* 102-107.

Milanovic, A., Milijasevic, D., Brankov, J. (2011). Assessment of polluting effects and surface water quality using water pollution index: a case study of Hydro-system Danube-Tisa-Danube, Serbia. *Carpathian Journal of Earth and Environmental Sciences. 6*, 269-277.

Mrozik, K., Przybyla, Cz, Pyszny, K. (2015). Problems of the Integrated Urban Water Management. The Case of the Poznan Metropolitan Area (Poland). *Rocznik Ochrona Środowiska, 17,* 230-245.

Pantelic, M., Dolinaj, D., Savic, S., Stojanovic, V., Nadj, I. (2012). Statistical analysis of water quality parameters of Veliki Bački Canal (Vojvodina, Serbia) in the period 2000-2009. *Carpathian Journal of Earth and Environmental Sciences. 7*, 255-264.

Pavic, D., Dolinaj, D., Dragicevic, S. (2009). Thermal regime of water and ice on the Tisza river in Serbia. [In Serbian]. *Collection of papers – Faculty of Geography at the University of Belgrade, 57*, 35-46.

Pavic D., Mesaros M. (2006). Navigability features of the Tisa River in Serbia as the main precondition for nautical tourism development. [In Serbian]. *Turizam, 10,* 112-115.

Pavic, D., Mesaros, M., Zivkovic, N. (2010). Water pollution and water quality of the Tisa River in Serbia. [In Serbian]. *Collection of papers – Faculty of Geography at the University of Belgrade, 58*, 47-62.

Regulation on the parameters of the ecological and chemical status of surface waters and the parameters of the chemical and quantitative status of groundwater. Official Gazette of the RS, No 74/2011.

Regulation on threshold values of limit values for pollutants in surface waters and ground waters and sediments and the deadlines for their achievement. Official Gazette of RS, No 50/2012.

Rodic, M.N., Vidovic, M.M., Vidovic, M.U. (2003). *Anthropological influences of the Tisa river.* The Sixth International Symposium and Exhibition on Environmental Contamination in Central and Eastern Europe and the Commonwealth of Independent States. Prague, 1-5.

Savic, R., Bezdan, A., Josimov Dundjerski, J., Letic, LJ., Nikolic, V., Ondrasek D. (2014). Water quality degradation of Krivaja watercourse. [In Serbian]. *Agro-knowledge Journal, 52*, 159-172.

Savic, R., Ondrasek, G., Letic, LJ., Nikolic, V., Tanaskovik, V. (2017). Nutrients accumulation in drainage channel sediments. *International Journal of Sediment Research*, *32(2)*, 180-185.

Savic, R., Pejic, B., Ondrasek, G., Vranesevic, M., Bezdan, A. (2013). Utilisation of natural resources for irrigation in Vojvodina. [In Serbian]. *Agro-knowledge Journal, 14*, 133-142.

Skoric, M. (2014). *The impact of emissions of pollution on the Tisa river and measures for improvement of the ecological and chemical status.* [In Serbian]. Master thesis. Faculty of Agriculture, University of Novi Sad.

Sojka, M., Murat-Blazejewska, S. (2009). Physico-chemical and Hydromorphological State of a Small Lowland River. [in Polish]. *Rocznik Ochrona Srodowiska, 11*, 727-737.

United States Environmental Protection Agency (US EPA) (2006). *Data Quality Assessment: Statistical Methods for Practitioners EPA QA/G-9S*. Washington, USA: Office of Environmental Information.

Veljkovic, N., Jovicic, M. (2009). Nitrate concentrations Trends in Serbian watercourses. [In Serbian]. *Voda i sanitarna tehnika (Water and Sanitary Engineering), 39(1)*, 23-30.

Vujovic, S., Kolakovic, S., Becelic-Tomin, M. (2013). Evaluation of significantly modified water bodies in Vojvodina by using multivariate statistical techniques. *Hemijska industrija, 67(5)*, 823-833.

Zelenakova, M., Purcz, P., Oravcova, A. (2015). Trends in water quality in Laborec River, Slovakia. *Procedia Engineering, 119*, 1161-1170.

Trendy zmian jakości wody rzeki Tisa wzdłuż jej biegu przez Serbię

Abstract

The problem of the paper is water quality of the water body Tisa which geographically belongs to Serbia. The scope of the analyses are water quality monitoring data of the Tisa River at tree measuring points along its flow through Serbia: Martonos, Novi Becej and Titel in period 2004-2014. The analyses encompassed conductivity, dissolved oxygen, BOD_5, COD, nitrates and total phosphorus. Assessment of water quality has been conducted by the application of contemporary classifications and criteria of the Republic of Serbia. Reference conditions for achieving excellent ecological status, I class of water quality are achieved for conductivity, dissolved oxygen, along investigated section (measuring points: Martonos, Novi Becej and Titel) and BOD_5 at the measuring point Martonos. Downstream at measuring points Novi Becej and Titel for BOD_5 water quality belongs to class II. According to concentrations of COD, nitrates and total phosphorus water quality belongs exclusively to class II. Linear regression analyses was applied for determining trend lines of parameters, while Mann-Kendell test in most cases (14/18), i.e. 78%, has confirmed non-existence of significant trend. Water quality during the past decade is stable. A statistically significant trend was confirmed in 4 cases: nitrates (measuring point Martonos, descending trend), BOD_5 and total phosphorus (measuring

point Novi Becej, descending trend), and dissolved oxygen (measuring point Titel, increasing trend). Signs of these trends speak in favor of future improvement of water quality of the Tisa River in Serbia.

Streszczenie

W artykule opisano jakość wody w rzece Tisa, która geograficznie należy do Serbii. Zakres analiz obejmuje są dane dotyczące jakości wody w rzece Tisa w punktach pomiarowych wzdłuż biegu przez Serbię: Martonos, Novi Becej i Titel w latach 2004-2014. Analizą objęto: przewodnictwo, tlen rozpuszczony, BZT_5, ChZT, azotany i fosfor ogólny. Ocena jakości wody została przeprowadzona przez zastosowanie aktualnej klasyfikacji i kryteriów w Republice Serbii. Warunki parametrów odpowiadające doskonałemu stanowi ekologicznemu, I klasy jakości wody, osiągnięto dla przewodności, tlenu rozpuszczonego, wzdłuż całego badanego odcinka (punkty pomiarowe: Martonos, Novi Becej i Titel) oraz BZT_5, w punkcie pomiarowym Martonos. W dolnym biegu rzeki, w punktach pomiarowych Novi Becej i Titel dla BZT_5 wody należą do klasy II. Jeśli chodzi o ChZT, azotany i fosfor całkowity jakość wody należy do klasy II. W celu określenia linii trendu parametrów zastosowano analizę regresji liniowej, a test Manna-Kendalla, w większości przypadków (14/18), tj. 78%, potwierdził brak znaczącego trendu. Jakość wody w ciągu ostatnich dziesięciu lat jest stabilna. W 4 przypadkach stwierdzono statystycznie istotną tendencję: azotany (punkt pomiarowy Martonos, tendencja spadkowa), BZT_5 i fosfor ogólny (punkt pomiarowy Novi Becej, tendencja spadkowa) oraz tlen rozpuszczony (punkt pomiarowy Titel, tendencja wzrostowa). Trendy mogą oznaczać poprawą jakości wody rzeki Tisa w Serbii w przyszłości.

Słowa kluczowe:
jakość wody, zanieczyszczenie, trend, test Manna-Kendalla, samooczyszczanie

Keywords:
water quality, pollution, trend, Mann-Kendall test, self-purification

MIDDLE POMERANIAN SCIENTIFIC SOCIETY OF THE ENVIRONMENT PROTECTION
ŚRODKOWO-POMORSKIE TOWARZYSTWO NAUKOWE OCHRONY ŚRODOWISKA

Annual Set The Environment Protection
Rocznik Ochrona Środowiska

Volume/Tom 19. Year/Rok 2017 ISSN 1506-218X 36-51

Comparative Study of Sustainable Key Performance Indicators in Metallurgical Industry

Radim Lenort[*], *David Staš*[*], *Pavel Wicher*[*], *David Holman*[*], *Katarzyna Ignatowicz*[**]
[*]*SKODA AUTO University,*
[**]*Bialystok University of Technology*

1. Introduction

The metallurgical industry faces many challenges in the recent global, competitive, and turbulent business environment. Sustainability is widely accepted as one of the most important approaches, which allows to reach a long-term success in the industry.

Metallurgical companies use reporting to measure, analyse and evaluate the sustainability strategy. This reporting should be based on key performance indicators (KPIs). The aim of the article is to identify and categorise the most often used sustainable KPIs and analyse methods of their evaluation in the metallurgical industry.

2. Literature review

Sustainability was presented as a new concept in "Our Common Future" report by the World Commission on Environment and Development (Brundtland Commission) in 1987 (World Commission on Environment and Development 1987).

Sustainability is practiced globally as a comprehensive strategy for improving the sustainability performance of the manufacturing industry (Li et al. 2012) and transportation (Chamier-Gliszczyński & Bohdal 2016), (Chamier-Gliszczyński & Bohdal 2016a). Although there exists a divergence of definitions of sustainability, most of them are based on

the Elkington's (2004) triple bottom line considering three fundamental sustainability dimensions: economic, environmental and social:

- Sustainability is a wise balance among economic development, environmental stewardship, and social equity (Sikdar 2003).
- Sustainability includes equal weightings for economic stability, ecological compatibility and social equilibrium (Goncz 2007).
- Sustainability is the complete plan of ethical action for an organization which is attempting to transform itself into sustainable, i.e. to become pro-environmental, pro-social, and traditional pro-economic (Lijo & Gopalakrishnan 2015).

This concept is increasingly reflected in corporations in order to derive specific sustainability performance indicators and to set related targets (Chamier-Gliszczyński & Bohdal 2016), (Kannegiesser & Gunther 2014).

Bateh et al. (2014) differentiate between internal and external sustainability. Internal sustainability is concerned with survival in a competitive market, which increasingly includes global competition. External sustainability takes into account societal needs that relate to quality of life issues worldwide.

Lijo & Gopalakrishnan (2015) suggest E3S model for sustainability, which contains four dimensions with the following components:

1. Economical – recycling natural resource, reusable packaging, long term customer relationship and loyalty, achieving scale economies, solution for resource scarcity, and competitive advantage (see also Chamier-Gliszczyński 2011).
2. Environmental – market pressure, life cycle assessment, product stewardship, value chain management, carbon credits, and customer perception.
3. Ethical – design consideration, utilitarian cost benefit, reduction of negative externalities, equitable responsibilities, and homogeneous business practices.
4. Social – organizational sustenance, building social identity, organizational social affiliation, psychological affiliation to social commitment, community support, and brand building.

3. Research methodology

Global Reporting Initiative (GRI) standards for sustainability reporting were used to carry out the comparative study. The GRI standards enable organizations to measure and understand their most critical impacts on the environment, society and the economy (Global Reporting Initiative 2016):

1. The economic dimension of sustainability concerns an organization's impacts on the economic conditions of its stakeholders, and on economic systems at local, national, and global levels.
2. The environmental dimension of sustainability concerns an organization's impacts on living and non-living natural systems, including land, air, water and ecosystems.
3. The social dimension of sustainability concerns an organization's impacts on the social systems within which it operates.

GRI defines the topic-specific standards for each dimension. Economic sustainability includes six topics, environmental sustainability eight topics, and social sustainability nineteen topics (see Table 1). Each topic contains one or more disclosures. For example, the environmental disclosures for Materials, Energy and Water topics are shown in Table 2.

Table 1. GRI sustainability topics (Global Reporting Initiative 2016)
Tabela 1. GRI obszary zrównoważonego rozwoju (Global Reporting Initiative 2016)

Economic Dimension	Environmental Dimension
Economic Performance	Materials
Market Presence	Energy
Indirect Economic Impacts	Water
Procurement Practices	Biodiversity
Anti-corruption	Emissions
Anti-competitive Behaviour	Effluents and Waste
	Environmental Compliance
	Supplier Environmental Assessment

Table 1. cont.
Tabela 1. cd.

Social Dimension	
Employment	Rights of Indigenous Peoples
Labour/Management Relations	Human Rights Assessment
Occupational Health and Safety	Local Communities
Training and Education	Supplier Social Assessment
Diversity and Equal Opportunity	Public Policy
Non-discrimination	Customer Health and Safety
Freedom of Association and Collective Bargaining	Marketing and Labelling
Child Labour	Customer Privacy
Forced or Compulsory Labour	Socioeconomic Compliance
Security Practices	

Table 2. GRI environmental disclosures – example of three topics (Global Reporting Initiative 2016)
Tabela 2. GRI przykłady poszczególnych obszarów środowiskowych (Global Reporting Initiative 2016)

Topic	Disclosure
Materials	Materials used by weight or volume
	Recycled input materials used
	Reclaimed products and their packaging materials
Energy	Energy consumption within the organization
	Energy consumption outside of the organization
	Energy intensity
	Reduction of energy consumption
	Reductions in energy requirements of products and services
Water	Water withdrawal by source
	Water sources significantly affected by withdrawal of water
	Water recycled and reused

GRI administers the GRI Sustainability Disclosure Database, which is a collection of all sustainability reports of which GRI is aware. To analyse sustainability KPIs and methods of their evaluation, top 15 steel-producing companies were selected (see Table 3).

The GRI column in Table 3 indicates the company has a sustainable report according to GRI. The KPI column shows, what

companies were selected for the detailed analysis. The selection criteria were:

1. The sustainability report is available in web sites of the company.
2. The sustainability report is in English language.
3. The report includes a comprehensive system of sustainable KPIs.

Table 3. Top 15 steel-producing companies in 2015, tonnage in million tonnes of crude steel production (World Steel Association 2016a)
Tabela 3. Wykaz największych przedsiębiorstw produkujących stal w 2015 roku, tonaż w mln ton produkcji stali surowej (World Steel Association 2016a)

Rank	Company	Country	Tonnage	GRI	KPIs
1	ArcelorMittal	Luxembourg	97.14	x	x
2	Hesteel Group	China	47.75		
3	NSSMC	Japan	46.37	x	
4	POSCO	South Korea	41.97	x	x
5	Baosteel Group	China	34.94	x	
6	Shagang Group	China	34.21		
7	Ansteel Group	China	32.50	x	
8	JFE Steel Corporation	Japan	29.83	x	
9	Shougang Group	China	28.55		
10	Tata Steel Group	India	26.31	x	
11	Wuhan Steel Group	China	25.78	x	
12	Shandong Steel Group	China	21.69	x	
13	Hyundai Steel	South Korea	20.48	x	x
14	Nucor Corporation	USA	19.62	x	
15	Maanshan Steel	China	18.82	x	

These criteria met only three companies and their reports:

1. ArcelorMittal (AM) – Annual Review 2015: Structural Resilience (ArcelorMittal 2016).
2. POSCO (PO) – POSCO Report 2015: Integrated Report of Economic, Environmental and Social Sustainability (POSCO 2016).
3. Hyundai Steel (HS) – Hyundai Steel Sustainability Report 2015 (Hyundai Steel 2015).

In addition, KPIs used by World Steel Association (WS) to report sustainability of the metallurgical industry at the global level (World Steel Association 2016b), were included to the comparative study.

5. Results and discussion

In the first step, sustainable KPIs from the analysed reports were assessed and categorised according to the GRI standards. The economic KPIs and their occurrence in the reports are shown in Table 4.

Table 4. Economic KPIs, based on the analysed sustainability reports
Tabela 4. Ekonomiczne kluczowe wskaźniki efektywności ujęte w raportach zrównoważonego rozwoju

GRI topic	KPI	WS	AM	PO	HS
Economic Performance	R&D investments	x	x	x	
	Economic Value Distributed (EVD)	x	x		x
	Direct economic value generated (revenues)		x	x	x
	Environmental investments		x	x	x
	Environmental costs			x	x
	Investments in STEM (Science, Technology, Engineering and Maths) projects		x	x	
	Number of beneficiaries of community projects		x		
	Social responsibility expenditures			x	x
	Donation to charity			x	
Anti-corruption	Number of Board self-assessments		x		
	Employees completed code of business conduct training		x	x	
	Employees completed anti-corruption training		x		
	Number of operations with a local confidential whistleblowing system		x		
	Complaints received via internal audit		x		
	Subsidiaries' implementation of compliance program			x	

The metallurgical industry representatives use KPIs only for measuring two GRI economic topics (of six defined): Economic Performance and Anti-corruption. They put the most emphasize on the direct and distributed economic value. Although the EVD includes all "responsible" investments, the metallurgical companies underline its economic sustainability using specific KPIs in the area of R&D, environmental and social

investments. R&D is necessary for the internal sustainability, and environmental and social investments especially for the external sustainability.

The environmental KPIs and their occurrence in the reports are presented in Table 5.

Table 5. Environmental KPIs, based on the analysed sustainability reports
Tabela 5. Środowiskowe kluczowe wskaźniki efektywności ujęte w raportach zrównoważonego rozwoju

GRI topic	KPI	WS	AM	PO	HS
Materials	Material efficiency	x			
	Raw materials used by weight		x		
	Steel scrap recycled		x		
	By-product recycling		x	x	x
Energy	Energy intensity	x	x		x
	Energy consumption		x	x	x
Water	Water intake		x	x	x
	Net water consumption		x		
Emissions	Greenhouse Gas (GHG) emissions	x	x	x	x
	Dust emissions		x	x	x
	NO_x emissions		x	x	x
	SO_x emissions		x	x	x
	Chemicals emissions			x	x
Effluents and Waste	Wastewater discharge			x	x
	Waste disposed (landfill, incineration)		x	x	
Environmental Compliance	Environmental Management Systems (EMS)	x	x		

The researched representatives use KPIs for measuring most GRI environmental topics (six of eight): Materials, Energy, Water, Emissions, Effluents and Waste, and Environmental Compliance. It indicates the environmental dimension is very crucial for the metallurgical industry due to very serious negative impacts on environment (Zwolińska 2013). Crucial topics are materials (with focus on by-product recycling), energy, emissions, and water because metallurgy belongs among industries with the biggest by-product production (especially slag, but also waste gases, sludge, and dust), energy consumption, emissions and water consumption.

The social KPIs and their occurrence in the reports are included in Table 6.

Table 6. Social KPIs, based on the analysed sustainability reports
Tabela 6. Społeczne kluczowe wskaźniki efektywności ujęte w raportach zrównoważonego rozwoju

GRI topic	KPI	WS	AM	PO	HS
Employment	Employee turnover rate		x	x	x
	Rate of return from parental/maternity leave			x	x
	Number of new hires			x	
	Retired employees			x	
	Retired employees who reached retirement age			x	x
Labour/ Management Relations	Number of strikes exceeding one week in duration		x		
	Number of formal consultations with the European Works Council		x		
	Employee satisfaction			x	
Occupational Health and Safety	Lost time injury frequency rate	x	x	x	
	Fatalities		x		
	Accidents		x	x	x
	Absenteeism rate		x		
	Industrial operations Certified o OHSAS 18001		x		x
Training and Education	Training time	x	x	x	
	Training expenses			x	
	Number of employees trained			x	
	Trainee satisfaction index			x	
Diversity and Equal Opportunity	Managers that are female		x	x	
	Female employees			x	x
	Employees by age			x	x
	Employees with disabilities			x	
Freedom of Association and Collective Bargaining	Employees covered by collective bargaining agreements		x		
Human Rights Assessment	Employees completed human rights training				
Local Communities	Volunteering hours			x	x
	Employee volunteer participation rate				x
Supplier Social Assessment	Global procurement suppliers evaluated against code for responsible sourcing		x		

This led authors to propose system for the aggregate evaluation of sustainable KPIs based on the Analytic Hierarchy Process (AHP) method. AHP method was chosen for two main reasons. Firstly, whole concept of sustainability is based on three main dimensions, which are further divided into different areas. Therefore, its basic logical structure corresponds with the hierarchical structure, which for its evaluation encourages the use of AHP method. This fact is confirmed by its relatively frequent application in the measurement and assessment of sustainability as it is shown in review articles (Tajbakhsh & Hassini 2015) and (Diaz-Balteiro et al. 2017). Secondly, AHP method is also relatively simple to understand and apply, and there are cheap, sophisticated and user-friendly software solutions. These benefits enable it to be used not only in a research work, but also in corporate practice.

6. Proposal of aggregate sustainability performance evaluation using AHP

Potential of AHP utilization in the sustainability measurement, analysis and evaluation was verified on the example of sustainability KPIs used by World Steel Association and its data series (World Steel Association 2016b).

The AHP is a multistage decomposition method used to solve decision-making problems involving more than one criterion of optimality developed by Saaty (2008). It belongs among the large family of the multi-criteria decision-making methods. The basic idea is to create a decision-making hierarchy and the subsequent evaluation of importance of the single links among the interconnected elements. These evaluations are represented by weights, which are determined on the basis of pairwise comparison. A detailed characteristic of the method and selected applications can be found in (Saaty & Vargas 2012). To verify AHP utilization in the sustainability performance assessment the Super Decisions software was used.

AHP model developed for the aggregated sustainability performance based on the World Steel Association KPIs and data from 2007 to 2015 is shown in Figure 1.

Provided the pairwise comparison matrices in Tables 7, 8, and 9, the global weights of the individual sustainable dimensions and KPIs are equal to the values in Table 10.

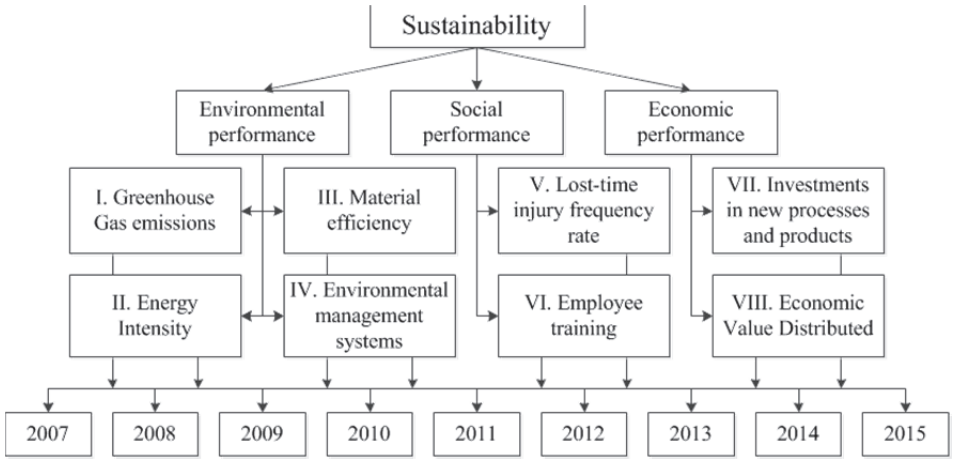

Fig. 1. AHP model of the World Steel Association sustainable KPIs
Rys. 1. Model AHP dla kluczowych wskaźników efektywności zrównoważonego rozwoju, World Steel Association

Table 7. Pairwise comparison matrix for the sustainable dimensions
Tabela 7. Macierz porównań parami dla wymiarów zrównoważonego rozwoju

Dimension	Environmental	Social	Economic
Environmental	1	2	1/2
Social	1/2	1	1/3
Economic	2	3	1

Table 8. Pairwise comparison matrix for the environmental dimension
Tabela 8. Macierz porównań parami dla wymiaru środowiskowego

Environmental KPI	I.	II.	III.	IV.
I.	1	2	3	4
II.	1/2	1	2	3
III.	1/3	1/2	1	2
IV.	1/4	1/3	1/2	1

Table 9. Pairwise comparison matrix for the social and economic dimensions
Tabela 9. Macierz porównań parami dla wymiaru społecznego i ekonomicznego

Social KPI	V.	VI.	Economic KPI	VII.	VIII.
V.	1	2	VII.	1	2
VI.	1/2	1	VIII.	1/2	1

Table 10. Global weights of sustainable dimensions and KPIs
Tabela 10. Globalne wagi wymiarów zrównoważonego rozwoju oraz kluczowych wskaźników efektywności

KPI	Weight (%)	Dimension	Weight (%)
I.	13.9	Environmental	29.7
II.	8.2		
III.	4.8		
IV.	2.8		
V.	10.9	Social	16.3
VI.	5.4		
VII.	36.0	Economic	54.0
VIII.	18.0		

The significance of the sustainability dimensions is in the following order: Economic (the most significant with weight of 54%), Environmental (29.7%), and Social (16.3%). The most significant KPIs are Investments in new processes and products (36%), Economic Value Distributed (18%), and Greenhouse Gas emissions (13.9%).

With respects to the global weights the AHP method allows to calculate the aggregated environmental, social, and economic performance (see Figure 2, 3, and 4) as well as the overall sustainable performance of the metallurgical industry (see Figure 5) in the analysed period. 2015 was determined as the base period.

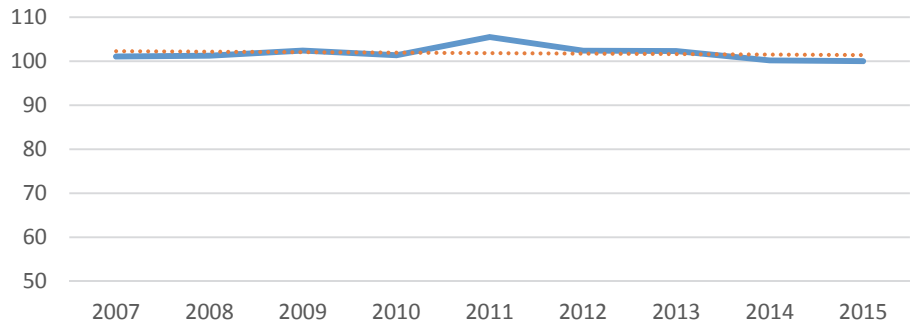

Rys. 2. Procentowa efektywność wymiaru środowiskowego w przemyśle metalurgicznym
Fig. 2. Environmental performance of the metallurgical industry [%]

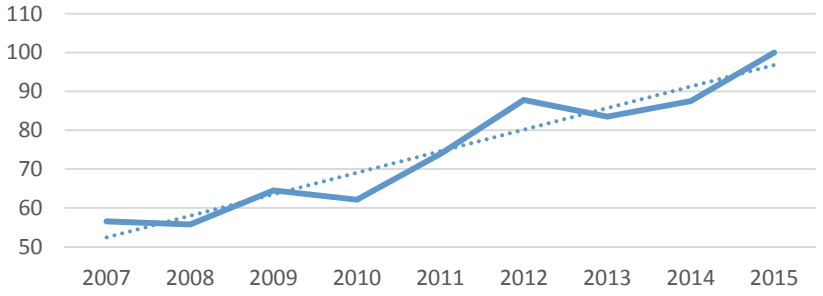

Rys. 3. Procentowa efektywność wymiaru społecznego w przemyśle metalurgicznym
Fig. 3. Social performance of the metallurgical industry [%]

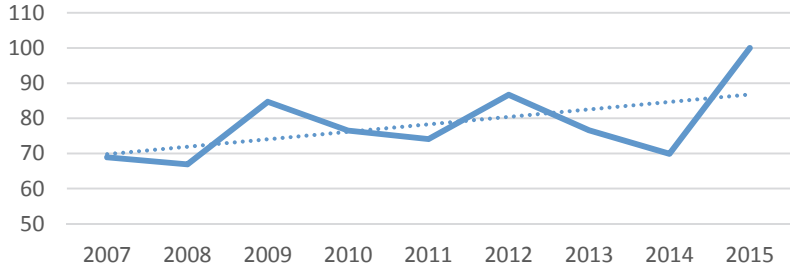

Rys. 4. Procentowa efektywność wymiaru ekonomicznego w przemyśle metalurgicznym
Fig. 4. Economic performance of the metallurgical industry [%]

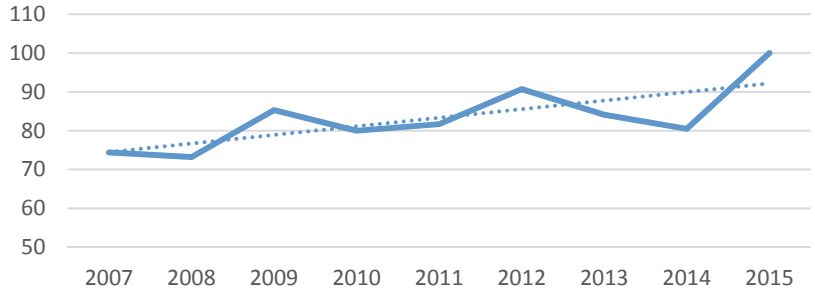

Rys. 5. Procentowa efektywność zrównoważonego rozwoju w ujęciu całkowity dla przemysłu metalurgicznego
Fig. 5. Overall sustainability performance of the metallurgical industry [%]

It is obvious the overall sustainability of the metallurgical industry gradually rises in the analysed period. This growth is caused by the social and economic performance. On the contrary, the environmental performance stagnates in the period.

7. Conclusion

The comparative study of KPIs in the metallurgical industry allows to identify the most important categories and indicators in the economic, environmental, and social sustainability dimensions. It has been confirmed an essential role of the economic dimension in the form of the direct and distributed economic value and a large importance of the environmental factors headed by materials, energy, emissions, and water KPIs. The article has also proven the AHP method is a suitable tool for the aggregate evaluation of sustainability, not only in the metallurgical industry.

Acknowledgement

The work is research output of the project "Green Solutions for Business and Industry", funded with the support of the European Union under the programme "Erasmus+", project registration number: 2014-1-CZ01-KA203-002096 and of the specific university research of Ministry of Education, Youth and Sports of the Czech Republic at SKODA AUTO University No. SGS/2015/02.

References

ArcelorMittal. (2016). *Annual Review 2015: Structural Resilience*. ArcelorMittal.

Bateh, J., Horner, D.H., Jr., Broadbent, A., Fish, D. (2014). Towards a theoretical integration of sustainability: A literature review and suggested way forward. *Journal of Sustainability Management, 2(1)*, 35-42.

Chamier-Gliszczyński, N. (2011). Environmental aspects of maintenance of transport means. End-of life stage of transport means. *Eksploatacja i Niezawodnosc (Maintenance and Reliability), 2*, 59-71.

Chamier-Gliszczyński, N., & Bohdal, T. (2016). Urban mobility assessment indicators in the perspective of the environment protection. *Rocznik Ochrona Srodowiska,* 18, 670-681.

Chamier-Gliszczyński, N., & Bohdal, T. (2016a). Mobility in urban areas in environment protection. *Rocznik Ochrona Srodowiska,* 18, 387-399.

Diaz-Balteiro, L., González-Pachón, J., Romero, C. (2017). Measuring systems sustainability with multi-criteria methods: A critical review. *European Journal of Operational Research, 258 (2)*, 607-616.

Elkington, J. (2004). Enter the Triple Bottom Line. In: Henriques, A., & Richardson, J. (Eds), *The Triple Bottom Line: Does It All Add up?* London: Earthscan, 1-16.

Global Reporting Initiative. (2016, January 10). *GRI Standards*, Retrieved from: https://www.globalreporting.org/standards/

Goncz, E., Skirke, U., Kleizen, H., Barber, M. (2007). Increasing the rate of sustainable change: a call for a redefinition of the concept and the model for its implementation. *Journal of Cleaner Production, 15(6)*, 525-37.

Hyundai Steel. (2015). *Hyundai Steel Sustainability Report 2015*. Hyundai Steel.

Kannegiesser, M. & Gunther, H. O. (2014). Sustainable development of global supply chains - part 1: sustainability optimization framework. *Flexible Services and Manufacturing Journal, 26*, 24-47.

Li, T., Zhang, H., Yuan, C., Liu, Z., Fan, C. (2012). A PCA-based method for construction of composite sustainability indicators. *The International Journal of Life Cycle Assessment, 17*, 593-603.

Lijo, J., & Gopalakrishnan, N. (2015). Converging sustainability definitions: industry independent dimensions. *World Journal of Science, Technology and Sustainable Development, 12(3)*, 206-232.

POSCO. (2016). *POSCO Report 2015: Integrated Report of Economic, Environmental and Social Sustainability*. POSCO.

Saaty, T. L. (2008). Decision making with the analytic hierarchy process. *International Journal of Services Sciences, 1(1)*, 83-98.

Saaty, T. L., & Vargas, L. G. (2012). *Models, Methods, Concepts & Applications of the Analytic Hierarchy Process*. New York: Springer.

Sikdar, S. K. (2003). Sustainable development and sustainability metrics. *AIChE Journal, 49(8)*, 1928-1932.
Tajbakhsh, A., & Hassini, E. (2015). Performance measurement of sustainable supply chains: a review and research questions. *International Journal of Productivity and Performance Management, 64(6)*, 744-783.
World Commission on Environment and Development. (1987). *Our Common Future*. Oxford: Oxford University.
World Steel Association. (2016a). *World Steel in Figures*. World Steel Association.
World Steel Association. (2016b). *Sustainability Indicators: Definitions, Relevance and Data 2003-2015*. World Steel Association.
Zwolińska, B. (2013). Types of waste streams created in steelworks. *From Conference Proceedings METAL 2013. 22nd International Conference on Metallurgy and Materials.* May 15th-17th 2013, Brno, Czech Republic.

Studium porównawcze wskaźników zrównoważonego rozwoju w przemyśle metalurgicznym

Abstract

The metallurgical industry faces many challenges in the recent global, competitive, and turbulent business environment. Contemporary, a sustainability belongs among the most important approaches, which allows to reach a long-term success in the metallurgical industry. In this study, the sustainability is understood as a balanced integration of an economic, environmental, and social performance. The aim of the article is to identify and categorise the most often used sustainable KPIs and analyse methods of their evaluation in the metallurgical industry. Global Reporting Initiative standards, World Steel Association sustainable KPIs, and sustainability reports of three global metallurgical companies were used to carry out the comparative study. It has been confirmed an essential role of the economic dimension in the form of the direct and distributed economic value and a large importance of the environmental factors headed by materials, energy, emissions, and water KPIs. Although the distributed economic value includes all "responsible" investments, the metallurgical companies underline its economic sustainability using specific KPIs in the area of R&D, environmental and social investments. From the social point of view, the metallurgical industry focuses especially on the employment, health and safety, and employee training KPIs. Based on the analysis it can be also stated that there is no aggregate evaluation used in the analysed reports. Therefore, the article proposes system for the aggregate evaluation of sustainable KPIs based on the Analytic Hierarchy Process (AHP) method. The AHP is a multi-

stage decomposition method that belongs among the large family of the multi-criteria decision-making methods. Potential of AHP utilization in the sustainability measurement, analysis and evaluation was verified on the example of sustainability KPIs used by World Steel Association and its data series. The article has proven the AHP method is a suitable tool for the aggregate evaluation of sustainability and their dimensions, not only in metallurgical industry.

Streszczenie

Funkcjonowanie współczesnego przemysłu metalurgicznego musi uwzględniać aspekt ekonomiczny, środowiskowy oraz społeczny w ujęciu koncepcji zrównoważonego rozwoju. Celem artykułu jest zidentyfikowanie, klasyfikacja oraz analiza wskaźników zrównoważonego rozwoju stosowanych w ocenie przemysłu metalurgicznego. W zaprezentowanych badaniach uwzględniono wytyczne do raportowania kwestii zrównoważonego rozwoju dla firm, kluczowe wskaźniki efektywności (KPIs) uwzględniane przez World Steel Association. Badania zostały przeprowadzone na przykładzie trzech globalnych przedsiębiorstwach metalurgicznych. Analiza sprawozdań udostępnionych przez przedsiębiorstwa pokazała, że w danych przedsiębiorstwach aspekt ekonomiczny stanowi wymiar podstawowy. Ujęcie środowiskowe zostało skoncentrowana na zużyciu materiałów, energii, wody i emisji zanieczyszczeń. Aspekt społeczny odniesiono do kwestii zatrudnienia, zdrowia, bezpieczeństwa i szkoleń pracowników zatrudnionych w przedsiębiorstwach metalurgicznych. Natomiast nie realizowana jest łączna ocena uwzględniająca wszystkie trzy aspekty zrównoważonego rozwoju. Realizując badania w przedstawionym artykule zaproponowano system łącznej oceny uwzględniający zrównoważone wskaźniki (ekonomiczne, środowiskowe i społeczne). System będzie bazował na wielokryterialnej metodzie hierarchicznej analizy problemów decyzyjnych AHP. Zaproponowana metoda umożliwia przeprowadzenie łącznej oceny ujmujące poszczególne wskaźniki zrównoważonego rozwoju. Wyniki badań zaprezentowane w artykule potwierdzają, że metoda AHP jest odpowiednim narzędziem do oceny przedsiębiorstw metalurgicznych w ujęciu koncepcji zrównoważonego rozwoju.

Słowa kluczowe:
zrównoważony rozwój, kluczowy wskaźnik efektywności,
przemysł metalurgiczny

Keywords:
sustainability, key performance indicator, metallurgical industry

MIDDLE POMERANIAN SCIENTIFIC SOCIETY OF THE ENVIRONMENT PROTECTION
ŚRODKOWO-POMORSKIE TOWARZYSTWO NAUKOWE OCHRONY ŚRODOWISKA

Annual Set The Environment Protection
Rocznik Ochrona Środowiska

Volume/Tom 19. Year/Rok 2017 ISSN 1506-218X 52-64

Wastewater Management in a Closed Cooling System of Professional Power Plant

Paweł Regucki[*], Renata Krzyżyńska[*], Zbyszek Szeliga[**]
[*]Wrocław University of Science and Technology, Poland
[**]VŠB – Technical University of Ostrava, Czech Republic

1. Introduction

In conventional and thermal power plants water is widely used in many technological processes including e.g.: water-steam cycle in power boiler, cooling system of power boiler, cooling installations of boiler's auxiliary equipment (Stańda 1999). Each of these processes requires constant access to sources of fresh water with its appropriate physical and chemical properties in order to maintain the continuity of the electricity and heat production (Hermanowicz *et al.* 2010). On the other hand, the power plants also are significant producers of pollutants and wastewater. Meaningful increase of production of wastewater and its influence on environment, recently reported e.g. by Blog (Blog 2016), indicates on the need for new restrictive regulations for water environment protection. Care for the environment results in the last industrial waste regulations of The Polish Ministry of Environment dated 18 November 2014 and the EU directive which imposed, with the beginning of 2016, new limits on the physical and chemical parameters of wastewater released to natural reservoirs (EU directive 2010/75/EU of 24 November 2010 on industrial emissions & regulation of the Polish Ministry of Environment dated 18 November 2014). The increase in environmental responsibility together with high penalties for exceeding allowable wastewater limits enforces the companies to look for the optimal management of industrial wastes. The efficient optimization process always bases on the scientific background

involving mathematical modeling and numerical approach which are more widely used in wastewater management (Skoczko *at al.* 2016).

In the paper, there is presented the mathematical model which allows to predict daily changes of sulphate ions concentration in water circulating in a close cooling system of power plant. According to the last regulations, the acceptable concentration of sulphate ions in wastewater is 500 g/m^3. Due to the fact that daily among of released water from cooling system as wastewater usually reaches the level of a several thousand m^3 its proper management could significantly reduce the cost of the system maintenance (Laudyn *et al.* 1997, Berman 1961).

2. Analysis of sulphate ions' changes in cooling system

A closed cooling system of power unit consists of condensers, cooling towers and connecting them concrete channels. Cold water from a cooling tower is transported to a condenser of power unit where is heated up receiving a latent heat during a spent steam condensation process. Next warm water returns to the cooling tower where is cooled down interacting with an air which is in counter flow motion. Cooling process of the circulating water depends on two mechanisms: its partial evaporation and heat exchange between water and the air. The most intensive evaporation is observed in summer when almost 90% of heat is exchanged through this process. The intensity of this process causes that approximately 1% of the flowing water is evaporated leading to the decrease of water temperature even about 10°C (Berman 1961). Depending on volumetric flow rates through the cooling towers, daily water loss in the system, due to its evaporation, reaches from several up to tens thousand m^3.

The understanding of thermal-flow processes inside the closed cooling system has a fundamental importance in an analysis of SO_4^{2-} concentration changes in circulating water because an increase of chemical components' concentrations in the circulating water is connected with its partial evaporation. Evaporated water is replenished by fresh one but its large demand causes that water delivered to the system cannot undergo through complex chemical treatment but mechanical cleaning only. On the other hand, sulphate ions are natural components of fresh water and its initial concentration depends on physic-chemical parameters of the local industrial water sources.

Continuous evaporation process in cooling towers and delivering of fresh water to closed cooling system causes permanent increase of SO_4^{2-} concentration. This is disadvantageous effect, for instance because an excessive increase in the concentration of SO_4^{2-} in the water may cause corrosion of concrete parts of channels and cooling tower as well as the increase in the concentration of calcium salts what can accelerate the process of their deposition on the exchanges' surfaces inside the condenser thereby impairing the heat exchange processes. In order to prevent an exceeding of the permissible SO_4^{2-} concentration limit, a part of water from the cooling system must be periodically removed to the sewage treatment plant.

3. Mathematical model of sulphate ions' concentration

Considering the changes of sulphate ions concentration in circulating water one has to take into account three main mechanisms mentioned in chapter 2:

- evaporation of water in cooling towers, $q_{\mathrm{v,ct}}$,
- discharge of wastewater to a sewage treatment plant, $q_{\mathrm{v,dw}}$,
- replenishment of fresh water, $q_{\mathrm{v,fw}}$.

Relationship between these three abovementioned processes is presented schematically at fig. 1.

Assuming that the total volume of water in the closed system V is conserved, mass conservation law must be satisfied:

$$q_{\mathrm{v,fw}}(t) = q_{\mathrm{v,dw}}(t) + q_{\mathrm{v,ct}}(t) \tag{1}$$

The analysis of losses and replenishment of water allows to formulate differential equation describing changes of SO_4^{2-} concentration in circulating water (t – time in days):

$$V \cdot \frac{dx(t)}{dt} = -q_{\mathrm{v,dw}}(t) \cdot x(t) - q_{\mathrm{v,ct}}(t) \cdot x_{\mathrm{ct}} + q_{\mathrm{v,fw}}(t) \cdot x_{\mathrm{fw}}(t) \tag{2}$$

where:
$x(t)$ – current concentration of sulphate ions in circulating water,
x_{ct} – sulphate ions concentration in vapor released in cooling tower,
$x_{\mathrm{fw}}(t)$ – concentration of sulphate ions in fresh water.

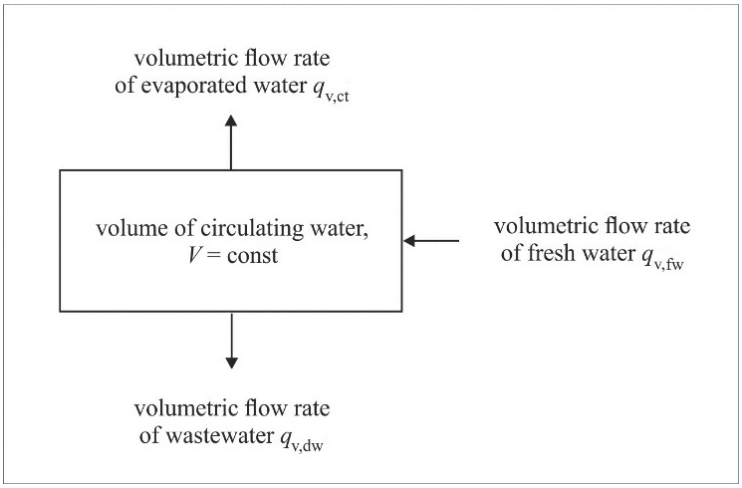

Fig. 1. Schematic balance of water in a closed cooling water system
Rys. 1. Poglądowy bilans wody chłodzącej w zamkniętym układzie chłodzenia

All concentrations are in g/m^3, volumetric flow rates in m^3/d and total volume V in m^3. Equation (2) can be analytically solved if one assumes that:

- volumetric flow rates $q_{v,dw}$ and $q_{v,ct}$ are constant over time,
- sulphate ions' concentration in fresh water is constant over time,
- vapor leaving cooling tower is chemically clean (x_{ct} = 0 g/m^3).

Taking into account above mentioned simplifications one can reduce (2) to the form of first order ordinary differential equation:

$$\frac{dx(t)}{dt} = -\alpha \cdot x(t) + \beta \tag{3}$$

where: $\alpha = q_{v,dw}/V$ and $\beta = (q_{v,dw} + q_{v,ct}) \cdot x_{fw}/V$. The solution of (3) is a function which describes change in SO_4^{2-} concentration over time:

$$x(t) = \frac{\beta}{\alpha} + \left(x_0 - \frac{\beta}{\alpha}\right) e^{-\alpha t} \tag{4}$$

where x_0 is an initial SO_4^{2-} concentration in the closed cooling system. On the fig. 2 there are shown two sample solutions of (4) for $q_{v,ct}$ = 43200 m^3/d and total water volume V = 100000 m^3. Red curve

(case A) shows function (4) for initial sulphate concentration x_0 = 60 g/m^3 and volumetric flow of wastewater $q_{v,dw}$ = 5000 m^3/d. One can notice that the SO_4^{2-} concentration increases with time up to the level of ~ 580 g/m^3 after 100 days. Blue curve (case B) shows the solution (4) for initial sulphate concentration x_0 = 600 g/m^3 and volumetric flow of wastewater $q_{v,dw}$ = 10000 m^3/d. In this case the sulphate ions concentration decreases with time reaching approximately 320 g/m^3 after 100 days.

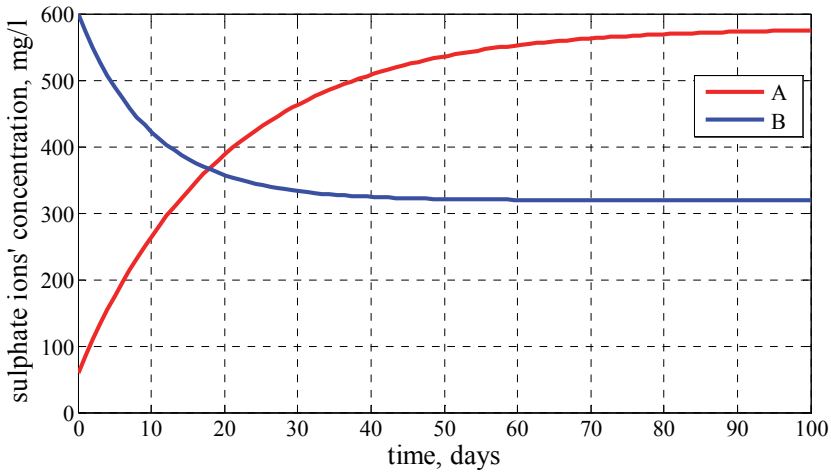

Fig. 2. Sample solutions of (4) for cases:
A (red color) – x_0 = 60 g/m^3, $q_{v,dw}$ = 5000 m^3/d;
B (blue color) – x_0 = 600 g/ m^3, $q_{v,dw}$ = 10000 m^3/d
Rys. 2. Przykładowe rozwiązania (4) dla przypadków:
A (czerwony kolor) – x_0 = 60 g/m^3, $q_{v,dw}$ = 5000 m^3/d;
B (niebieski kolor) – x_0 = 600 g/m^3, $q_{v,dw}$ = 10000 m^3/d

Figure 2 illustrates two different behaviors of the same function (4) depending on initial state of the closed cooling system. For the fixed value of SO_4^{2-} concentration in fresh water x_{fw}, the final concentration $x(t)$ depends only on the volumetric flow rate of wastewater $q_{v,dw}$. This is very important observation from economical point of view because operator, who controls the level of sulphate ions concentration in circulating water, can optimize the volumetric flow rate of wastewater keeping permissible SO_4^{2-} concentration in closed cooling system. Moreover, A and B curves at fig. 2 illustrate asymptotic behavior of the

function (4). Under given initial conditions, the solution of (3) tends to fixed value denoted by x_{asym}:

$$x_{\text{asym}} = \lim_{t\to\infty} \frac{\beta}{\alpha} + \left(x_0 - \frac{\beta}{\alpha}\right) e^{-\alpha t} = \frac{\beta}{\alpha} \tag{5}$$

The asymptotic value of $x(t)$ is determined by ratio $\beta/\alpha = x_{\text{fw}} \cdot q_{\text{v,fw}}/\ q_{\text{v,dw}}$ where $q_{\text{v,fw}}$ is calculated from (1). It is worth to mention that volumetric flow rate through the cooling towers $q_{\text{v,ct}}$ is directly connected with the number of working power units. Having knowledge about current SO_4^{2-} concentration in fresh water x_{fw} and volumetric flow rate of circulating water $q_{\text{v,ct}}$ one can reverse issue asking about minimal volumetric flow rate of wastewater $q_{\text{v,dw}}$ which satisfies legal regulations x_{legal}:

$$x_{\text{legal}} = \frac{x_{fw} \cdot \left(q_{\text{v,ct}} + q_{\text{v,dw}}\right)}{q_{\text{v,dw}}} \rightarrow \ q_{\text{v,dw}} = \frac{x_{\text{fw}} \cdot q_{\text{v,ct}}}{\left(x_{\text{legal}} - \ x_{\text{fw}}\right)} \tag{6}$$

Table 1 presents the example values of minimal volumetric flow rates $q_{\text{v,dw}}$ parametrized by sulphate ions concentration of fresh water x_{fw} and volumetric flow rate of circulating water $q_{\text{v,ct}}$.

Table 1. Example values of minimal volumetric flow rates $q_{\text{v,dw}}$ (in m^3/d), parametrized by sulphate ions concentration of fresh water x_{fw} and volumetric flow rate of circulating water $q_{\text{v,ct}}$, which satisfy legal regulations x_{legal}=500 g/m^3
Tabela 1. Przykładowe wartości minimalnych strumieni objętości odprowadzanych ścieków $q_{\text{v,dw}}$ (w m^3/d) z zamkniętego układu chłodzenia zapewniające spełnienie wymaganego limitu stężenia x_{legal} = 500 g/m^3

SO_4^{2-} ions' concentration x_{fw}, [g/m^3] / volumetric flow rate $q_{\text{v,ct}}$, [m^3/d]	40	50	60
28800	2504	3200	3927
36000	3130	4000	4909
43200	3757	4800	5891

Keeping the minimal volumetric flow rate $q_{\mathrm{v,dw}}$ which preserves legal regulations for SO_4^{2-} ions' concentration in wastewater operator can minimize operating costs of closed cooling water system both saving fresh water resources as well as minimizing the costs for industrial wastewater.

4. Comparison of the mathematical model with numerical calculation

The mathematical model (2) discussed in chapter 3 has analytical solution (4) under certain significant simplifications like fixed values of volumetric flow rates $q_{\mathrm{v,dw}}$ and $q_{\mathrm{v,ct}}$ as well as sulphate ions concentration x_{fw} in fresh water over time. It is worth to investigate an influence of variability of $q_{\mathrm{v,dw}}$, $q_{\mathrm{v,ct}}$ and x_{fw} parameters on a solution $x(t)$. Numerical solution of (2) could be found applying numerical procedure dedicated to solving ordinary differential equation of first order. The equation (2) could be discretized using Euler method with time step Δt (Mathews 1999):

$$x(t_{i+1}) = x(t_i) + \frac{\Delta t}{V}\Big(\big(q_{\mathrm{v,ct}}(t_i) + q_{\mathrm{v,dw}}(t_i)\big)\cdot x_{\mathrm{fw}}(t_i) - q_{\mathrm{v,dw}}(t_i)\cdot x(t_i)\Big) \quad (7)$$

where $t_{i+1} = t_i + \Delta t$ (Δt = 1 day). Volumetric flow rate $q_{\mathrm{v,fw}}(t)$ is calculated for each time step from the mass conservation law (1). The comparison of analytical solution (4) with numerical data obtained from (7) was derived for fixed values of volumetric flow rates $q_{\mathrm{v,dw}}$ and $q_{\mathrm{v,ct}}$ as well as sulphate ions concentration x_{fw} in fresh water over time. For better visualization of the agreement of these two curves, figure 3 presents the relative global discretization error e_i calculated from the formula:

$$e_i = \frac{\big(x_{\mathrm{a}}(t_i) - x(t_i)\big)}{x_{\mathrm{a}}(t_i)}\cdot 100\% \quad (8)$$

where: $x_{\mathrm{a}}(t_i)$ and $x(t_i)$ is analytical and numerical solution respectively.

Measurements done on real object indicate that, even if mean values of $q_{\mathrm{v,dw}}$, $q_{\mathrm{v,ct}}$ and x_{fw} are conserved, its daily values could change

over a dozen percent. This situation is illustrated at fig. 4 for volumetric flow rate of wastewater over a period of 100 days.

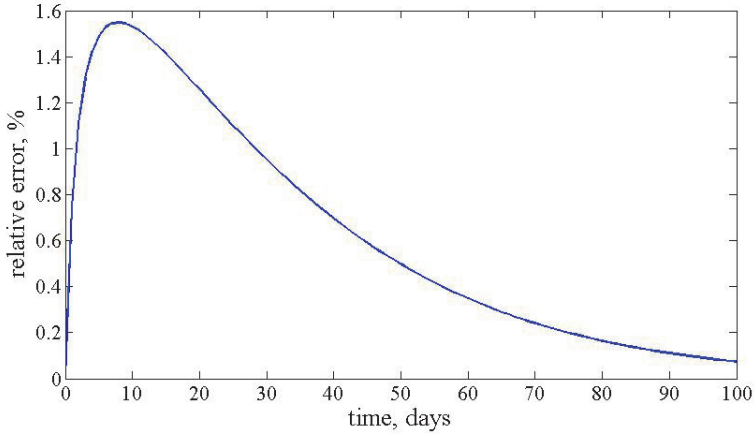

Fig. 3. Relative global discretization error e_i calculated from formula (8) for analytical and numerical solutions obtained for parameters: $x_0 = 60$ g/m^3, $q_{v,dw} = 5000$ m^3/d, $q_{v,ct} = 43200$ m^3/d and $V = 100000$ m^3

Rys. 3. Względny globalny błąd dyskretyzacji e_i obliczony ze wzoru (8) dla analitycznego i numerycznego rozwiązania otrzymanego dla parametrów: $x_0 = 60$ g/m^3, $q_{v,dw} = 5000$ m^3/d, $q_{v,ct} = 43200$ m^3/d oraz $V = 100000$ m^3

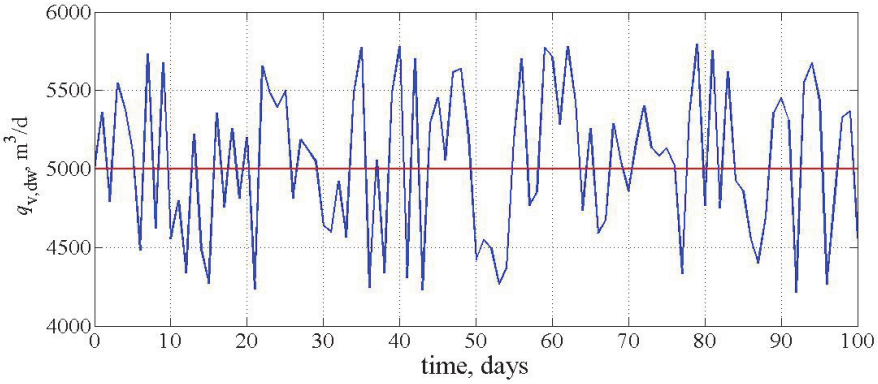

Fig. 4. Fluctuation (blue color) of volumetric flow rate of wastewater around mean value (red color) $q_{v,dw} = 5000$ m^3/d

Rys. 4. Fluktuacje strumienia objętości ścieków odprowadzanych z zamkniętego układu chłodzenia (niebieska linia) z zaznaczoną wartością średnią $q_{v,dw} = 5000$ m^3/d (czerwona linia)

In order to obtain more realistic changes of SO_4^{2-} concentration, the time fluctuations of $q_{v,dw}$, $q_{v,ct}$ and x_{fw} parameters were implemented to formula (7). An example of the numerical calculations including time variability of $q_{v,dw}$, $q_{v,ct}$ and x_{fw} is presented at fig. 5 in comparison with smooth analytical solution $x_a(t)$ calculated for mean values of $q_{v,dw}$, $q_{v,ct}$ and x_{fw}. The variability of $q_{v,dw}$, $q_{v,ct}$ and x_{fw} was at the level 20%, 16% and 10% respectively (detailed information is gathered in table 2).

Table 2. Maximum, minimum and mean values of $q_{v,dw}$, $q_{v,ct}$ and x_{fw} parameters noticed in numerical simulation illustrated at fig. 5
Tabela 2. Maksymalne, minimalne oraz średnie wartości parametrów $q_{v,dw}$, $q_{v,ct}$ i x_{fw} uzyskane podczas symulacji numerycznej przedstawionej na rysunku 5

observed value	$q_{v,dw}$, m^3/d	$q_{v,ct}$, m^3/d	x_{fw}, g/m^3
mean	5000	43200	60.0
maximum	5789	47406	71.8
minimum	4210	39008	48.1

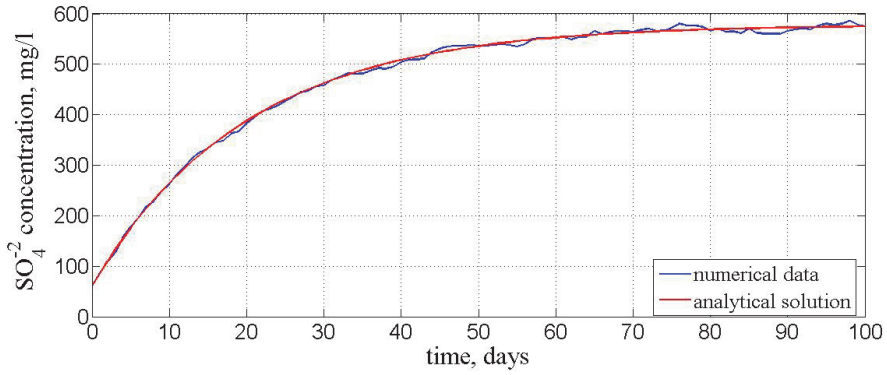

Fig. 5. Comparison of numerical calculation basing on (7) including random fluctuations of $q_{v,dw}$, $q_{v,ct}$ and x_{fw} parameters (blue color) with analytical solution (4) (red color) for the case discussed at fig. 3
Rys. 5. Porównanie rozwiązania numerycznego (7) z losową fluktuacją parametrów $q_{v,dw}$, $q_{v,ct}$ i x_{fw} (niebieski kolor) z rozwiązaniem analitycznym (4) (czerwony kolor) dla przykładu omawianego na rysunku 3

One can notice that numerical data (blue line) oscillate around analytical function (red line) and preserve its asymptotic behavior described by formula (5). The maximum value of relative global discretization error e_i, obtained in the calculation, was 3.2%. Presented example proves that analytical solution of the discussed mathematical model could be used both to optimize the volumetric flow rate of wastewater and fresh water in closed cooling system of power unit.

5. Optimization of wastewater management in closed cooling system

The advantage of the abovementioned mathematical model lies in fast and precise respond on the current working conditions of the cooling system. Using simplified analytical solution with average values of $q_{v,ct}$ and x_{fw} one can estimate optimal flow rate of wastewater $q_{v,dw}$ which preserves legal regulations - x_{legal} = 500 g/m^3. An example of the "on-line" modelling of changes of SO_4^{2-} ions concentrations is presented at fig. 6. The graph presents a simulation when during first 50 days in a power plant there operated six power units generating the volumetric flow rate of evaporated water through the cooling towers at the level of $q_{v,ct}$ = 43200 m^3/d (with x_{fw} = 50 g/m^3). Next one of these power units was stopped what caused reduction of $q_{v,ct}$ to the level of 36000 m^3/d. At this situation the actual volumetric flow rate of wastewater $q_{v,dw}$ = 4800 m^3/d was too high and the sulphate ions concentration started tend to x_{asym} = 425 g/m^3. In order to optimize the costs, after five days, a new volumetric flow rate $q_{v,dw}$ = 4000 m^3/d was applied. This corrected let to save 800 m^3 per day during the next 20 days. Finally the power unit returned to the operation and $q_{v,ct}$ increased again to the level of 43200 m^3/d. At this moment the current $q_{v,dw}$ was to low and SO_4^{2-} concentration could exceeding the permissible limits. In order to preserve this situation the flow rate of wastewater $q_{v,dw}$ returned to the old level of 4800 m^3/d.

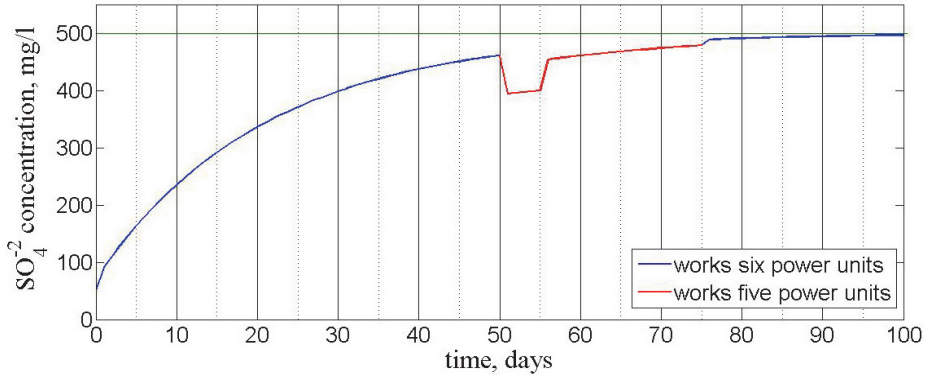

Fig. 6. Simulation of the SO_4^{2-} concentration changes in water under variable number of working power units (red part marks the analyzed period of 25 days)
Rys. 6. Symulacja zmian stężenia jonów SO_4^{2-} w cyrkulującej wodzie przy zmiennej liczbie pracujących bloków (czerwona linia wskazuje analizowany okres 25 dni)

6. Conclusions

Presented in the paper mathematical model allows not only to predict daily changes of SO_4^{2-} concentration in water circulating in closed cooling system but also to indicate asymptotic concentration of sulphate ions under given working parameters of the power system and to calculate minimal volumetric flow rate of wastewater required to keep the SO_4^{2-} concentration below legal regulations. This approach lets on an optimal utilization of water in the system and efficient management of wastewater reducing maintenance costs of the installation.

References

Berman, L. D. (1961). *Evaporative cooling of circulating water*. New York: Pergamon Press.

Blog, S. F. (Last cited 4 January 2016). Message to EPA: Time to Modernize America's Power Plants - Cooling Systems Included. http://switchboard. nrdc.org /blogs/sfleischli/message_to_epa_it_is_time_to_m.html

Council Directive 91/271 / EEC of 21 May 1991. Urban Waste Water Treatment (Acts. Office. EC L 135, 05.30.1991, p. 40, as amended. d.; Acts. Office. Polish special edition, ch. 15, v. 2, p. 26), the Directive of the European Parliament and of the Council 2010/75/EU of 24 November 2010 on industrial emissions (integrated pollution prevention and control) (recast) (OJ. office . EC L 334, 17.12.2010, p. 17, as amended. d.

Regulation of the Minister of Environment on conditions to be met when introducing waste into water or ground dated 18 November 2014 (Journal of Laws of 2014, pos. 1800).

Hermanowicz, W., *et al.* (2010). *Fizyczno-chemiczne badanie wody i ścieków*. Warszawa: Wydawnictwo Arkady.

Laudyn, D., Pawlik, M., Strzelczyk, F. (1997). *Elektrownie*. Warszawa: Wydawnictwo WNT.

Mathews, J. H., & Fink, K. D. (1999). *Numerical methods using Matlab*. New York: Prentice Hall.

Skoczko, I., Ofman, P., Szatyłowicz, E. (2016). Zastosowanie sztucznych sieci neuronowych do modelowania procesu oczyszczania ścieków w małej oczyszczalni ścieków. *Rocznik Ochrona Środowiska*, *18*, 493-506.

Stańda, J. (1999). *Woda do kotłów parowych i obiegów chłodzących siłowni cieplnych*. Warszawa: Wydawnictwo WNT.

Gospodarka wodno-ściekowa w zamkniętym układzie chłodzenia elektrowni

Abstract

The paper presents a mathematical model describing the changes in SO_4^{2-} concentration in a closed system of cooling water in a professional power plant. The analyzed installation consists of condensers and cooling towers connected by a system of channels. The main mechanism of heat transfer in the cooling tower bases on partial evaporation of water, resulting in the increase of concentration of SO_4^{2-} ions in the circulating liquid. The only mechanism to decrease concentration of undesirable chemicals in the circulating water is its periodic discharge to a wastewater treatment. According to the latest Polish Government Regulations (Regulation of the Ministry of Environment dated 18 November 2014) and the Directive of the European Parliament and of the Council (2010/75/EU of 24 November 2010 on industrial emissions) from the beginning of 2016 the new limits on the chemical components of a wastewater led to the natural tanks has been accepted, what forced planned and cost-effective wastewater treatment in a professional power plants. Presented mathematical model has an analytical solution which allows not only to predict daily changes of SO_4^{2-} concentration in circulating water but also to indicate asymptotic concentration of sulphate ions under given working parameters of the system and to calculate minimal volumetric flow rate of wastewater required to keep the SO_4^{2-} concentration below legal value.

Streszczenie

W pracy przedstawiono model matematyczny opisujący zmianę stężenia jonów siarczanowych SO_4^{2-} w zamkniętym obiegu wody chłodzącej bloku energetycznego. Analizowana instalacja obejmuje: skraplacze bloków energetycznych oraz chłodnie kominowe połączone systemem kanałów ssących i kolektorów tłocznych. Głównym mechanizmem wymiany ciepła w chłodni jest częściowe odparowanie przepływającej przez nią wody, co powoduje jednak wzrost stężeń związków chemicznych w cyrkulującej cieczy i wymusza okresowy zrzut części wody do przyzakładowej oczyszczalni ścieków. Zgodnie z najnowszymi rozporządzeniami prawnymi: Rozporządzeniem Ministra Środowiska z dnia 18 listopada 2014 roku oraz dyrektywą Parlamentu Europejskiego i Rady 2010/75/UE z dnia 24 listopada 2010 r. w sprawie emisji przemysłowych, od początku roku 2016 obowiązują nowe limity dotyczące składu chemicznego ścieków technologicznych kierowanych do zbiorników naturalnych, które wymuszają planową i oszczędną gospodarkę wodno-ściekową elektrowni. Prezentowany model matematyczny posiada analityczne rozwiązanie pozwalające nie tylko przewidzieć dobowe zmiany stężeń siarczanów w cyrkulującej wodzie, ale również określić graniczne stężenie jonów siarczanowych dla bieżących parametrów pracy układu oraz wyznaczyć minimalny strumień odprowadzanych ścieków zapewniający spełnienie norm emisji ścieków przemysłowych.

Keywords:
wastewater management, mathematical modeling, sulphate ions concentration, cooling system

Słowa kluczowe:
gospodarka wodno-ściekowa, modelowanie matematyczne, stężenie siarczanów, układ chłodzenia

MIDDLE POMERANIAN SCIENTIFIC SOCIETY OF THE ENVIRONMENT PROTECTION
ŚRODKOWO-POMORSKIE TOWARZYSTWO NAUKOWE OCHRONY ŚRODOWISKA

Annual Set The Environment Protection
Rocznik Ochrona Środowiska

Volume/Tom 19. Year/Rok 2017 ISSN 1506-218X 65-80

Hydropower Structures in the Natura 2000 Site on the River Radew: an Analysis in the Context of Sustainable Water Management

Mirosław Wiatkowski[*], *Czesława Rosik-Dulewska*[**], *Paweł Tomczyk*[*]
[*]*Wrocław University of Environmental and Life Sciences*
[**]*Institute of Environmental Engineering PAS, Zabrze*

1. Introduction

Hydropower is a potentially "clean" and "environment-friendly" renewable energy source (RES). In Poland, the interest in hydropower is stimulated by the international commitments of Poland to increase the share of RES in its overall gross energy usage. The "Energy Policy of Poland until 2030" assumes an increase of the use of RES up to 15% by 2020 and up to 20% by 2030. This indicator has been growing continuously since 2012, when it stood at 7.2% (Wiatkowski & Rosik-Dulewska 2012). Water energy – comprises to as much as 20% of power installed in various power plants around the world. In world's scale Norway and Brazil are among water tycoons (Pawłowski 2010). It is worth noting that the hydropower capacity of Poland is used only in 12% whereas, for example, France makes use of 100% of its capacity.

In the literature, one can find information on the advantages and drawbacks of small water power plants, as well as on their influence on the environment. These advantages include: there being no harmful pollution from the combustion of conventional fuels, an improvement in the saturation of water with oxygen down the dam, regulation of the water circulation system, integration into the landscape, reduction in flood risk and the formation of bird sanctuaries in the reservoirs used to drive the power plant (Fantin-Cruz et al. 2015; Kasperek & Wiatkowski 2014;

Malm Renöfält et al. 2010; Ždankus & Sabas 2006). However, in the literature information can also be found on the negative influence of such structures on the natural environment. The negative impact depends, among others, on the location of the plant and the adopted technical solution: the hydropower plants with a reservoir are more dangerous than the river hydro plants because of the outflow control and the impact on the hydrological regime down the dam (Anderson et al. 2015; Klaver et al. 2007; Jackson 2011; Malczewska 2010). Equally importantly, hydropower plants prevent the water organisms from migrating. Moreover, the power plants modify the temperatures down the dam and stimulate the bottom erosion which translates to a lower groundwater table. In what concerns the hydromorphology, new processes arise in the valley. In the case of reservoir hydro plants, sudden damming may result in the abrasion of water reservoirs (Benejam et al. 2014; Florek et al. 2008; Mihailova et al. 2013; Szoszkiewicz et al. 2014). Although the reaction of nature to the construction of a hydro plant is unpredictable (Jackson 2011; Vaikasas et al. 2015), one can take some mitigating measures such as, for example, building a fish ladder (Kasperek & Wiatkowski 2008). Therefore, the facilities should be monitored. The authors have begun research on the influence of such facilities on the natural environment. The aim of this paper is to analyze the operation of hydropower facilities "Rosnowo" and "Niedalino" within the network of protected areas Natura 2000, in the Radew river basin, north-west of Poland, in the context of sustainable water management. The natural conditions of the site are described, the legal conditions for Natura 2000 sites have been presented, and social conflicts related to the operation of water management projects in Natura 2000 areas have been highlighted. The article will contribute to the presentation of results of the assessment of the functioning of the hydro plant in the context of requirements for such objects for the protection of nature and the conditions under which they may operate.

2. Characterisation of the Radew river basin

The research area is located in the north-west of Poland, in the eastern part of the zachodniopomorskie province. According to Kondracki's classification, the area is located in the south-eastern part of the Pobrzeże Koszalińskie macro-region (Kostrzewski 1998).

The Radew is a lowland river, i.e. has a steady flow, muddy bottom and small slope. Side erosion is dominant, the course is strongly meandering and the river basin is located below 200 m ASL (KZGW 2014). The river is 93 km long, it flows out of the Kwiecko lake in the region of Żydowo and falls into the Parsęta in the region of Karlino. The surfrace area of the basin is 1082.4 km^2, which classifies this watercouse as the biggest–tributary of the Parsęta. The river has 20 tributaries. The river belongs to the water region of Przymorze Zachodnie. The basin of the river under study is part of two Natura 2000 sites, namely "Dolina Radwi, Chocieli i Chotli" and "Wiązogóra", and of other protected areas (GDOŚ 2015; Obolewski et al. 2016). The research area is shown on the map below (Fig. 1).

Fig. 1. The map of the research area (base map: geoportal.kzgw.gov.pl/imap/; date of access: 02/09/2017)
Rys. 1. Mapa obszaru badań (podkład: geoportal.kzgw.gov.pl/imap/; data dostępu: 02.09.2017 r.)

3. Hydropower use of the Radew

There are four hydropower plants operating on the Radew: "Żydowo", "Rosnowo", "Niedalino" and "Karlino". These facilities, with different power ratings, are located at different reaches of the watercourse. Although built in the 20th century, they correspond with the present EU policy on power generation. The key parameters of these small hydropower plants are given in Table 1.

Table 1. List of hydropower plants on the Radew with a short overview of each facility (Kostrzewski 1998; Obolewski et al. 2016)
Tabela 1. Wykaz elektrowni wodnych na rzece Radwi wraz z ich charakterystyką (Kostrzewski 1998; Obolewski i in. 2016)

No	Name of the plant	Km	Year built	Installed power [MW]
1.	Pumped storage power plant "Żydowo"	82+300	1971	157
2.	Hydropower plant "Rosnowo"	44+700	1922	3.3
3.	Hydropower plant "Niedalino"	36+000	1912	4.4
4.	Small hydropower plant "Karlino"	0+880	1926	0.1

Thanks to the properties of its basin and the hydrologic, geomorphic and climate conditions, the Radew has a hydropower potential and is an interesting option for water management projects despite its being part of a Natura 2000 site. As explained in, the reason for this is the high precipitation in the basin, but also the location of the river source high above its mouth and the favourable shape of the valley. The rough power of the river is 3.3 MW (Kostrzewski 1998; Obolewski et al. 2016).

There are three water sills in the middle course of the Radew, namely: the watermill at Niedalino (km 33.8, installed power: 220 kW) and the cooperating hydropower plants – Niedalino and Rosnowo. The damming of the Radew with an earth dam at km 44+700 of its course formed the Rosnowo reservoir. This reservoir supplies water for the hydropower plant Rosnowo through a supply channel. The water flows to another reservoir called Hajka, which supplies the power plant at Niedalino. Eventually, water is discharged through an outflow channel to the lower course of Radew at km 36 (Obolewski et al. 2016).

Initially, the rivers were used primarily for the generation of electricity in the pumped storage power plants of Rosnowo and Niedalino. They were also used as retention reservoirs during freshets (the idea of increasing the water retention is important due to the meager water resources of the Poland, as pointed out, among others, by Liberacki et. al 2016). Today the role of this entire hydrotechnical system has increased. It is also used for recreational purposes, as well as for fishing and as a water source in case of fire. At Mostowo, km 55+500, there are deep

water wells and water treatment stations – the water serve the city of Koszalin, as well as Mielno and Unieście (Obolewski et al. 2016).

4. Natural assets of the area

Because of the hydromorphological changes made to the middle reach of Radew, the natural conditions in a 8+ km long river section have changed drastically. The changes affected both the wetness of the terrain and its hydrological character. On a fast, shallow watercourse reservoirs were formed with a quiet flow, greater depths and a much broader channel than that of the Radew. Consequently, on the forested lands, in places with no constant presence of water ecosystems have formed characteristic of marshes. Water vegetation has appeared and these places have become a sanctuary for aquatic birds. Moreover, the area from Rosnowo to Hajka has value landscapes (GDOŚ 2015; Kostrzewski 1998).

All these factors have lead first to the creation of a protected landscape area "Dolina Radwi (Zegrze-Mostowo)" and then – in March 2009 – to the formation of a special protected habitat "Dolina Radwi, Chocieli i Chotli" in the framework of the European network of protected areas Natura 2000. The hydropower system described in this paper is part of this protected habitat. The entire site has an overall area of 22.000 ha including 4 priority sites and protects 39 species of flora and fauna listed in the annexes to the Habitats Directive and the Bird Directive (GDOŚ 2015; Kostrzewski 1998).

5. Legal factors for undertakings in the Natura 2000 sites and the principles of environmental protection and rational water management

The area being characterized is highly attractive, but its inclusion as a Natura 2000 site has also some consequences related to the specific, imposed type of usage. The main document which sets out the international policy on water is the Water Framework Directive. Being a member state, Poland is committed to adhere to its regulations. Consequently, its policies have been implemented in the Polish legal framework. For each member state there is an imposed time schedule. In the case of our country, the first deadline for the achievement of environmental goals is set to end of 2015. Consequently, important changes were made to the

Water Resources Law, the Environmental Protection Law and to many others. Lastly, new executory provisions were enacted.

In view of the above legal conditions and the new philosophy based on the approach to water as an "inherited resource", this paper thoroughly describes the hydropower plants starting from the water dam in Rosnowo and ending with the power plant in Niedalino. This description is made in the context of the requirements set out for the protected Natura 2000 sites (provided mainly in the Habitats Directive and in the Bird Directive), but also analyses the rational water management (Directive 2000; Okoński 2014).

In what concerns the provisions of the Bird Directive and the Habitats Directive, the most important principle is that of "not worsening", i.e. activities should be undertaken in such a way that the existing status of the environment. Importantly, a reference is made to the "current" status, i.e. that at the time when the Natura 2000 site was created. The main idea is to preserve at least those parts of the environment, because of which the site is considered notable, distinctive or locally representative. The reference point is the year in which the site was added to the European network of protected areas. Clearly, the actions aimed at improving the natural status are recommended, but not strictly necessary. The Natura 2000 sites are supposed to promote internationally a given area. Similar provisions can be found in Polish legislation, such as e.g. the Environmental Protection Act. Based on the example presented in our paper – the reservoirs formed about 100 years ago, the derivation channel, hydro-engineering structures and the hydropower plants in Rosnowo and Niedalino are an integral part of the landscape – this is precisely the status, to which one must refer when taking actions. The way they are they form a fully functional complete system with its specific environmental, social and economic conditions. Such unjustified actions would have been harmful not only to the environment, but also to the safety, health and well-being of people (Directive 2009; Directive 1992).

It is worth noting that at present the procedure of building a new hydropower plant in a Natura 2000 site would have been a lot more complicated. For any such investment an environmental impact assessment would have been required, in line with the Regulation of the Council of Ministers from 9 November 2010 on the undertakings with a significant potential impact on the environment. Since such an undertaking qualifies

to group II, i.e. an investment with a potentially significant impact on the environment, it would have been recommended to create a report on the environmental impact. As can be seen, the persons intending to launch new initiatives in water management will have to face several challenges, which were unheard of several dozen years ago (Rozporządzenie 2013; Ustawa 2008). This is consistent with the multidimensionality of sustainable development. As pointed out by Pawłowski should be taken into account, among others, the following aspects: the ethical dimension (the issue of humanity's responsibility for nature), the ecological dimension (nature conservation, protection of the environment created by humankind, spatial planning), the technical and technological dimension (new technologies, being economical with raw materials) (Pawłowski 2009).

6. The hydropower plants "Rosnowo" and "Niedalino" on the river Radew – an assessment of their operation in terms of the fulfilment of the environmental protection requirements

With reference to the hydropower plants "Rosnowo-Niedalino", several documents are in force which set out the rules for rational water management for the facility. These documents are based on the Water Resources Law and include: water management instructions, station instructions and operating instructions of the power plant, water permits and the aquatic legal surveys. These documents not only specify the function of the facility and its hydro-engineering structures, but also the methods and procedures for their safe operation so as to ensure a balance in the hydrographic conditions and safety of the staff and the population in line with the requirements of the current water policy (Ustawa 2001).

In what concerns the hydrotechnical system "Rosnowo", it consists of the following: the Rosnowo reservoir (formed by constructing a dam on the Radew, its retention capacity is 0.57 mln m^3 and an area of 154 ha); an earth dam with a weir, which directs the water from the reservoir to the old river bed; an evacuation channel leading to the power plant and to the Hajka reservoir, with an intake; the hydropower plant – the built part and the hydrotechnical part (3 water turbines – chambers with Francis turbines; power: 1100 kW and the nominal slope 16.4 m). Apart from these, there are also control structures (Obolewski et al. 2016).

Recently, during the period from June to August 2015, several works were completed, including the modernization of the intake lock and the supply channel. Moreover, several components in the power plant building were replaced. These works were necessary to ensure the correct functioning of the power plant and safety of the staff. Additionally, the grate at the intake to the power plant building was replaced.

Currently, the construction of a fish ladder is planned, which is the result of an order by the RZGW (Regional Board of Water Management) (RZGW 2014). Apart from that, renovation is also required for the sluice weir, which conducts the water in the case of a freshet, emergency or maintenance – an automatic weir will have to be installed, because the present capacity of the idle sluice exceeds the control discharge. In what concerns the Rosnowo reservoir, its maximum operating water level must not be exceeded and the minimum level must be maintained. This is required not only for the technical equipment to operate correctly, but also for the biological balance in the reservoir and because of safety concerns.

The silting up and shrinking of the Rosnowo reservoir is a well-documented and clearly perceivable environmental trend. Over the period of 40 years its surface decreased from 189 ha to 154 ha. Importantly, the present water permit points at the necessity of maintenance works on the river bed of the Bielica, which falls into the reservoir at a point within the reach of backwater. Such substantial works are scheduled for 2018. It is expected that this investment may not achieve some of the environmental goals under the Water Framework Directive and that some time derogation with regard to these goals should be considered. This reservation has been included in the updated draft Water Management Plan for the Odra drainage area (KZGW 2014).

The second hydropower plant "Niedalino" consists of the following structures: the Hajka reservoir with its dam (useful capacity: 0.242 mln m^3, surface area: 90 ha; dam length: 325 m and width: 4-80 m); the hydropower plant Niedalino – consisting of the above-ground part and the underground part (4 hydro-systems – turbine chambers with 3 operational Francis turbines and the following parameters: power: 1100 kW, flow rate: 5 m^3/s); a weir with a bottom sluice – a reinforced concrete weir with a 3-stage cascade and baffle piers in the spillway slab; evacuating channel, reinforced with stone material, in the Radew river bed.

Similar to the "Rosnowo" power plant, also here the usage of the Radew does not the water needs determined for the water region, i.e. the intake does not exceed the maximum flow rate determined for the hydro-engineering structures. Also the ordinates of damming between the minimum level are maintained, as well as those for letting the water pass so as to maintain the inviolable flow. The inviolable hydrobiological flow required for the maintenance of biological life and for the sake of landscape has also been determined. The hydro-engineering structures should fulfil their role, therefore their condition should be monitored and checked and maintenance should be provided. Hydrological measurements should be carried out for the flows and water levels and the Radew river bed below the dam should be kept in good condition. In what concerns the environmental protection and the consequences of operation on a Natura 2000 site, the owner is obliged to construct a fish ladder, and until this requirement is fulfilled – to restock the Hajka reservoir every year with eel, so as to maintain its population.

The latest document, which affected the direction in which the hydropower plants were rebuilt is the above mentioned order no 3/2013 of the Head of RZGW in Szczecin, dated 3 June 2014, on the terms and conditions of water usage for the regions of Dolna Odra and Przymorze Zachodnie. The most important goal of this document is to maintain the good status of the watercourses, which can be achieved by eliminating any obstacles to the inviolable flow. The most important decision is that all the hydro-engineering structures on rivers listed in a separate annex must be equipped with devices ensuring free fish migration. The changes must be made until the first rebuilding or development of the structure or until the deadline specified in the Water Management Plan for the Odra river basin area for the appropriate bodies of water. Another requirement is to install the grates with a maximum grid size of 15 mm at the entrance to the hydropower plants. These hydropower plants had such grates installed in June 2015 in Rosnowo and in August 2015 in Niedalino. The deadline for the completion of the solution for fish migration, specified in the water permit is end of 2021 for the hydropower plant in Niedalino and end of 2018 for the hydropower plant in Rosnowo (RZGW 2014). The plans outlined above prove a sensible approach to the issues of environmental protection.

7. Social conflicts related to water management in the Natura 2000 sites

Social conflicts related to water management undertakings implemented in the Natura 2000 sites stem from many various sources. The following are worth mentioning:

1) the concentrations of protected areas with valuable environmental assets and playing an important role in terms of water management;
2) ecological corridors in the areas important for water management;
3) neglect and poor financing of water management, and consequently the need to undertake tasks in protected natural sanctuaries;
4) non-compatibility between the legal framework of water management and the environmental protection laws; there being no cooperation procedures for the institutions supervising the environmental protection and those responsible for the water management system.

Such conflicts often result from decisions taken a long time ago; these conflicts were present already at the time of creation of a Natura 2000 site – in such cases it is necessary to take the right steps and find a solution. Simultaneously, a conflict is an obstacle in the implementation of water management goals or environmental protection goals for a Natura 2000 site. The causes and the course of social conflicts will be shown on the examples of the Trout Farm in Ubiedrze and the allegations of pollution into Chociel river (Badora 2013; Wiatkowski & Tomczyk 2015).

Some water management investments in the river basins located in the Natura 2000 sites are particularly controversial. One such example was the construction of a trout farm in Ubiedrze, which began in June 2011. The key charge made by the members of the Polish Angling Association was the destruction of habitats suitable for spawning grounds for endangered fish. Apart from this, the terrain includes protected wetlands, and the only known location of callitriche in Poland. Moreover, anglers voiced their concerns that the breeding of rainbow trout could adversely affect the water ecosystems by introducing a non-local species which might drive out the native species. Their observations hint that in the area of Mostowo a large proportion of the population of speckled trout has become extinct due to the fry being eaten by the "runaway" trout from the farm, leading to the homogenization of species found in the environment and to the disturbance of the biocenotic balance (Vowles et al.

2014). Therefore, there is a conflict of interests of the naturalists with those of the investor and the contractor.

The second example of social conflicts is the allegations of pollution in the upper reaches of the river – that is, discharges from the storm water treatment plant (storm outlet) of Bobolice, but also the leaky sewers of the sanitary sewage system, which overwhelmed the sewage system, significantly worsening oxygen conditions and physicochemical parameters of water. In July 2011 and in November-December 2012, inspections of the Voivodeship Inspectorate for Environmental Protection (WIOŚ), the Delegation in Koszalin, where no adverse changes were observed or legal actions were carried out. These were one-off checks, and those who had been watching for a long time noticed the change of color to dark brown and unpleasant odor – which caused death of fishes. It is worth mentioning, however, that the Regional Water Supply and Sewerage Company in Bialogard – Bobolice region, intervened several times to ensure the wells and their security. Eventually, in January 2013, appropriate action was taken, and there is currently no problem with leaks of impurities into the Chociel river (Atalap 2011, 2013).

8. Conclusions

The use of water management facilities, including those designed for power generation, located in the Natura 2000 sites requires cooperation between the specialists in the fields of both water management and environmental protection. Adhering to the principles of water management helps with achieving the targets of environmental protection.

The hydropower plants discussed in this paper have contributed to the formation of ecosystems related to water, already in existence at the time of creation of the "Dolina Radwi, Chocieli i Chotli" site. They also contributed to the specific species composition and the hydrological regime as well as other properties of the animate and inanimate world.

The hydropower plants play various roles in the environment and economy, they generate inexpensive clean energy to be used by man. This way both the power production policy and the environmental policy are implemented. The use of this alternative energy source should be promoted also in the Natura 2000 sites.

The analysis of the hydropower use of the river Radew in the "Dolina Radwi, Chocieli i Chotli" Natura 2000 site indicates that rational

actions are being taken to maintain sustainable water management in the hydrotechnical facilities in question, with particular emphasis on the principles of environmental protection. The operational assessment of the hydropower plants "Rosnowo" and "Niedalino" on the river Radew has shown that the hydropower facilities together with the entire hydro-engineering infrastructure contribute to the tasks of rational management of water resources, mainly in terms of maintaining the river and the hydrotechnical structures, using the water resources for power generation and providing protection against floods.

To sum up, the water management facilities located in the Natura 2000 sites may operate quite well; however, certain social, legal and environmental obstacles exist. These problems can be eliminated and the users manage the water resources in a more or less rational manner. Moreover, as can be seen in the paper, several water management works have been carried out in the Radew river basin and despite the rich hydro-engineering infrastructure in the area, the unique natural qualities of the site are preserved.

References

Anderson, D., Moggridge, H., Warren, P., Shucksmith, J. (2015). The impacts of 'run-of-river' hydropower on the physical and ecological condition of rivers. *Water and Environment Journal*, *29,* 268-276.

Atałap, B. (2011). Pismo DI.OW.0551/19/2011 (*w/s zanieczyszczenia wód rzeki Chocieli, spowodowanego odprowadzaniem ścieków wylotem burzowym*), WIOŚ w Szczecinie, Delegatura w Koszalinie, 14.07.2011 r.

Atałap, B. (2013). Pismo DI.1410.2.2013.AWI (*w/s stanu zrzutów ścieków do rzeki Chocieli ze studzienki na wysokości mleczarni w Bobolicach*), WIOŚ w Szczecinie, Delegatura w Koszalinie, 24.01.2013 r.

Badora, K. (2013). Feasibility of project related water management in Natura 2000 areas in Opole Province (in Polish). *In: Water retention in rural areas – selected issues*, ed. Wiatkowski M., Uniwersytet Opolski, Opole 217-232.

Benejam, L., Saura-Mas, S., Bardina, M., Solà, C. (2016). Ecological impacts of small hydropower plants on headwater stream fish: from individual to community effects. *Ecology of Freshwater Fish*, *25*, 295-306.

Directive 92/43/EEC, The Habitats Directive (1992).

Directive 2000/60/EC, Water Framework Directive (2000).

Directive 2009/147/EC, The Birds Directive (2009).

Fantin-Cruz, I., Pedrollo, O., Girard, P., Zeilhofer, P., Hamilton, S.K. (2015). Effects of a diversion hydropower facility on the hydrological regime of the Correntes River, Brazil. *Journal of Hydrology*, *531*, 810-820.

Florek, E., Florek, W., Łęczyński, L. (2008). Reservoirs of the Słupia river as morphogenetic agents (in Polish). *Landform Analysis*, *7*, 12-22.

GDOŚ (The General Directorate for Environmental Protection; 2015). *Geoserwis GDOŚ*, http://geoserwis.gdos.gov.pl/mapy/ (30.10.2015).

Jackson, A. (2011). RE vs. biodiversity: Policy conflicts and the future of nature conservation. *Global Environmental Change*, *21(4)*, 1195-1208.

Kasperek, R., & Wiatkowski, M. (2008). Field studies of fish pass operation on Michalice reservoir. *Rocznik Ochrona Środowiska*, *10*, 613-622.

Kasperek, R., & Wiatkowski, M. (2014). Hydropower generation on the Nysa Kłodzka river. *Ecological Chemistry and Engineering S, 21(2)*, 327-336.

Klaver, G., Van Os, B., Negrel, P., Petelet-Giraud, E. (2007). Influence of hydropower dams on the composition of the suspended and riverbank sediments in the Danube. *Environmental Pollution*, *148*, 718-728.

Kostrzewski, A. (1998). Struktura krajobrazowa dorzecza Parsęty w oparciu o dotychczasowe podziały fizyczno-geograficzne. *W: Funkcjonowanie geoekosystemów zlewni rzecznych, Środowisko przyrodnicze dorzecza Parsęty. Stan badań, zagospodarowanie, ochrona*, *1*, 131-141.

KZGW (2014). Opracowanie aktualizacji planów gospodarowania wodami na obszarach dorzeczy. (dorzecze Odry), Warszawa, grudzień 2014.

Liberacki, D., Korytowski, M., Kozaczyk, P., Stachowski, P., Stasik, R. (2016). Effects of Implementation of Small Retention Programme on the Example of Two Forest Districts of Lowland Area. *Rocznik Ochrona Środowiska, 10*, 428-438.

Malczewska, B. (2010). Environmental conditions of hydro-electric power station development based on example of river Bóbr. *Teka Komitetu Ochrony Kształtowania Środowiska Przyrodniczego – OL PAN*, *7*, 227-235.

Malm Renöfalt, B., Jansson, R., Nilsson, C. (2010). Effects of hydropower generation and opportunities for environmental flow management. Swedish riverine ecosystems in: *Freshwater Biology*, *55*, 49-67.

Mihailova, P., Traykov, I., Tosheva, A. (2013). Changes in biological and physicochemical parameters of river water in a small hydropower reservoir cascade. *Bulgarian Journal of Agricultural Science, 19(2)*, 286-289.

Obolewski, K., Strzelczak, A., Glińska-Lewczuk, K., Sadowski, Z., Astel, A., Timofte, C.M. (2016). Ecohydrological relationships between benthic communities and environmental conditions in the spring areas. *Environmental Engineering and Management Journal, 15(6)*, 1281-1291.

Okoński, B. (2014). *Analiza ustawy Prawo Wodne ze szczególnym uwzględnieniem Ramowej Dyrektywy Wodnej i określenia barier we wdrażaniu jej w Polsce*, Poznań, http://poznan.lasy.gov.pl/documents/688373/0/RDW_Baltic+Landscape.pdf (10.07.2016).

Pawłowski, A. (2009). Sustainable energy as a sine qua non condition for the achievement of sustainable development. *Problems of Sustainable Development*, *2,* 9-12.

Pawłowski, A. (2010). The role of environmental engineering in introducing sustainable development. *Ecological Chemistry and Engineering S*, *17(3)*, 263-278.

Rozporządzenie Rady Ministrów z 25.06.2013r. zmieniające rozp. w sprawie przedsięwzięć mogących znacząco oddziaływać na środowisko Poz. 817.

RZGW (Regional Water Management Board in Szczecin; 2014), *Rozporządzenie. nr 3/2014 Dyrektora z 3.06.2014 r. ws. ustalenia warunków korzystania z wód regionu wodnego Dolnej Odry i Przymorza Zachodniego*.

Szoszkiewicz, K., Pietruczuk, K., Strzeliński, P. (2014). Możliwości i założenia renaturyzacji rzek Wełny i Flinty. *W: Koncepcja lasu modelowego w zarządzaniu i ochronie różnorodności biologicznej rzek Wełny i Flinty,* eds. Bator J., et al., Bogucki Wyd. Nauk., Poznań, 127-140.

Ustawa (2001). (Water Law Act) (Dz.U. 115 poz. 1229, ze zm.).

Ustawa (2008). *Ustawa o udost. inf. o środ. i jego ochronie, udziale społ. w ochr. środ. oraz o ocenach oddział. na środ.* (Dz.U. 199 poz. 1227, ze zm.).

Vaikasas, S., Bastiene, N., Pliuraite, V. (2015). Impact of small hydropower plants on physicochemical and biotic environments in flatland riverbeds in Lithuania. *Journal of Water Security*, *1(1)*, 1-13.

Vowles, A.S., Karlsson, S.P., Uzunova, E.P., Kemp, P.S. (2014). The importance of behaviour in predicting the impact of a novelsmall-scale hydropower device on the survival of downstreammoving fish. *Ecological Engineering*, *69*, 151-159.

Wiatkowski, M., & Rosik-Dulewska, Cz. (2012). Present status and the possibilities of hydropower industry development in the Opole voivodeship (in Polish). *Water-Environment-Rural Areas*, *12(2)(38)*, 313-327.

Wiatkowski, W., & Tomczyk, P. (2015). The use of hydropower of the river Radew in Natura 2000 sites (in Polish). *Współczesne problemy energetyki III*, eds. Pikoń, K., & Czop, M., *Archiwum Gospodarki Odpadami i Ochrony Środowiska*, Gliwice, 175-185.

Ždankus, N., & Sabas, G. (2006). The Impact of Hydropower Plant on Downstream River Reach. *Environmental research, engineering and management*, *38(4)*, 24-31.

Analiza funkcjonowania obiektów hydroenergetycznych na obszarze Natura 2000 w zlewni rzeki Radew w aspekcie zrównoważonej gospodarki wodnej

Streszczenie

Praca dotyczy zagadnień dotyczących infrastruktury gospodarki wodnej ze szczególnym uwzględnieniem obiektów hydroenergetycznych i ochrony przyrody na obszarze Natura 2000 „Dolina Radwi, Chocieli i Chotli" w zlewni rzeki Radwi. Przedstawiono zalety i wady energetyki wodnej, charakterystykę zlewni rzeki Radew oraz wykorzystania hydroenergetycznego omawianego obszaru. Opisano warunki przyrodnicze terenu i scharakteryzowano uwarunkowania prawne dla przedsięwzięć na obszarach Natura 2000 (Ramowa Dyrektywa Wodna, Dyrektywa Ptasia i Siedliskowa, Ustawa Prawo wodne, akty wykonawcze w formie rozporządzeń i inne). W pracy przedstawiono ocenę funkcjonowania hydroelektrowni „Rosnowo" i „Niedalino" na rzece Radwi w kontekście wymagań stawianym takim obiektom ze względu na ochronę przyrody. Zwrócono także uwagę na konflikty społeczne związane z funkcjonowaniem przedsięwzięć z zakresu gospodarki wodnej na obszarach Natura 2000. Z pracy wynika, że na obszarze Natura 2000 „Dolina Radwi, Chocieli i Chotli" prowadzone są racjonalne działania mające na celu osiągnięcie zrównoważonej gospodarki wodnej na obiektach hydrotechnicznych, z zachowaniem zasad ochrony środowiska. Omawiane w artykule elektrownie wodne przyczyniły się do wykształcenia ekosystemów związanych z wodą, zastanych w momencie tworzenia „Doliny Radwi, Chocieli i Chotli", a także określonego składu gatunkowego, reżimu hydrologicznego oraz innych właściwości świata ożywionego i nieożywionego. Elektrownie wodne pełniąc różne zadania w środowisku i gospodarce wytwarzają energię, z której korzysta człowiek. W ten sposób realizuje się zarówno politykę energetyczną, jak również środowiskową. Obiekty związane z gospodarką wodną mogą dobrze funkcjonować, jednakże pod pewnymi warunkami społecznymi, prawnymi i środowiskowymi. Jakiekolwiek problemy są jednak minimalizowane, a użytkownicy w sposób racjonalny gospodarują poprawnie zasobami środowiska, planując i dokonując modernizacji tych budowli czy też stosując środki kompensujące. Ponadto w zlewni Radwi wykonano szereg prac z zakresu gospodarki wodnej i mimo bogatej infrastruktury wodnej na tym obszarze, zachowane zostały unikalne walory przyrodnicze terenu.

Abstract

This paper deals with the water management infrastructure, with a particular emphasis on the hydropower structures and environmental protection in the "Dolina Radwi, Chocieli i Chotli" Natura 2000 site in the Radew river basin

(the zachodniopomorskie province in the north-western Poland). Advantages and drawbacks (environmental, economic and social) of water power generation and a characterization of the Radew basin and characterization of hydropower usage of this area are discussed. The natural conditions of the terrain are described and the legal setting is characterized for undertakings in the Natura 2000 sites (Water Framework Directive, the Birds Directive, the Habitats Directive, Water Resources Law, the Nature Conservation Act, Act on Access to Information on the Environment and Its Protection and on Environmental Impact Assessments and executory provisions in the form of regulations). The paper presents an assessment of the operation of the hydropower plants "Rosnowo" and "Niedalino" on the river Radew in the context of the environment protection requirements for such facilities. Attention is also given to the social conflicts related to the operation of water management facilities in the Natura 2000 sites (on the example of the Trout Farm in Ubiedrze on the river Chociel). The authors conclude that in the "Dolina Radwi, Chocieli i Chotli" site rational actions are being taken for sustainable water management of hydraulic engineering facilities and that the principles of environmental protection are observed. The hydropower plants discussed in this paper have contributed to the formation of ecosystems related to water, already in existence at the time of creation of the "Dolina Radwi, Chocieli i Chotli" site. They also contributed to the specific species composition and the hydrological regime as well as other properties of the animate and inanimate world. The hydropower plants play various positive roles in the environment and economy, they generate inexpensive clean energy to be used by man. This way both the power production policy and the environmental policy are implemented. The use of this alternative energy source should be promoted also in the Natura 2000 sites. The structures related to water management may operate properly, but certain social, legal and environmental conditions apply. Any arising problems are minimized and users manage the natural resources in a rational and appropriate manner, both in terms of planning or modernizing these structures or by using compensation means. Moreover, several water management works have been carried out in the Radew river basin and despite the rich hydro-engineering infrastructure in the area, the unique natural qualities of the site are preserved.

Słowa kluczowe:
elektrownie wodne, odnawialne źródła energii, obszary Natura 2000,
rzeka Radew, Ramowa Dyrektywa Wodna, gospodarka wodna

Keywords:
hydropower plants, sustainable energy sources, Natura 2000 sites,
the Radew river, Water Framework Directive, water management

MIDDLE POMERANIAN SCIENTIFIC SOCIETY OF THE ENVIRONMENT PROTECTION
ŚRODKOWO-POMORSKIE TOWARZYSTWO NAUKOWE OCHRONY ŚRODOWISKA

Annual Set The Environment Protection
Rocznik Ochrona Środowiska

Volume/Tom 19. Year/Rok 2017 ISSN 1506-218X 81-95

Selected Mechanical Properties Analysis of Fibrous Composites Made on the Basis of Fine Waste Aggregate

Jacek Domski, Wiesława Głodkowska
Koszalin University of Technology

1. Introduction

The composites with dispersed reinforcement existed long before conventional reinforcement bars. Even before the birth of Christ people used various fibres such as animal dander or straw, mixing them with clay. The grounds for fibre reinforced concrete were laid by Joseph Lambot in the patent of 1847. Lambot suggested adding to the concrete fibres in the form of wires or nets (Naaman 1985). However, first use of steel components in concrete mix did not take place until year 1874, when A. Berard from California (USA) patented the strengthening of concrete by steel chips. In 1910 Porter was the first in the world to mention the possibility of using short steel wires in order to improve homogeneousness of concrete reinforced with only thick bars (Maidl 1995). The next patents, concerning various shapes of fibres and new methods of its application, were submitted as the first ones in the following countries by: H. Alfsen in France (1918), A. Kleinlogel in Germany (1920) and N. Zitkewic in England (1938). Yet, not until year 1963 in the USA, was elaborated the first theory of fine aggregate concrete containing steel fibres. The authors of the theory, J.P. Romualdi and G.B. Batson, proved that these steel fibres were able to inhibit development and propagation of cracks in concrete (Maidl 1995, Brandt 2008). This led to the possibility of introducing new technology of concrete reinforced with 25 mm fibres containing conventional fine aggregate. Guided by the rule that in

fibre reinforced concrete the amount of small fraction aggregate should be dominant, this article presents the comparison of the results obtained from the study on fibrous composites containing waste aggregate with maximum granulation of 4 mm. There are many publications, in which SFRC made on the basis of waste sand was analyzed (Domski 2016, Głodkowska & Laskowska-Bury 2015, Domski 2015, Głodkowska & Kobaka 2013). However, these studies mostly concerned the typically selected volumetric quantity of steel fibres, i.e. 0.5, 1.0, 1.5, 2.0 and 2.5%. The presented analysis was conducted based on practical aspects of quantitative use of steel fibres. The analysis was limited to two composites, in which the volume of steel fibres was 0.42% (Domski 2016) and 1.20% (Głodkowska & Laskowska-Bury 2015), considered accordingly as minimal and optimal.

2. Characteristics of composite

Concrete is the most popular construction material in the world. The basic component for concrete is aggregate, which constitutes approximately ¾ of its volume. It is estimated that annual demand on aggregate is 3,000 kg per one person. Such a big use of aggregate significantly influences the natural environment. Furthermore, the aggregate deposits are not evenly spread out around the world. It is the reason why the grading curves for concrete (e.g. reference concrete according to EN 1766) are difficult to obtain without additional activity. The regions with deficiency of coarse aggregate are in a particularly difficult situation as they are at risk of increased environmental degradation. This is due to the fact that more all-in aggregate is needed to prepare aggregate for concrete (e.g. the reference one).

In the analyzed composites the used aggregate was sand of 4 mm granulation, which is a waste material in aggregate mines located in northern Poland. In this area a significant part of the output is subjected to the process of hydroclassification which results in obtaining 80% of sand and only 20% of coarse aggregate. This disproportion leads to the situation where most of sand remains unused in numerous plies located nearby the aggregate mines (Fig. 1). The postulate to somehow utilise remaining waste sand dumps constitutes a world-wide tendency consisted with Sustainable Ecological Development (Sadowska-Buraczewska

& Rutkowski 2013, Błaszczyński & Król 2015, Meyer 2009, Hendriks & Janssen 2003, Siddique 2008, Soares et al. 2014, Ulsen et al. 2013). The similar phenomena of excessive sand fractions can be observed in other parts of the world, e.g. in Middle East or in North Africa (Al-Harthy et al. 2007).

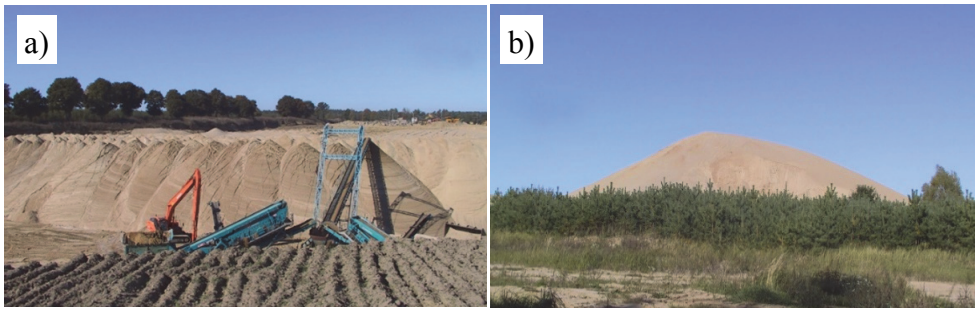

Fig. 1. Waste sand dumps in operative (a) and inoperative (b) aggregate mine (northern Poland area)
Rys. 1. Hałdy piasku w czynnej (a) i nieczynnej (b) kopalni kruszyw (obszar północnej Polski)

The figure 2 presents waste sand grading curves, appointed by various authors. These curves only insignificantly differ one from another, despite the fact that sand used in these studies originated all from various aggregate mines located in northern Poland. It proves that all these deposites are postglacial or fluvioglacial residues, developed in the same period. The used aggregates were additionally analyzed. Selected results are presented in table 1. Portland cements CEM II were used as binders in analyzed composites. Each cement mixture had different ash content. In case of cements of A-V series, the mixture was additionally sealed by silica dust (Głodkowska & Laskowska-Bury 2015). In every other analyzed composite, there was used a superplasticizer of FM series (Cartuxo et al. 2015). All composites were reinforced with steel fibres, which were 50 mm long and had 0.8 mm in diameter. Detailed analysis of the fibres is presented in (Katzer & Domski 2012). Figure 3 presents a histogram of tensile strength (R_m) of used steel fibres. The average value of strength, measured on 30 fibres, was 1155.2 MPa, and with standard deviation of 72.7 MPa. Described strength fits the range from 1153 to 1167 MPa, which is the range declared by the fibre producer. The conducted analysis

confirms that the used fibres comply with tensile strength declared by the producer.

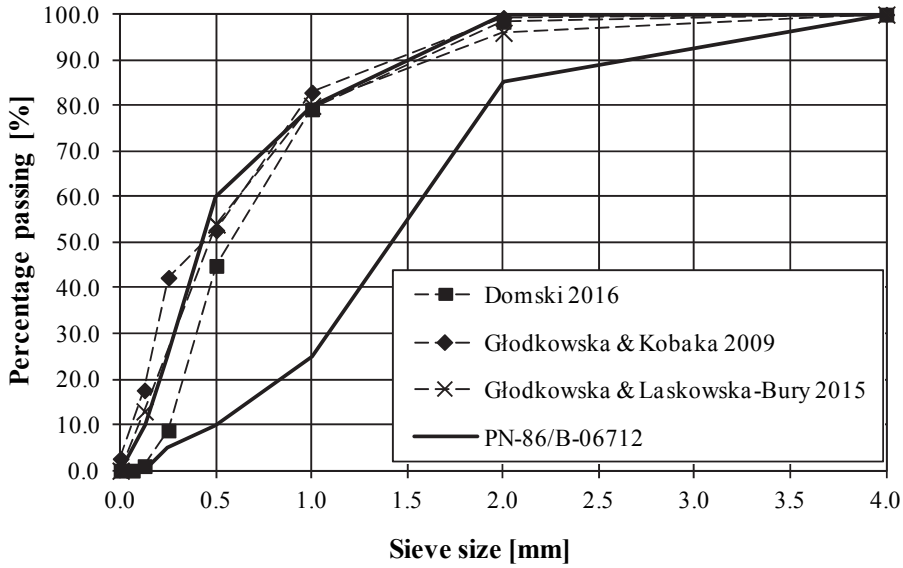

Fig. 2. Grading curves of waste aggregates
Rys. 2. Krzywe przesiewu kruszywa odpadowego

Table 1. Selected properties of waste aggregate
Tabela 1. Wybrane właściwości kruszywa odpadowego

Characteristics and origin of aggregate	Acc to (Głodkowska & Laskowska-Bury, 2015), mine in Lepino	Acc to (Domski 2016), mine in Sępólno Wielkie
Bulk density in loose state	1634 kg/m^3	1600 kg/m^3
Grain density	2632 kg/m^3	2600 kg/m^3
Quantity of mineral dust	1.3%	1.0%
Voids	32%	30%
Grain median	0.46 mm	0.28 mm
Foreign body content	0.0%	0.0%

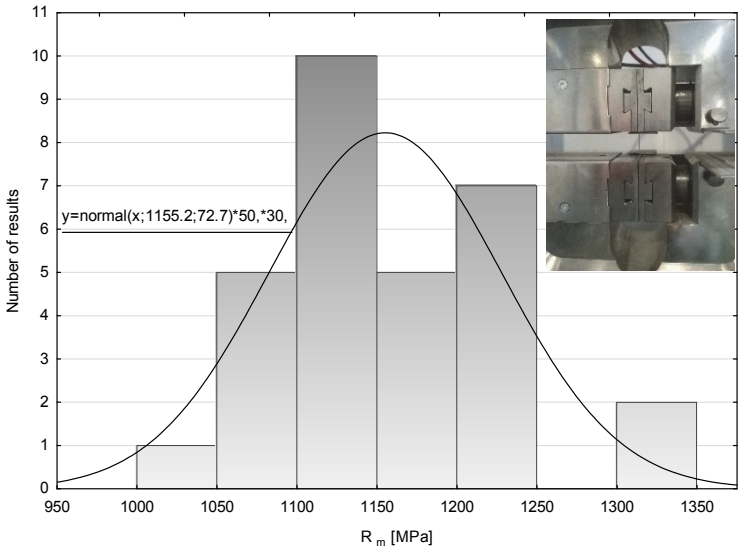

Fig. 3. Histogram of tensile strength and tensile strength test of steel fibres
Rys. 3. Histogram wytrzymałości na rozciąganie oraz badanie wytrzymałości na rozciąganie włókien stalowych

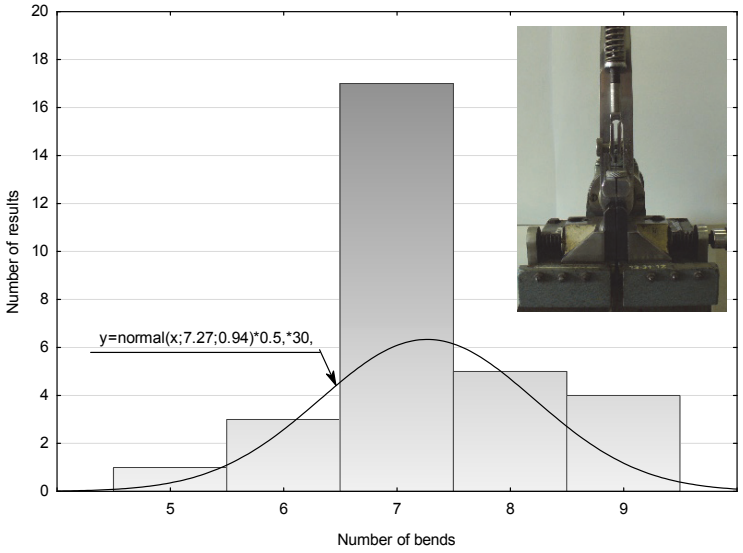

Fig. 4. Histogram of ductility and bend test of steel fibres
Rys. 4. Histogram odporności na przeginanie oraz badanie przeginania włókien stalowych

The fibres were also put to the bending test. It resulted in setting the number of bends necessary to break the fibres, accordingly to EN 10218-1:1994 (with reference to ISO 7801:1984 ‘‘Metallic materials: Wire: Reverse bend test). Figure 4 presents results of the bends measurements and a general view on the work stand. The average number of bends measured on 30 fibres was 7.3 at standard deviation of 0.94. The producer declares that the fibres should be resistant to at least 7 bends. The test results indicate that the analyzed fibres comply with this number.

3. Mechanical properties of composites with fibres made on the basis of waste sand

Analyzing any concrete or composite, it is necessary to measure its strength properties (Bywalski et al. 2015, Domski & Katzer 2013, Domski et al. 2012, Seitl et al. 2010, Yazıcı et al. 2007, Chiaia et al. 2007, Naaman 2003). This is essential to be able to describe the usefulness of a concrete or composite in various applications. First, using the correlation between compressive strength and a number of used fibres, determined in (Głodkowska & Kobaka 2013), it was verified if it also describes the properties of analyzed composites. Figure 5 presents the relation between compressive strength measured on 150 mm cubes and the fibre content percentage (V_f). The conducted analysis shows that no composite fits in the curve proposed in (Głodkowska & Kobaka 2013). Because of this and due to the new results from (Głodkowska & Laskowska-Bury 2015) and (Domski 2016), the proper correction was made. The least-square method was used to determine the quadratic function, for which the correlation ratio is 0.87.

Another analyzed quality was tensile strength while cracking, tested on cubic samples of 150 mm. In this case it was considered, also based on the function described in (Głodkowska & Kobaka 2013), whether the results of analyzed composites fit in the proposed range (fig. 6). According to the analysis of the composite with 1.2% of fibre content, the results fit the range of the curve proposed in (Głodkowska & Kobaka 2013). However, the composite with 0.42% of fibre amount slightly deviates from the curve and this is why a new curve was suggested (fig. 6). It was measured with the least square method using the test results from (Domski 2016, Głodkowska & Laskowska-Bury 2015 and Głodkowska

& Kobaka 2013). The new curve shows that the correlation ratio of 0.94 is lower than in (Głodkowska & Kobaka 2013), but still relatively high.

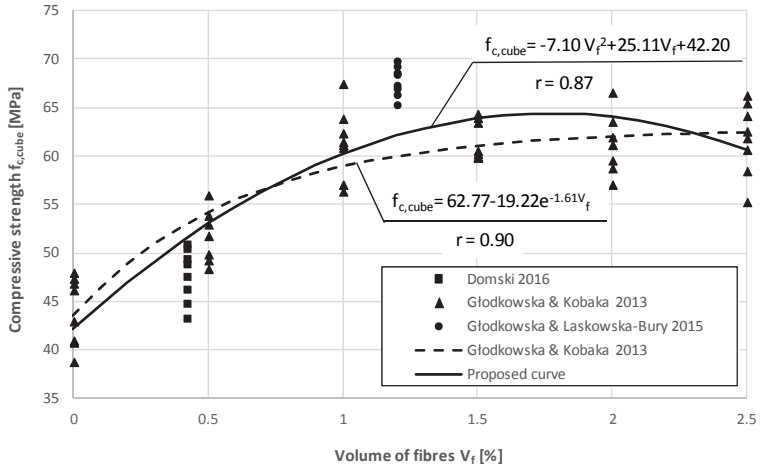

Fig. 5. Compressive strength vs. content of steel fibres
Rys. 5. Wytrzymałość na ściskanie w funkcji ilości włókien stalowych

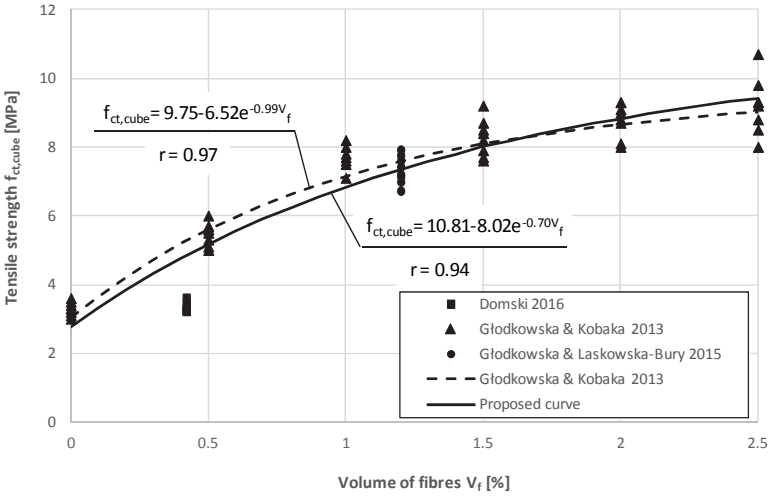

Fig. 6. Tensile strength at splintering vs. content of steel fibres
Rys. 6. Wytrzymałość na rozciąganie przy rozłupywaniu w funkcji ilości włókien stalowych

The study also included the analysis of modulus of elasticity. According to the literature (Naaman 1985, Maidl 1995, Brandt 2008, Głodkowska & Laskowska-Bury 2015, Błaszczyński & Przybylska-Fałek 2015), adding steel fibres to the composite results in a slight increase of static modulus of elasticity. Lack of significant influence of fibres on the modulus of elasticity can be caused by two factors. On the one hand, it can be caused by the increase of concrete compressive strength and on the other, by random setting of steel fibres and by the increase of air in hardened concrete (Rudzki et al. 2013, Bywalski & Kaminski 2011, Głodkowska & Kobaka 2012). Fig. 7 presents the relation between values of modulus of elasticity and compressive strength of several composites with fibres. These values were referred to the function presented in EN 1992-1-1. On the basis of this relation it can be stated that the function from EN 1992-1-1 does not describe variation of modulus of elasticity of tested composites. This is the reason why another function was proposed (fig. 7). It was set by the least-square method using test results from (Głodkowska & Kobaka 2009, Głodkowska & Laskowska-Bury 2015, Domski 2016). The correlation ratio for the proposed curve was 0.76.

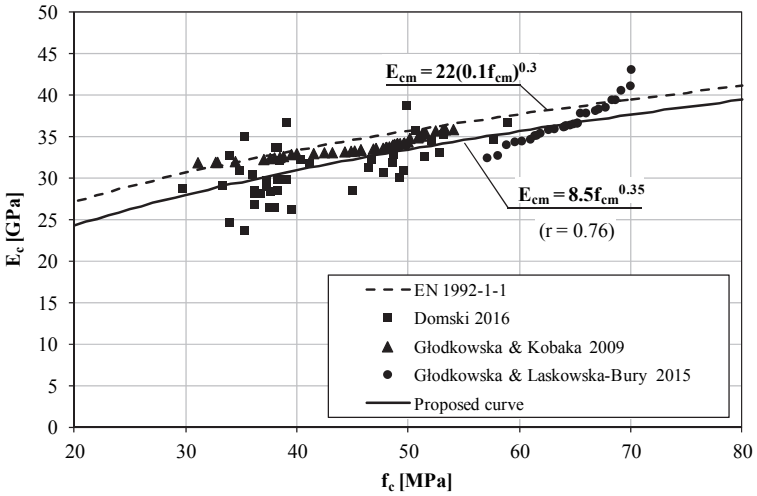

Fig. 7. Relation between modulus of elasticity and compressive strength
Rys. 7. Zależność pomiędzy modułem sprężystości a wytrzymałością na ściskanie

Figure 8 presents the relation between loading force and CMOD depending on the amount of steel fibres in concrete. Analyzing shape of each graph it can be stated that some composites, with steel fibres content of 0.42 and 1.20%, have the *pcs* attribute, i.e. decrease of destructive force together with increase of CMOD after the first crack appearance. On the other hand, for composites with steel fibre content of 0.90 and 0.50% the destructive force increases after appearance of the first crack. The test results of residual compressive strength clearly indicate on ductile nature of analyzed materials. It is caused by the fact that fibres significantly inhibit formation and expansion of cracks in composite with fibres. Thanks to applying dispersed reinforcement, composites are not so suddenly destroyed as it happens with ordinary concrete (Głodkowska & Kobaka 2012, Błaszczyński & Przybylska-Fałek 2015). Even the smallest amount of fibres, equal to 0.42%, comply with the minimal values of residual strength, specified in EN 14889-1 (1.5 MPa for COMD = 0.5 and 1.0 for CMOD = 3.5), which are declared by producers when their product contain adequate number of fibres (fig. 8 and tab. 2). Reaching these minimal values ($f_{R1,min}$ and $f_{R4,min}$) by every kind of steel fibres is essential for them to meet the assumed level of performance.

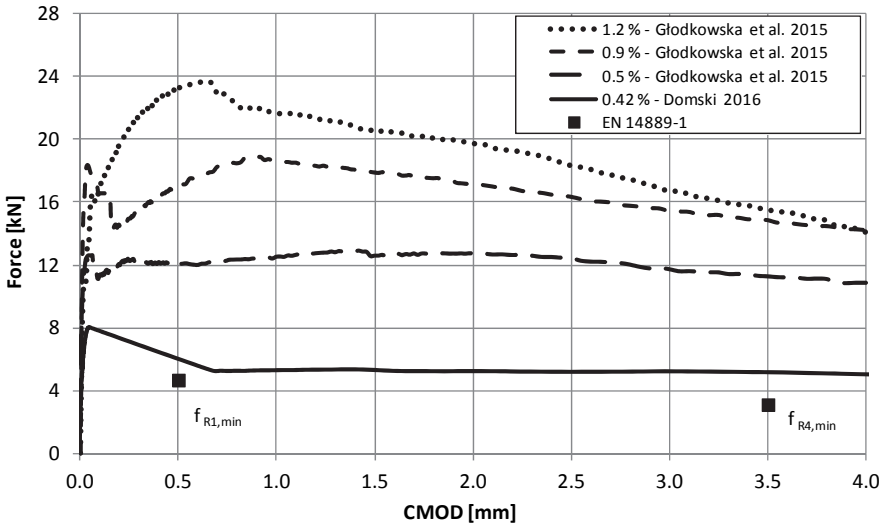

Fig. 8. Relation between loading force and CMOD
Rys. 8. Zależność pomiędzy siłą obciążającą a CMOD

Ultimately, based on fig. 8, the characteristic residual strengths were determined and the composites were classified given the proposal from Model Code 2010 (fib Bulletin 55 2010) (tab. 2). Classification 7b according to (fib Bulletin 55 2010, di Prisco et al. 2009) defines the analyzed material as composite with fibres (1.2%) of high f_{R1} value (range from 1÷8). The letter „b" in its name means that the composite has the *pcs* value, obtained from the f_{R3}/f_{R1} dependence („a" and „b" – *pcs*, „d" and „e" – *psh*).The composite with the level of fibre content of 0.42% reached the classification 2a. It can be presumed that there is a possibility of reaching even lower class (e.g. 1a). However, it should be noted that the obtained residual strength values are characteristic and should be reduced in case of designing bended and sheared construction elements.

Table 2. Average values of residual strength depending on the width of the opening crack (Głodkowska et al. 2015, Domski 2016)
Tabela 2. Średnie wartości wytrzymałości resztkowych zależne od szerokości rozwarcia rysy (Głodkowska i in. 2015, Domski 2016)

Crack mode opening displacement (CMOD) [mm]		0.5	1.5	2.5	3.5	$f_{R3} - f_{R1}$	Classification according to MC2010
Residual strengths [MPa]	1.20 [%]	7.45	6.55	5.85	4.95	0.78	**7b**
	0.90 [%]	5.45	5.72	5.23	4.75	0.96	**5c**
	0.50 [%]	3.38	4.04	3.99	3.62	1.18	**3d**
	0.42 [%]	2.39	1.43	1.41	1.40	0.59	**2a**
Residual strengths $f_{R,1}$, $f_{R,2}$, $f_{R,3}$ and $f_{R,4}$ were determined for crack mode opening displacement (CMOD), equal respectively to: 0.5, 1.5, 2.5, 3.5 mm.							

4. Summary

The results of conducted analysis prove that mechanical properties of fine aggregate composites made of waste sand with steel fibre content ranging from 0.42% to 2.5% comply with the requirements im-

posed on structural materials (fib Bulletin 55 2010, di Prisco et al. 2009). As it arises from (Głodkowska & Laskowska-Bury 2015) the most optimal quantity of steel fibres is 1.2% of the composite volume. Of course, the proper type of composite can be chosen depending on the strain level of construction elements. Ultimately, thanks to their properties, the analyzed composites can constitute in some cases an alternative for classic concrete as well as the material for creating construction elements such as: foundation plates, floor slabs, beams or shells (Domski 2015).

The possibility of using waste sand as aggregate of full value in the process of producing construction materials on an industrial scale would largely resolve the problem of managing waste sand dumps located in northern Poland. Large amounts of fine aggregate, occurring in a form of industrial waste, could become the basic component of materials used to produce construction elements and thanks to that, they could be the new regional treasure (Domski 2016, Głodkowska et al. 2015, Głodkowska & Laskowska-Bury 2015, Głodkowska & Kobaka 2009).

References

Al-Harthy, A.S., Abdel Halim, M., Taha, R., & Al-Jabri, K.S. (2007). The properties of concrete made with fine dune sand. *Construction and Building Materials, 21*, 1803-1808.

Błaszczyński, T., & Król, M. (2015). Usage of Green Concrete Technology in Civil Engineering. *Procedia Engineering, 122*, 296-301.

Błaszczyński, T., & Przybylska-Fałek, M. (2015). Steel Fibre Reinforced Concrete as a Structural Material. *Procedia Engineering, 122*, 282-289.

Brandt, A. M. (2008). Fibre reinforced cement-based (FRC) composites after over 40 years of development in building and civil engineering. *Composite Structures, 86(1-3)*, 3-9.

Bywalski, C., & Kaminski, M. (2011). Estimation of the bending stiffness of rectangular reinforced concrete beams made of steel fibre reinforced concrete. *Archives of Civil and Mechanical Engineering, 11(3)*, 553-571.

Bywalski, C., Kamiński, M., Maszczak, M., & Balbus, Ł. (2015). Influence of steel fibres addition on mechanical and selected rheological properties of steel fibre high-strength reinforced concrete. *Archives of Civil and Mechanical Engineering, 15(3)*, 742-750.

Cartuxo, F., de Brito, J., Evangelista, L., Jiménez, J.R., & Ledesma, E.F. (2015). Rheological behaviour of concrete made with fine recycled concrete aggregates – Influence of the superplasticizer. *Construction and Building Materials, 89*, 36-47.

Chiaia, B., Fantilli, A.P., & Vallini P.P. (2007). Evaluation of minimum reinforcement ratio in FRC members and application to tunnel linings. *Materials and Structures, 40*, 593-604.

di Prisco, M., Plizzari, G., & Vandewalle, L. (2009). Fibre reinforced concrete: new design perspectives. *Materials and Structures, 42(9)*, 1261-1281.

Domski, J. (2015). Long-term Study on Fibre Reinforced Fine Aggregate Concrete Beams Based on Waste Sand. *Rocznik Ochrona Środowiska, 17*, 188-199.

Domski, J. (2016). A blurred border between ordinary concrete and SFRC. *Construction and Building Materials, 112*, 247-252.

Domski, J., & Katzer, J. (2013). Load-deflection characteristic of fibre concrete based on waste ceramic aggregate. *Rocznik Ochrona Środowiska, 15*, 213-230.

Domski, J., Katzer, J., & Fajto, D. (2012). Load-CMOD characteristics of FRCC based on waste ceramic aggregate. *Rocznik Ochrona Środowiska, 14*, 69-80.

fib Bulletin 55. (2010). *Model Code* (wyd. First complete draft). Lausanne: International Federation for Structural Concrete.

Głodkowska, W., & Kobaka, J. (2009). Application of Waste Sands for Making Industrial Floors. *Rocznik Ochrona Środowiska, 11*, 193-206.

Głodkowska, W., & Kobaka, J. (2012). The Model of Brittle Matrix Composites for Distribution of Steel Fibres. *Journal of Civil Engineering and Management, 18(1)*, 145-150.

Głodkowska, W., & Kobaka, J. (2013). Modelling of properties and distribution of steel fibres within a fine aggregate concrete. *Construction and Building Materials, 44*, 645-653.

Głodkowska, W., & Laskowska-Bury, J. (2015). Waste Sands as a Valuable Aggregates to Produce Fibre-composites. *Rocznik Ochrona Środowiska, 17*, 507-525.

Głodkowska, W., Lehmann, M., & Ziarkiewicz, M. (2015). Wytrzymałości resztkowe fibrokompozytu na bazie piasku odpadowego. *Materiały budowlane, 513(5)*, 75-77.

Hendriks, C., & Janssen, G. (2003). Use of recycled materials in construction. *Materials and Structures, 36*, 604-608.

Katzer, J., & Domski, J. (2012). Quality and mechanical properties of engineered steel fibres used as reinforcement for concrete. *Construction and Building Materials, (34)*, 243-248.

Maidl, B.R. (1995). *Steel Fibre reinforced Concrete.* Berlin: Ernst & Sohn.

Meyer, C. (2009). The greening of the concrete industry. *Cement & Concrete composites, 31*, 601-605.

Naaman, A.E. (1985). Fiber reinforcement for concrete. *Concrete International: Design and Construction*, 21-25.

Naaman, A.E. (2003). Engineered Steel Fibres with Optimal Properties for Reinforcement of Cement Composites. *Journal of Advanced Concrete Technology, 1(3)*, 241-252.

Rudzki, M., Bugdol, M., & Ponikiewski, T. (2013). Determination of steel fibers orientation in SCC using computed tomography and digital image analysis methods. *Cement Wapno Beton, 18(5)*, 257-263.

Sadowska-Buraczewska, B., & Rutkowski, P. (2013). Concrete with Recycled HSC/HPC Aggregates in Sustainable Development. *Rocznik Ochrona Środowiska, 15*, 2175-2184.

Seitl, S., Keršner, Z., Bílek, V., & Knésl, Z. (2010). Fatigue parameters of cement-based composites with various types of fibers. *Key Engineering Materials, 417*, 129-132.

Siddique, R. (2008). *Waste Materials and By-Products in Concrete.* Berlin: Springer.

Soares, D., de Brito, J., Ferreira, J., & Pacheco, J. (2014). In situ materials characterization of full-scale recycled aggregates concrete structures. *Construction and Building Materials, 71*, 237-245.

Ulsen, C., Kahn, H., Hawlitschek, G., Masini, E. A., & Angulo , S. C. (2013). Separability studies of construction and demolition waste recycled sand. *Waste Management, 33*, 656–662.

Yazıcı, Ş., İnan, G., & Tabak, V. (2007). Effect of aspect ratio and volume fraction of steel fiber on the mechanical properties of SFRC. *Construction and Building Materials, 21*, 1250–1253.

Analiza wybranych właściwości mechanicznych fibrokompozytów na bazie drobnego kruszywa odpadowego

Streszczenie

Prezentowany artykuł dotyczy ochrony środowiska w aspekcie ograniczania zużycia surowców naturalnych oraz emisji dwutlenku węgla. Swoją tematyką wpisuje się on w ogólnoświatową tendencję związaną z tzw. Zrównoważonym Rozwojem Środowiska. Obszary Polski północnej są ubogie w kruszywo grube, które jest niezbędne przy produkcji tradycyjnych betonów. W tej sytuacji, aby uzyskać pełnowartościowe kruszywo do betonów, należy przerobić znacznie większą ilość urobku w postaci pospółki, przy jednoczesnym zwiększeniu nakładu pracy i energii. W efekcie tych zabiegów uzyskuje się różne frakcje kruszywa, jednak w znacznej części, bo w ponad 80%, jest to piasek o uziarnieniu do 4 mm. Sytuacja ta sprawia, że w obszarze kopalń kruszyw, znajdują się liczne hałdy piasku, traktowane jako odpad poprodukcyjny.

Argumenty te skłoniły autorów niniejszego artykułu, aby zaproponować rozwiązanie zaistniałego problemu. Przeprowadzono analizę wyników badań piasku, pochodzącego z dwóch kopalń z obszaru Polski północnej, która obejmowała: krzywą przesiewu, ziarno mediana, gęstość nasypową w stanie luźnym, gęstość ziaren, zawartość pyłów mineralnych, jamistość oraz zawartość ciał obcych. Wyniki z przeprowadzonej analizy potwierdziły możliwość wykorzystania piasku jako kruszywa w kompozytach cementowych z dodatkiem włókien stalowych. Dodatkowo przeanalizowano uzyskane, w ramach wcześniej przeprowadzonych badań, właściwości mechaniczne wybranych haczykowatych włókien stalowych o średnicy 0,8 mm i długości 50 mm. Zweryfikowano uzyskane wytrzymałości na rozciąganie oraz liczbę przegięć z parametrami deklarowanymi przez producenta włókien. Zasadnicza analiza dotyczyła dwóch specyficznych fibrokompozytów o objętościowej zawartości włókien 0,42% i 1,2%, uznanych za minimalną i optymalną ilość włókien w mieszance. Dla tych kompozytów przeprowadzono analizę statystyczną obejmującą wytrzymałości na ściskanie i rozciąganie przy rozłupywaniu, moduł sprężystości i wytrzymałości resztkowe badanych fibrokompozytów. Na podstawie przeprowadzonej analizy zaproponowano krzywe opisujące zmianę wytrzymałości na ściskanie, wytrzymałości na rozciąganie przy rozłupywaniu oraz modułu sprężystości w funkcji ilości dozowanych włókien. Przedstawione funkcje dobrze charakteryzują zmienność wyżej wymienionych cech, o czym świadczy współczynnik korelacji, który zawierał się w przedziale od 0,76 do 0,94. Przeanalizowano również zależność pomiędzy siłą obciążającą a szerokością rozwarcia rysy (CMOD). Na jej podstawie możliwe było określenie wytrzymałości resztkowych, zaś zgodnie z ModelCode 2010, ustalono klasy fibrokompozytów oraz ustalono, czy możliwe jest częściowe zastąpienie zbrojenia tradycyjnego fibrokompozytem. Wyniki z przeprowadzonych analiz dowodzą, że właściwości mechaniczne drobnokruszywowych kompozytów wykonanych na bazie piasków odpadowych ze zbrojeniem rozproszonym odpowiadają wymaganiom stawianym budowlanym materiałom konstrukcyjnym.

Abstract

The presented article concerns environmental protection in terms of limiting consumption of natural resources and carbon dioxide emission. Its subject matter fits in the world-wide tendency consisted with Sustainable Ecological Development. Northern Poland area lacks of coarse aggregate, which is essential to produce ordinary concrete. In this case, in order to obtain wholesome aggregate to concrete production, it is necessary to process much more output in the form of all-in aggregate, increasing work and energy input at the same time. This procedure results in obtaining various aggregate fractions,

however over 80% of it is sand with maximum granulation of 4 mm. As the result, most of sand remains unused in numerous piles located nearby the aggregate mines and is treated as post-production waste. These facts made the authors of the article to propose a solution of the existing issue. Therefore, there were analyzed the results of study on sand from two mines located in northern Poland. The analysis covered grading curves, grain median, bulk density in loose state, grain density, quantity of mineral dust, voids and foreign body content. The results of conducted analysis confirmed the possibility of using waste sand as aggregate in cement composites with steel fibres. Additionally, there were also analyzed the results of previous study on mechanical properties of selected hooked steel fibres, which were 50 mm long and had 0.8 mm in diameter. The tensile strength results and the number of bends, that were obtained, were verified with the parameters declared by fibre producers. The main analysis concerned two specific fibrous composites of volumetric content of fibres of 0.42% and 1.2%. These values are considered to be minimal as well as optimal for quantity of fibres in the mixture. In case of these composites, the statistical analysis also included compression strength and tension strength at splitting, modulus of elasticity and residual strength. On the basis of this analysis the curves were proposed describing value changes in compression strength, tension strength at splitting and modulus of elasticity in function of dosed fibres quantity. The presented functions well describe variability of aforementioned qualities, what is confirmed by correlation ratio, which was between 0.76 and 0.94. There was also analysed an interdependence between loading force and crack mode opening displacement (CMOD). On its basis it was possible to determine residual strength and to establish, according to Model Code 2010, fibrous composite classes and also whether it was possible to partially replace ordinary reinforcement with fibrous composites. The results of all these analysis prove that the mechanical properties of fine aggregate composites made on the basis of waste sand with dispersed reinforcement comply with the requirements imposed on construction materials.

Słowa kluczowe:
piasek odpadowy, kruszywo drobnoziarniste, kompozyt, włókna stalowe

Keywords:
waste sand, fine aggregate, composite, steel fibres

MIDDLE POMERANIAN SCIENTIFIC SOCIETY OF THE ENVIRONMENT PROTECTION
ŚRODKOWO-POMORSKIE TOWARZYSTWO NAUKOWE OCHRONY ŚRODOWISKA
Annual Set The Environment Protection
Rocznik Ochrona Środowiska
Volume/Tom 19. Year/Rok 2017 ISSN 1506-218X 96-121

Interpopulation Variation in Growth and Life-History Traits of the Non-Native Juvenile Pumpkinseed *Lepomis gibbosus* (L., 1758), in Cooling Water of a Power Plant in the Lower Stretch of the Oder River, Poland

Józef Domagała[*], *Przemysław Czerniejewski*[**], *Małgorzata Pilecka-Rapacz*[*]
[*]*University of Szczecin*
[**]*West Pomeranian University of Technology, Szczecin*

1. Introduction

Invasions of expansive species is a serious global issue and, according to the International Union for Conservation of Nature, and are one of the most significant threats to biodiversity due to unforeseeable effects that are caused by the appearance of a new species in the given area. One of the invasive foreign species is the North American pumpkinseed *Leppomis gibbosus* (L. 1758) (Casal 2006) introduced in European waters as a sporting and decorative fish (de Groot 1985) from where he reached natural conditions (Welcomme 1988, Copp & Fox 2007). Currently, populations of the pumpkinseed are typical of the water of Central and Western Europe (de Groot 1985, Welcomme 1992) and the Iberian Peninsula (Sostoa *et al.*, 1987) as well as the Black Sea in the south (Economidis *et al.*, 1981). The species predominantly occurs in stagnant waters, but also in lenitic segments of watercourses in which it feeds on available invertebrates and fish (Van Kleef *et al.*, 2008). It normally reaches puberty at the age of three years (Copp & Fox 2007) and seldom reaches the age of ten years (Copp *et al.,* 2004). The presence of the pumpkinseed in some European waters caused a clear decrease in

the water quality, zooplankton biomass (Angeler *et al.*, 2002), benthos organisms (Osenberg 1992) and most importantly a change in the structure of local fish, mainly due to feeding on the spawn and young fish and interspecific competition (Holcik 1991). For instance, in a Spanish lake of Albufera, *Mugil cephalus* was a dominant species until 2000. The introduction of the pumpkinseed caused elimination of the aforementioned species and more than a twofold increase in the number of the pumpkinseed (Blanco *et al.*, 2003). Moreover, in some Portugal rivers, the pumpkinseed not only reduced populations of local fish, but also became the dominant species (Godinho *et al.*, 1997). Another example of food competition between local fish species (the silver bream *Blicca bjoerkna*, the eel *Anguilla anguilla* and the pope *Gymnocephalus cernuus*) and the introduced pumpkinseed was observed in an Austrian lake of Neusiedler (Tomeček *et al.*, 2007) and the non-local Prussian carp (Guti *et al.*, 1991). Although the pumpkinseed is a typical generalist with high adaptability and tolerance of environmental conditions different from its natural habitat, it is not an invasive species everywhere in Europe and then its influence on the environment is slight due to its small populations (Copp *et al.*, 2002).

The pumpkinseed was first observed in the Polish waters in 1927 (Grabowska *et al.*, 2010) and currently, except for populations residing in warm waters with higher temperatures, single specimens of this species are caught sporadically in natural waters. The biggest population of the pumpkinseed occurs in warm waters of the Dolna Odra power plant (North-West of Poland) and, in comparison to other European populations, it is distinguished by significant populations, a rapid growth rate at each stage of life (Domagała *et al.*, 2016) and a long portion spawning season (Domagała *et al.*, 2014). However, little is known about seasonal changes in the increase in the length, mass and condition of young pumpkinseeds in these waters. The data obtained for this foreign species occurring in water with increased thermal conditions is important especially in connection with the global warming and may indicate possible expansion of this fish to natural surface waters in the future. The aim of the present paper is to assess the effect of increased thermal water conditions on the size of seasonal changes in the length, mass and condition and a detailed analysis of scales for the number of sclerites in each month of their lives and the time of development of annual growth rings in the population of young pumpkinseeds caught out in warm waters.

2. Material and Methods

The research material included 341 pumpkinseed individuals in age 0+ (305 ind.) and 1+ (36 ind.) caught during monthly catches (electrofishing) (Penczak 1967) in the waters of the lower Oder River. The site of the catch were the waters of the Warm Canal that cool the generators of the Dolna Odra power plant near Gryfino (Northwestern Poland). These waters characterized by an increased temperature with compared to natural waters Domagała et al. 2015), with similar values of other physical and chemical parameters of water (Domagała & Kondratowicz 2006, Domagała & Pilecka-Rapacz 2007).

Fig. 1. Location of the juvenile pumpkinseed catch site: (A) Odra River, from which water is supplied to the power plant 'Dolna Odra' (PDO), the canal receiving heated effluents (W) discharged in the cooling water, and Dąbie Lake
Rys. 1. Lokalizacja miejsc połowu młodocianego bassa słonecznego: (A) rzeka Odra, z której woda jest dostarczana do elektrowni "Dolna Odra" (PDO), kanał ciepły otrzymuje i odprowadza podgrzaną wodę pochłodniczą z elektrowni (W) i jezioro Dąbie

After catching all specimens were examined biologically: total length (TL) with the accuracy of 1 mm was established, individual weight (W) estimated on the electronic balance (type AXIS), with the accuracy of 0.1 g. The length-weight relationships were estimated using the equation W = aSLb , where W is total weight (g), SL - standard length (cm), a intercept, and b slope (Ricker 1975). Condition of fish was estimated on the basis of Fulton condition coefficient according to the formula: K = (W/SL3) * 100 (Bolger & Connolly 1989). Increases in length (Δ SL), weight (Δ W) and condition (Δ K) in each months of the year were estimated starting from June (May is the beginning of the breeding of pumpkinseed in the Warm Canal - Domagala et al. 2014) to May next year and expressed as the function of the size of fish at the start of the year's growth stanza (i. e. Wx, SLx) (Osenberg et al. 1988):

$$\Delta W = Wx+1 - Wx$$
$$\Delta SL = SL_{x+1} - SL_x$$

The scales were sampled following Uzunova et al. (2008) under the dorsal fin, next they were cleaned from of mucus in ammonia water and prepared for examination. On a Zeiss Stereo Discovery V12 microscope at various magnifications connected to PC using a special image analysis software "MultiScan" the age, number of sclerites (S) and the length of oral radius of scales (Po) from the center to the edge of scales in each month were determinated. It allowed indication of the time of setting up the annual ring on the scales of pumpkinseed, and calculation of SL_0 ie. the length at which in this species the scales start forming (Creaser 1926, Osenberg et al., 1988, Uzunova et al. 2008). This value was determined by the graphical method, by plotting the relationship between the standard length of fish (SL) and the scale radius (Po) (Fox & Crivelli 2001 Uzunova et al. 2008).

The obtained measurement results were processed using statistical methods (in Microsoft Excel and Statistica 6.0 software) to calculate arithmetic means ($\bar{x}$) and standard deviation (SD). Before the hypothesis of equal means was verified, the normality of distribution of the analysed characteristic was assessed (using the Shapiro–Wilk test and Levene's test of homogeneity of variance). The significance of differences was determined using Scheffe's test ($P < 0.05$) and analysis of variance (for multiple samples) (Stanisz 1998). To study correlations between

variables, regression analysis was used. The degree of match between function and empirical data was determined by calculating coefficients of correlation (R) and determination (R^2). The significance of correlation coefficient was established using t - test (Sokal & Rohlf 1995).

3. Results

Mean lengths (TL and SL) of young pumpkinseeds from the waters were 5.37 cm and 4.30 cm, respectively, and the lower standard deviation indicating smaller sample variation and the higher measurement accuracy were observed for SL (1.21) whereas for T1 the value was 1.52. Therefore, all the analyses and result discussion were conducted on the basis of SL. A statistically significant linear correlation was observed between TL and SL TL = 1.2451 SL + 0.012 ($R = 0.9945$ with $p<0.001$). The mean individual weight (W) of the caught fish was 3.20 g (±2.38). The lowest values SL and W were observed in the fish caught in June, which indicates that strong recruitment caused by intensive feeding of the youngest fish occurs in this period. The highest statistically significant increases in the standard length (Δ SL) (over 0.5 cm/month) and the individual weight (Δ W) (over 0.7 g/month) were observed in months with the highest water temperature (July, August) (ANOVA, $p<0.001$) (Fig. 2, 3). A statistically significant decrease in Δ SL and Δ W in comparison to the previous month was observed in September and October (ANOVA, $p<0.001$) and in the weight additionally in November and May. It seems it was caused by the autumn catch of fish which hatched at the end of August and at the beginning of September which lowered the mean SL and W values. A wide range of these parameters in the fish caught from September to November, 2.30-6.40 cm and 0.35-8.79g, relatively, indicates this phenomenon.

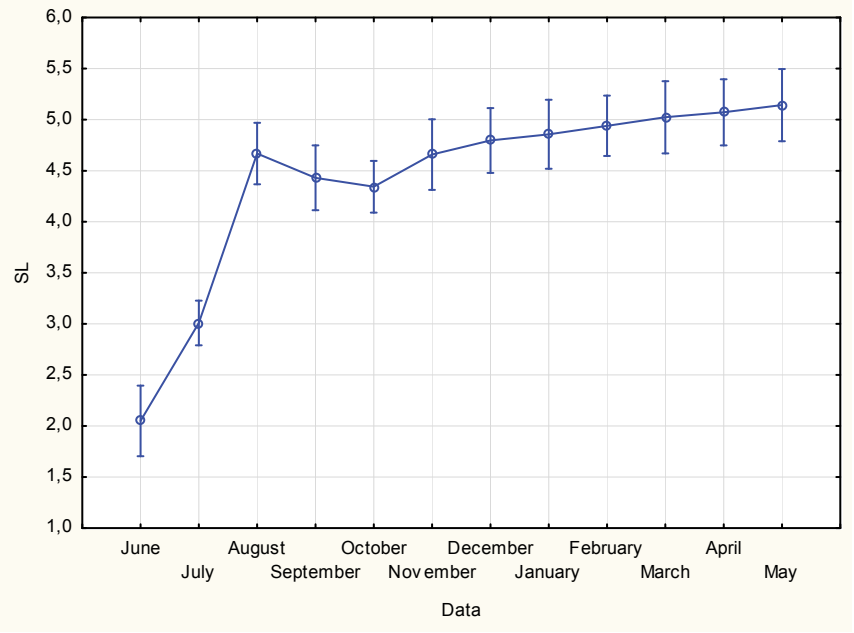

Fig. 2. Changes in standard length (SL) of the juvenile pumpkinseed in warm water
Rys. 2. Zmiany długości (SL) młodocianego bassa słonecznego w wodach pochłodniczych

The standard length (SL) and the individual weight in a young pumpkinseed from warm waters are significantly statistically correlated ($R = 0.9927$, $p<0.001$) and the equation looks as follows: $W = 0{,}0222SL^{3{,}2375}$. The high value of parameter b indicates the allometric increase in the weight in comparison to the increase in the body length of the fish.

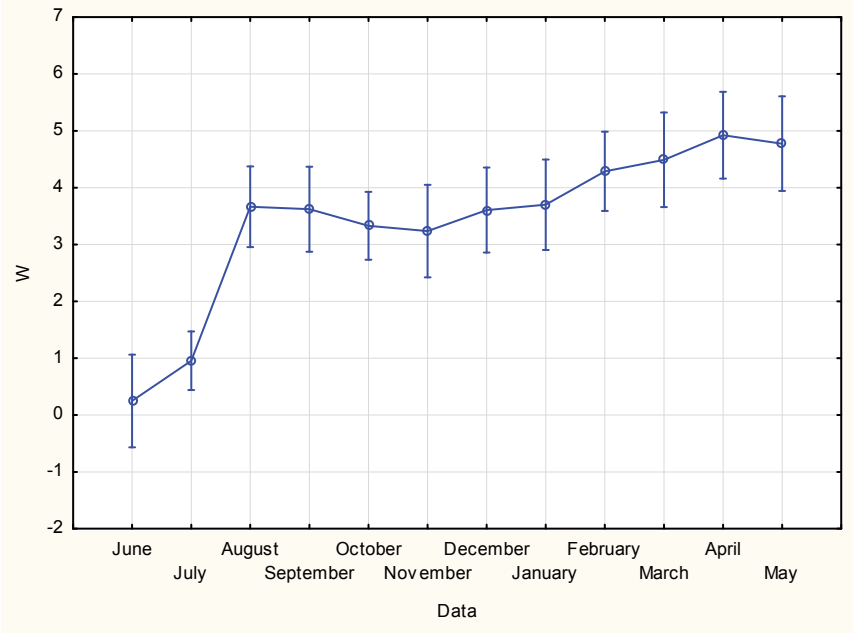

Fig. 3. Changes in individual weight (W) of the juvenile pumpkinseed in warm water
Rys. 3. Zmiany masy jednostkowej (W) młodocianego bassa słonecznego w wodach pochłodniczych

The mean value of the condition coefficient (K) of the caught fish was 3.14 ± 0.45. In the annual cycle, the highest mean K value belonged to the fish caught in April (K=3.60) whereas the significantly statistically lowest value of this parameter (K<3.0) in comparison to other months was observed in June and from November to December (ANOVA, $p<0.05$) (Fig. 4). The lowest values of condition coefficients in months with the lowest water temperature are typical of this thermophilic species.

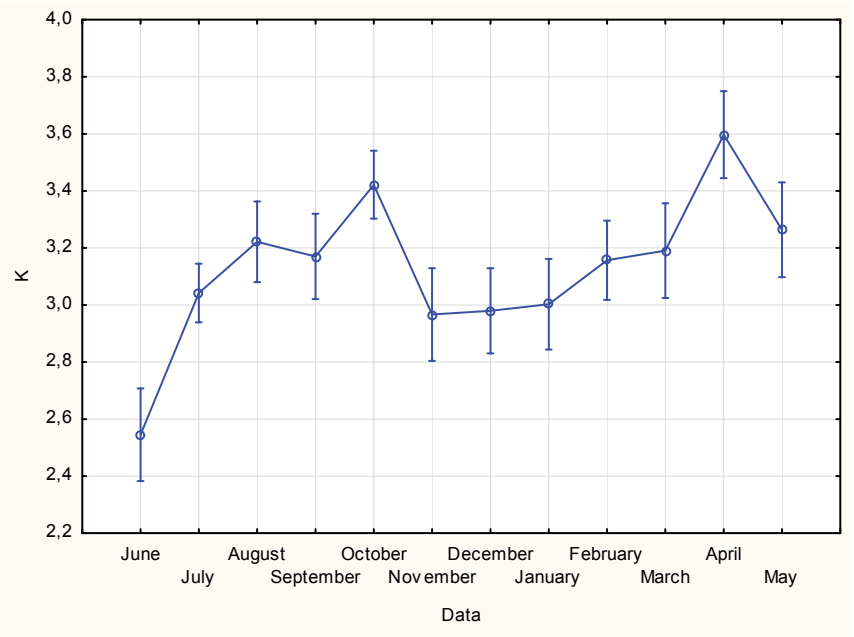

Fig. 4. Changes in condition coefficient (K) of the juvenile pumpkinseed in warm water
Rys. 4. Zmiany wartości współczynnika kondycji (K) młodocianego bassa słonecznego w wodach pochłodniczych

The age of the caught fish was estimated at 0+ (89.44%) and 1+ (10.56%). The fish aged 1+ were only caught in April and May. During the first year of life, the number of sclerites in a scale was on average 20.73 ±5.24 whereas the mean value for the oral ring was 0.892mm±0.241. The number of sclerites on a scale of the pumpkinseed grows proportionally to the increase in the length of this species according to the following formula: S = -0.8441 + 5.0880*SL (R = 0.95682, $p<0.001$). Also, the statistically significant increase in the length of the oral ring of the scale proved to be proportional to the length (SL) of the studied fish (ANOVA, $p<0.001$) (Fig. 5) and the length at which it is assumed that the scale in this species is 1.58 cm.

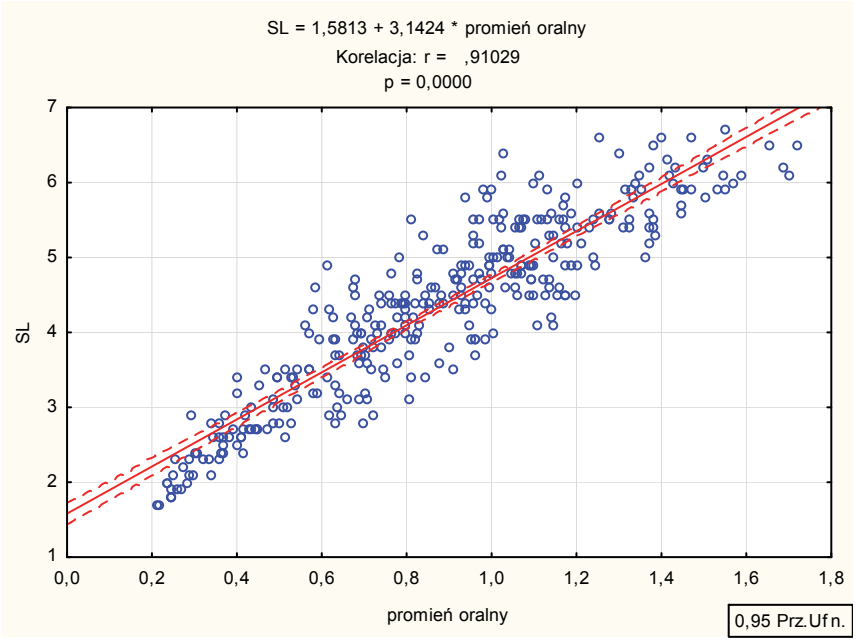

Fig. 5. Correlation between standard length (SL) and the scale radius (Po) of the juvenile pumpkinseed in warm water
Rys. 5. Korelacja prostoliniowa pomiędzy długością (SL) a długością promienia oralnego łuski młodocianego bassa słonecznego z wód pochłodniczych

It was observed that the number of sclerites (S) in an annual cycle increased in all the caught fish from 8,20 ±0.78 (in June) to 27.37 ±5.18 (in May). However, in 27.3 of the fish caught in April and in 56.7% in May the annual ring was already observed and on average 1.38 ±0.55 and 3.40 ±1.02 sclerites of the second year of life, respectively (Table 1). The fact indicates that the annual ring develops in the pumpkinseed in warm waters in this period. The highest statistically significant increases in the number of sclerities and the oral ring of the scale (respectively over 5 items and 0.3 mm) was observed on the scales of the fish caught from June to August (ANOVA, $p<0.05$) (Table 1). A statistically insignificant decrease in the number of sclerties and the lengths of oral rings of the scale in comparison to the previous month was observed in September as well as in January and February (ANOVA, $p<0.05$).

Table 1. Number of sclerites and the scale radius (Po) of the juvenile pumpkinseed in warm water
Tabela 1. Liczba sklerytów (szt.) i długości promienia oralnego łuski (mm) młodocianego bassa słonecznego z wód pochłodniczych

Month	Number of sclerites (pcs.)		The scale oral radius (mm)	
	Mean	SD	Mean	SD
June	8.20	0.78	0.261	0.039
July	14.32	3.26	0.601	0.239
August	22.18	4.59	0.931	0.665
September	21.08	5.88	0.715	0.295
October	21.31	4.74	0.747	0.197
November	23.21	3.79	0.946	0.240
December	24.69	4.41	1.036	0.262
January	24.41	3.92	1.019	0.239
February	22.88	5.14	0.913	0.324
March	25.02	4.46	1.133	0.290
April	25.89	4.56	1.118	0.251
May	27.37	5.18	1.279	0.241

In each month, the relative number of sclerties (S) crossing the oral ring in the pumpkinseed at 1 mm of the length of the oral ring decreases statistically insignificantly with the length SL according to the formula $S + 35.181 – 2.2 * SL$ ($R = -0.5523$ with $p<0.01$) and its annual average is 25.64 with small SD = 3.04.

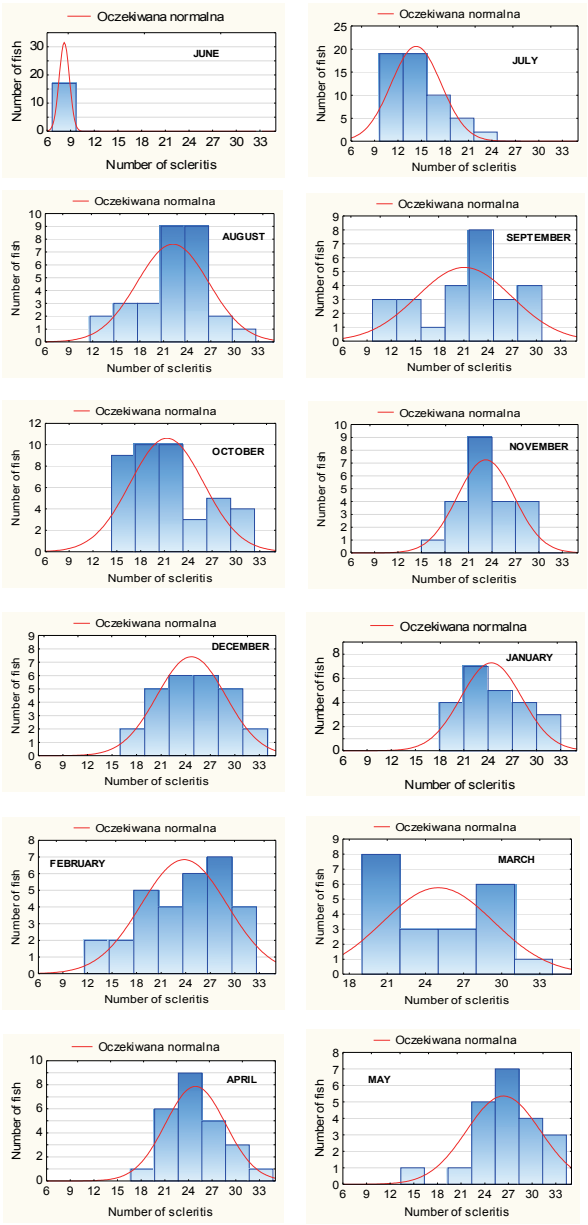

Fig. 6. Distribution of sclerites of pumpkinseed in warm water in annual cycle
Rys. 6. Rozkład liczby sklerytów bassa słonecznego z wód pochłodniczych w cyklu rocznym

Figure 6 presents the distribution of the number of sclerites in young pumpkinseeds in each month. It was assumed that in June the number of sclerites in the scale amounting to less than 14 corresponds to younger fish hatched in May although the pumpkinseed is a portion-spawning fish. From July, the fish were divided into groups in each month according to the number of sclerites. The younger ones from the June hatch were assumed to have up to 14 sclerites whereas the older ones from the May hatch were assumed to have over 14 sclerites. In June, the mean length (SL) of this fish in each group was 2.66 cm and 3.49 cm whereas the weight was 1.51 g and 1.69 g and differed statistically (ANOVA, $p<0.05$). In August, there were probably three age groups coming from the May, June and July hatches. Taking into account the distribution of sclerites in the fish from the catch from this month, it was assumed that we only caught two fishes with scales containing up to 14 sclerites (probably coming from the July hatch, the mean length SL was 3.25 cm and the weight was 0.90 g). Eight fishes featured from 14 to 22 sclerites (from the June hatch, SL = 4.06 cm and W = 2.26) whereas the other fish with the number of sclerites exceeding 22 belonged to the May hatch (SL = 5.26 cm and W = 4.97 g). In September, there were at least four groups differing in hatch season. However, only three groups were distinguished on the basis of the distribution of sclerites. Group I from the August hatch with the smallest number of sclerites (up to 14 sclerites) – 6 individuals (SL = 2.72 cm, W = 0.53 g), group II (July) which had from 14 to 22 sclerites – 8 individuals (SL = 4.31 cm, 2.85 g) and group III – older fish probably from the May and June hatches, over 22 sclerites (SL = 5.58 cm, W = 6.35 g). In October, the group from the September hatch was not caught, which is indicated by the lack of fish with the number of sclerites lower than 14. However, a large group of fish was caught probably from the August hatch which was characterised by up to 22 sclerites (SL = 3.77 cm, W = 1.65 g) and another group which consisted of older individuals (>22 sclerites, SL = 5.44 cm, W = 6.37 g). In November, the pumpkinseeds can only be divided into two groups according to the number of sclerites: up to 22 sclerites with the mean length of 4.01 cm and weight of 1.83 g and over 22 sclerites with SL = 5.29 cm and W = 4.35 g. In December and January, also two groups differing in the number of sclerites (group I <22, group II >22 sclerites) and in mean lengths (TL, SL), weights (W) and condition (K) were

distinguished (Table 2) whereas in February unexpectedly two fished with sclerites of up to 14 were caught, which may be caused by the catch of a small group of fish (2 individuals) coming from the September hatch. This group of fish featured low condition (K = 2.85), weight (W = 0.68 g) and length (TL = 3.61 cm and SL = 2.85 cm), which indicates that they encountered unfavourable environmental conditions after the hatch. In March, April and May two groups in each were observed with less than or more than 22 sclerites differing in lengths (TL and SL), weight (W) and condition (Table 2).

Table 2. The division of pumpkinseed from warm water into groups according to number of sclerites with mean lengths (SL and TL, mm), individual weight (W) and condition factor (K)
Tabela 2. Podział bassów na grupy według ilości sklerytów na łusce bassa słonecznego z wód pochłodniczych wraz z ich średnimi długościami (SL i TL, mm), masą (W) oraz współczynnikiem kondycji (K)

Month	Groups by numer of sclerites	Mean value of length (TL, SL, cm), individual weight (W, g) and condition (K) with standard deviation (SD)			
		TL±SD	SL±SD	W±SD	K±SD
June	<14	2.51±0.47	2.05±0.38	0.25±0.16	2.55±0.30
July	<14	3.28±0.37	2.66±0.22	1.51±0.18	2.83±0.42
	>14	4.38±0.51	3.49±0.43	1.69±0.22	3.34±0.31
August	<14	3.85±0.35	3.25±0.35	0.90±0.15	2.62±0.42
	14-22	5.09±0.55	4.06±0.50	2.26±1.01	3.18±0.59
	>22	6.54±0.52	5.26±0.36	4.97±1.44	3.33±0.40
September	<14	3.22±0.26	2.72±0.23	0.53±0.12	2.64±0.28
	14-22	5.37±0.90	4.31±0.75	2.85±1.69	3.15±0.41
	>22	7.09±0.64	5.58±0.44	6.35±1.74	3.56±0.32
October	<22	4.41±0.66	3.77±0.51	1.65±0.18	3.14±0.33
	>22	6.93±0.75	5.44±2.13	6.37±2.13	3.80±0.34
November	<22	5.01±0.57	4.01±0.51	1.83±0.65	2.72±0.24
	>22	6.53±0.60	5.29±0.45	4.35±0.15	2.87±0.35

Table 2. The division of pumpkinseed from warm water into groups according to number of sclerites with mean lengths (SL and TL, mm), individual weight (W) and condition factor (K)
Tabela 2. Podział bassów na grupy według ilości sklerytów na łusce bassa słonecznego z wód pochłodniczych wraz z ich średnimi długościami (SL i TL, mm), masą (W) oraz współczynnikiem kondycji (K)

Month	Groups by numer of sclerites	Mean value of length (TL, SL, cm), individual weight (W, g) and condition (K) with standard deviation (SD)			
		TL±SD	SL±SD	W±SD	K±SD
December	<22	5.01±0.71	4.03±0.57	1.94±0.83	2.79±0.13
	>22	6.40±0.64	5.20±0.59	4.49±1.71	3.08±0.29
January	<22	5.08±0.45	3.94±0.32	2.09±0.49	3.39±0.44
	>22	6.46±0.82	5.06±0.68	4.56±1.67	3.40±0.28
February	<14	3.61±0.57	2.85±0.49	0.68±0.29	2.85±0.23
	14-22	5.11±0.36	4.08±0.26	2.23±0.53	3.19±0.33
	>22	6.86±0.59	5.64±0.59	6.19±2.03	3.34±0.35
March	<22	5.21±0.23	4.19±0.22	2.13±0.21	2.92±0.35
	>22	6.78±0.76	5.49±0.65	5.85±2.19	3.37±0.37
April	<22	5.56±0.30	4.34±0.24	2.93±0.63	3.55±0.43
	>22	6.87±0.64	5.42±0.57	5.86±1.61	3.62±0.28
May	<22	5.50±0.42	4.35±0.31	2.61±0.66	3.12±0.31
	>22	6.81±0.83	5.33±0.67	5.29±2.15	3.30±0.25

4. Discussion

In 1880 the pumpkinseed was brought into European waters and currently it is one of the six species of the *Centrarchidae* family present in these waters (Tomeček *et al.*, 2007). In Europe it resides in reservoirs with various trophy and hydrology so the growth of this species (especially of the young ones) more depends on the environmental conditions than on their genetics (Heath & Roff 1987). However, as demonstrated by Copp *et al.*, (2004) growth of adult pumpkinseeds is generally lower in non-native European populations than in native American populations, probably due to the greater effect of reproduction and, therefore, greater populations of the fish in the first ones. However, as shown by the studies conducted in warm waters, growth of adult pumpkinseeds is greater than in natural waters of Europe (Dembski 2006, Domagała *et al.*, 2016) which might be caused by higher water temperatures (Domagała & Kondratowicz 2006, Domagała & Pilecka-Rapacz 2007). For instance, in warm waters of the Dolna Odra power plant, thermal conditions optimal for their growth remain from May to September, but the temperature of over 13ºC remains for 10 months (Domagała *et al.*, 2015). A confirmation of the conditions conducive to the growth of adult pumpkinseeds in warm waters of the Lower Oder (Domagała *et al.*, 2016) is a high, similar to the fast-growing populations of American waters, rate of the increase in the lengths of adult pumpkinseeds (Carlander 1977) and reaching the asymptotic length (L_∞) significantly exceeding the mean value of this parameter in European populations (Copp *et al.*, 2002, Godinho 2004, Domagała *et al*., 2016). Also, the growth of young (0+) individuals in warmed waters is higher than in natural waters (Dembski *et al.*, 2006, own studies). In European reservoirs young individuals reach the mean length (SL) of 40 mm in the first year of life (Copp *et al.*, 2004) whereas in waters with temperatures higher by 3.7ºC their length is 46.9 mm (Mirgenbach Reservoir, France) (Dembski *et al.*, 2006) whereas in warm waters of the Dolna Odra power plant it is as much as 51.4 cm (own data). Their rapid growth provides numerous benefits for the pumpkinseed, including reduced exposure to predator attacks, increased survival rate in winter, reduced interspecific and intraspecific competition as well as rapid transition to size classes (Arendt & Wilson 1999). However, rapid growth of the pumpkinseed

may be caused by earlier puberty than in natural waters although an important role is played by higher water temperatures (Zapata & Granadolorencio 1993, Dembski *et al.*, 2006, Domagała *et al.,* 2016). However, as demonstrated by Copp *et al.*, (2002), the pumpkinseed matures in the waters of Southern Europe at the age of two years and in the waters to the north even at the age of four whereas in warmed waters of the Mirgenbach Reservoir (France) at the age of one with the length of 56.8 mm (females) and 34.4 mm (males). Also, in the warm canal of the Lower Oder, part of the fish matures at the age of 1+ as early as in mid-May; females at the length of 57 mm and males at the length of over 54 mm, which was observed on the basis of the detailed analysis of gonads.

While assessing the growth of the fish through back-reading, it is important to collect the fish soon after the development of the annual ring and use the SL_0 value, i.e. when the scale develops in fish of a given species, to calculate the growth on the basis of back-reading (Osenberg *et al.*, 1988). The present studies demonstrated that the annual ring in the pumpkinseed develops at the turn of March and April. In this period, the biggest number of sclerites and the greatest edge increase on the scale (March) and a statistically significant decrease in the number of sclerites (ANOVA, $p<0.001$) after the development of the annual ring in April were observed in the analysed group of fish aged 0+. This is confirmed by the fact that part of the fish caught in April (27.3%) and May (56.7%) already had the first annual ring and a small number of sclerities of the new year of life (respectively 1.38 ±0.55 and 3.40 ±1.02). The length of the fish (SL) at which the scale develops in populations from warm waters is 1.58 cm and is slightly lower than in the waters of Southern Europe (1.71 cm) and Northern Europe (SL = 1.82 cm) (Uzunova *et al.*, 2008, Fox & Crivelli 2001), but in some populations of native waters of the USA this length for pumpkinseed is from 1.19 to 1.50 cm (Creaser 1926, Osenberg *et al.*, 1988).

The pumpkinseed population from warm waters is characterised by high variability of mean lengths and individual weights of the fish in each month. This probably results from the significantly longer reproduction cycle of this fish than in natural waters. Generally, the pumpkinseed spawns in portions. One female can lay spawn many times and the male milts the spawn of several females many times (Morris & Mischke 2000). For instance, in Lake Opinicon (Canada) females of the

species lay spawn on average 2.1 times (1-6 times) (Fox & Crivelli 1998). Also Kestemont & Philippart (1991) and Deacon & Keast (1987) indicate that the pumpkinseed females lay spawn at least three times every 20-30 days. The reproduction period of the native pumpkinseed populations normally begins in May or at the beginning of June (Bertschy & Fox 1999) and, depending on water temperature, lasts until the end of July or even the beginning of August (Forbes 1989, Vila-Gispert & Moreno-Amich 1998). Water temperature in this time should be 16-26ºC (Forbes 1989). Also a similar reproduction period for non-native populations occurring in Slovakian waters is reported by Holčik (1995), for Greek waters by Neophitou & Giapis (1994) and for Spain by Vila-Gispert & Moreno-Amich (1998). A significantly longer reproduction period is reported by Domagała *et al.* (2014) for the pumpkinseed population in warm waters of the Dolna Odra power plant (from May even to September). This is probably caused by higher water temperatures in comparison to natural waters (annually on average by 6-8ºC) remaining on the optimal level for this species until September (Fig. 7) (Domagała & Kondratowicz 2006). A similarly long reproduction period was observed in warm waters of the Mirgenbach Reservoir power plant in the south-east of France where the average annual water temperature is on average higher than in natural waters by 3.7ºC (Dembski *et al.*, 2006).

An effect of the variation of body lengths of the pumpkinseed may also be high food competition caused by large populations of the fish and cannibalism (Osenberg *et al.*, 1988), especially that individuals born in May are not only older by 5 months from the ones hatched in the last litter (September), but also encounter the most favourable thermal conditions as for the growth of this species (21-32ºC, as cited in Holtan 1989). However, individuals which hatched in September grow much more slowly only for 2-3 months (until November) and then the water temperature drops to 13ºC and remains below this level until mid-April (Fig. 7). Below this value, the pumpkinseed stops growing (Griffits 1978, as cited in Wismer & Christie 1987). This phenomenon was also observed in populations from warm waters of the Dolna Odra power plant, indicating that it is possible to determine fish groups from different hatch period on the basis of the number of sclerites on scales. Although the borders between the groups disappear, the groups differ in length

increases (TL and SL), individual weights (W) and condition (K) and probably in mortality in each month. Continuation of the studies of this issue will allow us to take a closer look at the population condition, including recruitment, population sizes and the number of the pumpkinseed in the largest population in Poland.

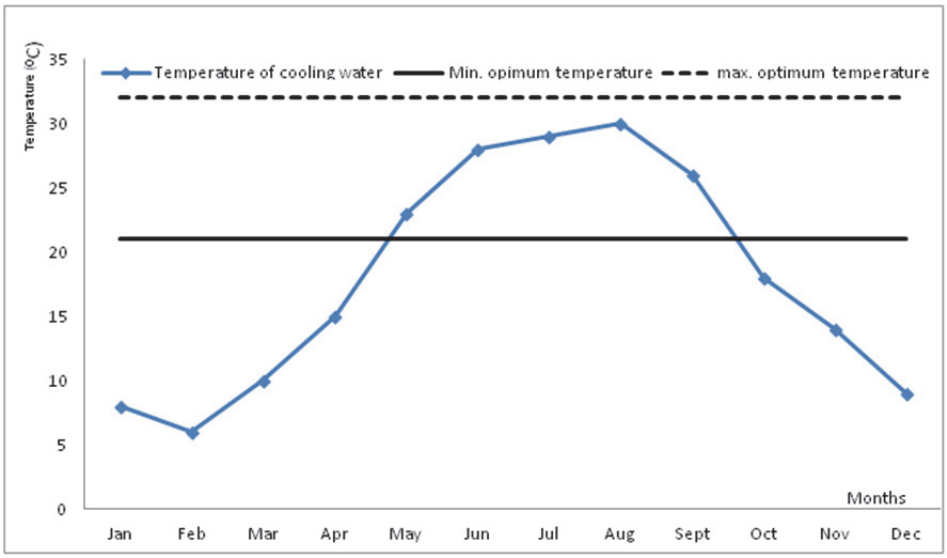

Fig. 7. Average monthly temperature of cooling water in 2009-2010, with an indication of the thermal optimum for the growth of the pumpikinseed (Domagala *et al.* 2015, modificated)
Rys. 7. Średniomiesięczne temperatury wód pochłodniczych w latach 2009-2010 wraz z zaznaczeniem optimum termicznego dla wzrostu bassa słonecznego (Domagała *et al.* 2015, zmienione)

4. Conclusions

An increase in the length and weight of a young pumpkinseed depends on water temperature. In warm waters of the Dolna Odra power plant with higher water temperatures than in natural waters, the fish is characterised by larger increases in lengths and weights in comparison to natural waters in Europe. This results from a longer period of optimal water temperature for the pumpkinseed to feed (Domagała *et al.*, 2015, Domagała *et al.,* 2016). This fact and richer food base in the warm canal explains why young pumpkinseeds do not leave the warm canal, excluding extreme situations. Also, the largest increases in lengths (Δ SL) (over 0.5 cm/month) and individual weights (Δ W) (over 0.7 g/month) which were observed in July and August are correlated with water temperature (over 26ºC). In successive months (autumn and winter), growth and values of the condition coefficient decrease despite temperatures higher by 5-8ºC in the warm canal than in neighbouring waters (Domagała & Kondratowicz 2006, Domagała & Pilecka-Rapacz 2007).

References

Angeler, D. G., Álvarez-Cobelas, M., Sánchez-Carrillo, S., Rodrigo, M. A. (2002). Assessment of exotic fish impacts on water quality and zooplankton in a degraded semi-arid floodplain wetland. *Aquatic Sciences* 64: 76-86. http://dx.doi.org/10.1007/ s00027-002-8056-y.

Arendt, J. D., Wilson, S. D. (1999). Countergradient selection for rapid growth in pumpkinseed sunfish: disentangling ecological and evolutionary effects. *Ecology.* 80: 2793-2798. DOI:10.1890/0012-9658(1999)080[2793:CSFRGI]2.0.CO;2.

Bertschy, K. A., Fox, M. G. (1999). The influence of age-specific survivorship on pumpkinseed sunfish life histories. *Ecology* 80 (7): 2299-2313. DOI: 10.1890/0012-9658(1999)080 [2299:TIOASS]2.0.CO;2.

Blanco, S., Romo, S., Villena, M. J., Martine´z, S. (2003). Fish communities and food web interactions in some shallow Mediterranean lakes. *Hydrobiologia* 506-509, 473-480.

Bolger, T, Connolly, P. L. (1989). The selection of suitable indices for the measurement and analysis of fish condition. *Journal of Fish Biology, 34*, 171-182.

Carlander, K. D. (1977). *Handbook of Freshwater Biology*. The Iowa State Press, Ames, *2.* 55-63.

Casal, C. M. V. (2006). Global documentation of fish introductions: the growing crisis and recommendations for action. *Biological Invasions* 8, 3-11, http://dx.doi.org/10.1007/s10530- 005-0231-3.

Copp, C., Fox, G. (2007). Growth and life history traits of introduced pumpkinseed (Lepomis gibbosus) in Europe, and the relevance to its potential invasiveness. In: Francesca Gherardi (Editor). *Biological invaders in inland waters: profiles, distribution, and threats*, 289-306.

Copp, G. H., Fox, M. G., Kováč, V. (2002). Growth, morphology and life history traits of a cool-water European population of pumpkinseed *Lepomis gibbosus*. *Archiv für Hydrobiologie 155*, 585-614.

Copp, H. G., Fox, M. G., Przybylski, M., Godinho, N., Vila-Gispert, A. (2004). Life-time growth patterns of pumpkinseed *Lepomis gibbosus* introduced to Europe, relative to native North American populations. *Folia Zoologica*, *53*, 237-254.

Creaser, C. W. (1926). Structure and growth of scales of fishes in relation to the interpretation of their life-history, with special reference to the sunfish *Eupomotis gibbosus*. *Univ. Mich. Misc. Pubs*. 17.

Deacon, L.I., Keast, J.A. (1987) Patterns of reproduction in two populations of pumpkinseed sunfish, *Lepomis gibbosus*, with differing food resources. *Environmental Biology of Fishes* 19 (4): 281-296. DOI: 10.1007/BF 00003229

Dembski, S., Masson, G., Monnier, D., Wagner, P., Pihan, J. C. (2006). Consequences of elevated temperatures on life-history traits of an introduced fish, pumpkinseed *Lepomis gibbosus*. *Journal of Fish Biology* 69 (2), 331-346. DOI: 10.1111/j.1095-8649.2006.01087.x.

Domagała, J., Czerniejewski, P., Pilecka-Rapacz, M. (2016). Growth rate, age and size structure of the alien pumpkinseed, *Lepomis gibbosus* (L., 1758) population from a heated-water discharge canal of a power plant in the lower stretch of the Oder river, Poland. *Rocznik Ochrona Środowiska, 18(1)*, 273-290.

Domagała, J., Dziewulska, K., Kirczuk, L., Pilecka-Rapacz., M. (2015). Sexual cycle of white bream, *Blicca bjoerkna (Actinopterygii, Cypriniformes, Cyprinidae*), from three sites of the lower Oder River (NW Poland) differing in temperature regimes. *Acta Ichthyologica et Piscatoria, 45(3)*, 285-298.

Domagała, J., Kirczuk, L., Dziewulska, K., Pilecka-Rapacz, M. (2014). Annual development of gonads of pumpkinseed, *Lepomis gibbosus (Actinopterygii: Perciformes: Centrarchidae*) from a heated-water discharge canal of a power plant in the lower stretch of the Oder River, Poland. *Acta Ichthyologica et Piscatoria, 44*, 131-143.

Domagała, J., Kondratowicz, A. (2006). Environmental Conditions of Waters of Cold and Warm Canals of "Dolna Odra" Power Station in the Second Half of the Nineties. *Rocznik Ochrona Środowiska, 22*, 355-360.

Domagała, J., Pilecka-Rapacz, M. (2007). Charakterystyka wód pochłodniczych Elektrowni Dolna Odra w latach 2004-2006. *Zeszyty Naukowe Wydziału Budownictwa i Inżynierii Środowiska*, *23*, 751-760.

Economidis, P. S., Kattoulas, M., Stephanidis, E. (1981). Fish fauna of the Aliakmon River and the adjacent waters (Macedonia, Greece). *Cybium* 5, 89-95.

Forbes, L. S. (1989). Spawning, growth, and mortality of three introduced fishes at Creston, British Columbia. *Canadian Field-Naturalist*, *103*, 520-523.

Fox, M. G., Crivelli, A. J. (2001). Life history traits of pumpkinseed (*Lepomis gibbosus*) populations introduced into warm thermal environments. *Archive fur Hydrobiologie 150*, 561-580.

Fox, M.G., Crivelli, A.J. (1998). Body size and reproductive allocation in a multiple spawning centrarchid. *Canadian Journal of Fisheries and Aquatic Sciences* 55 (3): 737-748. DOI: 10.1139/f97-269

Godinho, F. N. (2004). *The ecology of largemouth bass Micropterus salmoides, and pumpkinseed sunfish Lepomis gibbosus, in the lower Guadiana basin: the environmental mediation of biotic interactions*. Universidad Téchnica de Lisboa, Portugal

Godinho, F. N., Fereira, M. T., Cortes, R. V. (1997) The environmental basis of diet variation in pumpkinseed sunfish, *Lepomis gibbosus*, and largemouth bass, *Micropterus salmoides*, along an Iberian river basin. *Environmental Biology of Fishes* 50, 105-115, http://dx.doi.org/10.1023/A:1007302718072

Grabowska, J., Kotusz, J., Witkowski, A. (2010). Alien invasive fish species in Polish waters: an overview. *Folia Zoologica, 59*, 73-85.

Groot, de S. J. (1985). Introductions of non-indigenous fish species for release and culture in the Netherlands. *Aquaculture, 46*, 237-257.

Guti, G., Andrikowics, S., Bíró, P. (1991). Nahrung von Hecht (*Esox lucius*), Hundfisch (*Umbra crameri*), Karausche (*Carassius carassius*), Zwergwels (*Ictalurus nebulosus*) und Sonnenbarsch (*Lepomis gibbosus*) im Ócsa-Feuchtgebeit, Ungarn. *Fischökologie* 4, 45-66

Heath, D., Roff, D. A. (1987). Test of genetic differentiation in growth of stunted and nonstunted populations of yellow perch and pumpkinseed. *Transactions of the American Fisheries Society, 116*, 98-102.

Holčik, J. (1991). Fish introductions in Europe with particular reference to its central and eastern part. *Canadian Journal of Fisheries and Aquatic Science* 48, Suplement, *1*, 13-23.

Holčik, J. (1995). *Lepomis gibbosus* (Linnaeus, 1758). In: Baruš V., Oliva O. (eds.) *Mihulovci Petromyzontes a ryby Osteichthyes (2). [Cyclostomes Petromyzontes and fishes Osteichthyes (2).]* Academia, Praha, Czech Republic. [In Czech.]

Holtan, P. (1998). Pumpkinseed (*Lepomis gibbosus*). *Wisconsin Department of Natural Resources, Bureau of Fisheries Management*. Wisconsin, 1-6pp

Kestemont, P., Philippart, J. C. (1991) Considerations sur la croissance ovocytaire chez les poissons a ovogenese synchrone et asynchrone. *Belgian Journal of Zoology, 121(1)*, 87-98.

Morris, J. E., Mischke, C. C. (2000). A white paper on the status and needs of sunfish aquaculture in the north central region. *North Central Regional Aquaculture Center*, Ames, IA, 17.

Neophitou, C., Giapis, A. J. **(**1994). A study of the biology of pumpkinseed (*Lepomis gibbosus* (L.)) in Lake Kerkini (Greece). *Journal of Applied Ichthyology* 10 (2-3): 123-133. DOI: 10.1111/j.1439-0426.1994.tb00151.x

Osenberg, C. W., Mittelbach, G. G., Wainwright P. C. (1992). Two-stage life histories in fish: the interaction between juvenile competition and adult performance. *Ecology, 73*, 255-267.

Osenberg, C. W., Werner, E. E., Mittelbach, G. C., Hall, D. J. (1988). Growth patterns in bluegill (*Lepomis macrochirus*) and pumpkinseed (*L. gibbosus*) sunfish: environmental variation and the importance of ontogenic niche drifts. *Canadian Journal of Fisheries and Aquatic Science, 45*, 17-26.

Penczak, T. (1967). Biologiczne i techniczne podstawy połowu ryb stałym prądem. *Przeglad Zoologiczny*, 1*1*, 114-131.

Ricker, W. E. (1975). Computation and interpretation of biological statistics of fish populations. *Bulletin Fisheries Research Board of Canada*, *191*, 1-382.

Sokal, R. R., Rohlf, F. J. (1995). *Biometry: the principles and practice of statistics in biological research.* Third Edition, H. Freeman and Company, New York, 887.

Sostoa, A., Lobon-Cervia, J., Fernandez-Colome, V., Sostoa, F. J. (1987). La distribucion del pez sol (*Lepomis gibbosus* L.) en la Peninsula Iberica. *Acta Vertebrata, 14*, 121-123.

Stanisz, A. (1998). *Przystępny kurs statystyki*. StatSoft Poland. Kraków (in Polish).

Tomoček, J, Kováč, V, Katina, S (2007). The biological flexibility of the pumpkinseed: a successful colonizer throughout Europe. In: Gherardi F (ed), *Biological Invaders in Inland Waters: Profiles, Distribution, and Threats*. Invading Nature - Springer Series in Invasion Ecology, Volume 2. Springer, Dordrecht, The Netherlands, 307-336.

Uzunova, E. B., Velkov, S., Studenkov, M., Georgieva, M., Nikolova, L., Pehlivanov, D., Parvanov, D. (2008). Growth, age and size structure of the introduced pumpkinseed (*Lepomis gibbosus* L.) population from small ponds along the Vit River (Bulgaria). *Bulgarian Journal of Agricultural Sciences, 14*, 227-234.

Van Kleef, H, Van der Velde, G, Leuven, R. S. E. W., Esselink, H. (2008). Pumpkinseed sunfish (*Lepomis gibbosus*) invasions facilitated by introductions and nature management strongly reduce macroinvertebrate abundance in isolated water bodies. *Biological Invasions* 10, 1481-1490, http://dx.doi.org/10.1007/s 10530-008-9220-7

Vila-Gispert, A., Moreno-Amich, R. (1998). Periodic abundance and depth distribution of *Blennius fluviatilis* and introduced *Lepomis gibbosus*, in Lake Banyoles (Catalonia, Spain). *Hydrobiologia* 386, 95-101.

Welcomme, R. L. (1992). A history of international introductions of inland aquatic species. *ICES Marine Science*, 194, 3-14.

Wismer, D. A., Christie, A. E. (1987). *Temperature Relationships of Great Lakes Fishes: A Data Compilation.* Great Lakes Fishery Commission Special Publication, *87*, 1-165.

Zapata, S. C., Granadolorencio, C. (1993). Age, growth and feeding of the exotic species Lepomis gibbosus in a Spanish cooling reservoir. *Archiv für Hydrobiologie, 127*, 561-573.

Wewnątrzpopulacyjne zróżnicowanie wzrostu i życia młodocianych basów słonecznych wprowadzonych do wód pochłodniczych dolnej Odry, Polska

Streszczenie

Bass słoneczny *Lepomis gibbosus,* Linnaeus (1758) jest gatunkiem nierodzimym, którego najliczniejsza populacja w Polsce zasiedla kanał ciepły elektrowni "Dolna Odra". Dotychczas na osobnikach dorosłych tego gatunku przeprowadzono analizy wzrostu długości i masy oraz zmian dojrzałości gonad. Celem niniejszej pracy była ocena wpływu podwyższonej termiki wody na wielkość sezonowych zmian długości, masy i kondycji oraz liczby sklerytów, ze szczególnym uwzględnieniem długości (S_0) przy której zakłada się łuska. Materiał do badań stanowiły osobniki młodociane w wieku 0+ (305 szt.) i 1+ (36 sztuk.) złowione podczas prowadzenia comiesięcznych elektropołowów. Ryby ważono (W, g) z dokładnością do 0,1g, zmierzono (TL, SL, mm) oraz określano ich kondycje za pomocą współczynnika Fultona (K). Ponadto na łuskach oszacowano liczbę sklerytów oraz termin zawiązywania się pierścienia rocznego.

Największe miesięczne przyrosty długości SL (powyżej 0,5cm/miesiąc) oraz masy jednostkowej W (powyżej 0,7 g/miesiąc) u badanych ryb zanotowano w miesiącach o najwyższej termice wody (lipiec, sierpień) (ANOVA, $p<0,001$). Spadek temperatury wody w kanale ciepłym, w miesiącach jesienno- zimowych, powodował zmniejszanie się przyrostów miesięcznych ryb. Analiza regresji pomiędzy długością (SL) a długością promienia oralnego łuski (Po) przybrała postać funkcji liniowej: SL = 1,5813 + 3,1424*Po (R = 0,91029, p = 0,0000) i wykazała, iż długość przy której zakłada sie łuska u tego gatunku wynosi 1,58cm. Liczba sklerytów (S) na łuskach młodocianego bassa slonecznego wzrastała w cyklu rocznym od 8,20 szt. ±0,78 (w czerwcu) do 27,37 szt. ±5,18 (w maju następnego roku). W kwietniu i w maju u ryb zanotowano założony już pierścień roczny i odpowiednio średnio 1,38 szt. ±0,55 oraz 3,40 szt. ±1,02 sklerytów drugiego roku życia. Ponadto stwierdzono, że liczba sklerytów (S) na łusce bassa słonecznego rośnie proporcjonalnie do wzrostu długości tego gatunku zgodnie ze wzorem: S = -0,8441 + 5,0880*SL (R = 0,95682, $p<0,001$).

Abstract

Pumpkinseed *Lepomis gibbosus*, Linnaeus (1758) is a non-native fish species, which the largest population in Poland inhabits warm canal of a "Dolna Odra" Power Plant. Until now, the growth in length and weight and changes the gonad's maturity of adults individual of this species were carried out. The aim of this study was to evaluate the effect of high water temperature on the seasonal changes in the length, weight, condition, and the number of sclerites, with particular emphasis on length (S_0) at which in this species the scales start forming. The research material included 341 pumpkinseed individuals in age 0+ (305 ind.) and 1+ (36 ind.) caught during monthly catches (electrofishing). The fish was weighted (W, g) to the nearest 0.1 g, measured (TL, SL, mm) and their conditions was determined by the coefficient Fulton (K). In addition, number of sclerites (S) on scales and the time of setting up the annual ring were determinated. The biggest monthly increases in mean length - SL (more than 0.5 cm/month) and increases of mean weight W (above 0.7 g / month) in the fish were recorded in the months of highest thermals water (July, August) (ANOVA, $p <0.001$). The decrease of water temperature in the warm channel in the autumn and winter months, resulted in reduction of monthly growth of fish. Analysis of regression between length (SL) and the length of the scale radius (Po) took the form of a linear function: SL = 1.5813 + 3.1424 * Po (R = 0.91029, p = 0.0000) and showed that the length at which in this species the scales start forming is 1,58cm. Number of sclerites (S) on scales of juvenile pumpkinseed has grown at an annual cycle of 8.20 ± 0.78 (in June) to 27.37 ± 5.18 (in May of the following year). In April and May the fish were recorded

already formed on scales a year ring and respectively 1.38 ± 0.55 and 3.40 ± 1.02 sclerites of the second year of life. Moreover, the number of sclerites (S) on pumpkinseed's scales proportionally increased to the length of this species according to the formula: $S = -0.8441 + 5.0880 * SL$ ($R = 0.95682$, $p < 0.001$).

Słowa kluczowe:
gatunek nierodzimy, młodociany bass słoneczny, wzrost, kondycja, sezonowa zmienność

Keywords:
non-native species, juvenile pumpkinseed, growth rate, condition, seasonal variability

MIDDLE POMERANIAN SCIENTIFIC SOCIETY OF THE ENVIRONMENT PROTECTION
ŚRODKOWO-POMORSKIE TOWARZYSTWO NAUKOWE OCHRONY ŚRODOWISKA

Annual Set The Environment Protection
Rocznik Ochrona Środowiska

Volume/Tom 19. Year/Rok 2017 ISSN 1506-218X 122-142

Ecological and Economical Aspects of Modern Modeling of Thread Rolling Process

Krzysztof Kukiełka
Politechnika Koszalińska

1. Introduction

Modern methods of plastic metals processing such as cutting processes (Bohdal & Walczak 2013, Bohdal & Kukielka L. 2014), cutting and burnishing processes sliding (Bohdal et al. 2014), cutting by an abrasive single grain (Chodór 2014, Forysiewicz et al 2016, Kukielka L. & Kustra 2003, Kukielka L. et al 2005), drawpiece forming process (Kałduński & Kukielka L. 2014) thread rolling (Kukiełka K. 2009, Kukiełka K. & Kukielka L. 2013, Kukiełka K. 2014, Kukiełka K. et. al 2014, Kukiełka K. 2016, Kukiełka L. & Kukiełka K. 2007, Kukiełka L. & Kukiełka K. 2012), duplex burnishing (Patyk & Kukielka L. 2008, Patyk et al 2014), burnishing rolling (Kukiełka L. 1994, Kukiełka L. 1999, Kukiełka L. & Krzyżyński T. 2000, Kukiełka L. 2001, Kukiełka L. 2002, Kukiełka L. et al 2012, Kukiełka L. et al 2012, Kułakowska et al 2009, Kułakowska, Kukiełka L et al 2014, Myśliński et al 2004), rolling process (Kowalik, 2010), shot penning (Zaleski & Bławucki 2014), grinding process (Sutowski & Nadolny 2016, Nadolny et al 2014), plastic deformations of measured object surface (Kowalik et al. 2016), surface roughness measured after machining (Valicek et al 2012, Kusnerova et al 2013) other like water jet cutting (Perec 2016) and mechanical/abrasive polishing (MP), standard electropolishing (EP) and magnetoelectropolishing (MEP) (Rokosz 2016), plasma cutting (Skoczylas & Zaleski 2015) and modern material behaviour modelling (Malag et al 2014).

In applications using a theoretical calculations and modelling processes precision machining of modern parts (Kukiełka L. 1994, Kukiełka L. 1999, Kukiełka L. & Krzyżyński T. 2000, Kukiełka L. 2001, Kukiełka L. et al 2012, Kukiełka L. et al 2014, Kukiełka L. & Kukiełka K 2015, Myślński et al 2004) are geometrical, physical and thermal nonlinear boundary–initial problem, where there are nonlinear, movable and variable in time and in time and state of: stress, strain and space heat sources and boundary conditions were described by using the incremental models. Wherein, the boundary conditions are unknown in the contact zones between the tool and workpieces.

The implementation of a new process into industrial practice is long process, laborious-, energy- and material-consuming. The traditional methods are based on the on multiple improvements of the prototype solutions until the established requirements regarding the quality of the product.

Whereas, very often are made the assumption that the processes are isothermal treatment and are realized on cold (Kukiełka K. 2009, Kukiełka K. & Kukielka L. 2013, Kukiełka K. 2014, Kukiełka K. et al. 2014, Kukiełka K. 2016, Kukiełka L. & Kukiełka K. 2007, Kukiełka L. & Kukiełka K. 2012) do not take into account the variability of thermophysical constant with temperature. This results in significant errors in both qualitative and quantitative. For example on Fig. 1 shows the influence of temperature on variation of the Poisson ratio and Young's modulus.

At present is required that the prepare production of new products apply the principle of "eco-design product," which base on reduce the negative impact on the surrounding natural environment of man. The dominant role in this action plays the rational use of energy and environment protection. In this case, an important step is the correct development and the proper implementation of the process.

This article is about a new method of modelling machining processes, including thermodynamics of physical phenomena. The methodology was developed in team of prof. L. Kukiełka with the author (Kukielka L. 1994, Kukielka L. 1999, Kukielka, L. & Krzyzynski 2000, Kukielka L. et al. 2012, Kukielka L. et al., Kukiełka L. & Kukiełka K. 2015). The application of the developed general methodology to solve complex problems of modelling specific problems seen in several exam-

ples of technology. In particular, it shows examples of modelling of thread rolling process.

One of the post-machining methods used to form the outer layer, characterized by advantageous exploitational properties, is thread rolling (Domblesky & Feng 2002, Kukiełka K. 2009, Kukiełka K. & Kukielka L. 2013, Kukiełka K. 2014, Kukiełka K. et al. 2014, Kukiełka K. 2016, Kukiełka L.& Kukiełka K. 2007, Kukiełka L. & Kukiełka K. 2012, Łyczko 2010, Olszak 2008). The increase of life and reliability of a product are achieved, mainly, by means of the consolidation and hardening of the surface layer, by generating a resultant small-gradient compressive stress and by the decrease of roughness where the volume of the surface load is increased. Thread rolling is usually considered as a cold process with no pre-heating of the elements and with rigid (Fig. 2) pressure of the threaded element[1] onto object.

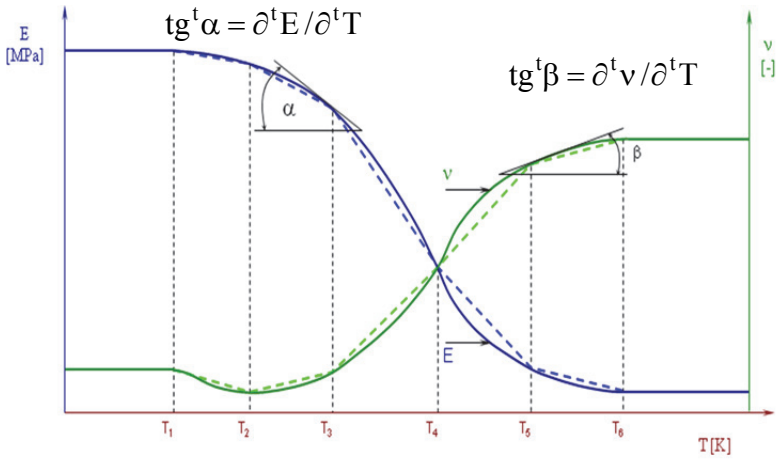

Fig. 1. Graphs of functions of Poisson's ratio ${}^t\nu = {}^t\nu({}^tT)$ and Young's modulus ${}^tE = {}^tE({}^tT)$ and a geometric interpretation of partial derivatives $\partial^t E/\partial^t T$ and $\partial^t \nu/\partial^t \nu$ in time t

Rys. 1. Wykresy funkcji współczynnika Poissona ${}^t\nu = {}^t\nu({}^tT)$ i modułu Younga ${}^tE = {}^tE({}^tT)$ oraz geometryczna interpretacja pochodnych cząstkowych $\partial^t E/\partial^t T$ i $\partial^t \nu/\partial^t \nu$ w chwili t

[1] The rolling element (roller) constitutes that part of the tool which is indirect contact with the rolled surface of the object.

The thread rolling process is a new technological process, such as the thread rolling quick pitch, therefore directly contributes to reduce the negative impact of this process on the surrounding environment. The new method of thread rolling, developed at the Department of Automatics, Mechanics and Constructions at the Faculty of Mechanical Engineering Technical University of Koszalin (Kukiełka K. & Kukielka L. 2013).

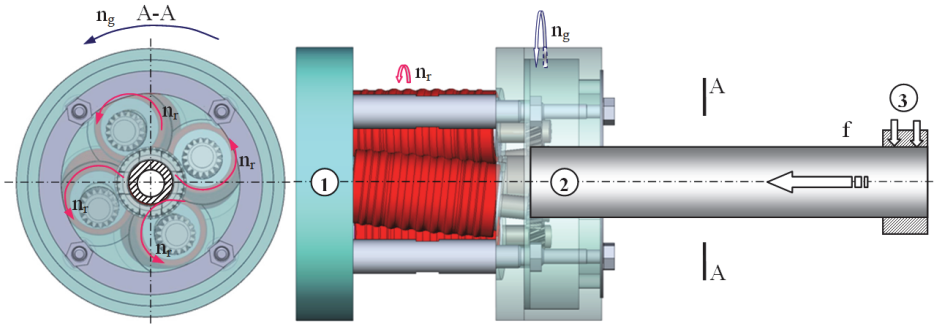

Fig. 2. The external thread rolling process schema on bars or pipe by rolling axial head with four rolls: 1 – head, 2 – blank, 3 – grip
Rys. 2. Schemat procesu walcowania gwintów łukowych na prętach lub rurach głowicą kątową czterorolkową metodą osiową: 1 – głowica, 2 – półwyrób, 3 – uchwyt

Knowledge of the physical phenomena with thermal phenomena occurring in the material in areas, where the threading element is in contact with the object and in the threading element while the thread process is carried out, is a basic necessity. It also enables the control of the properties of the outer layer of the product and achieving of the greatest shape-dimensional accuracy.

Thus, one of the most important technological problems in the thread rolling is the calculation of displacement, strain, stress and temperature in the surface layer.

So far there is no universal model of the thread rolling process and numerical algorithms for the analysis of these phenomena for various conditions of the process realization. The most frequently used regression equations obtained from the experimental investigations realized in accordance with the developed plan (Kukielka L. 1994, Kukielka L. 2002, Kukiełka K. 2009, Kukiełka K. 2014). Statistical relationships between

a random variable was determined with the use of a statistical method of identification from the experimental data.

The analysis of the literature on the rolling process, e.g. (Domblesky & Feng 2002, Kukiełka K. 2009, Kukiełka K. & Kukielka L. 2013, Kukiełka K. 2014, Kukiełka K. 2014, Kukiełka K. 2016, Kukiełka L.& Kukiełka K. 2007, Kukiełka L. & Kukiełka K. 2012, Łyczko 2010, Olszak 2008), own studies and computer simulations (Kukiełka K. 2009, Kukiełka K. & Kukielka L. 2013, Kukiełka K. 2014, Kukiełka K. et al. 2014, Kukiełka K. 2016, Kukiełka L. & Kukiełka K. 2006, Kukiełka L. & Kukiełka K. 2007, Kukiełka L. & Kukiełka K. 2012) shows that the technological quality of the rolled thread, can influence from the following factors:

1) Material factors: Young's modulus, Poisson ratio, initial yield point, plastic hardening modulus, sensitivity on the strain rate, plastic anisotropy, value of border-strain, inclination to brittle cracking;
2) Geometrical of the thread and tool factors: thread dimensions, outside diameter and wall thickness of the pipe, surface state and physical state of surface layer zones (state of stress) of the pipe after preceded treatment, roller geometry, number and spacing of the rolls, kind of the tool profile (in the shape of screw line or ring-shaped), material and set of the rest, single or multi-turn thread);
3) Technological parameters (depends of the rolling mill type and special head): speed of the roller put in, rolling speed, contact force;
4) Friction conditions in the contact zones (depends of the kind of lubricant): friction moment, friction forces;

and for its complex analysis it is necessary to develop adequate mathematical model and numerical methods of solving it.

This work describes the thread rolling as a real object and its physical and mathematical modelling. The update Lagranian description (Bathe 1982) has been used to describe nonlinear phenomena, on a typical incremental step, assuming the stepwise and co-rotational coordinate system. The states of strain and strain rate have been described by mean of nonlinear dependence without any linearization. The proper measures of strain and stress increments, i.e. the increment of Green-Lagrange's strain tensors and the increment of the second symmetric Pioli-Kirchhoff's strain tensors were applied. The nonlinearity of the material was described using the incremental model, making allowance for the

effects of strain, strain rate and temperature history. The work pieces (pipe or bar) have been considered treating an object as a body which can undergo elastic strains or thermo-elastic strains (in the reversible zone) and thermo-visco-plastic and phasis (in non-reversible zone). The material model was prepared making use of Huber-Mises-Hencky's nonlinear condition of thermo-plasticity, the associated law of flow and the mixed (isotropic-kinematical) strain hardening. The state of material after preprocessing was also taken into consideration introducing the initial conditions of displacement, strain, strain rate, stress and temperature. The incremental contact model obtained comprises the contact forces, contact rigidity, contact boundary conditions and friction conditions in this area (Kukiełka K. 2009). Then, the incremental functional of the total system energy and enthalpy, were derived. From stationary condition of this functionals derived variational, nonlinear two equations: one of motion and deformation of object and the second - heat transfer on the typical incremental step time $t \rightarrow \tau = t + \Delta t$. These equations has been solved with finite element spatial discretization, where the discrete system of motions and deformations equations of objects and heat transfer in the thread rolling process, were received. This model with initial and boundary conditions are used to numerical analysis of deformation and temperature in the thread rolled.

2. Algorithm of thermo-mechanical modelling and numerical analysis of the thread rolling process

The incremental mathematical model of thread rolling process, in the updated Lagrange formulation, contain the constitutive equations (model of thermo-dynamical yield stress, thermo-elastic/thermo-visco-plastic-phasis strains model, thermo-elastic/ thermo-visco-plastic-phasis stress model), the model of contact between tool-workpiece, dynamic equation of motion and deformation, equations of heat transfer, initial and boundary conditions.

First, variational method developed equation of motion and deformation, and heat transfer for a typical step time. Then, these equations with Finite Element Method (FEM) were discretized, given the equations of motion and deformation and heat transfer of a discrete object. Then, the explicit (DEM) scheme to step by step numerical solution is adopted.

The algorithms of numerical analysis without of temperature (on cold) in ANSYS program for different technological processes were elaborated (Domblesky & Feng 2002, Kukiełka K. 2009, Kukiełka K. & Kukielka L. 2013, Kukiełka K. 2014, Kukiełka K. et al. 2014, Kukiełka K. 2016, Kukiełka L. & Kukiełka K. 2006, Kukiełka L. & Kukiełka K. 2007, Kukiełka L. & Kukiełka K. 2012, Kukiełka L. & Kukiełka K. 2015), where discrete equations was applied together with initial and boundary conditions. Especially, modelling of the thread rolling process, including the mechanics of the process are shown in publications (Kukiełka K. 2009, Kukiełka K. 2016, Kukiełka L. & Kukiełka K. 2012, Kukiełka L. et al 2014) (Fig. 3).

For approve the design and control of thread rolling process, knowledge of the course of thermal distribution and temperature fields in the system (object-tool) is needed.

The paper presents a physical model of thermal phenomena in thread rolling process and description of the heat sources in an incremental differential equation with appropriate initial and boundary conditions for temperature.

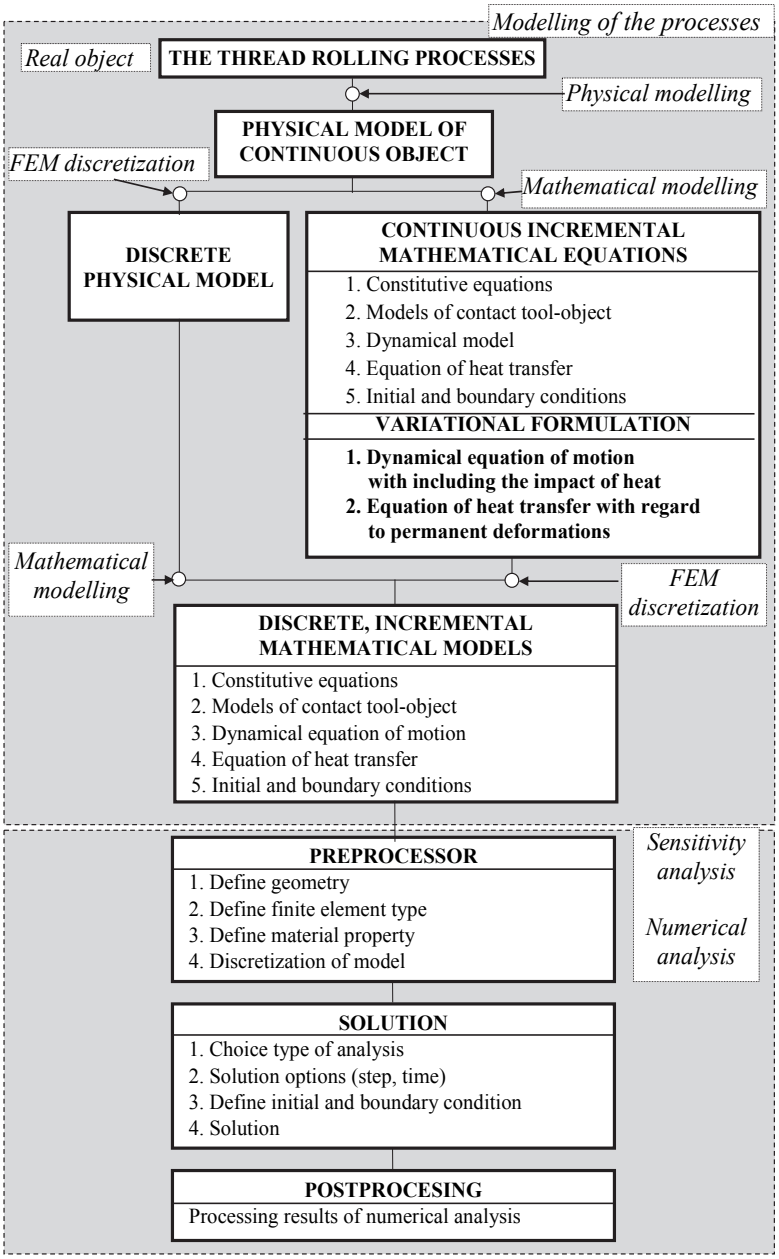

Fig. 3. Scheme of modern modelling and analysis of thread rolling process
Rys. 3. Schemat modelowania i analizy procesu walcowania gwintów

2.1. Mathematical incremental model of heat transfer

Uses an updated Lagrange description, assuming knowledge of the temperature field in the initial moments t_0 and present time t, while looking for a solution to the next time $\tau=t+\Delta t$, where Δt is a very small incremental of time (Bathe 1982). Then the equation for a typical incremental step $t \to \tau$, in the global coordinate $\{z\}$ is assumed:

$$\mathrm{div}\{\lambda(T)\cdot \mathrm{grad}[\Delta T(\boldsymbol{z},\Delta t)]\} + \Delta q_{VD}[\cdot] = C(T)\cdot\rho(T)\cdot\Delta\dot{T}(\boldsymbol{z},\Delta t), \tag{1}$$

where:

$$\Delta\dot{T}(\mathbf{z},\Delta t) = \frac{\partial[\Delta T(\mathbf{z},\Delta t)]}{\partial\, t} \tag{2}$$

is the speed of incremental of the temperature,
$\lambda(T), C(T), \rho(T)$ are depended on the temperature in the time t: heat conductivity, heat capacity and mass density, however:

$$\begin{aligned}\Delta q_{VD}[\cdot] = {} & \frac{(1-\xi)\cdot {}^{\tau}V}{t+\Delta t}\int_{{}_{t}\varepsilon_i^{(VP)}}^{{}_{\tau}^{\tau}\varepsilon_i^{(VP)}} {}_{\tau}^{\tau}\sigma_Y({}_{\tau}^{\tau}\varepsilon_i^{(VP)},\ {}_{\tau}^{\tau}\dot{\varepsilon}_i^{(VP)},\ {}^{\tau}T) + \\ & - \frac{(1-\xi)\cdot {}^{t}V}{t}\int_{{}_{t-\Delta t}^{t-\Delta t}\varepsilon_i^{(VP)}}^{{}_{t}^{t}\varepsilon_i^{(VP)}} {}_{t}^{t}\sigma_Y({}_{t}^{t}\varepsilon_i^{(VP)},\ {}_{t}^{t}\dot{\varepsilon}_i^{(VP)},\ {}^{t}T),\end{aligned} \tag{3}$$

are the rate of incremental spatial heat sources generated by visco-plastic deformation, where ${}_{\tau}^{\tau}\sigma_Y({}_{\tau}^{\tau}\varepsilon_i^{(VP)},\ {}_{\tau}^{\tau}\dot{\varepsilon}_i^{(VP)},\ {}^{\tau}T)$ is accumulated yield stress, depending on the history of visco-plastic strain $\varepsilon_i^{(VP)}$ and strain rate $\dot{\varepsilon}_i^{(VP)}$ and temperature T, $\xi=0.05\div0.1$ is the coefficient energy absorption.

2.2. Initial and boundary conditions for temperature

The equation of heat transfer (1) is completed with the initial condition and the four boundary conditions.

Initial condition

Initial condition describes the temperature field at time which is the initial moment:

$$T(\mathbf{z}, t = t_0) = T_0(\mathbf{z}), \quad \mathbf{z}\in V. \tag{4a}$$

In typical processing conditions thread rolling, the temperature of the object at time $t = t_0$ is constant then:

$$T(\mathbf{z}, t = t_0) = T_0 = \text{const}, \tag{4b}$$

where T_0 is ambient temperature.

Boundary conditions

- *conditions of I gender* - the temperature may be prescribed at specific points in the surfaces, denoted by Σ_T, and/or at the specific points in the volume of the body, denoted by V_T:

$$T(\mathbf{z}, t) = T_o(\mathbf{z}, t), \text{ or } \Delta T(\mathbf{z}, \Delta t) = \Delta T_o(\mathbf{z}, \Delta t), \ \mathbf{z} \in \Sigma_T \tag{5}$$

- *conditions of II gender* – in the contact area tool and object Σ_k, heat flows:

$$-\lambda_o(T)\, \mathbf{n} \circ \text{grad}\,[\Delta T_o(\mathbf{z}, \Delta t)] = b_o \Delta q_{F\mu}, \ \mathbf{z} \in \Sigma_k, \tag{6a}$$

$$-\lambda_b(T)\, \mathbf{n} \circ \text{grad}\,[\Delta T_b(\mathbf{z}, \Delta t)] = b_b \Delta q_{F\mu}, \ \mathbf{z} \in \Sigma_k, \tag{6b}$$

- *conditions of III gender* (continuity of the heat flows):

$$-\lambda_o(T)\mathbf{n} \circ \text{grad}[\Delta T_o(\mathbf{z}, \Delta t)] = \frac{\Delta T_o(\mathbf{z}, \Delta t) - \Delta T_b(\mathbf{z}, \Delta t)}{R_s(\mathbf{z}, \Delta t)} =$$

$$= -\lambda_b(T)\mathbf{n} \circ \text{grad}[\Delta T_b(\mathbf{z}, \Delta t)], \ \mathbf{z} \in \Sigma_k, \tag{7}$$

where R_s is the heat resistance in the surface contact (for ideal contact R_s=0), b_o and b_b is the heat division coefficients for roller (b) and object (o), $\mathbf{n} \circ \text{grad}[\Delta T(\cdot)]$ is the scalar product, $\Delta q_{S\mu}[\cdot]$ is the rate of incremental surface heat sources generated by fretting per unit surface,

- *conditions of IV gender* – they are in areas Σ_C i Σ_R, in which exchange heat is on road convection and radiation, then the boundary conditions is defined by:

$$\Delta q_C = \alpha_C(T) \cdot \Delta T = -\lambda(T)\mathbf{n} \circ \text{grad}[\Delta T(\mathbf{z}, \Delta t)], \mathbf{z} \in \Sigma_C, \tag{8a}$$

$$\Delta q_R = \alpha_R(T) \cdot \Delta T = -\lambda(T)\mathbf{n} \circ \text{grad}[\Delta T(\mathbf{z}, \Delta t)], \ \mathbf{z} \in \Sigma_R, \tag{8b}$$

where Δq_C and Δq_R are incremental intensity flow heat exchange with the environment by convection and radiation, $\alpha_C(T)$ and $\alpha_R(T)$ are temperature - dependent convection coefficient and radiation coefficient (Staniszewski 1982).

Equation (1) with initial condition (4) and boundary conditions (5)÷(8) are a full mathematical description of heat transfer during the thread rolling, at the typical incremental time step. The analytical solution is impossible, therefore variational formulation was introduced.

2.3. Variational formulation equations of heat transfer

For the variational formulation of the equations of heat transfer in the thread rolling, at the typical time step, introduced an incremental functional $\Delta\mathbf{F}(\Delta\dot{T}, \Delta T', \Delta T, ...)$, in which is one independent field – it is temperature field, and its derivatives: $\Delta\dot{T} = d(\Delta T)/dt$, $\Delta T' = d(\Delta T)/dy_3$. This functional has differential equation (1) in the global Cartesians coordinate $\{z\}$ and boundary conditions (5)÷(8). It is:

$$\begin{aligned}\Delta\mathbf{F}[\Delta\dot{T}, \Delta T', \Delta T] &= \frac{1}{2}\int_V \left(\sum_{i=1}^{3}\lambda_i(T)\cdot L_{zi}^2(\Delta T)\right)\cdot dV + \int_V \Delta\dot{T}\cdot c(T)\cdot\rho(T)\cdot\Delta T\cdot dV \\ &- \int_V \Delta q_{VD}[\cdot]\cdot\Delta T\cdot dV - \int_{\Sigma_k} b\cdot\Delta q_{S\mu}[\cdot]\cdot\Delta T\cdot d\Sigma_k + \int_{\Sigma_k}\frac{\Delta T_o - \Delta T_b}{2R_s}\cdot\Delta T\cdot d\Sigma_k \\ &\frac{1}{2}\int_{\Sigma_C}\alpha_C(T)\cdot\Delta T^2\cdot d\Sigma_C + \frac{1}{2}\int_{\Sigma_R}\alpha_R(T)\cdot\Delta T^2\cdot d\Sigma_R - \int_{\Sigma_T}\Delta T_b\cdot\Delta T\cdot d\Sigma_T,\end{aligned} \tag{9}$$

where the integrations are performed over the volume V and surface Σ of the body, respectively, $L_{zi}^2(\Delta T) = \partial^2(\Delta T)/\partial z_i^2$ is the differential operator.

Using the conditions of stationarity of functional (9):

$$\delta[\Delta\mathbf{F}(\Delta\dot{T}, \Delta T', \Delta T)] = \frac{\partial[\Delta\mathbf{F}(\cdot)]}{\partial(\Delta T)}\delta(\Delta T) = 0, \tag{10}$$

we obtain (because ΔT is the only variable) in the global system $\{z\}$:

$$\begin{aligned}\delta[\Delta\dot{T}, \Delta T', \Delta T] &= \int_V\left[\sum_{i=1}^{3}\lambda_i(T)\cdot\frac{\partial(\Delta T)}{\partial z_i}\cdot\delta\left(\frac{\partial(\Delta T)}{\partial z_i}\right)\right]\cdot dV \\ &+ \int_V\frac{\partial(\Delta T)}{\partial t}\cdot C(T)\cdot\rho(T)\cdot\delta(\Delta T)\cdot dV \\ &+ \int_V\delta\left(\frac{\partial(\Delta T)}{\partial t}\right)\cdot C(T)\cdot\rho(T)\cdot\Delta T\cdot dV \\ &- \int_V\Delta q_{VO}[\cdot]\cdot\delta(\Delta T)\cdot dV - \int_{\Sigma_k} b\cdot\Delta q_{F\mu}[\cdot]\cdot\delta(\Delta T)\cdot d\Sigma_k \\ &+ \int_{\Sigma_k}\frac{\Delta T_o - \Delta T_b}{2R_s}\cdot\delta(\Delta T)\cdot d\Sigma_k + \int_{\Sigma_C}\alpha_C(T)\cdot\delta(\Delta T)\cdot d\Sigma_C \\ &+ \int_{\Sigma_R}\alpha_R(T)\cdot\delta(\Delta T)\cdot d\Sigma_R - \int_{\Sigma_T}\Delta T\cdot\delta(\Delta T)\cdot d\Sigma_T = 0.\end{aligned} \tag{11}$$

Equation (11) is variational formulation of heat transfer at the typical step time in updated Lagrange's description in thread rolling process.

2.4. Implementation of the finite element method

Assume that the complete body under consideration has been idealised as an assemblage of finite elements, we have, at step time $t \rightarrow t+\Delta t$ for element e and m*:*

$$\begin{aligned}
&\Delta T^{(e)}(\cdot) = [\mathbf{H}^{(e)}(\cdot)] \cdot \{\Delta \boldsymbol{\Theta}^{(e)}\},\ \Delta T'^{(e)}(\cdot) = [\mathbf{B}^{(e)}(\cdot)] \cdot \{\Delta \boldsymbol{\Theta}^{(e)}\},\\
&\Delta T'^{(e)}(\cdot) = [\mathbf{B}_3{}^{(e)}(\cdot)] \cdot \{\Delta \boldsymbol{\Theta}^{(e)}\}, \Delta T^{(m)}(\cdot) = [\mathbf{H}^{S(m)}(\cdot)] \cdot \{\Delta \boldsymbol{\Theta}^{(m)}\},\\
&\Delta \dot{T}^{(e)}(\cdot) = [\mathbf{B}^{(e)}(\cdot)] \cdot \{\Delta \dot{\boldsymbol{\Theta}}^{(e)}\},
\end{aligned} \tag{12}$$

where: $\Delta T^{(e)}$ is the temperature increment of finite element *e*, $\{\Delta \boldsymbol{\Theta}^{(e)}\}$ and $\{\Delta \dot{\boldsymbol{\Theta}}^{(e)}\}$ are vectors of increments in the nodal point temperature and of increments in the nodal point temperature rate, at all *n* nodal points, respectively (Kukielka L. 1998). Using the relation in (12) and substituting into the variational equation (11), we obtain the discretized equation of heat transfer equilibrium in the global coordinate {z} (the non stabilized heat transfer):

$$[\mathbf{C}]\{\Delta \dot{\boldsymbol{\Theta}}\} + ([\mathbf{K}^{K}] + [\mathbf{K}^{C}] + [\mathbf{K}^{R}] + [\mathbf{K}^{IV}])\{\Delta \boldsymbol{\Theta}\} = \{\Delta \mathbf{Q}\} + \{\Delta \mathbf{Q}^{I}\} \tag{13}$$

where $[\mathbf{C}]$ and $[\mathbf{K}^{K}]$, $[\mathbf{K}^{C}]$, $[\mathbf{K}^{R}]$, $[\mathbf{K}^{IV}]$ are the heat capacities, conductivity, convection and radiation matrices and total nodal point conditions of IV gender, $\{\Delta \mathbf{Q}\}$ is the nodal point increment heat flow input vector, $\{\Delta \mathbf{Q}^{I}\}$ is the vector of nodal point of the boundary conditions of I gender.

The solution of equation (13) with initial (4a-4b) and boundary (5, 6a, 6b, 7, 8a and 8b) conditions and experimental verification of the results shown in article (Kukielka K. 2017).

3. Conclusions

Till now, the thread rolling process, was described by regression equations. This is the so-called phenomenological approach, using the principle of „black box". These equations although received correctly are limited to use in the same as treatment conditions when was examinated. Also, it is impossible to get established, particularly high requirements shaped thread. Also, it is not possible to obtain assumed, in particular

high requirements of the shaped thread. These imperfections can be eliminated by increasing the accuracy of the modeling and analysis of the machining process. The complexity of the occurring physical phenomena and geometrical, physical and thermal non-linearity of the process, the partial knowledge of the boundary conditions require the use of adequate incremental description. That descriptions is updated Lagrange description, in which all searched quainties on the incremental step are related to the configuration of the well-known, established on the previous step. For this description a dynamic model of rolling process was developed and specifies the conditions for uniqueness, assuming that the work-piece is made of thermo-elastic/thermo-visco-plastic-phasis material with nonlinear mixed hardening. Excessive complexity of the model means that it is impossible its analytical solution. It is possible an approximate solution on the numerical way.

In researches is made simplification like the thread rolling process is carried out on cold and doesn't include influence on variation of constant from temperature. As a result, there are significant differences in the predicted and obtained thread and are too large deviations of dimensions and shape of the thread.

Increasing the shaping accuracy of the thread technological quality makes it necessary to increase accuracy of modelling and analysis of physical phenomena occurring in the thread rolling process. Described in this paper thermo-mechanical contact problem is a basic problem. The complex nature of phenomena occurring during the contact and the difficulties in their study force us to look for a solutions in the theoretical way. Occurring geometrical, physical and thermal nonlinearity, also only a partial knowledge of boundary conditions, which are moving in the process make it necessary to apply incremental description.

The external thread rolling with round profile is a complex in process technological terms. The thread rolling process is a geometrical, physical and thermal non-linear initial and boundary problem. Measurement of a process parameters decide on the technological quality, such as: a displacement zone, a temperature, stress, structural change etc. during the thread rolling process with nowadays technique of a measurement is impossible. About their course, we could conclude on the property of the product after rolling.

It has been shown that the thread rolling process can be described by incremental mathematical models in an updated Lagrangian description: constitutive equations thermo-dynamic yield stress, strain and stress, the contact model, the equations of motion and deformation also equation of heat transfer of the object and the initial and boundary conditions.

Developed incremental mathematical models of motion and deformation of the object allow for complex analysis of the phenomena occurring during the thread rolling process by using Finite Element Method. Applied incremental models allow to solve many problems without knowing the boundary conditions in the contact zone. So far, in order to solve the equations of motion of the object and heat transfer with the corresponding boundary conditions for the displacements, these conditions had to be assumed or experimentally determined.

The paper presents a possibility of applying the variational and finite element methods for the analysis of heat transfer in thread rolling operation.

The developed methodology step by step solutions allows for:

- effective scheme solutions, various constitutive models,
- the ability to analyze a variety of physical problems: displacement, strain, stress and temperature,
- the opportunity to load a variety of boundary conditions and kinematic and thermal constraints,
- the opportunity to load a variety of initial conditions (and history),
- efficient algorithm for analysis of the contact issue.

An own application in ANSYS program for the thread rolling process were elaborated. Numerical analysis let for forecast behavior of rolled thread during whole multistage technological process. For the most important possibilities of the numerical analysis in application for the thread rolling is determination of:

- dimensions of the pipe before rolling (mainly nominal and outline diameter),
- local strain, stress and temperature states in the thread,
- geometry and thread outline during thread rolling and after elastic relieving,

- maximum strain – where crack of the thread is possible,
- expected rolling force,
- influence of the friction coefficient on the process flow and quality of the thread,
- number and geometry of the rolls, in that active rolls surface in the introducing, shaping, calibrating and outing zone,
- state of loads, stresses and strains of the tools,
- areas of contact, slip and stick.

The developed models and methodology for the analysis of physical phenomena in the thread rolling process increase the accuracy of the modeling and prediction of the thread properties and the quality of the thread on the design stage, without the need for complex, costly and harmful for the environment experimental research.

One of the major environmental advantages of the thread rolling process, unlike to the machining, is using rolling technology as volume plastic working, it is possible to make threads with usage of the full material (Kukiełka K. 2016, Łyczko 2010). The diameter of the workpieces (bar) for the rolled thread is smaller compared to the diameter of the machined thread, which results measurable savings of the material. This eliminates the chip waste management, which also reduces production costs.

Use of radial thread rolling method provides significant savings in the form of shortening the threading time due to the traditional of thread forming, which reduce production cost and saving energy (Kukiełka K. 2016). However, if those threads are made by turning process the threading time is extend minimum two time higher then rolling (Kukiełka K. 2009, Kukiełka K. 2016, Łyczko 2010).

References

Bathe, K.J. (1982). *Finite element procedures in engineering analysis*. Prentice-Hall, Englewood Cliffs, New Jersey, USA.

Bohdal, Ł., Walczak, P. (2013). Eco–modeling of metal sheet cutting with disc shears. *Rocznik Ochrona Środowiska (Annual Set of Environment Protection)*, *15*, 863-872.

Bohdal, L., Kukielka, L. (2014). Application of variational and FEM methods to the modelling and numerical analysis of guillotining process for geometrical and physical nonlinearity. *Mechanika*, *20(2)*, 197-204.

Bohdal, L., Kukielka, L., Kukielka, K., Kulakowska, A., Malag, L., Patyk, R. (2014). Three Dimensional Finite Element Simulation of Sheet Metal Blanking Process. *Mechanics and Materials "Novel Trends in Production Devices and Systems"*, *474*, 430-435.

Chodor, J., Kukielka, L. (2014). Using Nonlinear Contact Mechanics in Process of Tool Edge Movement on Deformable Body to Analysis of Cutting and Sliding Burnishing Processes. *Mechanics and Materials "Novel Trends in Production Devices and Systems"*, *474*, 339-344.

Domblesky, J.P., Feng F. (2002). Two-dimensional and three-dimensional finite element models of external thread rolling. *Professional Engineering Publishing*, *216(4)*, 507-517.

Forysiewicz, M., Kukielka, L., Gotowala, K. (2016). Finite element simulation of physical phenomena in real conditions of a single grain cutting process. *Novel Trends in Production Devices and Systems "Materials Science Forum"*, *862*, 288-297.

Kaldunski, P., Kukielka, L., (2014). Numerical Analysis and Simulation of Drawpiece Forming Process by Finite Element Method, *Mechanics and Materials "Novel Trends in Production Devices and Systems"*, *474*, 153-158.

Kowalik, M., Rucki, M., Paszta, P., Gołębski, R. (2016). *Plastic deformations of measured object surface in contact with undeformable surface of measuring tool*. Measurement Science Review. *16(5)*, 254-259.

Kukiełka, K. (2009). *Modelling and numerical analysis of the states of deformations and stresses in the surface layer of the trapezoidal and round threads rolled on cold*. PhD Thesis, Koszalin University of Technology. (in Polish).

Kukiełka, K., Kukiełka, L. (2013). *External thread rolling head*. The polish patent No PL402652–A1, PL220175–B1, 4.02.2013. (in Polish).

Kukiełka, K. (2014). Effective numerical model to analyze the trapezoidal thread rolling process with finite element method. *Mechanik*, *11*, 156-167. (in Polish).

Kukielka, K., Kukielka, L., Bohdal, L., Kulakowska, A., Malag, L., Patyk, R. (2014). 3D Numerical Analysis the State of Elastic/Visco–Plastic Strain in the External Round Thread Rolled on Cold. *Applied Mechanics and Materials „Novel Trends in Production Devices and Systems", 474*, 436-441.

Kukielka, K. (2016). Ecological Aspects of the Implementation of New Technologies Processing for Machinery Parts. *Rocznik Ochrona Środowiska (Annual Set of Environment Protection)*, *18*, 137-157.

Kukielka K. (2017). Numerical simulations of the thread rolling process as ecological and economical research tool in the implementation of modern technologies. *Rocznik Ochrona Środowiska (Annual Set of Environment Protection)*, *19*.

Kukiełka, L. (1994). *Theoretical and experimental foundations of surface roller burnishing with the electrocontact heating*. Book WM nr 47. WSI Koszalin. (in Polish)

Kukielka, L. (1999). Application of the variational and finite element methods to dynamic incremental nonlinear analysis in the burnishing rolling operation. *ESM'99 - Modelling And Simulation A Tool For The Next Millennium*, II, 221-225.

Kukielka, L., Krzyzynski T. (2000). New thermo-elastic thermo-visco-plastic material model and its application. *Zeitschrift Fur Angewandte Mathematik Und Mechanik*, Vol. 80, supplement: 3, S595-S596 (2000).

Kukielka, L. (2001). Mathematical modelling and numerical simulation of nonlinear deformation of the asperity in the burnishing cold rolling operation. *Computational Methods in Contact Mechanics V, Book Series: Computational and Experimental Methods*, *5*, 317-326.

Kukiełka, L. (2002). *Bases of engineering research*. PWN, Warsaw. (in Polish).

Kukielka, L. (2002). Non-linear analysis of heat transfer in burnishing rolling operation. *Advanced computational methods in heat transfer VII. Computational studies*, WITPRESS, *4*, 405-414.

Kukielka, L., Kustra, J. (2003). Numerical analysis of thermal phenomena and deformations in processing zone in the centerless continuous grinding process. *Surface treatment VI: computer methods and experimental measurements for surface treatment effects. Computational and experimental methods*, Eds Brebbia, C. A., DeHosson, J.T.M; Nishida, S. I., WITPRESS, *7*, 109-118.

Kukielka, L., Kustra, J., Kukielka, K. (2005). Numerical analysis of states of strain and stress of material during machining with a single abrasive grain. *Computer Methods and Experimental Measurements for Surface Effects and Contact Mechanics VII*, Southampton-Boston, WIT*PRESS*, 57-66.

Kukielka, L., Kukielka, K. (2006). Numerical analysis of the process of trapezoidal thread rolling. *High Performance Structures and Materials III*, Southampton-Boston, WIT*PRESS*, 663-672.

Kukielka, L., Kukielka, K. (2007). Numerical analysis of the physical phenomena in the working zone in the rolling process of the round thread. *Computer Methods and Experimental Measurements for Surface Effects and Contact Mechanics VIII*, Southampton-Boston, WIT*PRESS,* 125-124.

Kukiełka, L. (2010). New damping of models of metallic materials and its application in non–linear dynamical cold processes of metal forming. *The 13th International Conference Metal Forming 2010*, *Steel Research International*, Toyohashi, *81*, 1482-1485.

Kukielka, L., Geleta, K., Kukielka, K. (2012). Modelling and Analysis of Nonlinear Physical Phenomena in the Burnishing Rolling Operation with Electrical Current. *Steel Research International, Special Edition: 14th International Conference Metal Forming*, Kraków, 1379-1382.

Kukielka, L., Geleta, K., Kukielka, K. (2012). Modelling of Initial and Boundary Problems with Geometrical and Physical Nonlinearity and its Application in Burnishing Processes. *Steel Research International, Special Edition: 14th International Conference Metal Forming*, Krakow, 1375-1378.

Kukiełka, L., Kukiełka, K. (2012). The modern method of modeling and analysis precision machining processes auto parts. *Environmental aspects of the use of new technologies in transport, Book of Mechanical Engineering*, No 235 of Mechanical Faculty, Koszalin University of Technology. Koszalin, 109-128 (in Polish).

Kukiełka, L., Bohdal, Ł., Chodór, J., Forysiewicz, M., Geleta, K., Kałduński P., Kukiełka, K., Patyk, R., Szyc, M. (2012). Numerical analysis of selected processes precision machining of automotive parts. *Environmental aspects of the use of new technologies in transport, Book of Mechanical Engineering No 235 of Mechanical Faculty*, Koszalin University of Technology, Koszalin. 129-194.

Kukielka, L., Kukielka, K., Kulakowska, A., Patyk, R., Malag, L., Bohdal, L. (2014). Incremental Modelling and Numerical Solution of the Contact Problem between Movable Elastic and Elastic/Visco–Plastic Bodies and Application in the Technological Processes. *Applied Mechanics and Materials "Novel Trends in Production Devices and Systems", 474*, 159-165.

Kukiełka, L., Kukiełka, K. (2015). Modelling and analysis of the technological processes using finite element method. *Mechanik, 88*, 317-340.

Kukielka, L., Szczesniak, M., Patyk, R., Kulakowska, A., Kukielka, K., Patyk S., Gotowala, K., Kozak, D. (2016). Analysis of the states of deformation and stress in the surface layer of the product after the burnishing cold rolling operation. *Novel Trends in Production Devices and Systems "Materials Science Forum"*.

Kulakowska, A., Patyk, R., Kukielka, L. (2009). Numerical analysis and experimental researches of burnishing rolling process of workpieces with real surface. *WMSCI 2009 – The 13th World Multi–Conference on Systemics, Cybernetics and Informatics, Jointly with the 15th International Conference on Information Systems Analysis and Synthesis, ISAS, 2*, 63-68.

Kulakowska, A., Kukielka, L., Kukielka, K., Malag, L., Patyk, R., Bohdal, L. (2014). Possibility of steering of product surface layers properties in burnishing rolling process. *Applied Mechanics and Materials "Novel Trends in Production Devices and Systems", 474*, 442-447.

Kusnerova, M., Valicek, J., Harnicarova, M., Hryniewicz, T., Rokosz, K., Palkova, Z., Vaclavik, V., Repka, M., Bendova, M. (2013). A Proposal for Simplifying the Method of Evaluation of Uncertainties in Measurement Results. *Measurement Science Review*, *13(1)*, 1-6.

Łyczko, K. (2010). *External thread rolling technology*. WNT, Warszawa. (in polish).

Malag, L., Kukielka, L., Kukielka, K., Kulakowska, A., Patyk, R., Bohdal, L. (2014). Problems Determining of the Mechanical Properties of Metallic Materials from the Tensile Test in the Aspect of Numerical Calculations of the Technological Processes. *Applied Mechanics and Materials "Novel Trends in Production Devices and Systems", 474*, 454-459.

Myslinski, P., Precht, W., Kukielka, L, et al. (2004). A possibility of application of MTDIL to the residual stresses analysis – The hard coating-substrate system. *Journal Of Thermal Analysis And Calorimetry*, *77(1)*, 253-258 (2004).

Nadolny, K., Plichta, J., Sutowski, P. (2014). Regeneration of grinding wheel active surface using high-pressure hydro-jet. Journal Of Central South University, *21(8)*, 3107-3118.

Olszak, W. (2008). *Machining*. WNT, Warszawa. (in polish)

Patyk, R., Kukielka, L. (2008). Optimization of geometrical parameters of regular triangular asperities of surface put to smooth burnishing. *The 12th International Conference Metal Forming 2008, Steel Research International,* Kraków, *2*, 642-647.

Patyk, R. (2010). Theoretical and experimental basis of regular asperities about triangular outline embossing technology. *The 13th International Conference Metal Forming 2010, Steel Research International*, 81, Toyohashi, 190-193.

Patyk, R., Kukielka, L., Kukielka, K., Kulakowska, A., Malag, L., Bohdal, L. (2014). Numerical Study of the Influence of Surface Regular Asperities Prepared in Previous Treatment by Embossing Process on the Object Surface Layer State after Burnishing. *Applied Mechanics and Materials "Novel Trends in Production Devices and Systems"*, *474*, 448-453.

Perec, A. (2016). *Abrasive suspension water jet cutting optimization using orthogonal array design*. International Conference on Manufacturing Engineering and Materials, ICMEM 2016, 6-10 June 2016, Nový Smokovec. Procedia Engineering, *149*, 366- 373.

Perec, A., Pude, F., Stirnimann, J., Wegener, K. (2015). *Feasibility study on the use of fractal analysis for evaluating the surface quality generated by waterjet*. Tehnički vjesnik, *22(4)*, 879-883.

Rokosz, K., Hryniewicz, T. (2016). *XPS Analysis of nanolayers obtained on AISI 316L SS after Magnetoelectropolishing*. World Scientific News, *37*, 232-248.

Skoczylas, A., Zaleski K. (2015). Effect of Plasma Cutting Parameters upon Shapes of Bearing Curve of C45 Steel Surface. *Advances in Science and Technology Research Journal*, *9(27)*, 78-82.

Sutowski, P., Nadolny, K. (2016). The identification of abrasive grains in the decohesion process by acoustic emission signal patterns. *International Journal Of Advanced Manufacturing Technology*, *87(1-4)*, 437-450.

Staniszewski, B. (1980). *Heat transfer*. PWN, Warsaw.

Valicek, J., Drzik, M., Hryniewicz, T., Harnicarova M., Rokosz K, Kusnerova M., Barcova K., Brazina D. (2012). Non-Contact Method for Surface Roughness Measurement After. Machining. *Measurement Science Review*, *12(5)*, 184-188.

Zaleski, K., Bławucki, S. (2015). Evaluation of the Effectiveness of the Shot Peening Process for Thin-Walled Parts Based on the Diameter of Impression Produced by the Impact of Shot Media. *Advances in Science and Technology Research Journal, 9(26)*, 77-82.

Ekologiczne i ekonomiczne aspekty nowoczesnego modelowania procesu walcowania gwintów

Streszczenie

W pracy przedstawiono nowoczesny sposób opracowania numerycznego modelu procesu walcowania gwintów przy wykorzystaniu rachunku wariacyjnego i Metody Elementów Skończonych oraz analizowano wpływ najważniejszych parametrów obróbki. Proces walcowania gwintów rozpatrywano jako geometrycznie, fizycznie oraz termicznie nieliniowy problem, z nieznanymi warunkami brzegowymi w strefie kontaktu narzędzia i przedmiotem.

Opisu nieliniowości materiału dokonano modelem przyrostowym uwzględniając wpływ historii odkształceń, prędkości odkształceń i temperatury. Przedmiot (pręt lub rurę) traktuje się, jako ciało, w którym mogą wystąpić odkształcenia termo-sprężyste (w zakresie odkształceń odwracalnych) oraz termiczne, lepkie, plastyczne i fazowe (w zakresie odkształceń nieodwracalnych), z nieliniowym umocnieniem. Ciało to oznaczono skrótowo TE/TVPF (termo-sprężyste/termo-lepko-plastyczno-fazowe). Do budowy modelu materiałowego zastosowano nieliniowy warunek termo-plastyczności Hubera-Mises'a-

Hencky'ego, stowarzyszone prawo płynięcia oraz wzmocnienie mieszane (izotropowo-kinematyczne). Uwzględniono również stan materiału po obróbkach poprzedzających przez wprowadzenie początkowych stanów: przemieszczeń, naprężeń, odkształceń, temperatury i ich prędkości. Model matematyczny uzupełniono przyrostowymi równaniami ruchu ciepła oraz warunkami jednoznaczności. Następnie, wprowadzono funkcjonał przyrostowy całkowitej entalpii układu. Z warunku stacjonarności tego funkcjonału wyprowadzono wariacyjne, nieliniowe równanie ruchu ciepła w obiekcie dla typowego kroku przyrostowego.

Abstract

In this study, a modern way to develop a numerical model of the thread rolling process was shown by using variational formulation and the finite element method also the effect of the main process parameters were analyzed. The thread rolling process was considered a geometrical, physical and thermal nonlinear problem with unknown boundary conditions in the contact area of the system, such as the tool and workpiece.

The nonlinearity of the material was described using the incremental model, making allowance for the effects of strain, strain rate and temperature history. The work pieces (pipe or bar) have been considered treating an object as a body which can undergo thermo-elastic strains (in the range of reversible strain), thermo, viscous, plastic and phasis (in the range of permanent strains). This body (thermo-elastic/thermo-visco-plastic-phasis) has been designated as TE/TVPF. The material model was prepared making use of Huber-Mises-Hencky's nonlinear condition of thermo-plasticity, the associated law of flow and the mixed (isotropic-kinematical) strain hardening. The state of material after pre-processing was also taken into consideration introducing the initial conditions of displacements, strains, stresses, temperature and their rates. Then, the incremental functional as the total enthalpy of the system, were derived. From stationary condition of this functional, nonlinear variational equation of motion and heat transfer for object on the typical incremental step time was derived.

Słowa kluczowe:
walcowanie gwintów, eko-modelowanie, ekologiczne procesy technologiczne, sformułowanie wariacyjne, metoda elementów skończonych

Keywords:
thread rolling, eco-modelling, ecological technological process,
variational formulation, Finite Element Method

MIDDLE POMERANIAN SCIENTIFIC SOCIETY OF THE ENVIRONMENT PROTECTION
ŚRODKOWO-POMORSKIE TOWARZYSTWO NAUKOWE OCHRONY ŚRODOWISKA

Annual Set The Environment Protection
Rocznik Ochrona Środowiska

Volume/Tom 19. Year/Rok 2017 ISSN 1506-218X 143-160

Application of Eco-innovative Technologies of Nutrients Removal in Wastewater – Case Study BARITECH Project

Magda Kasprzyk, Kristian Pierzgalski, Ewa Wojciechowska, Hanna Obarska-Pempkowiak, Magdalena Gajewska
Gdansk University of Technology

1. Introduction

Eco-innovative technologies in wastewater treatment should provide not only stringent standards for the quality of treated wastewater but also ensure maximum recovery of energy and raw materials from wastewater. One of the ways to improve the removal efficiency of nitrogen and phosphorus compounds in existing conventional wastewater treatment plants is pretreatment of reject water generated during the mechanical dewatering of the digested sewage sludge.

In conventional wastewater treatment plants, where sludge treatment process is stabilized by fermentation, the most common way of handling return flow of reject water is recirculation to the mechanical part, resulting in small hydraulic load (not exceeding 1.5%) with high amount of nutrients in between 10 and 20% of raw wastewater load (Fux et al., 2003, 2006; Gajewska and Obarska-Pempkowiak, 2011a). Reject water (RW) generated during mechanical dewatering of digested sewage sludge is not only characterized by uneven formation in time but also irregular composition. Characteristic for RW are high concentrations of: organic matter in the form difficult to biodegradation (COD: 800-2850 mg O_2/dm^3), total nitrogen, primarily in the form of ammonium nitrogen ($N\text{-}NH_4^+$: 450-1710 mg/dm^3) and total phosphorus (up to 400 mg/dm^3) (Fux et al., 2003, Wett and Alex, 2003, Fux et al. 2006,

Gajewska and Obarska-Pempkowiak, 2008). Phosphorus compounds are usually removed in process of precipitation with aluminum or iron salts and are constantly lost by becoming difficult manageable chemical sludge which in the end causes loosing the possibility of recovering phosphorus. The removal of nitrogen compounds is causing difficulties, due to their high concentration and adverse composition. For several years, to remove nitrogen compounds from RW the unconventional technologies with shorten removal path have been used. These processes allow to remove nitrogen compounds with limited oxygen access (energy) and easily accessible source of carbon. Unfortunately, according to literature reports, these processes in full scale are characterized by high sensitivity and instability, which in consequence do not provide proper quality of treated effluent. On the basis of studies and available literature data, it has been shown that the quality of effluent discharged after the SBR reactor in the nitritation/anammox process is variable in time. Particularly noticeable are changes in concentration of total nitrogen from 120 up to 500 mg N/dm^3. At the same time the process of nitritation/anammox does not provide the removal of phosphorus compounds.

According to the concept of circular economy adopted on December 2nd 2015, treatment technology should support the reuse of water, including the secondary use of water produced from treated wastewater. The approach applied in this circular economy assumes the closure of the product life cycle in the following sequence: production – usage – waste utilization. The essence of this approach is the use of waste generated during applied processes while at the same time limiting raw material consumption, reducing the amount of waste deposited and increasing the waste stream used for recovery and recycling.

The aim of this research is to select the technological parameters of processes to ensure effective removal of nutrient elements (N, P) from RW treated in a SBR reactor in the nitritation/anammox process. In project „Integrated technology for improved energy balance and reduced greenhouse gas emissions at municipal wastewater treatment plants" (BARITECH 2013-2017) among others the following goals have been established: stable treatment and quality of RW which does not interfere with main stream treatment of recirculation and treatment processes with minimal use of energy and raw materials consumption and possibilities to phosphorus recovery, in natural ecological process.

2. Methodology of research

The study was divided into two stages. The first stage was carried out to optimize nitrogen removal and parallelly in the second stage the optimization of phosphates removal was carried out.

The idea of these innovative assumptions is in accordance with the principles of circular economy. There are many benefits of applying previously stated technical solutions, e.g resulting in reduction of generated secondary and chemical sludge during nutrient removal from the reject water. In case of a phosphorus compounds removal method, the product might be easily recirculated and used as natural fertilizer. These proposed methods are characterized by having low influence for environment (Gajewska M. and Obarska-Pempkowiak, H., 2011b, Nastawny et al., 2015, Pempkowiak J. and Obarska-Pempkowiak, H., 2002).

2.1. Methodology of research, experimental design – nitrogen removal

Material and experimental design

The installation consists of four single vertical subsurface flow (VSSF) beds located in stainless steel containers (LxWxH: 40 cm x 40 cm x 80 cm) working parallel marked as BED control "0", "I", "II" and "III". Each bed consists of a filtration layer (45 cm), a thin geotextile and a 10 cm drainage layer made of 16-32 mm gravel. The substrate for each filter is: I – 0.5-1.2 mm sand; "0", II and III – 2-8 mm gravel. Control bed remains unplanted, other three beds are planted with common reed. Each bed is equipped with a manual ball valve and a flexible ending pipe which are necessary in case of need to prolong the contact time for removal both forms of nitrogen (NH_4^+-N, NO_3^--N). The ending pipes are mounted to sampling tanks, which have a sealed lid to ensure minimum contact with atmospheric air. The effluent is discharged to the sewage system.

A main distribution stainless steel tank (LxWxH: 20 cm x 20 cm x 60 cm) is divided into five sections: 5, 10, 15, 20 and 24 dm^3. It is equipped with stainless steel pipes, solenoid valves and sprinkler heads for automatic feeding and even distribution of influent on each filter. All valves are controlled by electronic timers. A HDPE tank (IBC – Intermediate Bulk Container) of volume 1000 dm^3 for preparation of synthetic wastewater is equipped with a pump to supply the distribution tank.

Common reed plants, around 1.8 m height with 50 cm root length, were excavated from a natural wetland and planted in the filter beds. Prior main investigation, the filter beds were washed through for one week to avoid future clogging. Start of laboratory research with synthetic sewage was on the 21st August 2016.

Due to limited light conditions (indoor), two CFL 85W light bulbs were placed above the beds to ensure photosynthesis and better growth.

Sampling and chemical analysis

During the investigation, each day a new batch of synthetic wastewater was prepared with assumed concentrations of NH_4^+-N, NO_3^--N and 6 mg/dm^3 of carbon source (glucose). The compounds used in this research are NH_4Cl, KNO_3 and simple carbohydrates $C_6H_{12}O_6$.

The system was set for 4 feeds of 24 dm^3/d resulting in 96 dm^3 per each bed per day with assumed hydraulic load of 600 mm/m^{2}d. The filtration through the system lasts 1.5-2 hours depending on the bed. After the daily cycle samples were taken from each tank. Afterwards each tank was emptied to provide next day sampling. The temperature in the laboratory fluctuated from 19 to 21˚C.

The concentration of NH_4^+-N, NO_3^--N and NO_2^--N was measured with a spectrophotometer by using cuvette tests HACH Lange LCK 303 for ammonium (2.0-47.0 mg/dm^3 NH_4^+-N), LCK 340 for nitrate (5-35 mg/dm^3 NO_3^--N) and LCK 341 for nitrite (0.015-0.6 mg/dm^3 NO_2^--N).

2.2. Methodology of research, experimental design – phosphorus removal

Material and experimental design

Phoslock® is an adsorbent based on lanthanum-modified bentonite clay, characterized by high capacity of phosphate binding. Removal of phosphorus compounds is based on their adsorption on the surface of the material, where they form an insoluble complex of adsorbed ions of orthophosphorus ion: PO_4^{3-} sediment (Phoslock General Brochure).

Lanthanum is a chemical element that binds phosphate ions in a 1:1 ratio. The product of this reaction is rhabdophane. Rhabdophane, a stable mineral of low solubility, is the only product of this process, and the lack of by-products is a very important benefit during the wastewater treatment (Haghseresht et al., 2009, Zamparas et al., 2015). The relative-

ly small size of adsorbent particles, with high specific surface area and pore volume, still allow to use maximum of adsorption area. According to Haghseresht et al. (2009), the adsorption capacity of phosphorus cannot be higher than 10.6 mg per 1 gram of adsorbent.

Phoslock® is able to operate in pH values from 4 to 11 (Ross & Haghseresht, 2008). The optimal range of pH is 5.0-9.0, but the maximum efficiency for phosphorus removal using Phoslock® is achieved at pH of 5.0-7.0, (PWS Report Number: IR 019/12, 2012).

To determine the sorption capacity of Phoslock®, the model solution was prepared with distilled water and potassium dihydrogen phosphate KH_2PO_4. Four beakers, each with a capacity of 2 dm^3,were filled with 1.5 dm^3 of the model solution. The concentration of PO_4^{3-}-P was approx.15 mg/dm^3. Five series (repetitions) have been performed (Table 1).

Table 1. Initial concentration of PO_4^{3-}-P in control samples ("0") in each series
Tabela 1. Początkowe stężenia PO_4^{3-}-P w kontrolnych próbach ("0") w poszczególnych seriach

Series	1st (0 hour)	2nd (24 hours)	3rd (72 hours)	4th (96 hours)	5th (120 hours)
Initial concentration [mg/dm^3]	15.2	15.0	16.1	15.1	15.6

Before the addition of Phoslock®, the following parameters of the synthetic wastewater were determined: concentration of PO_4^{3-}-P, temperature, total suspended solids (TSS), conductivity, pH, turbidity and color. To each beaker 100 g of adsorbent was added. Stirring was provided by a magnetic stirrer (1000 rpm) in each beaker batches 5, 10, 20 and 30 minutes of mixing times followed by sedimentation. The sampling was made after 0.5, 1, 2, 3, 4, and 24 hours of sedimentation from each beaker. When reduction of the entire PO_4^{3-}-P from model solution was observed, the whole process was repeated five times until reaching the exhaustion of sorption capacity of Phoslock®. All tests were conducted at room temperature approx. 20°C. In total there were 5 series of investigation resulting in 7.5dm^3 synthetic wastewater treated per each batch reactor. 28 samples were taken from every beaker giving in total 112 samples.

Physical and chemical analysis

Prior to the designation of the parameters of synthetic wastewater, the samples were filtrated to define total suspended solids (TSS). The concentration of TSS was calculated by gravimetric method. The concentration of PO_4^{3-}-P was marked by using cuvette tests HACH Lange LCK 049 (1.6-30 mg/dm^3 PO_4-P), LCK 348 (0.5-5.0 mg/dm^3 PO_4-P) and LCK 349 (0.05-1.5 mg/dm^3 PO_4-P). Conductivity was defined by conductivity meter HACH Lange HQ40D Multi. Turbidity and color were measured by using a spectrophotometer HACH Lange DR3900. The temperature and pH were performed with a pH meter: WTW inoLab pH 720. Sorption capacity of Phoslock® was defined according to the following equation (Nastawny et al., 2015):

$$q = \frac{(C_0 - C)}{m} * V \quad (1)$$

where:
q – the value of sorption [mg/g],
C_0 – initial concentration of PO_4^{3-}-P [mg/dm^3],
C – final concentration of PO_4^{3-}-P [mg/dm^3],
m – mass of the adsorbent [g],
V – volume of solution [dm^3],
(C_0 – C) * V – load of absorbed phosphates [mg].

3. Results and discussion

3.1. Nitrogen removal

Influent concentration and working conditions

Based on literature information (Fux et al., 2003; van Loosdrecht & Salem, 2005; van Hulle et al., 2010; van Kempen et al., 2001) about anammox, reject water (RW) a hydraulic load of 600 mm/m^{2}d was assumed (Table 2). Additional source of carbon was used to enhance possible denitrification. After a few vegetation seasons decaying plant tissue will become a good source of. In this investigation a higher concentration of NH_4^+-N was assumed due to enhance nitrification process. The aim of the research was to define the influence and treatment efficiency of high concentrated anammox reject water on VSSFs with high hydraulic load.

Table 2. Parameters of synthetic reject water after SBR with ANAMMOX
Tabela 2. Parametry ścieków syntetycznych po reaktorze SBR z ANAMMOX

Parameter	Inflow [mg/dm^3]			MEAN load of TN [g/m^{2}d]	Synthetic influent load	
	Min.-Max.	MEAN	SD		Feed volume [dm^3/bed per day]	Hydraulic load [mm/m^{2}d]
NH_4^+-N	60.4-65.4	63.0	±1.51	37.8	96	600
NO_3^--N	23.8-28.2	26.0	±1.07	15.6		
NO_2^--N	–	0.00	–	0.0		
TN	86.2-92.5	89.0	±1.81	53.4		

Comparison of nitrogen compounds concentrations during treatment

The variation of influent and effluent concentrations of nitrogen compounds in each bed are presented in Table 3, 4, 5.

Table 3. Average characteristic of nitrogen form in outflow with efficiency removal
Tabela 3. Charakterystyka frakcji azotu w odpływie wraz ze skutecznością usuwania

Bed	Parameter	Outflow [mg/dm^3]			Efficiency of removal
		Min.- Max.	MEAN	SD	Mean ± SD
'0'	NH_4^+-N	21.3-63.0	43.0	±16.6	32.9±16.2
	NO_3^--N	5.0-26.0	14.4	±7.6	45.1±27.9
	NO_2^--N	0-2.5	1.3	±1.0	production
	TN	43.3- 89.0	57.5	± 11.8	34.3±17.8
'I'	NH_4^+-N	23.3-63.0	38.5	±13.9	40±21.4
	NO_3^--N	13-35,1	25.2	±8.7	2.3 ±35
	NO_2^--N	0-4.6	1.8	±1.3	production
	TN	41.9-89.0	63.7	±13.1	26.9 ±23.2
'II'	NH_4^+-N	25.4-63.0	35.7	±12.0	44.4±18.6
	NO_3^--N	7.0-39.1	21.6	±7.8	16.4 ±33.3
	NO_2^--N	0-3.6	1.7	±1.0	production
	TN	37.5-89.0	57.3	±14.7	33.8±15.6

In case of bed "I", with the smallest substrate, since 21st August 2016 until the first sampling no treatment was observed, a decrease of 2.2 mg/dm^3 of NH_4^+-N was indicated. Significant decrease of NH_4^+-N in the effluent was noticed in 2nd sample on 28th August resulting in a treatment

efficiency of 48.6% NH_4^+-N indicating that nitrification is occurring due to significant increase of NO_2^--N. In samples 2-10, there was a "stable" treatment efficiency from 48.6% up to 63.0%. A visual changes in plants was observed on 7th December 2016. A significant increase of NH_4^+-N in last sample from 15th December indicate end of any treatment processes. Those observation prove that the plants have finally finished their biological cycle and changed into winter sleep.

Table 4. Concentration of NH_4^+-N in effluent from analyzed beds "0" – control, "I" and "II"
Tabela 4. Stężenie NH_4^+-N w analizowanych złożach "0" – kontrola, "I" i "II"

Sampling date	NH_4^+-N [mg/dm^3]		
	Bed 0	Bed I	Bed II
23.08	60.8	54.6	34.8
28.08	32.4	37.8	39.7
30.08	28.9	30.5	46.3
01.09	24.0	25.5	38.9
03.09	29.5	31.3	46.8
07.09	23.0	25.4	41.7
09.09	31.6	26.5	45.7
15.09	23.3	28.1	43.5
01.11	28.7	20.3	21.3
04.11	31.2	29.3	35.5
07.11	44.3	34.0	32.8
09.11	44.0	33.7	35.8
17.11	45.1	38.7	50.5
07.12	44.4	37.6	52.3
15.12	62.0	55.1	60.7

For bed "II", with core sand as a substrate, similar pattern of NH_4^+-N changes has been noticed, but the removal efficiency was higher than in bed "I" with a minimum 46.0% on the 7th November and maximum 67.8% on 1st November. What is surprising, the second highest removal efficiency of NH_4^+-N was observed for the bed "0". On 1st November it reached 21.3 mg/dm^3 which gives a 66.2% efficiency. This high effectiveness of NH_4^+-N removal in the first period of VSSF bed exploitation could be explained by sorption process described by other researchers (Saeed & Sun, 2012; Wojciechowska et al., 2017). Important

is, that when the sorption capacity has been exhausted, other removal processes become more importance Table 4, 5.

Table 5. Concentration of NO_3^--N in effluent from analyzed beds "0" – control, "I" and "II"
Tabela 5. Stężenie NO_3^--N w analizowanych złożach "0" – kontrola, "I" i "II"

Sampling date	NO_3^--N [mg/dm^3]		
	Bed 0	Bed I	Bed II
23.08	60.8	54.6	34.8
28.08	32.4	37.8	39.7
30.08	28.9	30.5	46.3
01.09	24.0	25.5	38.9
03.09	29.5	31.3	46.8
07.09	23.0	25.4	41.7
09.09	31.6	26.5	45.7
15.09	23.3	28.1	43.5
01.11	28.7	20.3	21.3
04.11	31.2	29.3	35.5
07.11	44.3	34.0	32.8
09.11	44.0	33.7	35.8
17.11	45.1	38.7	50.5
07.12	44.4	37.6	52.3
15.12	62.0	55.1	60.7

Significant decrease of NO_3^--N in the effluent at the beginning of the process indicates either that sorption was occurring or assimilation by plans, more likely even both. The amount of NO_3^--N was rising till 7th August and staying stable up to 15th August indicating that production of NO_3^- was higher that the concentration assimilated by sorption and plants, possibly sorption capacity has been exhausted.

In general it has been already proven that faster and more effective nitrification occurs in beds with fine substrate – bed "I" (Kadlec & Wallace, 2009). In this research for the beginning of nitrification process the 1st November could be assumed since the concentration of NO_3^--N started to increase above the discharged concentration indicating the transformation of NH_4^+ into NO_3^- in nitrification process.

The NO_2^--N presence in the effluent could be explained only by occurrence of partial nitrification process. It is important to notice that in the first two weeks of investigation the concentration of NO_2^--N was very low and in the third week rapid growth appeared in beds inhabited by reed indicating the initiation of nitrification process. Since then concentration of NO_2^--N has been significantly various indicating that the transformation process was unstable. Concentration of NO_2^--N in bed "II" effluent between 28th August and 1st September indicates that the ammonia oxidizing bacteria (AOB) were in their highest function. AOB are the first group of nitrifiers in nitrification and are responsible for oxidizing ammonia to nitrite (Ward, 2013).

The input concentration of nitrogen is only present in the form of NH_4^+-N and NO_3^--N due to treatment in VSSF bed models show different pattern of processes responsible for their transformation and removal, depending on the bed substrate and vegetation cycle.

3.2. Results and discussion for phosphates removal

Effect of Phoslock® on phosphates reduction

This investigation showed a significant sorption capacity of Phoslock®. The total amount of adsorbed PO_4^{3-}-P and sorption value defined according to (Nastawny et al., 2015) are presented in Table 6.

The 1st series have shown that the concentration of phosphates ions rapidly decreased after 30 minutes of sedimentation with the effectiveness over 99%. During each mixing the concentration of PO_4^{3-}-P has been reduced from the initial quantity to a value of 0.1-0.2 mg/dm^3. In 4th series, a smaller decrease in concentration of PO_4^{3-}-P was observed, but the reduction rate oscillated around 90%. After 5th series, the phosphorus level decreased by only 80% to approx. 3 mg/dm^3, indicating the moment of exhaustion of Phoslock® sorption capacity. For each mixing time similar results were achieved.

During the field study presented by Haghseresht (2009), 95% reduction of phosphorus compounds were achieved. The research of Van Oosterhout and Luring (2013) shows binding of phosphates by Phoslock® with effectiveness close to 100%. According to Ross (2008), in the optimal pH range, sorption capacity reached 4.37 mg/g, therefore this investigation demonstrated a higher efficiency of Phoslock® (Table 6).

Table 6. The value of sorption capacity of Phoslock® material for each time of mixing
Tabela 6. Pojemność sorpcyjna preparatu Phoslock® dla poszczególnych czasów mieszania

Time of mixing	Summary load of PO_4^{3-}-P L_0 [mg]	Final load of PO_4^{3-}-P L [mg]	Quantity of adsorbed PO_4^{3-}-P [mg]	Sorption q [mg/g]	Removal efficiency [%]
5 min	77.00	2.41	74.59	5.59	96.9
10 min		2.39	74.61	5.60	96.9
20 min		3.33	73.67	5.53	95.7
30 min		2.70	74.30	5.57	96.5

Effect of Phoslock® on total suspended solids (TSS)

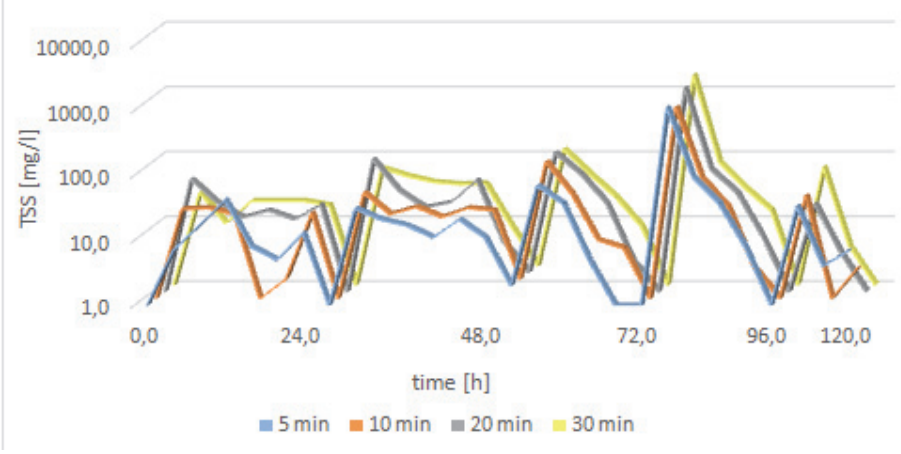

Fig. 1. Characteristic of total suspended solids (TSS) during the investigation (logarithmic scale)
Rys. 1. Charakterystyka zmian zawiesiny podczas trwania doświadczenia (skala logarytmiczna)

Figure 1 shows the variability in TSS concentration during the research. The initial value was 0-1 mg/dm^3 and was very low due to the use of model solution. Phoslock® caused the release of suspension after use. The increase in TSS concentration followed along with the course of the investigation.

The highest TSS concentration was noticed after 20 and 30 minutes of mixing time. In the 4th series (72 h) after 30 minutes of sedi-

mentation TSS reached approx. 1000 mg/dm^3 (for 5 and 10 minutes mixing time) and 1398 mg/dm^3 and 1740 mg/dm^3 for 20 and 30 minutes of mixing respectively. In 5th series, samples were not collected after 30 minutes of sedimentation, due to high concentration of solids. In each series TSS decreased to average value of 10 mg/dm^3 after 3 hours of sedimentation for 5 and 10 minutes mixing time, while for 20 and 30 minutes mixing time after 24 hours of sedimentation.

From the values of TSS, we can concluded, that the multiple use of the same deposits (resuspension) and extended mixing time have unfavorable influence to a solution with Phoslock®.

Effect of Phoslock® on conductivity

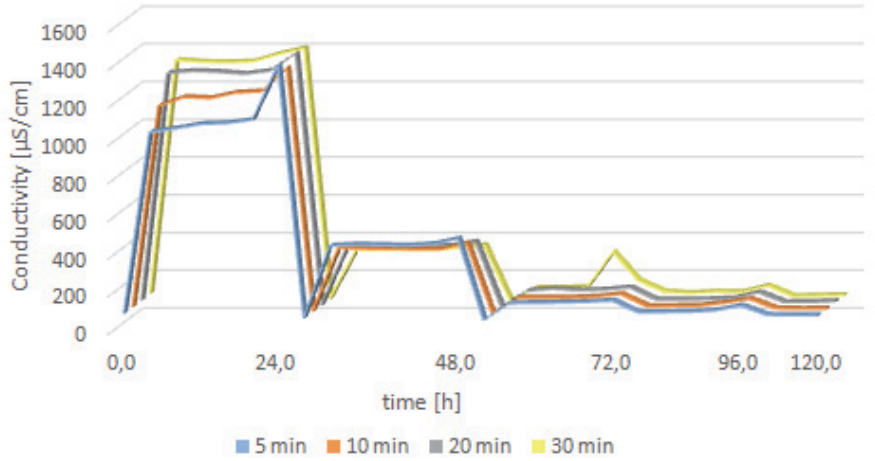

Fig. 2. Characteristic of the conductivity during the investigation
Rys. 2. Charakterystyka przewodności podczas trwania doświadczenia

The conductivity of the control samples was fluctuating significantly (Fig. 2). Over 1st series the conductivity has increased to values 1000-1400 µS/cm (longer time of mixing gave higher conductivity). In each next series conductivity decreased gradually to average values: after 2nd series to 400 µS/cm, after 3rd series to 150 µS/cm, after 4th series – 100 µS/cm. After 5th series dropped to approx. 90 µS/cm, so the value of conductivity was close to the control sample. Investigation has not shown

correlation between conductivity and time of mixing. The conclusion might be stated that Phoslock® material, releases dissolved substances in the early stage of process. After resuspension ensue resorption of dissolved compounds and conductivity values decrease again.

Effect of Phoslock® on pH

During the experiment no significant changes in the value of pH have been observed. Investigation has proceeded in pH from 6.45 to 7.50. Only in 3rd series, after 24 hours of sedimentation for 30 minutes mixing time an increase of pH to 8.74 was noticed. To achieve the highest effectiveness in reduction of phosphorus compounds the optimal pH values were from 6.0 to 9.0 (PWS Report Number: IR 019/12, 2012).

Effect of Phoslock® on color and turbidity

This research has shown a significant influence of Phoslock® on color and turbidity of the model solution. Results for control samples "0" for color and turbidity were 2-5 mg Pt/dm^3 and 0.1-1.0 mg/dm^3 respectively. After 1st series, color and turbidity fluctuated slightly, but over time of subsequent series, both color and turbidity increased notably. In 2nd series, color was changing between 400-500 mg Pt/dm^3 and turbidity value reached 143.7 mg/dm^3 for 20 minutes mixing time. For 30 minutes mixing time did not present any readings on the spectrophotometer (absorbance>3.5). After 24 hours of sedimentation, lower values were noticed: color 278 mg Pt/dm^3, turbidity 75.1 mg/dm^3. In every next series higher values were observed. Many samples values were impossible to be analyzed. In 4th series measurements have been made for control samples and after 24 hours of sedimentation time, which shows values of 300-400 mg Pt/dm^3 for color and 80-100 mg/dm^3 for turbidity. For 30 minutes mixing time content of color and turbidity could not be analyzed due to high values. In 5th series, only for 20 minutes mixing time and 24 hours of sedimentation readings were made and reached values for color – 372 mg Pt/dm^3 and for turbidity – 95.9 mg/dm^3.

Investigation described by Van Oosterhout and Luring (2013) either indicates a significant increase in turbidity after using Phoslock® from 0.15 mg/dm^3 to 218 mg/dm^3 and it decreases along with period of sedimentation. After 6 h turbidity values were about 13 mg/dm^3 and after 24 hours reached 6.5 mg/dm^3.

4. Conclusions

Applied technologies: removal of total nitrogen (TN) in VSSF beds connected with removal of PO_4^{3-}-P in batch reactors (beakers) using Phoslock® secured the assumptions of circular economy. Based on the carried out investigations following statements could be concluded:

1. The investigation has shown different pattern of processes responsible for nitrogen compounds transformation and removal efficiency, depending on the bed substrate and vegetation.
2. The initial high removal of ammonia nitrogen in the "0" bed can be attributed only to the sorption process in the substrate. After exhausting the sorption capacity (after four months) no further ammonium nitrogen removal was observed in this process
3. In VSSF reed beds ("I" and "II") NH_4^+-N concentration decreased in wastewater and NO_2-N production with simultaneous NO_3-N changes were observed, what indicated the nitrification process
4. VSSF reed beds("I" and "II") provide a better environment for the conversion of nitrogen compounds and in consequence they provide better removal of the N compounds.
5. Investigation has shown high sorption capacity of Phoslock® – 5.60 mg/g. The sorption of removed PO_4^{3-}-P was in average 5.5 mg/g and over 95.0% of phosphorus removal efficiency from model solution.
6. The optimal condition for adsorption in steady condition is: (1) mixing time should not exceeded 10 min and (2) sedimentation time is 3 h.
7. Conductivity of the solution was subjected to significant changes. It was noticed that resuspension of Phoslock® reduces its ability to increase the conductivity. The conductivity oscillation changes were not connected with mixing time.
8. Phoslock® material causes a slight fluctuation in pH, where the mixing time did not affect the changes.
9. Further investigation by using different loads and additional air input to recognized the processes responsible for N removal as well as working conditions of VSSF beds applied for treatment of effluent after the SBR with anammox need to be performed. In case of phosphorus removal there is necessity to lower the color and turbidity due to application of Phoslock®.

Acknowledgements

The research was carried out within the subtask 2.3 of the project entitled "Integrated technology for improved energy balance and reduced greenhouse gas emissions at municipal wastewater treatment plants" with the acronym "BARITECH" co-funded by the Norwegian funds, under the Polish-Norwegian Cooperation Research carried out by the National Centre for Research and Development [197025/37/2013].

References

Fux, Ch., Lange, K., Faesseler, A., Huber, P., Grueniger, B., Siegrist, H. (2003). Nitrogen removal from digester supernatant via nitrite-SBR or SHARON? *Water Science and Technology, 48(8)*, 9-18.

Fux, Ch.,Valten, S., Carozzi, V., Solley, D., Keller, J., (2006). Efficient and stable nitrification and denitrification of ammonium-rich sludge dewatering liquor using SBR with continuous loading. *Water Research, 40(14)*, 2765-2775.

Gajewska M., Obarska-Pempkowiak H. (2008). Wpływ zawracania odcieków z odwadniania osadów ściekowych na pracę oczyszczalni ścieków. *Przemysł Chemiczny, 87(5)*, 448-452

Gajewska M., Obarska-Pempkowiak, H. (2011b). Efficiency of pollutant removal by five multistage constructed wetlands in a temperate climate. *Environment Protection Engineering, 37(3)*, 27-36.

Gajewska, M., Obarska-Pempkowiak, H. (2011a). The role of SSVF and SSHF beds in concentrated wastewater treatment, design recommendation. *Water Science and Technology*, *64(2)*, 431-439.

Haghseresht, F., Wang, S., Do D.D., (2009). A novel lanthanum-modified bentonite, Phoslock, for phosphate removal from wastewaters. *Applied Clay Science, 46*, 369-375.

Kadlec, R. H., Wallace, S. D. (2009). *Treatment Wetlands*, Second Edition. CRC Press Taylor & Francis Group.

Nastawny, M., Jucherski, A., Walczowski, A., Jóźwiakowski, K., Pytka, A., Gizińska-Górna, M., Marzec, M., Gajewska, M., Marczuk, A., Zarajczyk, J. (2015). Preliminary evaluation of selected mineral adsorbents used to remove phosphorus from domestic wastewater (in Polish). *Przemysł Chemiczny*, *94(10)*, 1001-1004.

Pempkowiak, J., Obarska-Pempkowiak, H. (2002). Long-term changes in sewage sludge stored in a reed bed. *Science of The Total Environment*, *297(1-3)*, 59-65.

Phoslock General Brochure: http://www.phoslock.com.au/irm/content/scientificreport/genbrochureSara.pdf [cited 18 March 2017]

PWS (Phoslock Water Solutions Limited) Report Number: IR 019/12, (2012): http://www.phoslock.com.au/irm/content/scientificreport/AlumvsPhoslock-March2012.pdf [cited 18 March 2017]

Ross, G., Haghseresht, F., Cloete, T.E., (2008). The effect of pH and anoxia on the performance of Phoslock, a phosphorus binding clay. *Harmful Algae, 7*, 545-550.

Saeed, T., Sun, G. (2012). A review on nitrogen and organics removal mechanisms in subsurface flow constructed wetlands: dependency on environmental parameters, operating conditions and supporting media. *Journal of Environmental Management, 112*, 429-448.

Van Hulle, S., Yandeweyer, B. D., Meesschaert, P. A., Vanrolleghem, R., Dumoulin, A. (2010). Engineering aspects and practical application of autotrophic nitrogen removal from nitrogen rich streams. *Journal of Chemical Engineering, 162*, 1-20.

Van Kempen, R., Mulder, J. W., Uijterlinde, C.A., van Loosdrecht, M.C.M. (2001). Overview: full scale experience of the SHARON process for treatment of rejection water of digested sludge dewatering. *Water Science and Technology, 44*, 145-152.

Van Loosdrecht, M. C. M., Salem, S. (2005). Biological treatment of sludge digester liquids. *IWA Specialized Conference „Nutrient Management In Wastewater Treatment Processes and Recycle Streams",* 13-22.

Van Oosterhout, F., Lürling, M., (2013). The effect of phosforus binding clay (Phoslock®) in mitigating cyanobacterial nuisance: a laboratory study on the effects on water quality variables and plankton. *Hydrobiologia, 710*, 265-277.

Ward, B.B. (2013). *Reference Module in Earth Systems and Environmental Sciences.* Elsevier Inc.

Wett, B., Alex, J. (2003). Impact of separate reject water treatment on the overall plant performance. *Water Science and Technology, 48(4)*, 139-14.

Wojciechowska, E., Gajewska, M., Ostojski, A. (2017). Reliability of nitrogen removal processes in multistage treatment wetlands receiving high-strength wastewater. *Ecological Engineering, 98*, 365-371.

Zamparas, M., Gavriil, G., Coutelieris, F.A., Zacharias, I. (2015). A theoretical and experimental study on the P-adsorption capacity of Phoslock™. *Applied Clay Science, 335*, 147-152.

Zastosowanie innowacyjnych technologii do usuwania związków biogennych ze ścieków – studium przypadku (BARITECH)

Streszczenie

Innowacyjne technologie stosowane podczas oczyszczania ścieków powinny spełniać nie tylko wysokie wymagania dotyczące jakości oczyszczonych ścieków, ale także zapewnić maksymalny potencjał odzysku energii i surowców z ścieków. Jednym ze sposobów poprawy skuteczności usuwania związków azotu i fosforu w istniejących konwencjonalnych oczyszczalniach ścieków, jest wstępne oczyszczanie odcieków powstających podczas mechanicznego odwadniania osadu ściekowego po biologicznym oczyszczaniu ścieków. Celem badań było określenie charakterystycznych parametrów procesów technologicznych, dla zapewnienia skutecznego usuwania związków biogennych (N, P) ze ścieków po oczyszczaniu w procesie nitryfikacji/anammox zachodzącym w reaktorze typu SBR. Badanie zostało podzielone na dwa etapy. Pierwszy etap przeprowadzono w celu optymalizacji procesu usuwania związków azotu (NH_4-N, NO_3-N i NO_2-N) z odcieków powstających z mechanicznego odwadniania przefermentowanych osadów ściekowych. Odcieki oczyszczane były w reaktorze SBR w procesie ANAMMOX. Instalacja pilotowa składała się z pojedynczych złóż o przepływie pionowym umieszczonych w zbiornikach ze stali nierdzewnej, pracujących równolegle oznaczonych odpowiednio jako złoże "0", "I", "II". Próbki do analizy pobierano w celu określenia zmian NH_4-N, NO_3-N i NO_2-N w ściekach w każdym ze złóż. W złożu "0" (nie zasiedlonym trzciną) usuwanie związków azotu spowodowane było jedynie przed sorpcję, aż do wyczerpania jego pojemności sorpcyjnej. Natomiast zmiany stężenia NH_4-N i wytwarzanie NO_2-N przy jednoczesnych zmianach stężenia NO_3-N wskazywały na zachodzący proces nitryfikacji w złożach "I" i "II" (oba zasiedlone trzciną). Doświadczenia wykazały różne mechanizmy procesów odpowiedzialnych za przemiany związków azotu i skuteczność ich usuwania, w zależności od podłoża i wegetacji. W drugim etapie badań przeprowadzono optymalizację procesu usuwania fosforanów. Natomiast doświadczenia związane z usuwaniem fosforu zostało przeprowadzone w laboratorium w warunkach nieprzepływowych przy zastosowaniu modelu z czterema reaktorami. Każdy reaktor zawierający ścieki syntetyczne o stężeniu fosforanów 15 mg/dm^3 poddano mieszaniu. Próbki do analizy zostały pobierane z każdej zlewki po założonym czasie sedymentacji. Badania przeprowadzono w celu określenia optymalnej dawki preparatu Phoslock® przy znanym stężeniu anionów fosforanowych PO_4^{3-} w roztworze modelowym, oraz znalezienia optymalnego czasu mieszania i sedymentacji. Próbki poddano analizie i określono następujące parametry: pH, zawiesinę, przewodnictwo, mętność, barwę i stężenie fosforanów. Przeprowadzone badania potwierdziły wy-

soką skuteczność usuwania $PO4^{3-}$ (ponad 95%). Badanie nie wykazało zależności między czasem mieszania a stopniem redukcji związków fosforu.

Abstract

Eco-innovative technologies in wastewater treatment should provide not only stringent standards for the quality of treated wastewater but also ensure maximum recovery of energy and raw materials from wastewater. One of the ways to improve the removal efficiency of nitrogen and phosphorus compounds in existing conventional wastewater treatment plants is pretreatment of reject water generated during the mechanical dewatering of the digested sewage sludge. The aim of this research was to select the technological parameters of processes to ensure effective removal of nutrient elements (N, P) from RW treated in a SBR reactor in the nitritation/anammox process. The study was divided into two stages. The first stage was carried out to optimize nitrogen compounds removal in the effluent from ANAMMOX process used to treat reject water after centrifugation. The installation consists of single vertical subsurface flow (VSSF) beds located in stainless steel containers working parallel marked as BED control "0", "I", "II". Samples have been taken for analysis to determine the changes of NH_4-N, NO_3-N and NO_2-N in the effluent of each filter. In bed "0" the removal of nitrogen compounds was caused only by sorption at last until its capacity was reached. In bed "I" and "II" the NH_4-N concentration in effluent and production of NO_2-N with simultaneous changes of NO_3-N indicated that nitrification was occurring. The investigation has shown different pattern of processes responsible for nitrogen compounds transformation and removal efficiency, depending on the bed substrate and vegetation. In the second stage the optimization of phosphates removal was carried out. The investigation was conducted in steady conditions in laboratory model with four batch reactors. Each batch reactor of synthetic wastewater with given concentration of phosphates (15 mg/dm^3) was subjected to mixing. Samples for analyzing were taken from each beaker after assumed time of sedimentation. Studies were conducted to determine the optimal dose of Phoslock® with known concentration of phosphate anions PO_4^{3-} in model solution, time of mixing and time of sedimentation. Samples were analyzed with following parameters: pH, total suspended solids, conductivity, turbidity, color and phosphate concentration. The carried out investigations confirmed high efficiency of phosphate anions $PO4^{3-}$ removal (over 95%). Also study showed no relationship between the mixing time and the degree of reduction of phosphorus compounds.

Słowa kluczowe:
Usuwanie azotu, usuwanie fosforu, odcieki, oczyszczalnie hydrofitowe

Keywords:
Nitrogen removal, phosphorus removal, reject water, constructed wetlands

MIDDLE POMERANIAN SCIENTIFIC SOCIETY OF THE ENVIRONMENT PROTECTION
ŚRODKOWO-POMORSKIE TOWARZYSTWO NAUKOWE OCHRONY ŚRODOWISKA

Annual Set The Environment Protection
Rocznik Ochrona Środowiska

Volume/Tom 19. Year/Rok 2017 ISSN 1506-218X 161-180

Numerical Simulations of the Thread Rolling Process as Ecological and Economical Research Tool in the Implementation of Modern Technologies

Krzysztof Kukiełka
Politechnika Koszalińska

1. Introduction

In the twenty-first century, preparing the production of new products should be subject to "eco-design of the product," which consists to reduce the negative impact on the surrounding natural environment of man. The dominant role in this action plays the rational use of energy and environmental protection. In this aspect, it is important to develop a correct and proper implementation of technological process.

Volume plastic work on cold allows to achieve high accuracy of the product and high productivity in process like: thread rolling (Kukiełka K. 2009, Kukiełka K. & Kukielka L. 2013, Kukiełka K. 2014, Kukiełka K. et. al 2014, Kukiełka K. 2016, Kukiełka L. & Kukiełka K. 2007, Kukiełka L. & Kukiełka K. 2012), duplex burnishing (Patyk & Kukielka L. 2008, Patyk et al 2014), burnishing rolling (Kukiełka L. 1994, Kukiełka L. 1999, Kukiełka L. & Krzyżyński T. 2000, Kukiełka L. 2001, Kukiełka L. 2002, Kukiełka L. et al 2012, Kukiełka L. et al 2012, Kułakowska et al 2009, Kułakowska, Kukiełka L et al 2014, Myśliński et al 2004), drawpiece forming process (Kałduński & Kukielka L. 2014), shot penning (Zaleski & Bławucki 2014), grinding process (Sutowski & Nadolny 2016, Nadolny et al 2014), plastic deformations of measured object surface (Kowalik et al. 2016), surface roughness measured after machining (Valicek et al 2012, Kusnerova et al 2013), other like water jet

cutting (Perec 2016) and mechanical/abrasive polishing (MP), standard electropolishing (EP) and magnetoelectropolishing (MEP) (Rokosz 2016), plasma cutting (Skoczylas & Zaleski 2015) and modern material behaviour modelling (Malag et al 2014). The performance of machine parts using this technology, the use of the starting material is on average 85-97%, and material savings entail large energy savings. Savings should also include lower costs of storage material, the elimination of chips management, less need for cooling, lower expenditures on transport and depreciation of production equipment (Jednovicky & Streit 1998).

One of the post-machining methods employed to shape the outer layer, characterized by advantageous exploitation properties, is thread rolling. The thread rolling technology has many advantages, namely: saving material, extremely short times of execution, which affects on high performance of production, high durability of tools, make full use of existing machine park. In contrast to thread machining, after which the waste remains in the shape of chips, using a rolling technology as volume of the plastic working, it is possible to perform thread with total consumption of material. Diameter of the blank (bar or pipe) to the rolled thread is smaller than the diameter of the machined thread, and this results significant savings of material (Domblesky & Feng 2002, Kukiełka K. 2009, Kukiełka K. & Kukielka L. 2013, Kukiełka K. 2014, Kukiełka K. et al. 2014, Kukiełka K. 2016, Kukiełka L.& Kukiełka K. 2007, Kukiełka L. & Kukiełka K. 2012, Łyczko 2010, Olszak 2008).

Favourable strength (both static and dynamic) and exploitational properties of the rolled threads are the result of plastic deformation in the top layer of the part. In these threads, the material in the external layers is laid in the form of fibers covering the whole thread profile (Fig. 1), whereas in the threads made by cutting the fibers are cross-cut.

The heating of parts is realised whilst rolling, by means of visco-plastic deformation and fretting in the areas of contact between the roller and the objet (Fig. 2) (Kukielka L. 1994, Kukielka L. 1999, Kukielka, L. & Krzyzynski 2000, Kukielka L. et al. 2012, Kukielka L. et al., Kukiełka L. & Kukiełka K. 2015, Kukielka K. 2017).

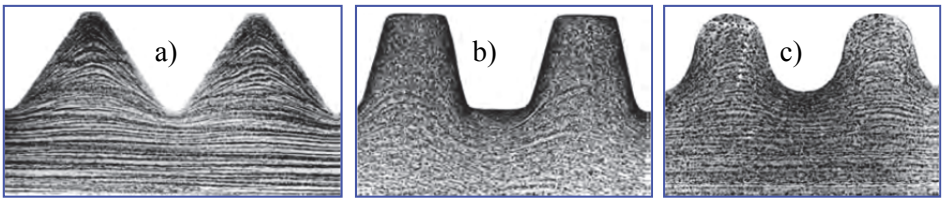

Fig. 1. Microstructure and texture of the rolled thread (St3 steel) a) M25 thread, b) trapezoidal thread, c) Round thread (Fette 2007)
Rys. 1. Mikrostruktura i tekstura gwintu wygniatanego (stal St3) a) gwint M25, b) gwint trapezowy, c) gwint okrągły (Fet2007)

Thread rolling is carried out with using a concentrated heat source, move together with the tool. These sources depending on their location are dived into plane and spatial sources. Plane sources appear in the contact zone of active surface of the roll with workpieces, while the spatial source occur inside the wok pieces and tools (Fig. 2).

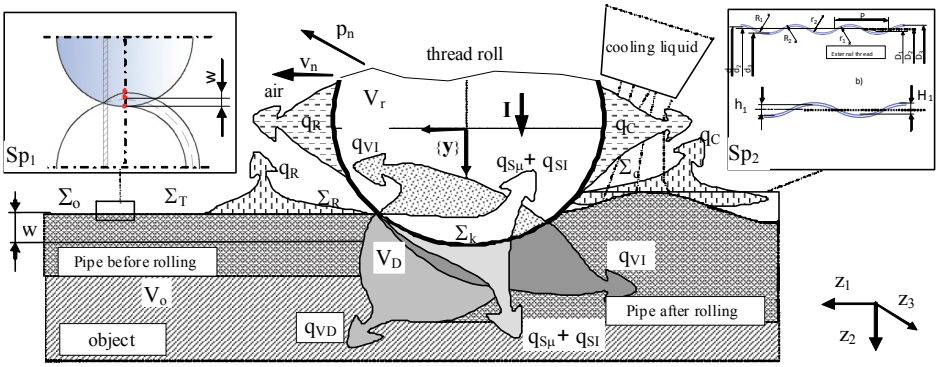

Fig. 2. Diagram of the system of heat fluxes arising in characteristic volumes V and areas ∑ during thread rolling: pipe before rolling and pipe after - surface of the object and outer layer after previous treatment and after rolling, respectively
Rys. 2. Schemat procesu z układem strumieni cieplnych powstających podczas obróbki, w charakterystycznych objętościach V i obszarach ∑ obiektu: Sp_1 i Sp_2 - rura odpowiednio po obróbce poprzedzającej i po walcowaniu

Energy of plane sources is the mechanical energy (friction roll-work pieces). During the friction heat is produced $q_{S\mu}$. Spatial sources of energy is the mechanical energy (plastic deformation of the material). During plastic deformation the heat q_{VD}. The total power of heat sources

is the sum of the mechanical power sources $q_{S\mu} + q_{VD}$, and wherein the value of the temperature distribution during the rolling process depends on the quotas for of those power sources. During the rolling, there are four variation stages of heat field, namely: the increase, almost stabilization, alignment, and decrease. Increase of the heat field it takes a place in the initial phase of rolling, upon commencement of operation of sources. The decrease of the heat field occurs in the final stage, once resolved these sources. For practical purposes it can be assumed that the temperature field is quasi-stationary, because instability the time periods are short and cooling conditions are selected as to achieve stable temperature field. Then, in any position of the tool, the temperature distribution is characterized by the presence of elongated isotherm (Fig. 3).

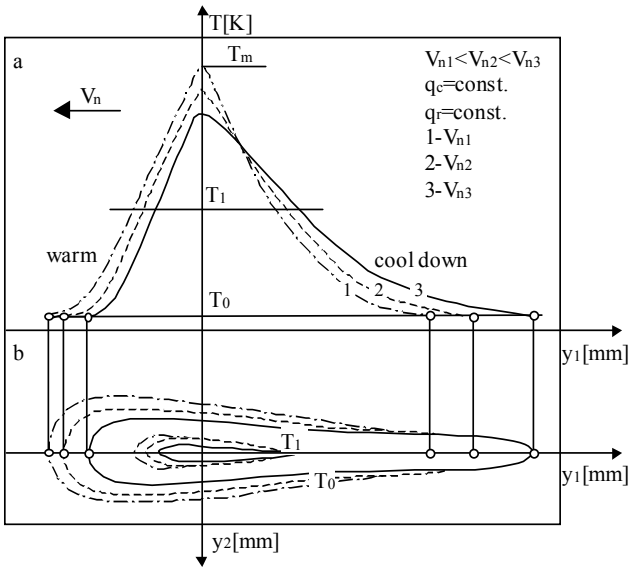

Fig. 3. Thermal cycle in massive body occurring during thread rolling at different speeds V_n and the constant cooling rate: a) the temperature distribution in the surface layer of the object in the direction of the velocity vector of the thread rolling b) isotherms T_0 and T_1

Rys. 3. Cykl cieplny w ciele masywnym zachodzący podczas walcowania z różnymi prędkościami V_n i stałej szybkości chłodzenia: a) rozkład temperatury w warstwie wierzchniej przedmiotu na kierunku wektora prędkości walcowania, b) rozkład izoterm T_0 i T_1.

The increase of the rolling speed at constant power of the heat sources and constant cooling rate causes elongated isotherm along y_1 axis (Fig. 3a) (on the direction of the rolling speed), while ahead of the source of the thermal field decreases. Followed by also narrowing of the isotherms perpendicular direction (Fig. 3b).

In the article (Kukielka K. 2017) shows the problem of modelling the thread rolling process with applying of advanced methods, which directly contributes to reduce the negative impact of this process on the surrounding environment. Ways to solve the received discrete equations of motion of the object together with an analysis and numerical simulation are presented in the work (Kukielka K. 2017).

In the this paper the solutions of discrete equations of the heat transfer of the object in the thread rolling process with applied explicit and implicit integrations methods, were shown. Described results of experimental investigations, which verify computational results and correctness of calculating model.

2. Algorithm of numerical analysis

In the paper (Kukielka K. 2017) the discretized equations of heat transfer equilibrium was obtained:

$$[{}^t\mathbf{C}]\{{}_t^{\tau}\Delta\dot{\boldsymbol{\Theta}}\} + ([{}^t\mathbf{K}^k]+[{}^t\mathbf{K}^c]+[{}^t\mathbf{K}^r]+[{}^t\mathbf{K}^{IV}])\{{}_t^{\tau}\Delta\boldsymbol{\Theta}\} = \{{}_t^{\tau}\Delta\mathbf{Q}\} + \{{}_t^{\tau}\Delta\mathbf{Q}^I\}, \quad (1)$$

where $[{}^t\mathbf{C}]$ and $[{}^t\mathbf{K}^k]$, $[{}^t\mathbf{K}^c]$, $[{}^t\mathbf{K}^r]$, $[{}^t\mathbf{K}^{IV}]$ are the convection and radiation, heat capacities, conductivity matrices and total nodal point conditions of IV gender, respectively:

$$\begin{aligned}
[{}^t\mathbf{C}] &= \sum_e^E \int_{{}^tV^{(e)}} {}^tc^{(e)}\,{}^t\rho^{(e)}[{}^t\mathbf{H}^{(e)}]^T[{}^t\mathbf{H}^{(e)}]\,d^tV^{(e)},\\
[{}^t\mathbf{K}^k] &= \sum_e^E \int_{{}^tV^{(e)}} [{}^t\mathbf{B}^{(e)}]^T[{}^t\lambda^{(e)}][{}^t\mathbf{B}^{(e)}]\,d^tV^{(e)},\\
[{}^t\mathbf{K}^c] &= \sum_{m=1}^{S_C} \int_{{}^t\Sigma_C^{(m)}} {}^t\alpha_C[{}^t\mathbf{H}^{S(m)}]^T[{}^t\mathbf{H}^{S(m)}]\,d^t\Sigma_C^{(m)}), \qquad (2)\\
[{}^t\mathbf{K}^r] &= \sum_{m=1}^{S_R} \int_{{}^t\Sigma_R^{(m)}} {}^t\alpha_R[{}^t\mathbf{H}^{S(m)}]^T[{}^t\mathbf{H}^{S(m)}]\,d^t\Sigma_R^{(m)}),\\
[{}^t\mathbf{K}^{IV}] &= \sum_{m=1}^{S_k} (\int_{{}^t\Sigma_k^{(m)}} \frac{[{}^t\mathbf{H}^{S(m)}]^T[{}^t\mathbf{H}^{S(m)}]}{{}^tR_s^{(m)}}\,d^t\Sigma_k^{(m)})
\end{aligned}$$

E is the total number of the finite elements in the system, S_R, S_C, S_k are the number of the finite elements in the zones Σ_R, Σ_C and Σ_k, respectively.

The nodal point increment heat flow input vector $\{{}_t^{\tau}\Delta\mathbf{Q}\}$ is given by:

$$\{{}_t^{\tau}\Delta\mathbf{Q}\} = \{{}_t^{\tau}\Delta\mathbf{Q}_{VD}\} + \{{}_t^{\tau}\Delta\mathbf{Q}_{S\mu}\}, \tag{3}$$

where:

$$\{{}_t^{\tau}\Delta\mathbf{Q}_{VD}\} = \sum_{e=1}^{E}\left(\int_{{}_tV_R^{(e)}} [{}^t\mathbf{H}^{(e)}]^T\, {}_t^{\tau}\Delta q_{VD}^{(e)}\, d^tV^{(e)}\right),$$
$$\{{}_t^{\tau}\Delta\mathbf{Q}_{S\mu}\} = \sum_{m=1}^{S_k}\left(\int_{{}_t\Sigma_k^{(m)}} [{}^t\mathbf{H}^{S(m)}]^T\, {}_t^{\tau}\Delta q_{S\mu}^{(m)}[\cdot]\, d^t\Sigma_k^{(m)}\right). \tag{4}$$

The vector $\{{}_t^{\tau}\Delta\mathbf{Q}^I\} = \{{}_t^{\tau}\Delta\mathbf{Q}_S^I\} + \{{}_t^{\tau}\Delta\mathbf{Q}_V^I\}$ of the boundary conditions of I gender is given by:

$$\{{}_t^{\tau}\Delta\mathbf{Q}_S^I\} = \sum_{m=1}^{S_T}\left(\int_{{}_t\Sigma_T^{(m)}} [{}^t\mathbf{H}^{S(m)}]^T [{}^t\mathbf{H}^{S(m)}]\, {}_t^{\tau}\Delta\Theta_b^{(m)}\}\, d^t\Sigma_T^{(m)}\right),$$
$$\{{}_t^{\tau}\Delta\mathbf{Q}_V^I\} = \sum_{e=1}^{E_T}\left(\int_{{}_t\Sigma_k^{(m)}} [{}^t\mathbf{H}^{(e)}]^T [{}^t\mathbf{H}^{(e)}]\, \{{}_t^{\tau}\Delta\Theta_b^{(m)}\}\, d^tV_T^{(e)}\right), \tag{5}$$

where S_T and E_T are the number of the finite elements in the zones Σ_T and volume V_T, respectively.

Use the principles of step-by-step integration scheme (Kukielka L. & Kukielka K. 2015) in this section is presented for the solution of transient heat transfer problems. To approximate the velocity component $\{{}_t^{\tau}\Delta\dot{\boldsymbol{\Theta}}\}$ in term of $\{{}_t^{\tau}\Delta\boldsymbol{\Theta}\}$ in the equation (1) we can use the Euler method (with the temperature varies linearly over the time interval Δt) and the direct integration methods: the Houbolt method, the Wilson Θ method, and the Newmark method. In this paper, an example to using the Houbolt method to solution the equation (1) is showed. The Houbolt method reduces directly to a static analysis. The following finite approximate of the velocity component $\{{}_t^{\tau}\Delta\dot{\boldsymbol{\Theta}}\}$ is employed:

$$\{{}_t^{\tau}\Delta\dot{\boldsymbol{\Theta}}\} = a_1\{{}_t^{\tau}\Delta\boldsymbol{\Theta}\} - a_2\{{}^t\boldsymbol{\Theta}\} + a_3\{{}^{t-\Delta t}\boldsymbol{\Theta}\} - a_4\{{}^{t-2\Delta t}\boldsymbol{\Theta}\}, \tag{6}$$

where:

$$a_1 = 11/(6\Delta t),\ a_2 = 7/(6\Delta t),\ a_3 = 3/(2\Delta t),\ a_4 = 1/(3\Delta t), \tag{7}$$

are the integral constants.

Substituting (6) into (1) and arranging all known vectors on the right-hand side, we obtain for the solution of $\{{}^{\tau}_{t}\Delta\boldsymbol{\Theta}\}$:

$$[{}^{t}\widetilde{\mathbf{K}}]\{{}^{\tau}_{t}\Delta\boldsymbol{\Theta}\} = \{{}^{\tau}_{t}\Delta\widetilde{\mathbf{Q}}\} + \{{}^{t}\widetilde{\mathbf{Q}}\}, \tag{8}$$

where:

$$[{}^{t}\widetilde{\mathbf{K}}] = a_1[{}^{t}\mathbf{C}] + [{}^{t}\mathbf{K}^{k}] + [{}^{t}\mathbf{K}^{c}] + [{}^{t}\mathbf{K}^{r}] + [{}^{t}\mathbf{K}^{IV}], \tag{9}$$

$$\{{}^{t}\widetilde{\mathbf{Q}}\} = [{}^{t}\mathbf{C}](a_2\{{}^{t}\boldsymbol{\Theta}\} - a_3\{{}^{t-\Delta t}\boldsymbol{\Theta}\} + a_4\{{}^{t-2\Delta t}\boldsymbol{\Theta}\}), \tag{10}$$

$$\{{}^{\tau}_{t}\Delta\widetilde{\mathbf{Q}}\} = \{{}^{\tau}_{t}\Delta\mathbf{Q}\} + \{{}^{\tau}_{t}\Delta\mathbf{Q}^{I}\}. \tag{11}$$

As shown in (10) the solution of $\{{}^{\tau}_{t}\Delta\boldsymbol{\Theta}\}$ required knowledge of $\{{}^{t}\boldsymbol{\Theta}\}$, $\{{}^{t-\Delta t}\boldsymbol{\Theta}\}$ and $\{{}^{t-2\Delta t}\boldsymbol{\Theta}\}$. Although the knowledge of $\{{}^{0}\Delta\boldsymbol{\Theta}\}$ and $\{{}^{0}\Delta\dot{\boldsymbol{\Theta}}\}$ is useful to start the Houbolt integration scheme, it is more accurate to calculate $\{{}^{\Delta t}\boldsymbol{\Theta}\}$ and $\{{}^{2\Delta t}\boldsymbol{\Theta}\}$ by some other means; i.e., we employ special starting procedures. One way of the proceeding is to integrate (1) for the solution of $\{{}^{\Delta t}\boldsymbol{\Theta}\}$ and $\{{}^{2\Delta t}\boldsymbol{\Theta}\}$ using a different integration scheme, possibly a conditionally stable method such as the central difference scheme such as the central difference scheme with a fraction of Δt as the time step. The complete algorithm used in the integration is given in Table 1.

Table 1. Step-By-Step Solution Using Houbolt Integration Method
Tabela 1. Rozwiązanie Krok po Kroku przy wykorzystaniu metody całkowania Houbolt

A. *Initial Calculations:*

1. Form matrix $[{}^{t}\mathbf{C}], [{}^{t}\mathbf{K}^{k}], [{}^{t}\mathbf{K}^{c}], [{}^{t}\mathbf{K}^{r}]$ and $[{}^{t}\mathbf{K}^{IV}]$.
2. Initialise $\{{}^{0}\boldsymbol{\Theta}\}$ and $\{{}^{0}\dot{\boldsymbol{\Theta}}\}$.
3. Select time step Δt and calculate integration constants:
   $a_1 = 11/(6\Delta t),\ a_2 = 7/(6\Delta t),\ a_3 = 3/(2\Delta t),\ a_4 = 1/(3\Delta t).$
4. Use special starting procedure to calculate $\{{}^{\Delta t}\boldsymbol{\Theta}\}$ and $\{{}^{2\Delta t}\boldsymbol{\Theta}\}$.
5. Calculate effective matrix $[{}^{t}\widetilde{\mathbf{K}}]$:

$$[{}^{t}\widetilde{\mathbf{K}}] = a_1[{}^{t}\mathbf{C}] + [{}^{t}\mathbf{K}^{k}] + [{}^{t}\mathbf{K}^{c}] + [{}^{t}\mathbf{K}^{r}] + [{}^{t}\mathbf{K}^{IV}].$$

B. *For Each Time Step*

1. Calculate effective heat load at time t:

$$\{{}^{t}\widetilde{\mathbf{Q}}\} = [{}^{t}\mathbf{C}](a_2\{{}^{t}\boldsymbol{\Theta}\} - a_3\{{}^{t-\Delta t}\boldsymbol{\Theta}\} + a_4\{{}^{t-2\Delta t}\boldsymbol{\Theta}\}).$$

2. Calculate effective incremental heat load at time step $t \rightarrow \tau$:

$$\{{}^{\tau}_{t}\Delta\widetilde{\mathbf{Q}}\} = \{{}^{\tau}_{t}\Delta\mathbf{Q}\} + \{{}^{\tau}_{t}\Delta\mathbf{Q}^{I}\}.$$

3. Partition of the heat equilibrium equation for two blocks, we can write the problem in the form:

$$\begin{bmatrix} [{}^{t}\widetilde{\mathbf{K}}_{11}^{nxn}] & [{}^{t}\widetilde{\mathbf{K}}_{12}^{nxw}] \\ [{}^{t}\widetilde{\mathbf{K}}_{21}^{wxn}] & [{}^{t}\widetilde{\mathbf{K}}_{22}^{wxw}] \end{bmatrix} \begin{Bmatrix} \{{}^{\tau}_{t}\Delta\boldsymbol{\Theta}_1^{nx1}\} \\ \{{}^{\tau}_{t}\Delta\boldsymbol{\Theta}_2^{wx1}\} \end{Bmatrix} = \begin{Bmatrix} \{{}^{\tau}_{t}\Delta\widetilde{\mathbf{Q}}_1^{nx1}\} \\ \{{}^{\tau}_{t}\Delta\widetilde{\mathbf{Q}}_2^{wx1}\} \end{Bmatrix} + \begin{Bmatrix} \{{}^{t}\widetilde{\mathbf{Q}}_1^{nx1}\} \\ \{{}^{t}\widetilde{\mathbf{Q}}_2^{wx1}\} \end{Bmatrix},$$

where vectors $\{{}^{\tau}_{t}\Delta\boldsymbol{\Theta}_2^{wx1}\}$, $\{{}^{\tau}_{t}\Delta\widetilde{\mathbf{Q}}_1^{nx1}\}$ are knows and $\{{}^{\tau}_{t}\Delta\boldsymbol{\Theta}_1^{nx1}\}$, $\{{}^{\tau}_{t}\Delta\widetilde{\mathbf{Q}}_2^{wx1}\}$ are not known.

4. Solve for temperature increment vector $\{{}^{\tau}_{t}\Delta\boldsymbol{\Theta}_2^{wx1}\}$ at time step using the modified Newton-Raphson iteration method:

$$[{}^{t}\widetilde{\mathbf{K}}_{11}]^{[i-1]}_{nxn}\{{}^{\tau}_{t}\Delta\boldsymbol{\Theta}_1\}^{[i]}_{nx1} = \{{}^{\tau}_{t}\Delta\widetilde{\mathbf{Q}}_1\}^{[i-1]}_{nx1} + \{{}^{t}\widetilde{\mathbf{Q}}_1\}_{nx1} - [{}^{t}\widetilde{\mathbf{K}}_{12}]^{[i-1]}_{nxw}\{{}^{\tau}_{t}\Delta\boldsymbol{\Theta}_2\}_{wx1}.$$

5. Substituting vector $\{{}^{\tau}_{t}\Delta\boldsymbol{\Theta}_1^{nx1}\}$ into equation:

$$\{{}^{t}\widetilde{\mathbf{Q}}_2\}^{[i]}_{wx1} = [{}^{t}\widetilde{\mathbf{K}}_{21}]^{[i-1]}_{wxn}\{{}^{\tau}_{t}\Delta\boldsymbol{\Theta}_1\}^{[i]}_{nx1} + [{}^{t}\widetilde{\mathbf{K}}_{22}]^{[i-1]}_{wxw}\{{}^{\tau}_{t}\Delta\boldsymbol{\Theta}_2\}_{wx1} - \{{}^{t}\widetilde{\mathbf{Q}}_2\}_{wx1},$$

and solve we obtain the vector $\{{}^{\tau}_{t}\Delta\widetilde{\mathbf{Q}}_2\}^{[i]}_{wx1}$.

6. Calculate the temperature vector at the end of iteration i:

$$\{{}^{\tau}\boldsymbol{\Theta}\}^{[i]} = \{{}^{t}\boldsymbol{\Theta}\}^{[i-1]} + \{{}^{\tau}_{t}\Delta\boldsymbol{\Theta}\}^{[i]}.$$

7. Calculate vector $\{{}^{\tau}_{t}\Delta\dot{\boldsymbol{\Theta}}\}$ at step time:

$$\{{}^{\tau}_{t}\Delta\dot{\boldsymbol{\Theta}}\} = a_1\{{}^{\tau}_{t}\Delta\boldsymbol{\Theta}\} - a_2\{{}^{t}\boldsymbol{\Theta}\} + a_3\{{}^{t-\Delta t}\boldsymbol{\Theta}\} - a_4\{{}^{t-2\Delta t}\boldsymbol{\Theta}\}.$$

3. THREAD ROLLING application for numerical analysis

Developed by author application THREAD ROLLING in ANSYS system fully satisfy advanced requirements and can be successfully used to simulate thread rolling process in real conditions. In this application the algorithm shown in point 2 were applied. Increasing technical and economic requirements also decrease negative impact on environment lead to search for new technology and materials, which require the development of new theoretical models and their numerical implementation. This article presents the practical application called THREAD ROLLING to modeling and simulation process of thread rolling with round outline. The purpose of a computer simulation is to restore investigated process base on a mathematical model by using a computer and examine the impact of the environment (input signals) and internal properties of an object (process parameters) on the characteristics of the object.

The main advantages of computer simulation in comparison with other methods of the process analysis are:

- the model flexibility – is easy to making changes in the simulated model also filling model with new phenomena,
- easy to introduce various types of extortion and disturbance (random) and extreme extortion and disturbance without destroying usually expensive material model,
- relatively low cost and short preparation time of simulation,
- the reliability of simulation results - especially when we can compare the simulation results with the results obtained from measurements on a real object.

Numerical calculations in ANSYS system were realized by the following sequence:

a) data preparation (PREPROCESSOR):

- defining the workpieces and the tool geometry,
- defining the material properties of the workpiece and tool (depends of temperature),
- generating the finite element grid (mesh),
- defining contact between tool-workpieces, by introducing the contact finite element TARGET and CONTA,
- applying boundary condition (displacement, forces, temperatures),

b) solving (SOLVER)
– introducing number of steps and iterations, convergence conditions, etc.
– setting the course of calculations,
c) analysis of solutions and edit the results (POSTPROCESSOR - General Postproc or Time History Postproc).

4. Examples of numerical solution

Elaborated application THREAD ROLLING for spatial (3D) and plane (2D), with assumption of spatial state of stress and plane state of displacement and strain. In the exemplary simulation is shown the possibility of using reduced model to simulate the impact of the flat profile of the working rollers active surface on the thread rolling process realization and quality. The tool is a rigid body $E \rightarrow \infty$, however the model material as an elasto/thermo-visco-plastic body with nonlinear hardening (Fig. 4). The model has discretized by finite element PLANE184 with linear function of the shape. Shape coefficient (SC=B/A=1) rectangular finite element is define as a ratio height B to width A of elements (Fig. 4).

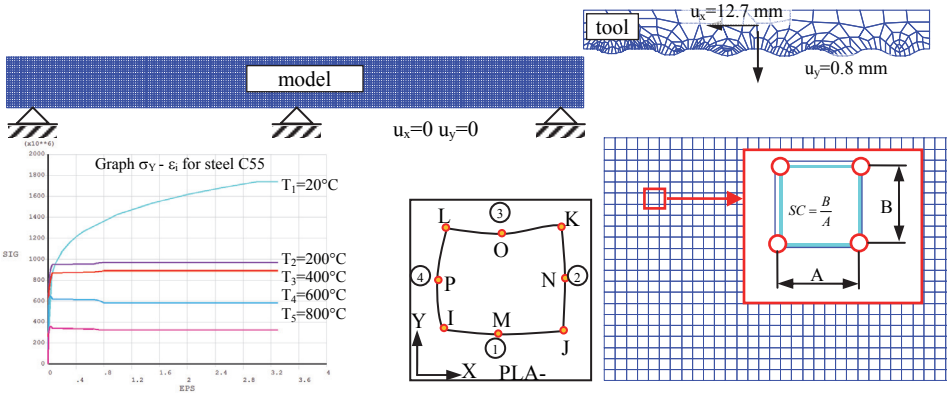

Fig. 4. Discretized computational model 2D for the external thread rolling with round profile
Rys. 4. Dyskretny model komputerowy 2D dla procesu walcowania gwintów zewnętrznych z okrągłym profilem

In the contact zone the boundary conditions for displacement are unknown. The calculation was carried out for following properties: rolling by means of a $D = 61$ mm diameter roller-shaped element; depth of rolling $w = 0.8$ mm; velocity of rolling $v_r = 0.025$, 0.05, 0.1 $m \cdot s^{-1}$; object material – steel C55, roller – 145Cr6; heat conductivity coefficients $\lambda_{(o)} = 42 - 0.012 \cdot \Delta T$ $W \cdot m^{-1} \cdot K^{-1}$; $\lambda_{(r)} = 13.2207 - 0.0032 \cdot \Delta T$ $W \cdot m^{-1} \cdot K^{-1}$; mass density $\rho = 7850/(1 + 3 \cdot \alpha \cdot \Delta T)$ $g \cdot m^{-3}$; heat capacity $c = 484 + 0.01 \cdot \Delta T$ $J \cdot (kg \cdot K)^{-1}$; coefficient of fretting $\mu = \mu_0 (1 - 0.003 \cdot v_r)(1 - 0.000015 \cdot \Delta T)$; heat resistance in the surface contact R_s=0 (ideal contact) and $R_S = 0.094$ $m^2 \cdot K \cdot W^{-1}$ (real contact), yield stress ${}^t_t\sigma_Y = 924(0.066 + {}^t_t\varepsilon_i^{(VP)})^{0.18} \times (1 + {}^t_t\dot{\varepsilon}_i^{(VP)})^{0.15}(1.737 - 0.043\,{}^t T^{1/2})$ MPa, where ${}^t_t\varepsilon_i^{(VP)}$ and ${}^t_t\dot{\varepsilon}_i^{(VP)}$ are intensity of true strain and strain rate at time t, respectively, Young's modulus $E = 5 \cdot 10^{11} \cdot T^{-0.259}$ GPa, Poisson's ratio $\nu = 0.299 \cdot T^{0.0193}$.

The nonlinear analysis of the temperature in the contact zone is demonstrated in the Figure 5-7.

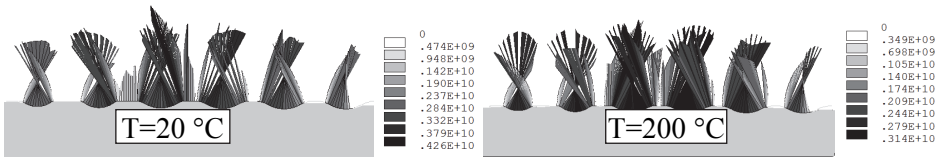

Fig. 5. Distribution of the contact pressure (MPa) for successive rings during the thread rolling process with round outline for various value of temperature
Rys. 5. Rozkład nacisków kontaktowych (MPa) dla kolejnych pierścieni rolki podczas procesu walcowania gwintów z okrągłym profilem dla różnych wartości temperatury

The results for contact pressure during the thread rolling process are shown on Fig. 5. We can observed that increase of the temperature of rolled materials decrease the value of contact pressure. The distribution of the displacement vector sum (1), m, maps of equivalent plastic total strain Huber-Mises-Hencky's (2), maps of equivalent total stress Huber-Mises-Hencky's, (3) after thread rolling process with round outline for temperature 20°C and 200°C we can observe respectively on Figs. 6 and

7. The value of displacement vector sum is still the same, but for strain and stress the value is smaller for higher temperature.

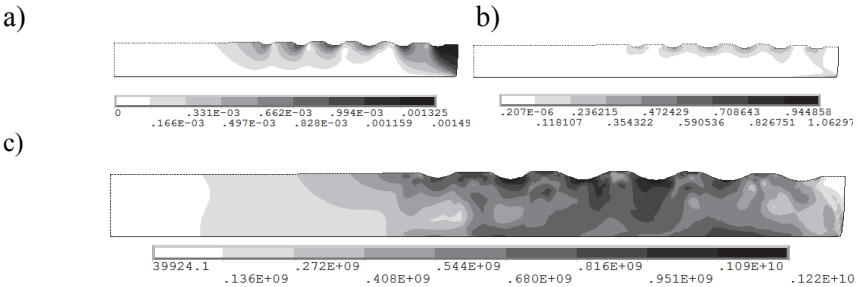

Fig. 6. Distribution of the displacement vector sum, m (a), maps of equivalent plastic total strain Huber-Mises-Hencky's (b), maps of equivalent total stress Huber-Mises-Hencky's, MPa (c) after thread rolling process with round outline for temperature 20°C

Rys. 6. Rozkład wektora przemieszczeń wypadkowych, m (a), mapa całkowitych plastycznych odkształceń zastępczych według hipotezy Hubera-Mises'a-Hencky'ego (b), mapa całkowitych naprężeń zastępczych według hipotezy Hubera-Mises'a-Hencky'ego, MPa (c) po procesie walcowania gwintów okrągłych dla temperatury 20°C

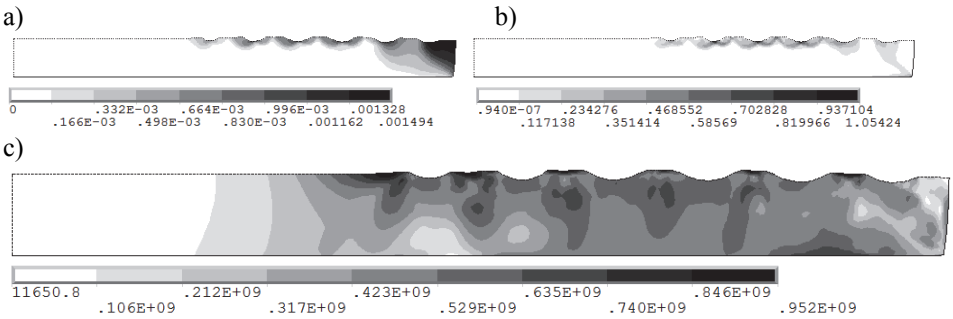

Fig. 7. Distribution of the displacement vector sum (a), m, maps of equivalent plastic total strain Huber-Mises-Hencky's (b), maps of equivalent total stress Huber-Mises-Hencky's, MPa (b) after round thread rolling process for temperature 200°C

Rys. 7. Rozkład wektora przemieszczeń wypadkowych (a) m, mapa całkowitych plastycznych odkształceń zastępczych według hipotezy Hubera-Mises'a-Hencky'ego (b), mapa całkowitych naprężeń zastępczych według hipotezy Hubera-Mises'a-Hencky'ego, MPa (c) po procesie walcowania gwintów okrągłych dla temperatury 200°C

From the environmental point of view must be increased rolling speed, since it reduces the processing time. In the figure 8 it shows the effect of rolling speed on the temperature field in object and tool for ideal contact and for the occurrence of thermal resistance and coefficient of friction $\mu_0 = 0.2$.

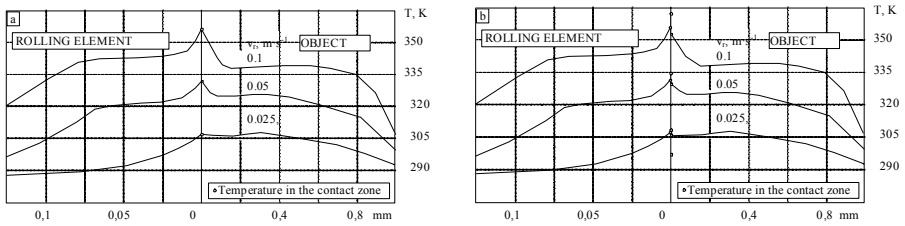

Fig. 8. Distribution of resultant temperature inside the roller and the object in axis z_2 for ideal contact (a) and with heat resistance in the surface contact (b)
Rys. 8. Rozkład wypadkowej temperatury wewnątrz rolki i na przedmiocie na osi z_2 dla idealnego kontaktu (a) oraz z opornością cieplną wewnątrz powierzchni kontaktu (b)

5. Experimental verification

Proposed in this paper a new way through the centerless rolling doesn't have the above drawbacks. The essence of this approach is to eliminate the fixed steady and the introduction of a system which contains four roller rolling surface (Fig. 9). The head is designed to conventional lathes and is fastened in place of the chuck. Head design allows for easy change of force and roller change (Kukiełka K. 2009, Kukiełka K. & Kukielka L. 2013, Kukiełka K. 2014, Kukiełka K. et al. 2014, Kukiełka K. 2016). In the working zone rolling fluid is given. The cyclic process of gradual loading, forming, calibrating and unloading is repeated until the desired length of thread is received. On the Fig 9. The real working head system during the thread rolling process is shown, where the temperature is measured by thermo visual hand camera made by Flir (Fig 9).

Figure 10 shows the temperature distributions during rolling of the pipes in the contact zone and outside it for different velocity rate, ie. $v = 0.025, 0.1\ m \cdot s^{-1}$. From conducted researches of measuring temperatures indicates the growth of rolling speed directly affects the growth of the temperature, the highest values is observed in the contact zone and after the roll-

ing process, that are the direct result of plastic deformation. For example, for a speed of $v = 0.025$ m·s^{-1} maximum measured temperature was 25.8°C, while the speed $v = 0.1$ m·s^{-1} reached value to 58.9°C.

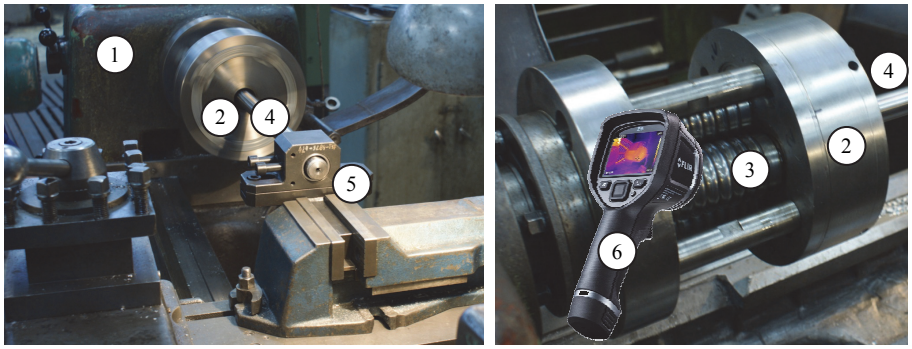

Fig. 9. Rolling system: 1 – conventional lathe, 2 – angular thread rolling head, 3 – rolling rolls, 4 – workpiece 5 – handle the workpieces in vice, 6 – manual thermal imaging camera Flir

Rys. 9. Układ obróbkowy: 1 – tokarka konwencjonalna, 2 – kątowa głowica do walcowania gwintów, 3– rolki walcujące, 4 – przedmiot obrabiany, 5 – uchwyt przedmiotu w imaku nożowym, 6 – ręczna kamera termowizyjna firmy Flir

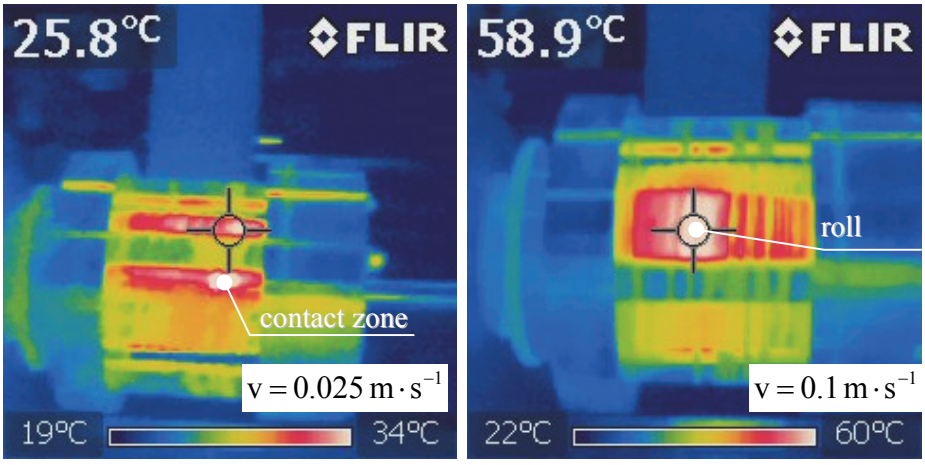

Fig. 10. The temperature distributions during rolling of the pipe for different velocity rate, ie. $v = 0.025, 0.1$ m·s^{-1}

Rys. 10. Rozkład temperatury podczas procesu walcowania rur dla różnych wartości prędkości, tj. $v = 0.025, 0.1$ m·s^{-1}

6. Conclusions

The presented method of numerical calculation of temperature fields is correct for any rolling conditions and the state of the output object and the history of his material. Using the application THREAD ROLLING it is possible to carry out a comprehensive analysis of thermal phenomena occurring during the thread rolling process. Can specify either the temperature distribution and the distribution of heat fluxes in the rolling zone for specified processing conditions, or conversely – for required temperature is possible to determined output state of the object and the conditions for implementation of rolling – include technological parameters (ie. velocity and depth of rolling).

The example shown illustrates how it affects the speed of rolling on temperature distribution, contact forces and the state of displacement, strain and stress in the object.

Application THREAD ROLLING in ANSYS system enables a complex time analysis of deformation (displacements, strains), forces, contact pressure, states of stresses and temperature occurring in object folding from a workpieces and a tool. It is possible to make a complete analysis for following data:

- any object geometry (eg. shaft, sleeve) and tools (an outline of the active surface, the number of rings, etc.)
- any material of workpieces and the tools material (Young's modulus, Poisson ratio, initial yield stress, tangent modulus, nonlinear dependence of the properties plastic materials: strain and strain rate, temperature and various models of hardening),
- different conditions of friction in the contact area,
- any horizontal and vertical movement of the tool in time.

The use of thread rolling process in place of the traditional methods of formulation through the loss of material gives a very large benefits in terms of environmental protection. Thread rolling process is carried out in about ten-fold less. In addition, the new processing technology is an innovation process and is a breakthrough character of technology because it replaces the machining method by plastic shaping threads. The use of traditional treatments produces waste in the form of chips sliced material,

dust, noise and waste coolant from machine tools – contaminated emulsion, which is hardly workable waste and require special disposal.

Additional benefits in terms of environmental protection resulting from the application of modern methods of production preparation, through the application of numerical simulation methods in place of the traditional long-term iterative process of reaching the required solution by experimental study.

References

Domblesk, J.P., Feng, F. (2002). Two-dimensional and three-dimensional finite element models of external thread rolling. *Professional Engineering Publishing*, *216(4)*, 507-517.

Jednovicky, B., Streit, J. (1998). *Cold volume treatment in market economy conditions*. Scientific-Technical Conference on Modern Cold Plastic Metalforming Technologies, Poznań- Kiekierz, 147-151. (in Polish).

Kaldunski, P., Kukielka, L., (2014). Numerical Analysis and Simulation of Drawpiece Forming Process by Finite Element Method, *Mechanics and Materials "Novel Trends in Production Devices and Systems", 474*, 153-158.

Kowalik, M., Rucki, M., Paszta, P., Gołębski, R. (2016). *Plastic deformations of measured object surface in contact with undeformable surface of measuring tool*. Measurement Science Review. *16*(*5)*, 254-259.

Kukiełka, K. (2009). *Modelling and numerical analysis of the states of deformations and stresses in the surface layer of the trapezoidal and round threads rolled on cold*. PhD Thesis, Koszalin University of Technology. (in Polish).

Kukiełka, K., Kukiełka, L. (2013). *External thread rolling head*. The polish patent No PL402652–A1, PL220175–B1, 4.02.2013. (in Polish).

Kukiełka, K. (2014). Effective numerical model to analyze the trapezoidal thread rolling process with finite element method. *Mechanik*, *11*, 156-167. (in Polish).

Kukielka, K., Kukielka, L., Bohdal, L., Kulakowska, A., Malag, L., Patyk, R. (2014). 3D Numerical Analysis the State of Elastic/Visco–Plastic Strain in the External Round Thread Rolled on Cold. *Applied Mechanics and Materials „Novel Trends in Production Devices and Systems", 474*, 436-441.

Kukielka, K. (2016). Ecological Aspects of the Implementation of New Technologies Processing for Machinery Parts. *Rocznik Ochrona Środowiska (Annual Set of Environment Protection)*, *18*, 137-157.

Kukielka, K. (2017). Ecological and economical aspects of modern modeling of thread rolling process. *Rocznik Ochrona Środowiska (Annual Set of Environment Protection)*, *19*.

Kukiełka, L. (1994). *Theoretical and experimental foundations of surface roller burnishing with the electrocontact heating*. Book WM nr 47. WSI Koszalin. (in Polish)

Kukielka, L. (1999). Application of the variational and finite element methods to dynamic incremental nonlinear analysis in the burnishing rolling operation. *ESM'99 - Modelling And Simulation A Tool For The Next Millennium*, Vol. II, 221-225.

Kukielka, L., Krzyzynski T. (2000). New thermo-elastic thermo-visco-plastic material model and its application. *Zeitschrift Fur Angewandte Mathematik Und Mechanik*, Vol. 80, supplement: 3, S595-S596.

Kukielka, L. (2001). Mathematical modelling and numerical simulation of nonlinear deformation of the asperity in the burnishing cold rolling operation. *Computational Methods in Contact Mechanics V, Book Series: Computational and Experimental Methods*, *5*, 317-326.

Kukiełka, L. (2002). *Bases of engineering research*. PWN, Warsaw. (in Polish).

Kukielka, L., Kustra, J., Kukielka, K. (2005). Numerical analysis of states of strain and stress of material during machining with a single abrasive grain. *Computer Methods and Experimental Measurements for Surface Effects and Contact Mechanics VII*, Southampton–Boston, WIT*PRESS*, 57-66.

Kukielka, L., Kukielka, K. (2006). Numerical analysis of the process of trapezoidal thread rolling. *High Performance Structures and Materials III*,. Southampton–Boston, WIT*PRESS*, 663-672.

Kukielka, L., Kukielka, K. (2007). Numerical analysis of the physical phenomena in the working zone in the rolling process of the round thread. *Computer Methods and Experimental Measurements for Surface Effects and Contact Mechanics VIII*, Southampton–Boston, WIT*PRESS,* 125-124.

Kukiełka, L. (2010). New damping of models of metallic materials and its application in non–linear dynamical cold processes of metal forming. *The 13th International Conference Metal Forming 2010*, *Steel Research International*, Toyohashi, *81*, 1482-1485.

Kukielka, L., Geleta, K., Kukielka, K. (2012). Modelling and Analysis of Nonlinear Physical Phenomena in the Burnishing Rolling Operation with Electrical Current. *Steel Research International, Special Edition: 14th International Conference Metal Forming*, Kraków, 1379-1382.

Kukielka, L., Geleta, K., Kukielka, K. (2012). Modelling of Initial and Boundary Problems with Geometrical and Physical Nonlinearity and its Application in Burnishing Processes. *Steel Research International, Special Edition: 14th International Conference Metal Forming*, Krakow, 1375-1378.

Kukiełka, L., Kukiełka, K. (2012). The modern method of modeling and analysis precision machining processes auto parts. *Environmental aspects of the use of new technologies in transport, Book of Mechanical Engineering*, No 235 of Mechanical Faculty, Koszalin University of Technology. Koszalin, 109-128 (in Polish)

Kukiełka, L., Bohdal, Ł., Chodór, J., Forysiewicz, M., Geleta, K., Kałduński P., Kukiełka, K., Patyk, R., Szyc, M. (2012). Numerical analysis of selected processes precision machining of automotive parts. *Environmental aspects of the use of new technologies in transport, Book of Mechanical Engineering No 235 of Mechanical Faculty*, Koszalin University of Technology, Koszalin, 129-194.

Kukielka, L., Kukielka, K., Kulakowska, A., Patyk, R., Malag, L., Bohdal, L. (2014). Incremental Modelling and Numerical Solution of the Contact Problem between Movable Elastic and Elastic/Visco–Plastic Bodies and Application in the Technological Processes. *Applied Mechanics and Materials "Novel Trends in Production Devices and Systems", 474*, 159-165.

Kukiełka, L., Kukiełka, K. (2015). Modelling and analysis of the technological processes using finite element method. *Mechanik, 88*, 317-340.

Kukielka, L., Szczesniak, M., Patyk, R., Kulakowska, A., Kukielka, K., Patyk S., Gotowala, K., Kozak, D. (2016). Analysis of the states of deformation and stress in the surface layer of the product after the burnishing cold rolling operation. *Novel Trends in Production Devices and Systems "Materials Science Forum"*.

Kulakowska, A., Patyk, R., Kukielka, L. (2009). Numerical analysis and experimental researches of burnishing rolling process of workpieces with real surface. *WMSCI 2009 – The 13th World Multi–Conference on Systemics, Cybernetics and Informatics, Jointly with the 15th International Conference on Information Systems Analysis and Synthesis, ISAS, 2*, 63-68.

Kulakowska, A., Kukielka, L., Kukielka, K., Malag, L., Patyk, R., Bohdal, L. (2014). Possibility of steering of product surface layers properties in burnishing rolling process. *Applied Mechanics and Materials "Novel Trends in Production Devices and Systems", 474*, 442-447.

Kusnerova, M., Valicek, J., Harnicarova, M., Hryniewicz, T., Rokosz, K., Palkova, Z., Vaclavik, V., Repka, M., Bendova, M. (2013). A Proposal for Simplifying the Method of Evaluation of Uncertainties in Measurement Results. *Measurement Science Review*, *13(1)*, 1-6.

Łyczko, K. (2010). *External thread rolling technology*. WNT, Warszawa. (in polish).

Malag, L., Kukielka, L., Kukielka, K., Kulakowska, A., Patyk, R., Bohdal, L. (2014). Problems Determining of the Mechanical Properties of Metallic Materials from the Tensile Test in the Aspect of Numerical Calculations of the Technological Processes. *Applied Mechanics and Materials "Novel Trends in Production Devices and Systems", 474*, 454-459.

Nadolny, K., Plichta, J., Sutowski, P. (2014). Regeneration of grinding wheel active surface using high-pressure hydro-jet. *Journal Of Central South University*, *21(8)*, 3107-3118.

Olszak, W. (2008). *Machining*. WNT, Warszawa. (in polish)

Patyk, R., Kukielka, L. (2008). Optimization of geometrical parameters of regular triangular asperities of surface put to smooth burnishing. *The 12th International Conference Metal Forming 2008, Steel Research International,* Kraków, *2*, 642-647.

Patyk, R. (2010). Theoretical and experimental basis of regular asperities about triangular outline embossing technology. *The 13th International Conference Metal Forming 2010, Steel Research International*, Toyohashi, *81*, 190-193.

Patyk, R., Kukielka, L., Kukielka, K., Kulakowska, A., Malag, L., Bohdal, L. (2014). Numerical Study of the Influence of Surface Regular Asperities Prepared in Previous Treatment by Embossing Process on the Object Surface Layer State after Burnishing. *Applied Mechanics and Materials "Novel Trends in Production Devices and Systems"*, *474*, 448-453.

Perec, A. (2016). *Abrasive suspension water jet cutting optimization using orthogonal array design*. International Conference on Manufacturing Engineering and Materials, ICMEM 2016,6-10 June 2016, Nový Smokovec. Procedia Engineering, *149*, 366-373.

Perec, A., Pude, F., Stirnimann, J., Wegener, K. (2015). *Feasibility study on the use of fractal analysis for evaluating the surface quality generated by waterjet*. Tehnički vjesnik, *22*, 4, 879-883.

Rokosz, K., Hryniewicz, T. (2016). *XPS Analysis of nanolayers obtained on AISI 316L SS after Magnetoelectropolishing*. World Scientific News, *37*, 232-248.

Skoczylas, A., Zaleski, K. (2015). Effect of Plasma Cutting Parameters upon Shapes of Bearing Curve of C45 Steel Surface. *Advances in Science and Technology Research Journal, 9(27)*, 78-82.

Staniszewski, B. (1980). *Heat transfer*. PWN, Warsaw.

Sutowski, P., Nadolny, K. (2016). The identification of abrasive grains in the decohesion process by acoustic emission signal patterns. *International Journal Of Advanced Manufacturing Technology*, *87(1-4)*, 437-450.

Valicek, J., Drzik, M., Hryniewicz, T., Harnicarova M., Rokosz K, Kusnerova M., Barcova K., Brazina D. (2012). Non-Contact Method for Surface Roughness Measurement After. Machining. *Measurement Science Review*, *12(5)*, 184-188.

Zaleski, K., Bławucki, S. (2015). Evaluation of the Effectiveness of the Shot Peening Process for Thin-Walled Parts Based on the Diameter of Impression Produced by the Impact of Shot Media. *Advances in Science and Technology Research Journal, 9(26)*, 77-82.

Symulacje numeryczne procesu walcowania gwintów jako ekologiczne i ekonomiczne narzędzie badawcze w procesie wdrażania nowoczesnych technologii

Streszczenie

W pracy przedstawiono sposób rozwiązywania dyskretnego równania ruchu ciepła w obiekcie podczas procesu walcowania gwintów przy wykorzystaniu metod jawnego i niejawnego całkowania. Zamieszczono przykładowe wyniki analiz numerycznych dla procesu walcowania gwintów w programie ANSYS. Pokazano również rozkłady temperatur dla różnych wartości prędkości walcowania.

Abstract

In the this paper the solutions of discrete equations of the heat transfer of the object in the thread rolling process with applied explicit and implicit integrations methods, were shown. Examples of simulations of the rolling process in ANSYS programs are presented. Also the temperature distributions for various value of rolling velocity were shown.

Słowa kluczowe:
walcowanie gwintów, eko-modelowanie, ekologiczne procesy technologiczne, sformułowanie wariacyjne, metoda elementów skończonych

Keywords:
thread rolling, eco-modelling, ecological technological process, variational formulation, Finite Element Method

MIDDLE POMERANIAN SCIENTIFIC SOCIETY OF THE ENVIRONMENT PROTECTION
ŚRODKOWO-POMORSKIE TOWARZYSTWO NAUKOWE OCHRONY ŚRODOWISKA

Annual Set The Environment Protection
Rocznik Ochrona Środowiska

Volume/Tom 19. Year/Rok 2017 ISSN 1506-218X 181-199

Microbiological Contamination of Water in Fountains Located in the Ciechocinek Health Resort

Katarzyna Budzińska, Natalia Pyrc, Bożena Szejniuk, Rafał Pasela, Adam Traczykowski, Magdalena Michalska, Krzysztof Berleć
University of Science and Technology, Bydgoszcz

1. Introduction

Municipal fountains, normally situated in parks and city centres, play mainly a recreational role for people, but they also serve as a habitat and watering place for birds and other animals. Shared use of fountains by animals and people may be conducive to the spread of pathogens and hazardous to the health and life of human beings (Biedunkiewicz 2009). Unlimited access to fountains often encourages people to use them for bathing as well, which leads to an enormous sanitary hazard (Burkowska-But et al. 2013, Eisenstein et al. 2008). Fountain water is characterised by a very good oxygenation and is not subject to disinfection, which is conducive to the growth of pathogens. Microorganisms detected in fountain water include coliform bacteria, staphylococci, streptococci, bacteria of genus *Salmonella* and microscopic fungi (Kirian et al. 2008). Their presence causes mainly gastrointestinal and skin infections (Minshew et al. 2000). Water particles carried by wind form the so-called water-air aerosol, which has the long-awaited soothing effect in summer. However, the aerosol may spread microbiological contamination, including the hazardous *Legionella* spp. bacteria. Inhalation of contaminated aerosol may cause the bacteria penetration into the lungs and may cause the respiratory disease called the Legionnaires' disease (Haupt et al. 2012). The lifespan of pathogens in the environment is generally sufficiently long to

pose a potential threat of spreading diseases by water. The viability of microorganisms in water depends on the type of microorganism and physical and chemical conditions and it may range from several days to several months (Szejniuk et al. 2013). Due to the fact that there are no legal regulations in Poland concerning the sanitary requirements for water from the fountains, it is justified to quote data concerning water used for recreational purposes. Therefore, the quality of water and air around such facilities is crucial for patients who use the fountains. Furthermore, the water is not legally subject of sanitary and epidemiological inspections. The facilities are not examined regularly, while sporadic water analyses are based on the requirements specified in the Regulation of the Minister of Health of 8 April 2011 on the water quality supervision in bathing facilities (Dz.U. 2011 no 86 item 478). The report entitled "Surveillance for Waterborne Disease Outbreaks and Other Health Events Associated with Recreational Water" indicates that between the years 2007 and 2008 in 38 countries a total of 134 recreational water epidemics were recorded that led to at least 13.966 disease cases. More than 60% of them involved gastrointestinal tract disorders, 18% – skin infections, and ca. 13% – respiratory system diseases. Their major epidemiological factors were parasites (64.5%), bacteria (21.0%), viruses (4.8%), chemical substances used (8.6%) and synergic impact of several factors (1.0%) (Office of Surveillance, Epidemiology, and Laboratory Services, Centers for disease control and prevention (CDC), U.S. Department of health and human services, 2011). Fountains located in health resorts frequently serve as therapeutic waters intended for recreational and balneological purposes (Walczak & Lalke-Porczyk 2011).

Conducted research aimed at the assessment of the degree of bacterial and fungal contamination of water samples taken from fountains located in the Ciechocinek health resort from the perspective of biosafety of tourists and patients.

2. Material and methods

2.1. Water sampling

Water samples for testing were taken from four fountains located in the Ciechocinek health resort in the Kujawsko-Pomorskie Province. Fountain A "Jaś i Małgosia" is the most famous fountain in Ciechocinek

situated in the central part of the "Park Zdrojowy". Fountain B "Żaba" is located at the medicinal water pump room in the "Park Zdrojowy". Fountain C "Grzybek" in the city centre serves as a natural inhalatorium due to the properties of brine water. Fountain D "Windsor 600" is the newest fountain located at the famous Hellwig Promenade in Ciechocinek. Closed circulation of water and mechanical filtration was applied in all fountains. Surface of water for individual fountains is respectively: A – 29.21 m^2; B – 66.15m^2; C – 66.60m^2; D – 23.32m^2. It attracts particular attention among tourists, because of its water jet that changes every several minutes. The research was conducted during the period from June to October 2014 in 7 research series. Water samples from individual fountains were taken to sterile glass 1000 ml bottles according to standard PN-EN ISO 19458:2007. The bottles were filled to the ¾ of their volume. Samples were transferred to the laboratory of the Department of Animal Hygiene and Microbiology of the Environment at University of Science and Technology in Bydgoszcz, where, on the same day. A total count of bacteria and fungi, a count of coliform bacteria, *Escherichia coli*, and a count of faecal staphylococci and streptococci were determined in the samples tested.

2.2. Microbiological contamination determination procedure

The sanitary analysis of fountain waters included:

- determination of total mesophilic bacteria count incubated at temperature 37°C during 24 hours on nutrient agar, according to the Polish standard PN-EN-ISO 8199:2010;
- determination of coliform bacteria count on Endo agar and *Escherichia coli* on Tergitol®7 agar with TTC, incubated at temperature 37°C during 24 hours, according to the standard PN-EN-ISO 9308-1:2004;
- determination of enterococci on agar with kanamycin, aesculin and azide, incubated at temperature 37°C during 24-48 hours, according to the Polish standard PN-ISO 7899-2: 2004;
- determination of staphylococci on Chapman agar, incubated at temperature 37°C during 24-48 hours, according to the standard PN-Z-11001-3:2000;
- determination of total fungi count on Sabouraud dextrose agar with chloramphenicol, incubated at temperature 26°C during 5-7 days, according to the Polish standard PN-EN-ISO 8199:2010.

The determination of a total count of mesophilic bacteria and a total count of fungi in the water samples was conducted by using plate method and surface culture technique. In order to detemine total bacterial and fungi count by usage of plate method, a series of decimal dilutions were performed in the range from 10^{-1} to 10^{-4} with condiseration of estimated degree of microbiological contamination in taken samples. The plate method results were read from plates taken from two consecutive dilutions, which demonstrated growth of 15-300 colonies of bacteria and 10-150 colonies of fungi.

The final result expressed in colony forming units (cfu) in a 1 ml of sample was calculated using the following formula:

$$L = \left[\frac{C}{(N_1+0{,}1N_2)\cdot d}\right] \cdot a \quad (1)$$

where:
L – a total count of bacteria or fungi (cfu in 1 ml), C – a total colony count on plates selected for counting, N_1 – number of plates of the first counted dilution, N_2 – number of plates of the second counted dilution, d – dilution factor corresponding to the first counted dilution, a – volume factor of culture material.

For the quantitative determination of coliform bacteria, *Escherichia coli*, staphylococci and streptococci, the membrane filter technique was used. Sterile cellulose ester filters with 0.45 μm pores were used in the tests. The first stage involved dilutions 10^{-1} of water samples. Then occurred filtration of 100 ml undiluted and diluted 10^{-1} water samples, filtered in three repetitions. Following the filtration of a water sample, the filter with retained microorganisms was transferred to a Petri dish with appropriate solid medium. Final result of determination was obtained through counting characteristic colonies that grew on the surface of the filter and taking into account the dilution factor; the result was expressed in cfu/100 ml.

The results of microbiological tests in a logarithmic form were calculated using the Microsoft Excel 2007 program. For calculating the basic statistical data, the Statistica 2010 program was used.

3. Results and discussion

Tests results regarding microbiological contamination of fountain water in the Ciechocinek health resort are presented in Tables 1-6 and Figures 1-6. Throughout the period of testing, the total bacteria count in research series from individual fountains ranged on average from $2.86 \cdot 10^2$ to $5.17 \cdot 10^2$ cfu/ml (Table1). Microorganisms were the most abundant in water taken from fountain B, while their lowest amount was isolated from water samples taken from fountain D, with the difference between the two results amounted to 0.24 log cfu/ml (Fig. 1). Research by Burkowska-But et al. (2013) indicates that the population size of mesophilic bacteria in water samples taken from fountains ranged from $5.0 \cdot 10^0$ to $1.52 \cdot 10^3$ cfu/ml. Furthermore, Burkowska & Donderski (2007) have found that the bacteria may enter air in the form of water aerosol, with their count ranging from 0 to $1.3 \cdot 10^3$ cfu/m^3 depending on the month. However, the mesophilic bacteria content in air ranged from 23 to 566 cfu/m^3, with their highest concentration occurring in August (Burkowska et al. 2012). Szczygłowska et al. (2012) have found that the bacteria content in water-air aerosol reached $1.4 \cdot 10^3$ cfu/m^3, while in contaminated water the number was higher and amounted to $1.9 \cdot 10^4$ cfu/ml.

Table 1. Total number of bacteria (cfu/ml) in the water samples of investigated fountains
Tabela 1. Ogólna liczba bakterii (jtk/ml) w próbkach wody z badanych fontann

Research series	Object			
	A	B	C	D
1	$2.64 \cdot 10^2$	$5{,}91 \cdot 10^2$	$2{,}64 \cdot 10^2$	$2.82 \cdot 10^2$
2	$4.73 \cdot 10^2$	$7.18 \cdot 10^2$	$1{,}81 \cdot 10^2$	$2.27 \cdot 10^2$
3	$8.55 \cdot 10^2$	$6.55 \cdot 10^2$	$5{,}73 \cdot 10^2$	$2.09 \cdot 10^2$
4	$3.27 \cdot 10^2$	$5.64 \cdot 10^2$	$3{,}55 \cdot 10^2$	$3.27 \cdot 10^2$
5	$4.91 \cdot 10^2$	$2.73 \cdot 10^2$	$4{,}09 \cdot 10^2$	$3.18 \cdot 10^2$
6	$4.36 \cdot 10^2$	$4.90 \cdot 10^2$	$3{,}36 \cdot 10^2$	$2.73 \cdot 10^2$
7	$6.45 \cdot 10^2$	$3.27 \cdot 10^2$	$2, 82 \cdot 10^2$	$3.64 \cdot 10^2$
Mean	$4.99 \cdot 10^2$	$5.17 \cdot 10^2$	$3{,}43 \cdot 10^2$	$2.86 \cdot 10^2$

Fungi were also identified in the water samples taken from the relevant municipal fountains (Table 2). Their highest mean count of $1.8 \cdot 10^3$ cfu/ml was recorded for fountain D, while the lowest for fountain B ($2.75 \cdot 10^2$ cfu/ml).

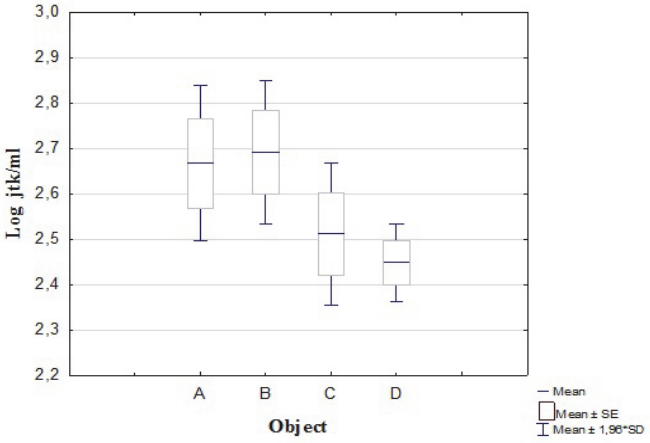

Fig. 1. Average number of bacteria in the water from individual fountains
Rys. 1. Średnia liczba bakterii w wodzie z poszczególnych fontann

In the water samples taken from fountain A, the mean fungi count amounted to $1.3 \cdot 10^3$ cfu/ml, while the water samples from fountain C contained $1.6 \cdot 10^3$ cfu/ml of these microorganisms. It must be noted that for all the fountains analysed, there were samples that did not contain any fungi at all. As the data presented in Figure 2 demonstrate, the largest difference in the total fungi count was recorded between fountain A and fountain B, while a similar count was found in the water samples taken from fountain C and fountain D. It should be noted that the water originating from all fountains was not deprived of spores of fungi, even the water taken from fountain "Grzybek" (C), which had highest degree of salinity, which exceeded 4,51%. Similar results were conducted by Biedunkiewicz (2009), who found a significant fungal contamination of fountain water, demonstrating that 14 out of 60 water samples taken from five municipal fountains contained microfungi. Among them, there were four species of mould fungi (*Aspergillus fumigatus*, *Aspergillus niger*, *Syncephalastrum racemosum* and *Trichoderma viridae*) and 23 species of yeast-like fungi, where *Candida* was the dominating genus (34.78%). During the research, none of the fountains was found to be completely free from fungal contamination (Biedunkiewicz 2009).

Fungal spores may also be present in water-air aerosol. Szczygłowska et al. (2012) argues that their population in air is higher

than that of bacteria and amounts to $5.3 \cdot 10^2$ cfu/m^3. On the other hand, research conducted by Burkowska & Donderski (2006) demonstrates that the highest amount of mould fungi in bioaerosol is reported in June (2600 cfu/m^3). Research by Burkowska-But et al. (2013) shows that bio-indicators of faecal contamination were found in the water of 74% of fountains examined.

Table 2. Total number of fungi (cfu/ml) in the water samples from individual fountains
Tabela 2. Ogólna liczba grzybów (jtk/ml) w próbkach wody z poszczególnych fontann

Research series	Object			
	A	B	C	D
1	$3.36 \cdot 10^2$	$1.09 \cdot 10^2$	$4.55 \cdot 10^2$	$3.00 \cdot 10^2$
2	0	0	$0.45 \cdot 10^0$	0
3	$9.09 \cdot 10^2$	$9.09 \cdot 10^2$	$9.09 \cdot 10^2$	$2.73 \cdot 10^3$
4	0	0	0	0
5	$4.55 \cdot 10^3$	0	9.09×10^3	$9.09 \cdot 10^3$
6	$5.73 \cdot 10^2$	0	7.27×10^2	$4.73 \cdot 10^2$
7	$2.73 \cdot 10^3$	$9.09 \cdot 10^2$	0	0
Mean	$1.30 \cdot 10^3$	$2.75 \cdot 10^2$	$1.60 \cdot 10^3$	$1.80 \cdot 10^3$

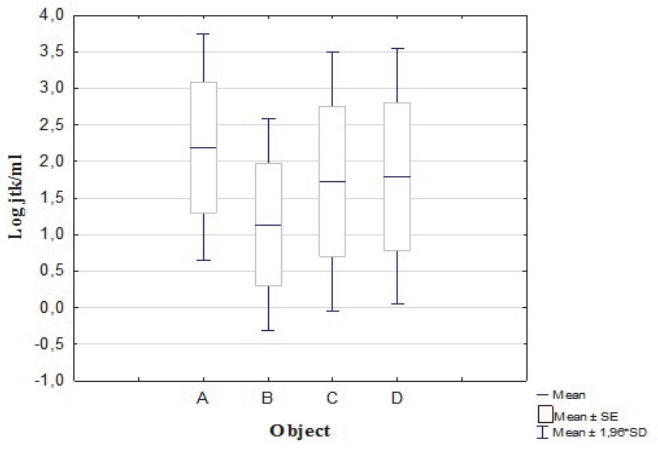

Fig. 2. Mean number of fungi in the water from individual fountains
Rys. 2. Średnia liczba grzybów w wodzie z poszczególnych fontann

Table 3. Number of faecal streptococci (cfu/100 ml) in the water from individual fountains
Tabela 3. Liczebność paciorkowców kałowych (jtk/100 ml) w wodzie z poszczególnych fontann

Research series	Object			
	A	B	C	D
1	0	$2.00 \cdot 10^0$	0	$6.00 \cdot 10^0$
2	$1.20 \cdot 10^1$	$2.50 \cdot 10^1$	0	$1.00 \cdot 10^0$
3	$1.40 \cdot 10^1$	$2.97 \cdot 10^1$	$7.00 \cdot 10^0$	$1.07 \cdot 10^1$
4	$8.67 \cdot 10^0$	0	0	0
5	$1.00 \cdot 10^0$	$1.33 \cdot 10^0$	0	$3.17 \cdot 10^1$
6	0	$2.50 \cdot 10^0$	$6.00 \cdot$	$1.03 \cdot 10^1$
7	0	$5.00 \cdot 10^0$	0	$4.33 \cdot 10^0$
Mean	$5.10 \cdot 10^0$	$9.36 \cdot 10^0$	$1.86 \cdot 10^0$	$9.14 \cdot 10^0$

Own studies indicate that the number of faecal streptococci in the water samples was relatively low (Table 3). Mean amount of these bacteria in the water samples from fountain B was $9.36 \cdot 10^0$ cfu/100 ml and was higher by only 0.22 cfu than the amount isolated from the samples taken from fountain D. The water samples from fountain A were characterised by the presence of faecal streptococci amounting to $5.10 \cdot 10^0$ cfu/100 ml. The water samples from fountain C contained the least amount of these bacteria ($1.86 \cdot 10^0$ cfu/100 ml). A maximum number of faecal streptococci was identified in research series 5 from fountain D ($3.17 \cdot 10^1$ cfu/100 ml). In samples number 4 from fountain B and D and in most of the water samples from fountain C, those bacteria were not found (Table 3). Figure 3 demonstrates the occurrence of faecal streptococci in the water samples taken from individual fountains. As the data indicate, the largest differences regarding the population of those microorganisms were between water samples taken from fountain B and C. Burkowska-But et al. (2013) demonstrate that the content of faecal streptococci in water samples taken from fountains ranged from $3.6 \cdot 10^1$ cfu/ml to $1.99 \cdot 10^3$ cfu/ml. The ratio of the amount of *E. coli* to the number of faecal streptococci FC/FS indicates contamination of animal origin in 3/4 of the fountains examined. According to Hoebe et al. (2004), the number of faecal streptococci in similar facilities amounts to an average of $3.5 \cdot 10^3$ cfu/100 ml. However, Flores et. al. (2013) argue

that the amount of enterococci in fountain water reaches an average of $4.10 \cdot 10^0$ cfu/100 ml. There are two species dominating in this genus: *Enterococcus faecium* and *E. faecalis*. Own studies indicate that the number of faecal streptococci in the water samples ranged from $1.86 \cdot 10^0$ to $9.14 \cdot 10^0$ cfu/100 ml.

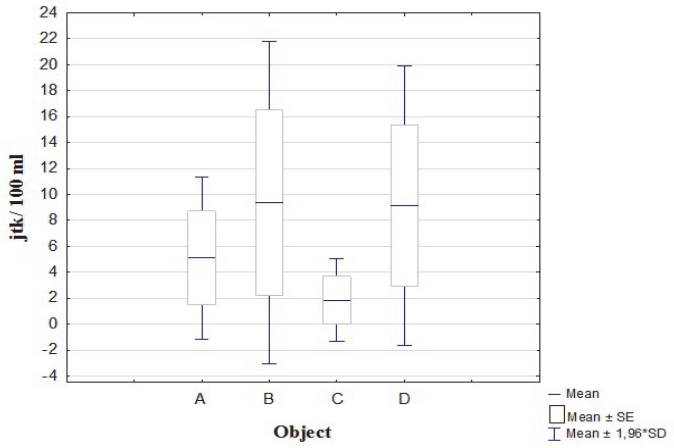

Fig. 3. Occurrence of faecal streptococci in the water from individual fountains
Rys. 3. Występowanie paciorkowców kałowych w wodzie pochodzącej z poszczególnych fontann

The occurrence of coliform bacteria in the water samples taken from the relevant fountains shows Table 4. During the entire period of research, the mean number of coliform bacteria in the water samples ranged from $0.29 \cdot 10^0$ cfu/100 ml to $7.10 \cdot 10^0$ cfu/100 ml. The highest amount of those bacteria was determined in research series 6 from fountain D ($2.27 \cdot 10^1$ cfu/100 ml). The highest frequency of occurrence of coliform bacteria was found for the water samples taken from fountain A, while within the entire period of research regarding the water samples taken from fountain C, only research series 5 contained those bacteria, the amount of which was 2 cfu in 100 ml of water. Figure 4 shows the distribution of coliform bacteria population in the water samples, with their sampling point indicated. The results obtained indicate that the highest differences in the number of coliform bacteria occurred between the water samples taken from fountain C and D.

Table 4. Occurrence of coliform bacteria (cfu/100 ml) in water from individual fountains
Tabela 4. Występowanie bakterii z grupy coli (jtk/100 ml) w wodzie z poszczególnych fontann

Research series	Object			
	A	B	C	D
1	$3.00 \cdot 10^0$	$1.10 \cdot 10^1$	0	$1.00 \cdot 10^1$
2	0	$4.00 \cdot 10^0$	0	0
3	$6.00 \cdot 10^0$	$2.00 \cdot 10^0$	0	0
4	$2.00 \cdot 10^0$	0	0	0
5	$1.47 \cdot 10^1$	$1.10 \cdot 10^1$	$2.00 \cdot 10^0$	$1.70 \cdot 10^1$
6	$1.00 \cdot 10^1$	$8.00 \cdot 10^0$	0	$2.27 \cdot 10^1$
7	$3.67 \cdot 10^0$	0	0	0
Mean	$5.62 \cdot 10^0$	$5.15 \cdot 10^0$	$0.29 \cdot 10^0$	$7.10 \cdot 10^0$

The water samples taken from the fountains contained an average of $9.0 \cdot 10^1$ cfu/100 ml to $2.5 \cdot 10^4$ cfu/100 ml of coliform bacteria, with the population of *E. coli* ranging from 0 to $1.96 \cdot 10^3$ cfu/100 ml (Burkowska-But et al. 2013). However, according to Hoebe et al. (2004), the population of coliform bacteria in fountain water amounts to $1.0 \cdot 10^3$ cfu/ml, while the number of *E. coli* reaches $7.7 \cdot 10^3$ cfu/100 ml. According to Fleming et al. (2000) the amount of *E. coli* in water was $5.0 \cdot 10^0$ cfu/100 ml. However, Flores et. al. (2013) detected *E. coli* in 13 fountains located in Porto (Portugal) a mean population these bacteria amounted to $3.52 \cdot 10^2$ cfu/100 ml. There were $2.1 \cdot 10^3$ cfu/ml of coliform bacteria in the water taken from an interactive fountain, with a mean population of *E. coli* amounting to 40 cfu/ml (Jones et al., 2006). Research by Roscoe et al. (2000) indicates that the water samples taken from fountains contained more than $4.8 \cdot 10^1$ cfu/100 ml of coliform bacteria. The highest number of these bacteria was more than $8.0 \cdot 10^1$ cfu/100 ml. Research by Sezen et al. (2012) indicates that the water samples contained from $3.8 \cdot 10^1$ to $3.0 \cdot 10^2$ cfu/100 ml of coliform bacteria. The number of *E. coli* ranged from 2.2 x 10^1 to $1.0 \cdot 10^2$ cfu/100 ml. Fernández et al. (2002) detected coliform bacteria and *E. coli* respectively in 75% and 49% of samples taken from five fountains located in Guadalajara (Mexico). Research by Hlavsa et al. (2014) confirms that *E. coli* occur also in recreational water in the USA. The use of treated water led to the infections with the strain *E. coli* O157:H7 – 14 cases were

reported. The contact with untreated water, on the other hand, caused infections in 17 people.

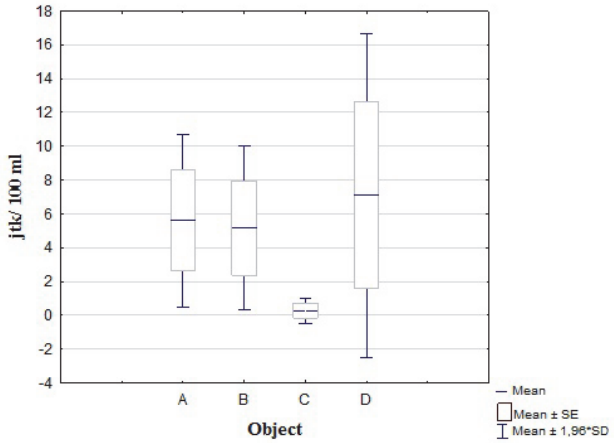

Fig. 4. Mean population of coliform bacteria isolated from water from individual fountains
Rys. 4. Średnia liczebność bakterii z grupy coli wyizolowana z wody z poszczególnych fontann

Table 5 demonstrates research findings regarding the occurrence of *Escherichia coli* isolated from the water samples taken from individual fountains.

Table 5. Number of *Escherichia coli* (cfu/100 ml) in the water from individual fountains
Tabela 5. Liczebność bakterii *Escherichia coli* (jtk/100 ml) w wodzie z poszczególnych fontann

Research series	Object			
	A	B	C	D
1	$3.00 \cdot 10^0$	$6.00 \cdot 10^0$	0	$8.00 \cdot 10^0$
2	0	$3.90 \cdot 10^0$	0	0
3	$3.00 \cdot 10^0$	$1.00 \cdot 10^0$	0	0
4	$2.00 \cdot 10^0$	0	0	0
5	$1.17 \cdot 10^1$	$1.10 \cdot 10^1$	$1.00 \cdot 10^0$	$1.20 \cdot 10^0$
6	$9.00 \cdot 10^0$	$7.67 \cdot 10^0$	0	$2.03 \cdot 10^1$
7	$1.50 \cdot 10^0$	0	0	0
Mean	$4.31 \cdot 10^0$	$4.22 \cdot 10^0$	$0.14 \cdot 10^0$	$5.76 \cdot 10^0$

The mean amount of these bacteria in the water samples taken from fountain D was $5.76 \cdot 10^0$ cfu/100 ml, which was more than 40 times higher than the mean population of these microorganisms isolated from the water taken from fountain C ($0.14 \cdot 10^0$ cfu/100 ml). Water samples taken from fountains A and B had similar content of *E. coli,* which amounted to respectively $4.31 \cdot 10^0$ cfu/100 ml and $4.22 \cdot 10^0$ cfu/100 ml. The highest amount of *Escherichia coli* was determined in research series 6 taken from fountain D ($2.03 \cdot 10^1$ cfu/100 ml). The highest frequency of the occurrence of the *E. coli* bacilli was recorded in fountain A, while they occurred once in research series 5 taken from fountain C Figure 5 demonstrates the occurrence of *E. coli* in water samples taken from individual fountains. Similar to other microorganisms, the highest discrepancies in their amount occurred in fountains C and D. Own studies demonstrate that the least number of coliform bacteria and *E. coli* was found in fountain C, where 4.51% brine water was used. Considering the fact that brine is used for medicinal purposes in Poland, there is insufficient data on the sanitary and hygiene condition of these waters. It is presumed that salt has negative effect on the growth and viability of microorganisms. Previous research indicated that *E. coli* occurred in brine water within the Ciechocinek spa resort and their content ranged from 10 to 140 cfu/ml (Walczak & Lalke-Porczyk 2011).

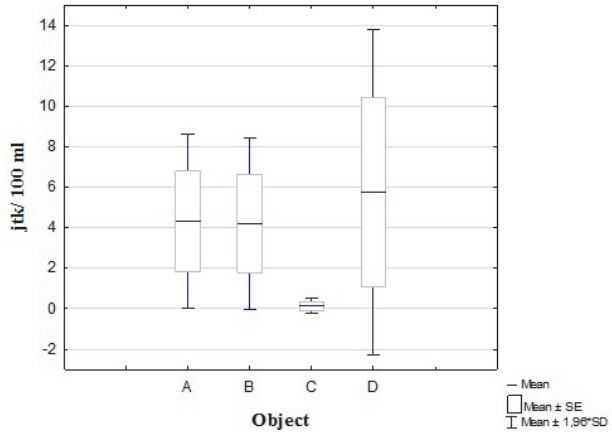

Fig. 5. Mean number of *E. coli* isolated from water from individual fountains
Rys. 5. Średnia liczebność bakterii *E. coli* wyizolowana z wody z poszczególnych fontann

Table 6 demonstrates research findings regarding the occurrence of staphylococci isolated from the water samples taken from individual fountains. The mean population of staphylococci in the water samples taken from fountains ranged from $1.88 \cdot 10^1$ to $3.85 \cdot 10^1$ cfu/100 ml. The water samples taken from fountain A contained an average of $3.25 \cdot 10^1$ cfu/100 ml, while from fountain B – $3.85 \cdot 10^1$ cfu/100 ml. The highest number of staphylococci during the entire research period was determined in water research series 3 taken from fountain D ($7.9 \cdot 10^1$ cfu/100 ml), while in water in research series 1 taken from fountains A and C and in research series 6 from fountain B, no such bacteria were found (Table 6).

Table 6. Number of staphylococci (cfu//100 ml) in water from individual fountains
Tabela 6. Liczebność gronkowców (jtk/100 ml) w wodzie z poszczególnych fontann

Research series	Object			
	A	B	C	D
1	0	$1.40 \cdot 10^1$	0	$2.90 \cdot 10^1$
2	$6.65 \cdot 10^1$	$5.00 \cdot 10^1$	$1.03 \cdot 10^1$	$1.30 \cdot 10^1$
3	$4.50 \cdot 10^1$	$6.12 \cdot 10^1$	$9.82 \cdot 10^0$	$7.90 \cdot 10^1$
4	$4.67 \cdot 10^0$	$5.04 \cdot 10^1$	$1.65 \cdot 10^1$	$2.47 \cdot 10^1$
5	$3.13 \cdot 10^1$	$6.33 \cdot 10^1$	$1.70 \cdot 10^1$	$4.07 \cdot 10^1$
6	$5.37 \cdot 10^1$	0	$7.50 \cdot 10^1$	$3.67 \cdot 10^1$
7	$2.63 \cdot 10^1$	$2.97 \cdot 10^1$	$3.00 \cdot 10^0$	$2.43 \cdot 10^1$
Mean	$3.25 \cdot 10^1$	$3.85 \cdot 10^1$	$1.88 \cdot 10^1$	$3.53 \cdot 10^1$

Figure 6 demonstrates the distribution of staphylococci population in the water samples, with their sampling point indicated. The data indicate that the highest differences were observed staphylococci identified in the water samples taken from fountain B and C. Burkowska & Donderski (2006) confirm that they are also present in water-air aerosol generated by fountains, with their mean amount reaching 140 cfu/m^3. At the same time, the researchers pointed out that the highest amount of those microorganisms occurred during the holiday season (Burkowska & Donderski, 2007).

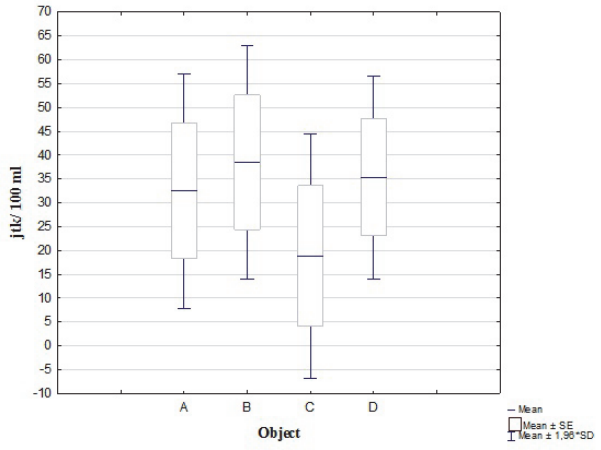

Fig. 6. Mean number of staphylococci in water from individual fountains
Rys. 6. Średnia liczebność gronkowców w wodzie z poszczególnych fontann

Own studies demonstrate that also in this case, the least number of staphylococci was found in fountain C (Table 6), which used brine water ($1.88 \cdot 10^1$ cfu/100 ml). Research conducted by Walczak & Lalke-Porczyk (2011) confirms that brine water from Ciechocinek does not contain *Staphylococcus aureus.*

4. Conclusions

1. The water from fountains located within the Ciechocinek health resort contained bacterial and fungal contamination, with microscopic fungi being the most abundant group, while the least contaminated was the water with highest degree of salinity.
2. Bioindicators, such as coliform bacteria, *Escherichia coli* and faecal streptococci, were found in the water samples taken from the fountains. The analyses also revealed the presence of mannitol positive staphylococci.
3. The microbiological contamination of water may pose a risk of diseases for people who use the fountains, that's why it is important to monitor the sanitary state of water originating from such sources.
4. The research indicated that it is necessary to monitor fountain water and introduce legal regulations regarding its sanitary and hygiene condition.

References

Biedunkiewicz, A. (2009). Microfungi of municipal fountains in environmental monitoring – an epidemiological threat. *Ochrona Środowiska i Zasoby Naturalne, 41,* 163-171.

Burkowska, A., Donderski, W. (2006). Wpływ otwartych inhalatoriów na mikrobiologiczny stan powietrza uzdrowiska Ciechocinek. *Acta Agraria et Silvestria. Series Agraria, 49*, 111-119.

Burkowska, A., Donderski, W. (2007). Bacterial pollution of air in health resort Ciechocinek. *Polish Journal of Natural Sciences, 22(4),* 633-644.

Burkowska, A., Kalwasińska, A., Walczak, M. (2012). Airborne mesophilic bacteria at the Ciechocinek health resort. *Polish Journal of Environmental Studies, 21(2)*, 307-3111.

Burkowska-But, A., Swiontek Brzezinska, M., Walczak, M. (2013). Microbiological contamination of water in fountains located in the city of Toruń. *Annals of Agricultural and Environmental Medicine, 20(4),* 645-648.

Dz.U. 2011 nr 86 poz. 478. *Rozporządzenie Ministra Zdrowia z dnia 8 kwietnia 2011 r. w sprawie prowadzenia nadzoru nad jakością wody w kąpielisku i miejscu wykorzystywanym do kąpieli.*

Eisenstein, L., Bodager, D., Ginzl, D. (2008). Outbreak of giardiasis and cryptosporidiosis associated with a neighborhood interactive water fountain – Florida, 2006. *Journal of Environmental Health, 71(3),* 18-22.

Fernández, E. E., Saldaña, L. J., Rodríguez, G. O., Cliver, D.O. (2002). Potential *Salmonella* transmission from ornamental fountains. *Journal of Environmental Health, 65(4),* 9-12, 22.

Fleming, C.A., Caron, D., Gunn, J.E., Horine, M.S., Matyas, B.T., Barry, M.A. (2000). An outbreak of *Shigella sonnei* associated with a recreational spray fountain. *American Journal Public Health, 90(10),* 1641-1642.

Flores C., Loureiro L., Bessa L., Martins da Costa P., 2013: Presence of multidrug-resistant *E.coli, Enterococcus spp*. and *Salmonella spp*. in lakes and fountains of Porto, Portugal. *Journal of Water Resource and Protection, 5(11),* 1117-1126.

Haupt, T.E., Heffernan, R.T., Kazmierczak, J.J., Nehls-Lowe, H., Rheineck, B., Powell, Ch., Leonhardt, K.K., Chitnis, A.S., Davis, J.P. (2012). An outbreak of legionnaires disease associated with a decorative water wall fountain in a hospital. *Infection Control & Hospital Epidemiology, 33(2),* 85-191.

Hlavsa, M.C., Roberts, V.A., Kahler, A.M., Hilborn, E.D., Wade, T.J., Backer, L.C., Yoder, J.S. (2014). Recreational water-associated disease outbreaks-United States, 2009-2010. *Morbidity and Mortality Weekly Report, 64(24),* 6-10.

Hoebe, C.J.P.A., Vennema, H., de Roda Husmna, A.M., van-Duynhoven, Y.T. (2004). Norovirus outbreak among primary schoolchildren who had played in a recreational water fountain. *The Journal of Infectious Diseases, 189(4),* 699-705.

Jones, M., Boccia, D., Kealy, M., Salkin, B., Ferrero, A., Nichols, G., Stuart, J.M. (2006). *Cryptosporidium* outbreak linked to interactive water feature, UK: importance of guidelines. *Eurosurveillance, 11(4-6),* 126-128.

Kirian, M.L., Merefillano, G., Gennette, D., Weintraub, J. M. (2008). Multi-jurisdictional investigation of interactive fountain associated cryptosporidiosis and salmonellosis outbreaks. *Epidemiology & Infection, 136(11),* 1547-1551.

Minshew, P., Ward, K., Mulla, Z., Hammond, R., Johnson, D., Heber, S., Hopkins, R. (2000). Outbreak of gastroenteritis associated with an interactive water fountain at a beachside park – Florida, 1999. *Morbidity and Mortality Weekly Report, 49(25),* 565-568.

Office of Surveillance, Epidemiology, and Laboratory Services, Centers for disease control and prevention (CDC), U.S. Department of health and human services, Atlanta, GA 30333, (2011). Surveillance for waterborne disease outbreaks and other health events associated with recreational water-United States, 2007-2008 and surveillance for waterborne disease outbreaks associated with drinking water – United States, 2007-2008. *Morbidity and Mortality Weekly Report, 60(12),* 1-75.

PN-EN ISO 19458:2007 (2007). *Pobieranie próbek wody do badań mikrobiologicznych*. Warszawa: Wydawnictwo PKN.

Roscoe, T., Sloan, D., Cooper, T., Morton, B., Hunter, I. (2000). A waterborne outbreak of Morbidity and Mortality Weekly Report Saintpaul. *Communicable Diseases Intelligence, 24(11),* 336-340.

Sezen, F., Aval, E., Agkurt, T., Yilmaz, Ş., Temel, F., Güleşen, R., Korukluoğlu, G., Sucakli, M.B., Torunoğlu, M.A. (2014). A large multi-pathogen gastroenteritis outbreak caused by drinking contaminated water from antique neighbourhood fountains, Erzurum city, Turkey, December 2012. *Epidemiology & Infection, 143(4),* 704-710.

Szczygłowska, R., Chyc, M., Burzała, B., Kołwzan, B. (2012). Ocena jakości bakteriologicznej i fizyko-chemicznej wody basenowej w wybranym krytym obiekcie rekreacyjnym. *Ochrona Środowiska, 34(4),* 52-56.

Szejniuk, B., Budzińska K., Jurek, A., Traczykowski, A., Berleć, K., Michalska, M., Piątkowski, J.K. (2013). Przeżywalność bakterii *Salmonella* Enteritidis w wodach powierzchniowych. *Rocznik Ochrona Środowiska, 15,* 2738-2749.

Walczak, M., Lalke-Porczyk, E. (2011). Przeżywalność bakterii w wodach geotermalnych. *Technika Poszukiwań Geologicznych, Geotermia, Zrównoważony Rozwój, 1-2,* 413-423.

Zanieczyszczenie mikrobiologiczne wody pochodzącej z fontann zlokalizowanych w uzdrowisku Ciechocinek

Abstract

Fountains located in health resorts frequently serve as therapeutic waters intended for recreational and balneological purposes. Therefore, the quality of water and air around such objects is crucial for patients using the fountains. Fountain water conducive to the occurrence of pathogen microorganisms, such as: coliform bacteria, staphylococci, streptococci, *Salmonella* spp. and microscopic fungi. They mostly cause a gastrointestinal and skin infections. The research here presented aimed at the assessment of the degree of bacterial and fungal contamination of water samples taken from fountains located in the Ciechocinek health resort from the perspective of biosafety of tourists and patients. Microbiological analysis of the water sample was taken from four fountains (object A-D), one of which (object C) was supplied with brine water.The plate method was used to determination of a total count of bacteria and a total count of fungi in the water samples. For the quantitative determination of coliform bacteria, *Escherichia coli*, staphylococci and streptococci, the membrane filter technique was employed. The studies showed that the samples of water from fountains contained bacteriological and mycological contamination in which microfungi being the most abundant group. The water samples contained a few cells of *E. coli*, fecal streptococci and staphylococci. The most frequently indentified indicator bacteria in sample water from fountain D were faecal streptococci ($3.17 \cdot 10^1$ cfu/100 ml). The water samples coming from the object B and D and in most water samples from the object C, there was no presence of these bacteria. As the data indicate, the largest differences regarding the population of those microorganisms were between water samples taken from Fountain B and C. The highest frequency of the occurrence of the *E. coli* bacilli was recorded in fountain A, while they occurred once in research series 5 taken from fountain C. The mean amount of these bacteria in the water samples taken from Fountain D was $5.76 \cdot 10^0$ cfu/100 ml, which was more than 40 times higher than the mean population of these microorganisms isolated from the water taken from Fountain C ($0.14 \cdot 10^0$ cfu/100 ml). The studies demonstrate that the least number of coliform bacteria and *E. coli* was found in fountain C, where 4.51% brine water was used. The highest number of staphylococci during the entire research period was determined in water sample taken from fountain D ($7.9 \cdot 10^1$ cfu/100 ml), while in water sample taken from fountains A and C and in sample from fountain B, no such bacteria were found. Occurrence of faecal bacteria, staphylococci and microscopic fungi in water may pose a risk of diseases for people who use the fountains. The research indicated that it is neces-

sary to perform monitoring of fountain water and introduce legal regulations regarding its sanitary and hygiene condition.

Streszczenie

Fontanny zlokalizowane na terenach uzdrowiskowych często są wykorzystywane jako wody lecznicze przeznaczone do celów rekreacyjnych oraz balneologicznych. W związku z tym bardzo ważna dla kuracjuszy korzystających z fontann jest jakość wody i powietrza wokół tych obiektów. Woda pochodząca z fontann sprzyja występowaniu mikroorganizmów chorobotwórczych takich jak: bakterie grupy coli, gronkowce, paciorkowce, pałeczki z rodzaju *Salmonella* oraz grzyby mikroskopowe. Powodują one przede wszystkim zakażenia o charakterze żołądkowo-jelitowym oraz infekcje skórne. Celem pracy była ocena stopnia zanieczyszczenia bakteriologicznego i mikologicznego próbek wody pobieranych z fontann, zlokalizowanych na terenie uzdrowiska Ciechocinek w aspekcie bezpieczeństwa sanitarnego turystów i kuracjuszy. Analizie mikrobiologicznej poddano próbki wody pobrane z czterech fontann (obiekty A-D), z których jedna (obiekt C) była zasilana wodą solankową. Metodą płytkową oznaczono ogólną liczbę bakterii i grzybów mikroskopowych. Do oznaczenia ilościowego bakterii grupy coli, *Escherichia coli*, paciorkowców kałowych oraz gronkowców wykorzystano metodę filtrów membranowych. W wyniku przeprowadzonych badań stwierdzono, że próbki wody pochodzące z fontann zawierały zanieczyszczenia bakteriologiczne i mikologiczne, przy czym najliczniej reprezentowane były grzyby mikroskopowe. W próbkach wody występowały pojedyncze komórki *E. coli* a także paciorkowce kałowe oraz gronkowce. Najliczniej paciorkowce kałowe identyfikowano w próbce wody pobranej z fontanny D ($3{,}17 \cdot 10^1$ jtk/100 ml). W próbkach wody pochodzących z obiektu B i D oraz w większości próbek wody z obiektu C nie stwierdzono obecności tych bakterii. Największe różnice dotyczące liczebności tych mikroorganizmów wystąpiły w przypadku próbek wody pochodzących z fontanny B i C. W obiekcie A notowano najwyższą częstotliwość występowania pałeczek *E. coli*, natomiast w przypadku fontanny C występowały one w jednym przypadku w wody pochodzącej z 5 serii badawczej. Średnia liczba bakterii *Escherichia coli* w próbkach wody pobranej z obiektu D wynosiła $5{,}76 \cdot 10^0$ jtk/100 ml i była ponad 40-krotnie wyższa od średniej liczebności tych drobnoustrojów izolowanych z wody pochodzącej z obiektu C ($0{,}14 \cdot 10^0$ jtk/100 ml). Badania wykazały, że najmniej bakterii grupy coli i *E. coli* stwierdzono w obiekcie C, w którym wykorzystywano wodę solankową o zasoleniu 4,51%. Największą liczbę gronkowców w ciągu całego okresu badań oznaczono w próbce wody pobranej z obiektu D ($7{,}9 \cdot 10^1$ jtk/100 ml), natomiast w niektórych próbkach wody ujętej z obiektu A i C oraz B nie stwierdzono obecności tych bakterii.

Występowanie w wodzie bakterii fekalnych, gronkowców, jak również grzybów mikroskopowych może stwarzać ryzyko zachorowań u ludzi korzystających z fontann. Przeprowadzone badania wskazują na konieczność prowadzenia monitoringu wody pochodzącej z fontann, a także na wprowadzenie regulacji prawnych dotyczących ich stanu sanitarno-higienicznego.

Słowa kluczowe:
woda, fontanny, zanieczyszczenie, bakterie, grzyby mikroskopowe

Keywords:
water, fountains, contamination, bacteria, microscopic fungi

MIDDLE POMERANIAN SCIENTIFIC SOCIETY OF THE ENVIRONMENT PROTECTION
ŚRODKOWO-POMORSKIE TOWARZYSTWO NAUKOWE OCHRONY ŚRODOWISKA

Annual Set The Environment Protection
Rocznik Ochrona Środowiska

Volume/Tom 19. Year/Rok 2017 ISSN 1506-218X 200-210

Application of Multilayer Perceptron for the Calculation of Pressure Losses in Water Supply Lines

Andrzej Czapczuk[*], *Jacek Dawidowicz*[**], *Jacek Piekarski*[***]
[*] *F.B.I. TASBUD a Joint-Stock Company*
[**] *Bialystok University of Technology*
[***] *Koszalin University of Technology*

1. Introduction

Numerical methods have been used widely for many years in the design and operation of water supply systems. Specialised computer programmes offer ever more facilities, especially for data entry and viewing, but they still function on the basis of predetermined algorithms. At the same time, we are also dealing with the game-changing development of artificial intelligence techniques, which are increasingly paving the way for practical applications. To this end, traditional calculation programmes are supplemented with artificial intelligence methods. This trend can also be seen in issues related to the supply of water. The aim of this article is to present the method of artificial neural networks for the calculation of pressure losses in water supply lines.

2. Artificial Neural Networks (ANN)

Intelligence is attributed solely to man, but since the creation of the first computer, many attempts have been made to build a machine with such a feature. This led to the creation of a field of science known as artificial intelligence AI (Negnevitsky 2004). There are several trends, but expert systems, artificial neural networks and various types of metaheuristics have gained the greatest popularity.

Such methods are based on the observation of the processes occurring in the natural world or functioning of the nervous system. This group includes, among other things, artificial neural networks (ANN) that simulate the processing of information in the nervous systems of animals and humans. The most commonly used type of uni-directional artificial neural network is the multi-layer perceptron, which consists of neurons arranged in layers (Bishop 1966).

3. The Current State of the Application of Artificial Neural Networks in the Design of Water Distribution Systems

In the works (Lingireddy & Ormsbee 1998, Saldarriaga et al., 2004), artificial neural networks, aimed at streamlining the process of taring a numerical model in a water distribution system, was described. Hydraulic calculations using the Darcy-Weisbach formula require determination of the coefficient of linear resistance, most often by the application of an iteration method. In the articles (Besarati et al. 2015, Brkić & Ćojbašić 2016, Salmasi et al. 2012, Shayya & Sablani 1998), the methods for calculating this factor, using artificial neural networks, in order to reduce calculation times, were presented.

Calculation modules based on artificial neural networks were also introduced into the simulation methods used in the real-time control of water supply networks. The task of neural computing in this case is to simplify the computational model and accelerate calculations (Bargiela 1995, Xu et al. 1997).

The problem of controlling the adjustment of control valves using neural networks was discussed in articles (Haytham et al. 2005, Van den Boogaard & Kruisbrink 1996).

In the study (Dawidowicz 2015), it was assumed that the hydraulic calculations of water distribution systems are a multi-stage process requiring performance evaluation, appropriate data correction and subsequent calculations. Therefore, the methodology of process diagnostics was used to evaluate the results of the calculations. Diagnostic methods were introduced to detect computational abnormalities using artificial neural networks. In the article (Dawidowicz 2017), an artificial neural network for evaluation of a pressure lines and pressure zones, in the water distribution system, was discussed.

An effective control of the water distribution system requires accurate information about the current state of the network. For economic reasons, some parameters must be calculated on the basis of the information available. In the group of parameter estimation methods, estimators based on artificial neural networks appear (Gabrys & Bargiela 1996). A computerised system for controlling pumping systems using genetic algorithms and artificial neural networks is described in the article (Lingireddy & Ormsbee 1995).

4. Development of Artificial Neural Network for Calculation of Pressure Losses in Water Supply Lines

The type of unidirectional artificial neural network most commonly used is the multi-layer perceptron, which consists of neurons arranged in layers (Bishop 1966). There are three basic types of layers, viz. the input layer, the hidden layer, and the output layer. Neurons are interconnected between layers on a *peer-to-peer* basis, whereas in one layer there are no connections between neurons. Each connection is assigned a weighing factor. The combined weight factors of the neural network creates the weight vector, viz., $\mathbf{W}=[w_1,\ w_2,\ldots,w_i,\ldots,\ w_N]^T$.

A multi-layered perceptron is taught by means of a strategy with a teacher that has an iterative nature and consists of repeatedly presenting a network of learning examples $\{X_i,d_i\}$, where $X = [x_1,\ x_2...,x_i...,x_N]^T$ is a vector of the input variables and d is a valid or *real* response to the set of specified input data. The artificial neural network learning algorithm consists in choosing the weights so that the differences- δ_i - between the value calculated by the network- y_i - and the correct value- d_i - for all training examples $i = 1, ...T$ was the smallest. An error function is used to evaluate the current quality of a neural network in the learning process, which is a measure of the compatibility of the prediction of a network with the value set. The error function is used to determine the magnitude of the neuronal weight corrections which are necessary at every stage of network learning. In this paper, the function of an error is the sum of the squares of differences:

$$E_{SOS} = \sum_{i=1}^{T} (y_i - d_i)^2 \tag{1}$$

where:
T – is the number of learning cases (input-output pairs),
y_i – is the network prediction (network output) for the i-th case of the training case,
d_i – is the correct (real) value of the i-th case.

In the neurons of the input layer, a linear activation function was applied, whereas in the hidden and output layer, a logistic function was applied:

$$y = \frac{1}{1 + e^{-\beta S}} \qquad y \in (0...+1) \tag{2}$$

where:
y – is the initial value of the neuron,
β – is a numerical factor, usually with the value of 1,
S – is the value of the post-synaptic potential function *PSP*.

The use of artificial neural networks requires a set of training examples describing the object or process being modelled. Neural network calculations in this example rely on the generation of pressure losses on the computational sections of the water supply lines. Therefore, it is a regression problem and the output variable is numeric in character. Input variables may be numerical or nominal. In the training data set, the following parameters of the computational sections are stored:

- nominal flow q [l/s],
- nominal diameter DN [mm], supplied to the network as a nominal value,
- length of the section/segment L [m],
- coefficient of absolute roughness k [mm],
- calculated level of pressure losses on the computational section Δ/segment H [m].

The hydraulic calculations were performed with the following assumptions:

- pressure losses were calculated using the Darcy-Weisbach formula,
- internal diameters of the water pipes were assumed for the calculations,

- PE100 polyethylene pressure pipes of the SDR17 series (EN 12201-2: 2011) for diameters up to DN225 and ductile iron pipes (EN 545: 2010) for higher diameters were applied,
- minimum cable diameter DN90,
- maximum cable diameter DN500,
- range of lengths of computational pipelines L = 50-3000 [m],
- range of reliable flow in the relation q = 0.5-570 [l/s],
- range of roughness coefficients was assumed at k = 0.01-2.0 [mm].

Nominal diameters were adopted as follows:

- DN90, DN110, DN160, DN225 for PE100 polyethylene pipes of the SDR17 series (EN 12201-2:2011),
- DN250, DN300, DN350, DN400, DN450, DN500 for ductile iron pipes (EN 545: 2010).

As a result of hydraulic pipeline calculations for various input parameters, 16,260 training examples were obtained.

An artificial neural network was investigated to determine the structure of the neural network, in order to obtain the results of pressure losses in the water pipes with the smallest error. In the learning process, the training data set was divided into three subsets, viz., the training set (70%), the validation subset (15%) and the test subset (15%):

- the training set – is used to teach the network,
- the validation set – cases in this set are not used to modify network parameters in the training process, but are used independently, in parallel to the training process, in quality assessment and generalisation ability,
- the test set – is not used at all during the training process, but enables a final, quality assessment of the network's performance to be carried out after the training process has been completed.

The network was taught by the BFGS method. As a result of training various structures of the multi-layer perceptron, a neural network composed of the following elements was assumed for the calculation of pressure losses in the water supply lines:

- a layer with 15 neurons for input variables, 12 of which correspond to the nominal diameter DN,
- a hidden layer built of 85 neurons with a logistic activation function,
- an output layer with 1 neuron and a logistic, activation function.

A schematic diagram of the neural network, with a shortened inner layer, is shown in Figure 1. The input of the nominal variable, describing diameters according to the "one of N" principle, is worth mentioning.

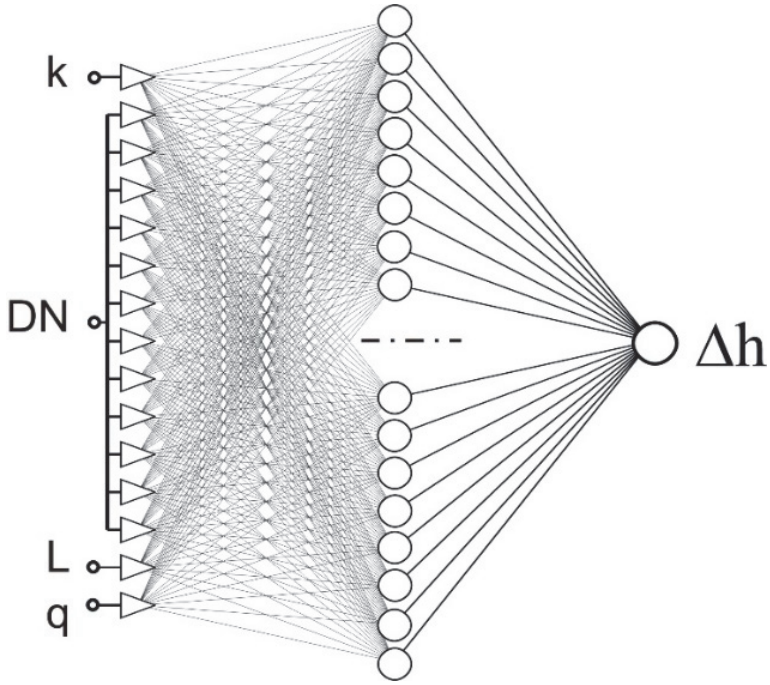

Fig. 1. A schematic diagram of the neural network for calculating pressure losses in water pipes
Rys. 1. Schemat sieci neuronowej do obliczeń strat ciśnienia w przewodach wodociągowych

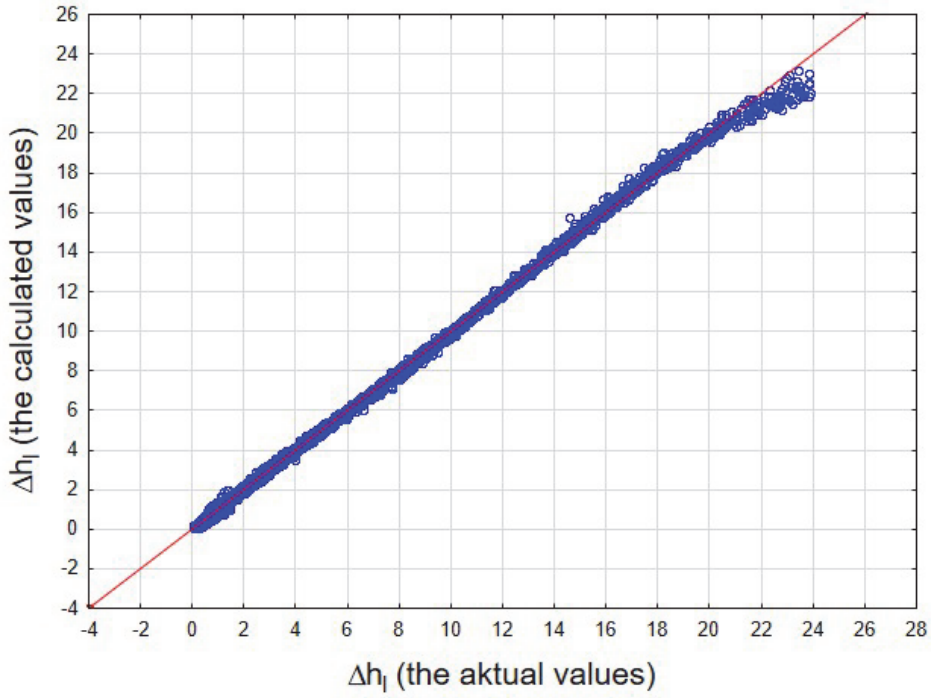

Fig. 2. The relationship between the actual values of pressure losses Δh_l and those calculated by the artificial neural network
Rys. 2. Zależność pomiędzy rzeczywistymi wartościami strat ciśnienia Δh_l a wyliczonymi przez sztuczną sieć neuronową

Table 1. Parameters of the multi-layer perceptron for calculating pressure losses in water supply lines
Tabela 1. Parametry perceptronu wielowarstwowego do obliczania strat ciśnienia w przewodach wodociągowych

Parameter	Training subset	Validation subset	Test subset
SOS error	0.007970	0.009528	0.009493
Correlation coefficient	0.999601	0.999486	0.999518

A very low SOS error value for the three subsets and a high value for the Pearson correlation coefficient r, between the actual values and the values calculated by the neural network, shows that it can be used to simplify the hydraulic calculation model. Artificial neural networks with parallel structures are characterised by very short data processing times and can be used in real-time control systems where calculation time is critical.

5. Summary and Conclusions

In the design of water distribution systems, hydraulic calculations are carried out together with calculations for the selection of the pumps, the reservoir sizes or optimisation of the components of the operating parameters of individual systems. Computational methods based on classical numerical algorithms have largely exhausted their development possibilities. Accelerating computing by using the latest generation of computers does not always deliver better results. Only the application of new calculation methods can significantly improve both the quality of the solutions obtained and the results of calculations. Increasingly, when dealing with a number of problems, artificial intelligence is referred to. It is used to solve problems that have not had classical computational algorithms, or significant amounts of required data, to date and where constraints have caused their use to be unfeasible.

This paper reviews the proposed use of artificial neural networks in the calculation of water distribution systems implemented by computer programmes. On the other hand, there are hardware-based software drives that use smart software, which greatly enhances the ability to use smart methods in practice. The wide range of solutions indicates that they pave the way for their implementation, in practice.

A computational example in the form of an artificial neural network calculating pressure losses in water supply pipes shows that artificial intelligence methods can play a significant role in the design, control, and management of water distribution systems in the future. A very high convergence was found between the results obtained from the EPANET calculation programme and the results generated by the multi-layer perceptron.

References

Bargiela, A. (1995). High performance neural optimization for real time pressure control. *Proceedings of High Performance Computing Conference HPC Asia'95*, Chap. AL34, Taipei, 1-8.

Besarati, S. M., Myers, P. D., Covey, D. C., & Jamali, A. (2015). Modeling friction factor in pipeline flow using a GMDH-type neural network. *Cogent Engineering, 2(1)*, 1-14.

Bishop, C. M. (1996). *Neural Networks for Pattern Recognition*. Oxford: University Press.

Brkić, D., & Ćojbašić, Ž. (2016). Intelligent flow friction estimation. *Computational intelligence and neuroscience 2016*, 1-10.

Dawidowicz, J. (2017). Evaluation of a pressure head and pressure zones in water distribution systems by artificial neural networks. *Neural Computing & Application.* doi:10.1007/s00521-017-2844-8

Dawidowicz, J. (2015). *Diagnostyka procesu obliczeń systemu dystrybucji wody z zastosowaniem modelowania neuronowego*. Rozprawy Naukowe. Białystok: Oficyna Wydawnicza Politechniki Białostockiej (in Polish).

Gabrys, B. & Bargiela, A. (1996). An integrated neural based system for state estimation and confidence limit analysis in water networks. *Proceedings of ESS 96. 8th European Simulation Symposium Simulation in Industry*, *2*, 398-402.

Haytham, A., Kwamura, A., & Jinno, K. (2005). Applications of artificial neural networks for optimal pressure regulation in supervisory water distribution networks. *Memoirs of the Faculty of Engineering, 65*, 29-51, Kyushu University, Fukuoka, Japan.

Lingireddy, S., & Ormsbee, L.E. (1998). Neural Networks in Optimal Calibration of Water Distribution Systems. In Flood I., Kartam N. (Eds), *Artificial Neural Networks for Civil Engineers: Advanced Features and Applications*, ASCE, 53-76.

Lingireddy, S., & Ormsbee, L.E. (1995). Optimal control of water supply pumping systems using genetic algorithms and artificial neural networks. *Proceedings of The International Federation for Automatic Control Symposium on Large Scale Systems '95*, London, UK.

Negnevitsky, M. (2004). *Artificial Intelligence: A Guide to Intelligent Systems*. Addison-Wesley.

Saldarriaga, J., Gómez, R., & Salas, D. (2004). Artificial intelligence methods applicability on water distribution networks calibration. *Critical Transitions in Water and Environmental Resources Management*, 1-11. https://doi.org/10.1061/40737(2004)248

Salmasi, F., Khatibi, R., & Ghorbani, M. A. (2012). A study of friction factor formulation in pipes using artificial intelligence techniques and explicit equations. *Turkish Journal of Engineering and Environmental Sciences, 36(2)*, 121-138.

Shayya, W.H., & Sablani, S.S. (1998) An artificial neural network for non-iterative calculation of the friction factor in pipeline flow. *Computers and Electronics in Agriculture*, 21(3), 219-228.

Van den Boogaard, H.F., & Kruisbrink, A.C.H. (1996) *Hybrid modeling by integrating neural networks and numerical models hydraulic engineering.* Proceedings of the Second International Conference on Hydroinformatics, 2, 471-477.

Xu C., Bouchart F., & Goulter I.C. (1997) *Neural networks for hydraulic analysis of water distribution systems.* Proceedings of the Innovation in Computer Methods for Civil and Structural Engineering, Civl-Comp Press, 129-136, Cambridge.

Zastosowanie perceptronu wielowarstwowego do obliczeń strat ciśnienia w przewodach wodociągowych

Streszczenie

Metody numeryczne stosuje się powszechnie od wielu lat w projektowaniu i eksploatacji systemów zaopatrzenia w wodę. Specjalistyczne programy komputerowe oferują coraz więcej udogodnień, szczególnie w zakresie wprowadzania danych oraz przeglądania wyników, lecz nadal funkcjonują na podstawie z góry określonych algorytmów. Obecnie dąży się jednak do stworzenia programów obliczeniowych, które będzie charakteryzować pewien stopień kreatywności, co powinno ułatwić użytkownikom podejmowanie decyzji na różnych etapach realizacji zadania i poprawić jakość rozwiązań. Zwiększająca się moc obliczeniowa komputerów samoistnie nie rozwiąże złożonych problemów. Dopiero wprowadzanie odpowiednich metod obliczeniowych, pozwala uzyskać właściwe efekty. Wydaje się, że klasyczne algorytmy o sformalizowanym przebiegu, można obecnie uzupełnić znacznie bardziej zaawansowanymi technikami obliczeniowymi. W niniejszej pracy dokonano przeglądu literatury w zakresie zastosowania sztucznych sieci neuronowych w projektowaniu systemów dystrybucji wody. W drugiej części artykułu zamieszczono omówienie sztucznej sieci neuronowej do obliczeń strat ciśnienia w przewodach wodociągowych. W wyniku obliczeń hydraulicznych przewodów wodociągowych za pomocą programu EPANET dla różnych wartości parametrów wejściowych uzyskano zbiór 16260 przykładów uczących. Parametry wejściowe sieci neuronowej to długość przewodu, przepływ miarodajny, współczynnik chropowatości bez-

względnej oraz średnica nominalna. Uzyskano bardzo wysoką zgodność pomiędzy wynikami obliczeń strat ciśnienia z programu EPANET i perceptronu wielowarstwowego z jedną warstwą ukrytą.

Abstract

Numerical methods have been widely used for many years in the design and operation of water supply systems. Specialised computer programmes offer more and more facilities, especially for data entry and viewing, but they still function on the basis of predetermined algorithms. At present, however, we strive to create computational programmes with a certain degree of creativity, which should make it easier for users to make decisions at various stages of the task and improve the quality of their solutions. The increasing power of computers will not solve complex problems alone. Only by introducing appropriate calculation methods can we obtain the right results. It seems that classical algorithms with a formalised course can be supplemented, nowadays, with far more advanced computational techniques. This paper presents an literature review on the use of artificial neural networks in the design and operation of water distribution systems. Presented in the second part of the paper, is an overview of the artificial neural network, developed for the calculation of pressure losses in water supply lines. The calculation of hydraulic piping with the EPANET programme for various input parameters resulted in a collection of 16,260 training examples. Input parameters of the neural network include pipe length, measurable flow, absolute roughness coefficient and the nominal diameter. Very high compatibility was obtained between the calculation results for those pressure losses obtained from the EPANET programme and those obtained from the multi-layered perceptron with one hidden layer.

Keywords:
water distribution systems, artificial intelligence, expert systems,
artificial neuronal networks, heuristic methods, calculation of pressure losses

Słowa kluczowe:
systemy dystrybucji wody, sztuczna inteligencja, systemy ekspertowe,
sztuczne sieci neuronowe, metody heurystyczne, obliczenia strat ciśnienia

MIDDLE POMERANIAN SCIENTIFIC SOCIETY OF THE ENVIRONMENT PROTECTION
ŚRODKOWO-POMORSKIE TOWARZYSTWO NAUKOWE OCHRONY ŚRODOWISKA

Annual Set The Environment Protection
Rocznik Ochrona Środowiska

Volume/Tom 19. Year/Rok 2017 ISSN 1506-218X 211-229

Vegetation and Birds Species Changes in Meadow Habitats in Polesie National Park, Eastern Poland

Mariusz Kulik[*]*, Ryszard Baryła*[*]*, Danuta Urban*[*]*,*
Grzegorz Grzywaczewski[*]*, Andrzej Bochniak*[*]*,*
Andrzej Różycki[**]*, Ewelina Tokarz*[*]
[*]*University of Life Sciences, Lublin*
[**]*Polesie National Park*

1. Introduction

Grasslands are one of the semi-natural ecosystems that require human activity and quickly degrades as a result of land use changes. Many agricultural lands, including grassland, are excluded from use (Harkot et al. 2011). Development of meadow communities depends upon flora composition (Nekrošienė & Skuodienė 2012), which is also one of the most sensitive indicators of landscape changes (Jutila 2003). Disturbance of the habitat conditions through regulating the hydrologic regime as well as limiting the intensity of use or its abandonment lead to changes in the species composition and range of the area covered by plant communities (Czyż et al. 2013, Myśliwy & Bosiacka 2009, Nekrošienė & Skuodienė 2012). The method and intensity of grassland use have an impact on the persistency and floristic diversity of that communities. The lack of use of meadows and pastures leads to their fast degradation (Stypiński & Grobelna 2000) and frequently irreversible habitat changes (Kozłowska & Burs 2013, Kulik 2014). Changes in grassland flora, mainly under the impact of too intensive livestock grazing and hay harvesting, can also be observed (Shushpannikova 2014).

These changes affect not only the vegetation cover but also birds. Many bird species that inhabit wet meadows, in particular, constitute one of the most endangered ecological groups in the whole of Europe. The

main threat is posed by changes in the humidity of habitats and abandonment of use (Chylarecki et al. 2006, Langgemach & Bellebaum 2005, Ławicki et al. 2011, Pehlak & Lohmus 2008, Vickery et al. 2001, Watkinson & Ormerod 2001). In the Lublin Region, for example, meadows and pastures are the habitats for about 20% of 213 breeding bird species, including those that are vulnerable and endangered (Grzywaczewski & Cios 2012). One of the areas, where the changes in land use were observed, is Polesie National Park in Eastern Poland.

The aim of the study was to: (1) identify the vegetation and bird species in the study area and compare it with the data collected 17 years ago, (2) analyse the changes in plant communities and bird species depending on grassland management and habitat as well as (3) analyse the climate and habitat changes based on Ellenberg's indicators.

2. Material and methods

2.1. The study area

Zienki Meadows are situated in Polesie National Park, Eastern Poland. The meadow complex discussed (51˚27-29' N; 23˚6-9' E), covering approx. 650 ha. The area encompasses the easternmost enclave of the Wieprz River catchment (Piwonia basin) and adjoins the western part of the Bug River catchment (Włodawka basin). The meadow complex has natural borders: in the north, it adjoins a natural mineral soil elevation, the so-called Włodawa Ridge; a forest complex in the west; a peat bog with Lake Moszne in the south; and a watershed on mineral soils in the east (Baryła & Urban 1999). The site encompasses vast natural basins of glacial origin, former bogs and peat bogs of varying humidity.

2.2. Field study

Previous research studies were carried out in 1996 and 2013 on Zienki Meadows. In that study, only complexes with the same phytosociological relevés in 1996 (marks as 7-302) and 2013 (marks as 7a-302a) were taken into account. The plant communities were classified using the Braun-Blanquet (1964) method, with 48 phytosociological relevés established each year on area of 25 m^2. Phytosociological taxonomy was based on Matuszkiewicz (2008), and the species names were provided according to Mirek et al. (2002).

Investigations concerning birds were conducted in the breeding period from mid-April to mid-July in the same periods as the vegetation cover; observations concerning the absence of certain bird species in the second period (2013) were confirmed over a period of several years (2009-2015). The observations, carried out in the morning from sunrise to 9-10 am, consisted of walking in the study area and recording the individual bird species and identifying their breeding distribution. Besides, dusk and night-time inspections were carried out to record species active at this time of day. Changes in bird species over a period of 17 years are presented in the overall table.

2.3. Data analysis

The pragmaTax program was used to carry out the numerical classification for all relevés based on the quantitative share of the species. The Weighted Pair Group Method of Arithmetic averages (WPGMA) was used. A comparison of the dendrograms obtained in the classification made it possible to include groups of relevés at alfa scale 0.5, similar in terms of community species composition. Changes of the climatic and edaphic conditions were assessed using ecological indicator values by Ellenberg et al. (1992). Climatic (L – light, T – temperature, K – continentality) and edaphic (F – moisture, R – reaction, N – nitrogen content) indicators were taken into account. Obtained results of ecological indicator values for every relevés were put to the ANOVA analysis complemented by the Tukey test ($p<0.05$) to estimate significant changes in study years for all plant communities and for the predominant *Arrhenatheretum elatioris* association and *Deschampsia caespitosa* community. The multidimensional Principal Component Analysis (PCA) was used to identify patterns occurring in the dataset. PCA helped determine which indices result in the greatest variance in the communities, and facilitated the visualisation of changes that occurred in the particular years of the investigation. Due to the identical scale of the indices examined, the PCA was based on a covariance matrix. The software used to carry out the analysis was Statistica v. 10.

3. Results and discussion

Phytosociological studies conducted in 1996 as part of the Polesie National Park Conservation Plan revealed the great diversity of habitats and plant communities in the area. Several communities were distinguished: from *Phragmitetea* class wetland communities to dry and poor habitat communities of the *Koelerio glauca-Corynopheretea canescentis* class. *Alopecurus* meadows (*Alopecuretum pratensis*) growing in more humid habitats and the *Poa pratensis-Festuca rubra* community in fresh habitats predominated in the analysed area. Tall oat-grass meadows (*Arrhenatheretum elatioris*), occurring in habitats on more fertile mineral soil and formerly used mainly as arable fields, were also frequently recorded (Baryła & Urban 1999). These communities were characterised by poor floristic diversity because their species composition was based on mixes of grasses with legumes sown in the past after the regulation of hydrologic conditions. Tall oat-grass meadows were the most stable plant communities, with the greatest floristic diversity. 85% of these meadows did not change; their species composition changed only slightly. These meadows were located in dry habitats on mineral soils, located close to agricultural farms and systematically used. The share of these meadows actually increased because it replaced the *Poa pratensis-Festuca rubra* community, *Arrhenatherion* representing the same alliance and a community with *Agrostis capillaris* (Fig. 1). The persistence of tall oat-grass meadows is linked with the occurrence of high plants, including *Arrhenatherum elatius*, which is indirectly shown by the largest light index among the dominant communities (7.58); these meadows are also characterised by the lowest soil humidity index (5.19; Fig. 2). Climate changes were observed based on the changes in the species composition of these meadows in the study period linked with the light and temperature indices (Fig. 4). Xerothermic species had a greater share in the sward. Based on the calculated Ellenberg's indicators (1992), a significant reduction of soil acidity (6.65 > 6.36) and trophism (6.23 > 5.59) was observed. This could result from the extensification of meadow use in these habitats, particularly linked with the reduction or complete lack of mineral fertilisation.

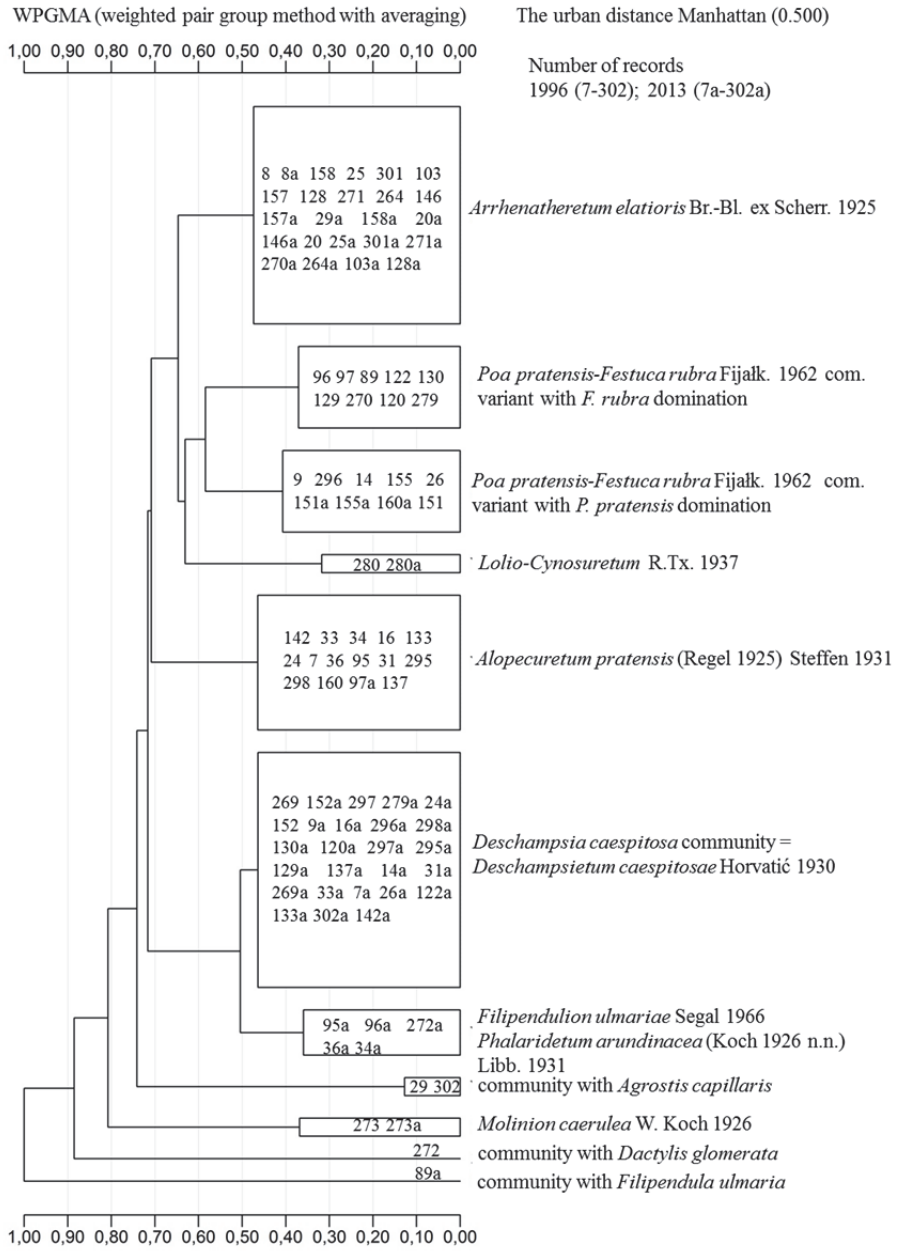

Fig. 1. Classification of the meadow plant communities
Rys. 1. Klasyfikacja łąkowych zbiorowisk roślinnych

The floristic composition of tall oat-grass meadows undergoes constant transformations and their restoration is limited by the existing use. It should be added that fresh meadows are one of the habitat types protected within the framework of the Nature 2000 network due to the presence of species of European importance (Klarzyńska & Kryszak 2015). In the last 25 years, in some European countries, including Poland, we have been observing a gradual disappearance of meadows from the *Arrhenatherion* alliance (Kucharski 2014, Vintu et al. 2011, Weigelt et al. 2009).

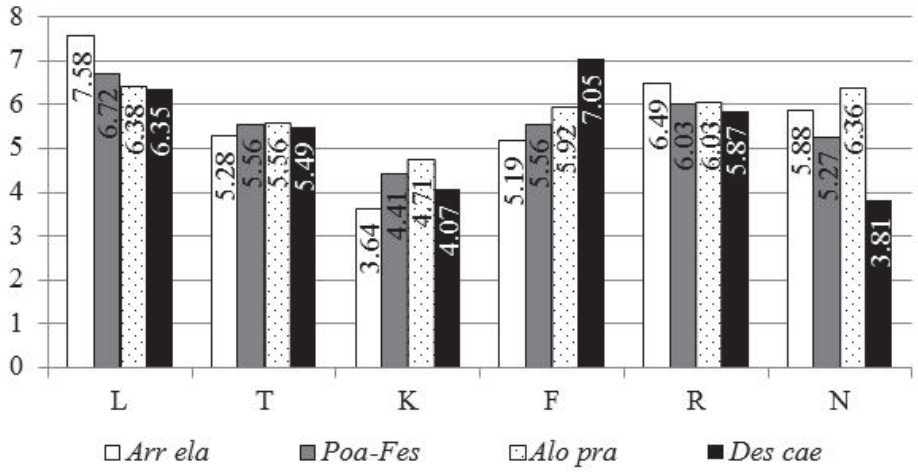

Fig. 2. Ellenberg's indicators (1996-2013) of dominant plant communities (L – light, T – temperature, K – continentality, F – soil moisture, R – acidity, N – trophism)
Rys. 2. Wskaźniki Ellenberga (1996-2013) dominujących zbiorowisk roślinnych (L – światło, T – temperatura, K – kontynentalizm, F – wilgotność gleby, R – kwasowość, N – trofizm)

The *Molinia* meadow and fertile *Lolio-Cynosuretum* pasture were also among the communities that did not change in the analysed period. The former needs to be mowed once a year, at a late date (Kulik 2014), and such extensive meadow management was conducted in most of the area of this complex. The latter community requires systematic grazing, which is rare not only in the Polesie National Park, but also throughout Europe. Grazing was conducted in this pasture in the years 1996-2013,

which significantly contributed to the stability of this community. It should be noted, however, that these were isolated grasslands.

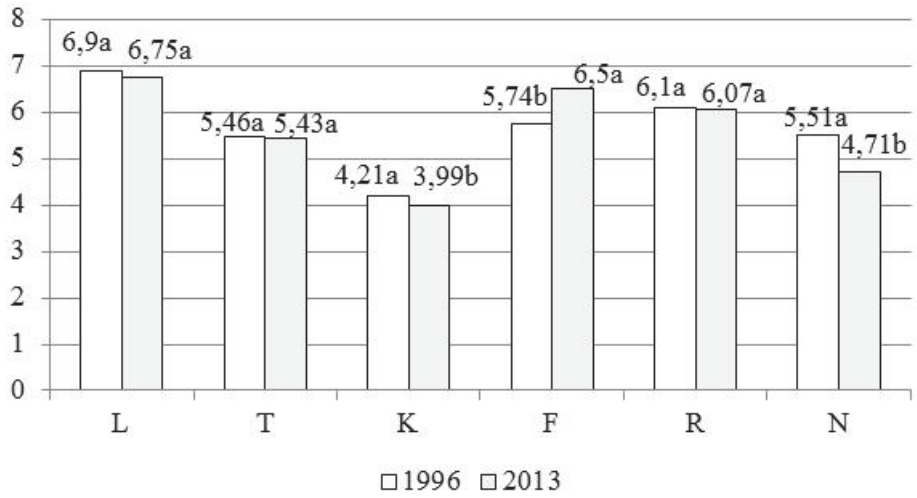

Fig. 3. Changes of Ellenberg's indicators mean values of all meadow communities (L – light, T – temperature, K – continentality, F – soil moisture, R – acidity, N – trophism; different letters indicate significant differences $p<0.05$)
Rys. 3. Zmiany średnich wartości wskaźników Ellenberga wszystkich zbiorowisk roślinnych (L – światło, T – temperatura, K – kontynentalizm, F – wilgotność gleby, R – kwasowość, N – trofizm; różne litery oznaczają istotne różnice $p<0.05$)

The biggest changes were observed in *Alopecurus* meadows that, in 1996, showed a predominance of *Alopecurus pratensis* and a large share of *Poa pratensis, Festuca rubra* and characteristic species of the *Molinietalia* order (*Lysimachia vulgaris, Lythrum salicaria, Deschampsia caespitosa*). Between 10 and 15 plant species were recorded in this community. After 17 years, most patches of this community (71%) transformed into communities with the predominance of *Deschampsia caespitosa*. Some *Alopecurus* meadows (21%), located in the proximity of waterlogged habitats under active protection of the Polesie National Park, transformed into floristically poor *Phalaris* meadows or herbaceous meadows of the *Filipendulion ulmariae* alliance (Fig. 1, 5). *Phalaris* meadows are characterized by predominance of *Phalaris arundinacea*

and usually the poorest species richness is observed in patches corresponding to the *Phragmitetea* class (Czyż et al. 2013). On the other hand, these meadows have an enormous significance for avifauna and mammal fauna (Wyłupek et al. 2015). Thus, *Alopecurus* meadows disappeared from the landscape of this complex in a very short period of time. It should be noted that the persistence of these meadows depends largely on their systematic use and optimum humidity conditions. The disappearance of that meadows was linked with the absence or very late date of mowing. After 1998, only a few fragments of this meadow complex were mowed, which limited the invasion of herbaceous and, subsequently, thicket communities. Systematic management was not introduced until 2009, but it was limited to mowing only once a year at a late date, which contributed to the continuously increasing share of *Deschampsia caespitosa.* In the years 2009-2013, about 40% of the meadow area in this complex was used systematically.

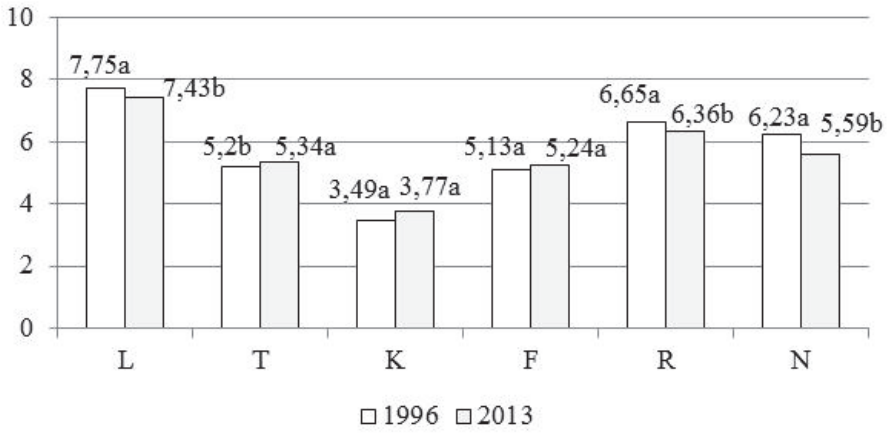

Fig. 4. Changes of Ellenberg's indicators mean values of *Arrhenatheretum elatioris* association (explanations like in Fig. 3)
Rys. 4. Zmiany średnich wartości wskaźników Ellenberga zespołu *Arrhenatheretum elatioris* (objaśnienia jak w Rys. 3)

Another example of meadows mowed for hay in the first period, but later transformed, was the *Poa pratensis-Festuca rubra* community represented by two variants: the more humid variant, with the predominance of *Poa pratensis*, and the drier variant, with *Festuca rubra* (Fig. 1,

5). During the 17-year study period, the species composition changed significantly in 84% of the meadows. Most of them (50%) transformed into *Deschampsia caespitosa* communities. Tussocks of this species can be safe sites for seedling recruitment in the succession of floristically rich wet meadows (Kostrakiewicz-Gierałt 2014). However, in this case, *D. caespitosa* predominates, which prevents the restoration of the original plant communities. Changes in the more humid variant with *P. pratensis* primarily resulted from the lack of mowing, while in the case of the drier variant, an additional reason was the increased humidity of the habitat due to the active protection measures conducted by the Polesie National Park. The groundwater level in the part of the meadow complex increased by 7 to 70 cm under conditions of precipitation volume similar to the previous period (Kulik & Baryła 2010). This is confirmed by the highest humidity index for the *D. caespitosa* community (7.05) among the dominant plant communities (Fig. 2). Due to the increased humidity, some *Poa-Festuca* meadows transformed into herbaceous meadows of the *Filipendulion ulmariae* alliance (Fig. 1). Only 16% of these meadows (variant with *P. pratensis*) did not change significantly. It resulted from the systematic mowing, often twice a year, which prevented the propagation of *D. caespitosa* occurring in the sward. *Poa-Festuca* meadows are Natura 2000 habitats (6510-2) but, according to Korzeniak (2012), these habitats only include floristically rich meadows whose species composition is similar to psammophilous grassland. However, cultivated meadows, with a predominance of grasses with a high fodder value, may not be included in this habitat. Such meadows with a large share of grasses and a small share of dicotyledons develop in more humid habitats (Klarzyńska & Kryszak 2015).

Principal Component Analysis shows that the first two components account for 82.6% (and the first for 62.3%) of the total variance of data. Figure 5 shows the share of the particular Ellenberg indicators (1992) in the structure of the principal components. It should be noted that climatic indicators underwent smaller changes (Fig. 3). Significant changes were recorded only in the case of the continentality index (4.21 > 3.99), which was manifested by the reduced cover of continental species. The most significant factors differentiating the data set under study are trophism (positive impact on first component) and soil humidity (negative impact on first component). The first study period was charac-

terised by a significantly lower soil humidity index (5.74) in comparison with the second period (6.50). The appearance or increase in the cover of humid habitat species resulted from the protective measures that had been conducted in the Polesie National Park. These measures consisted of reducing the drainage of water from the analysed meadow complex, which caused an increase of water retention and increase of humidity. This, in turn, led to the reduced intensity of the organic soil muck-formation process and reduced soil trophism, which was confirmed by the significantly lower trophism indices in the second study period (5.51 > 4.71; Fig. 3).

The lack of mineral fertilisation was an important factor that could have contributed to the reduced soil trophism. The smallest variance of the results was found for soil acidity, temperature and light indices. Fig. 5 also shows the distribution of dominant plant communities in the coordinate system determined by the first two principal components.

The community with *D. caespitosa* has higher values of the soil acidity index, while the *Arrhenatheretum elatioris* and *Alopecuretum pratensis* communities have higher values of the trophism indices. Phytosociological relevés of the *Poa pratensis-Festuca rubra* community are located neutrally in relation to the first principal component, and they show a tendency to be heliophytic – influence on the second principal component (Fig. 5).

Vegetation changes also affect birds changes. In the first study period, 73 bird species were found, while in the second period, the number of species increased to 78 (Table 1). Though the small increase in the number of species, negative changes were observed for two endangered *Charadriiformes* species in Poland and Europe: the black-tailed godwit *Limosa limosa* and the common redshank *Tringa totanus* (Beintema et al. 1991, Chodkiewicz et al. 2015). The withdrawal of these two bird species could have been caused by the changes that occurred in wet meadow habitats, including the transformation of *Alopecurus* meadows into *Deschampsia* meadows. Both the black-tailed godwit and redshank inhabit waterlogged open meadows, pastures or peat-bogs (Lewartowski & Piotrowska 1987, Świętochowski 2009). The appearance of large areas of more humid meadows dominated by the high tussocks of *Deschampsia caespitosa* was probably one of the reasons for the withdrawal of these *Charadriiformes* species from this complex.

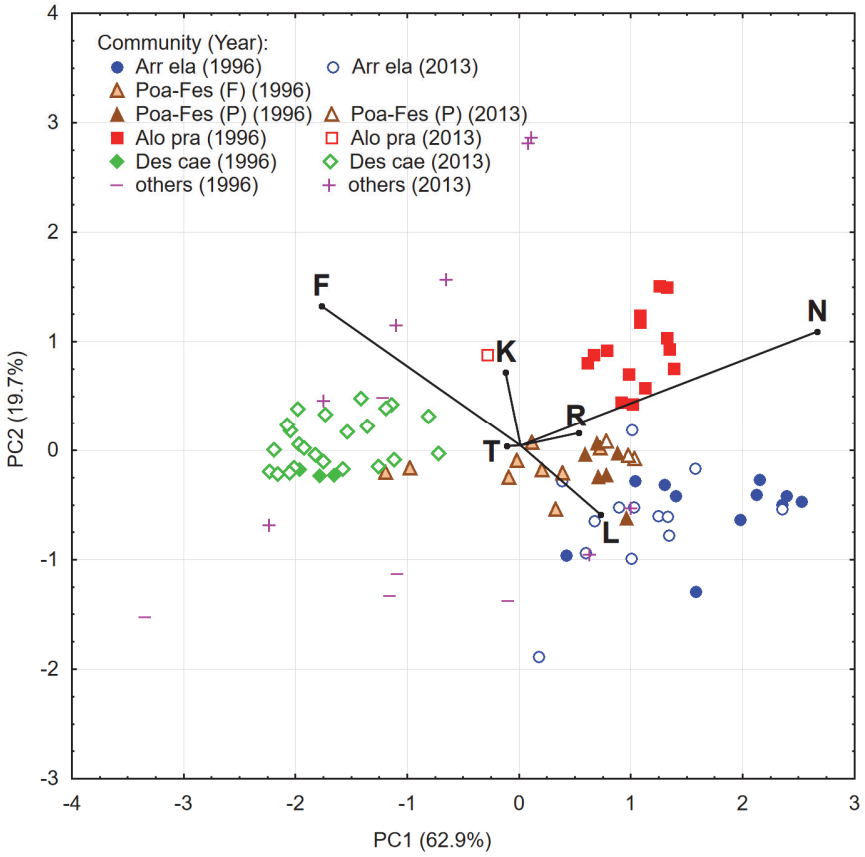

Fig. 5. The share of Ellenberg indices in principal components and distribution of plant communities (explanations like in Fig. 2)
Rys. 5. Udział wskaźników Ellenberga w składowych głównych oraz rozmieszczenie zbiorowisk roślinnych (objaśnienia jak w rysunku 2)

Table 1. List of bird species observed on "Zienkowskie Meadows"
Tabela 1. Lista gatunków ptaków obserwowanych na Łąkach Zienkowskich

Groups	Bird species	The main reasons for changes
bird species observed only in the first period	*Circus pygargus*, *Corvus cornix, C. frugilegus*, *Erythrina erythrina, Fulica atra*, *Limosa limosa*, *Tetrao tetrix*, *Tringa totanus*	transformation of *Alopecurus* meadows into meadows with the dominance of *Deschampsia caespitosa*, a high tussock grass species
bird species observed in both periods	*Accipiter gentilis*, *A. nisus*, *Acrocephalus palustris*, *A. schoenobaenus*, *A. scirpaceus*, *Actitis hypoleucos*, *Alauda arvensis*, *Anas crecca*, *A. platyrhynchos*, *A. querquedula*, *A. strepera*, *Anser anser*, *Ardea alba*, *Aythya ferina*, *A. fuligula*, *Buteo buteo*, *Calidris pugnax*, *Chlidonias hybrida*, *Ch. leucopterus*, *Chroicocephalus ridibundus*, *Ciconia ciconia*, *C. nigra*, *Circus aeruginosus*, *Clanga pomarina*, *Corvus corax*, *Crex crex*, *Cuculus canorus*, *Dendrocopos major*, *D. medius*, *Dryocopus martius*, *Emberiza citrinella*, *E. schoeniclus*, *Falco columbarius*, *F. subbuteo*, *Fringilla coelebs*, *Gallinago gallinago*, *Gallinula chloropus*, *Garrulus glandarius*, *Grus grus*, *Haliaeetus albicilla*, *Hirundo rustica*, *Lanius collurio*, *L. excubitor*, *Linaria cannabina*, *Locustella luscinioides*, *Luscinia luscinia*, *Motacilla flava*, *Oriolus oriolus*, *Phasianus colchicus*, *Phylloscopus collybita*, *P. trochilus*, *Porzana porzana*, *Rallus aquaticus*, *Saxicola rubetra*, *Sturnus vulgaris*, *Sylvia atricapilla*, *S. borin*, *S. communis*, *Tachybaptus ruficollis*, *Tringa erythropus*, *T. glareola*, *T. ochropus*, *Turdus merula*, *Upupa epops*, *Vanellus vanellus*	mosaic character of habitats diversity of plant communities diversity of habitat humidity preservation of extensive use involving mowing (very rarely pasture) in some parts of the area
bird species observed only in the second period	*Anthus pratensis, A. trivialis, Ardea cinerea, Chlidonias niger, Clanga clanga, Delichon urbicum, Gallinago media, Larus cachinnans, Locustella fluviatilis, L. naevia, Phalacrocorax carbo*	raising of the groundwater level and increase of humidity appearance of isolated shrubs due to the extensification of meadow management

On the other hand, the active protection of wet habitats conducted by the Polesie National Park in recent years, based on retaining water by building of sluices and weirs, led to the appearance of the greater spotted eagle *Clanga clanga*, a species vulnerable to extinction in Poland and Europe. The greater spotted eagle occurs in bogs in the vicinity of wet forests and in the vast areas of waterlogged meadows and wetlands. Besides, the restrictions on the use of these meadows not only led to changes in the plant communities, but also triggered secondary succession which occurs faster in forest meadows or meadows located in the vicinity of forest ecosystems (Szydłowska 2010). Isolated low shrubs that appeared in these meadows and shrubs growing along drainage ditches became a favourable habitat for the common grasshopper warbler *Locustella naevia* that had not occurred on the complex of Zienki Meadows before (Table 1).

4. Conclusions

The phytosociological studies conducted on Zienki Meadows in the Polesie National Park revealed a great diversity of habitats and plant communities.

1. It was found that the greatest changes occurred in *Alopecurus* and *Poa pratensis-Festuca rubra* meadows. After 17 years, most of them transformed into meadows with the predominance of *Deschampsia caespitosa*. Some *Alopecurus* meadows, located in the proximity of waterlogged habitats under active protection of the Polesie National Park, transformed into floristically poor *Phalaris* meadows or herbaceous meadows of the *Filipendulion ulmariae* alliance.
2. Tall oat-grass meadows 6510 (*Arrhenatherum elatioris*) were found to be the most stable plant communities, with the greatest floristic diversity. However, based on Ellenberg's indicators, a significant reduction of soil acidity and trophism of the habitat was observed, possibly as a result of the extensification of meadow use in these habitats (reduction or lack of mineral fertilisation).
3. Soil humidity and trophism were the most significant factors differentiating the data set under study. The appearance of large areas of such humid meadows was probably one of the reasons for the withdrawal

of two endangered bird species in Poland and Europe: the black-tailed godwit *Limosa limosa* and the common redshank *Tringa tetanus*.

4. Vegetation changes resulted from the lack of mowing as well as increased humidity of the habitat due to the active protection measures conducted by the Polesie National Park. On the other hand, the mosaic character of habitats with diverse humidity, diversity of plant communities and extensive utilisation ensured the stable number of bird species observed in both periods of the study.

References

Baryła, R. & Urban, D. (1999). Directions in grass community changes due to reduction and renunciation the agricultural performance following the example of Poleski National Park meadows. *Folia Universitatis Agriculturae Stetinensis*, *Agricultura*, *197(75)*, 25-29.

Beintema, A.J., Thissen, J.B., Tensen, D., Visser, G.H. (1991). Feeding ecology of Charadriiform chicks in agricultural grass land. *Ardea*, *79*, 31-43.

Braun-Blanquet, J. (1964). *Plant sociology. The study of plant communities*. Ed. 3. Wien-New York: Springer Publishing, 865.

Chodkiewicz, T., Kuczyński, L., Sikora, A., Chylarecki, P., Neubauer, G., Ławicki, Ł., Stawarczyk, T. (2015). Ocena liczebności populacji ptaków lęgowych w Polsce w latach 2008-2012. *Ornis Polonica, 56*, 149-189.

Chylarecki, P., Matyjasiak, P., Gmitruk, K., Kominek, E., Ogrodowczyk, P. (2006). Breeding success of waders in the Bug and Narew valleys, E Poland. *Wader Study Group Bulletin, 111*, 24-25.

Czyż, H., Malinowski, R., Kitczak, T., Przybyszewski, A. (2013). Charakterystyka chemiczna gleb i szaty roślinnej użytków zielonych w dolinie ujścia Warty. *Rocznik Ochrona Środowiska*, *15*, 694-713.

Ellenberg, H., Weber, H.E., Düll, R., Wirth, V., Werner, W., Paulißen, D. (1992). Zeigerwerte von Pflanzen in Mitteleuropa. *Scripta Geobotanica*, *18*, 258.

Grzywaczewski, G., Cios, Sz. (2012). Biological diversity of birds in the Lublin region - significance for the region. In: *Biodiversity and Regional Development* (eds. Bojar W., Diniz F., Junkuszew A.). Toruń: Towarzystwo Naukowe Organizacji i Kierownictwa, 213-236.

Harkot, W., Lipińska, H., Wyłupek, T. (2011). Directions of land management changes on a background of natural conditions of agricultural production space in Lublin region. *Acta Scientiarum Polonorum Administratio Locorum 10(1)*, 5-16.

Jutila, H.M. (2003). Germination in Baltic coastal wetland meadows: similarities and differences between vegetation and seed bank. *Plant Ecology 166(2)*, 275-293.

Klarzyńska, A. & Kryszak, A. (2015). Floristic diversity of extensively used fresh meadows (6510) in the Wielki Łęg Obrzański complex. *Acta Agrobotanica*, *68(2)*, 115-123.

Korzeniak, J. (2012). 6510 Extensively use hay lowland meadows (*Arrhenatherion*). In: *Monitoring of natural habitats. Methodical guidebook.* Part 3. (eds. Mróz W.). Chief Inspectorate of Environmental Protection, Warsaw, 79-94.

Kostrakiewicz-Gierałt, K. (2014). Are *Deschampsia caespitosa* (L.) Beauv. tussocks safe sites for seedling recruitment in the succession of wet meadows. *Polish Journal Ecology*, *62(4)*, 707-721.

Kozłowska, T. & Burs, W. (2013). Transformation of meadow communities due to the changes in soil moisture of meadow habitats. *Journal of Research and Applications in Agricultural Engineering, 58(4)*, 7-11.

Kucharski, L. (2014). Vegetation of oat-grass meadows in central Poland. *Steciana*, *18(3)*, 119-125.

Kulik, M. (2014). Changes of biodiversity and species composition of Molinia meadow depending on use method. *Polish Journal of Environmental Studies*, *23(3)*, 773-782.

Kulik, M. & Baryła, R. (2010). The changes of groundwater level at "Krasnoryki" meadow site in the Poleski National Park. *Teka Komisji Ochrony i Kształtowania Środowiska Przyrodniczego – OL PAN*, 7, 184-191.

Langgemach, T. & Bellebaum, J. (2005). Pradation und der Schutz bodenbrutender Vogelarten in Deutschland. *Vogelwelt*, *126*, 259-298.

Ławicki, Ł., Wylegała, P., Batycki, A., Kajzer, Z., Guentzel, S., Jasiński, M., Kruszyk, R., Rubacha, S., Żmihorski, M. (2011). Long-term decline of grassland waders in western Poland. *Vogelwelt*, *132*, 101-108.

Lewartowski, Z. & Piotrowska, M. (1987). Breeding birds in the valley of the Narew River. *Acta Ornithologica*, *23*, 215-272.

Matuszkiewicz, W. (2008). *Przewodnik do oznaczania zbiorowiska roślinnych Polski.* Warszawa: Wydawnictwo PWN, 536.

Mirek, Z., Piękoś-Mirkowa, H., Zając, A., Zając, M. (2002). *Flowering plants and pteridophytes of Poland a checklis*t. Kraków: Institute of Botany, Polish Academy of Sciences, 442.

Myśliwy, M. & Bosiacka, B. (2009). Disappearance of *Molinio-Arrhenatheretea* meadows diagnostic species in the Upper Płonia river valley (NW Poland). *Polish Journal of Environmental Studies*, *18(3)*, 513-519.

Nekrošienė, R. & Skuodienė, R. (2012). Changes in floristic composition of meadow phytocenoses, as landscape stability indicators, in protected areas in Western Lithuania. *Polish Journal of Environmental Studies, 21(3)*, 703-711.

Pehlak, H. & Lohmus A. (2008). An artificial nest experiment indicates equal nesting success of waders in costal meadows and mires. *Ornis Fennica, 85*, 66-71.

Shushpannikova, G. (2014). Formation and degradation of meadows under the impact of hay harvesting and grazing in the Vychegda and Pechora floodplains. *Russian Journal of Ecology*, *45(1)*, 33-37.

Stypiński, P. & Grobelna, D. (2000). Directions of succession of plant communities on the degraded and taken out from utilisation former grassland. *Łąkarstwo w Polsce, 3*, 151-157.

Świętochowski, P. (2009). Czynniki wpływające na sukces rozrodczy wybranych gatunków siewkowych *Charadriiformes* w strefie zalewowej doliny Biebrzy. *Dubelt*, *1*, 27-42.

Szydłowska, J. (2010). Charakterystyka florystyczna runi oraz ocena fitoindykacyjna warunków siedliskowych wybranych łąk śródleśnych. *Rocznik Ochrona Środowiska*, *12*, 299-312.

Vickery, J.A., Tallowin, J.R., Feber, R.E., Asteraki, E.J., Atkinson, P.W., Fuller, R.J., Brown, V.K. (2001). The management of lowland neutral grasslands in Britain: effects of agricultural practices on birds and their food resources. *Journal of Applied Ecology*, *38*, 647-664.

Vintu, V., Samuil, C., Rotar, I., Moisuc, A., Razec, I. (2011). Influence of the management on the phytocoenotic biodiversity of some Romanian representative grassland types. *Notulae Botanicae Horti Agrobotanici Cluj-Napoca*, *39(1)*, 119-125.

Watkinson, A. & Ormerod, S. (2001). Grasslands, grazing and biodiversity: editors introduction. *Journal of Applied Ecology*, *38*, 233-237.

Weigelt, A., Weisser, W.W., Buchmann, N., Scherer-Lorenzen, M. (2009). Biodiversity for multifunctional grasslands: equal productivity in high-diversity low-input and low-diversity high-input systems. *Biogeosciences*, *6(8)*, 1695-1706.

Wyłupek, T., Ziemińska-Smyk, M., Czarnecki, Z. (2015). Floristic diversity and agricultural value of *Phalaridetum arundinaceae* (Koch 1926 n.n.) Lib. 1931 in the selected river valleys of the Zamość region. *Acta Agrobotanica, 68(2)*, 109-113.

Zmiany szaty roślinnej i gatunków ptaków w siedliskach łąkowych w Poleskim Parku Narodowym, wschodnia Polska

Streszczenie

Celem badań była ocena szaty roślinnej i gatunków ptaków oraz porównanie wyników z danymi zebranymi 17 lat wcześniej, analiza zmian zbiorowisk roślinnych i gatunków ptaków w zależności od siedliska i gospodarki na użytkach zielonych, a także analiza zmian klimatycznych i siedliskowych na podstawie obliczonych ekologicznych liczb wskaźnikowych Ellenberga. Badania zostały przeprowadzone w latach 1996 i 2013 na Łąkach Zienkowskich w Poleskim Parku Narodowym, we wschodniej Polsce. Analizowany kompleks łąkowy (51˚27-29 'N; 23˚6-9' E), obejmuje powierzchnię ok. 650 ha i oddzielony jest naturalnymi granicami: od północy przylega on do naturalnego wyniesienia mineralnego, tzw. Garbu Włodawskiego, od zachodu otacza go kompleks leśny, od południa torfowisko z Jeziorem Moszne, a od wschodu mineralne wyniesienie wododziałowe. Zbiorowiska roślinne zostały zaklasyfikowane według metody Braun-Blanqueta. Badania dotyczące ptaków prowadzono w okresie lęgowym od połowy kwietnia do połowy lipca w okresach analogicznych do badań szaty roślinnej. Obszar badań charakteryzował się dużą różnorodnością siedlisk i zbiorowisk roślinnych. Największą stabilnością odznaczały się łąki rajgrasowe, które należą do jednego z typów cennych siedlisk przyrodniczych chronionych w ramach sieci Natura 2000 (6510). Te łąki świeże charakteryzowały się największą różnorodnością florystyczną, ale wskaźniki Ellenberga pokazały istotne zmniejszenie kwasowości gleby i trofizmu tych siedlisk w ciągu 17 lat. Zmiany te mogły być spowodowane ekstensywnym użytkowaniem łąk (zmniejszenie lub brak nawożenia mineralnego). Z kolei największe zmiany zaobserwowano na łąkach z *Alopecurus pratensis* i *Poa pratensis-Festuca rubra*. Większość z nich przekształciła się w łąki z dominacją *Deschampsia caespitosa*. Pojawienie się dużych powierzchni łąk bardziej wilgotnych mogło być prawdopodobnie jedną z przyczyn wycofania się dwóch zagrożonych wyginięciem w Europie ptaków: rycyka *Limosa limosa* i krwawodzioba *Tringa tetanus*. Wilgotność gleby i trofizm były bowiem czynnikami, które w największym stopniu wpływały na uzyskane dane. Z drugiej strony mozaikowaty charakter różnych siedlisk, zróżnicowanie zbiorowisk roślinnych i ekstensywne użytkowanie wpływało na stabilną liczbę gatunków ptaków w obydwu okresach badawczych. Czynna ochrona siedlisk podmokłych, która jest prowadzona w ostatnich latach przez Poleski Park Narodowy, przyczyniła się

do pojawienia się orlika grubodziobego *Clanga clanga*, ptaka, który jest zagrożony wyginięciem w Europie. Ponadto pojedyncze, niskie krzewy, pojawiające się na tych łąkach oraz krzewy, rosnące wzdłuż rowów melioracyjnych stały się korzystnym siedliskiem dla świerszczaka *Locustella naevia*, ptaka, który wcześniej nie występował na tym terenie.

Abstract

The aim of the study was to estimate the vegetation and bird species and compare it with the data collected 17 years ago, analyse the changes in plant communities and bird species depending on grassland management and habitat as well as analyse the climate and habitat changes based on Ellenberg's indicators. Studies were carried out in 1996 and 2013 on Zienki Meadows in Polesie National Park, Eastern Poland. The meadow complex discussed (51˚27-29' N; 23˚6-9' E), covering approx. 650 ha, has natural borders: in the north, it adjoins a natural mineral soil elevation, the so-called Włodawa Ridge; a forest complex in the west; a peat bog with Lake Moszne in the south; and a watershed on mineral soils in the east. The plant communities were classified using the Braun-Blanquet method. Investigations concerning birds were conducted in the breeding period from mid-April to mid-July in the same periods as the vegetation cover. The study area is characterized by the great diversity of habitats and plant communities. The most stable were tall oat-grass meadows, which are one of the habitat types protected within the framework of the Nature 2000 network (6510). That fresh meadows were characterized by the greatest floristic diversity, but Ellenberg's indicators showed a significant reduction of soil acidity and trophism of that habitat during 17 years. These changes could have been caused by extensification of meadow use (reduction or lack of mineral fertilisation). The biggest changes in *Alopecurus* and *Poa pratensis-Festuca rubra* meadows were observed. Most of them were transformed into meadows with the predominance of *Deschampsia caespitosa*. The appearance of large areas of such humid meadows was probably one of the reasons for the withdrawal of two endangered bird species in Europe: the black-tailed godwit *Limosa limosa* and the common redshank *Tringa tetanus*. The most significant factors differentiating the data set were soil humidity and trophism. On the other hand, a mosaic character of different habitats, diversity of plant communities and extensive utilisation ensured the stable number of bird species in both study periods. The active protection of wet habitats conducted by the Polesie National Park in recent years led even to the appearance of the greater spotted eagle *Clanga clanga*, a species that is vulnerable to extinction in Europe. Moreover, isolated low shrubs that appeared in

these meadows and shrubs growing along drainage ditches became a favourable habitat for the common grasshopper warbler *Locustella naevia* which had not occurred in this area before.

Słowa kluczowe:
gatunki ptaków, wskaźniki Ellenberga, łąka, zmiany szaty roślinnej

Key words:
bird species, Ellenberg's indicators, meadow, vegetation changes

MIDDLE POMERANIAN SCIENTIFIC SOCIETY OF THE ENVIRONMENT PROTECTION
ŚRODKOWO-POMORSKIE TOWARZYSTWO NAUKOWE OCHRONY ŚRODOWISKA

Annual Set The Environment Protection
Rocznik Ochrona Środowiska

Volume/Tom 19. Year/Rok 2017 ISSN 1506-218X 230-239

Analysis of Rheological Models of Modified Sewage Sludge

Paweł Wolski
Czestochowa University of Technology

1. Introduction

Sewage sludge represents a multi-phase system with complex flocculent structure with specific yield stress value (Zhou et al. 2014, Zhou et al. 2017). The composition of sewage sludge can be varied, which determines its physical, chemical and biological properties (Piecuch et al. 2013, Zawieja 2016). Evaluation of sludge properties often does not take into consideration the rheological parameters which are important for the hydraulic transport. Neglecting of these parameters may generate substantial design errors, thus functional difficulties of the whole system of sludge treatment (Fryźlewicz-Kozak et al. 2015). Rheological examinations are connected with non-Newtonian flow of sewage sludge (Wolny et al. 2008, Liu et al. 2015).

Rheology deals with examination of the response of real substances to stress (Travnicek et al. 2013). Rheological problems do not concern the motion of the body as a whole but the motion of certain body components with respect to the other. The aim of the rheology is to anticipate body behaviour with regards to the applied force system or to anticipate the system of forces that will result in specific body behaviour (Dong et al. 2012). The main task of rheology is to develop models used for description of behaviour of bodies exposed to the effect of force (Liang et al. 2017).

Rheological models allow for approximation of flow curves (Sozański et al. 1993). The flow curve becomes a straight line only at a very high shear rate. The logarithmic diagram of the dependency of the

shear stress and shear rate for the pseudoplastic fluid is often a straight line with the slope from 0 to 1. The simplest mathematical rheological model used to describe the flow curve for these fluids is the Ostwald-de Waele power model (Ferguson et al. 1995):

$$\tau = k \cdot (\gamma)^n \quad (1)$$

where: k – constant termed consistency coefficient, Pa·s; n – exponent, termed yield exponent.

In the Bingham model, fluids flow only after applying the shear stress τo, and, for smaller stress, they behave as a plastic solid:

$$\tau = \tau_o + \eta_{pl} \cdot \gamma \quad (2)$$

where: τ_o – yield stress, Pa; η_{pl} – plastic viscosity, Pa·s.

Herschel-Bulkley models are mostly composed of three parameters:

$$\tau = \tau_o + K \cdot (\gamma)^n \quad (3)$$

where: τ_o – yield stress, Pa; K – rheological parameter of the model; n – yield exponent.

The results of rheological measurements are approximated by means of specific rheological models, which can later be used for designing wastewater transport and storage or operation of wastewater treatment plants (Fryźlewicz-Kozak et al. 2008, Yang et al. 2009).

2. Materials and methods

Sewage sludge for the examinations was sampled from treatment of the wastewater from the cellulose and paper industry. Dry matter content was 16.82 g/dm^3, whereas initial hydration was 98.32%. Dry mass content and initial hydration of sludge was determined based on the standard PN-EN-12880. Modification of sludge was conducted using the process of sonication for 60s under static conditions. Sludge sonication used ultrasound field with intensity of: 2.2 (40%), 2.7 (60%); 3.2 (80%); 3.8 (100%) W/cm^2. The process of sewage sludge sonication used ultrasound processor Sonics VCX-1500 with maximal power output of 1,500 W. Frequency of ultrasound field vibration was 20 kHz whereas

maximal wavelength for the amplitude of 100% was 39.42 μm. The device is used to transform electricity into mechanical energy supplied to the titanium tip in the form of wave. Volume of the samples for sonication was 500 cm^3 for sludge after fermentation both in the flasks and in the bioreactor.

Fermentation of initially prepared sludge samples was performed in order to determine the effect of stabilization on rheological parameters. The process occurred in glass flasks that represented models of fermentation chambers and bioreactor. The sludge samples were placed in 10 laboratory flasks with volume of V = 0.5 dm^3. On each day of the process, rheological models were determined after removing one of the flasks from the thermostat in order to evaluate rheological parameters. Rheological parameters were determined using the rheometer RC20, with the shear rate of 0-200s^{-1}, for the period of 120s.

3. Results and discussion

The examinations conducted in this study were used to evaluate properties of sewage sludge exposed to the effect of ultrasound field wave with different length and fermentation time. Presentation of the values in the form of models allows for evaluation of rheological parameters of sewage sludge necessary for characterization of their pumpability or hydraulic transport. Flow curves, which represent the relationship between shear stresses and velocity gradient, illustrate the pattern in rheological models. The values obtained for the correlation coefficient were high and ranged, for the non-conditioned sludge: from 0.922-0.997; for sludge + UD40%: 0.847-0.999; for sludge + UD60%: 0.854-0.999; for sludge + UD80%: 0.822-0.999 and for sludge + UD100%: 0.882-0.999. Fig. 1 presents the relationship between the consistency constant *K* and flow index *n* for the model of Ostwald-de Waele at the temperature of 22°C.

An increase in flow index was found for each amplitude on each day of the fermentation process (see Fig. 1). For all the conditioning methods, the index value was below 1 ($n<1$), ranging, for the non-conditioned sludge from 0.521 (0 day of fermentation) to 0.629 (25th day of fermentation). For the sludge after conditioning with the ultrasound field with intensity of 3.8 W/cm^2, the flow index ranged from 0.382 (0 day of fermentation) to 0.539 (25th day of fermentation).

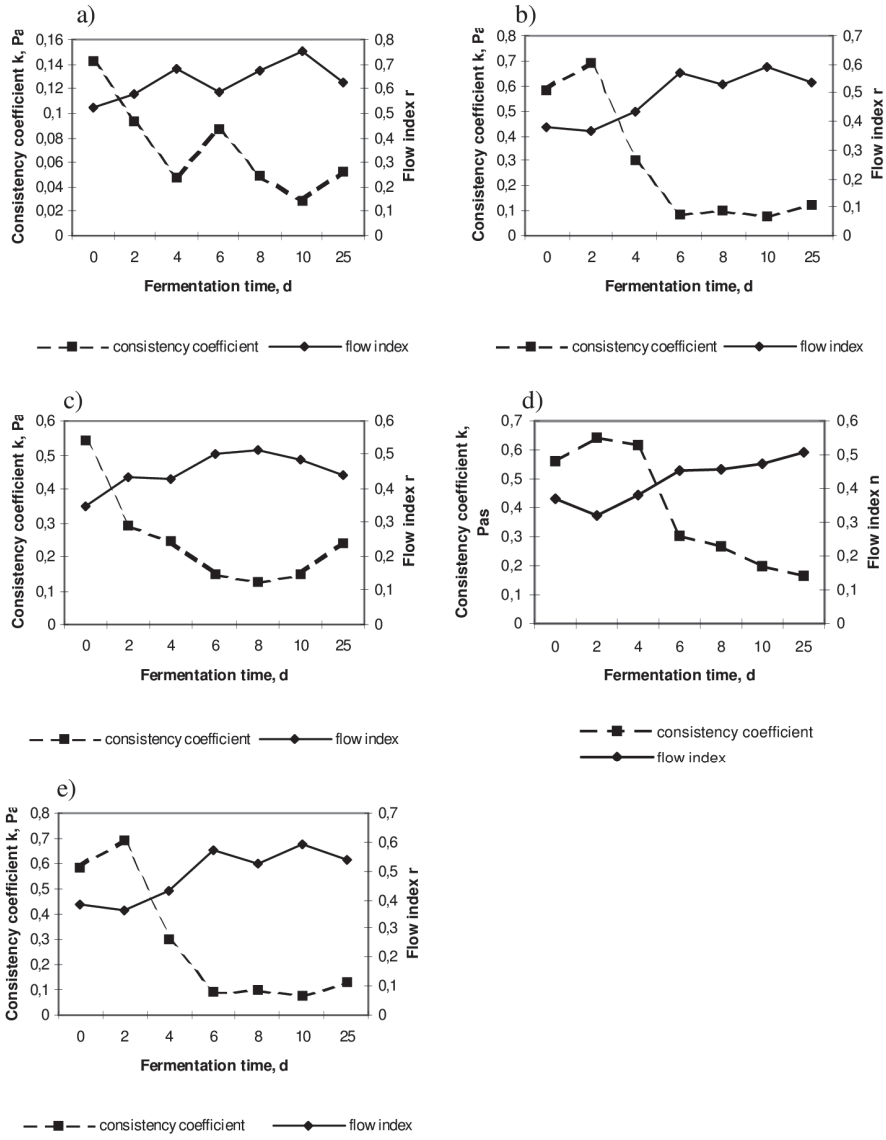

Fig. 1. Relationship between the consistency constant *K* and flow index *n* for Ostwald-de Waele model; a) non-conditioned sludge, b) sludge + UD40%, c) sludge + UD 60%, d) sludge + UD80%, e) sludge + UD100%
Rys. 1. Zależność stałej konsystencji *K* od wskaźnika płynięcia płynu *n* dla modelu Ostwalda-de Waele'a; a) osady niekondycjonowane, b) osady + UD40%, c) osady + UD 60%, d) osady + UD80%, e) osady + UD100%

Furthermore, sludge stabilization caused a reduction in consistency coefficient on each day of stabilization. The consistency constant, which is a measure of viscosity, was the lowest for the non-conditioned sludge compared to the sludge subjected to disintegration with ultrasound field (Table 1 to 5).

Table 1. Values of parameters of selected rheological models of unconditioned sewage sludge for γ = 0-200 s^{-1}; k – consistency coefficient, n – power exponent, τ_o – yield stress, η – viscosity, K – rheological model parameter
Tabela 1. Wartości parametrów wybranych modeli reologicznych niekondycjonowanych osadów ściekowych dla γ = 0-200 s^{-1}; k – współczynnik konsystencji, n – wykładnik potęgi, τ_o – granica płynięcia, η – lepkość, K – parametr reologiczny modelu

Rheological models		Fermentation time, d						
		0	2	4	6	8	10	25
Ostwald-de Waele	k	0.143	0.094	0.047	0.087	0.049	0.028	0.053
	n	0.521	0.575	0.683	0.584	0.671	0.754	0.629
Bingham	τ_o	0.466	0.348	0.227	0.325	0.225	0.154	0.196
	η_{pl}	0.1	0.009	0.008	0.009	0.008	0.007	0.007
Herschel-Bulkley	τ_o	0.157	0.057	0.074	0.091	0.011	0.073	0.181
	K	0.087	0.075	0.07	0.06	0.054	0.048	0.014
	n	0.604	0.613	0.611	0.648	0.656	0.661	0.87

Table 2. Values of parameters of selected rheological models of sewage sludge conditioned with the ultrasound field UD 40% for γ = 0-200 s^{-1}; k – consistency coefficient, n – power exponent, τ_o – yield stress, η – viscosity, K – rheological model parameter
Tabela 2. Wartości parametrów wybranych modeli reologicznych kondycjonowanych osadów ściekowych polem UD 40%, dla γ = 0-200 s^{-1}; k – współczynnik konsystencji, n – wykładnik potęgi, τ_o – granica płynięcia, η – lepkość, K – parametr reologiczny modelu

Rheological models		Fermentation time, d						
		0	2	4	6	8	10	25
Ostwald-de Waele	k	0.53	0.293	0.143	0.162	0.1	0.124	0.172
	n	0.344	0.416	0.498	0.452	0.539	0.501	0.474
Bingham	τ_o	1.093	0.707	0.417	0.418	0.326	0.357	0.474
	η_{pl}	0.013	0.011	0.009	0.008	0.008	0.008	0.009
Herschel-Bulkley	τ_o	0.856	0.677	0.374	0.422	0.258	0.356	0.444
	K	0.117	0.04	0.028	0.02	0.027	0.019	0.028
	n	0.58	0.747	0.782	0.807	0.766	0.83	0.781

Table 3. Values of parameters of selected rheological models of sewage sludge conditioned with the ultrasound field UD 60% for γ = 0-200 s^{-1}; k – consistency coefficient, n – power exponent, τ_o – yield stress, η – viscosity, K – rheological model parameter

Tabela 3. Wartości parametrów wybranych modeli reologicznych kondycjonowanych osadów ściekowych polem UD 60%, dla γ = 0-200 s^{-1}; k – współczynnik konsystencji, n – wykładnik potęgi, τ_o – granica płynięcia, η – lepkość, K – parametr reologiczny modelu

Rheological models		Fermentation time, d						
		0	2	4	6	8	10	25
Ostwald-de Waele	k	0.541	0.293	0.248	0.15	0.128	0.146	0.238
	n	0.351	0.437	0.428	0.503	0.514	0.484	0.44
Bingham	τ_o	1.134	0.758	0.633	0.439	0.382	0.403	0.602
	η_{pl}	0.014	0.013	0.01	0.01	0.009	0.008	0.011
Herschel-Bulkley	τ_o	0.877	0.584	0.469	0.4	0.371	0.425	0.616
	K	0.122	0.071	0.065	0.028	0.021	0.018	0.028
	n	0.584	0.672	0.649	0.79	0.825	0.848	0.803

Table 4. Values of parameters of selected rheological models of sewage sludge conditioned with the ultrasound field UD 80% for γ = 0-200 s^{-1}; k – consistency coefficient, n – power exponent, τ_o – yield stress, η – viscosity, K – rheological model parameter

Tabela 4. Wartości parametrów wybranych modeli reologicznych kondycjonowanych osadów ściekowych polem UD 80%, dla γ = 0-200 s^{-1}; k – współczynnik konsystencji, n – wykładnik potęgi, τ_o – granica płynięcia, η – lepkość, K – parametr reologiczny modelu

Rheological models		Fermentation time, d						
		0	2	4	6	8	10	25
Ostwald-de Waele	k	0.561	0.642	0.616	0.303	0.266	0.198	0.165
	n	0.37	0.32	0.381	0.453	0.457	0.473	0.507
Bingham	τ_o	1.227	2.161	1.387	0.808	0.707	0.526	0.481
	η_{pl}	0.016	0.023	0.019	0.014	0.013	0.011	0.011
Herschel-Bulkley	τ_o	1.059	1.606	1.107	0.666	0.653	0.581	0.464
	K	0.098	0.273	0.131	0.065	0.044	0.02	0.027
	n	0.651	0.535	0.63	0.712	0.763	0.871	0.819

Table 5. Values of parameters of selected rheological models of sewage sludge conditioned with the ultrasound field UD 100% for γ = 0-200 s^{-1};
k – consistency coefficient, n – power exponent, τ_o – yield stress, η – viscosity, K – rheological model parameter
Tabela 5. Wartości parametrów wybranych modeli reologicznych kondycjonowanych osadów ściekowych polem UD 100%, dla γ = 0-200 s^{-1};
k – współczynnik konsystencji, n – wykładnik potęgi, τ_o – granica płynięcia, η – lepkość, K – parametr reologiczny modelu

Rheological models		Fermentation time, d						
		0	2	4	6	8	10	25
Ostwald-de Waele	k	0.585	0.693	0.3	0.089	0.098	0.076	0.128
	n	0.382	0.364	0.432	0.574	0.528	0.59	0.539
Bingham	τ_o	1.325	1.502	0.749	0.308	0.29	0.276	0.404
	η_{pl}	0.018	0.019	0.013	0.009	0.007	0.008	0.01
Herschel-Bulkley	τ_o	1.046	1.109	0.732	0.208	0.319	0.189	0.364
	K	0.128	0.173	0.04	0.031	0.012	0.027	0.027
	n	0.627	0.583	0.771	0.759	0.893	0.769	0.811

The use of sludge conditioning with the ultrasound field increased the level of yield stress. In the Bingham model, the value τ_o for non-conditioned and non-stabilized sludge was 0.466Pa. In the case of modification with the ultrasound field, the value of yield stresses were: 1.093 (UD40%); 1.134 (UD60%); 1.227 (UD80%); 1.325Pa (UD100%). Exposure of sludge modified with energy of ultrasound field to fermentation led to a reduction in the values of the parameter discussed. They were lower on consecutive days of stabilization compared to the sludge which was not modified before. Similar relationship was found for the three-parameter Herschel-Bulkley model.

4. Conclusions

One of the most basic problems of contemporary civilization is manufacturing, processing, utilization and degradation of liquid compounds. Therefore, it is essential to properly determine physical properties and rheological and technological parameters of liquids. Proper adjustment of the rheological model to behaviour of real liquid minimizes errors of the calculated values, such as character of flow, flow resistance in the circulation system and particle sedimentation. This study aimed to evaluate rheological parameters of the sludge from the cellulose and pa-

per industry subjected to conditioning at different intensities of the ultrasound field and then stabilization in flasks and a bioreactor.

The findings of the study lead to the following conclusions:

- the sewage sludge analysed in the study belongs to shear-thinning fluids. The values of flow index for all the tests is n<1;
- the examined types of sewage sludge had a yield stress values. The values of the discussed index increased with the intensity of the ultrasound field wave. With the use of the fermentation process, yield stress decreased as fermentation time elongated;
- the rheological models used for characterization of sewage sludge represented the rheological parameters accurately for different values and modification methods. The consistency coefficient (which is a measure of viscosity) and plastic viscosity increased as the ultrasound field intensity rose, while it was decreasing on consecutive days of anaerobic stabilization.

Acknowledgements

The research was funded by the project No. BS-PB-401/303/12 and BS-PB-401/301/11

References

Dong, Y., Wang, Y. (2012). Steady rheological characteristics of the concentrated water treatment residuals (CWTR). *Acta Scientiae Circumstantiae,* 678-682.

Ferguson, J., Kembłowski, Z. (1995). *Reologia stosowana płynów*. Łódź: MARCUS,.

Fryźlewicz-Kozak, B., Jamróz, J., Pachołek, M. (2015). Badania właściwości reologicznych ścieków. *Inż. i Ap. Chem., 54(2)*, 33-35.

Fryźlewicz-Kozak, B., Tal-Figiel, B. (2008). Theoretical and experimental analysis of floc structure of an activated sludge under sonication. *Chemical Proc. Eng., 29*, 87-98.

Liang, F., Sauceau, M., Dusserre, G., Arlabosse, P. (2017). A uniaxial cyclic compression method for characterizing the rheological and textural behaviors of mechanically dewatered sewage sludge, mechanically dewatered sewage sludge. *Water Res., 113*, 171-180.

Liu, G.J., Liu, Y., Wang, Z.Y., Lei, Y.H., Chen, Z.A., Deng, L.W. (2015). The effects of temperature, organic matter and time-dependency on rheological properties of dry anaerobic digested swine manure. *Waste Manage., 38(1)*, 449-454.

Piecuch, T., Piekarsk,i J., Malatyńska, G. (2013). Filtration of mixtures forming compressible sediments. *Rocznik Ochrona Środowiska, 15*, 39-58.
PN-EN 12880 – charakterystyka osadów ściekowych. Oznaczanie suchej pozostałości i zawartości wody.
Sozański, M., Jeż-Walkowiak, J. (1993). Charakterystyki reologiczne osadów i ich znaczenie w rozwiązywaniu problemów projektowych i eksploatacyjnych. [w:] Bien J.,(red.). *Materiały Konf. Naukowo-Technicznej, Czestochowa.* 153-173.
Travnicek, P., Vitez, T., Junga, P., Krcalova, E., Sevcikova, J. (2013). Original research of rheological measurements of disintegrated activated sludge. *Pol. J. Environ. Stud*., 1209-1212.
Wolny, L. Wolski, P., Zawieja, I. (2008). Rheological parameters of dewatered sewage sludge after conditioning. *Desalination*, 382-387.
Yang, F., Bick, A., Shandalov, S., Brenner, A., Oron, G. (2009). Yield stress and rheological characteristics of activated sludge in an airlift membrane bioreactor. *J. Membrane Sci*., *334*, 83-90.
Zawieja, I. (2016). Characteristics of Excess Sludge Subjected to Disintegration. *Rocznik Ochrona Środowiska*, *18*, 124-136.
Zhou, C.H., Ling, Y., Zeng, M., Li, X.Y. (2017). Analysis of particle size distribution and water content on microwave/ultrasound pretreated sludge. *Chinese Journal of Environmental Engineering, 11(1)*, 529-534.
Zhou, C.H., Ling, Y., Zeng, M., Li, X.Y. (2014). Influence of microwave and ultrasound on sludge dewaterability. *Advanced Materials Research, 955-959*, 2074-2079.

Analiza modeli reologicznych modyfikowanych osadów ściekowych

Streszczenie

W artykule przedstawiono wyniki badań prowadzone na osadach ściekowych z przemysłu celulozowo-papierniczego. Celem prowadzonych badań było wyznaczenie modeli reologicznych (Ostwalda-de Waele, Binghama, Herschela-Bulkley'a) dla osadów ściekowych niekondycjonowanych oraz poddanych działaniu pola ultradźwiękowego przy różnych jego natężeniach, a następnie stabilizacji w kolbach i bioreaktorze. Poznanie właściwości reologicznych osadów umożliwia dokładną charakterystykę ich pompowalności oraz zdolności podczas transportu hydraulicznego. W wyniku przeprowadzonych badań stwierdzono zwiększenie granicy płynięcia, jak również konsystencji poprzez zastosowanie energii pola ultradźwiękowego. Wartości omawianych parametrów ulegały obniżenie podczas kolejnych dni prowadzenia procesy stabilizacji.

Abstract

This paper presents the results of examinations of sewage sludge from cellulose and paper industry. The aim of the study was to determine rheological models (the Ostwald-de Waele, Bingham and Herschel-Bulkley models) of non-conditioned sewage sludge and the sludge exposed to the effect of the ultrasound field at its different intensities and then stabilized in flasks and in the bioreactor. Evaluation of rheological properties of sewage sludge allows for a detailed characterization of their pumpability and abilities during the hydraulic transport. The examinations revealed the increase in the yield stress and consistency coefficient through application of the energy of the ultrasound field. The values of the parameters discussed were reduced on consecutive days of the stabilization process.

Słowa kluczowe:
osady ściekowe, modele reologiczne, nadźwiękawianie, stabilizacja

Keywords:
sewage sludge, rheological models, sonication, stabilization

MIDDLE POMERANIAN SCIENTIFIC SOCIETY OF THE ENVIRONMENT PROTECTION
ŚRODKOWO-POMORSKIE TOWARZYSTWO NAUKOWE OCHRONY ŚRODOWISKA
Annual Set The Environment Protection
Rocznik Ochrona Środowiska
Volume/Tom 19. Year/Rok 2017 ISSN 1506-218X 240-252

Studies on the Field Type Ground Heat Exchanger Coupled with the Compressor Heat Pump (Part 1)

Oktawia Dolna, Jarosław Mikielewicz
Institute of Fluid Flow Machinery of PASci

1. Introduction

This paper focuses on the CFD analysis of the vertical FGHE and its influence on the compressor heat pump performance. The numerical research were carried out for the FGHE varying geometry and ground's temperature boundary conditions. However, the primary aim was to improve the quasi-steady heat pump operation modelling.

In the engineering practice, it is common that the heat flux transferred to the heat pump's evaporator from the low heat source is being averaged with respect to the FGHE work time. On the other hand, it is well known that the heat flux value, varies in time, due to the soil and the ground heat exchanger external wall temperature variation.

In the cases having been analysed during numerical research, of which, the results are presented in the work, two FGHE's lengths were taken into account. Moreover, two different epsilon values were considered (Fig.1 and Fig.2).

There has been done a numerical analysis of 170 hours of continuous work (Dolna, 2016). The present work concentrates on the FGHE-compressor heat pump coupling.

2. Computaitonal model description and boundary conditios

The reference FGHE consisted of two 110 meters long coaxial pipes. The external one had an oval bottom. The FGHE was hooked in

the ground, which was divided into three layers, of different thermophysical properties. As a comparative case, 27.5 meters long FGHE surrounded by the soil of one type was examined. Fig.3 illustrates the outline of a computational domain.

In the calculations, there was taken into account the finite volume of the ground, simulating infinite half-space. The initial temperature profile of the ground, in the numerical computations, in the UDF (User Defined Function) was defined and it is easy to modify. The numerical simulation calculations of the described FGHE have been done using the commercial software.

Boundary conditions and implemented UDF are as follows:

- the temperature variation with depth was given in User's Defined Function (UDF) and interpreted in Fluent as a temperature boundary condition on the outline of the whole computational domain
- the temperature profile was defined by the conjunction of two linear functions as the ground's temperature increase varies with depth
- the soil types
  - gravel – from 0 level to the depth of 20 meters:
  - clay – at depth range of (20-110) meters:
  - limestones – under 110 meters:
- inlet fluid temperature (3[ºC]) and inlet fluid pressure (10[bar])
- working medium – ethylene glycol
- ground surface temperature (marked in green in Fig. 3) was set at 6[ºC] or -2 [ºC]

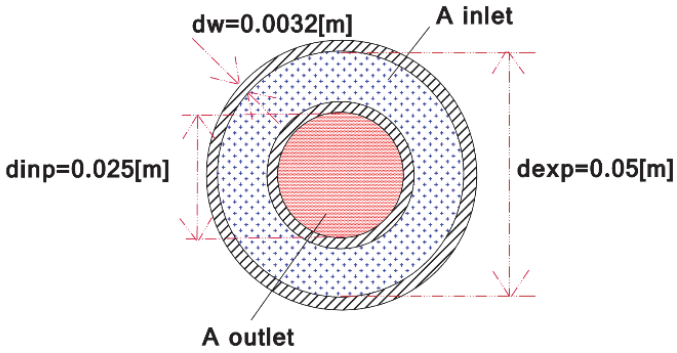

Fig. 1. Reference FGHE, $\varepsilon = 0.41$ (Dolna, 2016)
Rys. 1. Referencyjny GWCF, $\varepsilon = 0.41$ (Dolna, 2016)

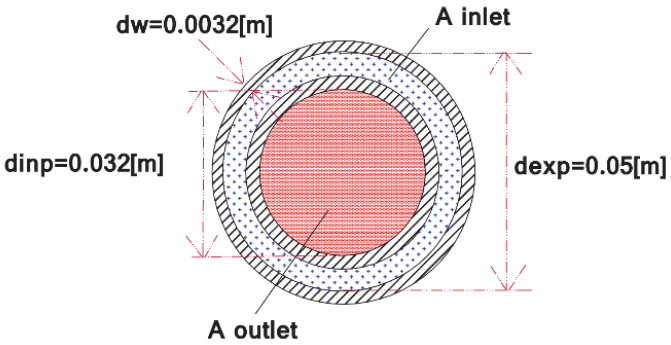

Fig. 2. Comparative FGHE, $\varepsilon = 1$ (Dolna, 2016)
Rys. 2. Porównawczy GWCF, $\varepsilon = 1$ (Dolna, 2016)

where: $\varepsilon = \frac{A_{outlet}}{A_{inlet}}$

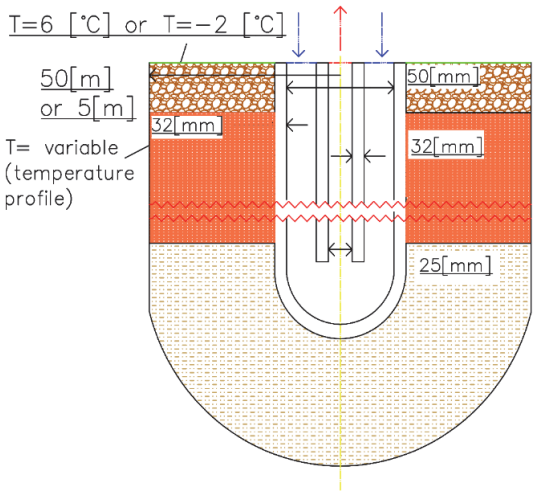

Fig. 3. Two-dimensional outline of the computational domain (Dolna, 2016)
Rys. 3. Dwuwymiarowy szkic domeny obliczeniowej (Dolna, 2016)

The FVM was used to discretise the computational domain. For the purpose of numerical calculations, the structural mesh was generated. Obviously, the mesh size varied according to the FGHE's length. The mesh influence was not discussed in the current paper however described problem is mesh independent as the proper analysis was caried out.

3. Conjunction of 0D-level (compressor heat pump cycle) and 3D-level (CFD FGHE) programming

In this section, there is described the conjunction of the compressor heat pump cycle author's programme with the CFD analysis results of the FGHEs of different lengths and outlet/inlet surface ratios. As a result of 0D-3D level programming, there was created a computational model, which provides the possibility of the heat pump system designing in a way, which hasn't been used before. Further work on this author's software development may result in creating a commercial programme, which could be widely used by the heat pump systems designers.

The numerical research, of which the results are discussed in this subsection, confirm the time dependent FGHE heat-flow parameters variation, what in conjunction with the geometry variation, influences the compressor heat pump work. According to the above, the 0D-3D programming conjunction is about the CFD (3D) analysis results implementation into author's code *COMPRESSOR HEAT PUMP* (0D). The FGHE varying heat-flow parameters are as follows, the mass flow rate and the temperature, and the heat flux transferred from the surrounding ground. The FGHE length variation results in the mass flow rate change. Consequently, the FGHE working fluid outlet temperature and the heat flux also change.

The FGHE outlet is identical with the GCHP evaporator's inlet. The FGHE working medium outlet temperature variation corresponds with the GCHP evaporator's heat flux value change. As the FGHE is coupled with the compressor heat pump, its factual influence should be taken into account. However, nowadays, for instance the FGHE outlet heat flux is mostly being averaged. The present work shows the importance of a quasi-steady GCHP system modelling as the FGHE outlet heat flux value decreases with the work time significantly.

This work concerns also the analysis of a case of a heat pump heating power decrease. It is obvious that the heating or cooling devices do not work with their nominal power all the time. Bearing on mind this fact, FGHE work under varying load was studied. Figure (Fig.4) presents heat characteristics of FGHE of different mass flow rate and corresponding heat pump heating power.

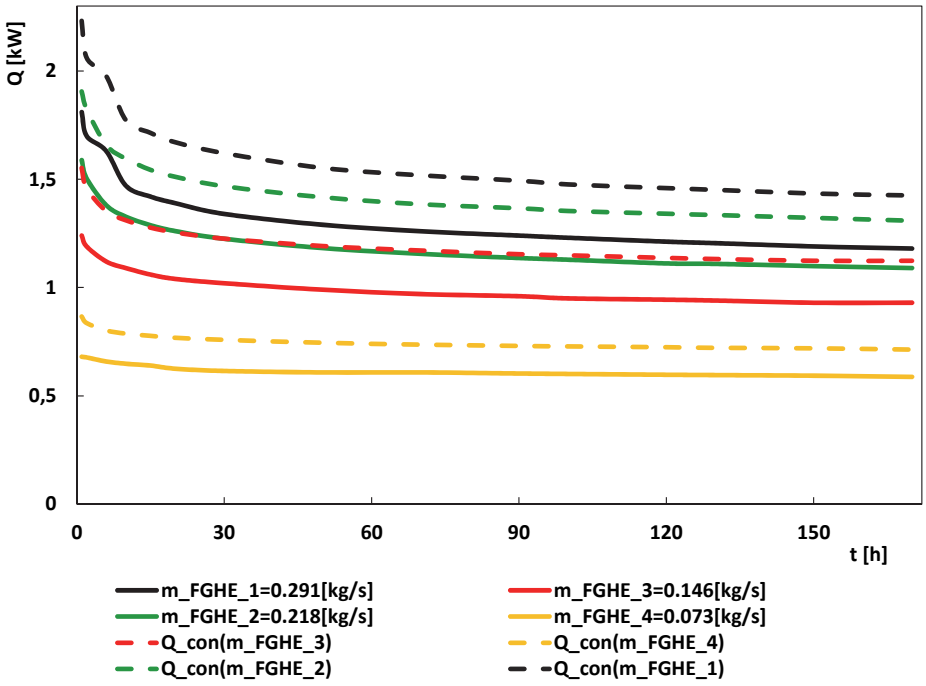

Fig. 4. Variation of the heat pump heating power resulting from the FGHE heat load variation during continuous quasi-steady work (Dolna, 2016)
Rys. 4. Zależność mocy grzewczej sprężarkowej pompy ciepła od zmiennego obciążenia GWCF (Dolna, 2016)

Continuous lines correspond to FGHE varying load, while the intermittent ones correspond to the varying heat pump heating power. For the cases of the FGHE, working under varying load, the COP value of the compressor heat pump was computed and is exposed in the figure attached below (Fig. 5). On the basis of this analysis having been carried out, it is now possible to estimate how will the FGHE work if the GCHP heating power decreases.

For the purpose of the FGHE-HP coupling, one hundred and seventy hours of continuous FGHE work had been analysed. Figure 6 and 7 visualise the results of FGHE-CHP conjunction reached through the 0D-3D level programming linkage.

On the basis of these studies it become possible to model quasi-steady heat pump's work.

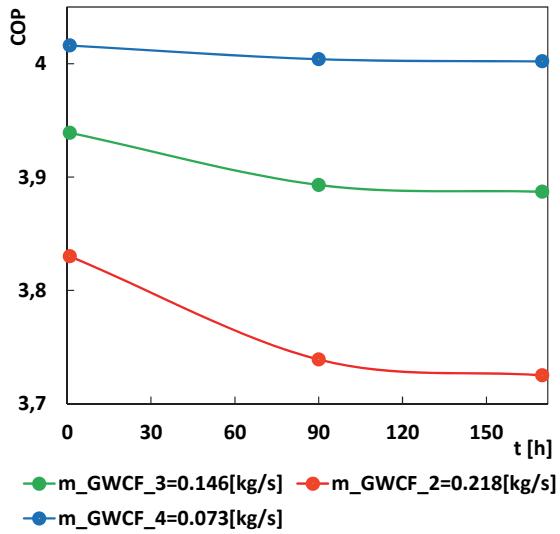

Fig. 5. Heat pump COP variation with FGHE load during quasi-steady continuous work (Dolna, 2016)
Rys. 5. Wahania wartości COP sprężarkowej pompy ciepła w czasie ciągłej quasi-stacjonarnej pracy, wynikające ze zmiany obciążenie GWCF (Dolna, 2016)

Figures exposed in the work (Figures 4-8) visualise the results received on the basis of the 0D and the 3D programming conjunction. The black continuous line (Fig. 6) refers to the FGHE reference model of the mass flow rate equal $\dot{m} = 0.291 \left[\frac{kg}{s}\right]$. The heat pump working medium used in these particular computations was R600a, however, the author's software provides the use of 13 different refrigerants, however the list of working fluids may be defined in any other way regarding user's needs.

The results presented in Fig. 5 concern the HP COP value variation with the FGHE circulating pump electric power, being dependent of the FGHE mass flow rate. Moreover, from the figure 6 it might be seen how does the COP value vary in time during the continuous 170 [h] work. The heat pump coefficient of performance value, was calculated on two ways, using author's code. First approach did not include the amount of the electric power having been consumed by the low heat source heat exchange system circulating pump. In the second approach, the FGHE circulating pump electric power was taken into account. However, from

the realistic point of view, the electric power of the circulating pumps of the low and high heat pump source should be taken into account when computing the COP value. The aim of the current analysis is to show the difference between the COP value having been computed in two different ways, described above. The results are as follows: $COP_1 = 4.081$ – the value of the heat pump COP computed without taking into account the electrical power of the low heat source circulating pump. $COP_2 = 3.323$ corresponds to the latter algorithm, which included the low heat source system (in this case it is the LFGHE) circulating pump electric power.

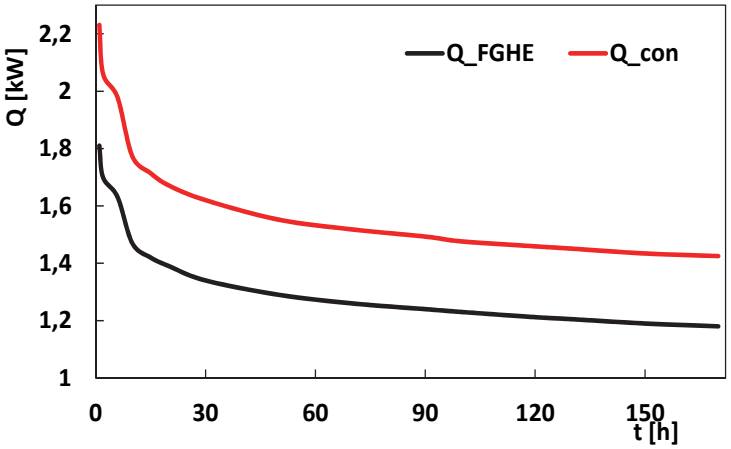

Fig. 6. Q_FGHE – time dependent thermal power of the FGHE; Q_con – time dependent heating power of the compressor heat pump (Dolna, 2016)
Rys. 6. Q_FGHE – moc cieplna GWCF zależna od czasu; Q_con – moc grzewcza sprężarkowej pompy ciepła zależna od czasu (Dolna, 2016)

The computations have been done in terms of a non-stationary analysis. Moreover, the computations have run in the transient mode from the very beginning. It means that, the simulations did not start from the steady state and then have turn into a transient mode. It was noticed, that when the steady state computations run, the computational tool (Fluent) predicts the solution (which may not be the correct one) and when it is turned into transient mode, the results are not that satisfactory as they should be. This is the main and only reason why the transient mode

should be switched on from the very beginning. The disadvantage of such a way of solving the problem is that it takes much more time, but the results are of a much better quality than in the case of steady – transient transition.

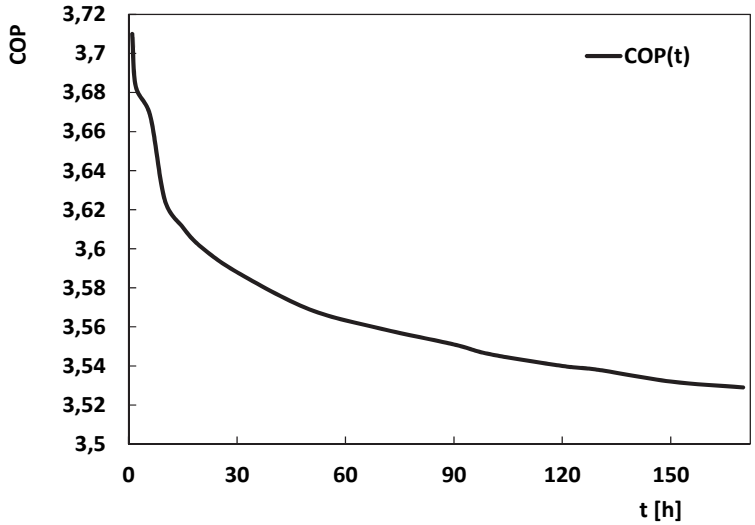

Fig. 7. Compressor heat pump COP value change during the quasi-steady 170 [h] continuous work (Dolna, 2016)
Rys. 7. Zależność wartości COP sprężarkowej pompy ciepła podczas 170 godzinnej quasi-stacjonarnej pracy (Dolna, 2016)

Characteristics presented in the following graph (Fig. 8) show the difference between one LFGHE and a set of four SFGHEs. The comparative criterion was the circulating power of the FGHE working medium as it is exposed in the table attached below (Table 1). From energetic point of view, one LFGHE is more efficient than four SFGHEs. However, sometimes environmental conditions unfavourable and it is not possible to drill as deep as 110 meters. From the graph (Fig. 8), we may see how much energy is being lost if the set of SFGHEs is applied instead of LFGHE.

Table 1. Juxtaposition of the comparative parameter values corresponding to a particular FGHE system (Dolna, 2016)
Tabela 1. Zestawienie wartości parametrów stanowiących kryterium porównawcze GWCF o różnej długości (Dolna, 2016)

Length [m]	Circulating power [W]
$L_{LFGHE} = 110$	26
$L_{SFGHE} = 27.5$	6 4 x 6= 24

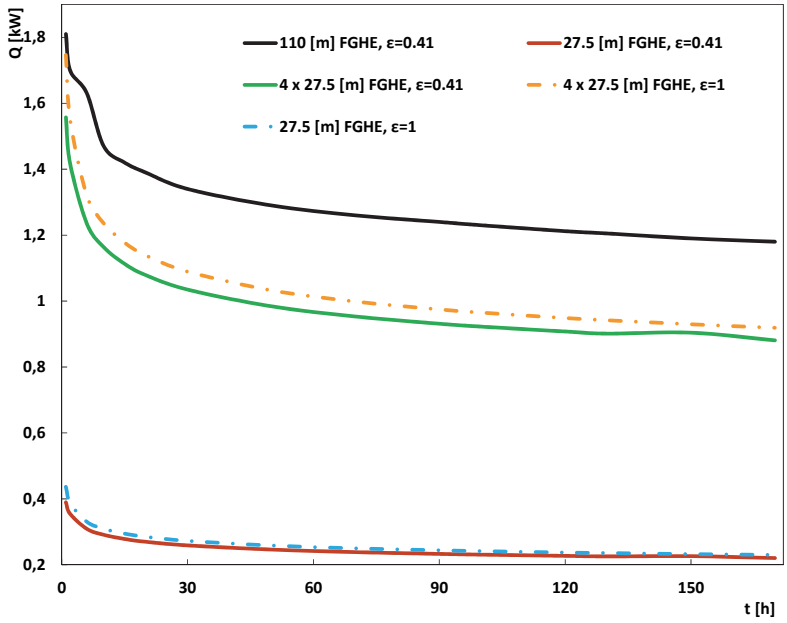

Fig. 8. Comparison of FGHEs of different length and time dependent epsilon values (Dolna, 2016)
Rys. 8. Porównanie GWCF o różnej długości i wartości współczynnika epsilon zależnego od czasu (Dolna, 2016)

Bearing on mind the need to consider whether the ground's surface (marked in green, in Fig. 3.) temperature strongly influence the borehole heat transfer or not, there was studied a case of a negative temperature value. Figure 9. presents the results of the analysis mentioned above, so it can be noticed that the temperature decrease at this particular surface did not influence the borehole heat transfer.

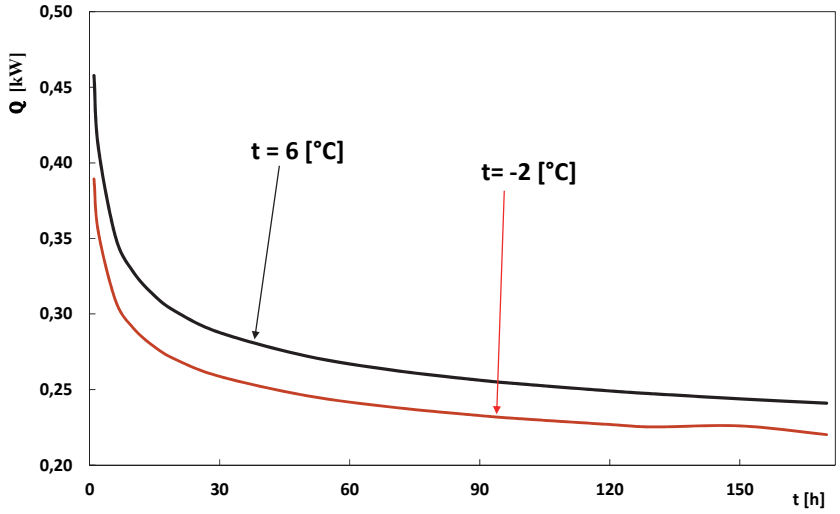

Fig. 9. FGHE time dependent thermal power for varying ground's surface tempearture boundary conditions (Dolna, 2016)
Rys. 9. Strumień ciepła, zależny od czasu, pozyskany przez GWCF dla zmiennych temperaturowych warunków brzegowych (Dolna, 2016)

4. Summary

On the basis of the results presented in the work, some assumptions were stated. First of all, the results confirm the thesis about the low heat source's (the ground) thermal efficiency depletion in time. It can be noticed in the graphs: Fig. 9, Fig. 8, Fig. 6 and Fig.4 that the thermal borehole power decrease in time significant. The quasi-steady character of the FGHE work should be taken into account in the GCHP system designing level as it was proven that the heat pump heating power varies in time. The latter is a result of not stable in time FGHE output heat flux. 0D-3D level programming coupling provided a computational tool to investigate the FGHE influence on the compressor heat pump and the quasi-steady CHP work could have been modelled.

Numerical research having been done, resulted in determining the FGHE performance working under varying load. For instance, 25 % reduction of the LFGHE mass flow rate resulted in 15 % decrease of the compressor heat pump heating power.

It was also noticed that, from energetic point of view, it is more efficient, to drill longer borehole instead of a set of short ones.

Nomenclature

FGHE – Field type ground heat exchanger,
CFD – computational fluid dynamics,
LFGHE – long FGHE (110 [m]),
SFGHE – short FGHE (27.5 [m]),
GCHP – ground coupled compressor heat pump,
GWCF – Field type ground heat exchanger (in Polish: gruntowy wymiennik ciepła typu Field'a),
HP – heat pump,
CHP – compressor heat pump,
COP – coefficient of performance,
FVM – Finite Volumes Method,
0D – zero-dimensional,
3D – three-dimensional,
$c_p \left[\frac{J}{kg\ K}\right]$ – specific heat,
$\dot{L}_{FGHE}[W]$ – FHGE circulating power,
$\dot{m} \left[\frac{kg}{s}\right]$ – FGHE working fluid mass flow rate,
t_{out}[℃] – FGHE working medium outlet temperature, which is identical to the GCHP evaporator's inlet,
$A\ [m^2]$ – inlet/outlet surface of the FGHE.

Greek symbols

$\boldsymbol{\varepsilon = \frac{A_{outlet}}{A_{inlet}}}$ – epsilon – inlet/outlet surface ratio,
$\lambda \left[\frac{W}{m\ K}\right]$ – thermal conductivity,
$\varrho \left[\frac{kg}{m^3}\right]$ – density.

Subscripts

con – condenser.

References

Bohdal, T., Charun, H., Sikora, M. (2015). Wybrane aspekty prawno-techniczne i ekologiczne stosowania sprężarkowych pomp ciepła. *Rocznik Ochrona Środowiska, 17*, 461-484

Dolna, O. (2016). *Influence of the ground heat exchanger design heat – flow parameters on the heat pump efficiency.* Institute of Fluid Flow Machinery, PhD dissertation.

Mikielewicz, J., Grochal, B., Polesek-Karczewska, S., Gumkowski, S., Mikielewicz, D. (1996). *Heat Exchange.* Gdańsk: Institute of Fluid Flow Machinery PASci (in Polish).

Yang, H., Cui, P., Fang, Z. (2010). Vertical-borehole ground-coupled heat pumps: A review and systems *Applied Energy*, *87*, 16-27.

Zalewski, W. (2001). *Compressor, Sorption and Thermoelectric Heat Pumps*. IPPU MASTA (in Polish).

Badania gruntowego wymiennika ciepła typu Field'a współpracującego ze sprężarkową pompą ciepła (część 1)

Streszczenie

Niniejsza praca dotyczy analizy CFD gruntowgo wymiennika ciepła typu Field'a oraz zbadania wpływu jego pracy na działanie sprężarkowej pompy ciepła. W pracy podjęto problem gruntowego pionowego wspólosiowego wymiennika ciepła, ponieważ zdecydowana część prac naukowo-bawdawczych poświęcona jest wymiennikom gruntowym typu U-rura (Yang et al., 2010). Wobec powyższego, brak jest w literaturze cieplno-przepływowych charakterystyk gruntowego wymiennika ciepła typu Fielda. W pracy przedstawiono analizę quasi-stacjonarnej pracy gruntowej sprężarkowej pompy ciepła, co było możliwe dzięki sprzęgnięciu programowania na poziomie 0D i 3D. Praca całego systemu miała charakter ciągły i trwała 170 godzin. Sprężarkowa gruntowa pompa ciepła może pokryć zapotrzebowanie na ciepło pracując nawet w obiegu monowalentnym, ale system wymiany ciepła dolnego źródła ciepła musi być prawidłowo zaprojektowany. Ponadto, należy starannie dobrać właściwy pod względem efektywności czynnik roboczy sprężarkowej pomy ciepła (Bohdal i in., 2015). Obliczenia CFD zostały przeprowadzone przy użyciu komercyjnego oprogramowania. Natomiast, obliczenia obiegu sprężarkowej pomy ciepła zostały wykonane przy użyciu autorskiego programu. Przeanalizowano pracę GWCF o zdywersyfikowanej geometrii w trybie pracy nieprzerywanej. Zaimplementowano zmienne temperaturowe warunki brzegowe na jednej powierzchni domeny obliczeniowej. Praca zawiera jakościową analizę systemu

gruntowej pompy ciepła, której wyniki mogłyby zostać wykorzystane w procesie projektowania gruntowych sprężarkowych pomp ciepła.

Abstract

Present work concerns the CFD analysis of the Field type ground heat exchanger and its influence on the compressor heat pump performance. The coaxial vertical ground heat exchanger has been chosen as in most studies the U-pipe is being considered (Yang et al., 2010). Therefore, Field type ground heat exchanger's heat-flow characteristics are not available in the literature. Conjunction of 0D-3D level programming enabled FGHE-coupled compressor heat pump system analysis in terms of a quasi-steady continuous work lasting 170 hours. The ground coupled compressor heat pump may work in the monovalent system and complitely fulfil demand on heat, however, the heat exchange system of the low heat source needs to be designed in a proper way. Additionally, the CHP working medium needs to be chosen carefully (Bohdal et al., 2015). The CFD simulations were executed using a commercial software. Compressor heat pump cycle calculations were carried out using the author's computational programme. The FGHE of varying geometry was investigated in terms of a long term continuous work. Varying temperature boundary conditions were taken into account. This work provides qualitative data, which may be useful at ground coupled compressor heat pump system modelling.

Słowa kluczowe:
Gruntowy wymiennik ciepła typu Fielda, 0D-3D, sprężarkowa pompa ciepła

Key words:
Field type ground heat exchanger, 0D-3D, compressor heat pump

MIDDLE POMERANIAN SCIENTIFIC SOCIETY OF THE ENVIRONMENT PROTECTION
ŚRODKOWO-POMORSKIE TOWARZYSTWO NAUKOWE OCHRONY ŚRODOWISKA

Annual Set The Environment Protection
Rocznik Ochrona Środowiska

Volume/Tom 19. Year/Rok 2017 ISSN 1506-218X 253-269

Studies on the Field Type Ground Heat Exchanger Coupled with the Compressor Heat Pump (Part 2)

Oktawia Dolna, Jarosław Mikielewicz
Institute of Fluid Flow Machinery of PASci

1. Introduction

Ground source heat pumps receive more and more attention and interest each day, because of their potential to reduce primary energy consumption. Consequently, lower amount of greenhouse gases is emitted to the atmosphere.

GSHPs are found to be highly efficient devices, which use renewable sources of energy for space heating and cooling. This technology exploits the phenomenon, which occurs naturally in our environment. Using the ground capacitance is regarded as a passive way of heating (cooling) of residual heat removal system. However, all benefits of GSHPs can be exploited only with the use of best management practices during installation, operation and decommissioning of these systems. It is really important to improve efficiency and quality of GSHPs, because use of the EESs can significantly reduce GGE. A.M. Omer (2011) states in his work that the GGE may by reduced even by 66 % compared to conventional energy supplying systems. Moreover, the GSHPs systems are meant to use 75 % less electricity than traditional ones, which work on fossil fuels (Omer, 2011). This technology is also very attractive from the economical point of view, because its operating cost is one-quarter of the conventional systems'.

Nowadays, researchers focus on ground heat exchangers mostly because the design heat-flow parameters of the working medium and the geometry of the heat exchanger have a huge influence on the heat pump

work. However, the studies found in the literature do not include research on coupling the ground heat exchangers with the heat pumps. In order to fill in this gap, the present paper aims at presenting the analysis of the ground heat exchanger and the compressor heat pump cooperation. Therefore, a complex heat pump system analysis was planned to be carried out in this work. The heat pump system needs to be understood in terms of a compressor heat pump joined with a vertical ground heat exchanger. To sum up, the subject of the present work is a numerical analysis of the coaxial vertical ground heat exchanger coupled with a compressor heat pump cycle. For this purpose, the "0D"-"3D" level programming conjunction was applied. This, according to the literature, has not been done in practice until now.

The problem being discussed in the paper concerns the ground coupled heat pump quasi-steady intermittent work. Aiming to reach the goal, FGHE CFD analysis was carried out as the outlet FGHE parameters, influencing the CHP work, vary in time. Diurnal programmed FGHE work time was equal approximately from 4 to 6 hours. It was done intentionally to provide the ground's much time for its thermal regeneration. However, even though the FGHE did not work continuously and the ground's thermal regeneration occurred, the ground's temperature did not reach the initial value. On the basis of the CFD analysis the regeneration tempo was determined. These numerical researches have shown that heat pump should operate in a reversible mode so the ground could undergo a better thermal regeneration. Considering the fact that ground thermal efficiency decreases with time, it seems clear that ground cannot be thought of as inexhaustible. This is stated on the basis of the present work and the literature (Fidorów et al., 2015) and also on the basis of the technical companies practice (e.g. Viessmann).

The FGHE impact zone was also estimated. Mentioned impact zone must be understood in terms of the width of the ground layer surrounding FGHE, in which there occurs a temperature decrease being caused by FGHE operation.

2. Theoretical and numerical ground heat exchanger designing methods being used nowadays

In general, the CFD analysis gives the user the possibility of improving the innovative concepts of solving a wide range thermodynamic problems. Nevertheless, the numerical computations will never replace experiments and real measurements, it is still a source of a real and valuable data. The studies of the vertical ground heat exchangers described in the literature, focus mainly on the U-pipe ground heat exchanger. However, many researchers working on the U-type vertical ground heat exchangers do not couple U-pipes with a heat pump device, which is crucial in the overall heat pump system analysis. The work of Hanuszkiewicz-Drapała (2009) includes wider analysis of the ground heat exchanger, because the circulating pump flow characteristics have been taken into account.

The importance of the CFD analysis is confirmed also by the fact that the ground properties vary with depth. Moreover, the ground heat exchanger analysis becomes even more complex with the occurrence of ground water. In the light of these facts, it is obvious that numerical simulations may simplify solving the problem as numerical computations do not include any simplifications, which are being found in the analytical considerations. Moreover, the analytical calculations concerning the ground water occurrence, understood in terms of a flow heat source of a high capability to regenerate, may be burdened with a great inaccuracy.

2.1. Experimental analysis of the ground heat exchangers being carried out so far

As it has been mentioned earlier in the work, the subject of the research on the vertical ground heat exchangers are being mainly devoted to U-pipe analysis. There are very few works on the Field type Ground Heat Exchangers (FGHE). However, in the work of Yuehong Bi et al. (2002), there has been analysed a vertical double spiral coil ground heat exchanger. The numerical results, compared with the experimental data, are of a good accuracy. Yuehong Bi et al. have then also confirmed the necessity of carrying out the numerical analysis as it is a source of a valuable data. The FGHE case analysis, presented in this paper, has been carried out, because it is hard to find such an example in the litera-

ture. Suggestions of the designing process of the vertical ground heat exchangers mainly concern the U-pipe type (PORT PC, 2013). Moreover, the CFD analysis could be shortened while using the axisymmetric Field type heat exchanger model.

2.2. Computational domain description

The subject of the CFD analysis was the Field type ground heat exchanger. Its length was equal to 27.5 [m]. FGHE was hooked in a volume of the ground of one type. Two temperature boundary conditions were applied to the volume of the ground and are exposed in Fig. 1. First of them was a constant value and it was set on the upper ground's surface marked in green in Fig. 1. The other one was applied to the envelope of the computational domain as a temperature profile. Latter one consists of two linear functions. These functions may be arbitrarily changed so the implementation of different seasons may be executed. However, from the given depth, the atmospheric conditions do not influence the ground's temperature, indeed. As it is exposed in Fig. 1, the FGHE consists of two coaxial pipes. The external one had an oval bottom so the hydraulic resistance could had been reduced. Two pipes were made of different materials. The internal one was made of teflon as its thermal conductivity is low what was desired. The external one was made of polyethylene.

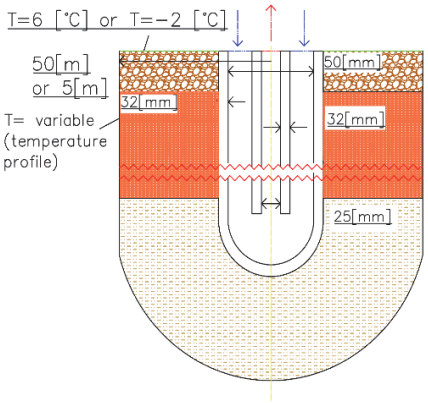

Fig. 1. Outline of the computational domain consisting of the FGHE and the ground (Dolna, 2016)
Rys. 1. Szkic domeny obliczeniowej, na którą składa się GWCF i grunt (Dolna, 2016)

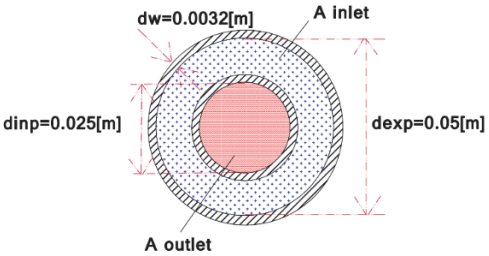

Fig. 2. Cross section of the FGHE, $\boldsymbol{\varepsilon}$ =0.41 (Dolna, 2016)
Rys. 2. Przekrój poprzeczny GWCF, $\boldsymbol{\varepsilon}$ =0.41 (Dolna, 2016)

The boundary conditions on the fluid side were as follows, the FGHE working medium inlet temperature, $t_{in} = 3[℃]$, and inlet pressure, $p = 10\ [bar]$.

The FVM was used to discretise the computational domain. For the purpose of numerical calculations, the structural mesh was generated. Obviously, the mesh size varied according to the FGHE's length. The mesh influence was not discussed in the current paper however described problem is mesh independent as the proper analysis was carried out.

2.3. Results of the 0D-3D level programming coupling

This paragraph is devoted to the numerical model validation description and resulting single FGHE impact zone estimation. Further, the results of the FGHE-CHP conjunction are presented. Bearing on mind the ground's thermal depletion in time, its regeneration process was implemented and is discussed in this work. Worth mentioning is that the ground's regeneration has been implemented in the case of non-reversible CHP work. During the regeneration period, the FGHE did not work at all. Thermal ground's regeneration has been overlapping due to the temperature boundary condition applied to the envelope of the computational domain. Simultanously, the ground heat exchanger has not been working. Of course, the regeneration process would be more effective, from the heat transfer point of view, if the use of a reversible heat pump cycle would has been exploited. However, for the purpose of the current studies such system was not applied as it was meant to estimate the tempo of the ground's thermal regeneration without any heat injection into the ground.

3. Computational fluid dynamics results validation

Numerical investigation having been carried out concern LFGHE and SFGHE, from which the LFGHE was the reference model. It's length was equal 110 meters and **ε** was equal 0.41. Calculus presented in this paragraph is devoted to the reference FGHE. As the laboratory bench was not available, the numerical simulations were validated using theoretical algorithms, presented in the literature. Two separate analytical methods were applied. First one was a penetration theory, modified by J. Mikielewicz (Mikielewicz et al., 1996). The second one was Bose-Parker's algorithm (Zalewski, 2001).

In this paragraph, there are presented the results of the numerical simulations and theoretical considerations. As mentioned earlier in the text, there have been analysed two analytical methods, providing the possibility to determine the impact zone of a single vertical ground heat exchanger. As it can be seen further, a great convergence of the analytical and numerical results was obtained. This fact confirms the good quality of the CFD simulation results. First algorithm, having been used, was a so called penetration theory. It defines the width of the impact zone (Mikielewicz et al., 1996) (5):

$$\delta_{iz,M} = \sqrt{\pi \cdot a \cdot \tau} \tag{1}$$

where:
$\delta_{iz,M}$ – total width of the impact zone $[m]$,
a – the ground diffusivity $\left[\frac{m^2}{s}\right]$,
τ – characteristic time [s].

In order to calculate the width of the FGHE impact zone there was used the time of the heat exchanger work $\tau = 138600\ [s]$ (1). However, further in this paragraph another specific time is used when calculating the heat transfer coefficient on the soil side. Brief explanation is described below.

The second algorithm, used to validate the numerical simulations results, was the Bose-Parker method (Zalewski, 2001). Full calculus is available in the work (Dolna, 2016).

Primarily, there was calculated the unitary ground heat resistance for a single borehole, (2) (Zalewski, 2001), (Dolna, 2016):

$$R_{u\_gr} = \frac{I(x)}{2 \cdot \pi \cdot \lambda_{gr}} \tag{2}$$

where:

R_{u_gr} – unitary ground heat resistance $\left[\frac{m^2 \cdot K}{W}\right]$

$$I(x) = -0.5\, E_i(-x^2) \tag{3}$$

where the function E_i is defined as follows:

$$E_i(x) = \int_{-\infty}^{x} \frac{e^t}{t}\, dt \tag{4}$$

$$E_i(x) = \gamma + \frac{1}{2}\ln x^2 + \sum_{k=1}^{\infty} \frac{x^k}{k \cdot k!} \tag{5}$$

where:

$\gamma = 0.5772$ – Euler's constant

$$x = \frac{r}{2\sqrt{a_{gr} \cdot \tau_p}} \tag{6}$$

where:

$r = \frac{d_h}{2}$ distinctive dimension $[m]$,

where:

d_h – hydraulic diameter $[m]$.

Solving the integral-exponential function E_i, needed while using the Bose-Parker algorithm , was possible by dint of using author's code, presented in the appendix of the work (Dolna, 2016).

Considering equations (7) and (8), we get (9), on the basis of which, it is possible to derive eq.(11):

$$\dot{Q} = \frac{2\pi\lambda L}{ln\frac{r_2}{r_1}} \cdot \Delta T \tag{7}$$

$$\dot{Q} = \frac{2\pi\lambda L}{I(x)} \cdot \Delta T \tag{8}$$

Comparing the Bose-Parker algorithm results for the infinitive width with the finite thickness, it might be stated that :

$$\frac{2\pi\lambda L}{ln\frac{r_2}{r_1}} = \frac{2\pi\lambda L}{I(x)} \tag{9}$$

where:

$$r_2 = r_1 + \delta_{z,B-P} \tag{10}$$

$r_1[m]$ – external radius of the external pipe of the FGHE
$\delta_{z,B-P}[m]$ – width of the FGHE impact zone, determined using Bose-Parker algorithm.

$$\delta_{z,B-P} = r_1(e^{I(x)} - 1) \tag{11}$$

Two algorithms, presented above, give the following results (18), (19), respectively. Obviously, these values, (12), (13), have been determined with the use of exactly the same parameters as in the numerical simulations (14).

However, results (18) and (19) differ from each other. This is being caused mainly by the differences of the methodology of two algorithms having been used. The penetration theory provides only estimation of the magnitude of the searched values. The Bose-Parker algorithm is more precise as it includes characteristic geometry parameters of the FGHE such as its length and hydraulic diameter. That is why a great convergence of the CFD (13) and Bose-Parker algorithm (14) results was obtained.

$$\delta_{z,M-K} = 0.77\ [m] \tag{12}$$

$$\delta_{z,B-P} = 1.19\ [m] \tag{13}$$

$$\delta_{CFD} = 1.22\ [m] \tag{14}$$

As mentioned earlier in this paragraph, the penetration theory was also used to estimate the value of the ground heat transfer coefficient, $\alpha_{gr}\ \left[\frac{W}{m^2K}\right]$ (21). In this particular case, the time $\tau_{pf} = 440\ [s]$ was the time of a particle flow from the top to the bottom of the LFGHE. As a result, the boundary layer thickness was obtained, $\delta_{bl} = 4 \cdot 10^{-4}\ [m]$, which allows to calculate the ground heat transfer coefficient, α_{gr} :

$$\alpha_{gr} = \frac{\lambda_{gr}}{\delta_{bl}} \left[\frac{W}{m^2 K}\right] \tag{21}$$

where:

$\lambda_{gr} = 2.18 \left[\frac{W}{mK}\right]$

$\alpha_{gr} = 54.5 \left[\frac{W}{m^2 K}\right]$.

The α_{gr} value is consistent with data presented by Zalewski (2001).

4. Intermittent quasi-steady GCHP work analysis

As it is commonly known, the GCHP compressor of a well-designed system should operate in the annual time range varying from 1800 to 2400 hours. Unfortunately, even though the heat pump systems have a long history, they are still being over- or undersized. This happens if the designing process does not overlap in a proper way. Nevertheless, this work concerns the ground's regeneration process and instability of the FGHE heat flux value during the intermittent GCHP work. The GCHP working medium having been used for the purpose of the current work was R600a. This fluid is thought to be one from equivalents for R134a (Bohdal et al., 2012). Bearing on mind this problem, the periodic GCHP system work was programmed. For the purpose of the FGHE – CHP conjunction, the 0D-3D level programming was applied. Regarding the fact that the FGHE diurnal work was equal 4 to 6 hours, interchangeably, much time for the ground's thermal regeneration was included. Even though, the soil has not been extremely exploited by the FGHE, the ground' s thermal regeneration proceeded in a long term, what is described further in this article.

The graph exposed in Fig. 3 shows the results of the FGHE intermittent work. The FGHE length was 27.5 [m]. The mass flow rate of the FGHE working fluid was equal 1.1 $\left[\frac{kg}{s}\right]$. As the analysis which has been carried out is mostly of a qualitative character, the FGHE working fluid was chosen from the commercial computational tool fluid database. The possible to use working medium was 100% ethylene glycol. However, in the practice the (30-60)% ethylene glycol brines are being used.

Application of the 100% ethylene glycol consequently resulted in higher hydraulic resistance, however for the purpose of the herby presented analysis it did not really matter that much as the analysis is mostly of a qualitative than quantitative character.

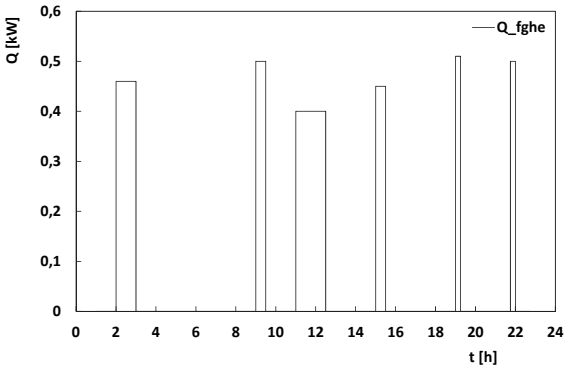

Fig. 3. Diurnal heat flux variation during the intermittent FGHE work (Dolna, 2016)
Rys. 3. Dobowe wahania wartości strumienia ciepła pozyskiwanego z gruntu za pośrednictwem GWCF podczas pracy przerywanej (Dolna, 2016)

As the heat flux received via FGHE varied during the work time, the GCHP COP also changed, consequently, what can be observed in Fig. 4.

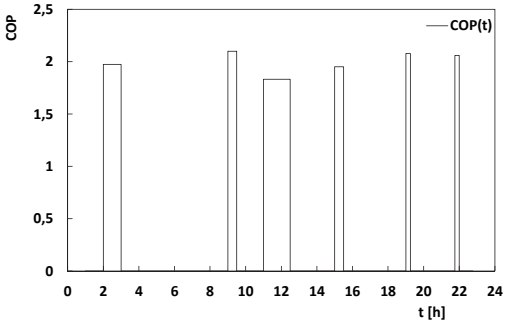

Fig. 4. GCHP COP value change during the intermittent work time (Dolna, 2016)
Rys. 4. Zależność wartości COP GCHP od czasu podczas pracy przerywanej (Dolna, 2016)

As it is presented in Fig. 3 and Fig. 4, it can be stated that even though the ground has had relatively much time for its thermal regeneration, the heat flux transferred from the borehole via FGHE was not constant during the intermittent work time period. This fact should be considered and taken into account at designing level. In the case, of which the results are discussed in the paper, the ground's regeneration has been executed through cutting off the FGHE working medium flow. The temperature boundary conditions, having been applied to the envelope of a studied domain, have forced the ground's temperature to increase. This phenomenon of thermal regeneration has taken much time. This fact is importing, because of the following assumption. The GCHP systems should work in the reversible mode. Applying this solution would extend the life cycle of the ground working as a low heat source. In other case the ground's degradation would overcome relatively fast and the ground would not regenerate in a proper way. It means that the ground could not be called a renewable source of energy as the ground's thermal efficiency would decrease significantly.

5. Influence of FGHE on the surrounding ground

This paragraph concerns the effect of FGHE operation in the soil, understood in terms of the ground's temperature decrease. Figure presented below (Fig. 5) exposes the work time and the depth dependent temperature distribution in LFGHE surroundings . On the x coordinate the distance from FGHE external wall is given. In the centre of the coordinate origin FGHE is placed. Fig. 5 presents the soil's temperature layout, starting from the FGHE external pipe surface. Data, visualised through this characteristics, was collected on the way of continuous FGHE work lasting 39 hours. Numerical simulations had run in transient mode. For each work hour and three different depths (10 [m], 30 [m], 110 [m]), the temperature profile was obtained.

From Fig. 5 it can be observed that the FGHE impact zone is of a cone shape and it is wider at lower depths, i.e. yellow and pink line in Fig. 5. It can be noticed that deeper FGHE reaches, the thinner FGHE impact zone is.

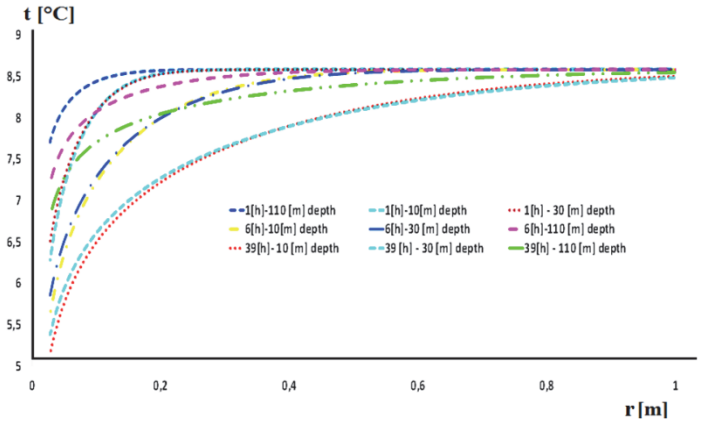

Fig. 5. Temperature distribution at different depths in the ground after 1[h], 6[h], 39[h] of FGHE continuous work (Dolna, 2016)
Rys. 5. Rozkład temperatury w gruncie na różnych głębokościach po 1[h], 6[h], 39[h] godzinach pracy GWCF (Dolna, 2016)

In the following graph, Fig. 6, results of the intermittent SFGHE work are displayed. During the intermittent SFGHE work, SFGHE operated in the time range described the previous paragraph of present paper. All lines, exposed in Fig. 6, correspond to stages of the ground regeneration which coincide with SFGHE no operation period during the intermittent SFGHE week work. The blue line is identical to the first regeneration period during the first day of work. As the ground regeneration occurred interchangeably with the SFGHE work the ground's temperature varied in an unpredictable way. The red line corresponds to the last regeneration period during the seventh work day. Other lines show how did the soil's temperature changed during following regeneration periods during the first work day. From Fig. 6 it can be seen that even though the ground had relatively much time for its thermal regeneration, this process had not proceed with a satisfactory efficiency as the soil's temperature decrease was equal $\Delta T = 1.4[℃]$.

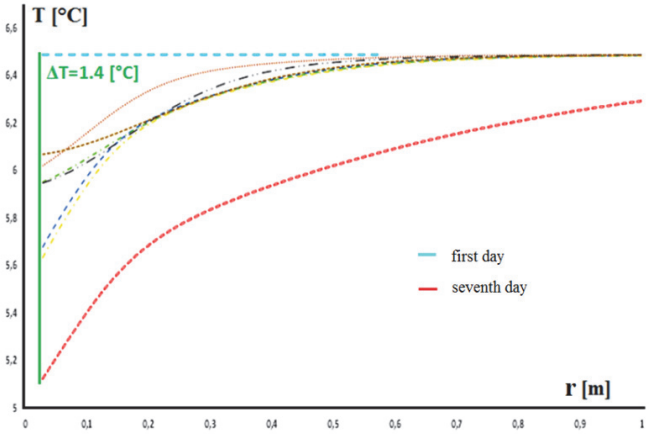

Fig. 6. Ground's thermal degradation (Dolna, 2016)
Rys. 6. Degradacja termiczna gruntu (Dolna, 2016)

Figures attached below(Fig. 7, Fig. 8, Fig. 9) present the CFD analysis results. The subject of investigation was SFGHE of ε =0.41. Its work was continuous and has been lasting for 446 hours. After that time, the ground's temperature decreased significantly (Fig. 7). During its work, FGHE mass flow rate was equal 1.1 $\left[\frac{kg}{s}\right]$. Then, the ground's thermal regeneration was implemented, for the purpose of which, FGHE working medium flow was stopped. The ground's temperature increased as well as the temperature profile, having been set as a boundary condition, forced it to. After 1060 hours of a continuous regeneration, the ground's temperature distribution was like it is exposed in Fig. 8. The ground's temperature reached its initial state value after 4131 hours of uninterrupted regeneration Fig. 9.

Temperature distribution exposed in Fig. 9 is forced by the temperature profile applied to the envelope of a studied computational domain. This isothermal surfaces layout corresponds to the initial state temperature distribution.

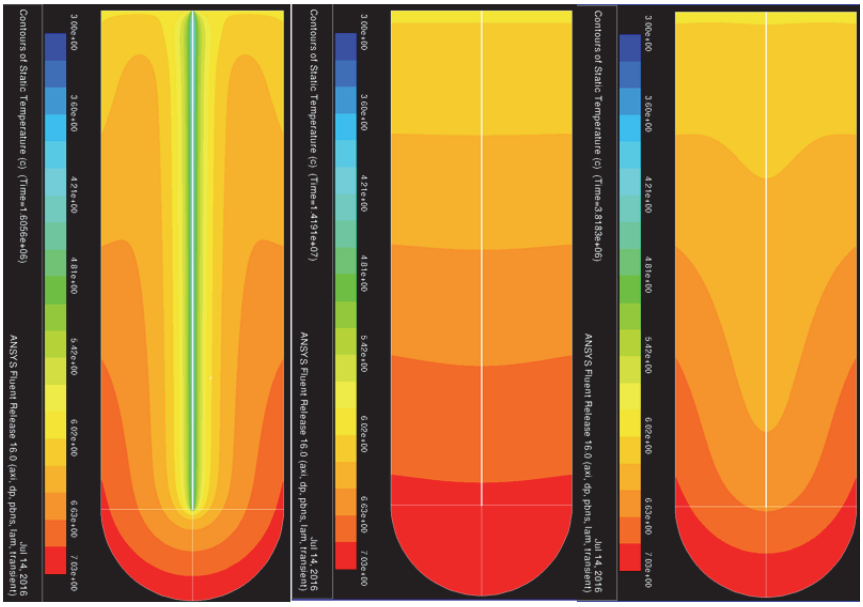

Fig. 7. **Fig. 8.** **Fig. 9.**

Fig. 7. Isothermal surfaces layout in the ground after 446 hours of SFGHE continuous work (Dolna, 2016)
Rys. 7. Rozkład powierzchni izotermicznych w gruncie po 446 godzinach ciągłej prac 27.5 [m] GWCF (Dolna, 2016)

Fig. 8. Ground's temperature increase after 1060 hours of thermal regeneration (Dolna, 2016)
Rys. 8. Wzrost temperatury gruntu po 1060 godzinnej regeneracji termicznej (Dolna, 2016)

Fig. 9. Isothermal surfaces layout after 4131 hours of the ground's thermal regeneration (Dolna, 2016)
Rys. 9. Rozkład powierzchni izotermicznych w gruncie po 4131 godzinach nieprzerwanej regeneracji termicznej gruntu (Dolna, 2016)

6. Summary

The numerical simulations results of the intermittent and continuous FGHE work, presented in the paper, have shown, how does the FGHE impact zone vary with the FGHE work time and its geometry. The results confirm the thesis about the low heat source's (the ground) thermal efficiency depletion in time. Despite the fact that the FGHE work

was of the intermittent character and the low heat source could regenerate, the surrounding ground did not reach the initial temperature value during the week work. On the basis of the CFD simulations having been carried out, an important assumption is stated. The ground's thermal efficiency decreases significant in time. According to this, the ground remains a renewable source of energy only if the condition of a well ground heat exchange system design is fulfilled. Moreover, the GCHP systems should operate in a reversible mode to improve the ground's thermal regeneration.

The results presented in the paper have shown that the quasi-steady FGHE work character should be taken into account at the GCHP system designing level.

Nomenclature

GGE – greenhouse gases emission,
FGHE – Field type ground heat exchanger,
CFD – computational fluid dynamics,
GWCF – gruntowy wymiennik ciepła typu Fielda,
GSHP – ground-source heat pumps,
GWHP – ground-water heat pump,
SWHP – surface-water heat pump,
GCHP – ground-coupled heat pump,
EESs – earth-energy systems,
LFGHE – long FGHE (110 [m]),
SFGHE – short FGHE (27.5 [m]),
HP – heat pump,
CHP – compressor heat pump,
COP – coefficient of performance,
0D – zero-dimensional,
3D – three-dimensional.

Greek symbols

$\varepsilon = \frac{A_{outlet}}{A_{inlet}}$ – epsilon – inlet/outlet surface ratio,
$\lambda \left[\frac{W}{m\,K}\right]$ – thermal conductivity,
$\varrho \left[\frac{kg}{m^3}\right]$ – density,
γ – Euler's constant.

Subscripts

gr – ground,
pf – particle flow,
bl – boundary layer,
iz – impact zone,
M – Mikielewicz,
$B\text{-}P$ – Bose-Parker,
h – hydraulic.

References

Bohdal, T., Charun, H. (2012). *Zasady transportu ciepła cz. 1*. Koszalin: Politechnika Koszalińska.

Bohdal, T., Charun, H., Sikora, M. (2015). Wybrane aspekty prawno-techniczne i ekologiczne stosowania sprężarkowych pomp ciepła. *Rocznik Ochrona Środowiska*, *17*, 461–484.

Dolna, O. (2016). *Influence of the ground heat exchanger design heat – flow parameters on the heat pump efficiency.* Institute of Fluid Flow Machinery, PhD dissertation.

Fidorów, N., Szulgowska-Zgrzywa, M. (2015). Temperature monitoring in the vertical borehole of the heat pump, *Rynek Instalacyjny*, *4*.

Hanuszkiewicz-Drapała, M. (2009). Modelowanie zjawisk cieplnych w gruntowych wymiennikach ciepła pomp grzejnych z uwzględnieniem oporów przepływu czynnika pośredniczącego. *Modelowanie Inżynierskie*, *38*, 57-68.

Mikielewicz, J., Grochal, B., Polesek-Karczewska, S., Gumkowski, S., Mikielewicz, D. (1996). *Heat Exchange*. Gdańsk: Institute of Fluid Flow Machinery PASci (in Polish).

Omer, A.M. (2008). Ground-source heat pumps systems and applications. *Renewable and Sustainable Energy Reviews*, *12*, 344-371.

Polska norma: PN-82-/B-02403 – Ogrzewnictwo. Temperatury obliczeniowe zewnętrzne.

PORT PC. (2013).Wytyczne projektowania, wykonania i odbioru instalacji z pompami ciepła, Cz. 1, Dolne źródła do pomp ciepła.

Xiao, C., Xiaoli, H., (2015). Exergy Analysis of a Ground-Coupled Heat Pump Heating Systems with Different Terminals. *Entropy, 17*, 2328-2340.

Yuehong, B., Lingen, C., Chin, W., (2002). Ground heat exchanger temperature distribution analysis and experimental verification. *Applied Thermal Engineering*, *22*, 183-189.

Zalewski, W. (2001). *Compressor, Sorption and Thermoelectric Heat Pumps.* IPPU MASTA (in Polish).

Badania gruntowego wymiennika ciepła typu Field'a współpracującego ze sprężarkową pompą ciepła (część 2)

Abstract

This work concerns the numerical research on the ground coupled compressor heat pump quasi-steady intermittent work. To reach the goal 0D-3D level programming coupling was applied. The work contains also the analysis of the influence of a single Field type vertical ground heat exchanger on the surrounding ground. Numerical model was validated using Bose-Parker's algorithm and penetration theory modified by J. Mikielewicz. In order to determine the ground's ability to thermal regeneration, CFD simulations of the Field type ground heat exchanger were carried out.

Streszczenie

Niniejsza praca poświęcona została badaniom numerycznym quasi-stacjonarnej przerywanej pracy gruntowej sprężarkowej pompy ciepła. By osiągnąć zamierzony cel sprzęgnięto programowanie na poziomie 0D i 3D. W pracy zawarto również analizę szerokości strefy wpływu pojedynczego GWCF. Powyższe należy rozumieć jako obszar termicznego oddziaływania na grunt pionowego współosiowego gruntowego wymiennika ciepła. Walidacja modelu numerycznego została przeprowadzona w oparciu o algorytm Bosego-Parkera oraz teorię penetracji zmodyfikowaną przez J. Mikielewicza. Chcąc określić zdolność gruntu do termicznej regeneracji przeprowadzono symulacje CFD, których wyniki załączono w niniejszej pracy.

Słowa kluczowe:
Wymiennik gruntowy typu Field'a, 0D-3D, CFD, sprężarkowa pompa ciepła

Key words:
Field type ground heat exchnager, 0D-3D, CFD, compressor heat pump

MIDDLE POMERANIAN SCIENTIFIC SOCIETY OF THE ENVIRONMENT PROTECTION
ŚRODKOWO-POMORSKIE TOWARZYSTWO NAUKOWE OCHRONY ŚRODOWISKA

Annual Set The Environment Protection
Rocznik Ochrona Środowiska

Volume/Tom 19. Year/Rok 2017 ISSN 1506-218X 270-287

Impact of Various Kinds of Straw and Other Raw Materials on Physical Characteristics of Pellets

Artur Kraszkiewicz[*], *Magdalena Kachel-Jakubowska*[*], *Ignacy Niedziółka*[*], *Beata Zaklika*[*], *Kazimierz Zawiślak*[*], *Rafał Nadulski*[*], *Paweł Sobczak*[*], *Janusz Wojdalski*[**], *Remigiusz Mruk*[**]

[*]*University of Life Sciences, Lublin*

[**]*Warsaw University of Life Sciences SGGW*

1. Introduction

Due to climate change and growing problems associated with the emission of excessive amounts of CO_2, not to mention the ubiquitous occurrence of smog in large cities, limitation of the use of fossil fuels is becoming a necessity. Replacing fossil fuels by energy produced from renewable energy sources such as biomass can significantly reduce greenhouse gas emissions, hence renewable energy sources are considered to be very important for the protection of the environment and the future of society (Piecuch 2010, Blaschke et al. 2013, Kuntal & Sudipta 2014, Malowaniec 2016). Sustainable energy systems will have to rely on the rational use of energy from renewable sources (Callejón-Ferre et al. 2011, Ibrahim et al. 2008, Hlavatá et. al 2014).

The energy use of biomass in heating devices favours refuse-derived fuels (RDF) with specified technical characteristics. However, due to better combustion process and easier handling of boilers, users of these fuels prefer the wood based ones. Also, automation of fuel supply to boilers results in pellets gaining bigger popularity than briquettes (Williams et al. 2012, Sypuła et. al 2010, Lisowski et. Al 2015, Wzorek & Krupa-Żuczek 2015). At the biomass market no chips or sawdust wood

with low prices are available, and hence other types of biomass and commonly available agricultural or fodder by-products that could replace those in deficit are searched for in order to be used in pellet production. Such materials may consist of waste from agricultural production and processing of plant products such as – straw of cereals, rapeseed and soya bean, or industrial waste known as rapeseed cake and soya bean hulls and spelt hulls (Caryalho et al. 2013, Ståhl & Berghel 2011). It is assumed that on average 1 tonne of rapeseed seeds yields approximately 650 kg of rapeseed cake or about 600 kg of post-extraction meal (Firrisa et al. 2014). According to the conducted studies rapeseed cake has appropriate parameters for power industry, as their net calorific value is approximately 19.8 $MJ \cdot kg^{-1}$ (Mc Kendry 2002, Ståhl & Berghel 2011). Also the results for mechanical strength of the pellets produced from rapeseed cake or with admixture thereof were characterised by high parameters, which are within the accepted quality standards (96.5%) (Ståhl & Berghel 2011).

The production of soya bean in the world is estimated to approximately 160 million tonnes. Assuming that hulls make up around 14% of it, a yearly average production of hulls equals to 22 million tonnes (Firrisa et al. 2014). Oil and microcrystalline cellulose, to name just a few, in large quantities obtained from soya beans are very important products for pharmaceutical, food and cosmetic industries (Uesu et al. 2000). Soya bean meal is the most important source of protein used in livestock feeding. During processing of soya bean hulls are obtained as waste product, which may be used for power production purposes, for example by using it in pellet production.

Pellets are produced in the process of pressure agglomeration, in which the pulverised material under the external forces (solidifying pressure) and internal ones (intermolecular forces and bonds) takes the permanent shape with specified geometric dimensions (Adapa et al. 2004, Theerarattananoon et al. 2011). Depending on the die used the end product are pellets of cylindrical shape with a diameter between 6 and 25 mm and length of up to few cm (Shawa et al. 2009). However, the process of pressure agglomeration of biomass entails many technical and operating difficulties related to high variability of physical and chemical properties of the materials that were subject to granulation (Adapa et al. 2004). Keeping in mind the above issues an examination was conducted on the

feasibility of pelleting cereal and rapeseed straw in compound with rapeseed cake and soya bean and spelt hulls. The physical characteristics of the obtained pellets and their possible use as solid biofuel were assessed.

2. Materials and methods

For the production of pellets rye straw, wheat straw, rapeseed straw and rapeseed cake, soya bean hulls and spelt hulls were used. The composition and mass fraction of the used kinds of straw and individual compounds are presented in Table 1. The particular ash content and average size of particle was presented in Table 2 in raw material. Prior to pelletizing the straw was initially pulverised using universal hammer crusher, driven by an electric motor with the power of 7.5 kW and fitted with 2 sieves with holes 20 mm in diameter. The final fragmentation of the straw was done by blade crusher, driven by an electric motor with the power of 5.5 kW and fitted with a sieve with holes 8 mm in diameter. All others raw materials used for the production of pellets were in pulverised form. For agglomeration of the plant raw materials a flat die pelleting machine with rotating compression rollers was used. It was driven by an electric motor with the power of 7.5 kW. The diameter of the holes in the pelleting machine die was 8 mm, and the length to diameter ratio (L/D) was 3.125.

Moisture content of raw materials and pellets was determined using a laboratory oven with forced air circulation. Samples of raw materials or pellets were placed in the oven and then dried at 105°C until reaching constant mass, in accordance with BS EN ISO 17225-6:2014 standard. Rapeseed straw, wheat straw and rye straw were moistened until the moisture content was equal to 18%.

The net calorific value of the produced pellets was calculated on the basis of the heat of combustion measured by calorimetric method using isoperibolic calorimeter, according to BS EN 14918:2009 standard. The ash content was measured after pellet sample ashing, at the final temperature of 550°C, according to BS EN 14775:2009 standard.

Measurements of the geometrical characteristics of the pellets produced in flat die pelleting machine included: diameter, length, and mass. Random samples of 20 pieces of pellets were collected for the measurements. The geometric measurements of the pellets were made

using a calliper with measurement accuracy of ±1 mm, and their mass – using laboratory scales with measurement accuracy of ±0.1 g.

Table 1. Types of plant raw materials and the produced pellets
Tabela 1. Rodzaje surowców roślinnych i wytworzonych peletów

Type of straw	Straw mass fraction [%]	Other compounds	Additive mass fraction [%]	Pellet designation
Rye straw	50	Rapeseed cake	50	A
Wheat straw	50	Rapeseed cake	50	B
Rapeseed straw	50	Rapeseed cake	50	C
Rye straw	50	Soya bean hulls	50	D
Wheat straw	50	Soya bean hulls	50	E
Rapeseed straw	50	Soya bean hulls	50	F
Rapeseed straw	50	Rapeseed cake	25	G
		Spelt hulls	25	
Rapeseed straw	50	Soya bean hulls	25	H
		Spelt hulls	25	
Rapeseed straw	25	Rapeseed cake	50	I
		Spelt hulls	25	
Rapeseed straw	25	Soya bean hulls	50	J
		Spelt hulls	25	

Table 2. Average particle size and ash content in raw material
Tabela 2. Średni rozmiar cząstek i zawartość popiołu w surowcu

Raw material	Average particle size [mm]	Ash content [%]
Rye straw	1.71	3.69
Wheat straw	1.97	4.71
Rapeseed straw	1.38	4.85
Rapeseed cake	0.90	5.49
Soya bean hulls	1.29	4.44
Spelt hulls	3.30	4.62

Particle density of the pellets was determined on the basis of measurements of their physical characteristics including geometric dimensions and mass, and was calculated according to the BS EN 15150:2011 standard. Bulk density of pellets was determined on the basis of measurements of their mass and volume according to BS EN

15103:2009 standard. After the pellets were poured into measurement container with capacity of 5 dm^3 and their excess was removed with a straight edge, they were weighed on laboratory scales and the density was calculated.

Measurements of mechanical strength of the pellets were carried out on a test bench in accordance to BS EN ISO 17831-1:2015 standard. The rotational speed of the drum was 50 $rpm \cdot min^{-1}$ (±0.1 $rpm \cdot min^{-1}$), the duration time of the measurement was 10 min, and the mass of the sample was 500 g (±10 g). After mechanical strength test the tested sample of pellets was sieved on a sieve with holes 1 mm smaller in diameter than the diameter of the pellet.

Crushing testing consisted of placing a pellet sample between work plates of a measuring head and then running a crushing test at a constant speed of 50 $mm \cdot min^{-1}$ until the point when a rupture or destruction of the structure of the sample occurred. The measurement of the pellet cutting strength was conducted using a blade set at 45° angle. On the basis of the obtained crushing and cutting strength curves for tested samples their respective values were specified. The tests were performed using TA.XT Plus TEXTURE ANALYZER.

Results of the measurements of the physical and energetic characteristics of the raw materials and pellets were statistically analysed using the one-way analysis of variance processed in STATISTICA 10.0 software. The significance of the differences between the means was defined using Tukey's test at the significance level of $\alpha = 0.05$.

3. Research results

The results of the determination of the moisture content, net calorific value and ash content in the produced pellets are shown in Table 3. The moisture content during the pelletizing process depended on the composition of the compound, and the differences were caused by various amounts of particular types of the raw materials (Table 3). The moisture content during the pelletizing process ranged between 9.0% and 13.65%. In similar conditions other authors were pelletizing barley straw using the moisture content within the limits of 9-17%. While the best quality pellets made from barley straw were obtained for moisture content between 19% and 23% (Serrano et al. 2011). Considering the pro-

duced pellets the highest ash content was measured for pellet from sample C – 5.17%, and the lowest for pellet from sample D – 4.06%, made of rye straw and rapeseed cake. When comparing these data with the data on the ash content in wheat straw (8.32%) or barley straw (10.72%), which was obtained by other authors in the course of research on pellets making (Mani et al. 2006), this content is low. According to the ISO standard 17225-6:2014, the ash content for cereal straw pellets should not be above 6%. The ash content of the biomass pellets due to the ash content in the raw material. Higher ash content may indicate contamination of raw material. Most are pollution from accidental admixture substrate storage area. The ash content of the presented pellets was below 6% which results from the ash content in the raw material (Table 2).

Table 3. Characteristics of the produced pellets
Tabela 3. Charakterystyka produkowanych peletów

Pellet designation	Moisture content of mixtures before pelleting [%]	Pellets moisture content [%]	Calorific value [MJ·kg^{-1}]	Ash content [%]
A	11.25	8.39	17.67	4.59
B	11.25	8.88	16.97	5.10
C	11.25	7.31	17.08	5.17
D	13.65	8.39	17.89	4.06
E	13.65	8.88	17.23	4.57
F	13.65	9.58	16.74	4.64
G	12.7	11.45	15.85	4.95
H	13.8	10.00	15.89	4.69
I	9.3	9.18	16.59	5.11
J	9.0	8.73	17.10	4.39

The net calorific value of the produced pellets varied to a small extent. The difference between the highest net calorific value and the lowest one was 2.04%. The lowest net calorific value was measured for pellets marked as G sample, made of rapeseed straw, rapeseed cake and spelt hulls (15.85 MJ·kg^{-1}), and the highest – for pellets from sample D, made of rye straw and soya bean hulls (17.89 MJ·kg^{-1}). In accordance with ISO standard 17225-6:2014, net calorific value of pellet should be within a range of 16.5-19.0 MJ·kg^{-1}. All tested pellets, with the exception

of the samples marked as G and H, complied with the specified standard. While only the pellets from sample G did not meet the established in the standard level of moisture content below 10%. In the so far conducted studies the net calorific value of pellets made exclusively of wheat straw, rapeseed straw, or corn straw, as well as of compounds thereof was investigated. The highest net calorific value was obtained for the pellets made of rapeseed straw and corn straw, and it was equal to 16.22 $MJ \cdot kg^{-1}$ (Niedziółka et al. 2015). Also, a research on the net calorific value of pellets made of buckwheat hulls with admixture of potato pulp was performed. The highest net calorific value was measured in the case of buckwheat pellet. It equalled to 18.89 $MJ \cdot kg^{-1}$. With the increasing amount of potato pulp compound the net calorific value of pellets was decreasing, to reach the value of 17.95 $MJ \cdot kg^{-1}$, in the case of 30% pulp content (Obidziński et al. 2016).

Figure 1 depicts the specific density of the pellets. Statistical analysis of the results showed that the pellets used in the research, despite being varied in terms of the raw material composition, did not significantly differ in terms of the specific density. Also the change of the initial moisture content, which ranged between 9% (for compound J) to 13.65% (in the case of compounds D, E and F) had no effect on the density of the pellets. However, in studies on the impact of varied moisture content of hay (within a range between 28 and 44%) on the specific density of the produced pellets certain dependence was ascertained – with the increase of the moisture content the specific density of pellets decreased.

At the same time, statistically significant differences were obtained in the bulk density of the examined pellets (Fig. 2). The lowest bulk density was determined for pellets of sample G, which were made of rapeseed straw, spelt hulls and rapeseed cake. Despite the fact that composition of the pellet compound have no impact on its specific density, statistically significant differences in the bulk density resulted from varying lengths of the pellets (Fig. 3).

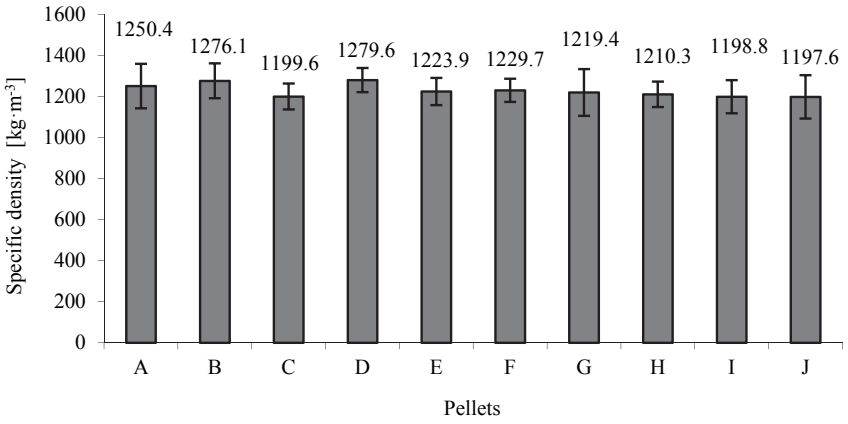

Fig. 1. Average specific density of the pellets with standard deviation
Rys. 1. Średnia gęstość właściwa peletów wraz z odchyleniem standardowym

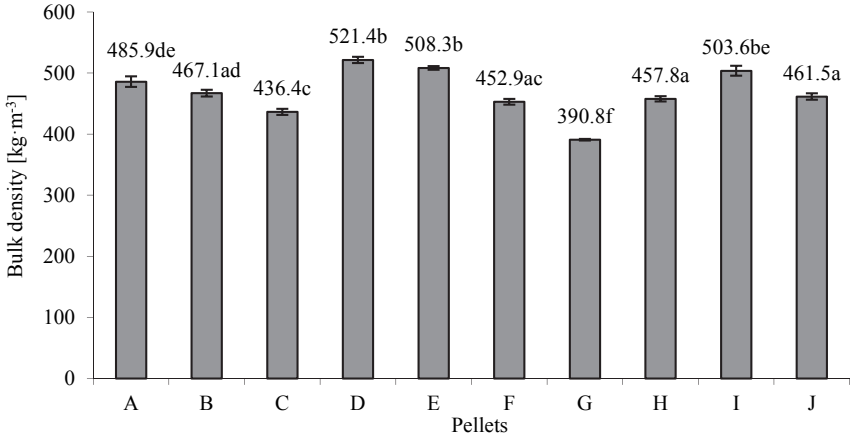

**the same letter stands for the lack of significant difference between mean values within given group at significance level =0.05*

Fig. 2. Average bulk density of the pellets with standard deviation
Rys. 2. Średnia gęstość nasypowa peletów wraz z odchyleniem standardowym

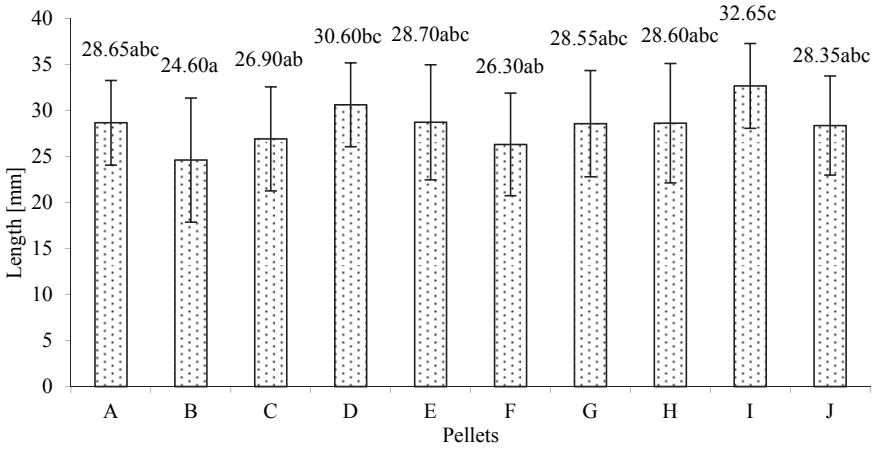

**the same letter stands for the lack of significant difference between mean values within given group at significance level =0.05*

Fig. 3. Average length of the pellets with standard deviation
Rys. 3. Średnia długość peletów wraz z odchyleniem standardowym

In the obtained results of the length measurements large standard deviation was observed, which testifies to high dimensional large of the pellets. The statistical differences was observed between B and I and C and I pellets. Varied length of the pellets resulted also in the varied mass of pellets. The statistical differences was observed also between pellets B and I, D and B. This was identified during mass measurement of the individual pellets (Fig. 4). According to the European Norms bulk density should be above 500 kg·m^{-3} (García-Maraver et al. 2011). Out of the tested pellets only the ones obtained from soya bean hulls and rye straw (sample D), wheat straw and soya bean hulls (sample E), and pellets of sample I made of rapeseed straw and spelt straw on the base of rapeseed cake complied with the specified standards. In so far completed studies on pellets made of different raw materials their bulk density was measured. Pellets were made of bamboo with addition of pine or rice straw, or of various kinds of straw (Liu et al. 2013, Liu et al. 2016). The bulk density of bamboo pellets increased with the increasing share of pine chips or rice straw admixture. After adding pine chips the bulk density of the pellet increased from 540 to 600 kg·m^{-3} (Liu et al. 2013, Liu et al. 2016). On the other hand, the bulk density of pellets made of straw was varied,

depending on the straw kind or the composition of used compounds. The highest bulk density characterised pellets made of corn straw and it was equal to 566.9 kg·m^{-3}, while the ones made of wheat straw had the bulk density of only 407.7 kg·m^{-3} (Niedziółka et al. 2015).

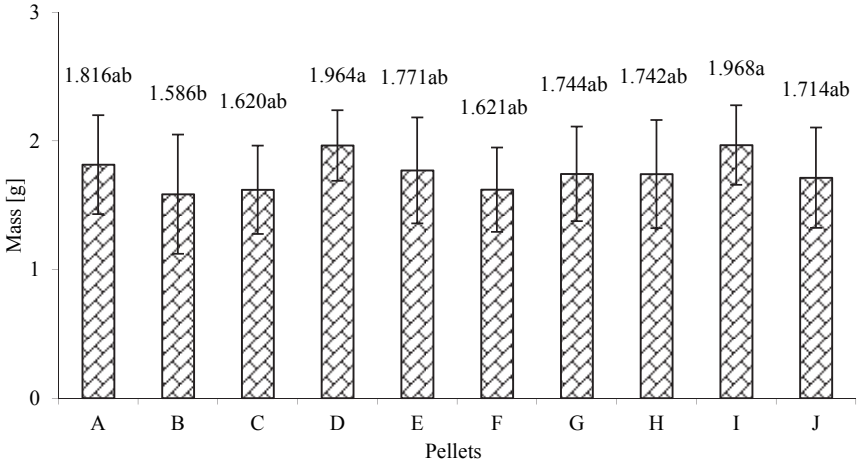

**the same letter stands for the lack of significant difference between mean values within given group at significance level =0.05*

Fig. 4. Average mass of the pellets with standard deviation
Rys. 4. Średnia masa peletów wraz z odchyleniem standardowym

The mechanical strength of the obtained pellets varied depending on the composition of their compound (Fig. 5). The highest strength characterised the pellets from sample I (95.9%) made of rapeseed straw, rapeseed cake and spelt hulls, while the lowest mechanical strength (85.4%) was determined in the case of the pellets from sample C, which were made of rapeseed straw and rapeseed cake. Statistically significant differences in the mechanical strength of pellets were observed after adding rapeseed cake to various kinds of straw. Pellets with rye straw in their compound (sample A) were characterised by greater mechanical strength (91.7%) than those with wheat straw composition (sample B – 87.7%), or rapeseed straw one (sample C – 85.4%). After introduction of soya bean hulls in the place of rapeseed cake the mechanical strength of pellets increased and amounted to 93.6% for compounds with rye straw (sample D), 94.0% for mixtures with wheat straw (sample E), and 90.2% for ones

with rapeseed straw (sample F). In the research conducted by Liu et al. (2013) mechanical strength of pellets made of bamboo and rice straw (at a ratio of 2:3) was 99%. The mechanical strength of pellets made of straw ranged between 96.1% in the case of rapeseed straw to 97.7% in the case of compound of wheat and corn straw (Niedziółka et al. 2015). Additionally, an examination was made on the mechanical strength of pellets made of wheat straw depending on the degree of straw pulverization. On the basis of the results obtained, it was ascertained that the increased particle size caused increased mechanical strength of pellets made of wheat straw (Kashaninejad et al. 2014).

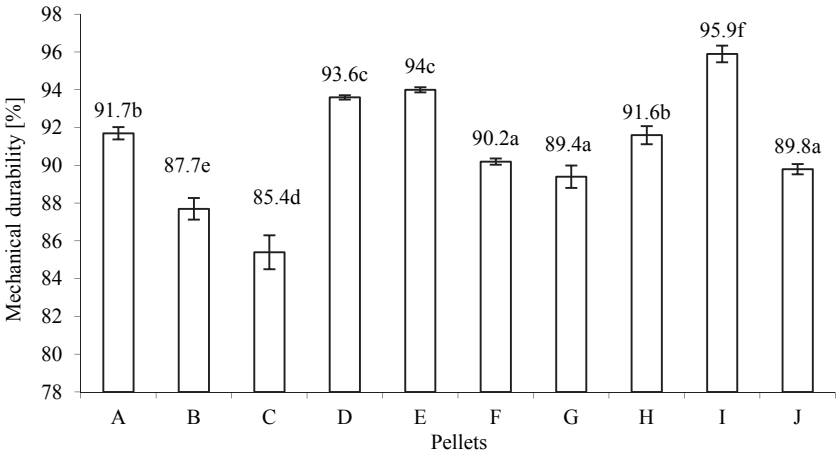

******the same letter stands for the lack of significant difference between mean values within given group at significance level =0.05*

Fig. 5. Average mechanical durability of the pellets with standard deviation
Rys. 5. Średnia wytrzymałość mechaniczna peletów wraz z odchyleniem standardowym

The pellet crushing strength determined in accordance with the agreed methodology varied for individual components (Fig. 6). Large differences in the results attest biological diversity of the material. The most resistant to compressive force turned out to be pellets from samples A, G, and I with 50% of rye straw or rapeseed cake, and the pellets with spelt hulls constituting 25% of the compound, which boosted the pellets compressive strength, and without soya bean hulls, which, in turn, lowered the compressive strength of the pellets. Research carried out by oth-

er authors on pellets compressive strength show that the highest resistance characterises the pellets made of rye straw and corn straw, somewhat smaller – the pellets made of rapeseed straw, and the lowest – ones made of wheat straw (Starek et al. 2014). In a research on the impact of size fraction of wheat bran on the compressive strength it was ascertained that the greatest resistance distinguish the pellets made of bran with the size of 0.5-1 mm. In turn, the pellets made of bran of the size of 1 to 2 mm had the lowest resistance (Zawiślak et al. 2014).

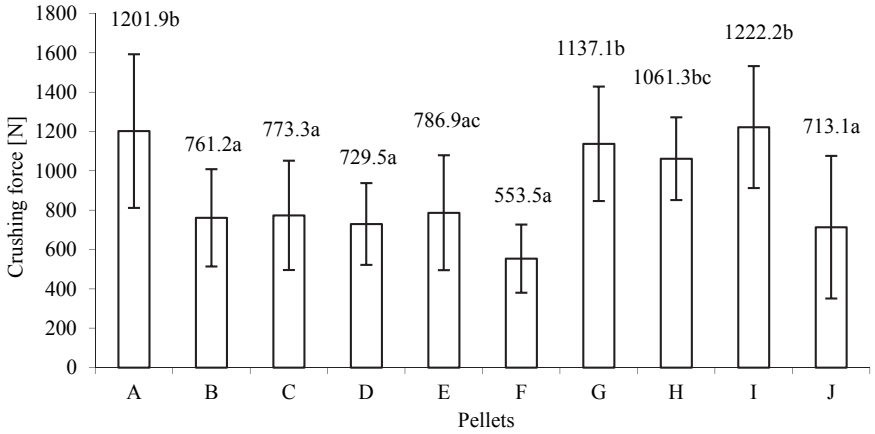

**the same letter stands for the lack of significant difference between mean values within given group at significance level =0.05*

Fig. 6. Average value of crushing force of the pellets with standard deviation
Rys. 6. Średnia wartość siły zgniatania peletów wraz z odchyleniem standardowym

The results of the cutting test of the produced pellets are presented on Figure 7. Similarly to the case of crushing strength measurement, there was a large variation in the results. The results for the pellet from sample I, which was characterised by the highest cutting strength, proved to be statistically significant. The pellets from I sample also had the highest resistance to crushing. Cutting tests performed by other researchers on pellets made of pine and poplar sawdust showed dependence on the moisture content during the process of compaction. In accordance to the obtained results, the increased initial moisture content in the sawdust decreased the cutting strength of the pellets (Millili & Schwartz 2008).

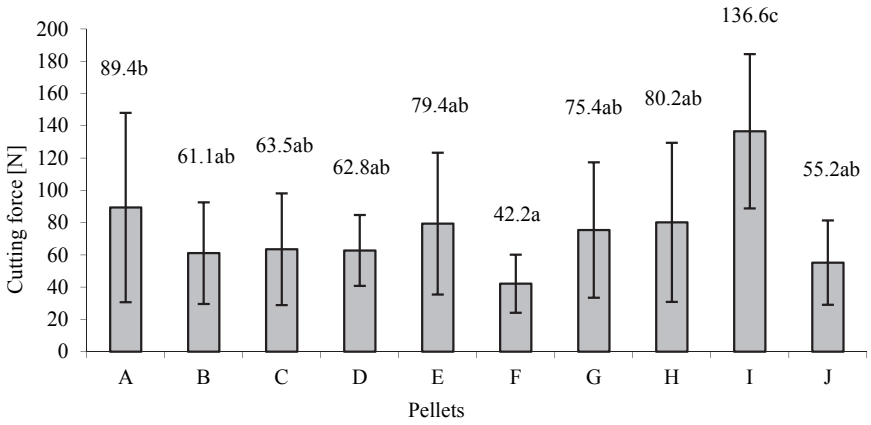

**the same letter stands for the lack of significant difference between mean values within given group at significance level =0.05*

Fig. 7. Average value of cutting force of the pellets with standard deviation
Rys. 7. Średnia wartość siły cięcia peletów wraz z odchyleniem standardowym

The effect of used different kinds of straw on the quality of the pellet was processed by statistical software Statistica 10.0, using the one-way analysis of variance (ANOVA) and Tukey's test. The results of statistical analysis for the individual parameters are displayed in Table 4. Statistically, varied raw material composition of the pellets did not affect the specific density thereof. Statistically significant differences were obtained for bulk density, length, mass, mechanical strength, as well as crushing and cutting. In conclusion, it can be inferred that the raw material composition has an impact on the evaluated physical parameters of pellets.

Table 4. Analysis of variance (ANOVA)
Tabela 4. Analiza wariancji (ANOVA)

Source variables	SS	df	MS	F value	Probability
Specific density [kg·m^{-3}]	132466.9	9	14718.54	2.01617	0.039
Bulk density [kg·m^{-3}]	40171.83	9	4463.536	98.4473	0.00
Length [mm]	884.38	9	98.26444	3.12253	0.0015
Mass [g]	3.196023	9	0.355114	2.54857	0.0087
Mechanical durability [%]	261.5939	9	29.06599	135.528	0.00
Crushing force [N]	10180415	9	1131157	14.0318	0.00
Cutting force [N]	119843.0	9	13315.89	8.57085	0.00

4. Conclusions

On the basis of the carried out studies on the influence of different raw materials used for production of pellets it was attested that statistically they do not affect the specific density of the pellets. However, there are differences in the bulk density of the pellets. Only three of the samples comply with European Norms regarding the pellet bulk density (samples: D, E and I). Further testing is necessary, in order to increase bulk density through the introduction of other raw materials. The pellet from sample I had the highest mechanical strength. It was made of rapeseed straw, rapeseed cake and spelt hulls. The same pellet had the highest crushing and cutting strength. When assessing the resistance to crushing and cutting it was concluded that there are significant statistical differences depending on the kind of straw and other raw materials used for pellet production. In terms of the analysed parameters pellet from sample G, made of rapeseed straw, soya bean hulls and spelt hulls, was the lowest rated one. The pellet from this sample had the lowest net calorific value, high moisture content, low bulk density, and low mechanical strength. Among the evaluated samples the highest rated were pellets from sample D, made of rye straw and soya bean hulls, which had the highest net calorific value of 17.89 $MJ \cdot kg^{-1}$, and complied with European standards in terms of bulk density, moisture content, and high mechanical strength.

References

Adapa, P.K., Tabil, L.G., Schoenau, G.J. & Sokhansanj, S. (2004). Pelleting characteristics of fractionated sun-cured and dehydrated alfalfa grinds. *Applied Engineering in Agriculture, (20)6,* 813-820.

Blaschke, T., Biberacher, M., Gadocha, S. & Schardinger, I. (2013). Energy landscapes: meeting energy demands and human aspirations. *Biomass Bioenergy, 55,* 3-16.

Callejón-Ferre, A.J., Velázquez-Martí, B., López-Martínez, J.A. & Manzano-Agügliaro, F. (2011). Greenhouse crop residues: energy potential and models for the prediction of their higher heating value. *Renewable & Sustainable. Energy Reviews, 15,* 948-955.

Caryalho, L., Wopierika, E., Pointner, C., Lundgren, J., Verma, V.K., Haslinger, W. & Schmidl C. (2013). Performance of a pellet boiler fired with agricultural fuels. *Applied Energy, 104,* 286-296.

Firrisa, M.T., van Duren, I. & Voinov, A. (2014). Energy efficiency for rapeseed biodiesel production in different farming systems. *Energy Efficiency, 7(1),* 79-95.

García-Maraver, V., Popov, V. & Zamorano, M. (2011). A review of European standards for pellet quality. *Renew. Energy, 36,* 3537-3540.

Hlavatá M., Čablíková L., Čablík V., Nowak A.K., Wzorek Z., Gorazda K., Serwatka K. (2014). Comparison of biomass and fossil fuels (Porównanie biomasy i paliw kopalnych). *Przemysł Chemiczny*, *6*, 93, 893-896.

Ibrahim, H., Ilinca, A. & Perron, J. (2008). Energy storage systems – characteristics and comparisons. *Renewable & Sustainable Energy Reviews, 12(5),* 1221-1250.

ISO 17225-6:2014. Solid biofuels – Fuel specifications and classes – Part 6: Graded non-woody pellets.

Kashaninejad, M., Tabil, L.G. & Knox, R. (2014). Effect of compressive load and particle size on compression characteristics of selected varieties of wheat straw grinds. *Biomass Bioenergy, 60,* 1-7.

Kuntal, J. & Sudipta, D. (2014). Biomass integrated gasification combined cogeneration with or without CO_2 capture – A comparative thermodynamic study. *Renew. Energy, 72*, 243-252.

Liu, Z., Liu, X., Fei, B., Jiang, Z., Cai, Z. & Yu, Y. (2013). The properties of pellets from mixing bamboo and rice straw. *Renew. Energy, 55,* 1-5.

Liu, Z., Mia, B., Jianga, Z., Fei, B., Cai, Z. & Liu, X. (2016). Improved bulk density of bamboo pellets as biomass for energy production. *Renew. Energy, 86,* 1-7.

Lisowski A., Grela M., Sypuła M., Świętochowski A., Dąbrowska-Salwin M., Stepień W., Korupczyński R. (2015). Pellets and briquettes from fruit trees wood. *Ann. Warsaw Univ. of Life Sci. – SGGW. Agricult. 66*, 127-136.

Malowaniec B. **(**2016**)**. European low-power renewable energy devices (Europejskie urządzenia małej mocy wykorzystujące odnawialne źródła energii). *Przemysł Chemiczny, 3*, 95, 512-518.

Mani, S., Tabil, L.G. & Sokhansanj, S. (2006). Effects of compressive force. particle size and moisture content on mechanical properties of biomass pellets from grasses. *Biomass Bioenergy, 30,* 648-654.

Mc Kendry, P. (2002). Energy production from biomass (part 1): overview of biomass. *Bioresource Technology, 83,* 37-46.

Millili, G.P. & Schwartz, J.B. (2008). The strength of microcrystalline cellulose pellets: The effect of granulating with water/ethanol mixtures. *Journal Drug Development and Industrial Pharmacy, 16(8),* 1411-1426.

Niedziółka, I., Szpryngiel, M., Kachel-Jakubowska, M., Kraszkiewicz, A., Zawiślak, K., Sobczak, P. & Nadulski, R. (2015). Assessment of the energetic and mechanical properties of pellets produced from agricultural biomass. *Renew. Energy, 76,* 312-317.

Obidziński, S., Piekut, J. & Dec, D. (2016). The influence of potato pulp content on the properties of pellets from buckwheat hulls. *Renew. Energy, 87,* 289-297.

Piecuch, T. (2010). Termiczna utylizacja odpadów. *Rocznik Ochrona Środowiska, 2*, 11-37.

Serrano, C., Monedero, E., Lapuerta, M. & Portero, H. (2011). Effect of moisture content. particle size and pine addition on quality parameters of barley straw pellets. *Fuel Process. Technology, 92,* 699-706.

Shawa, M.D., Karunakaranb, C. & Tabila, L.G. (2009). Physicochemical characteristics of densified untreated and steam exploded poplar wood and wheat straw grinds. *Biosystems Engineering, 103(2),* 198-207.

Ståhl, M. & Berghel, J. (2011). Energy efficient pilot-scale production of wood fuel pellets made from a raw material mix including sawdust and rapeseed cake. *Biomass and Bioenergy, 35(12),* 4849-4854.

Starek, A., Kośko, M., Zarajczyk, J., Kowalczuk, J., Tatarczak, J., Zawiślak, K., Sobczak, P., Mazur, J. & Szmigielski, M. (2014). Wpływ rodzaju surowca i parametrów roboczych granulatora nowej konstrukcji na odporność peletów na ściskanie. *Zeszyty Problemowe Postępów Nauk Rolniczych, 578,* 121-129.

Sypuła, M., Lisowski, A., Chlebowski, J., Nowakowski, T., Strużyk, A. (2010). Bulk density of chopped material of energetic plants. *Annals of Warsaw University of Life Sciences – SGGW. Agricult., 56*, 29-37.

Theerarattananoon, K., Xu, F. & Wilson, J. (2011). Physical properties of pellets made from sorghum stalk, corn stover, wheat straw, and big bluestem. *Industrial Crops and Products, 33(2),* 325-332.

Uesu, N.Y., Winkler, E.A.G. & Hechenleitner, A.A. (2000). Microcrystalline cellulose from soybean husk: effects of solvent treatments on its properties as acetylsalicylic acid carrier. *International Journal of Pharmaceutics, 206,* 85-96.

Williams, A., Jones, J.M., Ma, L. & Pourkashanian, M. (2012). Pollutants from the combustion of solid biomass fuels. *Progress in Energy and Combustion Science, 38(2),* 113-137.

Wzorek, Z., Krupa-Żuczek, K. (2015). Biomass from cultivation of sunflower and wheat as substitute of conventional fuels (Biomasa z uprawy słonecznika oraz pszenicy jako substytut paliw konwencjonalnych). *Przemysł Chemiczny, 8* , 94, 1344-1346.

Zawiślak, K., Sobczak, P., Panasiewicz, M., Mazur, J., Nadulski, R. & Starek, A. (2014). Wpływ wielkości frakcji otrąb pszennych na jakość granulatu. *Inżynieria Przetwórstwa Spożywczego, 3(4),* 25-28.

Wpływ rodzajów słomy i dodatków pochodzenia roślinnego na fizyczne cechy peletów

Streszczenie

W pracy przedstawiono wyniki badań nad peletowaniem różnych rodzajów słomy z dodatkiem makuchu rzepakowego, łuski sojowej i łuski orkiszowej. Uzyskane pelety poddano ocenie jakościowej badając: wytrzymałość mechaniczną peletów, siłę cięcia i zgniatania oraz podstawowe właściwości fizyczne. Otrzymane wyniki porównano z normą jakościową ISO 17225-6:2014 oceniając ich przydatność dla przemysłu. Wyniki opracowano statystycznie stwierdzając zależności wpływu dodatków i słomy na badane parametry.

Z badań wynika, że wilgotność mieszanek w procesie peletowania mieściła się w przedziale od 9,0 do 13,65%, a peletów – 7,31-11,45%. Wartość opałowa otrzymanych peletów była zróżnicowana w niewielkim stopniu (15,85-17,89 $MJ \cdot kg^{-1}$). Najmniejsza zawartość popiołu wyniosła dla peletu wytworzonego ze słomy żytniej i łuski sojowej (4,06%), a największa dla peletu ze słomy rzepakowej i makuchu rzepakowego (5,17%). Rodzaj słomy wraz z zastosowanymi dodatkami nie wpłynął na gęstość właściwą peletów. Otrzymano natomiast zróżnicowanie w gęstości nasypowej. Pelety uzyskane ze słomy rzepakowej z dodatkiem łuski orkiszowej i makuchu rzepakowego posiadały najniższą gęstość nasypową (380,9 $kg \cdot m^{-3}$). Tylko pelety uzyskane ze słomy żytniej i łuski sojowej, słomy pszennej i łuski sojowej oraz pelety uzyskane ze słomy rzepakowej i łuski orkiszowej na bazie makuchu rzepakowego posiadały gęstość nasypową powyżej 500 $kg \cdot m^{-3}$.

Najwyższą wytrzymałość mechaniczną posiadały pelety, wytworzone ze słomy rzepakowej z dodatkiem makuchu rzepakowego i łuski orkiszowej (95,9%), dla których uzyskano również najwyższą odporność na ściskanie (1222,2 N) oraz siłę cięcia (136,6 N). Pod względem analizowanych parametrów najniżej oceniono pelety, wykonane ze słomy rzepakowej z dodatkiem makuchu rzepakowego i łuski orkiszowej. Posiadały one najniższą wartość opałową (15,85 $MJ \cdot kg^{-1}$), wysoką wilgotność (11,45%), małą gęstość usypową (390,8 $kg \cdot m^{-3}$) oraz wytrzymałość mechaniczną (89,4%). Najkorzystniejsze z ocenianych peletów okazały się pelety, ze słomy żytniej i łuski sojowej o najwyższej wartości opałowej 17,89 $MJ \cdot kg^{-1}$.

Abstract

The paper presents the results of a research on pelletizing different kinds of straw with admixture of rapeseed cake, soya bean hulls and spelt hulls. Obtained pellets were qualitatively assessed by examining: mechanical strength of the pellets, cutting and crushing strength, and basic physical characteristics. The results were compared with the ISO 17225-6:2014 quality standard in order to assess their suitability for industry. The results were statistically processed to determine the effects the particular admixtures and straw kinds had on the test parameters.

The research testifies that moisture content of mixtures during the pelletizing process ranged between 9.0 and 13.65%, however pellets – 7.31-11.45%. The net calorific value of the produced pellets varied to a small extent (15.85-17.89 MJ·kg^{-1}). The lowest ash content was measured for pellet made of rye straw and soya bean hulls (4.06%), and the highest for pellet made of rapeseed straw and rapeseed cake (5.17%). The various kinds of straw with applied compounds do not affect the specific density of the pellets. However, the obtained bulk density varied. The pellets obtained from rapeseed straw with spelt hulls and rapeseed cake compounds had the lowest bulk density (380.9 kg·m^{-3}). Only the pellets made of soya bean hulls and rye straw, wheat straw and soya bean hulls, and the ones made of rapeseed straw and spelt hulls and based on rapeseed cake had bulk density > 500 kg·m^{-3}.

The highest mechanical strength was measured for the pellets made of rapeseed straw with admixture of rapeseed cake and spelt hulls (95.9%), for which also the highest crushing strength (1222.2 N) and cutting strength (136.6 N) were obtained. Considering the analysed parameters, the pellets made of rapeseed straw with rapeseed cake and spelt hulls admixture received the lowest ratings. They were characterised by the lowest net calorific value (15.85 MJ·kg^{-1}), high moisture content (11.45%), low bulk density (390.8 kg·m^{-3}) and low mechanical strength (89.4%). Out of the examined pellets, the one made of rye straw and soy bean hulls had the highest net calorific value of 17.89 MJ·kg^{-1} and received the highest ratings.

Słowa kluczowe:
biomasa roślinna, pelety, cechy fizyczne i energetyczne

Keywords:
plant biomass, pellets, energetic and physical properties

MIDDLE POMERANIAN SCIENTIFIC SOCIETY OF THE ENVIRONMENT PROTECTION
ŚRODKOWO-POMORSKIE TOWARZYSTWO NAUKOWE OCHRONY ŚRODOWISKA
Annual Set The Environment Protection
Rocznik Ochrona Środowiska
Volume/Tom 19. Year/Rok 2017 ISSN 1506-218X 288-301

Analysis of the Effect of Temperature Cycling on Phosphorus Fractionation in Activated Sludge

Elżbieta Bezak-Mazur, Renata Stoińska, Bartosz Szeląg
Kielce University of Technology

1. Introduction

Sewage treatment by the activated sludge method consists in the mineralization of organic pollutants by microorganisms in aerated bioreactors. Decomposing organic matter provides microbes with essential nutrients necessary for life, i.e. mineral forms of carbon, phosphorus, sulfur and nitrogen. Temperature is an important parameter affecting wastewater treatment since its increase accelerates the decomposition of organic compounds. The optimum temperature of this process falls within the range of 18-22°C (Bugajski et al., 2012). As far as the biological phosphorus removal is concerned, reference sources provide conflicting reports concerning the optimum temperature. According to Converti et al. (Converti et al., 1995) the biological phosphorus removal is most efficiently performed at the temperatures from 20 to 37°C, whereas Florentz M. et al. think a different range of temperatures is optimum for this process, i.e. 5-15°C (Florentz et al., 1987). The latter maintain it is associated with the metabolism of phosphorus bacteria since these microorganisms are believed to belong mainly to a psychrophilic group and can already grow at temperatures slightly above 5°C (Kaczor 2008). Similarly, Xiong Liu et al. (Xiong Liu et al. 2014) regard phosphorus accumulating bacteria as primarily psychrophilic, which accounts for the reduction in phosphorus removal at temperatures above 20°C. The studies of Bassin et al. (Bassin et al. 2012) also investigated the process of removing phosphorus from wastewater. Their research revealed that the efficiency of

phosphorus removal at 20°C (> 90%) was higher than that at 30°C (60%). Piaskowski et al. (Piaskowski et al., 2005) examined the effect of temperature on biological phosphorus removal in a wider temperature range (5-45°C). They demonstrated that in anaerobic conditions the rise in temperature from 5°C to 30°C was accompanied by the increase in the amount of the released orthophosphates from 13.25 to 27.4 mg P/dm^3. A similar relation was also observed during the accumulation of orthophosphates under aerobic conditions, with the highest intensity being registered for the range of 25-30°C. These authors point to a direct effect of wastewater temperature on the rate of enzymatic reaction involving PAO bacteria. The rate of the phosphorus removal reaction in the function of temperature observed by the authors is in accordance with van't Hoff's rule, determining a 2-3-fold increase in the rate of enzymatic reactions for each rise in temperature by 10°C within the range of 0-30°C and a reduction in the rate at temperatures above 30°C (Kaczkowska 2002; Rheinheimer 1977). Since there are discrepancies in reference sources with regard to the effect of sewage sludge temperature on the phosphorus removal process, this research paper presents the analysis results of phosphorus speciation in activated sludge in an annual cycle (in temperate climate) in which the sewage sludge temperature can range from 5°C to 25°C. The tests examined samples of sewage sludge from oxygenated zone which represents the first stage of phosphorus accumulation by rapidly multiplying PAO microbes.

2. Research methodology

In order to determine the effect of cyclic temperature changes on the phosphorus removal process, the investigation involved monthly analyses of phosphorus fractionation in activated sludge samples taken from six sewage treatment plants (Table 1).

The content of different phosphorus fractions was determined in the collected sludge samples using fractionation scheme presented by Golterman (Golterman 1996). This is a sequential extraction scheme method where each extraction stage is followed by permeating the sample and treating it with another reagent of increasing extraction force (Tab. 2) (Bezak Mazur et al.,2014). Each determination of phosphorus fractions was repeated three times.

Table 1. Sewage treatment plants that provided the activated sludge samples
Tabela 1. Prezentacja oczyszczalni z których pobierano osady czynne do badań

Type of plant		Treatment method	Nominal capacity
A	biological	three-stage activated sludge method	900 m^3/d
B	biological	three-stage activated sludge method	1200 m^3/d
C	biological	three-stage activated sludge method with a sequencing batch reactor operating in cycles	300 m^3/d
D	biological	three-stage activated sludge and the rotating biological bed methods	500 m^3/d
E	biological-chemical	three-stage activated sludge method and chemical precipitation with lime	500 m^3/d
F	biological-chemical	three-stage activated sludge method and chemical precipitation with the PIX coagulant	72000 m^3/d

Table 2. Modified extraction scheme according to Golterman (Golterman 1996)
Tabela 2. Zmodyfikowany schemat ekstrakcji wg Goltermana (Golterman 1996)

Stage	Extraction conditions	Fraction	Phosphorus fraction – description
1	4h, 0.05 M $CaNa_2$-EDTA	Ca-EDTA	phosphorus associated with oxides and hydroxides of iron, aluminum and manganese
2	18h, 0.1 M Na_2-EDTA	Na-EDTA	phosphorus associated with carbonates
3	2h, 0.5 M H_2SO_4	H_2SO_4	phosphorus found in soluble combinations with organic matter
4	2 M NaOH, 2h	NaOH	The remaining forms, including phosphorus bound with aluminosilicates and contained in organic matter in the form of combinations not affected by the sulfuric acid activity in stage 3.

The concentration of total phosphorus in the obtained permeates was determined by spectrophotometry using a UV-VIS Lambda 25 PERKIN ELMER spectrophotometer. During sampling the temperature of the activated sludge was measured by means of a portable thermometer.

3. Results analysis

Wastewater treatment is predominantly conducted in a continuous manner, which results in a constant supply of organic matter. Activated sludge is therefore a mixture of substances already mineralized (flowing out of the bioreactor as an excess sludge) and organic substances flowing into the bioreactor with raw sewage. This diversity of organic and inorganic matter in the activated sludge is also reflected in the results of the speciation analysis of phosphorus in the sludge. Phosphorus is a mineral contained both in organic and inorganic substances.

Fractionation analysis performed by Golterman method allows for distinguishing mineral fractions of phosphorus adsorbed on the sewage particle surface. These fractions are considered as the most mobile (Table 2), bioavailable (Ca-EDTA and Na-EDTA fractions). This method involves also the extraction of phosphorus bound in strong combinations with aluminosilicates (NaOH fraction) and phosphorus identified primarily with organic forms (Table 2), or phosphorus fractions found in soluble combinations with organic matter (H_2SO_4 fraction) and those contained in the organic matter (NaOH fraction). The fractions of phosphorus bound in combinations with aluminosilicates and identified with organic fractions are defined by Golterman as fractions difficult to access (H_2SO_4 and NaOH fractions).

Fractionation analysis showed that in an annual cycle the shares of phosphorus fractions in the examined specimens vary considerably. It is due, among others, to the constantly changing composition of raw waste flowing into the reactor and to the sludge temperature fluctuations in an annual cycle resulting from varying air temperature in the temperate climate. The samples of the analysis results are presented in Figure 1.

The percentage shares of different phosphorus fractions in the activated sludge demonstrate high variability of values, however, in the case of their classification into one of the two groups on the basis of bioavailability (form: mobile and difficult to access), one can notice a pattern occurring in the annual cycle. Figure 2 shows the percentage shares of phosphorus mobile fractions (the sum of the Ca-EDTA and Na-EDTA fractions shares) and the temperature of the activated sludge in particular months. The increase or decrease in the sludge temperature is noticeably accompanied by a rise or fall in the percentage share of phosphorus mobile fractions.

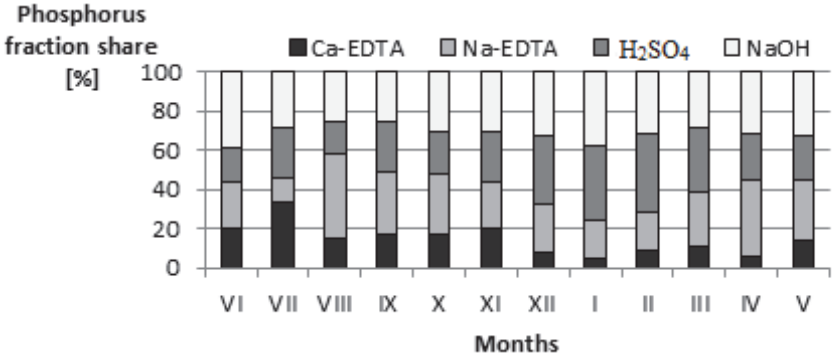

Fig. 1. Shares of different phosphorus fractions in the activated sludge collected at the *F* wastewater treatment plant
Rys. 1. Udział poszczególnych frakcji fosforu w osadach czynnych pochodzących z oczyszczalni F

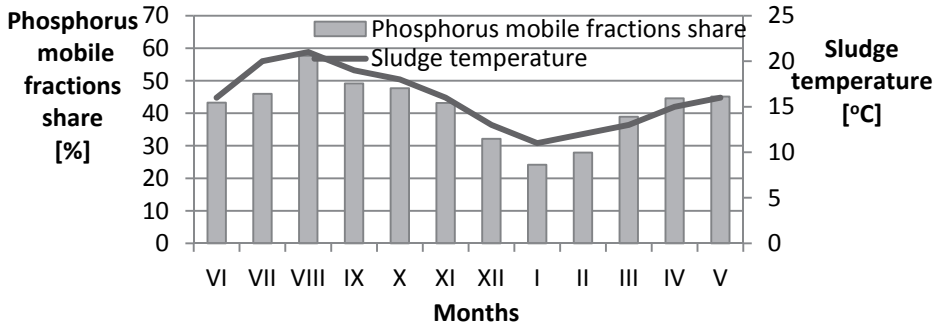

Fig. 2. Change dynamics in percentage shares of phosphorus mobile form and temperature in activated sludge collected at the *F* wastewater treatment plant
Rys. 2. Dynamika zmian udziałów procentowych frakcji fosforu oraz temperatury w osadzie czynnych pochodzącym z oczyszczalni *F*

In August, when the temperature of the sludge was 21°C, the share of phosphorus mobile fractions was the highest and amounted to 58%. In winter there occurs a decrease in the shares of mobile fractions and an increase in the shares of hard-accessible ones. In January, when the temperature of the activated sludge was the lowest at 11°C, the share of mobile phosphorus fractions was only 24%. Similar results were also obtained in the remaining treatment plants. Figure 3 presents the box

graphs of the mobile phosphorus fractions shares in the activated sludge collected at the six sewage treatment plants discussed in this paper. The ends of the box charts' whiskers represent the minimum and maximum values of the mobile fractions shares. In all the analyzed facilities the extreme values of the mobile fractions shares correspond to the extreme values of the activated sludge temperatures. Analyzing the six treatment plants it can be said that the mobile fractions shares varied within the range of 19-64%.

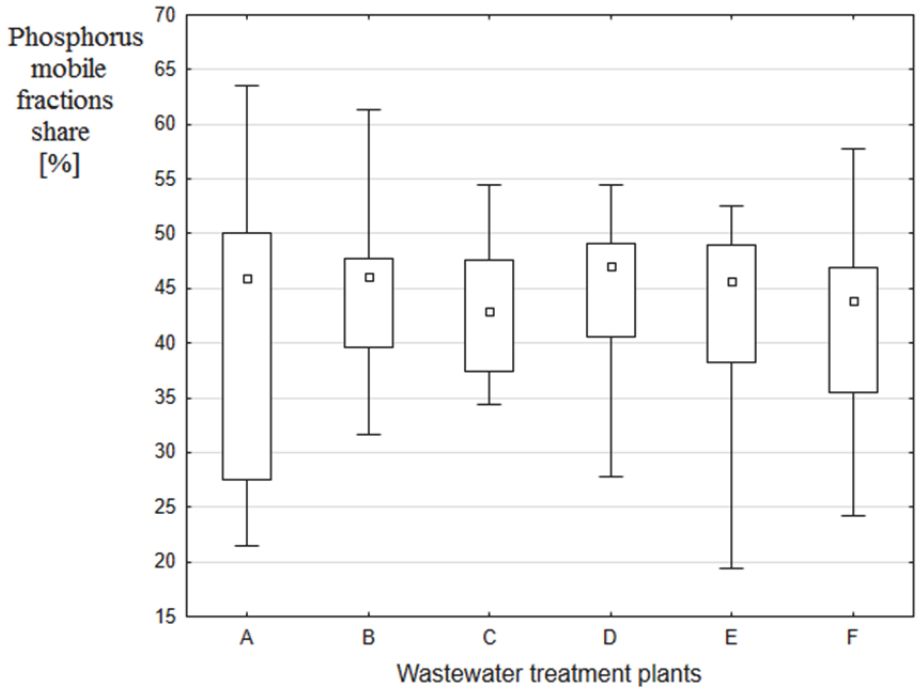

Fig. 3. Shares of phosphorus mobile fractions in activated sludge collected at *A, B, C, D, E* and *F* treatment plants
Rys. 3. Wartości udziałów form mobilnych fosforu w osadach czynnych pochodzących z oczyszczalni *A*, *B*, *C*, *D*, *E* i *F*

The values of the phosphorus mobile fractions shares (p.m.f.s) changing together with the temperature in an annual cycle (Figure 2 and 3) indicate the effect of temperature on phosphorus removal from wastewater. Therefore, in order to approximate the experimental relations

with empirical formulas, a separate regression model was developed for the analyzed parameters of the activated sludge collected at each treatment plant.

Prior to statistical analyses the Shapiro-Wilk test was applied, primarily to confirm the compliance of the statistical distributions of the analyzed sludge temperature sequences and the mobile form shares with the normal distribution. The probability value for all the analyzed parameters was higher than α=0.05, which means that the investigated variables have a normal distribution and it is possible to perform further statistical analyses.

The next analysis was aimed at establishing similarities and differences between the treatment plants under consideration. The cluster analysis was applied for this purpose. This method involves defining groups (clusters) of objects similar to each other on the basis of variables depicting the analyzed objects and showing how much one cluster differs from another. This methodology is discussed in detail in scientific literature (Licznar and Szeląg 2014). To determine the Euclidean distance (bond distance) between the emerging clusters, a popular single-bond method was applied. The results of the conducted calculations are presented in Figure 4.

On the basis of the dendrogram shown in Fig. 4 it can be concluded that the *F* and *E* treatment plants are most similar to each in terms of the analyzed variables, which may be associated with chemical dephosphatation used in these facilities. *C, B, D, F* and *E* treatment plants are similar with regard to the analyzed parameters. The bond distance for these facilities does not exceed 0.16, therefore they form a large cluster. Forming a cluster comprising five out of six investigated facilities may indicate that the joint analysis of parameters such as mobile forms share and activated sludge temperature is justified owing to the similarity of results obtained in the facilities. The sewage treatment plant *A* deviates most from the other plants presented in the dendrogram, which may be associated with the quality of the activated sludge in this facility. In the spring and summer filamentous microorganisms from the *Actinomycetes* group multiply very intensely in the bioreactors of this sewage treatment plant. These organisms have hydrophobic cell walls owing to which they stick to air bubbles and are carried up together with the sludge flocs to the surface of the reactor. They disrupt the homeostasis of the environ-

ment and thus the biochemical processes occurring in the activated sludge chamber.

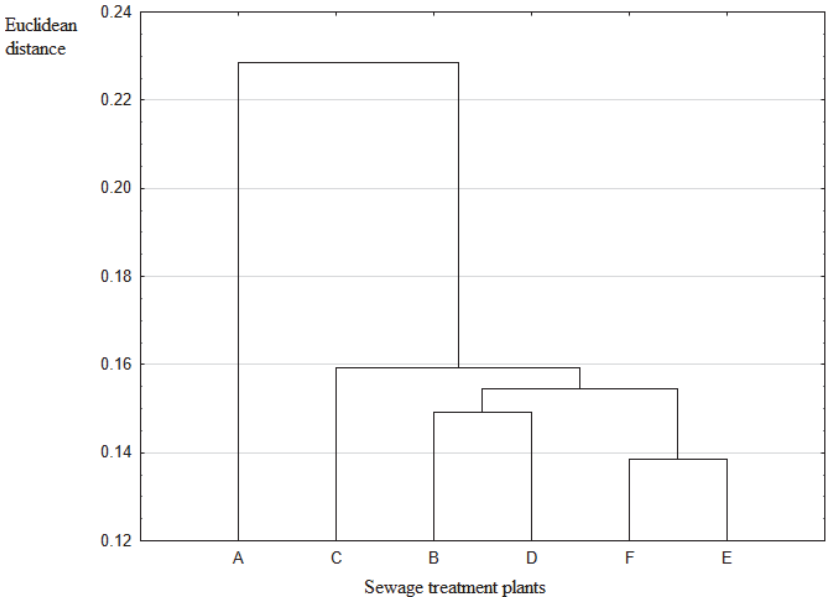

Fig. 4. Dendrogram determined for the investigated treatment plants based on the variable shares of the phosphorus mobile forms and the activated sludge temperature
Rys. 4. Dendrogram wyznaczony dla analizowanych oczyszczalni oparte na zmiennych udziałach form mobilnych i temperatury osadu czynnego

In the next stage an attempt was made to develop a mathematical model describing the dependence of the phosphorus mobile fractions share (p.m.f.s.) on temperature. Considering the observations made during the investigation, this relation was expressed as follows by the segmented regression (Seber et al. 2003):

$$p.m.f.s. = \begin{cases} \alpha_0 + \alpha_1 \cdot T \quad dla \quad T < T_{gr} & (1) \\ \alpha_0 - \alpha_2 \cdot T_{gr} + (\alpha_1 + \alpha_2) \cdot T \quad dla \quad T > T_{gr} & (2) \end{cases}$$

where α_0, α_1, α_2 – empirical model parameters estimated by Levenberg-Marquardt method, T_{gr} – limit temperature corresponding to the change of the dependence p.m.f.s. = f(T). It can be concluded on the basis of the performed calculations that, in the case of the *A, B, C, D* and *E* treatment plants, the p.m.f.s. = f (T) relation had a linear character and was described by equation (1), whereas for the *F* plant the dependence p.m.f.s. = f (T) was expressed by equation (2). The values of the determined parameters α_i and determination coefficients are given in Table 3.

Table 3. Parameter values of the m.f.s. = f(T) equation for the analyzed facilities
Tabela 3. Zestawienie wartości parametrów równania u.f.m. = f(T) dla analizowanych obiektów

Facility	Parameters				
	α_0	α_1	α_2	T_{gr}	R^2
A	0.029±(0.002)	0.0299±(0.003)			0.903
B	0.237±(0.039)	0.0166±(0.003)			0.771
C	0.279±(0.027)	0.0122±(0.002)			0.808
D	0.226±(0.036)	0.0169±(0.002)			0.778
E	0.013±(0.033)	0.0270±(0.004)			0.832
F	-0.206±(0.022)	0.080±(0.020)	0.072±(0.020)	7.77	0.906

In addition, Figure 5 shows a sample of a graphical representation of the p.m.f.s. = f (T) calculations for the *A* and *F* treatment plants. Based on the above, it can be stated that there is a statistically significant relationship between the activated sludge temperature and mobile fractions shares. In the case of the *A,B, C, D, E* treatment plants this relationship is linear. Based on the regression curves one can estimate how the mobile fractions share will change in the case of temperature alteration. The analysis of the parameters α_1 (Table 3) in equation (1) shows that in the case of the *A, B, C, D* and *E* treatment plants, the increase in the temperature of the activated sludge by 1°C will cause the rise in the share of mobile phosphorus fractions from 1.22 to 2.99%. It is a considerable change, because the annual amplitude of the activated sludge temperature is even 10°C. A piecewise regression curve was constructed for the sewage treatment plant *F* (Fig. 5).

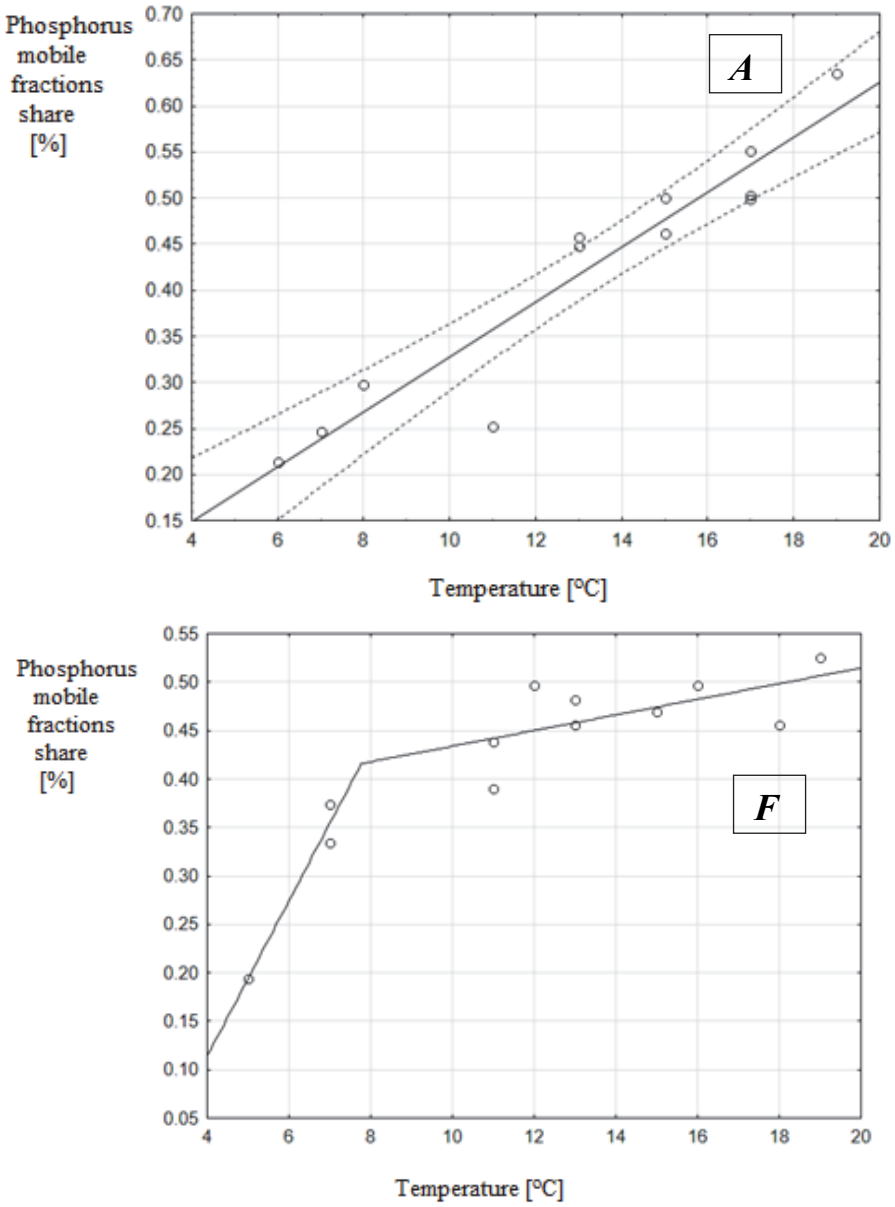

Fig. 5. Effect of activated sludge temperature on the share of mobile forms in wastewater treatment plants *A* and *F*
Rys. 5. Wpływ temperatury osadu czynnego na udział form mobilnych w oczyszczalniach *A* i *F*

The examination of the calculated parameters α_1 and α_2 in the regression model described by formula (2) leads to the conclusion that for the estimated limit temperature (T_{gr}) of 7.7 ^{o}C (Tab. 3) the increase in the temperature by 1°C causes the rise in the mobile fractions shares of phosphorus by 8%. However, above T_{gr} = 7.7°C the rise in temperature by 1°C leads to the increase in the mobile fractions shares of phosphorus merely by 7.2%.

4. Conclusions

The analysis of the above study provides ground for the conclusion that there is a statistically significant effect of temperature on the shares of phosphorus fractions in activated sludge. The increase in temperature is accompanied by the rise in the shares of phosphorus mobile fractions (Ca-EDTA and Na-EDTA) that can be identified with mineral fractions of this element adsorbed on the surface of sludge particles. The increase in the mineral fractions share under the influence of temperature may indicate the direct effect of the activated sludge temperature on the rate of enzymatic reactions and thus on the microbial mineralization of phosphorus contained in the organic matter reaching the bioreactor. This may mean that the rate of phosphorous bacteria metabolism increases together with the temperature in the analyzed range. Based on the estimated regression models obtained in this study it was found that the increase in the activated sludge temperature by 10°C can cause an increase in the mobile (mineral) phosphorus fractions share from 12% to 30%.

References

Bassin, J., Winkler, M., Kleerebezem, R., Dezotti, M., Loosdrecht, M. (2012). Improved phosphate removal by selective sludge discharge in aerobic granularsludge reactors. *Biotechnol Bioeng, 109*, 1919-28.

Bezak-Mazur, E., Mazur, A. Stoińska, R.(2014). Phosphorus speciation in sewage sludge. *Environment Protection Engineering, 40(3),* 161-175.

Bugajski, P., Kaczor, G.(2012). Influence of chosen factors on sewage temperature in the flow of biological reactor. *Infrastructure and Ecology of Rural Areas, 2(I)*, 75-85

Converti, A., Rovatti, M., Borghi, M.(1995). Biological removal of phosphorus from wastewaters by alternating aerobic and anaerobic conditions. *Water Res., 29(1)*, 263-269.

Florentz, M., Caille, D., Bourdon, F,, Sibony, J. (1987). Biological phosphorus removal in France. *Water Sci. Technol*., *19(4),* 1171-1183.

Golterman, H. L.(1996). Fractionation of sediment phosphate with chelating compounds: a simplification, and comparison with other methods. *Hydrobiologia, 335*, 87-95.

Kączkowski, J. (2002). *Foundations of biochemistry* [in Polish].Warsaw: WNT.

Licznar, P., Szeląg, B., (2014). Analysis of time-related variability of atmospheric precipitation in Warsaw [in Polish]. *Ochrona Środowiska, 3*, 23-28.

Piastowski, K., Ostrowska, M. (2005). The effect of environmental agents on biological phosphorus removal [in Polish]. *Gaz, woda i technika sanitarna, 3*, 34-40.

Rheinheimer, G.(1977). *Microbiology of Waters* [in Polish]. Warsaw: PWRiL.

Xiongliu, Z., Peide, S., Jingyi, H., Yingqi, S., Zhirong, H., Haiqing, F., Shuyu, L.(2014). Inhibitory factors affecting the process of enhanced biological phosphorus removal (EBPR) – A mini-review. *Process Biochemistry, 49*, 2207-2213.

Analiza wpływu cyklicznych zmian temperatury na specjacje fosforu w osadach czynnych

Abstract

Temperature is a significant parameter affecting wastewater treatment , because its increase accelerates decomposition of organic compounds. The optimum temperature of this process falls within the range of 18-22°C (Bugajski et al., 2012). As far as the biological phosphorus removal process is concerned, there are conflicting reports in reference sources with regard to the temperature optimum. Due to the existing discrepancies in the relevant literature on the effect of the sewage sludge temperature on the phosphorus removal processes, this study attempts to provide a speciation analysis of phosphorus in activated sludge in an annual cycle (in temperate climate), in which the sewage sludge temperature may range from 5°C to 25°C. The studies conducted to evaluate the effect of temperature cycling on the phosphorus speciation in activated sludge involved performing monthly speciation analyses of phosphorus in activated sludge collected at six sewage treatment plants. The content of different phosphorus fractions was determined in the sewage specimens using the fractionation scheme proposed by Golterman. The speciation analysis performed by this method allows to distinguish mineral phosphorus forms adsorbed on the surface of the sludge particles. These forms are considered as the most mobile, bioavailable (fractions of Ca-EDTA and Na-EDTA). This method is also used to extract phosphorus bound in strong combinations with aluminosilicates (NaOH

fraction) and phosphorus identified primarily with organic forms, i.e. forms of phosphorus found in soluble combinations with organic matter (H_2SO_4fraction) as well as the forms of phosphorus contained in organic matter (NaOH). Forms of phosphorous bound in combinations with aluminosilicates and identified with organic forms are distinguished by Golterman as forms difficult to access (H_2SO_4 and NaOH fractions). The results presented in the study show that the shares of different phosphorus fractions in activated sludge demonstrate high variability in value, however, in the case of their classification into one of the two groups on the basis of bioavailability (fractions: mobile and difficult to access), one can notice a pattern occurring in the annual cycle. There is a noticeable increase in the share of mobile (mineral) phosphorus forms which accompanies a rise in the sludge temperature (with the temperature increase by 1°C the mobile forms shares grow from 1.2% to 3%). The increase in the mineral forms share under the influence of temperature may indicate the direct effect of the activated sludge temperature on the rate of enzymatic reactions. The fact that the share of phosphorus forms difficult to access (H_2SO_4 and NaOH fractions), identified primarily with organic forms, is dominant in winter while the share of mobile forms is minor (24%), confirms the reduction of phosphorus removal at a low sludge temperature.

Streszczenie

Istotnym parametrem wpływającym na proces oczyszczania ścieków jest temperatura, ponieważ jej wzrost przyspiesza procesy rozkładu związków organicznych. Optymalna temperatura tych procesów mieści się w granicy 18-22°C (Bugajski i in. 2012). Z kolei w przypadku procesu defosfatacji biologicznej istnieją sprzeczne doniesienia literaturowe dotyczące optimum temperaturowego. Ze względu na występujące rozbieżności w doniesieniach literaturowych dotyczących wpływu temperatury osadu ściekowego na procesy defosfatacji, w niniejszej pracy podjęto się wykonania analizy specjacyjnej fosforu w osadach czynnych w cyklu rocznym (w klimacie umiarkowanym), w którym temperatura osadów ściekowych może wahać się od 5°C do 25°C. W celu oceny wpływu cyklicznych zmian temperatury na specjacje fosforu w osadach czynnych zostały wykonane badania, które polegały na wykonaniu comiesięcznych analiz specjacyjnych fosforu w osadach czynnych pochodzących z sześciu oczyszczalni ścieków. W pobranych próbach osadu oznaczano zawartość poszczególnych frakcji fosforu wykorzystując schemat frakcjonowania zaproponowany przez Golterman'a. Analiza specjacyjna wykonana tą metodą pozwala wyróżnić formy mineralne fosforu, zaadsorbowane na powierzchni cząstek osadów. Formy te uważane są jako najbardziej mobilne, biodostępne (frakcje Ca-EDTA i Na-EDTA). W metodzie tej ekstrahuje się również fosfor związany

w silnych połączeniach z glinokrzemianami(frakcja NaOH) oraz fosfor utożsamiany przede wszystkim z formami organicznymi, czyli formami fosforu występującymi w rozpuszczalnych połączeniach z materią organiczną (frakcja H_2SO_4) oraz formami fosforu zawartymi w materii organicznej (NaOH). Formy fosforu związanego w połączeniach z glinokrzemianami oraz utożsamiany z formami organicznymi Golterman wyróżnia jako formy trudnodostępne (frakcje H_2SO_4 i NaOH). Przedstawione w pracy wyniki świadczą iż wartości udziałów poszczególnych frakcji fosforu w osadach czynnych wykazują dużą zmienność, jednak w przypadku ich przyporządkowania do dwóch grup pod względem biodostępności (frakcje mobilne i trudnodostępne) można dostrzec występowanie tendencji w cyklu rocznym. Zauważalny jest wzrost udziału form mobilnych(mineralnych) fosforu wraz ze wzrostem temperatury osadu (przy wzroście temperatury o 1°C udziały form mobilnych wzrastają od 1,2% do 3%). Zwiększenie udziałów form mineralnych pod wpływem temperatury może świadczyć o bezpośrednim wpływie temperatury osadów czynnych na szybkość reakcji enzymatycznych. Dominujący w okresie zimowym udział form trudnodostępnych fosforu (frakcji H_2SO_4 i NaOH), utożsamianych przede wszystkim z formami organicznymi oraz niewielki udział form mobilnych (24%) potwierdza obniżenie procesów defosfatacji w przypadku niskiej temperatury osadu.

Słowa kluczowe:
formy specjacyjne fosforu, osad czynny, temperatura

Key words:
speciation forms of phosphorus, active sludge, temperature

MIDDLE POMERANIAN SCIENTIFIC SOCIETY OF THE ENVIRONMENT PROTECTION
ŚRODKOWO-POMORSKIE TOWARZYSTWO NAUKOWE OCHRONY ŚRODOWISKA

Annual Set The Environment Protection
Rocznik Ochrona Środowiska

Volume/Tom 19. Year/Rok 2017 ISSN 1506-218X 302-334

Physicochemical Properties of Seed Extraction Residues and Their Potential Uses in Energy Production

Monika Aniszewska[*], *Arkadiusz Gendek*[*],
Michał Drożdżek[*], *Marta Bożym*[**], *Janusz Wojdalski*[*]
[*]*Warsaw University of Life Sciences – SGGW*
[**]*Opole University of Technology*

1. Introduction

Biomonitoring involves observations and evaluations of changes in ecosystems with the use of bioindicators. Biomonitoring programs are implemented to analyze environmental parameters, in particular air and water pollution, accumulation of toxic substances in plants and the physicochemical parameters of plants in view of their potential uses (Coşkun 2006, Gdula-Argasińska et al. 2004, Greinert 2011, Karnosky et al. 2007, Masese et al. 2014, Wójcik et al. 2014). Not long ago, many biological materials did not have practical applications (Nanda et al. 2014). The advance of modern technologies for the production, bioconversion and generation of green energy and the introduction of legally binding targets for reducing CO_2 emissions brought far-reaching changes. The relevant progress has contributed to the significance of biomass as biofuel (Budzianowski 2012a,b; Gendek & Zychowicz 2014; Gołos & Kaliszewski 2015; Sawauchi et al. 2015; Yoshioka & Sakai 2005). Biomass is a highly recommended source of renewable energy because its combustion is associated with low sulfur and nitric oxide emissions. This sustainable resource is part of the carbon cycle (Kratzeisen & Müller 2013, Pindór & Preisner 2011). Biomass is used for generating heat and electricity, and it can be co-combusted with fossil fuels. (Basu et al.

2011, Coronado et al. 2011). Biomass includes forest waste (Aniszewska & Gendek 2016a, b; Gendek & Nurek 2016; Gendek & Zychowicz 2014, 2015; Risovič et al. 2008). Forests in Northern, Central and Eastern Europe, including Poland, are characterized by a predominance of coniferous stands. The most common tree species are the Scots pine (*Pinus Sylvestris* L.), Norway spruce (*Picea abies* H. Karst.), European larch (*Larix decidua* Mill) and Polish larch (*Larix polonica*) (Raciborski & Wóycicki-Domin). Their seeds have wings which promote seed dispersal by wind across considerable distances. Wings are separated from seeds in industrial plants where the husking process lasts 12 to 56 hours, depending on the species (Aniszewska 2012). Wings have to be removed before successive stages of seed production because they hinder sowing, in particular when precision seeders are used. Wings are separated by dry or wet dewinging methods. In the dry method, wings are removed mechanically by rubbing seeds against a hard surface, such as drum or studded rollers. In the increasingly popular wet dewinging method, seeds are moistened with water (Tylek & Walczyk 2009a,b). Seeds imbibe more water than wings, and wings become separated in the process. Wings are attached to seeds differently in the Scots pine and in the Norway spruce. In pines, wings encapsulate the entire seed, whereas in the spruce, the wing is attached to one side of the seed only.

Steven and Carlisle (1959) investigated the morphology of Scots pine seeds and observed that wing shape varies within the same cone and is determined by the size of the seed husk (Białobok et al. 1993).

Seed wings are classified as long, standard or broad based on the ratio of wing length to wing width (Sylven 1916, as cited in Białobok et al. 1993). According to Sylven (1916) & Zajączkowski (1949), the length of standard wings on Scots pine and Norway spruce seeds ranges from 11 to around 16 mm, and their width – from 4.5 to 6.1 mm. Seeds from trees growing in the mountains have smaller and relatively broad wings (Zajączkowski 1949). According to Zajączkowski (1949), the length and width of wings are closely correlated with the length and width of the cone.

Significant variations are observed in the color of seed wings (Białobok et al. 1993). In pines, wing color varies from yellow to red, reddish brown and purple-gray with light and dark streaks, whereas in spruces, wing color is less differentiated and ranges from fawn to light brown. The calorific value of wood, cones, needles and bark has been

extensively researched. The calorific value of wood was investigated by Günther et al. (2009), Haufa & Wojciechowska (1986), Komorowicz et al. (2009), Krzysik (1974), Lu et al. (2009), Monkielewicz & Pflaum (1967), Rembowski (2007), Reva et. al. (2012), So & Eberhardt (2013), Stolarski et al. (2013) and Uri et al. (2015). In the cited studies, this parameter was determined in the range of 19.2-21.2 $MJ \cdot kg^{-1}$ for pine wood and 18.8-20.5 $MJ \cdot kg^{-1}$ for spruce wood. In the work of Font et al. (2009), the calorific value of pine needles and cones was determined at 20.14 $MJ \cdot kg^{-1}$ and 18.78 $MJ \cdot kg^{-1}$, respectively. The calorific value of pine needles was established at 20.6 $MJ \cdot kg^{-1}$ by Zhao et al. (2014). Wanin (1953) determined the calorific value of Norway spruce needles and bark at 20.66 $MJ \cdot kg^{-1}$ and 20.33 $MJ \cdot kg^{-1}$, respectively, whereas in the work of Zhao et al. (2014), the calorific value of Scots pine bark reached 19.3 $MJ \cdot kg^{-1}$. The cited authors investigated mostly wood, bark and green parts of trees. The properties of seed extraction residues, including wings and empty seeds, have never been evaluated in view of their potential uses in energy generation. Biomonitoring studies revealed that higher plants are less resistant to high concentrations of heavy metals in soil. The most toxic metals are Cu, Pb, Cd, Co and Ni (Kabata-Pendias & Pendias 1999). Excessive metal levels in plants cause chlorosis, needle yellowing and inhabited growth. High concentrations of Hg, Cd and Pb in plant tissues can slow down photosynthesis, mitosis and water absorption (Kabata-Pendias & Pendias 1999). The ratios of heavy metals in plant tissues are also important for plant growth (Mandre & Ots 2012). The heavy metal content of plants is influenced by various factors, including environmental pollution (soil and air), weather conditions, soil properties, surface structure, age of plant tissues and the species' ability to accumulate and transport metals (Voutsa et al. 1996, Onder & Dursun 2006, Nkongolo et al. 2008, Mandre & Ots 2012). Trees take up heavy metals from soil via the root system. Mycorrhizae can limit the uptake of toxins by trees (Khan et al. 2000). The absorbed heavy metals are distributed to all plant parts, and their concentrations can differ significantly across organs. Needles accumulate less metals than the roots, trunks and branches of coniferous trees (Nkongolo et al. 2008, Sawidis et al. 1995, Fuentes et al. 2007, Onder & Dursun 2006). The highest concentrations of heavy metals are generally noted in bark on account of its porous

structure and the ability to absorb metals from atmospheric air. According to Coşkun (2006), bark is a reliable indicator of air pollution. Due to its sorptive properties, coniferous bark (pine, spruce) is used to remove metal ions from aqueous solutions, for example in industrial waste water treatment plants. According to Su et al. (2013), Argun et al. (2009) and Palma et al. (2003), ground cones have similar properties.

The accumulation of metals in different organs of coniferous trees has been extensively researched, but little is known about their impact on seed ecology. In comparison with other plant organs, seeds generally accumulate the smallest amounts of metals. Most heavy metals are microelements that occur naturally in tree seeds. Excessive metal concentrations can have adverse environmental effects, which is why they are controlled as part of biomonitoring programs. Coniferous seeds have a physiological barrier that protects generative reproduction organs against heavy metals (Palowski 2000). The reproductive organs of coniferous trees have a complex structure and a long reproductive cycle, which makes them most sensitive to the harmful effects of anthropogenic pollutants. Seeds harvested from trees growing near heavy-traffic roads were characterized by lower viability (Stvolinskaya 2000). The presence of heavy metals in seeds has a negative effect on the quality of genetic material. Excessive metal accumulation in seeds can inhibit germination and seedling development (Ganatsasa et al. 2011). Prus-Głowacki et al. (2006) subjected seeds to isoenzyme and cytology tests which revealed that heavy metal ions significantly influenced the genetic structure of the examined population of *Pinus sylvestris* L.

There is a general scarcity of published data on the morphology and characteristics of pine and spruce seed wings. The microscopic structure, chemical composition and calorific value of seed extraction residues have never been evaluated. Those parameters could constitute important data for biomonitoring.

2. Research objective

The aim of this study was to describe selected physicochemical properties, including microscopic structure, chemical composition, heat of combustion and calorific value, of seed wings and empty seeds of two coniferous species: Scots pine (*Pinus sylvestris* L.) and Norway spruce

(*Picea abies* H. Karst.). Wings and empty seeds, which constitute seed extraction residues, were evaluated as potential sources of energy. Heavy metal emissions during the combustion of seed discards were measured, and attempts were made to determine whether cell structure influences the calorific value of seeds. The results of this study will fill the existing knowledge gap and will have practical applications for environmental biomonitoring. The study will make a reference to the observations made by Bunse et al. (2011) who postulated the need to bridge the gap between academic research and the research needs of industry, as well as the work of Leturcq (2014) and Uliasz-Bocheńczyk & Mokrzycki (2015) who investigated alternative fuels.

3. Materials and methods

The wings and empty seeds of the Scots pine and Norway spruce were supplied by a seed extraction plant in Grotniki located on the territory managed by the Regional Directorate of State Forests in Łódź, Poland.

The morphology of wings was described based on microscopic observations. The size of cells in the longitudinal section and the cross-section was determined at x40, x100 and x400 magnification under the Nikon Alphaphot -2- TRIN microscope equipped with a camera and connected to a computer with MicroScan software. The surface of pine wings was also viewed at x80 and x1000 magnification under the Quanta 200 scanning electron microscope with a data recording system.

Cell length, cell width, cell wall thickness, cell perimeter and surface area were measured in the longitudinal section. Wing thickness at the widest point and cell lumina were measured in the cross-section. Measurements were performed in MicroScan v. 1.5 software to the nearest 1 μm.

Seed extraction residues were sorted with the use of mesh screens. The fraction that passed through the screen with 0.80 mm mesh size and was captured by the screen with 0.43 mm mesh size was used in chemical composition analysis. The sorted material was extracted with a chloroform-ethanol mixture (93:7) (Antczak et al. 2006) for 10 hours. The content of cellulose (Krutul 2002), lignin (PN-92/P-50092) and holocellulose (Kacik & Solar 1999) was determined in extracted material.

The content of substances soluble in 1% NaOH solution was determined in non-extracted residues. Ash content was analyzed in the powdery fraction which passed through the screen with 0.43 mm mesh size. The material was heated and roasted in a muffle furnace. The final roasting temperature of 600°C was maintained for 6 hours. The moisture content of the examined residues was determined before analysis by the gravimetric method, according to standard PN-EN 13183-1:2004 in three replications.

Heat of combustion and calorific value were determined calorimetrically according to standard PN-ISO 1928:2002. The material was pulverized in a mill, and it was dried to constant weight in the SLW 115 TOP laboratory drier at 104±1°C for 24 hours.

Analytical samples of 1.0 g each were weighed to the nearest 0.001 g on the WSP 210S scale. They were burned in an oxygen bomb calorimeter (KL10). Measurements were performed in 10-11 replications for every type of material. Indoor temperature and humidity were measured to the nearest ±0.1°C and ±0.1%, respectively, with the Rotronik HygroPalm HP23 series humidity meter. Heat of combustion Q_s was determined automatically by the bomb calorimeter.

Calorific value Q_{op} was calculated based on the following formula (PN-ISO 1928:2002):

$$Q_{op} = (Q_s - 206 \cdot H) \cdot (1 - 0.01 \cdot W_w) - 23.0 \cdot W_w \quad (1)$$

The calculated values of the heat of combustion of various wood components were used to derive empirical formula (2) (Telmo and Lousada, 2011):

$$Q_{ne} = 14.3377 + 0.1228(L) + 0.11353(Ext) \quad (2)$$

The CHNS (carbon, hydrogen, nitrogen, sulfur) analysis was performed in the Elementar Vario Macro Cube elemental analyzer based on the Alfalfa standard (B2273). Measurement error was: C – 6.7%, H – 18.4%, N – 15.5%, S – 16.4%.

The content of cadmium (Cd), lead (Pb), copper (Cu), zinc (Zn), nickel (Ni), chromium (Cr), molybdenum (Mo), cobalt (Co), iron (Fe), manganese (Mn), calcium (Ca), magnesium (Mg), potassium (K), sodium

(Na) and mercury (Hg) was determined in pine and spruce wings and empty seeds. The analyses were performed by flame absorption atomic spectroscopy (FAAS) with the Thermo Solaar 6M spectrometer. Samples were mineralized in Teflon-lined pressure vessels in a mixture of nitric acid and hydrogen peroxide according to procedure No. DG-EN-19 "Wood chips" for the Milestone Start D microwave mineralizer. Sample weight was 0.5 g, and measurements were performed to the nearest 0.001 g. The reaction mixture was composed of 8 cm^3 of nitric acid (65% HNO_3, ultra pure) and 2 cm^3 of hydrogen peroxide (30% H_2O_2, ultra pure). The temperature profile was as follows: 2 minutes – increase to 85°C, after 5 minutes – increase to 145°C, after 3 minutes – increase to 200°C, last 20 minutes – 200°C. Heating power during mineralization was 1000 W.

Data were processed in the Statistica v. 12 program (Stat Soft Inc. 2014) at a significance level of α=0.05. Differences were regarded as statistically significant at $p<0.05$.

4. Results and discussion

4.1. Microscopic structure of wings

Scots pine (Pinus sylvestris L.) wings

Every pine wing has two edges. The inner edge is located near the center of the husk axis, whereas the outer edge is situated near the edge of the husk. The inner edge (Fig. 1a) is composed of similarly sized and regularly overlapping cells with dark brown color. The outer edge consists of variously sized cells with irregular, elongated shape (Fig. 1b). Unlike the inner edge, the outer edge is convex. The tip and the outer edge of a wing comprise irregularly distributed cells with light brown color. Cells contain dark brown, differently sized bodies with an elliptical cross-section. The content of brown bodies in cells increases towards the tip of the wing.

The central part of the wing (Fig. 2a) consists of cells with regular, elongated cells and ribbed cell walls. In this segment, the cells are arranged in a pattern of lighter and darker streaks. Darker streaks are composed of cells with brown bodies (Fig. 2b), similarly to the cells distributed along the outer edge or at the tip of the wing. Light streaks consist of cells without brown bodies.

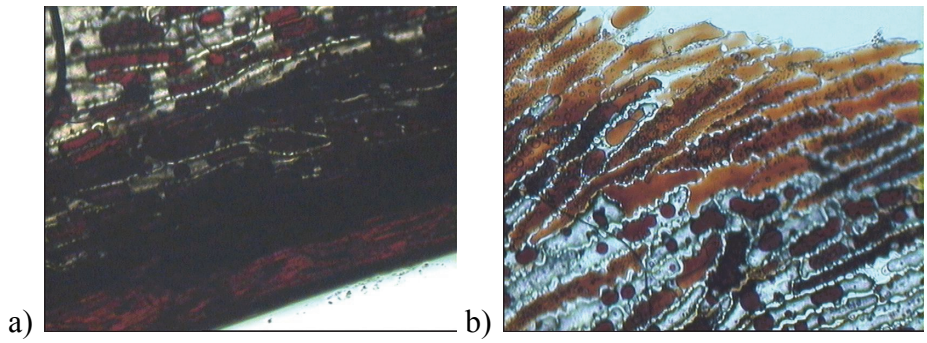

Fig. 1. View of cells along the edge of a Scots pine (*Pinus sylvestris* L.) wing, x100 magnification: a – inner edge, b – outer edge
Rys. 1. Widok krawędzi z komórkami skrzydełka sosny zwyczajnej (*Pinus sylvestris* L.) w powiększeniu x100: a – wewnętrznej, b – zewnętrznej

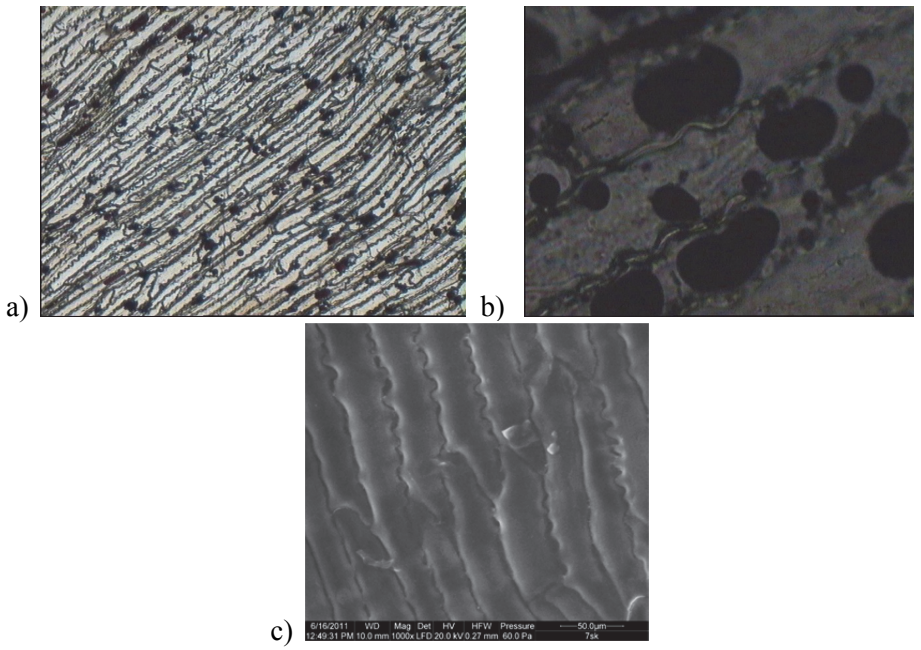

Fig. 2. View of cells in the central part of a Scots pine (*Pinus sylvestris* L.) wing: a – x40 magnification, b – x400 magnification under a light microscope, c – x1000 magnification under SEM
Rys. 2. Widok komórek skrzydełka sosny zwyczajnej (Pinus sylvestris L.) ze środkowej części: a – powiększenie x40, b – powiększenie x400 na mikroskopie świetlnym, c – na mikroskopie skaningowym (powiększenie x1000)

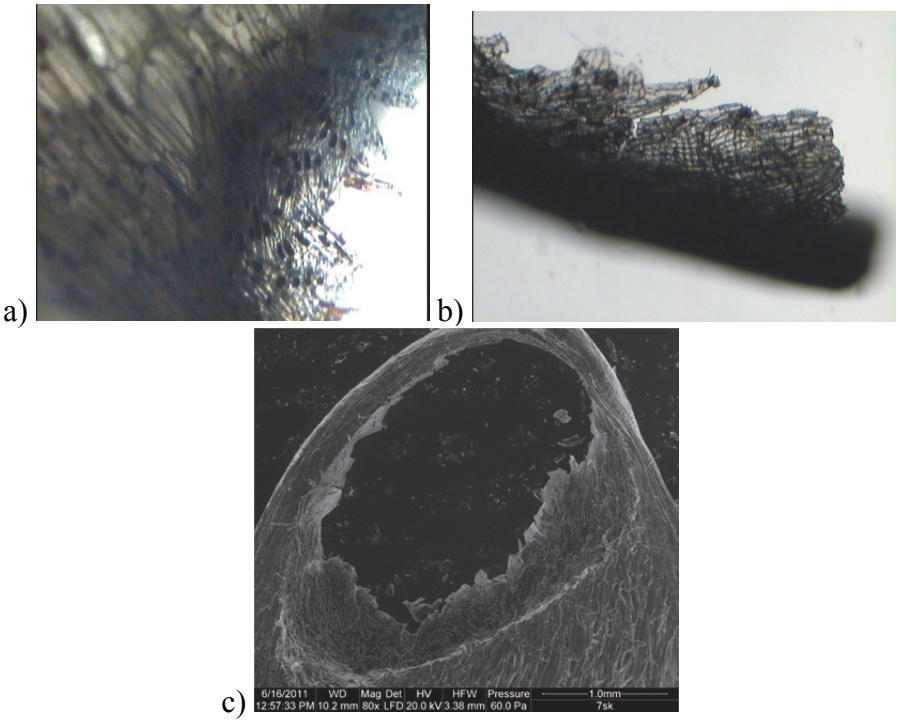

Fig. 3. The point of connection between a Scots pine (*Pinus sylvestris* L.) wing and seed (x40): a – in the central part, b – along the edge, viewed under a light microscope, c – whole, x80, viewed under SEM
Rys. 3. Miejsce połączenia skrzydełka sosny zwyczajnej (*Pinus sylvestris* L.) z nasieniem (powiększenie x40): a – w środkowej części, b – u brzegu kleszczowego zakończenia z mikroskopu świetlnego, c – całe, z mikroskopu skaningowego (powiększenie x80)

Cells with ribbed walls in the central part of the wing change shape at the place of contact with the seed. Several layers of jagged cells with variously shaped cross-sections and thin walls are visible (Fig. 3).

Norway spruce (Picea abies* H. Karst.) *wings

Similarly to a Scots pine wing, a Norway spruce wing also has an inner edge and an outer edge. The inner edge is straight (Fig. 4a), and it comprises regularly shaped cells. The outer edge is convex and jagged (Fig. 4b), and it is composed of irregularly shaped cells.

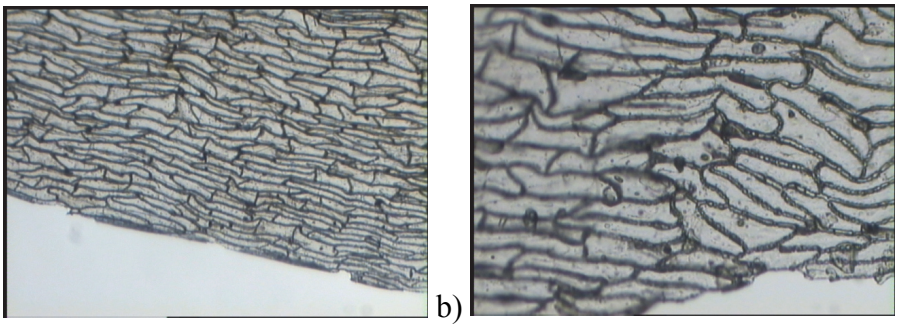

Fig. 4. Edges of a Norway spruce (*Picea abies* H. Karst.) wing: a – inner edge (x40), b – outer edge (x100)
Rys. 4. Krawędzie skrzydełka świerka pospolitego (Picea abies H. Karst.): a – wewnętrzna (x40), b – zewnętrzna (x100)

Cells at the tip and in the central part of the wing are lightly colored in various hues of yellow. Unlike the cells in Scots pine wings, they do not contain brown bodies.

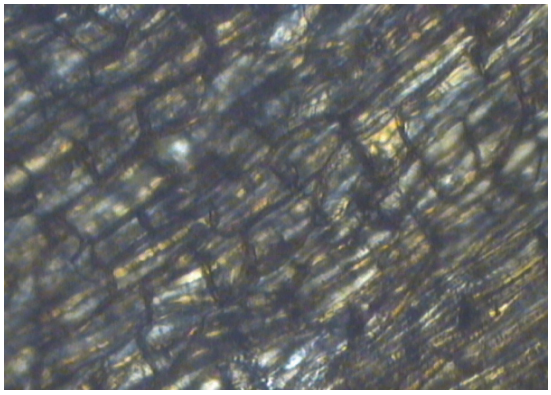

Fig. 5. View of a Norway spruce (*Picea abies* H. Karst.) wing under the seed (x100)
Rys. 5. Widok skrzydełka świerka pospolitego (*Picea abies* H. Karst.) pod nasieniem (x100)

Cells in the part of the wing that supports the seed (in the Norway spruce, the wing encapsulates the seed on one side only) are brown.

4.2. Cell size in Scots pine (*Pinus sylvestris* L.) and Norway spruce (*Picea abies* H. Karst.) wings

Cell parameters (mean, minimum and maximum cell length, cell width, cell wall thickness, cell area and perimeter) measured in the longitudinal section of pine and spruce wings are presented in Tables 1 and 2.

The cells in Scots pine wings had the average length of 305 μm, width of 28 μm, surface area of 8434 μm^2, and perimeter of 704 μm. Brown bodies were differently sized. In the outer (convex) part of the wing, brown bodies filled nearly the entire cell, and their average area was determined at 4759 μm^2. In inner and central segments of the wing, brown bodies were nearly seven-fold smaller (654 μm^2). Some brown bodies adhered to cell walls, and their area was estimated at 65 μm^2.

The analysis of variance confirmed an absence of significant differences in cell width between Scots pine and Norway spruce wings ($F_{(2,52)}$=1.57; p=0.218). Significant differences between Scots pine and Norway spruce were noted with respect to cell length ($F_{(2,46)}$=30.66; p<0.001), cell thickness ($F_{(2,47)}$=20.98; p<0.001), cell area ($F_{(2,69)}$=79.95; p<0.001) and perimeter ($F_{(2.68)}$=86.89; p<0.001)

The cells from outer and inner segments of Norway spruce wings were smaller than the cells from the central part, which is why they were analyzed separately. Their mean length was determined at 127 μm, and width – at 25 μm. Cells from the central part of the wing had the estimated length of 200 μm and width of more than 28 μm. Brown bodies were not observed inside spruce cells. Cell walls were 35% thicker in spruce than in pine wings.

The measured cell parameters were subjected to analysis of variance which did not reveal significant differences in the width of cells distributed in the center and in inner/outer segments of the wing ($F_{(1,15)}$=3.31; p=0.0890). Significant differences were observed in cell length ($F_{(1,15)}$=14.57; p=0.0017), wall thickness ($F_{(1,15)}$=4.91; p=0.0426), cell area ($F_{(1,15)}$=17.60; p=0.0008) and cell perimeter ($F_{(1,15)}$=13.68; p=0.0021), subject to location.

In the cross-section, the average thickness of pine wings (Fig. 6) was determined at 14.23 μm, whereas the thickness of spruce wings was nearly 4 μm smaller (Table 3). Wing cells observed in the cross-section formed a single layer with average lumen of 219 μm in pine and 149 μm in spruce.

Table 1. Cell parameters of Scots pine (*Pinus sylvestris* L.) wings in the longitudinal section (Statistica v. 12)
Tabela 1. Parametry wielkościowe komórek skrzydełek sosny zwyczajnej (*Pinus sylvestris* L.) na przekroju podłużnym (Statistica v. 12)

Parameter	Cell width	Cell length	Cell wall thickness	Cell perimeter	Cell area	Area of brown bodies in cells in wing sections:		
						outer	inner	central
	µm				µm^2			
m	27.81	305.08	3.68	703.54	8433.65	4759.24	654.21	64.66
Me	28.12	293.43	3.70	684.32	8617.24	3977.38	680.28	56.46
Min	15.01	129.65	2.27	387.49	3629.29	1355.39	147.68	38.70
Max	36.86	534.08	5.67	1007.12	12733.23	8266.81	1469.83	107.00
SD^2	29.6	8775.2	1.0	24507.0	5579412.0	7532146.0	64289.9	883.8
SD	5.440	93.676	0.992	156.547	2362.078	2744.476	253.555	29.729
V	19.56	30.71	26.96	22.25	28.01	57.67	38.76	45.98
SE	1.047	18.735	0.216	29.585	446.391	1037.314	39.599	14.864
SK E	-0.30	0.30	0.37	0.15	0.00	0.07	0.52	1.42
K	-0.04	0.49	-0.65	-0.38	-0.66	-1.91	1.56	2.29

Table 2. Cell parameters of Norway spruce (*Picea abies* H. Karst) wings in the longitudinal section
Tabela 2. Parametry wielkościowe komórek skrzydełek świerka pospolitego (*Picea abies* H. Karst.) na przekroju podłużnym

Parameter	Wing section									
	Outer and inner					Central				
	Width	Length	Wall thickness	Area	Perimeter	Width	Length	Wall thickness	Area	Perimeter
	µm			µm^2	µm	µm			µm^2	µm
m	24.91	126.74	5.63	2699.63	313.86	28.12	199.36	4.51	5143.53	439.36
Me	25.49	117.07	5.93	2635.95	303.8	27.97	205.67	4.37	4837.97	442.41
Min	16.60	88.57	3.70	1634.36	236.13	20.94	93.66	3.90	2892.31	278.79
Max	33.00	250.57	7.18	4466.71	408.46	34.4	269.62	5.23	7323.35	609.84
SD^2	26.20	1279.60	1.20	646439.20	2734.50	19.00	4227.00	0.00	1802260.00	6291.00
SD	5.11	35.77	1.08	804.02	52.29	4.40	65.01	0.49	1342.48	79.32
V	20.53	28.23	19.18	29.78	16.66	15.66	32.61	10.84	26.10	18.05
SE	1.542	8.432	0.248	154.733	10.255	1.068	26.542	0.155	325.600	19.237
SK E	-0.13	2.59	-0.50	0.45	0.27	-0.24	-0.73	0.43	0.22	0.14
K	-0.84	8.66	-0.86	-0.80	-1.21	-1.26	0.16	-1.26	-0.76	0.56

Table 3. Cell parameters of Scots pine (*Pinus sylvestris* L.) and Norway spruce (*Picea abies* H. Karst.) wings in the cross-section
Tabela 3. Parametry wielkościowe skrzydełka sosny zwyczajnej (*Pinus sylvestris* L.) i świerka pospolitego (*Picea abies* H. Karst.) w przekroju poprzecznym

Parameter	**Species**	***m***	***Me***	**Min**	**Max**	***SD*^{2}**	***SD***	***V***	***SE***	***SK E***	***K***
Thickness [µm]	P	14.23	13.98	9.92	19.59	5.44	2.33	16.40	0.344	0.36	-0.44
	S	10.06	10.02	2.32	14.75	7.38	2.72	27.01	0.430	-0.32	0.56
Cell lumen [µm^2]	P	218.94	208.55	145.07	314.97	3208.93	56.65	25.87	20.028	0.70	-0.24
	S	149.34	141.56	49.52	241.05	3752.89	61.26	41.02	20.420	0.30	0.09

a) 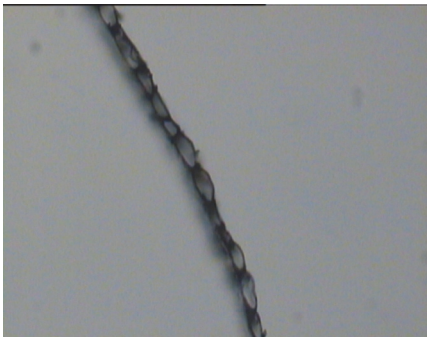 b) 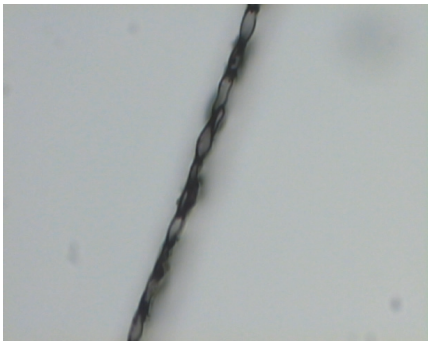

Fig. 6. Wings in the cross-section: a – Scots pine (*Pinus sylvestris* L.), b – Norway spruce (*Picea abies* H. Karst.)
Rys. 6. Skrzydełka w przekroju poprzecznym: a – sosny zwyczajnej (*Pinus sylvestris* L.), b – świerka pospolitego (*Picea abies* H. Karst.)

The analysis of variance confirmed significant differences in wing thickness ($F_{(1,84)}$=58.67; $p<0.001$) and cell lumen ($F_{(1,15)}$=5.86; $p=0.0286$) between the analyzed species.

4.3. Chemical composition of Scots pine (*Pinus sylvestris* L.) and Norway spruce (*Picea abies* H. Karst.) wings

The chemical analysis revealed differences in the composition of Scots pine and Norway spruce wings. The equilibrium moisture content of wings ranged from 10% to 11%, and in wood, this parameter is generally determined at 6% to 7% under identical conditions. The above difference can be attributed to the high content of extractive compounds in wings. At the drying temperature of 105°C, water and extractives evaporate from wings, and the same process is observed in pine wood. The resulting loss of mass increases the absolute moisture content of the analyzed material. The content of extractive substances was three times lower in pine wings (4.6%) than in spruce wings (14.5%). The content of structural compounds, i.e. cellulose, lignin and hemicellulose, varied between species. Pine wings contained more cellulose and holocellulose, but less lignin than spruce wings. Lignin concentration was higher in spruce wings. A two-fold difference in the content of substances soluble in 1% NaOH was also noted. The hemicellulose content, which can be theoretically determined from the difference in cellulose and holocellulose content, was similar in both species. The two-fold difference in

the content of substances that are soluble in 1% NaOH can be attributed to much higher concentrations of extractive substances (by around 10%) in spruce than in pine. Both species were characterized by relatively low ash content that did not exceed 2% (Figure 7).

The chemical composition analysis revealed that pine and spruce wings contained less cellulose, but significantly more lignin and extractive substances than pine and spruce wood (Sjöström 1993).

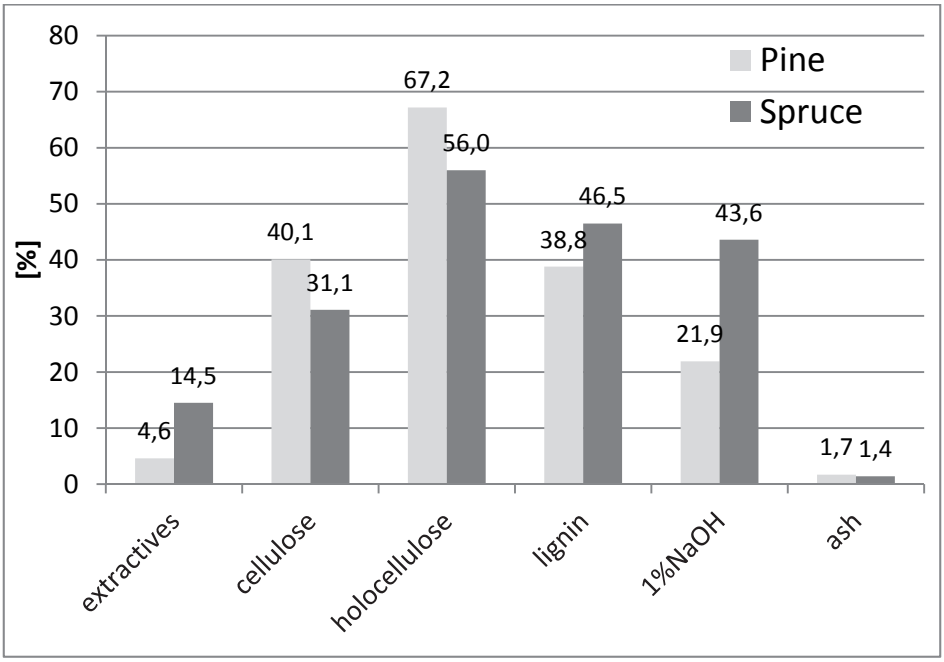

Fig. 7. Chemical composion of Scots pine (*Pinus sylvestris* L.) and Norway spruce (*Picea abies* H. Karst.) wings
Rys. 7. Skład chemiczny skrzydełek sosny zwyczajnej (*Pinus sylvestris* L.) I świerka pospolitego (*Picea abies* H. Karst.)

In wood, heat of combustion is determined by moisture content and composition, including the content of polysaccharides, lignin and extractive substances. The heat of combustion of structural and non-structural wood components was calculated by many authors. This parameter was determined at 17.3 $MJ \cdot kg^{-1}$ in cellulose and 27.7 $MJ \cdot kg^{-1}$ in lignin (Rowell 2012). Coniferous lignin has a different structure, and its

heat of combustion is 23.5 MJ·kg^{-1} (Bulk & Jenkins 2000). The highest heat of combustion in the range of 34.89 to 37.22 MJ·kg^{-1} was noted in coniferous extractives (Howard 1973).

Formula (2) was used to calculate the calorific value of wings based on their chemical composition. Calorific value was determined at 19.72 MJ·kg^{-1} for pine wings and at 22.01 MJ·kg^{-1} for spruce wings.

In a study by Font et al. (2009), the calorific value of pine needles and cones was calculated at 20.14 MJ·kg^{-1} and 18.78 MJ·kg^{-1}, respectively.

4.4. Heat of combustion and calorific value of Scots pine (*Pinus sylvestris* L.) and Norway spruce (*Picea abies* H. Karst.) wings and empty seeds

The carbon content of pine and spruce seeds was 45.19% (Table 4), and it was somewhat higher in wings (49.09%-49.15%). Hydrogen concentrations were similar in seeds and wings (5.72%-5.79%), and they were lower than in coniferous wood (6.3%) examined by Munalula & Martin (2009) and Reva et al. (2012). Frank & Cox (2009) determined carbon and hydrogen levels in the seeds of selected species of coniferous trees: Apache pine (*Pinus engelmannii*) – C 58.7%, H 8%, white fir (*Abies concolor*) – C 60.6%, H 8.2%, and the subalpine fir (*Abies lasiocarpa*) – C 63.1%, H 9.2%. According to the cited authors, the carbon and hydrogen content of coniferous seeds decreases during storage.

Seeds were significantly more abundant in nitrogen (2.62%) than wings (0.57%-0.59%). Plant seeds, including the seeds of coniferous trees, are generally rich in protein (Gifford 1988), which explains the higher content of nitrogen. Sulfur content was determined at 0.218%-0.315%. This parameter is generally lower in cones (Brebu et al. 2010, Font et al. 2009). Similarly to nitrogen, sulfur may be derived from seed proteins. In the elemental analysis conducted by Brebu et al. (2010), pine seeds contained 42.62% C, 5.56% H, 0.76% N and 0.05% S.

The heat of combustion and calorific value of pine and spruce wings and seeds are presented in Table 5. The mean heat of combustion was determined at 20.57 MJ·kg^{-1} in pine wings (19.75 to 22.10 MJ·kg^{-1}), 20.38 MJ·kg^{-1} in spruce wings (20.04 to 20.79 MJ·kg^{-1}) and 20.69 MJ·kg^{-1} in empty seeds (19.94 to 21.08 MJ·kg^{-1}).

Table 4. Elemental composition of samples
Tabela 4. Zawartość pierwiastków w badanych próbkach

Sample	C	H	N	S
	[%]			
Spruce wings	49.09	5.74	0.59	0.273
Pine/spruce seeds	45.19	5.79	2.62	0.315
Pine wings	49.15	5.72	0.57	0.218

In dry material, heat of combustion is higher than its calorific value by the amount of heat required to evaporate water from hydrogen combustion (Krzysik 1974). For this reason, the calorific value of all wings and seeds was lower than their heat of combustion. Calorific value was used in successive analyses as a parameter which has greater practical significance and is generally used to determine the energy efficiency of fuels.

In view of the general scarcity of published information about the calorific value of pine and spruce wings and empty seeds, the obtained values were compared with the calorific value of wood. According to the literature, pine wood has calorific value of 19.2-21.2 $MJ \cdot kg^{-1}$ and spruce wood – 18.8-20.5 $MJ \cdot kg^{-1}$ (Günther et al. 2009, Haufa & Wojciechowska 1986, Komorowicz et al. 2009, Krzysik 1974, Lu et al. 2009, Monkielewicz & Pflaum 1967, Rembowski 2007, Reva et al. 2012, So & Eberhardt 2013, Stolarski et al. 2013, Uri et al. 2015).

The mean calorific value of pine wings was determined at 19.38 $MJ \cdot kg^{-1}$ (18.57 to 20.91 $MJ \cdot kg^{-1}$), and it was 0.18 $MJ \cdot kg^{-1}$ (0.93%) higher than the minimal value and 1.82 $MJ \cdot kg^{-1}$ (8.58%) lower than the maximum value for pine wood.

The mean calorific value of spruce wings was determined at 19.20 $MJ \cdot kg^{-1}$ (18.86-19.62 $MJ \cdot kg^{-1}$), and it was 0.40 $MJ \cdot kg^{-1}$ (2.08%) higher than the minimal value and 1.30 $MJ \cdot kg^{-1}$ (6.34%) lower than the maximum value for spruce wood.

The mean calorific value of empty pine and spruce seeds was 19.49 $MJ \cdot kg^{-1}$ (18.75-19.89 $MJ \cdot kg^{-1}$), and it was 0.69 $MJ \cdot kg^{-1}$ (3.54%) higher than the minimal value for spruce wood and 1.71 $MJ \cdot kg^{-1}$ (8.07%) lower than the maximum value for pine wood.

The mean calorific value of all samples was 19.36 $MJ \cdot kg^{-1}$, and it was 0.56 $MJ \cdot kg^{-1}$ (2.89%) higher than the minimal value for spruce wood and 1.84 $MJ \cdot kg^{-1}$ (8.68%) lower than the maximum value for pine wood. In all cases, the results were closer to the minimum values reported in the literature for a given tree species.

The statistical analyzes presented in Table 5 for calorific value and combustion heat indicate high accuracy of measurement and reproducibility (max. SE = 0.23).

The calorific value of pine wings was 1.72% lower and the calorific value of spruce wings was 12.77% lower in comparison with the empirical values determined based on formula (2).

The analysis of variance ($F_{(2,28)}$=1.05; p=0.36) revealed an absence of significant differences in the calorific value of the examined residues, which implies that the analyzed material was homogeneous in this respect (Stat Soft, Inc. 2014; Luszniewicz & Słaby 2008; Rabiej 2012).

According to Aniszewska (2012), extraction residues such as wings and empty seeds account for approximately 0.5% of husked material. In 2009-2012, the total production of cones from four species of forest trees (Scots pine, Norway spruce, European larch and silver fir) reached 1432.3 Mg in Poland (Aniszewska & Kuszpit 2015). Therefore, the mean annual production of cones for seed husking was 35.8 Mg, including around 1.79 Mg of extraction residues that are suitable for energy generation. The total calorific value is estimated 34.46 GJ, and that energy can be used to heat drying cabinets or residential buildings. The energy obtained from the combustion of extraction residues would be sufficient to heat a residential building with a floor area of 100 m^2, standard insulation and energy use intensity of 100 $W \cdot m^{-2}$ for 39-40 days.

Table 5. Heat of combustion and calorific value of Scots pine (*Pinus sylvestris* L.) and Norway spruce (*Picea abies* H. Karst.) wings and empty seeds – descriptive statistics (Stat Soft Inc. 2014)
Tabela 5. Ciepło spalania, wartość opałowa skrzydełek sosny zwyczajnej (*Pinus sylvestris* L.) i świerka pospolitego (*Picea abies* H. Karst.) oraz mieszanki pustych nasion – statystyki opisowe (Stat Soft, Inc. 2014)

Material	*m*	+95% *m*	-95% *m*	Min	Max	SD^2	*SD*	*V*	*SE*	*SK E*	*K*
Heat of combustion [MJ·kg^{-1}]											
Pine wings	20.57	20.05	21.08	19.75	22.10	0.52	0.72	3.50	0.23	1.06	0.98
Empty seeds	20.69	20.48	20.89	19.94	21.08	0.10	0.31	1.49	0.09	-1.33	2.82
Spruce wings	20.38	20.19	20.56	20.04	20.79	0.07	0.26	1.26	0.08	0.23	-1.13
Total	**20.55**	**20.37**	**20.72**	**19.75**	**22.10**	**0.22**	**0.47**	**2.30**	**0.08**	**0.97**	**2.53**
Calorific value [MJ·kg^{-1}]											
Pine wings	19.38	18.87	19.90	18.57	20.91	0.51	0.72	3.69	0.23	1.05	0.97
Empty seeds	19.49	19.29	19.70	18.75	19.89	0.10	0.31	1.58	0.09	-1.29	2.71
Spruce wings	19.20	19.01	19.38	18.86	19.62	0.07	0.26	1.35	0.08	0.24	-1.12
Total	**19.36**	**19.19**	**19.54**	**18.57**	**20.91**	**0.22**	**0.47**	**2.43**	**0.08**	**0.98**	**2.56**

It should be noted that seed wings are very light, which implies high transportation costs. For this reason, the preferred solution would be to burn extraction residues locally in a seed extraction plant.

The macroelement and microelement content of pine and spruce seeds and wings are presented in Table 6. Mercury (Hg) is the most toxic heavy metal. Plants absorb mercury from soil via the root system or directly from air. The analyzed seeds and wings were characterized by low mercury levels which ranged from 0.0015 to 0.0032 $mg \cdot kg^{-1}$. The concentration of cadmium (Cd) in the mixture of pine and spruce seeds was determined at 1.607 (±0.016) $mg \cdot kg^{-1}$. Cadmium content was higher in wings at 1.866 (±0.103) $mg \cdot kg^{-1}$ (pine) and 2.600 (±0.032) $mg \cdot kg^{-1}$ (spruce). Cadmium is not a microelement, and excessive cadmium levels in seeds can lead to genomic changes (Prus-Głowacki et al. 2006, Stvolinskaya 2000). Similarly to cadmium, lead does not demonstrate biological activity. The described metals can disrupt plant metabolism and limit the uptake of other elements (Kabata-Pendias & Pendias 1999). Lead concentrations of 30-300 $mg \cdot kg^{-1}$ exert toxic effects on plants (Mandre & Ots 2012). In this study, the lead content of pine and spruce seeds was below 1 $mg \cdot kg^{-1}$. Similar results were reported by Ganatsasa et al. (<1 $mg \cdot kg^{-1}$) who did not observe excessive Pb levels in the seeds of pine trees growing at various distance from roads. Cadmium and lead concentrations are generally higher in the roots, wood and bark of coniferous trees (Schulz et al. 1999, Coşkun 2006, Nkongolo et al. 2008). In this study, the lead content of wings was determined at 6.75 (±0.179) $mg \cdot kg^{-1}$ (pine) and 1.88 (±0.067) $mg \cdot kg^{-1}$ (spruce), and it was higher than in seeds. Those differences could be attributed to the large area of wings capable of absorbing lead-containing dust.

Table 6. Elemental composition of Scots pine (*Pinus sylvestris* L.) and Norway spruce (*Picea abies* H. Karst.) wings and empty seeds [mg·kg^{-1} DM]
Tabela 6. Zawartość pierwiastków w skrzydełkach sosny zwyczajnej (*Pinus sylvestris* L.) i świerka pospolitego (*Picea abies* H. Karst.) oraz w pustych nasionach [mg·kg^{-1} s.m.]

	Pine wings				**Empty seeds**				**Spruce wings**				**GO**$^{*)}$	**u**$^{*)}$
	m	***SD***	***V***	***SE***	***m***	***SD***	***V***	***SE***	***m***	***SD***	***V***	***SE***		
Cd	1.87	0.10	5.51	0.06	1.61	0.02	0.97	0.01	2.60	0.03	1.24	0.02	0.5	10
Pb	6.75	0.18	2.66	0.10	0.56	0.27	48.57	0.16	1.88	0.07	3.56	0.04	1	10
Cu	3.84	0.25	6.55	0.15	9.93	0.06	0.59	0.03	3.75	0.15	3.92	0.08	1	20
Zn	42.23	0.88	2.09	0.51	83.43	1.23	1.48	0.71	33.59	1.55	4.61	0.89	1	20
Ni	3.27	0.13	3.93	0.07	13.16	0.31	2.36	0.18	3.66	0.12	3.26	0.07	1	20
Cr	0.50	0.08	15.52	0.04	8.27	0.15	1.79	0.09	0.58	0.15	25.22	0.09	1	10
Mo	1.12	0.48	42.98	0.28	33.03	2.24	6.77	1.29	0.82	0.23	28.23	0.13	2	15
Co	1.07	0.08	7.41	0.05	1.34	0.08	6.31	0.05	0.50	0.36	73.43	0.21	1	10
Fe	124.13	3.10	2.50	1.79	1130.33	30.92	2.74	17.85	22.00	1.71	7.78	0.99	2	15
Mn	39.20	1.07	2.73	0.62	65.40	2.76	4.22	1.59	12.49	0.81	6.46	0.47	1	10
Ca	992.33	7.02	0.71	4.06	1603.33	60.28	3.76	34.80	1059.67	60.87	5.74	35.14	2.5	13
Mg	1523.33	75.06	4.93	43.33	1226.67	60.28	4.91	34.80	950.47	23.09	2.43	13.33	2.5	10
K	2029.00	101.43	5.00	58.56	2062.00	52.12	2.53	30.09	3416.00	114.94	3.36	66.36	0.2	8
Na	132.33	10.69	8.08	6.17	91.03	1.38	1.52	0.80	127.01	2.16	1.70	1.25	0.2	10
Hg	0.0032	0.0003	8.27	0.0002	0.0028	0.0002	6.19	0.0001	0.0015	0.0002	13.33	0.0001	0.0007	15

*) limit of detection (*LOD*) and uncertainty (*u*) at k = 2 and α=0.95.

Copper is a microelement that influences enzymatic processes in plants, including photosynthesis. Copper and iron deficiencies lead to yellowing of needles, death of side shoots and inhibited seedling growth. However, coniferous trees are resistant to high environmental levels of Cu. Pine is a hyperaccumulator of Cu in strongly polluted environments (Kirchner et al. 2008). In this study, the copper content of pine and spruce seeds was determined at 9.93 (±0.059) $mg \cdot kg^{-1}$. In the work of Ganatsasa et al. (2011), copper levels in pine seeds reached 8.36-11.21 mg/kg, whereas Cheikh-Rouhou et al. (2006) determined the copper content of Aleppo pine (*Pinus halepensis*) seeds at 22.5 $mg \cdot kg^{-1}$. In this study, copper concentrations were much lower in wings at 3.84 (±0.25) $mg \cdot kg^{-1}$ (pine) and 3.75 (±0.147) $mg \cdot kg^{-1}$ (spruce). Zinc is a ubiquitous element with low toxicity, and excessive zinc levels in soil do not inhibit plant growth. This microelement is a component of plant growth regulators, mostly auxins and indoleacetic acid (IAA), and it participates in enzymatic reactions (Kabata-Pendias & Pendias 1999). The analyzed pine and spruce seeds contained 83.4 (±1.2) $mg \cdot kg^{-1}$ of zinc, whereas the zinc content of wings was significantly lower (33.6-42.2 $mg \cdot kg^{-1}$). Cheikh-Rouhou et al. (2006) determined the Zn content of pine seeds at 134.9 $mg \cdot kg^{-1}$. Nickel is used as a cofactor by numerous enzymes, and it affects nitrogen metabolism in plants (Kabata-Pendias & Pendias 1999). Plants have a low demand for this element. Similarly to Cd and Pb, excessive levels of Ni can inhibit growth and induce genomic changes in seeds (Kabata-Pendias 1999, Prus-Głowacki et al. 2006, Stvilinskaya 2000). Pines can act as hyperaccumulators of Ni in strongly polluted environments (Kirchner et al. 2008). In this study, the nickel content of pine and spruce seeds was determined at 13.16 (±0.31) $mg \cdot kg^{-1}$, and wings were significantly less abundant in this metal (3.27-3.66 $mg \cdot kg^{-1}$). Chromium is also an important plant microelement. Chromium levels reached 8.27 (±0.15) $mg \cdot kg^{-1}$ in pine and spruce seeds, but did not exceed LOD in wings (<1 $mg \cdot kg^{-1}$). Molybdenum is a component of nitrogen metabolizing enzymes (Kabata-Pendias & Pendias 1999), and its deficiency can compromise the quality of seeds. The Mo content of pine and spruce seeds was determined at 33.0 (±2.2) $mg \cdot kg^{-1}$ in pine and spruce seeds, and it was below LOD in wings (<2 $mg \cdot kg^{-1}$). Cobalt is not an essential microelement for most plants (Greinert 2011),

and its concentrations were determined at 1.337 (±0.084) mg·kg^{-1} in pine and spruce seeds, 1.072 (±0.079) mg·kg^{-1} in pine wings, and below 1 mg/kg in spruce wings. Iron plays a host of important roles in plants. It is involved in enzymatic reactions, it controls nitrogen metabolism and influences photosynthetic processes (Kabata-Pendias & Pendias 1999). Pine and spruce seeds contained 1130 (±31) mg·kg^{-1} of iron, whereas wings were significantly less abundant in this element at 124 (±3) mg·kg^{-1} (pine) and 22 (±2) mg·kg^{-1} (spruce). The iron content of pine seeds was determined at 271 mg·kg^{-1} by Cheikh-Rouhou et al. (2006) and at 94.38-135.05 mg·kg^{-1} by Ganatsasa et al. (2011). Manganese and calcium are iron antagonists in plant tissues (Kabata-Pendias & Pendias 1999, Mandre & Ots 2012). Similarly to iron, manganese participates in photosynthesis and is a component of many enzymes (Kabata-Pendias & Pendias 1999). Manganese concentrations were determined at 65.4 (±2.8) mg·kg^{-1} in seeds and 12.5-39.2 mg·kg^{-1} in wings. The manganese content of pine seeds was determined at 22.68-37.78 mg·kg^{-1} by Ganatsasa et al. (2011) and at 51.3 mg·kg^{-1} by Cheikh-Rouhou et al. (2006).

Light metals such as Ca, Mg, K and Na are macroelements essential for plant growth and development. According to Zhan et al. (2014), their concentrations in wood, bark and green parts of plants are influenced by seeding rate, which can also affect the content of those macroelements in seeds and wings. The examined seeds were most abundant in potassium, followed by calcium, magnesium and sodium. Cheikh-Rouhou et al. (2006) also reported high levels of essential macronutrients in the seeds of the Aleppo pine (*Pinus halepensis*). In their study, the predominant element was K (6171 mg·kg^{-1}), followed by Mg (3303 mg·kg^{-1}), Ca (1167 mg·kg^{-1}) and Na (69.6 mg·kg^{-1}). Sukhdolgor et al. (2003) also noted the highest levels of magnesium and calcium in Scots pine seeds. The predominant heavy metal was manganese, followed by copper, zinc and iron. The content of Ni, Cr, Mo and Pb was 10- to 100-fold lower in comparison with the above metals.

5. Conclusions

Biomonitoring is an essential part of environmental protection and resource management programs. The threats and potential outcomes of resource management projects have to be continuously monitored in

protected areas. Biomonitoring schemes are obligatory under the provisions of Polish and EU laws. Changes in ecosystems can be evaluated with the use of bioindicators, including seed extraction residues. This paper describes selected physicochemical parameters of extraction residues based on the results of microscopic and chemical analyses. Morphological differences were noted between the wings of Scots pine (*Pinus sylvestris* L.) and Norway spruce (*Picea abies* H. Karst.) seeds. Microscopic observations revealed that pine and spruce wings were composed of variously sized cells with different wall thickness. The cells in pine wings were longer and larger than the cells in spruce wings. Spruce cells had thicker walls, which contributed to greater rigidity and overall strength of spruce wings. The results of chemical analyses demonstrated that spruce wings contained 8% more lignin and 9% less cellulose than pine wings. The observed differences in the chemical composition of pine and spruce wings did not affect their calorific value. The cellulose content of pine wings is generally similar to the amount of cellulose found in pine cones, and it was determined at 39.3% by Font et al. (2009) and at 40.1% in this study. The lignin content of pine wings was 8% lower in comparison with the published data.

The heat of combustion and the calorific value of pine and spruce wings and empty seeds did not differ significantly and were determined at 19.25 $MJ \cdot kg^{-1}$ on average. The mean results noted in this study were within the range determined by various authors for pine and spruce wood, but they were only 0.36-3.14% higher than the minimum values.

Pine and spruce wings differed in color. Pine wings were darker along the edges, but they contained 10% less extractive substances and 21% less compounds soluble in NaOH than spruce wings. Spruce wings were lighter along the edges and in the center, but they were visibly darker under the seed (due to morphological differences, this part is not present in pine wings). The above segment of spruce wings probably has a high content of the analyzed chemical compounds.

Heavy metal concentrations were higher in seeds than in wings of the analyzed tree species. The only exception was lead. Contamination with lead could be attributed to the deposition of lead-containing dust on the surface of wings. The content of heavy metals in the examined seeds should not have adverse environmental effects, and it was similar to that

reported by other authors. The evaluated seeds were abundant in potassium, calcium and magnesium.

Wings and empty seeds separated from fully developed seeds in the cleaning process can be used for energy generation. In Poland, the annual production of seed extraction residues is estimated at 1790 kg, which would be sufficient to heat a medium-sized home for 40 days. However, seed wings are very light, which considerably increases transportation costs. For this reason, wings should be burned locally in a husking plant or added to pellets containing other types of biomass.

Abbreviations

Ext – content of extractive substances,
F – Fisher's F-test,
LOD – limit of detection,
H – hydrogen content, %,
K – coefficient of kurtosis,
L – content of Klason lignin relative to dry matter content of wood after extraction,
Me – median,
Q_{ne} – calorific value of wood before extraction, $MJ \cdot kg^{-1}$,
Q_{op} – calorific value, $MJ \cdot kg^{-1}$,
Q_s – heat of combustion, $MJ \cdot kg^{-1}$,
SD – standard deviation,
SD^2 – sample variance,
SE – standard error,
SK E – coefficient of skewness,
V – coefficient of variation,
W_w – relative moisture content, %,
m – mean,
p – probability at α=0.05,
u – uncertainty.

References

Aniszewska, M. (2012). *Dynamika procesu pozyskania nasion w jedno- i dwuetapowych procesach łuszczenia szyszek sosny zwyczajnej Pinus sylvestris L.* Warszawa: Wydawnictwo SGGW.

Aniszewska, M., & Gendek, A. (2014). Comparison of heat of combustion and calorific value of the cones and wood of selected forest tree species. *Forest Research Papers*, *75(3)*, 231-236.

Aniszewska, M., & Gendek, A. (2016a). Logistics of the supplies of selected forest tree species' cones. Part 1. Cone density and substitution coefficient. *Ann. Warsaw Univ. Life Sci. – SGGW, Agricult., 67*, 121-130.

Aniszewska, M., & Gendek, A. (2016b). Logistics of delivery of cones of selected species of forest trees. Part 2: Cone transport. *Ann. Warsaw Univ. Life Sci. – SGGW, Agricult., 68*, 113-121.

Aniszewska, M., & Kuszpit, D. (2015). Analysis of acquisition and potential usage of conifer cones from Polish seed extraction houses between 2009-2012. *Ann. Warsaw Univ. Life Sci. – SGGW, Agricult., 65*, 93-101.

Antczak, A., Radomski, A., & Zawadzki, J. (2006). Benzene Substitution in Wood Analysis. *Ann. WULS – SGGW, For. and Wood Technol., 58*, 15-19.

Argum, M.E, Dursun, S.,& Karatas, M. (2009). Removal of Cd(II), Pb(II), Cu(II) and Ni(II) from water using modified pine bark. *Desalination, 249(2)*, 519-527.

Białobok, S., Boratyński, A., & Bugała, W. (1993). *Biologia sosny zwyczajnej*. Polska Akademia Nauk Instytut Dendrologii. Poznań-Kórnik: Wydawnictwo Sorus.

Budzianowski, W. (2012). Sustainable biogas energy in Poland: Prospects and challenges. *Renewable and Sustainable Energy Reviews*, *16(1)*, 342-349.

Budzianowski, W. (2012). Target for national carbon intensity of energy by 2050: A case study of Poland's energy system. *Energy*, *46(1)*, 575-581.

Bunse, K., Vodicka, M., Schönsleben, P., Brülhart, M., & Ernst, F.O. (2011). Integrating energy efficiency performance in production management – gap analysis between industrial needs and scientific literature. *Journal of Cleaner Production*, *19*, 667-679.

Brebu, M., Ucar, S., Vasile, C., & Yanik, J. (2010). Co-pyrolysis of pine cone with synthetic polymers. *Fuel*, *89(8)*, 1911-1918.

Bulk, S. L., & Jenkins, B. M. (1999). Combustion properties of lignin residue from lignocellulose fermentation. *National Renewable Energy Laboratory*, *2*, 1385-1391.

Cheikh-Rouhou, S., Hentati, B., Besbes, S., Blecker, C., Deroanne, C., & Attia, H. (2006). Chemical composition and lipid fraction characteristics of Aleppo Pine (*Pinus halepensis* Mill.) seeds cultivated in Tunisia. *Food Sci Tech Int., 12(5)*, 407-415.

Coşkun, M., (2006). Toxic Metals in the Austrian Pine (Pinus Nigra) Bark in the Thrace Region, Turkey. *Environmental Monitoring and Assessment, 121*,173-178.

Font, R., Conesa, J.A., Molto, J., & Muñoz, M. (2009). Kinetics of pyrolysis and combustion of pine needles and cones. *Journal of Analytical and Applied Pyrolysis, 85(1-2)*, 276-286.

Frank, C.L., & Cox, S.R. (2009). *The adaptive significance of seed hoarding by the Mt. Graham Red Squirrel.* Rozdział monografii: "The Last Refuge of the Mt. Graham Red Squirrel: Ecology of Endangerment" (red.) H. Reed Sanderson, John L. Koprowski, University of Arizona Press, 427, 256-271.

Fuentes, D., Disante, K.B., Valdecantos, A., Cortina, J., & Vallejo, R. (2007). Sensitivity of Mediterranean woody seedlings to copper, nickel and zinc. *Chemosphere*, *66(3)*, 412-420.

Ganatsasa, P., Tsakaldimia, M., & Zachariadis, G. (2011). Effect of air traffic pollution on seed quality characteristics of *Pinus brutia. Environmental and Experimental Botany*, *74*, 157-161.

Gendek, A., Nurek, T. (2016). Variability of energy woodchips and their economic effects. *Folia Forestalia Polonica, Series A, 58(2)*, 62-71.

Gendek, A., & Zychowicz, W. (2014). Investigations on the calorific value of forest chips *Ann. Warsaw Univ. Life Sci. – SGGW, Agricult., 63*, 65-72.

Gendek, A., & Zychowicz, W. (2015). Analysis of wood chippings fractions utilized for energy purposes *Ann. Warsaw Univ. Life Sci. – SGGW, Agricult., 65*, 79-91.

Gdula-Argasińska, J., Appleton, J., Sawicka-Kapusta, K., & Spence, B. (2004). Further investigation of the heavy metal content of the teeth of the bank vole as an exposure indicator of environmental pollution in Poland. *Environmental Pollution*, *1(131)*, 71-79.

Gifford, D.J. (1988). An electrophoretic analysis of the seed proteins from Pinus monticola and eight other species of pine. *Canadian Journal of Botany*, *66(9)*, 1808-1812.

Gołos, P., & Kaliszewski, A. (2015). Aspects of using wood biomass for energy production. *Forest Research Papers*, *76 (1)*, 78-87.

Greinert, A. (2011). Kobalt w środowisku przyrodniczym i antropogenicznym. Zielona Góra: *Uniwersytet Zielonogórski*. DOI: 10.13140/2.1.2292.5764.

Günther, B., Gebauer, K., Barkowski, R., Rosenthal, M., & Bues, C.T. (2012). Calorific value of selected wood species and wood products. *Eur. J. Wood Prod*., *70*, 755-757.

Haufa, T., & Wojciechowska D. (1986). Leśne sortymenty opałowe – jako potencjalne źródło energii cieplnej. *Las Polski*, *20*, 12-14.

Howard, E. T. (1973). Heat of combustion of various southern pine materials. *Wood Science*, *5(3)*, 194-197.

Kabata-Pendias, A., & Pendias, H. (1999). *Biogeochemia pierwiastków śladowych.* Warszawa: PWN.

Kačik, F., & Solár, R. (1999). *Analiticka Chemia Dreva*. *Zvolen: Technicka Univerzita vo Zvolene* [in Slovak].

Karnosky, D. F., Skelly, J. M., Percy, K.E., & Chappelka, A.H. (2007). Perspectives regarding 50 years of research on effects of tropospheric ozone air pollution on US forest. *Environmental Pollution, 3(147)*, 489-506.

Khan, A.G., Kuek, C., Chaudhry, T.M., Khoo, C.S., & Hyes, W.J. (2000). Role of plants, mycorrhizae and phytochelators in heavy metal contaminated land remediation, *Chemosphere*, *41(1-2)*, 197-207.

Kirchner, P, Biondi, F, Edwards, R., & McConnell, J.R. (2008). Variability of trace metal concentrations in Jeffrey pine (*Pinus jeffreyi*) tree rings from the Tahoe Basin, California, USA. *Journal of Forest Research, 13*, 347-356.

Krutul, D. (2002). *Ćwiczenia z chemii drewna oraz wybranych zagadnień chemii organicznej.* Warszawa: Wydawnictwo SGGW.

Komorowicz, M., Wróblewska, H., & Pawłowski, J. (2009). Skład chemiczny i właściwości energetyczne biomasy z wybranych surowców odnawialnych. *Ochrona środowiska i zasobów naturalnych, 40*, 402-410.

Krzysik, F., (1974). *Nauka o drewnie.* Warszawa: PWN.

Leturcq, P. (2014). Wood preservation (carbon sequestration) or wood burning (fossil-fuel substitution), which is better for mitigating climate change? *Annals of Forest Science, 71(2)*, 117-124.

Lu, L., Tang Y., Xie, J., & Yuan, Y. (2009). The role of marginal agricultural land-based mulberry planting in biomass energy production. *Renewable Energy*, *34(7)*, 1789-1794.

Luszniewicz, A., & Słaby, T. (2008). *Statystyka z pakietem komputerowym STATISTICA PL. Teoria i zastosowania.* Warszawa: C.H. Beck.

Munalula, F., & Meincken, M. (2009). An evaluation of South African fuelwood with regards to calorific value and environmental impact. *Biomass and Bioenergy*, *33(3)*, 415-420.

Mandre, M., & Ots, K. (2012). Monitoring of heavy metals uptake and allocation in *Pinus sylvestris* organs in alkalised soil, *Environmental Monitoring and Assessment, 184(7)*, 4105-4117.

Masese, F.O., Kitaka, N., Kipkemboi, J., Gettel, G. M., I. K., & McClain, M.E. (2014). Litter processing and shredder distribution as indicators of riparian and catchment influences on ecological health of tropical streams. *Ecological Indicators, 46*, 23-37.

Monkielewicz, L., & Pflaum H. (1967). *Użytkowanie Lasu.* Warszawa: PWRiL.

Mikłaszewicz, M. (2002). Budowa anatomiczna szyszek świerka. *Sylwan*, *7*, 85-91.

Nanda, S.; Kozinski, J.A., & Dalai, A.K. (2013). Forestry biomass in a bioenergy perspective. *J-FOR-Journal of Science & Technology for Forest Products and Processes*, *3(6)*, 15-26.

Nkongolo, K.K, Vaillancourt, A., Dobrzeniecka, S., Mehes, M., & Beckett, P. (2008). Metal content in soil and black spruce (*Picea mariana*) trees in the Sudbury Region (Ontario, Canada): Low concentration of arsenic, cadmium, and nickel detected near smelter sources. *Bull Environ Contam Toxicology*, *80(2)*, 107-111.

Onder, S., & Dursun, S. (2006). Air borne heavy metal pollution on Cedrus libani (A. Rich.) in the city centre of Konya (Turkey), *Atmos. Environ., 40(6)*, 1122-1133.

Palma, G., Freer, J., & Baeza, J. (2003). Removal of metal ions by modified *Pinus radiata* bark and tannins from water solutions, *Water Res., 37(20)*, 4974-4980.

Palowski, B. (2000). Seed yield from polluted stands of *Pinus sylvestris* L. *New Forests*, *20(1)*, 15-22.

Pindór T., & Preisner, L. (2011). The use of selected renewable energy sources in the context of sustainable development criteria. *Research Papers of Wrocław University of Economics, 231*, 186-196.

PN-92/P-50092. Surowce dla przemysłu papierniczego. Drewno. Analiza chemiczna. *Polski Komitet Normalizacyjny*.

PN-EN 13183-1:2004. Wilgotność sztuki tarcicy. Część 1: Oznaczanie wilgotności metodą suszarkowo-wagową. *Polski Komitet Normalizacyjny*.

PN-ISO1928:2002. Paliwa stałe. Oznaczanie ciepła spalania metoda spalania w bombie kalorymetrycznej i obliczanie wartości opałowej. *Polski Komitet Normalizacyjny*.

Prus-Głowacki, W., Chudzińska, E., Wojnicka-Półtorak, A., Kozacki, L., & Fagiewicz, K. (2006). Effects of heavy metal pollution on genetic variation and cytological disturbances in the *Pinus sylvestris* L. population. *J. Appl. Genet*., *47(2)*, 99-108.

Rabiej, M. (2012). *Statystyka z programem STATISTICA.* Gliwice: Helion.

Rembowski, Ł. (2007). Wartość opałowa drewna. [http://agroenergetyka.pl/?a=article&id=146].

Reva, V., Fonseca, L., Lousada, J., Abrantes, I., & Viegas, D. (2012). Impact of the pinewood nematode, Bursaphelenchus xylophilus, on gross calorific value and chemical composition of Pinus pinaster woody biomass. *Eur. J. Forest Res*., *131*, 1025-1033.

Risovič, S., Đukič, I., & Vučkovič, K. (2008). Energy Analysis of Pellets Made of Wood Residues. *Croat. J. For. Eng*., *29(1)*, 95-107.

Rowell, R.M. (2012). *Handbook of Wood Chemistry and Wood Composites.* CRC Press.

Sawauchi, D., Kunii, D. & Yamamoto, Y. (2015) Carbon Dioxide Emissions and Energy Self-Sufficiency of Woody Biomass Utilization for Residential Heating: A Case Study of Nishiwaga, Japan. *Journal of Environmental. Protection*, *6*, 321-327.

Sawidis, T., Marnasidis, A., Zachariadis, G., & Stratis, J. (1995). A study of air pollution with heavy metals in Thessaloniki City (Greece) using trees as biological indicators. *Arch. Environ. Contam. Toxicol., 28(1)*, 118-124.

Schulz, H., Popp, P., Huhn, G., Stark, H. J., & Schüürmann, G. (1999). Biomonitoring of airborne inorganic and organic pollutants by means of pine tree barks. I. Temporal and spatial variations'. *The Science of Total Environment, 232(1-2)*, 49-58.

Sjöström, E. (1993). *Wood Chemistry. Fundamentals and Applications*. *Second edition ed.* San Diego: Academic press.

So, C.L., & Eberhardt, T.(2013). A mid-IR multivariate analysis study on the gross calorific value in longleaf pine: impact on correlations with lignin and extractive contents. *Wood Sci Technol., 47*, 993-1003.

StatSoft, Inc. (2014). STATISTICA (data analysis software system), version 12. www.statsoft.com.

Steven, H. M., & Carlisle, A. (1959). *The native pinewoods of Scotland.* Edinburgh, London: Oliver and Boyd.

Stolarski, M., Szczukowski, S., Tworkowski, J., Krzyżaniak, M., Gulczyński, P., & Mleczek, M. (2013). Comparison of quality and production cost of briquettes made from agricultural and forest origin biomass. *Renewable Energy*, *57*, 20-26.

Stvolinskaya, N.S. (2000). Viability of *Taraxacum officinale* Wigg. in populations of the city of Moscow in relation to motor transport pollution. *Russ. J. Ecol., 31(2)*, 129-131.

Su, P., Grandholm K., Pranovich A., Harju L., Holmbom B., & Ivaska A. (2013). Sorption of metal ions from aqueous solution to spruce bark, *Wood Sci Technol., 47(5)*, 1083-1097.

Sukhdolgor, J., Badamtsetseg, S., & Adyakhuu, D. (2003). Chemical composition and amount of macro and microelements of pine (*Pinus silvestris* L) and larch (*Larix sibirica* Ldb) trees in Mongolia, *Mongolian Journal of Biological Sciences*, *l(1)*, 81-83.

Sylven, N. (1916). Den nordsvenska tallen. *Medd. Statens Skogsförskninst, 13*, 9.

Telmo, C., & Lousada, J. (2011). The explained variation by lignin and extractive contents on higher heating value of wood. *Biomass and Bioenergy*, *35(5)*, 1663-1667.

Tylek, P., Walczyk, J., & Mateusiak, Ł. (2010). Prototyp separatora pneumatyczno-sitowego do nasion drzew leśnych z sitami cylindrycznymi. *Prace Komisji Nauk Rolniczych, Leśnych i Weterynaryjnych PAU, 14(II)*, 187-192.

Tylek, P., & Walczyk, J. (2009). Bębnowy odskrzydlacz nasion metodami suchą i mokrą. *Zeszyty Problemowe Postępów Nauk Rolniczych, 543*, 365-370.

Tylek, P., & Walczyk, J. (2009). Polish devices for the seeds de-winging, cleaning and sorting. [W:] *FORMEC, Czech University of Life Sciences*, Prague, 398-403.

Uliasz-Bocheńczyk, A., & Mokrzycki, E. (2015). Biomasa jako paliwo w energetyce. *Rocznik Ochrona Środowiska, 17*, 900-913.

Uri, V., Aosaar, J., Varik, M., Becker, H., Kukumägi, M., Ligi, K., Pärn, L., & Kanal, A. (2015). Biomass resource and environmental effects of Norway spruce (*Picea abies*) stump harvesting: An Estonian case study. *Forest Ecology and Management*, *335*, 207-215.

Voutsa, D., Grimanis, A., & Samara, C. (1996). Trace elements in vegetables grown in an industrial area in relation to soil and air particulate matter. *Environ. Pollut., 94*, 325-335.

Wójcik, M., Sugier, P., Siebielec, G. (2014). Metal accumulation strategies in plants spontaneously inhabiting Zn-Pb waste deposits. *Science of the Total Environment, 487,* 313-322.

Yoshioka, T., & Sakai, H. (2005). Amount and availability of forest biomass as an energy resource in a mountainous region in Japan: a GIS-based analysis. Croatian *Journal of Forest Engineering*, *26(2)*, 50-70.

Zajączkowski, M. (1949). Studia nad sosną zwyczajną w Tatrach i Pieninach. *Prace Roln.-Leśne PAU, 45*.

Zhao, D., Kane, M., Teskey, R., Markewitz, D., Greene, D., & Borders, B. (2014). Impact of management on nutrients, carbon, and energy in aboveground biomass components of mid-rotation loblolly pine (*Pinus taeda* L.) plantations. *Annals of Forest Science, 71(8),* 843-851.

Właściwości fizykochemiczne i możliwości energetycznego wykorzystania pozostałości wyłuszczarskich

Streszczenie

W przedstawionych badaniach określono ciepło spalania i wartość opałową pustych nasion i ich skrzydełek, które mogą być wykorzystane na cele energetyczne. Opisana została ich budowa komórkowa oraz zawartość toksycz-

nych metali i innych pierwiastków (Cd, Pb, Hg, Cu, Zn, Ni, Cr, Mo, Co, Fe, Mn, Ca, Mg, K, Na), które mogą być emitowane do środowiska. Ciepło spalania wyznaczono metodą kalorymetryczną, budowę komórkową określano na podstawie zdjęć z mikroskopu z kamerą Nikon Alphaphot -2- TRIN i mikroskopu skaningowego Quanta 200. Analizę elementarną i pierwiastkową wykonano analizatorem Elementar Vario Macro Cube oraz mineralizatorem mikrofalowym Milestone Start D. Uzyskano średnią wartość opałową badanych materiałów w zakresie 19,20-19,49 $MJ \cdot kg^{-1}$. Zawartość metali ciężkich w nasionach sosny i świerka jest wyższa niż w skrzydełkach, jednak ich ilość nie powinna powodować negatywnych skutków ekologicznych. Zawartość metali była zbliżona do wartości podawanych przez innych autorów. Nasiona były zasobne w potas, wapń i magnez. Skrzydełka i puste nasiona po procesie wyłuszczenia szyszek można spalać i wykorzystywać jako paliwo pochodzące z OZE.

Abstract

The heat of combustion and calorific value of empty seeds and seed wings were determined. The structure of seed and wing cells and the content of toxic metals and other elements (Cd, Pb, Hg, Cu, Zn, Ni, Cr, Mo, Co, Fe, Mn, Ca, Mg, K, Na) were described. Heat of combustion was measured in a bomb calorimeter. Cell structure was described based on microscopic images acquired with the Nikon Alphaphot -2- TRIN microscope and camera and the Quanta 200 scanning electron microscope. The elemental analysis was performed in the Elementar Vario Macro Cube analyzer and the Milestone Start D microwave digestion system. The mean calorific value of the tested materials ranged from 19.20 to 19.49 $MJ \cdot kg^{-1}$. Heavy metal content was higher in pine and spruce seeds than in wings, but the noted concentrations should not have adverse environmental effects. Metal concentrations were similar to those reported by other authors. The tested seeds were abundant in potassium, calcium and magnesium. Wings and empty seeds from extraction residues can be burned and used as sources of renewable energy.

Słowa kluczowe:
bioenergia, biomasa, biomonitoring, odpady leśne, metale,
pozostałości wyłuszczarskie

Keywords:
bioenergy, biomass, biomonitoring, forest waste, metals,
seed extraction residues

MIDDLE POMERANIAN SCIENTIFIC SOCIETY OF THE ENVIRONMENT PROTECTION
ŚRODKOWO-POMORSKIE TOWARZYSTWO NAUKOWE OCHRONY ŚRODOWISKA

Annual Set The Environment Protection
Rocznik Ochrona Środowiska

Volume/Tom 19. Year/Rok 2017 ISSN 1506-218X 335-354

Carbon Footprint as a Tool for Local Planning of Low Carbon Economy in Poland

Paweł Wiśniewski, Mariusz Kistowski
University of Gdansk

1. Introduction

In recent years, carbon footprint has become a popular and promising tool for estimating greenhouse gas emissions caused by human activity, as well as an important tool in raising awareness and creating environmentally friendly behaviors. Moreover, it could be used in the development and management of low carbon economy as well as in planning activities for climate protection and adaptation to its changes (Finkbeiner 2009, Ercin & Hoekstra 2012, Pandey & Agrawal 2014, Fantozzi & Bartocci 2016, Ibidhi et al. 2017). Despite its widespread application, however, there is no uniform, worldwide definition of carbon footprint and, what is more, there are also different methods of its estimation (Hammond 2007, Wiedmann & Minx 2008, Wang et al. 2013, Fang et al. 2014). Thus, it hinders the effective application of this tool in the analysis of quantitative greenhouse gas emissions, mitigating the effects of global warming and the adaptation of the various sectors and areas which are sensitive to changes. For example, Grubb and Ellis (2007) define carbon footprint as a measure of the amount of carbon dioxide emitted through the combustion of fossil fuels. In their view, in the case of a business organization, it is the amount of CO_2 emitted either directly or indirectly as a result of its everyday operations. It also might reflect the fossil energy represented in a product or commodity reaching market. The most extensive survey on the definition of the carbon footprint was done by Wiedmann and Minx (2008) who analyzed the apparent discrepancy between public and academic use of the term carbon footprint and

suggests a scientific definition based on commonly accepted accounting principles and modelling approaches. They suggest the definition of carbon footprint is a measure of the exclusive total amount of carbon dioxide emissions that is directly and indirectly caused by an activity or is accumulated over the life stages of a product. This includes activities of individuals, populations, governments, companies, organizations, processes, industry sectors, etc. Products include goods and services. All direct and indirect emissions need to be taken into account, but this definition does not include other substances with greenhouse warming potential. In most cases carbon footprint is used as a generic synonym for emissions of carbon dioxide and other greenhouse gases (including nitrous oxide and methane) produced to directly and indirectly support human activities, expressed in CO_2 equivalent (Patel 2006, POST 2006, Carbon Trust 2007, Pandey et al. 2011). This approach applies in this paper.

Poland, pursuing the aims of the EU climate policy, as well as striving to meet new challenges, must be prepared for the necessity to move to a low carbon economy. It has been recognized in the draft of the National Programme for Development of Low Carbon Economy, adopted by the Ministry of Economy (2015). Unfortunately, work on the final adoption of this project has been halted in 2016 and its status is currently not quite clear. The development of such an economy, which requires the integration of all its aspects around low carbon technologies and practices, efficient energy solutions, clean and renewable energy as well as environmentally friendly technological innovation, is one of the priorities adopted by the European Parliament and the Council of the European Union, the 7th General Union Environment Action Programme to 2020 (European Commission 2014). It also coincides with the objectives and priorities of the Europe 2020 Strategy for smart, sustainable and inclusive growth (European Commission 2010).

In order to effectively transform the Polish economy, appropriate actions at the local level should be planned. To this end, municipal low carbon economy plans are created. These are important strategic documents which are to determine the vision of municipal development towards a low carbon economy and to increase the chances of local authorities in applying for EU funds in the 2014-2020 financial perspective. They are equivalent to the Sustainable Energy Action Plans (SEAP) –

key documents developed by the signatories of the Covenant of Mayors for Climate and Energy, an association of more than 6 thousand local governments from Europe and beyond. The tasks which are included in these plans should focus on low carbon and resource-efficient activities, which would improve energy efficiency and use renewable energy sources in all sectors of the economy with the participation of entities which are producers and consumers of energy as well as residents, local authorities and institutions. It is noteworthy that municipalities have no formal obligation to prepare local low carbon economy plans. In most cases, they are created mainly to allow municipalities to benefit from EU funds for low carbon development activities. The detailed recommendations on the structure of plans for a low carbon economy, developed by the National Fund for Environmental Protection and Water Management (NFEP&WM), stress the need for including in these documents investment projects aimed at reducing energy consumption in transport, buildings or installations and in the scope of waste management and energy production, as well as noninvestment tasks, such as urban spatial planning, public procurement, communication strategy, promotional activities (NFEP&WM 2013). However, the agricultural regions as well as rural areas were ignored, which led to the situation wherein the plans accepted for execution by local municipalities, created mostly on the basis of the NFEP&WM, particular attention is being paid to the energy, construction and transport sectors while agriculture and rural areas are being treated marginally (Wiśniewski & Kistowski 2016, 2017).

The control of greenhouse gas emissions using the method of assessing carbon footprints should be an important tool to support local planning of a low carbon economy. The proper baseline emission inventory should be an important element in assessing local conditions as well as the reference point for the adopted bearing of low carbon development of individual local governments. The study attempted to evaluate the role and importance of carbon footprint as a tool for the local planning of a low carbon economy at local level in Poland, and to indicate necessary changes and modifications that will enable the effective management of the use of low carbon economy by local governments.

2. Material and methods

The research material consisted of local low carbon economy plans, adopted for implementation by the randomly selected rural, urban-rural and urban municipalities, representing all the provinces in Poland (Table 1). In total, the analysis covered 48 such documents – 3 for each province. The plans under study were evaluated taking into consideration the methodology of calculation of the carbon footprint, particularly in the choice of base year, gases and sectors covered by the inventory and the adopted emission factors. On the basis of the results of the inventory of greenhouse gases presented in the studied plans, the estimation of carbon footprint (total and per capita) was carried out both in the individual municipalities with the division of their type (rural, urban-rural and urban) as well as their inclusion in the inventory sectors. Due to the different approach of local governments with regards to the choice of base year and inventory control, the article presents the size of carbon footprint calculated for the previous year, as included in the document, so that all presented data come from the years 2010-2014. In order to standardize the results and carry out statistical and comparative analyses, greenhouse gas emissions was expressed as carbon dioxide equivalent (CO_2eq), adopting the global warming potential values (GWP) specified in the Fifth Assessment Report of the Intergovernmental Panel on Climate Change (IPCC 2013).

The size of the carbon footprint in the studied municipalities as well as the method of its determination and calculation were confronted with the results obtained using the model solution, implemented earlier in the Pilot programme of low carbon development of Starogard county, realized in the years 2014-2015 within the framework of the project "Good Climate for Counties" jointly carried out by the Institute for Sustainable Development (ISD), Association of Polish Counties and the Community Energy Plus in cooperation with other public authorities and institutions of the Starogard county. It is the first document of its type to be dedicated to low carbon economy, drawn up on county scale in Poland and developed with the participation of the co-author of this article (ISD 2015b, Wiśniewski 2015). The solution used in the Starogard county is in line with the methodology and standard indicators of the IPCC (IPCC 2000, 2006), and, in order to obtain more accurate emissions data, takes

into account the elements of national methodology and emission factors developed by the National Centre for Emission Management (KOBiZE) for the purposes of preparing annual inventory reports (ISD 2015a). Starogard county is located in the southern part of the Pomeranian Province. It covers an area of 1345 km^2, out of which 48% is agricultural areas and 42% – woodlands. The population of the county reaches 124 000 of which 50% live in the city. It consists of 13 municipalities – 9 rural, 1 urban-rural and 3 urban areas.

Table 1. General characteristics of the municipalities covered by the analysis
Tabela 1. Ogólna charakterystyka porównawcza gmin objętych analizą

No.	Municipality	Type of municipality*	Province	Area	Population		Agricultural areas	Woodland
					total	in cities		
				km^2	thous.	%	%	%
1	Bolesławiec	r	Lower Silesian	288	14,1	-	41	40
2	Żarów	u-r		87	12,6	54	77	11
3	Oleśnica	u		20	37,3	100	63	0
4	Aleksandrów Kujawski	r	Kuyavian-Pomeranian	131	11,6	-	74	16
5	Nakło nad Notecią	u-r		186	32,4	60	67	19
6	Golub-Dobrzyń	u		7	12,9	100	47	15
7	Karczmiska	r	Lublin	95	5,7	-	72	22
8	Tarnogród	u-r		113	6,9	48	69	26
9	Biłgoraj	u		20	27,2	100	55	9
10	Pszczew	r	Lubusz	177	4,3	-	40	49
11	Międzyrzecz	u-r		315	25,2	76	37	51
12	Żary	u		33	38,9	100	39	20
13	Tomaszów Mazowiecki	r	Lodz	151	10,8	-	45	44
14	Opoczno	u-r		190	35,2	62	69	19
15	Sieradz	u		51	43,4	100	69	3
16	Sułoszowa	r	Lesser Poland	53	5,8	-	89	7
17	Wieliczka	u-r		100	55,2	38	73	8
18	Nowy Targ	u		50	33,7	100	48	36

Table 1. cont.
Tabela 1. cd.

19	Regimin	r	Masovian	111	5,1	-	69	20
20	Konstancin-Jeziorna	u-r		78	24,8	71	63	13
21	Mława	u		24	30,9	100	58	7
22	Izbicko	r	Opole	84	5,4	-	51	38
23	Strzelce Opolskie	u-r		202	31,3	63	59	30
24	Kędzierzyn-Koźle	u		123	63,2	100	24	45
25	Przeworsk	r	Subcarpathian	90	14,9	-	88	1
26	Lesko	u-r		111	11,6	50	40	46
27	Dębica	u		33	46,9	100	42	19
28	Narewka	r	Podlachia	339	3,8	-	25	65
29	Rajgród	u-r		207	5,4	29	58	29
30	Bielsk Podlaski	u		26	26,3	100	72	2
31	Puck	r	Pomeranian	243	24,9	-	60	29
32	Kartuzy	u-r		205	33,0	50	42	46
33	Chojnice	u		21	40,1	100	57	5
34	Bestwina	r	Silesian	37	11,2	-	65	11
35	Skoczów	u-r		63	26,7	58	63	22
36	Żywiec	u		50	32,1	100	45	17
37	Morawica	r	Świętokrzy-skie	140	15,4	-	64	27
38	Staszów	u-r		225	26,4	56	59	34
39	Skarżysko-Kamienna	u		64	47,2	100	26	31
40	Gietrzwałd	r	Warmian-Masurian	174	6,5	-	37	48
41	Pisz	u-r		634	28,0	68	28	45
42	Działdowo	u		11	21,5	100	53	6
43	Kiszkowo	r	Greater Poland	114	5,4	-	80	8
44	Ślesin	u-r		145	14,0	23	59	21
45	Gniezno	u		40	69,9	100	46	13
46	Postomino	r	West Pomeranian	227	7,1	-	61	20
47	Gryfino	u-r		253	32,1	69	54	21
48	Białogard	u		25	24,9	100	48	9

*r – rural municipality; u-r – urban-rural municipality; u – urban municipality

3. Results and discussion

Conducted diagnosis showed that in all analyzed low carbon economy plans in greenhouse gas emission inventory used standard emission factors in line with the IPCC principles. They cover all the CO_2 emissions that occur due to energy consumption in the municipality, both direct emissions from the fuel combustion in buildings, installations and transport, as well as indirect emissions accompanying the production of electricity, heat and cold for inhabitants. The standard emission factors are based on the carbon content of each fuel, like in national greenhouse gas inventories in the context of the United Nations Framework Convention on Climate Change (UNFCCC) and the Kyoto protocol. The advantage of this method is the fact that Poland – a party to the UNFCCC – has already gained experience in applying this method (Burchard-Dziubińska 2014). However, in this approach, CO_2 is the most important greenhouse gas, and the emissions of CH_4 and N_2O do not need to be calculated. Furthermore, the CO_2 emissions from the sustainable use of biomass or biofuels, as well as emissions of certified green electricity, are considered to be zero, which usually is not consistent with reality (Bertoldi et al. 2010). The LCA (Life Cycle Assessment) emission factors were not applied in any of the surveyed municipalities. They take into consideration the overall life cycle of the energy carrier. This approach includes not only the emissions of the final combustion, but also all emissions of the supply chain. It includes emissions from exploitation, transport and processing steps in addition to the final combustion. Hence, this includes also emissions that take place outside the location where the fuel is used. In this approach, the greenhouse gas emissions from the use of biomass or biofuels, as well as emissions of certified green electricity, are higher than zero. In the case of this approach, greenhouse gases other than CO_2 may play an important role. LCA is a noteworthy standardized method used worldwide by many institutions and governments and can be applicable at the local level in Poland, in order to determine the carbon footprint, providing unified, integrated approach to the role of consumption at the product level, contributing to emission of greenhouse gases (Sinden 2009).

Polish local governments, in creating local plans for low carbon economy, base primarily on the principles and guidelines of Covenant of

Mayors for Climate and Energy, which refer to the principles for the development of Sustainable Energy Action Plans (SEAP) and the Baseline Emission Inventory (BEI). According to these guidelines, if the local authorities decide to use standard emission factors, it will be sufficient to apply inventory to CO_2 emissions. Such a solution was applied by 77% of the surveyed municipalities. In four cases, the emissions were expressed as carbon dioxide equivalent. However, with the exception of CO_2, it was not indicated which gases have been included in the inventory. Neither was it explained which GWP factors were adopted. In seven municipalities it was decided to include also other gases in emission (such as CH_4, N_2O, SO_2), however, their emission was not converted into CO_2 equivalent (Table 2).

According to the guidelines of the Covenant of Mayors, the baseline emission inventory should include direct emissions from fuel combustion in buildings, plants and in the transport sector; indirect emissions associated with the production of electricity; heat and cooling energy used by end users; as well as other direct emissions occurring on its territory, depending on the specifics of the municipality. Among the recommended sectors which are to be taken into account there are buildings, equipment and facilities municipal and service device (non-municipal); residential buildings; municipal public lighting; municipal road transport (municipal fleet, public, private and commercial transport); municipal rail transport as well as fuel consumption for heat and cold production. Other road transport, railway, local ferries and off-road transport (e.g. agricultural and construction machinery), industries not involved in EU ETS, wastewater treatment, solid waste treatment as well as fuel consumption for electricity production – should be included in the BEI, provided that the activities in these sectors are included in the SEAP. However, in accordance with the guidelines of the Covenant of Mayors, it is not mandatory to include industries involved in EU ETS, aviation, shipping and fluvial transport, fugitive emissions from production, transformation and distribution of fuels, process emissions of industrial plants, the use of products and fluorinated gases, agriculture and changes in carbon stocks due to the changes in land use. As a result, these sectors are rarely taken into account while calculating the carbon footprint by local governments in Poland. In the surveyed municipalities, the baseline inventory includes, primarily, emissions from public buildings and facili-

ties, housing, transport and public lighting. In a little less than half of the analyzed plans, when calculating the carbon footprint, the industrial sector was included, however, it was mostly limited to emissions from sources of heat in industrial plants with the exception of plants covered by the EU ETS and industry fed on medium and high voltage. Only in ten documents, emissions related to waste as well as water and sewage management were taken into account. The agricultural sector was included only in three plans for low carbon economy, while in case of Aleksandrów Kujawski municipality, the assessment of CO_2 emissions from agriculture along with the emission from residential buildings was carried out. In none of the analyzed plans have not made the balance of greenhouse gases from LULUCF sector (Land Use, Land-Use Change and Forestry), which has a great mitigation potential (IPCC 2003) (Table 2).

Table 2. Greenhouse gases and sectors included in the emission inventory in the analyzed municipalities
Tabela 2. Gazy cieplarniane i sektory ujęte w bazowej inwentaryzacji emisji w badanych gminach

No.	Municipality	Gases					Sectors*								
		CO_2	CO_2 eq	N_2O	CH_4	other	A	B	C	D	E	F	G	H	I
1	Bolesławiec	●						●		●	●	●			●
2	Żarów	●					●	●		●		●			
3	Oleśnica		●				●	●	●	●	●	●	●		
4	Aleksandrów Kujawski	●					●	○			●	●	○		●
5	Nakło nad Notecią	●					●	●		●	●	●			●
6	Golub-Dobrzyń	●					●	●	●	●		●			●
7	Karczmiska	●					●	●		●					●
8	Tarnogród	●		●		●	●	●	●	●		●			●
9	Biłgoraj	●		●		●	●	●	●	●		●			●
10	Pszczew	●					●	●		●		●			●
11	Międzyrzecz	●					●	●		●		●			●
12	Żary	●					●	●		●	●	●			●
13	Tomaszów Mazowiecki		●				●	●		●		●			●

Table 2. cont.
Tabela 2. cd.

14	Opoczno		●				●	●		●		●			●
15	Sieradz	●					●	●		●		●			●
16	Sułoszowa	●		●	●	●	●	●	●	●		●			●
17	Wieliczka	●					●	●		●		●			●
18	Nowy Targ	●					●	●	●	●		●			●
19	Regimin	●					●	●	●	●		●			●
20	Konstancin-Jeziorna	●					●	●	●	●		●			●
21	Mława	●					●	●	●	●		●			●
22	Izbicko	●					●	●	●	●		●			●
23	Strzelce Opolskie	●													
24	Kędzierzyn-Koźle	●					●	●		●	●	●			●
25	Przeworsk	●					●	●		●		●			●
26	Lesko	●					●	●	●	●		●			●
27	Dębica	●		●		●	○	●	●	●		●			○
28	Narewka	●					●	●	●	●		●			
29	Rajgród	●					●	●		●		●			
30	Bielsk Podlaski	●					●	●		●		●			●
31	Puck	●					●	●	○	●	●	●			○
32	Kartuzy	●					●	●		●	●	●			●
33	Chojnice	●					●	●	●	●					●
34	Bestwina	●					●	●		●		●			●
35	Skoczów	●						●	●	●					●
36	Żywiec	●					●	●	●	●					●
37	Morawica	●					●	●	●		●	●			●
38	Staszów	●					●	●	●	●		●			●
39	Skarżysko-Kamienna	●					●	●		●		●			●
40	Gietrzwałd	●					●	●		●		●			●
41	Pisz	●					●	●	●	●	●	●			●
42	Działdowo	●					●	●		●		●			●
43	Kiszkowo	●			●		●	●		●		●	●		●
44	Ślesin	●		●		●	●	●		●		●			●
45	Gniezno	●					●	●	●	●		●			●

Table 2. cont.
Tabela 2. cd.

46	Postomino	●					●	●		●		●			●
47	Gryfino		●				●	●		●		●			●
48	Białogard	●		●		●	●	●	●	●		●			●
Starogard county		●	●	●	●	●	●	●	●	●	●		●	●	●

*Sectors: A – public buildings and facilities, B – housing, C – industry, D – transport, E – waste management and wastewater treatment, F – public lighting, G – agriculture, H – LULUCF, I – other
● – considered, ○ – considered together with another sector

The guidelines of the Covenant of Mayors also recommended that in the emission inventory, as the base year – in relation to which local authorities will try to reduce emissions by 2020 – the year 1990 was chosen, as it is regarded as a starting point for reduction targets which are set in the EU climate and energy package as well as the Kyoto protocol.

However, municipal authorities in Poland rarely have data which enables the calculation of carbon footprint for the year 1990, which makes this practice inapplicable and the base year in the emission inventory is very different. In addition, not all communes decide to carry out an inventory control, making it difficult to compare results in terms of emission reductions achieved at the local level in Poland.

The size of the carbon footprint in individual communes, shown in Figure 1, and expressed in carbon dioxide equivalent in absolute terms and per capita, as well as the results of statistical analysis and benchmarking (Table 3) indicate considerable differences in the emission of greenhouse gases. These differences are probably due to the peculiarities of local governments, but also are the result of non-uniform methodological assumptions when estimating emission.

The value of carbon footprint in the surveyed municipalities range from 17.3 thousand Mg CO_2eq/year in Karczmiska rural municipality to 436.4 thousand Mg CO_2eq/year in Gniezno municipality, with the average absolute value of 131.1 thousand Mg CO_2eq/year and a standard deviation of 91.6 thousand Mg CO_2eq/year. In per capita terms, these values range from 2.9 Mg CO_2eq in Aleksandrów Kujawski and Karczmiska, rural municipalities, and up to 31.5 Mg CO_2eq in Gietrzwałd rural municipality, with an average of 6.6 Mg CO_2eq and a standard de-

viation of 4.5 Mg CO_2eq. Taking into consideration the type of municipalities, the average absolute CO_2eq emissions for the surveyed rural units it is twice as much less than in the urban-rural municipalities, and more than three times lower than in case of the urban municipalities. Rural municipalities are characterized by the highest carbon footprint per capita.

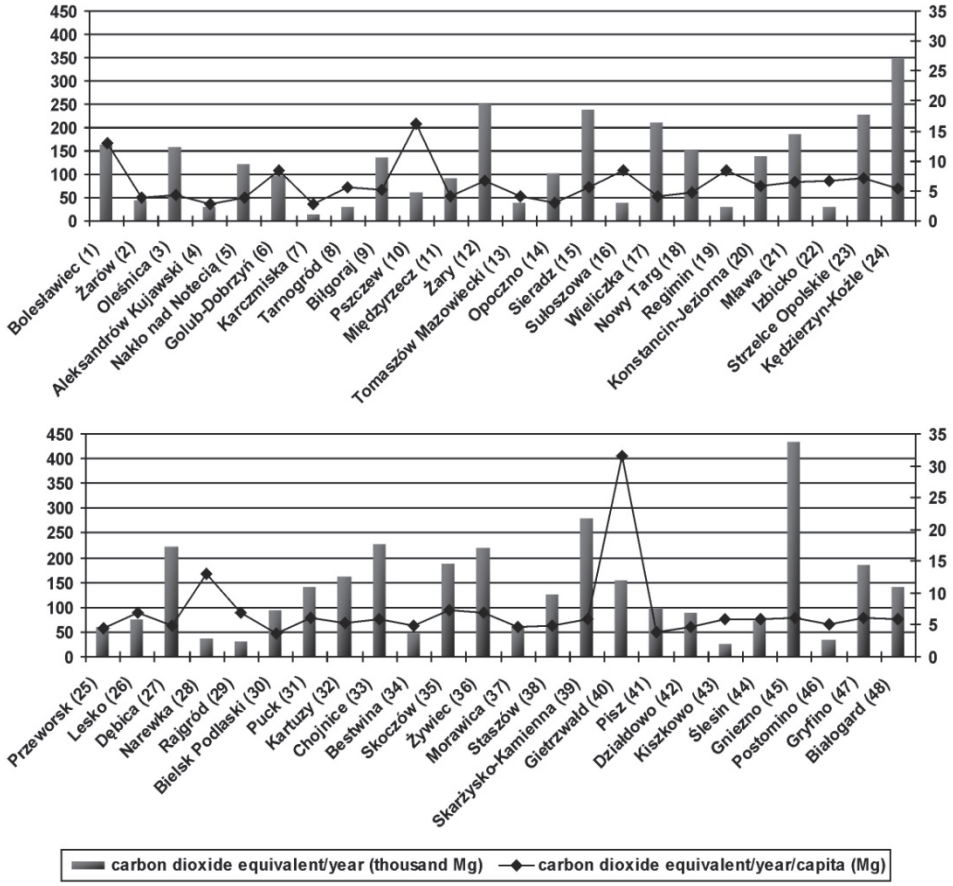

Fig. 1. Carbon footprint in the analyzed municipalities, expressed in carbon dioxide equivalent (global and per capita)
Rys. 1. Ślad węglowy w badanych gminach, wyrażony w ekwiwalencie dwutlenku węgla (w wartościach bezwzględnych i per capita)

Table 3. Descriptive statistics of the carbon footprint (in CO_2 equivalent) by sector and types of municipalities
Tabela 3. Statystyki opisowe wielkości śladu węglowego (w ekwiwalencie CO_2) z podziałem na sektory i typy gmin

Sector*	Rural municipalities				Urban-rural municipalities				Urban municipalities			
	min	max	average	σ	min	max	average	σ	min	max	average	σ
thousand Mg CO_2eq/year												
A	0.33	6.85	1.60	1.79	0.61	21.76	6.84	6.57	3.41	21.72	10.06	5.33
B	0.18	51.94	24.34	12.76	16.34	112.30	49.68	24.76	21.22	154.20	80.21	42.68
C	0.05	10.23	3.08	4.12	3.89	27.90	17.47	8.84	2.13	85.13	37.73	26.54
D	0.49	152.24	28.83	41.32	3.67	107.03	38.35	31.86	0.52	173.82	47.64	48.04
E	0.42	1.85	1.25	0.74	0.97	2.25	1.77	0.69	0.001	2.25	0.76	1.29
F	0.08	1.47	0.52	0.44	0.10	3.61	1.27	0.93	0.73	3.30	1.83	0.82
G		5.73		-			-			1.50		-
I	0.10	27.52	7.19	7.95	1.32	230.36	30.79	58.50	1.05	201.52	48.36	53.08
Total	17.27	167.43	63.46	48.06	33.59	230.36	122.36	62.33	92.76	436.37	207.42	94.41
Mg CO_2eq/year/capita												
A	0.02	1.37	0.27	0.38	0.01	1.56	0.40	0.45	0.15	0.59	0.29	0.13
B	0.01	8.17	3.49	2.18	1.46	3.27	2.28	0.59	1.13	3.92	2.17	0.79
C	0.01	3.41	0.88	1.44	0.65	1.50	0.94	0.36	0.18	2.01	1.06	0.68
D	0.05	18.45	3.77	5.17	0.15	3.59	1.66	1.02	0.01	5.78	1.34	1.47
E	0.03	0.13	0.08	0.05	0.03	0.08	0.06	0.03	0.00	0.03	0.01	0.02
F	0.01	0.19	0.06	0.04	0.01	0.28	0.06	0.07	0.03	0.09	0.05	0.02
G		1.15		-			-			0.04		-
I	0.01	3.30	0.77	0.82	0.04	7.20	1.03	1.80	0.06	5.30	1.30	1.37
Total	2.88	31.48	8.66	7.22	3.05	7.35	5.31	1.40	3.70	8.36	5.70	1.14

*Sectors: A – public buildings and facilities, B – housing, C – industry, D – transport, E – waste management and wastewater treatment, F – public lighting, G – agriculture, I – other
σ – standard deviation

An analysis of the carbon footprint by sectors shows that the largest share in the total CO_2 emissions in the surveyed municipalities have housing (38.4%) and transport (27.8%) sectors. The sector indicated in Tables 2 and 3 as I (others), comprising mainly buildings, equipment and service devices (non-communal) is responsible for 20.1% of total emission. Urban municipalities are characterized by a higher proportion (18.2%) of industry in overall emissions compared to rural (4.9%) and rural-urban municipalities (14.3%).

The average size of carbon footprint in the analyzed municipalities per capita is about 2.4 Mg CO_2eq lower than the carbon footprint calculated for the purposes of the pilot programme of low carbon development of Starogard county (Table 4). Clear differences are also noticeable in the division into particular sectors. The carbon footprint per capita in Starogard county in industry, energy and housing economy is about 2.8 Mg CO_2eq higher than the average carbon footprint produced in those sectors in the surveyed municipalities (including the emission from public buildings). The difference is even greater in case of the waste as well as water and wastewater management (3.23 Mg CO_2eq in Starogard county with an average value of 0.01 Mg CO_2eq in the studied municipalities). Similar values (sequentially 1.29 Mg CO_2eq and 1.57 Mg CO_2eq) apply to the transport.

Table 4. Carbon footprint in Starogard county in 2013 (in CO_2 equivalent)
Tabela 4. Ślad węglowy w powiecie starogradzkim w 2013 r.
(w ekwiwalencie CO_2)

Carbon footprint	Sectors*					Total
	I	II	III	IV	V	
Global (thous. Mg CO_2eq)	705.71	160.47	400.80	131.98	-277.65	1,121.31
Per capita (Mg CO_2eq)	5.69	1.29	3.23	1.06	-	9.04

*Sectors: I – industry, energy and housing economy; II – transport; III – waste management and wastewater treatment; IV – agriculture; V –LULUCF

It is worth noting that agriculture takes 9% share in the total greenhouse gas emissions in Starogard county. The carbon footprint from this sector, which is covered by the pilot programme for the county, is slightly more than 1 Mg CO_2eq/year/capita. In the analyzed municipalities, this sector was virtually ignored. In addition, the size of carbon footprint of Starogard county has been reduced by the balance of greenhouse gases in the LULUCF sector, which has not been done in any of the surveyed municipalities. In Starogard county – as in the studied municipalities – uniform methodology and standard IPCC emission factors were used. Moreover, in order to obtain more accurate data on emission – the national methodology and emission factors developed by KOBiZE were used in order to prepare the annual inventory reports (ISD 2015a). The average size of carbon footprint per capita calculated on the basis of the data contained in the plans for low carbon economy adopted for implementation by the studied municipalities is also lower by 1.5 Mg CO_2eq in relation to the size of the carbon footprint for Poland in 2013 and by 1.2 Mg CO_2eq compared to 2014, calculated and presented in the latest report on global trends in emissions of CO_2, published by the PBL Netherlands Environmental Assessment Agency and the European Commission's Joint Research Centre (JRC) (Olivier et al. 2015).

4. Conclusions

The assessment of the carbon footprint for particular local government units can be a useful tool for effective management of emissions of greenhouse gases and the choice of appropriate guidelines for low carbon development at the local level. Properly conducted emissions inventory enables the identification of its main sources and priority areas, which require low carbon actions, thereby increasing the effectiveness of local low carbon policy and contributing to the optimization of the costs of action in order to reduce emissions. According to the authors of the SEAP guidebook (Bertoldi et al. 2010), elaborating a baseline emission inventory is of critical importance. This is because the inventory will be the instrument allowing the local authority to measure the impact of its actions related to climate change. The inventory will show where the local authority was at the beginning, and the successive monitoring emission inventories will show the progress towards the objective. Emission

inventories are very important elements to maintain the motivation of all parties willing to contribute to the local authority's greenhouse gases reduction objective, allowing them to see the results of their efforts.

An analysis of 48 local low carbon economy plans, which are important strategic documents aiming to determine the vision of municipal development in a low carbon economy in Poland has, however, shown that the use of these methods for calculating the carbon footprint are ineffective and do not allow for the determination of the actual level of greenhouse gas emissions. The weaknesses of the applied solutions should include, primarily, focusing almost exclusively on CO_2 emissions without taking into account other gases, using only standard emission factors without taking into account the indices, which consider the life cycle of each energy carrier as well as skipping important sectors, among others agriculture, which is, particularly in the rural and urban-rural municipalities, unjustified. Polish local governments do not carry out the verification of carbon footprint through the balance of gases in the LULUCF sector, which is mostly a net absorbent.

The summary of the size of carbon footprint in the analyzed municipalities along with calculations carried out under a pilot programme of low carbon development of Starogard county, indicates that in majority of the local governments the numbers are underestimated. This is also confirmed by the calculations of carbon footprint for Poland, presented in national and international reports on CO_2 emissions.

Due to underestimation and significant differences in the size of carbon footprint in particular local governments, which result mainly from the non-uniform methodological assumptions, observed not only in Poland but also in other European countries (e.g. in Greece, Norway and Finland) (Larsen & Hertwich 2010, Heinonen & Junnila 2011, Angelakoglou et al. 2015, Zdeb 2015), there is an urgent need to create an effective, coherent and simplified model for the assessment of carbon footprint, which would be available for use by all local government units, extending beyond the guidelines of the Covenant of Mayors for Climate and Energy, which allows to take into account the specificity of local conditions.

References

Angelakoglou, K., Gaidajis, G., Lymperopoulos, K., Botsaris, P.N. (2015). Carbon Footprint Analysis of Municipalities – Evidence from Greece. *Journal of Engineering Science and Technology Review, 8(4),* 15-23.

Bertoldi, P., Cayuela, D.B., Monni, S., Raveschoot, R.P. (2010). *Guidebook „How to develop a sustainable energy action plan (SEAP)"*. Luxembourg: JRC Scientific and Technical Reports, Publications Office of the European Union.

Burchard-Dziubińska, M. (2014). Availability and quality of statistical data indispensable for low-emission development strategies in local government units. *Optimum. Economic Studies, 3(69)*, 144-155.

Carbon Trust (2006). *Carbon footprints in the supply chain: the next step for business*. London: The Carbon Trust.

Ercin, A.E., & Hoekstra, A.Y. (2012). *Carbon and Water Footprints. Concepts, Methodologies and Policy Responses*. Paris: United Nations Educational, Scientific and Cultural Organization.

European Commission (2010). *Europe 2020. A strategy for smart, sustainable and inclusive growth, COM (2010) 2020*. Brussels.

European Commission (2014). *General Union Environment Action Programme to 2020. Living well, within the limits of our planet*. Luxembourg.

Fang, K., Heijungs, R., de Snoo, G.R. (2014). Theoretical exploration for the combination of the ecological, energy, carbon, and water footprints: Overview of a footprint family. *Ecological Indicators, 36*, 508-518.

Fantozzi, F., & Bartocci, P. (2016). *Carbon Footprint as a Tool to Limit Greenhouse Gas Emissions*. Rijeka: InTech.

Finkbeiner, M. (2009). Carbon footprinting – opportunities and threats. *Int J Life Cycle Assess*, *14*, 91-94.

Grubb, E., & Ellis, C. (2007). *Meeting the Carbon Challenge: The Role of Commercial Real Estate Owners*. Chicago: Users & Managers.

Hammond, G. (2007). Time to give due weight to the 'carbon footprint' issue. *Nature, 445(18)*, 256.

Heinonen, J., & Junnila, S. (2011). A Carbon Consumption Comparison of Rural and Urban Lifestyles. *Sustainability, 3*, 1234-1249.

Ibidhi, R., Hoekstra, A.Y., Gerbens-Leenes, P.W., Chouchane, H. (2017). Water, land and carbon footprints of sheep and chicken meat produced in Tunisia under different farming systems. *Ecological Indicators, 77*, 304-313.

IPCC (2003). *Good Practice Guidance for Land Use, Land-Use Change and Forestry*. Hayama, Kanagawa.

IPCC (2013). *Climate Change 2013. The Physical Science Basis. Contribution of Working Group I to the Fifth Assessment Report of the Intergovernmental Panel on Climate Change*. Cambridge, United Kingdom and New York.

ISD (2015a). *Methods of assessing the level of greenhouse gas emissions in selected counties for the years 2005, 2010 and 2013 by sector*. Warsaw: Institute for Sustainable Development Foundation.

ISD (2015b). *Pilot programme of low carbon development of Starogard county*. Warsaw: Institute for Sustainable Development Foundation.

Larsen, H.N., & Hertwich, E.G. (2010). Implementing Carbon-Footprint-Based Calculation Tools in Municipal Greenhouse Gas Inventories: The Case of Norway. *Journal of Industrial Ecology, 14*, 965-977.

Ministry of Economy (2015). *National Programme for Development of Low Carbon Economy (draft)*, Warsaw.

NFEP&WM (2013). *Detailed recommendations on the structure of plans for a low carbon economy*. Warsaw: The National Fund for Environmental Protection and Water Management.

Olivier, J.G.J, Janssens-Maenhout, G., Muntean, M., Peters, J.A.H.W. (2015). *Trends in global CO_2 emissions: 2015 Report. PBL Netherlands Environmental Assessment Agency*. The Hague.

Pandey, D., & Agrawal, M. (2014). *Carbon Footprint Estimation in the Agriculture Sector*. Singapore: Springer.

Pandey, D., Agrawal, M., & Pandey, J.S. (2011). Carbon footprint: current methods of estimation. *Environmental Monitoring and Assessment, 178*, 135-160.

Patel, J. (2006). Green sky thinking. *Environment Business, 122*, 32.

POST (2006). *Carbon footprint of electricity generation*. London: Parliamentary Office of Science and Technology.

Sinden, S. (2009). The contribution of PAS 2050 to the evolution of international greenhouse gas emission standards. *Int J Life Cycle Assess, 14(3)*, 195-203.

Wang, Y., Zhang, H., Wang, T.Y. (2013). Structure Decomposition Analysis of the Carbon Footprint Differences between Beijing and Tianjin. *Advanced Materials Research*, *734-737*, 1960-1963.

Wiedmann, T., & Minx, J. (2008). *A Definition of 'Carbon Footprint'*. New York: Nova Science Publishers.

Wiśniewski, P. 2015. Agriculture and rural areas in local low carbon economy planning: a case study of the county of Starogard. *Water-Environment-Rural Areas, 4(52)*, 69-81.

Wiśniewski, P., & Kistowski, M. (2016). Local low carbon economy plans in the context of low carbon rural development. *Journal of Ecological Engineering, 17(4)*, 112-119.

Wiśniewski, P., & Kistowski, M. (2017). Agriculture and rural areas in the local planning of low carbon economy in light of the idea of sustainable development – results from a case study in north-central Poland. *Fresenius Environmental Bulletin, 26(8)*, 4927-4935.

Zdeb, M. (2015). Minimization of Methane and Selected Aromatic Hydrocarbons Emissions from Municipal Landfill in Biofilters – a Field Study. *Rocznik Ochrona Środowiska, 17*, 1053-1073.

Ślad węglowy jako narzędzie w lokalnym planowaniu gospodarki niskoemisyjnej w Polsce

Abstract

Based on the analysis of 48 local plans for a low carbon economy, adopted for implementation by randomly selected communes of various specificity, the assessment of the role and importance of carbon footprint as a tool in local planning of low carbon economy at local levels in Poland was carried out. The methodology of the inventory of greenhouse gas emissions applied in these documents was evaluated. On the basis of the results of the inventory of greenhouse gases presented in the studied plans, the estimation of carbon footprint was carried out for the individual municipalities, which was expressed in carbon dioxide equivalent. Furthermore, statistical and comparative analyzes were carried out. There were significant differences in the size of the carbon footprint in the individual municipalities and sectors, resulting mainly from the non-uniform methodological assumptions. Global values range from 17.3 thousand Mg CO_2eq/year to 436.4 thousand Mg CO_2eq/year (with an average of 131.1 thousand Mg CO_2eq/year and a standard deviation of 91.6 thousand Mg CO_2eq/year), while per capita from 2.9 Mg CO_2eq to 31.5 Mg CO_2eq (with an average of 6.6 Mg CO_2eq and a standard deviation of 4.5 Mg CO_2eq). Having compared the size of the carbon footprint in the analyzed municipalities with the calculations carried out for the Starogard county, which is under a pilot program of low carbon development, as well as estimate values for Poland, presented in national and international reports on CO_2 emissions, it was found that in most cases, the values are underestimated, which makes it difficult to identify the main sources of emissions and hence the implementation of effective low carbon policy at the local level in Poland.

Streszczenie

W oparciu o analizę 48 lokalnych planów gospodarki niskoemisyjnej, przyjętych do realizacji przez losowo wybrane gminy o zróżnicowanej charakterystyce, dokonano oceny roli i znaczenia śladu węglowego jako narzędzia w planowaniu gospodarki niskoemisyjnej na poziomie lokalnym w Polsce. Ocenie poddano zastosowaną w tych dokumentach metodologię inwentaryzacji emisji gazów cieplarnianych. W oparciu o przedstawione w badanych planach wyniki inwentaryzacji gazów cieplarnianych, dokonano obliczeń śladu węglowego w poszczególnych gminach, wyrażonego w ekwiwalencie dwutlenku węgla. Przeprowadzono również analizy statystyczne i porównawcze. Stwierdzono znaczne zróżnicowanie wielkości śladu węglowego w poszczególnych gminach i sektorach, wynikające przede wszystkim z niejednolitych założeń metodologicznych. Wartości globalne wahają się od 17.3 tys. Mg CO_2eq/rok do 436.4 tys. Mg CO_2eq/rok (przy średniej 131.1 tys. Mg CO_2eq/rok i odchyleniu standardowym 91.6 tys. Mg CO_2eq/rok), natomiast per capita od 2.9 Mg CO_2eq do 31.5 Mg CO_2eq (przy średniej 6.6 Mg CO_2eq i odchyleniu standardowym 4.5 Mg CO_2eq). Z porównania wielkości śladu węglowego w analizowanych gminach z obliczeniami przeprowadzonymi dla powiatu starogardzkiego, objętego pilotażowym programem niskowęglowego rozwoju, a także szacunkowymi wielkościami dla Polski, prezentowanymi w krajowych i międzynarodowych raportach dotyczących emisji CO_2, stwierdzono iż w większości przypadków są to wartości niedoszacowane, co utrudnia identyfikację głównych źródeł emisji oraz realizację skutecznej polityki niskowęglowej na poziomie lokalnym w Polsce.

Słowa kluczowe:
ślad węglowy, inwentaryzacja emisji, gazy cieplarniane, ekwiwalent dwutlenku węgla, plany gospodarki niskoemisyjnej

Keywords:
carbon footprint, emission inventory, greenhouse gases, carbon dioxide equivalent, low carbon economy plans

MIDDLE POMERANIAN SCIENTIFIC SOCIETY OF THE ENVIRONMENT PROTECTION
ŚRODKOWO-POMORSKIE TOWARZYSTWO NAUKOWE OCHRONY ŚRODOWISKA

Annual Set The Environment Protection
Rocznik Ochrona Środowiska

Volume/Tom 19. Year/Rok 2017 ISSN 1506-218X 355-369

Adsorption of Halogenophenols from Aqueous Solutions on Activated Carbon

Krzysztof Kuśmierek[*], *Katarzyna Bieniek*[*], *Lidia Dąbek*[**], *Andrzej Świątkowski*[*]
[*]*Military University of Technology, Warsaw*
[**]*Kielce University of Technology*

1. Introduction

The increase in industrial activity has led to the production of environmental impurities which are dangerous to the ecosystem and human health. Phenol and its derivatives are common water contaminants, which are generated by coal conversion, petrochemical, pharmaceutical, paper and pesticide producing industries. The toxicity and environmental impact of these compounds can vary depending upon the number, type and position of substituent groups on the phenol ring. Phenolic compounds impart an unpleasant taste and odor to drinking water. Many of them are not only toxic at lower concentrations but are also suspected carcinogens and endocrine disrupting chemicals (Michałowicz and Duda, 2007). Therefore, the removal of these compounds from an environment is necessary. Several methods are currently used for the removal of phenolic compounds from aqueous solutions. These methods have been classified in two principal categories: non-destructive processes e.g. adsorption, and destructive processes such as biodegradation, oxidation by Advanced Oxidation Processes, photochemical oxidation, photocatalytic oxidation (Pera-Titus et al., 2004) as well as catalytic hydrodechlorination (HDC) of chlorophenols based on the reductive cleavage of a C–Cl bond by highly reactive atomic hydrogen (Xia et al., 2009; Witońska et al., 2014).

The destructive methods, however, are often relatively expensive or do not provide complete mineralization. They can also generate toxic

decomposition intermediates, often more dangerous than the starting compound. The adsorption process by solid adsorbents is one of the most efficient methods for the removal of organic contaminants from water (Dąbrowski et al., 2005; Bansal and Goyal, 2009). Adsorption is attractive for its relative flexibility and simplicity of design, low cost, ease of operation as well as the no or low generation of toxic substances. Activated carbons are now the most commonly used adsorbents of proven adsorption efficiency for organic pollutants.

In this study, the adsorption of halogenated phenols including 4-fluorophenol (4-FP), 4-chlorophenol (4-CP) and 4-bromophenol (4-BP) from aqueous solution on powdered activated carbon was investigated. The kinetic studies and adsorption isotherms were studied and the results were analyzed by applying conventional theoretical models. The effect of solution pH on the adsorption was also investigated.

2. Materials and methods

The 4-fluorophenol (4-FP) was from PCR Incorporated (Gainesville, USA), 4-chlorophenol (4-CP) was from Sigma-Aldrich (St. Louis, USA) and 4-bromophenol (4-BP) was from Alfa Aesar (Karlsruhe, Germany). The physicochemical properties and molecular structures of the selected compounds are given in Table 1. The hydrochloric acid and sodium hydroxide were obtained from Avantor Performance Materials (Gliwice, Poland). As adsorbent the powdered activated carbon SX2 (Norit, The Netherlands) was chosen. Prior to use, the activated carbon was dried in an oven at 130°C to constant weight and stored in a desiccator until use. The BET surface area of the activated carbon was obtained on the basis determined low-temperature adsorption-desorption isotherms (ASAP 2020, Micromeritics, Norcross, USA).

The adsorption experiments were carried out in an Erlenmeyer flasks. For each time 0.02 g of the activated carbon and 0.04 L of 4-FP, 4-CP or 4-BP solutions were mixed and then shaken (200 rpm). After an appropriate time the solutions were filtered and concentration of the adsorbates was measured using a UV-Vis spectrophotometer (Carry 3E, Varian, USA) at the wavelengths of 270, 274 and 276 nm, which correspond to the maximum absorption peaks of the 4-FP, 4-CP or 4-BP, respectively. The calibration curves for the phenolic compounds were linear in the studied ranges (from 0.05 to 1.5 mmol/L) with correlation coef-

ficients (R^2) better than 0.998. The equations for the regression line (n = 3) were: $y = 1.977x + 0.080$ for 4-fluorophenol, $y = 1.362x + 0.032$ for 4-chlorophenol and $y = 1.262x + 0.010$ for 4-bromophenol (where y is the absorbance and x is the concentration of the adsorbate).

Table 1. Physicochemical properties of the halogenophenols
Tabela 1. Właściwości fizykochemiczne halogenofenoli

Compound	Chemical structure	Molecular weight	Solubility in water at 20°C (mg/L)	pK_a	$logK_{ow}$
4-fluorophenol	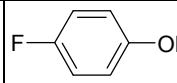	112.10	12.5	9.91	1.77
4-chlorophenol	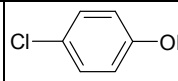	128.56	24.0	9.30	2.39
4-bromophenol	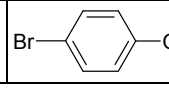	173.01	14.0	9.17	2.59

The kinetic studies were conducted for initial concentration of the phenols 1.0 mmol/L. The amount of adsorption at time t, q_t (mmol/g), was calculated by the equation:

$$q_t = \frac{(C_0 - C_t)V}{m} \tag{1}$$

where C_0 and C_t are the initial concentration and adsorbate concentration at time t (mmol/L), m is the mass of the adsorbent (g) and V is the volume of the solution (L).

In adsorption isotherm studies, the solutions of adsorbates with different initial concentrations (from 0.5 to 2.0 mmol/L) were added to an Erlenmeyer flasks containing 0.02 g of the activated carbon and shaken for 6 hours. The uptake of the adsorbates at equilibrium, q_e (mmol/g), was calculated by the following equation:

$$q_e = \frac{(C_0 - C_e)V}{m} \tag{2}$$

where: C_e is equilibrium concentration of adsorbates (mmol/L) in solution.

The effect of pH on the adsorption of halogenated phenols onto activated carbon was studied by varying the initial pH of the solutions from pH 2 to 11. The pH was adjusted (prior to the addition of the adsorbent) using 0.1 mol/L HCl or 0.1 mol/L NaOH and was measured using pH meter. The initial concentration of 4-FP, 4-CP and 4-BP was fixed at 1.0 mmol/L.

All of the experiments were carried out in duplicate, and the average values were used for further calculations. The experimental error being around 5% (mean value).

3. Results and discussion

3.1. Adsorbents characterization

Fig. 1 shows the adsorption-desorption isotherm of nitrogen at 77.4 K on the SX2 activated carbon. The specific surface area was calculated from the Brunauer-Emmett-Teller equation and was found to be 890 m^2/g. The micropore volume V_{mi} and mesopore volume V_{me} were 0.370 and 0.242 cm^3/g, respectively. The point of zero charge (pH_{PZC}) of the activated carbon was measured elsewhere (Dąbek et al., 2016) and was found to be 7.15.

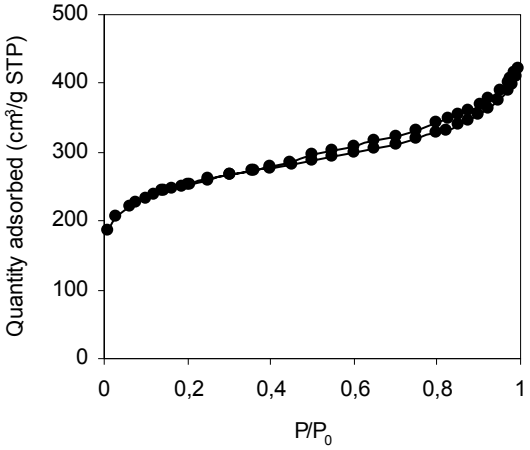

Fig. 1. Nitrogen adsorption-desorption isotherm of Norit SX2 activated carbons at 77.4 K

Rys. 1. Izoterma adsorpcji-desorpcji azotu na węglu aktywnym Norit SX2 w temperaturze 77,4 K

3.2. Kinetic studies

The adsorption kinetic curves of the 4-FP, 4-CP and 4-BP are shown in Fig. 2. As can be seen, the adsorption equilibriums were achieved after about 60 min.

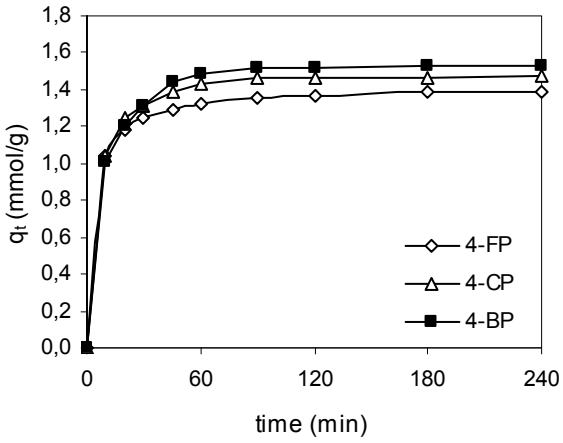

Fig. 2. Adsorption kinetics of the halogenated phenols on Norit SX2 activated carbon
Rys. 2. Kinetyka adsorpcji halogenofenoli na węglu aktywnym Norit SX2

For the description of the experimental data the pseudo-first order (Lagergren, 1898) and pseudo-second order (Ho and McKay, 1999) kinetic models were used. The pseudo-first order equation has the form:

$$\frac{dq_t}{dt} = k_1(q_e - q_t) \tag{3}$$

where k_1 is the pseudo-first order rate constant (1/min).

After integration and applying the initial conditions the integrated form of the Eq. 3 becomes:

$$\log(q_e - q_t) = \log q_e - \frac{k_1}{2.303}t \tag{4}$$

The values of k_1 were obtained from the intercept and the slope of the linear plot of $\log(q_e - q_t)$ versus t.

The pseudo-second order kinetic model is expressed in the form:

$$\frac{dq_t}{dt} = k_2(q_e - q_t)^2 \quad (5)$$

where k_2 is the pseudo-second order rate constant (g/mmol·min).

Integrating the Eq. 5 and applying the initial conditions we have:

$$\frac{t}{q_t} = \frac{1}{k_2 q_e^2} + \frac{1}{q_e} t \quad (6)$$

The rate constants of the pseudo-second order adsorption (k_2) were calculated from the straight line plots of t/q_t vs. t.

The kinetic parameters for the adsorption of the phenolic compounds on the SX2 activated carbon are presented in Table 2. As can be seen, the correlation coefficients for the pseudo-first order kinetic model are relatively low, whereas the R^2 values for the pseudo-second order kinetic model are higher than 0.997. This indicates that the adsorption system belongs to the pseudo-second order kinetic model. The k_2 values were 0.202, 0.186 and 0.153 g/mmol·min, for 4-FP, 4-CP and 4-BP, respectively. The adsorption rate followed the sequence: 4-bromophenol < 4-chlorophenol < 4-fluorophenol.

Table 2. The pseudo-first order and pseudo-second order kinetic parameters for 4-FP, 4-CP and 4-BP adsorption on the activated carbon
Tabela 2. Parametry kinetyczne równań pseudo 1. i pseudo 2. rzędu opisujące kinetykę adsorpcji 4-FP, 4-CP i 4-BP na węglu aktywnym

Adsorbate	pseudo-first order		pseudo-second order	
	k_1 (1/min)	R^2	k_2 (g/mmol·min)	R^2
4-FP	0.028	0.901	0.202	0.999
4-CP	0.025	0.892	0.186	0.998
4-BP	0.017	0.911	0.153	0.998

In order to investigate the mechanism of the adsorption, the intra-particle diffusion model (Weber and Morris, 1963) was used. The intra-particle diffusion equation is described as:

$$q_t = k_i t^{0.5} + C_i \quad (7)$$

where: k_i is the intra-particle diffusion rate constant (mmol/g·min$^{-0.5}$) and C_i is the thickness of the boundary layer (mmol/g). Both constants were determined experimentally from the slope and intercept of plot q_t versus $t^{0.5}$ (Fig. 3).

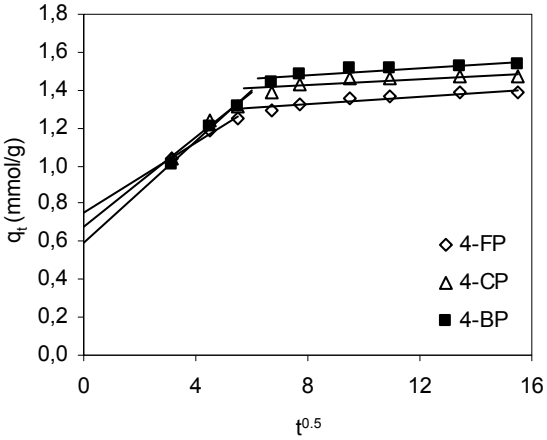

Fig. 3. Intra-particle diffusion kinetics for adsorption of phenols from aqueous solutions
Rys. 3. Kinetyka dyfuzji wewnątrzcząstkowej opisująca adsorpcję fenoli z roztworów wodnych

If the plot of q_t vs. $t^{0.5}$ passes through the origin, then the rate limiting process is only due to the intra-particle diffusion. If the plot is linear, then the diffusion is involved in the entire adsorption process (Lorenc-Grabowska et al., 2013). As shown in Fig. 3, none of the lines passed through the origin. This indicates that the intra-particle diffusion was not the only rate-controlling step. Moreover, the plots were not linear over the whole time range, suggesting that more than one process affected the adsorption. Similar adsorption mechanism of 4-chlorophenol was observed on the multi-walled carbon nanotubes (Kuśmierek & Świątkowski, 2015a; Kuśmierek et al., 2015; Strachowski & Bystrzejewski, 2015), carbon-encapsulated iron nanoparticles (Strachowski & Bystrzejewski, 2015), carbon black (Kuśmierek et al., 2015) and various activated carbons including Filtrasorb 400 (Kuśmierek and Świątkowski, 2015a), L2S Ceca (Kuśmierek et al., 2015), Sigma-Aldrich AC (Strachowski & Bystrzejewski, 2015), Norit ROW 0.8 Supra (Reczek et al., 2017) and modified granular activated carbon Norit R3ex (Kuśmierek et al., 2015).

3.3. Equilibrium studies

The adsorption isotherms of the 4-FP, 4-CP and 4-BP on the SX2 activated carbon are shown in Fig. 4. Two isotherm models (Freundlich,

1906 and Langmuir, 1916) were used to test the fitting of the experimental data. The Freundlich isotherm is widely applied for sorption surfaces with nonuniform energy distribution while the Langmuir isotherm is employed to monolayer adsorption.

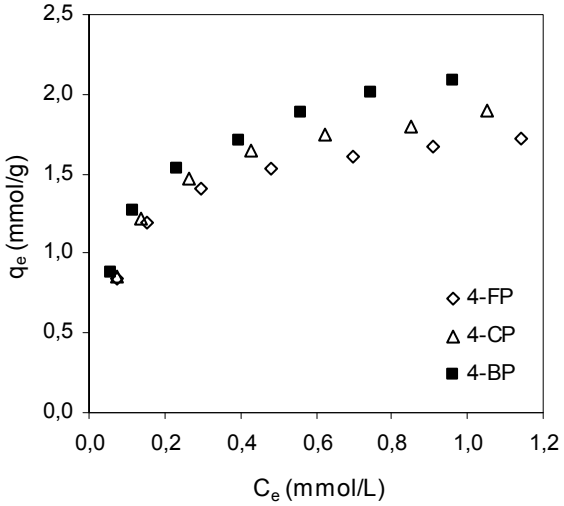

Fig. 4. Adsorption isotherms of halogenated phenols on Norit SX2 activated carbon
Rys. 4. Izotermy adsorpcji halogenofenoli na węglu aktywnym Norit SX2

The Freundlich isotherm is described by the formula:

$$q_e = K_F C_e^{1/n} \tag{8}$$

which can be converted to a linear form:

$$\ln q_e = \ln K_F + \frac{1}{n} \ln C_e \tag{9}$$

where K_F ((mmol/g) (L/mmol)$^{1/n}$) and n are the Freundlich equation constants which relate to adsorption capacity and adsorption intensity of the adsorbent. These constants were calculated from the intercept and slope of lnq_e vs. lnC_e plot.

The Langmuir isotherm is expressed as follows:

$$q_e = \frac{q_m b C_e}{1 + b C_e} \tag{10}$$

after conversion to a linear form the Eq. 10 becomes:

$$\frac{C_e}{q_e} = \frac{1}{q_m} C_e + \frac{1}{q_m b} \tag{11}$$

where q_m (mmol/g) is a monolayer adsorption capacity, and b (L/mmol) is the equilibrium adsorption constant. The values of the q_m and b were calculated from the intercept and slope of C_e/q_e vs. C_e plot.

The Freundlich and Langmuir adsorption isotherm model parameters as well as the correlation coefficients R^2 for the adsorption of the halogenated phenols on the activated carbon are listed in Table 3. The linear regression correlation coefficient values show that the equilibrium data obtained for all of the adsorbents were well represented by both models, nevertheless, a higher R^2 values (≥ 0.998) were observed for the Langmuir equation. The values of the Langmuir maximum adsorption capacity (q_m) as well as the Freundlich constant K_F increased in the order: 4-FP < 4-CP < 4-BP. The adsorption efficiency increased with respective increase in the molecular weight and octanol-water partition coefficient of the phenols.

Table 3. Parameters of the Freundlich and Langmuir adsorption isotherm models for the halogenated phenols
Tabela 3. Parametry równań izoterm Freundlicha i Langmuira opisujące adsorpcję halogenofenoli

Adsorbate	Freundlich			Langmuir		
	K_F (mmol/g) $(L/mmol)^{1/n}$	n	R^2	q_m (mmol/g)	b (L/mmol)	R^2
4-FP	1.493	0.188	0.986	1.603	12.04	0,998
4-CP	1.847	0.234	0.978	1.834	12.68	0.999
4-BP	1.927	0.261	0.968	2.004	10.51	0.999

The adsorption of the 4-CP on activated carbon was investigated by many authors. The Langmuir adsorption capacity (q_m) for the adsorption of 4-CP onto various activated carbons are presented in Table 4. As can be seen, the adsorption capacity of the SX2 activated carbon is more or less comparable with other adsorbents. Only a few papers describe the adsorption of 4-bromophenol and 4-fluorophenol. Bhatnagar (2007) studied the adsorption of 4-bromophenol from water on the activated carbon

obtained from Merck (S_{BET} = 710 m^2/g), activated carbon slurry waste (S_{BET} = 380 m^2/g), activated blast furnace sludge (S_{BET} = 28 m^2/g) and activated blast furnace dust (S_{BET} = 13 m^2/g). The maximum adsorption of the 4-BP was 0.502, 0.235, 0.073 and 0.055 mmol/g, respectively. Anbia and Amirmahmoodi (2011) investigated the adsorption of 4-bromophenol and 4-chlorophenol on untreated (SBA-15) and amino functionalized (NH_2-SBA-15) mesoporous silica materials. They found that the uptake of 4-chlorophenol was higher than 4-bromophenol. The Langmuir adsorption constants for adsorption of 4-CP and 4-BP were 0.447 and 0.185 mmol/g for SBA-15, and 1.633 and 0.647 mmol/g for NH_2-SBA-15, respectively. Recently, Oh and Seo (2016) studied the adsorption of pharmaceuticals and halogenated phenols including 4-FP, 4-CP and 4-BP on graphite powder (Aldrich), charcoal-based granular activated carbon (DC Chemical) and five types of biochar. The maximum adsorption capacity of the activated carbon (S_{BET} = 738.8 m^2/g) was found to be 1.133 mmol/g for 4-FP, 1.580 mmol/g for 4-CP and 0.988 mmol/g for 4-BP (4-BP < 4-FP < 4-CP).

Table 4. Comparison of 4-chlorophenol adsorption on various activated carbons
Tabela 4. Porównanie adsorpcji 4-chlorofenolu na różnych węglach aktywnych

Activated carbon	S_{BET} (m^2/g)	Adsorption capacity, q_m (mmol/g)	Reference
Norit SX2	890	1.834	this study
modified Norit R3ex	1530	3.004	Kuśmierek et al., 2015
Gryfskand CXZ 2	977	2.505	Lorenc-Grabowska et al., 2010
Sigma-Aldrich AC	1187	2.178	Strachowski and Bystrzejewski, 2015
Prolabo AC	929	1.980	Hamdaoui and Naffrechoux, 2007
L2S Ceca	925	1.981	Kuśmierek et al., 2015
DC Chemical AC	739	1.580	Oh and Seo, 2016
F-400	997	1.537	Kuśmierek and Świątkowski, 2015a
AC from rattan sawdust	1083	1.468	Hameed et al., 2008

3.4. Influence of solution pH

The pH of the solution is an important parameter as it strongly affects the surface charge of the adsorbent as well as the degree of ionization and speciation of adsorbate. The effect of the initial solution pH on the adsorption equilibrium of the halogenated phenols was studied in the range of 2 to 11 and the results are presented in Fig. 5.

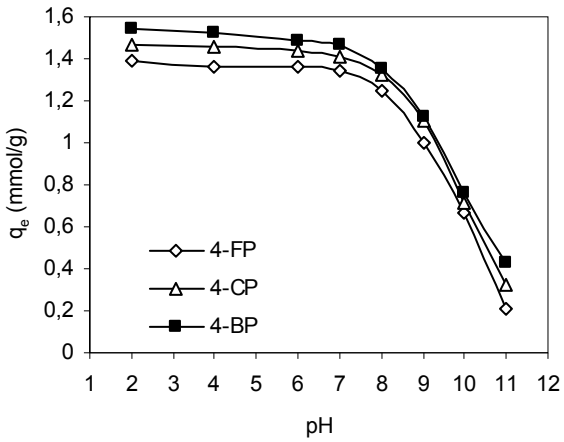

Fig. 5. The influence of the pH on the adsorption of phenols on the Norit SX2 activated carbon
Rys. 5. Wpływ pH na adsorpcję fenoli na węglu aktywnym Norit SX2

The data indicate that the adsorption behavior of the adsorbates on the activated carbon was similar. The adsorption of the phenols was almost constant at acidic pH range from 2 to 7 and decreased with the further increasing in the pH (from pH 7 to 11). In the pH range of 2-7, the surface of the activated carbon was positively charged ($pH_{PZC} = 7.15$), while at a pH greater than pH_{PZC}, the surface had a net negative charge. The pK_a of 4-FP, 4-CP and 4-BP is 9.91, 9.30 and 9.17, respectively. At a pH greater than the pK_a value, the adsorbates existed predominantly in anionic forms as negatively charged phenoxide ions. The results presented in Fig. 5 suggested that the non-dissociated forms of the phenols were preferred by the positively charged surface of the adsorbent. The large reduction in the adsorption at highly basic conditions can be attributed to the electrostatic repulsion between the negatively charged adsorbent sur-

face and the dissociated molecules of the adsorbates. A similar results were reported for the adsorption of 4-CP onto activated carbon prepared from rattan sawdust (Hameed et al., 2008) and Norit R3-ex granular activated carbon (Kuśmierek and Świątkowski, 2015b).

4. Conclusions

This study investigated the adsorption of 4-fluorophenol, 4-chlorophenol and 4-bromophenol from aqueous solutions on the powdered activated carbon. The adsorption kinetics was better represented by the pseudo-second order model. The adsorption rate increased in the order: 4-BP < 4-CP < 4-FP. The adsorption isotherms of the phenols were analyzed using the Freundlich and Langmuir models. The experimental data received were found to be well described by the Langmuir isotherm equation. The adsorption efficiency increased in the order: 4-FP < 4-CP < 4-BP. The adsorption was strongly pH dependent. The adsorption of the phenols was almost constant at acidic environment and decreased significantly at basic conditions.

References

Anbia, M., Amirmahmoodi, S. (2011). Adsorption of phenolic compounds from aqueous solutions using functionalized SBA-15 as a nano-sorbent. *Scientia Iranica C*, *18(3),* 446-452.

Bansal, R.C., Goyal, M. (2009) *Adsorpcja na węglu aktywnym.* Warszawa: Wydawnictwo Naukowo-Techniczne.

Bhatnagar, A. (2007). Removal of bromophenols from water using industrial wastes as low cost adsorbents. *Journal of Hazardous Materials*, *B139,* 93-102.

Dąbek, L., Kuśmierek, K., Świątkowski, A. (2016). Adsorpcja fenoli z roztworów wodnych na pylistych węglach aktywnych. *Inżynieria i Ochrona Środowiska*, *19(2),* 217-226.

Dąbrowski, A., Podkościelny, P., Hubicki, Z., Barczak, M. (2005). Adsorption of phenolic compounds by activated carbon-a critical review. *Chemosphere, 58*, 1049-1070.

Freundlich, H.M.F. (1906). Über die adsorption in lösungen. *Zeitschrift für Physikalische Chemie*, *57,* 385-470.

Hamdaoui, O., Naffrechoux, E. (2007). Modeling of adsorption isotherms of phenol and chlorophenols onto granular activated carbon. Part I. Two-parameter models and equations allowing determination of thermodynamic parameters. *Journal of Hazardous Materials*, *147,* 381-394.

Hameed, B.H., Chin, L.H., Rengaraj, S. (2008). Adsorption of 4-chlorophenol onto activated carbon prepared from rattan sawdust. *Desalination*, *225*, 185-198.

Ho, Y.S., McKay, G. (1999). Pseudo-second-order model for sorption processes. *Process Biochemistry, 34*, 451-465.

Kuśmierek, K., Sankowska, M., Skrzypczyńska, K., Świątkowski, A. (2015). The adsorptive properties of powdered carbon materials with a strongly differentiated porosity and their applications in electroanalysis and SPME-GC. *Journal of Colloid and Interface Science*, *446*, 91-97.

Kuśmierek, K., Świątkowski, A. (2015a). Influence of pH on adsorption kinetic of monochlorophenols from aqueous solutions on granular activated carbon. *Ecological Chemistry and Engineering S*, *22(1),* 95-105.

Kuśmierek, K., Świątkowski, A. (2015b). The influence of an electrolyte on the adsorption of 4-chlorophenol onto activated carbon and multi-walled carbon nanotubes. *Desalination and Water Treatment, 56,* 2807-2816.

Lagergren, S. (1898). Theorie der sogenannten adsorption geloester stoffe. *Vetenskapsakademiens Handlingar*, *24,* 1-39.

Langmuir, I. (1916). The constitution and fundamental properties of solids and liquids. *Journal of the American Chemical Society*, *38,* 2221-2295.

Lorenc-Grabowska, E., Gryglewicz, G., Diez, M.A. (2013). Kinetics and equilibrium study of phenol adsorption on nitrogen-enriched activated carbons. *Fuel*, *114*, 235-243.

Lorenc-Grabowska, E., Gryglewicz, G., Machnikowski, J. (2010). p-Chlorophenol adsorption on activated carbons with basic surface properties. *Applied Surface Science*, *256,* 4480-4487.

Michałowicz, J., Duda, W. (2007). Phenols – sources and toxicity. *Polish Journal of Environmental Studies, 16(3),* 347-362.

Oh, S.Y., Seo, Y.D. (2016). Sorption of halogenated phenols and pharmaceuticals to biochar: affecting factors and mechanisms. *Environmental Science and Pollution Research*, *23,* 951-961.

Pera-Titus, M., Garcia-Molina, V., Baños, M.A., Giménez, J., Esplugas, S. (2004). Degradation of chlorophenols by means of advanced oxidation processes: a general review. *Applied Catalysis B: Environmental*, *47,* 219-256.

Reczek, L., Michel, M.M., Kuśmierek, K., Świątkowski, A., Siwiec, T. (2017). Sorption of 4-chlorophenol and lead(II) on granular activated carbon: equilibrium, kinetics and thermodynamics. *Desalination and Water Treatment*, *62,* 369-376.

Strachowski, P., Bystrzejewski, M. (2015). Comparative studies of sorption of phenolic compounds onto carbon-encapsulated iron nanoparticles, carbon nanotubesand activated carbon. *Colloids and Surfaces A*, *467*, 113-123.

Weber, Jr. W., Morris, J. (1963). Kinetics of adsorption on carbon from solution, *Journal of the Sanitary Engineering Division*, *18,* 31-42.

Witońska, I.A., Walock, M.J., Binczarski, M., Lesiak, M., Stanishevsky, A.V., Karski, S. (2014). Pd-Fe/SiO_2 and Pd-Fe/Al_2O_3 catalysts for selective hydrodechlorination of 2,4-dichlorophenol into phenol. *Journal of Molecular Catalysis A: Chemical, 393*, 248-256.

Xia, C.H., Liu, Y., Zhou, S.W., Yang, C.Y., Liu, S.I., Xu, J., Yu, J.B., Chen, J.P., Liang, X.M. (2009). The Pd-catalyzed hydrodechlorination of chlorophenols in aqueous solutions under mild conditions: A promising approach to practical use in wastewater. *Journal of Hazardous Materials, 169*, 1029-1033.

Adsorpcja halogenofenoli z roztworów wodnych na węglu aktywnym

Streszczenie

Zbadano adsorpcję *para*-halogenopochodnych fenolu – 4-fluorofenolu (4-FP), 4-chlorofenolu (4-CP) oraz 4-bromofenolu (4-BP), z roztworów wodnych na pylistym węglu aktywnym Norit SX2. Zbadano kinetykę adsorpcji, adsorpcję w warunkach równowagowych oraz wpływ pH roztworu. Do opisu kinetyki adsorpcji zastosowano równania pseudo 1. rzędu, pseudo 2. rzędu oraz model dyfuzji wewnątrzcząstkowej. Stwierdzono, że kinetyka adsorpcji była najlepiej opisana równaniem pseudo 2. rzędu; najszybciej adsorbował się 4-fluorofenol, a najwolniej 4-bromofenol (4-FP > 4-CP > 4-BP). Do opisu adsorpcji w warunkach równowagowych zastosowano równania Freundlicha i Langmuira. Adsorpcję badanych fenoli najlepiej opisywał model izotermy Langmuira, dla którego uzyskano najwyższe wartości współczynników korelacji R^2. Obliczone wartości pojemności adsorpcyjnych q_m zwiększały się w kolejności 4-FP < 4-CP < 4-BP. Skuteczność adsorpcji fenoli była silnie zależna od pH roztworu.

Abstract

The adsorption of p-substituted halogenophenols – 4-fluorophenol (4-FP), 4-chlorophenol (4-CP) and 4-bromophenol (4-BP) from aqueous solutions on Norit SX2 powdered activated carbon was investigated. The adsorption kinetics, adsorption equilibrium as well as the effect of the solution pH were studied. The kinetic data were evaluated in terms of the pseudo-first order, pseudo-second order and intra-particle diffusion kinetic models. The adsorption kinetics was better represented by the pseudo-second order model. The adsorption rate decreased in the order: 4-FP > 4-CP > 4-BP. To describe the adsorption isotherms,

the Freundlich and Langmuir equations were applied. The Langmuir model provides the better correlation of the experimental data with higher R^2 values in comparison to the Freundlich equation. The values of the Langmuir maximum adsorption capacity (q_m) increased in the order: 4-FP < 4-CP < 4-BP. The results showed that the adsorption of the phenols was strongly pH dependent.

Słowa kluczowe:
adsorpcja, węgiel aktywny, 4-fluorofenol, 4-chlorofenol, 4-bromofenol

Keywords:
adsorption, activated carbon, 4-fluorophenol, 4-chlorophenol, 4-bromophenol

MIDDLE POMERANIAN SCIENTIFIC SOCIETY OF THE ENVIRONMENT PROTECTION
ŚRODKOWO-POMORSKIE TOWARZYSTWO NAUKOWE OCHRONY ŚRODOWISKA

Annual Set The Environment Protection
Rocznik Ochrona Środowiska

Volume/Tom 19. Year/Rok 2017 ISSN 1506-218X 370-393

Analysis of the Influence of a Hybrid Constructed Wetland Wastewater Treatment Plant on the Water Quality of the Receiver

Magdalena Gizińska-Górna, Krzysztof Jóźwiakowski, Michał Marzec, Aneta Pytka, Bożena Sosnowska, Monika Różańska-Boczula, Agnieszka Listosz
University of Life Sciences, Lublin

1. Introduction

The continuous development of civilization leads to the growth of human impact on aquatic environments. The concentrations of contaminants washed every day into rivers, lakes and coastal waters constantly increase, which poses a huge threat to these receivers. In extreme cases, pollutants may kill all organic life forms in a body of water, depriving it of all its self-cleaning abilities (Owczarczyk 2001, Gajewska et al. 2013).

Surface water are still an important source of water for large settlements and industry. That is why high levels of pollution create not only technical problems connected with water purification for technological and food and beverage applications but also generate secondary threats associated with the growing possibility that drinking water, fish and water for industrial aims may contain many different contaminants (Owczarczyk 2001).

The discharge of industrial and domestic wastewater into surface water seriously increases the level of their pollution (Andrulewicz 1997, Chen et al. 2004, Elhatip & Güllü 2005, Kowalkowski & Buszewski 2006). The constantly growing costs connected with wastewater treatment and water purification for consumption trigger more and more interest in studies concerning the interactions between sewage and receivers (Owczarczyk 2001).

Taking effective action in the field of water protection requires, besides the understanding of the wastewater treatment process, good transport and dilution of pollutants in natural water receivers. A body of running water can only be used as a receiver of treated wastewater when sewage outflow does not interfere with the biological functioning of the ecosystem. The choice of the receiver depends on its absorbency, i.e. the ability to take in a specific volume of effluents, and the load of pollutants. The load of pollutants should not restrict the process of water self-cleaning, because the receiver is involved in further steps of wastewater treatment (Juszkiewicz et al. 2006). The speed of mixing sewage with river water depends on the quantity of sewage, the volume of water and the speed of water flow, as well as the width and depth of the watercourse (Rajda & Kanownik 2007).

Numerous studies indicate that effluents from municipal wastewater treatment plants have some impact on the quality of water in sewage river-receivers, but not always so negative as to change their ecological status (Mosiej et al. 2007, Frąk 2010, Królak et al, 2011, Lewandowska-Robak et al. 2011, Wira 2011, Wiatkowski 2012, Policht-Latawiec et al. 2014). In recent years, more and more constructed wetland wastewater treatment plants have been used worldwide, often in order to protect water quality (Kivaisi 2001, Zhang et al. 2009, Gizińska et al. 2012, Avila et al. 2013, Jóźwiakowski et al. 2014, Gizińska-Górna et al. 2016). It has been found that their use complies with the principles of sustainable development (Jóźwiakowski et al. 2015). To date, however, not many studies have been devoted to the impact of wetland wastewater treatment plants on the quality of water in the receiving bodies of water. The aim of this work was to determine the impact of treated wastewater discharged from a hybrid constructed wetland wastewater treatment plant on the quality of water in the receiver (the Urzędówka River).

2. Methods

2.2. Study site

The Urzędówka River is a right tributary of the Wyżnica River, which, in turn, is a first class tributary of the Vistula River, km 318 + 500. The source of the Urzędówka River lies near Wilkołaz Village in Kraśnik county, and the estuary of the Wyżnica River is located in

Dzierzkowice Village (Wojciechowski 1972). The valley of the Urzędówka River lies in the Urzędowskie Hills, in the western part of the Lublin Upland, in South-Eastern Poland. This is an area with an extremely low density of the river network. The basin and some dry forms of erosion cut deep into the loess cover, under which lies a chalk underlay of cracked rocks (Zielinski 2011). In the 1960s, the Urzędówka River was regulated, and the grassland in the valley was reclaimed by draining (Dobrzański & Turski 1972).

The Urzędówka is one of the cleanest rivers of the region, though in the report regarding the state of plain surface water bodies issued in 2014 by Provincial Inspectorate for Environmental Protection in Lublin, the condition of its waters was assessed as bad. In terms of the biological profile, the Urzędówka was assigned to class IV (poor status), and in terms of the hydromorphological and physico-chemical profiles to class II (good status). Overall, its ecological potential was defined as weak (Provincial Inspectorate for Environmental Protection 2015). The Urzędówka belongs to rivers with a low and relatively stable water flow across the year. States of water are not read here, which is why we used data from a water gauge in Bór Village 6+100 km of the Wyżnica River, where hydrological observations had been carried out since 1996 to determine the characteristics of flow. The average flow of water in the estuary of the Urzędówka River was estimated to be about 0.625m^3/s (Zielinski 2011).

The Urzędówka River is the receiver of treated wastewater outflowing from a hybrid constructed wetland wastewater treatment plant in Skorczyce. This plant is used for the treatment of domestic wastewater from a multi-family building and has an average throughput of 2.5 m^3/d. It consists of a concrete three-chamber initial septic tank with a pumping station (with a total volume of 8.64 m^3). The main part of this system is composed of two constructed wetland beds (Fig. 1). A first bed with Vertical Subsurface Flow (VSSF type) with an area of 96 m^2 and a depth of 0.8 m has been planted with giant miscanthus (*Miscanthus* × *giganteus* Greef et Deu.). A second bed with Horizontal Subsurface Flow (HSSF type) with an area of 80 m^2 and a depth of 1.2 m has been planted with Jerusalem artichoke (*Helianthus tuberosus* L.) (Jóźwiakowski et al. 2011, Gizińska-Górna et al. 2016). The place where treated wastewater is discharged into the river is located at 12 + 662 km (Fig. 1).

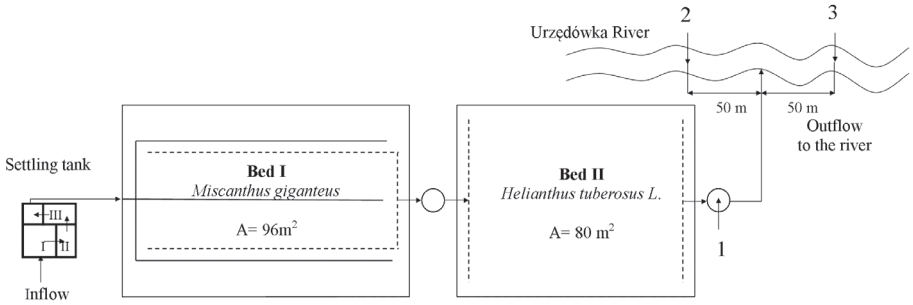

Fig. 1. Technological scheme of the hybrid constructed wetland wastewater treatment plant in Skorczyce (1, 2, 3 – sampling points of sewage to analysis) (Gizińska i in. 2012)
Rys. 1. Schemat technologiczny hybrydowej grutnowo-roślinnej oczyszczalni ścieków w Skorczycach (1, 2, 3 – punkty poboru prób do analiz)

Fot. 1. Urzędówka River – reciver of wastewater from the hybrid constructed wetland wastewater treatment plant in Skorczyce (fot. M. Gizińska)
Fot. 1. Rzeka Urzędówka – odbiornik ścieków oczyszczonych w Skorczycach (fot. M. Gizińska)

2.2. Experimental procedures

The influence of the hybrid constructed wetland wastewater treatment plant on the quality of water in the Urzędówka River was analyzed over a three-year period (2011-2013). The analyses of water and wastewater were carried out seasonally, at different times of the year: in winter (February), spring (May), summer (August), and autumn (October). Samples for analysis were taken at the outflow from the HF bed,

which, together with the drain collector, is the last element of the wastewater treatment plant. Samples of water from the Urzędówka River were taken at two points: 50 m downstream and 50 m upstream of the place where treated wastewater was discharged (Fig. 1). Sampling was done in accordance with the guidelines set out in the Polish Standards (PN-74\/C-04620\/00; PN-EN 25667-2:1999). In each series of experiments, the following parameters of collected water and wastewater were determined: temperature, pH, electrolytic conductance, concentration of dissolved oxygen, total suspension, BOD_5, COD_{cr}, concentration of total nitrogen, total phosphorus, nitrate nitrogen, nitrite nitrogen, ammonium nitrogen, sulfates, and chlorides.

2.3. Analytical methods

The analysis and the physico-chemical measurements of water and wastewater were according to the table of reference methods for the analysis of wastewater samples (Dz. U. 2009, nr 27, poz. 169 [Polish Journal of Laws 2009, no. 27, item 169]) and according to the reference methods for the analysis of samples of water (Dz. U. 2011, nr 257, poz. 1550). The quality of water in the Urzędówka River was compared with the requirements set out in the regulation of the Minister of the Environment of 9 November 2011 establishing the way of classifying the state of uniform parts of surface water and environmental quality standards for priority substances (Dz. U. 2011, nr 257, poz. 1550).

In 2013, four additional series of microbiological tests of water and wastewater were performed. The samples for the microbiological assays were taken in February, May, August, and November, in accordance with PN-74/C-04620/00 and PN-EN 25667-2:1999. Bacterial counts were performed for E. coli, fecal coliform bacteria, and fecal enterococci in accordance with the current standards (PN-C-04615-05:1975P; PN-C-04615-07:1977P; PN-C-04615-25:2008P). The results of the microbiological tests were compared to the requirements set out in the regulation of the Minister of the Environment of 11 February 2004 on the classification for presenting the status of surface water and groundwater and forms and methods of monitoring and interpreting the results and presenting the status of these waters (Dz. U. 2004 nr 32, poz. 284).

On the basis of test results, characteristic values (minimum, maximum, mean and standard deviation) of the analyzed pollution indicators were determined, and a statistical analysis was carried out. The effect of

the constructed wetland wastewater treatment plant on the quality of water was studied using a Shapiro-Wilk test followed by the nonparametric Wilcoxon matched-pairs signed-rank test. A dendrogram was constructed based on Euclidean distances using Ward's method, and k-means grouping was performed.

3. Results and discussion

In accordance with the regulation of the Minister of the Environment of 9 November 2011 (Dz. U. 2011, nr 258, poz. 1550), assignment of water to an appropriate class and its usefulness depend, among others, on biological and hydromorphological indicators, physico-chemical indicators, in particular salinity, acidification and nutrient conditions, and oxygen indicators. Monitoring of river waters carried out in the Lublin province in the year 2014 by the Provincial Inspectorate for Environmental Protection in Lublin, showed that the state of water in the Urzędówka River was poor. The river faced the threat of eutrophication of municipal origin and the ecological status of the river was identified as weak (Provincial Inspectorate for Environmental Protection 2015). It was supposed that one of the potential sources of these threats may be the constructed wetland wastewater treatment plant in Skorczyce.

The present study did not find any significant impact of the treated wastewater discharged from the hybrid constructed wetland wastewater treatment plant in Skorczyce on the quality of water in the Urzędówka River. This was an expected result, as the share of sewage flow in the total flow of the river was very small. The average flow of water (SSQ) at the measuring point Urzędówka – Skorczyce Bridge located at the outlet of the treated wastewater from the treatment plant, was about 0.457 m^3/s. The other characteristic flows, i.e. the medium low flow (SNQ) and the lowest flow (NNQ) were 0.242 m^3/s and 0.099 m^3/s, respectively (Structum SP. Z o.o. 2000; Zielinski, 2011). The designed wastewater treatment capacity was only 2.5 m^3/d, or about 0.00003 m^3/s, which represented 0.006% of the average flow of river water. In fact, due to the intensive transpiration from plants and beds, the volume of wastewater discharge from the treatment plant to the receiver was much smaller.

To investigate the effect of the Skorczyce treatment plant on the quality of water in the receiver, we used the nonparametric Wilcoxon matched-pairs signed-rank test, which made it possible to determine

whether the examined indicators of surface water quality differed significantly at two measuring points located on the Urzędówka River: upstream and downstream of the point of discharge of treated wastewater. The Wilcoxon test was selected because most of the analyzed parameters did not have a normal distribution, as determined by the Shapiro-Wilk test (Lewandowska-Robak et al. 2011). The results of the nonparametric test, which are shown in the table below, indicate that at the level of significance $\alpha = 0.05$, there was no significant difference between the investigated quality indicators of water collected upstream and downstream of the treatment plant outlet Table 1.

Table 1. The results of sequence pairs of Wilcoxon test (T) and p-value
Tabela 1. Wyniki sekwencyjnych par testu Wilcoxona (T) i wartości p

Parameters	T	Level p-value
Temperature	12.000	0.401
pH	24.000	0.721
Conductivity	15.000	0.374
Dissolved oxygen	24.000	0.721
TSS	22.000	0.575
BOD_5	20.000	0.767
COD	7.500	0.141
Ammonium	26.500	0.918
Nitrate	26.000	0.878
Nitrite	18.500	0.635
Total nitrogen	20.500	0.475
Total phosphorus	12.000	0.401
Chlorides	12.500	0.236
Sulphates	6.000	0.051

Further analysis was conducted using averaged values of the investigated indicators for three types of sample, (1) treated wastewater, (2) water collected from the river before the discharge of wastewater, and (3) water collected from the river after wastewater discharge. After standardization, the data were processed/analyzed using Ward's method, and a dendrogram was obtained on the basis of Euclidean distances (Fig. 2).

The dendrogram (Fig. 2) clearly shows two clusters. The first type of sample formed a distinct aggregation (cluster). The grouping performed by k-means (k = 2 clusters) demonstrated why this was the case.

A table 2 shows that the greatest impact on the separation of the first type of sample from the other two was exerted by a statistically significant influence (p value < 0.05) for the following indicators: oxygen, BOD5, nitrate nitrogen, nitrite nitrogen and total phosphorus.

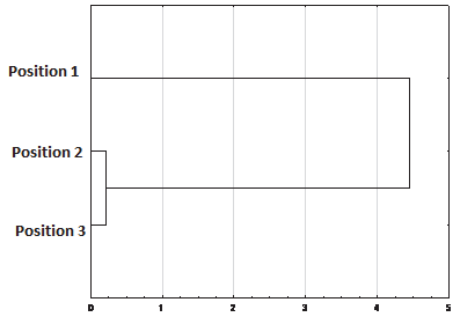

Fig. 2. Dendrogram
Rys. 2. Dendogram

Table 2. Analysis of variance (SS between – variability between clusters, df – degrees of freedom, SS variability within clusters, F – Fishera_Snedecora test)
Tabela 2. Analiza wariancji (SS pomiędzy - zmienność między klastrami, df - stopnie swobody, zmienność SS w obrębie klastrów, próba F – test Fishera_Snedecora)

Variable	SS between	df	SS within	df	F	P value
Temperature	1.237026	1	0.019795	1	62.49	0.080106
pH	0.096779	1	0.004135	1	23.41	0.129761
Dissolved oxygen	0.515685	1	0.000242	1	2128.54	0.013797
TSS	0.001840	1	0.000048	1	38.61	0.101582
BOD_5	0.000162	1	0.000000	1	18990.83	0.004620
CODcr	0.000600	1	0.000004	1	156.48	0.050784
$N\text{-}NO_2$	2.823230	1	0.000134	1	21095.28	0.004383
NO_3	1.983734	1	0.000819	1	2421.08	0.012936
N_{tot}	0.174237	1	0.000047	1	3731.85	0.010420

Both the temperature range and the average temperature of treated wastewater were very close to those of the water in the river (Table 3). Purification carried out in a ground-surface environment contributed to the cooling of treated wastewater, which was ultimately cooled down to ambient temperature when it passed through the 94 meter long outlet collector connecting the treatment plant with the receiver.

Together with the treated wastewater, about 17.4 mg/L of total suspended solids was drained to the Urzędówka River (Table 3). In the river, upstream of the discharge point, the average content of total suspended solids was 6.78 mg/L and downstream of this place we noted a slight increase in the concentration of total suspended solids to the average level of 8.58 mg/L (Table 3, Figure 3). In the case of mechanical pollutants, such as, it is difficult to talk about the impact of the hybrid constructed wetland wastewater treatment plant, because the result of the measurement may be reliant on a number of factors, e.g connected with the kinetics of water flow in the river or local eddies.

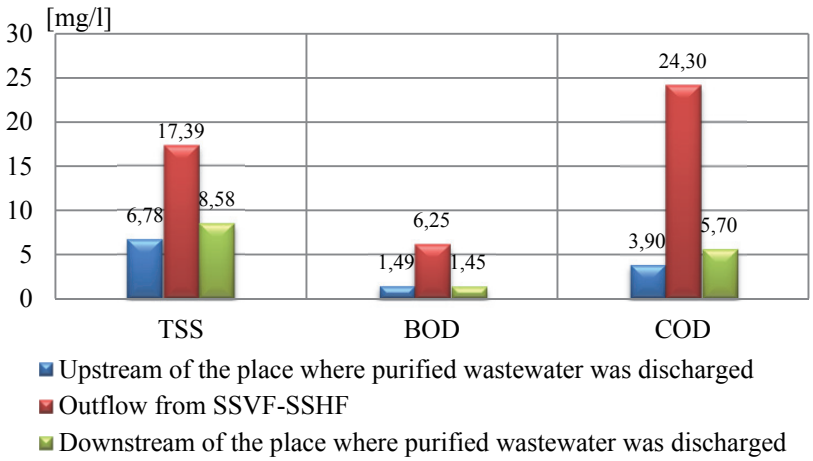

Fig. 3. Average values of pollutants in sewage discharged from the hybrid constructed wetland wastewater treatment plant and in water from Urzędówka River

Rys. 3. Średnie wartości zanieczyszczeń w ściekach odprowadzanych z hybrydowej gruntowo-roślinnej oczyszczalni ścieków komunalnych oraz w wodzie z rzeki Urzędówki

The average concentration of oxygen dissolved in treated wastewater was just over 6 mg $O_2 \cdot dm^{-3}$. The placement of the wastewater outlet high above the water surface of the receiver (Fig. 1) allowed additional oxygenation of sewage before it was mixed with river water. In the river, upstream and downstream of the discharge point, the ranges of oxygen concentration were similar at 8.98-12.80 mg O_2/L and 8.80-

12.24 mg O_2/L, respectively. The average oxygen contents at the measuring points differed only slightly (10.06 and 10.16 mg O_2/L, respectively) (Table 3) and were higher than the requirements for class I water purity (Dz. U. 2011, nr 258, poz. 1550).

The average value of BOD_5 in river water was constant over the distance between measuring points at about 1.5mg O_2/L. The concentration of BOD_5 in river water in all measuring series did not exceed the normative value specified for class I water purity (Dz. U. 2011, nr 258, poz. 1550). Treated wastewater, despite a clearly higher content of organic compounds (6.25 mg O_2/L) did not have a negative impact on the quality of water in the Urzędówka River (Table 3, Figure 3). This was due to the small participation of sewage in the total flow of the river and self-cleaning processes taking place in the surface water, especially the dilution of pollutants by the water from the receiver.

In the case of COD_{cr}, slightly larger fluctuations were observed. Upstream of the treated sewage outfall, the value of COD_{cr} was about 3.9 mg O_2/L, while downstream of this place, it was 5.7mg O_2/L (Table 3, Figure 3). Taking into consideration the fact that the average value of COD_{cr} in wastewater was 24.3 mg O_2/L, it can be stated that sewage may have had a small impact on the water in the receiver. Despite the fact that the quality of water in the Urzędówka River slightly deteriorated in terms of the concentration of organic pollutants (a 46% increase in COD_{cr}), the classification of the analyzed waters (class I) was not affected.

Indicators characterizing the salinity of water, i.e. conductivity, sulfates and chlorides, were not assayed in the treated sewage from the constructed wetland wastewater treatment plant; however, the regulation of the Minister of the Environment (Dz. U. 2011, nr 258, poz. 1550) makes it compulsory to analyze these indicators in surface water. In the investigated case, there was a slight increase in electrolytic conductivity and chlorides downstream of the outlet of the collector of the wastewater treatment plant. A study by Lewandowska-Robak et al. (2011) carried out in Kicz Creek in Tuchola shows that the changes in the concentration of chlorides may be a result of discharge of wastewater from treatment plants. The concentration of sulfates after wastewater disposal was slightly reduced. Average values of all three indicators upstream and downstream of the sewage discharge point were low compared to the values specified for high ecological status waters (class I) (Table 3).

Table 3. Selected physical and chemical indicators of purified sewage and water from Urzędówka River before and after the discharge of sewage from the hybrid constructed wetland wastewater treatment plant
Tabela 3. Skład fizyczno-chemiczny ścieków oczyszczonych oraz wód z rzeki Urzędówki przed i po dopływie ścieków z hybrydowej gruntowo-roślinnej oczyszczalni ścieków

Indicators	Purified sewage				Water from the river before discharge sewage				Water from the river after discharge sewage				The limit values*				
	min	max	$\bar{x}$	σ	min	max	$\bar{x}$	σ	min	max	$\bar{x}$	σ	I	II	III	IV	V
The indicators characterizing the physical condition, including thermal conditions																	
Temperature [°C]	10.60	20.80	**15.87**	**3.67**	10.70	20.40	**15.04**	**2.90**	9.60	20.70	**14.91**	**3.09**	≤22	≤24	Limits not determined		
TSS [mg·dm^{-3}]	2.04	65.10	**17.39**	**22.36**	1.20	14.20	**6.78**	**4.13**	0.70	25.00	**8.58**	**7.31**	≤25	≤50			
Indicators characterizing aerobic conditions (conditions oxygenation) and organic pollutants																	
Diss. oxygen [mg O_2·dm^{-3}]	1.27	11.42	**6.16**	**3.22**	8.98	12.80	**10.06**	**1.36**	8.81	12.24	**10.16**	**1.25**	≥7	≥5	Limits not determined		
BOD_5 [mg O_2·dm^{-3}]	0.78	36.90	**6.25**	**10.82**	0.41	2.40	**1.49**	**0.54**	0.17	2.40	**1.45**	**0.61**	≤3	≤6			
CODcr [mg O_2·dm^{-3}]	8.00	43.00	**24.30**	**11.71**	1.00	8.00	**3.90**	**2.51**	1.00	11.00	**5.70**	**4.00**	≤25	≤30			
Indicators characterizing the salinity																	
Conductivity [μS·cm^{-3}]	–	–	–	–	422.00	509.00	**469.06**	**30.74**	412.00	604.00	**491.62**	**58.92**	≤ 1000	≤ 1500	Limits not determined		
SO_4 [mg·dm^{-3}]	–	–	–	–	24.00	98.00	**60.20**	**19.62**	17.00	81	**53.30**	**18.90**	≤150	≤250			
Cl [mg·dm^{-3}]	–	–	–	–	1.90	23.1	**14.68**	**5.24**	1.50	48.40	**19.12**	**11.86**	≤200	≤300			
The indicators characterizing the acidification (as acidification)																	
pH	6.97	8.22	–	**0.42**	7.39	8.10	–	**0.24**	7.10	8.13	–	**0.29**	6-8.5	6-9	Limits not determined		

Table 3. cont.
Tabela 3. cd.

Indicators	Purified sewage				Water from the river before discharge sewage				Water from the river after discharge sewage				The limit values*				
	min	max	$\bar{x}$	σ	min	max	$\bar{x}$	σ	min	max	$\bar{x}$	σ	I	II	III	IV	V
The indicators characterizing the nutrient conditions (nutrients)																	
$N\text{-}NH_4$ [$mg \cdot dm^{-3}$]	0.10	41.50	**15.19**	**18.02**	0.07	0.35	**0.14**	**0.08**	0.06	0.44	**0.15**	**0.11**	≤0.78	≤1.56	Limits not determined		
$N\text{-}NO_3$ [$mg \cdot dm^{-3}$]	10.78	58.20	**32.96**	**18.60**	1.17	7.55	**4.77**	**1.85**	1.76	7.21	**4.55**	**1.85**	≤2.2	≤5			
N_{tot} [$mg \cdot dm^{-3}$]	10.00	150.00	**78.80**	**49.90**	1.50	2.40	**1.87**	**0.33**	0.50	2.70	**1.87**	**0.68**	≤5	≤10			
P_{tot} [$mg \cdot dm^{-3}$]	1.30	11.00	**5.85**	**3.14**	0.13	6.10	**0.99**	**1.82**	0.13	6.32	**1.08**	**1.87**	≤0.2	≤0.4			
Indicators	Purified sewage				Water from the river before discharge sewage				Water from the river after discharge sewage				The limit values**				
	min	max	$\bar{x}$	σ	min	max	$\bar{x}$	σ	min	max	$\bar{x}$	σ	I	II	III	IV	V
Biogenic indicator																	
NO_2 [$mg \cdot dm^{-3}$]	0.03	3.62	**0.93**	**1.31**	0.02	0.13	**0.05**	**0.03**	0.03	0.22	**0.07**	**0.06**	0.03	0.1	0.5	1.0	>1.0

*The limit values of indicators of water quality appropriate for the class by the Regulation of the Minister of the Environment [2011]
** The limit values of indicators of water quality appropriate for the class by the Regulation of the Minister of the Environment [2004]

Treated sewage had a slightly alkaline pH during the entire study period. At pH values in the range of 6.97-8.22, treated wastewater had an almost identical pH range to that of river water 7.10-8.13 (Table 3), hence it is difficult to speak of any impact of sewage pH on the wastewater – receiver system. In terms of pH, the waters of the Urzędówka River were assigned to class I (Dz. U. 2011, nr 258, poz. 1550).

The analyzed constructed wetland wastewater treatment plant did not have a total nitrogen limit due to the low throughput. Nevertheless, the average concentration of total nitrogen in wastewater discharged from the treatment plant (78.8 mg/L) was relatively high, far exceeding the maximum permissible value for small purification plants (PE < 2000). This, however, did not lead to an increase in the concentration of this component in the waters of the Urzędówka River. The average content of total nitrogen in river water at both measuring points was identical at 1.87 mg/L (Table 3, Figure 4). The analyzed section of the river (100 m) seems to be too short for metabolic processes leading to permanent removal of nitrogen compounds from the incoming sewage to take place. In this situation, the tendency observed can be explained by a lower-than-average wastewater inflow rate and complete lack of inflow in some periods. When it comes to the content of total nitrogen, the water from the Urzędówka River was assigned to water purity class I (Dz. U. 2011, nr 258, poz. 1550).

An analysis of the particular mineral nitrogen forms points to similar tendencies as in the case of total nitrogen and leads to the same conclusion. The average content of ammonium nitrogen was 15.19 mg/L in treated wastewater, 0.14 mg/L in river water upstream of the sewage discharge point, and 0.15 mg/L downstream of the discharge point (Table 3, Figure 4). The contents of $N\text{-}NH_4$ in the Urzędówka River during the research period were clearly lower than the limit value for the cleanest waters. Similar results were obtained by Królak et al. (2011), whose analysis of water quality of the watercourses Zielawa and Lutnia showed that wastewater treatment plants had little impact on the concentration of ammonium ions in sewage receivers.

The average concentration of nitrate nitrogen, which is an intermediate form of nitrogen transformation, may also be used as an indicator of water pollution, both at outlets of wastewater (Królak et al. 2011) and in water bodies contaminated with untreated sewage (Wiatkowski et

al. 2012). The average concentration of NO_3^- in the water from the Urzędówka River collected upstream of the sewage discharge point was 4.77 mg/L. The content of this component in the effluent disposed into the river reached an average level of 32.96 mg/L and at the measuring point located downstream of the sewage outlet, the average content of NO_3^- was slightly reduced to 4.55 mg/L (Table 3, Figure 4). The average content of NO_3^- in river water at both measuring points qualified this water for inclusion in purity class II. It is worth noting that during the research period, the content of nitrate nitrogen in river water occasionally exceeded the limit value for water purity class II (Dz. U. 2011, nr 258, poz. 1550).

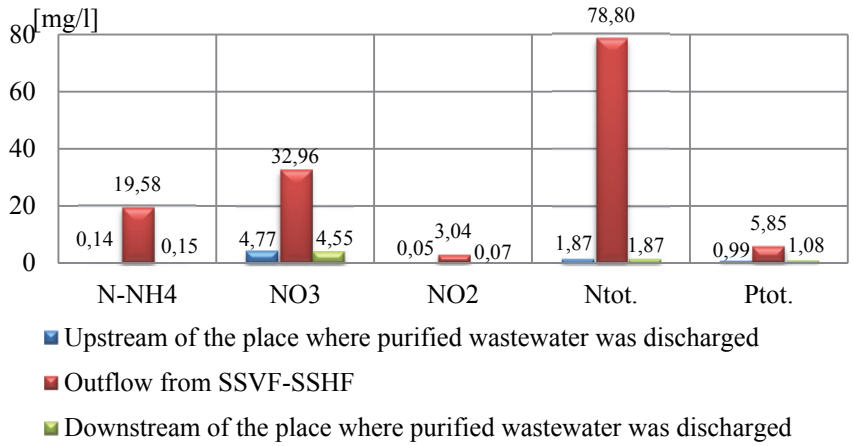

Fig. 4. Average values of nutrient compounds in sewage discharged from the hybrid constructed wetland wastewater treatment plant and in water from Urzędówka River
Rys. 4. Średnie wartości związków biogennych w ściekach odprowadzanych z hybrydowej gruntowo-roślinnej oczyszczalni ścieków komunalnych oraz w wodzie z rzeki Urzędówki

The average nitrite nitrogen content in the water collected from the river upstream of the sewage disposal point was 0.05 mg/L. Downstream of this point, there was a slight increase in the concentration of NO_2^- to 0.07 mg/L (Table 3, Figure 4). The average concentration of nitrite nitrogen in the effluent from the sewage treatment plant was

0.93 mg/L. The analyzed water could be assigned to water quality class II according to a 2004 classification of surface water (Dz. U. 2004, nr 32, poz. 284) – this parameter, however, is currently no longer used in the classification of surface water.

The average content of phosphorus in the effluent discharged from the constructed wetland wastewater treatment plant was 5.85 mg/L (range 1.3-11 mg/L) (Table 3). River water upstream of the sewage discharge point contained 0.13 to 6.10 mg/L of total phosphorus, with a mean of 0.99 mg/L. The content of this element in river water collected downstream of the discharge point was in a similar range from 0.13 to 6.32 mg/L, with a mean of 1.08 mg/L (Table 3). A comparison of the concentrations of total phosphorus (Table 3, Figure 4) for the two measuring points shows that after treated wastewater had been dropped into the river, the contents of that element in river water slightly increased, on average by 9%. The content of total phosphorus in the water from the river exceeded the standards established for water quality class II. As this situation applied to both measuring points (upstream and downstream of the place of discharge), it can be assumed that the increase was not a result of the impact of the treatment plant but of influx of phosphorus from other sources, such as agricultural land or farm buildings (Sapek & Sapek 2005).

From the data presented in Figures 5 and 6, it can be seen that water in the Urzędówka River upstream of the treatment plant already contained a certain concentration of coliform bacteria, fecal coliforms, and fecal enterococci.

The largest increases in the counts of coliform bacteria in the investigated section of the Urzędówka River were recorded in November (Table 4, Figure 5) – from $2.4 \cdot 10^3$ to $2.4 \cdot 10^4$ MPN (Maximum Possible Number) $\cdot 100$ cm^{-3}, and February – from $2.4 \cdot 10^2$ to $7 \cdot 10^2$ MPN$\cdot 100$ cm^{-3}. Only in those cases, could it be concluded that the wastewater from the Skorczyce treatment plant had an impact on the counts of the tested microorganisms in the water of the Urzędówka River. In the remaining periods (May and August), the counts of bacteria at the two measuring points in the river were similar and equalled or exceeded those in the effluents from the treatment plant. These findings leads to the conclusion that the presence of coliform bacteria was the result of the impact of other sources of contamination located in the upper reaches of the river, of

which the most likely were discharges of untreated domestic wastewater or organic fertilizers.

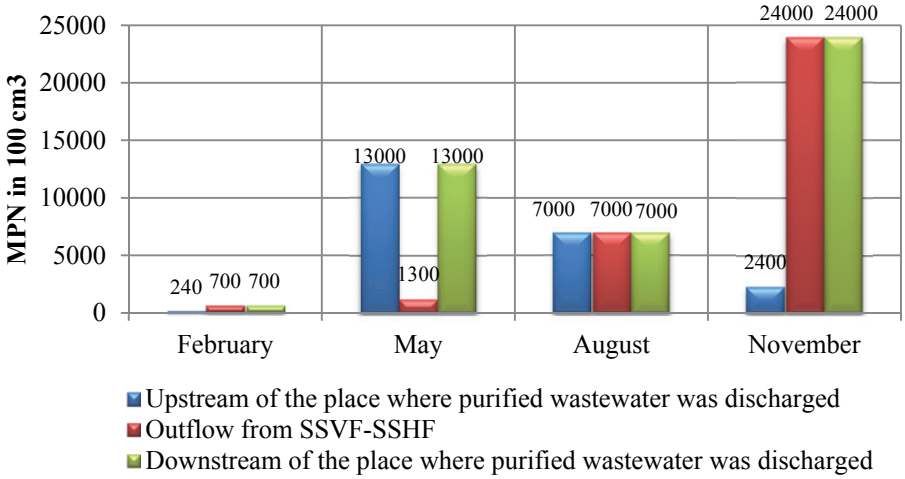

Fig. 5. Numbers of *coliform* bacteria in sewage discharged from the hybrid constructed wetland wastewater treatment plant and in water from Urzędówka River
Rys. 5. Liczebność bakterii grupy *coli* w ściekach odprowadzanych z hybrydowej gruntowo-roślinnej oczyszczalni ścieków komunalnych oraz w wodzie z rzeki Urzędówki

A similar trend could be observed in the case of fecal coliform bacteria. During spring and summer (May and August), the numbers of microorganisms upstream of the sewage discharge point were slightly higher than downstream of this point (Fig. 5, Table 4). In February and November, the number of these bacteria in the samples of water collected upstream of the wastewater outlet was low, but increased in the samples of water collected downstream of the outlet. In November, an increase in those numbers from $1.3 \cdot 10^2$ to $2.4 \cdot 10^3$ MPN·100 cm^{-3} was observed, and in February there was a much smaller increase from $2.4 \cdot 10^2$ to $7 \cdot 10^2$ MPN·100 cm^{-3}.It is not without significance that in this period treated sewage was characterized by a high concentration of fecal coliforms, which could have had a direct impact on the quality of river water (Fig-

ure 6, Table 4). A similar relationship was observed by Wira (2011) in her study of the Wełna River (a right tributary of the Warta River), which receives substantial concentrations of sewage discharged from collectors situated in surrounding towns.

Table 4. Selected indicators of microbial purified sewage and water from Urzędówka River before and after the discharge of sewage from the hybrid constructed wetland wastewater treatment plant in 2013
Tabela 4. Skład zanieczyszczeń mikrobiologicznych ścieków oczyszczonych oraz wód z rzeki Urzędówki przed i po dopływie ścieków z hybrydowej gruntowo-roślinnej oczyszczalni ścieków w 2013 roku

Indicators	Purified sewage				Water from the river before discharge sewage				Water from the river after discharge sewage				The limit values of indicators of water quality appropriate for the class by the Regulation of the Minister of the Environment [2004]				
	II	V	VIII	XI	II	V	VIII	XI	II	V	VIII	XI	I	II	III	IV	V
Numbers of *coliform* bacteria [MPN·100 cm^{-3}]	$7 \cdot 10^2$	$1{,}3 \cdot 10^3$	$7 \cdot 10^3$	$2{,}4 \cdot 10^4$	$2{,}4 \cdot 10^2$	$1{,}3 \cdot 10^4$	$7 \cdot 10^3$	$2{,}4 \cdot 10^3$	$7 \cdot 10^2$	$1{,}3 \cdot 10^4$	$7 \cdot 10^3$	$2{,}4 \cdot 10^4$	50	500	5000	50000	>50000
Numbers of fecal *coliform* bacteria [MPN·100 cm^{-3}]	$7 \cdot 10^2$	$7 \cdot 10^2$	$2{,}4 \cdot 10^3$	$2{,}4 \cdot 10^3$	$2{,}4 \cdot 10^2$	$2{,}4 \cdot 10^3$	$7 \cdot 10^3$	$1{,}3 \cdot 10^2$	$7 \cdot 10^2$	$7 \cdot 10^2$	$2{,}4 \cdot 10^3$	$2{,}4 \cdot 10^3$	20	200	2000	20000	>20000
Indicator does not mean in surface waters according to the regulations outlined																	
Numbers of fecal *enterococci* [MPN·100 cm^{-3}]	-	$1{,}1 \cdot 10^3$	$2{,}4 \cdot 10^3$	$4{,}6 \cdot 10^2$	-	$4{,}6 \cdot 10^2$	$4{,}6 \cdot 10^3$	$1{,}1 \cdot 10^4$	-	$1{,}1 \cdot 10^3$	$2{,}4 \cdot 10^3$	$4{,}6 \cdot 10^2$	-	-	-	-	-

According to the requirements concerning the concentration of coliform bacteria and fecal coliforms in bodies of water, set out in the Regulation of the Minister of the Environment of 2004 (Dz. U. 2004 nr 32, poz. 284), water collected from the Urzędówka River upstream of the sewage discharge point in May and August had the characteristics of class IV waters and that collected in February and November met class III water quality standards. The numbers of coliform bacteria in water collected downstream of the treatment plant in May, August and November were characteristic of class IV waters, and samples collected in February met class III standards. When described in terms of the concentration of fecal coliforms,water samples from February and May met the standards for class III waters and those from August and November met class IV water quality standards (Table 4).

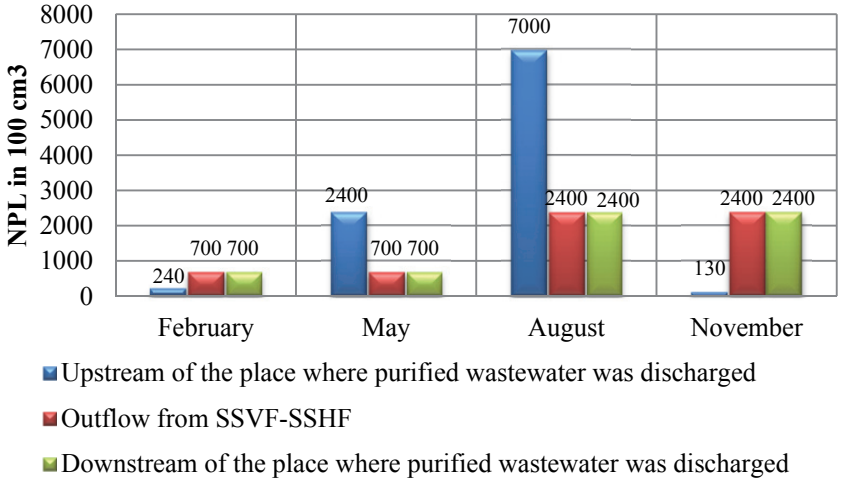

Fig. 6. Numbers of fecal coliform bacteria in sewage discharged from the hybrid constructed wetland wastewater treatment plant and in water from Urzędówka River
Rys. 6. Liczebność bakterii grupy *coli* typu kałowego w ściekach odprowadzanych z hybrydowej gruntowo-roślinnej oczyszczalni ścieków komunalnych oraz w wodzie z rzeki Urzędówki

The numbers of fecal enterococci in the effluent and in river water were analyzed three times, in May, August, and November. In those months, the largest numbers of these microorganisms were found in the water collected upstream of the sewage discharge point. Bacterial counts in the other two types of samples were much lower. Only in May, did the number of fecal enterococci in the effluent ($1.1 \cdot 10^3$ MPN·100 cm^{-3}) exceed that found in the water collected from the Urzędówka River upstream of the discharge point ($4.6 \cdot 10^2$ MPN·100 cm^{-3}) (Figure 7, Table 4). The presence of micro-organisms in the water which did not come into contact with sewage from the Skorczyce treatment plant shows a negative effect of some other sources of microbial contamination.

A close vicinity of rural settlements suggests that the large numbers of fecal bacteria may have been an effect of uncontrolled disposal of domestic wastewater. Similar conclusions were drawn by Frąk (2010), who examined the quality of water in the Biebrza River. In her samples, she found a large number of psychrophilic microorganisms and fecal

coliform bacteria. In our study, fecal pollutants were also probably washed into the receiver from the grazing fields situated in the Valley of the Urzędówka River.

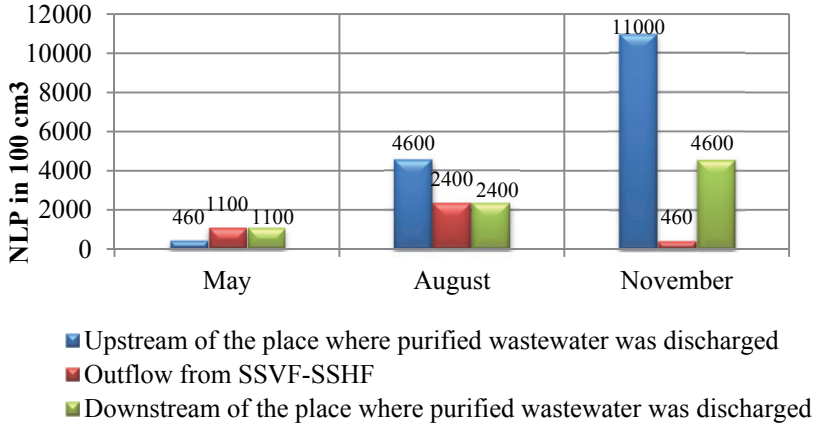

Fig. 7. Numbers of fecal enterococci in sewage discharged from the hybrid constructed wetland wastewater treatment plant and in water from Urzędówka River

Rys. 7. Liczebność bakterii enterokoków kałowych w ściekach odprowadzanych z hybrydowej gruntowo-roślinnej oczyszczalni ścieków komunalnych oraz w wodzie z rzeki Urzędówki

4. Conclusions

The wastewater treated in the investigated constructed wetland wastewater treatment plant was characterized by a small content of total suspended solids, organic matter, and other pollutants (except for nitrogen and phosphorus), and its introduction into the Urzędówka River did not have any statistically significant impact on the quality of the water in the river. The water of the Urzędówka River met water quality standards for class I waters; only the contents of phosphorus and nitrate nitrogen exceeded the limits specified for purity class II. In the autumn-winter period (February and November), a correlation was observed between the concentrations of coliform bacteria, fecal coliform bacteria and fecal enterococci found in the wastewater discharged from the constructed wetland wastewater treatment plant and those found in river water collected

downstream of the sewage discharge point. In the summer months, the discharge of treated wastewater from the constructed wetland wastewater treatment plant did not increase number of microorganism in water samples from the Urzędówka River. Large numbers of fecal coliform bacteria and fecal enterococci found in the water collected from the river upstream of the place where wastewater was discharged from the treatment plant indicated the existence of other sources of microbial contamination. The impact of the investigated VF-HF treatment plant on water quality in the Urzędówka River was insignificant. This was mainly due to the high efficiency of the wastewater treatment system and the low rate of inflow of treated wastewater into the receiver relative to the flow of water in the river, which allowed self-cleaning processes to run smoothly and efficiently.

References

Andrulewicz, E. (1997). An overview on lagoons in the Polish coastal area of the Baltic Sea. *International Journal of Salt Lake Research*, *6 (2),* 121-134.

Ávila, C., Salas, J. J., Martín, I., Aragón, C., & García, J. (2013). Integrated treatment of combined sewer wastewater and stormwater in a hybrid constructed wetland system in southern Spain and its further reuse. *Ecological Engineering*, *50*, 13-20.

Chen, J., He, D., Zhang, N. & Cui, S. (2004). Characteristics of and human influences on nitrogen contamination in Yellow River system, China. *Environmental Monitoring and Assessment, 93 (1-3),* 125-138.

Dobrzański, B. & Turski, R. (1972). *Soil cover* (in Polish). [In] Spatial zoning of agricultural production in the Lublin province. Lublin, 30-36..

Elhatip, H. & Güllü, Ö. (2005). Influences of wastewater discharges on the water quality of Mamasın dam watershed in Aksaray, Central Anatolian part of Turkey. *Environmental Geology*, *48(7)*, 829-834.

Frąk, M. (2010). Bacterial pollution in the assessment of the Biebrza River water quality (in Polish). *Woda-Środowisko-Obszary Wiejskie, 10*, 73-82.

Gajewska M., Stosik M., Wojciechowska E. & Obarska-Pempkowiak H. (2013). Wpływ technologii oczyszczania ścieków na spektrum rozmiarów cząstek w odpływie. *Rocznik Ochrona Środowiska, 15*, 1191-1206.

Gizińska, M., Jóźwiakowski, K., Marzec, M. & Pytka, A. (2012). The problems of construction and commissioning of a constructed wetland wastewater treatment plant without planting of vegetation: the example of a wastewater treatment facility in Skorczyce (in Polish). *Infrastruktura i Ekologia Terenów Wiejskich, (3/I)*, 97-110.

Gizińska-Górna, M., Czekała, W., Jóźwiakowski, K., Lewicki, A., Dach, J., Marzec, M., Pytka, A., Janczak, D., Kowalczyk-Juśko, A. & Listosz, A. (2016). The possibility of using plants from a hybrid constructed wetland wastewater treatment plant for energy purposes. *Ecological Engineering, 95*, 534-541.

Jóźwiakowski, K., Marzec, M., Gizińska, M., Pytka, A. & Goral, R. (2011). An annex to the construction design of a domestic wastewater treatment plant for a residential building in the village of Skorczyce (commune of Urzędów) (in Polish). *Maszynopis Katedry Inżynierii Kształtowania Środowiska i Geodezji UP w Lublinie*, 10-20.

Jóźwiakowski, K., Marzec, M., Gizińska-Górna, M., Pytka, A., Skwarzyńska, A., Słowik, T., Kowalczyk-Juśko, A., Gajewska, M., Steszuk, A., Grabowski, T. & Szarawa, Z. (2014). The concept of construction of a hybrid constructed wetland for wastewater treatment in the Roztocze National Park. *Barometr Regionalny. Analizy i Prognozy, 12(4)*, 91-102.

Jóźwiakowski, K., Mucha, Z., Generowicz, A., Baran, S., Bielińska, J., & Wójcik, W. (2015). The use of multi-criteria analysis for selection of technology for a household WWTP compatible with sustainable development. *Archives of Environmental Protection*, *41(3)*, 76-82.

Juszkiewicz, A., Bartynowska-Meus, Z., Kawałek, M., Meus, M., & Łaptaś, A. (2006). The impact of a wastewater treatment plant on water quality in the Rudawa River basin (in Polish). *Aura, 6*, 12-13.

Kivaisi, A. K. (2001). The potential for constructed wetlands for wastewater treatment and reuse in developing countries: a review. *Ecological engineering, 16(4)*, 545-560.

Kowalkowski, T. & Buszewski, B. (2006). Emission of nitrogen and phosphorus in polish rivers: past, present, and future trends in the vistula river catchment. *Environmental Engineering Science*, *23(4)*, 615-622.

Królak, E., Korycinska, M., Diadik, K. & Godziuk, S. (2011). Do local sewage treatment plants influence the quality of water in sewage receiving rivers? (in Polish). *Ochrona Środowiska i Zasobów Naturalnych, 48*, 343-352.

Lewandowska-Robak, M., Górski, Ł., Kowalkowski, T., Dąbkowska-Naskręt, H. & Miesikowska, I. (2011). The influence of treated sewage discharged from a wastewater treatment plant in Tuchola on water quality of Kicz Creek (in Polish). *Inżynieria i Ochrona Środowiska*, *14*, 209-221.

Mosiej, J., Komorowski, H., Karczmarczyk, A. & Suska, A. (2007). Effect of pollutants discharged from the Łódź conurbation on the quality of water in the Ner and the Warta rivers (in Polish). *Acta Sci. Pol., Formatio Circumiectus, 6 (2)*, 19-30.

Owczarczyk, A. (2001). Radiotracer studies of natural and artificial water reservoirs (in Polish). http://www.iaea.org/inis/collection/NCLCollectionStore/_Public/32/032/32032495.pdf (accessed on 19.05.2016)

PN-74/C-04620/00 Water and sewage. Sampling. General provisions and scope of the standard (in Polish).

PN-C-04615-05:1975P. Water and sewage. Microbiological testing. Determination of coliform bacteria by the multi-tube fermentation (in Polish).

PN-C-04615-07:1977P. Water and sewage. Microbiological testing. Determination of fecal coliform bacteria by the multi-tube fermentation (in Polish).

PN-C-04615-25:2008P. Water and sewage. Microbiological testing. Part 25. Determination of fecal enterococci by the by the multi-tube fermentation (in Polish).

PN-EN 25667-2: 1999 Water quality. Sampling. Guidelines for sampling techniques (in Polish).

Policht-Latawiec, A., Bogdał, A., Kanownik, W., Kowalik, T., Ostrowski, K., & Gryboś, P. (2014). Quality and usable values of small flysch river water (in Polish). *Rocznik Ochrona Środowiska, 16(1)*, 546-561.

Provincial Inspectorate for Environmental Protection 2015 Report on the state of the environment of the Lublin Region in 2014 (in Polish). *Biblioteka Monitoringu Środowiska Lublin*, 28-46.

Rajda, W. & Kanownik, W. (2007). Some water quality indices in small watercourses in urbanized areas. *Archives of Environmental Protection*, *33(4)*, 31-38.

Regulation of the Minister of the Environment of 11 February 2004 on the classification for the present status of surface water and groundwater and how to conduct the monitoring and interpret the results and presentation of the status of these waters. Dz. U. 2004 no. 32 pos. 284 (in Polish).

Regulation of the Minister of the Environment of 15 November 2011 on the forms and manner of monitoring of surface water bodies and groundwater. Dz. U. 2011, no. 258, pos. 1550 (in Polish).

Regulation of the Minister of the Environment of 28 January 2009 amending the regulation on the conditions to be met when discharging sewage into water or soil and on substances particularly harmful to the aquatic environment. Dz. U. 2009, no. 27, pos. 169 (in Polish).

Regulation of the Minister of the Environment of 9 November 2011 on the classification of the status of homogenous parts of surface water and environmental quality standards for priority substances. Dz. U. (Journal of Laws) no. 257, pos. 1545 (in Polish).

Sapek, A. & Sapek, B. (2005). Strategy of nitrogen and phosphorus management in agriculture for the protection of waters of the Baltic Sea (in Polish). *Zeszyty Edukacyjne. Rolnictwo Polskie i Ochrona Jakości Wody, 10*, 67-69.

Structum Sp. z o.o. (2000). Hydrological expert study for the Wyżnica River (in Polish).

Wiatkowski, M., Rosik-Dulewska, C. & Gruss, L. (2012). Profile of water quality indicators changes in Stobrawa river (in Polish). *Infrastruktura i Ekologia Terenów Wiejskich, (3/IV)*, 21-35.

Wira, J. (2011). Evaluation of the impact of selected physical and biological indices on the quality of water in the Wełna (in Polish). *Zeszyty Naukowe. Inżynieria Lądowa i Wodna w Kształtowaniu Środowiska, 3*, 71-76.

Wojciechowski, K. (1972). Hydrographic conditions and guidelines for their use (in Polish). *In: Projekt rejonizacji produkcji rolniczej w województwie lubelskim. Lublin*, 90-121.

Zhang, D., Gersberg, R. M. & Keat, T. S. (2009). Constructed wetlands in China. *Ecological Engineering, 35(10)*, 1367-1378.

Zieliński, M. (2011). *An expert study of water-related and legal aspects of discharge of treated wastewater from a domestic wastewater treatment plant into the Urzędówka River at 12+662 km* (in Polish). Biuro Projektowe „SKALA".

Analiza wpływu hybrydowej gruntowo-roślinnej oczyszczalni ścieków na jakość wód odbiornika

Abstract

This paper presents the results of research on the impact of the composition of wastewater discharged from a hybrid constructed wetland wastewater treatment plant on the quality of water in the Urzędówka River, a right tributary of the Wyżnica River. During the years 2011-2013, samples of treated wastewater and water from the river were collected (upstream and downstream of the wastewater discharge point) and subjected to physicochemical analysis and, in 2013, also to microbiological analysis. The study showed that the treated wastewater outflowing from the treatment plant did not have any negative influence on the quality of the water in the receiver. Water from the Urzędówka River met clarity standards for class I waters; only the concentrations of total phosphorus and nitrate nitrogen exceeded the limit values for water clarity class II. The studies have shown that waters from the Urzędówka River upstream of the treatment plant contained a huge concentration of E. coli bacteria, fecal coliform bacteria and fecal enterococci, which indicates the impact of other sources of microbiological pollution.

Streszczenie

W pracy przedstawiono wyniki badań dotyczące wpływu ścieków odprowadzanych z hybrydowej oczyszczalni hydrofitowej na jakość wód z rzeki Urzędówki, prawostronnego dopływu rzeki Wyżnicy. Próby ścieków oczyszczonych oraz wód z rzeki (powyżej i poniżej miejsca zrzutu ścieków) do analiz fizyczno-chemicznych pobierano w latach 2011-2013, a do analiz mikrobiologicznych w 2013 roku. Na podstawie wyników badań stwierdzono, że ścieki oczyszczone, odpływające z gruntowo-roślinnej oczyszczalni nie miały negatywnego wpływu na jakość wód odbiornika. Wody rzeki Urzędówki odpowiadały I kasy czystości, jedynie zawartość fosforu ogólnego oraz azotu azotanowego przekraczała wartości graniczne określone dla II klasy czystości. W wodzie z rzeki przed zrzutem ścieków oczyszczonych notowano wysoką liczebność bakterii grupy *coli* i *coli* typu kałowego oraz enterokoków kałowych, co wskazuje na oddziaływanie innych źródeł zanieczyszczeń mikrobiologicznych.

Słowa kluczowe:
oczyszczalnie gruntowo-roślinne, oczyszczalnie ścieków,
wody powierzchniowe, odbiornik ścieków, rzeka, jakość wód

Keywords:
constructed wetland system, wastewater treatment, surface water,
sewage receiver, river, water quality

MIDDLE POMERANIAN SCIENTIFIC SOCIETY OF THE ENVIRONMENT PROTECTION
ŚRODKOWO-POMORSKIE TOWARZYSTWO NAUKOWE OCHRONY ŚRODOWISKA
Annual Set The Environment Protection
Rocznik Ochrona Środowiska
Volume/Tom 19. Year/Rok 2017 ISSN 1506-218X 394-410

Analysis of Properties of Synthetic Hydrocarbons Produced Using the ETG Method and Selected Conventional Biofuels Made in Poland in the Context of Environmental Effects Achieved

Małgorzata Krzywonos[*], *Karol Tucki*[**], *Janusz Wojdalski*[**], *Adam Kupczyk*[**], *Michał Sikora*[**]
[*]*University of Economy, Wrocław,*
[**]*Warsaw University of Life Sciences*

1. Introduction

For many years, the Polish energy mix has been based on traditional, non-renewable carriers of primary energy, in particular, brown coal and hard coal. End use of fuels in transport is also dominated by non-renewable fuels, that is, Diesel oil and unleaded petrol. The climate and energy policy of the European Union, the so-called 3x20% + 10% package, indicates activity aimed at promotion of renewable energy sources both in power engineering and in transport. According to provisions of Directive 2009/28/EC, until year 2020, the share of biofuels in total fuel consumption is to reach at least 10% in terms of energy (Krzywonos et al. 2015). The new long-term objectives for the climate and energy policy have been agreed and accepted in October of 2014 by the European Council. They require a 40% reduction in CO_2 emission and at least a 27% share of energy from renewable sources (RES) at the EU level in final energy consumed by the end of year 2030. The new energy policy took into account the motion for amendment of directive on renewable energy sources and sustainable use of bioenergy. The Community activities include incentives to use financial instruments to

support development of new RES generation capacity and promotion of cooperation between member states.

In April 2015, the European Parliament and the Council agreed to amend, until the end of year 2020, the directive on fuel quality and the RES directive in order to take into account the effects of indirect change in the mode of land use, caused by increase in specific crops, used for biofuel production. The following assumptions have been made in the new legal framework:

- The level of maximum 7% share of biofuels made of edible raw materials, which are to be designated for achievement of the objective of 10% share of energy from renewable sources in transport until 2020;
- A target estimated level of 0.5% is to be introduced with regard to advanced biofuels; and
- The Commission will be obliged to take into account the effects of indirect change of land use (ILUC) through inclusion of emission indicators in the reports (European Commission 2015).

The components, listed above, have been taken into account in the prepared draft of amendment of the act on amendment of the act on biocomponents and liquid biofuels of August 31st, 2016, which is now in the course of social consultations (Ministry of Energy, 2016).

Increase in the share of renewable energy in the transport sector is implemented mainly through introduction of transport biofuels on the market, primarily by mixing biocomponents with traditional fuels. For more than 10 years, a well developed technical infrastructure has been present in Poland, allowing for ethanol production, which is translated to very high production capacity for bioethanol, amounting nearly to 750 million dm^3,while the real consumption level remained relatively low, at the level of 24.4%. Overall generation capacity for biocomponents, bioethanol and methyl esters in Poland exceed 2 bln l/year (Borowski 2014, Krzywonos et al. 2015, Antczak et al. 2016).

In the recent years, a number of amendments have been made to the legislation (Act of 2015) regulating the domestic sector of transport biofuels, aimed at reducing energy consumption and emission levels of production processes, as well as partial replacement of the raw materials used.

These amendments concerned, among other things, introduction of the Sustainable Development Criteria (*SDC*) with regard to minimum levels of CO_2 emission reduction, which must be met by all biofuels and biocomponents marketed.

At present, many production plants have had to undergo detailed energy audits of their production lines in order to optimize primary energy, heat and electricity consumption. Modernization and/or modification tasks were based largely on application of natural gas as the process fuel, which is processed by highly efficient cogeneration. These activities are based mainly on the previously identified (e.g. Borowski et al. 2014) problems with regard to sustainability, including reduction of CO_2 emission for selected biofuels made of raw materials originating from the food industry – in particular, these apply to bioethanol produced in two phases (distillery – dehydration facility).

At present, the minimum levels are 50% starting from 2018 and 60% for biofuels generated in new installations (Act of 2015). All of these additional regulations are aimed at stimulating and accelerating implementation of the technology for production of 2nd generation biofuel (advanced biofuels), which are made of non-food, waste or post-production biomass (Act of 2015). Such biofuels include, for instance, bioethanol, made in the process of fermentation of lignocellulosic biomass (Wang 2012,Wilk 2015, Munoz 2016), originating from waste from baking industry, as well as biodiesel, originating, among others, from fat processing waste.

These biofuels are characterized by much higher (more beneficial) levels of CO_2 emission reduction (Wang 2012), and they do not compete with food crops (Munoz 2016, Krzywonos 2014). It should be noted that legislation on marketing of 2nd generation biofuels have been subject to substantial fluctuations lately, in particular, with regard to their eligibility for double counting for the purpose of achievement of the National Indicative Target (*NIT*). A substantial part of the production capacity of bioethanol can be still potentially used, in particular, in the case of more favorable market conditions of increased demand. This leads to the conclusion that the Polish market of bioethanol seems to have a great potential for unconventional technologies of ethanol processing to synthetic hydrocarbons, in particular, ETG (Ethanol to Gasoline). Moreover, it can be predicted that development of this technology will lead to a posi-

tive change on the market of bioethanol and result in increased demand for ethyl alcohol produced by Polish distilleries (Krzywonos 2015). One of such new ETG installations will soon start to produce advanced biofuels in the process of catalytic hydrogenation of ethanol, obtaining synthetic hydrocarbons (Book EkoBenz 2016). The installation will allow, on the industrial scale (22 500 Mg/year), of processing of ethanol to receive synthetic hydrocarbons of parameters consistent with the present quality standards for motor fuels to be marketed.

Alcohols were used as motor fuels already in the 19th century. Among alcohols, ethanol is most popular, and lately, it has been presented as a renewable, biomass-based, environment-friendly motor fuel for spark-ignition engines (Faber 2011, Rodriguez-Anton et al. 2016, Sikora 2016).

Ethanol is a promising alternative for biomass fuel thanks to its chemical properties as well as the fact that it is biodegradable (He et al. 2003). Addition of ethanol and/or ETBE to gasoline may change some fuel properties and gas emission, mechanical capacity and reliability of the engine, at the same time warranting maintenance of good performance standards (Rodriguez-Anton et al. 2016) and increasing the octane rating of mixed fuels and reducing distillation temperature (He et al. 2003, Sikora 2016).

Catalytic ethanol transformation to synthetic hydrocarbons in the ETG technology (Fig. 1) can be divided into three stages: ethanol dehydration to ethylene, secondary reactions (oligomerization of ethylene), production of aromatic compounds/ paraffin through hydrogen transfer (HT) (Sun 2014).

Research on conversion of bioethanol to dimethyl esthers has been conducted, among others, by Nazimek et al. (2015a,b) using copper ion-exchanged zeolite catalysts. The properties of hydrocarbons obtained in the ETG process have been presented in Tabela 1.

Dimethyl ether (DME) has been considered one of the substitutes of Diesel fuel. This has been due to development of cheaper and simpler technologies of its production. The reason for it use as diesel fuel include low self-ignition temperature and high cetane number, which improve the engine performance qualities. Moreover, in comparison with diesel fuel, emission levels of greenhouse gases and other harmful substances have been reduced. Thanks to use of bioethanol for DME production, it can be used as biofuel (BioDME) (Nazimek 2015).

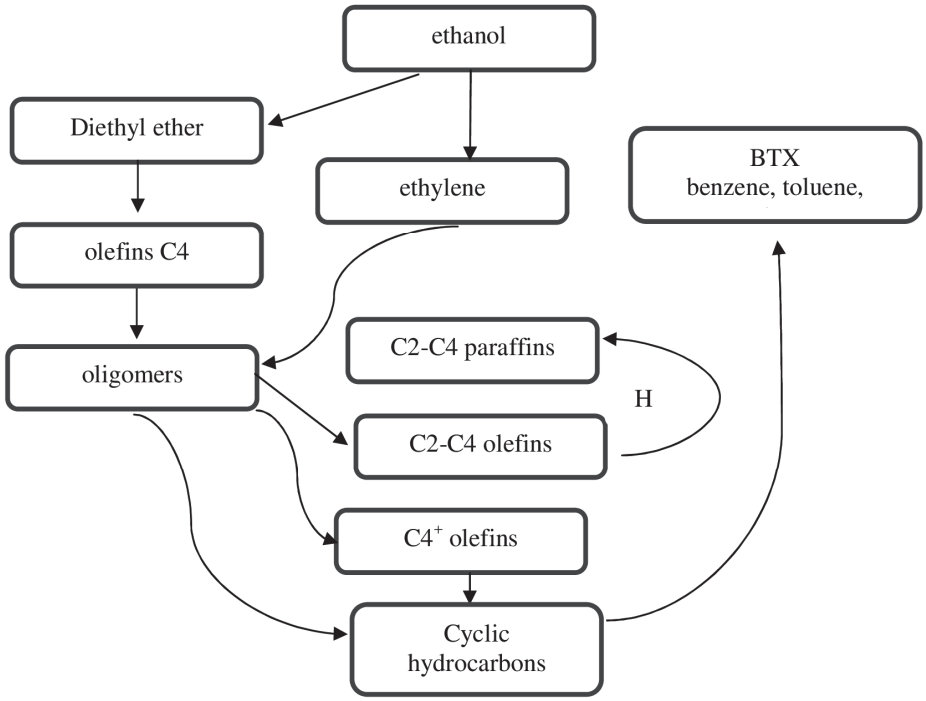

Fig. 1. Conversion of ethanol to gasoline (ETG)
Rys. 1. Proces konwersji etanolu do benzyny (ang. ethanol to gasoline ETG)
Source: Own compilation on the basis of (Viswanadham 2012)

Refineries will be forced to produce increasingly environment-friendly fuels. Adding of synthetic hydrocarbons seems to be an ideal/ advantageous solution. If attractive unit price can be attained for synthetic hydrocarbons, ethanol can be completely replaced as a biocomponent. In production of ethanol of 1st generation, the share of the cost of purchase of enzymes in relation to total production cost of alcohol is not significant, while in production of 2nd generation ethanol, the enzyme cost can reach even 15% of total cost. Thus, the present efforts in the field of 2nd generation ethanol are aimed at increasing enzyme performance and activity. At present, enzyme cost for production of 2nd generation ethanol, according to ABENGOA company, are estimated to range between USD 0.10 and 0.13 per 1 dm^3 of ethanol (Ramos 2016).

Table 1. Chemical composition of synthetic carbohydrates obtained using ETG method
Tabela 1. Skład chemiczny węglowodorów syntetycznych uzyskanych metodą ETG

Chemical composition	Synthetic hydrocarbons after fractioning at capacity of 80%	Synthetic hydrocarbons obtained using ETG method (raw material: ethanol)	Synthetic hydrocarbons obtained using ETG method (raw material: methanol)	Synthetic hydrocarbons obtained using ETG method (raw material: butanol)	Nazimek and Niećko (2010)	Quality requirements for motor gasolines (Resolution of 2008)
MeOH, % vol/vol	<0,17					3
MeOH, % vol/vol	<0,17					5
ETBE Ethyl tert-butyl ether, % vol/vol					22.7	
Oxygen % [m/m]	<0,17	0.42	0.59	0.15	3.28	2.7
Benzene, % vol/vol	<0,1	0.08	0.00	0.01	–	1.0
Olefin type hydrocarbon content, % vol/vol	4.4	7.5	15.8	10.1	8.57	0-18,00
Saturated compounds, % vol/vol		59.8	58.3	31.4	52.35	
Aromatic hydrocarbon content, % vol/vol	28.5	30.7	23.6	26.8	16.35	0-35
Xylene, % vol/vol		4.9	2.6	1.9	-	
RON (Research Octane Number)		94.8	86.5	84.9	107.9	95-

Source: Own compilation

An economically efficient solution could be withdrawal of excise

tax on ethanol for energy production purposes. This could substantially increase the attractiveness of ethyl alcohol as a raw material for synthetic gasoline production. At present, excise tax for motor gasolines and products of mixing of these with biocomponents is PLN 1540 / 1000 l. The rate for diesel fuels with CN code is PLN 1171/ 1000 l. In relation to biocomponents constituting independent fuels (CN code is of no significance), which meet the specific quality requirements, the rate of PLN 1171/1000 l is also applicable. For other motor fuels, it is PLN 1797/1000 l. The excise tax for ethyl alcohol is even higher, amounting to PLN 5704 /100 l of 100% ethanol (Resolution of 2015). Such high financial burden leads to a substantial slowdown in research on potential uses of alcohol as an energy source.

At present, a very significant factor, which determines the possibility of marketing of innovative, advanced biofuels and biocomponents for the *NIT* is compliance with the requirements of the *SDC*. These criteria reflect the minimum acceptable levels of the environmental (ecological) effect obtained as a result of use of biofuels and they are expressed as reduction in CO_2 emission. In this work, we focused on comparative analysis of selected conventional 1st generation biofuels and the advanced biofuel (synthetic biohydrocarbons) obtained using ETG methods with regard to environmental effect.

The aim of this work was to conduct a comparative analysis for synthetic biohydrocarbons produced using the ETG method and selected conventional biofuels (of 1st generation), made of food components, from the perspective of the environmental effect achieved, expressed as CO_2 emission reduction.

2. Analysis methodology

The comparative analysis was conducted for selected biofuels produced in various regions of Poland. The research was conducted using the LCA (Life Cycle Assessment) technique and the BIOGRACE 4.0 d procedure/ tool. It has been approved by the European Commission (BioGrace GHG 2016) as compliant with the greenhouse gas emission assessment methodology in association with production processes and use of transport fuels, biofuels and bioliquids, specified in Directive 2009/28/EC. The tool is generally available and used for determination of

CO_2 emission reduction levels and compliance of transport biofuel production systems with the sustainable development criteria (Biograce GHG, 2016). Moreover, within the framework of the analysis conducted, it is possible to assess energy crop biomasses designated for biofuel production. As for processing of biomass for energy production purposes, the tool allows for calculation of agricultural emissions, as well as emissions and emission reductions in the full life cycle of plants generally used for bioethanol and biodiesel production, as well as for determination of direct impact of the value of a given parameter of the unit biomass and/or biofuel production process on the final emission value, expressed in relation to the functional unit applied (1 MJ of biofuel) throughout the full life cycle.

Research was conducted using detailed data, typical for the selected biofuel production technologies, including in particular: i. bioethanol made of corn (1 phase method), ii. synthetic biohydrocarbons using the ETG method (advanced biofuel). As a supplement for missing, unavailable data, standardized indicator values were used, typical for selected links of the production chain. In order to reflect the cases analyzed more precisely, modified indicator values, typical for Poland, were also applied, e.g. with regard to emission from nitrogen-based fertilizers.

2.1. Analysis of parameters of synthetic biohydrocarbon production using ETG method (case 1)

The production process was analyzed using the LCA (Life Cycle Assessment). The process of production of synthetic biohydrocarbons consists of the following unit processes:

1) Production of ethanol, including
   - Plant cultivation,
   - Transport of grains/ plants to the plant
2) Transport of ethanol to the plant for production of synthetic biohydrocarbons using the ETG method,
3) Production of synthetic biohydrocarbons,
4) Transport to production site.

A simplified diagram of production for the analyzed life cycle of the process of production of synthetic biohydrocarbons using the ETG methods, divided into unit processes, has been presented in Figure 2.

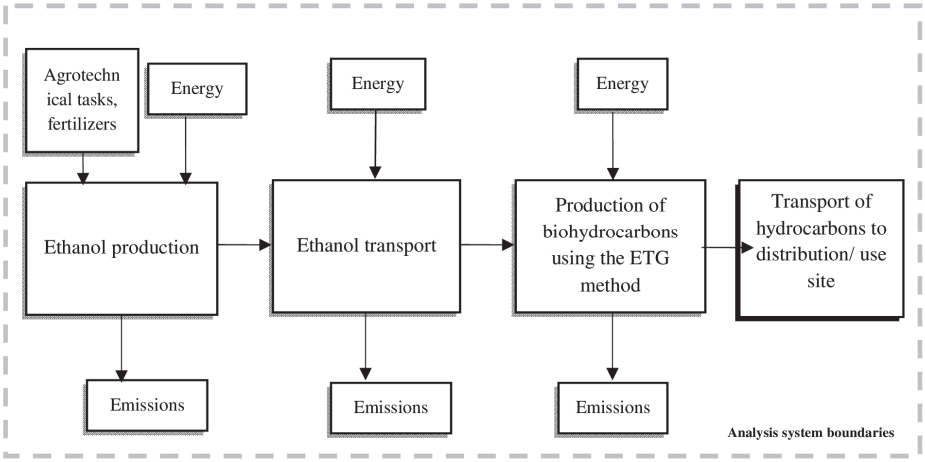

Fig. 2. Scheme of the life cycle of the process of synthetic biohydrocarbons produced by ETG
Rys. 2. Schemat cyklu życia procesu wytwarzania biowęglowodorów syntetycznych metodą ETG
Source: own compilation

Indicated in figure 2 are the main material and energy flows in the life cycle. For the sake of simplification, a detailed division of the ethanol production process has not been presented – it has been explained in the further part of the text (see chapter 2.3), however, the authors indicate that in the final results of analysis of the ecological effect, its energy consumption and the resulting emission values have been taken into account. The process of production of synthetic biohydrocarbons by ETG is much more complex than the processes of production of conventional biofuels. This is mainly due to the possibility of replacing a part of the main stream of substrate (pure ethanol) with substances constituting waste and/or byproducts of alcohol production processes. This has a very positive impact on the final energy and emission balance of the production process. An overall block diagram of the manufacturing process for synthetic biohydrocarbons has been presented in Fig. 3.

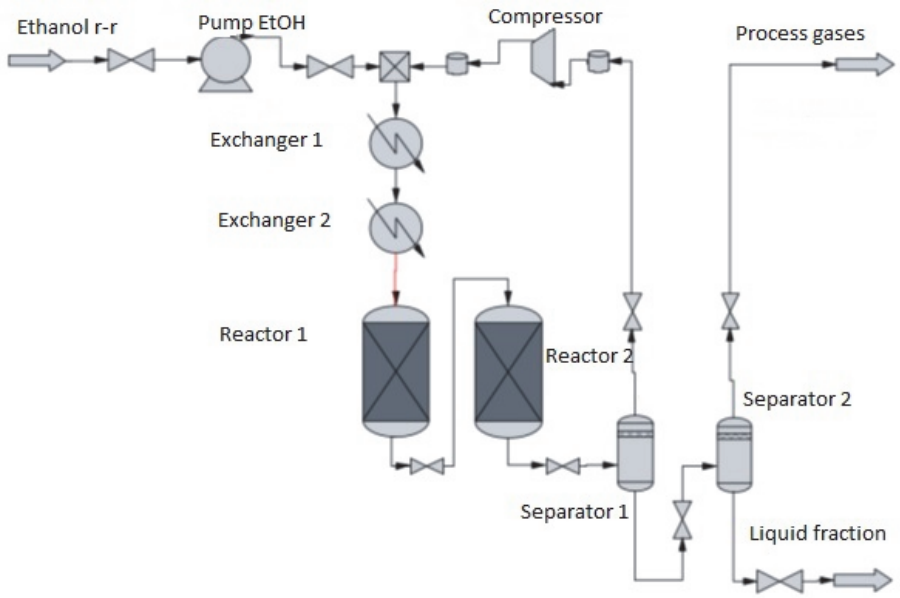

Fig. 3. Block diagram of the process of manufacturing of synthetic biohydrocarbons by ETG method
Rys. 3. Blokowy schemat poglądowy procesu wytwarzania biowęglowodorów syntetycznych metodą ETG
Source: own compilation on the basis of materials of Ekobenz Sp. z o.o.

In this analysis was taken the production of biohydrocarbons (the drained ethanol), which is the low wine produced in the 1-phase method from beet molasses, in the plant where the source of technological heat is natural gas, which is burned in the high-efficiency steam generators (without cogeneration).

2.2. Analysis of parameters of the process of bioethanol production from corn using the 1-phase method (case 3)

The life cycle of bioethanol production from corn using the 1-phase method consisted of three main unit processes:

1) Corn cultivation
2) Transport of corn grains to bioethanol production plant,
3) Production of bioethanol at the plant using the 1-phase method,
4) Transport of bioethanol to the final use/distribution site.

The block diagram of life cycle of bioethanol production from corn has been presented in figure 4.

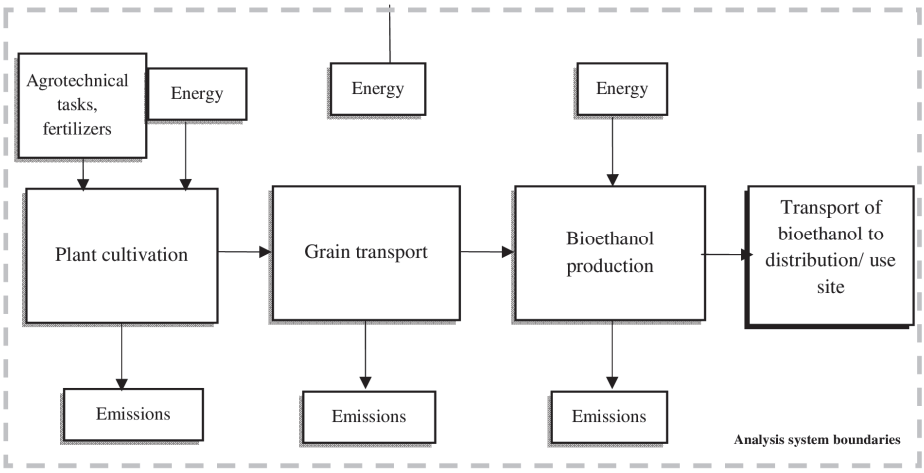

Fig. 4. A block diagram of the life cycle manufacturing process of bioethanol of corn in a 1-phase process
Rys. 4. Schemat blokowy cyklu życia procesu wytwarzania bioetanolu z kukurydzy metodą I-fazową
Source: own compilation

It presents an outline of a block diagram of the life cycle of the process of bioethanol production from corn using a 1-phase method, including the main unit processes and the key input and output streams of mass and/or energy. Bioethanol was produced using the pressure method with enzymatic hydrolysis of substrates. The process fuel was natural gas, combusted in highly efficient steam generators (processing efficiency at the level of 85%). It was assumed that the total transport distance for individual raw materials and products would be 350 km. The production scale at the plant under concern was 30 000 dm^3/24h. A block diagram of the production process has been presented in Fig. 5.

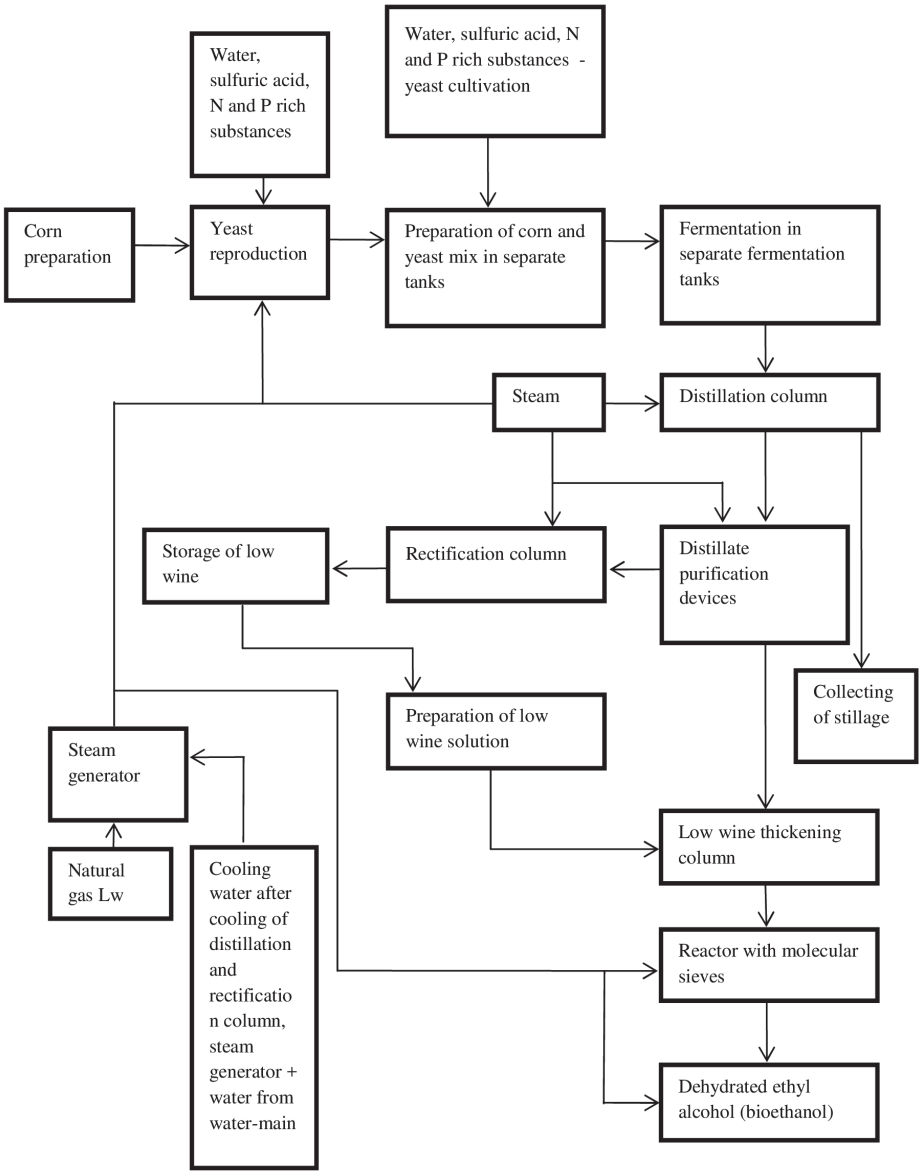

Fig. 5. Block model (technological path)of bioethanol producing-plant from corn by single-phase method
Rys. 5. Model (ścieżka technologiczna) zakładu produkującego bioetanol metodą jednofazową z kukurydzy
Source: Kupczyk, et al. (2016).

3. Analysis results

Table 2 presents results of the comparative analyses conducted, environmental effects (CO_2 emission reduction for synthetic biohydrocarbons produced using the ETG method and conventional biofuels of the 1st generation).

Table 2. Compilation of the results of the calculations for bioethanol production from corn by using single-phase method and and advanced biofuels (ETG)
Tabela 2. Zestawianie wyników obliczeń dla przeanalizowanych procesów wytwarzania biowęglowodorów syntetycznych metodą ETG oraz konwencjonalnych biopaliw 1. generacji

SYNTHETIC BIOHYDROCARBONS (case 1)	
Emission value for transport of ethanol to production plant [g CO_2eq/MJ]	< 1
Emission value for the production process [gCO_2eq/MJ]	< 28
Emission reduction for the production process calculated using BIOGRACE [%]	**< 60**
1-PHASE BIOETHANOL (case 3)	
Quantity of bioethanol produced, dm^3	30,000.00
Quantity of bioethanol produced, MJ	649,874.40
CO_2 emission in corn cultivation, g/MJ of ethanol	26.08
CO_2 emission in cultivation of plants to be used for bio-ethanol production, g/kg of corn	179.85
CO_2 emission in bioethanol production, g/MJ of ethanol	60.30
CO_2 emission in transport throughout the entire life cycle in total, g/MJ of ethanol	1.9
Total emission after allocation, g/MJ of bioethanol	49.0
CO_2 emission for bioethanol production [%]	**41,5-43**

Source: own compilation and Kupczyk et al.(2016)

The results obtained for the synthetic biohydrocarbon production process (case 1) indicate the environmental effect values above 60% of CO_2 emission reduction throughout the entire life cycle. These are also the highest among all transport biofuels analyzed. This indicates that the final energy consumption for this production process is the lowest, in comparison with the remaining cases. The main factors that determine

the above correlations include *i*. use of waste and/or zero emission semi-finished products as a significant part of the substrate feed, *ii*. low losses in energy transmission at the plant, *iii*. high efficiency of processing of primary energy carriers to heat.

For the case of bioethanol made of corn, they indicate the environmental effect and emission level at ~49 g CO_{2eq}/MJ of bioethanol, which is sufficient to achieve CO_2 emission reduction at the level of 41,5-43%. This means that the plant meets the defined criteria for CO_2 emission reduction, and bioethanol produced at the plant can be marketed. At the same time, it should be noted that at present, the biofuel does not meet the reduction threshold of 50%, which is to be applicable starting from January 1st, 2018. At the same time, it has been indicated that such installation, after the loss limitation and energy consumption optimization processes, may meet the required criterion of CO_2 at the level of 50%. The results presented refer to the works of Kijeński (2007), Gąsiorek and Wilk (2011), Manzetti & Andersen (2015, 2016).

4. Summary

Hydrocarbons produced using the ETG method can be used as a biocomponent in fuels for spark-ignition engines. The synthetic hydrocarbons obtained, from chemical point of view, meet the quality requirements for motor fuels used in vehicles with spark-ignition engines. The environmental effect values achieved (above 60%) indicate that this modern fuel may successfully be used in the future as an innovative renewable fuel. In comparison with conventional biofuels, generally used on the Polish market of biofuels of the 1st generation, the environmental effect achieved is higher by more than 20 percentage points. High values of CO_2 emission reduction are, among other things, attributable to use of substrates consisting of zero emission waste and/or semi-finished products and high efficiency of processing of primary energy. Further works on development and implementation of ETG technology may bring further improvement in optimum energy consumption, enhancing the environmental effect of CO_2 emission reduction.

References

Act of January 15th, 2015 On amendment of the act on biocomponents and liquid biofuels and some other acts, Journal of Laws of 2015 item 151.

Announcement of the Minister of Finance of December 4th, 2015 on excise tax for engine fuels applicable in year 2016, MP of 2015, item O 1253.

Antczak, A. et al. (2016). *Results of selected research tasks in project WOODTECH.* Warszawa: Oficyna Wydawniczo-Poligraficzna i Reklamowo-Handlowa „Adam".

BioGrace GHG – biograce.net/img/files/EC_approval_BG-I-v4d.pdf – dostęp na dzień 08.12.2016.

Book EkoBenz. (2016). Produkcja paliw syntetycznych.

Borowski, P., Gawron, J., Golisz, E. et al. (2014). *Wpływ redukcji emisji CO_2 na funkcjonowanie sektorów biopaliw transportowych w Polsce.* Warszawa: Oficyna Wydawniczo-Poligraficzna i Reklamowo-Handlowa „Adam".

Directive 2009/28/EC of the European Parliament and of the Council of 23 April 2009 on the promotion of the use of energy from renewable sources and amending and subsequently repealing Directives 2001/77/EC and 2003/30/EC.

European Commission (2015). Climate action progress report, including the report on the functioning of the European carbon market and the report on the review of Directive 2009/31/EC on the geological storage of carbon dioxide.

Faber, A. et al. (2011). *Poziom emisji gazów cieplarnianych (CO_2, N_2O i CH_4) dla upraw pszenicy, pszenżyta, kukurydzy i żyta przeznaczonych do produkcji bioetanolu oraz upraw rzepaku przeznaczonych do produkcji biodiesla.* Ekspertyza wykonana na zlecenie Ministerstwa Rolnictwa i Rozwoju Wsi.

Gąsiorek, E., Wilk, M. (2011). Possibilities of utilizing the solid by-products of biodiesel production – a review. *Polish Journal of Chemical Technology, 13(1)*, 58-62.

He, B.-Q., Wang, J.-X., Hao, J.-M., Yan, X.-G., Xiao, J.-H. (2003). A study on emission characteristics of an EFI engine with ethanol blended gasoline fuels. *Atmospheric Environment, 37*, 949-957.

http://legislacja.gov.pl/projekt/12289553/katalog/12377157#12377157

Kijeński, J. (2007). Biorefineries – from biofuels to the chemicalization of agricultural products. *Polish Journal of Chemical Technology, 9(3)*, 42-45.

Krzywonos, M., Borowski, P.F., Kupczyk, A., Zabochnicka-Swiątek, M. (2014). Ograniczenie emisji CO_2 poprzez stosowanie biopaliw motorowych. *Przemysł Chemiczny, 93/7*, 1124-1127.

Krzywonos, M., Skudlarski, J., Kupczyk, A., Wojdalski, J., Tucki, K. (2015). Prognoza rozwoju sektora biopaliw transportowych w Polsce w latach 2020-2030. *Przemysł Chemiczny, 94*, 2218-2222.

Kupczyk, A., Tucki, K., Sikora, M., Zubrzycka, M., Bączyk, A. (2016). Porównanie nakładów energetycznych i emisji CO_2 w procesach wytwarzania sprężonego metanu z kiszonki kukurydzianej i gnojowicy oraz bioetanolu z kukurydzy. *Przemysł Chemiczny, 95/8*, 1624-1629.

Manzetti S., Andersen O. (2015). A review of emission products from bioethanol and its blends with gasoline. Background for new guidelines for emission control. *Fuel, 140(15)*, 293-301.

Manzetti S., Andersen O. (2016). A molecular dynamics study of nanoparticle-formation from bioethanol-gasoline blend emissions. *Fuel, 183(1)*, 55-63.

Munoz, I., Flury, K., Jungbluth N., Rigarlsford, G., Canals, L.M., King, H. (2013). Life cycle assessment of bio-based ethanol produced from different agricultural feedstocks. *Int. J. Life Cycle Assess, 19*, 109-119.

Nazimek, D., Niećko, J. (2010). Coupling ethanol with synthetic fuel. *Pol J Environ Stud., 19(3)*, 507-514.

Nazimek, D., Słowik, T., Zając, G., Krzaczek, P., Kuranc, A., Szyszlak-Bargłowicz, J., Piekarski, W., Marczuk, A. (2015a). Badania fizykochemicznych właściwości prekursorów katalizatorów do otrzymywania DME z etanolu. *Przemysł Chemiczny, 94(10)*, 1772-1777.

Nazimek, D., Zając, G., Słowik, T., Kuranc, A., Krzaczek, P., Szyszlak-Bargłowicz, J., Piekarski, W., Marczuk, A. (2015b). Badania kinetyki konwersji bioetanolu do eteru dimetylowego na katalizatorach zeolitowych zawierających miedź. *Przemysł Chemiczny, 94(10)*, 1778-1782.

Ramos, J., Valdivia, M., García-Lorente, F., Segura, A. (2016). Benefits and perspectives on the use of biofuels. *Microbial Biotechnology, 9*, 436-40.

Rodriguez-Anton, L.M., Gutierrez-Martin, F., Martinez-Arevalo, C. (2016). Experimental determination of some physical properties of gasoline, ethanol and ETBE ternary blends. *Fuel, 156*, 81-86.

Rozporządzenie Ministra Gospodarki z dnia 9 grudnia 2008 r. w sprawie wymagań jakościowych dla paliw ciekłych, Dz.U. z 2013, poz. 1058.

Sikora, M. (2016). *Badanie redukcji emisji CO_2 dla bioetanolu wytwarzanego z topoli energetycznej i założenia do budowy biorafinerii.* In: A. Antczak et al. Results of selected research tasks in the project WOODTECH, Warszawa: Oficyna Wydawniczo-Poligraficzna i Reklamowo-Handlowa „Adam".

Sikora, M., Stasiak-Panek, J., Kupczyk, A., Zubrzycka, M., Bączyk, A., Mączyńska, J. (2016). Aktualny stan i atrakcyjność biopaliw w Polsce. Cz. 2. *Przemysł Fermentacyjny i Owocowo-Warzywny, 5*.

Sun, J., Wang, Y. (2014). Recent Advances in Catalytic Conversion of Ethanol to Chemicals. *ACS Catal, 4 (4)*, 1078-1090.

Viswanadham, N., Saxena, S.K., Kumar, J., Sreenivasulu, P., Nandan, D. (2012). Catalytic performance of nano crystalline H-ZSM-5 in ethanol to gasoline (ETG) reaction. *Fuel, 95*, 298-304.

Wang, M., Han, J., Dunn, J.B., Cai, H., Elgowainy, A. (2012). Well-to-wheels energy use and greenhouse gas emissions of ethanol from corn, sugarcane and cellulosic biomass for US use. *Environmental Research Letters, 7*, 045905.
Wilk, M., Krzywonos, M. (2015). Metody wstępnej obróbki surowców lignocelulozowych w procesie produkcji bioetanolu drugiej generacji. *Przemysł Chemiczny, 94*, 599-604.

Analiza właściwości syntetycznych węglowodorów wytwarzanych metodą ETG i wybranych konwencjonalnych biopaliw wytwarzanych w Polsce w kontekście osiąganych efektów środowiskowych

Abstract

The aim of the work was to analyze the properties and to compare the processes of production of synthetic biohydrocarbons using the ETG method and the selected conventional transport biofuels produced in Poland, from the perspective of the environmental effect achieved, expressed as CO_2 emission reduction. Research was conducted using the BIOGRACE 4.0 d. method. Within the framework of the research conducted, detailed data ,typical for selected biofuel production methods, was used. The comparative analysis encompassed: *i*. synthetic biohydrocarbons produced using the ETG method (advanced biofuel), *ii*. bioethanol made of wheat (2-phase method), *iii*. bioethanol made of corn (1-phase method).

Streszczenie

Celem pracy było przenalizowanie właściwości oraz porównanie procesów wytwarzania biowęglowodorów syntetycznych wytwarzanych metodą ETG oraz wybranych konwencjonalnych biopaliw transportowych wytwarzanych w Polsce, pod kątem osiąganego efektu ekologicznego, wyrażonego jako redukcja emisji CO_2. Badania przeprowadzone zostały z zastosowaniem metody BIOGRACE 4.0 d. W ramach przeprowadzonych badań zostały wykorzystane dane szczegółowe, charakterystyczne dla wybranych, technologii wytwarzania biopaliw. Analizą porównawczą objęto: *i*. biowęglowodory syntetyczne wytwarzane metodą ETG (biopaliwo zaawansowane), *ii*. bioetanol wytwarzany z pszenicy (metoda II-fazowa), *iii*. bioetanolu wytwarzany z kukurydzy (metoda I-fazowa),

Słowa kluczowe:
bioetanol, redukcja emisji, węglowodory syntetyczne, nakłady energetyczne

Key words:
bioethanol, emission reduction, synthetic hydrocarbons, energy expenditures

MIDDLE POMERANIAN SCIENTIFIC SOCIETY OF THE ENVIRONMENT PROTECTION
ŚRODKOWO-POMORSKIE TOWARZYSTWO NAUKOWE OCHRONY ŚRODOWISKA

Annual Set The Environment Protection
Rocznik Ochrona Środowiska

Volume/Tom 19. Year/Rok 2017 ISSN 1506-218X 411-422

The Effect of Hard Coal Mine Drainage Water on the Quality of Surface and Ground Waters

Małgorzata Ciosmak[*], *Antoni Grzywna*[**], *Andrzej Bochniak*[**]
[*]*Lublin University of Technology*
[**]*University of Life Sciences, Lublin*

1. Introduction

The working and exploitation of most beds with usable minerals requires rock mass dewatering. In turn, the exploitation of such chemical materials as sulphur and salts involves forcing in water. These processes lead to significant transformations of the water relation in the geological environment. The lowering of the natural drainage base to dewatering levels, the formation of voids in rock mass, the fracture of rock strata above the bed, the unsealing of fault planes, the deformation of rock strata and the depression of surface area – all these give rise to hydrodynamically and hydrochemically complex systems of groundwater and surface water circulation. From the point of view of regulations, any water from dewatering is treated as wastewater. The range and scale of influence of mining on the changes in the water relation following intensive exploitation of mineral resources are illustrated on the map of hydrogeological transformation (Wilk ed. 1990, Wilk 1999).

The area of supply of water-bearing levels under mine drainage in Poland is approximately 5000 km^2 – 1.5% of the country's area. 3 mln $m^3 \cdot day^{-1}$ water was pumped from underground and surface mines per year (Witkowski 2005). The chemical composition and quality classes of mine waters discharged into water depend on the location of exploited and drained beds in the groundwater circulation system. These waters have different quality classes, from fresh to salt water. The latter were

15.6% of the total amount of pumped mine waters containing 2.5 million tons of chlorides and sulphates per year, and nearly all of them (94%) were discharged into water waste. Most mine waters were and still are discharged into surface watercourses either directly or following their use for technological purposes. As a result, nearly half of the rivers in Silesia are characterized by waters with abnormal composition and higher mineralization (Różkowski 1995, Macioszczyk & Dobrzyński 2002, Szczepański 2004).

The Bogdanka mine pumps $14 \cdot 10^3$ $m^3 \cdot day^{-1}$ of waters classified according to mining classification as normal and industrial waters. $13.5 \cdot 10^3$ $m^3 \cdot day^{-1}$ of these waters is drained to wastewater, while $0.5 \cdot 10^3$ $m^3 \cdot day^{-1}$ is used by the mine. In the Lublin Coal Basin the degree of nuisance caused by draining waters from the Bogdanka mine to the watercourse is not significant (Wilk & Bocheńska ed. 2003, Michalczyk et al. 2007). The mine dumps industrial waters classified as fourth class quality into the river Świnka, its waters being classified also as second class quality. The waters drained to the watercourse are multi-ionic with higher concentrations of chlorides and sulphates.

2. Methods and material

The study was performed from 2014 to 2015 by analysing the physical and chemical indicators of water samples. The samples were taken from the following sources: piezometers a depth to 120 m; points groundwater; drainage ditch; water feed, the river Świnka (eight samples for each site). The analyses were performed at a chemical laboratory of the Central Mining Institute in Lublin. A number of physical and chemical indicators were determined using a multispectral analyser. The following parameters were examined: pH, electrolytic conductivity, dissolved substances, total hardness, calcium, magnesium, sodium, nitrates, sulphates and chlorides. The examined indicators were subjected to Friedman's nonparametric univariate analysis (ANOVA) for measurements repeated using the Statistica software. The aim of this work is to investigate the effect of the Bogdanka mine's activity on the drainage of ground water as well as the physical and chemical indicators of both ground and surface waters.

3. Hydrogeological conditions

The study was conducted in the Lublin Coal Basin in the area of mining activity of the "Bogdanka" mine. The mining area is 57 km^2. It comprises three mining regions: Bogdanka, Nadrybie and Stefanów. Aside from the mining activity, the area is marked by increased tourism (Chmielewski ed. 2009, Sawicki & Łyszczarz 2009).

One can distinguish four main aquifers in the Lublin Coal Basin: I – Quaternary and Upper Cretaceous; II – Lower Cretaceous; III – the Upper and Middle Jurassic; IV – Carboniferous complexes. It has been found that there is no hydraulic communication between the waters at use level and the waters located below. The upper hydrodynamic zone comprises the Quaternary and Upper Cretaceous aquifers down to a depth of approximately 170 m. Quaternary aquifers are bound with sand and gravels forming free water table levels. Quaternary waters are therefore exposed to anthropopressure, which can lead to changes in their chemical composition and physical properties as well as variations in water quantity. Ground waters at lower water levels are separated at a depth of 320-563 m from the first aquifer waters by an over layer of impermeable Cretaceous formations with a mining floor of approximately 250 m (Wilk ed. 2003, Porzycki & Zdanowski 1995).

The central hydrodynamic zone with a mining floor of about 830 m comprises formations from Jurassic. The aquifer forming a huge water reservoir in the roof of productive Carboniferous formation has a direct effect on flooding of mining excavations. Carbonate, fractured-porous, locally fractured karst rock formations are characterized by hindered water exchange in the hydrogeological profile and different water-bearing properties. Starting at a depth of about 1000 m, the lower hydrodynamic zone comprising water levels of older Paleozoic elements is contained in the range of the hydrodynamic stagnant zone. In the section of the productive Carboniferous aquifer Westphalian and Namurian formations occurred. The aquifers are beds of porous fractured sandstone. The hydrodynamic zonation of the Lublin Coal Basin is confirmed by hydrochemical zonation, which means that the total mineralization of waters increases with increasing depth. The higher mineralization and changes in ionic composition reflect the dip layers and regional water flow (Różkowski & Rudzińska-Zapaśnik 1987, Szczepański et al. 2007).

Due to safety reasons, waters from all aquifers, particularly the first and third ones, must be taken and drained from the excavation area. The water from water intakes around the mine is used for living and farming purposes. As a result, the safety requirements for mining works and coal production partly meet the demand for water of both the mine and nearby communities. More deeply located Jurassic formation waters are also a huge reservoir of very high quality waters which can be used for municipal purposes. The results of examination of the concentration of Jurassic waters demonstrate that these waters have the properties of curative mineral waters (Ciosmak 2002).

4. Results

The impact of the ”Bogdanka” mine on hydrosphere is connected with the drainage of deep-seated waters for correct operation of the mine. The mean annual inflow of water to the excavations in the Bogdanka mine is 14 000 $m^3 \cdot day^{-1}$ and the average total mineralization is 2100 $mg \cdot dm^{-3}$. Given the concentration of chloride and sulfuric ions, mine waters are classified as second class industrial waters. The hydrogeological study of the groundwater condition revealed that there exists insulation between individual aquifers located at different depths underground and the lack of water drainage from Jurassic Carboniferous rocks in the zone of coal seams exploitation to the Quaternary and Upper Cretaceous level. The results of regular analyses of radioactive substances in the inflowing mine waters also reveal that the concentration of Rad226 ranges to 0.174 $KBq \cdot m^{-3}$. The results of water radioactivity are stable and significantly below the tolerable limits (Ciosmak 2012).

Figure 1 shows the box plots illustrating the variations and scatter in the values of the selected physical and chemical parameters depending on 4 categories of waters: ground waters (piezometres), drinking waters (well), surface waters in the ditches and rivers.

The highest conductivity was measured in a drainage ditch where it amounted average 3200 $\mu S \cdot cm^{-1}$. In turn, the lowest conductivity was measured in ground water where it amounted to 383 $\mu S \cdot cm^{-1}$. With regard to conductivity, ground water was included in quality class I and quality class II [Dz. U. 2016.85]. For surface water, the limit values are not determined [Dz. U. 2016.1187]. A similar situation can be observed

for dissolved substances. The highest value dissolved substances was measured in drainage ditch where it amounted average 2400 mg·dm^{-3}. The lowest value measured in river, average 300 mg·dm^{-3}. For surface water, the limit values are not determined.

The highest average value pH was measured in a water feed. The lowest average electrolytic conductivity was measured in coal water. Ground water is characterized by neutral pH, whereas surface water is slightly alkaline. With regard to value pH alls water was included in quality class I. The highest average total hardness was measured in drainage ditch. The lowest average total hardness in ground water (Fig. 1). In terms of total hardness, all waters were classified as hard water.

The highest average value calcium was measured in drainage ditch, where it amounted 233 mg Ca^{+}·dm^{-3}. The lowest average value calcium was measured in ground water, where it amounted 57 mg Ca^{+}·dm^{-3} was included in quality class II. Surface water was included in quality class I. The highest value magnesium was measured in drainage ditch, where it amounted 68 mg Mg^{+}·dm^{-3}. The lowest value was measured in ground water, where it amounted 10 mg Mg^{+}·dm^{-3}. With regard to Mg^{+} ground water was included in quality class I and II. Surface water was included in quality class I (river) or II (ditch). The highest value sodium was measured in drainage ditch, where it amounted 608 mg Na^{+}·dm^{-3}. The lowest value was in ground water, where it amounted average 17 mg Na^{+}·dm^{-3}. With regard to value Na^{+} ground water was included in quality class I. For surface water, the limit values are not determined.

The highest value sulfates was measured in drainage ditch, where it amounted 1200 mg SO_4^{-}·dm^{-3}. The lowest value was measured in river, where it amounted 77 mg SO_4^{-}·dm^{-3}. With regard to SO_4^{-} ground water was included in quality class II [Dz. U. 2016 poz. 85]. Surface water was included in quality class I [Dz. U. 2016 poz. 1187]. The highest value chlorides was measured in water feed. The lowest value was in ground water (Fig. 1). With regard to Cl^{-} ground water was included in quality class III. Surface water was included in quality class I (river).

The highest value nitrates was measured in ditch, where it amounted 100 mg NO_3^{-}·dm^{-3}. The lowest value was in ground water (well). With regard value NO_3^{-} ground water was included in quality class I. For surface water, the limit values are not determined.

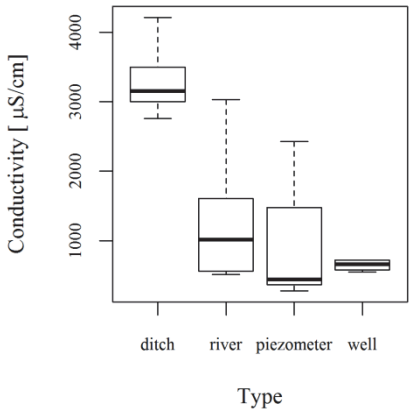
Conductivity [µS/cm]
1000
2000
3000
4000
ditch
river
piezometer
well
Type

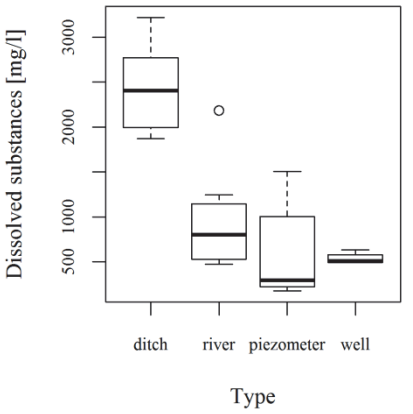
Dissolved substances [mg/l]
500
1000
2000
3000
ditch
river
piezometer
well
Type

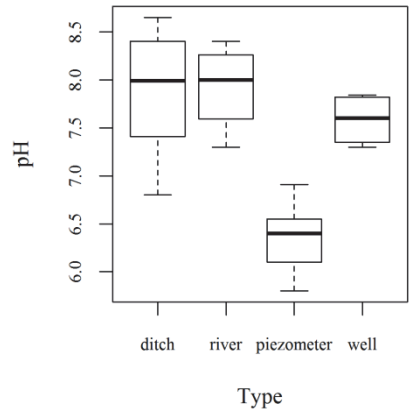
pH
6.0
6.5
7.0
7.5
8.0
8.5
ditch
river
piezometer
well
Type

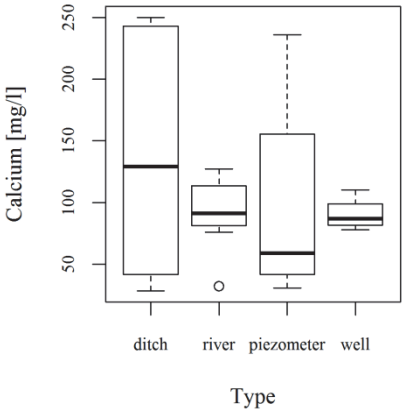
Calcium [mg/l]
50
100
150
200
250
ditch
river
piezometer
well
Type

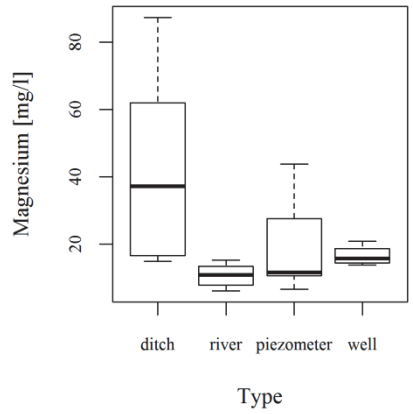
Magnesium [mg/l]
20
40
60
80
ditch
river
piezometer
well
Type

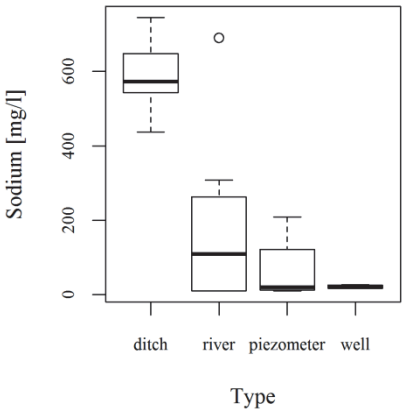
Sodium [mg/l]
0
200
400
600
ditch
river
piezometer
well
Type

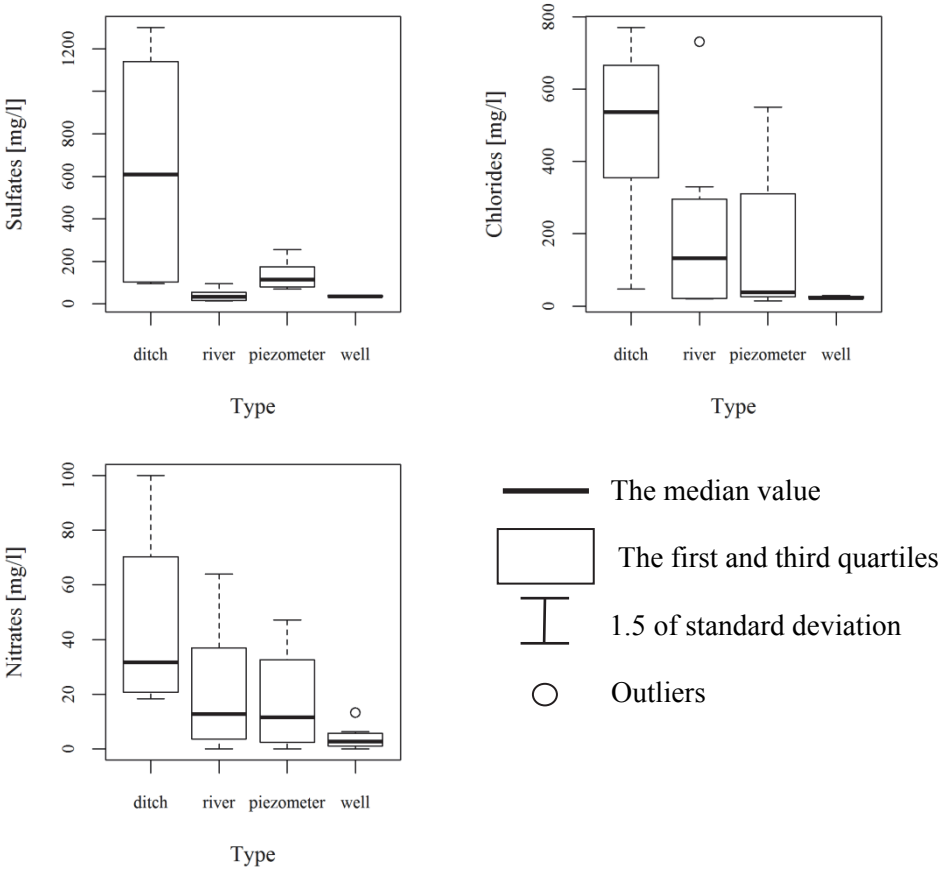

Fig. 1. Box plots comparing the selected parameters for types of water
Rys. 1. Wykresy pudełkowe wybranych parametrów dla rodzajów wód

The results of statistical analysis point to significant differences between both the types of water (except of calcium) and no differences in the measurements (except pH value) (Tab. 1). The highest concentrations of analysed pollutants were recorded most frequently in the drainage ditch, and the lowest in ground water. The situation was different for pH value and nitrates. In the case of pH the highest values were recorded in water feed. In the case of nitrates the highest values were recorded in river and the lowest in water feed. The highest pH value and the lowest concentration of nitrates in water feed is a result of the fact that the water

was drained from protected areas with a very low level of use. The high quality of the water from the ditches may be due to the small quantity and weak flow of water.

Table 1. p-values of chemical parameters obtained from the Freidman test by water type and measurements
Tabela 1. Wartości testu Friedmana dla parametrów chemicznych wg rodzaju wód i pomiarów

Parameter	Type	Value
Conductivity	0,0074 *	0,8254
pH	0,0129 *	0,0336 *
Total hardness	0,0256 *	0,3080
Calcium	0,0576	0,9600
Magnesium	0,0256 *	0,4402
Sodium	0,0074 *	0,5519
Nitrates	0,0440 *	0,0503
Sulfates	0,0112 *	0,6149
Chlorides	0,0129 *	0,2725
Dissolved substances	0,0112 *	0,3916

* statistically significant differences

5. Conclusions

The results of this study together with the examination of water and sewage management enable assessment of physical and chemical indicators describing waters in the mining area in the Lublin Coal Basin. The rate of changes in these indicators is best illustrated by the way in which surface waters react in contact with mine waters (Michalczyk et al. 2007, Staniszewski & Jusik 2013).

Although one can observe changes in the examined parameters describing the quality of the river Świnka waters, it must be stressed that the significant increase in mining activity had no effect whatsoever on its water quality. The increase in chemical concentrations in mine waters drained to the river are not so high as to cause irreversible changes in this ecosystem. This is shown by a rapid (after a distance of 1 km) return of water quality in the river to the pre-drainage condition. Comparing their current state to the beginning of mining activity in the Lublin Coal Basin, the majority of mine water indicators show stability (Ciosmak 2012). The

observed single increases in concentrations do not remain fixed. The actions applied for environment protection are effective.

Waters taken from the piezometers, the well and the river were classified as second class water quality, while the waters from the land improvement ditches did not meet these criteria (there are no standards for lower classes). The highest quality was observed for groundwater, which is often classified as second class quality. This means that the aquifers provide good insulation and are not affected by the Bogdanka mine's activity.

References

Chmielewski, T. J. (red.) (2009). *Ekologia krajobrazów hydrogenicznych Rezerwatu Biosfery „Polesie Zachodnie”*. Lublin: Uniwersytet Przyrodniczy w Lublinie.

Ciosmak, M. (2002). Evaluation of hydrogeochemical stability of Jurassic waters of Lublin Coal Basin as the basis for using them in balneology. *Archives of Environmental Protection, 28(4)*, 15-25.

Ciosmak, M. (2012). Zmiany parametrów wód kopalnianych lubelskiego zagłębia węglowego (LZW) podczas intensywnej eksploatacji i ich wpływ na jakość wód rzeki Świnki. *Inżynieria Ekologiczna, 28,* 20-29.

Czernaś, K., Sawicki, B. & Zawiślak, J. (2003). Właściwości fizyczno-chemiczne wody z rowu opaskowego wokół składowiska odpadów powęglowych w Bogdance w aspekcie ich gospodarczego wykorzystania. *Acta Agrophysica, 1,* 55-60.

Dz. U. 2016 poz. 85. Rozporządzenie Ministra Środowiska z dnia 21 grudnia 2015 r. w sprawie kryteriów i sposobu oceny stanu jednolitych części wód podziemnych.

Dz. U. 2016 poz. 1187. Rozporządzenie Ministra Środowiska z dnia 21 lipca 2016 r. w sprawie sposobu klasyfikacji stanu jednolitych części wód powierzchniowych oraz środowiskowych norm jakości dla substancji priorytetowych.

Macioszczyk, A. & Dobrzyński, D. (2002). *Hydrogeochemia strefy aktywnej wymiany wód podziemnych*. Warszawa: PWN.

Michalczyk, Z., Chmiel, S., Chmielewski, J. & Turczyński, M. (2007). Hydrologiczne konsekwencje eksploatacji złoża węgla kamiennego w rejonie Bogdanki (LZW). *Biuletyn Państwowego Instytutu Geologicznego, 422,* 113-125.

Porzycki, J. & Zdanowski, A. (1995). Lublin Coal Basin. *Prace Państwowego Instytutu Geologicznego, 148,* 159-164.

Sawicki, B. & Łyszczarz, L. (2009). Zagospodarowanie turystyczne i rekreacyjne jako szansa rozwoju dla terenów zdegradowanych obszaru górniczego kopalni węgla w Bogdance. *Inżynieria Ekologiczna, 21,* 121-131.
Staniszewski, R. & Jusik, Sz. (2013). Wpływ zrzutu wód kopalnianych z odkrywki węgla brunatnego na jakość wód rzecznych. *Rocznik Ochrona Środowiska, 15,* 2652-2665.
Szczepański, A. (2004). Wpływ górnictwa na środowisko wodne. *Przegląd Geologiczny, 52,* 968-971.
Szczepański, A., Różkowski, A. & Rudzińska-Zapaśnik, T. (2007). *Hydrogeologia regionalna Polski*. Warszawa: Państwowy Instytut Geologiczny.
Wilk, Z. (red.) (1990). *Mapa przeobrażeń hydrogeologicznych pod wpływem działalności górnictwa w Polsce na tle warunków środowiskowych 1:500 000*. Warszawa: Państwowy Instytut Geologiczny.
Wilk, Z. (1999). Hydrogeologiczna górnicza w Polsce – wczoraj, dziś i jutro. *Biuletyn Państwowego Instytutu Geologicznego, 388,* 229-247.
Wilk, Z. (red.) (2003). *Hydrogeologia polskich złóż kopalin i problemy wodne górnictwa*. Kraków: Akademia Górniczo-Hutnicza.
Wilk, Z. & Bocheńska, T. (red.) (2003). *Hydrogeologia polskich złóż kopalin i rejonów górniczych*. Kraków: Akademia Górniczo-Hutnicza.
Witkowski, A. J. (2005). Contemporary reviews of mine water studies in Europe, part 2: Poland. *Journal International Mine Water Assessment, 24(1),* 13-16.

Wpływ wód z odwodnienia kopalni węgla kamiennego na jakość wód powierzchniowych i gruntowych

Streszczenie

Ocenę wpływu wód kopalnianych na właściwości fizyczne i chemiczne wód powierzchniowych i gruntowych prowadzono w 2014 i 2015 roku na terenie Lubelskiego Zagłębia Węglowego. Pobierano 2 razy co roku próbki wody do analiz właściwości fizykochemicznych. Próbki wody pobierano z piezometrów, studni, rowów melioracyjnych oraz rzeki Świnki. Analizie poddano następujące parametry: pH, przewodność, substancje rozpuszczone, twardość ogólna, wapń, magnes, sód, azotany, siarczany i chlorki. Badane wskaźniki poddano nieparametrycznej analizie Friedmana (ANOVA) dla powtarzanych pomiarów przy użyciu oprogramowania Statistica.

Przeprowadzane badania oraz analiza gospodarki wodno-ściekowej, pozwalają na ocenę parametrów fizykochemicznych wód w obszarze prowadzonej eksploatacji w Lubelskim Zagłębiu Węglowym. Najlepszą oceną intensywności

zmian parametrów może być to, w jaki sposób środowisko wód powierzchniowych, odpowiada na kontakt z wodami kopalnianymi.

Wody podziemne charakteryzowały się niskimi wartościami wskaźników chemicznych. Wody pitne ze studni we wszystkich przypadkach zaliczane były do I klasy jakości. Wody gruntowe z piezometrów były najczęściej zaliczane do II klasy jakości. Maksymalne wartości przewodności nie przekraczały 2500 $\mu S \cdot cm^{-1}$, zaś substancji rozpuszczonych 1500 $mg \cdot dm^{-3}$. Jedynie w przypadku wapnia i chlorków zdarzały się przypadki zaliczenia wody do III klasy jakości. Maksymalne wartości wapnia wynosiły 2500 mg $Ca^{+} \cdot dm^{-3}$, zaś chlorków 300 mg $Cl \cdot dm^{-3}$. Woda w rzece charakteryzowała się wartościami parametrów zbliżonymi do wody podziemnej. Pozwalało to zaliczyć ją do II klasy jakości (wartość graniczna przewodności wynosi 2000 $\mu S \cdot cm^{-1}$, zaś substancji rozpuszczonych 1000 $mg \cdot dm^{-3}$. Odmiennie sytuacja wyglądała w przypadku wody z rowów. Wartości wskaźników jakości wody były tu nawet trzykrotnie wyższe niż w rzece. W tym przypadku zostały przekroczone wartości graniczne dla II klasy jakości, a dla pozostałych klas ich się nie wyznacza.

Dają się zaobserwować zmiany w analizowanych głównych parametrach jakościowych wód rzeki Świnki, jednak znaczne zwiększenie intensywności wydobycia nie wpłynęło na jakość. Podwyższone stężenia składników wód kopalnianych, jakie spływają do rzeki, nie są jednak o tak dużych wartościach, aby doszło do nieodwracalnych zmian w tym ekosystemie. Świadczy o tym szybki powrót jakości wód w tej rzece do stanu sprzed miejsca zrzutu. Większość parametrów wód kopalnianych, porównywanych od początku istnienia kopalni ze stanem obecnym, wykazuje stabilność. Obserwowane pojedyncze wzrosty stężeń nie ulegają utrwaleniu. Wodę pochodzącą z piezometrów, studni i rzeki zakwalifikowano do drugiej klasy jakości, zaś woda z rowów nie spełnia tych parametrów. Najwyższą jakości charakteryzują się wody gruntowe zaliczane najczęściej do pierwszej klasy czystości. To wskazuje na dobrą izolację warstw wodonośnych i brak wpływu na nie działalności kopalni.

Abstract

The effect of mining waters on the physical and chemical properties of surface and ground waters was evaluated in 2014 and 2015 within the Lublin Coal Basin. Samples of water for physicochemical analyses were taken twice a year. Water was sampled from piezometers, wells, drainage ditches and from the river Świnka. The following parameters were analyzed: pH, conductivity, dissolved substances, general hardness, calcium, magnesium, sodium, nitrates, sulphates and chlorides. The examined indicators were subjected to Friedman's nonparametric univariate analysis (ANOVA) for measurements repeated using the Statistica software.

The tests and analysis of water and sewage management make it possible to evaluate the physicochemical parameters of waters within the mining area in the Lublin Coal Basin. The best measure of the intensity of parameter changes can be the response of the surface water environment to contact with mining waters.

Underground waters featured low values of chemical indicators. Drinking water drawn from wells in all cases was classified as quality class I. Ground waters sampled from piezometers were most often classified as quality class II. The value of maximum conductivity did not exceed 2500 $\mu S \cdot cm^{-1}$, while that of dissolved substances, 1500 $mg \cdot dm^{-3}$. Only with regard to the content of calcium and chlorides were some cases of water quality class III recorded. The maximum value for calcium was 2500 mg $Ca^{+} \cdot dm^{-3}$, while for chlorides this was 300 mg $Cl \cdot dm^{-3}$. Water in the river featured parameter values similar to those recorded for underground water. Therefore, it could be included in quality class II (the limit value for conductivity is 2000 $\mu S \cdot cm^{-1}$, for dissolved substances 1000 $mg \cdot dm^{-3}$). The situation was different for water sampled from ditches. Here, water quality indicators were even three times higher than in the river. In this case the limit values for quality class II were exceeded. Such limit values are not determined for other classes.

Can observe changes in the examined parameters describing the quality of river Świnka waters, it must be stressed that the significant increase in mining activity had no effect whatsoever on its water quality. The increase in chemical concentrations in mine waters drained to the river are not that high so as to cause irreversible changes in this ecosystem. This is proved by a fast return of water quality in the river to the pre-drainage condition. Comparing their current state to the beginning of mining activity, the majority of mine water indicators show stability. The observed single increases in concentrations do not remain fixed. Waters taken from the piezometers, the well and the river were classified as second water quality, while the waters from the land improvement ditches did not meet these criteria. The highest quality was observed for groundwater which is often classified as Type I water quality. This means that the aquifers provide good insulation and are not affected by the Bogdanka mine's activity.

Keywords:
chemical indicators, water inflows, Lublin Coal Mine

Słowa kluczowe:
wskaźniki chemiczne, dopływ wody, Lubelskie Zagłębie Węglowe

MIDDLE POMERANIAN SCIENTIFIC SOCIETY OF THE ENVIRONMENT PROTECTION
ŚRODKOWO-POMORSKIE TOWARZYSTWO NAUKOWE OCHRONY ŚRODOWISKA

Annual Set The Environment Protection
Rocznik Ochrona Środowiska

Volume/Tom 19. Year/Rok 2017 ISSN 1506-218X 423-438

Slurry Management on Family Farms Using Acidification System to Reduce Ammonia Emissions

Andrzej Borusiewicz[*], *Jan Barwicki*[**]
[*]*Higher School of Agribusiness, Lomza*
[**]*Institute of Technology and Life Sciences, Warsaw Branch*

1. Introduction

When discussing the problem of slurry influence on country side environment, it is important to provide some analysis of animal production, what has substantial influence on manure presence in close distance to houses and flats. In Figure 1 it is presented number of different animals, which are grown on farms in different countries of EU.

The size of a herd is either expressed in term of head (number of animal) or Livestock Unit (LSU) where one LSU is the grazing equivalent of one adult dairy cow. The data in Table 1 were used to convert from head to LSU when needed.

According to the data of Polish Ministry of Agriculture on March 2017 there were in Poland 3 732 616 cows in the age of more than 1 year old. When counting beef cattle of the same age there are 1 024 616 animals. Taking into account pigs, there are 11 824 300 animals of these breed. In these number there were 1 009 700 sows.

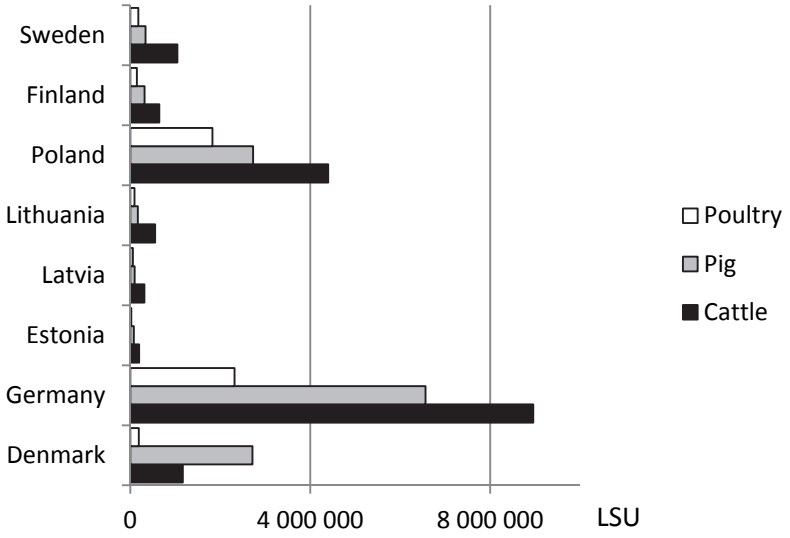

Fig. 1. Population of cattle, pig and poultry in different countries in LSU* (Eurostat 2014)
Rys. 1. Populacja bydła, świń i drobiu w różnych krajach w LSU (Eurostat 2014)
*****_The reference unit used for the calculation of livestock units (=1 LSU) – is the grazing equivalent of one adult dairy cow producing 3 000 kg of milk annually, without additional concentrated foodstuffs._

Table 1. Conversion head to LSU (Eurostat 2014)
Tabela 1. Współczynnik przeliczania sztuk rzeczywistych na LSU (Eurostat 2014)

Bovine animals	Under 1 year old	0.4
	1 but less than 2 years old	0.7
	Male, 2 years old and over	1
	Heifers, 2 years old and over	0.8
	Dairy cows	1
	Other cows, 2 years old and over	0.8
Pigs	Piglets having a live weight of under 20 kg	0.027
	Breeding sows weighing 50 kg and over	0.5
	Other pigs	0.3
Poultry	Broilers	0.007
	Laying hens	0.014

Recently more and more livestock barns, in which animals are kept on slotted floor, instead of manure as organic fertilizer we gain here liquid manure – a mixture of manure, urine and water. The composition and value of natural fertilizer depend on the breeding technology, feeding and water delivery system. Cow manure and swine manure are different and they show different effect on environment. Slurry is, usually mixed with some bedding material and some water during management to give a liquid manure with a dry matter content in the range from about 1 to 10%. Although potassium is available almost immediately after the application of the manure to the soil, with nitrogen, and especially with phosphorus is not so easy. For phosphorus and a large part of nitrogen, they may be available for plants as nutrients, when a process of mineralization occurs, and generally speaking, must become the activity of soil micro flora to provide simple mineral compounds, that can be absorbed by the plant. So the activity of the soil micro flora depends on the degree of use of manure as fertilizer (Pain et al. 1994). Thus, many studies shows that the efficiency of nitrogen supplied in the slurry varies in very wide range from 30 to 70%. In addition to the mineralization we have to take into account the time – because we want to release the ingredients gradually, along with the course of the growing season. Here, nature favors us, because in the period from April to the end of August the temperatures are highest, which promotes the development of micro flora. To the development of micro flora was the most intense, you should provide them with more nutrient components. Slurry as organic fertilizer is used mainly before vegetation. It is important that large doses of manure (especially on light soils) is not preceded directly sown plants, as emitted from the manure ammonia can damage and even destroy the root system of rising plants. This assumes that the nutrients and organic matter contained in the slurry should help to increase soil fertility and increase crop yields without the risk of contamination with biogenic compounds of environmental ground water (Nyord et al. 2013).

The use of slurry in an uncontrolled way is a threat to the environment. European Union legislation allow for the use of natural fertilizers (solid manure, liquid manure, urine) an amount not exceeded 170 kg of nitrogen (N) in pure ingredient per 1 hectare of agricultural land per year (Lyngsø 2016). Requirements for agricultural construction sites, utilized for solid manure, slurry and urine storage, gives the Act of 10 July 2007 concerning fertilizers and fertilization technology. In case of

utilization liquid manure for many years in doses exceeding the nutritional needs of plants, it can reveal symptoms of soil fatigue manifested by reduced yield of plants. It should, however, take into account the slurry in the fertilization of crops on the farm, as part of the supplementary nutrition. Well-applied manure improves soil physicochemical properties.

The amount slurry produced in EU countries brings all governments to establish special regulations to avoid its harmful influence on environment in country side surroundings.

2. Development of new technology for slurry treatment in the aspect of its harmful influence on environment

The international interest for slurry acidification is big and the current draft BREF (Reference Document for Best Available Techniques) has recognised slurry acidification, which will become a compulsory to Best Available Technic (BAT) in all EU member states. There are three main technologies, namely in-house, tank and in-field acidification. Their effects in reducing ammonia emissions from stables, stores and fields are substantial, and in the range of 40 to 64% according official tests, among other the Verification Statement (VERA) of technology verification programme set up in cooperation between Danish, German and Dutch environmental authorities (Biocover A/S 2012). Slurry acidification can be explained as equilibrium between the water bound ammonium (NH_4^+) and the volatile ammonia (NH_3) is moved towards ammonium by adding acid to the slurry. Normally, concentrated sulphuric acid is used, and the costs of the acid in many cases outweighed by savings on purchase of S fertiliser. The nitrogen that is captured via avoided ammonia evaporation is turned into savings on purchase of N fertiliser, or in higher crop yields. Slurry acidification also has a considerable climate effect by increasing the carbon sequestration in soil. Reducing the loss of nitrogen from agriculture is key to reducing eutrophication of the Baltic Sea. Most of the airborne eutrophication to the Baltic Sea comes from ammonia emissions, and in the Baltic State Region (BSR) almost all ammonia emissions are from livestock manure. Annual deposition of ammonia nitrogen to the Baltic Sea has been increasing during recent years and was greater in 2012 than in 1995. While emissions are decreasing slightly in some countries, Baltic Sea Action Plan (HELCOM 2013) calls for a reduction of 118,000 tonnes of nitrogen annually to the Baltic

Sea, and the Revised Gothenburg Protocol (UNECE 2012) calls for ambitious reductions in ammonia emissions from all Baltic See Region (BSR) countries. Slurry acidification also affects solid/liquid slurry separation efficiency positively; DM is higher, N lower and P higher in the solid fraction. A combined treatment should efficiently prevent gaseous emissions, increase fertilizer value of slurry and reduce transport and energy costs.

3. Acidification systems possible to utilize in practice

Acidification of animal slurry has proved to be an efficient solution to minimize NH_3 emissions in-house, during storage, and after soil application, as well as to increase the fertilizer value of slurry, without negative impacts on other gaseous emissions.

Mobile acidification equipment could be suitable for acidifying the slurry in storage during mixing just before spreading. Such equipment could be invested in by the farmer. Mobile equipment implies that the cost can be shared if the same equipment is used on several farms. The service could also be hired from a contractor, under the conditions that there is a contractor in the neighborhood providing this service.

Just to explain, why ammonia evaporation doesn't exists, it can be explained by drawing the following equilibrium in slurry between ammonium salt and ammonia gas

$$NH_4^+ + OH \leftrightarrow NH_3 + H_2O$$

At pH=6,4 all mineralized N is found as ammonium, and no evaporation takes place (Fangueiro at al. 2014).

In Denmark, the slurry should after lowering the pH <6 be spread within 24 hours according to rules. As the spreading season last for longer times, this could mean a period of several weeks per year. Economical calculations are needed to compare which solution is most profitable for individual farms. When hiring the service of acidification, the technology will be available also for smaller farms. Also, if surplus storage volume is needed because of foaming when adding acid, may make the alternative non-profitable compared to the other two alternatives (Shi et al. 2001).

Orum Smeden's appeared after in field acidification system as much simpler and cheaper. Using this equipment it causes foam formation in top of the slurry tank, what means that that part of storage capacity is reduced (Nørgaard et al. 2010). Such acidification is usually

done a few hours or days before spreading on the field, what makes lower ammonia evaporation when spreading such slurry on crops. So far there are about 40 such installation working in Denmark.

In regards to the type of housing, different systems may be used within the same farm. Therefore, livestock within production having more than one type of housing system are counted once for each housing system used on the farm. However, some housing systems only represent a minor share of the actual production (Ribeiro 2009). In order to avoid this double counting, the number of places for each type of housing system is used.

For instance, many farms combine different housing system like having slatted floor for the milking cows but solid dung management (deep bed) for the cows about to farrow. Thus, the number of heads on each system changes during the year whereas the number of places is more of an average and represent that actual share of each system (Semitela et al. 2013).

To estimate the potential for each Slurry Acidification Technology (SAT), we should know for each country what are the most represented animal production systems including animal species and what are the most used manure management systems in these most common productions. The manure management systems include the housing types, the storage systems, and the spreading techniques. It is assumed, that the SAT is only used for slurry.

The last step of a manure handling system is the spreading stage. There are different technics for spreading slurry. Some of them like injection or incorporation have been proven to reduce ammonia emissions (Moset et al. 2012). Therefore, Slurry Acidification Technology (SAT) could be seen as an alternative to those techniques. Band-spreading is the used technique in Denmark to apply acidified slurry with as it place the slurry on the soil surface and gives a rather even distribution of the slurry transversal direction.

Figure 2 presents two slurry tanks, one for fresh slurry and one for acidified slurry. Each one has capacity of 12,5 m^3. It is experimental system, but it can be utilized for small family farms as stationary acidification system, where preparing acidified slurry just before spreading it in the field.

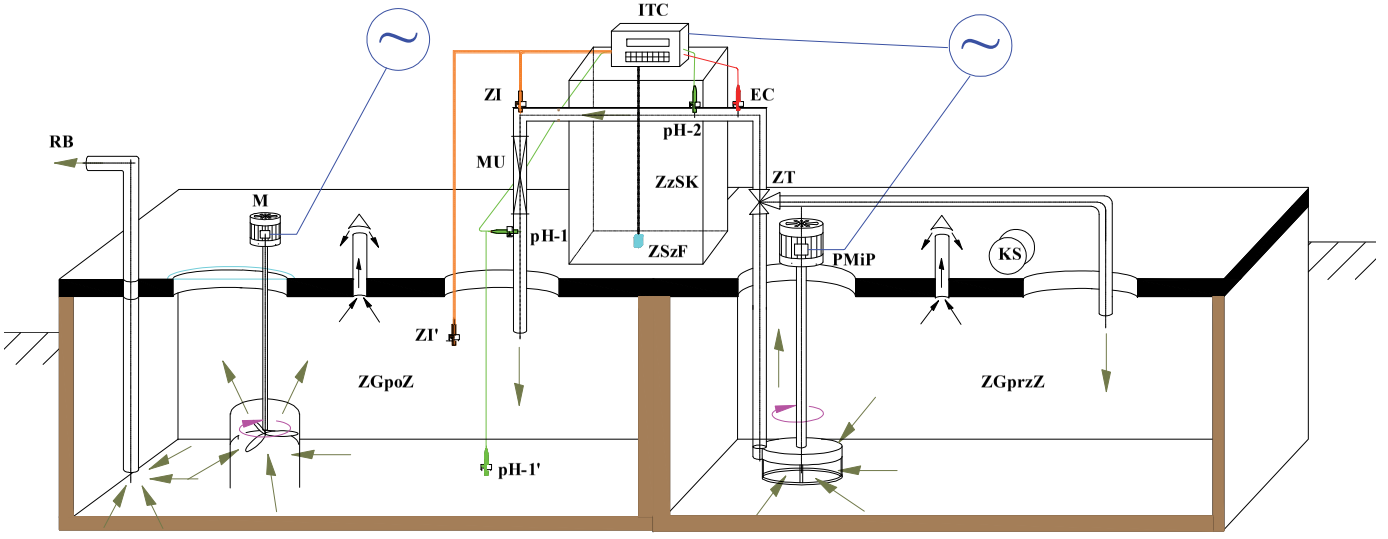

Fig. 2. Experimental pumping of fresh slurry to acidification tank (own elaboration); ITC – dosing pump with pH meter, ZzSK – container with acid, M – mixer, PMiP – pump, ZT – three way valve, ZGprzZ – tank with fresh slurry, ZGpoZ – tank with acidified slurry, RB – discharge pipe

Rys. 2. Przykładowy schemat przepompowywania gnojowicy do zbiornika z kwasem (opracowanie własne)

System contains: slurry pump, slurry mixer, acid pump, pH meter, nozzle, temperature meter, acid tank, electronic steering unit. Slurry from the barn is coming to right tank and when it is full, pump provides mixing and pumping all its capacity to left tank, where acidification process starts.

When slurry get proper pH level than tractor with tanker is coming and takes all acidified slurry into the field for spreading using trailing hoses. This type of experimental system will be very helpful when doing field experimentation on the small plots.

Figure 3 presents components from electronic system, which provides complete automated work, when providing acidification process. The whole system was elaborated with cooperation of FAPO Co. to provide all experiments in SAT Interreg project on experimental farm in Falenty near Warsaw.

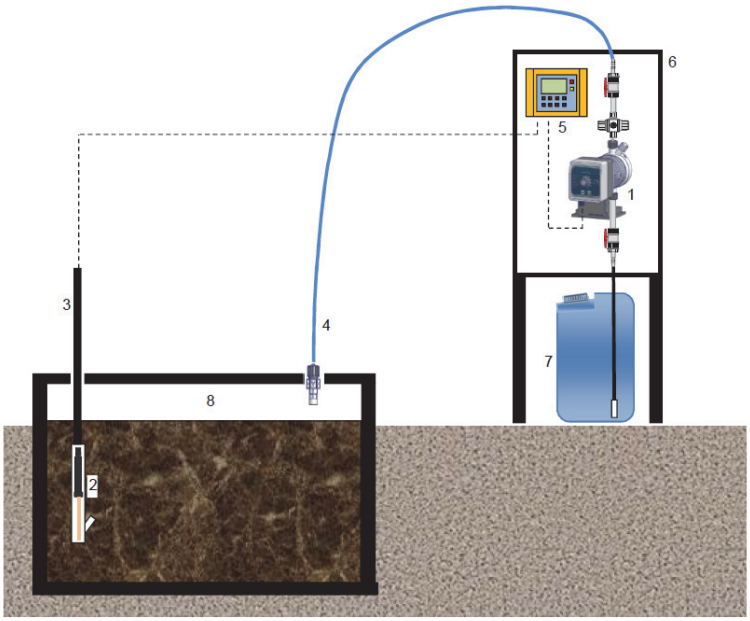

Fig. 3. Fully automated acid delivery system depending on the slurry pH content (FAPO and own elaboration); 1 – acid dosing pump type AMSPLUS, 2 – pH probe type EPHL, 3 – pH probe holder with perfusion system type PECAP-E, 4 – injection line with discharge valve, 5 – control box, 6 – safety cabinet, 7 – container with acid, 8 – slurry tank

Rys. 3. Zautomatyzowany układ dostarczania kwasu w zależności od zawartości pH w gnojowicy (FAPO i opracowanie własne)

Normal field acidification tests on a bigger scale will be provided with the help of Orum Semeden's acidified system presented on Figure 4. This system is quite simple in construction, not much automated units, what can be an advantage, when working in very difficult conditions. This system is very mobile and can be moved from farm to farm and preparing slurry to put acid, than mixing with acid and finally pumping to the tanker and spreading on the field using trailing hoses (Rotz 2004).

Fig. 4. Orum Smeden's "in storage" acidification system at work (Orum Semden's)
Rys. 4. System zakwaszania gnojowicy w zbiorniku firmy Orum Smeden podczas pracy **(**Orum Semden's)

Orum Smeden's system www.oerum-smeden.dk is based on a slurry mixer, equipped in pipes for adding 98% concentrated sulfuric acid. Slurry is pumped directly in the direction of activity of the mixer, what makes easer to obtain slurry mixture uniformity with acid. This is presented on Figure 5.

Acid pipes are located very close to the slurry mixing screw.

Fig. 5 Detailed view on acid discharge system of ORUM Co.– construction of "in storage" unit (Orum Semden's)
Rys. 5. Widok urządzenia ORUM Co do rozprowadzania i mieszania kwasu w gnojowicy (Orum Semden's)

4. Results and discussion

Description of processes when adding Sulphur acid to slurry is presented below:

NH_3(ammonia) + H+= NH_4+(ammonium)

NH_3= gas – may evaporate NH_4^+= salt – does not evaporate)

H_2SO_4 (Sulphur acid) = Hydrogen – Sulphur – Oxygen = Sustainable

The concept of reducing slurry pH to get lower nitrogen losses to the air relies on the equilibrium between NH_4 and NH_3 what is presented in Figure 6.

The effect of pig and cattle slurry acidification on equivalent of mineral fertilizer is presented on Figure 7.

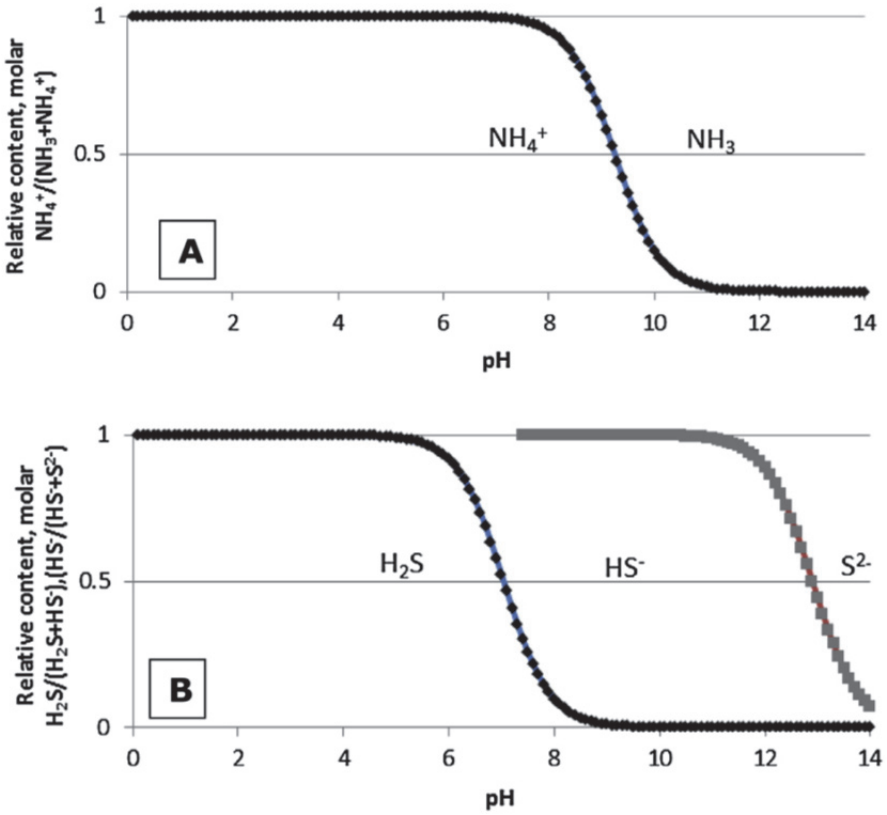

Fig. 6. Effect of slurry pH on its relative content of NH_4^+ (A) and H_2S (B) (Fangueiro et al. 2013)
Rys. 6. Wpływ zawartości pH gnojowicy na względną zawartość NH_4^+ (A) i H_2S (B) (Fangueiro i in. 2013)

There was a strong relationship between NH_3 emissions and ventilation rate during spring and autumn, but less so during summer where ventilation rates were generally high. It was concluded that the contribution from floors to NH3 emissions was <50%. There was some evidence for reduced CH_4 emissions from acidified slurry, but CH_4 emissions were generally low and apparently dominated by enteric fermentation (Moset et al. 2012). No effect on N_2O emissions was observed. The effect of acidification on emissions of H_2S differed between experiments. Implications of slurry acidification on the field state, depends also on N and S availability, and soil pH value (Roboredo et al. 2012).

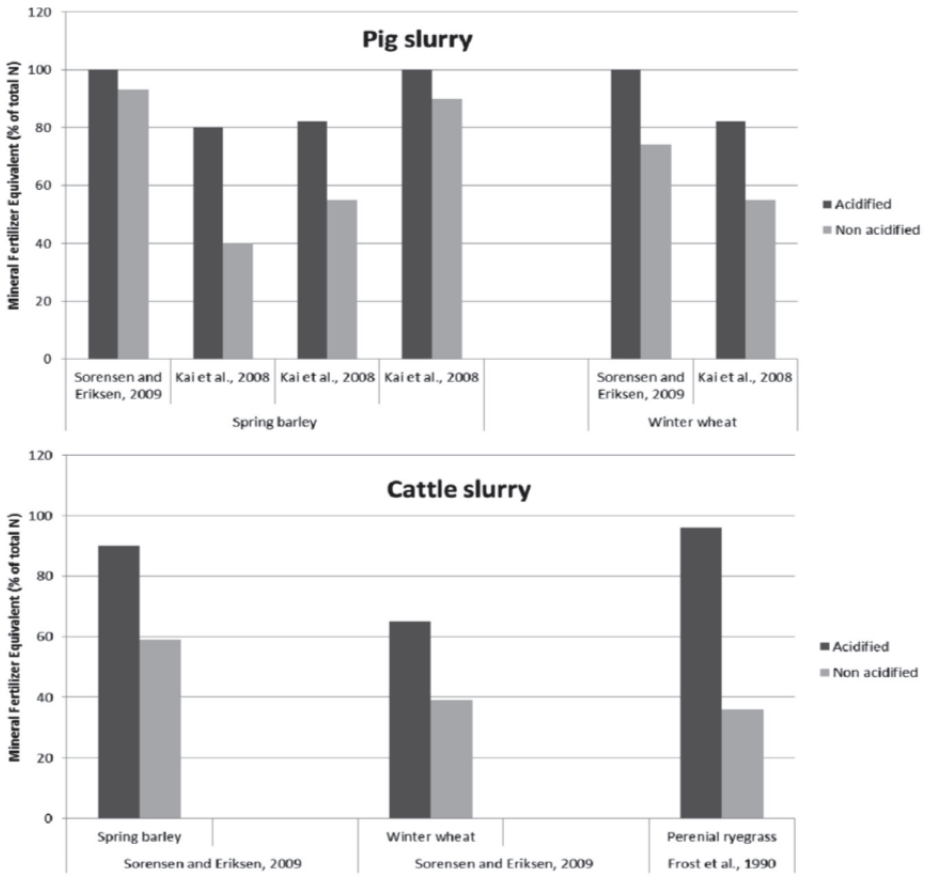

Fig. 7. Effect of pig and cattle slurry acidification on equivalent of mineral fertilizer (Fangueiro et al. 2014)
Rys. 7. Wpływ zakwaszania gnojowicy trzody chlewnej i bydła na równoważnik azotu w nawozie (Fangueiro i in. 2014)

5. Conclusions

1. Slurry acidification technology gives many advantages from the point of view soil fertilization and also the limiting of ammonia emission. Of course it requires provide safety procedures to avoid direct contact of farm workers with harmful activity of the acid. But heaving good acidification technology, which doesn't allow to have direct contact either in the storage area or in the field with the acid, this job is rather safe while fulfilling the procedures.

2. Acidification of animal slurry has proved to be an efficient solution to minimize NH_3 emissions in-house, during storage, and after soil application, as well as to increase the fertilizer value of slurry, without negative impacts on other gaseous emissions.
3. Furthermore, acidification impacts positively on other slurry treatments such as solid liquid separation or composting; upon the use of a non-sulphur containing additive, it may also impact positively on biogas production. Nevertheless, acidification of slurry might induce higher losses by leaching, due to solubilisation of mineral elements.
4. Alternatives to concentrated acids already exist but more research is still needed to improve both their technical and economic aspects. Moreover, the lack of specific equipment for the acidification of solid manures and the separated solid fraction narrows the possible fields of application of the treatment.
5. pH level of 5,5-6,4 is not very acidic, and no more acidic than rain water, which has a normal pH range from 4,5 to 8,5.
6. Corrosion of concrete in stables due to use of slurry acidification has never been an issue in Denmark, as it isn't for an outdoor concrete construction like this exposed to rain.
7. Acidification reduces NH_3 emission from pig houses by 70% compared with the standard housing treatment. Little loss was observed from stored slurry, and the NH_3 emission from applied slurry was reduced by 67%. In consequence, a 43% (S.E. 27%) increase in mineral fertilizer equivalent (MFE) was measured in field studies. The slurry acidification system is approved Best Available Technology (BAT) in Denmark.

References

BalticManure.http://www.balticmanure.eu/en/news/acidification_of_slurry_and_biogas_can_go_hand_in_hand.htm (accessed 06.05.2014).

Biocover A/S. (2012). Vera Statement. http://www.veracert.eu/-/media/DS/Files/Downloads/Artikler/VERA_erklaering_2012_okt_enkeltside.pdf (accessed 07.05.2014).

Fangueiro, D., Surgy, S., Coutinho, J., Vasconcelos, E. (2013). Impact of cattle slurry acidification on carbon and nitrogen dynamics during storage and after soil incorporation. *J. Plant Nutr. Soil Sci. 176,* 540-550.

Fangueiro, D., Surgy, S., Napier, V., Menaia, J., Vasconcelos, E., Coutinho, J. (2014). Impact of slurry management strategies on potential leaching of nutrients and pathogens in a sandy soil amended with cattle slurry. *J. Environ. Manag. 146,* 198-205.

HELCOM. (2013). Revised nutrient targets. http://www.helcom.fi/baltic-sea-action-plan/nutrient-reductionscheme/targets (accessed 06.05.2015).

Interreg EU – Baltic Sea Region – Baltic Slurry Acidification Project 2016-2019.

Lyngsø H. F. (2016). *Agricultural biogas production in a EU policy context, and ways to enhance effects with slurry acidification technologies.* Warsaw: International ITP Conference Monograph.

Moset, V., Cerisuelo, A., Sutaryo, S., Møller, H.B. (2012). Process performance of anaerobic co-digestion of raw and acidified pig slurry. *Water Res. 46,* 5019-5027.

Nørgaard, J.V., Fernandez, J.A., Sørensen, K.U., Wamberg, S., Poulsen, H.D., Kristensen, N.B. (2010). Urine acidification and mineral metabolism in growing pigs fed diets supplemented with dietary methionine and benzoic acid. *Livest. Sci. 134,* 116-118.

Nyord, T., Liu, D., Eriksen, J., Adamsen, A.P.S. (2013). *Effect of acidification and soil injection of animal slurry on ammonia and odour emission.* In: Proceedings from the 15th RAMIRAN Conference, Versailles, France.

Pain, B.F., Misselbrook, T.H., Rees, Y.J. (1994). Effects of nitrification inhibitor and acid naddition to cattle slurry on nitrogen losses and herbage. *Grass Forage Sci. 49,* 209-215.

Ribeiro, H., Vasconcelos, E., Coutinho, J., Cabral, F. (2009). Treatment by acidification followed by solid-liquid separation affects slurry and slurry fractions composition and their potential of N mineralization. *Bioresour. Technol. 100 (20),* 4914-4917.

Roboredo, M., Fangueiro, D., Lage, S., Coutiho, J. (2012). Phosphorus dynamics in soils amended with acidified pig slurry and derived solid fraction. *Geoderma, 189-190,* 328-333.

Rotz, C.A. (2004). Management to reduce nitrogen losses in animal production. *J. Anim. Sci. (Suppl), 82,* 119-137.

Semitela, S., Martins, F., Coutinho, J., Cabral, F., Fangueiro, D. (2013). *Ammonia emissions and potential nitrate leaching in soil amended with cattle slurry: effect of slurry pre-treatment by acidification and/or soil application method.* In: Proceedings from the 15th RAMIRAN Conference, Versailles, France.

Shi, Y., Parker, D.B., Cole, N.A., Auvermann, B.W., Mehlhorn, J.E. (2001). *Surface amendments to minimize ammonia emissions from beef cattle feedlots.* Trans.

UNECE. (2012). Parties to UNECE Air Pollution Convention approve new emission reduction commitments for main air pollutants by 2020 (revised Gothenburg Protocol). http://www.unece.org/ (accessed 15.05.2014).
Project implementation contract BIOSTRATEG1/269056/5/NCBR/2015, dated 11.08.2015.

Zagospodarowanie gnojowicy w gospodarstwach rodzinnych z wykorzystaniem systemu zakwaszania w celu zmniejszenia emisji amoniaku

Abstract

Most of dairy and beef cattle when grown in barn with slotted floor is connected with high concentration of slurry what creates ammonia emission problems. The article presents some proposals for development of new technology in this area. Using slurry acidification technology in the barn, in the storage or in the field we can avoid many environmental problems concerning ammonia emission. Besides that we can save on overall fertilizers usage on the farm. Ammonia emissions is a major problem associated with animal slurry management, and solutions to overcome this problem are developed worldwide by farmers and scientists. An obvious way to minimize ammonia emissions from slurry is to decrease slurry pH by addition of acids or other substances acting in similar way. This solution has been used commonly in Denmark, and its efficiency with regard to the minimization of NH_3 emissions has been documented in some studies. Acidification reduced NH_3 emission from stored slurry to less than 10% of the emission from untreated slurry, and the NH_3 emission from applied slurry on the field was reduced by 67%.

Streszczenie

Większość bydła mlecznego i mięsnego utrzymywana jest w budynkach inwentarskich wyposażonych w podłogi szczelinowe co powoduje wysoką koncentrację gnojowicy i jest przyczyną emisji dużej ilości amoniaku. W artykule przedstawiono wybrane propozycje dla rozwoju nowoczesnych technologii w tej dziedzinie. Wykorzystanie technologii systemu zakwaszenia gnojowicy w budynkach inwentarskich, zbiornikach lub bezpośrednio na polu pozwala na zmniejszenie emisji amoniaku, co wpływa pozytywnie na ochronę środowiska. Ponadto, możemy zaoszczędzić na ilości nawozów stosowanych w gospodarstwie. Rozwiązaniem tego problemu zajmują się naukowcy, farmerzy na całym świecie. Oczywistym sposobem minimalizacji emisji amoniaku jest zmniejszenie pH gnojowicy poprzez dodawanie kwasów lub innych substancji, działają-

cych w podobny sposób. Takie rozwiązania stosowane są w Danii, a jego skuteczność minimalizacji emisji NH_3 zostało udokumentowane w pracach naukowych. Zakwaszenie zmniejsza emisje NH_3 przechowywanej gnojowicy do 10% w porównaniu z gnojowicą bez zakwaszenia, a emisja NH_3 w polu była mniejsza o 63%.

Słowa kluczowe:
nowe technologie, zakwaszenie gnojowicy, emisja amoniaku, ochrona środowiska

Key words:
new technology, slurry acidification technology, ammonia emission, environment protection

MIDDLE POMERANIAN SCIENTIFIC SOCIETY OF THE ENVIRONMENT PROTECTION
ŚRODKOWO-POMORSKIE TOWARZYSTWO NAUKOWE OCHRONY ŚRODOWISKA

Annual Set The Environment Protection
Rocznik Ochrona Środowiska

Volume/Tom 19. Year/Rok 2017 ISSN 1506-218X 439-450

Analysis of the Ecological Status of Surface Waters in the Region of the Lublin Conurbation

Antoni Grzywna, Joanna Sender, Urszula Bronowicka-Mielniczuk
University of Life Sciences, Lublin

1. Introduction

The chemistry of waters is a result of landscape geochemistry, chemical composition and distribution of precipitation, soil water management, land development and use, and plant cover (Ryszkowski 1992). The chemistry of waters can also differ depending on their terrain situation (Grzywna 2010). Therefore, it is of major importance to identify the processes causing the pollutants to move in water in the case of increasing small retention resources. A significant pressure factor is precipitation water or melt-water taken in sewerage systems, flowing from polluted areas, including city centres, industrial areas and roads with heavy traffic as well as car parks. The waters taken in sewerage systems require treatment, otherwise they become a source of pollution for surface waters and groundwaters. Leachate must also be treated both during and after the operation of the landfill (Mouri et al. 2012; Kowalik et al. 2014).

Eutrophication is a process in which the productivity of water increases because of improper agrarian activity and water and sewage management. This process causes mass growth of algae and cyanobacteria. Consequently, water becomes cloudy and biological life disappears (Balcerzak & Rybicki 2011). The issue of agricultural pollution of water was identified in the member states of the European Union (EU) a long time ago. The EU set the rules for handling such pollution (Directive 2000). Poland transposed the provisions of the EU directive into the Water Law act (Dz. U. 2001.115.1229).

The purpose of monitoring surface waters, according to the Water Framework Directive, is to obtain information about the status of waters in river basins for the needs of water management planning and evaluating the accomplishment of environmental goals. The ecological status of waters is determined by biological elements (phytoplankton, phytobenthos, macrophytes) and chemical elements (oxygen conditions, salt content, nutrients) (Pietruczuk & Szoszkiewicz 2012; Lai et al. 2013; Kowalik et al. 2014; Grzywna et al. 2015).

The changes in the quality of water were evaluated using the macrophyte and phytobenthos index and major physico-chemical parameters of waters in the rivers of the Lublin region. The aim of the work was to determine the ecological potential of watercourses using biological and chemical elements.

2. Material and methods

The Bystrzyca – a left-bank tributary of the River Wieprz, has its source in Sulów (at 227 m above sea level). The total length of the river is 70.3 km, and the area of the river basin 1315.5 km^2. Below Spiczyn (at 152 m above sea level) it flows into the River Wieprz. In Osmolice the River Kosarzewka flows into the Bystrzyca. Within the limits of Lublin three more tributaries flow into the river: Krężniczanka from the west, Czerniejówka from the south and Czechówka from the northwest. The last tributary outside the city limits is Ciemięga. The storage reservoir Zalew Zemborzycki is situated on the river in the southern part of Lublin – a place for leisure and recreation, with a base of tourist and sports services (Michalczyk & Wilgat 1998).

The paper presents the results of surveys into the ecological status of rivers in the Lublin region. Lublin is the largest city in Poland east of the Vistula, situated on the northern edge of the Lublin Highland, on the River Bystrzyca, at 163-238 m above sea level. It is ranked ninth in Poland in terms of population (300,000 inhabitants), and 16th in terms of area (147 km²). The River Bystrzyca, and its tributaries Czerniejówka and Czechówka, flow through Lublin city from the south to the northeast. The Bystrzyca Valley divides the city into two parts with separate landscapes: the left-bank portion forming a part of the Nałęczów Plateau with a varied relief, deep valleys and old loess gorges and the right-bank por-

tion forming a part of the Świdnica Plateau and the Giełczew Elevations, with flatter and less varied relief. Industry is mainly concentrated in the north-eastern and south-eastern parts of the city. Single-family housing estates are intermingled with blocks of flats. Recreation grounds are concentrated in the south-western part of the city around lake Zalew Zemborzycki. The Campus is a compact area (GUS 2015, Kozyra 2002).

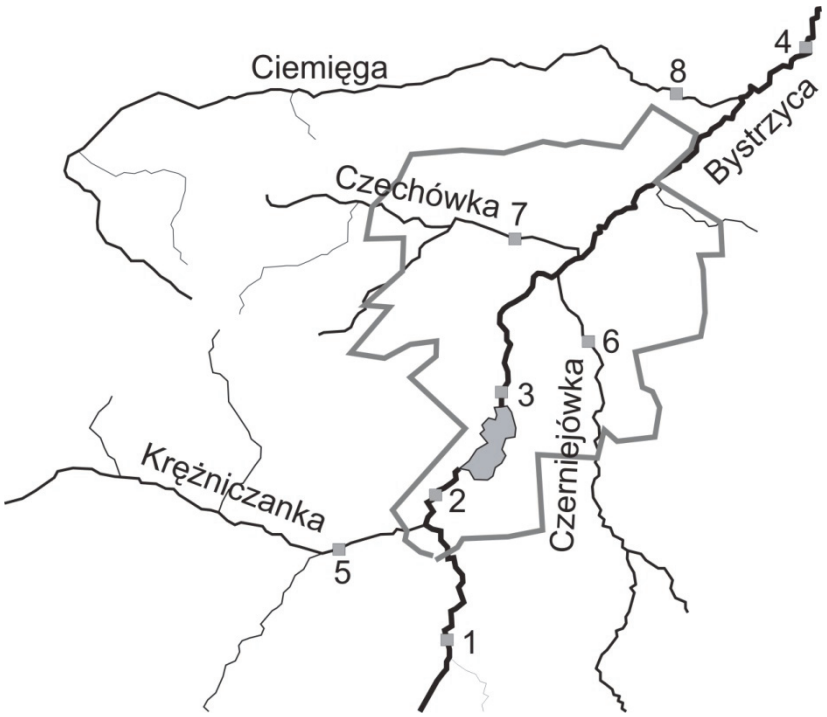

Fig. 1. The hydrographic network in the region of Lublin; 1-8 locations of checkpoints
Rys. 1. Sieć hydrograficzna w rejonie Lublina. 1-8 lokalizacja punktów badań

Biological and chemical elements were analysed between 2012-2014. Analyses were carried out at the following checkpoints on the rivers (Fig. 1): Bystrzyca (No. 1 – Osmolice, 48th km of the river, No. 2 m^3/s flow rate; No. 2 – Zemborzyce, 38th km; No. 3 – Dąbrowa, 34th km; No. 4 – Spiczyn, 5th km, 4.5 m^3/s flow rate, sub-catchment 838 km^2), Krężniczanka (No. 5 – Krężnica, tributary of the Bystrzyca on 40th km,

0.6 m^3/s flow rate, catchment 225 km^2); Czerniejówka (No. 6 – Fabryczna, tributary on 25th km, 0.5 m^3/s flow rate, catchment 172 km^2), Czechówka (No. 7 – Botanik, tributary on 24th km, 0.16 m^3/s flow rate, catchment 78 km^2), Ciemięga (No. 8 – Pliszczyn, tributary on 12th km, 0.5 m^3/s flow rate, catchment 158 km^2) (Czarnecka 2005).

The following chemical indicators were determined in water samples: conductivity at 20^oC (Con), BOD_5, general hardness (Hard), total nitrogen (N), Kjeldahl nitrogen (N-K), ammonia nitrogen ($N\text{-}NH_4$) and nitrate nitrogen ($N\text{-}NO_2$), phosphates (PO_4), total phosphorus (P). In addition, biological indicators were determined: Polish Macrophyte Index for Rivers (MIR) according to macrophyte species, diatom index (IO) according to the species of diatoms (Picińska-Fałtynowicz & Błachuta 2008; Szoszkiewicz et al. 2010; Grzywna et al. 2015).

The planning of a surface waters monitoring network was based on the regulation concerning the forms and method of monitoring of uniform parts of surface waters and groundwaters. The quality of water was evaluated according to the regulation on the method of classification of uniform parts of surface waters and environmental quality standards for priority substances.

The results obtained were processed by statistical methods including the determination of the differentiation of water quality ratios as regards the checkpoint (measuring site) and the year of measurement. To this end, methods of descriptive statistics were used, including box-plots. The data was analysed using Statistica 10 software.

3. Results

At the end of 2013, seven wastewater treatment plants were in operation in the conurbation of Lublin: two municipal and five industrial. Despite this fact, evaluation of the level of the risk of eutrophication caused by sewage effluents from municipal sources revealed that the phenomenon did occur. Agriculture is another source of pressure on the aquatic environment. The widespread use of mineral fertilizers and pesticides leads to an increased load of nitrogen and phosphorus compounds in waters (GUS 2015).

It is assumed that the life of the analysed biological, physicochemical and hydromorphological elements in operating monitoring is 3

years. Every biological element has different sensitivity to specific pressure. For example, diatom phytobenthos (IO) is a sensitive indicator of eutrophication. However, this is a short-term indicator referring to a river habitat. Short life cycles of diatoms and fast production rate prevent conclusions on long-term changes in the environment. On the other hand, these organisms quickly respond to the deteriorating condition of the environment (Gołub 2010; Tarkowska-Kukuryk 2013).

The IO values were average and they mostly ranged from 0.3-0.5. However, for checkpoints 2, 7 and 8 the value was lower than 0.3 (tab. 1, fig. 2). In single cases for checkpoint 1 the value of the index exceeded 0.5. Depending on the checkpoint and year of study, the watercourses are classified as waters of II, III or IV quality class. Irrespective of the checkpoint, diatoms were predominantly species with a wide range of ecological tolerance, often found in waters subject to anthropogenic pollution from surface run-off.

Tabela 1. Wartości średnie analizowanych wskaźników jakości wody
Table 1. The mean values of the analyzed indicators of water quality

Point	1	2	3	4	5	6	7	8	Mean
IO	0.50	0.29	0.46	0.33	0.41	0.34	0.28	0.28	0.36
MIR	40.9	36.5	39.3	38.4	39.5	34.8	33.4	37.9	37.6
Con	491	518	358	552	546	529	641	576	526
Hard	301	316	288	237	347	356	384	363	324
BOD_5	2.4	2.7	7.4	3.2	3.7	5.5	4.7	3.4	3.5
$N\text{-}NH_4$	0.090	0.128	0.183	0.271	0.282	0.123	0.189	0.169	0.18
N-K	0.92	1.03	1.16	1.41	1.38	1.19	1.54	0.93	1.20
$N\text{-}NO_2$	2.15	2.55	1.23	1.97	3.68	3.39	2.18	1.41	2.32
N	3.15	3.77	2.52	3.46	4.92	4.40	3.81	2.33	3.54
PO_4	0.28	0.36	0.17	0.29	0.46	0.35	0.43	0.29	0.32
P	0.15	0.17	0.15	0.21	0.27	0.19	0.33	0.16	0.20

Depending on the year, MIR values enabled classifying the watercourses into class II and III of water quality. The overall number of macrophyte species was average and ranged from 5 to 15. In the structure of dominance, the largest share was that of emergent macrophytes and pleustonic species. The structure of macrophyte species was typical of anthropogenic reservoirs or was subject to continuing influx of nutrients from the catchment area. MIR values most often ranged from 37 to 41. However, for checkpoints 2, 6 and 7 they were lower than 37.

In terms of BOD_5 at checkpoint 3 the mean value exceeded the acceptable limit (6 mg $O_2 \cdot dm^{-3}$) for class II. At checkpoints 1 and 2 above Lublin BOD_5 was within the range acceptable for waters of very good quality. At other checkpoints, surface waters were classified as II class of purity in terms of BOD_5. Statistical analysis revealed that biochemical oxygen demand was higher below checkpoint 4. Electrolytic conductivity was low in comparison to values acceptable for waters with class I ecological status.

Below the city of Lublin, at checkpoint 4, the mean concentrations of all nutrient indicators were higher than recorded above the city at checkpoint 1 (Tab. 1). However, in the case of nitrate nitrogen the values were identical, while for other indicators the concentrations were significantly higher than those recorded at checkpoint 1 – from 1.3 (total nitrogen) to 3 times (ammonia nitrogen). Despite large differences between checkpoints, the ecological status of water was very good since the average values of total nitrogen and ammonia nitrogen did not exceed standard limits for class I. The watercourses were most varied in terms of nitrate nitrogen content (limit value 2.2 mg $N\text{-}NO_3 \cdot dm^{-3}$) and total phosphorus (limit value 0.2 mg $P \cdot dm^{-3}$), and depending on the checkpoint, waters were classified as purity class I or II (Fig. 2). In the case of Kjeldahl nitrogen (1-2 mg $N \cdot dm^{-3}$) and phosphates (0.2-0.4 mg $PO_4 \cdot dm^{-3}$) the analysed waters are classified as quality class II. However, the limit value for class II was exceeded for checkpoints 5 and 7 (no limit values given for other classes). The River Czechówka, flowing along the streets of Lublin, featured the worst parameters.

Water in the rivers can be considered hard as its general hardness at most study periods ranged from 300 to 400 mg $CaCO_3 \cdot dm^{-3}$ (Tab. 1). The mean values of salt content from many years at the checkpoint below and above the city were 301 and 238 mg $Ca\text{-}CO_3 \cdot dm^{-3}$ respectively, which made the water eligible for class I.

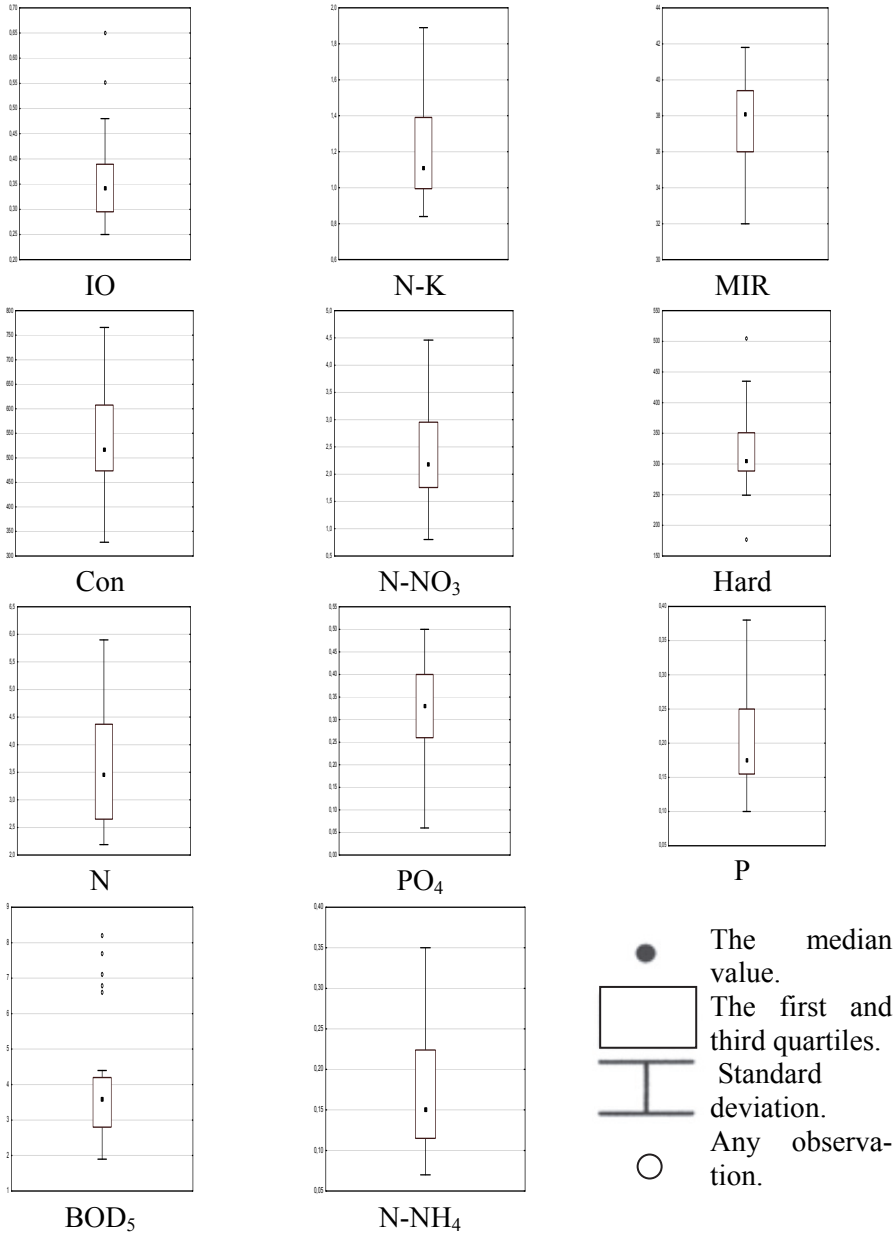

Fig. 2. Box-plot of water quality indicators in 2012-2014
Rys. 2. Zmienność wskaźników jakości wody w latach 2012-2014.

4. Summary

The analysed river waters were characterised by very low content of ammonia nitrogen below 0.4 mg $N\text{-}NH_4$/l, total nitrogen below 5 mg $N \cdot dm^{-3}$ and conductivity below 600 uS/cm. These values are characteristic of class I water purity. The content of Kjeldahl nitrogen within the range of 1-2 mg $N \cdot dm^{-3}$, phosphates within the range 0.2-0.4 mg $PO_4 \cdot dm^{-3}$, nitrate nitrogen 2-5 mg $N\text{-}NO_3 \cdot dm^{-3}$ and phosphorus 0.2-0.4 mg $P \cdot dm^{-3}$ makes the analysed waters eligible for purity class II. Sometimes the content of phosphates in the region of Lublin exceeds the limit value for class II – 0.4 mg $PO_4 \cdot dm^{-3}$. BOD_5 in lake Zalew Zemborzycki continuously exceeded the limit value for class II – 6 mg $O_2 \cdot dm^{-3}$.

The results were considerably worse for biological indicators. For MIR the index was 37-41, which made the waters eligible for purity class II. At some checkpoints within the limits of Lublin city the value of the index lower than 37 made the water eligible for purity class III. For IO the index most often ranged from 0.3 to 0.4, which corresponds to class III water purity. A decrease in the index below 0.3 in Ciemięga and Czechówka rivers made the water eligible for purity class IV.

The main reason for the poor ecological status of water was a high content of phosphates and a low diatom index. The largest variability in the value of the index was characteristic of the analysed watercourses for nitrate nitrogen and ammonia nitrogen and oxygen level. The watercourses are not very wide (1-3 m) and not very deep (0.2-1.0 m), they have a low flow and their beds are modified (profiled bed, concrete slabs). Watercourses located outside the city are characterised by moderate ecological potential (quality class III), whereas watercourses in Lublin are characterised by insufficient ecological potential (class IV).

Anova analysis showed a significant variability in values between the analysed checkpoints, which is not applicable to MIR only. In most cases no significant variability in the values of indicators was recorded between years at respective checkpoints, which is not applicable to phosphates and total phosphorus.

References

Balcerzak, W. P. & Rybicki S. M. (2011). Ocena stopnia zagrożenia wody eutrofizacją na przykładzie zbiornika zaporowego w Świnnej Porębie. *Ochrona Środowiska, 33(4)*, 67-69.

Czarnecka, H. (2005). *Atlas podziału hydrograficznego Polski*. Warszawa: Wydawnictwo PWN.

Directive 2000/60/EC of the European Parliament and of the Council establishing a framework for Community action in the field of water police.

Dz. U. 2001.115.1229. *Ustawa Prawo wodne*.

Gołub, M. (2010). Ocena stanu ekologicznego jezior na podstawie makrobezkręgowców bentosowych zgodna z wymaganiami ramowej dyrektywy wodnej – przegląd rozwiązań metodycznych w Europie. *Ochrona Środowiska i Zasobów Naturalnych, 45*, 30-45.

Grzywna, A. (2010). Chemiczne wskaźniki jakości wody w zlewni Lasów Parczewskich. *Inżynieria Ekologiczna, 36*, 120-127.

Grzywna, A., Tarkowska-Kukuryk, M., Bochniak, A., Marczuk, A., Jóźwiakowski, K., Marzec, M., Mazur, A., Obroślak, R., Nieścioruk, K. & Zarajczyk, J. (2015). Zastosowanie wskaźników chemicznych i biologicznych do oceny potencjału ekologicznego sztucznych cieków wodnych. *Przemysł Chemiczny, 94(11)*, 1954-1957.

GUS 2015. *Rocznik statystyczny*.

Kowalik, T., Kanownik, W., Bogdał, A. & Policht-Latawiec, A. (2014) Wpływ zmian użytkowania zlewni wyżynnej na kształtowanie jakości wody powierzchniowej. *Rocznik Ochrona Środowiska, 16*, 223-238.

Kozyra, W. (2002). *Lublin w dziejach najnowszych*. Lublin: Wydawnictwo LTN.

Lai, Y.C., Tu, Y.T., Yang, C.P., Surampalli, R.Y. & Kao C.M. (2013). Development of a water quality modeling system for river pollution index and suspended solid loading evaluation. *Journal of Hydrology, 478*, 89-99.

Mouri, G., Shinoda, S. & Oki, T. (2012). Assessing environmental improvement options from a water quality perspective for an urbane rural catchment. *Environmental Modelling & Software, 32*, 16-26.

Michalczyk, Z. & Wilgat, T. (1998). *Stosunki wodne Lubelszczyzny*. Lublin: Wydawnictwo UMCS.

Picińska-Fałtynowicz, J., Błachuta, J. (2008). *Wytyczne metodyczne do przeprowadzenia oceny stanu ekologicznego jednolitych części wód rzek i jezior oraz potencjału ekologicznego sztucznych i silnie zmienionych jednolitych części wód płynących Polski na podstawie badań fitobentosu*. Warszawa: Wydawnictwo GIOŚ.

Pietruczuk, K., Szoszkiewicz, K. (2012). Zależność między klasyfikacją rzek opartą na makrolitach a jakością fizyczno-chemiczną wody na przykładzie rzek województwa wielkopolskiego. *Ochrona Środowiska, 34(1)*, 41-46.

Ryszkowski, L. (1992). Rolnictwo a zanieczyszczenia obszarowe środowiska. *Zeszyty Problemowe Postępów Nauk Rolniczych, 504*, 3-14.

Szoszkiewicz, K., Zbierska, J., Jusik, Sz. & Zgoła, T. (2010). *Makrofitowa metoda oceny rzek. Podręcznik metodyczny do oceny i klasyfikacji stanu ekologicznego wód płynących w oparciu o rośliny wodne*. Poznań: Wydawnictwo Naukowe Bogucki.

Tarkowska-Kukuryk, M. (2013). Effect of phosphorous loadings on macrophytes structure and trophic state of dam reservoir on a small lowland river (Eastern Poland). *Archives of Environmental Protection, 39(3)*, 33-46.

Analiza stanu ekologicznego wód powierzchniowych w rejonie aglomeracji lubelskiej

Streszczenie

W pracy przedstawiono wyniki prowadzonych badań stanu ekologicznego rzek w rejonie Lublina. Analizie poddano elementy biologiczne i chemiczne za lata 2012-14. Do analizy wytypowano 8 punktów kontrolnych na rzekach. W próbkach wody oznaczano wskaźniki chemiczne oraz elementy biologiczne. Na podstawie uzyskanych wyników badań przeprowadzono analizy statystyczne, które obejmowały określenie zróżnicowania wskaźników jakości wody ze względu na stanowisko oraz rok pomiarów. Wykorzystano w tym celu metody statystyki opisowej z wizualizacją w postaci wykresów pudełkowych. Analiza danych przeprowadzona została w programie Statisica.

Badane wody rzeczne charakteryzowały się bardzo niską zawartością azotu amonowego poniżej 0,4 mg $N\text{-}NH_4$/l, azotu ogólnego poniżej 5 mg $N \cdot dm^{-3}$ oraz przewodnością poniżej 600 uS/cm. Są to wartości charakterystyczne dla I klasy czystości wody. Zawartość azotu Kjeldahla w zakresie 1-2 mg $N \cdot dm^{-3}$, fosforanów w zakresie 0,2-0,4 mg $PO_4 \cdot dm^{-3}$, azotu azotanowego 2-5 mg $N\text{-}NO_3 \cdot dm^{-3}$ i fosforu 0,2-0,4 mg $P \cdot dm^{-3}$ klasyfikuje badane wody do II klasy czystości. W rejonie miasta Lublin niekiedy zawartość fosforanów przekracza wartość graniczną dla II klasy. W przypadku wielkości BZT_5 w Zalewie Zemborzyckim stale była przekroczona wartość graniczna dla II klasy. Znacznie gorsze wyniki otrzymano w przypadku wskaźników biologicznych. W przypadku MIR wartość indeksu wynosiła 37-41, co pozwalało na zaliczenie wód do II klasy czystości. W niektórych punktach położonych w granicach Lublina wartość indeksu wynosząca poniżej 37 powodowała zaliczenie wody do III klasy czystości. W przypadku IO wartość indeksu mieściła się najczęściej w zakresie

0,3-0,4 co odpowiada III klasie czystości wody. Spadek tego indeksu poniżej wartości 0,3 w rzekach Ciemięga i Czechówka powodował zaliczenie wody do IV klasy czystości.

Główną przyczyną złego stanu ekologicznego wody była wysoka zawartość fosforanów oraz niski indeks okrzemkowy. Największą zmiennością wartości wskaźnika charakteryzowały się badane cieki w przypadku azotu azotanowego i amonowego oraz natlenienia. Cieki charakteryzuje niewielka szerokość (1-3 m) oraz głębokość (0,2-1,0 m), mały przepływ wody, jak również modyfikacje koryta (koryto profilowane, płyty betonowe). Cieki zlokalizowane poza miastem charakteryzują się umiarkowanym potencjałem ekologicznym (III klasa jakości), zaś cieki na terenie Lublina charakteryzują się niedostatecznym potencjałem ekologicznym (IV klasa jakości).

Analiza Anova wykazała istotną zmienność wartości wskaźników między badanymi stanowiskami, co nie dotyczy tylko MIR. W większości przypadków nie stwierdzono istotnej zmienności wartości wskaźników między latami w poszczególnych stanowiskach, co nie dotyczy fosforanów i fosforu ogólnego.

Abstract

The paper presents the results of surveys into the ecological status of rivers in the region of Lublin. Biological and chemical elements were analysed between 2012-2014. Analyses were carried out at the following 8 checkpoints on the rivers. The following chemical and biological indicators were determined in water samples. The obtained results were processed by statistical methods including determining the differentiation of water quality indicators as regards the checkpoint (measuring site) and the year of measurement. To this end, methods of descriptive statistics were used, including box-plots. The data was analysed using Statistica software.

The analysed river waters were characterised by very low content of ammonia nitrogen below 0.4 mg $N\text{-}NH_4$/l, total nitrogen below 5 mg $N \cdot dm^{-3}$ and conductivity below 600 uS/cm. These values are characteristic of class I water purity. The content of Kjeldahl nitrogen within the range of 1-2 mg $N \cdot dm^{-3}$, phosphates within the range 0.2-0.4 mg $PO_4 \cdot dm^{-3}$, nitrate nitrogen 2-5 mg $N\text{-}NO_3 \cdot dm^{-3}$ and phosphorus 0.2-0.4 mg $P \cdot dm^{-3}$ makes the analysed waters eligible for purity class II. Sometimes the content of phosphates in the region of Lublin exceeds the limit value for class II – 0.4 mg $PO_4 \cdot dm^{-3}$. BOD_5 in lake Zalew Zemborzycki continuously exceeded the limit value for class II – 6 mg $O_2 \cdot dm^{-3}$.

The results were considerably worse for biological indicators. For MIR the index was 37-41, which made the waters eligible for purity class II. At some checkpoints located within the limits of Lublin city the value of the index lower than 37 made the water eligible for purity class III. For IO the index most often

ranged from 0.3 to 0.4, which corresponds to class III water purity. A decrease in the index below 0.3 in Ciemięga and Czechówka rivers made the water eligible for purity class IV.

The main reason for the poor ecological status of water was a high content of phosphates and a low diatom index. The largest variability in the value of the index was characteristic of the analysed watercourses for nitrate nitrogen and ammonia nitrogen and oxygen level. The watercourses are not very wide (1-3 m) and not very deep (0.2-1.0 m), they have a low flow and their beds are modified (profiled bed, concrete slabs). Watercourses located outside the city are characterised by moderate ecological potential (quality class III), whereas watercourses in Lublin are characterised by insufficient ecological potential (quality class IV).

Anova analysis showed a significant variability in values between checkpoints, which is not applicable to MIR only. In most cases, no significant variability in the values of indicators was recorded between years at respective checkpoints, which is not applicable to phosphates and total phosphorus.

Słowa kluczowe:
rejon Lublina, woda, stan ekologiczny, wskaźniki jakości

Keywords:
region of Lublin, water, ecological status, quality indicators

MIDDLE POMERANIAN SCIENTIFIC SOCIETY OF THE ENVIRONMENT PROTECTION
ŚRODKOWO-POMORSKIE TOWARZYSTWO NAUKOWE OCHRONY ŚRODOWISKA

Annual Set The Environment Protection
Rocznik Ochrona Środowiska

Volume/Tom 19. Year/Rok 2017 ISSN 1506-218X 451-464

Stymulacja rozkładu 3-pierścieniowych WWA podczas fermentacji osadów ściekowych

Maria Włodarczyk-Makuła[*], *Bartłomiej Macherzyński*[**]
[*]*Politechnika Częstochowska*
[**]*Uniwersytet Kardynała Stefana Wyszyńskiego w Warszawie*

1. Wstęp

Osady ściekowe wydzielane podczas oczyszczania ścieków zarówno komunalnych jak i przemysłowych zawierają znaczne ilości związków organicznych, w tym także wielopierścieniowych węglowodorów aromatycznych (WWA) (Bień & Wystalska 2011, Jędrczak 2008, Sadecka i in. 2011, Włodarczyk-Makuła 2007). Do najczęściej stosowanych procesów przeróbki osadów należą procesy odwadniania i stabilizacja biologiczna lub chemiczna. Głównym celem przeróbki osadów ściekowych jest rozkład związków organicznych, zmniejszenie objętości osadów, przygotowanie do dalszej przeróbki, wykorzystania lub zagospodarowania (Bień & Wystalska 2011, Dymaczewski i in. 20011, Kalderis i in. 2010, Macherzyński & Włodarczyk-Makuła 2015). Cennym pod względem energetycznym produktem stabilizacji beztlenowej jest metan (Gazda i in. 2012, Kardos i in. 2011, Myszograj 2011, Szaflik i in. 2014, Pawłowska & Siepak 2009).

Obecność WWA w osadach wydzielonych ze ścieków miejskich wielokrotnie zostało potwierdzone w literaturze (Bernacka & Pawłowska 2000, Hua i in. 2008, Khadhar i in. 2010, Park i in. 2009, Barret i in. 2010, Bernal-Martinez i in. 2005, Bernal-Martinez i in. 2009). WWA są związkami hydrofobowymi. Wprawdzie słabo rozpuszczają się w wodzie, ale obecność np. substancji powierzchniowo czynnych co jest charakterystyczne dla ścieków bytowo-gospodarczych, wpływa na zwięk-

szenie ich rozpuszczalności. Ponadto dobrze rozpuszczają się w tłuszczach, olejach oraz rozpuszczalnikach organicznych. WWA są związkami wykazującymi silne powinowactwo do cząstek stałych, zatem w układzie dwufazowym ścieki-osady ściekowe, występują przede wszystkim w formie zaadsorbowanej na cząstkach stałych. Występują także w cieczach osadowych, co zwykle jest pomijane w literaturze, z wyjątkiem badań autorskich zapoczątkowanych w Politechnice Częstochowskiej (Macherzyński & Włodarczyk-Makuła 2011, Macherzyński & Włodarczyk-Makuła 2015,Macherzyński i in. 2014, Włodarczyk-Makuła 2010). Podczas fermentacji metanowej zachodzą wielokierunkowe przemiany WWA takie jak bioakumulacja, ulatnianie, reakcje z innymi składnikami, adsorpcja/desorpcja oraz biodegradacja (Christensen i in. 2004, Bernal-Martinez i in. 2005). Z uwagi na fakt, że procesy te zachodzą równocześnie, wyniki badań opisane w literaturze są często rozbieżne. Dla przykładu przedstawione są wyniki badań, które potwierdzają, że podczas beztlenowej stabilizacji zachodzi biodegradacja WWA (Christensen i in. 2004, Li i in. 2008) jak i takie, które wskazują na silną sorpcję utrudniającą przemiany biologiczne (Chang i in. 2002). Skuteczność i szybkość biodegradacji WWA zależy od struktury oraz od warunków środowiska tzn. odczynu, temperatury, obecności mikroorganizmów zdolnych do rozkładu tych związków, łatwo przyswajalnego źródła węgla, obecności lub brak akceptorów elektronów oraz inhibitorów i stymulatorów przemian metabolicznych mikroorganizmów (Barret i in. 2010).

2. Cel badań

Celem badań było określenie stopnia degradacji WWA w osadach komunalnych i w mieszaninie osadów komunalnych z koksowniczymi podczas procesu fermentacji. Zmiany ilościowe WWA analizowano równolegle w osadach ściekowych oraz w cieczach nadosadowych, co pozwoliło na zbilansowanie WWA w obu fazach.

3. Metodyka badań

3.1. Substraty

Badania prowadzono z wykorzystaniem osadów pobranych z oczyszczalni miejskiej oraz z oczyszczalni zakładowej. Do badań technologicznych z oczyszczalni ścieków miejskich pobierano osady komu-

nalne (surowe, nadmierne) przeznaczane do fermentacji w warunkach technicznych oraz osady przefermentowane (do zaszczepienia). Osady koksownicze pobrano z osadnika wtórnego biologicznej oczyszczalni eksploatowanej na terenie koksowni.

3.2. Badania technologiczne

Badania fermentacji prowadzono w szklanych reaktorach porcjowych przy ograniczonym dostępie światła z możliwością pomiaru ciśnienia biogazu. Proces prowadzono w termostacie w stałej temperaturze na poziomie 37±2ºC. Do badań fermentacji przygotowano: osady komunalne (wstępne osady kontrolne K) oraz mieszaninę osadów komunalnych z koksowniczymi w proporcji 20:1 (osady badane B). Proporcja ta odpowiada ilości osadów koksowniczych jakie nie wpływają negatywnie na efektywność procesu fermentacji. Zarówno w osadach jak i cieczach nadosadowych oznaczano wielopierścieniowe węglowodory aromatyczne przed procesem fermentacji oraz po jego zakończeniu. Na podstawie zawartości WWA w osadach ściekowych w odniesieniu do suchej masy oraz stężeń w cieczach nadosadowych wyznaczono bilans masowy WWA. Do określenia istotności zmian WWA w fazie stałej i cieczach nadosadowych wykorzystano test t-*Studenta*. Poziom ufności przyjęto na poziomie 0,95. Liczba określająca stopień swobody wyniosła 3, dla tego parametru wartość teoretyczna rozkładu t-*Studenta* t_d wynosiła 2,776.

3.3. Metodyka analityczna oznaczania WWA

Do badań pobierano 10 g odwirowanych osadów ściekowych oraz 500 cm^3 cieczy nadosadowych. Wydzielenie matrycy organicznej z osadów realizowano w procesie sonolizy z wykorzystaniem mieszaniny rozpuszczalników cykloheksanu i dichlorometanu (5:1 v/v). Związki organiczne wydzielano z cieczy osadowych podczas ekstrakcji ciecz-ciecz z dodatkiem metanolu, cykloheksanu i dichlorometanu (20:5:1 v/v/v). Oddzielanie ekstraktów od cieczy odbywało się w rozdzielaczu szklanym. Do wyizolowania analitów z ekstraktów od równocześnie wyekstrahowanych innych substancji organicznych używano żelu krzemionkowego. Oczyszczone ekstrakty zatężano w strumieniu azotu. Oznaczenia wykonywano przy użyciu chromatografu gazowego sprzężonego ze spektrometrem mas (model GC800/MS800 firmy Fisons). Ilościowo oznaczono 2-pierścieniowy naftalen, 3-pierścieniowe węglowodory takie

jak acenaftylen, acenaften, fluoren, fenantren, antracen oraz 4-pierścieniowe: fluoranten, piren, benzo(a)antracen i chryzen.

4. Wyniki badań i dyskusja

4.1. Zmiany zawartości WWA w osadach ściekowych

Wyniki oznaczeń jakościowo-ilościowych poszczególnych WWA podczas kofermentacji osadów kontrolnych przedstawiono na rysunku 1. Sumaryczna początkowa zawartość 10 WWA w osadach kontrolnych wynosiła 1162 µg/kg s.m. Po procesie fermentacji sumaryczna zawartość analizowanych WWA w osadach była 4-krotnie mniejsza i wynosiła 302 µg/kg s.m. W osadach kontrolnych po procesie fermentacji odnotowano mniejsze zawartości analizowanych WWA w porównaniu z początkowymi z wyjątkiem naftalenu, acenaftalenu oraz acenaftenu czyli najbardziej lotnych węglowodorów. Wzrost tych związków mógł być spowodowany rozpadem innych węglowodorów o bardziej rozbudowanej strukturze.

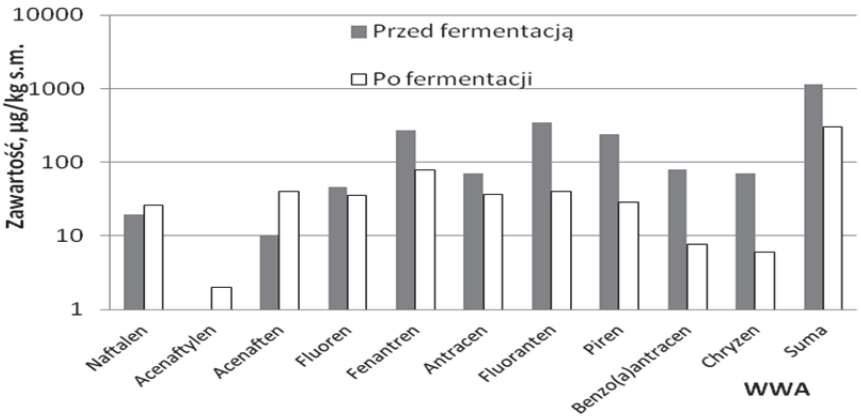

Rys. 1. Zmiany stężeń poszczególnych WWA w osadach kontrolnych – K
Fig. 1. Changes of individual PAHs concentration in control sewage sludge – K

W mieszaninie osadów komunalnych z koksowniczymi sumaryczna zawartość 10 WWA wynosiła 2872 µg/kg s.m. Podczas fermentacji odnotowano 73% ubytek sumarycznej ilości WWA (rys. 2). W tym przypadku stężenia wszystkich węglowodorów po procesie fermentacji były mniejsze od początkowych.

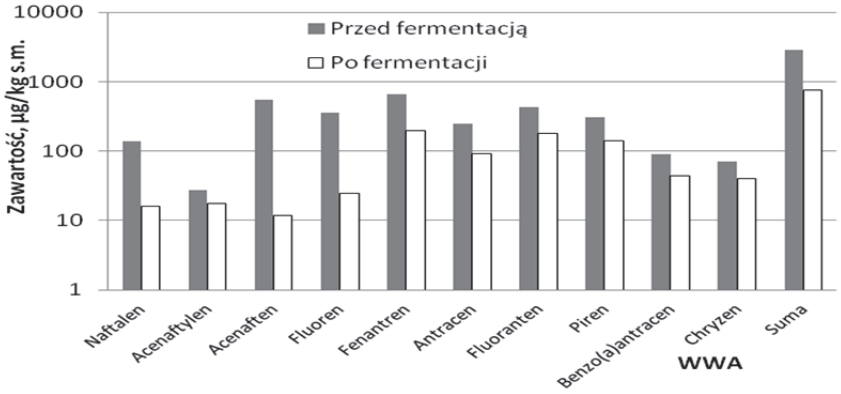

Rys. 2. Zmiany stężeń poszczególnych WWA w osadach badanych – B
Fig. 2. Changes of individual PAHs concentration in examined sewage sludge –B

4.2. Zmiany stężeń WWA w cieczach nadosadowych

Stężenie dziesięciu WWA w cieczach nadosadowych wydzielonych z osadów kontrolnych przed procesem fermentacji wynosiło 0,7 µg/dm^3. Po 16 dobowej fermentacji nastąpił prawie 4-krotny wzrost ilości WWA w cieczach nadosadowych do wartości 2,5 µg/dm^3. Zmiany stężeń WWA w cieczach nadosadowych z kontrolnych osadów ściekowych przedstawiono na rysunku 3.

Wartości oznaczonych stężeń poszczególnych wielopierścieniowych węglowodorów aromatycznych w cieczach nadosadowych wydzielonych z mieszaniny osadów komunalnych z osadami koksowniczymi przedstawiono na rysunku 4. Przed procesem sumaryczne stężenie 10 WWA w cieczach nadosadowych wynosiło 0,9 µg/dm^3. Po procesie kofermentacji nastąpił wzrost stężeń wszystkich oznaczanych węglowodorów, a w najwyższym stężeniu oznaczono fenantren, którego stężenie wzrosło ponad 5-krotnie.

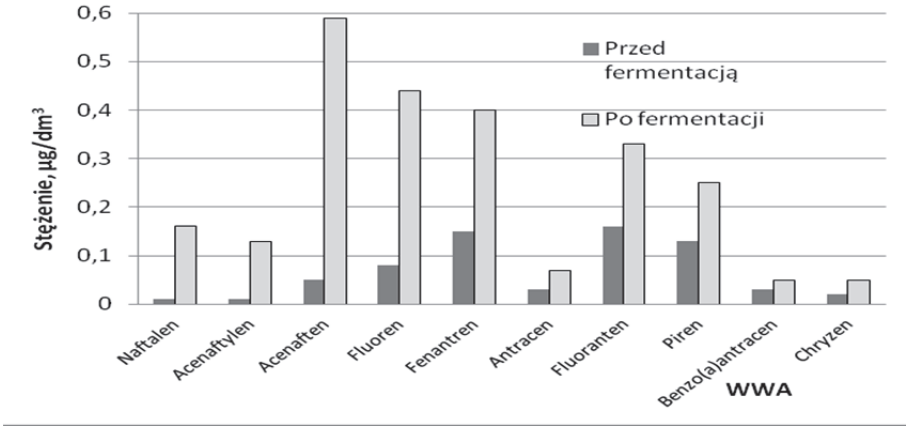

Rys. 3. Zmiany stężeń poszczególnych WWA cieczach nadosadowych – K
Fig. 3. Changes of individual PAHs concentration in supernatant – K

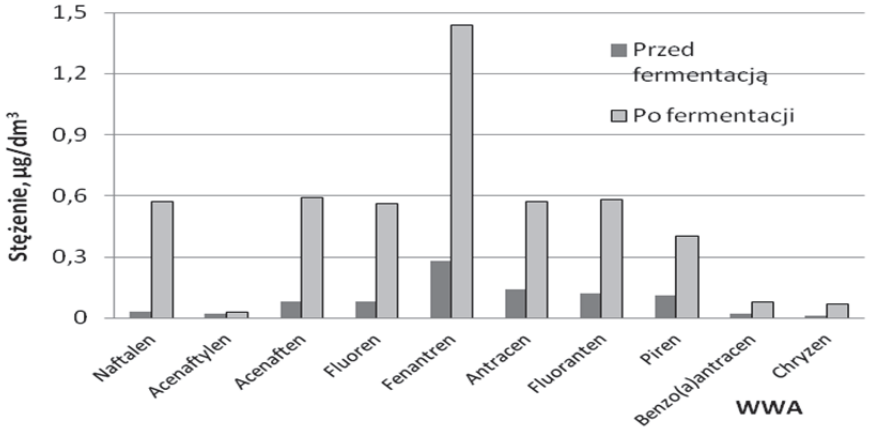

Rys. 4. Zmiany stężeń poszczególnych WWA cieczach nadosadowych – B
Fig. 4. Changes of individual PAHs concentration in supernatant – B

4.3. Bilans WWA

Bilans WWA dla osadów kontrolnych przedstawiono w tabeli 1. Podczas fermentacji osadów kontrolnych ilość WWA w jednostkowej objętości zmalała z 22,59 do 6,91 μg. W osadach ściekowych nastąpił zatem ubytek ilości WWA podczas fermentacji na poziomie 15,68 μg. Uwzględniając oddzielnie fazę stałą i ciekłą osadów, odnotowano ubytek WWA w fazie stałej przy wzroście stężenia tych związków w fazie ciekłej. Ubytek ten jednak nie bilansuje się ze wzrostem, gdyż ubytek wynosił 17,42 μg a wzrost – 1,74 μg. Przed procesem fermentacji w osadach zawartość 10 WWA wynosiła 21,93 μg, natomiast po procesie – 4,51 μg. W cieczach nadosadowych natomiast początkowa ilość WWA wynosiła 0,66 μg, a końcowa – 2,4 μg.

Tabela 1. Bilans masowy WWA w osadach i cieczach nadosadowych przed i po procesie fermentacji dla osadów kontrolnych (K)
Table 1. Mass balance of PAHs in the sewage sludge and supernatant before and after the fermentation process for control sewage sludge (K)

Ilość pierścieni	WWA	Przed fermentacją, μg		Po fermentacji, μg		Ubytek
		Osady	Ciecze	Osady	Ciecze	
2	Naftalen	0,37	0,01	0,40	0,16	–
3	Acenaftylen	0,00	0,01	0,03	0,12	–
	Acenaften	0,20	0,05	0,59	0,57	–
	Fluoren	0,86	0,08	0,53	0,43	–
	Fenantren	5,19	0,15	1,17	0,39	3,78
	Antracen	1,33	0,03	0,55	0,07	0,74
4	Fluoranten	6,55	0,15	0,60	0,32	5,78
	Piren	4,56	0,13	0,43	0,24	4,02
	Benzo(a)antracen	1,53	0,03	0,12	0,05	1,39
	Chryzen	1,34	0,02	0,09	0,05	1,22
Suma 10 WWA		21,93	0,66	4,51	2,40	15,68

Bilans masy WWA dla mieszaniny osadów komunalnych z koksowniczymi (B) przedstawiono w tabeli 2. Z bilansu masy wynika, że w fazie stałej przed kofermentacją zawartość 10 WWA była na poziomie 50,03 µg, a po procesie kofermentacji – 12,00 µg. Zatem ubytek węglowodorów w fazie stałej wynosił 38,03 µg. W cieczach nadosadowych po fermentacji odnotowano zwiększoną ilość WWA o 3,90 µg w porównaniu z zawartością początkową. Uwzględniając obie fazy ubytek WWA był na poziomie 34,13 µg. Wskazuje to na możliwość degradacji analizowanych węglowodorów w przyjętych warunkach doświadczenia. Stopień degradacji WWA w tym przypadku był większy niż w przypadku osadów kontrolnych (komunalnych). Dotyczyło to naftalenu i węglowodorów 3-pierścieniowych. Ubytek pozostałych węglowodorów w mieszaninie osadów z udziałem koksowniczych był mniejszy niż bez ich udziału.

Tabela 2. Bilans masowy WWA w osadach i cieczach nadosadowych przed i po procesie fermentacji dla osadów badanych (B)
Table 2. Mass balance of PAHs in the sewage sludge and supernatant before and after the fermentation process for examined sewage sludge (B)

Ilość pierścieni	WWA	Przed fermentacją, µg		Po fermentacji, µg		Ubytek
		Osady	Ciecze	Osady	Ciecze	
2	Naftalen	2,42	0,03	0,25	0,55	1,65
3	Acenaftylen	0,48	0,02	0,27	0,03	0,20
	Acenaften	9,46	0,07	0,19	0,57	8,77
	Fluoren	6,21	0,08	0,38	0,54	5,37
	Fenantren	11,53	0,27	3,11	1,40	7,29
	Antracen	4,33	0,13	1,43	0,55	2,48
4	Fluoranten	7,45	0,11	2,85	0,56	4,15
	Piren	5,36	0,10	2,19	0,39	2,88
	Benzo(a)antracen	1,57	0,02	0,69	0,08	0,82
	Chryzen	1,22	0,01	0,64	0,07	0,52
Suma 10 WWA		50,03	0,84	12,00	4,74	34,13

Zmiany stężenia WWA w osadach ściekowych, jak i cieczach nadosadowych odnotowane w badaniach wskazują, że podczas fermentacji osadów ściekowych występuje biodegradacja tych związków. Odnotowano ubytek większości analizowanych węglowodorów. Większy ubytek WWA podczas fermentacji odnotowano w przypadku obecności osadów koksowniczych. Zatem te osady mogły zawierać mikroorganizmy zdolne do biodegradacji WWA. Takimi mikroorganizmami są archeany metanogenne, które wykazują zdolność degradacji węglowodorów (Anielak 2013). Mikroorganizmy te zasiedlające osady koksownicze rozwijały się w obecności WWA i dlatego były przystosowane do enzymatycznych przemian tych związków. Wzrost natomiast stężenia niektórych węglowodorów może świadczyć o desorpcji tych związków z osadów do cieczy nadosadowych, w tym także o uwalnianiu, wcześniej zaabsorbowanych związków, w komórkach mikroorganizmów. Zarówno w osadach jak i cieczach nadosadowych wyniki obliczeń wskazują, że dla większości węglowodorów odnotowane zmiany zawartości w osadach i cieczach były istotne pod względem statystycznym. Wyjątkiem był benzo(a)antracen w osadach kontrolnych dla którego obliczona wartość t_d nie przekraczała wartości charakterystycznej dla testu t-*Studenta*.

Opisane w literaturze badania zmian ilościowych wielopierścieniowych węglowodorów aromatycznych dotyczą przede wszystkim osadów z oczyszczalni miejskich. Wyniki badań zawartości WWA w osadach koksowniczych są nieliczne. Zawartość WWA w osadach wydzielonych podczas oczyszczania ścieków koksowniczych na terenie Chin sięgała 4490 mg/kg (Zhang i in. 2012). We wcześniejszych badaniach autorów oznaczone zawartości WWA były mniejsze i przyjmowały wartości od kilku µg do kilkuset mg/kg s.m. Sumaryczna zawartość 16 WWA w osadach sięgała 740 mg/kg s.m. natomiast w cieczach nadosadowych 17 µg/dm^3 (Włodarczyk-Makuła 2007, Włodarczyk-Makuła 2010).

Jak wspomniano na wstępie w osadach przefermentowanych oznacza się zarówno wyższe jak i niższe zawartości WWA niż przed procesem. Przykładowo w badaniach prowadzonych przez Bernal-Martinez i in. zawartość 13 WWA w osadach ściekowych podczas fermentacji wzrosła o 1,8 mg/kg (Bernal-Martinez i in.2005). Wyniki innych badań wskazują na obniżenie zawartości tych związków w osadach o 1,1 mg/kg i w cieczach nadosadowych (w zakresie 48-51% zawartości początkowej) (Bernal-Martinez i in. 2009). Rozbieżności te wynikają ze

zmiennego składu chemicznego osadów, różnych warunków procesowych oraz zróżnicowanej aktywności mikroorganizmów zdolnych do biodegradacji WWA.

5. Wnioski

Na podstawie wyników badań przeprowadzonych w ustalonych warunkach można sformułować następujące wnioski:

- Bilans masy w odniesieniu do jednostkowej objętości osadów świadczy o degradacji tych związków podczas fermentacji metanowej osadów komunalnych i ich mieszaniny z koksowniczymi.
- Wykazano, że dodatek osadów koksowniczych stymulował degradację naftalenu i 3-pierścieniowych WWA, gdyż ubytek tych związków był większy w obecności tych osadów niż bez ich udziału.
- Możliwy jest wzrost stężenia WWA w cieczach osadowych po procesie fermentacji co może mieć znaczenie w przypadku zawracania tych cieczy do ciągu oczyszczania ścieków.

Pracę zrealizowano w ramach BS-PB-402-301/11

Literatura

Anielak, A. (2013). *Czy archeany najstarsze mikroorganizmy świata mogą współtworzyć nowoczesne systemy oczyszczania*? Materiały konferencyjne „Gospodarka wodno-ściekowa i odpadowa miast i wsi" Wyższa Szkoła Zarządzania Środowiskiem w Tucholi, 7-8.

Barret, M., Carrere, H., Delgadillo, L., Patureau, D. (2010). PAH fate during the anaerobic digestion of contaminated sludge: Do bioavailability and/or cometabolism limit their biodegradation? *Water Research*, *44*, 3797-3806.

Bernal-Martinez, A., Carrere, H., Patureau ,D., Delgenes, J.P. (2005). Combining anaerobic digestion and ozonation to removal PAH from urban sludge. *Process Biochemistry*, *40*, 3244-3250.

Bernal-Martinez, A., Patureau, D., Delgenes, J.P., Carrere, H. (2009). Removal of polycyclic aromatic hydrocarbons (PAH) during anaerobic digestion with recirculation of ozonated digested sludge. *Journal of Hazardous Materials*, *162*, 1145-1150.

Bernacka, J., Pawłowska, L. (2000). *Substancje potencjalnie toksyczne w osadach z komunalnych oczyszczalni ścieków*. Warszawa: Instytut Ochrony Środowiska.

Bień, J., Wystalska, K. (2011). *Osady Ściekowe. Teoria i praktyka*. Częstochowa: Wydawnictwo Politechniki Częstochowskiej.

Chang, B., Shiung, L., Yuan, S. (2002). Anaerobic biodegradation of polycyclic aromatic hydrocarbon in soil. *Chemosphere*, *48*, 717-724.

Christensen, N., Batstone, D.J., He, Z., Angelidaki, I., Schmidt, J.E. (2004). Removal of polycyclic aromatic hydrocarbons (PAHs) from sewage sludge by anaerobic degradation. *Water Science and Technology*, *50*, 237-244.

Dymaszewski, Z., Sozański, M. *Poradnik eksploatatora oczyszczalni ścieków*. (2011). Poznań: Wydanie III, PZITS.

Gazda M., Rak A., Sudak, M. (2012). Badania kofermentacji osadów ściekowych z tłuszczami odpadowymi w oczyszczalni ścieków w Brzegu. *Infrastruktura i Ekologia Terenów Wiejskich, Polska Akademia Nauk*, *3*, 79-90.

Hua, L., Wu, W.X., Tientchen, C.M., Chen, Y-X. (2008). Heavy metals and PAHs in sewage sludge from twelve wastewater treatment plants in Zhejiang Province. *Biomedical and Environmental Sciences*, *4*, 345-352.

Jędrczak, A.(2008). *Biologiczne przetwarzanie odpadów*. Warszawa: Wydawnictwo Naukowe PWN.

Kalderis, D., Aivalioti, M., Gidarakos, E. (2010). Options for sustainable sewage sludge management in small wastewater treatment plants on islands: The case of Crete. *Desalination*, *260(1)*, 211-217.

Kardos, L., Juhasz, A., Palko, GY., Olah, J., Barkacs, K., Zaray, GY. (2011). Comparing of mesophilic and thermophilic anaerobic fermented sewage sludge based on chemical and biochemical tests. *Applied Ecology and Environmental Research*, *9(3)*, 293-302.

Khadhar, S., Higashi, T., Hamdi, H., S. Matsuyama, S. Charef A. (2010). Distribution of 16 EPA-priority polycyclic aromatic hydrocarbons (PAHs) in sludges collected from nine Tunisian wastewater treatment plants. *Journal of Hazardous Materials*, *183*, 98-102.

Li, X., Li, P., Lin, X., Zhang, C., Li, Q., Gong, Z. (2008). Biodegradation of aged polycyclic aromatic hydrocarbons (PAHs) by microbial consortia in soil and slurry phases. *Journal of Hazardous Materials*, *150*, 21-62.

Macherzyński, B., Włodarczyk-Makuła, M. (2011). Ekstrakcja WWA z osadów wydzielonych ze ścieków koksowniczych. *Inżynieria i Ochrona Środowiska*, *4*, 333-343.

Macherzyński, B., Włodarczyk-Makuła, M. (2015). Ocena możliwości unieszkodliwiania osadów koksowniczych w procesie kofermentacji. *Rocznik Ochrona Środowiska (Annual Set The Environment Protection)*, *17*, 1142-1161.

Macherzyński, B., Włodarczyk-Makuła, M., Nowacka, A. (2012). Simplification of procedure of preparing samples for PAHs and PCBs determination. *Archives of Environmental Protection*, *4*, 22-33.

Myszograj, S. (2011). Produkcja metanu wskaźnikiem oceny biodegradowalności substratów w procesie fermentacji metanowej., *Rocznik Ochrona Środowiska (Annual Set The Environment Protection)*, *13*, 1245-1260.

Park, J.M., Lee, B.J., Kim, J.P., Kim, M.J., Kwon, O.S., Jung, D.I. (2009). Behavior of PAHs from sewage sludge incinerators in Korea. *Waste Management*, *29*, 690-695.

Pawłowska, M., Jerzy Siepak, J. (2009). Współfermentacja odpadów komunalnych i osadów ściekowych na składowisku odpadów. Polska *Inżynieria Środowiska pięć lat po wstąpieniu do Unii Europejskiej, Monografie Komitetu Inżynierii Środowiska, 60(3)*, 191-198.

Sadecka, Z., Myszograj, S., Suchowska-Kisielewicz, M. (2011). Aspekty prawne przyrodniczego wykorzystania osadów ściekowych. *Zeszyty Naukowe Uniwersytetu Zielonogórskiego, Inżynieria Środowiska*, *24(144)*, 5-17.

Szaflik, W., Iżewska, A., Dominowska, M. (2014). Bilans energii chemicznej przefermentowanych osadów Oczyszczalni Ścieków Pomorzany w Szczecinie. *Rocznik Ochrona Środowiska (Annual Set The Environment Protection)*, *16*, 16-33.

Włodarczyk-Makuła, M. (2010). Ilościowe zmiany WWA w osadach i cieczach nadosadowych podczas fermentacji prowadzonej w warunkach denitryfikacji. *Inżynieria i Ochrona Środowiska*, *4*, 311-319.

Włodarczyk-Makuła, M. (2007). *Zmiany ilościowe WWA podczas oczyszczania ścieków i przeróbki osadów*. Częstochowa: Wydawnictwo Politechniki Częstochowskiej.

Zhang, W., Wei, C., Chai, X., He, J., Cai, Y., Ren, M., Yan, B., Peng, P., Fu, J. (2012). The behaviors and fate of polycyclic aromatic hydrocarbons (PAHs) in a coking wastewater treatment plant. *Chemosphere*, *88*, 174-182.

The Stimulation of Degradation of 3-ring of PAHs in Sewage Sludge During Fermentation Process

Abstract

The paper presents the results of co-digestion of municipal and coke sewage sludge. The fermentation process was carried out at 37°C, in glass bioreactors in the dark. Fermentation research was carried out for two mixtures. The first one was municipal sewage sludge (a mixture of preliminary sewage sludge, excess sewage sludge and inoculum), and the second – a mixture of municipal sewage sludge (composition as above) with the addition of coke sewage sludge in the amount of 5% by volume. Determination of PAHs was performed two times parallel in the sewage sludge and in supernatants: before fermentation and at the end of the process. Naphtalene, acenaphtylene, acenaph-

tene, fluorine, phenanthrene, anthracene, fluoranthene, pyrene, benzo(a)anthracene and chrysene was determined using a gas chromatograph coupled with a mass detector. On the basis of designated concentrations of PAHs and dry matter content in sewage sludge amounts of these compounds in solid and liquid phase in relation to the unit volume was calculated. In municipal sewage sludge amount of low molecular weight (2-, 3- and 4-ring) PAHs before the process in sewage sludge and separated from them supernatants was 1162 μg in total, while after the stabilization process – 302 μg. In liquid phase an increase of 10 PAHs by 1,8μg was obtained, while in the solid phase – 74% decrease. In the case of the mixture fermentation, in which 5% of the volume was coke sewage sludge, the total hydrocarbon content in the solid phase after the process was less than the initial by about 73%. While in the liquid phase, reported increase in PAHs concentration during the process. The total amount of PAHs in both phases (solid and liquid) before the process was 51μg, and after fermentation process – 17 μg. The addition of coke sewage sludge stimulated decomposition of naphthalene and 3-ring of PAHs.

Streszczenie

W artykule zaprezentowano wyniki badań kofermentacji osadów wydzielonych ze ścieków miejskich i ze ścieków koksowniczych. Proces fermentacji prowadzono w temperaturze 37°C, w szklanych bioreaktorach. Fermentację prowadzono w dwóch próbach: jedną stanowiły osady osady komunalne (mieszanina osadów wstępnych, nadmiernych oraz inokulum), drugą – mieszanina osadów komunalnych (jak wyżej) z dodatkiem osadów koksowniczych w ilości stanowiącej 5% objętościowo. Oznaczanie WWA było prowadzone równolegle dwukrotnie w osadach ściekowych i w cieczach nadosadowych: przed procesem fermentacji oraz po jego zakończeniu. Oznaczono ilościowo takie WWA jak: naftalen, acenaftylen, acenaften, fluoren, fenantren, antracen, fluoranten, piren, benzo(a)antracen oraz chryzen z wykorzystaniem chromatografu gazowego z detektorem masowym. Na podstawie stężeń WWA w przeliczeniu na suchą masę osadów, zawartości suchej masy oraz stężenia w cieczy nadosadowej i jej objętości wyznaczono ilości WWA w jednostkowej objętości osadów. W osadach komunalnych zawartość małocząsteczkowych (2-, 3- i 4-pierścieniowych) WWA przed procesem fermentacji w jednostce objętości osadów była na poziomie 1162 μg l, natomiast po procesie fermentacji wynosiła 302 μg. W cieczach nadosadowych odnotowano wzrost 10 WWA do wartości 1,8 μg, podczas gdy w fazie stałej, spadek wartości wyniósł 74%. W przypadku mieszaniny osadów, w której 5% objętości stanowiły osady koksownicze, całkowita zawartość WWA w fazie stałej po procesie fermentacji była mniejsza od początkowej o 73%. W tym samym czasie w fazie ciekłej odnotowano wzrost

ilości WWA. Całkowita zawartość WWA w obu fazach (osadach i cieczach) wynosiła przed procesem fermentacji 51 μg, natomiast po procesie – 17 μg. Dodatek osadów koksowniczych wpływał stymulująco na degradację naftalenu i 3-pierścieniowych WWA.

Słowa kluczowe:
WWA, osady ściekowe, osady koksownicze, ciecze nadosadowe, kofermentacja

Keywords:
PAHs, sewage sludge, coke sludge, supernatants, co-fermentation

MIDDLE POMERANIAN SCIENTIFIC SOCIETY OF THE ENVIRONMENT PROTECTION
ŚRODKOWO-POMORSKIE TOWARZYSTWO NAUKOWE OCHRONY ŚRODOWISKA

Annual Set The Environment Protection
Rocznik Ochrona Środowiska

Volume/Tom 19. Year/Rok 2017 ISSN 1506-218X 465-479

Metodologia tworzenia numerycznej aplikacji do symulacji rozprzestrzeniania się zanieczyszczeń w powietrzu atmosferycznym

Aleksandra Kowalska, Jacek Piekarski
Politechnika Koszalińska

1. Wstęp

W prawie polskim kwestie związane z ochroną powietrza reguluje m.in. rozporządzenie Ministra Środowiska z dnia 24 sierpnia 2012 r. w sprawie poziomów niektórych substancji w powietrzu (Dz.U. z 2012 r., poz. 1031) oraz rozporządzenie Ministra Środowiska z dnia 26 stycznia 2010 r. w sprawie wartości odniesienia dla niektórych substancji w powietrzu (Dz.U. z 2010 r., poz. 87). Jedno z ww. rozporządzeń, a mianowicie rozporządzenie Ministra Środowiska w sprawie wartości odniesienia dla niektórych substancji w powietrzu (Dz.U. z 2010 r., poz. 87) określa metodykę modelowania stężenia zanieczyszczeń w powietrzu atmosferycznym, emitowanych ze źródeł punktowych, powierzchniowych i liniowych. Zgodnie z ww. rozporządzeniem opracowano szereg modeli matematycznych analityczno-empirycznych. Powyższe modele wykorzystywane są przy tworzeniu systemów alarmowych oraz do specyfikacji obszarów zagrożeń na wypadek wystąpienia dużych emisji losowych (Rozporządzenie 2012, Rozporządzenie 2010, Kościelnik & Dąbrowski 2015, Piekarski & Lubierski 2003). Analizowane modele znajdują swoje odzwierciedlenie podczas sporządzania symulacji występujących stężeń w atmosferze (Konieczyński 2012, Michalczyk & Murawski 2001, Sówka et al. 2016). Znając parametry emitora, warunki meteorologiczne oraz terenowe przy użyciu tego typu modeli można obliczyć stężenia zanieczyszczeń w punktach receptorowych.

Równanie Pasquilla jest najczęściej wykorzystywane w praktyce ze względu prostotę obliczeniową i łatwość zastosowania. Stężenie substancji gazowej *Sxyz* w lokalizacji receptora oblicza się według wzoru (Rozporządzenie 2012, Rozporządzenie 2010, Kościelnik & Dąbrowski 2015, Piekarski & Lubierski 2003):

$$S_{xyz}=\frac{E_g}{2\pi\bar{u}\sigma_y\sigma_z}\exp\left(-\frac{y^2}{2\sigma_y^2}\right)\left\{\exp\left[-\frac{(z-H)^2}{2\sigma_z^2}\right]+\exp\left[-\frac{(z+H)^2}{2\sigma_z^2}\right]\right\} \quad (1)$$

Istnieje wiele programów, przy pomocy których można dokonywać obliczeń rozprzestrzeniania się zanieczyszczeń w atmosferze (pakiet OPERAT FB, system OPA03, program EMITOR, program COPDIMO). Np. autorzy pracy (Holnicki i in. 2017), jako narzędzie analizy jakości powietrza w Warszawie wykorzystali system CALMET/CALPUFF, którego zadaniem było powiązanie danych emisyjnych z rozkładami średniorocznych stężeń zanieczyszczeń atmosferycznych. Większość tego typu aplikacji to rozbudowane programy o charakterze komercyjnym. Dlatego w niniejszym artykule przedstawiono prostą metodę tworzenia w darmowym środowisku programistycznym aplikacji do symulacji rozprzestrzeniania się zanieczyszczeń w powietrzu atmosferycznym.

2. Charakterystyka opracowanego programu

2.1. Informacje wprowadzające

Na podstawie algorytmu (Piekarski & Lubierski 2003) oraz aktów prawnych (Rozporządzenie 2012, Rozporządzenie 2012) w programistycznym środowisku darmowego LAZARUSA v. 1.6.4 skompilowano (Free Pascal na licencji GPL) kod źródłowy w systemie 32-bitowego Windowsa, tworząc wersję wykonywalną programu ATMO – rysunek 1. Aplikacja jest rozwinięciem programu ATMO ver. 1.0, z 2002 roku który powstał w środowisku DELPHI (Piekarski & Lubierski 2003).

W ramach prowadzonych prac opracowano cztery podstawowe moduły, których zadaniem jest wprowadzenie danych wstępnych oraz dwa moduły wynikowe, służące wizualizacji symulacji poprzez przedstawienie zmian wartości stężenia 1-godzinnego substancji gazowej w zależności od odległości receptorów od emitora oraz wykresów profili. Program wyposażono w możliwość zapisu do pliku oraz odczytu z pliku wprowadzonych danych początkowych (*.atx). Ponadto, program gene-

ruje raport końcowy oraz daje możliwość wydruku wprowadzonych danych początkowych i wyników obliczeń.

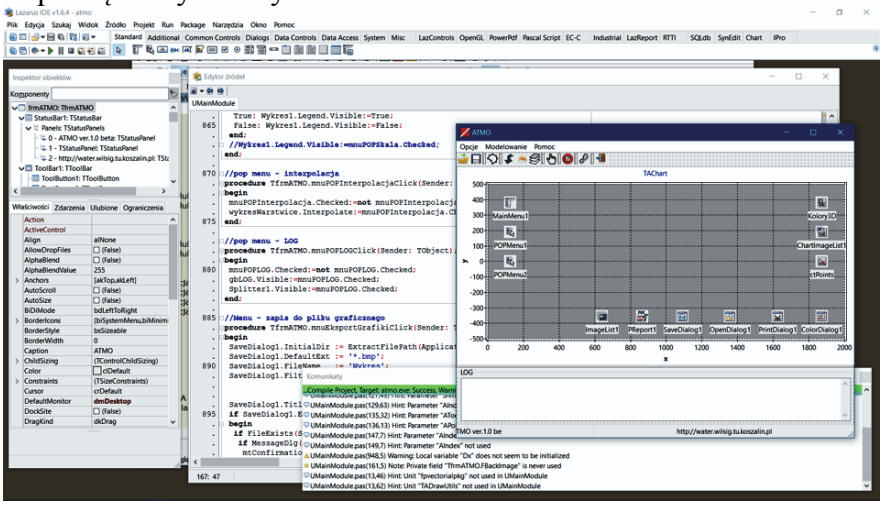

Rys. 1. Widok środowiska LAZARUS z fragmentem kodu źródłowego ATMO
Fig. 1. View of LAZARUS environment with fragment of ATMO source code

2.2. Funkcjonalności opracowanego programu

Po uruchomieniu opracowanej aplikacji należy wybrać z menu górnego opcję „Ustawienia” (Ctrl+U), która spowoduje otwarcie okna (rysunek 2), umożliwiającego początkową konfigurację modelowanego obszaru poprzez wprowadzenie maksymalnej wartości na osi X [m] (wartość domyślna X=3000 m) oraz Y [m] (wartość domyślna Y=300 m).

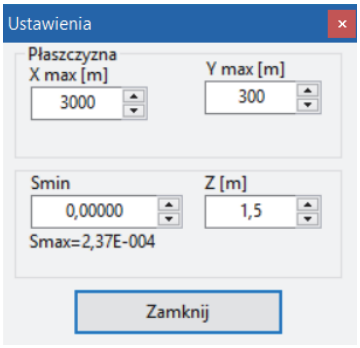

Rys. 2. Podstawowe ustawienia aplikacji
Fig. 2. Basic application settings

Ponadto wprowadzono możliwość ustalenia wartości minimalnej *Smin*, będącej podstawą generowania wizualizacji symulacji zmian wartości stężenia 1-godzinnego substancji gazowej (wartość domyślna *Smin*=0). Aplikacja w trybie rzeczywistym wyświetla wartość *Smax* dla domyślnych wartości wszystkich zmiennych niezależnych (wartość domyślna *Smax*=2,37E-004). Daje również możliwość wprowadzenia wartości poziomu odniesienia względem osi *Z* [m] (wartość domyślna *Z* = 0) – rysunek 2.

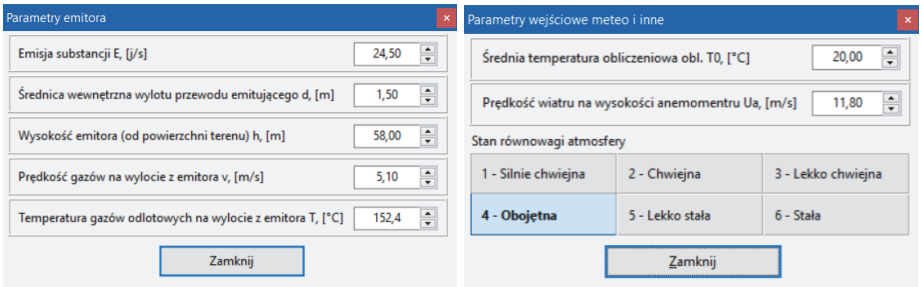

Rys. 3. Parametry emitora oraz meteorologiczne
Fig. 3. Emitter and meteorological parameters

Mając na uwadze stworzenie jak najprostszej aplikacji pod względem użyteczności, program wyposażono w oddzielne moduły, które są uruchamiane niezależnie od siebie i odnoszą się do danych wstępnych, m.in.: parametrów emitora, danych meteorologicznych, współczynnika aerodynamicznej szorstkości terenu oraz lokalizacji receptorów – rysunek 3 i 4.

Moduł 1 wywoływany z menu górnego opcją „Emitor" (Ctrl+W), charakteryzuje parametry techniczne emitora, tj.: maksymalną emisję substancji gazowej *E*, średnicę wewnętrzną wylotu przewodu emitującego substancje *d*, geometryczną wysokość emitora *h*, prędkość gazów na wylocie z emitora *v* oraz temperaturę gazów odlotowych na wylocie z emitora *T* – rysunek 3.

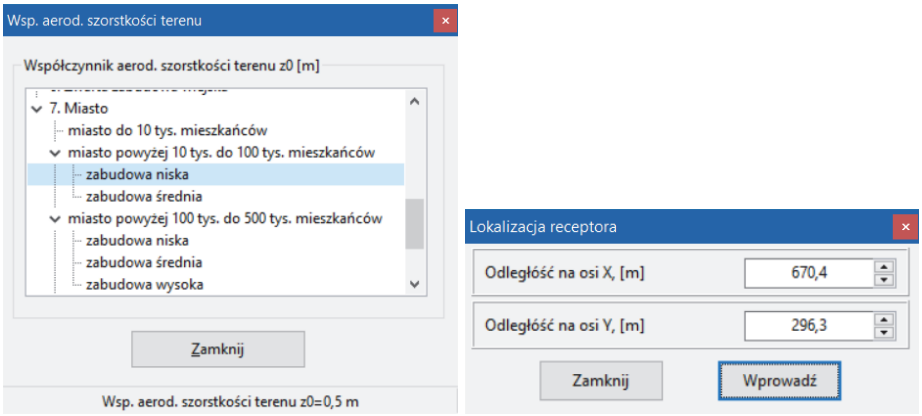

Rys. 4. Współczynnik aerodynamicznej szorstkości terenu oraz lokalizacja receptora
Fig. 4. Aerodynamic coefficient of terrain roughness and location of the receptor

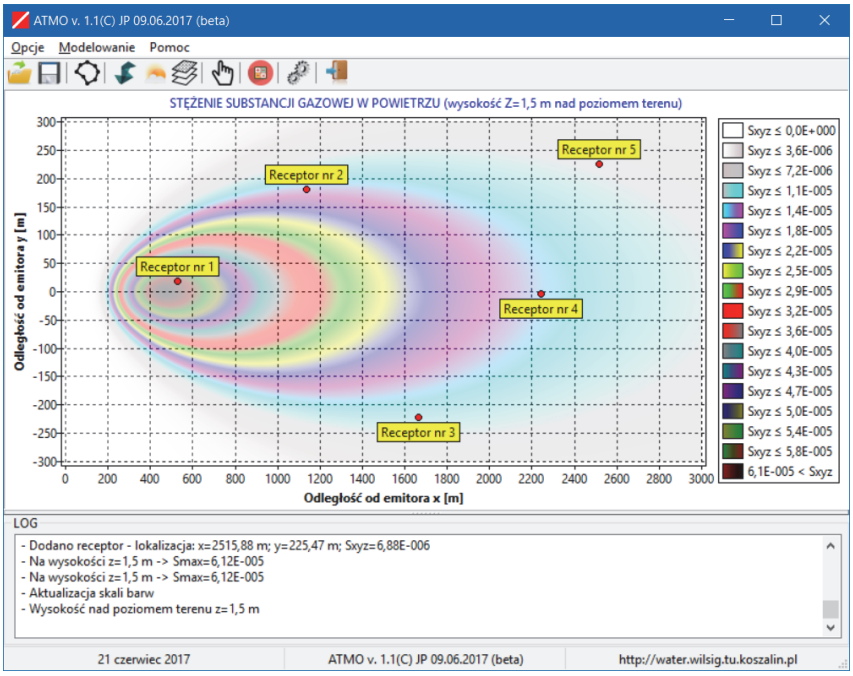

Rys. 5. Symulacja rozprzestrzeniania się zanieczyszczeń w powietrzu atmosferycznym
Fig. 5. Simulation of the spread of pollutants in atmospheric air

Moduł 2 uruchamiany z menu górnego opcją „Meteo" (Ctrl+M), odnosi się do parametrów meteorologicznych, tj.: średniej temperatury powietrza w okresie obliczeniowym *T0*, prędkości wiatru mierzonej na wysokości anemometru *Ua* oraz stanu równowagi atmosfery *ATM* – rysunek 3. Moduł 3 wywoływany z menu górnego opcją „Szorstkość terenu" (Ctrl+T), umożliwia poprzez wybór wprowadzenie wartości współczynnika aerodynamicznej szorstkości terenu *z0* – rysunek 4. Moduł 4 uruchamiany z menu górnego opcją „Lokalizacja receptora" (Ctrl+L) służy do deklaracji lokalizacji receptora podawanej w formie odległości od emitora: *X* (równolegle z kierunkiem wiatru) i *Y* (prostopadle do kierunku wiatru) dla której wykonuje się szczegółowe obliczenia – rysunek 4.

Po zamknięciu dowolnego okna modułów wstępnych przedstawionych na rysunkach 1-4, następuje wywołanie wewnętrznej procedury, która na podstawie wszystkich wprowadzonych wartości parametrów zmiennych niezależnych realizuje obliczenia zgodnie z algorytmem (Rozporządzenie 2012, Rozporządzenie 2010, Piekarski & Lubierski 2003) i formułą (1). Wynikiem realizacji obliczeń jest symulacja rozprzestrzeniania się zanieczyszczeń w powietrzu atmosferycznym zawarta w podstawowym oknie aplikacji i przedstawiona na rysunku 5.

Na podstawie wartości stanu równowagi atmosfery *ATM* [–], która zmienia się w granicach od 1 do 6, program dobiera poprzez zaimplementowaną procedurę pozostałe stałe obliczeniowe *m, a* i *b*. W zależności od wysokości emitora *h* oblicza prędkość wiatru na wysokości wylotu z emitora *Uh*. W przypadku, gdy obliczona wartość *Uh* będzie mniejsza niż 0,5 m/s do dalszych obliczeń aplikacja przyjmie wartość 0,5 m/s. W kolejnym kroku program oblicza emisję ciepła z emitora *Q*, która zależy od średnicy emitora *d*, prędkości gazów na wylocie z emitora *v* oraz temperatury otoczenia *T0* i temperatury gazów na wylocie z emitora *T*. Następnie na podstawie emisji ciepła z emitora *Q* program dobiera i wyświetla nazwę formuły, według której następnie oblicza wartość parametru termiczno-dynamicznego wyniesienia gazów odlotowych *Dh*. Dla $Q < 16000$ kJ/s zastosowana zostaje formuła Hollanda, w której w zależności od stosunku prędkości wiatru na wysokości wylotu z emitora *Uh* do prędkości gazów na wylocie z emitora *v* jest obliczana wartość *Dh*, jako funkcja emisji ciepła *Q* , średnicy emitora *d* oraz prędkości gazów *v*. Dla $Q > 24000$ kJ/s stosowana jest formuła CONCAWE, gdzie *Dh* jest obliczane na podstawie wartości emisji *Q* i prędkości wiatru *Uh*. W przypadku, gdy *Q* będzie zawierać się w przedziale wartości od 16000 do 24000

kJ/s zastosowane zostaną obie formuły, odpowiednio pomniejszone o różnicę pomiędzy wartością Q, a wartościami granicznymi. Suma wartości parametrów wysokości geometrycznej emitora h oraz wyniesienia gazów odlotowych Dh stanowi efektywną wysokość emitora Hp. W zależności od efektywnej wysokości emitora Hp oraz wysokości geometrycznej emitora h program oblicza średnią prędkość wiatru Usr w warstwie, której wysokość waha się od $z=h$ do $z=Hp$. Wartość Usr zależy od efektywnej wysokości emitora Hp, wysokości geometrycznej emitora h oraz prędkości wiatru na wysokości anemometru Ua. Program, podobnie jak dla Uh, przyjmie Usr=0,5 m/s, gdy średnia prędkość wiatru będzie mniejsza niż 0,5 m/s. Następnie dokonywana zostaje weryfikacja ilorazu efektywnej wysokości emitera Hp oraz współczynnika aerodynamicznej szorstkości terenu $z0$.

Kolejnym etapem realizacji algorytmu jest obliczanie współczynników topograficznych A i B zależnych od współczynnika meteorologicznego m oraz ilorazu efektywnej wysokości emitora Hp i współczynnika aerodynamicznej szorstkości terenu $z0$. Na podstawie obliczonych współczynników topograficznych A i B, dobranych wcześniej współczynników empirycznych a i b (zależnych od stanu równowagi) oraz odległości receptora od emitora x [m] obliczone zostają współczynniki dyspersji poziomej Sy i pionowej Sz. Ostatnim parametrem, który program oblicza w zależności od wartości emisji gazów Eg, średniej prędkości wiatru Usr, odległości emitora od receptora y, wysokości receptora z oraz współczynników dyspersji Sy i Sz jest stężenie jednogodzinne substancji gazowej S. Ta wartość finalnie umieszczana jest na wykresie w postaci graficznych pasm przedstawionych na rysunku 5. Z prawej strony wykresu automatycznie generowana jest legenda, z opisem wartości poszczególnych barw.

W celu ułatwienia obsługi aplikacji w obrębie podstawowego wykresu funkcjonują opcje dostępne po wybraniu prawego przycisku myszki (POPMENU) – rysunek 6.

Po wyborze z podręcznego menu (rysunek 6) opcji „Wstaw receptor" program umożliwia umieszczenia receptora w postaci graficznej na podstawowym wykresie w danej lokalizacji kursora (rysunek 5). Ponadto program wzbogacono w możliwość zmiany lokalizacji poszczególnych, wprowadzonych wcześniej receptorów, poprzez wybór receptora oraz wciśnięcie przycisku SHIFT i wskazanie nowej lokalizacji.

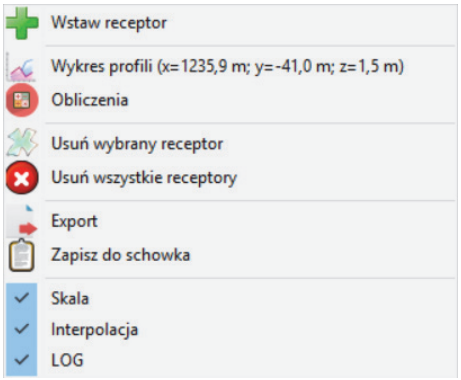

Rys. 6. Menu podręczne
Fig. 6. Popup menu

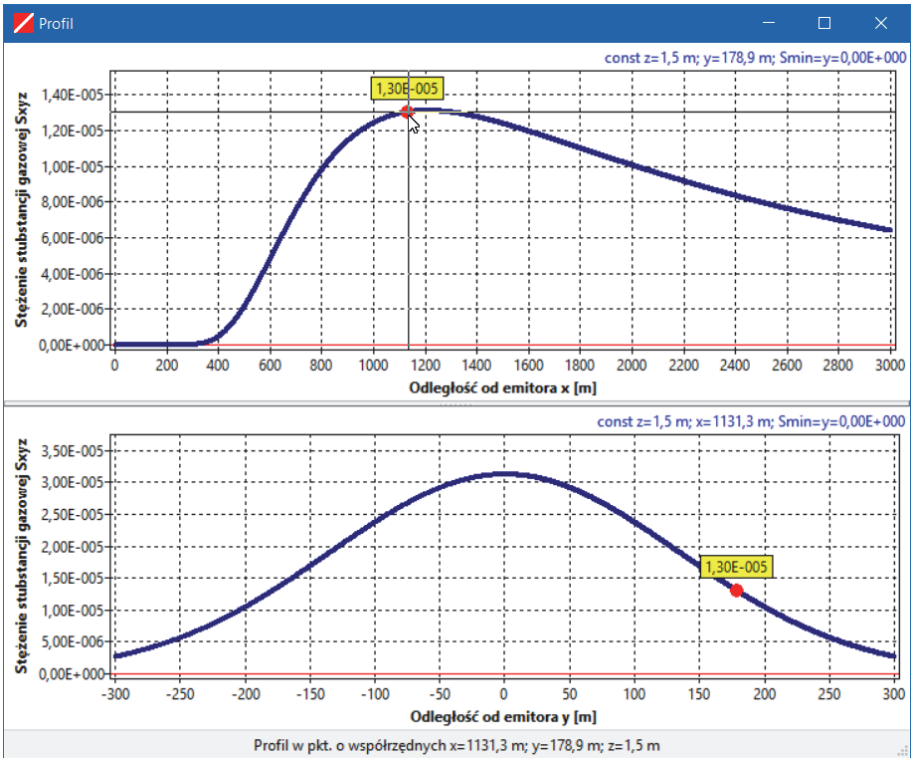

Rys. 7. Graficzne przedstawienie rozkładu stężenia zanieczyszczeń
Fig. 7. Graphical representation of pollution concentration distribution

Opcja „Wykres profili" służy do generowania wykresów przedstawionych na rysunku 7. Wykres górny prezentuje zmianę wartości stężenia substancji gazowej *Sxyz* w zależności od odległości od emitora w osi *X*. W tym przypadku parametrami stałymi są: *z*, *y* oraz *Smin*. Czerwony punkt na wykresie symbolizuje wybrany punkt w lokalizacji kursora na wykresie podstawowym. Z kolei wykres dolny przedstawia zmianę wartości stężenia substancji gazowej *Sxyz* w zależności od odległości od emitora w osi *Y*. Parametrami stałymi są wartości: *z*, *x* oraz *Smin*. Również i na tym wykresie czerwony punkt symbolizuje wybrany punkt w lokalizacji kursora na wykresie podstawowym.

Po wyborze z podręcznego menu (rysunek 6) opcji „Obliczenia" aplikacja otwiera okno tekstowe, które zawiera szczegółowe wyniki obliczeń, podzielone jest pod względem informacyjnym na trzy części. Część pierwsza zawiera dane początkowe, tj.: parametry emitora (emisja substancji, wysokość emitora, średnica wewnętrzna wylotu przewodu emitującego, prędkość gazów na wylocie z emitora, temperatura gazów odlotowych na wylocie z emitora), parametry meteorologiczne (prędkość wiatru na wysokości anemometru, średnia temperatura obliczeniowa, stan równowagi atmosfery, współczynnik aerodynamicznej szorstkości terenu). W części drugiej raportu przedstawione są ogólne wyniki obliczeń, tj. wartości: współczynników *m*, *a* i *b*, prędkości wiatru na wysokości wylotu z emitora, emisji ciepła z emitera, wyniesienia gazów odlotowych, efektywnej wysokość emitera, średniej prędkość wiatru w warstwie od z=h do z=Hp oraz współczynników obliczeniowych *A* i *B*. Natomiast w części trzeciej raportu zawarte są wyniki obliczeń w lokalizacji wprowadzonych receptorów, tzn. wartości: współczynników dyspersji poziomej i pionowej oraz stężenia 1-godzinnego substancji gazowej.

Pozostałe opcje zawarte w podręcznym menu (rysunek 6) umożliwiają usuwanie z podstawowego wykresu (rysunek 5) zarówno wskazanych pojedynczych („Usuń wybrany receptor"), jak również i wszystkich receptorów („Usuń wszystkie receptory"). Ponadto program wyposażono w możliwość eksportu podstawowego wykresu do postaci zewnętrznego pliku graficznego („Eksport"). Do wyboru udostępniono zapis do postaci: *.bmp, *.jpg, *.png, *.wmf oraz *.tiff. Po wyborze z podręcznego menu opcji „Zapisz do schowka" program umieszcza w systemowym schowku podstawowy wykres, który można w zależności od potrzeb poddać dowolnej edycji.

W trakcie pracy z programem, poprzez wybranie opcji „Skala" istnieje możliwość wizualizacji legendy wykresu podstawowego w zakresie zmiany wartości *Sxyz* od 0 do *Smax*. Natomiast po wybraniu opcji „Interpolacja" opracowano procedurę interpolowanego przejścia pomiędzy poszczególnymi barwami symbolizującymi różne wartości *Sxyz*. Opcja „LOG" umożliwia wyświetlenie w dolnej części okna, w którym wyprowadzane są w formie komentarzy wszystkie kluczowe operacje wykonywane w trakcie działania aplikacji. Uzupełniającym elementem programu jest możliwość generowania raportu w postaci pliku MICROSOFT WORD (*.docx). Raport zawiera szczegółowe wyniki obliczeń.

3. Przykład zastosowania programu

Celem przetestowania opracowanego oprogramowania wraz z jego funkcjonalnościami wykonano symulację numeryczną dla źródła emisji o charakterystyce i parametrach oraz towarzyszących warunkach meteorologicznych (tabela 1).

Tabela 1. Dane wstępne
Table 1. Preliminary data

Parametry emitora				
Lp.	Parametr	Symbol	Jednostka	Wartość
1	Emisja substancji	Eg	g/s	24,5
2	Średnica wewnętrzna wylotu przewodu emitującego	D	m	1,50
3	Wysokość geometryczna emitora (od powierzchni terenu)	H	m	58,00
4	Prędkość gazów na wylocie z emitora	V	m/s	5,10
5	Temperatura gazów odlotowych na wylocie z emitora	T	°C	152,4

Tabela 1. cd.
Table 1. cont.

Parametry meteorologiczne i inne				
Lp.	Parametr	Symbol	Jednostka	Wartość
1	Średnia temperatura obliczeniowa	T_0	°C	20,00
2	Prędkość wiatru na wysokości anemometru	Ua	°C	11,80
3	Stan równowagi atmosfery	ATM	ATM	4
4	Współ. aerodynamicznej szorstkości terenu (miasto powyżej 10 tys. do 100 tys. mieszkańców – zabudowa niska)	–	m	0,5

Tabela 2. Ogólne wyniki obliczeń
Table 2. General calculation results

Obliczenia ogólne				
Lp.	Parametr	Symbol	Jednostka	Wartość
1	Współczynnik	M	-	0,270
2	Współczynnik	A	-	0,818
3	Współczynnik	B	-	0,822
4	Prędkość wiatru na wysokości wylotu z emitora	Uh	m	17,32
5	Emisja ciepła z emitora	Q	kJ/s	996
6	Wyniesienie gazów odlotowych	Dh	m	0,00
7	Efektywna wysokość emitera	Hp	m	58,00
8	Średnia prędkość wiatru w warstwie od z=h do z=Hp	Usr	m/s	17,30
9	Współczynnik	A	-	0,45
10	Współczynnik	B	-	0,27

Tabela 3. Wyniki obliczeń w lokalizacji receptora
Table 3. Calculation results at the receptor location

Receptor nr 1 (Lokalizacja: x=530,0 m; y=18,50 m; z=1,50 m)				
Lp.	Parametr	Symbol	Jednostka	Wartość
1	Współ. dyspersji poziomej	Sy	m	76,15
2	Współ. dyspersji pionowej	Sz	m	46,85
3	Stężenie 1-godzinne substancji gazowej	Sxyz	$\mu g/m^3$	5,7E-05
Receptor nr 2 (Lokalizacja: x=1600,0 m; y=150 m; z=1,50 m)				
Lp.	Parametr	Symbol	Jednostka	Wartość
1	Współ. dyspersji poziomej	Sy	m	188,01
2	Współ. dyspersji pionowej	Sz	m	116,19
3	Stężenie 1-godzinne substancji gazowej	Sxyz	$\mu g/m^3$	1,33E-05
Receptor nr 3 (Lokalizacja: x=2400,0 m; y=-150 m; z=1,50 m)				
Lp.	Parametr	Symbol	Jednostka	Wartość
1	Współ. dyspersji poziomej	Sy	m	261,95
2	Współ. dyspersji pionowej	Sz	m	162,14
3	Stężenie 1-godzinne substancji gazowej	Sxyz	$\mu g/m^3$	8,45E-06

Na rysunku 8 przedstawiono wygenerowany przez program rozkład stężeń zanieczyszczeń w zależności od odległości od emitora z uwzględnieniem receptorów na wysokości 1,5 m nad poziomem terenu. Wykres przedstawia płaszczyznę o wymiarach: 3000 m (odległość od emitora wzdłuż osi x), ±300 m (odległość od emitora prostopadle osi x). Z prawej strony wykresu znajduje się legenda, z opisem wartości poszczególnych barw, gdzie wartość maksymalna $Sxyz_{max}$=6,1E-05 $\mu g/m^3$. Na płaszczyźnie przedstawiono trzy receptory, które szczegółowo opisuje tabela 3.

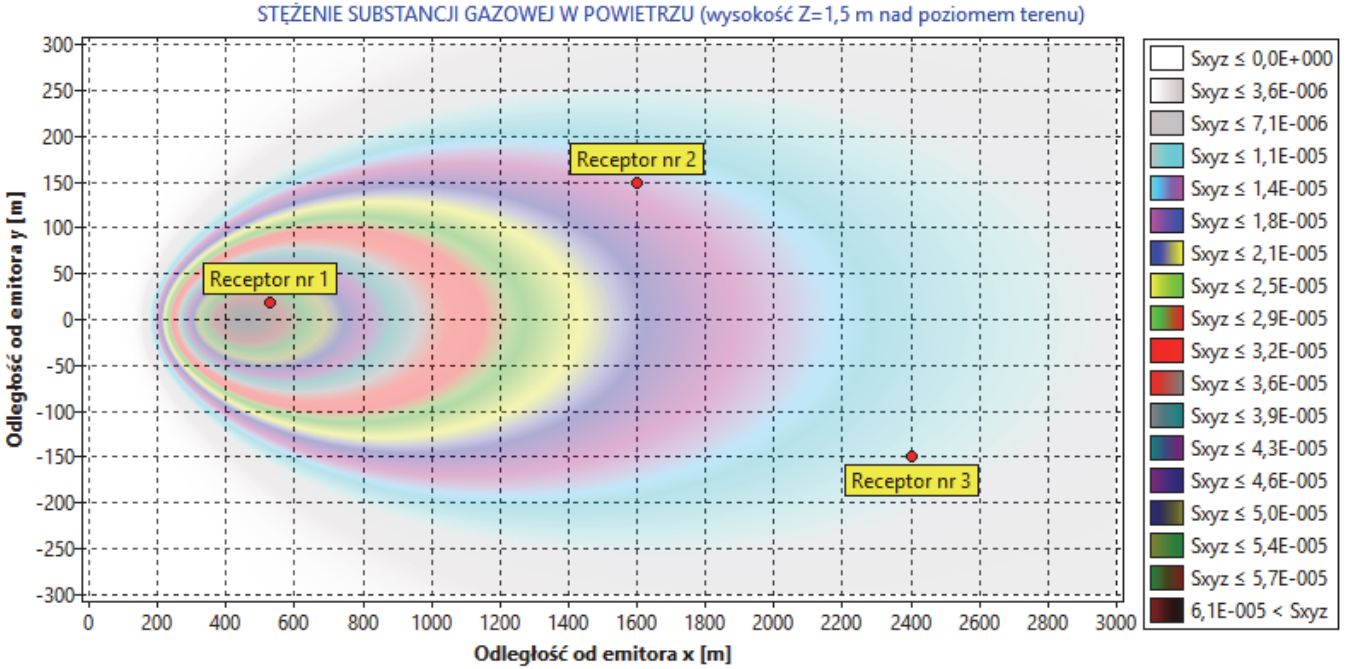

Rys. 8. Rozkład stężeń zanieczyszczeń w zależności od odległości od emitora z uwzględnieniem receptorów
Fig. 8. Distribution of pollutant concentrations depending on the distance from the emitter including emitters

4. Podsumowanie

W niniejszym artykule przedstawiono prostą metodę tworzenia aplikacji numerycznej do symulacji rozprzestrzeniania się zanieczyszczeń w powietrzu atmosferycznym. Aplikacja na podstawie danych wejściowych charakteryzujących emitor, parametry meteorologiczne oraz współczynnik szorstkości terenu umożliwia wyprowadzenie w oparciu o formułę Pasquilla, w sposób graficzny rozkładu stężeń substancji gazowej w zależności od odległości od emitora. Program stanowi niewątpliwie alternatywę dla aplikacji komercyjnych, ponieważ powstał w oparciu o darmowe środowisko programistyczne LAZARUS. W związku z tym intencją autorów programu ATMO jest udostępnienie w sposób wolny i otwarty kodu źródłowego oraz wersji wynikowej na stronie internetowej Rocznika Ochrona Środowiska celem umożliwienia dalszego rozwijania i weryfikacji działania aplikacji w aspekcie symulacji rozprzestrzeniania standardowych oraz specyficznych zanieczyszczeń powietrza atmosferycznego np. odorów.

Literatura

Rozporządzenie Ministra Środowiska z dnia 24 2012 r. sierpnia w sprawie poziomów niektórych substancji w powietrzu (Dz.U. z 2012 r., poz. 1031).

Rozporządzenie Ministra Środowiska z dnia 26 stycznia 2010 r. w sprawie wartości odniesienia dla niektórych substancji w powietrzu (Dz.U. nr 87).

Głodkowska, W., Kobaka, J. (2012). The model of brittle matrix composites for distribution of steel fibres. *Journal of Civil Engineering and Management, 18(1)*, 145-150.

Głodkowska, W., Kobaka, J. (2013). Modelling of properties and distribution of steel fibres within a fine aggregate concrete. *Construction and Building Materials*, 44(7), 645-653.

Holnicki, P., Kałuszko, A., Nahorski Z., Stankiewicz K., Trapp W. (2017). Air quality modeling for Warsaw agglomeration. *Archives of Environmental Protection 43(1)*, 48-64.

Konieczyński, J. (2012). *Ochrona powietrza w teorii i praktyce*, Instytut Podstaw Inżynierii Środowiska Polskiej Akademii Nauk w Zabrzu, Zabrze, 2, 153-161.

Kościelnik, B., Dąbrowski, T. (2015). *Podstawy Ochrony Atmosfery*, Koszalin: Wydawnictwo Politechniki Koszalińskiej.

Michalczyk, J.K., Murawski, K. (2001). Symulacje numeryczne dyspersji zanieczyszczeń gazowych w atmosferze. *Ochrona Powietrza i Problemy Odpadów*, *35(5),* 175-185.
Piekarski, J. (2003). *Wybrane przykłady obliczeń komputerowych zastosowanych w inżynierii środowiska*. Koszalin: Wydawnictwo Politechniki Koszalińskiej, Koszalin.
Piekarski, J., Lubierski, M. (2003). *Komputerowa symulacja rozprzestrzeniania zanieczyszczeń*. Koszalin: Wydawnictwo Politechniki Koszalińskiej.
Piekarski, J. (2009). *Numeryczne modelowanie procesu filtracji i sorpcji*. Monografia, Koszalin: Wydawnictwo Politechniki Koszalińskiej.
Sówka, I., Miller, U., Sobczyński, P. (2015). Dynamic olfactometry and modeling as methods for the assessment of odour impact of public utility objects. *Environment Protection Engineering,* 42(3).

Methodology of Creating Numerical Application for Simulation Pollutants Diffusion in the Atmosphere

Abstract

There is many programs that allow doing calculations of spreading pollution in the atmosphere. Most programs are very complicated and commercial. In this article are shown easy methods of creating simulations of spreading pollution in atmosphere applications in free, numeric programming environment. Application is free and open source software to make a possibility to its verification and further development.

Streszczenie

Istnieje wiele programów, przy pomocy których można dokonywać obliczeń rozprzestrzeniania się zanieczyszczeń w atmosferze. Większość tego typu aplikacji to skomplikowane programy o charakterze komercyjnym. W niniejszym artykule przedstawiono prostą metodę tworzenia w darmowym numerycznym środowisku programistycznym aplikacji do symulacji rozprzestrzeniania się zanieczyszczeń w powietrzu atmosferycznym. Aplikacja ma charakter wolnego i otwartego oprogramowania (WiOO) w celu umożliwienia zainteresowanym weryfikacji i dalszego rozwijania.

Słowa kluczowe:
metody numeryczne, modelowanie, rozprzestrzenianie zanieczyszczeń

Keywords:
numerical methods, modeling, diffusion of pollutants

MIDDLE POMERANIAN SCIENTIFIC SOCIETY OF THE ENVIRONMENT PROTECTION
ŚRODKOWO-POMORSKIE TOWARZYSTWO NAUKOWE OCHRONY ŚRODOWISKA
Annual Set The Environment Protection
Rocznik Ochrona Środowiska
Volume/Tom 19. Year/Rok 2017 ISSN 1506-218X 480-496

Badania wstępne nad ograniczeniem zawartości rtęci w energetycznym węglu kamiennym poprzez zastosowanie wibracyjnego powietrznego stołu koncentracyjnego

Ireneusz Baic, Wiesław Blaschke
Instytut Mechanizacji Budownictwa i Górnictwa Skalnego
Oddział Zamiejscowy, Katowice

1. Wprowadzenie

Celem podjętej przez Instytut pracy było zbadanie możliwości usuwania rtęci z surowego urobku energetycznego węgla kamiennego i z produktów handlowych uzyskiwanych w procesach tradycyjnej (metodami mokrymi) przeróbki węgla na będącym, w dyspozycji IMBiGS, wibracyjnym powietrznym stole koncentracyjnym. Dotychczas wykonane prace badawcze z zastosowaniem metody suchej separacji produktów węglowych pozwalają na postawienie tezy, że istnieje możliwość, oprócz odkamieniania i odpopielania, usuwania rtęci występującej w składnikach mineralnych znajdujących się w warstwach stropowych i spągowych pokładów węgla kamiennego oraz w przerostach węglowych.

2. Rtęć – źródła emisji, zawartość w węglach kamiennych

2.1. Źródła emisji rtęci

Rtęć emitowana jest do środowiska ze źródeł naturalnych i antropogenicznych. W skali roku ze źródeł naturalnych emitowane jest około 6,2 tys. Mg rtęci, natomiast ze źródeł antropogenicznych około 2,6 tys. Mg rtęci. Strukturę naturalnej i antropogenicznej emisji rtęci przedstawiono w tabeli 1. (Pirrone i in. 2010; Sloss 2015; UNEP 2013)

Tabela 1. Wielkość naturalnej i antropogenicznej emisji rtęci
Table 1. Value of the natural and anthropogenic mercury emissions

Lp.	Emisja naturalna		Emisja antropogeniczna	
	Źródło emisji	**Wielkość [%]**	**Źródło emisji**	**Wielkość [%]**
1.	Oceany	52	Procesy spalania paliw kopalnych na cele energetyczne	24
2.	Jeziora	2	Produkcja cementu	9
3.	Lasy	7	Produkcja metali (w tym hutnictwo stali)	18
4.	Tundra, łąki, sawanny, prerie	9	Przemysł chloro-alkaliczny	1
5.	Pustynie	10	Rzemiosło artystyczne i produkcja złota	37
6.	Obszary rolne	2	Zagospodarowanie odpadów	5
7.	Uwalnianie rtęci po procesach jej akumulowania	4	Inne	6
8.	Procesy spalania biomasy	13		
9.	Wulkany i tereny geotermalne	2		

Obecnie obserwowany jest spadek emisji rtęci w Europie i Ameryce Północnej. Jest on spowodowany wprowadzaniem nowoczesnych systemów oczyszczania spalin, jak również systemów kontroli emisji zanieczyszczeń. Polska jest za jednym z największych emitentów rtęci w Unii Europejskiej. Ilość rtęci emitowanej w Polsce w latach 2010-2014 wahała się w granicach od 9,6-10,3 Mg/rok. Wielkość emisji rtęci w Polsce z poszczególnych źródeł zaprezentowano w tabeli 2. (KOBIZE 2013, 2014, 2015, 2016).

W oparciu o dane przedstawiono w tabeli 2, można zauważyć, że procesy spalania są odpowiedzialne za blisko 94% emisji rtęci, z czego emisja w sektorze wytwarzania energii stanowi 54%. Z uwagi na fakt, że procesy spalania węgla są jednym z głównych źródeł antropogenicznej emisji rtęci w Polsce i na świecie, przystąpiono w wielu krajach do opracowania programów ograniczających tę emisję. Problem ten jest szczególnie istotny dla Polski, której sektor wytwarzania energii elektrycznej i ciepła oparty jest głównie na węglu kamiennym.

Tabela 2. Wielkość emisji rtęci w Polsce w latach 2010-2014
Table 2. Mercury emissions in Poland in 2010-2014

Źródło emisji	Wielkość emisji [kg]				
	2010	**2011**	**2012**	**2013**	**2014**
Procesy spalania w sektorze produkcji i transformacji energii	5 640,4	5 588,2	5 776,6	5 687,2	5 210,2
Procesy spalania poza przemysłem	1 782,5	1 476,4	1 546,5	1 112,2	1 011,2
Procesy spalania w przemyśle	2 095,4	2 271,7	2 390,2	2 655,3	2 817,2
Procesy produkcyjne	552,6	600,9	588,7	517,4	519,6
Zagospodarowanie odpadów	45,0	43,4	55,7	55,1	34,8
Inne pojazdy i urządzenia	0,1	0,1	0,1	0,1	0,1
Ogółem	**10 116,0**	**9 980,7**	**10 357,8**	**10 027,3**	**9 593,1**

2.2. Zawartość rtęci w węglu kamiennym

Zawartość rtęci w węglu kamiennym jest relatywnie niska i wynosi od kilkudziesięciu do kilkuset μg/kg. Analiza wyników badań wskazuje na różne sposoby występowania rtęci w węglu (Meij & Winkel 2009; Strezov i in. 2010; Yudovich & Ketris 2005; Zhang i in. 2009). Występuje ona w substancji mineralnej jak również w substancji organicznej. Rtęć w substancji mineralnej węgla występuje głównie w pirycie i markasycie. Jej wartość może wynosić nawet 10 000 μg/kg (Hower i in. 2008). Rtęć w substancji organicznej występuje w połączeniach siarkowych, głównie w powiązaniu z grupami tiolowymi (R-SH).

W Polsce w zależności od położenia i rodzajów pokładów z których eksploatowany jest węgiel kamienny zawartość rtęci jest zróżnicowana i waha się w granicach od 10 do 800 μg/kg. W tabeli 3 zaprezentowano zakresy zawartości rtęci w wybranych kopalniach eksploatujących w Polsce węgiel kamienny (Bukowski & Burczyk 2008; Michalska & Białecka 2012; Smoliński 2007).

W ostatnich latach zrealizowano kilka projektów badawczych, w których badano poziom zawartości rtęci w krajowych węglach. Do najważniejszych z nich zaliczyć należy projekt pn. „*Opracowanie bazy danych zawartości rtęci w krajowych węglach, wytycznych technologicznych jej dalszej redukcji wraz ze zdefiniowaniem benchmarków dla krajowych wskaźników emisji rtęci"* o akronimie „*Baza-Hg"*.

W ramach tego projektu badaniom poddano 179 próbek węgli energetycznych pochodzących z wielu kopalń węgla kamiennego. Analiza uzyskanych wyników potwierdziła, że zawartość rtęci w węglach kamiennych jest relatywnie niska (Białecka & Pyka 2016).

Tabela 3. Zawartość rtęci w polskich węglach kamiennych
Table 3. Mercury content in Polish steam coal

Nazwa Spółki	Kopalnia	Zakres zawartości rtęci, [µg/kg]
Polska Grupa Górnicza S.A. KWK ROW	Ruch Jankowice	b.d.
	Ruch Chwałowice	b.d.
	Ruch Marcel	15-113
	Ruch Rydułtowy	b.d.
Polska Grupa Górnicza S.A. KWK Ruda	Ruch Bielszowice	b.d.
	Ruch Halemba	1-758
	Ruch Pokój	b.d.
Polska Grupa Górnicza S.A. KWK Piast-Ziemowit	Ruch Piast	99-126
	Ruch Ziemowit	45-169
Polska Grupa Górnicza S.A	KWK „Bolesław Śmiały”	b.d.
Polska Grupa Górnicza S.A	KWK „Sośnica”	95-130
Katowicki Holding Węglowy S.A.	KWK „Murcki - Staszic” Ruch Staszic	20-120
Katowicki Holding Węglowy S.A.	KWK „Murcki - Staszic” Ruch Murcki	20-160
Katowicki Holding Węglowy S.A.	KWK „Mysłowice -Wesoła” Ruch Mysłowice	68-101
Katowicki Holding Węglowy S.A.	KWK „Mysłowice - Wesoła” Ruch Wesoła	37-73
Katowicki Holding Węglowy S.A.	KWK „Wieczorek”	30-50
Katowicki Holding Węglowy S.A.	KWK „Wujek”	95-260
Jastrzębska Spółka Węglowa S.A.	KWK „Borynia – Zofiówka – Jastrzębie Ruch Borynia	73-185
Jastrzębska Spółka Węglowa S.A.	KWK „Borynia – Zofiówka – Jastrzębie Ruch Zofiówka	43-173
Jastrzębska Spółka Węglowa S.A.	KWK „Borynia – Zofiówka – Jastrzębie Ruch Jastrzębie	b.d.
Jastrzębska Spółka Węglowa S.A.	KWK „Budryk”	153-202
Jastrzębska Spółka Węglowa S.A.	KWK „Knurów-Szczygłowice”	b.d.
Jastrzębska Spółka Węglowa S.A.	KWK „Krupiński”	5-195
Jastrzębska Spółka Węglowa S.A.	KWK „Pniówek”	90-202

Tabela 3. cd.
Table 3. cont.

Nazwa Spółki	Kopalnia	Zakres zawartości rtęci, [µg/kg]
TAURON Wydobycie S.A.	ZG „Janina”	18-198
TAURON Wydobycie S.A.	ZG „Sobieski”	24-74
TAURON Wydobycie S.A.	ZG „Nowe Brzeszcze”	11-518
WĘGLOKOKS KRAJ Sp. z o. o.	KWK „Bobrek”	b.d.
WĘGLOKOKS KRAJ Sp. z o. o.	KWK „Piekary”	51-71
PG Silesia Sp. z o.o.	–	6-113
Lubelski Węgiel Bogdanka S.A.	–	18-561
Spółka Restrukturyzacji Kopalń S.A.	KWK „Kazimierz – Juliusz”	136-159
Spółka Restrukturyzacji Kopalń S.A.	KWK „Anna”	1-83
Spółka Restrukturyzacji Kopalń S.A.	KWK „Jas-Mos”	5-123
Spółka Restrukturyzacji Kopalń S.A.	KWK „Murcki-Staszic” Ruch Boże Dary	75-120

3. Uwarunkowania prawne dotyczące emisji rtęci

W Polsce jak i w Unii Europejskiej brak obecnie regulacji prawnych i norm dotyczących zawartości rtęci w węglu jak i limitów emisji rtęci z elektrowni węglowych. We wszystkich krajach UE prowadzony jest natomiast Europejski Rejestr Uwalniania i Transferu zanieczyszczeń E-PRTR (European Pollutant Release and Transfer Register), którego celem jest ewidencjonowanie danych dotyczących emisji zanieczyszczeń w tym rtęci z instalacji przemysłowych. Rejestr ten zawiera obecnie dane z blisko 30 tys. różnego typu instalacji przemysłowych w tym również z sektora energetycznego (E-PRTR 2014). Dane do powyższego rejestru wprowadzane są na podstawie Krajowych Rejestrów Uwalniania i Transferu Zanieczyszczeń (PRTR), do których sporządzania zobligowane są wszystkie państwa członkowskie UE na mocy Rozporządzenia (WE) nr 166/2006 Parlamentu Europejskiego i Rady (Rozp. 2006).

W przypadku emisji rtęci i jej związków do powietrza obowiązek raportowania spoczywa na jednostkach o rocznej emisji rtęci powyżej 10 kg. W Polsce rejestr zanieczyszczeń, w tym rtęci prowadzony jest przez Krajowy Ośrodek Bilansowania i Zarządzania Emisjami – KOBiZE.

Pomimo braku unijnych norm emisji rtęci z elektrowni węglowych takie normy obowiązują już w Holandii i USA, a w Niemczech zapowiedziano ich wprowadzenie. W tabeli 4 przedstawiono dopuszczalne w tych krajach wartości emisji rtęci z elektrowni węglowych. Ponadto w USA wprowadzono ogólnokrajowe standardy mające na celu ograniczenie emisji zanieczyszczeń, w tym rtęci, z elektrowni węglowych – MATS (Mercury and Air Toxics Standard). Przepisy te dotyczą wszystkich jednostek wytwarzających energię elektryczną o mocy powyżej 25 MW (EPA 2015). Mają one na celu ograniczyć aktualną emisję rtęci w USA o 90% (Gołaś & Strugała 2014).

Tabela 4. Normy emisji rtęci dla elektrowni węglowych
Table 4. Mercury emission standards for coal power plant

Kraj	Norma emisji rtęci [µg/Nm^3 spalin]	
	Obiekty istniejące	Obiekty nowe
USA	5	3
Holandia	2,4	2,8
Niemcy	3 (wartość planowa)	

Wśród regulacji prawnych dotyczących emisji rtęci ważnym dokumentem jest Konwencja Minamata (Konwencja rtęciowa), która została przyjęta w 2013 roku (Adamska 2014; Chmielarz 2014). Zapisy zawarte w Konwencji poparła w 2014 roku również Polska. Głównym celem konwencji jest ochrona zdrowia ludzi i środowiska przed antropogeniczną emisją rtęci i jej związków. Konwencja rtęciowa reguluje następujące obszary: podaż i handel rtęcią, emisję i uwolnienia rtęci do środowiska, produkty zawierające i procesy wykorzystujące rtęć, odpady, składowanie, zanieczyszczenia terenu rtęcią, aspekty zdrowotne, finansowanie i pomoc techniczną oraz wymianę informacji, badania i rozwój.

W konsekwencji wprowadzenia Konwencji rtęciowej sformułowane zostały w Unii Europejskiej Konkluzje BAT w zakresie emisji rtęci ze spalania paliw stałych (węgla kamiennego i brunatnego) w jednostkach energetycznych, które będą podstawą do określenia limitów emisyj-

nych. W tabeli 5 przedstawiono powiązane z BAT dopuszczalne zawartości rtęci w spalinach w roku 2016 (Wdowiak & Henc 2016).

Tabela 5. BAT – poziomy emisji rtęci do powietrza ze spalania węgla
Table 5. BAT – levels of mercury emission to air from coal combustion

Typ węgla	Moc obiektu [MW]	Dopuszczalna zawartość rtęci w spalinach [µg/Nm^3]	
		Nowe instalacje	Istniejące instalacje
Kamienny	< 300	<3	<9
	> 300	<2	<4
Brunatny	< 300	<5	<10
	> 300	<4	<7

4. Metody ograniczenia zawartość rtęci w węglach

Metody ograniczenia zawartości rtęci w węglach przed jego energetycznym wykorzystaniem należą do metod pierwotnych (pre-combustion) w odróżnieniu od metod wtórnych (post-combustion) polegających na usuwaniu rtęci ze spalin lub gazów podprocesowych (Krzyżyńska i in. 2011, Wdowin i in. 2015).

Skuteczność pierwotnych metod usuwania węgla zależy od formy jej występowania w danym złożu. Do podstawowych metod pierwotnych ograniczających zawartość rtęci w węglach zaliczyć należy:

- przeróbkę mechaniczną węgla,
- wstępną preparację termiczną węgla,
- selektywną eksploatację pokładów węglowych,
- ekstrakcję wodną w warunkach podkrytycznych,
- chemiczną obróbkę węgla,
- roztwarzanie pirytu z wykorzystaniem SO_2,
- metody biologiczne,
- metodę Hyper-Coal.

4.1. Przeróbka mechaniczna węgla

Węgiel kamienny wydobywany w kopalni, czyli tzw. niesort jest zbiorem różnej wielkości ziaren węgla, a także skały płonnej, przerostów węglowo-kamiennych i łupków węglowych. W takiej postaci nie nadaje

się do bezpośredniego wykorzystania i musi być poddany procesom przeróbczym. W przypadku węgla energetycznego, jeśli parametry jakościowe odpowiadają wymaganiom potencjalnych odbiorców (wartość opałowa, zawartość popiołu, wilgoci i siarki) wystarczy go rozdzielić na węższe klasy ziarnowe. W większości przypadków surowy węgiel energetyczny nie spełnia jednak wymogów jakościowych odbiorców. Z kolei węgiel koksowy w stanie surowym nie nadaje się do bezpośredniego wykorzystania. Aby spełnić wymagania jakościowe odbiorców węgiel poddany musi być procesom przeróbki mechanicznej mającym na celu usunięcie kamienia, łupków, części przerostów kamienno-węglowych, piasku posadzkowego i pirytu. Procesy te nazywane są wzbogacaniem. Wzbogacanie węgla może być prowadzone w ośrodku wodnym lub powietrznym. W procesach wzbogacania wykorzystywane są różnice właściwości fizycznych substancji mineralnej i organicznej takich jak: gęstość rzeczywista czy właściwości powierzchniowe. (Blaschke 2009). Procesy wzbogacania węgla oprócz usuwania z nich niepożądanych z uwagi na parametry energetyczne zanieczyszczeń przyczyniają się również do obniżenia w węglu zawartości pierwiastków szkodliwych m.in. rtęci i siarki (Baic i in. 2015A, 2015B, 2015C). Skuteczność usuwania rtęci w procesie jego wzbogacania jest różna dla różnych typów węgli. Zadowalające rezultaty w zakresie obniżenia zawartości rtęci uzyskuje się w przypadku wzbogacania węgli bogatych w piryt. Proces wzbogacania umożliwia blisko 90% redukcję zawartości rtęci, a jego skuteczność jest proporcjonalna do skuteczności usunięcia substancji mineralnej. Dla węgli o niskiej zawartości pirytu metody wzbogacania są mało efektywne, a uzyskiwana skuteczność nie przekraczać 10%.

Należy w tym miejscu podkreślić, że efektywność usunięcia rtęci nie jest jedynie zależna od zawartości pirytu w węglu, ale również od jego formy. Piryt pochodzenia epigenetycznego, tzw. piryt gruboziarnisty jest łatwy do usunięcia na drodze wzbogacania, w odróżnieniu od pirytu syngenetycznego, tzw. pirytu drobnoziarnistego. Według danych literaturowych najlepsze rezultaty w usunięciu pirytu uzyskać można dla pirytu pochodzenia epigenetycznego występującego w postaci dużych wtrąceń nierównomiernie rozsianych w strukturze węgla oraz stosując proces głębokiego rozdrobnienia węgla. (Aleksa i in. 2007).

4.1.1. Wzbogacanie na mokro

W warunkach krajowych procesy wzbogacania realizowane są najczęściej w środowisku wodnym. Stosowane metody wykorzystują różnice w gęstości substancji organicznej i mineralnej węgla. Są to procesy wzbogacania grawitacyjnego. Wzbogacanie grawitacyjne stosowane jest najczęściej dla ziaren urobku powyżej 10-20 mm, choć wzbogaca się też urobek o uziarnieniu powyżej 1-3 mm. Drobniejsze ziarna urobku węglowego wzbogaca się metodami fizykochemicznymi. Wykorzystują one różnice we właściwościach powierzchniowych ziaren węgla i zanieczyszczeń. Przykładem takiego procesu może być flotacja (Blaschke 2009).

W Polsce najczęściej stosowanymi procesami wzbogacania na mokro są:

- wzbogacanie w cieczy ciężkiej,
- wzbogacanie osadzarkowe,
- wzbogacanie flotacyjne.

4.1.2. Wzbogacanie na sucho

Procesy suchej separacji, zwane również procesami suchego odkamieniania, odbywają się bez udziału wody lub z niewielką jej ilością, co sprzyja ochronie środowiska i pozwala zmniejszyć nakłady inwestycyjne oraz koszty eksploatacyjne (Baic i in. 2015A, 2015B, 2015C). W niektórych krajach sucha separacja węgla stosowana jest przed poddaniem go procesowi wzbogacania na mokro. Wstępne usunięcie skały płonnej pozwala uprościć schemat technologiczny zakładu przeróbczego, zmniejsza ilość nadawy, zmniejsza ilość niezbędnych maszyn i urządzeń, ogranicza zużycie energii oraz obniża koszty wzbogacania na mokro. Co więcej, wydzielone produkty odpadowe, z uwagi na brak kontaktu z wodą mogą być z powodzeniem stosowane jako substytut kruszyw naturalnych. Dla suchej separacji zastosowanie mogą znaleźć m.in. powietrzne wibracyjne stoły koncentracyjne (Baic & Blaschke 2013).

Powietrzny wibracyjny stół koncentracyjny składa się z perforowanego stołu roboczego, urządzenia wibracyjnego, komory powietrznej, napędu oraz mechanizmu pozwalającego zmieniać kąty nachylenia stołu i częstotliwość wibracji. Nadawa surowego węgla kierowana jest na stół wprawiany w ruch wibracyjny. Spod stołu z komór powietrznych podawane jest powietrze powodujące unoszenie złoża węglowego. W wyniku

przepływu powietrza następuje separacja złoża węglowego. Materiał o małej gęstości (węgiel) koncentruje się na powierzchni złoża, a materiał o dużej gęstości (odpad) w strefie dolnej złoża. Z uwagi na to, że stół jest pochylony w kierunku poprzecznym, materiał o małej gęstości znajdujący się na powierzchni złoża ma tendencję do przesuwania się po tej powierzchni i spadania pod wypływem siły grawitacji poprzez przegrodę usytuowaną na brzegu stołu. Materiał o wyższej gęstości koncentruje się w dolnej części złoża i przesuwa się w kierunku wylotu odpadów (Baic & Blaschke 2013).

Możliwość obniżenia zawartości rtęci w węglu przy wykorzystaniu powietrznych wibracyjnych stołów koncentracyjnych została potwierdzona przez amerykańskich uczonych. (Honaker 2007). Podczas separacji węgla uzyskano obniżenie zawartości rtęci na poziomie 67%.

5. Metodyka badań

Realizacja pracy wymagała przygotowania i zbadania szeregu próbek badawczych: nadawy (węglowych produktów handlowych) oraz otrzymywanych w wyniku procesu suchej separacji z wykorzystaniem powietrznego wibracyjnego stołu koncentracyjnego produktów rozdziału (koncentratów, produktów pośrednich, pyłów i odpadów), dla oceny zmian zawartości rtęci w węglu kamiennym poprzez zastosowanie tego procesu. Badane próbki pobrano z instalacji badawczej do suchej separacji węgla kamiennego wyposażonej w powietrzny wibracyjny stół koncentracyjny typu FGX-1. Uproszczony schemat instalacji badawczej z zaznaczeniem miejsca pobrania próbek oraz ich oznaczeniem przedstawiono na rysunku 1.

Wszystkie pobrane próbki poddane zostały analizie technicznej i elementarnej.

Pomiaru zawartości rtęci w badanych próbkach dokonano za pomocą analizatora rtęci MA-2 japońskiej firmy Nippon Instruments Corporation według metody EPA Method 7473. Aparat wykorzystuje metodę Atomowej Spektrometrii Absorpcyjnej z techniką zimnych par (CVAAS), zgodną z aktualnie obowiązującą w Polsce normą PN-ISO 15237:2007 Paliwa stałe – Oznaczanie rtęci całkowitej w węglu. Jest to powszechnie stosowana metoda oznaczania zawartości rtęci w próbkach stałych, w tym w węglu (Lopez-Anton i in. 2012). Analizator odznacza

się szerokim zakresem pomiarowym z granicą wykrywalności na poziomie $2 \cdot 10^{-6}$ µg i górnym zakresem pomiarowym do 1 µg rtęci w badanej próbce. Urządzenie cechuje się także wysoką liniowością metody (R^2 równym 0,999). Oznaczenia zawartości rtęci wykonano w Laboratorium Paliw Alternatywnych i Odpadów, Centrum Energetyki, Akademia Górniczo-Hutnicza w Krakowie.

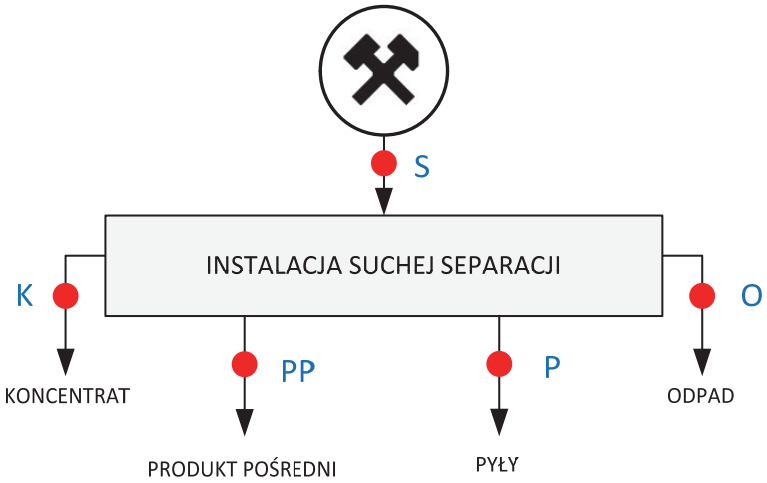

Rys. 1. Uproszczony schemat technologiczny instalacji badawczej do suchej separacji węgla energetycznego (kropką oznaczono miejsca pobrania próbek)
Fig. 1. A simplified flowsheet of pilot plant for dry separation of steam coal (dot indicates the place of sampling)

6. Analiza zamian zawartości rtęci w węglu energetycznym po procesie suchej separacji

Celem przeprowadzonych badań z zastosowaniem procesu suchej separacji węgla energetycznego na instalacji badawczej wyposażonej w powietrzny wibracyjny stół koncentracyjny była:

- ocena możliwości usuwania rtęci z energetycznego węgla kamiennego z wykorzystaniem tego procesu,
- określenie dystrybucji rtęci pomiędzy produkty rozdziału powstające w tym procesie.

W tabelach 6.1.-6.3. zaprezentowano otrzymane wyniki badań.

Tabela 6.1. Wynik badań wstępnych nad możliwością usuwania rtęci z węgla o granulacji 20-0 mm
Table 6.1. Test result of preliminary research on the possibility of removing mercury from raw coal granulation 20-0 mm

Parametr	Ozn.	Jedn.	Nadawa [S]	Koncentrat [K]	Produkt pośredni [PP]	Odpad [O]	Pyły [P]
Wilgoć przemijająca	W_{ex}^{r}	%	5,1	1,2	1,2	0,9	1,1
Wilgoć analityczna	W^{a}	%	4,6	5,3	4,1	1,8	4,8
Wilgoć robocza	W_{t}^{r}	%	9,5	6,4	5,3	2,7	5,8
Popiół	A^{a}	%	25,0	13,4	33,3	81,3	27,8
Ciepło spalania	Q_{s}^{a}	kJ/kg	21979	26431	18530	2566	20942
Wartość opałowa	Q_{i}^{a}	kJ/kg	21105	25411	17747	2315	20109
Rtęć	**Hg_{t}^{d}**	**µg/kg**	**113**	**72**	**143**	**319**	**153**
Wychód	**γ**	**%**	**100**	**60**	**27**	**7**	**6**

Tabela 6.2. Wynik badań wstępnych nad możliwością usuwania rtęci z węgla o granulacji 25-10 mm
Table 6.2. Test result of preliminary research on the possibility of removing mercury from raw coal granulation 25-10 mm

Parametr	Ozn.	Jedn.	Nadawa [S]	Koncentrat [K]	Produkt pośredni [PP]	Odpad [O]
Wilgoć przemijająca	W_{ex}^{r}	%	1,6	1,9	1,6	2,1
Wilgoć analityczna	W^{a}	%	2,0	3,4	2,9	0,9
Wilgoć robocza	W_{t}^{r}	%	3,6	5,2	4,5	3,0
Popiół	A^{a}	%	50,5	8,1	24,3	86,2
Ciepło spalania	Q_{s}^{a}	kJ/kg	11852	29169	20837	0
Wartość opałowa	Q_{i}^{a}	kJ/kg	11233	28018	19899	0
Rtęć	**Hg_{t}^{d}**	**µg/kg**	**65**	**51**	**90**	**78**
Wychód	**γ**	**%**	**100**	**33,3**	**7,5**	**59,1**

Tabela 6.3. Wynik badań wstępnych nad możliwością usuwania rtęci z węgla o granulacji 25-6 mm
Table 6.3. Test result of preliminary research on the possibility of removing mercury from raw coal granulation 25-6 mm

Parametr	Ozn.	Jedn.	Nadawa [S]	Koncentrat [K]	Produkt pośredni [PP]	Odpad [O]
Wilgoć przemijająca	W_{ex}^{r}	%	6,4	7,0	5,6	6,3
Wilgoć analityczna	W^{a}	%	9,7	9,6	9,7	8,3
Wilgoć robocza	W_{t}^{r}	%	15,5	15,9	14,8	14,1
Popiół	A^{a}	%	8,4	6,1	7,6	14,8
Ciepło spalania	Q_{s}^{a}	kJ/kg	25893	26624	26096	23802
Wartość opałowa	Q_{i}^{a}	kJ/kg	24752	25464	24957	22840
Rtęć	**Hg_{t}^{d}**	**µg/kg**	**88**	**61**	**110**	**162**
Wychód	**γ**	**%**	**100**	**66,5**	**18,5**	**15**

6. Podsumowanie

Przeprowadzone wstępne badania dla trzech próbek węgla o różnej granulacji pochodzących z różnych kopalń wykazały, że istnieje możliwość usuwania rtęci z węglowych produktów handlowych poprzez zastosowanie metody suchej separacji. Zastosowanie powietrznego wibracyjnego stołu koncentracyjnego umożliwiło redukcję całkowitej zawartości rtęci w badanych próbkach węgla energetycznego z efektywnością od 21 do 36%. Jest to związane z faktem, że urządzenia tego typu umożliwiają usunięcie tylko rtęci występującej w formach mineralnych. Otrzymane wyniki pokazały, że rtęć w wyniku procesu suchej separacji kumuluje się głównie w odpadach oraz w produktach pośrednich. Z tego też względu skuteczność usuwania rtęci zależy od ilości wydzielonych w procesie suchej separacji odpadów i produktów pośrednich oraz formy występowania rtęci w węglu (w substancji organicznej czy mineralnej).

Zdaniem autorów efektywność usuwania rtęci będzie można zwiększyć poprzez zmianę parametrów technologicznych pracy powietrznego wibracyjnego stołu koncentracyjnego oraz rozszerzenie zakresu badań analitycznych o formę występowania rtęci w węglu.

Efektem końcowym zaplanowanych do realizacji prac będzie propozycja układu technologicznego usuwania rtęci z energetycznych węglowych produktów handlowych wraz z podaniem warunków skutecznego prowadzenia takiego procesu.

Literatura

Adamska, B. (2014). Konwencja Minamata w sprawie rtęci. *Rtęć w przemyśle – Konwencja, ograniczanie emisji, technologia. Warszawa, 26.11.2014.*

Aleksa, H., Dyduch, F., Wiechowski, K. (2007). Chlor i rtęć w węglu i możliwości ich obniżenia metodami przeróbki mechanicznej. *Górnictwo i Geoinżynieria, 31(3/1)*, 35-48.

Baic, I., Blaschke, W. (2013). Analiza możliwości wykorzystania powietrznych stołów koncentracyjnych do otrzymywania węglowych paliw kwalifikowanych i substytutów kruszyw. *Polityka Energetyczna, 16(3)*, 247-260.

Bai,c I., Blaschke, W., Sobko, W., Fraś, A. (2015A). Application of air concentrating table for improvement in the Quality parameters of the commercial product "Jaret". *Journal of the Polish Mineral Engineering Society – Inżynieria Mineralna, tom. 16(1),* 221-226.

Baic, I., Blaschke, W., Góralczyk, S., Szafarczyk, J., Buchalik, G. (2015B). Nowa ekologiczna metoda usuwania zanieczyszczeń skałą płonną z urobku węgla kamiennego. *Rocznik Ochrona Środowiska, 17,* 1274-1285.

Baic, I., Blaschk,e W., Sobko, W. (2015C). Badania nad odkamienianiem energetycznego węgla kamiennego na powietrznych stołach koncentracyjnych. *Rocznik Ochrona Środowiska, 17*. 958-972.

Białecka, B., Pyka, I. (2016). *Rtęć w polskim węglu kamiennym do celów energetycznych i w produktach jego przeróbki.* Katowice: Główny Instytut Górnictwa.

Blaschke, W. (2009). *Przeróbka węgla kamiennego – wzbogacanie grawitacyjne.* Kraków: Wydawnictwo Instytutu Gospodarki Surowcami Mineralnymi i Energią PAN.

Bukowski, Z., Burczyk, A. (2008). Oznaczanie rtęci w węglach koksujących. Analiza korelacji. *Konferencja Koksownictwo, Zakopane, 8-10.10.2008*.

Chmielarz, A. (2014). Propozycja BAT/BEP w dokumentach roboczych grupy eksperckiej konwencji Minamata w sprawie rtęci. *Rtęć w przemyśle – Konwencja, ograniczanie emisji, technologia, Warszawa, 26.11.2014.*

E-PRTR (2014). European Pollutant Release and Transfer Register, (*http://prtr.ec.europa.eu*).

Gołaś, J., Strugała, A. (2014). *Mercury As a Coal Combustion Pollutant. Monograph AGH University of Science and Technology*. Kraków: Oficyna Drukarska – J. Chmielewski.

Honaker, R.Q. (2007). *Development of an advanced deshaling technology to improve the energy efficiency of coal handling, processing, and utilization operations.* U. S. Department of Energy, Industrial Technologies Program, Mining of the Future, ID Number: DE-FC26-05NT42501.

Hower, J.C., Campbell, J.L., Teesdale, W.J., Nejedly, Z., Robertson, J.D. (2008). Scanning proton microprobe analysis of mercury and other trace elements in Fe-sulfides from a Kentucky coal. *International Journal of Coal Geology, 75,* 88-92.

KOBiZE (2013). Krajowy Ośrodek Bilansowania i Zarządzania Emisjami: *Krajowy bilans emisji SO_2, NO_x, CO, NH_3, NMLZO, pyłów, metali ciężkich i TZO za lata 2010-2011 w układzie klasyfikacji SNAP.* Warszawa, 2013.

KOBiZE (2014). Krajowy Ośrodek Bilansowania i Zarządzania Emisjami: *Krajowy bilans emisji SO_2, NO_x, CO, NH_3, NMLZO, pyłów, metali ciężkich i TZO za lata 2011-2012 w układzie klasyfikacji SNAP.* Warszawa, 2014.

KOBiZE (2015). Krajowy Ośrodek Bilansowania i Zarządzania Emisjami: *Krajowy bilans emisji SO_2, NO_x, CO, NH_3, NMLZO, pyłów, metali ciężkich i TZO w układzie klasyfikacji SNAP i NFR.* Warszawa, 2015.

KOBiZE (2016). Krajowy Ośrodek Bilansowania i Zarządzania Emisjami: *Krajowy bilans emisji SO_2, NO_x, CO, NH_3, NMLZO, pyłów, metali ciężkich i TZO za lata 2013-2014 w układzie klasyfikacji SNAP i NFR.* Warszawa 2016.

Krzyżyńska, R., Zhao, Y, Hutson, N.D. (2011). Bench- and Pilot-scale Investigation of Integrated Removal of Sulfur Dioxide, Nitrogen Oxides and Mercury in a Wet Limestone Scrubler. *Rocznik Ochrona Środowiska 13,* 29-50.

Lopez-Anton, M.A., Diaz-Somoano, M., Ochoa-Gonzalez, R., Martinez-Tarazona, M.R. (2012). Analytical methods for mercury analysis in coal and coal combustion by-products. *International Journal of Coal Geology, 94*, 44-53.

Meij, R., Winkel, B.H. (2009). Trace elements in world steam coal and their behavior in Dutch coal-fired power stations – A review. *International Journal of Coal Geology, 77,* 289-293.

Michalska, A., Białecka, B. (2012). Zawartość rtęci w węglu i odpadach górniczych. *Prace Naukowe GIG Górnictwo i Środowisko, 3,* 73-87.

Pirrone, N. Cinnirella, S., Feng, X., Finkelman, R.B., Friedli, H.R., Mason, R., Mukherjee, A.B., Stracher, G.B., Streets, D.G., Telmer, K. (2010). Global mercury emissions to the atmosphere from anthropogenic and natural sources. *Atmospheric Chemistry and Physics, 10,* 5951-5964.

Rozporządzenie (WE) Nr 166/2006 Parlamentu Europejskiego I Rady z dnia 18 stycznia 2006 r. |w sprawie ustanowienia Europejskiego Rejestru Uwalniania i Transferu Zanieczyszczeń.

Sloss, L.L. (2015). Issue of mercury emissions from an EU perspective. *Konferencja naukowo-przemysłowa pt. „Emisja rtęci i możliwości jej ograniczenia w polskim sektorze energetycznym". Kraków 13-14.05.2015r.*

Smoliński, A. (2007). Energetyczne wykorzystanie węgla źródłem emisji rtęci – porównanie zawartości tego pierwiastka w węglach. *Ochrona Powietrza i Problemy Odpadów, 41(2),* 45-53.

Strezov, V., Evans, T.J., Ziółkowski, A., Nelson, P.F. (2010). Mode of Occurrence and Thermal Stability of Mercury in Coal. *Energy Fuels, 24,* 53-57.
UNEP (2013). United Nations Environment Programme: *Global mercury assessment 2013. Sources, emissions, releases and environmental transport.* Geneva: Switzerland.
Wdowiak, M., Henc, M. (2016). Redukcja rtęci w jednostkach wytwórczych PGE GiEK S.A. w kontekście wymagań Konkluzji BAT. *XI Konferencja Naukowo-Techniczna, Ochrona Środowiska w Energetyce, Katowice, 8-9 lutego 2016.*
Wdowin, M., Baran, P., Panek, R., Zarębska, K., Franus, W. (2015). Analiza możliwości oczyszczania gazów wylotowych z Hg i CO^2 na zeolitach otrzymanych z popiołów lotnych. *Rocznik Ochrona Środowiska, 17,* 1306-1319.
Yudovich, Y.E., Ketris, M.P. (2005). Mercury in coal: a review – Part 1. Geochemistry. *International Journal of Coal Geology, 62,* 107-134.
Zhang, C., Chen, G., Gupta, R., Xu, Z. (2009). Emission control of mercury and sulfur by mild thermal upgrading of coal. *Energy Fuels, 23,* 766-733.

Preliminary Studies on the Reduction of Mercury Content in Steam Coal through the Use of Air-vibrating Concentration Table

Abstract

Mercury content in hard coal is relatively small. However, when a large amount of coal is burned in Poland, the considerable quantities of mercury reach the atmosphere. The mercury is mainly pyrite and marcasite included in mineral coal substance. It is also present in the organic carbon substance. Certain, sometimes substantial quantities of mercury are found in the roof and bottom layers of coal field which during the exploitation reach the run-of-mine. During the enrichment (mechanical processing) it is possible to remove impurities with a gangue coming from these layers and from inserts of stone outstripping coal seams. It is also possible to remove the released iron sulphide particles. But, as practice shows wet enrichment methods (jigging, flotation) are often inaccurate. The concentrates contain certain amounts of gangue and sulphur compounds. This results in a transition to commercial products of mercury compounds.

The Institute of Mechanized Construction and Rock Mining, a Branch in Katowice conducts for several years the research on the deshaling method of dry run-of-mine. It uses possessed installation equipped with air-vibrating concentration table. This device, with good regulation, allows effective removal of these contaminants. There is therefore the possibility of deshaling the excavated

material and in addition removing mercury compounds that are found in the fractions with a high density.

This article discusses the sources and emissions of mercury, its content in hard coal and legal considerations regarding mercury emissions. Also presented are the preliminary results of research activities on mercury removal using a air-vibrating concentration table.

Streszczenie

Zawartość rtęci w węglach kamiennych jest stosunkowo niewielka. Jednak przy dużej ilości spalanego węgla w Polsce do atmosfery przedostają się jej znaczne ilości. Rtęć występuje głównie w pirycie i markazycie wchodzących w skład substancji mineralnej węgla. Występuje także w substancji organicznej węgla. Pewne, czasami znaczne, ilości rtęci znajdują się w warstwach stropowych i spągowych pokładów węglowych, które podczas eksploatacji trafiają do urobku węglowego. Podczas wzbogacania (przeróbki mechanicznej) istnieje możliwość usuwania zanieczyszczeń skałą płonną pochodzącą z tych warstw a także z wkładek kamiennych przerastających pokłady węglowe. Możliwe jest też usuwanie uwolnionych ziarn siarczków żelaza. Jak jednak pokazuje praktyka wzbogacania metodami mokrymi (osadzarki, flotacja) procesy te są często niedokładne. W koncentratach pozostają pewne ilości skały płonnej i związków siarki. Skutkuje to przechodzeniem do produktów handlowych związków rtęci.

W Instytucie Mechanizacji Budownictwa i Górnictwa Skalnego w Oddziale Katowickim prowadzone są od kilku lat badania nad odkamienianiem urobku węglowego metodą suchą. Wykorzystuje się posiadaną instalację wyposażoną w wibracyjny powietrzny stół koncentracyjny. Urządzenie to, przy dobrym uregulowaniu, pozwala na skuteczne usuwanie wspomnianych zanieczyszczeń. Istnieje więc możliwość aby oprócz odkamieniania urobku usuwać związki rtęci, które znajdują się we frakcjach o dużej gęstości.

W niniejszym artykule omówiono źródła i wielkości emisji rtęci, jej zawartość w węglach kamiennych oraz uwarunkowania prawne dotyczące emisji rtęci. Przedstawiono też wstępne wyniki badań nad możliwościami usuwania rtęci przy wykorzystaniu wibracyjnego powietrznego stołu koncentracyjnego.

Słowa kluczowe:
węgiel energetyczny, sucha separacja, usuwanie rtęci z węgla,
powietrzny wibracyjny stół koncentracyjny

Keywords:
steam coal, dry separation, removing mercury from raw coal,
air-vibrating concentration table

MIDDLE POMERANIAN SCIENTIFIC SOCIETY OF THE ENVIRONMENT PROTECTION
ŚRODKOWO-POMORSKIE TOWARZYSTWO NAUKOWE OCHRONY ŚRODOWISKA

Annual Set The Environment Protection
Rocznik Ochrona Środowiska

Volume/Tom 19. Year/Rok 2017 ISSN 1506-218X 497-510

Wtrysk balastu wodnego jako metoda zmniejszenia emisji tlenków azotu

Aleksander Szkarowski[,**], Sylwia Janta-Lipińska[*], Magdalena Orłowska[*], Shirali Mamedov[***]*
[*]Politechnika Koszalińska,
[**]St.Petersburg Polytechnic University,
[***]St.Petersburg University of Architecture & Civil Engineering

1. Wstęp

W niniejszej publikacji autorzy kontynuują przedstawienie wyników swoich badań związanych z obniżeniem emisji tlenków azotu (NO_x) powstających podczas spalania paliwa w kotłach przemysłowo-grzewczych (Szkarowski 2001, 2002, Szkarowski et al. 2011, 2013, 2015, 2016). Wysokie wskaźniki pod względem ekonomiczności i ekologiczności procesu spalania posiada metoda strefowego wtryskiwania balastu wodnego do płomienia. Wcześniejsze badania i skuteczne wdrożenia metody dotyczyły kotłów parowych, głównie konstrukcji dwuwalczakowej, poziomej np. DKVR i DE (Szkarowski et al. 2009, 2016). Kolejnym etapem badań było opracowanie i wdrożenie tej metody dla kotłów wodnych o dużej mocy (30-50 MW) o przeznaczeniu ciepłowniczym. Jako obiekt badań wybrano kotły PTVM, których konstrukcja szybowa powoduje całkiem inne warunki spalania i aerodynamikę płomienia niż we wcześniej opracowanych przypadkach.

2. Charakterystyka obiektu badań

Druga Krasnogwadiejska kotłownia w Sankt-Petersburgu wyposażona jest w 2 kotły PTVM-50 o mocy nominalnej 50 MW wyprodukowane w Czechach, pracujące bezpośrednio na sieć cieplną. Kotły mają

konstrukcję szybową bez regulatorów ciągu, a pęczki konwekcyjne znajdują się bezpośrednio nad ekranowanym paleniskiem. Kotły wyposażone są w 12 standardowych palników typu DKZ, umieszczonych w blokach po 6 sztuk na przeciwległych ścianach kotła. Każdy palnik ma własny wentylator nadmuchowy. Palniki przeznaczone są do spalania gazu ziemnego i wyposażone we wtryskiwacze mazutu o rozpylaniu mechanicznym (Jemieljanow 1992, Charun et al. 2016, Czapp et al. 2016, Pavlenko et al. 2014) (rys. 1).

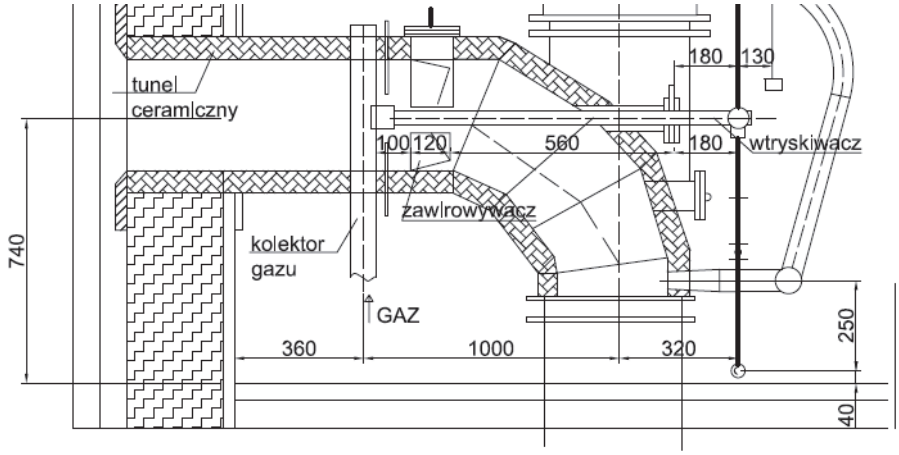

Rys. 1. Przekrój palnika DKZ z wtryskiwaczem mazutu wykorzystywanym do doprowadzania balastu wodnego
Fig. 1. Cross section view of DKZ burner with the black oil atomizer used for injection of water ballast

W kotłowni znajdują się także 3 kotły parowe DKVR-10 co daje możliwość wykorzystania produkowanej pary jako balastu wodnego. Praca kotłowni przewiduje wykorzystanie mazutu jako paliwa rezerwowego i jest on wykorzystywany skrajnie rzadko. Dlatego celem pracy było opracowanie i wdrożenie systemu zmniejszenia emisji tlenków azotu podczas spalania gazu z możliwością płynnego przejścia na spalanie mazutu bez jakichkolwiek zakłóceń i przeszkód.

3. Teoretyczne uzasadnienie zastosowania metody

Metoda balastowania strefy spalania wilgocią zapewnia efektywne zdławienie powstawania tlenku azotu wskutek złożonego działania kilku mechanizmów (Szkarowski 1997, 2001, 2002, 2003). Przesłanką do uzasadnienia tej metody jest zjawisko niejednorodności płomienia wzdłuż paleniska zarówno ze względu na jego skład jak i temperaturę. Przy czym różne strefy płomienia w różnym stopniu „odpowiedzialne" są za powstawanie poszczególnych składników. Temperaturowe warunki i koncentracje komponentów reakcji chemicznych w tych strefach wyznaczają intensywność generacji tlenków azotu (NO_x) i ich końcowe stężenie w spalinach (Roslakow 1986). Z kolei oddziaływanie na warunki temperaturowe i koncentracyjne w takich strefach jest potężnym narzędziem dla zdławienia powstania NO_x i zmniejszenia zanieczyszczenia atmosfery jednym z najbardziej niebezpiecznych produktów spalania każdego paliwa organicznego.

Po pierwsze wtrysk wilgoci do dokładnie określonych stref płomienia obniża ich temperaturę będącą głównym czynnikiem przyśpieszającym generację NO_x. Po drugie wtrysk pozwala zapewnić zupełne spalanie przy obniżonym stężeniu wolnego tlenu, co również przyczynia się do zdławienia powstawania tlenków azotu.

Ten drugi mechanizm z kolei jest bardzo złożony. Wtryskiwanie z dużą prędkością pary do dokładnie określonych stref jądra płomienia znacznie intensyfikuje mieszanie się strumieni gazu i powietrza i co za tym idzie – również procesy wewnątrzpłomieniowe. Ponadto część wilgoci dysocjuje w wysokotemperaturowej strefie na rodniki H i OH, co także sprzyja przyśpieszeniu procesów spalania, ponieważ rodniki te włączają się do reakcji z udziałem pośrednich produktów spalania.

Należy zauważyć, że zwiększenie stężenia gazów trójatomowych w przestrzeni paleniskowej skutkuje wzrostem stopnia czarności tej przestrzeni i przyczynia się do zwiększenia intensywności wymiany ciepła powierzchni ekranowych na drodze promieniowania. Wstępne obliczenia wykazały, że metoda zapewnić może zmniejszenie emisji NO_x o 25 do 30% przy wtryskiwaniu balastu w ilości do 1% ekwiwalentnej wydajności parowej kotła. Z kolei zmniejszenie nadmiaru powietrza i towarzyszące temu obniżenie strat ciepła spalinowych (Orłowska et al. 2012) powinno pozwolić na zwiększenie sprawności kotła brutto o około 1%.

W ten sposób zdławienie tlenków azotu osiągnięte zostanie bez zmniejszenia sprawności kotłowni netto.

4. Opracowanie systemu zmniejszenia emisji NO_x

Występowanie w konstrukcji palników wtryskiwaczy mazutu spowodowało naturalne rozwiązanie o ich wykorzystaniu do wtryskiwania wilgoci (zobacz rys. 1). Ze względu na zaspokojenie obciążenia cieplnego sieci cieplnej oraz wysoką kaloryczność paliwa gazowego, nawet przy obciążeniu zbliżonym do nominalnego (50 MW) w kotle nr 4 wykorzystuje się najwyżej 9 palników zaś w kotle nr 5 tylko 10. Dlatego po wstępnym modelowaniu procesu paleniskowego podjęto decyzję o doprowadzaniu pary tylko do 4 środkowych palników po każdej ze stron (rys. 2).

W trakcie obszernych badań eksperymentalnych opracowano optymalną konstrukcję głowicy do wtryskiwania wilgoci nakręcanej w miejscu głowicy rozpylającej mazut (rys. 3). W podobny sposób ustalone zostało, że obecne położenie głowicy mazutowej najlepiej odpowiada miejscu doprowadzania wilgoci. Dalsze sterowanie strugami pary w celu balastowania wybranych stref w płomieniu zapewnia kąt rozwarcia chmury parowej oraz ciśnienie pary.

5. Badania eksperymentalne

Program badań eksperymentalnych przewidywał:

1. Określenie faktycznego poziomu emisji w eksploatacyjnym stanie technicznym kotłów, będącego poziomem odniesienia.
2. Możliwość optymalizacji pracy kotłów skierowanej na zmniejszenie emisji NO_x bez zastosowania dodatkowych środków technicznych (Кузнецова, Н. и др. 1973).
3. Określenie najlepszych konstruktywnych parametrów głowic rozpylających.
4. Ustalenie najkorzystniejszego, pod względem zużycia pary, trybu pracy układu zapewniającego wymagane osiągi.

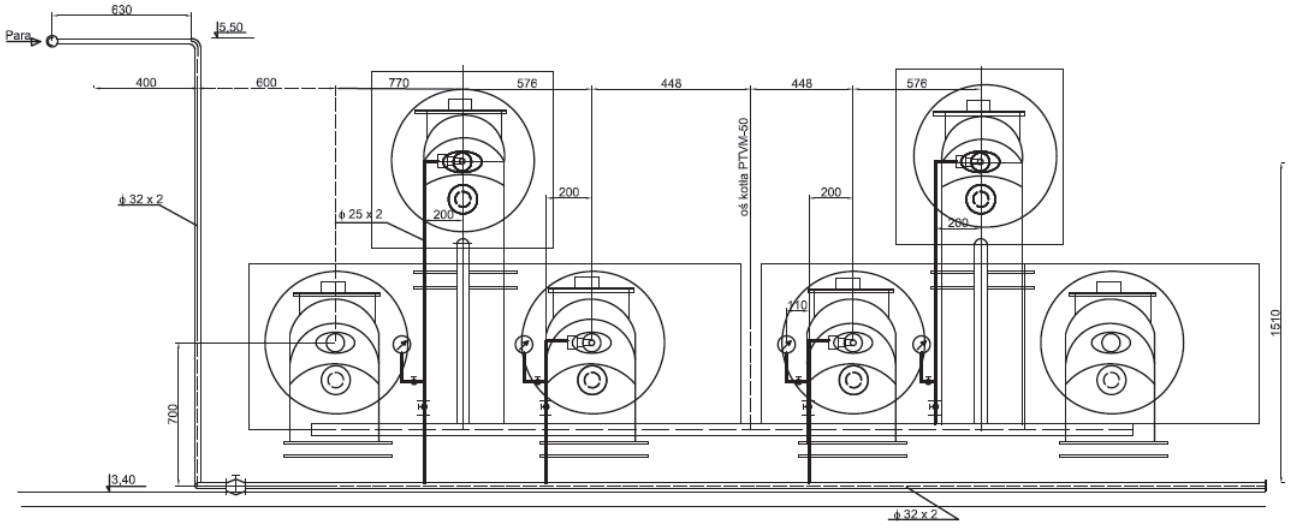

Rys. 2. Schemat doprowadzania pary do wtryskiwaczy dla bloku palników na prawej ścianie kotła
Fig. 2. Steam supply scheme of the injectors for the burner block on the right side of boil

Wstępnie oszacowana maksymalna obliczeniowa emisję tlenków azotu emitowana do atmosfery [g/s] w przeliczeniu na NO_2 wyniósł 4,709 [g/s] (Сборник (1986)). Taki poziom można uważać za wstępne oszacowanie emisji. Za bardziej wiarygodny poziom odniesienia, w stosunku, do którego określa się działanie środków ekologicznych uznano rzeczywistą maksymalną emisję.

Doprowadzenie pary do strefy spalania w celu zmniejszenia intensywności generacji NO_x wykorzystano wchodzące w skład palników DKZ wtryskiwacze mazutu. Wygląd chmury parowej znajdującej się dokładnie w wymaganym miejscu jądra płomienia udowodnił słuszność tej decyzji.

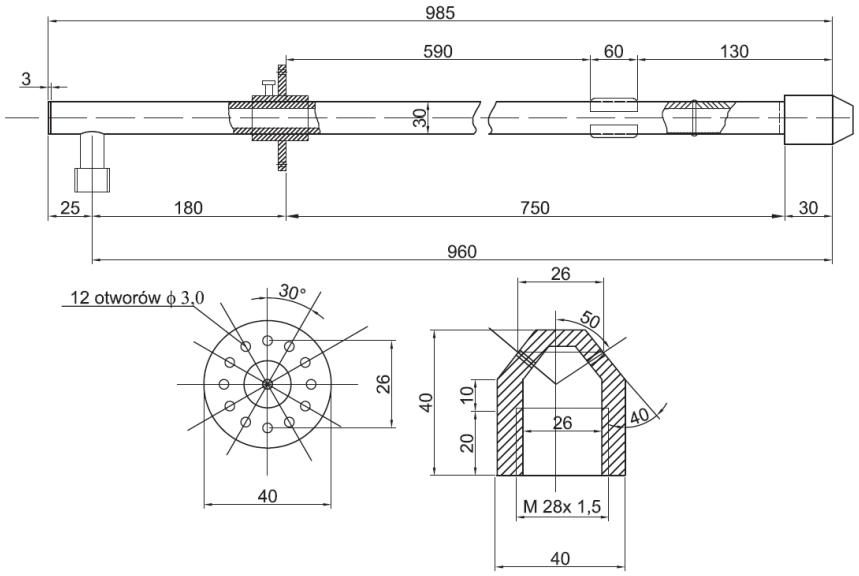

Rys. 3. Wtryskiwacz mazutu z opracowaną głowicą do rozpylania wilgoci
Fig. 3. Black oil atomizer with a developed nozzle for injection of moisture

W celu uzyskania optymalnego wyniku (maksymalnego zmniejszenia emisji NO_x przy minimalnym zużyciu pary i minimalnym wpływie na sprawność kotła) zmieniano:
– typ i wymiary głowic rozpylających;
– kształt chmury parowej;
– miejsce doprowadzania pary do strefy spalania.

Zrealizowanie powyższego programu badań pozwoliło na określenie optymalnych konstruktywnych i reżimowych parametrów systemu zdławienia emisji NO_x, zakładając oczekiwany poziom zmniejszenia emisji o 25%.

6. Wyniki badań

Emisję NO_x podaje się w przeliczeniu na masową emisję tlenków azotu G_{NOx} [g/s], ponieważ właśnie ten wskaźniki charakteryzuje bezwzględny wpływ emisji szkodliwych składników spalin na zanieczyszczenie atmosfery.

W trakcie analizy wyników badań rozpatrywano trzy poziomy ewentualnego wpływu emisji ze spalinami kotłów na zanieczyszczenia atmosfery:

1. Maksymalny obliczeniowy poziom emisji, który dla kotłów PTVM-50 wynosił 4,709 g/s.
2. Maksymalny faktyczny poziom określony doświadczalnie podczas inwentaryzacji kotłowni, przy praktycznie maksymalnie osiąganych trybach pracy kotłów wyniósł:
   – dla kotła nr 4 – 4,285 g/s
   – dla kotła nr 5 – 4,374 g/s
3. Zmniejszony zgodnie z zadaniem o 25% poziom emisji. W związku z tym, że w żadnym z kotłów faktyczny poziom emisji nie przekraczał obliczeniowego za poziom odniesienia przyjęto faktyczną maksymalną emisję tlenków azotu:
   – dla kotła nr 4 – 3,21 g/s
   – dla kotła nr 5 – 3,28 g/s

Przy nałożeniu na wspomniane poziomy danych optymalizacji-system zdławienia emisji NO_x przedstawiono na rysunkach 4 i 5. Przytoczone dane w postaci masowej emisji substancji wymagają specjalnej obróbki wyników pomiarów i kwalifikowanych obliczeń, co raczej jest trudno osiągalne w praktyce.

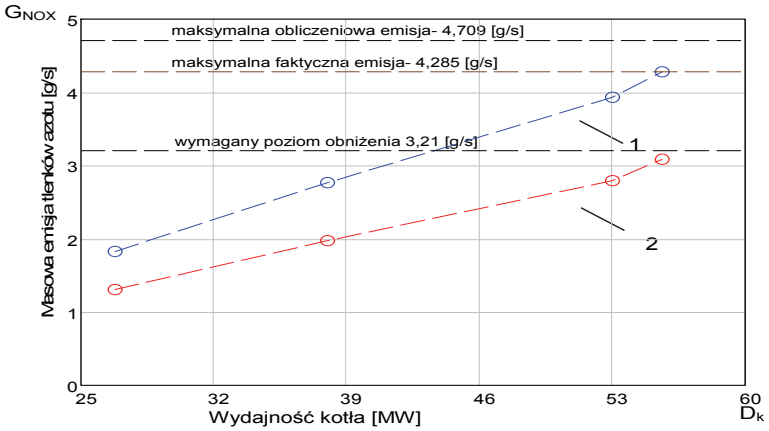

Rys. 4. Masowa emisja NO_x dla kotła PTVM-50 nr 4: 1 – w stanie eksploatacyjnym; 2 – z włączonym systemem zdławienia emisji tlenków azotu
Fig. 4. Mass emissions of NO_x boiler PTVM-50 No 4: 1 – in operating condition; 2 - enabled system to stifle emissions of nitrogen oxides

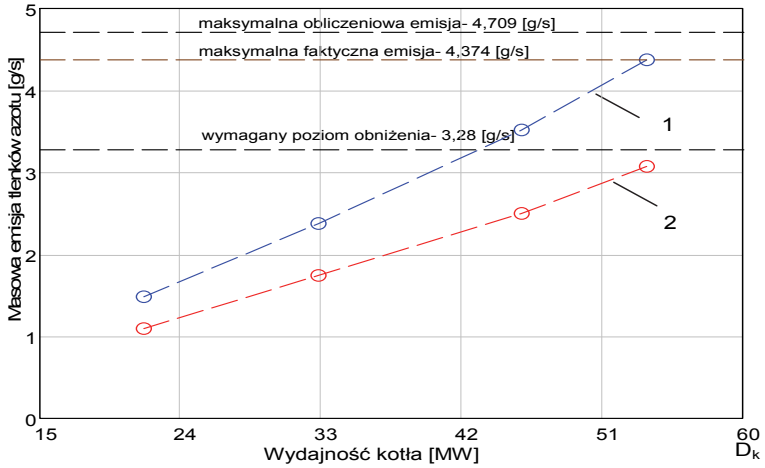

Rys. 5. Masowa emisja NO_x dla kotła PTVM-50 nr 5: 1 – w stanie eksploatacyjnym; 2 – z włączonym systemem zdławienia emisji tlenków azotu
Fig. 5. Mass emissions of NO_x boiler PTVM-50 No 5: 1 – in operating condition; 2 – enabled system to stifle emissions of nitrogen oxides

Dlatego zestawienie głównych opomiarowanych i obliczanych wartości charakteryzujących pracę kotłów przy działaniu opracowanego systemu przedstawiono w tabelach 1 i 2.

Tabela 1. Zestawienie wyników badań emisji tlenków azotu dla kotła PTVM-50 nr 4 na paliwie gazowym
Table 1. Summary of the results of the testing of emissions of nitrogen oxides for fuel gas boiler PTVM-50 No 4

Wskaźniki	Ilość pracujących palników			
	4	6	8	9
1. Wydajność kotła [MW]	26,79	37,96	52,95	55,56
2. Zużycie gazu [m^3/h]	3150	4470	5980	6600
3. Strumień objętości spalin (α=1, t=20°C)[m^3/s]	7,98	11,32	15,14	16,71
4. Stężenie NO_x w spalinach (α=1, t=20°C) [mg/m^3]:				
a) faktyczna eksploatacyjna	230	245	260	265
b) z włączonym systemem	165	175	185	185
5. Emisja masowa tlenków azotu [g/s]:				
a) maksymalna obliczeniowa	4,709			
b) maksymalna faktyczna	4,285			
c) faktyczna eksploatacyjna	1,835	2,773	3,936	4,285
d) z włączonym systemem	1,317	1,981	2,801	3,091
6. Ciśnienie pary przed wtryskiwaczami systemu [bar]	1,0	1,0	1,0	1,8
7. Zużycie pary na wtrysk [kg/h]	275	410	550	735

Tabela 2. Zestawienie wyników badań emisji tlenków azotu dla kotła PTVM-50 nr 5 na paliwie gazowym
Table 2. Summary of the results of the testing of emissions of nitrogen oxides for fuel gas boiler PTVM-50 No 5

Wskaźniki	Ilość pracujących palników			
	4	6	8	10
1. Wydajność kotła [Gkcal/h]	21,63	32,80	45,79	53,79
2. Zużycie gazu [m^3/h]	2560	3840	5348	6400
3. Strumień objętości spalin (α=1, t=20°C)[m^3/s]	6,48	9,72	13,54	16,20
4. Stężenie NO_x w spalinach (α=1, t=20°C) [mg/m^3]:				
a) faktyczna eksploatacyjna	230	245	260	270
b) z włączonym systemem	170	180	185	190
5. Emisja masowa tlenków azotu [g/s]:				
a) maksymalna obliczeniowa	4,709			
b) maksymalna faktyczna	4,374			
c) faktyczna eksploatacyjna	1,490	2,381	3,520	4,374
d) z włączonym systemem	1,102	1,750	2,505	3,078
6. Ciśnienie pary przed wtryskiwaczami systemu [bar]	1,0	1,0	1,0	1,8
7. Zużycie pary na wtrysk [kg/h]	275	410	550	735

7. Wnioski

1. Został opracowany, zbadany i wdrożony układ zmniejszenia emisji tlenków azotu dla kotłów PTVM-50 metodą wtryskiwania pary z konkretnym typem urządzenia rozpylającego dla kotłów parowych, sposobem jego montażu oraz miejscem i ilością wtryskiwanej pary.
2. Określono optymalny tryb pracy systemu zmniejszenia emisji tlenków azotu, który pozwala osiągnąć wymagane zmniejszenie emisji o 25% przy ograniczonym zużyciu pary na wtryskiwanie (nie więcej 1 % ekwiwalentnej wydajności parowej kotła).
3. Ponieważ wtrysk pary wg autorskiej technologii pozwala zwiększyć sprawność pracy kotła netto średnio o 1% zalecane tryby pracy kotłów z włączonym systemem zmniejszenia emisji tlenków azotu nie powodują obniżenia sprawności kotłowni brutto.

Literatura

Сборник методик по расчету выбросов в атмосферу загрязняющихвеществ различными производствами (1986). Л. Гидрометеоиздат. Госкомгидромет.

Charun H., Czapp M., Czapp S., Orłowska M., (2016). Effect of the inclination angle of the condenser on the heat transfer coefficient value – experimental study. *Zeszyty Naukowe Politechniki Rzeszowskiej* 293, *Mechanika 88, RUTMech, tom 33, zeszyt 88 (4/16),* 307-315.

Czapp S., Czapp M. and Orłowska M. (2016). Numerical and experimental investigation of thermal convection near electric devices with vertical channels. *International Conference on Information and Digital Technologies (IDT), Rzeszów*, 54-59.

Jemieljanow, A. A., (1992). *Opracowanie urządzeń wtryskających dla zdławienia tlenków azotu przy spalaniu gazu i mazutu w paleniskach kotłów*. Autoreferat rozprawy doktorskiej. Sankt – Petersburg.

Кузнецова, Н. и др. (1973). Тепловой расчет котельных агрегатов: Норматив. метод. *М.: Энергия*.

Orłowska M., Czapp M., (2012). Analiza numeryczna wydajności cieplnej konwekcyjnego wymiennika ciepła obudowanego poziomymi płytami, *Rocznik Ochrona Środowiska, 14*, 582-585.

Pavlenko, A., Szarowski, A., Janta-Lipińska, S. (2014). Badania spalania emulsji paliwowych. *Rocznik Ochrona Środowiska,16,* 376-385.

Roslakow, P. W. (1986). Obliczenie wytwarzania się paliwowych tlenków azotu przy spalaniu paliwa zawierającego azot. *Energetyka cieplna, 1(1)*, 37-41.

Szkarowski, A. (1997). *Podwyższenie efektywności ochrony atmosfery przy spalaniu gazowego i ciekłego paliwa.* Autoreferat rozprawy habilitacyjnej. Sankt-Petersburg.

Szkarowski, A. (2001). Technologia redukcji emisji NO_x metoda dozowanego skierowanego balastowania płomienia. *Rocznik Ochrona Środowiska, 3*, 53-73.

Szkarowski, A. (2002). Zasady obliczeń zdławienia NO_x metodą dozowanego skierowanego wtrysku balastu wodnego. *Rocznik Ochrona Środowiska,4*, 365-378.

Szkarowski, A. (2003). Szczegółowe problemy sprawnego i ekologicznego spalania paliwa w przedpaleniskach pieców. *Rocznik Ochrona Środowiska, 5*, 67-78.

Szkarowski, A., Janta- Lipińska, S. (2009). Automatyczne sterowanie jakością spalania paliwa stałego w kotłach przemysłowo-grzewczych. *Rocznik Ochrona Środowiska, 11,* 241-255

Szkarowski, A., Janta-Lipińska, S. (2011). Modelowanie optymalnego spalania w kotłach przemysłowo-grzewczych. *Rocznik Ochrona Środowiska, 13*, 511-524.

Szkarowski, A., Janta-Lipińska, S. (2013). Badania energo-ekologicznych wskaźników pracy kotłów przy spalaniu paliwa ze sterowanym resztkowym niedopałem chemicznym. *Rocznik Ochrona Środowiska, 15,* 981-995.

Szkarowski, A., Janta-Lipińska, S. (2015). Badania doświadczalne a dokładność opracowanego modelu. *Rocznik Ochrona Środowiska, 17*, 576-584.

Szkarowski, A., Janta-Lipińska, S., Gawin, R. (2016). Obniżenie emisji tlenków azotu z kotłów DKVR. *Rocznik Ochrona Środowiska, 18*, 565-578.

Injection of Water Ballast as a Method to Reduce Nitrogen Oxide Emissions

Abstract

The water ballast injection method is one of the most prospective scientific and technical solutions. Its chief purpose is to reduce the pollution of air with harmful products of organic fuel combustion. The analysis conducted demonstrates that the injection method is characterized by unique energy efficiency and environmental friendly indices as compared to other air quality protection methods.

The phenomenon of the heterogeneity of the flame along the furnace considering both its composition and temperature constitutes the grounds of this method. Various flame areas are "responsible" to a different extent for the occurrence of individual components. The temperature conditions and the concentrations of the components of chemical reactions in these areas determine the intensity of the generation of nitrogen oxides (NO_x) and their final concentration in fumes. An injection of humidity into accurately specified flame areas lowers their temperature, which constitutes the main factor that accelerates the generation of NO_x. Furthermore, this method guarantees complete combustion with a reduced concentration of free oxygen, which also contributes to a suppressed occurrence of nitrogen oxides.

The present study was performed for two PTVM-50 boilers with DKZ burners (Fig. 1) that are installed in the Second Krasnogwadiejski Boiler Plant in Sankt-Petersburg. Preliminary calculations demonstrated that this method may guarantee a reduction of NO_x emissions by 30 per cent with a balance injection in a quantity up to 1 per cent of the equivalent steam boiler performance.

A reduction of excess air and the accompanying reduction of fume heat loss should permit an increased gross boiler efficiency by ca. 1 per cent.

The aforementioned assumptions were realized during the studies. Furthermore, an optimal design was developed of a head for humidity injection, which was installed in the place of a head that sprays mazut (Fig. 3). The use of this solution permitted measurements of NO_x emission in fumes, which are presented in the study (Fig. 4 and Fig. 5). In the analysis conducted, three levels were taken into account of the possible impact of the emissions of fumes from boiler on air pollution.

Streszczenie

Metoda wtrysku balastu wodnego jest jednym z najbardziej perspektywistycznych rozwiązań naukowo-technicznych. Skierowana jest ona przede wszystkim na zmniejszenie zanieczyszczeń atmosfery szkodliwymi produktami spalania paliwa organicznego. Przeprowadzona analiza pokazuje, że metoda wtrysku charakteryzuje się unikalnymi energo-ekologicznymi i techniczno-ekonomicznymi wskaźnikami spośród innych technologii ochrony atmosfery.

Przesłanką do uzasadnienia tej metody jest zjawisko niejednorodności płomienia wzdłuż paleniska zarówno ze względu na jego skład jak i temperaturę. Przy czym różne strefy płomienia w różnym stopniu „odpowiedzialne" są za powstawanie poszczególnych składników. Temperaturowe warunki i koncentracje komponentów reakcji chemicznych w tych strefach wyznaczają intensywność generacji tlenków azotu (NO_x) i ich końcowe stężenie w spalinach. Wtrysk wilgoci do dokładnie określonych stref płomienia obniża ich temperaturę będącą głównym czynnikiem przyśpieszającym generację NO_x. Ponadto metoda ta pozwala zapewnić zupełne spalanie przy obniżonym stężeniu wolnego tlenu, co również przyczynia się do zdławienia powstawania tlenków azotu. Opracowanie wykonane zostało dla dwóch kotłów PTVM-50 z palnikami DKZ (rys. 1) zainstalowanych w Drugiej Krasnogwadiejskiej kotłowni w Sankt-Petersburgu. Wstępne obliczenia wykazały, że metoda ta zapewnić może zmniejszenie emisji NO_x o 25 do 30% przy wtryskiwaniu balastu w ilości do 1% ekwiwalentnej wydajności parowej kotła. Z kolei zmniejszenie nadmiaru powietrza i towarzyszące temu obniżenie strat ciepła spalinowych powinno pozwolić na zwiększenie sprawności kotła brutto o około 1%.

Powyższe założenia zrealizowane zostały w trakcie badań. Ponadto opracowana została optymalna konstrukcja głowicy do wtryskiwania wilgoci, która nakręcana była w miejscu głowicy rozpylającej mazut (rys. 3). Wykorzystanie takiego rozwiązania pozwoliło na pomiary emisji NO_x w spalinach, które zaprezentowane zostały w pracy (rys. 4 i rys. 5). W trakcie przeprowadzonej

analizy uwzględniane zostały trzy poziomy ewentualnego wpływu emisji ze spalinami kotłów na zanieczyszczenie atmosfery.

Key words:
emissions, injection of humidity, boiler, nitrogen oxides

Słowa kluczowe:
emisja, wtrysk wilgoci, kocioł, tlenki azotu

MIDDLE POMERANIAN SCIENTIFIC SOCIETY OF THE ENVIRONMENT PROTECTION
ŚRODKOWO-POMORSKIE TOWARZYSTWO NAUKOWE OCHRONY ŚRODOWISKA

Annual Set The Environment Protection
Rocznik Ochrona Środowiska

Volume/Tom 19. Year/Rok 2017 ISSN 1506-218X 511-526

Pożar – czynnik kształtujący liczebność mikroorganizmów i mezofauny w glebach leśnych

Izabella Olejniczak[*], Ewa Beata Górska[**], Marek Kondras[**], Lidia Oktaba[**], Dariusz Gozdowski[**], Urszula Jankiewicz[**], Anna Prędecka[***], Jakub Dobrzyński[**], Anna Otręba[****], Łukasz Tyburski[****], Małgorzata Mickiewicz[****], Edyta Hewelke[**]

[*]*Uniwersytet Kardynała Stefana Wyszyńskiego, Warszawa*
[**]*Szkoła Główna Gospodarstwa Wiejskiego, Warszawa*
[***]*Szkoła Główna Służby Pożarniczej, Warszawa*
[****]*Kampinoski Park Narodowy, Izabelin*

1. Wstęp

Zespoły mikroorganizmów i mezofauny, w tym roztoczy (*Acari*) i skoczogonek (*Collembola*) zasiedlające środowisko glebowe zaangażowane są w rozkład i mineralizację substancji organicznej, przez co odgrywają znaczącą funkcję w biogeochemicznych cyklach pierwiastków, w tworzeniu próchnicy glebowej, co przekłada się na żyzność gleby i jej produkcyjność (Seastedt 1984, Gardi i in. 2009, Mummey i in. 2010; Carrillo i in. 2011, Scharenbroch i in. 2012, de Vries i in. 2013). Mezofauna może wpływać na mikroorganizmy zarówno bezpośrednio poprzez zjadanie bakterii i grzybów a także pośrednio, rozdrabniając materię organiczną ułatwiając w ten sposób mikroorganizmom zasiedlanie jej i rozkład (Lussenhop 1992, Heneghan & Bolger 1996, Berg i in. 2001). Z drugiej zaś strony rozwój, liczebność i różnorodność edafonu zależy między innymi od własności fizycznych i chemicznych gleby, wilgotności i temperatury oraz typu i bogactwa gatunkowego roślinności pokrywającej glebę (Petersen 1980, Huhta & Mikkonen 1982, Dighton i in. 1997).

Jednym z czynników stresowych, poważnie zaburzającym równowagę biologiczną gleby jest pożar (Dress & Boerner 2004, Banning i in. 2011, Mataix-Solera i in. 2009, Smith i in. 2008, Zaitsev i in. 2015, Xingjia i in. 2014, Sulwiński i in. 2017). Zaburzenia powodowane przez pożar zależą od siły, czasu trwania, sezonu i częstotliwości pojawiania się pożaru oraz jego natury, tj. czy jest 'naturalny' czy 'antropogeniczny' (Wikars & Schimmel 2001, Saint-Germain i in. 2005, Malmström 2010). Pożary podobnie jak zanieczyszczenia atmosfery wpływają na fizyczne, chemiczne i biologiczne własności gleby. Przyczyniają się do zmniejszenia liczebności mezo – i makrofauny (Wikars & Schimmel 2001), wpływają także na mikroorganizmy glebowe oraz aktywność enzymatyczną gleb (Dunn i in. 1985, Neary i in. 1999, De Vries i in. 2013, Köster i in. 2017, Pietikäinen i in.1995). Na terenach popożarowych ekspansywnie rozwijają się grzyby pasożytnicze, które pogarszają strukturę zdrowotną drzewostanów, a tym samym obniżają wartość hodowlaną oraz zdolności produkcyjne gleb leśnych. Wiadomo przy tym, że charakter i siła zaburzeń decyduje o możliwościach odbudowy ekosystemów (Bengtsson 2002, Malmström i in. 2008, Malmström 2010).

Ponieważ zespoły mikroorganizmów i mezofauny glebowej mają kluczowe znaczenie w funkcjonowaniu ekosystemów leśnych (Decaëns 2010, Carrillo i in. 2011) ważnym jest zrozumieć reakcję organizmów glebowych na pożary, zwłaszcza pochodzenia antropogenicznego.

Liczba pożarów z roku na rok zwiększa się, w tym również na obszarze Polski dlatego wydaje się koniecznym prowadzenie badań na obszarach pożarzysk.

Celem podjętych badań jest ocena wpływu intensywności pożaru na liczebność wybranych grup edafonu glebowego w tym bakterii heterotroficznych, grzybów mikroskopowych oraz mezofauny glebowej roztoczy (*Acari*) i skoczogonków (*Collembola*) w ściółce i w glebie na pożarzysku w Puszczy Kampinoskiej. Podczas pożaru powierzchniowego (jaki miał miejsce w Puszczy Kampinoskiej) organizmy zasiedlające wierzchnie warstwy gleby, są bezpośrednio narażone na działanie pożaru (Swengel 2001, Adeniyi 2010, Malmström 2010). Założono więc, że liczebność organizmów związanych z warstwą organiczną gleb powinna być znacznie niższa na obszarach wypalonych w porównaniu z niewypalonymi.

2. Metodyka badań

Badania środowiska glebowego oraz mezofauny przeprowadzono w północno-wschodniej części Kampinoskiego Parku Narodowego, w Obrębie Ochronnym Laski, w Obwodzie Ochronnym Kaliszki, 15 miesięcy po pożarze. Dokładna lokalizacja pożarzyska to tereny oddziałów 76 oraz 77. Obejmowały one częściowo Obszar Ochrony Ścisłej Sieraków, stanowiący największy i najbardziej wartościowy teren KPN oraz jeden z bardziej atrakcyjnych terenów kraju. Wszystkie badane powierzchnie porastał zespół rośliny *Peucedano-pinetum* (Subkontynentalny bór sosnowy świeży), jako typ siedliskowy lasu określono bór świeży. Gleby zaklasyfikowano według Klasyfikacji gleb leśnych Polski (Biały i in. 2000) do gleb rdzawych właściwych o zasadniczej budowie profilu: Ol-Ofh-A-Bv-BvC-C oraz rdzawych bielicowych o profilu: Ol-Ofh-AEes-BvBfeh-Bv-C. Próchnicę glebową zaklasyfikowano, jako typ moder-mor świeży. Utwory z których wykształciły się badane gleby rdzawe, to dobrze wysortowane piaski eoliczne o uziarnieniu piasków luźnych.

Na badanym terenie doszło do dwóch pożarów, które objęły łącznie powierzchnię ponad 11 hektarów. Były to pożary przyziemne – spaleniu uległa w dużym stopniu pokrywa gleby (poziomy organiczne). Wydarzenia te miały miejsce odpowiednio 7 maja 2015 roku oraz 4 czerwca 2015 roku.

Ustalono pozycję systematyczną gleb według Klasyfikacji gleb leśnych Polski (Biały i in. 2000). Określono typ siedliskowy lasu oraz zespół roślinny. Z wyróżnionych w profilach gleb poziomów genetycznych pobrano próbki, w których oznaczono właściwości fizykochemiczne następującymi metodami Ostrowska i in. 1991; Bednarek i in. 2004: pH – w H_2O i 1M KCL·dm^{-3} potencjometrycznie; zawartość węgla organicznego ogółem (C_{org}) za pomocą automatycznego analizatora węgla firmy Shimadzu TOC 5000A; ogólną zawartość azotu (N_{og}) – zmodyfikowaną metodą Kjeldahla stosując analizator Kjeltec-Tecator.

Do badań wytypowano stanowiska po mocnym i słabym pożarze oraz nie objęte ogniem oddalone o 10 m od linii ognia – stanowiące kontrolę, każde o łącznej powierzchni 10 m^2. Próbki do analiz chemicznych i mikrobiologicznych pobrano z zachowaniem zasad aseptyczności do pojemników jałowych z warstwy organicznej i poziomu mineralnego gleby (0-20 cm). Próbki były pobierane z 6 losowo wybranych punktów

na każdej powierzchni, z których przygotowywano próbę zbiorczą dla danego poziomu.

Na tych samych poletkach pobierano losowo po 6 prób do analizy mezofauny glebowej. Próby pobierano wycinakiem glebowym o powierzchni 10 cm^2 do głębokości 10 cm. Następnie tak pobrane walce gleby dzielono na dwie podpróbki, umieszczane w osobnych pojemnikach: pierwszą obejmującą warstwę 0-5 cm (organiczną) oraz drugą obejmującą warstwę 5-10 cm (mineralną). Mezofaunę z prób glebowych wypłaszano w aparacie MacFadyena i konserwowano w 70% alkoholu etylenowym.

W poziomie organicznym i mineralnym gleb oznaczono metodą posiewu wgłębnego ogólną liczbę bakterii heterotroficznych na podłożu Bunta i Roviry z dodatkiem wyciągu glebowego i cyklohexamidu – 50 $\mu g \cdot cm^{-3}$ (Bunt i Rovira 1955) oraz grzybów mikroskopowych na podłożu Martina z dodatkiem streptomycyny – 50 $\mu g \cdot cm^{-3}$ (Martin 1950). Liczebność mikroorganizmów wyrażano w jednostkach tworzących kolonie (jtk) w przeliczeniu na kg suchej masy ściółki i gleby.

Wyniki badań dotyczące wpływu pożaru na liczebność organizmów glebowych zweryfikowano jednoczynnikową analizą wariancji, grupy jednorodne wyróżniono testem Tukey'a dla $\alpha = 0{,}05$ stosując program Statgraphics ver. plus 4.1. Zależności między badanymi cechami oraz wielocechowe zróżnicowanie badanych obiektów oceniono stosując analizę składowych głównych (PCA).

3. Wyniki i dyskusja

Pożar lasu podczas jego trwania i po nim kształtuje właściwości abiotyczne i biotyczne środowiska, w tym zmienia liczebność i różnorodność taksonomiczną, a wraz z nią również metaboliczną wspólnoty mikroorganizmów oraz zespołów mezofauny glebowej (Dunn i in. 1985, Sgardelis & Margaris 1993, Neary i in. 1999, DeBano 2000). Powodem tych zmian jest między innymi drastyczny wzrost temperatury, zmniejszenie ilości łatwo przyswajalnej dla organizmów substancji organicznej w glebie, a także wytworzenie substancji toksycznych jako wynik spalania celulozy, lignin, żywic i innych aromatycznych związków chemicznych (Certin i in. 2005).

Badane poziomy organiczne oraz mineralne w zależności od intensywności pożaru różniły się właściwościami chemicznymi, co przedstawia tabela 1. Zwykle obserwuje się zubożenie gleby w główne makroskładniki. W wyniku pożaru może nastąpić wyraźne wzbogacenie w poziomach popiołowych w dostępne formy wapnia, magnezu, sodu i potasu. Pożar w istotny sposób wpływa na wzrost pH gleby. Spowodowane to jest z jednej strony powstawaniem tlenków metali alkalicznych, a także wodorotlenków i węglanów, z drugiej – spalanie materii organicznej wiąże się z uwolnieniem do atmosfery związków o charakterze zasadowym (Neary i in. 1999, Kennard & Gholz 2001, Otsuka i in. 2008). W badanych glebach stwierdzono alkalizację poziomów organicznych na powierzchniach objętych pożarem w stosunku do powierzchni kontrolnych. Wykazano także znaczny spadek zawartości węgla organicznego oraz azotu ogólnego na powierzchniach objętych mocnym pożarem w stosunku do kontroli oraz powierzchni objętych słabym pożarem. Proporcja C/N w glebach objętych mocnym pożarem ma wyższą wartość, niż na pozostałych stanowiskach. Świadczy to o większym ubytku azotu ogólnego w stosunku do węgla organicznego.

Literatura przedmiotu wykazuje niejednoznaczny wpływ pożarów i ich następstwa na właściwości biologiczne gleby, w tym na liczebność i różnorodność taksonomiczną mikroorganizmów (Ditomaso i in. 2006, Dunn i in. 1985, Neary i in. 1999, Guerro i in. 2005, Mataix-Solera i in. 2009). W krótkim okresie po pożarze wielu badaczy obserwowało wzrost liczebności bakterii na wypalonych obszarach (Badia & Marti 2003, Guerro i in. 2005), co mogłoby mieć związek ze wzrostem pH gleby i dostępnością nutrientów (Jokinen i in. 2006) czy brakiem konkurencji o zasoby pokarmowe (Bauhus i in.1993). Przy czym wraz z upływem czasu od pożaru notowano spadek liczebności bakterii do poziomu sprzed pożaru i związane było to z sukcesją roślinności (Grasso i in. 1996). Wyniki badań prezentowanych w pracy wykazały, że w rok po pożarze liczebność bakterii heterotroficznych zmniejszyła się w ściółce (nieistotne statystycznie) i glebie mineralnej na terenie który był objęty mocnym pożarem porównując z liczebnością na powierzchni kontrolnej, co nie zawsze potwierdziła analiza statystyczna (tab. 2). Być może uzyskane wyniki odzwierciedlają opisane powyżej zjawisko. Odmienne relacje stwierdzono w obu badanych poziomach genetycznych w przypadku grzybów mikroskopowych. Obszar po słabym pożarze charakteryzował

się zmniejszoną liczebnością grzybów w porównaniu z powierzchnią objętą mocnym ogniem (tab. 2).

Grzyby dzięki intensywniejszemu zarodnikowaniu po pożarze, który jest wynikiem wzrostu pH w środowisku oraz dzięki zdolności do wytwarzania tzw. propaguli (artrospory, sklerocja, artrospory, zoospory i inne) mogą przetrwać niesprzyjające warunki środowiska (w tym działanie ognia) dzięki czemu biorą udział w regeneracji wspólnoty grzybów po pożarze. Tworzenie propaguli przez grzyby mikoryzowe może być również sprowokowane przez zmniejszenie ilości łatwo przyswajalnej substancji w tkankach drzewa w wyniku powolnego obumierania systemu korzeniowego roślin po pożarze (Cerda & Robichaud 2009). Wspólnota bakterii w glebie po pożarze ulega regeneracji, między innymi dzięki endosporom, cystom, zarodnikom konidialnym, jak również może być naniesiona z odtwarzającej się na pożarzysku flory i/lub z liści naniesionych w wyniku ruchów powietrza z innych terenów.

Pożar selekcjonuje liczebność mikroorganizmów (Pizarro-Tobías i in. 2014), które dominowały w środowisku w okresie poprzedzającym pożar, stąd zmiana warunków fizycznych i chemicznych w glebie po pożarze mogła wpłynąć na zwiększenie liczebności grzybów między innymi dlatego, że stopniowo mogły rozwijać się wszystkie grzyby mikroskopowe, które przeżyły w formie propaguli, a nie tylko te które dominowały przed pożarem.

W przypadku mezofauny: roztoczy i skoczogonek obserwowano pewne trendy w kształtowaniu się ich liczebności. Wydają się one mniejsze na obszarach po słabym pożarze (różnice jednak nie są istotne statystycznie) w porównaniu z obszarem po silnym (tab. 3). Reakcja mezofauny na zaburzenia spowodowane przez pożar są niejednoznaczne. Lussenhop (1976) nie stwierdzał różnic w liczebności mezofauny w krótkim czasie po pożarze. Podczas gdy Sgardelis i Margaris (1993) stwierdzili mniejsze liczebności mezofauny na obszarach wypalonych w porównaniu z niewypalonymi po 3 latach od pożaru a Malmström ze współpracownikami (2009) nawet po 5 latach po pożarze. Ponadto Malmström i in. (2009) stwierdzili, że odbudowa zespołów mezofauny może trwać nawet dłużej niż 5 lat. Także Huhta i in. (1969) uważają że fluktuacje liczebności skoczogonek i roztoczy mogą trwać kilka lat. Spadek liczebności mezofauny może wynikać z faktu, że pożary niszczą warstwę ściółki i próchnicy, w których zwierzęta te najliczniej występują (Malmström

2010). Znajdują tam nie tylko optymalne warunki mikroklimatyczne i możliwość ochrony przed drapieżnikami, ale także źródło pokarmu.

Skoczogonki odżywiają się różnorodnym pokarmem, najłatwiej dostępnym w środowisku (Ngosong i in. 2009). Nie dziwi, więc ścisła korelacja skoczogonek z licznie występującymi na pożarzysku grzybami (rys. 1 i rys. 2). Podobnie na obszarach kontrolnych, w warstwie organicznej, dużej obfitości grzybów towarzyszyła duża liczebność skoczogonek (rys. 3). Można przypuszczać, że zarówno na pożarzysku jak i obszarach kontrolnych przeważały skoczogonki grzybożerne lub że skoczogonki wybierały najłatwiej dostępny pokarm.

Roztocza obejmują różne grupy troficzne (Boczek & Błaszak 2005). Są wśród nich gatunki drapieżne, które mogą odżywiać się skoczogonkami, ale także grzybożerne czy saprofagiczne, które mogą konkurować ze skoczogonkami o pokarm. W prezentowanej pracy stwierdzono ujemne relacje między liczebnościami skoczogonków i roztoczy (rys. 1 i rys. 2). Z jednej strony mogły tu działać zależności ofiara-drapieżca (rys. 2), z drugiej zaś konkurencja (rys. 1) efektem której było wykorzystywanie przez skoczogonki i roztocza odmiennych źródeł pokarmu.

Otrzymane wyniki badań zweryfikowane analizą statystyczną uprawniają do stwierdzenia, że w ponad rok od pożaru na pożarzysku zachodzi stopniowa regeneracja populacji mikroorganizmów zarówno w poziomie organicznym jak również w poziomie mineralnym gleby.

Tabela 1. Właściwości chemiczne gleby
Table 1. Chemical properties of soil

Intensywność pożaru	C-org $g \cdot kg^{-1}$		N-og $g \cdot kg^{-1}$		C:N		pH w KCl		pH w H_2O	
	Poziom genetyczny gleby									
	org.	min.	org.	min.	org.	min.	org.	min.	org.	min.
K – kontrola	351,7	9,62	7,23	0,37	48,6	26,0	3,13	3,91	3,27	4,46
Sp – słaby pożar	387,1	10,9	7,17	0,30	53,9	36,0	3,04	4,11	3,30	4,22
Mp – mocny pożar	317,3	12,6	5,67	0,21	55,9	60,0	3,46	3,43	3,68	3,62

Tabela 2. Wpływ intensywności pożaru na wybrane wskaźniki mikrobiologiczne gleby, grupy jednorodne – a, b wyróżniono testem Tukeya dla α = 0,05
Table 2. The influence of fire intensity on the selected microbiological indicators of soils, homogeneous groups – a, b were distinguished by the Tukey test for α = 0,05

Intensywność pożaru	Liczebność bakterii $\cdot 10^7$ jtk$\cdot$kg^{-1} suchej masy gleby		Liczebność grzybów mikroskopowych $\cdot 10^6$ jtk$\cdot$kg^{-1} suchej masy gleby	
	Poziom genetyczny gleby			
	org.	min.	org.	min.
K – kontrola	354,0 a	38,0 ab	177,0 b	8,1 a
Sp – słaby pożar	254,0 a	41,0 b	35,0 a	4,8 a
Mp – mocny pożar	199,4 a	22,0 a	174,0 b	17,0 b
Odchylenie standardowe	102,5	14,1	69,7	6,1

Tabela 3. Wpływ intensywności pożaru na liczebność wybranych grup mezofauny glebowej, grupy jednorodne – a, b wyróżniono testem Tukey'a dla α = 0,05
Table 3. The influence of fire intensity on the number of selected soils mesofauna groups, homogeneous groups – a, b were distinguished by the Tukey test for α = 0,05

Intensywność pożaru	Liczebność roztoczy (*Acari*) $\cdot 10^3 \cdot$m^{-2}		Liczebność skoczogonków (*Collembola*) $\cdot 10^3 \cdot$m^{-2}	
	Poziom genetyczny gleby			
	Organiczny	Mineralny	Organiczny	Mineralny
K – kontrola	21,0 b	0,3 a	23,5 a	0,0 a
Sp – słaby pożar	8,5 ab	0,3 a	1,7 a	0,0 a
Mp – mocny pożar	9,8 a	0,2 a	12,9 a	0,2 a
Odchylenie standardowe	9,74	0,48	18,45	0,28

Na podstawie rysunku 1 można określić powiązania między poszczególnymi cechami ocenionymi dla warstwy organicznej. Np. stwierdzono silną ujemną korelację między zawartością węgla organicznego (C-org) a pH. Ponadto dodatni związek stwierdzono między liczebnością bakterii, zawartością azotu ogólnego (N-og) i liczebnością roztoczy (*Acari*). Te trzy cechy były dodatnio, lecz słabo skorelowane z liczebnością grzybów i skoczogonków (*Collembola*).

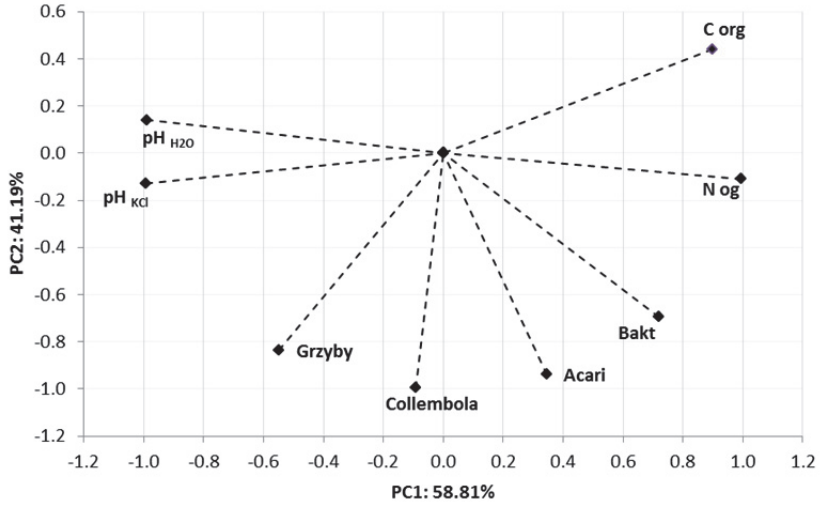

Rys. 1. Wyniki analizy składowych głównych (PCA) dla warstwy organicznej przedstawiające powiązania między badanymi cechami
Fig. 1. The results of main component analysis (PCA) for the organic layer showing the relationships between the tested features

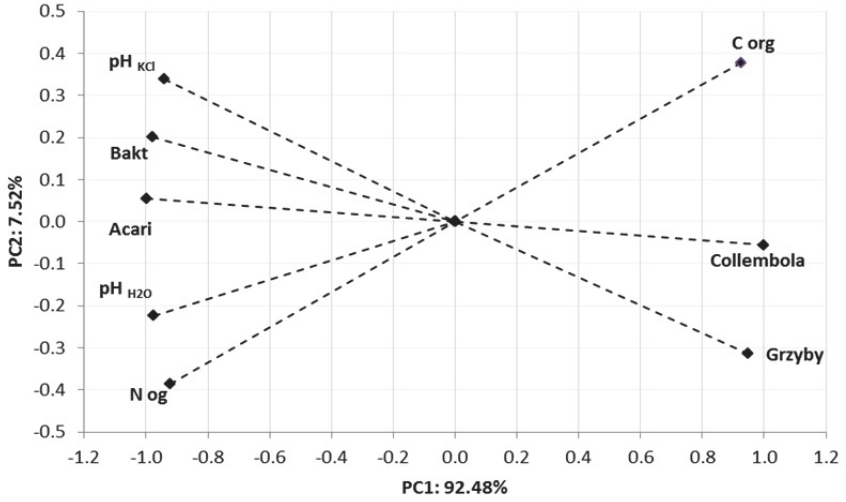

Rys. 2. Wyniki analizy składowych głównych (PCA) dla warstwy mineralnej przedstawiające powiązania między badanymi cechami
Fig. 2. The results of main components analysis (PCA) for the mineral layer showing the relationships between the tested features

Na podstawie rysunku 2 można określić powiązania między poszczególnymi cechami ocenionymi dla warstwy mineralnej. Np. stwierdzono dodatnią silną korelację między zawartością C-org i liczebnością skoczogonków (*Collembola*) oraz grzybów, a jednocześnie ujemną korelację tych trzech cech z wszystkimi pozostałymi cechami, tj. pH, bakteriami, zawartością N i liczebnością roztoczy (*Acari*). Ponadto te cechy (pH, liczebnością bakterii, zawartością N-og i liczebnością roztoczy (*Acari*) były ze sobą dodatnio powiązane.

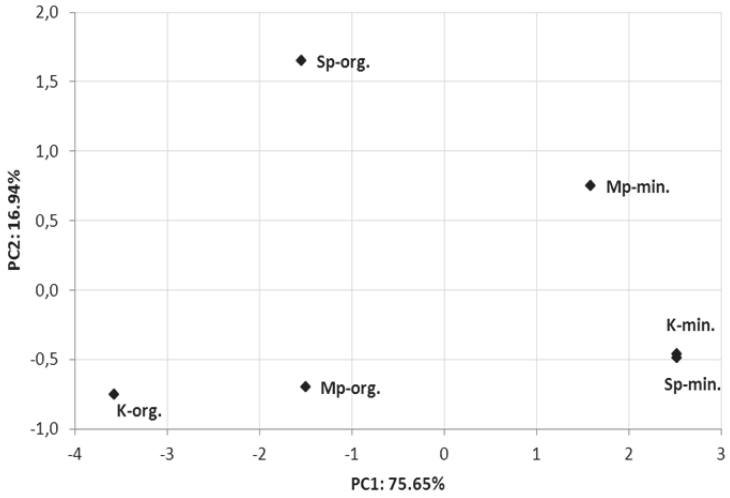

Rys. 3. Wyniki analizy składowych głównych (PCA) dla warstwy organicznej i mineralnej przedstawiające wielocechowe zróżnicowanie badanych obiektów
Fig. 3. The results of main components analysis (PCA) for organic and mineral layer presenting multifocal differentiation of examined objects

Natomiast na podstawie wykresu 3 można stwierdzić, że największa zmienność między obiektami była oznaczona dla PC1 (ponad 75% zmienności), czyli dla osi X, co oznacza, że znacznie ważniejsze są różnice między obiektami w poziomie, niż w pionie. Obiekty K-min. i Sp-min. charakteryzowały się wysokim pH gleby, a jednocześnie dość niskimi wartościami dla pozostałych cech. Obiekt Mp-min. charakteryzował się dość niskimi wartościami większości cech. W przypadku warstwy organicznej wyróżniał się najbardziej obiekt K-org, który charakteryzował się wysokimi zawartościami grzybów mikroskopowych i skoczogonków (*Collembola*), jak również niskim pH.

4. Wnioski

- Właściwości chemiczne i biologiczne gleby ulegają stopniowej regeneracji w glebie i ściółce w 15 miesięcy po pożarze.
- Intensywność pożaru ma istotne znaczenie w odtwarzaniu liczebności mikroorganizmów i mezofauny. Słaby pożar działa bardziej selekcjonująco na mikroorganizmy i mezofaunę niż pożar mocny.
- Uzyskane wyniki badań uprawniają do stwierdzenia, że pożar może być jednym z czynników stymulujących rozwój grzybów zarówno w poziomie organicznym jak i mineralnym gleb leśnych

Badania zrealizowano w ramach zadania badawczego „Właściwości fizyczne, chemiczne gleb, różnorodność roślin, grzybów, mikrofauny na pożarzysku w Palmirach w Kampinoskim Parku Narodowym – etap I" dofinansowanego ze środków Funduszu Leśnego PRL LP w 2016 roku.

Literatura

Adeniyi, A. S. (2010). Effect of slash and burning on soil microbial diversity and abundance in the tropical rainforest ecosystem, Ondo State, Nigeria, *African Journal of Plant Science, 4(9)*, 322-329.

Badia, D., Marti, C. (2003). Effect of simulated fire on organic matter and selected microbiological properties of twocontrasting soils. *Arid Land Researchand Management, 17*, 55-69.

Banning, N. C., Gleeson, D. B., Grigg, A. H., Grant, C. D., Andersen, G. L., Brodie, E. L., and Murphy, D. V. (2011). Soil microbial community successional patterns during forest ecosystem restoration. *Applied and environmental microbiology*, *77(17)*, 6158-64.

Bauhus, J., Khanna, P.K., Raison, R.J. (1993). The effect of fire on carbon and nitrogen mineralization and nitrification in Australian forest soil. *Australian Journal of Soil Research, 31*, 621-639.

Bednarek, R., Charzyński P., Kabała C. (2009). *Klasyfikacja zasobów glebowych Świata*. Toruń: Wyd. UMK.

Bengtssone, J.(2002). Disturbance and resilience in soil animal communities. *Europen Journal of Soil Biology, 38*, 119-125.

Berg, M., De Ruitter ,P., Didden, W., Janssen, M., Schouten, T., Vrhoef, H. (2001). Community food web, decomposition and nitrogen mineralisation in a stratified Scots pine forest soil. *Oikos, 94*, 130-142.

Biały, K., Brożk, S., Chojnicki, J., Czępińska-Kamońska, D., Januszek, K., Kowalkowski, A., Krzyżanowski, A., Okołowicz, M., Sienkiewicz, A., Skiba, S., Wójcik, J., Zielony, R. (2000). *Klasyfikacja gleb leśnych Polski*. Warszawa: Centrum Informacyjne Lasów Państwowych.

Boczek, J., Błaszak, C. (2005). *Roztocze (Acari). Znaczenie w życiu i gospodarce człowieka*. Warszawa: Wydawnictwo.

Bunt, Y.S., Rovira, A.D. (1955). Microbiological studies of some subarctic soils. *Journal of Soil Sciences, 6*, 119-128.

Carrillo, Y., Ball, B.A., Bradford, M.A., Jordan, C.F., Molina, M. (2011). Soil fauna alter the effects of litter composition on nitrogen cycling in a mineral soil. *Soil Biology and Biochemistry, 43*, 1440-1449.

Cerda, A., Robichaud, P.R. (2009). *Fire effects on soils and restoration strategies*. Taylor and Francis.

Certin, G., (2005). Effects of fire on properties of forest soils: a review. *Oecologia, 143*, 1-10.

DeBano, L.F. (2000). Water repellent soils: a historical overview. *Journal of Hydrology, 231*, 4-32.

Decaëns, T. (2010). Macroecological patterns in soil communities. *Global Ecology and Biogeography, 19*, 287-302.

De Vries, F.T., Thébault, E., Liiri, M., Birkhofer, K., Tsiafouli, M.A., Bjørnlund, L., Jørgensen, H.B., Brady, M.V., Christensen, S., De Ruiter, P., d'Hertefeldt, T., Frouz, J., Hedlund, K., Hemerik, I., Holk, W.H.G., Hotes, S., Mortimer, S.N., Setälä, H., Sgardelis, S.P., Uteseny, K., van der Putten, W.R., Wolters, V., Bargett, R.D. (2013) Soil food web properties explain ecosystem services across European land use systems. *Proceedings of the National Academy of Sciences*, *110*, 14296-14301.

Dighton, J., Jones, H.E., Robinson, C.H., Becken, J. (1997). The role of abiotic factors, cultivation practices and soil fauna in the dispersal of genetically modified microorganisms in soils. *Applied Soil Ecology, 5*, 109-131.

Ditomaso, J.M., Brooks, M.L., Allen, E. B., Minnich, R., Rice, P.M., Kyser, G.B. (2006). Control of Invasive Weeds with Prescribed Burning Review Article, *Weed Technology*, *20*, 535-548,

Dress, W.J., Boerner, R.E.J. (2004). Patterns of microarthropod abundance in oak-hickory forest ecosystems in relation to prescribed fire and lanscape position. *Pedobiologia, 48*, 1-8.

Dunn, P.H., Barro, S.C., Poth, M. (1985). Soil moisture affects survival of microorganisms in heated chaparral fire. *Soil Biology and Biochemistry, 17*, 143-148.

Gardi, C., Montanarella, L., Arrouays, D., Bispo, a., Lemanceau, P., Jolivet, C., Menta, C. (2009). Soil biodiversity monitoring in Europe: ongoing activities and challenges. *European Journal of Soil Science*, *60(5)*, 807-819.

Grasso, G.M., Ripabelli, G., Sammarco, M.L., Mazzoleni, S. (1996). Effects of heating on the microbial populations of grassland soil. *International Journal of Wildland Fire, 6*, 67-70.

Guerro, C., Mataix-Solera, J., Gómez, I., García-Orenes, F., Jordán, M.M. (2005). Microbial recolonization and chemical changes in soil heated at different temperatures. *International Journal of Wildland Fire, 14*, 385-400.

Heneghan, L., Bolger, T. (1996). Effects of component of ‚acid' rain on soil microarthropods' contribution to ecosystemfunction. *Journal Applied of Ecology, 33*, 1329-1344.

Huhta, V., Nurminen, M., Valpas, A. (1969). Further notes on the effects of silvicultural practices upon soil fauna of coniferous forest soil. *Annales Zoologici Fennici*, *6*, 327-334.

Huhta, V., Mikkonen, M. (1982). Population structure of *Entomobryidae* (*Collembola*) in mature spruce stand and in a clear-cut reforested area in Finland. *Pedobiologia, 24*, 231-240.

Jokinen, H.K., Kiikkilä, O., Fritze, H. (2006). Exploring the mechanisms behind elevated microbial activity after wood ahs application. *Soil Biology and Biochemistry, 38*, 2285-2291.

Kennard, D.K., Gholz, H.L. (2001). Effects of high – and low – intensity fires on soil properties and plant growth in a Bolivian dry forest. *Plant and Soil*, *234*, 119-129.

Köster, K., Berninger, F., Heinonsalo, J., Lindén, A., Köster, E., Ilvesniemi, H., Pumpanen, J. (2017) The long-term impact of low-intensity surface fires on litter decomposition and enzyme activities in boreal coniferous forests. *International Journal of Wildland Fire, 25(2)*, 213-223.

Lussenhop, J. (1976). Soil arthropod response to praire burning. *Ecology, 57*, 88-98.

Lussenhop, J. (1992). Mechanisms of microarthropod - microbial interactions in the soil. *Advances in Ecological Research, 23*, 1-33.

Malmström, A., Persson, T., Ahlström, K. (2008). Effects of fire intensity on survival and recovery of soil microarthropods after clearcut burning. *Canadian Journal of Forest Research, 38*, 2465-2475.

Malmström, A., Persson T., Ahlström K., Gongalsky K.B., Bengtsson J. (2009). Dynamics of soil meso- and macrofauna during a 5-year period after clearcut burning in a boreal forest. *Applied and Soil Ecology, 43*, 61-74.

Malmström, A. (2010). The importance of measuring fire severity-Evidence from microarthropod studies. *Forest Ecological Management, 260*, 62-70.

Martin, J.P. (1950). Use of acide rose Bengal and steeptomycin in the plate method for estimating of fungi. *Soil Sciences, 69*, 215-233.

Mataix-Solera, J., G.Barcenas-Moreno, F. Garcia-Orenes, (2009). Forest fire effects on soil microbiology. http//www.researchgate.net/publication/ 229163976, DOI:101201/9781439843338-c5.

Mummey, D. L., Clarke, J. T., Cole, C. A., O'Connor, B. G., Gannon, J. E., Ramsey, P. W. (2010). Spatial analysis reveals differences in soil microbial community interactions between adjacent coniferous forest and clearcut ecosystems. *Soil Biology and Biochemistry, 42(7)*, 1138-1147.

Neary, D.G., Klopatek, C.C., DeBano, L.F., Folliott, F. (1999). Fire effects on belowground suistainability: a review and synthesis. *Forest Ecology and Management, 122*, 51-71.

Ngosong, C, Raupp, J, Scheu, S, Ruess, L. (2009). Low importance for a fungal based food web in arable soils under mineral and organic fertilization indicated by *Collembola* grazers. *Soil Biology and Biochemistry, 41*, 2308-2317.

Ostrowska, A., Gawliński, S., Szczubiałka Z. (1991). *Metody analizy i oceny właściwości gleb i roślin*. Warszawa: Instytut Ochrony Środowiska.

Otsuka, S, Sudiana, I, Komori, A, (2008). Community structure of soil bacteria in a tropical rainforest several years after fire. *Microbes and Environments*, *23(1)*, 49-56.

Petersen, H. (1980). Population dynamic and metabolic characterization of *Collembola* species in a beech forest ecosystem. *Soil Biology as Related to Land Use Practices. Ed. D.L. Dindal* EPA, Washington, 806-833.

Pietikäinen,J., Fritze, H. (1995). Clear-cutting and prescribed burning in coniferous forest: comparison of effects on soil fungal and total microbial biomass, respiration activity and nitrification. *Soil Biology and Biochemistry, 27,* 101-109.

Pizarro-Tobías, P., Fernández, J. L., Niqui, J. Solano, E. Duque, J.-L. Ramos, Roca, A. (2014). Restoration of a Mediterranean forest after a fire: bioremediation and rhizoremediation field-scale trial. *Applied Microbiology, Microbial Biotechnology, 8*, 77-92.

Saint-Germain, M., Larrivée, M., Drapeau, P., Fahrig, L., Buddle, Ch.M. (2005). Short-term response of ground beetles (*Coleoptera: Carabidae*) to fire and Logging in a spruce-dominated boreal landscape. *Forest Ecological Management, 212*, 118-126.

Scharenbroch, B. C., Nix, B., Jacobs, K. A., and Bowles, M. L. (2012). Two decades of low-severity prescribed fire increases soil nutrient availability in a Midwestern, USA oak (Quercus) forest. *Geoderma*, *183-184*, 80-91.

Seastedt, T.R. (1984). The role of microarthropods in decomposition and mineralization processes. *Annual Review of Entomology, 29*, 25-46.
Sgardelis, S.P., Margaris, N.S. (1993). Effects of fire on soil microarthropods of a phryganic ecosystem. *Pedobiologia*, *37*, 83-94.
Smith, N. R., Kishchuk, B. E., Mohn, W.W. (2008). Effects of wildfire and harvest disturbances on forest soil bacterial communities. *Applied and Environmental Microbiology, 74*, 216-224.
Sulwiński, M., Mętrak, M., Suska-Malawska, M. (2017). Study of old ecological hazards, oil seeps and contaminations using earth observation methods – spectral library for oil seep. *Archives of Environmental Protection, 43(1)*, 11-19.
Swengel, A. B. (2001). A literature review of insect responses to fire, compared to other conservation managements of open habitat. *Biodiversity Conservation, 10*, 1141-1169.
Wikars, L.O., Schimmel, J. (2001). Immediate effects of fire-severity on soil invertebrates in cut and uncut pine forest. *Forest Ecological Management, 141*, 189-200.
Xingjia XiangYu Shi,Jian Yang, Jianjian Kong, Xiangui Lin, Huayong Zhang, Jun Zeng, Haiyan Chu, (2014). Rapid recovery of soil bacterial communities after wildfire in a Chinese boreal forest. *Scientific Reports, 4*, 3829.
Zaitsev, A.S., Gongalsky, K.B., Malmström, A., Persson, T. (2015). Why are forest fires generally neglected in soil fauna research? A mini-review. *Applied of Soil Ecology, 98*, 261-271.

Fire – a Factor Forming the Numbers of Microorganisms and Mesofauna in Forest Soils

Streszczenie

Jednym z czynników stresogennych poważnie zakłócającym równowagę biologiczną gleby jest pożar. Charakter zaburzeń powodowanych przez pożar zależy od siły, czasu trwania, sezonu i częstotliwości jego pojawiania się. Pożary wpływają na fizyczne, chemiczne i biologiczne własności gleby. Przyczyniają się do zmniejszenia liczebności mezo – i makrofauny oraz wpływają na mikroorganizmy glebowe. Celem podjętych badań była ocena wpływu intensywności pożaru na liczebność wybranych grup edafonu glebowego w tym bakterii heterotroficznych, grzybów mikroskopowych oraz mezofauny glebowej roztoczy (*Acari*) i skoczogonek (*Collembola*) w ściółce i w glebie na pożarzysku w Puszczy Kampinoskiej. Podczas pożaru powierzchniowego (jaki miał miejsce w Puszczy Kampinoskiej) organizmy zasiedlające wierzchnie warstwy gleby, są bezpośrednio narażone na działanie pożaru. Założono, że liczebność organizmów związanych z warstwą organiczną gleb powinna być znacznie niższa na

obszarach wypalonych w porównaniu z niewypalonymi. Do badań wytypowano stanowiska po mocnym i słabym pożarze oraz nie objęte ogniem oddalone o 10 m od linii ognia – stanowiące kontrolę, każda o łącznej powierzchni 10 m^2. Na podstawie uzyskanych wyników stwierdzono, że właściwości chemiczne i biologiczne gleby ulegają stopniowej regeneracji w glebie i ściółce w 15 miesięcy po pożarze. Ponadto intensywność pożaru ma istotne znaczenie w odtwarzaniu liczebności mikroorganizmów i mezofauny. Słaby pożar działa bardziej selekcjonująco na mikroorganizmy i mezofaunę, niż pożar mocny. Uzyskane wyniki badań uprawniają do stwierdzenia, że pożar może być jednym z czynników stymulujących liczebność grzybów zarówno w poziomie organicznym, jak i mineralnym gleb leśnych.

Abstract

One of the stressors that seriously disturbs the biological balance of soil is fire. The nature of disorder caused by the fire depends on the strength, duration, season and the frequency of occurrence. Fires affect physical, chemical and biological properties of soil. They contribute to reducing the population of meso- and macrofauna and affect micro-organisms living in the soil. The purpose of the study was to evaluate the effect of fire intensity on the number of selected soil edafon groups including heterotrophic bacteria, microscopic fungi, *Acari* and *Collembola*, both in the leaf litter and soil in Kampinos Forest. During the surface fire (which took place in Kampinos National Park) organisms inhabiting the surface of the soil were directly exposed to fire. It was assumed that the number of organisms in the organic layer should be considerably lower in areas burned compared to non-burned. Research was conducted on sites that had encountered high severity fires, low severity fires and on those not affected - 10 m from the fire line - each with a total area of 10 m^2. Based on the obtained results, it was found that the chemical and biological properties of soil gradually recovered in the soil and litter within 15 months from the fire. In addition, the intensity of the fire is important in reproducing the population of microorganisms and mesofauna. A low severity fire works more selectively on microorganisms and mesofauna than a severe one. The results of the research indicate that the fire can be one of the factors stimulating fungal growth both in the organic and mineral layers of the forest soils.

Słowa kluczowe:
pożar, liczebność mikroorganizmów, mezofauna, gleby leśne

Keywords:
fire, number of microorganisms, mezofauna, forest soils

MIDDLE POMERANIAN SCIENTIFIC SOCIETY OF THE ENVIRONMENT PROTECTION
ŚRODKOWO-POMORSKIE TOWARZYSTWO NAUKOWE OCHRONY ŚRODOWISKA

Annual Set The Environment Protection
Rocznik Ochrona Środowiska

Volume/Tom 19. Year/Rok 2017 ISSN 1506-218X 527-539

Wyniki pomiarów i analiz oddziaływania farm elektrowni wiatrowych na klimat akustyczny

Adam Zagubień
Politechnika Koszalińska

1. Wstęp

Jednym z podstawowych oddziaływań towarzyszącym eksploatacji farm wiatrowych jest hałas emitowany do środowiska. Dlatego też, każda projektowana lokalizacja farmy wiatrowej powinna być poddana ocenie wpływu na środowisko ze względu na emitowany hałas. Na etapie projektowania prognoza skutków lokalizacji farmy wiatrowej ze względu na emitowany hałas może być wykonana jedynie na drodze obliczeniowej (Zagubień & Ingielewicz 2017). Po uruchomieniu farmy wiatrowej prowadzone są pomiary terenowe hałasu przy najbliższych terenach chronionych akustycznie zlokalizowanych w otoczeniu farmy wiatrowej, a na podstawie uzyskanych wyników wykonywana jest ocena zagrożenia dla środowiska. Aktualnie w Polsce do pomiarów hałasu farm wiatrowych stosowane są metody referencyjne obowiązujące w pomiarach hałasu przemysłowego (Dz. U. poz. 1542. 2014). Ponadto należy mieć na uwadze, że w widmie hałasu emitowanego od elektrowni wiatrowych występują również składowe z zakresu infradźwiękowego (Boczar i in. 2012, Ingielewicz & Zagubień 2013, Ingielewicz & Zagubień 2014, Jabben & Verheijen 2012, Jacobsen 2001, Pierzga i in. 2013, Pleban & Radosz 2015, Szulczyk & Cempel 2010).

Oceniając oddziaływanie na środowisko elektrowni wiatrowych w zakresie hałasu, należy mieć na uwadze trzy podstawowe aspekty:

1. Ograniczenia w postaci dopuszczalnych poziomów hałasu w środowisku dla otaczających farmę terenów, dotyczące zakresu częstotliwości słyszalnych korygowanych krzywą A.

2. Specyfikę zjawisk akustycznych związanych z pracą turbin wiatrowych, dotyczącą zmian poziomów mocy akustycznych zastosowanych turbin i poziomu tła w otoczeniu, w zależności od prędkości wiatru.
3. Emisję infradźwięków przez turbiny wiatrowe.

Obszerny opis tych zagadnień został zamieszczony w publikacji (Ingielewicz & Zagubień 2016).

W artykule podjęto próbę dokonania oceny zmierzonych poziomów równoważnego poziomu dźwięku w odniesieniu do poziomów dopuszczalnych hałasu słyszalnego obowiązujących w różnych krajach na świecie. Badania terenowe prowadzono zgodnie z polską metodyką pomiarową (Dz. U. poz. 1542. 2014). Dlatego do porównań wybrano tylko te kraje, w których poziom dopuszczalny hałasu wyrażony jest wskaźnikiem – równoważny poziom dźwięku korygowany krzywą A. Nie uwzględniono wskaźników zależnych od prędkości wiatru, które występują przykładowo w Danii lub Kandzie (Ontario). Obszerne zestawienie poziomów dopuszczalnych hałasu pochodzącego od turbin wiatrowych w różnych krajach prezentują (Koppen & Fowler 2015).

W różnych krajach na świecie oceny oddziaływania farm wiatrowych na środowisko prowadzi się odmiennymi metodami. Ustalanie poziomów dopuszczalnych odbywa się głównie za pomocą trzech metod. Pierwszy sposób realizowany jest poprzez ustalenie bezwzględnych wskaźników, uzależnionych najczęściej od pory doby i sposobu zagospodarowania terenu. Drugi sposób, polega na ustalaniu wskaźników względnych, które zależą od aktualnego stanu warunków akustycznych na analizowanym terenie. Trzeci sposób, to połączenie dwóch wcześniejszych, czyli stosowanie łącznie wskaźników względnych i bezwzględnych.

Należy zauważyć, że część krajów uzależnia swoje wskaźniki hałasu od prędkości wiatru i precyzuje poziomy dopuszczalne dla źródła hałasu, jakim są turbiny wiatrowe.

2. Metodyka pomiarowa

W Polsce pomiary hałasu przemysłowego, w tym hałasu od farm wiatrowych prowadzone są zgodnie z referencyjną metodyką pomiarową zawartą w Rozporządzeniu Ministra Środowiska (Dz. U. poz. 1542. 2014). Metodyka pomiarowa ustala szereg ograniczeń, co do warunków

atmosferycznych panujących podczas pomiarów, lokalizacji punktów pomiarowych, zestawów pomiarowych oraz określa sposób wykonywania pomiaru.

Ustalony podczas pomiaru wynik w postaci równoważnego poziomu dźwięku A, porównywany jest z poziomami dopuszczalnymi określonymi dla pory dziennej i pory nocnej (Ingielewicz & Zagubień 2016).

Zasadniczym problemem podczas rejestracji hałasu farm wiatrowych jest dobór optymalnych parametrów prędkości wiatru napędzającego turbiny, przy jednoczesnym zachowaniu warunków meteorologicznych określonych metodyką referencyjną. Fakt ten potwierdzają także autorzy innych opracowań jak np. w publikacji (Wszołek & Kłaczyński 2014). Prowadząc pomiary należy dążyć do takich warunków, by prędkość wiatru na wysokości osi wirników turbin wiatrowych osiągała wartości odpowiadające maksymalnej mocy akustycznej turbin lub bliskie tym wartościom. Wykonując pomiary zgodnie z polską metodyką referencyjną należy spełnić warunek prowadzenia pomiarów przy średniej prędkości wiatru w punkcie kontrolnym (najczęściej 4,0 m nad terenem) nie przekraczającej wartości 5 m/s. Zachowanie tego warunku łącznie z dążeniem do sytuacji, by pomiary wykonać przy maksymalnym poziomie mocy akustycznej turbin w praktyce jest trudne do osiągnięcia, a możliwości jego spełnienia zależą od konfiguracji i zagospodarowania terenu (Bullmore i in. 2009), lokalizacji punktów pomiarowych i występujących w otoczeniu elementów ekranujących. Zdarza się jednak, że podczas pomiarów zostają spełnione oba warunki, czyli turbiny pracują z pełną mocą, a prędkość wiatru nie przekracza 5 m/s na wysokości 4,0 m w punkcie pomiarowym. Wynika to z nieprzewidywalnej zmienności pionowych profili prędkości wiatru w czasie (Ro & Hunt 2007).

Do najbardziej istotnych aspektów dotyczących pomiarów hałasu turbin wiatrowych należy zaliczyć:

- Wybór metody pomiarów, tj. pomiar ciągły lub metoda próbkowania.
- Czas pomiaru próbki w przypadku metody próbkowania.
- Lokalizację punktów pomiarowych.
- Sposób pomiaru tła akustycznego.
- Warunki atmosferyczne podczas pomiarów, a w szczególności prędkość i kierunek wiatru.

2.1. Wybór metody pomiarów

Prowadząc pomiary dążono do wykluczenia wszelkich zakłóceń od innych źródeł hałasu, niezwiązanych z pracą farmy wiatrowej. Najczęściej spotykanymi w praktyce źródłami zakłócającymi pomiar jest ruch samochodowy na pobliskich drogach, praca maszyn rolniczych, wszelkie prace gospodarskie w gospodarstwach domowych, porywy wiatru oraz tak prozaiczne, jak szczekanie psa, pianie koguta, czy śpiew ptaków i inne odgłosy przyrody. Opisane zakłócenia należy eliminować zarówno w czasie pomiarów hałasu od źródeł, jak i podczas pomiarów tła akustycznego. Stosowanie zapisów pomiarów ciągłych i późniejsze próby eliminacji zakłóceń mogą prowadzić do zbyt dużych błędów. W związku z powyższym prezentowane wyniki uzyskano stosując metodę próbkowania.

2.2. Metoda próbkowania

Liczebność próbek oraz czas pomiaru pojedynczej próbki ustalano w zależności od sytuacji akustycznej towarzyszącej pomiarom. Zaobserwowano, że czas pomiaru próbki umożliwiający eliminację wpływu zakłóceń, nie przekracza 60 s, a często wymaga skrócenia do 10 s. Taki dobór czasu pomiaru dotyczy zarówno rejestracji hałasu turbin wiatrowych, jak i tła akustycznego po ich wyłączeniu i zatrzymaniu. Liczba próbek w poszczególnych punktach pomiarowych zawierała się w przedziale 3 do 5.

2.3. Lokalizacja punktów pomiarowych

Położenie punktu pomiarowego określa jego lokalizacja w terenie np. współrzędne geograficzne oraz wysokość nad poziomem terenu.

Wysokość pomiarową ustalono na 4,0 m nad poziomem terenu. Lokalizację punktów pomiarowych przyjęto na granicach działek terenów chronionych akustycznie, najbliższych w stosunku do farmy wiatrowej. Sytuowanie punktów przy elewacji budynków zwiększa odległość od najbliższych turbin, ogranicza możliwość rozbudowy obiektów chronionych w przyszłości i wymaga korekty zmniejszającej wyniki pomiarów kontrolnych o 3 dB. Wykonywanie pomiarów kontrolnych, w punktach położonych na granicy działek najbliższych terenów akustycznych, jest bardziej bezpieczne dla środowiska i ludzi.

2.4. Pomiar tła akustycznego

Pomiary tła akustycznego wykonywano po zatrzymaniu wszystkich turbin wiatrowych. Pomiary prowadzono w tych samych punktach pomiarowych, w których mierzono hałas, przyjmując ten sam czas pomiaru próbki i zasady eliminacji zakłóceń. Podczas pomiarów nie napotykano problemów z zatrzymaniem turbin na czas pomiarów tła, mając stałą łączność podczas pomiarów z operatorem farmy wiatrowej.

Nieodłącznym składnikiem wpływającym na wynik pomiaru jest hałas powodowany wiejącym wiatrem, szumem drzew, zawirowaniami wiatru na przeszkodach, itp. Składowa hałasu wywołana wiatrem jest możliwa do określenia, ponieważ stanowi podstawowy składnik tła akustycznego mierzonego po zatrzymaniu turbin, z zastrzeżeniem, że pomiary tła wykonuje się eliminując zakłócenia od innych źródeł hałasu w otoczeniu farmy. Po zakończonych badaniach wynik pomiaru tła akustycznego odejmowano od wyniku pomiaru hałasu farm wiatrowych zmierzonego łącznie z tłem akustycznym.

2.5. Warunki atmosferyczne podczas pomiarów

Obowiązująca w Polsce referencyjna metoda wykonywania pomiarów hałasu ogranicza prędkość wiatru podczas pomiarów hałasu do wartości średniej 5 m/s na wysokości min. 3,5 m nad poziomem terenu. Warunek ten dotyczy wszystkich pomiarów środowiskowych i wynika z faktu, że przy prędkościach wiatru na wysokości mikrofonu powyżej 5 m/s, pomiary stają się nierozróżnialne z tłem, ze względu na wysoki poziom tła akustycznego. Wartości średniej prędkości wiatru rejestrowane w punktach pomiarowych zestawiono w tabelach 1 i 3. W tabelach podano również wartości prędkości wiatru rejestrowane podczas pomiarów na wysokości wież turbin wiatrowych. Wyniki tych rejestracji otrzymano po zakończeniu pomiarów od operatorów farm wiatrowych.

Pozostałe parametry meteorologiczne, takie jak: ciśnienie atmosferyczne, wilgotność i temperatura, zawierały się w granicach dopuszczalnych określonych w rozporządzeniu (Dz. U. poz. 1542. 2014).

3. Wyniki pomiarów

W artykule przedstawiono materiał zebrany podczas pomiarów terenowych hałasu na 5 farmach elektrowni wiatrowych liczących od 6 do 15 turbin wiatrowych, o mocach od 2,5 MW do 3,0 MW i wysokości wieży w przedziale 100-120 m. Ze względu na zachowanie poufności nie podano informacji szczegółowych o lokalizacji farm, wynikach ocen akustycznych oraz konkretnych typach turbin. Przedstawiono jedynie wyniki pomiarów i ogólne dane istotne dla ocen akustycznych, umożliwiające sformułowanie wniosków.

W tabeli 1 zestawiono prędkości wiatru zarejestrowane podczas pomiarów na wysokości punktów pomiarowych (4,0 m nad terenem) oraz na wysokości osi turbin (120 m nad terenem).

Tabela 1. Wyniki pomiarów wiatru w poszczególnych porach roku w czasie wykonywanych pomiarów
Table 1. Results of wind speed measurements in particular seasons at the time of making measurements

Pora roku	Średnie prędkości wiatru na poszczególnych turbinach	Średnia prędkość wiatru na farmie wiatrowej	Kierunek wiatru	Średnie prędkości wiatru w punktach pomiarowych
	[m/s]	[m/s]	-	[m/s]
Jesień	10,2 – 11,9	10,7	SW	4,3 – 5,0
Zima	8,3 – 9,5	9,1	NE	3,1 – 4,4
Wiosna	7,2 – 9,1	8,5	W	2,9 – 4,6
Lato	8,8 – 9,5	9,0	E	3,5 – 4,8

W tabeli 2 przedstawiono wyniki pomiarów wykonanych czterokrotnie w ciągu roku (jesień, zima, wiosna, lato) na farmie złożonej z 11 elektrowni wiatrowych o mocy 3,0 MW i wysokości wieży 120 m. Pomiary wykonano w 5 punktach pomiarowych, których najmniejsza odległość od najbliższej turbiny wynosiła 540 m, natomiast największa 660 m. W otoczeniu wszystkich punktów pomiarowych, w odległościach do 10 m, występowały skupiska wysokich drzew wpływających na poziomy mierzonego tła i hałasu, szczególnie przy wzrastających prędkościach wiatru. Wszystkie pomiary dotyczą pory nocnej.

Tabela 2. Wyniki rocznych pomiarów hałasu na farmie wiatrowej
Table 2. Results of annual noise measurements on a wind farm

Nr	L_{Aeq}	L_{AT}	$L_{Aeq,im}$	L_{Aeq}	L_{AT}	$L_{Aeq,im}$	L_{Aeq}	L_{AT}	$L_{Aeq,im}$	L_{Aeq}	L_{AT}	$L_{Aeq,im}$
	[dBA]											
	Jesień			Zima			Wiosna			Lato		
P1	44,5	43,2		43,1	41,8	w tle	44,2	39,7	42,2	44,3	40,1	42,2
P2	44,0	42,6		43,7	40,2	41,1	43,0	40,4	w tle	44,8	41,0	42,4
P3	45,1	44,7	w tle	43,9	41,6	w tle	43,6	41,8	w tle	43,9	41,5	w tle
P4	43,9	42,7		43,4	39,8	41,0	43,0	38,8	40,9	43,2	38,9	41,2
P5	44,4	42,8		42,8	38,5	40,8	43,4	38,9	41,6	43,6	39,0	41,8

Oznaczenia w tabeli 2.:
Nr – numer punktu pomiarowego,
L_{Aeq} – wyniki pomiaru łącznie z tłem,
L_{AT} – wynik pomiaru tła,
$L_{Aeq,im}$ – wynik pomiaru po odjęciu tła – równoważny poziom dźwięku A w czasie odniesienia.

W tabeli 4 zestawiono przedziały uzyskanych wyników pomiarów hałasu dla czterech farm elektrowni wiatrowych, o różnej liczbie i typach turbin wiatrowych, ale o zbliżonych mocach. Wyniki pomiaru hałasu, które zawierały się w tle pomiarowym odrzucono z zestawienia. W otoczeniu wybranych punktów nie występowały przeszkody znacznie wpływające na wyniki pomiarów hałasu i tła akustycznego spowodowane wzrostem siły wiatru (kompleksy leśne, sady, szpalery drzew itp.). Punkty oddalone były od dróg o znaczącym natężeniu ruchu o co najmniej 400 m. Ogólne dane farm wraz z wynikami pomiarów prędkości wiatru w czasie prowadzonych badań zestawiono w tabeli 3.

Pomiary hałasu wykonano w punktach położonych w najmniejszych odległościach od skrajnych turbin farmy na wysokości 4,0 m. Wybrano punkty, których odległości zawierały się w przedziale 450 m do 650 m, a więc stanowiły najczęściej wynikające z obliczeń numerycznych odległości, umożliwiające zachowanie poziomów dopuszczalnych hałasu w środowisku.

Przedstawione wyniki zmierzonego równoważnego poziomu dźwięku A uzyskano przy zachowaniu przedziałów niepewności rozszerzonej U_{95} mniejszej od ± 2,0.

Tabela 3. Dane ogólne przykładowych farm wraz z wynikami pomiarów wiatru w czasie prowadzonych badań
Table 3. General data of sample wind farms with results of wind measurements at the time of making measurements

Numer Farmy	Liczba turbin (Moc jednej turbiny)	Wysokość wieży	Średnie prędkości wiatru na poszczególnych turbinach		Średnia prędkość wiatru na farmie wiatrowej		Średnie prędkości wiatru w punktach pomiarowych	
			Dzień	Noc	Dzień	Noc	Dzień	Noc
	[szt.] [MW]	[m]	[m/s]					
WF 1	15 (2,5)	100	7,4÷9,5	6,5÷8,6	9,1	7,9	2,8÷4,6	2,9÷4,5
WF 2	16 (2,5)	100	9,1÷9,4	9,6÷10,1	9,2	9,8	3,1÷4,4	3,0÷4,7
WF 3	6 (2,5)	100	6,6÷7,7	6,7 – 8,0	7,3	7,4	2,7÷4,1	2,9÷4,3
WF 4	7 (3,0)	105	6,8÷9,0	6,5 – 8,6	8,2	7,8	2,9÷4,6	2,6÷4,3

Tabela 4. Zakres wartości wyników pomiarów hałasu dla 4 farm wiatrowych
Table 4. The ranges of values of noise measurements results at 4 wind farms

Oznaczenie farmy	Pora	Wynik pomiaru łącznie z tłem akustycznym L_{Aeq}	Wynik pomiaru tła akustycznego L_{AT}	Wynik poziomu imisji po uwzględnieniu tła $L_{Aeq,im}$
		[dBA]		
WF 1	dzień	43,1 ÷ 44,8	38,4 ÷ 42,0	41,8 ÷ 43,3
	noc	41,9÷ 43,9	36,9 ÷ 38,9	39,5 ÷ 42,8
WF 2	dzień	40,7 ÷ 44,9	38,6 ÷ 41,9	40,9 ÷ 43,1
	noc	41,2 ÷ 44,7	38,2 ÷ 42,1	42,9 ÷ 43,5
WF 3	dzień	39,0 ÷ 42,3	36,3 ÷ 39,2	37,3 ÷ 40,3
	noc	39,6 ÷ 42,6	36,0 ÷ 38,6	37,5 ÷ 40 6
WF 4	dzień	40,7 ÷ 44,6	37,6 ÷ 40,1	39,8 ÷ 42,9
	noc	40,1 ÷ 44,0	36,3 ÷ 38,4	37,4 ÷ 42,8

4. Podsumowanie i wnioski

Porównanie uzyskanych wyników pomiarów z wybranymi obowiązującymi poziomami dopuszczalnymi w różnych krajach na świecie pokazano w tabeli 5. W tabeli zestawiono tylko te kraje w których podobnie jak w Polsce wskaźnikiem oceny jest równoważny poziom dźwięku A – L_{Aeq}.

Tabela 5. Porównanie wyników pomiarów z wybranymi poziomami dopuszczalnymi
Table 5. Comparison measurements with selected permissible noise levels

Kraj	Poziom dopuszczalny dla zabudowy zagrodowej L_{Aeq}		Przekroczenie poziomu dopuszczalnego	
	Dzień	Noc	Dzień	Noc
Polska	55	45	nie	nie
Finlandia	45	40	nie	tak
Belgia (Flandria)	48	43	nie	tak (nieznacznie)
Belgia (Walonia)	45	45	nie	nie
Kanada (Alberta)	50	40	nie	tak
Niemcy	60	45	nie	nie
USA (Georgia)	55	55	nie	nie
USA (Minnesota)	50	50	nie	nie
USA (Wisconsin)	50	45	nie	nie
USA (Wyoming)	50	50	nie	nie

Analiza wyników pomiarów prowadzonych dla pięciu farm elektrowni wiatrowych oraz zaobserwowanych zjawisk i uwarunkowań występujących podczas pomiarów pozwoliły sformułować następujące wnioski ogólne:

1. W przypadku pomiarów i oceny hałasu farm elektrowni wiatrowych prowadzenie pomiarów w porze dziennej, z praktycznego punktu widzenia, jest nieuzasadnione. Najniższy z zestawionych w tabeli 5 poziomów dopuszczalnych pory dziennej dla terenów wiejskich, przeważających w otoczeniu farm wiatrowych wynosi 45 dB.
2. W Europie poziomy dopuszczalne hałasu w porze nocnej, określone wskaźnikiem L_{AeqN} (poziom równoważny dźwięku A) zawierają się w przedziale 40-45 dB. Ewentualne obniżanie tych poziomów skutkować będzie uzyskiwaniem wyników pomiarów nierozróżnialnych z tłem pomiarowym (LUBW 2016).
3. Prowadzenie badań terenowych metodą próbkowania pozwala na wybranie najkorzystniejszego czasu pomiaru. Jest to istotne ze względu na dużą zmienność prędkości wiatru i innych parametrów meteorologicznych w ciągu doby.
4. Podczas oceny pomiarowej imisji hałasu w punktach kontrolnych, należy mieć na uwadze również fakt, że w tym samym czasie poszczególne turbiny farmy wiatrowej pracują z różnymi poziomami mocy akustycznej.

5. W celu uzyskania kompleksowych informacji o emisji hałasu badanej farmy elektrowni wiatrowych wskazane jest prowadzenie pomiarów w okresie rocznym, np. w kolejnych 4 porach roku. Można wtedy uzyskać wyniki dla różnych warunków atmosferycznych, a w szczególności przy różnych kierunkach i prędkościach wiatru. Wykonanie czterokrotnych pomiarów w ciągu roku daje większe prawdopodobieństwo wykonania pomiarów przy prędkości wiatru odpowiadającej maksymalnym lub bliskim maksymalnym poziomom mocy akustycznej turbin. Stosując tę zasadę uzyskuje się znacznie szerszy materiał do analizy, co umożliwia kompleksowe wykonanie oceny.
6. W przypadkach, gdy zmierzony poziom imisji hałasu jest nierozróżnialny z tłem akustycznym, a jednocześnie poziom imisji nie przekracza wartości poziomów dopuszczalnych pory dziennej i nocnej w danym punkcie, celowym byłoby wprowadzić zapis interpretacyjny, że w takim przypadku poziom imisji hałasu w danym punkcie nie stanowi zagrożenia dla środowiska i ludzi.

Literatura

Boczar, T., Malec, T., Wotzka, D. (2012). Studies on Infrasound Noise Emitted by Wind Turbines of Large Power. *Acta Physica Polonica A. 122, (5)*, 850-853.

Bullmore, A., Adcock, J., Jiggins, M., Cand, M. (2009). Wind Farm Noise Predictions and Comparison with Measurements. *Third International Meeting on Wind Turbine Noise.* Aalborg, Denmark.

Dz. U. 2012 Nr 0 poz. 1109. (2012). *Rozporządzenie Ministra Środowiska z dnia 1 października 2012 r. zmieniającym rozporządzenie w sprawie dopuszczalnych poziomów hałasu w środowisku.* Warszawa: Dziennik Ustaw.

Dz. U. 2014 Nr 0 poz. 1542. (2014). *Rozporządzenie Ministra Środowiska z dnia 30 października 2014 r. w sprawie wymagań w zakresie prowadzenia pomiarów wielkości emisji oraz pomiarów ilości pobieranej wody.* Warszawa: Dziennik Ustaw.

Dz. U. Nr 120 poz. 826 (2007). *Rozporządzenie Ministra Środowiska z dnia 14 czerwca 2007 r. w sprawie dopuszczalnych poziomów hałasu w środowisku.* Warszawa: Dziennik Ustaw.

Ingielewicz, R., & Zagubień, A. (2013). The infrasound noise measurement emitted by wind farm. *Measurement Automation and Monitoring. 59, (7)*, 725-727.

Ingielewicz, R., & Zagubień, A. (2014). Infrasound noise of natural sources in environment and infrasound noise of wind turbines. *Pol. J. Environ. Stud. 23*, 1323-1327.

Ingielewicz, R., & Zagubień, A. (2016). Problemy oceny hałasu farm elektrowni wiatrowych na podstawie terenowych pomiarów kontrolnych. *Rocznik Ochrona Środowiska. 18*, 531-549.

Jabben, J., & Verheijen, E. (2012). Options for Assessment and Regulation of Low Frequency Noise. *Journal of Low Frequency Noise, Vibration and Active Control. 31(4)*, 225-238.

Jacobsen J. (2001), *Danish guidelines on environmental low frequency noise, infrasound and vibration*, Journal of Low Frequency Noise. Vibration and Active Control, *20(3),* 141-148.

Koppen, E., & Fowler, K. (2015). International legislation for wind turbine noise. *Tenth European Conference on Noise Control, EuroNoise 2015.* Maastricht, Netherlands.

LUBW – Landesanstalt für Umwelt, Messungen und Naturschutz Baden-Württemberg (2016). *Hałas niskoczęstotliwościowy zawierający infradźwięki pochodzący od turbin wiatrowych i innych źródeł*. Germany: Baden-Württemberg.

Pierzga, R., Boczar, T., Wotzka, D., Zmarzły, D. (2013). Studies on Infrasound Noise Generated by Operation of Low-Power Wind Turbine. *Acta Physica Polonica A. 124(3)*, 542-545.

Pleban, D., Radosz, J. (2015). Hałas emitowany przez turbinę wiatrową podczas pracy. *Rynek Energii. 3(118)*, 109-114.

Ro, K.S., Hunt, P.G. (2007). Characteristic Wind Speed Distributions and Reliability of the Logarithmic Wind Profile. *Journal of Environmental Engineering, 133(3),* 313-318.

Szulczyk, J., & Cempel, Cz. (2010). Hałas turbin wiatrowych w zakresie infradźwięków. *Międzynarodowa konferencja Monitoring Środowiska.* Kraków.

Wszołek, T., & Kłaczyński, M. (2014). Problems in Measurements of Noise Indicators for Wind Turbines in Poland. *Forum Acusticum*. Poland: Cracow.

Zagubień, A., & Ingielewicz, R. (2017). The Analysis of Similarity of Calculation Results and Local Measurements of Wind Farm Noise. *Measurement, 106,* 211-220.

The Results of the Measurements and Analyses of Impact of Wind Farms on Acoustic Climate

Abstract

Noise emitted to environment is one of the basic factors connected with wind farm operation. That is the reason why each wind farm localization should be analysed to assess the impact on environment considering noise. At the stage of the project, the prognosis of localization results considering emitted noise may be only predicted theoretically, mostly by computer simulation. The exist-

ing farm can be assessed by performing local measurements. Conducting local measurements of wind farms, minding the specificity of their work, requires generally applied and suggested modifications of noise measuring methods. The basic problem while carrying out noise measurements is choosing the proper wind speed, which should not exceed 5 m/s at the height of measurement point (usually 4 m). In the article there are presented examples of own local measurements conducted at more than 5 big wind farms. It was proved that at the distance of more than 500 m from the farm, lots of results of measurements are comparable to measurements of existing acoustic background. For cases when noise measurement results, including background noise, were unrecognizable when compared with only acoustic background and the values were lower than permissible level in the measurement point, some interpretations of such situations were suggested. In the article, there has been made an attempt to assess measured levels of equivalent sound level regarding admissible levels of audible noise applicable in various countries in the world. Local measurements were carried out according to Polish measurement methodology. That is why, for comparison, there have been chosen only those countries in which admissible level of noise is defined by index A - which is an equivalent sound level. Indices dependent on wind speed - which are used in Denmark or Canada (Ontario) for example, were not considered. To get complex info about noise emission of analyzed windfarm it is suggested to conduct measurements in a year period for example in four following seasons. Then we can get results for different weather conditions and especially for different directions and speeds of wind. Conducting such measurements four times a year give us greater probability of making measurements at wind speed equal or close to maximum levels of acoustic power of turbines. Applying this rule we can get wilder material for analysis which preparing complex assessment.

Streszczenie

Hałas emitowany do środowiska jest podstawowym negatywnym czynnikiem towarzyszącym eksploatacji elektrowni wiatrowych. Dlatego też, każda projektowana lokalizacja farmy wiatrowej powinna być poddana ocenie wpływu na środowisko ze względu na emitowany hałas. Na etapie projektu, prognoza skutków lokalizacji farmy wiatrowej ze względu na emitowany hałas, może być wykonana jedynie na drodze teoretycznej, najczęściej są to symulacje komputerowe. Istniejącą farmę wiatrową ocenia się przy wykorzystaniu pomiarów terenowych. Metodyka wykonywania pomiarów terenowych, ze względu na specyfikę pracy elektrowni wiatrowych, różni się od ogólnie przyjętych i zalecanych metod pomiaru hałasu środowiskowego. Podstawową różnicą jest zalecana w typowych pomiarach środowiskowych dopuszczalna prędkość wiatru

podczas pomiarów, która w zgodzie z ogólnie przyjętą metodyką pomiarów środowiskowych w Polsce nie powinna przekraczać 5 m/s na wysokości 4 m. Natomiast podczas pomiaru hałasu pochodzącego od turbin wiatrowych należy dążyć do pomiaru przy prędkości wiatru bliskiej 5 m/s. W artykule przedstawiono przykłady własnych pomiarów terenowych przeprowadzonych na pięciu istniejących farmach wiatrowych. Wykazano, że w odległościach powyżej 500 m od skrajnej turbiny farmy wiatrowej wiele wyników pomiarów hałasu zawarte jest w tle pomiarowym. Część wyników mimo nierozróżnialności z tłem akustycznym miała wartość poniżej poziomu dopuszczalnego. Zaproponowano własną interpretację tej sytuacji pomiarowej.

W artykule podjęto próbę dokonania oceny zmierzonych poziomów równoważnego poziomu dźwięku w odniesieniu do poziomów dopuszczalnych hałasu słyszalnego obowiązujących w różnych krajach na świecie. Badania terenowe prowadzono zgodnie z polską metodyką pomiarową. Dlatego do porównań wybrano tylko te kraje w których poziom dopuszczalny hałasu wyrażony jest wskaźnikiem – równoważny poziom dźwięku korygowany krzywą A. Nie uwzględniono wskaźników zależnych od prędkości wiatru które występują przykładowo w Danii lub Kandzie (Ontario). W celu uzyskania kompleksowych informacji o emisji hałasu badanej farmy elektrowni wiatrowych wskazane jest prowadzenie pomiarów w okresie rocznym, np. w kolejnych czterech porach roku. Uzyskuje się wtedy wyniki dla różnych warunków atmosferycznych, a w szczególności przy różnych kierunkach i prędkościach wiatru. Wykonanie czterokrotnych pomiarów w ciągu roku daje większe prawdopodobieństwem wykonania pomiarów przy prędkości wiatru odpowiadającej maksymalnym lub bliskim maksymalnych poziomów mocy akustycznej turbin. Stosując tę zasadę uzyskujemy znacznie szerszy materiał do analizy, co umożliwia kompleksowe wykonanie oceny.

Słowa kluczowe:
pomiar hałasu, farma wiatrowa, poziomy hałasu

Keywords:
noise measurement, wind farm, noise levels

MIDDLE POMERANIAN SCIENTIFIC SOCIETY OF THE ENVIRONMENT PROTECTION
ŚRODKOWO-POMORSKIE TOWARZYSTWO NAUKOWE OCHRONY ŚRODOWISKA
Annual Set The Environment Protection
Rocznik Ochrona Środowiska
Volume/Tom 19. Year/Rok 2017 ISSN 1506-218X 540-556

Analiza i ocena efektywności filtracji na wybranych masach

Iwona Skoczko, Ewa Szatyłowicz, Radosław Kulesza
Politechnika Białostocka

1. Wstęp

Najczęściej występującym procesem jednostkowym w układach technologicznych w uzdatnianiu wód podziemnych bądź powierzchniowych jest filtracja. Sprawność tego procesu uzależniona jest od zastosowanego złoża filtracyjnego. Wypełnienie układów filtracyjnych powinno być efektywne pod względem usuwania zanieczyszczeń z wody, nie powinno stwarzać problemów podczas eksploatacji, nie wprowadzać także żadnych toksycznych substancji do wody oraz być odporne na działanie silnych kwasów i zasad. Niezmiernie istotny jest także aspekt ekonomiczny (Skoczko, Kisło 2014, Jeż-Walkowiak 2013). W doborze złoża filtracyjnego liczy się nie tylko cena, ale też dostępność w miejscu zastosowania oraz koszty eksploatacji, które wiążą się z długością trwania cykli filtracyjnych, z wymaganą ilością wody bądź środka do regeneracji, z koniecznością zastosowania powietrza w procesie czy też trwałością i wytrzymałością masy filtracyjnej (Jeż-Walkowiak 2013, Weber, Jeż-Walkowiak, 2006). Do wypełniania filtrów można zastosować materiały filtracyjne, które są pochodzenia syntetycznego, a także naturalnego. Do materiałów filtracyjnych naturalnych można zaliczyć: piasek kwarcowy, grys marmurowy, kruszony granit, diatomit, antracyt, zeolity, piroluzyt itp. Wyróżnia się także materiały filtracyjne pochodzenia naturalnego, które zostały poddane obróbce termicznej lub chemicznej. Zaliczamy do nich m.in.: węgiel aktywny, keramzyt, koks, keramzyt rozdrobniony, prażony dolomit. Syntetyczne materiały filtracyjne stanowią materiały uzyskiwane z tworzyw sztucznych (Nawrocki 2010, Kaleta i in. 2009,

Skoczko, Szatyłowicz 2016). Znaczną grupą mas filtracyjnych są wyżej wymienione naturalne minerały w postaci kopalnianej, którymi są zeolity. Należą one do klasy materiałów „low cost" spełanijących wymagania stawiane złożom filtracyjnym (Wang, Peng 2010).

Stałe poszukiwanie nowych mas filtracyjnych, jak i doskonalenie już istniejących, pozwala znaleźć optymalne rozwiązania, łączące zarówno wysoką sprawność procesu jak i niskie koszty użytkowania. Nie mniej jednak, by nowe złoże znalazło swoje miejsce w technologii wody, należy rozpocząć badania zmierzające do określenia jego przydatności w procesie filtracji. Istotnym aspektem jest, aby prowadzone badania laboratoryjne posłużyły do uzyskania wyników, które pozwolą opracować wytyczne dotyczące doboru uziarnienia, parametrów procesu filtracji, parametrów płukania bądź regeneracji lub zakresu składu fizykochemicznego wody przeznaczonej do oczyszczania na danym złożu. Zakres poziomu zanieczyszczeń w oczyszczanej wodzie, w którym masa filtracyjna cechuje się najlepszą efektywnością jest jedną z najważniejszych cech (Kaleta i in. 2009, Jeż-Walkowiak 2011). Ponadto rodzaj złoża zależy także od celu procesu filtracji, co wiąże się na przykład z zdolnością do adsorpcji zanieczyszczeń, klarowania wody, dekarbonizacji, zmiękczania, wymiany jonowej, koagulacji kontaktowej czy katalitycznego utleniania (Jeż-Walkowiak 2013).

Celem prowadzonych badań była analiza i ocena efektywności filtracji na dwóch nie przebadanych w tym aspekcie masach filtracyjnych pochodzenia naturalnego. W związku z tym sprawdzono zachowanie badanych mas filtracyjnych w procesie filtracji w warunkach laboratoryjnych, aby ocenić efektywność usuwania poszczególnych zanieczyszczeń z wody. Oceniono wskaźniki chemiczne w wodzie modelowej przepływającej przez masy takie jak: odczyn, przewodność elektrolityczna, $ChZT_{Mn}$, sucha pozostałość, stężenie chlorków, stężenie azotu amonowego, stężenie azotanów (V), twardość ogólna, stężenie żelaza oraz stężenie manganu.

2. Metodyka i obiekt badań

Badania zostały przeprowadzone w laboratorium Katedry Technologii w Inżynierii i Ochronie Środowiska Politechniki Białostockiej. Stanowisko badawcze składało się z dwóch rozdzielaczy, które wypełnione były masami filtracyjnymi X_1 oraz X_2 o właściwościach zmieszczonych

w tabeli 2. Na rysunku 1 przedstawiono badane złoża służące do filtracji. Badane masy filtracyjne różniły się kolorem oraz uziarnieniem:
- masa X_1 – czarna i drobnoziarnista,
- masa X_2 – jasnobrązowa i gruboziarnista.

Rys. 1. Po prawej stronie masa X_1, po lewej masa X_2
Fig. 1. On the right mass X_1, on the left mass X_2

W tabeli 1 umieszczono dla obu mas wartości gęstości nasypowej, wyniki analizy sitowej, średnice równoważne ziaren, współczynniki nierównomierności oraz wartości porowatości obu złóż obliczone dwoma sposobami (Skoczko, Szatyłowicz 2016).

Tabela 1. Obliczone parametry fizyczne mas filtracyjnych X_1 i X_2
Table 1. The calculated parameters of the physical mass X_1 and X_2

Parametr	**Masa X_1**	**Masa X_2**
Granulacja	1-10 mm	1-10 mm
Gęstość nasypowa	0,921 kg/dm^3	0,900 kg/m^3
Sumaryczny przesiew złoża	1,22→38,89→82,22→ 98,11→100 [%]	0,8→9,6→19,8→ 81,4→100 [%]
Średnica równoważna złoża	4,68 mm	7,01 mm
Współczynnik równomierności	2,76 mm	2,70 mm
Porowatość złoża I sposób (metoda określająca przybliżoną porowatość złoża) II sposób (określenie stosunku objętości wolnych przestrzeni między ziarnami złoża do jego objętości całkowitej)	56% 55%	65% 64%

Źródło: (Skoczko, Szatyłowicz 2016)

Objętość rozdzielaczy wynosiła 1 dm^3, wysokość – 24 cm, średnica – 12 cm. Zanieczyszczona woda była pompowana przewodami gumowymi o średnicy ϕ3 mm przez pompę perystaltyczną typu PP1B – 05A firmy ZALIMP na złoża filtracyjne z beczki o pojemności 120 dm^3. Wydatek pompy wynosił 20 cm^3/min. Każde ze złóż przed właściwym procesem filtracji zostało przepłukane wodą wodociągową. Okres płukania mas filtracyjnych trwał 7 dni w systemie ciągłym. Badania wody prowadzono przez okres 5 tygodni aż do momentu wyczerpania właściwości oczyszczających złoża. Punkt ten określono na podstawie znacznego zmniejszenia efektywności usuwania z wody związków manganu. Masy filtracyjne pracowały w systemie ciągłym, 24 godziny na dobę i 7 dni w tygodniu. Pobór próbek do analizy był wykonywany co 7 dni. Do badań użyto równą objętości obu mas filtracyjnych równą 0,9 dm^3. Obciążenie hydrauliczne podczas pracy złóż filtracyjnych było równe 0,21 $m^3/m^2 \cdot h$, wydatek roztworu natomiast wynosił 0,0012 m^3/h, natomiast temperatura pracy mieściła się w zakresie 21-24°C. Badania analityczne poszczególnych wskaźników jakości wody obejmowały badanie wody surowej oraz próbek wody przefiltrowanej. Woda surowa była preparowana na bazie wody wodociągowej poprzez dawkowanie na 120 litrów wody wodociągowej: 1 g siarczanu amonu żelaza (II), 0,02 g siarczanu manganu oraz 3 g bulionu wzbogaconego. Wodę modelową przygotowywano do badań 5 razy w tygodniu, dlatego jej skład ulegał niewielkim zmianom. Zakres wartości badanych wskaźników w wodzie surowej zestawiono w tabeli 2.

Tabela 2. Skład wody surowej
Table 2. Composition of raw water

Lp.	Parametr	Zawartość w wodzie surowej	Jednostka
1	Azot amonowy	0,75-1,38	mg/dm^3
2	Stężenie azotanów (V)	2,03-2,15	mg/dm^3
3	Stężenie chlorków	15-23	mg Cl^-/dm^3
4	Stężenie manganu	0,97-1,24	mg Mn/dm^3
5	pH	6,85-7,6	–
6	Przewodność	410,6-501,2	μS/cm
7	Sucha pozostałość	310,05-325,65	mg/dm^3
8	Twardość ogólna	278,22-344,28	mg $CaCO_3/dm^3$
9	$ChZT_{Mn}$	10,3-16,5	mg O_2/dm^3
11	Stężenie żelaza	2,49-2,73	mg Fe/dm^3

Metodyka badań analitycznych:

- pH zmierzono metodą potencjometryczną na podstawie normy PN-EN ISO 10523,
- stężenie chlorków oznaczono stosując metodę miareczkową z azotanem (V) srebra w obecności dichromianu (VI) potasu jako wskaźnika (metoda Mohra), zgodnie z normą PN-ISO 9297,
- przewodność elektrolityczną zmierzono metodą konduktometryczną zgodnie z normą PN-EN 27888.
- stężenie żelaza oznaczono za pomocą metody spektrofotometryczną z tiocyjanianem amonu (Hermanowicz i in. 1999),
- stężenie manganu określano stosując metodę spektrofotometryczną z nadsiarczanem amonu (Hermanowicz i in. 1999),
- $ChZT_{Mn}$ oznaczono metodą miareczkową z nadmanganianem potasu (VII) w zgodności z normą PN/C-04578.02,
- twardość ogólną oznaczono metodą miareczkowaną z EDTA zgodnie z normą PN-ISO 6059.

3. Analiza wyników badań

Pomimo wysokiego stopnia zaawansowania metod oczyszczana wody ciągle poszukuje się nowych, skutecznych i ekonomicznie zasadnych sposobów usuwania z wody poszczególnych zanieczyszczeń. Obecnie panuje trend poszukiwań nowych naturalnych bądź odpadowych materiałów filtracyjnych, które niekiedy cechują się doskonałymi właściwościami usuwania poszczególnych zanieczyszczeń w procesie filtracji. Ponadto naturalne materiały dostępne są w dużych ilościach stąd są potencjalnymi niedrogimi złożami filtracyjnymi. Celowym zatem wydało się przeprowadzenie badań i dokonanie oceny przydatności dwóch nowych mas filtracyjnych pochodzenia naturalnego do oczyszczania wody głównie z popularnych zanieczyszczeń wyrażonych następującymi wskaźnikami jakości wody: $ChZT_{Mn}$, sucha pozostałość, stężenie chlorków, stężenie azotu amonowego, stężenie azotanów (V), twardość ogólna, stężenie żelaza oraz stężenie manganu.

W oparciu o przeprowadzone badania (tabela 3) stwierdzono, że skuteczniejszym złożem do usuwania substancji organicznych wyrażonych $ChZT_{Mn}$ okazało się złoże X_2. Efektywność usuwania substancji

organicznych wyrażonych $ChZT_{Mn}$ zmniejsza się wraz z czasem badań (rysunek 2 i 3). Następuje proporcjonalne do ilości przefiltrowanej wody kolmatacja złóż filtracyjnych. Nad zjawiskiem tym prowadziła badania grupa badawcza Piecucha (Piecuch, Piekarski, Maltyńska 2014). Kolmatacja kształtowała się w granicach od 20,4% tj. w pierwszym tygodniu do 11,5% w ostatnim tygodni analizując złoże X_2, natomiast w przypadku masy filtracyjne X_1 najlepszy efekt nastąpił w środku cyklu tj. po trzecim tygodniu i wyniósł 13,2%. Przez ostatnie dwa tygodnie poziom usuwania $ChZT_{Mn}$ na złożu X_1 nieznacznie obniżał się i wyniósł 9,1%. W przypadku złoża X_2 zawartość $ChZT_{Mn}$ w badanej wodzie mieści się w granicach od 8,2 do 14,6 mg O_2/dm^3, biorąc pod uwagę złoże X_1 zawartość wskaźnika w badanej wodzie mieści się w granicach od 9,8 do 15 mg O_2/dm^3. Badania Skoczko i in. (Skoczko, Piekutin, Roszczenko 2015) dowodzą, że substancje organiczne wyrażone np. parametrem $ChZT_{Mn}$ trudno jest znacznie obniżyć w wyniku procesu samej filtracji.

Analizując zmniejszenie suchej pozostałości (tabela 3) w wodzie surowej i w wodzie po filtracji przez masy filtracyjne X_1 i X_2 zaobserwowano po pierwszym tygodniu badań zmniejszenie zawartości suchej pozostałości w wodzie z 310,1 do 266,8 mg/dm^3 w przypadku masy X_1, natomiast w przypadku złoża X_2 do 250,0 mg/dm^3. Efektywność usuwania suchej pozostałości (rysunek 2 i 3) jest więc niewielka na obu nieznanych masach X_1 i X_2.

Zawartość chlorków w wodzie przed i po filtracji na złożu X_1 i X_2 przedstawiono w tabeli 3 oraz rysunku 2 i 3. Z analizy wyników można stwierdzić, że największa efektywność usuwania chlorków nastąpiła po pierwszych dwóch tygodniach filtracji i wyniosła: 18,8% po pierwszym tygodniu i 21,7% po drugim tygodniu badań na złożu X_1. Natomiast na złożu X_2 po drugim tygodniu badań i wynosił 13% tj. ok. 21 mg/dm^3. Po pierwszym i trzecim tygodniu efekt usuwania chlorków mieści się w granicach 5,9-6,3%, gdzie stężenie parametru obniżyło się o 1 mg/dm^3 Właściwości filtracyjne wobec usuwania chlorów zarówno złoża X_1 jak i X_2 są bardzo niewielkie. Można stwierdzić, że w wyniku filtracji wody przez masy X_1 i X_2 nie zachodzi wymiana jonowa. Chlorki z wody są w znacznym stopniu usuwane przez złoża jonowymienne bądź w procesach filtracji membranowej (Nawrocki 2010). Ponadto stężenie chlorków w wodzie surowej było niewielkie i wartości stężenia jonów chlorko-

wych nie przekraczały wartości normatywnych z Rozporządzenia Ministra Zdrowia.

Stężenie azotu amonowego w wodzie przed i po procesie filtracji na złożu X_1 przedstawiono w tabeli 3. W czasie całego cyklu filtracyjnego wartości amoniaku w badanej wodzie były niższe w porównaniu z woda surową i mieściły się w granicach od 0,52 do 1,3 mg/dm^3. Najwyższy efekt usunięcia zaobserwowano jednak po pierwszym tygodniu procesu filtracji, gdzie wyniósł on 40,6%, azot amonowy obniżył się z 1,38 do 0,82 mg/dm^3 (rysunek 2). Najniższy efekt usunięcia zaobserwowano po trzecim tygodniu badań (18,7%), gdzie obniżenie stężenia wyniosło zaledwie 0,3 mg/dm^3. W dwóch ostatnich tygodniach efekt usunięcia azotu amonowego mieści się w granicach od 0,22 do 0,25 mg/dm^3. Analizując złoże filtracyjne X_2 można zaobserwować, że wartości tego wskaźnika kształtowały się w przedziale od 0,65 do 1,4 mg/dm^3 w wodzie oczyszczonej. W czasie całego cyklu filtracyjnego wartości amoniaku w badanej wodzie były niższe w porównaniu z woda surową. Najwyższy efekt usunięcia zaobserwowano jednak po pierwszym tygodniu procesu filtracji, gdzie wyniósł on 33,3% tj. o 0,46 mg/dm^3. Natomiast najwyższe stężenie badanego parametru przed i po filtracji zaobserwowano po trzecim tygodniu cyklu filtracyjnego, gdzie wyniosło 1,4 mg/dm^3. Największą różnicę w usuwaniu azotu amonowego można zauważyć w dwóch ostatnich tygodniach badań, gdzie efektywność filtracji wody na złożu X_1 kształtuje się na poziomie 22,4% po czwartym i 24,2% w ostatnim tygodniu, a na złożu X_2 wynosi poniżej 5%. Zestawione wyniki świadczą o lepszych właściwościach sorpcyjnych masy filtracyjnej X_1. Obniżenie stężenia amoniaku przyczyniło się do podwyższenia azotanów (V) w wodzie po filtracji. Usunięcie azotu amonowego na złożach X_1 oraz X_2 prawdopodobnie zachodzi w procesie nitryfikacji (Papciak i in. 2009). Literatura podaje, że na utlenienie 1 mg amoniaku do azotanów (V) zużywane jest 4,57 mg tlenu rozpuszczonego (Klimiuk, Łebkowska 2003).

Analizując masę filtracyjną X_1 pod kątem usuwania azotanów (V) zaobserwowano wzrost stężenia od 0,1 do 0,34 mg/dm^3 w porównaniu do wody surowej. Wzrost tego parametru następuje w całym okresie cyklu filtracyjnego w przypadku masy filtracyjnej X_1. Największy wzrost stężenia azotanów (V) w badanej wodzie nastąpił po dwóch tygodniach filtracji przez złoże X_1 i wyniósł 16,6% tj. od 2,05 do 2,39 mg/dm^3.

W czasie kolejnych badań nie przekroczył on 10%. Wyższa wartość badanego wskaźnika prawdopodobnie jest spowodowana chemicznym utlenianiem się jonów amonu do azotanów (III) i azotanów (V) (Papciak, Zamorska 2008).

Wyniki badań twardości ogólnej wody przed i po filtracji na złożu X_1 zaprezentowano w tabeli 3. Wartości te wahały się od 240,19 do 280,22 mg $CaCO_3/dm^3$. Najwyższy efekt usunięcia twardości ogólnej odnotowano w pierwszych dwóch tygodniach prowadzonych badań – 17,2% po pierwszym tygodniu i 23,35% po drugim tygodniu (rysunek 2 i 3). W następnych cyklach badań można zauważyć obniżenie efektywności usuwania. W przypadku złoża X_2 wartości te wahały się od 258,21 do 278,22 mg $CaCO_3/dm^3$. Największy efekt usuwania twardości ogólnej nastąpił po dwóch pierwszych tygodniach badań tj. 11% w pierwszym oraz 19,2% w drugim tygodniu. W kolejnych tygodniach skuteczność obniżyła się do 2.8% w ostatnim tygodniu. Masa filtracyjna X_2 okazała się mało efektywna jeśli chodzi o usuwanie twardości wody w porównaniu do X_1. Twardość ogólna wody na poziomie 240-280 mg $CaCO_3/dm^3$ klasyfikuje wodę jako średnio twardą (III) (Olesiak, Stępniak 2013).

Stężenia żelaza w wodzie po filtracji wahały się w przedziale od 1,66 do 1,87 mg/dm^3. Najniższa zawartość wystąpiła po pierwszym tygodniu filtracji i wynosiła 1,66 mg/dm^3, natomiast najwyższa w ostatnim tygodniu – 1,87 mg/dm^3. Porównując efektywność usuwania żelaza w wodzie można stwierdzić, iż największe obniżenie nastąpiło w pierwszym cyklu badań (36,4%). Wraz z czasem filtracji stopień usuwania nieznacznie malał i w ostatnim badaniu wyniósł 25,2%. Spowodowane jest to obniżeniem wydajności materiału filtracyjnego jakim jest masa X_1. Stężenia żelaza w wodzie po filtracji wahały się w przedziale od 1,58 do 2,09 mg/dm^3. W całym cyklu filtracyjnym poziom efektywności usuwania żelaza analizując masę filtracyjną X_2 malał wraz z upływem czasu filtracji. Najlepszy efekt zaobserwowano w pierwszym tygodniu badań – 39,5%, gdzie stężenie żelaza obniżyło się o 1,03 mg/dm^3. W dwóch ostatnich tygodniach poziom ten spadł poniżej 25%. Podobnie jak w przypadku złoża X_1, właściwości filtracyjne złoża X_2 zmniejszały się wraz z upływem czasu badań. Porównując skuteczność usuwania żelaza na badanych złożach X_1 i X_2 do naturalnych zeolitów można wnioskować, że eliminacja żelaza jest niska, ponieważ filtrując wodę przez zeolity można otrzymać efektywność powyżej 90% (Anielak, Arendacz 2007).

Tabela 3. Zestawienie otrzymanych wyników przed i po filtracji na złożu X_1 i X_2
Table 3. Results before and after filtration through a bed of X_1 and X_2

Czas pracy złoża [tygodnie]	Odczyn pH			Przewodność [µS/cm]			$ChZT_{Mn}$ [mg O_2/dm^3]			Sucha pozostałość [mg/dm^3]			Stężenie chlorów [mg Cl^-/dm^3]		
	*S	*1	*2	*S	*1	*2	*S	*1	*2	*S	*1	*2	*S	*1	*2
1	7,6	7,52	7,44	474,6	410,0	447,5	10,3	9,8	8,2	310,1	266,8	250	16	13	15
2	6,85	7,21	7,25	501,2	492,1	497,4	11,8	11	9,5	325,7	323,7	320,4	23	18	20
3	7,06	7,29	7,17	484,2	464,5	476,3	12,1	10,5	10,2	314,6	309,5	304,85	17	15	16
4	7,4	7,58	7,62	491,0	490,4	490,9	13,5	11,8	11,5	319,2	318,5	319,15	15	15	15
5	7,01	7,47	7,60	410,6	396,0	408,5	16,5	15	14,6	316,6	315,5	316,6	17	17	17
Czas pracy złoża [tygodnie]	**Azot amonowy [mg NH_4^+/dm^3]**			**Azot azotanowy [mg NO_3^-/dm^3]**			**Twardość ogólna [mg $CaCO_3/dm^3$]**			**Stężenie żelaza [mg Fe/dm^3]**			**Stężenie manganu [mg Mn/dm^3]**		
	*S	*1	*2	*S	*1	*2	*S	*1	*2	*S	*1	*2	*S	*1	*2
1	1,38	0,82	0,92	–	–	–	290,23	240,19	258,21	2,61	1,66	1,58	1,24	1,01	1,1
2	0,75	0,52	0,65	2,05	2,39	2,56	344,28	264,21	278,22	2,73	1,86	1,84	1,2	1,07	1,1
3	1,6	1,3	1,4	2,08	2,18	2,26	280,22	242,6	260,21	2,51	1,73	1,8	0,98	0,96	0,94
4	1,03	0,78	0,98	2,03	2,22	2,34	278,22	250,2	270,22	2,49	1,74	1,94	0,97	0,94	0,96
5	0,98	0,76	0,94	2,15	2,28	2,32	284,23	260,21	276,22	2,5	1,87	2,09	0,97	0,94	0,96

*S – woda surowa, *1 – masa X_1, *2 – masa X_2

Usuwanie manganu w czasie trwania całego cyklu filtracyjnego na złożu X_1 zachodziło znacznie gorzej w porównaniu do innych materiałów filtracyjnych przeznaczonych do usuwania manganu. Najlepszą efektywność usuwania manganu z wody osiągają masy aktywne i oksydacyjne zostało to potwierdzone licznymi wynikami badań, prowadzonymi przez polskie światowe ośrodki badawcze (Jeż-Walkowiak i in. 2011; Kim, Jung 2008; Piispanen, Sallanko 2010, Nowak 2013). Zawartość manganu po procesie filtracji kształtowała się w granicach od 0,94 do 1,01 mg/dm^3. Natomiast efektywność usuwania mieści się w granicach od 18,5% do 2,0%. Po pierwszym tygodniu badań wynosi 18,5%, natomiast w dwóch ostatnich tygodniach filtracji spada do 3,1%. Spadek ten, podobnie jak w przypadku żelaza, może być spowodowany zużywaniem się materiału filtracyjnego wraz z upływem czasu poprzez zapychanie porów.

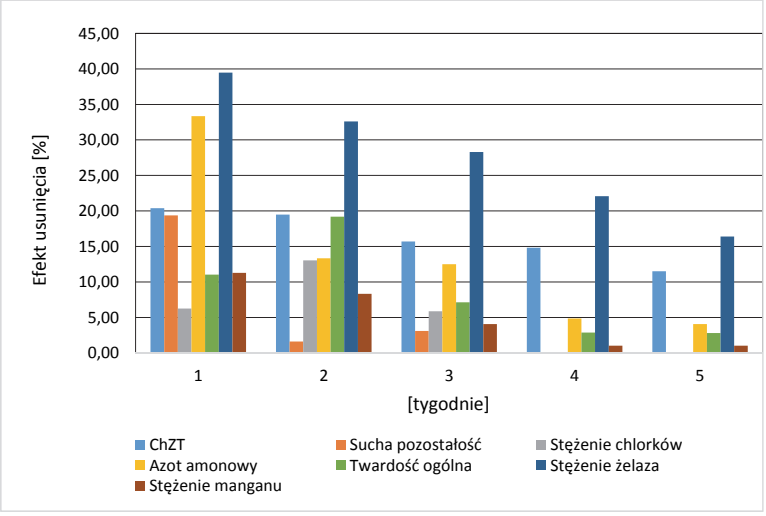

Rys. 2. Wykres efektywności usuwania poszczególnych zanieczyszczeń w procesie filtracji na złożu X_1
Fig. 2. Graph of removal efficiency of various pollutants in the filtration bed X_1

Analizując złoże X_2 można stwierdzić, że najwyższe stężenie manganu w wodzie przed filtracją wystąpiło w pierwszym tygodniu badań i wyniosło 1,24 mg/dm^3. Wraz z upływem badań wartość ta malała i wyniosła 0,97 mg/dm^3 w ostatnim tygodniu. Po pierwszym tygodniu

stężenie manganu po filtracji na złożu X_1 obniżyło się z wartości 1,24 mg/dm^3 do 1,01 mg/dm^3. Natomiast w przypadku złoża X_2 z wartości 1,24 mg/dm^3 do 1,11 mg/dm^3. Wraz z upływem czasu filtracji poziom efektywności usuwania znacznie zmniejszał się. W dwóch ostatnich tygodniach obniżenie stężenia po filtracji na złożu X_1 wyniosło zaledwie 0,03 mg/dm^3, a w przypadku złoża X_2 – 0,01 mg/dm^3. Efektywność usuwania manganu na tych dwóch złożach nie była duża. Wahała się w przedziale od 18,5 do 2% – złoże X_1 – oraz od 10,5 do 1% – złoże X_2.

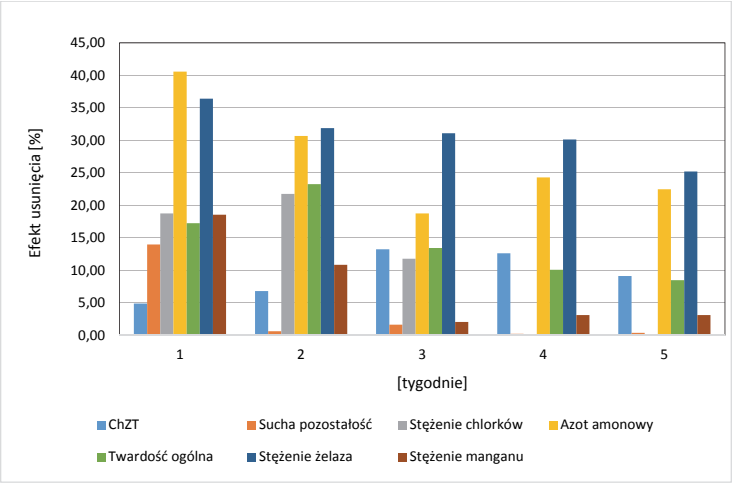

Rys. 3. Wykres efektywności usuwania poszczególnych zanieczyszczeń w procesie filtracji na złożu X_2
Fig. 3. Graph of removal efficiency of various pollutants in the filtration bed X_2

4. Podsumowanie

Wynikiem rozwoju technologii, które mają zastosowanie w oczyszczaniu wody jest między innymi wprowadzanie do użytku nowych mas filtracyjnych, które niekiedy cechują się selektywnym działaniem, albo przypominają skutecznością popularne złoża filtracyjne. Nowe materiały posiadają różną charakterystykę granulometryczną, chemiczną i fizyczną, są stosowane w określonych celach i różnych miejscach ciągu technologicznego na podstawie uzyskanych badań i porównań w skali laboratoryjnej (Jeż-Walkowiak 2013).

W wyniku przeprowadzonych badań wody przed jak i po filtracji pod względem jej przydatności do spożycia przez ludzi według Rozporządzenia Ministra Zdrowia z dnia 13 listopada 2015 r. w sprawie jakości wody przeznaczonej do spożycia przez ludzi. W tym celu mierzono poszczególne wskaźniki jakości wody, tj. odczyn (pH), przewodność, twardość ogólną, suchą pozostałość, azot amonowy, azotany (V), utlenialność, stężenie chlorków, zwartość żelaza, zawartość manganu. Proces filtracji przeprowadzono na dwóch złożach naturalnych, porowatych o nazwie X_1 oraz X_2, które poddano charakterystyce oraz efektywności usuwania poszczególnych związków. Skuteczniejszym złożem okazała się masa filtracyjna X_1 o drobniejszej frakcji. Jednak różnica w efektywności usuwania poszczególnych wskaźników jakości wody nie była duża. Większa część wskaźników jakości wody mieściła się w normie zawartej w powyższym rozporządzeniu, jeszcze w wodzie przed procesem filtracji, tj. odczyn (pH), przewodność, sucha pozostałość, stężenie chlorków, azot azotanowy (V), twardość ogólna. Wartości przekraczające dopuszczalne stężenia posiadały następujące wskaźniki: azot amonowy, utlenialność, stężenie żelaza, stężenie manganu. Żadne z badanych złóż filtracyjnych nie obniżyło stężenia tych parametrów do wartości wymaganych dla wód przeznaczonych do spożycia przez ludzi. Efektywność usuwania w każdym przypadku nie przekroczyła 50%.

Porównując skuteczność usuwania poszczególnych zanieczyszczeń z wody w wyniku filtracji masy X_1 i X_2 ze skutecznością filtracji piasku kwarcowego można odwołać się do badań prowadzonych przez Kaletę, Papciak i Puszkarewicz (2009), które w swojej pracy prowadziły badania technologiczne wody pochodzącej ze studni głębinowej zlokalizowanej w miejscowości Lubenia (woj. podkarpackie). Otrzymana przez wymienioną grupę badawczą efektywność usuwania żelaza wyniosła 79%, manganu <5% i amoniaku 44%. W przypadku mas filtracyjnych X_1 oraz X_2 badanych w niniejszej pracy, efekt usuwania żelaza był zdecydowanie niższy niż w przypadku piasku kwarcowego i wynosił 36,4% (X_1) i 39,5% (X_2) po pierwszym tygodniu badań. Jednak stężenie żelaza w wodzie surowej było znacznie mniejsze i mieściło się w przedziale 2,73-2,49 mg/dm^3 niż w badaniach Kalety, Papciak i Puszkarewicz (2009), gdzie zawartość żelaza w wodzie surowej wynosiła 8,60 mg/dm^3. Jeśli chodzi o mangan nieznacznie lepsze efekty uzyskano na złożu X_1 (18,5,6%) oraz X_2 (10,5%) w porównaniu do piasku kwarcowego. Stęże-

nia manganu w wodzie surowej wahały się w przedziale 0,97-1,24 mg/dm^3. Wartości te były więc nieznacznie mniejsze od stężenia manganu w wodzie ze studni w Lubaniu, gdzie zwartość manganu w wodzie surowej była równa 1,98 mg/dm^3. Efektywność usuwania amoniaku na złożu X_1 wynosiła 40,6%, a na złożu X_2 33,3% po pierwszym tygodniu badań, gdzie wyjściowe stężenie w wodzie surowej mieściło się w przedziale 0,75-1,6 mg/dm^3. Nieznacznie efektywniejszy jest piasek kwarcowy, które efektywność usuwania azotu amonowego w badaniach grupy badawczej Kalety (2009) wyniosła około 55,5%, nastąpiło obniżenie stężenia azotu amonowego z 2,7 mg/dm^3 do 1,5 mg/dm^3. Porównując złoża X_1 oraz X_2 do piasku kwarcowego można zauważyć, iż żadne złoże nie obniżyło badanych wskaźników jakości wody do wartości normatywnych zgodnych z Rozporządzeniem Ministra Zdrowia z dnia 13 listopada 2015 r. w sprawie jakości wody przeznaczonej do spożycia przez ludzi. Wody podziemne zawierające ponadnormatywne ilości żelaza, manganu i azotu amonowego powinny być poddawane dwustopniowej filtracji. Kaleta, Papciak i Puszkarewicz (2009) wskazują, iż pierwszy stopień filtracji powinien odbywać się na złożu z piasku kwarcowego w celu zatrzymania żelaza łatwo wytrącalnego. Być może badane masy X_1 i X_2 znalazłyby zastosowanie w filtracji dwustopniowej jako drugi etap filtracji. Wyniki badań prowadzone przez Papciak, Zamorską, Kaletę oraz Puszkarewicz (2009) dowiodły, że usuwanie azotu amonowego i manganu z wód to procesy konkurencyjne. Obecność w wodzie manganu ma wpływ na przebieg procesu nitryfikacji i skuteczność usuwania azotu amonowego, a proces nitryfikacji może zakłócać skuteczność odmanganianie w okresie wpracowywania złóż nitryfikacyjnych. Istnieje hipoteza ,że powstałe w pierwszym etapie nitryfikacji azotany (III) powodują redukcję ditlenku manganu, a same ulegają utlenieniu do azotanów (V) (Łomotowski, Haliniak 1997). Z kolei Nowak i Anielak (1998) podają, że usuwanie manganu z wody jest wynikiem nie tylko zachodzenia procesów fizyko-chemicznych, ale także udziału bakterii utleniających mangan, mogących odgrywać rolę w procesie formowania katalitycznej warstwy tlenków manganu. Równoważne wnioski można wyciągnąć z niniejszej pracy, gdzie procesy usuwania amoniaku i manganu konkurowały ze sobą i skuteczność ich usuwania była niewystarczająca do wartości normatywnych. Właściwym rozwiązaniem byłoby usuwanie tych parametrów na dwóch oddzielnych złożach filtracyjnych wdrażając filtrację dwustopniową.

5. Wnioski

1. W przeprowadzonych badaniach udokumentowano, że efektywniejszym złożem naturalnym pod względem eliminacji większości popularnych zanieczyszczeń z wody było złoże X_1 (drobnoziarniste), które charakteryzowało się mniejszą od złoża X_2 średnicą równoważna złoża.
2. Efektywność usuwania badanych wskaźników jakości wody obniżała się wraz z czasem przeprowadzonych badań. Niskie stężenia wyjściowe badanych parametrów, były przyczyną ich małej eliminacji.
3. Na żadnym z badanych złóż nie uzyskano obniżenia stężeń do wartości normatywnych takich wskaźników jak: stężenie żelaza, stężenie azotu amonowego, stężenie mangan i utlenialność.
4. Według badań zwartych w literaturze usuwanie azotu amonowego i manganu z wód to procesy konkurencyjne. Właściwym rozwiązaniem byłoby usuwanie tych parametrów na dwóch oddzielnych złożach filtracyjnych wdrażając filtracje dwustopniową. Ponadto badania wykazały, że wraz ze wzrostem twardości wody zmniejsza się zdolność jonowymienna złoża w stosunku do jonu amonowego.

Badania zostały zrealizowane w ramach pracy nr S/WBiIŚ/3/2014 i sfinansowane ze środków na naukę MNiSW.

Literatura

Anielak, A.M., Arendacz, M. (2007). Iron and manganese removal effects using zeolites, *Rocznik Ochrona Środowiska*, *9*, 9-18.

Hermanowicz, W., Dojlido, J., Dożańska, W. (1999). *Fizyczno-chemiczne badanie wody i ścieków.* Warszawa: Arkady.

Jeż-Walkowiak, J. (2013). Wymagania stawiane materiałom filtracyjnym. *Ekonomia i Środowisko, 2(45)*, 70-80.

Jeż-Walkowiak, J., Dymaczewski, Z., Sozański, M. (2011). Parametry technologiczne procesu filtracji pospiesznej wód podziemnych przez złoża oksydacyjne i chemicznie nieaktywne. *Inżynieria Ekologiczna, 26*, 112-121.

Kaleta, J. (2005). Evaluation of usability of selected adsorbents for removing of organic pollutants from water. *Monografie Komitetu Inżynierii Środowiska PAN, 32*, 179-186.

Kaleta, J., Papciak, D., Puszkarewicz, A. (2009). Naturalne i modyfikowane minerały w uzdatnianiu wód podziemnych. *Gaz, Woda i Technika Sanitarna*, *25*, 51-63.

Kim, J., Jung, S. (2008). Soluble manganese removal by porous media filtration. *Environmental Technology, 12(29)*, 1265-1273.

Klimiuk, E., Łebkowska, M. (2003). *Biotechnologia w ochronie środowiska*. Warszawa: Wydawnictwo Naukowe PWN.

Łomotowski, J., Haliniak, J. (1997). Usuwanie azotu amonowego z wody na filtrach biologicznie aktywnych. *Ochrona Środowiska*, *3(66)*, 15-17.

Nawrocki, J. (2010). *Uzdatnianie wody. Procesy fizyczne, chemiczne i biologiczne.* Warszawa: Wydawnictwo Naukowe PWN.

Nowak, R. (2013). Wpływ wybranych składników uzdatnianej wody na skuteczność jej odmanganiania w obecności mas aktywnych. *Rocznik Ochrona Środowiska, 15*, 714-728.

Nowak, R., Anielak, A.M. (1998). Filtracyjne złoża stosowane do odmanganiania wody. Matreiały *Szkoła Jakości Wody*, Ustronie Morskie, 311-325.

Olesiak, P., Stępniak, L. (2013). Wpływ twardości wody i pH roztworów na efektywność sonosorpcji substancji humusowych na węglu aktywnym, *Inżynieria i Ochrona Środowiska, 16(3)*, 405-415.

Papciak, D, Zamorska, J., Kaleta, J., Puszkarewicz, A. (2009). Effect of manganese(II) on the time of biofilm formation and on the effectiveness of ammonium nitrogen removal from water in biofiltration process. *Polish Journal of Environmental Studies, 2*, 43-50.

Papciak, D., Zamorska, J. (2008). Jedno- i dwuwarstwowe złoża nitryfikacyjne jako biotechnologiczna metoda usuwania azotu amonowego z wody. *Biotechnologia*, *1(80)*, 189-201.

Papciak, D., Zamorska, J., Kaleta, J., Puszkarewicz, A. (2009). Effect of manganese (II) on the time of biofilm formation and on the effectiveness of amonium nitrogen removal from water in biofiltration process. *Polish Journal of Environmental Studies, 2*, 43-50.

Piekarski, J., Piecuch, T., Malatyńska, G. (2014). Filtracja z tworzeniem osadu ściśliwego na złożu bez kolmatacji. *Gospodarka Surowcami Mineralnymi, 30(3)*, 83-98.

Piispanen, J.K., Sallanko, J.T. (2010). Mn(II) removal from groundwater with manganese oxide-coated filter media. *Journal of Environmental Science and Health, 13(45)*, 1732-1740.

PN/C-04578.02 – Jakość wody – Oznaczanie chemicznego zapotrzebowania tlenu (ChZT) metodą nadmanganianową.

PN-EN 27888 – Jakość wody – Oznaczanie przewodności elektrycznej właściwej.

PN-EN ISO 10523 – Jakość wody – Oznaczanie pH.

PN-ISO 6059 – Jakość wody – Oznaczanie sumarycznej zawartości wapnia i magnezu – Metoda miareczkowa z EDTA.
PN-ISO 9297 – Jakość wody – Oznaczanie chlorków – Metoda miareczkowania azotanem srebra w obecności chromianu jako wskaźnika (Metoda Mohra).
Rozporządzenie Ministra Zdrowia z dnia 13 listopada 2015 r. w sprawie jakości wody przeznaczonej do spożycia przez ludzi (Dz.U. 2015 poz. 1989).
Skoczko, I., Kisło, A. (2014). Analysis of ecological activity of Podlasie province. *Journal of Ecological Engineering, 15(1)*, 1-6.
Skoczko, I., Piekutin, J., Roszczenko, A. (2015). Usuwanie z wody związków żelaza i manganu. *Rocznik Ochrona Środowiska, 17*, 1587-1608.
Skoczko, I., Szatyłowicz, E. (2016), The analysis of physico-chemical properties of two unknown filter materials. *Journal of Ecological Engineering, 17(3)*, 148-154.
Wang, S., Peng, Y. (2010). Natural zeolites as effective adsorbents in water and wastewater treatment. *Chemical Engineering Journal, 156*, 11-24.
Weber, Ł., Jeż-Walkowiak, J. (2006). Rodzaje złóż filtracyjnych: Porównanie efektywności procesu filtracji. *Wodociągi – Kanalizacja, 11*, 53-57.

The Analysis and Assessment of the Effectiveness of Filtration on Selected Masses

Abstract

The constant search for new mass filter, as well as improving existing ones, contributing to the search for optimal solutions, combining both high process efficiency and low operation costs. However, that the new deposit found its place in water technology, should start research to determine its usefulness in the process of filtration. The aim of this study was to analyzed and evaluated the effectiveness of filtration two unknown, porous filter masses. Therefore, it was examined the behavior of filter bed by filtration in the laboratory, to assess the efficiency of removal of particular contaminants from the water. Chemical indicators were examined in the model water flowing through the mass, such as: pH, electrolytic conductivity, COD_{Mn}, dry residue, chloride concentration, ammonium concentration, nitrate (V) concentration, total hardness, iron and manganese concentration. It has been proved that the bed X_1, which has an less equivalent particle diameter, efficiently removed contaminants from the water compared to filter bed X_2. Filter beds X_1 and X_2 does not purify the water to the value of the regulation of the minister of health. The parameters have exceeded values after filtration are: iron concentration, ammonia concentration, manganese concentration and COD_{Mn}. It is concluded that probably gave to the second stage of a two-stage filtration.

Streszczenie

Stałe poszukiwanie nowych mas filtracyjnych, jak i doskonalenie już istniejących, przyczynia się do poszukiwań optymalnych rozwiązań, łączących zarówno wysoką sprawność procesu jak i niskie koszty użytkowania. Jednak, aby nowe złoże znalazło swoje miejsce w technologii wody, należy rozpocząć badania zmierzające do określenia jego przydatności w procesie filtracji. Celem prowadzonych badań była analiza i ocena efektywności filtracji na dwóch nieznanych, porowatych masach filtracyjnych pochodzenia naturalnego. W związku z tym sprawdzono zachowanie badanych mas filtracyjnych w procesie filtracji w warunkach laboratoryjnych, aby ocenić efektywność usuwania poszczególnych zanieczyszczeń z wody. Zbadano wskaźniki chemiczne w wodzie modelowej przepływającej przez masy takie jak: odczyn, przewodność elektrolityczna, $ChZT_{Mn}$, sucha pozostałość, stężenie chlorków, stężenie azotu amonowego, stężenie azotanów (V), twardość ogólna, stężenie żelaza oraz stężenie manganu. Udowodniono, iż złoże X_1, które charakteryzuje się mniejszą średnicą równoważną ziaren efektywniej usuwa zanieczyszczenia z wody w porównaniu do złoża X_2. Złoża filtracyjne X_1 i X_2 nie usuwają parametrów jakości wodny takich jak: stężenie żelaza, stężenie azotu amonowego, stężenie mangan i $ChZT_{Mn}$ do wartości z Rozporządzenia Ministra Zdrowia. Wywnioskowano, iż prawdopodobnie nadawały by się do II etapu filtracji dwustopniowej.

Słowa kluczowe:
złoża filtracyjne, sprawność filtracji, jakość wody

Keywords:
filter beds, filtration efficiency, water quality

MIDDLE POMERANIAN SCIENTIFIC SOCIETY OF THE ENVIRONMENT PROTECTION
ŚRODKOWO-POMORSKIE TOWARZYSTWO NAUKOWE OCHRONY ŚRODOWISKA

Annual Set The Environment Protection
Rocznik Ochrona Środowiska

Volume/Tom 19. Year/Rok 2017 ISSN 1506-218X 557-571

Podczyszczanie ścieków organicznych metodą koagulacji siarczanem glinu

Barbara Kościelnik, Aleksandra Kowalska
Politechnika Koszalińska

1. Wstęp

Warunki jakie należy spełnić przy wprowadzaniu ścieków do wód lub do ziemi oraz w sprawie substancji szczególnie szkodliwych dla środowiska wodnego określa Rozporządzenie Ministra Środowiska z dnia 18 grudnia 2014 roku (Rozporządzenie). Wprowadzone do wód lub do ziemi ścieki nie powinny wywoływać żadnych zmian chemicznych, fizycznych oraz biologicznych. Każda powyższa zmiana utrudniłaby lub uniemożliwiłaby prawidłową pracę odbiornika, przez co nie zostałyby spełnione określone wymagania jakościowe zgodne z ich użytkowaniem.

Wymagany efekt oczyszczania ścieków, nazywany także stopniem oczyszczania lub sprawnością działania oczyszczalni ścieków, jest wynikiem obecności zanieczyszczeń w ściekach doprowadzanych do oczyszczalni oraz związany jest z warunkami jakie powinny spełniać ścieki oczyszczone wprowadzane do odbiornika. Obowiązujące przepisy prawne określają więc, jaka powinna być jakość ścieków odprowadzanych do odbiornika (Puchlik i in. 2016).

W technologii oczyszczania ścieków, w tym także ścieków technologicznych, wykorzystuje się metody fizyczne, fizykochemiczne, chemiczne i biologiczne. Procesy fizyczne i fizykochemiczne, np. usuwanie barwników ze ścieków przemysłu włókienniczego, są efektywne, lecz bardzo kosztowne (Kyzioł-Komosińska i in. 2011). Jedną z metod chemicznych podczyszczania ścieków jest proces koagulacji. Zapewnienie optymalnych parametrów technologicznych przebiegu procesu koagulacji (rodzaju i dawki koagulantu) umożliwia częściowe usunięcie rozpusz-

czonych domieszek/zanieczyszczeń z wody oraz minimalizację niepożądanych skutków procesu koagulacji. Efektem skutecznej koagulacji oprócz zmniejszenia mętności i intensywności barwy jest również zmniejszenie ilości prekursorów ubocznych produktów dezynfekcji i utleniania chemicznego, mikrozanieczyszczeń takich jak WWA, DDT, metali ciężkich, a także bakterii i wirusów (Krupińska & Konkol 2015).

Dynamicznie rozwijający się przemysł wodochłonny, wzrastające zużycie wody na cele bytowo-gospodarcze stanowią zagrożenie wyczerpania zasobów wód. Coraz wyższe ceny za wodę skłaniają wielu przedsiębiorców do zastosowania najprostszego i najbardziej ekonomicznego systemu zaopatrywania w wodę, czyli „systemu zamkniętego". Działanie systemu polega na wykorzystaniu zużytej wody po jej uprzednim oczyszczeniu. Coraz więcej zakładów przemysłowych stosuje obiegi zamknięte, w których do pobranej wody dostarcza się niewielkie ilości uzupełniające. Takie rozwiązania są bardzo korzystne dla całego ekosystemu, gdyż nie naruszają zasobów wody i nie powodują ich zanieczyszczenia ściekami (Królikowski i in. 1991, Królikowski 1994, Królikowski 1993, Królikowski 1990, Magrel 2000).

Do podczyszczania ścieków zawierających substancje szkodliwe jak np. kleje organiczne można stosować różne metody. Jedną z nich jest proces pogłębionego chemicznego utleniania (AOPs – Advanced Oxidation Processes) za pomocą odczynnika Fentona (Piaskowski & Świderska-Dąbrowska 2006). Proces polega na chemicznym rozkładzie trudno lub niebiodegradowalnych związków zawartych w ściekach do prostszych form, wykazujących podatność na biodegradację. Z tego względu metody AOPs znalazły szerokie zastosowanie do podczyszczania ścieków przemysłowych z produkcji klejów mocznikowych, pestycydów, ścieków włókienniczych, pofarbiarskich. Do dalszej degradacji ścieków Autorzy prowadzili biologiczne doczyszczanie ścieków osadem czynnym metodą przesiewową (Piaskowski & Świderska-Dąbrowska 2006).

Układ technologiczny podczyszczania ścieków z produkcji paneli wytwarzanych z udziałem klejów na bazie żywic mocznikowo-formaldehydowych zaproponowali Żak i inni (Żak i in. 2005). Ścieki podczyszczano w dwóch etapach: proces koagulacji z udziałem koagulanta PIX 113. Po koagulacji podawano 1,0% roztwór flokulanta (PRAESTOL 862 BC), w ilościach umożliwiających wytworzenie flokuł podatnych na flotację chemiczną. Drugi etap pomocą polegał na chemicz-

nym utlenieniu za pomocą 30% roztworu nadtlenku wodoru o stężeniu 8,0-15,0 kg H_2O_2/m^3. Przyjęcie dwustopniowego podczyszczania ścieków według Żaka i innych (Żak i in. 2005) pozwoliło na uzyskanie redukcji wskaźników zanieczyszczeń na poziomie umożliwiającym dalsze bezkolizyjne oczyszczanie metodami biologicznymi, których efektywność była przedmiotem badań Maleja (Malej & Hołubowicz 1996, Malej 1997a, Malej 1997b).

Na podstawie wielu lat badań prowadzonych w Zakładzie Techniki Wodno-Ściekowej i Utylizacji Odpadów Politechniki Koszalińskiej, zaproponowano układ technologiczny podczyszczania ścieków poprodukcyjnych w procesach mechanicznych i fizykochemicznych (Juraszka & Piecuch 2008a, Juraszka & Piecuch 2008b, Juraszka & Piecuch 2007).

W pracy poddano ocenie wyniki badań jednego węzła układu technologicznego podczyszczania ścieków przemysłowych zawierających kleje organiczne, za pomocą koagulacji siarczanem glinu $Al_2(SO_4)_3$. Wyniki badań podczyszczania ścieków klejowych metodą koagulacji z zastosowaniem innych odczynników oraz wyniki badań doczyszczania ścieków w kolejnych węzłach zaproponowanego układu technologicznego opublikowano w pracach (Juraszka & Piecuch 2008a, Juraszka & Piecuch 2008b, Juraszka & Piecuch 2007).

2. Metodyka badań

Badaniami objęto ścieki powstające w wyniku mycia i płukania instalacji klejowych, nazywane dalej ściekami klejowymi. W celu przeprowadzenia dokładnej analizy, ścieki z istniejącego przedsiębiorstwa pobierano w różnych dniach pracy zakładu. Przedstawiony powyżej sposób poboru prób umożliwił pobranie ścieków o różnych ładunkach zanieczyszczeń. Ścieki przewożono w karnistrach i przechowywano w warunkach laboratoryjnych. Głównymi składnikami ścieków były resztki kleju dyspersyjnego oraz utwardzacza, zawierające m.in.: polioctan i kopolimer winylu, chlorek glinu oraz azotan glinu. Charakteryzowały się one wysoką lepkością oraz mleczną barwą.

W tabeli 1 przedstawiono charakterystykę ścieków klejowych użytych do badań własnych procesu koagulacji i sedymentacji grawitacyjnej.

Jako parametry zmienne w procesie przyjęto:
x_1 – dawkę koagulanta – D [g/dm^3],
x_2 – czas sedymentacji – t_s [h].

Jako parametry wynikowe oznaczono następujące wskaźniki:
Y_1 – ogólny węgiel organiczny – *OWO* [mg C/dm^3],
Y_2 – chemiczne zapotrzebowanie tlenu – *ChZT* [mg O_2/dm^3],
Y_3 – ekstrakt eterowy – E_E [mg/dm^3],
Y_4 – zawiesina ogólna – Z_O [mg/dm^3].

Proces koagulacji prowadzono równolegle w 5 kolbach stożkowych o objętości 500 ml, do których dodawano roztwór siarczanu glinu $Al_2(SO_4)_3 \cdot 18H_2O$ w zakresie stężeń od 0,0 do 1,5 g/dm^3. Ze względu na niski odczyn ścieków (pH 4,18) dodawano 0,2 g/dm^3 NaOH, w celu korekty odczynu do pH 7,5-8,0. Próby mieszano za pomocą urządzenia zwanego testerem flokulacji ET720. Po dodaniu odczynników ścieki poddawano najpierw szybkiemu mieszaniu przez 1 minutę, a następnie powolnemu mieszaniu przez 20 min przy obrotach 30 min^{-1}.

W pierwszym etapie jako parametr stały przyjęto czas sedymentacji grawitacyjnej wynoszący 2 godziny. Jego wartość stanowiła centralny punkt aproksymacji tego parametru. Jako parametr zmienny przyjęto dawkę koagulanta (x_1), która wynosiła: 0,3; 0,6; 1,0 i 1,5 g/dm^3.

W kolejnym etapie badań jako parametr stały przyjęto dawkę odczynnika, która wynosiła 0,6 g/dm^3. Wartość ta była jednocześnie centralnym punktem aproksymacji dla tego parametru. Jako parametr zmienny przyjęto czas sedymentacji grawitacyjnej (x_2), który wynosił 1; 2; 4 i 6 godzin.

Po procesie sedymentacji grawitacyjnej wykonano oznaczenia analityczne badanych wskaźników zanieczyszczeń. Badania przeprowadzono w trzech powtarzalnych seriach, a prezentowane wyniki są średnią arytmetyczną.

W tabeli 1 zostały przedstawione wyniki badań laboratoryjnych dla ścieków surowych z Zakładu DREWEXiM. Podane wyniki stanowiły dane wejściowe w pracach naukowych z użyciem różnego rodzaju koagulantów, tj. w niniejszej pracy oraz w pozostałych opublikowanych źródłach fizykochemicznych (Juraszka & Piecuch 2008a, Juraszka & Piecuch 2008b, Juraszka & Piecuch 2007).

Tabela 1. Wartości wskaźników zanieczyszczeń w ściekach przemysłowych pobieranych losowo z Zakładu DREWEXiM
Table 1. Values of pollution indicators of in raw wastewater sampled randomly at the DREWEXiM Company

Wskaźnik	Jednostka	Wartości wskaźników zanieczyszczeń				
Odczyn	pH	4,18	4,25	4,02	4,00	4,40
BZT_5	mg O_2/dm^3	0,9	0,7	0,4	0,7	0,3
ChZT	mg O_2/dm^3	45850	32500	28000	31200	56380
Zawiesina ogólna Z_O	mg/dm^3	16570	13980	21670	14600	20580
Ekstrakt eterowy E_E	mg/dm^3	120	185	98	78	112
Ogólny węgiel organiczny *OWO*	mg C/dm^3	18200	20700	15390	16820	11300
Substancje rozpuszczone S_r	mg/dm^3	6310	4280	7420	5850	6950

3. Wyniki badań i dyskusja

Ogólny węgiel organiczny (OWO). Analiza wyników badań wskazuje, że przy zmianie pierwszej zmiennej niezależnej (x_1), tzn. dawce koagulantu $Al_2(SO_4)_3$ od 0,00 g/dm^3 do 1,5 g/dm^3, stężenie OWO obniżyło się z 18200 mg C/dm^3 do 3320 mg C/dm^3 (dla najwyższej dawki koagulanta), co odpowiada sprawności koagulacji około 81% (rys. 1). Wyniki doświadczeń przedstawione na krzywej wskazują, że wraz ze wzrostem dawki $Al_2(SO_4)_3$ rośnie stopień usunięcia *OWO*, a optymalna dawka zastosowanego koagulantu powinna wynosić około 0,6 g/dm^3. Na podstawie przebiegu krzywej można stwierdzić, że stosowanie większych dawek koagulantu nie zmieni w sposób znaczący stężenia *OWO* w wodzie osadowej po koagulacji i sedymentacji.

Przy zmianie drugiej zmiennej niezależnej (x_2), tj. czasu sedymentacji od 0 do 6 h stężenie *OWO* obniżyło się z 18200 mg C/dm^3 do 4110 mg C/dm^3. Analiza wyników badań pozwala stwierdzić, że wraz ze wzrostem czasu sedymentacji grawitacyjnej maleje wartość wskaźnika *OWO* w cieczy nadosadowej (rys. 2). W tym przypadku optymalny czas sedymentacji wyniósł t = 2 h. Wydłużanie czasu sedymentacji powyżej dwóch godzin nie miała znaczącego wpływu na stężenie *OWO* w cieczy nadosadowej.

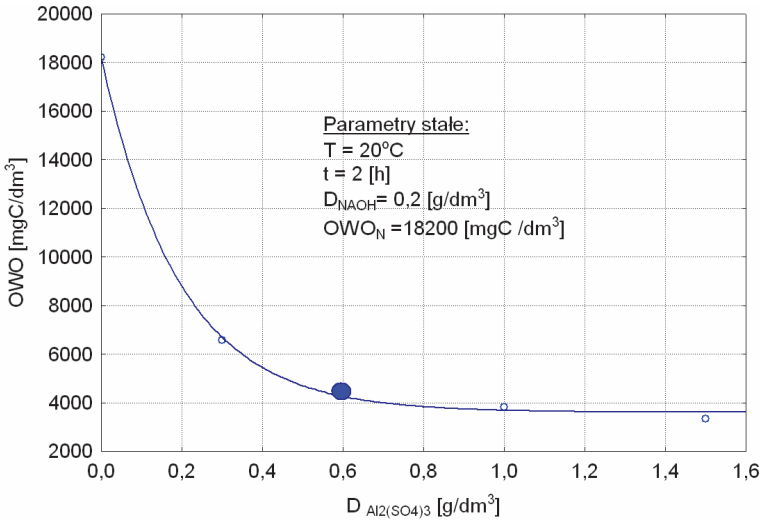

Rys. 1. Wpływ dawki $Al_2(SO_4)_3$ na stężenie węgla organicznego *OWO* w cieczy nadosadowej
Fig. 1. Influence of $Al_2(SO_4)_3$ dose on total organic carbon *TOC* concentration in wastewater after coagulation

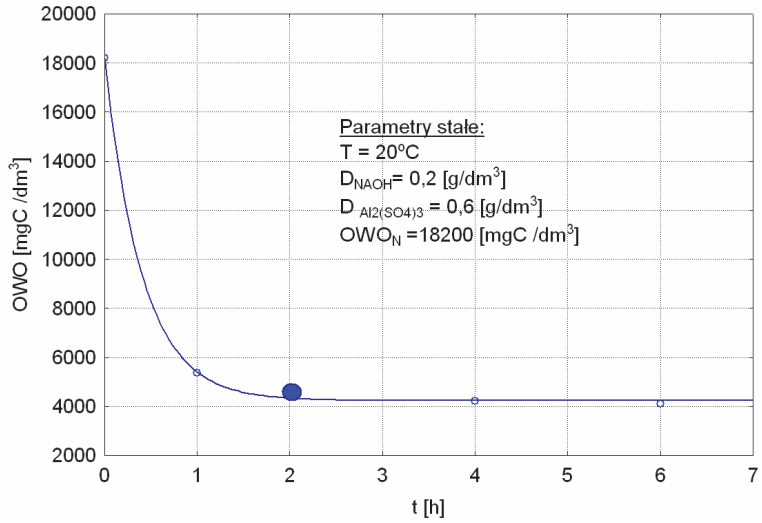

Rys. 2. Wpływ czasu sedymentacji t_S na wartość węgla organicznego *OWO* w cieczy nadosadowej
Fig. 2. Influence of sedimentation time t_S on organic karbon *TOC* value in wastewater after coagulation

Równanie aproksymacyjne po pierwszym i drugim stopniu, wyznaczone na podstawie wyników badań, ma następującą postać:

$$OWO(D, t_s) = \exp(9{,}59 - 5{,}17 \cdot D) + \exp(9{,}54 - 2{,}47 \cdot t_s) - 3823 \qquad (1)$$

gdzie:
OWO – ogólny węgiel organiczny [mg C/dm^3],
D – dawka $Al_2(SO_4)_3 \cdot 18H_2O$ [g/dm^3],
t_S – czas sedymentacji [h].

Chemiczne zapotrzebowanie tlenu (ChZT). Analiza wyników badań (rys. 3) wskazuje, że po zmianie dawki koagulanta $Al_2(SO_4)_3$ do 1,5 g/dm^3, przy czasie sedymentacji t wynoszącym 2h wartość *ChZT* obniżyła się z 45850 mg O_2/dm^3 do 8510 mg O_2/dm^3, czyli o 81%. Wraz ze wzrostem czasu sedymentacji grawitacyjnej maleje stężenie związków organicznych mierzonych wskaźnikiem *ChZT* w cieczy nadosadowej (rys. 4). Zaobserwowano największy spadek wskaźnika *ChZT* w czasie pierwszej godziny sedymentacji. Mechanizm przyczynowo-skutkowy przebiegu wykresu 4 można tłumaczyć tym, że zdecydowanie większość cząstek stałych (zawiesin) sedymentuje w pierwszej godzinie, a z tym łączy się właśnie obniżenie wartości wskaźnika *ChZT*.

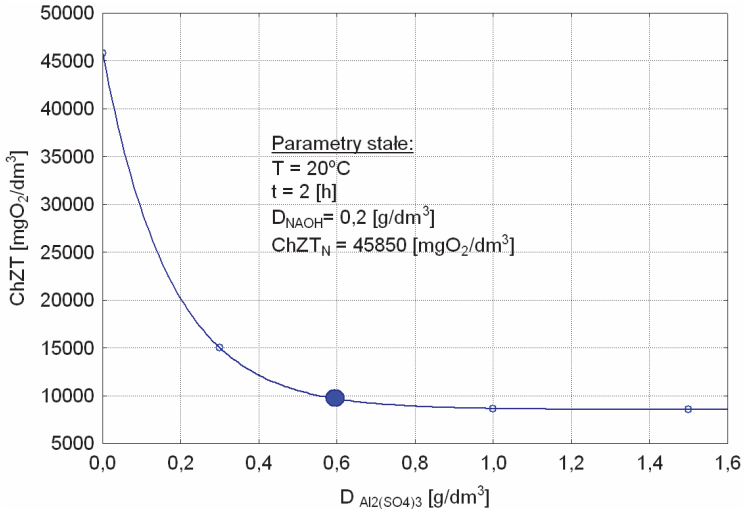

Rys. 3. Wpływ dawki $Al_2(SO_4)_3$ na wartość *ChZT* w cieczy nadosadowej
Fig. 3. Influence of $Al_2(SO_4)_3$ dose on *COD* value in wastewater after coagulation

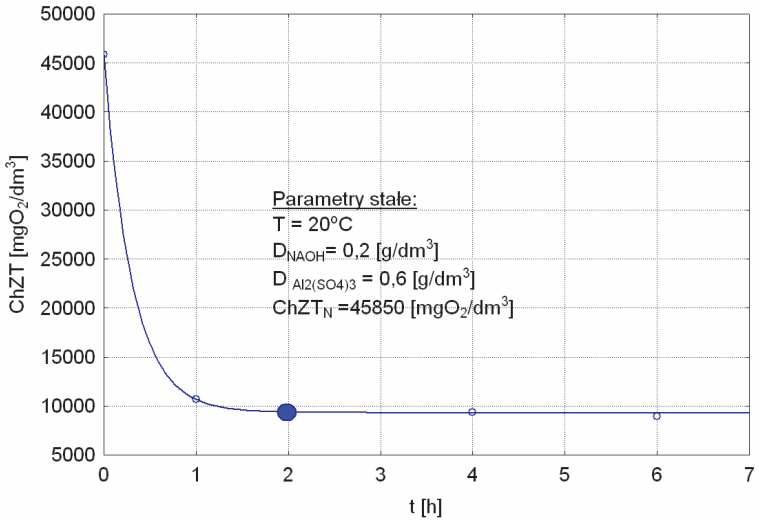

Rys. 4. Wpływ czasu sedymentacji t_S na wartość *ChZT* w cieczy nadosadowej po koagulacji
Fig. 4. Influence of sedimentation time t_S on *COD* value in wastewater after coagulation

Równanie aproksymacyjne po pierwszym i drugim stopniu ma postać:

$$ChZT(D, t_s)=\exp(10{,}53 - 5{,}84\cdot D) +\exp(1010{,}51 - 3{,}29\cdot t_s) +2504 \quad (2)$$

gdzie:
ChZT – chemiczne zapotrzebowanie na tlen [mg O_2/dm^3],
D – dawka $Al_2(SO_4)_3\cdot 18H_2O$ [g/dm^3],
t_S – czas sedymentacji [h].

Ekstrakt eterowy (E_E). Przy zmianie pierwszej zmiennej niezależnej (x_1), tj. dawce koagulantu $Al_2(SO_4)_3$ w przedziale od 0,00 g/dm^3 do 1,5 g/dm^3 oraz przy czasie sedymentacji t wynoszącym 2h wartość E_E obniżyła się z 120 mg/dm^3 do 71 mg/dm^3 – (dla największej dawki koagulanta), co odpowiada sprawności około 41% (rys. 5).

Znajduje to potwierdzenie w literaturze, gdyż koagulant powoduje powstawanie kłaczków o dużej powierzchni właściwej, na której adsorbują się substancje ekstrahujące eterem naftowym (Anielak 2000, Kowal & Świderska-Bróż 1997).

Przy zmianie drugiej zmiennej niezależnej (x_2), tj. czasu sedymentacji w przedziale od 0 do 6 godzin wartość E_E obniżyła się z wartości 120 mg/dm^3 do 84 mg/dm^3 po 6 godzinach sedymentacji. Ze wzrostem czasu sedymentacji grawitacyjnej maleje wartość wskaźnika E_E w cieczy nadosadowej. Przy czym wyraźne obniżenie się tej wartości odnotowano po 2,5 godzinnym czasie sedymentacji (rys. 6).

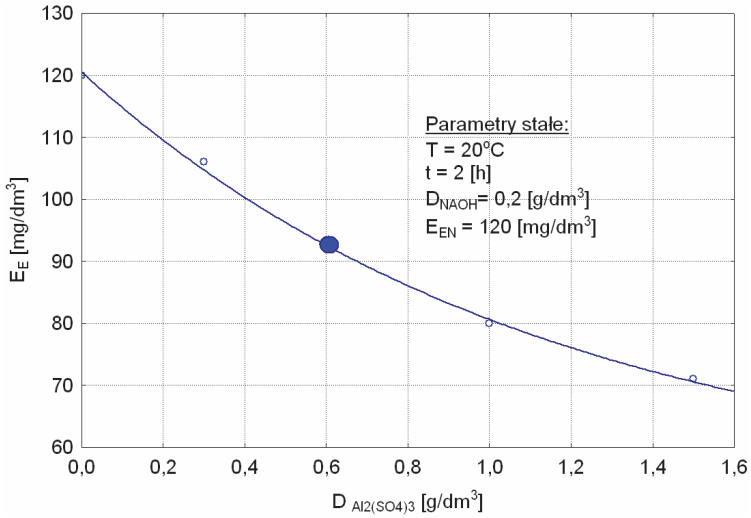

Rys. 5. Wpływ dawki $Al_2(SO_4)_3$ na stężenie ekstraktu eterowego E_E w cieczy nadosadowej po koagulacji
Fig. 5. Influence of $Al_2(SO_4)_3$ dose on ether extract E_E value in wastewater after coagulation

Równanie aproksymacyjne po pierwszym i drugim stopniu, wyznaczone na podstawie wyników badań, przyjęło następującą postać:

$$E_E(D, t_s) = \exp(4{,}22 - 0{,}88 \cdot D) + \exp(3{,}57 - 0{,}83 \cdot t_s) - 79 \qquad (3)$$

gdzie:
E_E – parametr wynikowy – ekstrakt eterowy [mg/dm^3],
D – dawka $Al_2(SO_4)_3 \cdot 18H_2O$ [g/dm^3],
t_S – czas sedymentacji [h].

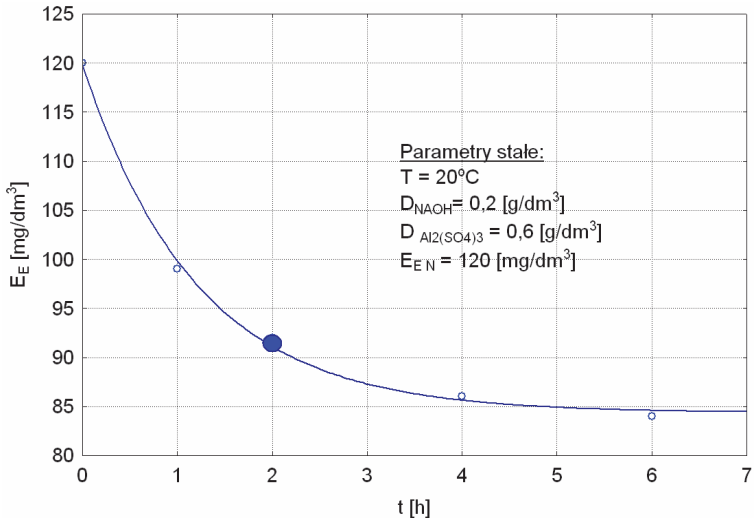

Rys. 6. Wpływ czasu sedymentacji t_S na stężenie substancji ekstrahujących się eterem E_E w cieczy nadosadowej po koagulacji
Fig. 6. Influence of sedimentation time t_S on ether extract E_E value in wastewater after coagulation

Zawiesina ogólna (Zo). Analiza wyników badań wskazuje, że przy zmianie pierwszej zmiennej niezależnej (x_1), tj. dawce koagulantu $Al_2(SO_4)_3$ w przedziale od 0,00 g/dm^3 do 1,5 g/dm^3, wartość Z_O obniżyła się z 16570 mg/dm^3 do 500 mg/dm^3(dla największej dawki koagulanta) (rys. 7). Stanowi to obniżkę rozpatrywanego parametru zmiennego wynikowego o 95,4%. Mechanizm przyczynowo-skutkowy tego przebiegu tłumaczy się tym, że w zakresie odczynu pH 5,5-7,5 wodorotlenek glinowy jest praktycznie nierozpuszczalny. W zakresie niskich wartości pH cząstki koloidu są obdarzone ładunkiem dodatnim, który nadają im kationy Al^{+3} i mogą wówczas destabilizować ujemnie naładowane koloidy powodujące mętność i barwę. Proces ten prowadzi do wytworzenia łatwo opadających kłaczków (Anielak 2000, Kowal & Świderska-Bróż 1997). Przy zmianie drugiej zmiennej niezależnej (x_2), tzn. czasu sedymentacji w przedziale od 0 do 6 godzin wartość Z_O obniżyła się z wartości 16570 mg/dm^3 do 680 mg/dm^3. Z analizy przebiegu krzywej wynika, że w przypadku tego wskaźnika czas sedymentacji wynoszący 1 h okazał się wystarczający (rys. 8).

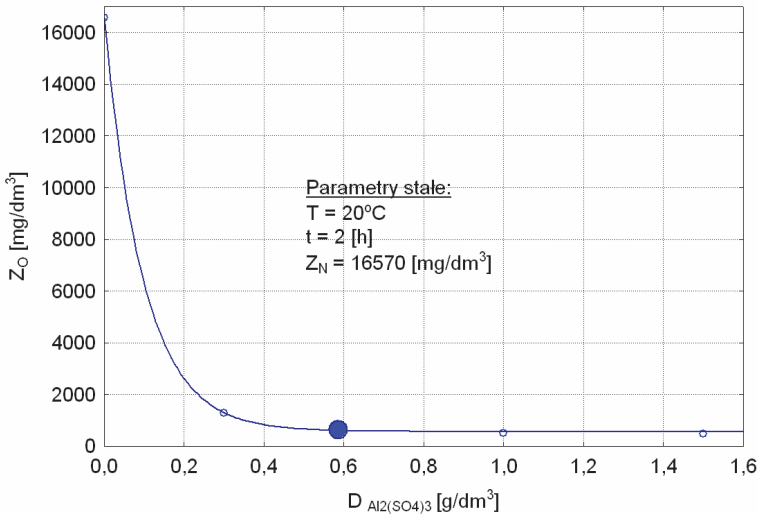

Rys.7. Wpływ dawki $Al_2(SO_4)_3$·na stężenie zawiesiny ogólnej w cieczy nadosadowej Z_O
Fig. 7. Influence $Al_2(SO_4)_3$·dose on total suspension Z_O value in wastewater after koagulation

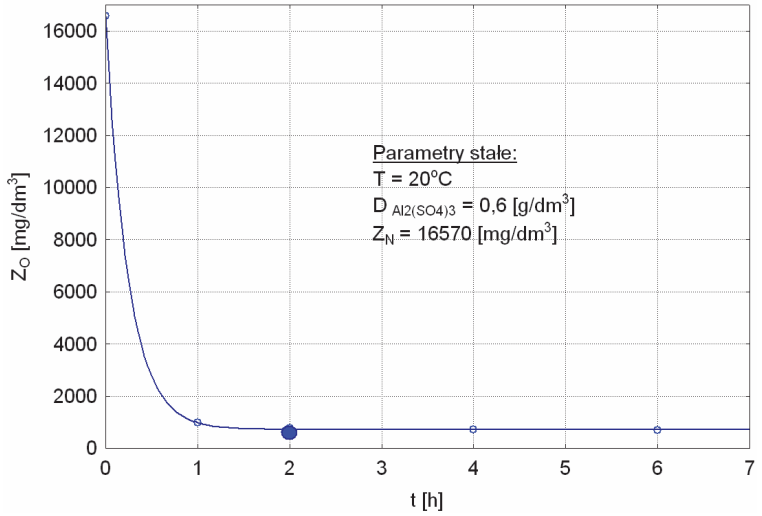

Rys. 8. Wpływ czasu sedymentacji grawitacyjnej t_S na stężenie zawiesiny ogólnej w cieczy nadosadowej Z_O po koagulacji
Fig. 8. Influence of sedimentation time t_S on total suspension Z_O value in wastewater after coagulation

Równanie po aproksymacji na pierwszym i drugim stopniu przyjmie postać:

$$Z_O(D, t_s) = \exp(9{,}68 - 10{,}28 \cdot D) + \exp(99{,}67 - 4{,}09 \cdot t_s) - 53{,}32 \quad (4)$$

gdzie:
Z_O – parametr wynikowy – zawiesina ogólna [mg/dm^3],
D – dawka $Al_2(SO_4)_3 \cdot 18H_2O$ [g/dm^3],
t_S – czas sedymentacji [h].

4. Wnioski

Podczyszczanie ścieków klejowych w procesie koagulacji siarczanem glinu umożliwia zmniejszenia stężenia badanych wskaźników zanieczyszczeń, ale wymaga doczyszczenia ścieków w kolejnych węzłach technologicznych, tj. w procesie filtracji grawitacyjnej oraz sorpcji.

Wykonane badania pozwoliły ustalić optymalne warunki procesu, tj. dawkę koagulanta $Al_2(SO_4)_3$ – 0,6 g/dm^3, czas sedymentacji t_s = 2 godziny, dla których odnotowano następującą obniżkę stężenia badanych wskaźników zanieczyszczeń: 77% ogólnego węgla organicznego (dla początkowej wartości 18200 mg C/dm^3), 80% substancji organicznych wyrażonych *ChZT* (dla stężenia początkowego 45850 mg O_2/dm^3), 20% substancji ekstrahujących się eterem (dla stężenia początkowego 120 mg/dm^3), 95% zawiesiny ogólnej (dla początkowej wartości 16570 mg/dm^3) oraz stężenia glinu o 67%.

Można również zaobserwować, że większa dawka $Al_2(SO_4)_3$ nie zmienia w sposób istotny stężenia parametrów wynikowych pozostających w ściekach po procesie koagulacji.

Podobne stwierdzenie można odnieść do czasu sedymentacji. Wydłużanie czasu sedymentacji powyżej 2 godzin nie wpłynie znacząco na badane wskaźniki zanieczyszczeń.

Literatura

Anielak, A.M. (2000). *Chemiczne i fizykochemiczne oczyszczanie ścieków*. Warszawa: Wydawnictwo Naukowe PWN.

Juraszka, B., Piecuch, T. (2008a). Badania podczyszczania ścieków poprodukcyjnych zawierających kleje organiczne w procesie filtracji grawitacyjnej. *Gaz, Woda i Technika Sanitarna, 4/2008*, 29-34.

Juraszka, B., Piecuch, T. (2008b). Podczyszczanie ścieków poprodukcyjnych zawierających kleje organiczne metodą koagulacji chlorkiem żelaza. *Rocznik Ochrona Środowiska, 10*, 221-242.

Juraszka, B., Piecuch, T. (2007). Podczyszczanie ścieków zawierających kleje organiczne w procesie sorpcji. *Inżynieria i Ochrona Środowiska, 10(3)*, 173-192.

Kowal, A.L., Świderska-Bróż, M. (1997). *Oczyszczanie wody*. Warszawa: Wydawnictwo Naukowe PWN.

Królikowski, A.J., Bartkowska, I., Rodowska, M. (1991). *Gospodarka wodno-ściekowa w zakładach przemysłowych.* Wydawnictwo Politechniki Białostockiej.

Królikowski, A.J. (1994). *Gospodarka wodno-ściekowa na obszarach niezurbanizowanych.* Wydawnictwo Politechniki Białostockiej.

Królikowski, A.J. (1993). *Pozyskiwanie i uzdatnianie wody.* Łódź: NOT.

Królikowski, A.J. (1990). *Problemy zaopatrzenia w wodę.* Wydawnictwo Politechniki Białostockiej.

Krupińska, I., Konkol A. (2015). Wpływ wybranych parametrów technologicznych na przebieg i skuteczność procesu koagulacji w oczyszczaniu wód podziemnych. *Zeszyty naukowe Uniwersytetu Zielonogórskiego. Inżynieria Środowiska, 157*, 152-163.

Kyzioł-Komosińska, J., Rosik-Dulewska, Cz., Dzieniszewska, A., Pająk, M. (2011). Compost as Biosorbent for Removal of Acid Dyes from the Wastewater Generated by the Textile Industry. *Archives of Environmental Protection, 37(4)*, 3-14.

Magrel, L. (2000). *Uzdatnianie wody i oczyszczanie ścieków, urządzenia, procesy, metody*. Białystok: Wydawnictwo Ekonomia i Środowisko.

Malej, J., Hołubowicz, D. (1996). Badania technologiczne nad oczyszczaniem ścieków z Zakładu płyt pilśniowych Alpex w Karlinie. *Zeszyty Naukowe Wydziału Budownictwa i Inżynierii Środowiska, 11*, 77-87.

Malej, J. (1997a). Usuwanie zawiesin ziarnistych i trudno opadających ze ścieków przemysłu drzewnego. *III Ogólnopolska Konferencja Naukowa nt.: Kompleksowe i szczegółowe Problemy Ochrony Środowiska,* 369-374.

Malej, J. (1997b). Zastosowanie osadu czynnego w procesie oczyszczania ścieków z przemysłu drzewnego. *Materiały konferencyjne pt. Współczesne problemy gospodarki wodno-ściekowej*, 305-314.

Piaskowski, K., Świderska-Dąbrowska R. (2006). Badania wstępne podatności ścieków klejowych na rozkład chemiczno-biologiczny. *Inżynieria i Ochrona Środowiska, 9(4)*, 379-394.

Puchlik, M., Struk-Sokołowska, J., Wołejko, E., Wydro, U. (2016). Problem oczyszczania ścieków z przemysłu spożywczego w małych i średnich przedsiębiorstwach. *Interdyscyplinarne Zagadnienia w Inżynierii i Ochronie Środowiska, 7,* 165-173.

Rozporządzenie Ministra Środowiska z dnia 18 listopada 2014 r. w sprawie warunków, jakie należy spełnić przy wprowadzaniu ścieków do wód lub do ziemi, oraz w sprawie substancji szczególnie szkodliwych dla środowiska wodnego (Dz.U. 2014 poz. 1800).

Żak, S., Zabłocki, L., Żółtowski, D. (2005). Technologia podczyszczania ścieków z produkcji klejów wytwarzanych na bazie żywic mocznikowo – formaldehydowych. *Monografie Komitetu Inżynierii Środowiska, 32,* 1007-1014.

Pre-treatment of Organic Wastewater by Coagulation with Aluminium Sulphate

Streszczenie

W pracy przedstawiono wyniki badań laboratoryjnych jednego węzła układu technologicznego podczyszczania ścieków przemysłowych, których dominującym składnikiem były resztki kleju oraz utwardzacza. Badania dotyczyły koagulacji siarczanem glinu $Al_2(SO_4)_3$ i sedymentacji grawitacyjnej. Ponadto, oceniono wpływ dawki koagulanta, czasu sedymentacji oraz stężenia początkowego zanieczyszczeń na efektywność procesu.

Zastosowanie koagulacji siarczanem glinu umożliwiło zmniejszenie o około 80% stężenia substancji organicznych trudno rozkładalnych wyrażonych jako ChZT oraz o 75% stężenia węgla organicznego. Jako optymalne warunki procesu przyjęto dawkę $Al_2(SO_4)_3$ wynoszącą 0,6 g/dm^3 oraz czas sedymentacji t_s 2 godziny. Wartości wskaźników zanieczyszczeń w wodzie nadosadowej po koagulacji zależały ściśle od stężenia początkowego w ściekach, przy czym zależność ta (spadek) była liniowa.

Zaproponowano, aby ścieki po koagulacji i sedymentacji grawitacyjnej były doczyszczane w kolejnych węzłach, tj. w procesie filtracji grawitacyjnej oraz sorpcji.

Na podstawie uzyskanych wyników badań wyznaczono, stosując metodę punktu centralnego, równania analityczno-empiryczne opisujące wpływ poszczególnych parametrów niezależnych na wartości parametrów wynikowych.

Abstract

This paper presents results of laboratory investigations on one node of proposed technological setup for pre-treatment of industrial wastewater, which contain mainly residual glue and hardener. The investigations concern coagulation process with application of $Al_2(SO_4)_3$ and sedimentation process. Authors estimated influence of coagulant dose, sedimentation time and initial concentration of contaminants on process effectiveness.

Applied process of coagulation with $Al_2(SO_4)_3$ reduces concentration of organic substances hardy digestible (COD) almost 80% and 75% of organic carbon . The investigations allowed to determine optimal values of process parameters: $Al_2(SO_4)_3$ dose – 0.6 g/dm^3, sedimentation time – 2 hours. The values of contamination parameters in wastewater after sedimentation depended strictly on their concentration before process, and this dependence (decrease) was linear.

Pre-treatment of wastewater containing glue using coagulation with $Al_2(SO_4)_3$ allowed to decrease concentrations of all contamination parameters, which were investigated in this work. However, when compared with requirements for wastewater inflowing to sewage system, wastewater after coagulation should undergo next processes proposed in technological setup, including filtration ad sorption.

On the basis of investigation results, analytical and empirical equations, which describe influence of individual independent parameters on resulting parameters, were determined using method of central point.

Słowa kluczowe:
podczyszczanie ścieków organicznych, kleje organiczne, przetwórstwo drewna, oczyszczanie ścieków, koagulacja, siarczan glinu

Keywords:
organic sewage sludge, organic adhesives, wood processing, sewage treatment, coagulation, aluminum sulphate

MIDDLE POMERANIAN SCIENTIFIC SOCIETY OF THE ENVIRONMENT PROTECTION
ŚRODKOWO-POMORSKIE TOWARZYSTWO NAUKOWE OCHRONY ŚRODOWISKA
Annual Set The Environment Protection
Rocznik Ochrona Środowiska
Volume/Tom 19. Year/Rok 2017 ISSN 1506-218X 572-589

Badania rozmieszczenia metali ciężkich w osadach dennych zbiorników retencyjnych na terenie zlewni zurbanizowanej

Ewa Wojciechowska, Aneta Rackiewicz, Nicole Nawrot, Karolina Matej-Łukowicz, Hanna Obarska-Pempkowiak
Politechnika Gdańska

1. Wstęp

Dopływ zanieczyszczeń ze zlewni zurbanizowanych prowadzi do degradacji wód powierzchniowych na terenie miast. Zagrożenie dla jakości cieków, zbiorników retencyjnych oraz gromadzących się w nich osadów stanowią ścieki deszczowe oraz bezpośredni spływ powierzchniowy z terenu zlewni. Źródłem zanieczyszczeń ścieków deszczowych na terenie zlewni zurbanizowanej jest przede wszystkim motoryzacja, pyły atmosferyczne, produkty spalania paliw oraz w mniejszym stopniu nawozy i środki ochrony roślin na terenach zielonych (Królikowski i in. 2005, Rosik-Dulewska i in. 2008). Zanieczyszczenia transportowane są wraz ze ściekami deszczowymi do odbiorników, którymi są przeważnie potoki i rzeki na terenie miast. W wielu miastach, m.in. w Gdańsku, są jednocześnie odbiornikami wylotów kanalizacji deszczowej a zarazem stanowiąc w praktyce otwarte kolektory kanalizacji deszczowej, które na części odcinków przechodzą w kolektory kryte (Suligowski 2017). Zanieczyszczenia obecne w ściekach deszczowych oraz w spływach powierzchniowych kumulują się w osadach gromadzących się w obiektach kanalizacji deszczowej (wpusty deszczowe, separatory, osadniki) oraz w zbiornikach retencyjnych zlokalizowanych na odbiornikach. Sedymentująca w tych obiektach zawiesina stanowi nie tylko najważniejsze pod względem ilościowym zanieczyszczenie ścieków opadowych, ale dodatkowo jest nośni-

kiem innych zanieczyszczeń, m.in. metali ciężkich, które adsorbują się na powierzchni cząstek zawiesiny (Gajewska i in. 2013, Obarska-Pempkowiak i in. 2015, Ociepa i in. 2015). Źródłem metali ciężkich, np. cynku jest przede wszystkim ruch uliczny: produkty ścierania nawierzchni ulic, tarcz hamulcowych i opon, ale także dachy lub rynny posiadające metalowe elementy (ocynkowane lub z blachy miedzianej) (Polkowska i Namieśnik 2008, Tobiszewski i in. 2010, Charters i in 2016) Istotnym źródłem metali jest również depozycja atmosferyczna (Murphy i in. 2015). W dotychczasowych badaniach (Królikowski i in. 2005) osadów pochodzących z obiektów kanalizacji deszczowej stwierdzono wyraźną zależność zawartości metali ciężkich od położenia obiektów. Osady z wpustów deszczowych zlokalizowanych w ulicach o dużym natężeniu ruchu charakteryzowały się wyraźnie wyższymi stężeniami metali niż osady z wpustów znajdujących się na ścieżce rowerowej. W bezpośrednim sąsiedztwie pasa drogowego (20-40 m) stwierdza się wysokie stężenia metali ciężkich (kadmu, miedzi, ołowiu, cynku oraz niklu) w glebach i roślinach, które maleje ze wzrostem odległości (Gawroński 2002). Oceny zawartości metali ciężkich w wodach zbiorników retencyjnych na terenie miast prowadzono m.in. w Poznaniu (Sojka i in. 2013) oraz w Kielcach (Bąk i in. 2012), wykazując obecność przede wszystkim cynku, ołowiu, miedzi i niklu. Metale ciężkie są toksyczne dla organizmów żywych, mają działanie kancerogenne i mutagenne oraz charakteryzują się zdolnością do kumulacji w łańcuchach troficznych (Ergönül i Altindağ 2014). Z tego powodu ocena zawartości metali ciężkich w osadach ze zbiorników retencyjnych na terenie zurbanizowanym jest istotna ze względu na konieczność właściwego zagospodarowania usuwanych okresowo osadów. W Polsce nie ma obecnie regulacji prawnych dotyczących jakości osadów pochodzących z kanalizacji deszczowej ani ze zbiorników retencyjnych oraz wytycznych ich oczyszczania i bezpiecznego zagospodarowania. Pomocne w ocenie jakości osadów z kanalizacji deszczowej mogą być kryteria geochemiczne opracowane przez Państwowy Instytut Geologiczny PIB (Bojakowska i Sokołowska 1998) oraz klasyfikacja niemiecka LAWA (Lander-Arbeitsgemeinschaft Wasser 1998).

Celem badań była wstępna ocena zawartości metali ciężkich: cynku, miedzi, ołowiu i kadmu w osadach dennych pochodzących z pięciu zbiorników retencyjnych zlokalizowanych na Potoku Oliwskim, będącym jednym z większych cieków na terenie Gdańska. Metale wytypo-

wano do badań na podstawie doniesień literaturowych, wskazujących na najczęstsze występowanie tych pierwiastków w spływach powierzchniowych z terenów zurbanizowanych (Królikowski i in. 2005, Gőbel i in. 2007,Wei i in. 2010).

2. Metodyka badań

2.1. Charakterystyka Potoku Oliwskiego

Badania prowadzono na pięciu zbiornikach retencyjnych zlokalizowanych na Potoku Oliwskim w Gdańsku. Potok Oliwski ma długość około 10 km i jest drugim pod względem długości ciekiem na terenie Gdańska. Jego źródło znajduje się w Złotej Karczmie, w pobliżu obwodnicy Trójmiasta (drogi S6), a powierzchnia zlewni całkowitej wynosi około 3050 ha. Potok posiada pięć dopływów, a jego ujście do Zatoki Gdańskiej znajduje się na plaży w dzielnicy Jelitkowo. Zlewnia Potoku ma charakter zróżnicowany: w górnym biegu są to głównie tereny leśne i rekreacyjne, zaś w biegu środkowych i dolnym koryto Potoku biegnie przez tereny o gęstej zabudowie mieszkaniowej, w pobliżu ruchliwych arterii komunikacyjnych (rys. 1). Również w swym górnym biegu Potok oraz jego dopływy narażone są na zanieczyszczenia pochodzące z ciągów komunikacyjnych (droga S6, ulica Spacerowa), a dodatkowo zlokalizowane są tu stawy rybne. Na całej swojej długości Potok pełni również funkcję odbiornika dla kanalizacji deszczowej. Na Potoku Oliwskim zlokalizowanych jest trzynaście zbiorników retencyjnych, o łącznej pojemności 70 000 m^3 i łącznej powierzchni około 13,5 ha, które oprócz ochrony przeciwpowodziowej pełnią funkcję rekreacyjną.

2.2. Pobieranie próbek wody i osadów

Próbki osadów pobierano w okresie kwiecień-czerwiec 2016 roku z pięciu zbiorników zlokalizowanych na Potoku Oliwskim (3 serie badawcze). Położenie zbiorników przedstawiono na rysunku 1, natomiast w tabeli 1 podano krótką ich charakterystykę.

Próbki osadów dennych pobierano w dwóch punktach każdego ze zbiorników, zlokalizowanych w rejonie dopływu (punkt A) i odpływu ze zbiorników (punkt B). Wierzchnią warstwę osadów dennych o miąższości ok. 20-25 cm pobierano z dna za pomocą narzędzi z tworzyw sztucznych, a następnie umieszczono w plastikowych pojemnikach (pojemność

120 ml). Próbki wody powierzchniowej pobierane były w dwóch punktach każdego zbiornika, zlokalizowanych w odległości około 1,5 m od brzegu, w pobliżu dopływu (punkt C) oraz odpływu ze zbiornika (punkt D). Próbki wody pobierano z głębokości ok. 30-50 cm poniżej zwierciadła wody do szklanych naczyń o pojemności 1 dm^3. Próbki wody oraz osadów dennych dostarczono w warunkach chłodniczych w czasie nie dłuższym niż 4 godziny do laboratorium w celu wykonania analizy chemicznej. Współrzędne punktów pobierania próbek wody i osadów dennych przedstawione zostały w tabeli 2.

Rys. 1. Lokalizacja badanych zbiorników retencyjnych na Potoku Oliwskim
Fig. 1. Location of analyzed retention tanks on Oliwski Stream

Tabela 1. Charakterystyka badanych zbiorników retencyjnych na Potoku Oliwskim
Table 1. Characteristics of analyzed retention tanks on Oliwski Stream

Nazwa zbiornika retencyjnego	Położenie	Powierzchnia	Pojemność retencyjna
	[km]	[ha]	[m^3]
Nr 2 „Orłowska”	0+920	0,58	2 900
Nr 3 „Chłopska”	1+411	1,20	6 000
Nr 4 „Subisława”	2+143	3,10	15 500
Nr 5 „Grunwaldzka”	2+819	1,69	8 450
Nr 8 „Spacerowa”	4+010	1,08	5 040

Tabela 2. Współrzędne punktów pobierania próbek wody i osadów dennych ze zbiorników retencyjnych na Potoku Oliwskim
Table 2. Coordinates of water sampling points and bottom sediments of analyzed retention tanks on Oliwski Stream

Nazwa zbiornika retencyjnego	Współrzędne punktów pobierania próbek wody i osadów dennych ze zbiorników retencyjnych			
	A:	B:	C	D
Nr 2 „Orłowska”	54°25’15.5”N 18°35’17.7” E	54°25’15.1”N 18°35’22.6”E	54°25’14.7”N 18°35’17.5”E	54°25’15.2”N 18°35’22.9”E
Nr 3 „Chłopska”	54°25’05.4”N, 18°35’05.9”E	54°25’03.6”N 18°35’05.9”E	54°25’05.2”N 18°35’05.8”E	54°25’03.1”N 18°35’00.4”E
Nr 4 „Subisława”	54°24’55.7”N, 18°34’24.7”E	54°24’56.0”N 18°34’29.3”E	54°24’55.7”N 18°34’25.1”E	54°24’58.8”N 18°34’34.0”E
Nr 5 „Grunwaldzka”	54°24’44.8”N 18°34’01.6”E	54°24’45.2”N 18°34’03.8”E	54°24’44.8”N 18°34’01.7”E	54°24’31.8”N 18°33’06.8”E
Nr 8 „Spacerowa”	54°24’33.5”N 18°33’15.9”E	54°24’32.9”N, 18°33’06.9”E	54°24’33.5”N 18°33’15.9”E	54°24’32.9”N 18°33’06.9”E

2.3. Metodyka oznaczeń

W pobranych próbkach wody powierzchniowej i osadów dennych ze zbiorników retencyjnych oznaczono stężenia metali: Zn, Cu, Pb oraz Cd. Próbki wody sączono przez sączek szklany GF/C wyprażony w temp. 450°C. Uzyskany przesącz poddawano mineralizacji i roztworzeniu. Próbki osadów przeniesiono do szalek Petriego, liofilizowano, a następnie poddawano mineralizacji materii organicznej na mokro i roztworzeniu. Naważkę 0,5 g próbki wysuszonego osadu umieszczano w bombach teflonowych. Następnie dodawano 2cm^3 kwasu nadchlorowego oraz wygrzewano przez 4 godziny w temperaturze 130°C. Kolejno dodawano – dwuetapowo w odstępie co 2 godziny – po 3 cm^3 kwasu fluorowodorowego (łącznie 6 cm^3) i ponownie wygrzewano w temperaturze 110°C. Bomby teflonowe ostudzono, odkręcono i umieszczono w płaszczach metalowych na noc na maszynce grzewczej. Drugiego dnia po odparowaniu kwasu fluorowodorowego próbki przeniesiono ilościowo do parownic kwarcowych za pomocą 6M kwasu solnego. Odparowano do białych dymów, dalej pod przykryciem ogrzewano do momentu zżółknięcia. Szkiełka zegarkowe opłukano kwasem solnym i próbki odparowano bez przykrycia. Zmineralizowane próbki rozpuszczono w 10 cm^3 0,1M kwasu azotowego. Przy każdej serii

próbek poddawanych mineralizacji uwzględniano jedną próbę ślepą, która pozwalała na wykrycie ewentualnych zanieczyszczeń wprowadzonych na etapie przetwarzania próbek. Dodatkowo do analiz wykonano rozcieńczenia dziesięcio-, stu- i tysiąckrotne próbek bazowych. Naczynia stosowane podczas kolejnych etapów przygotowania próbek uprzednio trawiono w czystym spektralnie kwasie azotowym, płukano trzykrotnie w wodzie destylowanej oraz redestylowanej.

Oznaczenia metali w tak przygotowanych roztworach wykonano techniką absorpcyjnej spektrometrii atomowej (AAS) z korekcją tła przy pomocy lampy deuterowej (Zn, Cu, Pb) oraz metodą spektrometrii mas sprzężoną z plazmą wzbudzaną indukcyjnie (ICP-MS) (Cd). W technice ASS atomizację próbki przeprowadzono z wykorzystaniem atomizera płomieniowego z wykorzystaniem mieszaniny gazów acetylen- powietrze. Każdorazowo przed wykonaniem analizy danego pierwiastka sporządzano krzywą wzorcową. Kontrolę uzyskiwanych wyników przeprowadzano poprzez zastosowanie certyfikowanych wzorców o odpowiednich stężeniach badanych metali ciężkich. Granica oznaczalności dla Zn oraz Cu przy zastosowaniu techniki ASA wynosi 0,05 μg/kg, a dla Pb 0,15 μg/kg. W przypadku Cd limit detekcji ASA wynosi 0,02 μg/kg. Zadeklarowano trzykrotne powtórzenia we wprowadzaniu próbek do urządzenia. Kontrolowano precyzję pomiaru w zakresie maksymalnym do 5%. Analizę zawartości Cd w próbkach osadów, ze względu na niskie zawartości tego pierwiastka, przeprowadzono przy pomocy bardziej czułej metody - ICP-MS. Spektrometr ICP-MS wykorzystany do analizy próbek zaopatrzony jest w standardowy kwarcowy palnik ICP, nebulizer, stożki niklowe, a próbki i wzorce podawane są za pomocą pompy perystaltycznej. Spektrometr poddawany jest codziennej optymalizacji, z zastosowaniem roztworu 10 μg/l (Mg, Cu, Rh, Cd, In, Ba, Ce, Pb, U) w 1% HNO_3. System wprowadzający składa się z rozpylacza i komory mgielnej. Podczas pomiarów stosowano próbę ślepą, która jest miarą czystości stosowanych odczynników oraz warunków panujących w pomieszczeniu pomiarowym. W przypadku licznych interferencji izobarycznych i poliatomowych spowodowanych przez powstanie różnych połączeń indywiduów pochodzących od gazu plazmowego (36Ar+, 38Ar+, 40Ar+ i ich dimerów), powietrza (28N2+, 29N2H, 14N), wody (16O, 17O, H i ich kombinacji z Ar, N, C) oraz kwasów zawierających S, Cl, P (i ich połączeń z Ar, O, N, H, C) zostały one wyeliminowane poprzez wybór odpowiedniego izotopu oraz wprowadzenie ewentualnej korekty matematycznej.

3. Wyniki i dyskusja

Potok Oliwski przepływa przez atrakcyjne rekreacyjnie i turystycznie rejony Gdańska, m.in. Dolinę Radości i Park Oliwski. Jednak charakter użytkowania zlewni sprawia, że Potok narażony jest na dopływ zanieczyszczeń antropogennych. Ze względu na bezpośrednie ujście do Zatoki Gdańskiej w rejonie popularnego kąpieliska morskiego i plaży w Jelitkowie, jakość wód Potoku jest systematycznie monitorowana przez Gminę Miasto Gdańsk. Analizowane są stężenia podstawowych wskaźników zanieczyszczeń (OWO, azot ogólny, fosfor ogólny, zawiesina ogólna), brak jest analiz stężeń metali w wodach czy osadach dennych. Zgodnie z danymi publikowanymi przez Urząd Miasta (http://www.gdansk.pl/urzad/zielony-gdansk) wskaźnik OWO przekracza wartość graniczną II klasy, natomiast średnie roczne wartości pozostałych wskaźników fizykochemicznych nie przekraczają wartości granicznych dla I klasy jakości wód. Potwierdzają to analizy prowadzone przez Matej-Łukowicz i Wojciechowską (2017), w których stwierdzono wzrost stężeń zanieczyszczeń w wyniku opadów.

Stężenia metali w próbkach wody pobranych z pięciu zbiorników na Potoku Oliwskim przedstawiono w tabeli 3. Rozporządzenie Ministra Środowiska z dnia 21 lipca 2016 r. w sprawie sposobu klasyfikacji stanu jednolitych części wód powierzchniowych oraz środowiskowych norm jakości dla substancji priorytetowych (Dz.U. 2016 poz. 1187) podaje kryterium zawartości metali dla wód powierzchniowych. Zgodnie z Rozporządzeniem stężenia cynku nie mogą przekraczać 1 mg/dm^3, zaś miedzi - 0,05 mg/dm^3 dla I i II klasy czystości. Porównanie stężeń zmierzonych w zbiornikach na Potoku Oliwskim do wartości określonych w Rozporządzeniu wskazuje, że stężenia cynku i miedzi odpowiadały klasie czystości I i II i były wyraźnie niższe od wartości granicznych. W tym samym Rozporządzeniu określono również dopuszczalne stężenia ołowiu dla wód powierzchniowych śródlądowych. Wyróżniono w tym wypadku wartość średnią roczną stężenia ołowiu i jego związków, wynoszącą 1,2 μg/dm^3 oraz maksymalne stężenie dopuszczalne (chwilowe) wynoszące 14 μg/dm^3. W przypadku trzech punktów pomiarowych (Orłowska C, Chłopska D i Subisława D) średnie stężenia ołowiu przekraczały wartość średnią roczną określoną w Rozporządzeniu. W żadnym punkcie pomiarowym nie stwierdzono przekroczenia maksymalnego stężenia dopuszczalnego.

Tabela 3. Stężenia metali w próbkach wody ze zbiorników retencyjnych na Potoku Oliwskim [μg/dm^3]; wartości średnie ± odchylenie standardowe
Table 3. Concentrations of metals in water samples collected from retention tanks on Oliwski Stream [μg/dm^3]; mean ± standard deviation

Punkt poboru	Pb	Cd	Zn	Cu
Orłowska C	1,5±0,0	0,02±0,00	2,0±0,2	1,3±0,1
Orłowska D	1,6±0,0	0,01±0,00	3,5±0,1	0,9±0,0
Chłopska C	0,8±0,0	0,04±0,00	0,1±0,0	0,7±0,1
Chłopska D	2,0±0,0	0,03±0,00	4,1±0,1	1,3±0,0
Subisława C	0,3±0,0	0,01±0,00	1,4±0,0	0,4±0,0
Subisława D	1,2±0,0	0,01±0,00	2,5±0,0	2,6±0,1
Grunwaldzka C	0,2±0,0	0,01±0,00	0,9±0,0	0,2±0,01
Grunwaldzka D	0,3±0,0	0,01±0,00	1,8±0,0	0,5±0,0
Spacerowa C	0,5±0,0	0,01±0,00	2,6±0,1	0,3±0,0
Spacerowa D	0,2±0,0	0,00±0,00	0,7±0,0	0,0±0,0

Na rysunkach 2-5 przedstawiono stężenia analizowanych metali ciężkich w osadach dennych. Dodatkowo, na każdym z rysunków pokazano wartości graniczne dla poszczególnych klas czystości według klasyfikacji osadów opracowanej przez Federalną Agencję Ochrony Środowiska (Umweltbundesamt) w Niemczech – tzw. klasyfikacja LAWA (Lander-Arbeitsgemeinschaft Wasser 1998) (tabela 4). Klasyfikacja ta dzieli wody, osady denne oraz zawiesiny na siedem klas czystości, w zależności od zawartości metali ciężkich. Klasa I charakteryzuje osady niezanieczyszczone, bez ingerencji antropogenicznej. Klasa I-II określa osady niezanieczyszczone lub z niewielką ingerencją antropogeniczną. Klasa II odpowiada osadom umiarkowanie zanieczyszczonym, a jednocześnie stanowi odniesienie dla pozostałych poziomów zanieczyszczania. Klasa II-III określa umiarkowane do znacznego zanieczyszczenie osadów, klasa III–znaczne zanieczyszczenie, klasa III-IV – bardzo silne zanieczyszczenie, klasa IV najwyższy poziom zanieczyszczenia.

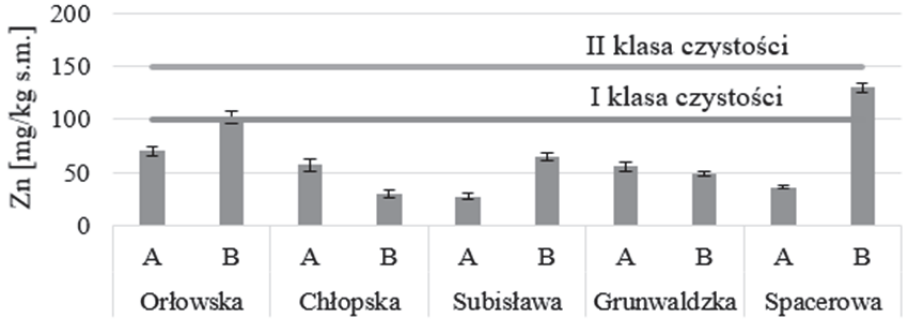

Rys. 2. Stężenia cynku w osadach dennych zbiorników retencyjnych na Potoku Oliwskim
Fig. 2. Concentrations of zinc in bottom sediments of retention tanks on Oliwski Stream

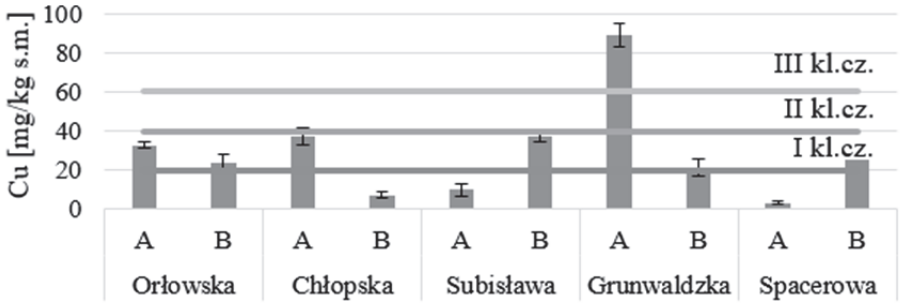

Rys. 3. Stężenia miedzi w osadach dennych zbiorników retencyjnych na Potoku Oliwskim
Fig. 3. Concentrations of copper in bottom sediments of retention tanks on Oliwski Stream

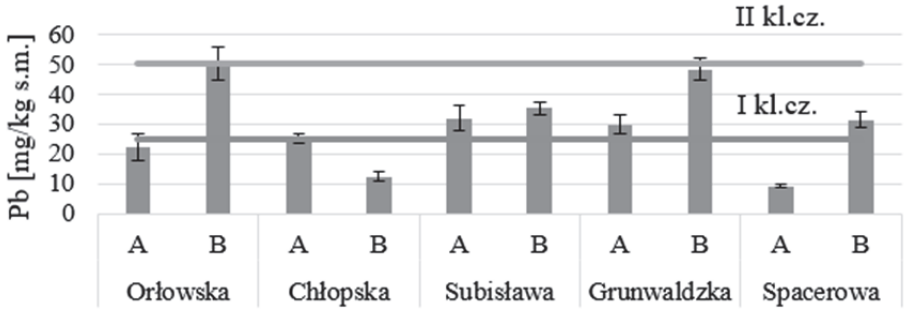

Rys. 4. Stężenia ołowiu w osadach dennych zbiorników retencyjnych na Potoku Oliwskim
Fig. 4. Concentrations of lead in bottom sediments of retention tanks on Oliwski Stream

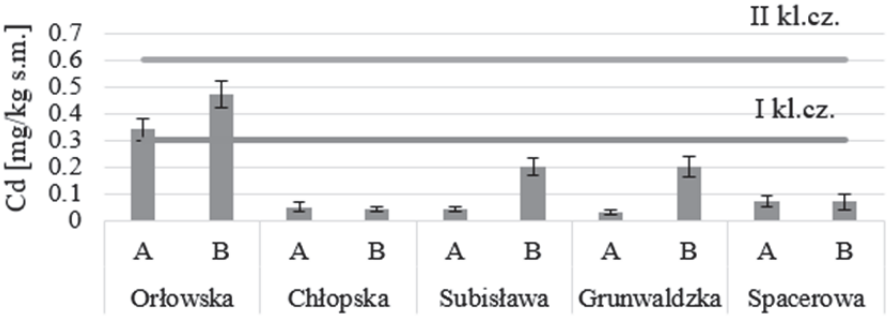

Rys. 5. Stężenia kadmu w osadach dennych zbiorników retencyjnych na Potoku Oliwskim
Fig. 5. Concentrations of cadmium in bottom sediments of retention tanks on Oliwski Stream

Tabela 4. Stężenia Zn, Pb, Cu i Cd w [mg/kg s.m.] dla poszczególnych klas czystości osadów według klasyfikacji Lander-Arbeitsgemeinschaft Wasser (1998)
Table 4. Concentrations of Zn, Pb, Cu and Cd [mg/kg s.m.] for each quality class according to Lander-Arbeitsgemeinschaft Wasser (1998)

Metal	Klasa czystości						
	I	I-II	II*	II-III	III	III-IV	IV
Cynk (Zn)	≤100	≤150	≤200	≤400	≤800	≤1600	>1600
Ołów (Pb)	≤25	≤50	≤100	≤200	≤400	≤800	>800
Miedź (Cu)	≤20	≤40	≤60	≤120	≤240	≤480	>480
Kadm (Cd)	≤0,3	≤0,6	≤1,2	≤2,4	≤4,8	≤9,6	>9,6

Stężenia metali w osadach dennych na ogół kształtowały się na poziomie I lub I-II klasy czystości według klasyfikacji LAWA, co odpowiada osadom niezanieczyszczonym, bez lub z niewielką ingerencją o charakterze antropogenicznym. W przypadku ołowiu w dwóch punktach pomiarowych (Orłowska B oraz Grunwaldzka B) stwierdzono wartości na pograniczu II klasy czystości (osady umiarkowanie zanieczyszczone) (rys. 5). Oba zbiorniki położone są w pobliżu ulic o dużym natężeniu ruchu, który prawdopodobnie stanowił źródło ołowiu w osadach. Mając na uwadze przekroczone w kilku punktach pomiarowych dopuszczalne średnie roczne stężenia ołowiu w próbkach wody, można stwierdzić, że ruchliwe arterie komunikacyjne przebiegające wzdłuż Potoku Oliwskiego stanowią zagrożenie dla jakości jego wód. Z drugiej strony, archiwalne wyniki badań wód i osadów z niektórych zbiorników na Potoku Oliwskim (Kasterka i in., 2010) wskazywały na wyższe stężenia ołowiu w osadach (w granicach 16-63 mg/kg s.m.). Może to świadczyć o zmniejszeniu depozycji ołowiu wskutek postępu w dziedzinie motoryzacji, który polegał na zastosowaniu katalizatorów i benzyn bezołowiowych.

Również na pograniczu II klasy czystości kształtowały się stężenia miedzi w osadach punktach pomiarowych Chłopska B i Subisława B (rys. 4). Natomiast w punkcie pomiarowym Grunwaldzka A stężenie miedzi odpowiadało klasie II-III, co oznacza umiarkowane do silnego zanieczyszczenie osadów tym metalem.

Propozycję klasyfikacji geochemicznej osadów wodnych opracował Państwowy Instytut Geologiczny (Bojakowska i Sokołowska 1998). Klasyfikacja ta przedstawia trzy klasy czystości osadów oraz podaje wartości tła geochemicznego dla poszczególnych pierwiastków (tabela 5).

Tabela 5. Klasyfikacja osadów na podstawie kryteriów geochemicznych, zawartości metali podane w ppm [mg/kg s.m.]
Table 5. Classification of bottom sediments according to geochemical criteria, concentrations of metals in ppm [mg/kg s.m.]

Metal	Tło geochemiczne	Klasa czystości		
		I	II	III
Cynk (Zn)	48	<200	<1000	<2000
Ołów (Pb)	10	<50	<200	<500
Miedź (Cu)	6	<20	<100	<200
Kadm (Cd)	<0,5	<1	<5	<20

Zgodnie z kryteriami Państwowego Instytutu Geologicznego (PIG) stężenia cynku, ołowiu i kadmu w osadach ze zbiorników na Potoku Oliwskim odpowiadają I klasie czystości. Stężenia kadmu we wszystkich punktach pomiarowych oraz stężenia cynku w punktach pomiarowych Chłopska A, Subisława A oraz Spacerowa B nie przekraczają wartości tła geochemicznego. Natomiast stężenia miedzi w 7. spośród 10. punktach pomiarowych (Orłowska A i B, Chłopska B, Subisława B, Grunwaldzka A i B oraz Spacerowa A) odpowiadały II klasie czystości. Stężenie miedzi w punkcie Grunwaldzka B wprawdzie mieści się w II klasie czystości osadów dennych według PIG, jednak zbliża się do górnej granicy tej klasy. Zbiornik Grunwaldzka zlokalizowany jest w dzielnicy stara Oliwa, w której część dachów wykonana jest w całości z blachy miedzianej lub posiada elementy wykonane z miedzi. Między innymi w podzlewni zbiornika, w odległości poniżej 1 km, znajduje się Archikatedra Oliwska, której dach (107 m długości, 19 m szerokości) wykonany jest w całości z blachy miedzianej. Występowanie dachów wykonanych z miedzi w obrębie podzlewni zbiornika Grunwaldzka, sugeruje związek z dość wysokimi stężeniami miedzi w analizowanych próbkach osadów, na poziomie wyraźnie wyższym niż stwierdzono w pozostałych punktach pomiarowych, których podzlewnie pozbawione są elementów miedzia-

nych pokryć dachowych. W badaniach Chartersa i in. (2016) stwierdzono wysokie stężenia miedzi w spływach z dachów Uniwersytetu w Canterbury i ich znaczący udział w ładunku miedzi odprowadzanych ze spływami powierzchniowymi ze zlewni. Z drugiej strony, według Wallindera i in. (2001) dachy wykonane z blachy miedzianej lub ocynkowanej, które są dłużej eksploatowane, pokryte są powierzchniową warstwą filmu, która chroni je przed korozją i zapobiega wymywaniu metali przez wodę opadową. Większość dachów, m.in. największy pod względem powierzchni dach Archikatedry, pokryte są wyraźnym zielonym nalotem patyny. Według badań Michelsa i in. (2017) odpływ z nowego dachu miedzianego zawierał 3630+/-1760 μg Cu/dm^3, natomiast odpływ z dachu pokrytego warstwą filmu 1460 +/-840 μg Cu/dm^3. Pennington i Webster-Brown (2008) również stwierdziły obecność miedzi w odpływie z dachów miedzianych pokrytych patyną (773-4000 μg Cu/dm^3), choć w mniejszych stężeniach niż w odpływie z dachów nowych (1000-6830 μg Cu/dm^3). Wskazuje to, że jakkolwiek w mniejszym stopniu niż dachy nowe, dachy pokryte patyną nadal mogą być źródłem miedzi. Miedź w osadach ze zbiornika Grunwaldzka mogła również zostać zdeponowana podczas wcześniejszych remontów elementów pokryć dachowych, tym bardziej, że osady nie były usuwane przez kilka lat poprzedzających okres badawczy. Badania Chartersa i in. (2016) wykazały również wysokie stężenia miedzi w spływach z parkingów i tras komunikacyjnych, zaś punkt pomiarowy Grunwaldzka A zlokalizowany jest bezpośrednio przy jednej z najbardziej ruchliwych arterii komunikacyjnych Trójmiasta.

4. Wnioski

1. Wody pochodzące ze zbiorników retencyjnych zlokalizowanych na Potoku Oliwskim nie wykazywały podwyższonych stężeń cynku, miedzi i kadmu. W punktach pomiarowych zlokalizowanych na trzech zbiornikach stwierdzono przekroczenia średniego rocznego dopuszczalnego stężenia ołowiu według Rozporządzenia Ministra Środowiska (Dz.U. 2016 poz. 1187).
2. Stężenia cynku, ołowiu i kadmu w osadach dennych ze zbiorników retencyjnych na Potoku Oliwskim odpowiadały I lub I-II klasie czystości według niemieckiej klasyfikacji LAWA oraz I klasie czystości

według klasyfikacji Państwowego Instytut Geologicznego. Stężenia kadmu we wszystkich punktach pomiarowych oraz cynku w 3. spośród 10. punktów pomiarowych nie przekraczały wartości tła geochemicznego.

3. Stężenia miedzi w analizowanych osadach były na wyższym poziomie w odniesieniu do wartości przedstawionych w klasyfikacjach osadów niż stężenia pozostałych osadów. Najwyższe zawartości miedzi występowały w osadach ze zbiornika Grunwaldzka, zlokalizowanego w dzielnicy stara Oliwa, w której występują stosunkowo liczne pokrycia dachowe z blachy miedzianej.

Podziękowania

Praca została wykonana w ramach grantu GRAM przyznawanego na zasadach konkursu przez Dziekana Wydziału Inżynierii Lądowej i Środowiska Politechniki Gdańskiej. Granty finansowane są ze środków na naukę zgodnie z Dz. U. Nr 96, poz. 615 ze zm.

Literatura

Bąk, Ł., Dąbek, L., Ozimina, E., & Sałata, A. (2012). Ocena jakości osadów pochodzących ze zbiornika otwartego miejskiej kanalizacji deszczowej w kontekście zagrożenia dla środowiska oraz możliwości ich zagospodarowania. W M. R. Dudzińska (Red.), *Polska inżynieria środowiska: prace; [IV Kongres Inżynierii Środowiska]*. *Lublin, 2,* 17-25.

Bojakowska, I., & Sokołowska, G. (1998). Geochemiczne klasy czystości osadów wodnych. *Przegląd geologiczny*, *46(1)*, 49-54.

Charters, F., Cochrane, T. A., & O'Sullivan, A. (2016). Predicting event-based stormwater contaminant loads from individual urban surfaces. Zaprezentowano na 11th South Pacific Stormwater Conference, New Zealand.

Ergönül, M. B., & Altindağ, A. (2014). Heavy Metal Concentrations in the Muscle Tissues of Seven Commercial Fish Species from Sinop Coasts of the Black Sea. *Rocznik Ochrona Środowiska*, *(Annual Set the Environment Protection)*, *16(1)*, 34-51.

Gajewska, M., Stosik, M., Wojciechowska, E., & Obarska-Pempkowiak, H. (2013). Wpływ technologii oczyszczania ścieków na spektrum rozmiarów cząstek w odpływie. *Rocznik Ochrona Środowiska*, *(Annual Set the Environment Protection)*, *15(11)*, 1191-1206.

Gawroński, K. (2002). Zanieczyszczenie gleb metalami ciężkimi i siarką na tle struktury funkcjonalno-przestrzennej gmin województwa małopolskiego. *Rocznik Ochrona Środowiska*, *4*, 379-401.

Gdańsk – oficjalny portal miasta. (2017). http://www.gdansk.pl/urzad/zielony-gdansk,781.html

Gőbel P., Dierkes C., Coldewey W.G. (2007). Storm water runoff concentration matrix for urban areas. *Journal of Contaminant Hydrology*, *91,* 26-42.

Kasterka, B., Kasterka, B., Ganczarek, P., & Klofczyńska, D. (2010). Badania jakości osadów dennych zbiornika Z-14 Potok Oliwski. niepublikowane.

Królikowski, A., Garbarczyk, K., Gwoździej-Mazur, J., & Butarewicz, A. (2005). *Osady powstające w obiektach systemu kanalizacji deszczowej*. Lublin: Polska Akademia Nauk.

Länderarbeitsgemeinschaft Wasser (LAWA). (1998). Beurteilung der Wasserbeschaffenheit von Fließgewässern in der Bundesrepublik Deutschland – Chemische Gewässergűteklassifikation.

Matej-Łukowicz, K., & Wojciechowska, E. (2017). Ocena stężenia form azotu w zurbanizowanej zlewni na przykładzie Potoku Oliwskiego. *Inżyniera Ekologiczna*, (w druku).

Michels, H. T., Boulanger, B. B., & Nikolaidis, N. P. (2017). Copper Roof Stormwater Runoff – Corrosion And The Environment. https://www. copper.org/environment/impact/NACE02225/

Murphy, L. U., Cochrane, T. A., & O'Sullivan, A. (2015). The Influence of Different Pavement Surfaces on Atmospheric Copper, Lead, Zinc, and Suspended Solids Attenuation and Wash-Off. *Water, Air, & Soil Pollution*, *226*(8). https://doi.org/10.1007/s11270-015-2487-2

Obarska-Pempkowiak, H., Gajewska, M., Wojciechowska, E., & Pempkowiak, J. (2015). Storm Water Treatment in TWs. W H. Obarska-Pempkowiak, M. Gajewska, E. Wojciechowska, & J. Pempkowiak, *Treatment Wetlands for Environmental Pollution Control* (105-120). Cham: Springer International Publishing. https://doi.org/10.1007/978-3-319-13794-0_6

Ociepa, E., Mrowiec, M., Deska, I., & Okoniewska, E. (2015). Pokrywa śnieżna jako ośrodek depozycji zanieczyszczeń. *Rocznik Ochrona Środowiska*, *(Annual Set the Environment Protection)*, *17(1)*, 560-575.

Pennington, S. L., & Webster□Brown, J. G. (2008). Stormwater runoff quality from copper roofing, Auckland, New Zealand. *New Zealand Journal of Marine and Freshwater Research*, *42(1)*, 99-108. https://doi.org/10.1080/00288330809509940.

Polkowska, Ż., & Namieśnik, J. (2008). Road and roof runoff waters as a source of pollution in a big urban agglomeration (Gdansk, Poland). *Ecological Chemistry and Engineering. 15(3)*, 375-385.

Rozporządzenie Ministra Środowiska z dnia 21 lipca 2016 r. w sprawie sposobu klasyfikacji stanu jednolitych części wód powierzchniowych oraz środowi-

skowych norm jakości dla substancji priorytetowych (Dz.U. 2016 poz. 1187). (2016).

Rosik-Dulewska, Cz., Głowala, K., Karwaczyńska, U., Robak, J. (2008). Elution of Heavy Metals from Granulates Produced from Municipal Sewage Deposits and Fly-Ash of Hard and Brown Coal in the Aspect of Recycling for Fertilization Purposes. *Archives of Environmental Protection, 34(2)*, 63-71.

Sojka, M., Siepak, M., & Gnojska, E. (2013). Ocena zawartości metali ciężkich w osadach dennych wstępnej części zbiornika retencyjnego Stare Miasto na rzece Powie. *Rocznik Ochrona Środowiska (Annual Set the Environment Protection)*, *15*, 1916–1928.

Suligowski, Z. (2017). Ochrona przed wodami opadowymi. Problem o znaczeniu strategicznym. *Forum Eksploatatora*, *1(88)*, 46-54.

Tobiszewski, M., Polkowska, Ż., Konieczka, P., Namieśnik, J., & others. (2010). Roofing materials as pollution emitters–concentration changes during runoff. *Pol. J. Environ. Stud*, *19(5)*, 1019-1028.

Wallinder, I. O., Leygraf, C., Karlén, C., Heijerick, D., & Janssen, C. R. (2001). Atmospheric corrosion of zinc-based materials: runoff rates, chemical speciation and ecotoxicity effects. *Corrosion Science*, *43(5)*, 809-816. https://doi.org/10.1016/S0010-938X(00)00136-0

Wei, Q., Zhu, G., Wu, P., Cui, L., Zhang, K., Zhou, J., Zhang, W. (2010). Distributions of typical contaminant species in urban short-term storm runoff and their fates during rain events: A case of Xiamen City. *Journal of Environmental Sciences, 22(4)*, 533-539.

Investigations of Heavy Metals Distribution in Bottom Sediments from Retention Tanks in the Urbanized Watershed

Streszczenie

Potoki na terenach miejskich stanowią odbiornik dla kolektorów kanalizacji deszczowej oraz dla spływów powierzchniowych, które spłukują zanieczyszczenia z terenu zlewni. W zbiornikach retencyjnych budowanych na potokach m.in. w celu ochrony przed powodzią, następuje sedymentacja zawiesiny ogólnej, stanowiącej nośnik dla innych zanieczyszczeń, między innymi metali ciężkich. Źródłem metali ciężkich w zlewni miejskiej jest przede wszystkim ruch uliczny (wycieki paliw i płynów samochodowych, zużywanie się opon, klocków hamulcowych, ścieranie się nawierzchni drogowej), ale również spływy z dachów, pyły atmosferyczne itd. Ocena zawartości metali ciężkich w osa-

dach jest istotna z punktu widzenia dalszego zagospodarowania lub unieszkodliwiania osadów okresowo usuwanych ze zbiorników. Osady denne zdeponowane w zbiornikach retencyjnych są bardzo dobrym wskaźnikiem jakości wody i ekosystemu wodnego oraz zapisem działalności antropogenicznej. W artykule przedstawiono wyniki analiz stężeń wybranych metali ciężkich (cynk, ołów, miedź, kadm) w próbkach wody oraz osadów dennych pobieranych z pięciu zbiorników retencyjnych znajdujących się na Potoku Oliwskim w okresie od kwietnia do czerwca 2016 roku. Potoki Oliwski to jeden z najdłuższych potoków na terenie Gdańska. Potok przepływa przez Dolinę Radości, Park Oliwski, Żabiankę i uchodzi bezpośrednio do Zatoki Gdańskiej w rejonie dzielnicy Jelitkowo, słynącej z popularnej plaży i kąpieliska morskiego. W próbkach wody stężenia cynku, miedzi i kadmu były na niskim poziomie, natomiast w trzech zbiornikach stwierdzono przekroczenie dopuszczalnego średniego rocznego stężenia ołowiu według Rozporządzenia Ministra Środowiska (Dz.U. 2016 poz. 1187). Stężenia metali w osadach dennych wykazały zróżnicowanie ilościowe i przestrzenne. Stężenia cynku wynosiły od 27 do 130 mg/kg s.m., miedzi od 2,3 do 89 mg/kg s.m, zaś stężenia ołowiu od 7 do 50 mg/kg s.m, w zależności od położenia zbiornika retencyjnego i charakterystyki jego zlewni. Najwyższe stężenia miedzi odnotowano w osadach pobranych ze zbiornika retencyjnego Grunwaldzka zlokalizowanego w dzielnicy Stara Oliwa, w której stosunkowo liczne są dachy wykonane z blachy miedzianej lub posiadające miedziane elementy. W celu oceny stopnia zanieczyszczenia osadów, stężenia metali w osadach porównano do wytycznych zawartych w klasyfikacjach osadów, np. klasyfikacji osadów dennych według kryteriów geochemicznych opracowanych przez Państwowy Instytut Geologiczny oraz niemieckiej klasyfikacji LAWA (Lander- Arbeitsgemeinschaft Wasser) z 1998 roku. W odniesieniu do cynku, ołowiu i kadmu stwierdzono dobrą jakość osadów. Stężenia kadmu nie przekraczały wartości tła geochemicznego według kryteriów podanych przez Państwowy Instytut Geologiczny. Natomiast stężenia miedzi w osadach dennych kształtowały się na poziomie oznaczającym umiarkowane zanieczyszczenie.

Abstract

Streams flowing through the urbanized areas receive surface runoff which washes out pollutants from the watershed. At many streams the outlets of urban drainage systems are also located, contributing to the pollution discharged with the runoff directly to the streams. In retention tanks built on urban streams for flooding protection needs, sedimentation of total suspended solids takes place. Along with the suspended solid also the pollutants adsorbed on solid particle surfaces, including heavy metals, accumulate in the sediments. The main source of heavy metals is urban traffic (spills fuel and automotive

fluids, tire wear, brake pads, attrition of the road surface), but metals are also washed out from the roofs surfaces, deposited with dust etc. Assessment of heavy metals concentration is important for future methods of sediments disposal. Sediments deposited in the reservoirs are a very good indicrato of water quality, aquatic ecosystem and also a proper track record of antropogenic. In the article concentrations of four heavy metals: zinc, copper, lead and cadmium was analysed in water and sediment samples collected from five retention tanks along Oliwski Stream. Oliwski Stream is one of the longests streams in gdańsk. It flows through the Valley of Joy, Oliwa Park, Zabianka and outflows directly to the Gulf of Gdańsk near the popular beach and bathing place in Jelitkowo. Concentrations of zinc, copper and cadmium in water samples were low. In case of lead the admissible mean annual concentrations were exceeded in three locations. Metals concentrations in collected sediment samples were on different levels depending on retention tank and some characteristics of its watershed. Concentrations of zinc varied from 27 to 130 mg/kg d.m., copper from 2,3 do 89 mg/kg d.m, and lead from 7 to 50 mg/kg d.m. The highest concentrations of copper were measured in the bottom sediments from retention tank Grunwaldzka situated in the district old Oliwa, whith relatively high numer of copper roofs. In order to facilitate the quality assessment, concentrations of heavy metals were compared to the geochemical criteria proposed by Polish Geological Insitute and to the German sediment classification LAWA (Lander- Arbeitsgemeinschaft Wasser) from 1998. The concentrations of zinc, lead and cadmiumwere on low level, comparing with both classifications. The concentrations of cadmium did not exceed the level of geochemical background, according to Polish Geological Insitute. In case of copper the moderate level of pollution was observed.

Słowa kluczowe:
klasyfikacja osadów, cynk, miedź, ołów

Keywords
sediment classification, zinc, copper, lead

MIDDLE POMERANIAN SCIENTIFIC SOCIETY OF THE ENVIRONMENT PROTECTION
ŚRODKOWO-POMORSKIE TOWARZYSTWO NAUKOWE OCHRONY ŚRODOWISKA
Annual Set The Environment Protection
Rocznik Ochrona Środowiska
Volume/Tom 19. Year/Rok 2017 ISSN 1506-218X 590-599

Badania numeryczne wpływu zabudowy grzejnika konwekcyjnego półką poziomą z zakrzywieniem na rozkład pól temperatury i prędkości powietrza w pomieszczeniu

Magdalena Orłowska, Aleksander Szkarowski,
Sylwia Janta-Lipińska
Politechnika Koszalińska

1. Wprowadzenie

W dzisiejszych czasach wystrój wnętrz odgrywa znaczącą rolę. Ludzie decydują się na różne elementy ozdobne, architektoniczne, nie myśląc do końca o ich wpływie na cyrkulację powietrza w pomieszczeniu. "Współczesne techniki wytwarzania nie są pozbawione problemów związanych z zapewnieniem odpowiedniej jakości wytwarzanych wyrobów przy jednoczesnej minimalizacji kosztów ich produkcji jak i wzroście wydajności procesu. Dominującą rolę w tym działaniu odgrywa racjonalne wykorzystanie energii i ochrona środowiska". (Bohdal i Walczak 2013)

Grzejniki powinny zapewniać odczucie komfortu w pomieszczeniu. Ogólne wymagania stawiane grzejnikom przede wszystkim to:

- zapewnienie odpowiedniej wydajności cieplnej,
- bezpieczna konstrukcja,
- regulacja oddawanego ciepła,
- łatwość demontażu i czyszczenia,
- niewielkie gabaryty przy intensywnej wymianie ciepła,
- niski ciężar i pojemność cieplna,
- odporność na korozję,

- łatwy i szybki montaż,
- niski koszt,
- optyczne dopasowanie do pomieszczenia.

O powszechnym zastosowaniu płytowych wymienników zdecydowały niewątpliwie zalety wynikające z samej konstrukcji czy zasady działania, związane m. in. z warunkami wymiany ciepła (współ- lub przeciwprąd), zakresem wydajności, czynnościami serwisowymi itd.

Płytowe wymienniki ciepła charakteryzują się:

- dużą mocą cieplną przy niewielkich różnicach temperatury współdziałających termicznie czynników,
- wysokimi wartościami współczynników przekazywania ciepła, a więc i dużą sprawnością,
- małą pojemnością cieplną,
- szerokim zakresem wydajności,
- wysoką wytrzymałością na ciśnienie i temperaturę,
- możliwością współpracy z substancjami agresywnymi,
- zwartą konstrukcją, a przez to małym ciężarem,
- bezpieczeństwem eksploatacji i niezawodnością działania dzięki zastosowaniu wielu innowacyjnych rozwiązań (m.in. komory bezpieczeństwa, podwójne ścianki płyt, system rozdzielania czynnika i in.),
- elastycznością konfiguracji i łatwością rozbudowy,
- prostymi czynnościami montażowymi oraz konserwacyjnymi (Florek i Pawlus 2006).

Informacje o zaleceniach montażowych grzejników nie pokrywają się ze sobą, co oznacza brak jednoznacznych danych! Przy montażu okien nieodzownie montowane są popularne półki poziome − parapety. Często mając na względzie zabiegi estetyczno-architektoniczne robi się to nieprzemyślanie, przez co można pogorszyć wymianę ciepła, a co za tym idzie wydajność cieplną grzejnika. Szerokość i budowa parapetów jest różna. Niektóre posiadają nawet swoiste zakrzywienia, zaokrąglenia. W tym momencie powstaje pytanie? Czy takie elementy poprawiają warunki cieplne w pomieszczeniu, czy może blokują swobodny przepływ powietrza? Autorzy artykułu (Orłowska i Czapp 2012) stwierdzili, że im węższy i wyżej położony nad grzejnikiem parapet tym wydajność cieplna

grzejnika większa przy czym najkorzystniejsza cyrkulacja powietrza pozostaje w przypadku układu bez parapetu. Artykuł jest kontynuacją bardzo szerokiego zagadnienia badania konwekcyjnego wymiennika ciepła pracującego przy różnych warunkach brzegowych. Niniejsza publikacja ma na celu podjęcie próby porównania wymiennika ciepła pracującego bez osłonięcia parapetem (rys. 1a) oraz z parapetem zakrzywionym (rys. 1b).

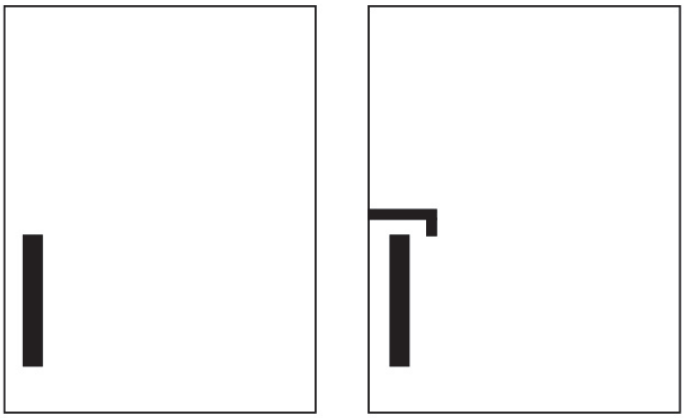

Rys. 1. Schemat pomieszczenia z konwekcyjnym wymiennikiem ciepła a) i zakrzywionym parapetem b)
Fig. 1. Diagram of room with convection heat exchanger a) and curved sill b)

2. Obliczenia numeryczne

Obliczenia numeryczne wykonano przy użyciu kodu komercyjnego Ansys, Flotran. Program ten oparty jest na rozwiązaniu równań bilansu energii, pędu i masy, stosowanych w Numerycznej Termomechanice Płynów (ang. CFD – Computational Fluid Dynamic). Wersja standardowa kodu obliczeniowego umożliwia prowadzenie modelowania w oparciu o tradycyjne zależności fenomenologiczne oraz dodatkowe równania domknięcia, opisujące wspomniane wcześniej turbulentne strumienie pędu i energii. Badany układ zamodelowano w przestrzeni dwuwymiarowej. Dwuwymiarowy tzw. model domknięcia opracowany został przez *Laundera*. W przypadku niewielkich prędkości przepływu czynnika przyjmuje się często model turbulencji dla niskich wartości liczby Reynoldsa (Szpakowska 2010).

Założenia dla modelu:

- pomieszczenie o wymiarach 2 x 2 m,
- grzejnik o szerokości 0,1 m i wysokości 0,5 m umieszczony na ścianie bez okna,
- stan ustalony,
- ruch turbulentny lub laminarny w zależności od rozpatrywanego układu,
- temperatura powierzchni grzejnej 328 K,
- temperatura otoczenia 293 K,
- prędkość na ściankach 0 m/s.

Po zadaniu odpowiednich parametrów dla powietrza, określeniu temperatury i prędkości ścianek pomieszczenia oraz grzejnika program wykonuje obliczenia dla zadanej liczby iteracji.

3. Wyniki obliczeń numerycznych

Uzyskane wyniki obliczeń przedstawiono na rysunkach 2-7. Obejmują one otrzymane pola temperatury i prędkości powietrza oraz współczynnik przejmowania ciepła α, który decyduje o intensywności wymiany ciepła.

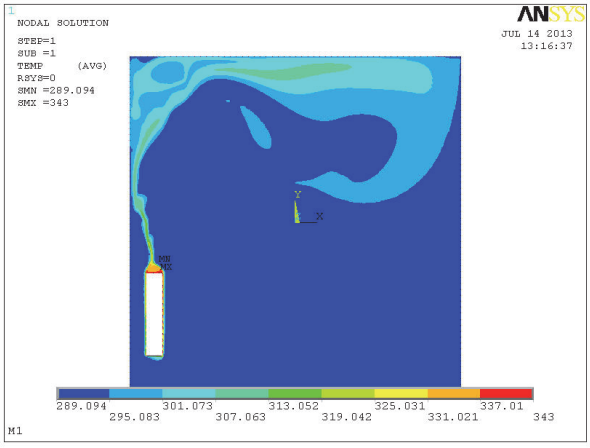

Rys. 2. Rozkłady pól temperatury powietrza w układzie bez półki poziomej (Ansys)
Fig. 2. Distribution of air temperature fields in a system without a horizontal shelf (Ansys)

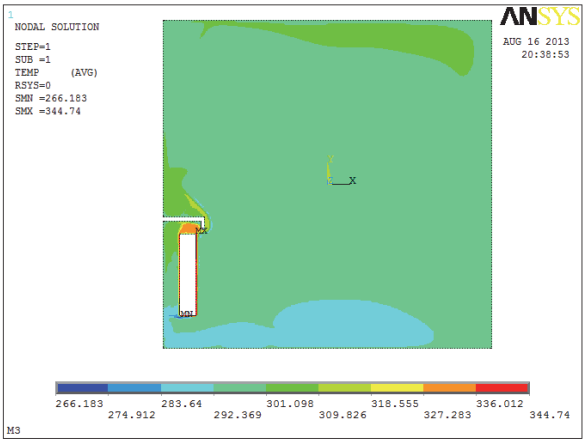

Rys. 3. Rozkłady pól temperatury powietrza w układzie z półką poziomą posiadającą zakrzywienie (Ansys)
Fig. 3. Distribution of air temperature fields in a system with a horizontal curved shelf (Ansys)

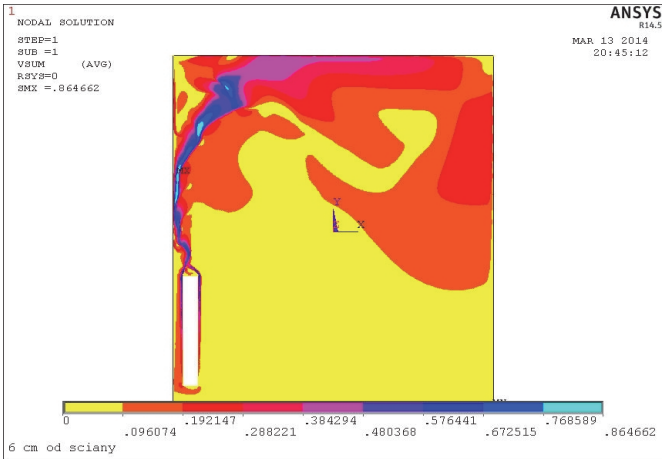

Rys. 4. Rozkłady pól prędkości powietrza w układzie bez półki poziomej (Ansys)
Fig. 4. Distribution of air velocity fields in a system without an horizontal shelf (Ansys)

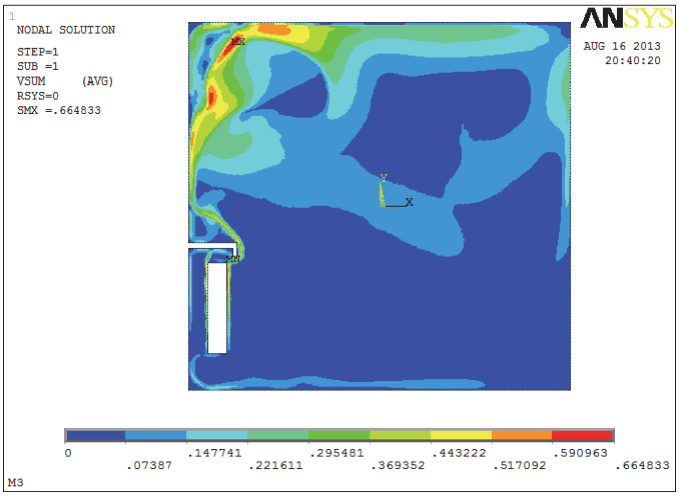

Rys. 5. Rozkłady pól prędkości powietrza w układzie z półką poziomą z zakrzywieniem (Ansys)
Fig. 5. Distribution of air velocity fields in a system with a horizontal curved shelf (Ansys)

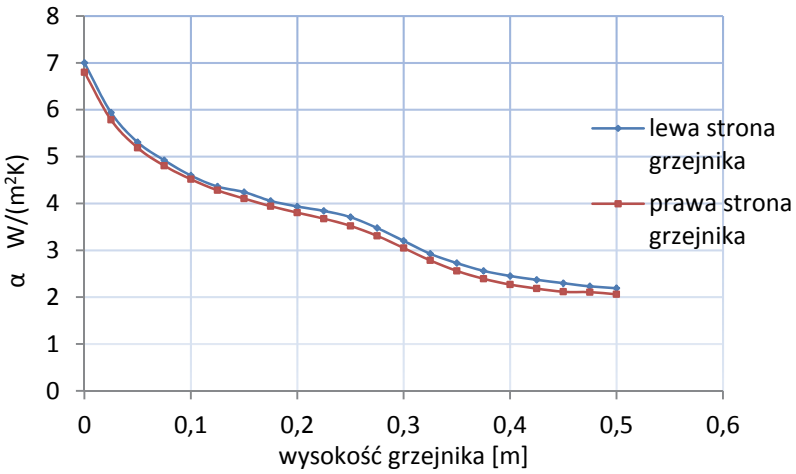

Rys. 6. Współczynnik przejmowania ciepła α po prawej i lewej stronie grzejnika przy zabudowie półką z zakrzywieniem w funkcji wysokości grzejnika
Fig. 6. Heat transfer coefficient α on the right and left side of the radiator with a curved shelf as a function of radiator height

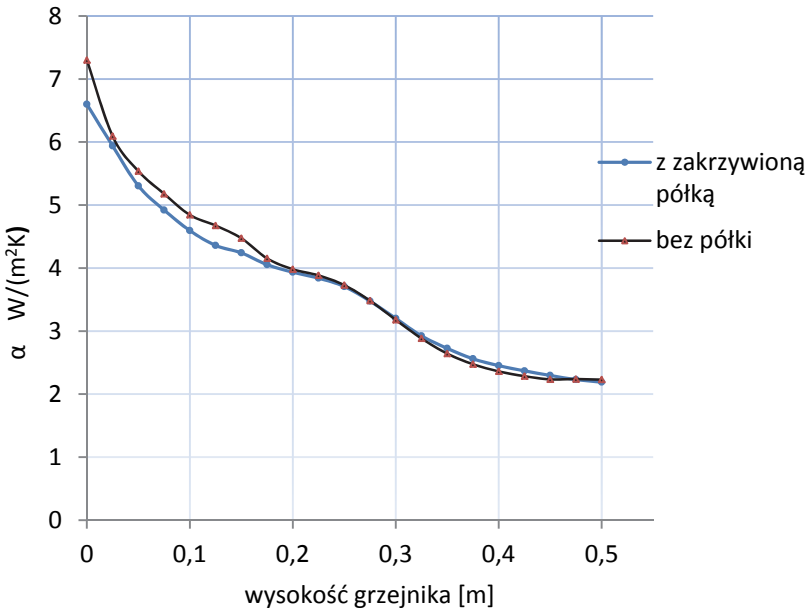

Rys. 7. Współczynnik przejmowania ciepła α przy zabudowie półką poziomą z zakrzywieniem oraz bez półki w funkcji wysokości grzejnika
Fig. 6. Heat transfer coefficient α for radiator with a curved shelf and without shelf as a function of radiator height

4. Wnioski

Z przeprowadzonych symulacji komputerowych jasno wynika, iż stosowanie półek z zakrzywieniem pogarsza cyrkulację powietrza w pomieszczeniu. Korzystniejsze pola temperatury i prędkości powietrza otrzymano w układzie bez półki. Podobnie przedstawia się przebieg współczynnika przejmowania ciepła α. Dla większej czytelności zobrazowano go w formie wykresu wzdłuż wysokości grzejnika. Widać wyraźnie, że od dolnej strony grzejnika współczynnik przejmowania ciepła α maleje wraz ze wzrostem wysokości, przy czym większe wartości przyjmuje w układzie bez półki poziomej (rys. 7). Malejące wartości współczynnika przejmowania ciepła α wzdłuż wysokości grzejnika spowodowane są wzrostem grubości warstwy przyściennej, a więc większymi oporami przepływu. Dodatkowo przedstawiono również zależność współczynnika przejmowania ciepła α po prawej i lewej stronie grzejnika

(rys. 6). Z lewej strony grzejnik znajduje się przy ścianie pomieszczenia. Ściana pozostaje nie bez znaczenia. Tworzy się w ten sposób kanał konwekcyjny, w którym powstaje ciąg. W związku z tym wartości alfa są wyższe niż w przypadku prawej strony grzejnika, która pozostaje niczym nie osłonięta.

Literatura

Ansys Flotran CFD.

Bohdal, Ł., Walczak, P., (2013). Ekomodelowanie cięcia blach nożycami krążkowymi. *Rocznik Ochrona Środowiska, 15*, 863-872.

Florek, R., Pawlus, J., (2006). Płytowe wymienniki ciepła w instalacjach chłodniczych – charakterystyka konstrukcyjna i przepływowa. *Technika Chłodnicza i Klimatyzacyjna, 5/2006*, 18.

Orłowska, M., Czapp, M., (2012). Analiza numeryczna wydajności cieplnej konwekcyjnego wymiennika ciepła obudowanego poziomymi płytami. *Rocznik Ochrona Środowiska, 14*, 582-586.

Szpakowska M./Orłowska M., (2010) *Badanie wpływu warunków brzegowych i na intensyfikację konwekcyjnej wymiany ciepła od płyty pionowej w przestrzeni częściowo ograniczonej*. Praca doktorska.

Research on the Impact of a Curved Horizontal Shelf over Radiator on the Distribution of Air Temperature and Velocity Fields

Abstract

Main objective of this work was to perform numerical studies with heat exchanger covered in horizontal shelves. Today's possibilities of commercial computer programs are impressive. Calculations were performed using the simulation code Ansys Flotran. One can simulate flows under the given boundary conditions. In the future, the author wants to expand the study to verify the numerical calculations on the laboratory measuring station.

This article concerns plate heat exchangers. These are the most popular and currently used in c.h. types of heaters. There are a whole range of different sizes, colors, visual effects and high thermal inertia determine the choice.

Very often, such heaters are installed according to installation conditions. Sometimes, improper installation or cover may be associated with decreased heat output efficiency. This applies not only to furnitures but also a very popular horizontal shelves – window sills, which have different depths and width and they are made of various materials, for example – plastic or marble.

Sometimes, they have a curvature of the edge. The question is, how this type of structures influence the thermal effect – the performance of the radiator?

This article presents selected results of numerical research on the convective heat exchanger. Heat was encased in a horizontal plate with curvation – Fig. 1. Temperature field, velocity and air density – Fig. 2-5. were obtained. heat transfer coefficient α, which determines the intensity of heat exchange was set on that basis.

It turned out that the curvature of the enclosure and heater sill affects the distribution of the heat transfer coefficient α. Therefore, no horizontal shelf is preferred. we should pay attention to this type of decorative elements and think about mounting conditions to take full advantage of the heat exchanger when we deciding on the cover.

Streszczenie

Celem pracy było wykonanie badań numerycznych płytowego wymiennika ciepła obudowanego półką poziomą z zakrzywieniem. Dzisiejsze możliwości komercyjnych programów komputerowych są imponujące. Obliczenia wykonano przy użyciu kodu obliczeniowego Ansys Flotran. Dzięki niemu można symulować przepływy przy zadanych warunkach brzegowych. W przyszłości autorka pragnie poszerzyć badania o weryfikację obliczeń numerycznych na stanowisku pomiarowym laboratoryjnym.

Artykuł traktuje o zabudowie płytowych wymienników ciepła. Są to najbardziej popularne i wykorzystywane obecnie w c.o. typy grzejników. Istnieje ich cała gama a rozmaite wymiary, kolory, efekty wizualne oraz duża bezwładność cieplna decydują o wyborze.

Często grzejniki takie montowane są wg warunków montażowych osób je instalujących. Nie zawsze przynoszą oczekiwany efekt cieplny. Niekiedy niewłaściwy montaż lub przysłonięcie może wiązać się ze zmniejszeniem efektywności – wydajności cieplnej. Mowa tutaj nie tylko o meblach czy osłonach je przysłaniających ale również o bardzo popularnych półkach poziomych – parapetach. Parapety mają różne głębokości i szerokości. Wykonywane są z rozmaitych materiałów, np. plastik czy marmur. Bywa, że posiadają zakrzywienia krawędzi. Pojawia się pytanie jak tego typu konstrukcje wpływają na efekt cieplny – wydajność grzejnika?

W artykule przedstawiono wybrane wyniki badań numerycznych dotyczących konwekcyjnego wymiennika ciepła. Wymiennik obudowano poziomą płytą z zakrzywieniem (rys. 1). Uzyskano pola temperatury i prędkości – rysunki 2-5. Na ich podstawie wyznaczono współczynnik przejmowania ciepła α, który decyduje o intensywności wymiany ciepła.

Okazało się, że zakrzywienie i obudowanie grzejnika parapetem niekorzystnie wpływa na rozkład współczynnika przejmowania ciepła α. Dlatego też korzystniejszy jest układ bez półki poziomej. Decydując się na obudowę powinniśmy zwrócić uwagę na tego typu elementy ozdobne i przemyśleć warunki montażowe aby w pełni wykorzystać możliwości grzewcze wymiennika ciepła.

Słowa kluczowe:
grzejnik, współczynnik przejmowania ciepła α, wymiana ciepła

Keywords:
radiator, heat transfer coefficient α, heat exchange

MIDDLE POMERANIAN SCIENTIFIC SOCIETY OF THE ENVIRONMENT PROTECTION
ŚRODKOWO-POMORSKIE TOWARZYSTWO NAUKOWE OCHRONY ŚRODOWISKA

Annual Set The Environment Protection
Rocznik Ochrona Środowiska

Volume/Tom 19. Year/Rok 2017 ISSN 1506-218X 600-617

Analiza skuteczności odmulania zbiorników wodnych Cierpisz i Kamionka jako efektywnej metody rekultywacji ekosystemów eutroficznych

Lilianna Bartoszek, Renata Gruca-Rokosz, Piotr Koszelnik
Politechnika Rzeszowska

1. Wprowadzenie

Większość stosowanych obecnie metod rekultywacji zbiorników wodnych skupia się albo na wyeliminowaniu zanieczyszczenia wtórnego wody substancjami uwalnianymi z osadów dennych lub chociaż na ograniczeniu jego wpływu na dalszą degradację zbiornika. Działania takie muszą zostać poprzedzone właściwym rozpoznaniem i eliminacją innych źródeł zanieczyszczeń biogenicznych (Wojtkowska & Dmochowski 2009, Koszelnik & Gruca-Rokosz 2013, Wiatkowski i in. 2015). Najwięcej uwagi poświęcono zahamowaniu zasilania wewnętrznego toni wodnej w związki fosforu, ze względu na intensywność krążenia tego pierwiastka biogennego w interfazie woda-osad i jego znaczący wkład w nasilenie procesu eutrofizacji wód (Dondajewska 2008, Dunalska i in. 2012). Jedną z takich metod jest bagrowanie, czyli usuwanie osadów dennych ze zbiornika wodnego. Wraz z wierzchnią warstwą osadów dennych usuwa się z ekosystemu znaczną część zgromadzonych w nich substancji organicznych i nieorganicznych, w tym związków biogennych oraz metali ciężkich, wskutek czego powinno ulec zahamowaniu wydzielanie i powrót tych substancji do toni wodnej, co w konsekwencji ma wpłynąć na poprawę jakości wody i spowolnić proces eutrofizacji wód. Właściwe składowanie, zapobiegające powrotom zanieczyszczonej wody, a następnie zagospodarowanie wydobytego osadu jest bardzo ważnym i często decydującym problemem, również z uwagi na dodatkowe znaczne nakła-

dy techniczne i finansowe, podnoszące koszty rekultywacji (Wiśniewski 1999). Osady denne mogą być przeznaczone do przyrodniczego wykorzystania na glebach pod uprawy rolnicze lub do rekultywacji terenów zdegradowanych (Ciesielczuk i in. 2011, Bartoszek i in. 2015), pod warunkiem, że będą odpowiednio żyzne (Koszelnik i in. 2008, Bartoszek i in. 2015), a zawartość w nich zanieczyszczeń, w tym metali ciężkich i niebezpiecznych substancji organicznych nie będzie przekraczała dopuszczalnych wartości granicznych dla gruntów występujących w miejscu przeznaczenia (Dz.U. 2016r. Poz. 1395.). Osady umiarkowanie zanieczyszczone lub ubogie w substancje biogenne mogą być wykorzystane w budownictwie po spełnieniu odpowiednich kryteriów geotechnicznych np. do budowy nasypów hydrotechnicznych, drogowych, albo w energetyce pod warunkiem posiadania odpowiednio wysokiej wartości opałowej, co wiąże się z zasobnością w materię organiczną (Kozielska-Sroka & Chęć 2009, Borsuk i in. 2012). W przypadku silnie zanieczyszczonych osadów dennych pozostaje deponowanie na odpowiednio zabezpieczonych składowiskach lub zastosowanie pirolitycznej utylizacji osadów (Wiśniewski & Wojtasik 2014). W Polsce bagrowanie zastosowano bezskutecznie na jeziorze Wegner (1984 r.), Mogileńskim (1991 r.) oraz w zbiorniku Maltańskim (1980-1990). Głównym powodem braku uzyskania trwałych efektów było niewyeliminowanie przyczyn degradacji zbiorników (Jankowski 2007, Szczepańska & Szpakowska 2009). Najczęściej stosowaną metodą rekultywacji płytkich, silnie zdegradowanych zbiorników małej retencji jest odmulanie. Odmulanie, jako przedsięwzięcie hydrotechniczne zaliczane jest do tzw. „prac utrzymaniowych" i ma na celu pogłębienie oraz zwiększenie pojemności użytkowej zbiornika, poprzez usunięcie z jego czaszy nagromadzonych przez lata osadów dennych.

Celem pracy była ocena tempa kumulacji zanieczyszczeń w osadach dennych dwóch zbiorników małej retencji położonych w jednym kontinuum rzecznym, w których przeprowadzono zabieg odmulania, w aspekcie ich wzmożonej eutrofizacji wód i potrzeb rekultywacyjnych.

2. Teren badań

W miejscowości Cierpisz na Podkarpaciu w 23,7 km biegu rzeki Tuszymka Duża przez przegrodzenie jej małą zaporą utworzono w 1953 roku zbiornik wodny o pojemności początkowej 34,5 tys. m^3. Wskutek znacznego zamulenia (stopień zamulenia 43,5%) w latach 1990-1991 przeprowadzono odmulanie zbiornika. Usunięto wówczas ok. 15 tyś m^3 osadu, jednocześnie pogłębiając go (Michalec i in. 2013). Zbiornik Kamionka został utworzony w roku 1957 ok. cztery kilometry niżej w 19,2 km biegu rzeki.

Tabela 1. Parametry morfometryczne zbiorników zaporowych Cierpisz i Kamionka (Madeyski i in. 2008, PB 2005)
Table 1. Morphometrics parameters of the Cierpisz and Kamionka reservoirs (Madeyski et al. 2008, PB 2005)

Parametr	Cierpisz	Kamionka
Powierzchnia [ha]	2,3	7,0
Objętość [tys. m^3]	22	105
Długość zbiornika [m]	340	950
Głębokość średnia (maks.) [m]	0,9 (1,5)	1,5 (3,0)
Powierzchnia zlewni [km^2]	54,5	90
Czas retencji wody [d]	1,2	4,8

Zbiornik został zmodernizowany i odmulony w 2007 roku, przy okazji odbudowy zapory zniszczonej podczas powodzi w 2005 roku (PB 2005). Zlewnia całkowita rzeki Tuszymka Duża zajmuje obszar o powierzchni 144,0 km^2, z czego zlewnia cząstkowa do zbiornika w Cierpiszu 54,5 km^2, do zbiornika Kamionka 90 km^2 (tabela 1). Zlewnia posiada charakter nizinny, rolniczo-leśny. Lasy stanowią ok. 48%, grunty orne 35%, użytki zielone 24% jej powierzchni całkowitej. Na obszarze zlewni przeważają piaski na glinach zwałowych (Madeyski i in. 2008).

3. Metodyka badań

Badania prowadzono w dwóch sezonach wegetacyjnych lat 2013 i 2014. Próbki wody i osadów dennych pobrano czterokrotnie w 2013 roku oraz pięciokrotnie w 2014 roku z 2 stanowisk badawczych na zbiorniku Cierpisz (St. 1 w pobliżu dopływu, St. 2 w pobliżu zapory) i 3 sta-

nowisk badawczych na zbiorniku Kamionka (w pobliżu dopływu St. 1, w okolicy środka zbiornika St. 2 i w pobliżu zapory St. 3) (rys. 1). Osady denne pobierano za pomocą czerpacza rurowego typu Kajak. Na każdym ze stanowisk pobierano po trzy próby osadów. Do badań laboratoryjnych brano wierzchnią, pięciocentymetrową warstwę osadu z każdej próby, które uśredniono. W próbkach wody na miejscu mierzono temperaturę, pH i zawartość tlenu rozpuszczonego (O_2) za pomocą wieloparametrowego miernika Hach Lange HQ40D.

Rys. 1. Rozmieszczenie stanowisk badawczych (St) na zbiornikach wodnych w Cierpiszu i Kamionce
Fig. 1. Location of the sampling stations (St) in the Cierpisz and Kamionka reservoirs

W laboratorium dokonano oznaczenia azotu ogólnego (TN) wykorzystując analizator TOC-VCPN (Shimadzu). Metodą spektrofotometryczną oznaczono stężenie fosforu fosforanowego ($P\text{-}PO_4^{3-}$) (reakcja z molibdenianem amonowym), fosforu ogólnego (TP) (po mineralizacji w środowisku H_2SO_4 i peroksodisiarczanów) oraz chlorofilu „a" (Chla) (Aquamate, Thermo Spectronic). Na potrzeby tej pracy poziom trofii

wód badanych obiektów określono na podstawie wartości indeksów troficznych (fosforowego – TSI_{TP} i chlorofilowego – TSI_{Chla}) według Carlsona. Osady po wysuszeniu i zhomogenizowaniu poddano prażeniu w temp. 550°C przez 4 h, na podstawie pozostałości po prażeniu obliczono zawartość materii organicznej (OM). Mineralizację osadów przeprowadzono w stężonym HNO_3 przy ciśnieniu 2-4,5 MPa w mineralizatorze mikrofalowym (UniClever II, Plazmatronika). W mineralizatach oznaczono metale (spektrometr ICP Integra) i fosfor całkowity (spektrofotometrycznie jako fosforany). Zawartość azotu w osadach oznaczono za pomocą analizatora elementarnego CNS (Flash EA 1112 Finnigan Mat). Do oceny stopnia zanieczyszczenia osadów dennych metalami ciężkimi wykorzystano kryterium geochemiczne oraz ekotoksykologiczne TEC (Treshold Effect Concentration) i PEC (Probable Effect Concentration) (MacDonald i in. 2000, Bojakowska 2001), a także Rozporządzenie Ministra Środowiska z dnia 1 września 2016 r. w sprawie sposobu prowadzenia oceny zanieczyszczenia powierzchni ziemi (Dz.U. 2016r. Poz. 1395.).

4. Wyniki badań i dyskusja

Osady denne omawianych obiektów okazały się bardzo ubogie w materię organiczną, fosfor i azot (tabela 2). Zaobserwowano analogiczną tendencję w zróżnicowaniu zawartości większości analizowanych parametrów w osadach w poszczególnych strefach zbiorników. Wyższe zawartości materii organicznej, fosforu, azotu, a także metali ciężkich obserwowano w osadach zbiornika Cierpisz na stanowisku 1 zlokalizowanym w pobliżu dopływu rzeki Tuszymka w porównaniu do stanowiska 2 w pobliżu zapory (tabela 2).

W większym i o mniejszej dynamice przepływu wód zbiorniku Kamionka na podstawie rozkładu średnich zawartości analizowanych parametrów można było wyróżnić trzy strefy kumulacji substancji w osadach. W osadach w pobliżu dopływu (St. 1) zaobserwowano wyższe zawartości substancji organicznych, fosforu, azotu oraz metali ciężkich. W strefie przejściowej w pobliżu środka zbiornika (St. 2) zawartości w/w parametrów malały, by znów wzrosnąć w strefie w pobliżu zapory (St. 3) za wyjątkiem miedzi. W osadach w pobliżu dopływu stwierdzono największą ilość materii organicznej, azotu, kadmu, miedzi, niklu, ołowiu

i cynku, co wskazuje na rzekę Tuszymkę, jako główne źródło tych zanieczyszczeń dla wód zbiornika Kamionka. W osadach w pobliżu zapory zaobserwowano najwyższe zawartości fosforu oraz chromu.

Tabela 2. Średnie zawartości materii organicznej, pierwiastków biogennych i metali ciężkich w osadach dennych zbiorników wodnych Cierpisz i Kamionka. Wartości tła geochemicznego, TEC i PEC (MacDonald i in. 2000, Bojakowska 2001)
Table 2. Average contents of organic matter, biogenic elements and heavy metals in the bottom sediments of the Cierpisz and Kamionka reservoirs. The values of geochemical background, TEC and PEC (MacDonald et al. 2000, Bojakowska 2001)

Zbiornik		**n = 9**	**OM**	**TP**	**N**	**Cd**	**Cu**	**Cr**	**Ni**	**Pb**	**Zn**
			[%]	[mg·g^{-1} s.m.o.]		[mg·kg^{-1} s.m.o.]					
Cierpisz	St. 1	Średnia	1,78	0,126	0,741	1,50	2,77	4,93	2,62	9,44	27,2
		SD	1,0	0,04	0,39	0,3	0,9	1,8	0,8	4,6	6,1
	St. 2	Średnia	1,38	0,079	0,643	0,88	1,82	2,75	2,03	6,02	17,6
		SD	0,5	0,03	0,14	0,4	1,6	1,1	0,9	2,3	6,9
	Zbiornik	Średnia	1,58	0,103	0,692	1,19	2,29	3,84	2,33	7,73	22,4
		SD	0,8	0,04	0,29	0,5	1,3	1,8	0,9	3,9	8,0
Kamionka	St. 1	Średnia	2,75	0,246	1,15	1,85	3,58	13,1	4,40	16,4	31,5
		SD	2,5	0,20	0,9	0,8	2,0	7,6	2,4	10	15
	St. 2	Średnia	2,19	0,157	0,907	1,15	3,47	4,86	2,24	5,01	17,5
		SD	2,0	0,16	0,72	0,5	3,2	3,4	1,4	2,7	7,6
	St. 3	Średnia	2,47	0,394	0,993	1,59	1,53	17,7	3,21	10,1	29,3
		SD	1,0	0,17	0,59	0,3	0,5	9,5	1,2	5,0	11
	Zbiornik	Średnia	2,47	0,266	1,02	1,53	2,86	11,9	3,28	10,5	26,1
		SD	1,9	0,20	0,7	0,6	2,3	8,8	1,9	8,1	13
Tło geochemiczne						0,5	7,0	6,0	5,0	15,0	73,0
TEC						0,99	31,6	43,4	22,7	35,8	121
PEC						4,98	149	111	48,6	128	459

Analizując zanieczyszczenie osadów dennych metalami ciężkimi stwierdzono, że zawartości kadmu, chromu i ołowiu przekroczyły wartości tła geochemicznego, czyli naturalnej zawartości tych pierwiastków wyznaczone dla osadów zbiorników wodnych Polski (tabela 2) (Bojakowska 2001). Tło geochemiczne zostało przekroczone w przypadku kadmu w osadach na wszystkich stanowiskach w obu zbiornikach. Wartość tła geochemicznego dla chromu została przekroczona w osadach zbiornika Kamionka w rejonie dopływu (St. 1) i w rejonie zapory (St. 3), natomiast dla ołowiu w rejonie dopływu (St. 1). Dla porównania prze-

ciętna zawartość kadmu, chromu i ołowiu w osadach dennych zbiorników świata wynosi 0,14; 68; 31 $mg \cdot kg^{-1}$ s.m.o. (odpowiednio) (Wiechuła 2004).

W celu określenia stopnia potencjalnego zagrożenia dla biosfery osadów dennych zanieczyszczonych metalami ciężkimi posłużono się metodą wskaźników numerycznych jakości osadów TEC (Treshold Effect Concentration) i PEC (Probable Effect Concentration) (MacDonald i in. 2000). Wartość progowa TEC została przekroczona przez kadm w osadach zbiornika Kamionka i na stanowisku w pobliżu dopływu (St. 1) zbiornika Cierpisz. Wartości progowe PEC nie zostały przekroczone w przypadku żadnego z metali w osadach obu zbiorników. Przekroczenie wartości progowej TEC przez kadm oznacza, że może już pojawiać się szkodliwe oddziaływanie tego pierwiastka na organizmy wodne, zwłaszcza żerujące przy dnie. Gdyby wartość progowa PEC została przekroczona, toksyczne działanie tego metalu występowałoby stale i takie osady stanowią już poważne zagrożenie dla środowiska wodnego, a pośrednio dla człowieka. Jedną z głównych przyczyn zanieczyszczenia środowiska wodnego kadmem w zlewniach rolniczych jest spływ powierzchniowy z pól uprawnych, na których przez wiele lat stosowano nawozy mineralne i środki ochrony roślin (Bojakowska 2001).

Biorąc pod uwagę zawartości analizowanych metali ciężkich wydobyte osady w razie odmulania obu zbiorników mogą być wykorzystane w pracach ziemnych dla dowolnej grupy gruntów, ponieważ ich stężenia nie przekraczają dopuszczalnych zawartości w glebie oraz ziemi dla wszystkich czterech grup gruntów wyszczególnionych w Rozporządzeniu Ministra Środowiska z 2016 r., uwzględniając głębokość warstwy, właściwości gleby i jej wodoprzepuszczalność (Dz.U. 2016r. poz. 1395.). Osady analizowanych obiektów, pomimo tego, że nie stwarzają zagrożenia dla środowiska glebowego, nie byłyby przydatne do spożytkowania na glebach wykorzystywanych pod uprawy rolnicze, ponieważ okazały się bardzo ubogie pod względem zawartości materii organicznej, azotu i fosforu. Brak jest odpowiednich kryteriów określających minimalne zawartości materii organicznej i substancji biogennych w wydobytych ze zbiornika osadach kwalifikujących je do zagospodarowania w rolnictwie. W przypadku wprowadzenia do obrotu takiego osadu, jako nawozu lub środka wspomagającego uprawę roślin decyzję w sprawie pozwolenia wydaje Minister właściwy do spraw rolnictwa **(**Dz.U. 2007 nr 147 poz. 1033**)**. Dla dostępnego w handlu nawozu organicznego, który według

informacji dystrybutora jest osadem dennym zbiorników słodkowodnych, Minister Rolnictwa i Rozwoju Wsi wydając pozwolenie na wprowadzenie do obrotu określił w decyzji wymagania jakościowe, które zawierają m.in. minimalną zawartość substancji organicznej w suchej masie na poziomie 30%, azotu całkowitego 3 $mg \cdot g^{-1}$ s.m.o, fosforu całkowitego 0,87 $mg \cdot g^{-1}$ s.m.o (Mat. Sapropel). Takie wymagania ostatecznie dyskwalifikują osady denne większości zbiorników zaporowych w spożytkowaniu, jako nawóz w uprawach rolnych, gdyż mają one przeważnie charakter mineralny i zawartość w nich materii organicznej rzadko przekracza 30%. Dla porównania zawartość materii organicznej w osadach jeziornych może nawet przekraczać 90% (Ciesielczuk i in. 2011). Osady badanych zbiorników mogą być natomiast wykorzystane do piaskowania torfów w celu poprawienia przepuszczalności i przewiewności gleby, a także np. do niwelacji terenu i rekultywacji terenów zdewastowanych.

Wyjątkowo niska zawartość fosforu i materii organicznej w osadach dennych nie wskazuje na możliwość występowania zasilania toni wodnej w fosforany i inne produkty rozkładu związków organicznych. Litoralne osady płytkich, eutroficznych jezior charakteryzujące się niską zawartością fosforu (0,3-0,6 mg g^{-1} s.m.o.) mogą być jednak znaczącym źródłem fosforanów, zwłaszcza w warunkach deficytu tlenu w wodzie nadosadowej podczas lata (Güde i in. 2000). W płytkich, małych zbiornikach ze względu na niewielką głębokość i intensywne mieszanie do dna, tlen powinien występować bez zakłóceń w całym profilu słupa wody. Z uwagi na niską zawartość materii organicznej w osadach zbiorników Cierpisz i Kamionka, nawet w upalne, bezwietrzne lata i przy bardzo niewielkiej ruchliwości wody nie powinno dochodzić do wystąpienia okresowego zaniku tlenu w strefie nadosadowej.

Szczegółowe wyniki oceny stanu troficznego wód zbiornika Kamionka (na podstawie jednego roku badań) i zbiornika Cierpisz (dla obu lat badawczych) z wykorzystaniem kryteriów stężeniowych Vollenweidera, OECD, Nürnberg oraz Forsberga i Rydinga, a także indeksów troficznych (TSI) Carlsona oraz Walkera przedstawiono w publikowanych już pracach (Bartoszek & Koszelnik 2014, Miąsik i in. 2014). Aktualna ocena stanu troficznego w oparciu o wartości indeksów troficznych (TSI) Carlsona wykazała zaawansowany poziom trofii wód obu zbiorników (tabela 3). Obliczone wartości indeksu troficznego fosforowego (TSI_{TP}) wskazywały na hypertrofię wód w zbiorniku Cierpisz, natomiast wartości

indeksu troficznego chlorofilowego (TSI_{Chla}) jeszcze na eutrofię. Ponieważ wartości TSI_{TP} były niewiele wyższe od 70 (TSI >70 – hypertrofia) można uznać, że stan troficzny wód zbiornika Cierpisz to eutrofia na pograniczu z hypertrofią. Rozpatrując zbiornik Kamionka obliczone wartości obu indeksów troficznych Carlsona, czyli fosforowego (TSI_{TP}) i chlorofilowego (TSI_{Chla}) wskazały na eutrofię wód w tym akwenie. Obliczone indeksy osiągnęły wartości w miarę zbliżone na poszczególnych stanowiskach, aczkolwiek indeks chlorofilowy wskazał na nieznacznie wyższą trofię wód w środkowym i przyzaporowym rejonie zbiornika Kamionka.

Tabela 3. Średnie wartości indeksów troficznych Carlsona (TSI_{TP}, TSI_{Chla}), stężenia azotu i fosforu w wodach zbiorników Cierpisz i Kamionka, ± SD
Table 3. Mean Carlson trophic index values (TSI_{TP}, TSI_{Chla}), nitrogen and phosphorus concentration in water of the Cierpisz and Kamionka reservoirs, ± SD

Zbiornik n = 9		**TN**	**TP**	**TSI_{TP}**	**Trofia**	**TSI_{Chla}**	**Trofia**
		[mg·dm^{-3}]					
Cier-pisz	St1	1,06±0,6	0,097±0,05	73	H	64	E
	St2	1,00±0,4	0,124±0,08	73	H	62	E
	zbiornik	1,03±0,5	0,110±0,06	73	H	63	E
Kamionka	St1	0,96±0,4	0,082±0,03	69	E	62	E
	St2	1,08±0,5	0,075±0,03	68	E	67	E
	St3	0,98±0,4	0,073±0,03	67	E	65	E
	zbiornik	1,00±0,4	0,076±0,03	68	E	65	E

W wodach zbiornika Kamionka odnotowano wyższą zawartość chlorofilu „a" (wskaźnika biomasy fitoplanktonu), przy czym najintensywniej proces wewnętrznej produkcji materii zachodził w rejonie środka zbiornika (St. 2) (rys. 2). Również w wodach zbiornika Kamionka częściej występowało zjawisko przesycenia wody tlenem wskazujące na wzmożony proces fotosyntezy. Najwyższe nasycenie wody tlenem (134%) zaobserwowano w strefie przejściowej tego zbiornika (rys. 2). Warunki tlenowe sprzyjały mineralizacji materii organicznej w obydwu zbiornikach.

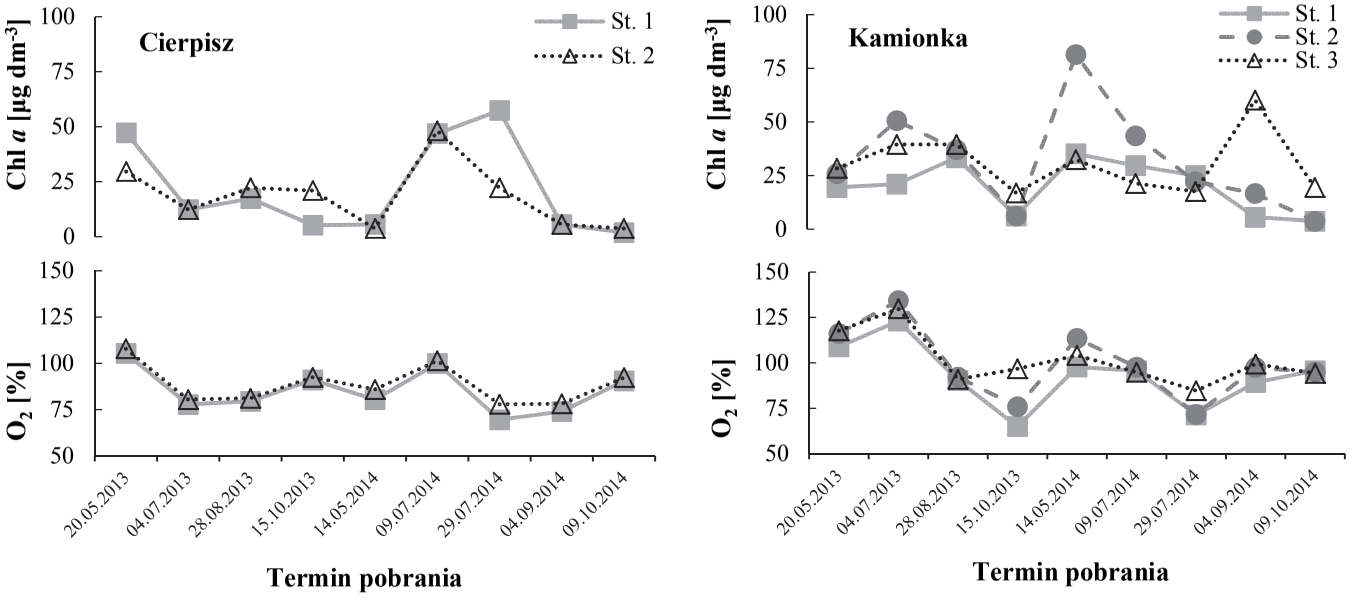

Rys. 2. Zmienność zawartości chlorofilu „a" [µg·dm^{-3}] i tlenu [%] w wodzie zbiorników Cierpisz i Kamionka
Fig. 2. Variability of chlorophyll "a" [µg·dm^{-3}] and oxygen [%] in water of the Cierpisz and Kamionka reservoirs

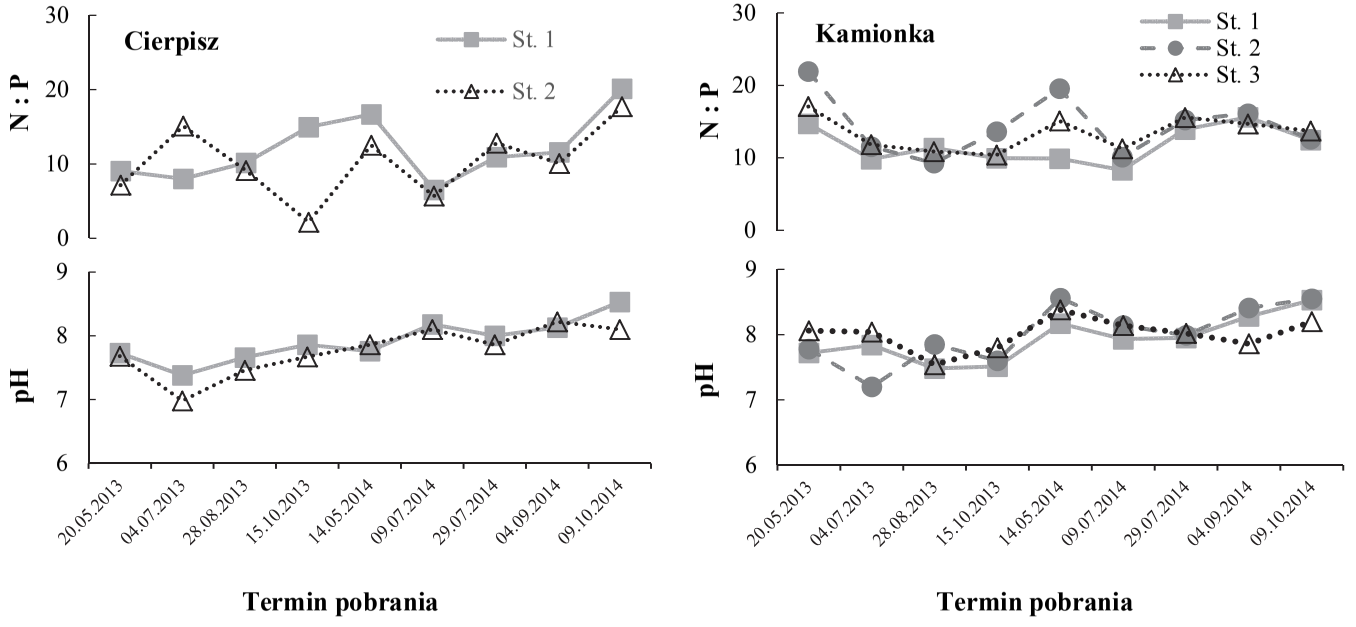

Rys. 3. Zmienność ilorazu N:P i pH w wodzie zbiorników Cierpisz i Kamionka
Fig. 3. Variability of N:P ratio and pH in the water Cierpisz and Kamionka reservoirs

Częściej pierwiastkiem limitującym rozwój fitoplanktonu w wodach zbiornika Cierpisz mógł być azot (N:P < 10:1) (rys. 3), stąd uzyskane rozbieżności pomiędzy indeksami troficznymi fosforowym (substratu) i chlorofilowym (produktu) dla tego obiektu. Wartość graniczna stężenia fosforu w wodzie, powyżej której występuje proces przeżyźnienia wód wynosi 0,1 $mg \cdot dm^{-3}$ (Berleć i in. 2015). Takie stężenia występowały często w wodzie zbiornika Cierpisz. Na rysunku 3 można zaobserwować postępującą alkalizację wód, wynikającą z postępu procesu eutrofizacji, z bardziej wyraźną tendencją wzrostową pH wody dla zbiornika Cierpisz.

Poziom trofii wód obu akwenów nie znajdował odzwierciedlenia w niewielkim wzbogaceniu osadów dennych w materię organiczną i substancje biogenne. Było to z jednej strony następstwem przeprowadzonych w przeszłości zabiegów odmulania obu obiektów, z drugiej silnie przepływowego charakteru wód obu zbiorników. W osadach zbiornika Kamionka pomimo stosunkowo niedawno przeprowadzonego odmulania (ok. 6 lat temu) zaobserwowano wyższą kumulację wszystkich analizowanych substancji niż w osadach zbiornika Cierpisz poddanego odmulaniu znacznie wcześniej (ok. 22 lata temu). Od tamtego czasu zbiornik w Cierpiszu został zagospodarowany przez wędkarzy. Z przeprowadzonej analizy wynika, że większy wpływ na zanieczyszczenie wód zbiornika Cierpisz miała ta część zlewni całkowitej, z której zanieczyszczenia dostarczane były za pośrednictwem dopływu, niż teren bezpośrednio go otaczający. W strefie w pobliżu dopływu panują warunki rzeczne, wpływające wody cieku bogate są w zawiesinę i substancje rozpuszczone (Wiatkowski i in. 2015), a niewielka głębokość i intensywne mieszanie wód sprzyja występowaniu zjawiska resuspensji osadów i sorpcji w nich zanieczyszczeń. W strefie przy zaporze dominują na ogół procesy wewnętrznej produkcji materii, wskutek czego następuje jej odkładanie po zakończonym sezonie wegetacyjnym w osadach dennych. Jednakże w małych zbiornikach charakter rzeczny często występuje na całej ich długości (Ligęza & Smal 2003). Zbiornik Cierpisz położony ok. 4 km wyżej, mógłby pełnić rolę zbiornika wstępnego przejmując część materii pochodzącej z terenu zlewni rzeki Tuszymka. Jednakże z uwagi na jego silnie przepływowy charakter (czas retencji wody 1,2 doby) znaczna część ładunku zanieczyszczeń transportowana była dalej do zbiornika Kamionka. Ponadto pomiędzy badanymi obiektami rzeka Tuszymka przepływa na odcinku ok. 4 km przez użytki rolne i dwie nieskanalizowane miejscowości.

Przyczyną wyższej kumulacji w osadach dennych w strefie przyzaporowej, jak również ogólnie większego zanieczyszczenia osadów zbiornika Kamionka w porównaniu do położonego wcześniej zbiornika Cierpisz mogła być nieuporządkowana gospodarka wodno-ściekowa w miejscowości, na pograniczu której znajduje się zbiornik. Nie bez wpływu pozostaje też bezpośrednie sąsiedztwo infrastruktury turystyczno-rekreacyjnej oraz szlaków komunikacyjnych.

Pomiary zamulania zbiornika Cierpisz wykonane w latach 2009 i 2011 wykazały, że od 1990 roku (od zabiegu odmulania) do 2011 roku, czyli w ciągu 22 lat eksploatacji stopień zamulenia wyniósł 27,45%, a wyliczone zmniejszenie pojemności tego obiektu o 50% może nastąpić po upływie 40 lat eksploatacji (Michalec i in. 2013). Brak jest danych dotyczących zamulania zbiornika Kamionka, z uwagi na stosunkowo niedawną jego modernizację. Głównym celem odmulania małych, płytkich, lokalnych zbiorników było ich pogłębienie i zwiększenie pojemności użytkowej. Dlatego też osady nie były badane pod kątem ich zanieczyszczenia i możliwości zagospodarowania. Wydobyte z dna osady najczęściej wykorzystywano do wzmocnienia skarp, tworzenia wysp, grobli, plaż i niwelacji terenu. W przypadku dużego zanieczyszczenia, zagospodarowanie ich w bezpośrednim otoczeniu rekultywowanego obiektu stwarza zagrożenie dla jakości jego wód, poprzez ich wtórne zanieczyszczenie.

5. Podsumowanie

Zbiorniki małej retencji są szczególnie narażone na degradację, ponieważ odkładanie w osadach dennych części materii transportowanej przez cieki oraz pochodzącej ze zlewni bezpośredniej powoduje ich szybkie wypłycanie. Zarówno w zbiorniku Kamionka, jak i w zbiorniku Cierpisz pomimo ok. 60 letniego funkcjonowania obu obiektów i zaawansowanego poziomu trofii wód, osady denne okazały się bardzo ubogie pod względem zawartości materii organicznej, substancji biogennych oraz stosunkowo umiarkowanie zanieczyszczone metalami ciężkimi. Bez wątpienia do niewielkiego nagromadzenia substancji w osadach analizowanych zbiorników przyczyniły się zabiegi odmulania przeprowadzone w różnym okresie eksploatacji obu obiektów oraz ich silnie przepływowy charakter. Ze względu na krótki czas retencji wody zbiornik Cierpisz nie przejmował znaczącej ilości zanieczyszczeń transportowanych przez

rzekę. Ilość nagromadzonych substancji w osadach obu zbiorników była nieco zróżnicowana i nie było to powiązane z okresem odmulania, lecz z oddziaływaniem antropogenicznym zlewni i warunkami hydrologicznymi. Analiza wzbogacenia osadów dennych i zagospodarowania terenu wykazała, że zbiornik Kamionka, zwłaszcza w rejonie dopływu narażony był na wyższą presję antropogeniczną ze strony zlewni. Wyższa trofia wód w środkowej części zbiornika Kamionka przy silnie przepływowym ich charakterze może oddziaływać na osady z pewnym opóźnieniem, znajdując odzwierciedlenie w ich użyźnieniu w rejonie strefy przyzaporowej. Ogólnie niska zawartość fosforu i materii organicznej nie wskazuje na możliwość występowania zasilania wewnętrznego toni wodnej i wpływu osadów na postęp procesu eutrofizacji w obu zbiornikach. Umiarkowany stopień zanieczyszczenia osadów metalami ciężkimi nie wyklucza możliwości wykorzystania ich w pracach ziemnych dla dowolnej grupy gruntów, jednak z uwagi na niską zawartość materii organicznej i substancji biogennych zagospodarowanie ich na użytkach rolnych może prowadzić do obniżenia żyzności gleby. Na chwilę obecną brak jest odpowiednich kryteriów pozwalających na właściwą kwalifikację wydobytych podczas bagrowania osadów pod kątem ich zagospodarowania w rolnictwie.

Podziękowanie

Badania były finansowane przez Narodowe Centrum Nauki w ramach projektu badawczego nr 2011/03/B/ST10/04998.

Literatura

Bartoszek, L., & Koszelnik, P. (2014). *Zagrożenie eutroficzne wód podkarpackich zbiorników Kamionka i Ożanna*. [w:] *Zaopatrzenie w wodę, jakość i ochrona wód*., (pod red.) Dymczewski, Z., Jeż-Walkowiak, J. Poznań: PZITS O/ Wielkopolski, 213-229.

Bartoszek, L., Koszelnik, P., Gruca-Rokosz, R., & Kida, M. (2015). Assessment of agricultural use of the bottom sediments from eutrophic Rzeszów reservoir. *Rocznik Ochrona środowiska*, 17, 396-409.

Berleć, K., Traczykowski, A., Budzińska, K., Szejniuk, B., Michalska, M., Jurek, A., Guścior, A., Majewska, M. (2015). Wpływ niewłaściwej gospodarki ściekowej i rolnej na stan fizykochemiczny wód jeziora Głęboczek kilka lat po rekultywacji. *Rocznik Ochrona Środowiska*, 17, 1449-1462.

Bojakowska, I. (2001). Kryteria oceny zanieczyszczenia osadów wodnych. *Przegląd Geologiczny*, 49(3), 213-218.

Borsuk, S., Kujawski, E., Borsuk, M. (2012). *Naturalny osad denny (NOD) jako potencjalne źródło ekologicznej energii odnawialnej*. [w:] *Inżynieria i Ochrona Środowiska*., (pod red.) Granops, M. Bydgoszcz: Wydawnictwo Uczelniane UTP, 43-52.

Ciesielczuk, T., Kusza, G., Karwaczyńska, U. (2011). Przyrodnicze wykorzystanie osadów dennych w świetle obowiązujących przepisów. *Rocznik Ochrona Środowiska*, 13, 1327-1338.

Dondajewska, R. (2008). Internal phosphorus loading from bottom sediments of a shallow preliminary reservoir. *Oceanological and Hydrobiological Studies*, XXXVII(2), 89-97.

Dunalska, J.A., Górniak, D., Jaworska, B., Gaiser, E.E. (2012). Effect of temperature on organic matter transformation in a different ambient nutrient availability. *Ecological Engineering*, 49, 27-34.

Dz.U. 2016r. Poz. 1395. Rozporządzenie Ministra Środowiska z dnia 1 września 2016 r. w sprawie sposobu prowadzenia oceny zanieczyszczenia powierzchni ziemi.

Dz.U. 2007 Nr 147 poz. 1033. Ustawa z dnia 10 lipca 2007 r. O nawozach i nawożeniu.

Güde, H., Seidel, M., Teiber, P., Weyhmüller, M. (2000). P-release from littoral sediments in Lake Constance. *Verh. Internat. Verein. Limnol*., 27, 2624-2627.

Jankowski, J. (2007). *Stan prac rekultywacyjnych w Polsce*. VI Konferencja Naukowo-Techniczna: *Ochrona i Rekultywacja Jezior*. Toruń: PZIiTS Oddział Toruń, 83-94.

Koszelnik, P., Tomaszek, J., & Gruca-Rokosz, R. (2008). Carbon and nitrogen and their elemental and isotopic ratios in the bottom sediment of the Solina-Myczkowce complex of reservoirs. *Oceanological and Hydrobiological Studies*, 37(3), 71-78.

Koszelnik, P., & Gruca-Rokosz, R. (2013). Determination of nitrate isotopic signature in waters of different sources by analysing the nitrogen and oxygen isotopic ratio, *Environmental Science: Processes & Impacts*, 15(4), 751-759.

Kozielska-Sroka, E., & Chęć, M. (2009). Właściwości osadów dennych Jeziora Czorsztyńskiego w aspekcie ich wykorzystania w budownictwie ziemnym. *Górnictwo i Geoinżynieria*, 33(1), 369-376.

Ligęza, S., & Smal, H. (2003). Skład granulometryczny osadów dennych zbiornika wód zrzutowych zakładów azotowych Puławy. *Acta Agrophysica*, 1(2), 271-277.

MacDonald, D.D., Ingersoll, C.*G.*, Berger, T.A. (2000). Development and evaluation of consensus-based sediment quality guidelines for freshwater ecosystems. *Archives of Environmental Contamination and Toxicology*, 39, 20-31.

Madeyski, M., Michalec, B., Tarnawski, M. (2008). *Zamulanie małych zbiorników wodnych i jakość osadów dennych*. Infrastruktura i ekologia terenów wiejskich: Kraków: PAN Komisja technicznej infrastruktury wsi.

Mat. Sapropel - Materiały firmy Sapropel. Nawóz organiczny http://www.sapropel.pl/ (data ostatniego dostępu 8.04.2016).

Miąsik, M., Koszelnik, P., Bartoszek, L. (2014). Trophic water assessment of the small retention reservoirs Blizne and Cierpisz in the Podkarpacie Region (Subcarpathian Province). *Limnological Review*, 14(4), 181-186.

Michalec, B., Tarnawski, M., Koniarz, T. (2013). Zamulenie jako czynnik ograniczający zasoby wodne zbiorników małej retencji. *Czasopismo Inżynierii Lądowej, Środowiska i Architektury*, 60(3), 129-142.

PB 2005 - Projekt budowlany, Budowa zapory ziemno-betonowej na rzece Tuszymka Duża w miejscowości Kamionka gm. Ostrów, woj. podkarpackie. Zespół Usług Technicznych NOT 2005.

Szczepańska, M., & Szpakowska, B. (2009). Rekreacyjne znaczenie zbiornika Maltańskiego i problemy związane z jego użytkowaniem. *Nauka Przyroda Technologie*, 3(1), 1-10.

Wiatkowski, M., Rosik-Dulewska, C., Kasperek, R. (2015). Inflow of Pollutants to the Bukówka Drinking Water Reservoir from the Transboundary Bóbr River Basin. *Rocznik Ochrona Środowiska*, 17, 316-336.

Wiechuła, D. (2004). *Ekotoksykologia osadów dennych zbiorników o różnej charakterystyce limnologicznej*. Katowice: Wydawnictwo Śląska Akademia Medyczna.

Wiśniewski, R. (1999). *Próby inaktywacji fosforanów w osadach dennych i zahamowania zakwitu sinic w jeziorze Łasińskim jako potencjalne metody rekultywacji*. I Ogólnopolska Konferencja Naukowo-Techniczna: *Postęp w Inżynierii Środowiska*. Rzeszów-Polańczyk: Oficyna Wydawnicza PRz. 189-202.

Wiśniewski, W., & Wojtasik, B. (2014). *Wyprażacz zanieczyszczonych osadów półpłynnych*. Patent nr 218690, Urząd patentowy RP.

Wojtkowska, M., & Dmochowski, D. (2009). Seasonal character of changes in nitrogen forms in waters of Korytów and Łąki Korytowskie retention reservoirs. *Environment Protection Engineering*, 35(2), 57-66.

Analysis of the Desludging Effectiveness of the Cierpisz and Kamionka Reservoirs as an Effective Method of the Eutrophic Ecosystems Recultivation

Abstract

Reservoir desludging is its simultaneous deepening and involves the removal of the accumulated over the years sediments from the bowl. It is the most commonly used method of recultivation of the shallow, strongly degraded small retention reservoirs. Two small retention reservoirs created on the river Tuszymka Duża (Sub-Carpathian region) were the research objects. The reservoir in Cierpisz (with a capacity of 22,000 m^3) was formed in 1953 and was subjected to desludging in 1990, whereas the reservoir in Kamionka (with a capacity of 105,000 m^3) was formed in 1957 and modernized and dredged in 2007. The research was conducted in two vegetation seasons the years 2013 and 2014. The samples of water and sediments were collected four times in 2013 and five in 2014 from 2 stations on the Cierpisz reservoir and 3 stations on the Kamionka reservoir. The sediments both of Kamionka and Cierpisz reservoirs despite the advanced eutrophication were very poor in terms of organic matter, phosphorus and nitrogen contents. Also, contamination of the sediments with heavy metals was moderate and except for cadmium, chromium and lead did not exceed the geochemical background. Generally, low content of phosphorus and organic matter does not indicate possibility of the occurrence of the internal supply of the water column and the sediment impact on the progress of eutrophication in both reservoirs. The amount of the accumulated substances in the sediments of the two reservoirs was slightly differentiated, and it was not related to the period of the desludging, but with the anthropogenic impact of the catchment and hydrological conditions.

Streszczenie

Odmulanie zbiornika jest jego jednoczesnym pogłębieniem i polega na usunięciu z jego czaszy nagromadzonych przez lata osadów dennych. Jest to najczęściej stosowana metoda rekultywacji płytkich, silnie zdegradowanych zbiorników małej retencji. Obiektami badawczymi były dwa zbiorniki małej retencji utworzone na rzece Tuszymka Duża na Podkarpaciu. Zbiornik wodny w Cierpiszu (o pojemności 22 tyś m^3) powstał w roku 1953 i był poddany odmulaniu w roku 1990, natomiast zbiornik wodny w Kamionce (o pojemności 105 tyś m^3) powstał w roku 1957 i został zmodernizowany oraz odmulony w roku 2007. Badania prowadzono w dwóch sezonach wegetacyjnych lat 2013 i 2014. Próbki wody i osadów dennych pobrano czterokrotnie w 2013 roku oraz

pięciokrotnie w 2014 roku z 2 stanowisk badawczych na zbiorniku Cierpisz i 3 stanowisk badawczych na zbiorniku Kamionka. Zarówno w zbiorniku Kamionka, jak i w zbiorniku Cierpisz pomimo zaawansowanej eutrofizacji wód osady denne były bardzo ubogie pod względem zawartości materii organicznej, fosforu i azotu. Również zanieczyszczenie osadów metalami ciężkimi było umiarkowane i za wyjątkiem kadmu, chromu i ołowiu nie przekraczało tła geochemicznego. Ogólnie niska zawartość fosforu i materii organicznej nie wskazuje na możliwość występowania zasilania wewnętrznego toni wodnej i wpływu osadów na postęp procesu eutrofizacji w obu zbiornikach. Ilość nagromadzonych substancji w osadach obu zbiorników była nieco zróżnicowana i nie było to powiązane z okresem odmulania, lecz z oddziaływaniem antropogenicznym zlewni i warunkami hydrologicznymi.

Słowa kluczowe:
małe zbiorniki wodne, odmulanie, osady denne, poziom zanieczyszczenia

Keywords:
small reservoirs, desludging, bottom sediments, pollution levels

MIDDLE POMERANIAN SCIENTIFIC SOCIETY OF THE ENVIRONMENT PROTECTION
ŚRODKOWO-POMORSKIE TOWARZYSTWO NAUKOWE OCHRONY ŚRODOWISKA

Annual Set The Environment Protection
Rocznik Ochrona Środowiska

Volume/Tom 19. Year/Rok 2017 ISSN 1506-218X 618-632

Wpływ nawożenia kompostem z osadów komunalnych na jakość gleby lekkiej pod uprawą wierzby wiciowej w czteroletnim cyklu uprawy

Leszek Styszko, Diana Fijałkowska, Janusz Dąbrowski
Politechnika Koszalińska

1. Wstęp

Podstawowym źródłem energii odnawialnej w Polce nadal jest biomasa. Wykorzystanie słabej jakości gruntów ornych do założenia plantacji wierzby energetycznej, stwarza szansę poprawy bilansu biomasy. W rejonach, gdzie dominują gleby lekkie, nawożenie kompostem z komunalnych osadów ściekowych lub też osadami ściekowymi, może zwiększyć ich produktywność, retencję wody opadowej oraz nasilić proces glebotwórczy (Krzywy i in. 2003). Osady są kłopotliwym odpadem w oczyszczalniach ścieków i są nadal trudne do zagospodarowania (Rosik-Dulewska i in. 2009). Wykorzystanie osadów ściekowych do produkcji kompostu, który następnie będzie zużyty m. in. do nawożenia upraw roślin energetycznych, pozwoli także na aktywne włączenie się do realizacji celów UE w odniesieniu do energetyki. Na glebach marginalnych możliwa jest uprawa roślin lignino-celulozowych przeznaczonych na cele energetyczne, ale plony biomasy w tych warunkach są niskie. Stąd zachodzi potrzeba podniesienia żyzności gleb lekkich przez stosowanie nawożenia organicznego oraz mineralnego. Do uprawy roślin na cele energetyczne można stosować nawożenie osadami ściekowymi i kompostami z osadów komunalnych (Ociepa-Kubicka & Pachura 2013).

Celem pracy była ocena niektórych zmian w jakości gleby lekkiej w warstwie 0-90 cm, pod uprawą wierzby wiciowej (*Salix viminalis*) w 4-letnim cyklu, na skutek zastosowania nawożenia kompostem z osadów komunalnych i nawożenia mineralnego.

2. Materiał i metoda

Doświadczenie dwuczynnikowe realizowano metodą losowanych podbloków w układzie zależnym, w trzech powtórzeniach, w latach 2006–2009 na polu doświadczalnym Politechniki Koszalińskiej w Kościernicy, gmina Polanów (16°24´N i 54°8´E). Doświadczenie założono na glebie lekkiej klasy IVb – V, kompleksu żytniego dobrego, o składzie granulometrycznym piasku gliniastego lekkiego do głębokości 100 cm oraz gliny lekkiej poniżej 100 cm. Przed zastosowaniem nawożenia kompostem wiosną 2006 roku pobrano próbki z trzech warstw gleby do głębokości 90 cm, a wyniki tych analiz zestawiono w tabeli 1.

Tabela 1. Chemiczne właściwości gleby przed założeniem doświadczenia
Table 1. Chemical properties of the soil before the experiment

Chemiczna właściwość gleby	Jednostka miary	Zawartość w warstwach profilu gleby (cm)				
		0-30	31-60	61-90	suma	średnia
Odczyn gleby	pH	5,08	5,21	5,16	–	5,15
Zawartość próchnicy	%	1,6	–	–	–	–
Zawartość N amonowego	mg· kg^{-1} s.m.	0,81	0,59	0,67	2,07	0,69
Zawartość N azotanowego	mg· kg^{-1} s.m.	2,13	1,83	2,42	6,38	2,13
Zawartość N mineralnego	mg· kg^{-1} s.m.	2,94	2,42	3,09	8,45	2,82
Zawartość N mineralnego	kg N·ha^{-1}	12,6	10,4	13,3	36,3	12,1

W doświadczeniu czynnikami I rzędu były cztery kombinacje nawozowe: (a) bez nawożenia, (b) kompost z osadów komunalnych (10 t·ha^{-1} s. m.), (c) kompost z osadów komunalnych (10 t·ha^{-1} s.m.) i azot mineralny w ilości 90 kg N·ha^{-1} oraz (d) kompost z osadów komunalnych (10 t·ha^{-1} s. m.) i azot mineralny w ilości 180 kg N·ha^{-1}. Kompost charakte-

ryzował się: pH_{KCl} – 6,63, zawartość suchej masy – 68,4%, a zawartość w suchej masie wyniosła: materii organicznej – 39,1%, N – 1,8%, P – 1,6%, K – 0,1%, Ca – 3,4% i Mg – 0,3%. Kompost zastosowano wiosną 2006 roku, a nawóz azotowy wysiewano corocznie przed rozpoczęciem wegetacji wierzby w latach 2006-2009. Czynnikiem II rzędu było dziewięć klonów wierzby wiciowej: 1047, 1054, 1023, 1013, 1052, 1047D, 1056, 1033 i 1018, które wysadzono w trzech powtórzeniach. Poletko miało powierzchnię 34,5 m^2, na którym wysadzono 120 zrzezów (34782 zrzezów na hektarze). Przed założeniem doświadczenia oraz corocznie po zakończeniu wegetacji wierzby pobierano z każdego poletka próbki gleby z trzech głębokości: 0-30 cm, 31-60 cm i 61-90 cm. Na bazie tych próbek przygotowano do analiz średnią próbkę z powtórzeń i złożono do zamrażarki (-18°C). W próbkach określono zawartość suchej masy według normy PB-R-0428, próchnicy i węgla organicznego metodą Tiurina, azotu ogólnego metodą Kjeldahla, azotu amonowego, azotanowego i azotu mineralnego według normy PB-R-04028 oraz odczynu gleby według normy PN-ISO 10390. Dane o rozkładzie opadów i temperatur w latach 2006-2009, uzyskano ze stacji meteorologicznej IHAR w Boninie, oddalonej w linii prostej o 10 km od pola doświadczalnego w Kościernicy (Styszko i in. 2010). Dla scharakteryzowania hydrotermicznych warunków wegetacji wierzby posłużono się współczynnikiem Sielianinowa (K) obliczonego z wzoru $K = P/0{,}1 \cdot \sum t$ (Molga 1986), gdzie P oznacza miesięczną sumę opadów atmosferycznych w mm, a $\sum t$ – miesięczną sumę temperatury powietrza >0°C. Hydrotermiczne warunki ekstremalne (skrajnie suche i bardzo suche oraz bardzo wilgotne i skrajnie wilgotne) oznaczone współczynnikiem Sielianinowa (K) mieszczą się w przedziałach < 0,7 oraz > 2,5 (Skowera & Puła 2004). Warunki skrajnie suche i bardzo suche (K< 0,7) wystąpiły w kwietniu 2009 roku, w maju 2008 roku i w lipcu 2006 roku. Natomiast warunki bardzo wilgotne (K > 2,5) wystąpiły w kwietniu 2006 i 2008 roku, w czerwcu 2009 roku, w lipcu 2007 roku, w sierpniu 2006 i 2008 roku, we wrześniu 2007 roku i październiku 2009 roku. Dla zebranych empirycznych cech wykonano standardową 3- lub 4-czynnikową analizę wariancji w programie AWA. W opracowaniu statystycznym wyniki klasyfikowano według czynników: A – 4 lata wegetacji wierzby, B – 3 głębokości w profilu glebowym, C – 4 kombinacje nawożenia i D – 9 klonów wierzby wiciowej. Istotność źródeł zmienności testowano testem F, a strukturę komponentów wariancyjnych zestawiono w tabeli 2 (Trętowski & Wójcik 1988).

3. Wyniki i dyskusja

Wyniki analiz dotyczących zawartości próchnicy i węgla organicznego dotyczą warstwy gleby 0-30 cm, a przy pozostałych cechach warstw: 0-30 cm, 31-60 cm i 61-90 cm. Zmienność w doświadczeniu spowodowana działaniem efektów głównych na poziomie ponad 50% zmienności całkowitej była przy zawartości: N ogólnego (72,9%), N azotanowego (61,5%), oraz próchnicy i C organicznego (po 51,9%). Spośród czynników głównych największy efekt wyodrębniono przy oddziaływaniu głębokości w profilu glebowym przy analizach: N ogólnego (63,4%), N mineralnego (37,8%) oraz lat wegetacji wierzby w analizie N azotanowego (37,2%). Spośród interakcji największe znaczenie miały współdziałania: lat wegetacji z głębokością w profilu glebowym przy zawartości azotu amonowego (25,5%) i kombinacji nawożenia z klonami wierzby przy odczynie gleby (14,6%).

Tabela 2. Wpływ analizowanych czynników na zmienność cech jakości gleby
Table 2. Effect of studied factors on the variability of soil quality

Komponent wariancyjny	Struktura komponentów wariancyjnych [%] w analizach (1-8)							
	1	2	3	4	5	6	7	8
Lata wegetacji [A]	46,2 ***	46,2 ***	8,4 ***	7,4 ***	37,2 ***	3,3 ***	3,3 ***	0,9 **
Głębokość w profilu gleby [B]	–	–	63,4 ***	14,6 ***	16,5 ***	37,8 ***	37,8 ***	2,9* **
Kombinacje nawożenia [C]	5,7 **	5,7 **	0,6 ***	0,0	6,9 ***	3,2 ***	3,2 ***	9,8 ***
Klony wierzby [D]	0,0	0,0	0,5 **	1,8 ***	0,9 ***	1,9 ***	1,9 ***	5,7 ***
Efekty główne	51,9	51,9	72,9	23,8	61,5	46,2	46,2	19,3
Interakcja AB	–	–	1,2 ***	25,5 ***	5,6 ***	2,8 ***	2,8 ***	0,1
Interakcja AC	2,0	2,0	1,3 ***	4,0 ***	2,9 ***	1,3 *	1,3 *	7,2 ***
Interakcja AD	0,0	0,0	1,4 **	0,9	0,6	0,7	0,7	4,4 ***

Tabela 2. cd.
Table 2. cont.

Komponent wariancyjny	Struktura komponentów wariancyjnych [%] w analizach (1-8)							
	1	2	3	4	5	6	7	8
Interakcja BC	–	–	0,6 *	2,2 **	6,0 ***	3,4 ***	3,4 ***	1,4 *
Interakcja BD	–	–	0,2	0,9	2,0 ***	1,7 *	1,7 *	3,2 ***
Interakcja CD	1,5	1,5	3,4 ***	2,1 *	2,0 ***	2,8 **	2,8 **	14,6 ***
Pozostałe interakcje	48,4	48,4	19,0	40,6	19,4	41,1	41,1	49,9
Suma	100	100	100	100	100	100	100	100

*Istotność różnic przy poziomie: *α = 0,05; **α = 0,01;***α = 0,001*
Analizy (1-8): 1 – zawartość próchnicy; 2 – zawartość C organicznego; 3 – zawartość N ogólnego; 4 – zawartość N amonowego; 5 – zawartość N azotanowego; 6 – zawartość N mineralnego w $mg \cdot kg^{-1}$ s.m.; 7 – zawartość N mineralnego w $kg \cdot ha^{-1}$; 8 – odczyn gleby.

W tabeli 3 zestawiono efekty przeciętne analizowanych czynników. W ciągu 4 lat uprawy w glebie nastąpiła akumulacja próchnicy i węgla organicznego (1,39-krotnie), a spadek zawartości N ogólnego (1,32 krotnie) i odczynu gleby (1,02-krotnie).

Zawartość N ogólnego w wierzchniej warstwie gleby zawierała się w przedziale 0,084-0,094%, wyższa była w kombinacjach nawozowych „c" i „d" roku wegetacji niż w „a" i „b" (tabela 4). Zawartość N amonowego w wierzchniej warstwie gleby zawierała się w przedziale 3,33-4,25 $mg \cdot kg^{-1}$ s.m, była najwyższa była w kombinacji „b", niższa w kombinacjach „d" i „c", a najniższa w na obiektach „a". Zawartość N azotanowego w wierzchniej warstwie gleby wahała się w przedziale 2,38-4,65 $mg \cdot kg^{-1}$ s.m, była najwyższa była w kombinacji „d", niższa w kombinacji „c", a najniższa wkombinacjach „a" i „b". Zawartość N mineralnego w wierzchniej war stwie gleby zawierała się w przedziale 5,79-8,14 $mg \cdot kg^{-1}$ s.m lub 24,9-35,0 $kg \cdot ha^{-1}$ N, była najwyższa była w kombinacji „d", niższa w kombinacjach „c" i „b", a najniższa w kombinacjach „a".

Tabela 3. Wpływ analizowanych czynników na jakość gleby
Table 3. Effect of studied factors on the properties of soil quality

Badany czynnik	Poziom czynnika	Analizy chemicznych właściwości gleby[(1-8)]							
		1	2	3	4	5	6	7	8
		[%]			[mg·kg^{-1} s.m.]			[kg N·ha^{-1}]	[pH]
Lata wegetacji wierzby [A]	1	1,77	1,03	0,074	1,89	3,90	5,79	24,9	5,13
	2	1,79	1,04	0,052	3,04	1,80	4,84	20,8	5,09
	3	2,38	1,38	0,057	3,51	1,01	4,52	19,4	5,10
	4	2,46	1,43	0,056	2,46	2,84	5,30	22,8	5,04
	$NIR_{0,05}$	0,17***	0,10***	0,003***	0,36***	0,20***	0,41***	1,78***	0,05**
Głębokość w profilu gleby w cm [B]	0-30	-	-	0,088	3,74	3,30	7,04	30,3	5,03
	31-60	-	-	0,058	2,63	2,22	4,85	20,9	5,09
	61-90	-	-	0,034	1,80	1,64	3,44	14,8	5,16
	$NIR_{0,05}$	-	-	0,003***	0,31***	0,17***	0,36***	1,54***	0,05***
Kombinacje nawożenia [C]	„a”	1,94	1,13	00,58	2,62	1,94	4,56	19,6	5,08
	„b”	2,04	1,19	0,058	2,77	2,04	4,81	20,7	5,26
	„c”	2,28	1,32	0,064	2,84	2,44	5,28	22,7	5,01
	„d”	2,14	1,24	0,060	2,67	3,14	5,81	25,0	5,03
	$NIR_{0,05}$	0,17**	0,10**	0,003***	0,36 n.i.	0,20***	0,41***	1,78***	0,05***

[(1-8)]: Oznaczenia analiz właściwości gleby podano w tabeli 2
*Istotność różnic: n.i. – brak istotności; **α = 0,01; ***α = 0,001*
Dla NIR podano wartość liczbową dla poziomu istotności α = 0,05

Tabela 3. cd.
Table 3. cont.

Badany czynnik	Poziom czynnika	Analizy chemicznych właściwości gleby[1-8]							
		1	2	3	4	5	6	7	8
		[%]			[mg·kg^{-1} s.m.]			[kg N·ha^{-1}]	[pH]
Klony wierzby [D]	1047	2,05	1,19	0,058	2,55	2,53	5,08	21,8	5,14
	1054	1,96	1,14	0,061	2,30	2,18	4,48	19,3	5,09
	1023	2,14	1,24	0,059	2,95	2,18	5,13	22,0	5,11
	1013	1,97	1,14	0,065	2,89	2,35	5,24	22,5	5,03
	1052	2,16	1,25	0,061	2,54	2,44	4,98	21,4	5,09
	1047D	2,20	1,27	0,061	2,22	2,19	4,41	19,0	5,13
	1056	2,14	1,24	0,056	2,67	2,56	5,23	22,5	4,99
	1018	2,12	1,23	0,061	3,52	2,24	5,76	24,8	5,28
	1033	2,17	1,26	0,056	2,88	2,82	5,70	24,5	5,00
	$NIR_{0,05}$	**0,25 n.i.**	**0,15 n.i.**	**0,005*****	**0,54*****	**0,30*****	**0,62*****	**2,67*****	**0,08*****
Średnia		2,10	1,22	0,060	2,72	2,39	5,11	22,0	5,09

[1-8]: Oznaczenia analiz właściwości gleby podano w tabeli 2
*Istotność różnic: n.i. – brak istotności; **α = 0,01;***α = 0,001*
Dla NIR podano wartość liczbową dla poziomu istotności α = 0,05

Tabela 4. Wpływ kombinacji nawozowych na cechy jakości w poziomach profilu gleby
Table 4. Effect of fertilizer combinations on quality properties at levels of the soil profile

Kombinacje nawozowe [C]	Głębokość w profilu gleby [B]	Analizy chemicznych właściwości gleby(1-8)					
		3	4	5	6	7	8
		[%]	[mg·kg^{-1} s.m.]			[kg N·ha^{-1}]	[pH]
a	0-30 cm	0,084	3,33	2,47	5,79	24,9	4,95
	31-60 cm	0,054	2,74	1,81	4,55	19,6	5,07
	61-90 cm	0,035	1,80	1,53	3,34	14,4	5,21
b	0-30 cm	0,084	4,25	2,38	6,63	28,5	5,25
	31-60 cm	0,056	2,36	2,00	4,36	18,7	5,25
	61-90 cm	0,033	1,70	1,74	3,44	14,8	5,27
c	0-30 cm	0,094	3,90	3,68	7,59	32,6	4,92
	31-60 cm	0,065	3,12	2,30	5,41	23,3	5,04
	61-90 cm	0,033	1,50	1,33	2,83	12,2	5,06
d	0-30 cm	0,090	3,48	4,65	8,14	35,0	4,99
	31-60 cm	0,056	2,32	2,79	5,10	21,9	5,01
	61-90 cm	0,034	2,20	1,97	4,17	17,9	5,08
$NIR_{0,05}$		0,006 *	0,06 *	0,35 ***	0,72 ***	3,08 ***	0,09 *

(1-8): Oznaczenia analiz właściwości gleby podano w tabeli 2
*Istotność różnic: *α = 0,05; **α = 0,01;***α = 0,001*
Dla NIR podano wartość liczbową dla poziomu istotności α = 0,05

W tabeli 5 zestawiono wyniki analiz regresji dla niektórych właściwości chemicznych gleby, a przy składnikach równań zaznaczono poziom ich istotności. Utworzone równania regresji najlepiej opisywały zmienność zawartości N ogólnego (69,7%) i N azotanowego (61,5%), wyraźnie słabiej zmienność zawartości próchnicy i C organicznego (po 44,7%), N mineralnego (41,6%), i N amonowego (24,4%), a najmniej przy odczynie gleby (9,8%). Kierunek oddziaływania badanych czynników na skład chemiczny gleby był różny.

Po kolejnych latach wegetacji malała zawartość w glebie azotu ogólnego, azotanowego i mineralnego, a wzrastała zawartość azotu amonowego. Nawożenie wierzby kompostem z osadów komunalnych zwiększało zawartość w glebie próchnicy i węgla organicznego oraz podnosiło odczyn gleby, a nie wpływało istotnie na zawartość mineralnych form azotu. Stosowanie nawożenia wierzby mineralnym nawozem azotowym podnosiło w glebie zawartość azotanów i azotu mineralnego, obniżało odczyn gleby, a nie wpływało na zawartość próchnicy, węgla organicznego, azotu ogólnego i amonowego.

W głębszych warstwach profilu gleby malała zawartość wszystkich form azotu, ale podwyższał się odczyn gleby. Opady w okresie wegetacji wierzby (IV-X) obniżały istotnie zawartość w glebie azotu ogólnego, azotanowego i mineralnego, a podwyższały zawartość azotu amonowego.

W literaturze opracowania dotyczące zmian w jakości gleby przy uprawie wierzby są cząstkowe. Uprawa roślin energetycznych (wierzba, miskant i ślazowiec pensylwański) wpływa na zmiany zawartości węgla organicznego w glebie, ale kierunek i wielkość tych zmian są zróżnicowane i zależą od wieku plantacji i warunków glebowych (Grabiński i in. 2010a, Matthews & Grogan 2001, Borzęcka-Walker i in. 2008). W pierwszych 2-3 latach uprawy tych roślin następuje zmniejszenie zawartość C organicznego, a w dalszych (lata 5-7) zwiększenie, szczególnie w wierzchniej warstwie gleby (0-10 cm). W badaniach własnych zawartość C organicznego w glebie również podlegała istotnym zmianom w kolejnych sezonach wegetacji, przy czym w 3 i 4 roku od założenia plantacji zaobserwowano wyraźny wzrost tej formy węgla w stosunku do jego ilości w czasie zakładania plantacji.

Tabela 5. Analiza regresji właściwości chemicznych gleby
Table 5. Regression analysis of chemical properties of soil

Parametr gleby	Składniki równań regresji							D [%]
	stała	lata	kompost, $t \cdot ha^{-1}$	azot, $kg \cdot ha^{-1}$	głębokość, cm	opad IV-X, mm	wsp. K	
Próchnica [%]	2,789 ***	0,143	0,011 *	0,0010	–	0,008	1,675	44,7 ***
C organiczny [%]	1,616 ***	0,083	0,06 *	0,0003	–	0,0046	0,972	44,7 ***
N ogólny $[mg \cdot kg^{-1}$ s.m.]	0,247 ***	-0,025 ***	0,0001	0,0001	-0,001 ***	-0,001 ***	0,287 ***	69,7 ***
$N\text{-}NH_4$ $[mg \cdot kg^{-1}$ s.m.]	-3,782 *	2,091 ***	0,012	-0,001	-0,032 ***	0,098 ***	-26,22 ***	24,4 ***
$N\text{-}NO_3$ $[mg \cdot kg^{-1}$ s.m.]	18,761 ***	-3,762 ***	0,004	0,006 ***	-0,028 ***	-0,177 ***	47,094 ***	61,5 ***
N mineralny $[mg \cdot kg^{-1}$ s.m.]	14,979 ***	-1,671 ***	0,016	0,006 ***	-0,060 ***	-0,078 ***	20,875 ***	41,6 ***
N mineralny $[kg \cdot ha^{-1}]$	64,408 ***	-7,187 ***	0,068	0,024 ***	-0,258 ***	-0,337 ***	89,761 ***	41,6 ***
Odczyn gleby [pH]	5,102 ***	-0,020	0,009 ***	-0,001 ***	0,002 ***	0,0001	-0,099	9,8 ***

*Istotność współczynników regresji: *α = 0,05; **α = 0,01;***α = 0,001*

W literaturze podaje się, że sekwestracja węgla w wierzchniej warstwie gleby przy uprawie wierzby wynosi od 0,30 t C·ha^{-1} (Borzęcka i in. 2008) do 0,41 t C·ha^{-1}(Mattews & Grogan 2001). Potwierdzono dane w literatury, że więcej C organicznego w glebie było po 3 i 4 niż po 1 i 2 roku uprawy. Te same zależności miały miejsce przy zawartości próchnicy w glebie. Na znaczenie próchnicy w kształtowaniu jakości gleby zwraca uwagę Pałosz (2009). Gleby zawierają przeważnie nieduże ilości azotu ogólnego 0,02-0,35%, głównie w formie organicznej, a tylko 1-5% azotu glebowego występuje w formie mineralnej. W badaniach Grabińskiego i in. (2010b), przeciętnie z pięciu grup granulometrycznych gleb w warstwie 0-90 cm było po zakończeniu wegetacji wierzby azotu amonowego – 23,9 kg N·ha^{-1} i azotanowego – 47,1 kg N·ha^{-1}, czyli łącznie azotu mineralnego – 71,0 kg. N·ha^{-1}. Na uprawach tych stosowano co 2 lub 3 lata skomasowaną dawkę azotu 160 lub 240 kg N·ha^{-1} po zbiorze wierzby. W badaniach własnych nawożenie azotem stosowano corocznie wiosną przed ruszeniem wegetacji w dawkach 90 i 180 kg N·ha^{-1}. Przy takim systemie nawożenia pozostałości azotu mineralnego jesienią w glebie wyniosły przeciętnie przy dawce 90 kg N·ha^{-1} – 22,7 kg N·ha^{-1}, a przy dawce 180 kg N·ha^{-1} – 25,0 kg N·ha^{-1}. Są to ilości bardzo małe i dlatego przy uprawie wierzby krzewiastej jest znikoma obawa o niebezpieczeństwo strat azotu mineralnego do środowiska (Obarska-Pempkowiak & Kołecka 2005). W badaniach własnych oraz Grabińskiego i in. (2010c), gleby miały odczyn kwaśny, a pH było wyższe w głębszych warstwach profilu niż w warstwie 0-30 cm.

4. Wnioski

1. Po kolejnych sezonach wegetacji wierzby malała zawartość w glebie azotu ogólnego, azotanowego i mineralnego, a wzrastała zawartość azotu amonowego, węgla organicznego i próchnicy.
2. Nawożenie wierzby kompostem z osadów komunalnych zwiększało zawartość w glebie próchnicy i węgla organicznego oraz podnosiło odczyn gleby, a nie wpływało na zawartość mineralnych form azotu.
3. Stosowanie mineralnego nawożenia azotowego pod wierzbę energetyczną zwiększało w glebie zawartość azotanów i azotu mineralnego, obniżało odczyn gleby, a nie wpływało na zawartość próchnicy, węgla organicznego, azotu ogólnego i amonowego.

Powyższa praca była finansowana przez MNiSW ze środków na naukę w latach 2010-2013 jako projekt badawczy.

Literatura

Borzęcka-Walker, M., Faber, A., Borek, R. (2008). Evaluation of carbon sequestration in energetic crops (*Miscanthus* and coppice willow). *Inst.Agrophysics*, 22, 185-190.

Grabiński, J., Nieróbca, P., Szeleźniak E. (2010a). Wpływ uprawy roślin energetycznych na zawartość węgla organicznego w glebie. *Modelowanie energetycznego wykorzystania biomasy.* Falenty-Warszawa Wydawnictwo IT-P, 22-32.

Grabiński, J., Nieróbca, P., Szeleźniak E. (2010b). Zawartość azotu mineralnego w glebie na plantacjach roslin energetycznych. *Modelowanie energetycznego wykorzystania biomasy.* Falenty-Warszawa Wydawnictwo IT-P, 33-32.

Grabiński, J., Nieróbca, P., Szeleźniak E. (2010c). Zmiany właściwości chemicznych gleby na plantacjach roślin energetycznych. *Modelowanie energetycznego wykorzystania biomasy.* Falenty-Warszawa Wydawnictwo IT-P, 47-56.

Krzywy, E., Iżewska, A., Jeżowski, S. (2003) Wpływ komunalnego osadu ściekowego na zmiany niektórych wskaźników żyzności gleby. *Zesz. Probl. Post. Nauk Rol.,* 494, 215-223.

Matthews, R.B., Grogan, P. (2001). Potential C-sequestration rates under short-rotation coppiced willow and *Miscanthus* biomass crop: a modeling study. *Aspects of Applied Biology*, 65, 303-312.

Molga, M. *Meteorologia rolnicza*. PWRiL Warszawa, 1986.

Obarska-Pempkowiak, H., Kołecka, K. (2005). Doświadczenia związane z wykorzystaniem wikliny *Salix viminalis* w usuwaniu zanieczyszczeń z wód i ścieków. *Rocznik Ochrona Środowiska*, 7, 56-69.

Ociepa-Kubicka, A., Pachura, P. (2013). Wykorzystanie osadów ściekowych i kompostu w nawożeniu roślin energetycznych na przykładzie miskanta i ślazowca. *Rocznik Ochrona Środowiska*, 15, 2267-2278.

Pałosz, T. (2009). Rolnicze i środowiskowe znaczenie bilansu próchnicy glebowej i metodyka jej bilansu. *Rocznik Ochrona Środowiska*, 11, 329-338.

Rosik-Dulewska, Cz., Karwaczyńska, U., Ciesielczuk, T., Głowala, K. (2009). Możliwości nieprzemysłowego wykorzystania odpadów z uwzględnieniem zasad obowiązujących w ochronie środowiska, *Rocznik Ochrona Środowiska,* 11(2), 863-874.

Skowera, B., Puła, J. 2004. Skrajne warunki pluwiometryczne w okresie wiosennym na obszarze Polski w latach 1971–2000. *Acta Agrophysica* 3(1), 171-177.
Styszko, L., Fijałkowska, D., Sztyma, M., Ignatowicz, M. (2010). Wpływ warunków uprawy na pozyskanie biomasy wierzby energetycznej w czteroletnim cyklu. *Rocznik Ochrona Środowiska*, 12, 575-586.
Trętowski, J., Wójcik, A.R. (1988). Metodyka doświadczeń rolniczych. *Wydawnictwo WSRP*, Siedlce.

The Effect of Fertilization with Compost from Municipal Sewage Sludge on the Quality of Light Soil under Cultivation of Coppice Willow during Four-year Cycle

Abstract

The aim of the study was to evaluate selected changes of the quality of light soil in a layer of 0-90 cm, under cultivation of willow coppice (*Salix viminalis*) in the 4-year cycle, due to fertilization with compost from municipal sewage sludge and mineral fertilizers. The experiment was carried out in 2006-2009 on the experimental field of Koszalin University of Technology in Kościernica, Polanów municipality (16°24'N and 54°8'E). The experiment was established on light soil of class IVb-V, of good rye complex, and granulometric composition of light loamy sand to a depth of 100 cm and light loam below 100 cm.

The experiment factors were: fertilization (I) – (a) objects without fertilization, (b) fertilized with compost from municipal sewage sludge (10 $t \cdot ha^{-1}$ d.m.), (c) fertilized with compost from municipal sewage sludge (10 $t \cdot ha^{-1}$ d.m.) and mineral nitrogen in the amount of 90 kg $N \cdot ha^{-1}$, and (d) fertilized with compost from municipal sewage sludge (10 $t \cdot ha^{-1}$ d.m.) and mineral nitrogen in the amount of 180 kg $N \cdot ha^{-1}$ and clones of willow (II) – 1047, 1054, 1023, 1013, 1052, 1047D, 1056, 1033 and 1018. Compost characterized by: pH_{KCl} – 6.63, dry mass content – 68.42%, and content in dry mass was as follows: organic matter – 39.06%, N – 1.75%, P – 1.60%, K – 0.112%, Ca – 3,426% and Mg – 0.325%. Compost was applied in the spring of 2006, and nitrogen fertilizer was applied each year before start of vegetation of willow in the years 2006-2009. The field area was 34.5 m2, it was planted 120 cuttings (34782) pieces$\cdot ha^{-1}$. Each year, after vegetation period of willow soil samples were taken from each plot from three depths: 0-30 cm, 31-60 cm, 61-90 cm. Analysis of soil after first (2006), second (2007), third (2008) and fourth year (2009) the willow vegetation periods included assessment of the content of dry matter, humus and organic carbon, total, ammonium, nitrate and mineral nitrogen and soil pH. Studies

show that during years of shoots regrowth of willow content of total, nitrate and mineral nitrogen decreased in soil and content of ammonium nitrogen, organic carbon and humus increased. Fertilization of willow with compost from municipal sewage sludge caused increase of the content of humus and organic carbon in soil and raised soil pH. It did not affect the content of mineral nitrogen forms. Fertilization of willow with mineral nitrogen caused increase of nitrate and mineral nitrogen content in the soil, and decrease of soil pH, and did not affect the content of humus, organic carbon, total and ammonium nitrogen.

Streszczenie

Celem pracy była ocena niektórych zmian w jakości gleby lekkiej w warstwie 0-90 cm, pod uprawą wierzby wiciowej (*Salix viminalis*) w 4-letnim cyklu, na skutek zastosowania nawożenia kompostem z osadów komunalnych i nawożenia mineralnego. Doświadczenie realizowano w latach 2006-2009 na polu doświadczalnym Politechniki Koszalińskiej w Kościernicy, gmina Polanów (16°24´N i 54°8´E). Doświadczenie założono na glebie lekkiej klasy IVb – V, kompleksu żytniego dobrego, o składzie granulometrycznym piasku gliniastego lekkiego do głębokości 100 cm oraz gliny lekkiej poniżej 100 cm.

Czynnikami doświadczenia były: nawożenie (I) – (a) obiekty bez nawożenia, (b) nawożone kompostem z osadów komunalnych (10 $t \cdot ha^{-1}$ s. m.), (c) nawożone kompostem z osadów komunalnych (10 $t \cdot ha^{-1}$ s. m.) i azotem mineralnym w ilości 90 kg $N \cdot ha^{-1}$ oraz (d) nawożone kompostem z osadów komunalnych (10 $t \cdot ha^{-1}$ s. m.) i azotem mineralnym w ilości 180 kg $N \cdot ha^{-1}$ oraz klony wierzby wiciowej (II) – 1047, 1054, 1023, 1013, 1052, 1047D, 1056, 1033 i 1018. Kompost charakteryzował się: pH_{KCl} – 6,63, zawartość suchej masy – 68,42%, a zawartość w suchej masie wyniosła: materii organicznej – 39,06%, N – 1,75%, P – 1,60%, K – 0,112%, Ca – 3,426% i Mg – 0,325%. Kompost zastosowano wiosną 2006 roku, a nawóz azotowy wysiewano corocznie przed ruszeniem wegetacji wierzby w latach 2006-2009. Poletko miało powierzchnię 34,5 m^2, na którym wysadzono 120 zrzezów (34782 $sztuk \cdot ha^{-1}$). Corocznie po zakończeniu wegetacji wierzby pobierano z każdego poletka próby gleby z trzech głębokości: 0-30 cm, 31-60 cm i 61-90 cm. Analiza gleby po zakończeniu wegetacji wierzby po pierwszym (2006 r.), po drugim (2007 r.), po trzecim (2008 r.) oraz po czwartym roku (2009) obejmowała ocenę na zawartość: suchej masy, próchnicy i węgla organicznego, azotu ogólnego, amonowego, azotanowego i mineralnego oraz odczynu gleby. Badania wykazały, w miarę upływu lat odstania pędów wierzby malała zawartość w glebie azotu ogólnego, azotanowego i mineralnego, a wzrastała zawartość azotu amonowego, węgla organicznego i próchnicy. Nawożenie wierzby kompostem z osadów komunalnych zwiększało zawartość w glebie próchnicy i węgla organicznego oraz pod-

nosiło odczyn gleby, a nie wpływało na zawartość mineralnych form azotu. Stosowanie mineralnego nawożenia azotowego uprawy wierzby energetycznej podnosiło w glebie zawartość azotanów i azotu mineralnego, obniżało odczyn gleby, a nie wpływało na zawartość próchnicy, węgla organicznego, azotu ogólnego i amonowego.

Słowa kluczowe:
gleba, wierzba, nawożenie, kompost, zawartość w glebie: próchnicy, C org., N ogólny, N amonowy, N azotanowy, N mineralny, odczyn gleby

Keywords:
soil, willow, fertilization, compost, content in the soil of: humus, C org., total N, ammonium N, nitrate N, mineral N, soil pH

MIDDLE POMERANIAN SCIENTIFIC SOCIETY OF THE ENVIRONMENT PROTECTION
ŚRODKOWO-POMORSKIE TOWARZYSTWO NAUKOWE OCHRONY ŚRODOWISKA

Annual Set The Environment Protection
Rocznik Ochrona Środowiska

Volume/Tom 19. Year/Rok 2017 ISSN 1506-218X 633-650

Modelowanie zmian parametrów ścieków oczyszczonych z wykorzystaniem sztucznych sieci neuronowych

Iwona Skoczko, Joanna Struk-Sokołowska, Piotr Ofman
Politechnika Białostocka

1. Wprowadzenie

Modelowanie matematyczne coraz częściej wykorzystywane jest w niemal każdej gałęzi przemysłu. Możliwość przewidywania efektów pracy obiektów technologicznych w dzisiejszych czasach jest bardzo pożądana, szczególnie gdy możliwa jest aproksymacja zmian zachodzących w układach biologicznych, takich jak oczyszczalnie ścieków (Baczyński 2010, Sochacki i in. 2010). Czasochłonne, a niejednokrotnie kłopotliwe, badania technologiczne wypierane są wynikami modelowania matematycznego prowadzonego na bazie symulacji komputerowych (Çinar 2005, Ráduly i in. 2007, Piekarski 2011). Tego typu podejście pozwala na znaczne zaoszczędzenie czasu, potrzebnego w innym wypadku na analizy laboratoryjne (Tomenko i in. 2007, Dymaczewski 2008, Sadecka i in. 2011, Haimi i in. 2013), a także umożliwia dobre odzwierciedlenie zmian, jakie zachodzą w trakcie całego procesu (Szetela & Dymaczewski 2002, Dymaczewski 2008, Ou i in. 2015). Ponadto, podejście modelowe w oczyszczaniu ścieków może wskazać momenty, w których występują nieprawidłowości w ciągu technologicznym obiektu lub okresy, gdy parametry ścieków oczyszczonych ulegną pogorszeniu (Mjalli i in. 2007). Zgodnie z pozwoleniami wodno-prawnymi ścieki oczyszczone odprowadzane do środowiska wodnego powinny spełniać określone normy (Hong i in. 2007, Eriksson i in. 2008, Andraka & Dzienis 2013). Dlatego też, możliwość wcześniejszego wykrycia potencjalnej awarii lub

nieprawidłowości w pracy oczyszczalni ścieków jest uzasadniona i pożądana z punktu ekonomicznego i środowiskowego.

Powszechnie wykorzystywane modele ASM w układach oczyszczania ścieków znajdują zastosowanie podczas planowania koncepcji technologicznych. Algorytmy te są rozbudowane do takiego stopnia, że na etapie projektowania pozwalają na stosunkowo dokładny opis zmian zachodzących w ściekach podczas ich oczyszczania (Moral i in. 2008, Benintendi 2015). Ze względu na stopień dokładności modeli ASM przed stworzeniem ciągu technologicznego oczyszczalni ścieków należy przeprowadzić szereg badań laboratoryjnych, uwzględniających między innymi frakcje ChZT czy alkaliczność ścieków. Oprócz tego modele ASM wymagają uwzględnienia parametrów technologicznych osadu czynnego (Gernaey i in. 2004, Lee i in. 2011, Heranandez i in. 2013), a zaawansowanie modelowanie wymaga od użytkownika znajomości stopnia kinetyki rozkładu danego związku w trakcie jego usuwania ze ścieków (Pomiès i in. 2013). Z tych powodów opis pracy oczyszczalni ścieków z wykorzystaniem gotowego oprogramowania jest trudny i czasochłonny.

Przez wzgląd na dokładność i ilość parametrów, które należy uwzględnić w modelu ASM ich wykorzystanie ogranicza się do wąskiego grona specjalistów z zakresu technologii oczyszczania ścieków. Stąd wynika potrzeba prostszego i niemniej skutecznego odwzorowania zmian zachodzących podczas oczyszczania ścieków (Gontarski i in. 2000, Skoczko i in. 2016). W literaturze tematu coraz częściej spotykane jest wykorzystanie sztucznych sieci neuronowych, które umożliwiają odzwierciedlenie pracy oczyszczalni ścieków na zasadzie tak zwanego modelu czarnej skrzynki (Moreno-Alfonso i Redondo 2001, Tomenko i in. 2007, Lee i in. 2011, Ou i in. 2015). W odróżnieniu od modeli ASM sztuczne sieci neuronowe, pozwalają na dowolność w przyjmowaniu zmiennych do prognozy jakości ścieków oczyszczonych (Dellana & West 2009, Gawdzik i in. 2016). Poprzez poszukiwanie najprostszej relacji pomiędzy zmiennymi wejściowymi i wyjściowymi, sieci neuronowe mogę uwzględniać jedynie parametry opisujące skład chemiczny ścieków surowych i oczyszczonych (Moreno-Alfonso i Redondo 2001, Czapczuk i in. 2015). Swobodny dobór zmiennych uwzględnianych w modelu teoretycznie pozwala na dokładniejsze odzwierciedlenie procesu oczyszczania ścieków. Ta własność jest szczególnie istotna w przypadku oczyszczalni przemysłowych lub oczyszczalni komunalnych przyjmujących

ścieki przemysłowe. Stwierdzenie te uzasadnione jest możliwością uwzględnienia w modelu parametrów potencjalnie toksycznych dla mikroorganizmów bytujących w osadzie czynnym (Sánchez-Avila i in. 2009, Sponza & Gök, 2010, Badawy i in. 2010, Deblonde i in. 2011).

W pracy przedstawiono i oceniono opracowany model sztucznej sieci neuronowej stworzonej na podstawie wyników badań prowadzonych w oczyszczalni ścieków, do której dopływają ścieki komunalne z udziałem ścieków mleczarskich pochodzących z zakładu zlokalizowanego w Bystrym koło Giżycka.

2. Metodyka

Model sztucznej sieci neuronowej aproksymujący stężenia i wartości wybranych parametrów ścieków oczyszczonych stworzono na podstawie wyników badań udostępnionych przez Przedsiębiorstwo Wodociągów i Kanalizacji w Giżycku. Analizy laboratoryjne prowadzone były w odstępach 7 dniowych w latach 2014 i 2015. Zakres badań obejmował BZT_5 i $ChZT_{Cr}$, azot ogólny, fosfor ogólny, zawiesiny ogólne w ściekach surowych i oczyszczonych. Dodatkowo w ściekach surowych badano odczyn i temperaturę. Analizy wykonywano zgodnie z następującymi normami:

- Odczyn – PN-EN ISO 10523:2012
- BZT_5 – PN-EN 1899-1:2002
- $ChZT_{Cr}$ – PN- ISO 6060:2006
- Azot ogólny – PB-13/2006/PG wyd. 3 z 02.012013
- Fosfor ogólny – PN-EN ISO 6878:2006+Ap1. 2010+Ap2.:2010 p.7
- Zawiesiny ogólne – PN-EN 872:2007+Ap1:2007

Ścieki surowe dopływają do oczyszczalni systemem kanalizacji grawitacyjnej i tłocznej. Wstępne mechanicznie oczyszczanie ścieków (rys. 1) następuje w budynku krat. Kolejnym etapem oczyszczania mechanicznego jest piaskownik, w którym wskutek zwolnienia przepływu ścieków następuje wytrącenie i sedymentacja zawiesiny mineralnej. Dodatkowo piaskownik jest napowietrzany sprężonym powietrzem w celu lepszego flotowania części pływających. Po oczyszczeniu mechanicznym ścieki przepływają do układu komór biologicznych, pełniących podstawową funkcję oczyszczania biologicznego. W pierwszym etapie ścieki dopływają do komory defosfatacji (beztlenowej), następnie do komór

denitryfikacji (niedotlenionych), do której recyrkulowany jest strumień azotanów z komór nitryfikacji (recyrkulacja wewnętrzna). Ścieki z komory denitryfikacji przepływają do komór nitryfikacji (tlenowych). Po oczyszczeniu w reaktorach biologicznych mieszanina osadu czynnego i ścieków dopływa poprzez przelewy do komór rozdziału i dalej do dwóch osadników wtórnych. W osadnikach następuje rozdział osadu czynnego od ścieków oczyszczonych w warunkach zwolnionego przepływu. Badana oczyszczalnia ścieków charakteryzowała się RLM na poziomie 98615. Fragment schematu technologicznego oczyszczalni ścieków w Bystrym koło Giżycka, istotny z punktu przeprowadzonych badań, przedstawiono na rysunku 1.

Wyniki przeprowadzonych badań poddano analizie statystycznej, która obejmowała wyznaczenie średniej arytmetycznej, mediany, odchylenia standardowego, minimum, maksimum oraz opracowanie modelu sztucznej sieci neuronowej. Obliczenia wykonano przy użyciu licencjonowanego oprogramowania Statistica 12.5 w polskiej wersji językowej pracującej na platformie Windows 10. Do analiz statystycznych wykorzystano łącznie około 2200 wyników pomiarów.

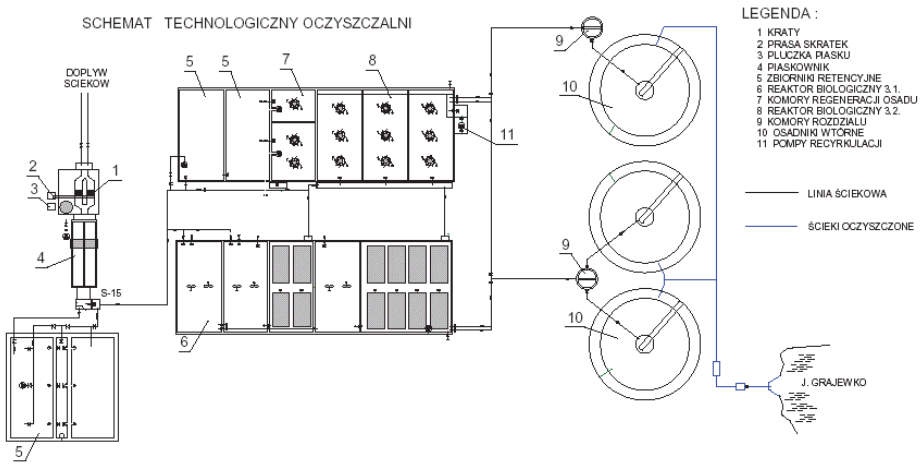

Rys. 1. Fragment schematu technologicznego oczyszczalni ścieków w Bystrym koło Giżycka

Fig. 1. Fragment of Bystre wastewater treatment plant technological scheme

Do budowy sztucznej sieci neuronowej zastosowano próbkowanie w ilości 6000 sieci, do którego wykorzystano sieci z wielowarstwowym perceptronem. W etapie próbkowania pominięto funkcję liniową do aktywacji perceptronu. Po wyborze spośród 6000 sieci, najlepszą z nich, poddano ponownemu uczeniu, które przebiegało w dwóch etapach. W pierwszej fazie jako algorytm uczący wykorzystano wsteczną propagację błędu, natomiast w drugiej fazie gradienty sprzężone. W pierwszym etapie ponownego uczenia zadano 5000 epok, a w drugim 1000. Prędkość uczenia sztucznej sieci neuronowej w obu fazach przyjęto za równą 0,001, natomiast za funkcje aktywujące warstwę ukrytą i wyjściową neuronów przyjęto odpowiednio logistyczną i wykładniczą.

3. Wyniki badań i dyskusja

Badane parametry ścieków dopływających do oczyszczalni wykazywały dużą zmienność w ciągu okresu badawczego. Wartości minimalne i maksymalne, jakie zaobserwowano w trakcie badań dla BZT_5 równe były odpowiednio 370,00 i 1450,00 mg $O_2 \cdot dm^{-3}$. Mimo dużej rozpiętości pomiędzy wartościami ekstremalnymi, zmienność BZT_5 w ciągu okresu badawczego zrównoważona, o czym świadczą zbliżone wartości średniej arytmetycznej (655,38 mg $O_2 \cdot dm^{-3}$) i mediany (620,00 mg $O_2 \cdot dm^{-3}$) oraz odchylenie standardowe, stanowiące około 26% średniej arytmetycznej (171,38 mg $O_2 \cdot dm^{-3}$).Wartości $ChZT_{Cr}$ zmieniały się w zakresie od 640,00 do 1840,00 mg $O_2 \cdot dm^{-3}$. Podobnie jak w przypadku BZT_5 nie obserwowano nagłych zmian wartości $ChZT_{Cr}$ w ściekach surowych. Zmiany w stężeniu azotu ogólnego w ściekach surowych wahały się od 58,00 do 126 mg $N \cdot dm^{-3}$. Na podstawie średniego stężenia tego parametru w okresie badawczym (88,85 mg $N \cdot dm^{-3}$) i mediany (89,00 mg $N \cdot dm^{-3}$) oraz odchylenia standardowego na poziomie 11,47 mg $N \cdot dm^{-3}$ stwierdzono, że zmiany w stężeniu azotu ogólnego były stopniowe i wynikały z wielkości produkcji w Zakładzie Przetwórstwa Mleka. Podobną prawidłowość obserwowano w przypadku fosforu ogólnego. Średnia arytmetyczna na poziomie 12,94 mg $P \cdot dm^{-3}$ i mediana równa 12,55 mg $P \cdot dm^{-3}$, przy zakresie od 8,40 do 24,40 mg $P \cdot dm^{-3}$ świadczą o stopniowych zmianach tego parametru w trakcie badań.

Tabela 1. Statystyki podstawowe wyników badań
Table 1. Basic statistics of studies results

Zmienna	Jednostka	Średnia arytmetyczna	Mediana	Odchylenie standardowe	Minimum	Maksimum
Q	$m^3 \cdot d^{-1}$	6469,54	6286,50	±676,11	4803,00	8438,00
BZT_5 – ŚS	mg $O_2 \cdot dm^{-3}$	655,38	620,00	±171,38	370,00	1450,00
$ChZT_{Cr}$ – ŚS	mg $O_2 \cdot dm^{-3}$	1246,33	1215,00	±252,11	640,00	1840,00
N_{og} – ŚS	mg $N \cdot dm^{-3}$	88,85	89,00	±11,47	58,00	126,00
P_{og} – ŚS	mg $P \cdot dm^{-3}$	12,94	12,55	±2,25	8,40	24,40
Z_{og} – ŚS	mg $\cdot dm^{-3}$	651,27	585,00	±220,86	330,00	1450,00
T – ŚS	°C	16,94	16,30	±2,65	11,60	21,30
pH – ŚS	–	–	–	–	7,00	7,90
BZT_5 – ŚO	mg $O_2 \cdot dm^{-3}$	4,61	4,50	±1,46	2,00	11,00
$ChZT_{Cr}$ – ŚO	mg $O_2 \cdot dm^{-3}$	61,44	60,00	±7,90	45,00	86,00
N_{og} – ŚO	mg $N \cdot dm^{-3}$	6,77	6,55	±2,17	2,70	15,20
P_{og} – ŚO	mg $P \cdot dm^{-3}$	0,52	0,47	±0,18	0,29	1,82
Z_{og} – ŚO	mg $\cdot dm^{-3}$	6,97	6,75	±2,11	3,30	16,00

Q – ilość ścieków dopływająca z zakładu na oczyszczalnię,
ŚS – wartości i stężenia w ściekach surowych,
ŚO – wartości i stężenia w ściekach oczyszczonych.

Spośród wszystkich badanych parametrów największą zmiennością charakteryzowały się zawiesiny ogólne. Mimo zbliżonych wartości średniej arytmetycznej (651,27 $mg \cdot dm^{-3}$) i mediany (585,00 $mg \cdot dm^{-3}$) odchylenie standardowe równe było 220,86 $mg \cdot dm^{-3}$ i stanowiło około 34% średniej arytmetycznej tego parametru.

Badane parametry jakościowe ścieków były zbliżone do tych, które prezentowali Demirel i inni (2007) w pracy poświęconej przeglądowi parametrów ścieków mleczarskich na terenie Holandii. Podobne wielkości poszczególnych parametrów w ściekach surowych zaobserwowała Bartkowska i inni (2011) w badaniach poświęconym jakości ścieków w oczyszczalni ścieków w Hajnówce, która oczyszcza zmieszane ścieki komunalne i mleczarskie. Nieznacznie mniejsze wartości i stężenie poszczególnych parametrów, w porównaniu z obserwowanymi w Giżycku, uzyskała Zielińska i inni (2013). Znacznie mniejsze wartości BZT_5 i ChZT w mieszaninie ścieków komunalnych i mleczarskich obserwowała Krzemińska i inni (2013) oraz Struk-Sokołowska na oczyszczalni w Olecku (2011) i Hajnówce (2013).

Proces mechaniczno-biologicznego oczyszczania ścieków w badanym obiekcie przebiegał stabilnie w ciągu okresu badawczego. Świadczą o tym niewielkie zmiany wartości i stężenia poszczególnych parametrów podlegających kontroli. Wartości średnich arytmetycznych i median wszystkich analizowanych składników były zbliżone do siebie. Największe zróżnicowanie w wartościach badanych parametrów zaobserwowano dla azotu ogólnego i zawiesin ogólnych. Odchylenia standardowe tych wskaźników równe były odpowiednio 2,17 i 2,11 przy zakresie zmienności dla azotu –2,7-15,2 mg $N \cdot dm^{-3}$ i zawiesin ogólnych – 3,3-16,0 $mg \cdot dm^{-3}$.

Najlepsza z uzyskanych sieci neuronowych charakteryzowała się topologią 8-13-8-5. Oznacza to, że w warstwie wejściowej, w trakcie toku obliczeniowego, nie odrzucono żadnej ze zmiennych badanych w ściekach surowych. Następnie model uwzględniał dwie warstwy ukryte, które składały się kolejno z 13 i 8 neuronów. Warstwę wyjściową stanowiły neurony opisujące wartości poszczególnych wskaźników jakościowych, badanych w ściekach oczyszczonych. Topologię uzyskanego modelu przedstawiono na rysunku 2.

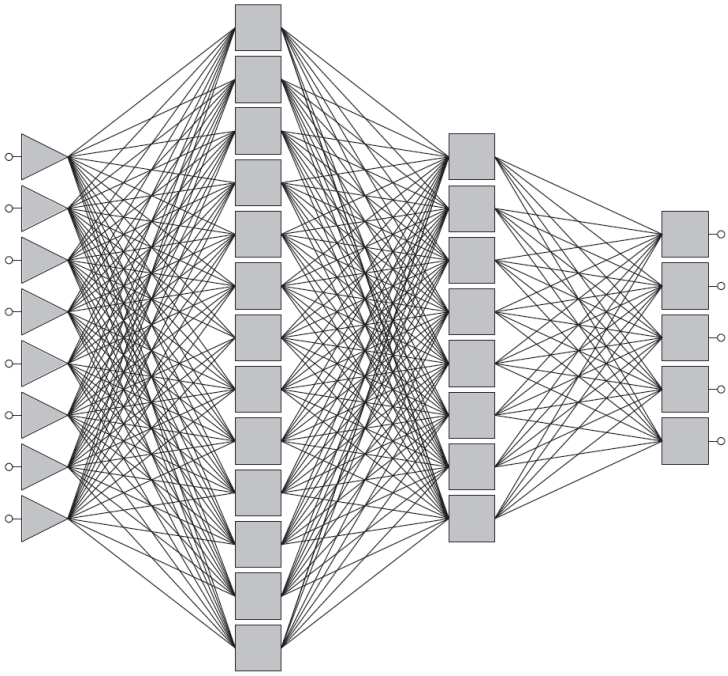

Rys. 2. Struktura modelu sztucznej sieci neuronowej
Fig. 2. Structure of artificial neural network model

Opracowany model sztucznej sieci neuronowej pozwolił na uzyskanie dobrego dopasowania wartości aproksymowanych do rzeczywistych. Wartości średnich arytmetycznych i odchyleń standardowych estymowanych wielkości zbliżone były do tych, które obserwowano w ściekach surowych w trakcie badań. Średnia wartość BZT_5 uzyskana w modelu równa była 4,51 mg $O_2 \cdot dm^{-3}$ i była mniejsza o około 2% w stosunku do średniej wartości tego parametru obserwowanej w ściekach. W przypadku $ChZT_{Cr}$ średnia wartość równa była 61,81 mg $O_2 \cdot dm^{-3}$. Wynik ten różnił się o około 1% w odniesieniu do wartości rzeczywistej. Średnie stężenie azotu ogólnego jakie było aproksymowane przez model wynosiło 7,07 mg $N \cdot dm^{-3}$ i było większe o około 4% od wartości średniej uzyskanej w ściekach oczyszczonych w ciągu okresu badawczego. Fosfor ogólny, zgodnie z aproksymacją modelu, średnią wartość przyjmował na poziomie 0,52 mg $P \cdot dm^{-3}$. Uzyskany wynik nie różnił się od wartości średniej arytmetycznej tego parametru obserwowanej w ściekach. W przy-

padku zawiesin ogólnych różnica pomiędzy średnią wartością tego parametru obserwowanego w ściekach i wartościach, jakie były aproksymowane przez model wynosiła około 2%.

Tabela 2. Statystyki opisowe zmiennych aproksymowanych przez model sztucznej sieci neuronowej
Table 2. Basic statistics of approximated variables in artificial neural network model

Parametr statystyczny	Zmienne wyjściowe, aproksymowane przez model				
	BZT_5 [mg $O_2 \cdot dm^{-3}$]	$ChZT_{Cr}$ [mg $O_2 \cdot dm^{-3}$]	N_{og} [mg $N \cdot dm^{-3}$]	P_{og} [mg $P \cdot dm^{-3}$]	Z_{og} [mg $\cdot dm^{-3}$]
Średnia	4,51	61,81	7,07	0,52	6,87
Odchylenie standardowe	1,35	8,15	2,36	0,14	2,04
Średni błąd bezwzględny	0,86	5,80	1,49	0,08	1,09
Korelacja	0,47	0,46	0,66	0,68	0,73
R^2	0,46	0,58	0,70	0,70	0,75

Średni błąd bezwzględny z jakim estymowano parametry jakościowe ścieków surowych dla wartości BZT_5 przyjmował wartość 0,86, w przypadku $ChZT_{Cr}$ równy był 5,80, dla azotu i fosforu ogólnego, odpowiednio, 1,49 i 0,08, a dla zawiesin ogólnych 1,09. Średnie błędy szacowania nie przekraczały 22% wartości średniej arytmetycznej poszczególnych wskaźników obserwowanych w ściekach oczyszczonych.

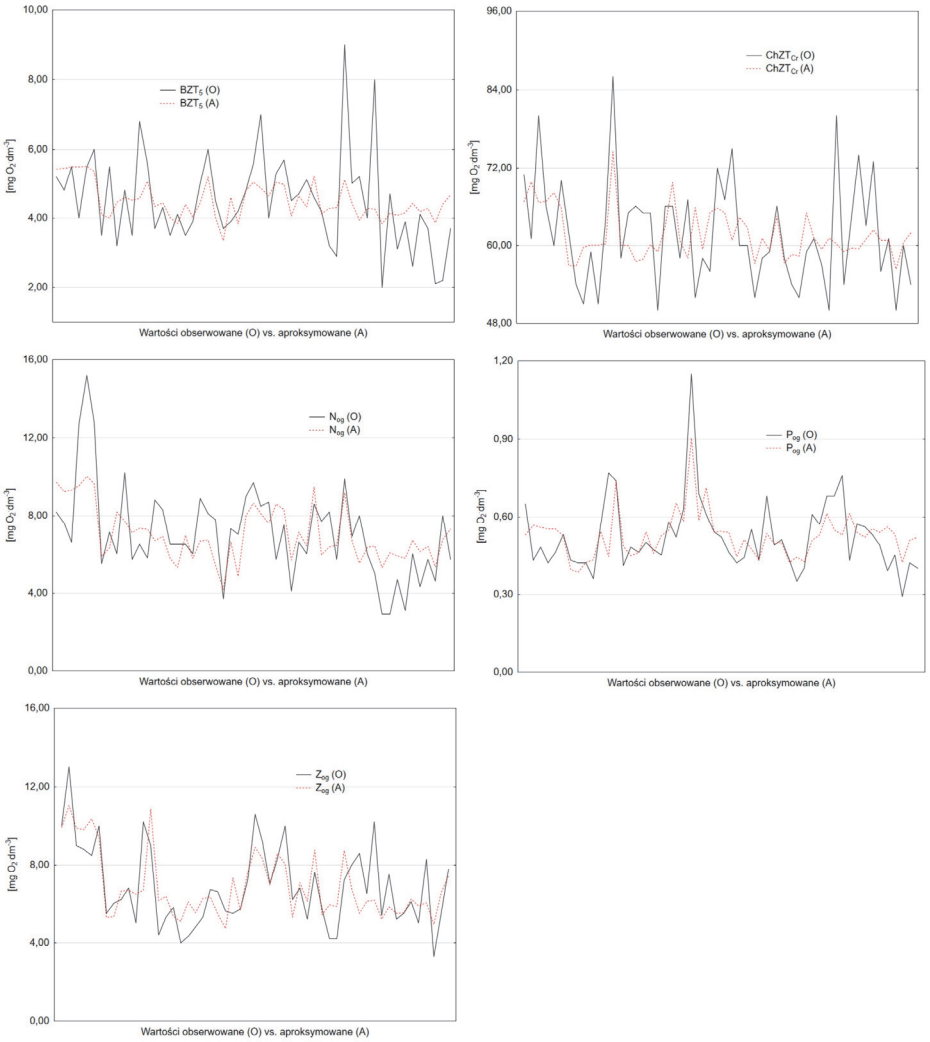

Rys. 3. Dopasowanie modelu sztucznej sieci neuronowej do rzeczywistych parametrów ścieków
Fig. 3. Artificial neural network model fit to observed wastewater parameters

Odnosząc się do miar dokładności dopasowania modelu do wartości obserwowanych, zaobserwowano, że model sztucznej sieci neuronowej najlepiej odzwierciedlił zmiany w wartościach zawiesin ogólnych. Wskaźnik ten, charakteryzował się współczynnikiem korelacji na poziomie 0,73 i współczynnikiem R^2 równym 0,75. Nieco mniejsze dopasowanie uzyskano w stosunku do azotu i fosforu ogólnego. Uzyskane wartości korelacji wynosiły, odpowiednio dla azotu i fosforu, 0,66 i 0,68. Natomiast współczynniki determinancji dla obu parametrów przyjęły tożsamą wartość równą 0,70. Mniejsze dopasowanie, w odniesieniu do pozostałych parametrów, uzyskano dla $ChZT_{Cr}$. Wartości współczynników korelacji i R^2 tego parametru równe były, odpowiednio, 0,46 i 0,58. Opracowany model w najmniejszym stopniu odwzorował zmiany, jakie zachodziły, w wartościach BZT_5. Współczynnika korelacji w tym przypadku równy był 0,47, a współczynnik R^2 0,46.

Model sztucznej sieci neuronowej aproksymujący zmiany w wartości zawiesin ogólnych, prezentowany przez Hanaby i współautorów (2008) dobrze odzwierciedlał trend zmian jakim podlegał ten parametr, jednakże wyniki uzyskane na drodze obliczeń były o około 20% większe w stosunku do wartości obserwowanych. Podobną relację wykazywał model prezentowany w tej pracy. Verma i inni (2013) uzyskali zbliżone do przedstawionego dopasowanie modelu sieci neuronowej w predykcji $ChZT_{Cr}$. Dokładność aproksymacji uzyskana przez autorkę wynosiła od 73,00 do 79,00%. Podobne dopasowanie wartości $ChZT_{Cr}$ i zawiesin ogólnych otrzymali Gieru i współautorzy (2006) w modelach aproksymujący wartości tych parametrów w ściekach. Prezentowane modele charakteryzowały się błędami estymacji z zakresu od 9,70 do 13,70% w stosunku do $ChZT_{Cr}$ i od 10,20 do 14,20% w stosunku do zawiesin ogólnych. Mniejsze, w porównaniu z prezentowanym modelem, dopasowanie aproksymowanych wartości $ChZT_{Cr}$ uzyskali Fang i inni (2010) oraz Kriger i Tzoneva (2007). Model prezentowany przez Fanga i współautorów charakteryzował się współczynnikiem determinancji na poziomie 0,01, natomiast Kriger uzyskał korelację równą 0,36. Kriger i Tzoneva (2007) oraz Akratos i inni (2009) przedstawili w pracach wyniki aproksymacji stężenia azotu ogólnego. Kriger i Tzoneva uzyskali mniejszy niż prezentowany współczynnik korelacji (0,52), natomiast dopasowanie modelu Akratosa było zbliżone ze względu na współczynnik determinacji (R^2=0,69). Nieco lepsze dopasowanie w przypadku aproksy-

macji wartości BZT_5 uzyskali Akratos i współautorzy (2008), gdzie współczynnik R^2 wynosił 0,52. Nieznacznie lepsze dopasowanie w stosunku do predykcji fosforu ogólnego uzyskali Akratos i inni (2009a). Współczynnik determinancji dla tego wskaźnika wynosił 0,83.

Wskaźniki, które zgodnie z miarami dopasowania modelu (korelacje i R^2), cechowały się najmniejszym dopasowaniem nie były aproksymowane z największym błędem. Mniejsze, w porównaniu z pozostałymi wskaźnikami, dopasowanie BZT_5 i $ChZT_{Cr}$ powodowane było brakiem odwzorowania w modelu wartości skrajnych występujących epizodycznie w trakcie okresu badawczego. W przypadku pozostałych zmiennych model umożliwił dobre odwzorowanie wartości ekstremalnych. Szczegółowy przebieg zmian badanych parametrów w ściekach oczyszczonych zestawiono na rysunku 3.

Tabela 3. Analiza wrażliwości modelu
Table 3. Model sensivity analysis

Miara istotności i ranga	Zmienna wejściowa w modelu							
	Q	BZT_5	$ChZT_{Cr}$	N_{og}	P_{og}	Z_{og}	T	pH
Iloraz	1,12	1,09	1,07	1,01	1,01	1,17	1,07	1,04
Ranga	2,00	3,00	4,00	8,00	7,00	1,00	5,00	6,00

Odnosząc się do analizy wrażliwości modelu sztucznej sieci neuronowej przedstawionej w tabeli 4, zaobserwowano, że największy wpływ na predykcję poszczególnych wskaźników w ściekach oczyszczonych miało stężenie azotu ogólnego, które odznaczało się największą rangą. Kolejnymi ze względu na istotność predykcji zmiennymi było stężenie fosforu ogólnego stężenie fosforu ogólnego, odczyn ścieków dopływających do oczyszczalni, temperatura ścieków surowych, stężenie związków organicznych charakteryzowanych parametrami $ChZT_{Cr}$ i BZT_5. Ilość zawiesin ogólnych w ściekach surowych oraz ich ilość trafiająca na oczyszczalnię miały najmniejszy wpływ na aproksymację zmiennych wyjściowych. Ze względu na ilorazy stężenie azotu i fosforu ogólnego miały prawie równoważny wpływ na proces oczyszczania ścieków. Podobna relacja występowała pomiędzy wartością $ChZT_{Cr}$ i temperaturą ścieków surowych.

4. Podsumowanie

Ścieki surowe należą do jednych z najbardziej skomplikowanych pod względem chemicznym cieczy. W trakcie ich biologicznego oczyszczania zachodzą tysiące reakcji jednostkowych, których celem jest biodegradacja zanieczyszczeń. Dokładny opis matematyczny takich zjawisk jest niezwykle trudny, a niejednokrotnie niemożliwy. Stąd, potrzeba stosowania rozbudowanych i złożonych algorytmów, które pozwolą możliwie dokładnie oddać charakter zmian mających miejsce w reaktorach biologicznych. W takim przypadku zadaniem sztucznych sieci neuronowych jest odnalezienie najprostszej relacji, jaka występuje pomiędzy dobranymi parametrami jakościowymi w układzie ściek surowy-ściek oczyszczony.

W niniejszej pracy przedstawiono model, którego zadaniem była predykcja pięciu podstawowych parametrów ścieków oczyszczonych, podlegających okresowej kontroli. W większość prac poświęconych modelowaniu matematycznemu procesów oczyszczania ścieków prezentowane są modele aproksymujące jedną zmienną. Rzadziej spotykane są algorytmy jednocześnie estymujące więcej niż trzy zmienne. Wynika to ze stopnia złożoności i częstotliwości występowania jednostkowych zmian w trakcie procesów biologicznych. Nie mniej prezentowany model pozwolił z dość dużą dokładnością odwzorować zmiany ilościowe podstawowych wskaźników charakteryzujących ścieki oczyszczone.

Literatura

Akratos, C. S., Papspyros, J. N. E., Tsihrintzis, V. A. (2008). An artificial neural network model and design equations for BOD and COD removal prediction in horizontal subsurface flow constructed wetland. *Chemical Engineering Journal*, *143*, 96-110.

Akratos, C. S., Papspyros, J. N. E., Tsihrintzis, V. A. (2009). Total nitrogen and ammonia removal prediction in horizontal subsurface flow constructed wetlands: Use of artificial neural networks and development of a design equation. *Biosource Technology*, *100*, 586-596.

Akratos, C. S., Papspyros, J. N. E., Tsihrintzis, V. A. (2009a). Artifical neural network use in ortho-phosphate and total phosphorus removal prediction in horizontal subsurface flow constructed wetlands. *Biosystems Engineering*, *102*, 190-201.

Andraka, D., Dzienis, L. (2013). Modelowanie ryzyka w eksploatacji oczyszczalni ścieków, *Rocznik Ochrona Środowiska*. *15*, 1111-1125.

Baczyński, T. (2010). Przegląd metod służących wyznaczaniu frakcji ChZT w ściekach. *Gaz, Woda i Technika Sanitarna, X*, 29-35.

Badawy, M. I., El-Wahaab, R. A., Moawad, A., Ali, M. E. M. (2010). Assessment of the performance of aerated oxidation ponds in the removal of Persistent Organic Pollutants (POPs): A case study. *Desalination, 251*, 29-33.

Bartkowska, I., Dzienis, L., Wawrentowicz, D. (2011). Efektywność pracy oczyszczalni ścieków w Hajnówce i propozycja jej modernizacji. *Inżynieria Ekologiczna, 24*, 226–235.

Benintendi, R. (2015). Modeling and experimental investigation of activated sludge VOCs adsorption and degradation. *Process Safety and Environmental Protection, 575*, 1-9.

Czapczuk, A., Dawidowicz, J., Piekarski, J. (2015). Metody sztucznej inteligencji w projektowaniu i eksploatacji systemów zaopatrzenia w wodę. *Rocznik Ochrona Środowiska, 17*, 1527-1544.

Deblonde, T., Cossu-Leguille, C., Hartemann, P. (2011). Emerging pollutants in wastewater: A review of the literature. *International Journal of Hygiene and Environmental Health, 214*, 442-448.

Dellana, S. A., West, D. (2009). Predictive modeling for wastewater applications: Linear and nonlinear approaches. *Environmental Modeling and Software, 24*, 96-106.

Demirel, B., Yenigun, O., Onay, T. T. (2005). Anaerobic treatment of dairy wastewaters: a review. *Process Biochemistry, 40*, 2583-2595.

Dymaczewski, Z. (2008). Charakterystyka frakcji organicznych ścieków miejskich pod kątem modelu osadu czynnego ASM2d. *Przemysł Chemiczny, 87/5*, 440–442.

Eriksson, E., Christensen, N., Schmidt, J. E., Ledin, A. (2008). Potential priority pollutants in sewage sludge. *Desalination, 226*, 371-388.

Fang, F., Ni, B-J., Xie, W-M., Sheng, G-P., Liu, S-G., Tong, Z-H., Yu, H-Q. (2010). An integrated dynamic model for simulating a full-scale municipal wastewater treatment plant under fluctuating conditions. *Chemical Engineering Journal, 160*, 522-529.

Gawdzik J., Szeląg B., Bezak-Mazur E., Stoińska R. (2016). Zastosowanie wybranych modeli nieliniowych do prognozy ilości osadu nadmiernego. *Rocznik Ochrona Środowiska, 18*, 695-708

Gernaey, K. V., van Loosdrecht, M. C. M., Henze, M., Lind, M., Jørgensen, B. (2004). Activated sludge wastewater treatment plant modeling and simulation: state of the art. *Environmental Modeling and Software, 19*, 763-783.

Gieru, S., Thiery, F., Traoré, A., Nguyen, T. P., Barreau, M., Polit, M. (2006). KSOM and MLP neural networks for on-line estimating the efficiency of an activated sludge process. *Chemical Engineering Journal, 116*, 1-11.

Gontarski, C. A., Rodrigues, P. R., Mori,M., Prenem, L. F. (2000). Simulation of an industrial wastewater treatment plant using artificial neural networks. *Computer and Chemical Engineering, 24*, 1719-1723.

Haimi, H., Mulas, M., Corona, F., Vahala, R. (2013). Data-derived soft-sensors for biological wastewater treatment plants: An overview. *Environmental Modeling and Software, 47*, 88-107.

Hamed, M., Khalafallah, M. G., Hassanein, E. A. (2004). Prediction of wastewater treatment plant performace using artificial neural network. *Environmental Modeling and Software, 19*, 919-928.

Hanaby, D., Turkoglu, I., Demir, Y. (2008). Prediction of wastewater treatment plant performance based on wavelet packet decomposition and neural networks. *Expert Systems with Applications, 34*, 1038-1043.

Hernandez, S. C., Bueno, J. A., Sanchez, E. N., Diaz-Jimenez, L. (2013). State Estimation by Artificial Neural Networks in a Continuous Bioreactor. *IFAC Proceedings Volumes, 46*, 215-220.

Hong, S. H., Lee, M. W., Lee, D. S., Park, J. M. (2007). Monitoring of sequencing batch reactor for nitrogen and phosphorus removal using neural networks. *Biochemical Engineering Journal, 35*, 365-370.

Kriger, C., Tzoneva, R. (2007). A neural network model for control of wastewater treatment process. *IFAC Proceedings Volumes, 40*, 981-986.

Krzemińska, D., Neczaj, E., Parkitna, K. (2013). Zastosowanie reakcji Fentona do wspomagania biologicznego oczyszczania ścieków z przemysłu mleczarskiego. *Rocznik Ochrona Środowiska, 15*, 2381-2397.

Lee, J-W., Suh, C., Hong, Y-S. T., Shin, H-S. (2011). Sequential modeling of full-scale wastewater treatment plant using and artificial neural network. *Bioprocesses and Biosystems Engineering, 34*, 963-973.

Lee, J-W., Suh, C., Hong, Y-S. T., Shin, H-S., (2011). Sequential modeling of full-scale wastewater treatment plant using and artificial neural network, *Bioprocesses and Biosystems Engineering*, 34, 963-973.

Mjalli, F. S., Al-Asheh, S., Alfadala, H. E. (2007). Use of artificial neural network black-box modeling for prediction of wastewater treatment plants performance. *Journal of Environmental Management, 83*, 329-338.

Moral, H., Aksoy, A., Gokcay, C. F. (2008). Modeling of the activated process by using artificial neural networks with automated architecture screening. *Computers and Chemical Engineering, 32*, 2471-2478.

Moreno-Alfonso, N., Redondo, C. F. A. (2001). Intelligent waste-water treatment with neural-networks. *Water Policy, 3*, 267- 271.

Ou, H-S., Wei, C-H., Wu, H-Z., He, B-Y. (2015). Sequential dynamic artificial neural network modeling of a full-scale coking wastewater treatment plant with fluidized bed reactors. *Environmental Science and Pollution Research, 22*, 15910-15919.

Ou, H-S., Wei, C-H., Wu, H-Z., He, B-Y. (2015). Sequential dynamic artificial neural network modeling of a full-scale coking wastewater treatment plant with fluidized bed reactors. *Environmental Science and Pollution Research, 22*, 15910-15919.

Piekarski, J. (2011). Zastosowanie metod numerycznych do modelowania procesu filtracji grawitacyjnej. *Rocznik Ochrona Środowiska, 13*, 315-332.

Pomiès M., Choubert J. M., Wisniewski C., Coquery M. (2013). Modeling of micropollutant removal in biological wastewater treatments: A review. *Science of the Total Environment, 443*, 733- 748

Ráduly, B., Gernaey, K. V., Capodaglio, A. G., Mikkelsen, P. S. (2007). Artificial neural network for rapid WWTP performance evaluation: Methodology and case study. *Environmental Modeling and Software, 22*, 1208-1216.

Sadecka, Z., Płuciennik-Koropczuk, E., Sieciechowicz, A. (2011). Frakcje ChZT ścieków w modelach biokinetycznych. *Forum Eksploatatora, 54*, 72-77.

Sánchez-Avila, J., Bonet, J., Velasco, G., Lacorte, S. (2009). Determination and occurrence of phthalates, alkylophenols, bisphenol A, PBDEs and PAHs in an industrial sewage grid discharging to a Municipal Wastewater Treatment Plant. *Science of The Total Environment, 407*, 4157-4167.

Skoczko, I., Ofman, P., Szatyłowicz, E. (2016). Zastosowanie sztucznych sieci neuronowych do modelowania procesu oczyszczania ścieków w małej oczyszczalni ścieków. *Rocznik Ochrony Środowiska, 18*, 493-506.

Sochacki, A., Płonka, L., Miksch, K. (2010). Zastosowanie modeli matematycznych w symulacji procesów oczyszczania ścieków metodą osadu czynnego. *Forum Eksploatatora, I/II*, 5-56.

Sponza D. T., Gök O. (2010). Effect of rhamnolipid on the aerobic removal of polyaromatic hydrocarbons (PAHs) and COD components form petrochemical wastewater. *Bioresource Technology, 101*, 914- 924

Struk-Sokołowska, J. (2011). Zmiany udziału frakcji ChZT podczas oczyszczania ścieków z dużym udziałem ścieków mleczarskich. *Rocznik Ochrona Środowiska, 12*, 2015- 2032.

Struk-Sokołowska, J., Ignatowicz, K. (2013). Współoczyszczanie ścieków komunalnych i mleczarskich przy zastosowaniu technologii SBR. *Rocznik Ochrona Środowiska, 15*, 1881-1898.

Szetela, R., Dymaczewski, Z. (2002). Modyfikacja obecnej postaci modelu osadu czynnego ASM2d. *Ochrona Środodowiska, 1/84*, 3-8.

Tomenko, V., Ahmed, S., Popov, S. (2007). Modelling constructed wetland treatment system performace. *Ecological Modelling, 24*, 355-364.
Verma, A., Wei, X., Kusiak, A. (2013). Predicting the total suspended solid in wastewater: A data-mining approach. *Engineering Applications of Artificial Intelligence, 26*, 1366-1372.
Zielińska, M., Cydzik-Kwiatkowska, A., Zieliński, M., Dębowski, M. (2013). Impact of temperature, microwave radiation and organic loading rate on methanogenic community and biogas production during fermentation of dairy wastewater. *Biosource Technology, 129*, 308-314.
Çinar, Ö. (2005). New tool for evaluation of performance of wastewater treatment plant: Artificial neural network. *Process Biochemistry, 40*, 2980-2984.

Modelling Changes in the Parameters of Treated Sewage Using Artificial Neural Networks

Abstract

Aim of this study was to develop a model of artificial neural network for changes approximation in concentration and values of basic quality parameters of treated wastewater. Studies were carried out in years 2014 and 2015 in Bystre wastewater treatment plant, located near Giżycko. To Bystre sewage treatment plant inflows mixed domestic and dairy wastewater. In model as input variables were taken seven chemical parameters of raw wastewater and the amount of sewage inflowing to facility. Chosen chemical indicators were describing values of biological and chemical oxygen demand, concentrations of total nitrogen and phosphorus, amount of total suspended solids, pH and temperature of raw wastewater. In presented model the greatest impact on variables approximation had concentrations of total nitrogen and phosphorus. Developed model at it best reflected changes in total suspended solid in treated wastewater.

Streszczenie

Celem pracy było opracowanie modelu sztucznej sieci neuronowej aproksymującej zmiany w stężeniach i wartościach podstawowych parametrów jakościowych ścieków oczyszczonych. Badania prowadzone były w latach 2014 i 2015 w oczyszczalni ścieków w Bystrym koło Giżycka. Obiekt ten oczyszcza zmieszane ścieki komunalne i mleczarskie. W modelu jako zmienne wejściowe wybrano siedem parametrów chemicznych ścieków surowych i ilość ścieków dopływającą do oczyszczalni. Wskaźniki chemiczne uwzględniały wartości biologicznego i chemicznego zapotrzebowania na tlen, stężenia azotu i fosforu ogólnego, ilość zawiesin ogólnych, odczyn oraz temperaturę ścieków. W pre-

zentowanym modelu największy wpływ na aproksymację zmiennych wyjściowych miały stężenia azotu i fosforu ogólnego. Opracowany algorytm najlepiej oddał charakter zmian zawiesin ogólnych w ściekach oczyszczonych.

Słowa kluczowe:
oczyszczanie ścieków, ścieki mleczarskie, sztuczne sieci neuronowe

Keywords:
wastewater treatment, dairy wastewater, artificial neural networks

MIDDLE POMERANIAN SCIENTIFIC SOCIETY OF THE ENVIRONMENT PROTECTION
ŚRODKOWO-POMORSKIE TOWARZYSTWO NAUKOWE OCHRONY ŚRODOWISKA

Annual Set The Environment Protection
Rocznik Ochrona Środowiska

Volume/Tom 19. Year/Rok 2017 ISSN 1506-218X 651-667

Modelowanie parametrów migracji zanieczyszczeń chemicznych w podłożu gruntowym składowisk odpadów komunalnych

Kazimierz Szymański, Robert Sidełko, Beata Janowska,
Izabela Siebielska, Bartosz Walendzik
Politechnika Koszalińska

1. Wstęp

Migracja zanieczyszczeń obecnych w odciekach składowiskowych w podłożu gruntowym składowisk, zarówno w strefie aeracji, jak i saturacji jest tematem wielu prac naukowych (Brun A. & Engesgaard P. 2002, Castrillón L. i in. 2010, Cooke A.J. i in. 2005, Cuevas J. i in. 2012, Ghosh P. i in. 2014, Islam J. & Singhal N. 2004, Janowska B. & Szymański K. 2009, Koda E. i in. 2009, Lacerda C.V. i in. 2014, Szymański K. i in. 2007, Szymański K. & Janowska B. 2016, Mahmood K. i in. 2017). Szacuje się, że w Polsce znajduje się obecnie 2371 składowisk o nieuregulowanym stanie prawnym (GUS – 2015), głównie nieczynnych składowisk odpadów, które powstały po dawnych wyrobiskach piaskowych, bez żadnego uszczelnienia podłoża. Tym samym stanowią one poważne zagrożenie dla jakości wód podziemnych. Znajomość migracji odcieków do podłoża gruntowego a następnie do tych wód umożliwia podjęcie działań technicznych ograniczających ten proces (Poradnik 2000, Regadío M. i in. 2012, Reyes-López J.A. i in. 2008, Schiopu, A.M. & Gavrilescu M. 2010, Sidełko R. & Chmielińska-Bernacka A. 2013, Siebielska I. & Sidełko R. 2015, Szymański K. 1987, Nowak R., Włodarczyk Makuła., Wiśniowska E., Grabarczyk K. 2016). Celem pracy było określania właściwości oczyszczających gruntu porowatego, przez który migrują preparowane laboratoryjnie odcieki składowiskowe o skła-

dzie zbliżonym do naturalnych. W badaniach uwzględniono dwa wskaźniki zanieczyszczenia obecne w odciekach ze składowisk odpadów komunalnych (Szymański K. & Nowak R. 2012, Szymański K. & Thomas O. 1987, Szymański K. & Siebielska I. 2000, Tałałaj I. A. & Dzienis L. 2007, Wysocka M. E. 2015). Wskaźnikami tymi była ogólna zawartość substancji organicznych (lotnych), jako straty prażenia oraz związki żelaza ogólnego. Są one łatwo oznaczalne zarówno w odciekach, jak również w filtratach.

2. Część eksperymentalna

2.1. Badania modelowe procesów migracji odcieków w ośrodku gruntowym

Badania modelowe migracji sztucznie preparowanych odcieków składowiskowych prowadzono w warunkach laboratoryjnych, symulujących strefę aeracji (rys. 1). Opisano je funkcją pozwalającą przewidywać masę zanieczyszczeń migrujących do porowatego podłoża gruntowego i wypływających z tego ośrodka, w zależności od miąższości tej warstwy, masy doprowadzanych zanieczyszczeń i intensywności doprowadzanych odcieków. Funkcja ta stanowi analizę warunków podobieństwa i podaje sposób obliczania stężenia zanieczyszczeń, przykładowo wypływających poza obręb składowiska odpadów.

Parametrami zmiennymi w prowadzonych badaniach była: intensywność doprowadzanych odcieków **ω** (objętość odcieków przypadająca na jednostkę powierzchni i czasu), masa doprowadzanych zanieczyszczeń m_d oraz miąższość gruntu l**.** Analizę zmian masy zanieczyszczeń przefiltrowanych przez warstwę modelową m_f, w zależności od tych parametrów, wykonano dla dwu istotnych wskaźników zanieczyszczenia, a mianowicie: strat prażenia, jako ogólną zawartość substancji organicznych i związków żelaza (Skoczko I. i in. 2015)

2.2. Stanowisko badawcze

Badania prowadzono w walcowych kolumnach filtracyjnych (rys. 1). Kolumny te zbudowano z tworzywa sztucznego (plexi), o wysokości 1,0 m i średnicy 0,1 m. (Szymański K. 1987). Przez okres 90 dni do górnej powierzchni warstwy filtracyjnej doprowadzano określoną dawkę odcieku. Odciek dozowano specjalnie skonstruowanym do-

zownikiem, umożliwiającym równomierne rozprowadzenie go na powierzchni kolumny filtracyjnej.

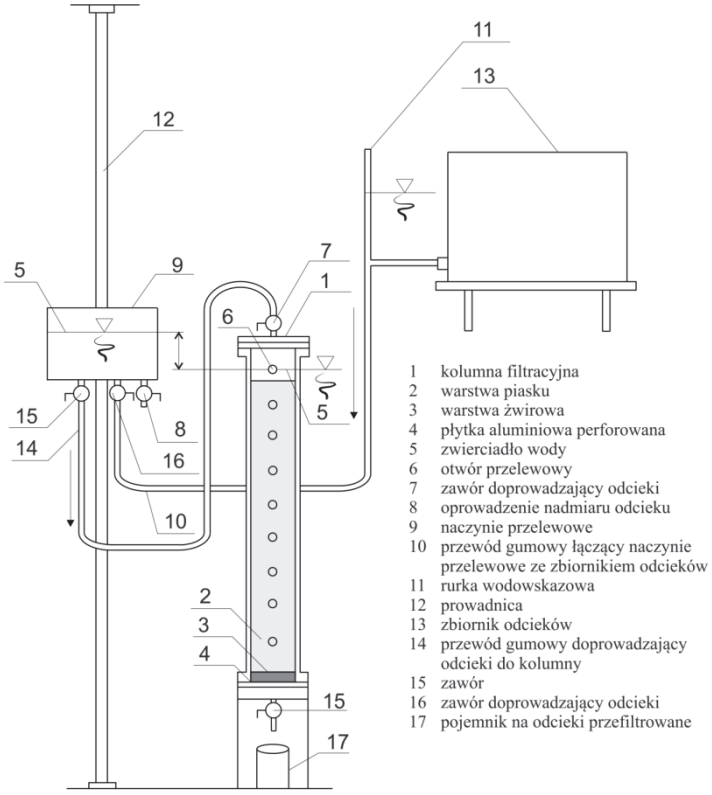

Rys. 1. Stanowisko badawcze stosowane w badaniach modelowych
Fig. 1. Test place used in model tests

Po wypełnieniu pojemności sorpcyjnej materiału filtracyjnego, zależnym od rodzaju i miąższości warstwy oraz objętości doprowadzonych odcieków, filtrat wypływał z dolnej strefy kolumny. W trakcie doświadczenia rejestrowano czas rozpoczęcia wypływu (liczony od momentu doprowadzenia pierwszej dawki odcieku), objętość filtratu oraz wysokość warstwy filtracyjnej. Odcieki doprowadzane do kolumny, jak i filtrat, poddawane były badaniom chemicznym. Wypełnieniem kolumny był piasek średni. Jego maksymalna i minimalna gęstość, określona w warunkach zerowej wilgotności, wynosiła odpowiednio $(\rho_d)_{max} = 1{,}79 \cdot 10^3$ kg/m^3,

$(\rho_d)_{min}$= 1,63·10^3 kg/m^3, zaś maksymalna gęstość przy wilgotności (w = 2,3%) była równa ρ_{max} = 1,83·10^3 kg/m^3. Stałym parametrem badań był skład chemiczny syntetycznych odcieków składowiskowych, przygotowanych w warunkach laboratoryjnych. Zawierał on m.in.: $FeCl_2$, $FeCl_3$, NaCl, $NaNO_3$, NH_4NO_3, Na_2CO_3, $MgSO_4$, KH_2PO_4, K_2SO_4 oraz kwas octowy, L-Serynę, DL-Valinę, Sacharozę, Ninhydrynę i L-izo-Leucynę. Stężenie tych składników dobrze symulowało odcieki składowiskowe w warunkach rzeczywistych.

2.3. Metodyka badań

Badania modelowe obejmowały trzy serie, różniące się miąższością warstwy (l_1 = 0,3 m, l_2 = 0,6 m, l_3 = 0,9 m). W każdej serii doprowadzano codziennie odciek z różną intensywnością (ω_1 = 0,026 m^3/m^{2}d, ω_2 = 0,052 m^3/m^{2}d, ω_3 = 0,104 m^3/m^{2}d). Oznacza to, że każdego dnia do jednej warstwy każdej serii wprowadzono objętość odcieku wynoszącą v_1 = 195·10^{-6} m^3, do drugiej v_2 = 390·10^{-6} m^3 a do trzeciej v_3 = 780·10^{-6} m^3. W trakcie całego badania do każdej warstwy doprowadzono około pięćdziesięciu dawek odcieku. Sumaryczną objętość doprowadzonego do kolumny filtracyjnej odcieku oznaczono literą W. Poszczególne serie badań zilustrowano na rysunkach 2, 3 i 4.

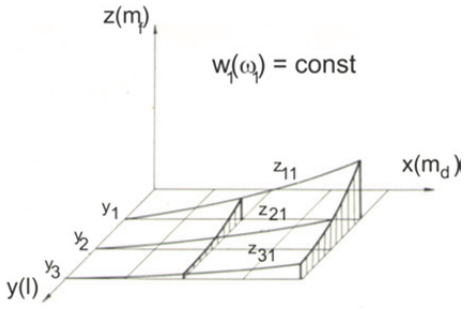

Rys. 2. Schematyczny wykres prowadzonych badań dla $W_1 = \omega_1$ = const.
Fig. 2. Schematic diagram of conducted research for $W_1 = \omega_1$ = const.

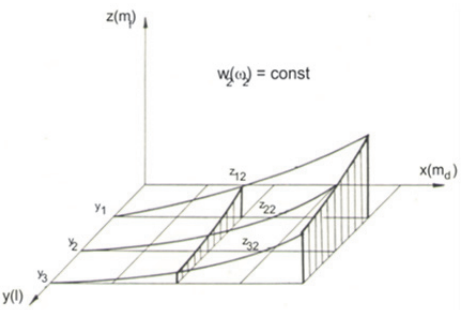

Rys. 3. Schematyczny wykres prowadzonych badań dla $W_2 = \omega_2$ = const.
Fig. 3. Schematic diagram of conducted research for $W_2 = \omega_2$ = const.

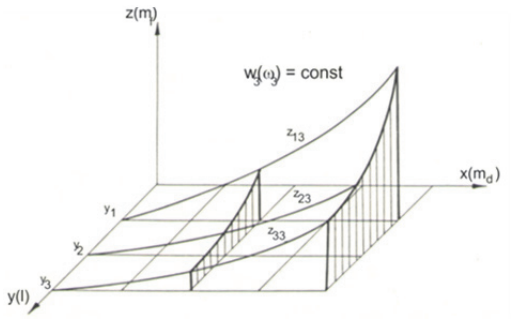

Rys. 4. Schematyczny wykres prowadzonych badań dla $W_3 = \omega_3 = \text{const}$.
Fig. 4. Schematic diagram of conducted research for $W_3 = \omega_3 = \text{const}$.

3. Wyniki badań

Graficzny przebieg badania, ilustrujący objętość odcieków doprowadzonych do złoża (V_d) i otrzymanych filtratów (V_f) oraz stopnia eliminacji poszczególnych zanieczyszczeń w zależności od liczby dawek doprowadzonego odcieku, dla wszystkich warstw piasku, zilustrowano na rysunkach 5-10. Z wykresów przedstawionych na tych rysunkach wynika, że im większa jest intensywność doprowadzanych odcieków (ω), tym krótszy jest okres pomiędzy wprowadzeniem odcieku a jego wypływem oraz, że wzrastają nieco różnice pomiędzy objętością doprowadzonego odcieku i filtratem. Wzrost miąższości warstwy opóźnia jedynie wypływ filtratu z dolnej jej powierzchni.

W warstwie o miąższości $l_2 = 0{,}6$ m, do której doprowadzono odciek o intensywności ω_3, widoczne są nieco większe różnice pomiędzy V_d i V_f w porównaniu do pozostałych przypadków. Prawdopodobnie przyczyna tego zjawiska była różnica gęstości złoża filtracyjnego. Gęstość jej była równa $\rho = 1{,}79 \cdot 10^3$ kg/m^3, podczas gdy w pozostałych warstwach była wyższa i wynosiła: $\rho_{śr} = 1{,}83 \cdot 10^3 \pm 0{,}018$ kg/m^3.

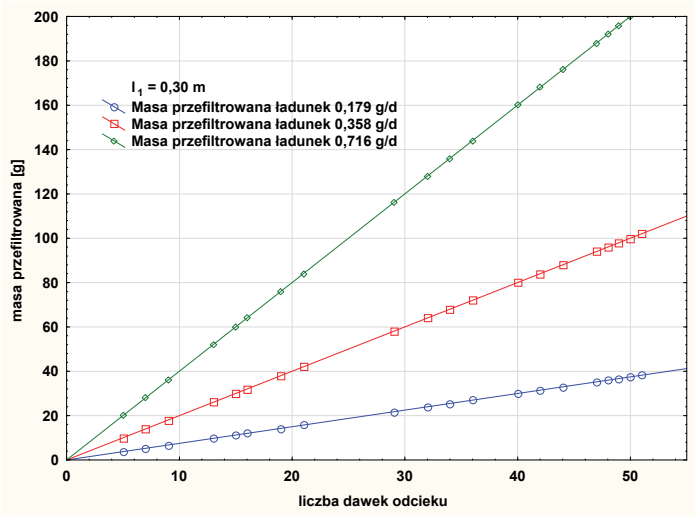

Rys. 5. Stopień eliminacji związków organicznych zawartych w odciekach w wyniku filtracji przez złoże l_1 = 0,30 m
Fig. 5. The degree of elimination of organic compounds contained in leachates by the filtration through the bed l_1 = 0.30 m

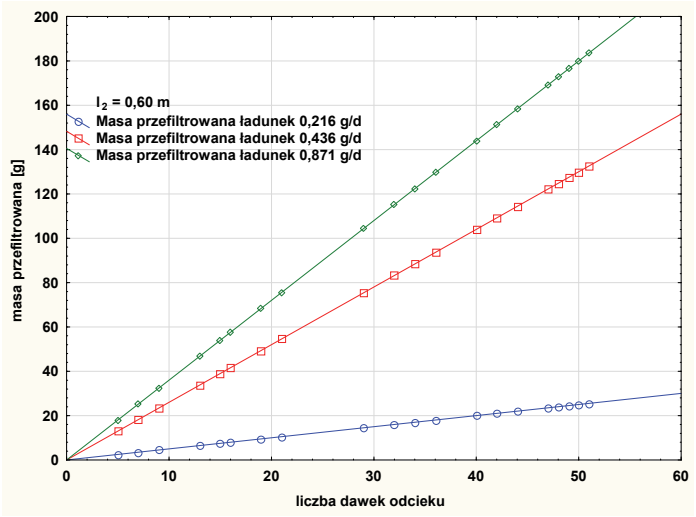

Rys. 6. Stopień eliminacji związków organicznych zawartych w odciekach w wyniku filtracji przez złoże l_1 = 0,60 m
Fig. 6. The degree of elimination of organic compounds contained in leachates by the filtration through the bed l_1 = 0.60 m

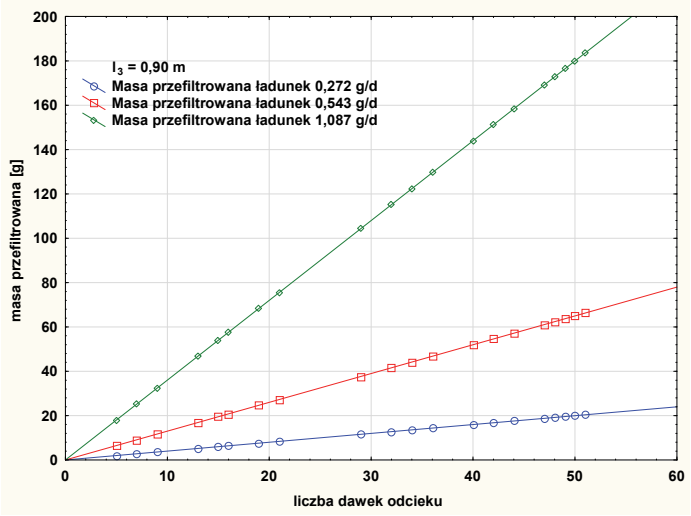

Rys. 7. Stopień eliminacji związków organicznych zawartych w odciekach w wyniku filtracji przez złoże l_1 = 0,90 m
Fig. 7. The degree of elimination of organic compounds contained in leachates by the filtration through the bed l_1 = 0.90 m

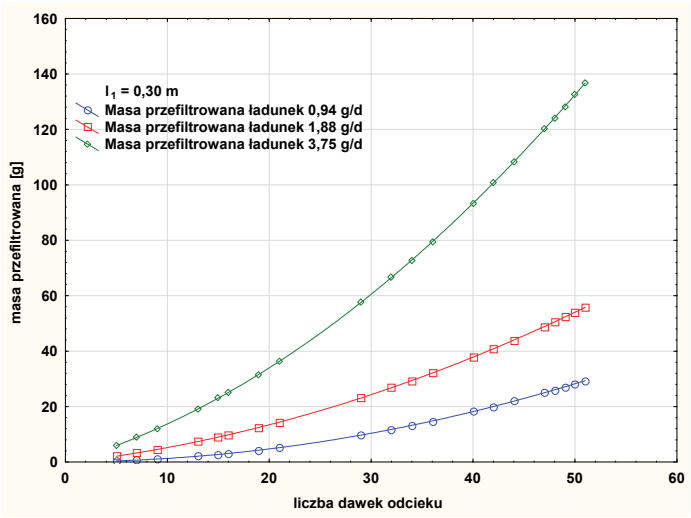

Rys. 8. Stopień eliminacji związków żelaza zawartych w odciekach w wyniku filtracji przez złoże l_1 = 0,30 m
Fig. 8. The degree of elimination of iron compounds contained in leachates by the filtration through the bed l_1 = 0.30 m

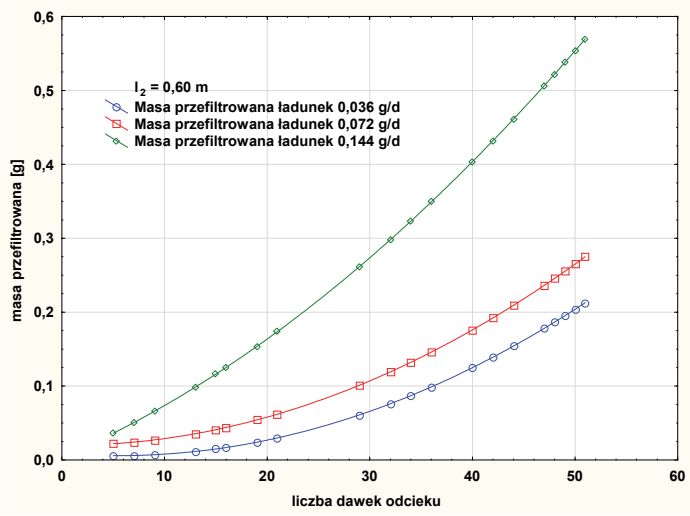

Rys. 9. Stopień eliminacji związków żelaza zawartych w odciekach w wyniku filtracji przez złoże l_1 = 0,60 m
Fig. 9. The degree of elimination of iron compounds contained in leachates by the filtration through the bed l_1 = 0.60 m

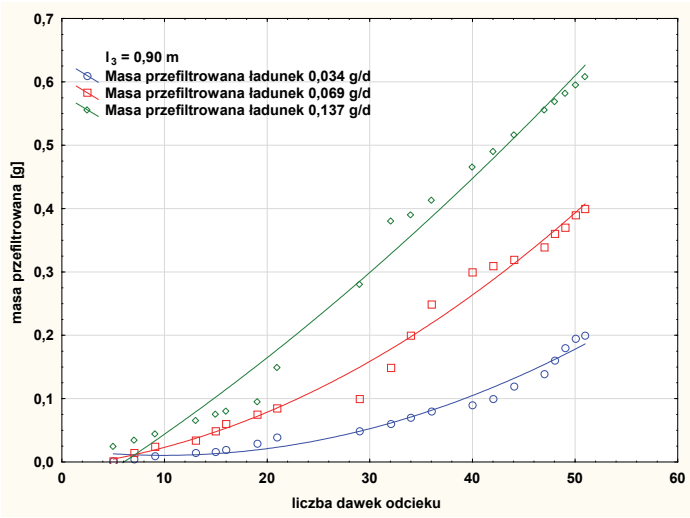

Rys. 10. Stopień eliminacji związków żelaza zawartych w odciekach w wyniku filtracji przez złoże l_1 = 0,90 m
Fig. 10. The degree of elimination of iron compounds contained in leachates by the filtration through the bed l_1 = 0.90 m

W trakcie trwania doświadczenia określano, zarówno w odcieku doprowadzanym, jak i filtracie, stężenie wymienionych wcześniej wskaźników zanieczyszczeń. W oparciu o znane wartości stężenia i objętości V_d i V_f, obliczono masę odpowiednich zanieczyszczeń doprowadzonych (m_d) i w filtracie (m_f), na każdym etapie badania. Do obliczeń m_d i m_f przyjmowano średnie wartości stężeń doprowadzonych zanieczyszczeń w poszczególnych seriach badań (l = const.). W konsekwencji takiego postępowania, w każdej serii badań była inna zawartość zanieczyszczeń w dawce doprowadzanego odcieku. Wartość ładunku rozpatrywanych zanieczyszczeń, w poszczególnych doświadczeniach, podano na rysunkach 5-10. Ilustrują one ładunek zanieczyszczeń zawartych w filtracie w zależności od liczby doprowadzonych dawek odcieku dla wszystkich trzech serii badań. Do każdej warstwy danej serii (l = const.) doprowadzono różną objętość odcieków (V_1, V_2 lub V_3), a więc różna była intensywność (ω_1, ω_2 lub ω_3) i masa doprowadzanych zanieczyszczeń. Na wykresach tych widać wyraźną tendencję wzrostu masy przefiltrowanych zanieczyszczeń w miarę zwiększania liczby i objętości dawek doprowadzanego odcieku. Z przebiegu tych wykresów można zauważyć, że wraz ze wzrostem masy doprowadzanych zanieczyszczeń rośnie masa zanieczyszczeń zawartych w filtracie. Ilość masy zanieczyszczeń w filtracie zależna jest od miąższości warstwy i intensywności doprowadzanych odcieków.

4. Analiza wyników badań

Przepływ odcieku przez warstwę gruntu powoduje zmiany właściwości fizyko-chemicznych ośrodka porowatego, tworzącego tę warstwę. Dotyczy to przede wszystkim porowatości (obserwowano zmniejszenie wysokości warstwy), uziarnienia (wypłukiwane były cząstki i drobniejsze ziarna gruntu) i przepuszczalności (zmniejszała się nieco prędkość przepływu cieczy). Zmiany tych wielkości były szczególnie wyraźne w pierwszej fazie badania. Intensywność tych zmian zależała od objętości jednorazowo doprowadzanych dawek odcieku oraz miąższości warstwy gruntu. Ogólnie można stwierdzić, że im mniejsze były dawki odcieku i im większa była miąższość warstwy, tym wolniej zachodziły procesy zagęszczania i wypłukiwania cząstek gruntu. W miarę doprowadzania kolejnych dawek odcieku, procesy te stopniowo zanikały, co

wskazywało na ustalenie się właściwości fizyko-chemicznych warstwy gruntu. Im większa była intensywność doprowadzania odcieków i mniejsza miąższość warstwy, tym mniejsza była objętość doprowadzanych odcieków, konieczna do osiągnięcia takiego stanu.

Zmiany właściwości fizyko-chemicznych wypełnienia kolumn filtracyjnych miały niewątpliwie istotny wpływ na właściwości sorpcyjne tego ośrodka. Względną zmianę masy doprowadzanych (m_d) i masy (m_f) zanieczyszczeń w filtracie do masy zanieczyszczeń doprowadzanych na jednostkę powierzchni warstwy (m'_d), przez którą one przepływają w formie odcieków. Względną zmianę masy $\overline{m}$ danego zanieczyszczenia można wyznaczyć ze wzoru:

$$\overline{m} = \frac{m_d - m_f}{m_d} \tag{1}$$

gdzie wartości m_d i m_f przyjmowano każdorazowo od początku doświadczenia.

Względna zmiana masy może przyjmować wartości $\overline{m} \leq 1{,}0$, w tym również ujemne. Wartości $\overline{m} = 1{,}0$ występują wówczas, gdy $m_f = 0$, $\overline{m} = 0$, gdy $m_f = m_d$, zaś ujemne, gdy $m_f > m_d$. Wzrostowi wielkości m'_d odpowiada spadek wartości $\overline{m}$. Taką tendencję, niezależnie od intensywności doprowadzania odcieków i miąższości warstwy, stwierdzono w przypadku żelaza ogólnego ($\overline{m} > 0$) oraz związków organicznych wyrażonych stratami prażenia ($\overline{m} < 0$). W początkowym etapie prowadzenia doświadczenia, prawie dla wszystkich wskaźników zanieczyszczenia, można zauważyć spadek wartości $\overline{m}$. Wydaje się uzasadnione stwierdzenie, że na tym etapie badania przeważają procesy wypłukiwania drobniejszych elementów gruntu (potwierdzają to ujemne wartości $\overline{m}$ strat prażenia), co pociąga za sobą zwiększenie prędkości przepływu odcieku przez warstwę. Kolejna faza badania, w której można zaobserwować lokalny wzrost względnej zmiany masy, odpowiada zagęszczaniu gruntu, w efekcie czego maleje zarówno objętość porów, jak i prędkość przepływu odcieku. W konsekwencji zmniejszania się porowatości i wydłużania czasu kontaktu odcieku z ośrodkiem gruntowym rośnie rola oczyszczania mechanicznego i fizyko-chemicznego. Ujawnia się ona wzrostem wartości $\overline{m}$. W miarę wyczerpywania się zdolności sorpcyjnych i jonowymiennych ośrodka gruntowego wartości $\overline{m}$ systematycznie spadają, po czym wykazują tendencję do przyjmowania wartości stałych. Wartość m'_d odpowiadająca osiąganiu podobnych wartości $\overline{m}$, niezależnie od in-

tensywności doprowadzania odcieków, zmniejsza się wraz ze zmniejszaniem miąższości l złoża. Można przypuszczać, że odpowiada ona osiągnięciu przez ośrodek gruntowy stałych właściwości fizyko-mechanicznych.

Podobne wnioski można formułować mając na uwadze poczynione obserwacje, że niezależnie od intensywności doprowadzanych odcieków, na pewnym etapie badania, warstwa gruntu wykazuje podobne właściwości filtracyjne. Osiągnięcie stałej wartości tego stosunku jest wyraźnie widoczne w doświadczeniach o największej intensywności ($\omega_3 = 4 \cdot \omega_1$), gdzie największa była masa doprowadzonych zanieczyszczeń.

W miarę sukcesywnego dostarczania odcieków do ośrodka porowatego, zawartość tlenu w jego porach ulega stopniowo wyczerpywaniu, wytwarzając ostatecznie środowisko beztlenowe. Jednocześnie wzrasta zagęszczenie i kolmatacja złoża w wyniku neutralizacji i wytrącania niektórych związków zawartych w odcieku. Powoduje to zmniejszenie porowatości ośrodka, a w konsekwencji wydłużenie czasu przepływu odcieku przez warstwę filtracyjną. Ponadto pory wypełniają się w coraz większym stopniu cieczą wypierającą fazę gazową. Ta zmiana warunków musi wpłynąć na udział poszczególnych procesów zachodzących w złożu a tym samym na ostateczny efekt usuwania zanieczyszczeń.

Stopniowe zmniejszanie się porowatości ośrodka wpływa na wzrost mechanicznego oczyszczania infiltrujących odcieków. Jeżeli w ośrodku tym obecne są minerały ilaste, możliwości odparowania wody będą się zmniejszały, lecz jednocześnie wzrośnie rola sorpcji i wymiany jonowej. Procesy utleniania będą coraz mniej intensywne i wraz ze spadkiem stężenia tlenu i zmiany warunków na anaerobowe. Nowe produkty, będące efektem wytrącania się z filtrującego przez badane złoże odcieku, w coraz większym stopniu będą zatrzymywane w porach. W złożu filtracyjnym mogą przebiegać także przemiany biologiczne. Należy przypuszczać, że wówczas po ustaleniu się równowagi fizyko-mechanicznej ośrodka oraz warunków tlenowych, właściwości oczyszczające tego ośrodka również nie będą ulegały radykalnej zmianie (Reyes-López J.A. i in. 2008, Schiopu, A.M. & Gavrilescu M. 2010).

Wyniki przeprowadzonych badań modelowych wyraźnie wskazują, że o masie zanieczyszczeń zawartych w odcieku, filtrowanych przez warstwę gruntu porowatego (m_f) decyduje masa doprowadzonych zanie-

czyszczeń (m_d), intensywność doprowadzonego odcieku (ω) oraz miąższość warstwy (l).

W celu określenia funkcji:

$$m_f = m_f(m_d, l, \omega) \tag{2}$$

wykorzystano metody statystyczne oraz zaproponowano rozwiązanie analityczne (Li Y. i in. 2012, Liu Z.J. i in. 2010, Luszniewicz A. & Słaby T. 2009, Nayak S. i in. 2007).

Rozwinięta forma funkcji (2) przyjmuje postać:

$$Z(x, y, w) = Z_1(x, y) \cdot K_1 + Z_2(x, y) \cdot K_2 + Z_3(x, y) \cdot K_3 \tag{3}$$

Obliczenie wartości tej funkcji wymaga określenia funkcji $Z_{ij} = Z_{ij}(x)$ dla przyjętych w badaniach modelowych wartości y_i i w_j.

Zaproponowana funkcja (3) pod względem formalnym spełnia przyjęte założenia i można ją wykorzystać do opisu masy zanieczyszczenia zawartego w filtracie, wypływającego z badanej warstwy piasku (m_f), w zależności od masy doprowadzonych zanieczyszczeń (m_d), miąższości warstwy (l) i intensywności doprowadzanych odcieków (ω).

Zakładając, że $Z = m_f$, $x = m_d$, $y = l$, $w = \omega$, można na podstawie wyników badań modelowych wyznaczyć zależność pomiędzy Z i x, (m_f i m_d). Wyniki tych obliczeń zestawiono w tabeli 1. Podano w niej dla rozpatrywanych wskaźników zanieczyszczenia równania funkcji regresji. Obliczenia wykonano przyjmując kolejno funkcje potęgową, liniową i wielomian drugiego stopnia. Wybór najbardziej właściwej funkcji powinien być dokonany w oparciu o wartość współczynnika korelacji oraz przebieg funkcji zgodny z przeprowadzonymi badaniami modelowymi.

Ogólnie można stwierdzić, że wszystkie trzy rodzaje analizowanych funkcji dają bardzo wysokie wartości współczynników korelacji (tabela 1).Wyniki badań wskazują, że masa przefiltrowanych zanieczyszczeń może osiągnąć tylko wartości $m_f \geq 0$. Najniższą wartością m_f jest zero i może ono wystąpić dla $m_d = 0$ lub $m_d > 0$, zależnie od intensywności doprowadzania odcieków i miąższości warstwy. Oznacza to, że zarówno funkcja liniowa, jak i dwumian kwadratowy tracą swoją ważność odpowiednio dla $x < \frac{-b}{a}$ i $x < \frac{-b+\sqrt{\Delta}}{2a}$.

Tabela 1. Liniowe funkcje regresji wielorakiej dla odcieków infiltrujących przez warstwę piasku średniego
Table 1. Functions of multiple linear regression for leachate infiltrating through a layer of medium sand

Wskaźnik zanieczyszczenia	Funkcja regresji $m_f' = m_f'(m_d, l, \omega)$	Współczynnik korelacji wielorakiej R
Związki organiczne	$m_f' = 2{,}98\ m_d' - 6.241{,}35\ l + 55.879{,}35\ \omega + 1.479{,}78$	0,9976
Żelazo ogólne	$m_f' = -0{,}02\ m_d' - 19{,}54\ l + 434{,}80\ \omega + 19{,}13$	0,9887

Oznaczenia:
m_f' – masa przefiltrowanego zanieczyszczenia przez jednostkę powierzchni [g/m^2],
m_d' – masa doprowadzonego zanieczyszczenia do jednostkowej powierzchni gruntu [g/m^2],
l – miąższość warstwy [m],
ω – intensywność doprowadzania odcieków [m^3/m^{2}d].

Dla przedziału od zera do x należy więc przyjąć $m_f = 0$. W przypadku funkcji liniowej, gdy $b > 0$ i funkcji kwadratowej, gdy $c > 0$, należy skorygować te funkcje w taki sposób, aby przechodziły one przez początek układu współrzędnych. Praktycznie można to wykonać łącząc rzędną pierwszego punktu, uzyskanego z badań (m_f) z początkiem układu współrzędnych. W przeprowadzonych badaniach wartości $y_i = l_i$ wynosiły $y_1 = 0{,}3$ m; $y_2 = 0{,}6$ m oraz $y_3 = 0{,}9$ m, zaś $w_j = \omega_j$ przyjmowały wartości $\omega_1 = 0{,}026$ m^3/m^{2}d, $\omega_2 = 0{,}052$ m^3/m^{2}d i $\omega_3 = 0{,}104$ m^3/m^{2}d. Stężenie zanieczyszczeń w wodzie gruntowej, przepływającej w warstwie wodonośnej o miąższości a, przepływającej z prędkością v, pod składowiskiem o szerokości b, można obliczyć zgodnie z pracą (Szymański K. 1987). Obliczenia polegają na określeniu elementarnej objętości przefiltrowanych przez strefę aeracji odcieków dV_f, wpływającej w czasie dt, zgodnie z równaniem różniczkowym wyznaczonym w badaniach wcześniejszych do wód podziemnych strefy aeracji, przy założeniu, że powierzchnia tych wód o wymiarach db 1,0 m^2. Objętość ta wynosi:

$$dV_f = v_a \cdot db \cdot 1{,}0 \cdot dt \qquad (4)$$

gdzie v_a oznacza prędkość przepływu odcieków w strefie aeracji**.**

5. Podsumowanie

Z przeprowadzonych badań wynikają następujące wnioski:

1. Masa zanieczyszczeń wypływających ze strefy aeracji jest funkcją zanieczyszczeń doprowadzonych do warstwy gruntu, jej miąższości oraz intensywności doprowadzania odcieków. Zależności te są różne dla różnych wskaźników zanieczyszczenia zawartych w odciekach.
2. Wzrost ilości doprowadzonych odcieków do złoża filtracyjnego powoduje stały wzrost masy zanieczyszczeń w filtratach, niezależnie od intensywności doprowadzonych odcieków. Im mniejsza jest miąższość warstwy, tym przy mniejszej wartości masy doprowadzonych zanieczyszczeń, warstwa złoża piaskowego spełnia funkcje warstwy filtracyjnej.
3. Przepływ odcieków przez złoże filtracyjne (piasek średni) powoduje, szczególnie w początkowym okresie filtracji, zagęszczenie złoża oraz wypłukiwanie drobnych cząstek gruntu, na których osadzają się zanieczyszczenia mineralne i organiczne.
4. Opisane badania modelowe oraz interpretacja ich wyników, w oparciu o zaproponowaną funkcję regresji wielorakiej, umożliwia adaptację tej funkcji w zróżnicowanych warunków gruntowych i różnych rodzajach zanieczyszczeń, zawartych w wodach infiltrujących do ośrodka gruntowego.

Literatura

Brun, A. & Engesgaard, P. (2002). Modeling of transport and biogeochemical processes in pollution plumes: literature review and model development. *Journal of Hydrology, 256*, 211-227.

Castrillón, L., Fernández-Nava, Y., Ulmanu, M., Anger, I. & Marañón, E. (2010). Physico-chemical and biological treatment of MSW landfill leachate. *Waste Management, 30*, 228-235.

Cooke, A.J., Rowe, R.K. & Rittmann, B.E. (2005). Modelling species fate and porous media effects for landfill leachate flow. *Canadian Geotechnical Journal, 42*, 1116-1132.

Cuevas, J., Ruiz, A.I., de Soto, I.S., Sevilla, T., Procopio, J.R., Da Silva, P., Gismera, M.J., Regadío, M., Sánchez Jiménez, N., Rodríguez Rastrero, M. & Leguey, S. (2012). The performance of natural clay as a barrier to the diffusion of municipal solid waste landfill leachates. *Journal of Environmental Management, 95*, 175-181.

Ghosh, P., Swati, & Thakur, I.S. (2014). Enhanced removal of COD and color from landfill leachate in a sequential bioreactor. *Bioresource Technology, 170*, 10-19.

Islam, J. & Singhal, N. (2004). A laboratory study of landfill leachate transport in soils. *Water Research, 38*, 2035-2042.

Janowska, B. & Szymański, K. (2009).Transformation of selected trace elements during the composting process of sewage sludge and municipal solid waste. *Fresenius Environmental Bulletin, 18*, 7, 1110-1117.

Koda, E., Wiencław, E. & Martelli, L. (2009).Transport modelling and monitoring research use for efficiency assessment of vertical barrier surrounding old sanitary landfill. *Annals of Warsaw University of Life Sciences – SGGW Land Reclamation, 41*, 41-48.

Lacerda, C.V., Ritter, E., da Costa Pires, J.A. & de Castro, J.A. (2014). Migration of inorganic ions from the leachate of the Rio das Ostras landfill: A comparison of three different configurations of protective barriers. *Waste Management, 34*, 2285-2291.

Li, Y., Li, J., Chen, S. & Diao, W. (2012). Establishing indices for groundwater contamination risk assessment in the vicinity of hazardous waste landfills in China. *Environmental Pollution, 165*, 77-90.

Liu, Z.J., Li, X.K. & Tanga, L.Q. (2010). The Numerical Simulation of Coupling Behavior of Soil with Chemical Pollutant Effects. *AIP Conference Proceedings, 1233(1)*, 690-695.

Luszniewicz, A. & Słaby, T. (2009). *Statistics with computer package of STATISTICA PL. Theory and Applications.* Warszawa: CH Beck (in Polish).

Mahmood, K., Batool, S.A., Chaudhary, M.N., Ul-Haq, Z. (2017). Ranking criteria for assessment of municipal solid waste dumping sites. *Archives of Environmental Protection, 43(1)*, 95-105.

Nayak, S., Sunil, B.M. & Shrihari, S. (2007). Hydraulic and compaction characteristics of leachate-contaminated lateritic soil. *Engineering Geology, 94(3-4)2*, 137-144.

Nowak, R., Włodarczyk-Makuła, M., Wiśniowska, E., Grabarczyk, K. (2016). Porównanie efektywności podczyszczania odcieków składowiskowych. *Rocznik Ochrona Środowiska, 18*, 122-133.

Poradnik (2000). *Metody badania i rozpoznawania wpływu na środowisko gruntowo-wodne składowisk odpadów stałych.* Warszawa: Ministerstwo Środowiska – Departament Geologii (in Polish).

Regadío, M., Ruiz, A.I., de Soto, I.S., Rodriguez Rastrero, M., Sánchez, N., Gismera, M.J., Sevilla, M.T., da Silva, P., Rodríguez Procopio, J. & Cuevas, J. (2012). Pollution profiles and physicochemical parameters in old uncontrolled landfills. *Waste Management, 32*, 482-497.

Reyes-López, J.A., Ramírez-Hernández, J., Lázaro-Mancilla, O., Carreón-Diazcontia, C. & Martín-Loeches Garrido M. (2008). Assessment of groundwater contamination by landfill leachate: A case in México. *Waste Management, 28*, S33-S39.

Schiopu, A.M. & Gavrilescu, M. (2010). Options for the Treatment and Management of Municipal Landfill Leachate: Common and Specific. *Clean: Soil, Air, Water, 38(12)*, 1101-1110.
Sidełko, R., Chmielińska-Bernacka, A. (2013). Application of compact reactor for methane fermentation of municipal waste. *Rocznik Ochrona Środowiska, 15*, 683-693.
Siebielska, I. & Sidełko, R. (2015). Polychlorinated biphenyl concentration changes in sewage sludge and organic municipal waste mixtures during composting and anaerobic digestion. *Chemosphere, 126*, 88-95.
Szymański, K. & Nowak, R. (2012). Transformations of leachate as a result of technical treatment at municipal waste landfills (in Polish). *Rocznik Ochrona Środowiska, 14*, 337-350.
Szymański, K. & Siebielska, I. (2000). Evaluation of groundwater pollution: analytical problems (in Polish). *Ochrona Środowiska, 76(1)*, 15-18.
Szymański, K. (1987). *Migracja odcieków z wysypisk odpadów komunalnych w gruncie.* Koszalin: Wydawnictwo WSInż.
Szymański, K., Janowska, B. (2016). Migration of pollutants in porous soil environment. *Archives of Environmental Protection, 42(3)*, 87-95.
Szymański, K., Sidełko, R., Janowska, B., Siebielska, I. (2007). Monitoring of waste landfills. *Zeszyty Naukowe Wydziału Budownictwa i Inżynierii Środowiska, 23*, 75-133.
Szymański, K., Thomas, O. (1987). Wpływ odcieków wysypiskowych na procesy mineralizacji wód podziemnych (in Polish). *Gaz, woda i Technika Sanitarna, 11-12*.
Tałałaj, I.A. & Dzienis, L. (2007). Influence of Leachate on Quality of Underground Waters. *Polish Journal of Environmental Studies, 16(1)*, 139-144.
Wysocka, M.E. (2015). Wpływ lokalizacji składowisk odpadów na jakość wód podziemnych. *Rocznik Ochrona Środowiska, 17*, 1074-1094.

Modelling the Parameters of Migration of Chemical Pollutants in the Soil Base of Municipal Landfills

Streszczenie

Migracja zanieczyszczeń w ośrodku gruntowym jest procesem złożonym, zależnym od wielu czynników. Model matematyczny tego procesu, oparty na założeniach hydromechaniki fizykochemicznej, uwzględniający specyfikę środowiska gruntowego i odcieku składowiskowego, ciągle jest niedoskonały. Dokładność oceny migracji skażonych wód gruntowych zależy również, w istotnym stopniu, od rozpoznania warunków gruntowo-wodnych. Dotyczy to przede wszystkim rodzaju i właściwości gruntu zalegającego w otoczeniu źródła skażenia, miąższości strefy aeracji i warstwy wodonośnej oraz kierunku

i prędkości przepływu wód gruntowych. Z praktyki wiadomo, że wielkości te, określane w oparciu o badania geotechniczne, są często mylące. Wyniki badań modelowych migracji odcieków składowiskowych w podłożu gruntowym na przykładzie zmian stężenia żelaza ogólnego oraz związków organicznych wyrażonych przez straty prażenia, interpretowane za pomocą liniowej funkcje regresji wielorakiej, wskazują na możliwość ich adaptacji do określonych warunków gruntowych oraz prognozowania rodzajów zanieczyszczeń zawartych w odciekach składowiskowych, infiltrujących do podłoża zbudowanego z materiału porowatego, a tym samym do strefy saturacji.

Abstract

Closed municipal and industrial waste landfill sites create potential hazard of ground water pollution. Pollutants that occur in leachate infiltrate to the soil substratum, where they are carried to in underground water. A municipal waste landfill substratum can be used for elimination of pollutants contained in leachates. Model research was performed with use of a sand bed and artificially prepared leachates. Efficiency of filtration in a bed of defined thickness was assessed based on change of iron, organic compounds value. Results of the model tests have indicated that the mass of pollutants contained in leachate filtered through porous ground layer *(m_f)* depends on the mass of supplied pollutants *(m_d)*, intensity of supplied leachate *(ω)* and layer thickness *(l)*. Increase of the mass of pollutants supplied to a unit area of ground layer causes reduction of the relative value of mass. Determined regression functions indicate compatibility with linear model of empiric values of variable m_f'. Determined regression functions allow for estimation of qualitative and quantitative influence of analysed independent variables *(m_d', l, ω)* onto values of the mass of pollutants flowing out from the medium sand layer. The method of evaluation of quality of water seeping through the aeration layer presented in this paper allows for estimation of the flowing out pollutants mass. Based on the test results obtained, efficiency of purification in the aeration zone can be assessed; likewise, safe thickness of the filtration layer under the landfill site can be designed.

Słowa kluczowe:
odcieki składowiskowe, strefa aeracji, zanieczyszczenie wody, migracja, żelazo ogólne, związki organiczne

Keywords:
landfill leachate, aeration zone, water pollution, migration, total iron, organic compounds

MIDDLE POMERANIAN SCIENTIFIC SOCIETY OF THE ENVIRONMENT PROTECTION
ŚRODKOWO-POMORSKIE TOWARZYSTWO NAUKOWE OCHRONY ŚRODOWISKA
Annual Set The Environment Protection
Rocznik Ochrona Środowiska
Volume/Tom 19. Year/Rok 2017 ISSN 1506-218X 668-681

Wpływ sumy rocznej opadów atmosferycznych na objętość wód przypadkowych dopływających do kanalizacji sanitarnej

Grzegorz Kaczor, Krzysztof Chmielowski, Piotr Bugajski
Uniwersytet Rolniczy im. H. Kołłątaja, Kraków

1. Wprowadzenie

Od wdrożenia do realizacji wytycznych zawartych w Dyrektywie 91/271/EWG z dnia 21 maja 1991 roku podjęto w poszczególnych krajach Unii Europejskiej działania zmierzające do uporządkowania oraz poprawy stanu gospodarki ściekowej. W latach 2007-2013 na ten cel przeznaczono 14 mld €. W Polsce, w ramach realizacji Krajowego Programu Oczyszczania Ścieków Komunalnych (zgodnie z jego aktualizacją z 2009 roku), podjęto decyzję o budowie 177 nowych oczyszczalni ścieków oraz modernizacji lub rozbudowie kolejnych 596 takich obiektów. Zadeklarowano także budowę 30 641 km nowej sieci kanalizacyjnej oraz modernizację 2 883 km sieci istniejącej. Wszelkie działania podejmowane w celu ochrony i poprawy jakości wód powierzchniowych i podziemnych nie powinny jednak skupiać się wyłącznie na budowie nowych i modernizacji istniejących systemów do odprowadzania i oczyszczania ścieków. Równie ważną kwestią jest utrzymanie odpowiedniej skuteczności i niezawodności działania sieci kanalizacyjnych oraz oczyszczalni ścieków już istniejących, a niekwalifikujących się jeszcze pod względem ekonomicznym do modernizacji (Bielińska i in. 2014, Jóźwiakowski i in. 2015, Kotowski i in. 2014).

W przypadku istniejących i funkcjonujących sieci kanalizacyjnych najważniejszym priorytetem powinno być utrzymywanie ich szczelności, niezawodność działania oraz wymaganej przepustowości

(Madryas i in. 2010). Poprzez szczelność sieci kanalizacyjnej należy rozumieć przede wszystkim zabezpieczenie kanałów ściekowych przed dopływami wód infiltracyjnych i przypadkowych oraz ewentualną eksfiltracją ścieków z wnętrza kolektorów do gruntu (Kaczor 2012).

Eksfiltracja to niekontrolowany, podziemny wypływ ścieków z kanałów sanitarnych lub studni kanalizacyjnych poprzez uszkodzenia ich ścian, dna lub nieszczelności połączeń poszczególnych elementów sieci i jej uzbrojenia (Ellis & Bertrand-Krajewski 2010).

Wody infiltracyjne to głównie wody gruntowe dopływające do kanalizacji poprzez uszkodzenia przewodów, ich połączeń oraz nieszczelności ścian i dna studni kanalizacyjnych (Cieślak & Pawełek 2014). Dopływ ten następuje wtedy, gdy przewody kanalizacyjne lub obiekty sieciowe ułożone są poniżej zwierciadła wody gruntowej. Intensywność dopływu wód infiltracyjnych do kanałów ściekowych jest wprost proporcjonalna do wysokości zwierciadła wody gruntowej nad przewodem (Madryas i in. 2010).

Jednym z najpoważniejszych problemów eksploatacyjnych sieci kanalizacyjnych i oczyszczalni ścieków jest dopływ do tych obiektów wód przypadkowych (De Bénédittis 2004). Wody przypadkowe to najczęściej wody opadowe (deszczowe) lub roztopowe, przedostające się do wnętrza kanałów sanitarnych przez otwory włazowe lub wentylacyjne studni kanalizacyjnych, a także poprzez nielegalnie wykonywane przez mieszkańców włączenia do przykanalików rynien dachowych (Butler & Davis 2011), wpustów podwórzowych (Kaczor 2012) lub drenaży służących do odwodnienia posesji (Pecher 1999). Do wód przypadkowych zalicza się także kierowane do kanalizacji, w sposób zamierzony lub niezamierzony, wody odprowadzane podczas wykonywanych prac budowlanych lub remontowych, wody chłodnicze, a także wody przedostające się do kanalizacji przez otwory we włazach studzienek po spłukiwaniu nawierzchni ulic lub myciu pojazdów.

Podczas eksploatacji sieci kanalizacyjnych wody przypadkowe, pojawiające się najczęściej podczas intensywnych opadów atmosferycznych, powodują przepełnienie kanałów, przeciążenie przepompowni ścieków, okresowe przepływy ścieków w kanałach grawitacyjnych w warunkach ciśnieniowych lub nawet w sytuacjach ekstremalnych wypływ ścieków ze studzienek kanalizacyjnych na powierzchnię terenu. Najbardziej negatywny wpływ wody przypadkowe wywierają na funk-

cjonowanie oczyszczalni, w których wymiary i pojemności poszczególnych obiektów technologicznych nie są przystosowane do okresowo zwiększonej przepustowości. Dopływ wód przypadkowych wpływa na przeciążenia hydrauliczne głównie takich obiektów jak piaskowniki oraz osadniki wstępne oraz wtórne. Wpływają one także negatywnie na funkcjonowanie reaktorów biologicznych, powodując obniżenie temperatury ścieków (zwłaszcza podczas roztopów śniegu) oraz skracają czas zatrzymania ścieków w poszczególnych komorach lub strefach reaktora (Kaczor 2011, Kaczor & Bugajski 2012). Nie bez znaczenia jest także obniżenie stężeń zanieczyszczeń w ściekach poprzez ich rozcieńczenie wodą deszczową, a tym samym ich zubożenie w substancje organiczne niezbędne dla rozwoju mikroorganizmów osadu czynnego (Kaczor i in. 2015, Bugajski i in. 2016). Oddziaływanie wód przypadkowych na wiele aspektów funkcjonowania oczyszczalni ścieków prowadzi w konsekwencji do okresowego obniżenie jej sprawności działania, a tym samym występowania zagrożenia zanieczyszczenia wód odbiornika ściekami niedostatecznie oczyszczonymi (Kowalik i in. 2015).

Objętość wód przypadkowych dopływających do sieci kanalizacyjnej zależy od warunków atmosferycznych (Wałęga i in. 2014). Jednak w literaturze dotyczącej problematyki wód obcych brakuje informacji oraz wyników badań potwierdzających, że objętość wód przypadkowych dopływających do kolektorów ściekowych zależy od sumy rocznej opadów atmosferycznych. Taka analiza możliwa jest do przeprowadzenia dopiero po uzyskaniu długoletnich ciągów pomiarowych. W ramach niniejszej publikacji, na postawie 12 letniego ciągu obserwacyjnego, podjęto próbę określenia siły związku korelacyjnego pomiędzy omawianymi parametrami.

2. Cel i zakres badań

Celem badań była ocena siły związku korelacyjnego pomiędzy roczną sumą opadów atmosferycznych oraz roczną objętością wód przypadkowych dopływających do 3 wybranych sieci kanalizacyjnych. W analizie wykorzystano 12 letnie ciągi pomiarowe, obejmujące sumy roczne opadów atmosferycznych dla Krakowa oraz roczne objętości wód przypadkowych dopływających do 3 rozdzielczych sieci kanalizacyjnych, odprowadzających ścieki bytowe z osiedli mieszkalnych, w latach 2004-2015.

3. Metodyka badań

Roczną sumę opadów atmosferycznych dla aglomeracji krakowskiej odczytano dla analizowanych lat 2004-2015 z Roczników Statystycznych Rzeczypospolitej Polskiej.

Roczne objętości wód przypadkowych określono na podstawie analizy dobowych dopływów ścieków do trzech badanych sieci kanalizacyjnych podczas pogody bezdeszczowej (tzw. suchej) oraz pogody deszczowej (tzw. mokrej). Przepływy ścieków mierzono na terenie oczyszczalni, do których były one odprowadzane z analizowanych sieci kanalizacyjnych. Pomiar dobowych przepływów ścieków, w przypadku każdego obiektów, wykonywano za pomocą takich samych układów pomiarowych, składających się z sondy poziomu nad przelewem trójkątnym. W rocznym ciągu pomiarowym dany dobowy odpływ ścieków z kanalizacji zaliczano do pogody suchej, jeżeli w tym dniu oraz w pięciu dniach poprzedzających nie wystąpił żaden opad atmosferyczny, lub wystąpił, ale jego wysokość dobowa nie przekraczała 1 mm. Informację o braku lub występowaniu opadów atmosferycznych odczytano z dzienników eksploatacyjnych poszczególnych oczyszczalni.

Średni dobowy odpływ ścieków z kanalizacji, w danym roku, podczas pogody bezdeszczowej posłużył do ustalenia przeciętnej ilości tzw. ścieków właściwych, czyli nie zawierających wód przypadkowych. Podczas pogody mokrej, czyli w okresie opadów atmosferycznych, części dobowych przepływów ścieków wyższe od ustalonego przeciętnego poziomu ścieków właściwych zaliczano do wód przypadkowych. Zatem dobową objętość wód przypadkowych obliczano według wzoru (1):

$$Q_{dp} = Q_{dm} - Q_{ds} \tag{1}$$

gdzie:
Q_{dp} – dobowy dopływ do kanalizacji wód przypadkowych ($m^3 \cdot d^{-1}$),
Q_{dm} – dobowy dopływ do kanalizacji mieszaniny ścieków właściwych i wód przypadkowych podczas pogody mokrej ($m^3 \cdot d^{-1}$),
Q_{ds} – średni dobowy dopływ do kanalizacji ścieków właściwych (bez wód przypadkowych) podczas pogody suchej ($m^3 \cdot d^{-1}$).

W analizach porównawczych roczną objętość wód przypadkowych, która dopłynęła do kanalizacji, opisuje się najczęściej za pomocą dwóch wskaźników wyrażanych w procentach. Są to udział wód przy-

padkowych oraz dodatek wód przypadkowych (Pecher 1999). Roczny udział wód przypadkowych, w odniesieniu do rocznej objętości mieszaniny ścieków właściwych i wód przypadkowych, oblicza się według wzoru (2):

$$UWP = \frac{Q_{rp}}{Q_r} \cdot 100 \tag{2}$$

gdzie:
UWP – roczny udział wód przypadkowych w kanalizacji (%),
Q_{rp} – roczna objętość wód przypadkowych dopływających do kanalizacji (m^3),
Q_r – roczna objętość mieszaniny ścieków właściwych i wód przypadkowych dopływających do kanalizacji (m^3).

Roczny dodatek wód przypadkowych ustala się natomiast zgodnie ze wzorem (3):

$$DWP = \frac{Q_{rp}}{Q_{r\acute{s}w}} \cdot 100 \tag{3}$$

gdzie:
DWP – roczny dodatek wód przypadkowych w kanalizacji (%),
Q_{rp} – roczna objętość wód przypadkowych dopływających do kanalizacji (m^3),
$Q_{r\acute{s}w}$ – roczna objętość ścieków właściwych (bez wód przypadkowych) dopływająca do kanalizacji (m^3).

Obliczone dla każdego roku wielolecia wartości Q_{dp}, *UWP*, *DWP* zestawiono z rocznymi sumami opadów, a następnie poddano analizie statystycznej. Analizę korelacji pomiędzy badanymi zmiennymi przeprowadzono za pomocą odpowiednich funkcji i procedur obliczeniowych programu komputerowego Statistica.

4. Opis obiektów badań

Badaniami objęto 3 wybrane sieci grawitacyjnej kanalizacji rozdzielczej, wykonane z kamionki, odprowadzające ścieki bytowe z osiedli domów jednorodzinnych zlokalizowanych w bliskim sąsiedztwie Krakowa (województwo małopolskie). Ze względu na brak zgody ze strony eksploatatorów obiektów na ujawnienie nazw miejscowości, w niniejszej pracy badane sieci kanalizacyjne oznaczono indeksami A, B i C. Ogólną

charakterystykę poddanych analizie porównawczej obiektów badań przedstawiono w tabeli 1.

Długość poddanych analizie sieci kanalizacyjnych waha się od 9,0 do 15,2 km. Wiek kanalizacji jest zbliżony, ponieważ ich budowę rozpoczęto w tym samym okresie. We wszystkich analizowanych sieciach kanalizacyjnych, w okresie pogody mokrej, zaobserwowano zwiększone przepływy ścieków powodowane wodami przypadkowymi. Wizje terenowe oraz wywiady z eksploatatorami kanalizacji wykazały, że przyczyn dopływu wód przypadkowych do kolektorów należy upatrywać głównie w nielegalnie wykonanych przez mieszkańców podłączeń rynien dachowych oraz wpustów podwórzowych do kanalizacji sanitarnej.

Tabela 1. Ogólna charakterystyka analizowanych sieci kanalizacyjnych
Table 1. General characteristics of the investigated sewerage networks

Parametr	Kanalizacja		
	A	B	C
Długość sieci [km]	9,0	11,0	15,2
Materiał rur [–]	kamionka		
Wiek kanalizacji [lata]	18	17	17
Liczba przyłączy [szt]	330	470	455
Liczba mieszkańców [–]	1485	2120	2050
Odległość od stacji opadowej [km]	8,7	10,7	8,5

W trakcie wizji lokalnych na trasie kanalizacji zaważono wiele włazów studni kanalizacyjnych obniżonych względem powierzchni drogi lub chodnika. W okresie opadów spływające wody deszczowe gromadzą się nad takim włazem i przedostają do wnętrza studzienek przez otwory w pokrywie.

5. Analiza wyników badań

W pierwszym etapie badań, oddzielnie dla każdej kanalizacji oraz roku, obliczono sumaryczną objętość ścieków oraz sumaryczną objętość wód przypadkowych. Uzyskane wyniki zestawiono w tabeli 2. W tabeli tej zamieszczono dodatkowo roczne sumy opadów dla poszczególnych lat badań oraz obliczoną dla każdego roku wartość udziału oraz dodatku wód przypadkowych. Oznaczenia poszczególnych zmiennych w nagłówkach kolumn tabeli 2 są zgodne z podanymi we wzorach (2) i (3).

Tabela 2. Roczne objętości ścieków i wód przypadkowych dopływające do poszczególnych kanalizacji na tle rocznych sum opadów
Table 2. Annual volume of sewage and accidental water entering individual sewerage systems compared with total annual precipitation

Rok	Σ roczna opadów (mm)	Q_r (m^3)	$Q_{rśw}$ (m^3)	Q_{rp} (m^3)	UWP (%)	DWP (%)
Kanalizacja A						
2015	551	67277,5	61208,6	6068,9	9,0	9,9
2014	627	71463,0	64867,2	6595,8	9,2	10,2
2013	644	79829,0	66760,8	13068,2	16,4	19,6
2012	619	72017,0	63805,7	8211,3	11,4	12,9
2011	467	76823,0	69665,2	7157,8	9,3	10,3
2010	1150	95007,0	72374,6	22632,4	23,8	31,3
2009	735	84176,0	70093,1	14082,9	16,7	20,1
2008	619	79288,0	71291,9	7996,1	10,1	11,2
2007	834	86902,0	74222,9	12679,1	14,6	17,1
2006	552	76423,0	65188,6	11234,4	14,7	17,2
2005	637	65977,0	55572,1	10404,9	15,8	18,7
2004	598	63953,0	54363,5	9589,5	15,0	17,6
Średnia	669,4	76594,6	65784,5	10810,1	14,1	16,4
Kanalizacja B						
2015	551	158511,1	116033,5	42477,5	26,8	36,6
2014	627	167634,5	123082,9	44551,6	26,6	36,2
2013	644	152599,5	100099,2	52500,3	34,4	52,4
2012	619	120696,0	88099,9	32596,1	27,0	37,0
2011	467	119888,0	79864,1	40023,9	33,4	50,1
2010	1150	165155,0	88887,2	76267,8	46,2	85,8
2009	735	159640,0	108144,8	51495,2	32,3	47,6
2008	619	117350,0	81448,4	35901,6	30,6	44,1
2007	834	113225,0	64975,0	48250,0	42,6	74,3
2006	552	80593,0	55071,1	25521,9	31,7	46,3
2005	637	78835,0	47426,9	31408,1	39,8	66,2
2004	598	74930,0	45640,1	29289,9	39,1	64,2
Średnia	669,4	125754,8	83231,1	42523,7	33,8	51,1
Kanalizacja C						
2015	551	313814,0	257156,0	56658,0	18,1	22,0
2014	627	361749,0	293871,7	67877,3	18,8	23,1
2013	644	392220,0	316828,0	75392,0	19,2	23,8
2012	619	309180,0	250786,2	58393,8	18,9	23,3
2011	467	292348,0	237148,1	55199,9	18,9	23,3
2010	1150	367381,0	224123,0	143258,0	39,0	63,9
2009	735	297120,0	191677,6	105442,4	35,5	55,0
2008	619	246326,0	169550,9	76775,1	31,2	45,3
2007	834	289903,0	192571,1	97331,9	33,6	50,5
2006	552	224183,0	179181,3	45001,7	20,1	25,1
2005	637	259933,0	199147,7	60785,3	23,4	30,5
2004	598	240797,0	187916,2	52880,8	22,0	28,1
Średnia	669,4	299579,5	224996,5	74583,0	24,9	33,1

Przeprowadzone badania wykazały, że w analizowanym wieloleciu 2004-2015 największe objętości wód przypadkowych dopływały do kanalizacji C. Średnia roczna objętość tych wód wynosiła 74 583 m^3.

Objętość ta stanowiła 24,0% średniego rocznego odpływu ścieków z tej kanalizacji. Najmniejsze ilości wód przypadkowych dopływały natomiast do kanalizacji A. Średnia roczna objętość tych wód w analizowanym wieloleciu wyniosła 10 810 m^3, co stanowiło 14,1% średniego rocznego odpływu ścieków z tej kanalizacji. W obiekcie badawczym B roczna objętość wód przypadkowych była o 32 059 m^3 mniejsza niż w C, ale udział tych wód stanowił aż 33,8% średniego rocznego odpływu wszystkich ścieków z tej kanalizacji.

Obliczona w tabeli 2 wartość dodatku wód przypadkowych (DWP) wskazuje, że podczas pogody mokrej wody te powodują wzrost dobowego przepływu ścieków w kanalizacji A – średnio o 16,5%, w kanalizacji B – średnio o 51,1% a w kanalizacji C – średnio o 33,1%.

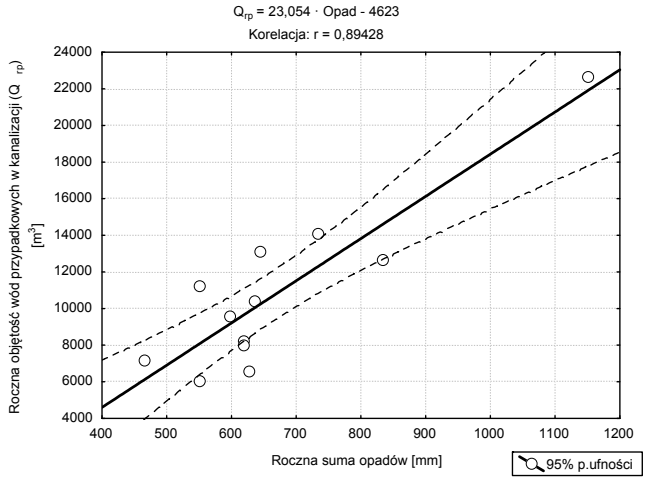

Rys. 1. Przykładowy wykres rozrzutu wpływu rocznej sumy opadów atmosferycznych na roczną objętość wód przypadkowych dopływających do kanalizacji A
Fig. 1. Example scatterplot relationship between annual precipitation totals and annual volume accidental water entering into sewer A

Drugi etap przeprowadzonych badań obejmował ocenę siły korelacji pomiędzy sumą roczną opadów atmosferycznych i roczną objętością wód przypadkowych dopływających do analizowanych sieci kanalizacyjnych (rys. 1). Dodatkowo przeanalizowano zależność korelacyjną

pomiędzy sumą roczną opadów atmosferycznych oraz wartością udziału lub dodatku wód przypadkowych. Analizę korelacji, a następnie regresji liniowej wykonano za pomocą programu komputerowego Statistica. Szczegółowe wyniki tej analizy zamieszczono w tabeli 3.

Tabela 3. Zestawienie wyników analizy korelacji oraz regresji liniowej
Table 3. Summary results of the correlation analysis and linear regression

Obiekt badań	$\overline{x}$	σ	r	Siła korelacji	r^2	t	p	b	a
Wpływ sumy rocznej opadów na roczną objętość wód przypadkowych (Q_{rp})									
A	10810,1	4564,2	0,89	bardzo wysoka	0,80	6,32	**0,000087**	-4622,71	23,05
B	42523,7	13790,6	0,82	bardzo wysoka	0,67	4,55	**0,001057**	-295,31	63,70
C	74583,0	28174,8	0,93	niemal pełna	0,87	8,28	**0,000009**	-24929,70	148,66
Wpływ sumy rocznej opadów na wartość udziału wód przypadkowych (UWP)									
A	13,8	4,3	0,81	bardzo wysoka	0,65	4,30	**0,001568**	0,66	0,02
B	34,2	6,5	0,70	bardzo wysoka	0,49	3,03	**0,012754**	17,34	0,03
C	24,9	7,7	0,81	bardzo wysoka	0,66	4,39	**0,001355**	1,34	0,04
Wpływ sumy rocznej opadów na wartość dodatku wód przypadkowych (DWP)									
A	16,3	6,1	0,83	bardzo wysoka	0,69	4,72	**0,000817**	-2,86	0,03
B	53,4	15,9	0,74	bardzo wysoka	0,55	3,48	**0,005907**	8,78	0,07
C	34,5	14,9	0,84	bardzo wysoka	0,70	4,82	**0,000704**	-12,72	0,07

Oznaczenia zmiennych zawartych w tabeli 3: $\overline{x}$ – średnia arytmetyczna danej zmiennej, σ – odchylenie standardowe danej zmiennej, r – wartość współczynnika korelacji Pearsona, r^2 – wartość współczynnika determinacji, t – wartość statystyki t-Studenta badającej istotność współczynnika korelacji, p – wyliczony poziom istotności (powinien być mniejszy od założonego poziomu istotności wynoszącego 0,05), b – wyraz wolny regresji liniowej, a – współczynnik kierunkowy regresji liniowej.

Przeprowadzone badania wykazały, że istnieje bardzo wysoka w przypadku obiektu A i B oraz niemal pełna w przypadku obiektu C korelacja pomiędzy roczną sumą opadów i roczną objętością wód przypadkowych dopływających do analizowanych sieci kanalizacyjnych. Dodatkowo wykazano, że istnieje także bardzo wysoka korelacja pomiędzy roczną sumą opadów i rocznym udziałem oraz dodatkiem wód przypad-

kowych. Wszystkie obliczone wartości współczynnika korelacji Pearsona okazały się istotne statystycznie na przyjętym poziomie 0,05. Wyniki analizy korelacji potwierdziły, że badane sieci kanalizacyjne są zasilane wodami opadowymi, przez co w konsekwencji funkcjonują one podobnie jak kanalizacja ogólnospławna.

Za pomocą analizy regresji dla każdego obiektu badań obliczono parametry równań funkcji liniowych, pozwalających na podstawie sumy rocznej opadów, wyrażonej w mm, prognozować roczną objętość wód przypadkowych oraz ich udział i dodatek: $Q_{rp} = a \cdot \Sigma$ roczna opadów + b, UWP = $a \cdot \Sigma$ roczna opadów + b, DWP = $a \cdot \Sigma$ roczna opadów + b. Parametry „a" oraz „b" wymienionych równań zamieszczono w tabeli 3.

Po podstawieniu wartości liczbowych do poszczególnych równań obliczono, że wzrost sumy rocznej opadów o 100 mm spowoduje wzrost rocznej objętości wód przypadkowych dopływających do kanalizacji A o 2 305 m^3, do kanalizacji B o 6 379 m^3, a do kanalizacji C aż o 14 866 m^3. Analogicznie wzrost rocznej sumy opadów o 100 mm będzie powodować wzrost wartości UWP w przypadku obiektu A o 2%, obiektu B o 3%, natomiast obiektu C aż o 4%.

W ostatnich czterech latach (2012-2015) suma roczna opadów dla Krakowa wahała się od 467 do 644 mm. Takie sumy roczne dla tej miejscowości charakteryzują według systematyki Kaczorowskiej (1962) odpowiednio lata od bardzo suchych do normalnych. W okresie tym wartości UWP w badanych kanalizacjach nie przekraczały 17% w przypadku obiektu A, 35% w przypadku obiektu B i 20% w przypadku obiektu C. Jednak przeprowadzona analiza regresji wskazuje, że jeżeli pojawią się na terenie zlewni tych kanalizacji opady o sumie rocznej takiej, jaka miała miejsce przykładowo w roku 2010 (1150 mm), to wartości UWP mogą wzrosnąć, w przypadku obiektu A o 6%, w przypadku obiektu B o 11%, natomiast w przypadku obiektu C aż o 19%.

Uzyskane na podstawie analiz wyniki badań dają podstawy do zintensyfikowania działań mających na celu wyeliminowanie nielegalnych podłączeń rynien dachowych lub wpustów podwórzowych do analizowanych sieci kanalizacyjnych. Jest to szczególnie istotne w przypadku kanalizacji B i C.

6. Wnioski

Na podstawie przeprowadzonych badań oraz wyników analiz sformułowano następujące wnioski:

- W odniesieniu do analizowanych obiektów badań występuje bardzo wysoka lub w niektórych przypadkach niemal pewna, zależność korelacyjna pomiędzy roczną sumą opadów atmosferycznych oraz roczną objętością wód przypadkowych dopływających do kolektorów kanalizacyjnych.
- Stwierdzono występowanie bardzo silnej korelacji pomiędzy roczną sumą opadów atmosferycznych a wartością udziału oraz dodatku wód przypadkowych dopływających wszystkich badanych kanalizacji.
- Obliczone parametry równań regresji pozwalają prognozować obciążenie hydrauliczne badanych sieci kanalizacyjnych wodami przypadkowymi w sytuacji wystąpienia lat wilgotnych lub skrajnie wilgotnych, charakteryzujących się wysoką roczną sumą opadów.
- Na podstawie sformułowanych równań liniowej funkcji regresji obliczono, że wzrost sumy rocznej opadów o 100 mm spowoduje wzrost rocznej objętości wód przypadkowych dopływających do kanalizacji A o 2 305 m^3, do kanalizacji B o 6 379 m^3, a do kanalizacji C o 14 866 m^3. Analogicznie wzrost rocznej sumy opadów o 100 mm będzie powodować wzrost wartości UWP w przypadku obiektu A o 2%, obiektu B o 3%, natomiast obiektu C – aż o 4%.
- Uzyskane wyniki badań, po przekazaniu ich eksploatatorom analizowanych sieci kanalizacyjnych, powinny stać się przyczynkiem do podjęcia intensywnych i skutecznych działań mających na celu wyeliminowanie nielegalnych podłączeń rynien dachowych lub wpustów podwórzowych do kanalizacji sanitarnej. Jednocześnie powinien być wykonany przegląd zwieńczeń studni kanalizacyjnych w aspekcie zalewania wodami opadowymi pokryw włazów obniżonych w stosunku do powierzchni terenu.

Literatura

Andraka, D., Dzienis, L. (2013). Modelowanie ryzyka w eksploatacji oczyszczalni ścieków. *Rocznik Ochrona Środowiska, 15*, 1111-1125.

Bielińska, E.J., Baran, S., Pawłowski, L., Jóźwiakowski, K., Futa, B., Bik-Małodzińska, M., Mucha, Z., Generowicz, A. (2014). Theoretical aspects of integrated protection of suburban areas. *Problems of sustainable development, 9(1)*, 127-139.

Bugajski, P., Chmielowski, K., Kaczor, G. (2016). Wpływ dopływu wód opadowych na jakość ścieków w małym systemie kanalizacyjnym. *Acta Scientarum Polonorum (Formatio Circumiectus), 15(2)*, 1-9.

Butler, D., Davies, J.W. (2011). *Urban Drainage*. 3rd Edition. London and New York: Spon Press an imprint of Taylor & Francis.

Cieślak, O., Pawełek, J. (2014). Dopływ wód obcych do kanalizacji sanitarnej na przykładzie gminy Mézos we Francji. *Instal, 7-8*, 90-95.

De Bénédittis, J. (2004). *Mesurage de l'infiltration et de l'exfiltration dans les réseaux d'assainissement. Le grade de docteur*. INSA de Lyon, Villeurbanne, France.

Ellis, J.B., Bertrand-Krajewski, J.L. (2010). *Assessing Infiltration and Exfiltration on the Performance of Urban Sewer Systems.* IWA Publishing.

Jóźwiakowski, K., Mucha, Z., Generowicz, A., Baran, S., Bielińska, J. (2015). The use of multi-criteria analysis for selection of technology for a household WWTP compatible with sustainable development. *Archives Of Environmental Protection, 41(3)*, 76-82.

Kaczor, G. (2011). Wpływ wiosennych roztopów śniegu na dopływ wód przypadkowych do oczyszczalni ścieków bytowych. *Acta Scientiarum Polonorum (Formatio Circumiectus), 10(2)*, 27-34.

Kaczor, G. (2012). Wpływ wód infiltracyjnych i przypadkowych na funkcjonowanie małych systemów kanalizacyjnych. Rozprawa habilitacyjna, nr 372, *Zeszyty Naukowe Uniwersytetu Rolniczego w Krakowie*, nr 495.

Kaczor, G., Bergel, T., Bugajski, P. (2015). Impact of extraneous waters on the proportion of sewage pollution indices regarding its biological treatment. *Infrastruktura i Ekologia Terenów Wiejskich*, *IV/3/2015*, 1251-1260.

Kaczor, G., Bugajski, P. (2012). Impact of Snowmelt Inflow on Temperature of Sewage Discharged to Treatment Plants. *Polish Journal of Environmental Studies*, *21(2)*, 381-386.

Kaczorowska, Z. (1962). *Opady w Polsce w przekroju wieloletnim. Prace Geograficzne, 33*, Instytut Geograficzny PAN.

Kotowski, A., Kaźmierczak, B., Nowakowska, M. (2014). Analiza przeciążeń kanalizacji deszczowej na osiedlu Rakowiec we Wrocławiu wywołanych zmianami klimatu. *Rocznik Ochrona Środowiska, 16*, 608-626.

Kowalik, T., Bogdał, A., Borek, Ł., Kogut, A. (2015). The effect of treated sewage outflow from a modernized sewage treatment plant on water quality of the Breń river. *Journal of Ecological Engineering, 16(4)*, 96-102.

Madryas, C., Przybyła, B., Wysocki, L. (2010). *Badania i ocena stanu technicznego przewodów kanalizacyjnych*. Wrocław: Dolnośląskie Wydawnictwo Edukacyjne.

Pecher, R. (1999). Wody przypadkowe w sieci kanalizacyjnej – problem gospodarki wodnej. *Gaz, Woda i Technika Sanitarna*, *12/1999*, 1-6.

Wałęga, A., Cupak, A., Pawełek, J., Michalec, B. (2014). Transformation of Pollutants in the Stormwater Treatment Process. *Polish Journal of Environmental Studies, 23(3)*, 909-916.

The Effect of Total Annual Precipitation on the Volume of Accidental Water Entering Sanitary Sewage System

Abstract

The aim of the study was to find out the strength of the correlation between total annual precipitation and annual volume of accidental water entering three selected sewerage systems. Accidental water is usually precipitation or melt water entering the sanitary sewers via manhole wells or the outlets of rain gutters, yard gullies or local drainage systems illegally connected to the drains. The analysis included 12-year measurement series covering total annual precipitation for Kraków and annual volume of accidental water entering three distribution sewerage networks discharging domestic sewage from residential areas in the years 2004-2005. The study revealed a significant and very strong correlation between total annual precipitation and annual volume of accidental water entering the investigated sewerage systems. Results if regression equations showed that a 100 mm increase in total annual precipitation would enhance will the annual volume of accidental water supplied to the analyzed sewerage systems from 2 305 up to 14 866 m^3. This clearly indicates the need to intensify the efforts aimed at elimination of illegal connections of rain gutters and yard gullies to the investigated sewerage systems.

Streszczenie

Celem badań była ocena siły korelacji pomiędzy roczną sumą opadów atmosferycznych i roczną objętością wód przypadkowych dopływających do 3 wybranych sieci kanalizacyjnych. Wody przypadkowe to najczęściej wody opadowe lub roztopowe przedostające się do wnętrza kanałów sanitarnych przez włazy studni kanalizacyjnych oraz nielegalnie wykonywane włączenia do przykanalików wylotów rynien dachowych, wpustów podwórzowych lub wylotów

drenaży służących do odwodnienia posesji. Analizę oparto na 12 letnich ciągach pomiarowych, obejmujących sumy roczne opadów atmosferycznych dla Krakowa oraz roczne objętości wód przypadkowych dopływających do 3 rozdzielczych sieci kanalizacyjnych, odprowadzających ścieki bytowe z osiedli mieszkaniowych w latach 2004-2015. Przeprowadzone badania wykazały istotną statystycznie, bardzo wysoka korelację pomiędzy roczną sumą opadów atmosferycznych i roczną objętością wód przypadkowych dopływających do badanych sieci kanalizacyjnych. Na podstawie równań funkcji regresji obliczono, że wzrost sumy rocznej opadów o 100 mm spowoduje wzrost rocznej objętości wód przypadkowych dopływających do analizowanych kanalizacji od 2 305 aż do 14 866 m^3. Uzyskane wyniki badań, powinny być sygnałem do podjęcia przez eksploatatorów sieci kanalizacyjnych intensywnych i skutecznych działań mających na celu wyeliminowanie nielegalnych podłączeń rynien dachowych lub wpustów podwórzowych do kolektorów sanitarnych.

Słowa kluczowe:
kanalizacja, ścieki, wody przypadkowe, opady, oczyszczalnia ścieków

Keywords:
sewerage system, sewage, accidental water, precipitation,
sewage treatment plant

MIDDLE POMERANIAN SCIENTIFIC SOCIETY OF THE ENVIRONMENT PROTECTION
ŚRODKOWO-POMORSKIE TOWARZYSTWO NAUKOWE OCHRONY ŚRODOWISKA
Annual Set The Environment Protection
Rocznik Ochrona Środowiska
Volume/Tom 19. Year/Rok 2017 ISSN 1506-218X 682-693

Domowe źródła hałasu niskoczęstotliwościowego

Adam Zagubień, Katarzyna Wolniewicz
Politechnika Koszalińska

1. Wstęp

W artykule autorzy podjęli próbę oceny oddziaływania hałasu niskoczęstotliwościowego w typowym domu jednorodzinnym. Ze względu na nadal fragmentaryczne badania wpływu infradźwięków i hałasu niskoczęstotliwościowego na zdrowie człowieka, szczególnie podczas długotrwałej ekspozycji, trudno jest określić odpowiednie poziomy dopuszczalne. Przyjmowanie poziomów dopuszczalnych infradźwięków i hałasu niskoczęstotliwościowego na granicy progów słyszenia i odczuwania, a często poniżej tej granicy (Leventhall 2003) spowodowane jest małą ilością dostępnych badań, które prowadzą do zachowawczego podejścia przy określaniu ujednoliconych regulacji prawnych (Pawlas i in. 2013). Norma ISO 1996-1:2003 (ISO 1996 2003) wspomina jedynie w części C o dźwiękach z silnymi składowymi niskich częstotliwości w widmie, prezentując zakres tych częstotliwości od 5 Hz do 100 Hz.

Pomiary oraz ocena zagrożenia hałasem infradźwiękowym i niskoczęstotliwościowym prowadzona jest głównie w miejscach pracy (Pawlaczyk-Łuszczyńska i in. 2006). Natomiast narażenie to nie kończy się wraz z opuszczeniem budynku zakładu pracy. Pomiędzy środowiskiem pracy, a środowiskiem naturalnym istnieje jeszcze codzienna ekspozycja pracownika na hałas w miejscu zamieszkania, np. podczas rozrywki (Smeatham 2002, Dudarewicz i in. 2007) oraz w czasie dojazdu do pracy (Zagubień 2016). Zwiększanie świadomości społecznej dotyczącej zagrożeń akustycznych w codziennym życiu człowieka pozwoli na świadomą identyfikację problemu oraz poprawę jakości wypoczynku i wydajności w pracy

(Lis i in. 2015). W artykule hałas niskoczęstotliwościowy oznaczony został skrótem LFN (z angielskiego: Low Frequency Noise).

Źródłem hałasu niskoczęstotliwościowego LFN mogą być urządzenia usytuowane w pobliżu miejsc odpoczynku lub w budynkach mieszkalnych. Są to między innymi: windy, transformatory, agregaty chłodnicze, pompy, gazowe piece grzewcze itp. W ostatnich latach montowane są na dachach budynków małe turbiny wiatrowe (Pierzga i in. 2015). Jednak nie zawsze są to urządzenia techniczne obsługujące wybrane funkcje w budynku, często są to małe urządzenia domowe jak: lodówki, pralki, zmywarki, pochłaniacze kuchenne czy gazowe podgrzewacze wody. W artykule podjęto próbę oceny klimatu akustycznego w budynku jednorodzinnym w zakresie hałasu LFN pochodzącego od urządzeń codziennego użytku.

W niniejszym artykule infradźwiękami nazwano dźwięki o częstotliwościach od 1 do 20 Hz zgodnie z normą ISO 7196:1995 (ISO 7196 1995). Brak jest standaryzacji dźwięków o niskich częstotliwościach, jednak większość naukowców zakres tych częstotliwości określa w granicach 10 do 200 Hz (Pawlas i in. 2013). Natomiast dźwięki powszechnie uważane za tzw. słyszalne, to dźwięki w zakresie częstotliwości 20-20 000 Hz mimo, że formalnie krzywe równej głośności dotyczą częstotliwości 20 do 12 500 Hz (ISO 226 2003). Propozycję standaryzacji zakresu częstości hałasu niskoczęstotliwościowego – LFN w Polsce oraz metodykę ustalania uciążliwości w budynkach mieszkalnych zaproponowała w 2001 roku M. Mirowska (Mirowska 2001). Wiele państw europejskich ma znormalizowany hałas niskoczęstotliwościowy. Przykładowe zestawienie zakresów hałasu LFN stosowanych w Europie zawarto w tabeli 1.

Tabela 1. Zestawienie zakresów niskich częstości w różnych krajach
Table 1. Summary of low frequency range in different countries

Kraj	Norma	Zakres częstotliwości [Hz]
Szwecja	SP INFO 1996:17	31,5-200
Dania	Nr. 9 1997	5- 160
Niemcy	DIN 45680	8- 125
Holandia	NSG 1999	20- 100
Finlandia	Asumisterveysohje 2003	20- 200
Litwa	LST ISO 1996- 2:2008	8- 200
Austria	ÖNORM S 5007	10- 80
Polska	Propozycja M. Mirowska	10- 250

Ze względu na obowiązujące w różnych krajach na świecie odmienne metody wykonywania pomiarów i ocen oddziaływania hałasu w zakresie niskich częstotliwości, powstają trudności w porównywaniu wyników oraz ustaleniu wspólnej polityki w tym zakresie. Przeprowadzona w pracy ocena wykonana została według kryterium uciążliwości zaproponowanego przez M. Mirowską (Mirowska 2001).

2. Metodologia i zakres wykonanych badań

Pomiary ciśnienia akustycznego wykonano cyfrowym analizatorem i miernikiem poziomu dźwięku oraz drgań SVAN 912AE klasy 1. Zestaw wyposażony był w analizator i rejestrator dźwięku, przedwzmacniacz mikrofonowy SV01A, mikrofon SV02/C4L, osłonę przeciwwietrzną oraz kalibrator akustyczny. Cały zestaw posiadał ważne świadectwo wzorcowania. Analizy rejestrowane były w pasmach tercjowych (1/3 oktawy) w przedziale od 1 Hz do 16 kHz bez korekcji. Następnie cyfrowo na wyniki nakładano filtr korekcyjny A oraz odrzucano wyniki powyżej 250 Hz. Czas pojedynczego pomiaru odpowiadał czasowi trwania zadania lub czynności. Podczas pomiarów mikrofon ustawiano na wysokości odpowiadającej położeniu ucha osoby wykonującej określoną czynność codzienną – średnio 1,2-1,5 m nad podłogą. Pomiary każdej czynności wykonywano trzykrotnie, biorąc do dalszych analiz wyniki najbliższe średniej. Warunki meteorologiczne w pomieszczeniach podczas realizacji pomiarów hałasu wynosiły: temperatura 18-23°C, wilgotność 65-82%, ciśnienie 960-1010 hPa.

Pomiary wykonano wewnątrz pomieszczeń domu jednorodzinnego, parterowego z poddaszem użytkowym. W pobliżu domu przebiegają ulice miejskie o małym natężeniu ruchu. Centralną część domu stanowi otwarty pokój dzienny, wokół którego zlokalizowane są pozostałe pomieszczenia. Ściany domu wykonane zostały w postaci przegrody warstwowej z pustaków ceramicznych, styropianu i okładziny z cegły pełnej, mur był obustronnie otynkowany. Źródłem dźwięku będącym podstawą analiz w niniejszym artykule były codzienne dźwięki związane z domową aktywnością człowieka. Zatem przed przystąpieniem do pomiarów ustalono harmonogram codziennych zajęć domowników. Ze względu na fakt najdłuższego czasu przebywania w domu gospodyni domowej dalsze analizy prowadzono dla tej osoby. Ustalenia zestawiono w tabeli 2.

Tabela 2. Harmonogram zajęć gospodyni domowej
Table 2. Schedule of activities of a housewife

Nr	Nr analizy pomiarowej	Nazwa czynności	Włączone urządzenia
1	A59	Higiena codzienna, mycie pod prysznicem	Prysznic, pralka, spłukiwanie toalety, lodówka w oddaleniu
2	A58	Pranie	Pralka, lodówka w oddaleniu
3	A50	Przygotowanie posiłków	Czajnik elektryczny, lodówka, zmywarka
4	A51	Gotowanie obiadu	Wentylacja mechaniczna nad palnikami, lodówka
5	A53	Odkurzanie	Odkurzacz, lodówka w oddaleniu
6	A60	Oglądanie TV	Telewizor, lodówka w oddaleniu
7	A5	Sen	W oddaleniu lodówka i piec grzewczy
8	A43	Tło pomiarowe	W oddaleniu lodówka

Kryterium oceny uzyskanych wyników pomiarów oparto na propozycji M. Mirowskiej (Mirowska 2001). W celu oceny widma mierzonych w mieszkaniu dźwięków stosowano charakterystyczną krzywą A10 oznaczoną na rysunkach MIR A10. Krzywa A10 wyznaczana jest w przedziale częstotliwości od 10 Hz do 250 Hz z zależności $L_{A10} = 10 - k_A$, gdzie k_A jest korekcją A zgodnie z normą PN-EN 61672-1 (PN-EN 61672-1:2014-03 2014). Według przyjętego kryterium niska częstotliwość hałasu LFN jest irytująca, gdy poziom ciśnienia akustycznego hałasu przekracza krzywą A10 i jednocześnie przekroczone są poziomy szumów tła o więcej niż 10 dB dla hałasów tonalnych oraz o 6 dB dla hałasów szerokopasmowych. Zatem spełnione muszą być jednocześnie dwa warunki:

- $\Delta L1 > 0$,
- $\Delta L2 > 10$ dla hałasów tonalnych lub $\Delta L2 > 6$ dla hałasów szerokopasmowych.

gdzie:
$\Delta L1 = L_H - L_{A10}$ – różnica pomiędzy mierzonym poziomem ciśnienia akustycznego, a poziomem ciśnienia akustycznego określonego krzywą A10,
$\Delta L2 = L_H - L_T$ – różnica pomiędzy mierzonym poziomem ciśnienia akustycznego, a poziomem tła akustycznego.

3. Analiza uzyskanych wyników

Symbole prezentowane na rysunkach 1- 4, np. A50, oznaczają nazwy prowadzonych analiz związane z czynnościami domowymi i odpowiadającą im pracą urządzeń domowych zgodnie z zestawieniem w tabeli 2. Oznaczenie HP np. A50HP, w symbolu analizy pomiarowej oznacza, że wynik podawany jest bez korekcji. Symbolem BG oznaczono wyniki analizy widmowej tła.

Wyniki analiz tercjowych wskazują występowanie dźwięków z zakresu LFN powyżej przyjętego kryterium w porze dziennej. W porze nocnej mieszkańcy analizowanego domu mają pełny komfort akustyczny w zakresie niskich częstości dźwięków, zgodnie z przyjętym kryterium. Dlatego dalszą ocenę uciążliwości hałasu LFN przeprowadzono tylko dla pory dziennej.

Na rysunku 3 zaprezentowano przekroczenia pierwszego warunku przyjętego do oceny kryterium $\Delta L1 > 0$. Wynik wskazuje na przekroczenia progu uciążliwości w częstościach środkowych powyżej 100 Hz dla wszystkich czynności domowych. Podobne rezultaty analiz prowadzonych w pomieszczeniach mieszkalnych uzyskali japońscy badacze (Yamada i in. 2012).

Na rysunku 4 zaprezentowano przekroczenia drugiego warunku przyjętego do oceny kryterium, $\Delta L2 > 10$ dla hałasów tonalnych lub $\Delta L2 > 6$ dla hałasów szerokopasmowych.

Stwierdzono, że przekroczenia drugiego warunku (rys. 4) dla hałasu szerokopasmowego występują od częstości 25 Hz ($\Delta L2 > 6$), a dla hałasu tonalnego od częstości 100 Hz ($\Delta L2 > 10$) z jednym wyjątkiem dla częstości 31,5 Hz. Spełnienie obu warunków uciążliwości hałasu LFN jednocześnie (przedstawionych na rysunku 3 i 4), występuje dla częstości w zakresie od 100 Hz do 250 Hz.

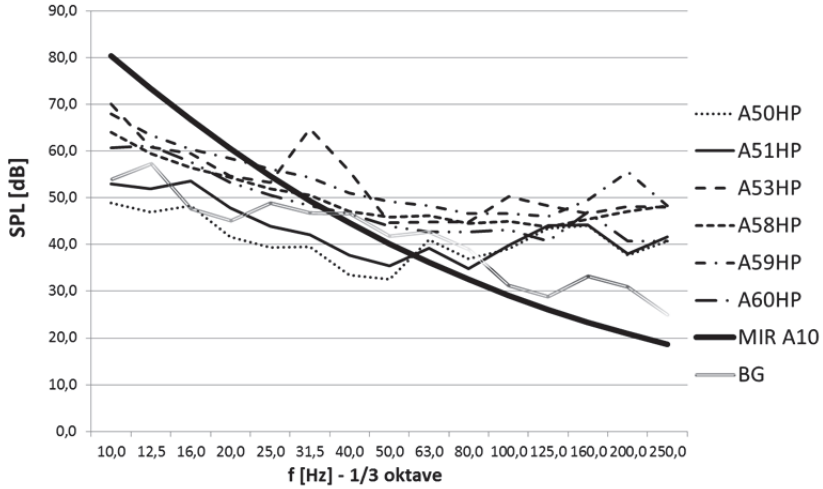

Rys. 1. Analizy tercjowe hałasu w domu przy zamkniętych oknach w porze dziennej
Fig. 1. One-third octave analyses of noise inside home with closed windows in the daytime

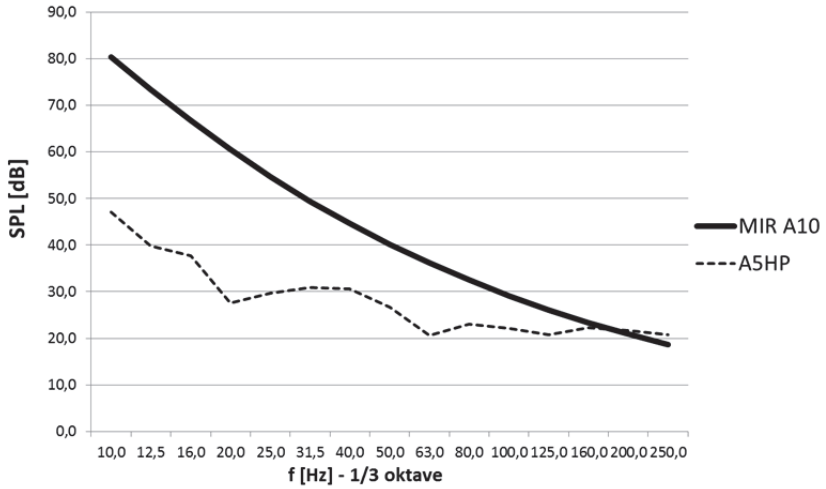

Rys. 2. Analizy tercjowe hałasu w domu przy zamkniętych oknach w porze nocnej
Fig. 2. One-third octave analyses of noise inside home with closed windows at night time

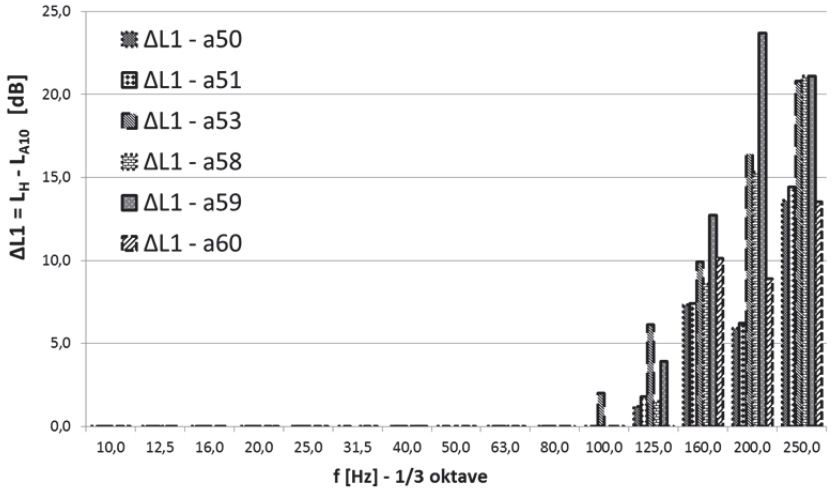

Rys. 3. Różnica pomiędzy mierzonym poziomem ciśnienia akustycznego (L_H), a poziomem ciśnienia akustycznego określonego krzywą A10
Fig. 3. Difference between measured sound pressure level in one-third octave bands for noise (L_H) and the appropriate sound pressure level for the A10 rating curve

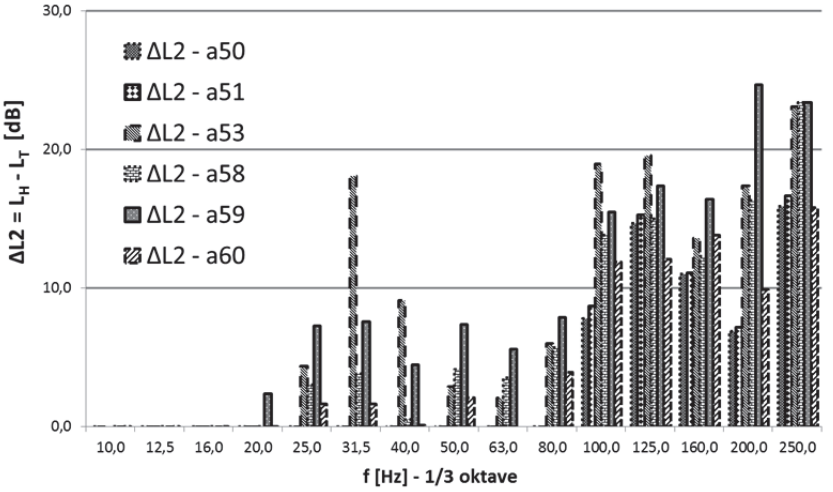

Rys. 4. Różnica pomiędzy mierzonym poziomem ciśnienia akustycznego (L_H), a poziomem tła akustycznego (L_T)
Fig. 4. Difference between the sound pressure level for noise (L_H) and the background noise level (L_T)

4. Wnioski

Prowadzenie łącznie ocen przy zastosowaniu korekcji A i G pozwala pełniej uwzględnić odziaływanie na organizm człowieka dźwięków w szerszym zakresie częstotliwości (Salt & Hullar 2010, Zagubień 2016).

Zagubień i Wolniewicz (Zagubień & Wolniewicz 2016) przedstawili również ocenę narażenia na hałas infradźwiękowy w domu, który był przedmiotem niniejszych analiz. Obliczony poziom ekspozycji dobowej w tym samym miejscu zamieszkania nie przekraczał 85 dB(G).

Przeprowadzone analizy hałasu LFN według wybranego kryterium (Mirowska 2001) wskazują przekroczenia progu uciążliwości w częstościach środkowych analiz tercjowych powyżej 100 Hz. Należy w tym miejscu zauważyć, że przyjęte kryterium ma szeroki zakres częstotliwości od 10 Hz do 250 Hz. Biorąc pod uwagę zawarte w tabeli 1 wybiórcze zestawienie metodyk LFN, to w takich krajach jak Austria, Niemcy lub Holandia w ogóle nie byłaby prowadzona ocena powyżej częstości 100 Hz.

Ze względu na powszechne występowanie podobnych poziomów LFN w większości mieszkań wyposażonych w lodówkę, pralkę, zmywarkę, telewizor czy odkurzacz, zaproponowane kryterium (Mirowska 2001) może mieć zastosowanie w porze nocnej w celu zachowania komfortu snu. Przeniesienie tego kryterium wprost do analiz hałasu LFN dla pory dziennej skutkowałoby wykluczeniem z użytkowania wielu niezbędnych przedmiotów AGD.

Prezentowane wyniki pomiarów wskazują na zagrożenia dla komfortu akustycznego pory dziennej w zakresie częstości LFN w miejscu zamieszkania. Ze względu na fakt jednoczesnej emisji hałasu słyszalnego przez wskazane wyposażenie mieszkania można przypuszczać, że mieszkańcy nie będą nadmiernie nadużywać tych przedmiotów. Ekspozycja na hałas LFN będzie trwała niezbędne minimum, tylko w czasie wykonywania określonych czynności w gospodarstwie domowym. Jednocześnie wykazano, że osoby zatrudnione jako pomoc domowa oraz gospodynie domowe mogą być narażone na hałas niskoczęstotliwościowy podczas wielogodzinnej ekspozycji w porze dziennej.

Część autorów (Leventhall i in. 2003, Jabben & Verheijen 2012, Ziaran 2013) uważa, że prowadzenie analiz i ocen przy zastosowaniu korekcji C pozwoliłoby uwzględnić dźwięki o niskich częstotliwościach

w mierzonym poziomie hałasu. Jednak autorzy ci zauważają również, że stosowanie korekcji C niesie za sobą problem obliczeniowy wykonywanych prognoz akustycznych, ponieważ większość źródeł hałasu zdefiniowana jest w dB(A), do których dostosowane są powszechnie używane i sprawdzone algorytmy obliczeniowe. Wymagałoby to konieczności określenia zupełnie nowych poziomów dopuszczalnych opisanych charakterystyką C, zdefiniowanych dla poszczególnych częstości środkowych widma.

Literatura

Dudarewicz, A., Pawlaczyk-Łuszczyńsk,a M., Śliwińska-Kowalska, M. (2007). Developing the metod for assessing non-occupational exposure to noise. *Med. Pracy, 58(3)*, 231-242.

ISO 226:2003 (2003). *Acoustics – Normal equal-loudness level contours*. Geneva: International Organization for Standardization.

ISO 1996-1:2003 (2003). *Acoustics. Description, measurement and assessment of environmental noise. Part 1: Basic quantities and assessment procedures.* Geneva: International Organization for Standardization.

ISO 7196:1995 (1995). *Acoustics – Frequency weighting characteristic for infrasound measurements*. Geneva: International Organization for Standardization.

Jabben, J. & Verheijen, E. (2012). Options for Assessment and Regulation of Low Frequency Noise. *Journal of Low Frequency Noise, Vibration and Active Control, 31(4)*, 225-238.

Leventhall, G., Pelmear, P., Benton, S. (2003). *A review of Published Research on Low Frequency Noise and Its Effects*. London: Defra Publications.

Lis, T., Nowacki, K., Bendkowska-Senator, K. (2015). Kształtowanie optymalnych warunków pracy przy występowaniu hałasu zawodowego i pozazawodowego, *XVIII Konferencja Innowacje w zarządzaniu i inżynierii produkcji, Zakopane 1-03.03.2015*.

Mirowska, M. (2001). Evaluation of Low-Frequency Noise in Dwellings. New Polish Recommendations. *Journal of Low Frequency Noise, Vibration and Active Control, 20(2)*, 67-74.

Pawlaczyk-Łuszczyńska, M., Szymczak, W., Dudarewicz, A., Śliwińska-Kowalska, M. (2006). Proposed Criteria for Assessing Low Frequency Noise Annoyance in Occupational Settings. *International Journal of Occupational Medicine and Environmental Health, 19(3)*, 185-197.

Pawlas, K., Pawlas, N., Boroń, M., Szłapa, P., Zachara, J. (2013). Infrasound and low frequency noise assessment at workplaces and environment – review of criteria. *Environmental Medicine, 16(1)*, 82-89.

Pierzga, R., Boczar, T., Wotzka, D. (2015). Measurements and Acoustic Analyses of Infrasound Noise Emitted by Operation of Small, Building Mounted Wind Farm. *Acta Physica Polonica A, 128(2)*, 294-299.

PN-EN 61672-1:2014-03 (2014). *Elektroakustyka – Mierniki poziomu dźwięku – Część 1: Wymagania.* Warszawa: PKN.

PN-Z 01338:2010 (2010). *Akustyka. Pomiar i ocena hałasu infradźwiękowego na stanowiskach pracy*. Warszawa: PKN.

Salt, A.N., & Hullar, T.E. (2010). Responses of the ear to low frequency sounds, infrasound and wind turbines. *Hearing Research, 268*, 12-21.

Smeatham, D. (2002). *Noise levels and noise exposure of workers in pubs and clubs — A review of the literature. Prepared by the Health and Safety Laboratory for the Health and Safety Executive. Research Report 026*. United Kingdom: *www.hse.gov.uk/research/rrpdf/rr026.pdf*

Vercammen, M. (2007). Criteria for low frequency noise. *Proceedings of the 19th International Congress on Acoustics, Madrid*.

Yamada, S., Inukai, Y., Takagi, K., Sebayashi, T., Koyama, S., Tanaka, Y., Horie, Y. (2012). Case Studies of Field Measurements of Low Frequency Sound and Complaints by a Non Profit Organization for Supporting Noise, Vibration and Low Frequency Noise Complainants in Japan. *Journal of Low Frequency Noise, Vibration and Active Control, 31(4)*, 257-266.

Zagubień, A. (2016). Pozazawodowe narażenie na hałas niskoczęstotliwościowy – analiza na podstawie wybranego środka transportu. *Rocznik Ochrona Środowiska, 18,* 626-641.

Zagubień, A. & Wolniewicz, K. (2016). Everyday exposure to occupational/non-occupational infrasound noise in our life. *Archives of Acoustics, 41(4)*, 659-668.

Ziaran, S. (2013). Low Frequency Noise and Its Assessment and Evaluation. *Archives of Acoustics, 38(2)*, 265-270.

Home Sources of Low Frequency Noise

Abstract

The authors of the article made an attempt to assess the impact of low frequency noise in a typical detached house. Much attention was paid to low frequency noise exposure in places other than the ones defined as potentially of great risk. There were presented own results of measurements which have proved that it is possible and necessary to carry out analysis of noise in a wide range of frequency. It has been noticed that assessments of impact and permissible levels of low frequency noise should concern not only workplace but also dwellings.

Minding the fact that all over the world there are different methods of conducing measurements ad assessments of low frequency noise impact, there are problems in comparing the results and setting up a mutual policy in this topic. The assessment presented in this research was conducted according to arduousness criteria by M. Mirowska.

The sources of sound which was the base of the analyses were the sounds connected with daily human activity. The measurement were made by digital analyser and by the meter of sound and vibration level SVAN 912AE class 1.The set was equipped with the analyser and sound register device and microphonic pre-amplifier SVA, microphone SV02/C4L and a windscreen and acoustic calibrator. The measurements inside the building where made in a detached house with a usable attic. The central part of a house was an open living room with other rooms around it.

Conducted analysis of low frequency noise according to chosen criteria show the exceeding of arduousness threshold in frequencies of middle 1/3 octave analysis above 100 Hz. Minding the fact the similarity of low frequency noise in most homes equipped with a fridge, a washing machine, dishwasher, a TV set or a vacuum cleaner, suggested criteria may be applied in night time in order to keep the sleep comfort. Applying these criteria in analysis during day time would result in excluding all necessary home equipment.

In the same time it has been proved that housewives and other people working for long hours as house cleaners can be exposed to low frequency noise. Increasing social awareness of acoustic threat in everyday life allows us to identify the problem and in the same improve the quality of rest and efficiency at work.

Conducting assessments by applying A and G correction allow to fully assess the impact of sounds of wider frequency on human body.

Streszczenie

W artykule autorzy podjęli próbę oceny oddziaływania hałasu niskoczęstotliwościowego w typowym domu jednorodzinnym. Zwrócono uwagę na ekspozycję na hałas niskoczęstotliwościowy odbywającą się poza miejscami zdefiniowanymi jako potencjalne zagrożenie takim hałasem. Przedstawiono własne wyniki pomiarów które wskazują, że są możliwości i potrzeby prowadzenia analiz hałasu w szerokim zakresie częstotliwości. Zauważono, że oceny wpływu narażenia oraz poziomy dopuszczalne na hałas niskoczęstotliwościowy powinny dotyczyć nie tylko miejsc pracy ale również miejsc zamieszkania.

Ze względu na obowiązujące w różnych krajach na świecie odmienne metody wykonywania pomiarów i ocen oddziaływania hałasu w zakresie niskich częstotliwości, powstają trudności w porównywaniu wyników oraz usta-

leniu wspólnej polityki w tym zakresie. Przeprowadzona w pracy ocena wykonana została według kryterium uciążliwości zaproponowanego przez M. Mirowską.

Źródłem dźwięku będącym podstawą analiz w niniejszym artykule były codzienne dźwięki związane z domową aktywnością człowieka. Pomiary wykonano cyfrowym analizatorem i miernikiem poziomu dźwięku oraz drgań SVAN 912AE klasy 1. Zestaw wyposażony był w analizator i rejestrator dźwięku, przedwzmacniacz mikrofonowy SV 01A, mikrofon SV 02/C4L, osłonę przeciwwietrzną oraz kalibrator akustyczny. Pomiary wewnątrz pomieszczeń wykonano w domu jednorodzinnym, parterowym z poddaszem użytkowym. Centralną część domu stanowi otwarty pokój dzienny, a wokół niego zlokalizowane są pozostałe pomieszczenia.

Przeprowadzone analizy hałasu niskoczęstotliwościowego według wybranego kryterium wskazują przekroczenia progu uciążliwości w częstościach środkowych analiz tercjowych powyżej 100 Hz. Ze względu na powszechne występowanie podobnych poziomów hałasu niskoczęstotliwościowego w większości mieszkań wyposażonych w lodówkę, pralkę, zmywarkę, telewizor czy odkurzacz, zaproponowane kryterium może mieć zastosowanie w porze nocnej w celu zachowania komfortu snu. Przeniesienie tego kryterium wprost do analiz hałasu niskoczęstotliwościowego dla pory dziennej skutkowałoby wykluczeniem z użytkowania wielu niezbędnych przedmiotów AGD.

Jednocześnie wykazano, że osoby zatrudnione jako pomoc domowa oraz gospodynie domowe mogą być narażone na hałas niskoczęstotliwościowy podczas wielogodzinnej ekspozycji. Zwiększanie świadomości społecznej na temat zagrożeń akustycznych w codziennym życiu człowieka pozwala na świadomą identyfikację problemu przez zainteresowanych oraz poprawę jakości wypoczynku i wydajności w pracy.

Prowadzenie łącznie ocen przy zastosowaniu korekcji A i G pozwala pełniej uwzględnić oddziaływanie na organizm człowieka dźwięków w szerszym zakresie częstotliwości.

Słowa kluczowe:
poziom ekspozycji na hałas pozazawodowy, poziomy hałasu, pomiary hałasu, infradźwięki, hałas niskoczęstotliwościowy

Keywords:
non-occupational noise exposure level, noise levels, noise measurements, infrasound, low frequency noise

MIDDLE POMERANIAN SCIENTIFIC SOCIETY OF THE ENVIRONMENT PROTECTION
ŚRODKOWO-POMORSKIE TOWARZYSTWO NAUKOWE OCHRONY ŚRODOWISKA

Annual Set The Environment Protection
Rocznik Ochrona Środowiska

Volume/Tom 19. Year/Rok 2017 ISSN 1506-218X 694-714

Środowiskowe sterowanie technologią elektrowni wiatrowej

Andrzej Tomporowski, Józef Flizikowski,
Robert Kasner, Weronika Kruszelnicka
Uniwersytet Technologiczno-Przyrodniczy, Bydgoszcz

1. Wprowadzenie

Obecnie, częstą przeszkodą w eksploatacji elektrowni wiatrowych w przemyśle są stany ekstremalne mocy, a przede wszystkim energii ich działania, i związana z tym nieprzewidywalność zyskowności (rentowności). Wartości ekstremalne ze względu na swój istotny – w większości przypadków negatywny – wpływ na wiele dziedzin życia i nauki są, od długiego czasu,tematem zainteresowań nie tylko naukowców i badaczy z wielu dziedzin. Negatywny wpływ ekstremalnych wartości określonych charakterystyk obserwuje się m.in. w takich dziedzinach, jak energetyka, ekonomia, a dokładnie rynki finansowe, szeroko rozumiana meteorologia ze szczególnym uwzględnieniem środowiskowych procesorów energii, np. elektrowni wiatrowych (Adaramola i in. 2014, Iglesias i in. 2010, Kusiak i in. 2013).

Rentowność sprzedaży netto (ang. net profit margin) mocy i energii, również emisji CO_2 w przypadku elektrowni wiatrowych – informuje, ile zysku (straty) po opodatkowaniu (netto) wypracowują w eksploatacji przychody z działalności. Innymi słowy, jaką część lub jaki procent wszystkich przychodów stanowi zysk po opodatkowaniu. Im wyższy wskaźnik sprzedaży netto tym lepiej, gdyż przedsiębiorstwo generuje większe przychody z działalności energetycznej i ekologicznej, a dzięki temu przynosi większy zysk energetyczny, finansowy i środowiskowy (Baseer i in. 2017, Diaf&Notton 2013, Ouarda i in. 2016).

Wysokie zyski ekonomiczne i niskie szkodliwości ekologiczne są stanami pożądanymi, ale asekuracja i szeroko rozumiane interdyscyplinarne bezpieczeństwo energetyczne powoduje, że główne zainteresowania poznawcze skupiają się na problemie: w jaki sposób zabezpieczyć się przed negatywnym oddziaływaniem ekstremalnie wysokich lub niskich wartości energetycznych charakterystyk użytkowych, czy też aerodynamicznych i meteorologicznych, które są bezpośrednią przyczyną powstawania negatywnych zjawisk (Deluga 2013, Gawłowski i in. 2010, Maatallah i in. 2013, Schweizer i in. 2016, Zohbi i in. 2015).

Mimo dynamicznego rozwoju wielu dziedzin nauki wciąż nie możliwym jest skuteczne przeciwdziałanie występowania ekstremalnych stanów meteorologicznych i ich negatywnym następstwom w przemysłowych stanach użytkowo-eksploatacyjnych. Jedyne, co można zrobić, to odpowiednio przewidywać efekt ich oddziaływania przez dobrze przygotowany system prognoz (Gawłowski i in. 2010, Khahro i in. 2014).

System prognoz warunków technicznych i stanów postulowanych oparty na teorii rozkładów ekstremalnych i związany jest z koniecznością badania określonych ciągów zmiennych losowych, które stanowią monitorowane, eksploatacyjne charakterystyki prędkości wiatru, natężenia przepływu odpowiadające za występowanie zjawisk niepożądanych. W większości przypadków rozpatrywane ciągi zmiennych losowych są w określonym stopniu od siebie zależne. Dlatego ważne są graniczne rozkłady wartości ekstremalnych w przypadku zależnych zmiennych losowych (Goh i in. 2016).

2. Cel badań

Celem badań jest weryfikacja modeli matematycznych, oszacowanie średniej i wariancji energetycznej, ekonomicznej i ekologicznej zyskowności elektrowni wiatrowej dla uaktualnionego, eksploatacyjnego rozkładu wietrzności na podstawie średniej i wariancji rocznej zyskowności elektrowni wiatrowej dla „starszego" oraz bieżącego rozkładu wietrzności.

Założono zakresy prędkości i wydatku wiatru: podkrytyczny, efektywny i nadkrytyczny. Problem badawczy, dla osiągnięcia celu badań, sformułowano w postaci pytania: jakie modele matematyczne można utworzyć, zastosować i wykorzystać dla osiągnięcia niezawodności

działania i energetycznej, ekonomicznej oraz ekologicznej zyskowności elektrowni wiatrowej w dowolnym okresie jej eksploatacji?

3. Model matematyczny

W pracy (Miziuła& Rychlik 2014, Miziuła& Rychlik 2015) rozważany jestnastępujący model: niech dla danego przedziału $\Theta \subseteq \mathbb{R}$ rodzina $\{F_\theta\}_{\theta\in\Theta}$ będzie rodziną dystrybuant o tej własności, że

$$\theta_1 < \theta_2 \Longrightarrow F_{\theta_1}(x) \leq F_{\theta_2}(x) \tag{1}$$

dla wszystkich $x \in \mathbb{R}$. Niech S i T będą danymi dwiema dystrybuantami mieszającymi. Do ograniczeń dla zależności w ciągach stacjonarnych należy silne mieszanie (*strongmixing*) (wprowadzone po raz pierwszy przez Rosenblatta w 1956 r.). Ciąg { Xn} spełnia założenie silnego mieszania, jeżeli istnieje funkcja mieszająca, funkcja g(k) (*mixingfunction*) dążąca do zera, jeżeli k→∞ i taka, że:

$$|P(A \cap B) - P(A)P(B)| < g(k) \tag{2}$$

gdzie:
$A \in \Gamma(X_1, \ldots, X_p)$
$B \in \Gamma(X_{p+k+1}, \ldots, X_{p+k+2}, \ldots)$
dla pewnego *p* i *k*, gdzie Γ(•) oznacza – ciało generowane przez wskazane zmienne losowe. Tak więc jeżeli ciąg zmiennych jest mieszający, to pewne zdarzenie A „na podstawie przeszłości do czasu p" jest blisko niezależne od zdarzenia B „na podstawie przyszłości od czasu p + k +1 naprzód", kiedy k jest duże. Na uwagę w tym miejscu zasługuje fakt, że warunek mieszający jest jednostajny, tzn. że funkcja g(k) nie jest zależna od A i B. Inne sposoby definiowania zależności wraz z ich zastosowaniami są omówione m.in. w pracach (Nor i in. 2014, Okeniyi i in. 2015).

Zdefiniowano dystrybuanty G i H jako mieszanki tej samej rodziny dystrybuant $\{F_\theta\}_{\theta\in\Theta}$ względem dwóch różnych dystrybuant mieszających – odpowiednio S i T:

$$G(x) = \int_\Theta F_\theta(x)S(d\theta), \; H(x) = \int_\Theta F_\theta(x)T(d\theta) \tag{3}$$

Ponadto przyjmujemy, że zmienne losowe X i Y mają dystrybuanty odpowiednio G i H:

$$X \sim G, \qquad Y \sim H.$$

Przy powyższych założeniach Miziuła udowodnił, że wartość oczekiwana $E(Y)$ i wariancja $Var(Y)$ zmiennej losowej Y mogą być oszacowane na podstawie analogicznych parametrów zmiennej losowej X i prostej funkcji dystrybuant mieszających G i H. Mianowicie:

$$\frac{r-L}{2} \wedge 0 \leq \frac{E(Y)-E(X)}{E(|X-E(X)|)} \leq \frac{R-l}{2} \vee 0,\ l \wedge r \leq \frac{Var(Y)}{Var(X)} \leq L \vee R, \tag{4}$$

gdzie:

$$l = \inf_{\theta\in\Theta}\left\{\frac{T(\theta)}{S(\theta)}\right\},\ L = \sup_{\theta\in\Theta}\left\{\frac{T(\theta)}{S(\theta)}\right\}, \tag{5}$$

$$r = \inf_{\theta\in\Theta}\left\{\frac{1-T(\theta)}{1-S(\theta)}\right\},\ R = \sup_{\theta\in\Theta}\left\{\frac{1-T(\theta)}{1-S(\theta)}\right\}, \tag{6}$$

natomiast $\wedge$ i $\vee$ oznaczają odpowiednio minimum i maksimum. Oszacowania te są optymalne w tym sensie, że dla danych dystrybuant mieszających S i T istnieje rodzina dystrybuant $\{F_\theta\}_{\theta\in\Theta}$, dla której wybrana nierówność staje się równością.

Oszacowania we wzorach (4) są tym dokładniejsze, im wartości l, L, r i R są bliższe 1. Jako, że zbiór parametrów Θ oraz dystrybuanty mieszające S i T są dowolnie wybierane przez użytkownia modelu. Warto tu zwrócić szczególną uwagę na możliwie doskonały dobór tych wielkości, co pozwoli na otrzymanie z zależności (4) jak najlepszych oszacowań.

4. Zastosowania teoretycznego modelu

4.1. Pod- i nadkrytyczne stany wietrzności

Przedstawiony model znalazł zastosowanie w teorii systemów niezawodnościowych do szacowania wartości oczekiwanej, wariancji i ogólnych miar rozproszenia czasu życia systemu w jednostkach analogicznych parametrów czasu życia pojedynczego elementu systemu przy założeniu, że elementy systemu są przestawialne (p. Goh i in. 2016, Lun & Lam 2000).

Innym kontekstem, w którym powyższe rozumowanie okazało się użyteczne i który omówiony zostanie tu nieco szerzej, jest analiza strat wywołanych przez ponad krytyczne prędkości (przepływy) wiatru przez elektrownie wiatrowe. W tym przypadku:

- $\Theta = [b, B]$, b oznacza podkrytyczną, najmniejszą prędkość wiatru powodującą ruch wirnika, natomiast B oznacza nadkrytyczną prędkość wiatru, dla której z przyczyn bezpieczeństwa należy wyłączyć turbinę,
- θ – oznacza roczne maksimum przepływu wiatru w okolicy kompleksu elektrowni (mierzone w $m^3 \cdot s^{-1}$),
- F_θ – oznacza dystrybuantę strat w kompleksie elektrowni wiatrowej spowodowanych krytycznym przepływem wiatru o wartości θ.

Przez b oznaczono najmniejszy przepływ powodujący efektywnie użyteczną pracę turbiny, natomiast B oznacza przepływ, którego przekroczenie może spowodować uszkodzenie elementów konstrukcyjnych wirnika. Dystrybuanty strat wydatku F_θ dla danych przepływów θ nie są znane, natomiast warunek (1) jest naturalnie spełniony: większy przepływ krytyczny powoduje większe straty. Dalej:

- S – oznaczna dystrybuantę rocznego maksimum przepływu wiatru wyznaczoną na podstawie starszych danych empirycznych,
- T – oznaczna dystrybuantę rocznego maksimum przepływu wiatru wyznaczoną na podstawie uaktualnionych danych empirycznych.

Dla potrzeb prowadzonych rozważań przyjęto założenie, że realizacja procesu przetwórczego następuje w oparciu o energię dostarczoną z krajowego systemu elektroenergetycznego (KSE) oraz, że analizowany proces energetyczno-przetwórczy w elektrowni wiatrowej jest częścią składową tego systemu. Tym samym staje się pośrednio źródłem zyskowności dla produkcji przemysłowej. Dystrybuanta S została wyestymowana na podstawie dostępnych danych empirycznych a nie w procesie bieżącego monitorowania. Dystybuantę T natomiast wyznacza się na podstawie na bieżąco aktualizowanych danych empirycznych. Przy takiej interpretacji zdefiniowano następujące dystrybuanty strat:

- G – oznacza dystrybuantę rocznych strat w kompleksie elektrowni przy użytej „starszej" dystrybuancie przepływu wiatru S,
- H – oznacza dystrybuantę rocznych strat w kompleksie elektrowni przy użytej uaktualnionej dystrybuancie przepływu wiatru T,
- X – oznacza losowe roczne straty w kompleksie elektrowni (mierzone w zł) przy użytej „starszej"dystrybuancie przepływu wiatru S,

- Y – oznacza losowe roczne straty w kompleksie elektrowni (mierzone w zł) przy użytej uaktualnionej dystrybuancie przepływu wiatru T.

Prowadzone analizy ukierunkowane były na zaktualizowanie parametrów $E(Y)$ i $Var(Y)$, czyli średniej i wariancji rocznych strat energetycznych farm wiatrowych przy użyciu zaktualizowanych danych. Co prawda wielkości te mogą zostać wyestymowane bezpośrednio, wymaga to jednak przeprowadzenia symulacji bardzo czaso- i pracochłonnych, a przez to bardzo drogich. Można ich uniknąć. Wystarczy użyć posiadanych już parametrów $E(X)$, $E(|X - E(X)|)$ i $Var(X)$ dla strat wyznaczonych na podstawie „starszych" danych, obliczyć l, L, r i R (co dla danych S i T nie stanowi problemu) i zastosować je we wzorach (4).

4.2. Zyskowność elektrowni wiatrowej

Celem badań jest oszacowanie średniej i wariancji dziennej energetycznej, ekonomicznej i ekologicznej zyskowności elektrowni wiatrowej dla uaktualnionego rozkładu dziennej wietrzności na podstawie średniej i wariancji rocznej zyskowności elektrowni wiatrowej na podstawie rozkładu dziennej wietrzności. W prowadzonych rozważaniach wielkości zdefiniowane w ogólnym modelu mają następujące interpretacje:

- $\Theta = [b, B]$,
- θ – oznacza prędkość wiatru (mierzoną w $m \cdot s^{-1}$),
- F_θ – oznacza dystrybuantę dziennych zysków energetycznych, ekonomicznych i ekologicznych uzyskanych z działania elektrowni wiatrowej przy prędkości wiatru θ.

Przez b oznaczono najmniejszą prędkość wiatru powodującąruch wirnika, natomiast B oznacza prędkość wiatru, dla której z przyczyn bezpieczeństwa należy wyłączyć turbinę.Dla danej prędkości wiatru θ zyski są losowe z nieznaną dystrybuantą F_θ.Warunek (1) jest spełniony w naturalny sposób: im mocniej wieje(większe prędkości wiatru) w przedziale efektywnych prędkości i przepływów, tym większy finalny zysk energetyczny, ekonomiczny i ekologiczny. Niech ponadto:

- S – oznaczna dystrybuantę dziennej wietrzności wyznaczoną na podstawie starszych danych empirycznych,

- T – oznaczna dystrybuantę dziennej wietrzności wyznaczoną na podstawie uaktualnionych danych empirycznych.

Wtedy:

- G – oznacza dystrybuantę dziennych zysków energetycznych, ekonomicznych i ekologicznych przy użytej „starszej" dystrybuancie wietrzności S,
- H – oznacza dystrybuantę dziennych zysków przy użytej uaktualnionej dystrybuancie wietrzności T,
- X – oznacza losowy dzienny zysk(mierzony w MWh, zł, $t_{eq}CO_2$) przy użytej „starszej" dystrybuancie wietrzności S,
- Y – oznacza losowy dzienny zysk (mierzony w MWh, zł, $t_{eq}CO_2$) przy użytej uaktualnionej dystrybuancie wietrzności T.

W tym miejscy analiza skierowana jest na zaktualizowanie parametrów E(Y) i Var(Y), czyli średniej i wariancji dziennych zysków przy użyciu zaktualizowanych danych. W tym celu użyto znanych już parametrów E(X), $E(|X - E(X)|)$ i Var(X) dla zysków wyznaczonych na podstawie „starszych" danych, by wyznaczyć: l, L, r i R i podstawić je do wzorów (4).

5. Studium przypadku

Zmienne warunki wietrzności utrudniają teoretyczne oszacowanie produktywności elektrowni wiatrowej. Szacunki dokonane na podstawie teoretycznych zależności i obliczeń obarczone są błędem – właśnie ze względu na zmienność i nieprzewidywalność warunków wietrznych.

W opracowaniu, analizę produktywności, w zależności od wietrzności w warunkach rzeczywistych, przeprowadzono dla elektrowni Vestas V90 o mocy 2 MW zlokalizowanej w gminie Błaszki. Wirnik elektrowni znajduje się na wysokości 105 m nad poziomem gruntu, a jego średnica to 90 m. Analizę stanu rzeczywistego przeprowadzono dla trzech kolejnych lat użytkowania elektrowni – 2013-2015.

W tabeli 1 przedstawiono średnie miesięczne wartości prędkości wiatru w analizowanym przedziale czasu i dla lokalizacji posadowienia przyjętego obiektu badań (gmina Błaszki). Z analizy danych zauważa się zmiany prędkości wiatru w poszczególnych miesiącach, w ciągu roku.

Tabela 1. Średnie miesięczne prędkości wiatru na wysokości 105 m w latach 2013-2015 w gminie Błaszki [badania własne]
Table 1. Average monthly wind speed at a height of 105m in 2013-2015 in Błaszki [Own research]

Miesięczne średnie prędkości wiatru w poszczególnych latach, $m \cdot s^{-1}$			
Miesiąc	**2013**	**2014**	**2015**
Styczeń	6,493	7,711	8,583
Luty	5,290	7,142	6,250
Marzec	6,757	6,044	7,062
Kwiecień	5,750	5,585	6,472
Maj	5,200	6,250	5,271
Czerwiec	4,429	4,830	4,914
Lipiec	4,784	5,120	5,566
Sierpień	4,839	5,100	5,872
Wrzesień	5,599	5,257	5,840
Październik	6,435	5,567	5,664
Listopad	6,512	5,811	6,995
Grudzień	8,479	7,361	7,950
Rocznie	**6,24**	**6,22**	**6,70**

Miesiącem o najwyższej prędkości wiatru jest styczeń i grudzień, najniższe średnie prędkości zanotowano w czerwcu. Dla wyznaczenia prędkości wiatru na dowolnej wysokości możliwe jest przeliczenie (Carvalho i in. 2014):

$$v_2 = v_1 \left(\frac{H_2}{H_1}\right)^{\propto} \tag{7}$$

gdzie:
v_1,v_2- prędkość wiatru na wysokości H_1, H_2
α – współczynnik wykładniczy zależny od szorstkości terenu
lub:

$$v_2 = v_1 \left(\frac{\ln\left(\frac{H_2}{z_0}\right)}{\ln\left(\frac{H_1}{z_0}\right)}\right) \tag{8}$$

Zależność współczynnika α i z_0 jest następująca:

$$\propto = \frac{1}{\ln\left(\frac{H}{z_0}\right)} \tag{9}$$

gdzie:
H – wysokość, na której porównywane są współczynniki.

Zmiennym parametrem jest nie tylko prędkość wiatru w danej chwili, zmienne są także czasy występowania danych prędkości wiatru. Aby określić częstość występowania i czasy trwania poszczególnych prędkości wiatru posłużono się teorią Weibulla, wg. której rozkład częstości występowania prędkości wiatru,w postaci analitycznej można opisać funkcją (Usta 2016):

$$F(C, k, v) = \frac{k}{C} \cdot \left(\frac{v}{C}\right)^{(k-1)} \exp\left\{-\left(\frac{v}{C}\right)^{k}\right\} \tag{10}$$

oznaczonej dwoma parametrami:
- parametrem kształtu – C,
- parametrem skali – k, gdzie: v – prędkość wiatru, $m \cdot s^{-1}$.

Na rysunku 1 przedstawiono rozkłady prędkości wiatru w latach 2013-2015, w miejscu posadowienia analizowanej elektrowni wiatrowej, wyznaczone na podstawie pomiarów oraz rozkład Weibulla dla tej lokalizacji wyznaczony metodami numerycznymi. Przy wyznaczaniu rozkładu Weibulla przyjęto współczynniki: k = 2,15 oraz C = 7,10.

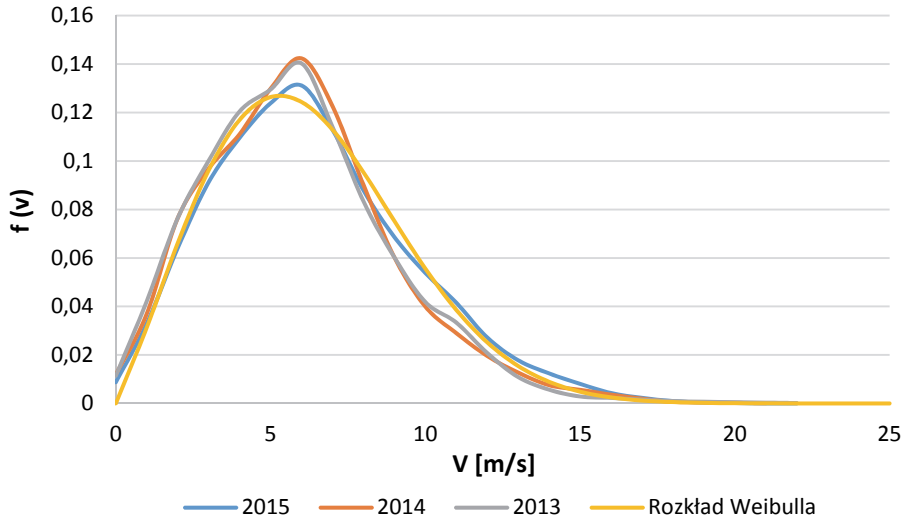

Rys. 1. Rozkłady prędkości wiatru dla lat: 2013-2015 i funkcja Weibulla częstości występowania prędkości wiatru w gminie Błaszki [badania własne]
Fig. 1. Distributions of wind speeds for years: 2013-2015 and function of Weibull frequency of wind speed in Błaszki [own research]

Tabela 2. Miesięczne czasy występowania danej prędkości wiatru w gminie Błaszki w 2013 roku [badania własne]
Table 2. Monthly prevalence of times the wind speed in Błaszki in 2013 [own research]

Czasy występowania danej prędkości wiatru w roku 2013, h												
V $m \cdot s^{-1}$	**Miesiąc**											
	Sty	Lut	Mar	Kwie	Maj	Czer	Lip	Sie	Wrze	Paź	List	Gru
0	15,6	2,0	3,7	10,8	12,6	25,9	5,2	3,7	5,8	4,5	8,6	1,5
1	37,9	24,2	14,9	29,5	44,6	79,2	29,8	28,3	36,0	17,9	24,5	3,0
2	37,2	66,5	26,8	60,5	52,1	105,8	84,1	87,8	56,2	37,2	44,6	10,4
3	46,1	110,9	46,9	67,7	74,4	82,8	105,6	128,0	73,4	69,9	49,0	22,3
4	89,3	105,5	58,0	74,9	101,2	90,7	126,5	132,4	98,6	61,0	57,6	59,5
5	103,4	92,1	106,4	82,1	104,9	90,0	122,8	95,2	100,8	83,3	80,6	72,9
6	98,2	72,6	117,6	105,1	135,4	90,0	117,6	87,8	102,2	119,0	98,6	84,8
7	74,4	54,4	85,6	100,1	102,7	57,6	74,4	78,9	82,8	100,4	100,8	87,8

Tabela 2. cd.
Table 2. cont.

Czasy występowania danej prędkości wiatru w roku 2013, h												
V $m \cdot s^{-1}$	Miesiąc											
	Sty	Lut	Mar	Kwie	Maj	Czer	Lip	Sie	Wrze	Paź	List	Gru
8	47,6	48,4	69,9	77,8	57,3	40,3	37,9	46,9	61,9	87,0	78,5	77,4
9	40,9	39,6	75,9	44,6	29,8	27,4	20,8	21,6	39,6	59,5	57,6	70,7
10	37,2	23,5	60,3	30,2	16,4	14,4	11,9	16,4	20,9	35,7	42,5	57,3
11	41,7	17,5	41,7	24,5	8,9	10,8	3,7	13,4	14,4	30,5	33,1	52,1
12	29,0	6,7	28,3	10,1	2,2	3,6	0,7	0,7	13,7	20,8	21,6	44,6
13	14,9	3,4	7,4	1,4	0,4	1,4	3,0	3,0	7,2	10,4	13,0	29,8
14	8,9	2,0	0,7	0,7	0,4	0,0	0,0	0,0	4,3	4,5	7,2	20,8
15	7,4	1,3	0,0	0,0	0,4	0,0	0,0	0,0	1,4	1,5	1,8	11,2
16	7,4	1,0	0,0	0,0	0,4	0,0	0,0	0,0	0,4	0,4	0,4	10,0
17	3,7	0,3	0,0	0,0	0,0	0,0	0,0	0,0	0,4	0,4	0,0	8,9
18	1,5	0,0	0,0	0,0	0,0	0,0	0,0	0,0	0,0	0,0	0,0	7,1
19	1,1	0,0	0,0	0,0	0,0	0,0	0,0	0,0	0,0	0,0	0,0	4,8
20	0,4	0,0	0,0	0,0	0,0	0,0	0,0	0,0	0,0	0,0	0,0	4,1
21	0,0	0,0	0,0	0,0	0,0	0,0	0,0	0,0	0,0	0,0	0,0	3,0
22	0,0	0,0	0,0	0,0	0,0	0,0	0,0	0,0	0,0	0,0	0,0	1,5
23	0,0	0,0	0,0	0,0	0,0	0,0	0,0	0,0	0,0	0,0	0,0	0,0
24	0,0	0,0	0,0	0,0	0,0	0,0	0,0	0,0	0,0	0,0	0,0	0,0
25	0,0	0,0	0,0	0,0	0,0	0,0	0,0	0,0	0,0	0,0	0,0	0,0
Tp, h	653,2	579,3	698,6	619,2	634,6	509,0	625,0	624,2	622,1	684,5	642,2	730,6

Dodatkowo w tabeli 2 zestawiono czasy występowania danej prędkości wiatru w poszczególnych miesiącach 2013 roku.

Przyjęto, że podstawową wielkością użytkową, charakteryzującą pracę elektrowni wiatrowej jest ilość wytworzonej energii elektrycznej w czasie – Ea (za czas rozliczeniowy przyjęto okres jednego roku ze względu na pewne charakterystyczne i podobnie, powtarzalne przebiegi rocznych rozkładów prędkości wiatru). Tę ilość wyznaczano z obliczeń, wykorzystując parametry funkcji Weibulla: C, k.

$$E_a = \int_0^{T_a} P(t)dt = \int_{v_0}^{v_{max}} P(v) \cdot F(C, k, v)dv, \ \ kW \cdot h \cdot a^{-1} \qquad (11)$$

gdzie:
T_a – okres czasu jednego roku, T_a = 8 760 h,
v_0 – startowa prędkość wiatru, przy której uruchamia się elektrownia wiatrowa (na ogół: v_0= 4 m·s^{-1}),
v_{max} – prędkość wiatru, przy której następuje zatrzymanie elektrowni wiatrowej i wyłączenie jej z ruchu (na ogół: w_{max} = 25 m·s^{-1}),
P(t) – moc elektrowni wiatrowej w chwili „*t*”, kW
P(v) – moc elektrowni wiatrowej przy prędkości wiatru (v), kW

Rzeczywiste wartości miesięcznej energii wyprodukowane przez analizowaną elektrownię wiatrową Vestas V90, o mocy 2 MW przedstawiono w tabeli 3.

Tabela 3. Miesięczna produkcja energii elektrycznej (w MWh) przez pojedynczą elektrownię wiatrową w trzech kolejnych latach [opracowanie własne]
Table 3. Monthly production of electricity (in MWh) by a single wind power plant in the next three years [own research]

Miesięczna produkcja energii elektrycznej w poszczególnych latach, MWh			
Miesiąc	**2013**	**2014**	**2015**
Styczeń	535	593	778
Luty	316	572	427
Marzec	588	444	575
Kwiecień	416	367	535
Maj	321	460	330
Czerwiec	241	269	246
Lipiec	245	292	347
Sierpień	270	287	375
Wrzesień	378	318	397
Październik	526	370	416
Listopad	523	428	602
Grudzień	710	639	798
Razem	**5069**	**5039**	**5826**

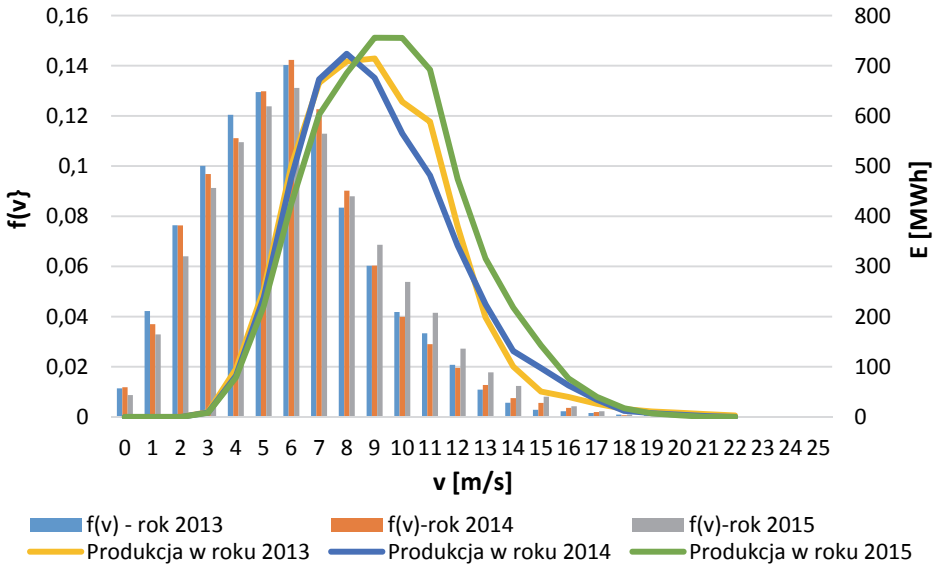

Rys. 2. Produktywność elektrowni wiatrowej Vestas V90, 2 MW w zależności od prędkości wiatru oraz rozkład częstości występowania danej prędkości wiatru w gminie Błaszki w latach 2013-2015 [badania własne]
Fig. 2. The productivity of a wind turbine Vestas V90 2 MW depending on the wind speed and the frequency distribution of the wind speed in Błaszki 2013-2015 [own research]

Porównując zestawienie produktywności w poszczególnych miesiącach z prędkościami wiatru w poszczególnych miesiącach łatwo zauważyć, że miesiące o najniższej (czerwiec) i najwyższej produktywności (styczeń, grudzień) pokrywają się z miesiącami o najniższej i najwyższej prędkości wiatru. Produktywność (zyskowność) zależy więc od prędkości wiatru a także częstości jego występowania. Dla badanej elektrowni wyznaczono produktywność w zależności od prędkości wiatru w latach 2013-2015 oraz naniesiono rozkłady częstości występowania danej prędkości wiatru (rys. 2).

Elektrownia wiatrowa zgodnie z prawem Betze'a nie jest w stanie przetworzyć więcej niż 60% dostępnej energii wiatru. Na rysunku 3 przedstawiono ilość energii możliwej do pozyskania z wiatru w miejscu lokalizacji analizowanego obiektu badań oraz ilość energii jaką wyprodukowała elektrownia wiatrowa w 2013 roku.

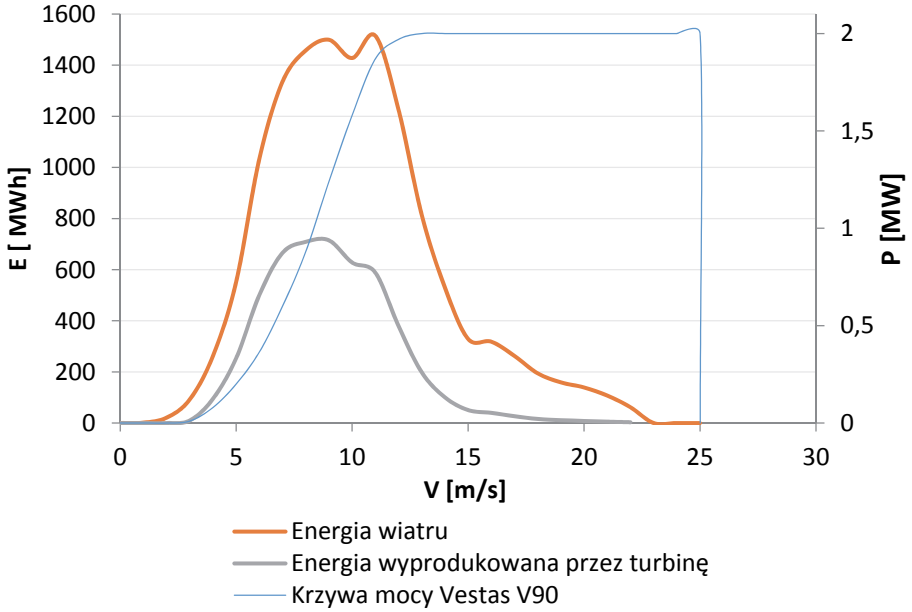

Rys. 3. Dostępna energia wiatru, energia wyprodukowana przez turbinę I krzywa mocy w zależności od prędkości wiatru dla elektrowni Vestas V90 zlokalizowanej w gminie Błaszki w roku 2013 [badania własne]
Fig. 3. Available wind energy, the energy produced by the turbine and power curve depending on wind speeds for power Vestas V90 located in Błaszki in 2013 [own research]

Na podstawie danych o dostępnej energii wiatru i produktywności w poszczególnych latach wyznaczono rzeczywiste, uzyskiwane sprawności elektrowni wiatrowej w zależności od prędkości wiatru w badanym okresie trzech lat (rys. 4). Maksymalne sprawności uzyskiwane są przy prędkości wiatru równej około 7 m/s.

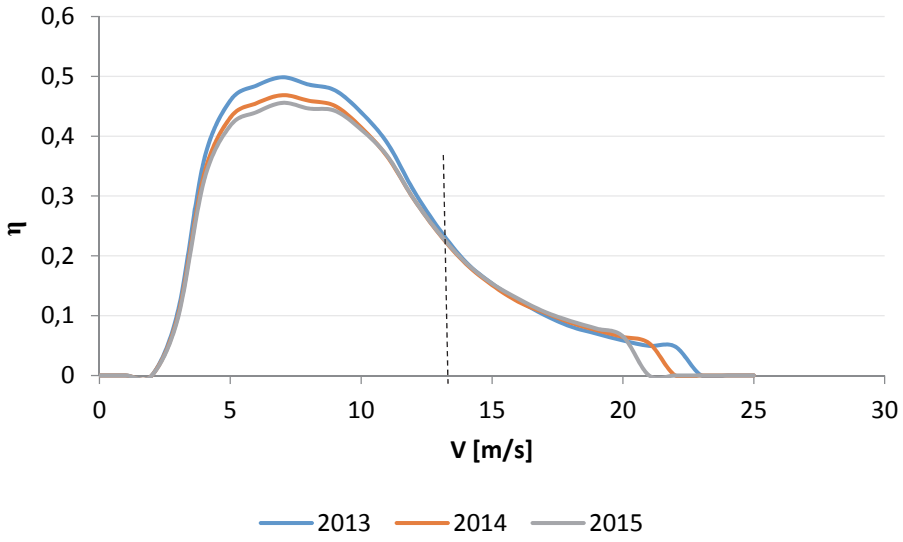

Rys. 4. Zależność sprawności turbiny Vestas V90 od prędkości wiatru w gminie Błaszki w trzech kolejnych latach [badania własne]
Fig. 4. The dependence of the efficiency of the turbine Vestas V90 wind speed in Błaszki in three consecutive years [own research]

Roczna produkcja energii elektrycznej może stanowić kryterium dopasowania danej elektrowni do zadanej lokalizacji produkcji przemysłowej z jej warunkami meteorologicznymi.

$$A = \frac{\int_0^{T_a} P(t)dt}{P_i} = \frac{\int_0^{T_a} P(v)\cdot F(C,k,v)dv}{P_i} = T(C,k,v),\ h\cdot a^{-1} \qquad (12)$$

Równoważnym i jednocześnie uzupełniającym kryterium dopasowania jest czas użytkowania mocy zainstalowanej – Ti. Tu: pojęcie „moc zainstalowana -Pi" – dla elektrowni wiatrowych może być traktowane jako równoznaczne z pojęciem „moc znamionowa – Pn".

W zależnościach (9) i (10) wielkości E_a oraz T_i są zależne od parametrów funkcji Weibulla. Można więc na płaszczyźnie (C, x, k) wyznaczyć linie stałych wartości E_a lub/i T_i. Rodzina takich wykresów stanowi **charakterystykę wytwórczą** elektrowni wiatrowej. Dla badanej elektrowni w zadanej lokalizacji parametry C, k do wyznaczenia charakterystyki wytwórczej elektrowni wiatrowej przedstawiono w tabeli 4.

Tabela 4. Parametry C i k charakterystyki wytwórczej elektrowni wiatrowej Vestas V90 w gminie Błaszki [badania własne]
Table 4. Parameters C and k of the productivity characteristics of the wind turbine Vestas V90 in Błaszki [own research]

Parametr	Lata		
	2013	2014	2015
C	7,10	7,06	7,61
k	2,15	2,13	2,50

Tabela 5. Wskaźniki rocznych korzyści ekonomicznych, energetycznych I ekologicznych badanej elektrowni wiatrowej Vestas V90, 2 MW w latach 2013-2015 [badania własne]
Table 5. Indicators of annual economic, energy and environmental benefits of wind turbine Vestas V90 2 MW in years 2013-2015 [own research]

Wskaźnik zyskowności		2013	2014	2015
Korzyści ekonomiczne, $k_e=f^*(v,n_e,p_e)$, tys. PLN	Przychody	1761	1878	1589
	Nakłady	493	442	441
	Korzyści	1268	1436	1148
Korzyści energetyczne, $k_{en}=f(v,n_{en},p_{en})$, MWh	Produktywność	4995	4841	5518
	Nakłady	21	18	14
	Korzyści	4974	4823	5504
Korzyści ekologiczne, $k_{ekol}=f(v,n_{ekol},p_{ekol})$, $t_{eq}CO_2$	Pożytki	4056	3930	4481
	Nakłady	24	24	24
	Korzyści	4032	3906	4457

f* – funkcja prędkości wiatru, nakładów i produktywności, odpowiednio: ekonomicznych, energetycznych i ekologicznych

W tabeli 5. zestawiono wskaźniki korzyści ekonomicznych, energetycznych i ekologicznych, definiowane jako różnica produktywności i nakładów na jej uzyskanie w warunkach rocznych wietrzności miejsca osadzenia elektrowni wiatrowej w latach (2013-2015).

Wskaźniki w tabeli 5 pełnią rolę relatywizująca techniki wytwarzania energii i w tym kontekście okazały się bardzo użyteczne. Sama rentowność sprzedaży netto mocy, energii elektrycznej, również świadectw zaoszczędzonych emisji CO_2 równa jest zyskowi netto, dzielone-

mu przez: przychody netto z ich sprzedaży powiększone o pozostałe przychody operacyjne, przychody finansowe i zyski nadzwyczajne.

6. Podsumowanie

Zweryfikowano modele matematyczne produktywności, oszacowano możliwości średniej i wariancji „zyskowności" energetycznej, ekonomicznej i ekologicznej elektrowni wiatrowej dla uaktualnionego rozkładu wietrzności, na podstawie średniej i wariancji rocznej zyskowności elektrowni wiatrowej oraz dla bieżąco monitorowanej wietrzności w gminie Błaszki, w latach: 2013, 2014 i 2015. Pozytywnie sprawdzono i oceniono założenie o zakresach prędkości i wydatku wiatru: podkrytycznym, efektywnym i nadkrytycznym.–Zestawiono roczne wskaźniki korzyści ekonomicznych, energetycznych i ekologicznych, definiowane jako różnice produktywności i nakładów eksploatacyjnych na jej uzyskanie w warunkach rocznych wietrzności (2013-2015).Najwyższe wartości, w badanych latach uzyskano: w roku 2013 dla korzyści ekonomiczne, $k_e=f^*(v,n_e,p_e)$ 1436 tys. PLN; w roku 2014 dla korzyści energetyczne, $k_{en}=f(v,n_{en},p_{en})$ 5504 MWh; również w roku 2014 dla korzyści ekologiczne, $k_{ekol}=f(v,n_{ekol},p_{ekol})$ 4457 $t_{eq}CO_2$.

Planowanie aplikacji/wdrożenia innowacji, a w dalszej kolejności użytkowania w procesie eksploatacji elektrowni wiatrowej, to etapy wymagające znacznych nakładów energetycznych, ekonomicznych i ekologicznych. Zatem już na etapie projektowania winny być weryfikowane wszelkie wątpliwości i ograniczenia przeciwdziałające innowacyjnym rozwiązaniom. W tym właśnie momencie należy stworzyć strategię innowacyjnego wdrożania oraz podjąć decyzje formalne i finansowe. Jak pokazano na rysunkach 1 i 2, funkcje rozkładu częstości prędkości wiatru są nie tylko zróżnicowane w poszczególnych latach, ale wykazują w kolejnych latach bardzo wyraźną tendencję zmniejszania się częstości występowania użytecznych prędkości wiatru na rzecz wzrostu częstości występowania małych prędkości wiatru.

Potwierdzono założenie, że realizacja zasilania technologii wytwórczej mocą i energią następuje z krajowego systemu elektroenergetycznego (KSE), również sprzedaż mocy i energii wytworzonej w elektrowni wiatrowej następuje do tego systemu, co staje się źródłem uzasadnionej zyskowności dla produkcji przemysłowej. Potwierdzają to dane

empiryczne z bieżącego monitorowania prędkości wiatru, mocy i energii elektrycznej elektrowni wiatrowej ujęte w modele matematyczne wspomagające projektowanie oraz ekologiczne rozwiązania innowacyjne w przemyśle.

Literatura

Adaramola, M., Agelin-Chaab, M., Paul, S. S. (2014). Assessment of Wind Power Generation Along the Coast of Ghana. *Energy Conversion and Management*, *77,* 61-69.

Baseer, M. A., Meyer, J. P., Rehman, S., Alam, Md. M. (2017). Wind power characteristics of seven data collection sites in Jubail, Saudi Arabia using Weibull parameters. *Renewable Energy, 102*, 35-49.

Carvalho, D., Rocha, A., Gómez-Gesteira, M., Silva Santos, C. (2014). WRF wind simulation and wind energy production estimates forced by different reanalyses: Comparison with observed data for Portugal. *Applied Energy, 117*, 116-126.

Deluga, W. (2013). Grupa energetyczna energa na krajowym rynku energii. *Rocznik Ochrona Środowiska, 15*, 944-965.

Diaf, S., Notton, G. (2013). Technical and economic analysis of large-scale wind energy conversion systems in Algeria. *Renewable and Sustainable Energy Reviews, 19*, 37-51.

Gawłowski, S., Listowska-Gawłowska, R., Piecuch, T. (2010). Uwarunkowania i prognoza bezpieczeństwa energetycznego Polski na lata 2010-2110. *Rocznik Ochrona Środowiska, 12,* 127-176.

Goh, H. H., Lee, S. W., Chua, Q. S., Goh, K. C., Teo, K. T. K. (2016).Wind energy assessment considering wind speed correlation in Malaysia. *Renewable and Sustainable Energy Reviews, 54,* 1389-1400.

Iglesias,G., Castellanos, P., Seijas, A. (2010).Measurement of productive efficiency with frontier methods: A case study for wind farms, *Energy Economics, 32(5)*, 1199-1208.

Khahro, S. F., Tabbassum, K., Soomro, A. M., Dong, L., Liao, X. (2014) Evaluation of wind power production prospective and Weibull parameter estimation methods for Babaurband, Sindh Pakistan, *Energy Conversion and Management, 78,* 956-967.

Kusiak, A., Zhang, Z., Verma, A. (2013).Prediction, operations, and condition monitoring in wind energy. *Energy, 60,* 1-12.

Lun, I. Y. F., Lam, J. C. A. (2000). Study of Weibull parameters using long-term wind observations. *Renewable Energy 2000, 20(2)*, 145-153.

Maatallah, T., Alimi, S. E., Dahmouni, A. W.,Nasrallah, S. B. (2013). Wind power assessment and evaluation of electricity generation in the Gulf of Tunis, Tunisia. *Sustainable Cities and Society, 6,* 1-10.

Miziuła, P., Rychlik, T.(2014). Sharp bounds for lifetime variances of reliability systems with exchangeable components. *IEEE Trans. Reliab., 63(4)*, 850-857.

Miziuła, P., Rychlik, T. (2015). Extreme dispersions of semicoherent and mixed system lifetimes. *J. Appl. Probab., 52(1),* 117-128.

Nor, K. M., Shaaban, M., Rahman, H. A. (2014). Feasibility assessment of wind energy resources in Malaysia based on NWP models. *Renewable Energy, 62,* 147-154.

Okeniyi, J. O., Moses, I. F., Okeniyi, E. T. (2015). Wind characteristics and energy potential assessment in Akure, South West Nigeria: econometrics and policy implications. *International Journal of Ambient Energy, 36(6),* 282-300.

Ouarda, T. B. M. J., Charron, C., Chebana, F. (2016). Review of criteria for the selection of probability distributions for wind speed data and introduction of the moment and L-moment ratio diagram methods, with a case study. *Energy Conversion and Management, 124*, 247-265.

Schweizer, J., Antonini, A., Govoni, L., Gottardi, G., Archetti, R., Supino, E., Berretta, C., Casadei, C., Ozzi, C. (2016). Investigating the potential and feasibility of an offshore wind farm in the Northern Adriatic Sea. *Applied Energy, 177,* 449-463.

Usta, I. (2016). An innovative estimation method regarding Weibull parameters for wind energy applications. *Energy, 106,* 301-314.

Zohbi, G. A., Hendrick, P., Bouillard, P. (2015). Wind characteristics and wind energy potential analysis in five sites in Lebanon. *International Journal of Hydrogen Energy, 40(44)*, 15311-15319.

Environmental Control of Wind Power Technology

Abstract

Currently, a common obstacle to the operation of wind turbines are states of extreme power, and above all the power of their actions, and the associated unpredictability of profitability. Net profit margin of power and energy, also the CO_2 emissions in the case of wind turbines – indicates how much profit (loss) after tax (net) generate income from operations.High economic profits and low ecological mischievousness of activities of wind power plant are desirable states, but energy security requires to Effectively counteract the negative effects of extremely high or low value of the energy characteristics utilities, or the aerodynamic and meteorological conditions, which are a direct cause of negative phenomena.

In the paper for the aim of research adopted to verify mathematical models to estimate the mean and variance of energy, economic and environmental profitability of wind power for the updated distribution of wind on the basis of the mean and variance of the annual profitability of a wind turbine for "elderly" and the current distribution of wind.

The article presents issues related to the operational management and exploitation of complex technical objects on the example of large wind turbine. In the paper developed the mathematical model of wind turbine productivity depending on variable wind speed and localization. Considered operational profits and losses of energy in sub- and supercritical wind conditions. Research of productivity for the real object was carried out on the basis of the research results of the wind turbine Vestas V90 / 105m 2 MW located in the municipality of Błaszki.It is assumed that the basic utility characteristic, characterizing the work of wind power is the amount of electricity generated in time. For determination this characteristic the parameters C and K of Weibull function was used.

Positively tested and rated the assumption of speed ranges and wind flow: subcritical, supercritical and effective. Variable wind conditions make it difficult to estimate the theoretical productivity of a wind power plant. Estimates made on the basis of theoretical dependence and calculations are burdened with mistake – precisely because of the volatility and unpredictability of wind conditions.

The study did not assess the short-term (eg. Monthly), specific profitability, due to the volatility of prices and the value of certificates of energy origin in different periods of research. Compiled while the annual economic, energy and environmental indicators of benefits defined as differences in productivity and operational costs to obtain it in terms of annual wind (2013-2015). The highest values were obtained in the studied years: in 2013 for economic benefits, $k_e = f^*(v, n_e p_e)$ 1436 thousand PLN; in 2014 for the of energy benefit $k_{en} = f(v, n_{en}, p_{en})$ 5504 MWh; also in 2014 for the environmental benefits $k_{ekol} = f(v, n_{ekol}, p_{ekol})$ 4457 teqCO_2.

Streszczenie

Częstą przeszkodą w eksploatacji elektrowni wiatrowych są stany ekstremalne mocy, a przede wszystkim energii ich działania, i związana z tym nieprzewidywalność zyskowności (rentowności). Rentowność sprzedaży netto (ang. net profit margin) mocy i energii, również emisji CO_2 w przypadku elektrowni wiatrowych – informuje, ile zysku (straty) po opodatkowaniu (netto) wypracowują przychody z działalności. Wysokie zyski ekonomiczne i niskie szkodliwości ekologiczne działania elektrowni wiatrowej są stanami pożądanymi, jednak bezpieczeństwo energetyczne wymaga by skutecznie przeciwdziałać negatywnym

oddziaływaniom ekstremalnie wysokich lub niskich wartości energetycznych charakterystyk użytkowych, czy też aerodynamicznych i meteorologicznych, które są bezpośrednią przyczyną powstawania negatywnych zjawisk.

W pracy za cel badań przyjęto weryfikację modeli matematycznych, oszacowanie średniej i wariancji energetycznej, ekonomicznej i ekologicznej zyskowności elektrowni wiatrowej dla uaktualnionego rozkładu wietrzności na podstawie średniej i wariancji rocznej zyskowności elektrowni wiatrowej dla „starszego" oraz bieżącego rozkładu wietrzności.

W artykule przedstawiono zagadnienia związane z eksploatacyjnym użytkowaniem złożonych obiektów technicznych na przykładzie turbin wiatrowych dużej mocy. W pracy opracowano model matematyczny produktywności turbiny wiatrowej w zależności od zmiennych prędkości wiatru i lokalizacji. Rozpatrywano eksploatacyjne zyski i straty energii w pod- i nadkrytycznych warunkach wietrzności. Badania produktywności dla rzeczywistego obiektu przeprowadzono na podstawie wyników badań turbiny wiatrowej Vestas V90 / 105m o mocy 2 MW zlokalizowanej w gminie Błaszki. Przyjęto, że podstawową wielkością użytkową, charakteryzującą pracę elektrowni wiatrowej jest ilość wytworzonej energii elektrycznej w czasie. Do jej wyznaczenia wykorzystano parametry C i k funkcji Weibulla.

Pozytywnie sprawdzono i oceniono założenie o zakresach prędkości i wydatku wiatru: podkrytycznym, efektywnym i nadkrytycznym. Zmienne warunki wietrzności utrudniają teoretyczne oszacowanie produktywności elektrowni wiatrowej. Szacunki dokonane na podstawie teoretycznych zależności i obliczeń obarczone są błędem – właśnie ze względu na zmienność i nieprzewidywalność warunków wietrznych.

W pracy nie dokonano oceny krótkoterminowej (np. miesięcznej), konkretnej zyskowności, ze względu na zmienność cen i wartości świadectw pochodzenia energii w poszczególnych okresach badań. Zestawiono natomiast roczne wskaźniki korzyści ekonomicznych, energetycznych i ekologicznych, definiowane jako różnice produktywności i nakładów eksploatacyjnych na jej uzyskanie w warunkach rocznych wietrzności (2013-2015). Najwyższe wartości, w badanych latach uzyskano: w roku 2013 dla korzyści ekonomicznnych, $k_e=f^*(v,n_e,p_e)$ 1436 tys. PLN; w roku 2014 dla korzyści energetycznych, $k_{en}=f(v,n_{en},p_{en})$ 5504 MWh; również w roku 2014 dla korzyści ekologicznych, $k_{ekol}=f(v,n_{ekol},p_{ekol})$ 4457 $t_{eq}CO_2$.

Słowa kluczowe:
technologia wytworzenia mocy, technologia przetwarzania energii, prognozowanie środowiska

Keywords:
power generation technology, energy conversion technology, forecasting environment

MIDDLE POMERANIAN SCIENTIFIC SOCIETY OF THE ENVIRONMENT PROTECTION
ŚRODKOWO-POMORSKIE TOWARZYSTWO NAUKOWE OCHRONY ŚRODOWISKA

Annual Set The Environment Protection
Rocznik Ochrona Środowiska

Volume/Tom 19. Year/Rok 2017 ISSN 1506-218X 715-730

Badanie emisji wybranych zanieczyszczeń gazowych podczas spalania peletów z agro biomasy w kotle małej mocy

Joanna Szyszlak-Bargłowicz, Grzegorz Zając, Tomasz Słowik
Uniwersytet Przyrodniczy, Lublin

1. Wprowadzenie

W polskim klimacie (typowym także dla wielu regionów w Europie), najefektywniejszym sposobem ogrzewania gospodarstw domowych jest wykorzystanie energii istniejącego potencjału biomasy w oparciu o lokalnie dostępne surowce biomasy (Gula & Goryl, 2014). Ponadto uregulowania krajowe, jak i unijne zmuszą producentów energii do wykorzystania biomasy rolniczej, takiej jak słoma i biomasa uzyskana z trwałych plantacji roślin energetycznych (Krzyżaniak i in., 2016).

Aby ułatwić wykorzystanie energetyczne biomasy (transport, składowanie i spalanie) jest ona przetwarzana do postaci peletów i brykietów. W porównaniu do tradycyjnego drewna opałowego, pelety mogą zapewnić możliwość automatyzacji i optymalizacji spalania, podobne do oleju opałowego czy gazu ziemnego w połączeniu z wysoką sprawnością spalania i niską ilością szkodliwych pozostałości spalania (Mirowski, 2016).

Aspekty ekologiczne i zagrożenia zanieczyszczeniem środowiska wskazują, że pelety drzewne powinny być wykorzystywane przede wszystkim w kotłach małej mocy do ogrzewania gospodarstw domowych.

Dynamiczny rozwój rynku biomasy powoduje, że tradycyjne jej źródła nie dają możliwości pokrycia zapotrzebowania na nią. Alternatywą może być biomasa pozyskiwana z innych źródeł, które mogłyby zastąpić tradycyjne paliwa stałe czy pelety drzewne stosowane w indywidualnym ogrzewnictwie (Castellano i in., 2015; Frączek, Mudryk, & Wróbel, 2011;

Niedziółka i in., 2015; Nilsson, Bernesson, & Hansson, 2011; Obidziński, 2014; Szlachta & Jakubowska, 2013; Szmigielski i in., 2014). Przed ich szerszym wprowadzeniem do użytkowania należy wziąć pod uwagę, że efektywność techniczna i eksploatacyjna generowania ciepła w źródłach małej mocy uzależniona jest zarówno od paliwa jak i od urządzenia grzewczego. Charakterystyka techniczna urządzenia grzewczego determinuje dobór paliwa, z kolei jakość paliwa wpływa na organizację procesu spalania (Dias, Costa, & Azevedo, 2004; Juszczak, 2014; Liu i in., 2013; Ozgen i in., 2014; Roy, Dutta, & Corscadden, 2013). Należy mieć na uwadze, że ilość i rodzaj zanieczyszczeń powstających w procesie spalania biomasy są zależne nie tylko od czynników procesowych ale również od rodzaju spalanej biomasy (Zajac i in., 2017, Konieczyński i in., 2017). W instalacjach małej mocy pelety są spalane najczęściej w kotłach automatycznych. Zazwyczaj palniki i układy podające paliwo tych kotłów są dostosowane do peletów drzewnych. Rozważając spalanie w nich peletów z innych rodzajów biomasy, należy prowadzić proces w sposób kontrolowany, tak aby nie destabilizować procesu spalania a tym samym zwiększać strat i emisji (Carvalho i in., 2013; Czop & Kajda-Szcześniak, 2013; Olsson & Kjällstrand, 2004; Qiu, 2013).

Celem przeprowadzonych badań było wykazanie i przeanalizowanie efektów ekologicznych oraz problemów eksploatacyjnych wynikających ze stosowania peletów z biomasy typu agro w kotle małej mocy przystosowanym do spalania peletów drzewnych. Określono emisję CO, NO, SO_2, podczas spalania peletów: drzewnych, ze ślazowca pensylwańskiego, miskanta olbrzymiego, słomy rzepakowej i z łusek słonecznika. Instalacja zastosowana w badaniach była typową instalacją wykorzystywaną do ogrzewania domów jednorodzinnych, przeznaczoną do spalania peletów drzewnych. Aby określić efekty ekologiczne spalania peletów innych niż drzewne podczas prowadzenia testów nie ingerowano w nastawy sterownika kotła tzn. kocioł pracował z nastawami fabrycznymi dostosowanymi do spalania peletów drzewnych. Uzyskane w trakcie badań wyniki nie stanowią ścisłych danych, lecz tylko przykłady zanotowane jednorazowo, wskazujące w przybliżeniu poziom emisji poszczególnych związków i obrazują efekty ekologiczne stosowania alternatywnych peletów.

2. Materiał i metody badań

Badania emisji podczas spalania peletów drzewnych, peletów ze ślazowca pensylwańskiego, miskanta olbrzymiego, słomy rzepakowej i łusek słonecznika wykonano z wykorzystaniem kotła z automatycznym załadunkiem paliwa o mocy 10 kW. Jest to kocioł przystosowany do spalania peletów drzewnych. Wyposażony jest w palnik wykonany ze stali ogniotrwałej, który ma wloty powietrza na kilku poziomach co powoduje zwiększenie efektywności procesu spalania. Pelety są transportowane z zasobnika do palnika za pomocą podajnika ślimakowego. Podczas zetknięcia z żarem oraz w połączeniu z odpowiednią ilością powietrza dostarczanego przez liczne kanały następuje proces pirolizy biopaliwa. Powstałe podczas spalania spaliny kierowane są przez wymiennik do wylotu kominowego za pośrednictwem ciągu kominowego, wspieranego pracą wentylatora, który dodatkowo ma za zadanie dostarczenie odpowiedniej ilości powietrza dla procesu spalania. Ilość podawanego do spalania paliwa jak również ilość powietrza, które jest potrzebne do prawidłowego procesu spalania jest automatycznie dobierana przez sterownik, na podstawie wyników pomiarów zawartości tlenu w spalinach, dostarczonych przez sondę lambda.

Testy spalania prowadzono w ustalonych warunkach pracy kotła przy nastawach znamionowych. Przed rozpoczęciem pomiarów kocioł był wygrzewany przez okres 1 h, test spalania poszczególnych peletów trwał 3 h. Strumień masy paliwa wynosił około 4 $kg \cdot h^{-1}$.

Pelety drzewne wykorzystane w badaniach, pochodziły od jednego z największych producentów peletów w Polsce i zakupione zostały w ogólnej sieci dystrybucji. Pelety z łusek słonecznika pochodziły z Ukrainy i zostały również zakupione u dystrybutora. Pelety ze słomy rzepakowej zostały zakupione w wytwórni peletów na terenie woj. lubelskiego. Natomiast pelety ze ślazowca pensylwańskiego i miskanta olbrzymiego zostały przygotowane na potrzeby prowadzonych badań w laboratorium własnym. W celu określenia właściwości fizykochemicznych pelety zostały poddane analizie elementarnej i technicznej, wyniki analiz zestawiono w tabeli 1.

Skład spalin na wylocie z kotła mierzono za pomocą układu analizatorów produkcji firmy SIEMENS. W skład układu weszły analizatory typu ULTRAMAT 23 umożliwiające pomiar CO w zakresach 0-5%

i 0-50%, CO_2 w zakresie 0-50%, SO_2 w zakresie 0-2500 ppm i dwóch analizatorów NO o zakresach 0-1000 ppm, w tym jednego współpracującego z konwertorem NO_2 do NO. Pomiary te były prowadzone z wykorzystaniem referencyjnej metody IR. Pomiar stężenia O_2 w gazie odbywał się za pomocą analizatora typu OXYMAT 5, działającego w oparciu o referencyjną metodę wykorzystującą zjawisko paramagnetyzmu. Analizator ten posiada zakres 0-25% O_2. Spaliny były próbkowane w sposób ciągły za pomocą układu sondy grzanej z filtrem ceramicznym, węża grzanego oraz układu kondycjonowania gazu.

Tabela 1. Właściwości fizykochemiczne badanych peletów [badania własne]
Table 1. Physicochemical properties of tested pellets [own research]

Parametr	Symbol	Jednostka	Pelety drzewne	Pelety ze słomy rzepakowej	Pelety ze ślazowca pensylwańskiego	Pelet z miskanta olbrzymiego	Pelety z łusek słonecznika
Wilgoć całkowita	W_t^r	%	6,3	9,4	6,4	7,1	9,4
Popiół	A^a	%	1,3	10,4	3,8	3,16	9,9
Zawartość części lotnych	V^{daf}	%	73,5	64,7	73,3	72,5	69,3
Węgiel	C^a	%	46,8	40,1	44,6	46,3	43,6
Wodór	H^a	%	6,2	5,8	6,4	6,4	6,4
Azot	N^a	%	4,3	0,8	0,52	0,49	1,7
Siarka	S^a_A	%	0,01	0,31	0,07	0,056	0,17
Ciepło spalania	Q_s^a	$kJ \cdot kg^{-1}$	18 235	15 972	17 956	17 975	17 956
Wartość opałowa	Q_i^r	$kJ \cdot kg^{-1}$	16 741	14 476	16 402	16 440	16 457

3. Wyniki badań i dyskusja

W wyniku przeprowadzonych pomiarów podczas spalania poszczególnych peletów otrzymano szeregi czasowe zmian stężenia poszczególnych zanieczyszczeń, które przedstawiono na rysunkach 1-3.

Uśrednione wyniki badań emisji toksycznych składników spalin podczas spalania badanych peletów przedstawiono w tabeli 2 i porównano na rysunku 4.

Ilość i rodzaj zanieczyszczeń powstających w procesie spalania biomasy są zależne są zarówno od czynników procesowych, ale również od rodzaju spalanej biomasy (García-Maraver, Popov, & Zamorano, 2011; Rajczyk i in., 2014; Verma, Bram, & De Ruyck, 2009; Zajemska i in., 2014), co potwierdzają również otrzymane wyniki badań.

Tabela 2. Emisja toksycznych składników spalin podczas testów spalania [badania własne]
Table 2. Emission of toxic components of exhaust gases during the tests combustion [own research]

Rodzaj peletów	CO	NO	SO_2	CO	NO	SO_2
	$mg \cdot m^{-3}$			$mg \cdot m^{-3}$ (10% O_2)		
Drzewne	87,50	338,89	0,0817	70,16	271,73	0,0655
Ze słomy rzepakowej	447,50	151,02	0,7414	405,21	136,76	0,310
Ze ślazowca pensylwańskiego	241,25	238,04	0,2443	118,85	248,31	0,120
Z miskanta olbrzymiego	613,75	170,00	0,1978	273,65	75,79	0,0882
Z łusek słonecznika	983,75	122,65	0,2895	470,21	58,62	0,1384

Emisja CO podczas testów spalania wybranych peletów różni się w sposób znaczący, najniższą wartość stwierdzono dla peletów drzewnych (tabela 2) 70,16 $mg \cdot m^{-3}$ (10% O_2), najwyższą dla peletów ze słomy rzepakowej 405,21 $mg \cdot m^{-3}$ (10% O_2). Obserwując dynamikę zmienności stężeń CO (rys. 1) widać, że podczas spalania peletów drzewnych po początkowym okresie znacznych wahań stężenia, następowało ustabilizowanie emisji tego gazu na najniższym poziomie w odniesieniu do pozostałych badanych peletów. Problemy z ustabilizowaniem pracy kotła

zaobserwowano przy zasilaniu go peletami z łusek słonecznika, zwłaszcza w końcowej fazie testu. Związane to było ze zbrylaniem się żużla, co uniemożliwiało przesypywanie popiołu do popielnika i jednocześnie utrudniało dostęp powietrza do retorty uniemożliwiając dopalanie CO do CO_2. Małą dynamiką zmian stężenia CO, świadczącą o stabilnym spalaniu, charakteryzowały się również pelety z miskanta olbrzymiego i ślazowca pensylwańskiego, jednak emisje te były wyższe w stosunku do emisji podczas spalania peletów drzewnych. Chwilowymi problemami z dozowaniem paliwa wywołanymi zbrylaniem się popiołu charakteryzowało się spalanie peletów z słomy rzepakowej co odzwierciedla się w przebiegu czasowym zmian stężenia CO.

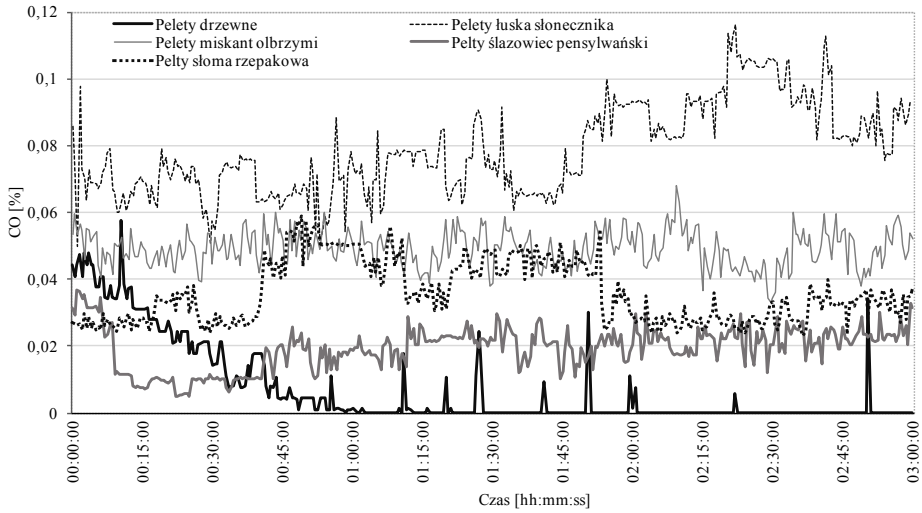

Rys. 1. Przebieg czasowy zmian stężenia CO podczas testów spalania [badania własne]
Fig. 1. Time line of the change CO concentration in the tests combustion [own research]

Podobne efekty spalania peletów z biomasy agro zaobserwowali w swoich badaniach inni autorzy. (Hardy i in., 2012; Musialik-Piotrowska i in., 2010).

Doniesienie literaturowe Kordylewskiego i Mościckiego (2010), opisujące doświadczenia przy spalaniu biomasy typu agro wskazuje, że ograniczenie emisji CO w palnikach retortowych poprzez zmianę współ-

czynnika nadmiaru powietrza nie zawsze jest możliwe. Zwiększenie współczynnika nadmiaru powietrza niejednokrotnie skutkuje zwiększeniem emisji CO (Dias i in., 2004; Wielgosiński & Łechtańska, 2010).

Na cele energetyczne wykorzystuje się również pozostałości po produkcji rolno-spożywczej, po wcześniejszym wysuszeniu np. pozostałości z pomidorów (González i in., 2004), winogron (Mediavilla, Fernández, & Esteban, 2009), czy oliwek (Lajili i in., 2015). Jednak stężenia CO sięgają często kilku tysięcy $mg \cdot m_n^{-3}$ (dla 10% zawartości tlenu w spalinach) i są znacznie wyższe niż stężenia ze spalania peletów drzewnych (w dobrych paleniskach znacznie poniżej 1000 $mg \cdot m_n^{-3}$ (Kjällstrand & Olsson, 2004)).

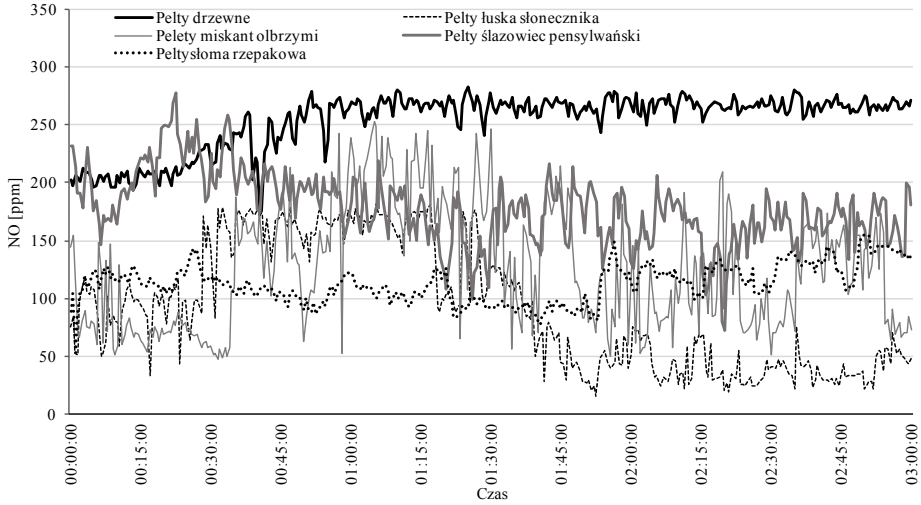

Rys. 2. Przebieg czasowy zmian stężenia NO podczas testów spalania [badania własne]
Fig. 2. Time line of the change NO concentration in the tests combustion [own research]

Stężenie NO oscylowało w zakresie 58,62 $mg \cdot m^{-3}$ (10% O_2) dla peletów z łuski słonecznika do 271,73 $mg \cdot m^{-3}$ (10% O_2) dla peletów drzewnych (tabela 2). Dynamika zmian stężenia NO (rys. 2) jest odzwierciedleniem zmian stężenia CO. Najwyższym poziomem emisji NO charakteryzowało się spalanie peletów drzewnych, najniższym peletów z łuski słonecznika. O końcowym poziomie emisji tlenków azotu decyduje zawartość azotu w paliwie i warunki spalania. Małej emisji tlenków azotu sprzy-

ja zatem mała zawartość azotu w paliwie, mała wartość współczynnika nadmiaru powietrza i niska temperatura spalania (Rybak, 2006).

Badania emisji NO podczas przeprowadzonych testów spalania peletów z biomasy agro korespondują z wynikami badań przeprowadzony przez Musialik-Piotrowską i in. (2010) oraz Kordylewskiego i Mościckiego (2010), realizowanych na kotle o mocy 15 kW.

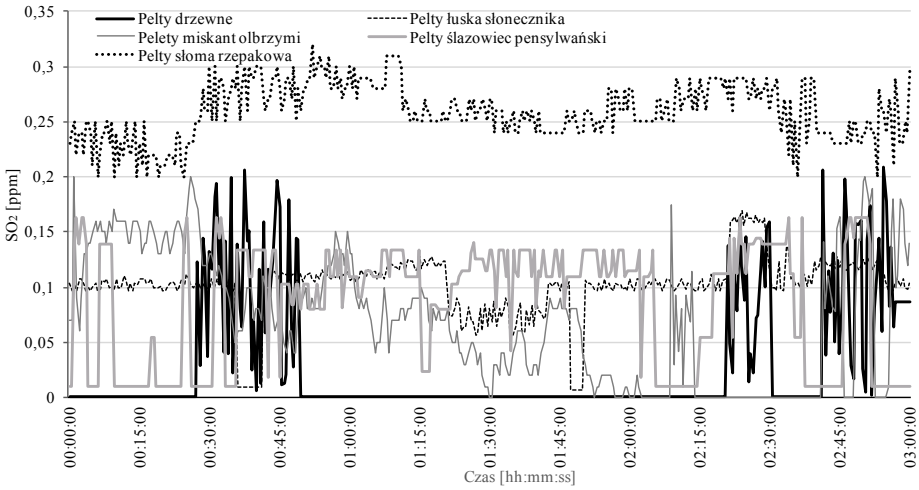

Rys. 3. Przebieg czasowy zmian stężenia SO_2 podczas testów spalania [badania własne]
Fig. 3. Time line of the change SO_2 concentration in the tests combustion [own research]

Najniższe stężenie SO_2 stwierdzono podczas testu spalania petów drzewnych (rys. 3). Wynosiło ono, po przeliczeniu na 10% zawartości O_2 w spalinach, 0,0655 $mg \cdot m^{-3}$, a najwyższe stężenie SO_2 odnotowano podczas testu spalania peletów słomy rzepakowej 0,1384 $mg \cdot m^{-3}$ (10% O_2) (tabela 2). Otrzymane wyniki badań emisji SO_2 korespondują z zwartością siarki w spalanych peletach (tabela 1). Najwyższą zwartość tego pierwiastka stwierdzono w peletach ze słomy rzepakowej (0,31%), najniższą w peletach drzewnych (0,01%). Ilość emitowanego SO_2 jest zależna od zawrotności siarki w paliwie. Im jest ona wyższa tym większy jest ładunek SO_2 wprowadzany do środowiska (Ściążko, Zieliński, & Chmielniak, 2003).

W pracy za efekt ekologiczny przyjęto korzyści powstałe w środowisku w związku wykorzystaniem energii ze źródeł odnawialnych. Wy-

twarzanie energii z zasobów odnawialnych jest również związane z pewnym ujemnym wpływem na środowisko, a zatem efekt ekologiczny wynikający wykorzystania poszczególnych odnawialnych źródeł energii jest zróżnicowany. W przypadku spalania biopaliw stałych do głównych czynników szkodliwych powstających w procesach wytwarzania energii zaliczono: emisje CO, SO_2, NO; związki te emitowane do atmosfery wywierają największy wpływ na środowisko i generują wysokie straty ekologiczne. Porównując emisję tych składników spalin podczas testów spalania (rys. 4) stwierdzono, że najniższa emisja CO i SO_2 miała miejsce podczas spalania peletów drzewnych, co predestynuje to biopaliwo jako najbardziej przyjazne środowisku, podczas spalania go w tego typu instalacjach.

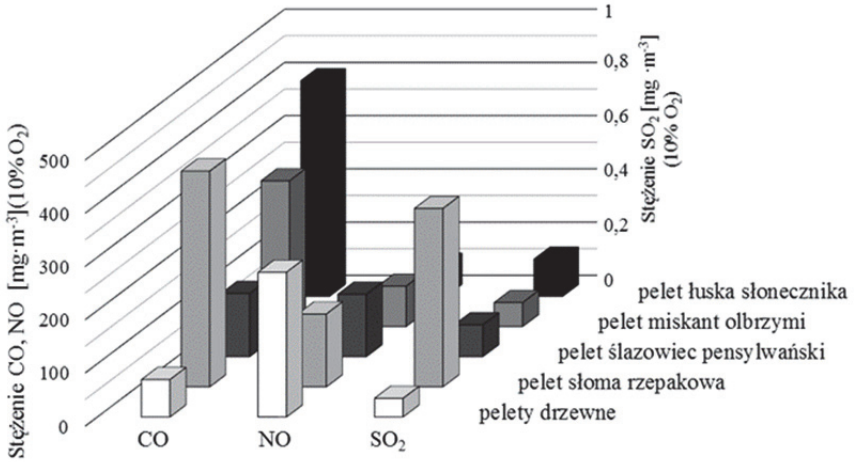

Rys. 4. Porównanie emisji toksycznych składników spalin podczas testów spalania (przy 10% zawartości O_2) [badania własne]
Fig. 4. Comparison of emission of toxic components of exhaust gases during the tests combustion (at 10% content O_2) [own research]

Również pelety ze ślazowca pensylwańskiego charakteryzowały się pozytywnym efektem ekologicznym, a emisja CO i SO_2 podczas testu spalania była nieznacznie wyższa niż podczas testu spalania peletów drzewnych. Należy jednak odnotować, że przy spalaniu peletów drzewnych stwierdzono najwyższy poziom emisji NO (rys. 4). Ze względu na śladową ilość tego składnika w paliwie głównej przyczyny tej emisji należy upatrywać w mechanizmach termicznych powstawania NO_x. Emisja NO zależy od temperatury procesu spalania, ponieważ podczas sprawnego,

procesu spalania paliwa temperatura jest wysoka, to skutkuje to wyższą emisją NO. Jednak dzięki wysokiej temperaturze spalania źródła te emitują mniej CO, benzo(a)pirenu, sadzy i węglowodorów (Pająk & Tomaszewska, 2016).

W biomasie pochodzenia roślinnego zawartość siarki jest znikoma, ilość tego pierwiastka w roślinach zależna jest od gatunku rośliny oraz od jej zawartości w glebach. Emisja SO_2 zależy od zawartości siarki w spalanych biopaliwach, co potwierdziły również przeprowadzone badania (tabela 1, tabela 2,). Spalane biopaliwa charakteryzowały się zróżnicowaną zawartością tego pierwiastka (tabela 1), najmniej zawierały go pelety drzewne a emisja SO_2 podczas testu spalania tego biopaliwa była najmniejsza, wysoką zawartość siarki stwierdzono w peletach ze słomy rzepakowej a spalaniu ich towarzyszyła największa emisja SO_2.

Najmniej korzystny efekt ekologiczny odnotowano podczas testu spalania peletów z łuski słonecznika i słomy rzepakowej, szczególnie w odniesieniu do emisji CO, a w przypadku słomy peletów ze słomy rzepakowej także w odniesieniu do emisji SO_2. Emisja NO byłą niska, co wynikało między innymi z powstałych problemów eksploatacyjnych.

Stosowanie peletów z różnego rodzaju biomasy rolniczej do kotłów przystosowanych do spalania peletów drzewnych może skutkować aglomeracją popiołu, stwarzając problemy w eksploatacji palnika i wpływając na zwiększenie emisji CO oraz zmniejszenie sprawności cieplnej kotła. Zaobserwowano to w szczególności podczas testu spalania peletów z łusek słonecznika, umiarkowane uciążliwości odnotowano spalając pelety ze słomy rzepakowej, ślazowca pensylwańskiego i miskanta olbrzymiego, a nie stwierdzono ich podczas spalania peletów drzewnych. Podobne spostrzeżenia mieli Kordylewski i Mościcki (2010) spalając pelety z biomasy agro w kotłach innej konstrukcji.

4. Podsumowanie

Na skład jakościowy i ilościowy zanieczyszczeń emitowanych do powietrza ma wpływ technologia i warunki spalania paliwa, konstrukcja paleniska oraz rodzaj i jakość użytego paliwa (Szkarowski & Janta-Lipinska, 2013). Nie mniej jednak, niezależnie od konstrukcji paleniska, na skład spalin ma przede wszystkim wpływ odpowiedni nadmiar powie-

trza podawanego do spalania i jakość paliwa (Musialik-Piotrowska & Ciołek, 2012).

Aspekty ekologiczne i zagrożenia zanieczyszczeniem środowiska wskazują, że pelety drzewne powinny być wykorzystywane przede wszystkim w kotłach małej mocy do ogrzewania gospodarstw domowych, podczas gdy pelety z innych rodzajów biomasy, w tym odpadowej, powinny być spalane na dużą skalę, w sposób kontrolowany (Olsson & Kjällstrand, 2004; Czop & Kajda-Szcześniak, 2013; Carvalho i in., 2013; Qiu, 2013), co potwierdzają również zaprezentowany wyniki badań własnych.

Efekt ekologiczny wynikający z wykorzystania badanych rodzajów biopaliw kompaktowanych był zróżnicowany, najniższą emisję CO i SO_2 odnotowano podczas testu spalania peletów drzewnych, co predestynuje to biopaliwo jako najbardziej przyjazne środowisku. Co prawda przy spalaniu peletów drzewnych zanotowano najwyższy poziom emisji NO jednak przy niskiej zawartości azotu w paliwie wynikało to z efektywności procesu spalania.

Najmniej korzystny efekt ekologiczny stwierdzono podczas testu spalania peletów z łuski słonecznika i słomy rzepakowej, szczególnie w odniesieniu do emisji CO, a w przypadku słomy peletów ze słomy rzepakowej także w odniesieniu do emisji SO_2 (co wynikało z wysokiej zawartości siarki w tym biopaliwie).

Przeprowadzone testy emisyjne wykazały, że zastępowanie peletów drzewnych peletami z innych rodzajów biomasy w kotłach małej mocy nie gwarantuje poprawności spalania i zmniejszenia emisji zanieczyszczeń emitowanych do atmosfery. Zaleca się spalać w tego typu kotłach pelety drzewne najwyższej jakości.

Wobec powyższego konieczne jest prowadzenie dalszych badań prowadzących do opracowania niskoemisyjnych i wysoko sprawnych technologii spalania paliw w kotłach małej mocy.

Literatura

Carvalho, L., Wopienka, E., Pointner, C., Lundgren, J., Verma, V. K., Haslinger, W., & Schmidl, C. (2013). Performance of a pellet boiler fired with agricultural fuels. *Applied Energy, 104,* 286-296.

Castellano, J. M., Gómez, M., Fernández, M., Esteban, L. S., & Carrasco, J. E. (2015). Study on the effects of raw materials composition and pelletization conditions on the quality and properties of pellets obtained from different woody and non woody biomasses. *Fuel*, *139*, 629-636.

Czop, M., & Kajda-Szcześniak, M. (2013). Environmental impact of straw based fuel combustion. *Archives of Environmental Protection*, *39(4)*, 71-80.

Dias, J., Costa, M., & Azevedo, J. L. T. (2004). Test of a small domestic boiler using different pellets. *Biomass and Bioenergy*, *27(6)*, 531-539.

Frączek, J., Mudryk, K., & Wróbel, M. (2011). Rożnik przerośnięty Silphium perfoliatum L. - źródło biomasy do produkcji biopaliw stałych. *Inżynieria Rolnicza*, *15(6)*, 21-27.

García-Maraver, A., Popov, V., & Zamorano, M. (2011). A review of European standards for pellet quality. *Renewable Energy*, *36(12)*, 3537-3540.

González, J. F., González-García, C. M., Ramiro, A., González, J., Sabio, E., Gañán, J., & Rodríguez, M. A. (2004). Combustion optimisation of biomass residue pellets for domestic heating with a mural boiler. *Biomass and Bioenergy*, *27(2)*, 145-154.

Gula, A., & Goryl, W. (2014). Toward a More Environmentally Friendly Use of Biomass for Energy Purposes in Poland. *Polish Journal of Environmental Studies*, *23(4)*, 1377-1380.

Hardy, T., Musialik-Piotrowska, A., Ciołek, J., Mościcki, K., & Kordylewski, W. (2012). Negative effects of biomass combustion and co-combustion in boilers. *Environment Protection Engineering*, *38(1)*, 25-33.

Juszczak, M. (2014). Concentrations of carbon monoxide and nitrogen oxides from a 15 kW heating boiler supplied periodically with a mixture of sunflower husk and wood pellets. *Environment Protection Engineering*, *40(2)*, 65-74.

Kjällstrand, J., & Olsson, M. (2004). Chimney emissions from small-scale burning of pellets and fuelwood—examples referring to different combustion appliances. *Biomass and Bioenergy*, *27(6)*, 557-561.

Konieczyński, J., Komosiński, B., Cieślik, E., Konieczny T., Mathews, B., Rachwał, T., Rzońca, G. (2017). Research into properties of dust from domestic central heating boiler fi red with coal and solid biofuels. *Archives of Environmental Protection, 43(2)*, 20-27.

Kordylewski, W., & Mościcki, K. (2010). Charakterystyka procesu spalania granulatów biomasowych w palenisku retortowym. *Archiwum Spalania*, *10(3-4)*, 99-108.

Krzyżaniak, M., Stolarski, M. J., Niksa, D., Tworkowski, J., & Szczukowski, S. (2016). Effect of storage methods on willow chips quality. *Biomass and Bioenergy*, *92*, 61-69.

Lajili, M., Jeguirim, M., Kraiem, N., & Limousy, L. (2015). Performance of a household boiler fed with agropellets blended from olive mill solid waste and pine sawdust. *Fuel*, *153*, 431-436.

Liu, H., Chaney, J., Li, J., & Sun, C. (2013). Control of NOx emissions of a domestic/small-scale biomass pellet boiler by air staging. *Fuel*, *103*, 792-798.

Mediavilla, I., Fernández, M., & Esteban, L. (2009). Optimization of pelletisation and combustion in a boiler of 17.5 kW th for vine shoots and industrial cork residue. *Fuel Processing Technology*, *90(4)*, 621-628.

Mirowski, T. (2016). Wykorzystanie biomasy na cele grzewcze a ograniczenie emisji zanieczyszczeń powietrza z sektora komunalno-bytowego. *Rocznik Ochrona Środowiska*, *18*, 466-477.

Musialik-Piotrowska, A., & Ciołek, J. (2012). Porównanie emisji lotnych związków organicznych podczas spalania drewna. W. *Ochrona powietrza atmosferycznego : wybrane zagadnienia. red. A. Musialik-Piotrowska , J. D. Rutkowski.* 215-221. Wrocław.

Musialik-Piotrowska, A., Kordylewski, W., Ciołek, J., & Mościcki, K. (2010). Characteristics of air pollutants emitted from biomass combustion in small retort boiler. *Environment Protection Engineering*, *36(2)*, 123-131.

Niedziółka, I., Szpryngiel, M., Kachel-Jakubowska, M., Kraszkiewicz, A., Zawiślak, K., Sobczak, P., & Nadulski, R. (2015). Assessment of the energetic and mechanical properties of pellets produced from agricultural biomass. *Renewable Energy*, *76*, 312-317.

Nilsson, D., Bernesson, S., & Hansson, P.-A. (2011). Pellet production from agricultural raw materials – A systems study. *Biomass and Bioenergy*, *35(1)*, 679-689.

Obidziński, S. (2014). Pelletization of biomass waste with potato pulp content. *International Agrophysics*, *28(1)*, 85-91.

Olsson, M., & Kjällstrand, J. (2004). Emissions from burning of softwood pellets. *Biomass and Bioenergy*, *27(6)*, 607-611.

Ozgen, S., Caserini, S., Galante, S., Giugliano, M., Angelino, E., Marongiu, A., & Morreale, C. (2014). Emission factors from small scale appliances burning wood and pellets. *Atmospheric Environment*, *94*, 144-153.

Pająk, L., & Tomaszewska, B. (2016). Porównanie efektów energetycznych, ekonomicznych i ekologicznych wykorzystania pompy ciepła typu woda/woda i solanka/woda do ogrzewania domu jednorodzinnego. *Ciepłownictwo, Ogrzewnictwo, Wentylacja*, *47,* 152-157.

Qiu, G. (2013). Testing of flue gas emissions of a biomass pellet boiler and abatement of particle emissions. *Renewable Energy*, *50*, 94-102.

Rajczyk, R., Bień, J., Palka, H., Pogodziński, A., & Smorąg, H. (2014). Co-Combustion of Municipal Sewage Sludge and Hard Coal on Fluidized Bed Boiler WF-6. *Archives of Environmental Protection*, *40(3)*, 101-113.

Roy, M. M., Dutta, A., & Corscadden, K. (2013). An experimental study of combustion and emissions of biomass pellets in a prototype pellet furnace. *Applied Energy*, *108*, 298-307.

Rybak, W. (2006). *Spalanie i współspalanie biopaliw stałych*. Wrocław: Oficyna Wydawnicza Politechniki Wrocławskiej.

Szkarowski, A., & Janta-Lipinska, S. (2013). Examination of Boiler Operation Energy-ecological Indicators During Fuel Burning with Controlled Residual Chemical Underburn. *Rocznik Ochrona Srodowiska*, *15*, 981-995.

Szlachta, J., & Jakubowska, J. (2013). Analiza procesu peletowania słomy zbożowej oraz zasadności dodawania otrąb zbożowych na przykładzie wybranego zakładu produkcyjnego. *Inżynieria Rolnicza*, *4(147)*, 365-374.

Szmigielski, M., Zarajczyk, J., Kowalczyk-Juśko, A., Kowalczuk, J., Rydzak, L., Ślaska-Grzywna, B., Krzysiak, Z., Cycan, D., Szczepanik, M. (2014). Jakość brykietów z biomasy jako surowca do termochemicznego przetwarzania i produkcji gazu syntezowego. *Przemysł Chemiczny*, *93(11)*, 1986-1990.

Ściążko, M., Zieliński, H., & Chmielniak, T. (2003). *Termochemiczne przetwórstwo węgla i biomasy*. Zabrze: IChPW.

Verma, V., Bram, S., & De Ruyck, J. (2009). Small scale biomass heating systems: standards, quality labelling and market driving factors-an EU outlook. *Biomass and bioenergy*, *33(10)*, 1393-1402.

Wielgosiński, G., & Łechtańska, P. (2010). Emisja zanieczyszczeń z procesu spalania biomasy. *W: A. Musialik-Piotrowska, JD Rutkowski [red.]: Współczesne osiągnięcia w ochronie powietrza atmosferycznego. PZITS Oddział Dolnośląski, Wrocław,* 391-400.

Zajac, G., Szyszlak-Barglowicz, J., Slowik, T., Wasilewski, J., & Kuranc, A. (2017). Emission characteristics of biomass combustion in a domestic heating boiler fed with wood and Virginia Mallow pellets. *Fresenius Environmental Bulletin*, *26(7)*, 4663-4670.

Zajemska, M., Musiał, D., Radomiak, H., Poskart, A., Wyleciał, T., & Urbaniak, D. (2014). Formation of Pollutants in the Process of Co-Combustion of Different Biomass Grades. *Polish Journal of Environmental Studies*, *23(4)*, 1445-1448.

Research on Emissions from Combustion of Pellets in Agro Biomass Low Power Boiler

Abstract

The dynamic development of the biomass market makes its traditional sources are not capable of covering demand for it. Alternatively, biomass can be obtained from other sources including biomass agro type that could replace wood

pellets used in individual heating systems. Before to its introduction to the wider use should be taken into account that the effectiveness of technical and operational generating heat sources of low power depends on both the fuel and the heating device. Technical characteristics of the heating equipment determines the choice of fuel, in turn, affects the quality of fuel organization of the combustion process. Considering the combustion of these pellets in other types of biomass, the process should be carried out in a controlled manner so as not to destabilize the combustion process and thereby increase the losses and emissions.

The aim of the study was to demonstrate and analyze the effects of environmental and operational problems arising from the use of pellets from biomass in agro-type boiler low power adapted to burn wood pellets. Specified emission of CO, NO, SO_2, during combustion in the boiler automatic 10 kW pellets: wood, from Virginia mallow, giant miscanthus, rape straw and sunflower husk. The installation used in the study was a typical installation, used for heating houses designed to burn wood pellets.

The lowest concentration of CO and SO_2 were found during the combustion test wood pets. It was, after conversion to 10% excl. O_2 in the exhaust gasses, respectively, CO 70.16 $mg \cdot m^{-3;}$ SO_2 0.0655 $mg \cdot m^{-3}$. The highest concentration of CO were found during the combustion test pellets from sunflower husk: 470.21 $mg \cdot m^{-3}$ (10% excl. O_2), and the highest concentration of SO_2 was recorded during the combustion test pellets from rape straw 0.1384 $mg \cdot m^{-3}$ (10% excl. O_2). The results obtained SO_2 emissions correspond to the sulfur concentration in burned pallets. The highest concentration of NO (10% excl. O_2) found during the combustion test wood pellets 271.73 $mg \cdot m^{-3}$ and pellets from Virginia mallow 248.31 $mg \cdot m^{-3}$, slightly lower than the combustion of rape straw 136.76 $mg \cdot m^{-3}$ and the lowest during the combustion of pellets from giant miscanthus and sunflower husk 75.79 $mg \cdot m^{-3}$ and 58.62 $mg \cdot m^{-3}$.

The biggest problems with the stabilization of the boiler occurred while burning pellets from sunflower husk, which resulted in the highest emissions of carbon monoxide in the exhaust gasses resulting from incomplete combustion of fuel.

Streszczenie

Dynamiczny rozwój rynku biomasy powoduje, że jej tradycyjne źródła nie dają możliwości pokrycia zapotrzebowania na nią. Alternatywą może być biomasa pozyskiwana z innych źródeł w tym biomasa typu agro, która mogłyby zastąpić pelety drzewne stosowane w indywidualnym ogrzewnictwie. Przed jej szerszym wprowadzeniem do użytkowania należy wziąć pod uwagę, że efektywność techniczna i eksploatacyjna generowania ciepła w źródłach małej mocy uzależniona jest zarówno od paliwa jak i od urządzenia grzewczego. Charakterystyka

techniczna urządzenia grzewczego determinuje dobór paliwa, z kolei jakość paliwa wpływa na organizację procesu spalania. Rozważając spalanie w nich peletów z innych rodzajów biomasy, należy prowadzić proces w sposób kontrolowany, tak aby nie destabilizować procesu spalania a tym samym zwiększać strat i emisji.

Celem przeprowadzonych badań było wykazanie i przeanalizowanie efektów ekologicznych i problemów eksploatacyjnych wynikających ze stosowania peletów z biomasy typu agro w kotle małej mocy przystosowanym do spalania peletów drzewnych. Określono emisję CO, NO, SO_2, podczas spalania w kotle automatycznym, o mocy 10 kW peletów: drzewnych, ze ślazowca pensylwańskiego, miskanta olbrzymiego, słomy rzepakowej i z łusek słonecznika. Instalacja zastosowana w badaniach była typową instalacją wykorzystywaną do ogrzewania domów jednorodzinnych przeznaczoną do spalania peletów drzewnych.

Najniższe stężenie CO i SO_2 stwierdzono podczas testu spalania petów drzewnych. Wynosiło ono, po przeliczeniu na 10% zaw. O_2 w spalinach, odpowiednio: CO 70,16 $mg \cdot m^{-3}$; SO_2 0,0655 $mg \cdot m^{-3}$. Najwyższe stężenie CO stwierdzono podczas testu spalania peletów z łusek słonecznika: 470,21 $mg \cdot m^{-3}$ (10% zaw. O_2), a najwyższe stężenie SO_2 odnotowano podczas testu spalania peletów ze słomy rzepakowej 0,1384 $mg \cdot m^{-3}$ (10% zaw. O_2). Otrzymane wyniki badań emisji SO_2 korespondują z badaniami zwartości siarki w spalanych paletach. Najwyższe stężenie NO (10% zaw. O_2) stwierdzono podczas spalania peletów drzewnych 271,73 $mg \cdot m^{-3}$ i peletów ze ślazowca pensylwańskiego 248,31 $mg \cdot m^{-3}$, nieco niższa podczas spalania słomy rzepakowej 136,76 $mg \cdot m^{-3}$ a najniższe podczas spalania peletów z miskanta olbrzymiego i łusek słonecznika 75,79 $mg \cdot m^{-3}$ i 58,62 $mg \cdot m^{-3}$.

Największe problemy z ustabilizowaniem pracy kotła wystąpił podczas spalania peletów z łusek słonecznika, co przełożyło się na najwyższą emisję tlenku węgla w spalinach, wynikającą z niezupełnego spalania paliwa.

Słowa kluczowe:
pelety, spalanie biomasy, kotły biomasowe

Keywords:
pellets, biomass combustion, biomass boilers

MIDDLE POMERANIAN SCIENTIFIC SOCIETY OF THE ENVIRONMENT PROTECTION
ŚRODKOWO-POMORSKIE TOWARZYSTWO NAUKOWE OCHRONY ŚRODOWISKA

Annual Set The Environment Protection
Rocznik Ochrona Środowiska

Volume/Tom 19. Year/Rok 2017 ISSN 1506-218X 731-744

Środowiskowe aspekty eksploatacji kruszyw żwirowo-piaskowych spod wody w Polsce

Wiesław Kozioł[*], Ireneusz Baic[*], Stefan Góralczyk[*], Łukasz Machniak[**], Adrian Borcz[**]
[*]Instytut Mechanizacji Budownictwa i Górnictwa Skalnego
[**]Akademia Górniczo-Hutnicza, Kraków

1. Wprowadzenie

Kruszywa naturalne (żwirowo-piaskowe i łamane) stanowią największą grupę wydobywanych i zużywanych w świecie surowców mineralnych. Światowa produkcja kruszyw szacowana jest na około 40 mld Mg (brak jest dokładnych danych z kilku krajów, m.in. z Chin). Kruszywa zużywane są głównie w budownictwie do produkcji betonów, dróg, mieszkań i innych obiektów budowlanych, w energetyce, chemii budowlanej itd. Kruszywa odpowiednio uszlachetnione stosuje się również poza budownictwem w wielu gałęziach gospodarki takich jak przemysł szklarski, odlewnictwo, filtracja wody i ścieków itp. Drobne piaski o wysokiej zawartości kwarcu stosowane są niemal w całej współczesnej elektronice (telefony komórkowe, komputery, telewizory, panele słoneczne itp.). Ostatnio kruszywa stosowane są również do wydobycia węglowodorów metodą szczelinowania hydraulicznego, do budowy i utrzymania infrastruktury sportowej i rekreacyjnej (boiska, pola golfowe) itd. Szeroki zakres zastosowań kruszyw naturalnych, a przede wszystkim rozwój w wielu bogatych krajach arabskich i innych, wysoko uprzemysłowionych, bardzo wysokiego budownictwa kubaturowego i inżynieryjnego, sprawia, że w niektórych krajach lub regionach występuje duży niedobór kruszyw naturalnych i konieczność ich importu niekiedy z odległych krajów czy złóż, a ceny importowanych kruszyw wynoszą od 50 do 100 USD/Mg, czyli przekraczają aktualne ceny węgla kamiennego (Kozioł 2016).

W Polsce w okresie ostatnich 25 lat odnotowano około czterokrotny wzrost wydobycia kruszyw z 63,0 (1991 r.) do 232,0 mln Mg/rok (2015 r.). Rekordową wielkość wydobycia osiągnięto w 2011 r. – 333,0 mln Mg/rok. W przeliczeniu na mieszkańca daje to obecnie wskaźnik produkcji ok. 6,0 Mg/mieszkańca (Kozioł i in. 2015; Kozioł 2016). Wskaźnik ten jest wyższy w porównaniu do średniej europejskiej (ok. 5,0 Mg/m.), ale równocześnie jest niższy od produkcji kruszyw w wielu krajach europejskich (Norwegia – 16,7 Mg/m., Finlandia – 15,7, Austria 12,2, Niemcy – 7 itd.) (UEPG 2016).

W produkcji kruszyw naturalnych w Polsce zdecydowaną przewagę mają kruszywa żwirowo-piaskowe, które stanowią ok. 2/3 produkowanych kruszyw. W porównaniu do produkcji kruszyw w UE i w innych krajach europejskich struktura ta znacznie się różni. W krajach tych przewagę ma produkcja kruszyw łamanych. Wynika to oczywiście głównie z uwarunkowań złożowych. W Polsce kruszywa naturalne eksploatowane są wyłącznie odkrywkowo. Piaski i żwiry wydobywane są głównie spod lustra wody (ok. 75% wydobycia), a surowce skalne do produkcji kruszyw łamanych eksploatowane są w wyrobiskach naziemnych stokowych, wgłębnych lub stokowo-wgłębnych (Kozioł 2016).

2. Technologie eksploatacji kruszyw żwirowo-piaskowych

Do wydobycia kruszyw żwirowo-piaskowych stosowane są trzy podstawowe technologie wydobycia: lądowa (sucha), spod wody (wodna) i mieszana (lądowo-wodna).

Zastosowanie jednej z tych technologii uzależnione jest od usytuowania poziomu wodonośnego względem stropu i spągu złoża (tabela 1). W złożach zawodnionych, eksploatowanych spod wody, zwierciadło wody utrzymywane jest co najmniej 1,5 m powyżej stropu złoża. Tego typu złoża najczęściej zalegają w południowej części kraju, gdyż związane są z obszarami akumulacji rzecznej lub wodnolodowcowej. Eksploatacja lądowa najczęściej występuje w obszarze Polski Północnej (zlodowacenie północnopolskie), a produkcja odpowiedniej jakości kruszyw wymaga ich płukania i dostarczenia odpowiedniej ilości wody przemysłowej.

W wielu kopalniach stosowana bywa również eksploatacja mieszana, z urabianiem górnego poziomu z lądu, a poziomu dolnego spod lustra wody. Głębokość zalegania spągu złoża najczęściej nie przekracza

10 m poniżej lustra wody. Złoża te eksploatowane są wyrobiskami wgłębnymi lub stokowo-wgłębnymi. W eksploatacji spod wody w zależności od głębokości zalegania złoża stosuje się urabianie koparkami z lądu (przy płytkiej eksploatacji 5-10 m) lub urabianie pogłębiarkami pływającymi. Piaski i żwiry eksploatuje się również z rzek i zbiorników wodnych w ramach prac regulacyjnych i pogłębiających koryta. Ta eksploatacja nie podlega jednak nadzorowi górniczemu i odbywa się zgodnie z wymogami prawa wodnego.

Tabela 1. Typy eksploatacji kruszyw żwirowo-piaskowych (Kozioł i in. 2011a; 2011b)
Table 1. Types of sand and gravel aggregates exploitation (Kozioł i in. 2011a; 2011b)

Typ eksploatacji	Rodzaj wyrobiska	Usytuowanie górnego poziomu wodonośnego względem złoża
Lądowa (sucha)	stokowe, stokowo-wgłębne, wgłębne	Poniżej spągu złoża lub spągu wyrobiska
Spod lustra wody (wodna)	wgłębne	Powyżej stropu złoża (min. 1,5 m)
Mieszana (lądowo-wodna)	stokowo-wgłębne, wgłębne	Poniżej stropu i powyżej spągu złoża

Ze względu na postępującą eksploatację złóż zalegających na większych głębokościach i pod grubszym nadkładem, systematycznie wzrasta udział wydobycia kruszyw spod lustra wody, który na przestrzeni ostatnich 40 lat przedstawiał się następująco:

- 1975 r. – 54% (wydobywanych żwirów i piasków),
- 1985 r. – 65%,
- 2015 r. – ok. 75%.

Specjalną technologią wydobycia kruszyw jest eksploatacja podmorska, w niektórych krajach stosowana na znaczna skalę (w UE ok. 55 mln Mg/rok) (UEPG 2016). W Polsce w 2015 roku wydobycie z Bałtyckiego Obszaru Morskiego wyniosło 0,485 mln Mg (PIG-PIB 2016).

Urabianie piasków i żwirów polega na pokonaniu sił spójności, które odbywa się w wyniku procesu mechanicznego (skrawanie), hydraulicznego lub pneumatycznego (Bęben 2008). Najczęściej urabianie zwią-

zane jest z zaczerpywaniem urobku do organu roboczego pogłębiarki lub innej maszyny (koparki, zgarniarki) wydobywczej, w którym równocześnie zapoczątkowane zostaje wynoszenie urobku ku powierzchni wody. Łącząc proces urabiania z transportem pionowym i poziomym urobku (po wodzie i na lądzie) stosuje się różne warianty układów technologicznych.

W tabeli 2 zestawiono podstawowe sposoby urabiania i wydobycia piasków i żwirów spod wody. Do najczęściej obecnie stosowanych maszyn wydobywczych należą (Jacaszek 2015):

- pogłębiarki ssące z głowicami spulchniającymi (pogłębiarka ssąco-refulująca – rysunek 1a),
- pogłębiarki chwytakowe,
- koparki łyżkowe (podsiębierne) lub zgarniakowe,
- zgarniarki linowe (rysunek 1b),
- pogłębiarki wieloczerpakowe.

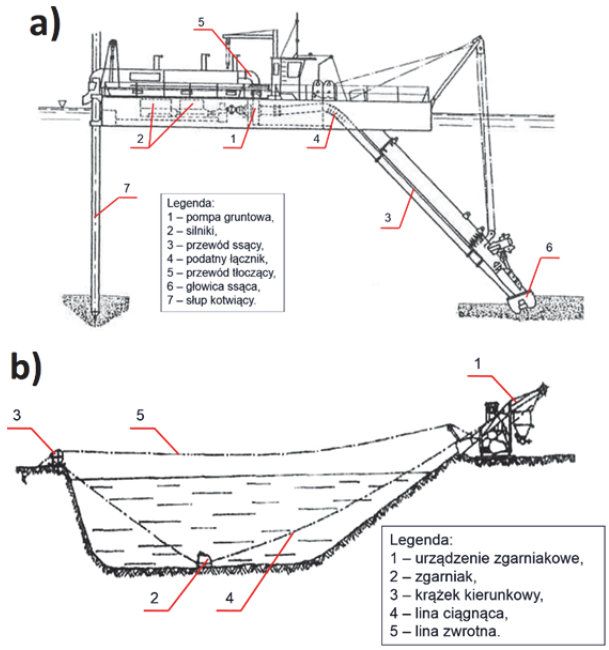

Rys. 1. a) Pogłębiarka ssąca z głowicą spulchniającą, b) Zgarniarka linowa z krążkiem zwrotnym (kierunkowym) (Bęben 2008)
Fig. 1. a) Trailing suction dredger, b) Dragline scraper with turning disc (Bęben 2008)

Tabela 2. Układy technologiczne stosowane do eksploatacji żwirów i piasków spod wody (Kozioł i in. 2011a; 2011b)
Table 2. Technological systems used in sand and gravel aggregates exploitation from under the water (Kozioł i in. 2011a; 2011b)

Sposób urabiania	Technika urabiania (maszyny i urządzenia)	Urabianie a – z lądu b – spod wody	Transport urobku	
			Po wodzie	Na lądzie
Mechaniczny	Koparki (pogłębiarki) łyżkowe podsiębierne	a	–	Samochody technolog. Przenośnik taśmowy
		b	Przenośnik taśmowy Barka, szalanda	Samochody technolog. Przenośnik taśmowy
	Koparki (pogłębiarki) chwytakowe	a	–	Przenośnik taśmowy Samochody technolog.
		b	Przenośnik taśmowy Barka, szalanda	Samochody technolog. Przenośnik taśmowy
	Koparki (pogłębiarki) zgarniakowe	a	–	Samochody technolog. Przenośnik taśmowy
		b	Przenośnik taśmowy Barka, szalanda	Samochody technolog. Przenośnik taśmowy
	Zgarniarki (pogłębiarki) linowe	a	–	Samochody technolog. Przenośnik taśmowy
		b	Przenośnik taśmowy Barka, szalanda	Samochody technolog. Przenośnik taśmowy
	Koparki (pogłębiarki) wielonaczyniowe	a	–	Przenośnik taśmowy Samochody technolog.
		b	Przenośnik taśmowy Barka, szalanda	Przenośnik taśmowy
Hydrauliczny	Pogłębiarki ssące	b	Rurociąg Przenośnik taśmowy	Rurociąg Przenośnik taśmowy
	Pogłębiarki ssące z głowicą spulchniającą	b	Rurociąg Przenośnik taśmowy	Rurociąg Przenośnik taśmowy
	Pogłębiarki hydropneumatyczne	b	Rurociąg Przenośnik taśmowy	Rurociąg Przenośnik taśmowy
	Pogłębiarki (statki)	b	Pogłębiarka (własne zbiorniki) Szalanda, barki	Samochody technolog. Przenośnik taśmowy
Mieszany	Pogłębiarki ssąco-frezujące	b	Rurociąg Przenośnik taśmowy	Rurociąg Przenośnik taśmowy

3. Środowiskowe aspekty podwodnej eksploatacji kruszyw żwirowo-piaskowych

Eksploatacja złóż surowców mineralnych w znacznej części społeczeństwa postrzegana jest jako działalność szkodliwa dla krajobrazu

i przyrody ożywionej. Za negatywny obraz tej działalności w dużym stopniu odpowiadają niektóre technologie, mechanizmy gospodarcze, ekonomiczne i prawne oraz niestety także zaniedbania środowiska górniczego. Na szczęście sytuacja ta ulega dużym zmianom, a stosowane obecnie technologie i zasady zagospodarowania złóż i terenów poeksploatacyjnych na ogół nie powodują istotnych szkodliwych oddziaływań na środowisko przyrodnicze i coraz częściej przynoszą satysfakcję zarówno przedsiębiorcom górniczym jak również przyrodnikom (ekologom). Liczne przykłady atrakcyjności przyrodniczej, krajobrazowej i kulturowej terenów poeksploatacyjnych skłaniają do spojrzenia na eksploatację kopalin jako na działalność wzbogacającą wartość przyrodniczą terenów pogórniczych. Dotyczy to w znacznym stopniu eksploatacji odkrywkowej złóż kruszyw naturalnych w tym szczególnie eksploatacji żwirów i piasków spod wody.

Porównanie poszczególnych technik i technologii eksploatacji (tabela 2) jest trudne ze względu na złożoność procesów i oddziaływań. W celu podjęcia takiej oceny niezbędne jest określenie najważniejszych kryteriów wrażliwości ekologicznej. Kryteria oceny oddziaływania eksploatacji na środowisko przyrodnicze zostały między innymi podane w wytycznych UE dotyczących obszarów Natura 2000 związanych z ochroną rzadkich i zagrożonych ptaków i innych siedlisk i gatunków (Kozioł i in. 2011a; 2011b):

- zakłócenie funkcjonowania zagrożonych gatunków lub ich przemieszczenie,
- utrata rzadkich lub zagrożonych gatunków,
- możliwość zasiedlenia przez obce inwazyjne gatunki,
- zmiany w ekosystemach wodnych lub ich degradacja.

Eksploatacja kruszyw spod wody praktycznie nie powoduje obniżenia zwierciadła wód, zatem nie powinna mieć szkodliwego wpływu na środowisko wodne. Do czynników branych pod uwagę przy opracowywaniu raportów oddziaływania eksploatacji na środowisko należą również hałas i pylenie. Praktycznie skala oddziaływania na czynniki środowiskowe w małym stopniu uzależniona jest od techniki i technologii eksploatacji (tabela 3), zależy natomiast głównie od wrażliwości środowiska, wyboru lokalizacji, kolejności eksploatacji, koncentracji wydobycia itp.

Tabela 3. Porównanie technologii eksploatacji kruszyw żwirowo-piaskowych ze względu na wybrane czynniki środowiskowe (Kozioł i in. 2011a; 2011b)
Table 3. Comparison of sand and gravel aggregates exploitation technologies due to selected environmental factors (Kozioł i in. 2011a; 2011b)

Sposób urabiania	Technika urabiania (maszyny i urządzenia)	Urabianie a – z lądu b – spod wody	Bezpieczeństwo pracy	Odwodnienie, obniżenie zwierciadła wody	Zanieczyszczenie wody	Hałas
Mechaniczny	Koparki (pogłębiarki) łyżkowe podsiębierne	a	±	nie	±	±
		b	±	nie	±	±
	Koparki (pogłębiarki) chwytakowe	a	+	nie	±	±
		b	+	nie	±	±
	Koparki (pogłębiarki) zgarniakowe	a	±	nie	–	±
		b	±	nie	–	±
	Zgarniarki linowe	a	+	nie	–	–
		b	+	nie	–	–
	Koparki wielonaczyniowe	a	+	nie	–	±
		b	+	nie	–	±
Hydrauliczny	Pogłębiarki ssące	b	+	nie	±	–
	Pogłębiarki ssące z głowicą spulchniającą	b	+	nie	±	–
	Pogłębiarki hydropneumatyczne	b	+	nie	±	±
	Pogłębiarki (statki)	b	+	nie	±	±
Mieszany	Pogłębiarki ssąco-frezujące	b	+	nie	±	±

\+ – poniżej średniej,
± – średnio,
– – powyżej średniej (mniej korzystne),
nie – praktycznie nie występuje.

Dotychczasowa praktyka górnicza wskazuje, że dzięki odpowiednio zaprojektowanej i wykonanej rekultywacji wyrobisk poeksploatacyjnych tereny pogórnicze stają się schronieniem rzadkich i zagrożonych gatunków ptaków, gadów, płazów itp. Obszary te w wielu przypadkach można określić mianem wybitnych ostoi przyrody, chroniących zjawiska przyrodnicze nie występujące lub bardzo rzadko występujące gdzie indziej. Prowadzone prace we Francji, w Niemczech a również i w Polsce potwierdziły, że niektóre gatunki chronione, które w tych krajach lub

regionach były bardzo nieliczne, znajdują schronienie w nowych siedliskach mieszczących się w dawnych lub też w czynnych wyrobiskach odkrywkowych. Za granicą mamy przykłady, że byłe wyrobiska włączane są do obszarów Natura 2000.

Na rysunku 2 mamy przykład rekultywacji jednego z wyrobisk po podwodnej eksploatacji żwirów i piasków w województwie małopolskim, zaś na rysunku 3 podano przykład planowanej rekultywacji wyrobiska po eksploatacji żwiru i piasku z podziałem na trzy zróżnicowane strefy pod względem intensywności użytkowania i rodzaju docelowego zagospodarowania. Ze względu, że złoże zlokalizowane jest w bliskim sąsiedztwie obszarów Natura 2000 oraz ośrodków przemysłowych na całym obszarze (ok. 60 ha) wydzielono trzy strefy: przyrodniczą (amazonia), cichego wypoczynku i aktywnej rekreacji. W ramach tych stref zaproponowano 6 kierunków rekultywacji (wodny, przyrodniczy, leśny, rekreacyjno-wypoczynkowy, gospodarczy, dydaktyczno-badawczy), a obszary zrekultywowane w jednym z kierunków mogą spełnić różne funkcje w zależności od położenia strefy. Biorąc pod uwagę uwarunkowania środowiskowe założono, że strefy rekreacyjne powinny być podporządkowane wymogom strefy przyrodniczej z kierunkiem rekultywacji dydaktyczno-badawczym (Kozioł i in. 2011c).

Rys. 2. Przykład zrekultywowanego wyrobiska po eksploatacji kruszyw żwirowo-piaskowych (Zając 2011)
Fig. 2. Example of reclamated mine after the sand and gravel aggregates exploitation (Zając 2011)

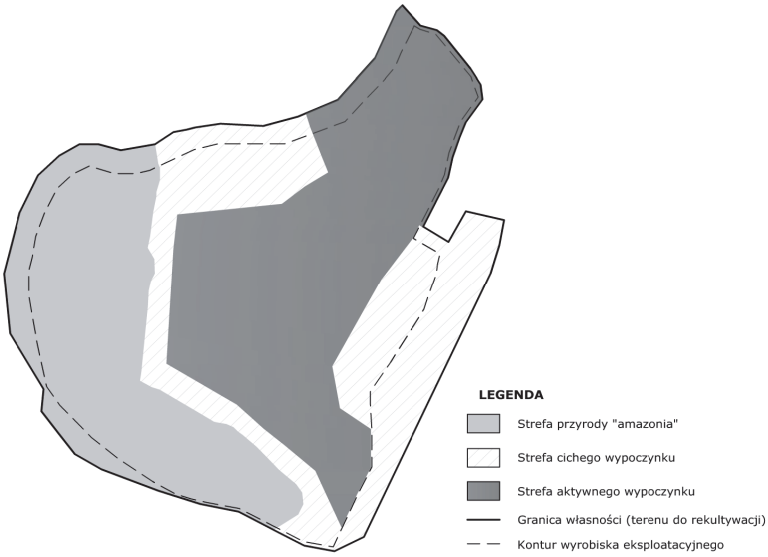

Rys. 3. Przykładowa koncepcja rekultywacji wyrobiska poeksploatacyjnego kruszyw żwirowo-piaskowych (Kozioł i in. 2011c)
Fig. 3. An example conception of reclamation of sand and gravel aggregates former mining areas (Kozioł i in. 2011c)

4. Wnioski końcowe

1. Złoża kruszyw żwirowo-piaskowych ze względu na trudności z ich odwodnieniem (duży zasięg leja depresji) w większości (w Polsce ok. 75%) eksploatuje się spod lustra wody, co praktycznie nie powoduje lokalnego obniżenia zwierciadła wód podziemnych.
2. W zależności od warunków geologiczno-górniczych eksploatacji (wielkość zasobów, głębokość zalegania i miąższość złoża, warunki urabiania, wielkość wydobycia itp.) stosowane są różne techniki i technologie wydobycia.
3. W pracy przedstawiono próbę porównania możliwych do stosowania technologii eksploatacji z uwagi na niektóre ważniejsze czynniki środowiskowe.
4. Dotychczas na wybór technologii wydobycia praktycznie w większości przypadków mają wpływ czynniki techniczne i ekonomiczne (wydajność, wielkość produkcji, koszty inwestycyjne i eksploatacyjne, efektywność produkcji).

5. Realizacja zrównoważonego rozwoju i ochrona środowiska naturalnego wymagają uwzględnienia również czynników środowiskowych zarówno w górniczych projektach jak również w analizach ekonomicznych efektywności eksploatacji (czynnik środowiskowy).
6. Z analizy porównawczej poszczególnych technologii wydobycia wynika, że do technologii bardziej sprzyjających środowisku naturalnemu można zaliczyć urabianie pogłębiarkami ssącymi i koparkami podsiębiernymi.
7. Ważne znaczenie dla ochrony środowiska mają prace koncepcyjno-projektowe eksploatacji złoża i wybór odpowiedniego wariantu. Do szczególnie istotnych czynników mających wpływ na środowisko, poza technologią, zaliczyć należy:
   - określenie wielkości wydobycia i produkcji kruszyw,
   - ustalenie obszaru (granic) eksploatacji,
   - wybór lokalizacji udostępnienia i postępu eksploatacji,
   - wybór lokalizacji zakładu przeróbczego oraz technologii przeróbki,
   - wybór miejsc składowania i zwałowania.
8. Uwzględniając konieczność ochrony terenów przyrodniczo cennych i równocześnie ograniczoną ilość nieodnawialnych zasobów surowców mineralnych, konieczne jest wypracowanie racjonalnych, modelowych metod zagospodarowania złóż (projektowanie, eksploatacja) oraz rekultywacji i rewitalizacji terenów poeksploatacyjnych w warunkach możliwego oddziaływania na środowisko przyrodnicze (Poros, Sobczyk 2014; Sobczyk i in. 2012; Zając 2011).

Literatura

Bęben, A. (2008). *Maszyny i urządzenia do wydobywania kopalin pospolitych bez użycia materiałów wybuchowych*. Wyd. AGH.

Jacaszek, C. (2015). *Metoda doboru technologii urabiania złóż żwirowo-piaskowych spod wody*. Praca doktorska, AGH, Kraków.

Kozioł, W., Ciepliński, A., Machniak, Ł., Jacaszek, C., Borcz, A. (2014). Wydobycie i produkcja kruszyw naturalnych w Polsce i w Unii Europejskiej. *Przegląd Górniczy, 10*, 23-29.

Kozioł, W., Machniak, Ł., Borcz, A., Baic, I. (2016). Górnictwo kruszyw w Polsce – szanse i zagrożenia. *Inżynieria Mineralna, 2*, 175-182.

Kozioł, W., Machniak, Ł., Ciepliński, A. (2011a). Technologia wydobycia kruszyw żwirowo-piaskowych spod wody. *Przegląd Górniczy, 7-8*, 207-214.

Kozioł, W., Machniak, Ł., Ciepliński, A., Borcz, A. (2015). Produkcja i zużycie kruszyw naturalnych w Polsce – aktualny stan i prognozy. *Górnictwo Odkrywkowe, 4*, 41-50.

Kozioł, W., Machniak, Ł., Goleniewska, J. (2011b). *Technologie eksploatacji złóż kruszyw naturalnych i ich wpływ na środowisko.* Konferencja „Problemy eksploatacji złóż kruszyw naturalnych na obszarach przyrodniczo-cennych". AGH, Kraków.

Kozioł, W., Machniak, Ł., Musiał, J., Ciepliński, A. (2011c). *Wariantowa koncepcja zagospodarowania terenów poeksploatacyjnych zakładu górniczego „Wiślicz"*. AGH, Kraków.

PIG-PIB (2016). *Bilans zasobów kopalin i wód podziemnych w Polsce*. Warszawa.

Poros, M., Sobczyk, W. (2014). Kierunki rekultywacji terenów pogórniczych obszaru chęcińsko-kieleckiego w kontekście ich wykorzystania w aktywnej edukacji geologicznej. *Rocznik Ochrona Środowiska, 16*, 386-403.

UEPG Annual Review 2015-2016 (2016). *European Aggregates Association*. Brussels.

Sobczyk, W., Biedrawa-Kozik, A., Kowalska, A. (2012). Threats to areas of natural interest. *Rocznik Ochrona Środowiska, 14*, 262-273.

Zając, T. (2011). *Uwarunkowania przyrodnicze eksploatacji złóż żwirowo-piaskowych.* Konferencja „Problemy eksploatacji złóż kruszyw naturalnych na obszarach przyrodniczo-cennych". AGH, Kraków.

Environmental Aspects of Sand and Gravel Aggregates Exploitation from under the Water in Poland

Streszczenie

Przemysłowa działalność człowieka w różnym stopniu oddziałuje na środowisko naturalne. Górnictwo związane z odkrywkową eksploatacją kopalin, charakteryzuje się przede wszystkim przekształcaniem morfologii terenu, ale również często wpływa na stosunki wodne (konieczność odwadniania złoża), na zasiedlenie obszarów przyległych przez różne gatunki zwierząt, ptaków, płazów, a także na lokalną florę.

Szeroki zakres zastosowań a także wielkość popytu na kruszywa naturalne żwirowo-piaskowe i łamane powoduje, iż stanowią największą grupę wydobywanych i zużywanych w świecie surowców mineralnych. W Polsce zdecydowaną przewagę mają żwiry i piaski. Górnictwo kruszyw naturalnych żwirowo-piaskowych w Polsce związane jest w większości (ok. 3/4 kopalń) z eksploatacją prowadzoną spod lustra wody. Kopalnie tego typu nie mają praktycznie wpływu na poziom zwierciadła wód podziemnych nie powodując osuszania

przyległych akwenów oraz terenów objętych ochroną. W przeciwieństwie do wielu obszarów, w których działalność człowieka związana jest np. ze wzmożoną turystyką i rekreacją, z produkcją odpadów w obszarach przyrodniczo cennych i innych aktywności człowieka, w tym związanych z urbanizacją, w których dochodzi do dewastacji lokalnego środowiska, prowadzenie działalności wydobywczej obliguje na przedsiębiorcy górniczym w ramach obowiązkowej rekultywacji terenów poeksploatacyjnych konieczność przywracania naturze obszarów cennych, co często w efekcie polepsza stan środowiska. Oczywiście również w górnictwie dochodzi do zaniedbań związanych z ochroną przyrody. Jednak pomimo początkowego i trwającego niejednokrotnie podczas prowadzenia eksploatacji wpływu na zmniejszenie liczebności gatunków zwierząt i roślin, takie przekształcanie środowiska daje nierzadko dużo skutków pozytywnych często przyczyniając się do tworzenia nowych i bogatszych siedlisk w stosunku do tych, które dotychczas występowały na badanym obszarze.

Artykuł przedstawia podział technologii wydobywczych stosowanych w Polsce do eksploatacji żwirów i piasków i skalę ich oddziaływania na środowisko. Wytypowano technologie eksploatacji, które najmniej oddziałują na środowisko naturalne. Podano najważniejsze kryteria wrażliwości ekologicznej, które są niezbędne do podjęcia oceny oddziaływania eksploatacji na środowisko. Są to kryteria, które podawane są między innymi w wytycznych UE dotyczących obszarów związanych z ochroną rzadkich gatunków zwierząt i roślin. Krajowe górnictwo kruszyw żwirowo-piaskowych eksploatowanych spod wody oparte jest o rozwiązania techniczne, które nie wpływają na obniżanie zwierciadła wód. Siła oddziaływania kopalń na środowisko w stosunkowo małym stopniu zależna jest od czynników technicznych, zależy zaś głównie od innych czynników, w tym od samego środowiska, które podlega ochronie. Dotychczasowa praktyka górnicza wskazuje, że dzięki odpowiednio zaprojektowanej i wykonanej rekultywacji wyrobisk poeksploatacyjnych tereny pogórnicze stają się schronieniem rzadkich i zagrożonych gatunków ptaków, gadów, płazów itp. Obszary te w wielu przypadkach można określić mianem wybitnych ostoi przyrody, chroniących zjawiska przyrodnicze nie występujące lub bardzo rzadko występujące gdzie indziej. Prowadzone prace we Francji, w Niemczech a również i w Polsce potwierdziły, że niektóre gatunki chronione, które w tych krajach lub regionach były bardzo nieliczne, znajdują schronienie w nowych siedliskach mieszczących się w dawnych lub też w czynnych wyrobiskach odkrywkowych. Za granicą mamy przykłady, że byłe wyrobiska włączane są do obszarów Natura 2000.

Abstract

Industrial human activities impacts in different levels on the environment. Mining related to the surface exploitation of minerals, is mainly characterized by the transformation of the terrain morphology, but also often affects water conditions (the necessity of deposits dewatering), for settlement adjoining areas for different species of animals, birds, amphibians, as well as the local flora.

Wide range of applications as well as the demand for sand and gravel and crushed stones natural aggregates causes that they represent the largest group of extracted and consumed minerals in the world. In Poland decisive advantage have gravels and sands. Mining of these aggregates in Poland is related mainly (approx. 3/4 of mine) to the operations from under the water. Mines of this type do not have a real impact on the level of groundwater without causing drainage adjacent basins and protected areas. Unlike many areas in which human activity is related to for example with increased tourism and recreation, the production of waste in environmentally valuable areas and other human activities, including those related to urbanization, which comes to the devastation of the local environment, mining activities obliges mining entrepreneurs for mandatory reclamation, which need to restore valuable nature areas, often resulting in improving the environment. Of course, also in the mining industry it comes to failures related to nature conservation. However, despite the initial and ongoing frequently, during exploitation, impact on reducing the number of animals and plants species, including the transformation of the environment, often gives a lot of positive effects contributing to the creation of new and richer habitats in comparison to those that so far have been observed in studied areas.

The article presents the division of mining technologies used in Poland to exploitation of gravels and sands and the scale of their impact on the environment. Technologies of exploitation were selected which has the lowest impact on the environment. The most important criterias of environmental sensitivity, that are needed to make impact assessment of exploitation on the environment, were given. These are the criterias that are given among other things in the EU guidelines on areas related to the protection of animals and plants rare species. Polish mining of sand and gravel aggregates exploited from under the water is based on technical solutions that do not affect lowering of the groundwater level. The impact of mines on the environment in a relatively low degree is dependent on technical factors and it mostly depends on other factors, including the environment itself which is subject to be protected. The current practice of mining shows that with properly designed and made reclamation of excavation workings mining areas have become shelter for rare and endangered species of birds, reptiles, amphibians, etc. These areas in many cases can be described as outstanding wildlife shelters, protecting natural phenomena which do

not occur, or are very rare elsewhere. Work carried out in France, Germany and Poland also confirmed that some protected species which in those countries or regions were very rare found shelter in the new habitats coming up in the old or in operating workings of surface mines. Outside Poland we have examples of the former workings which are included in the Natura 2000 areas.

Słowa kluczowe:
górnictwo odkrywkowe, kruszywa naturalne, oddziaływanie na środowisko, przywracanie naturze

Keywords:
surface mining, natural aggregates, environmental impact, restoration to nature

MIDDLE POMERANIAN SCIENTIFIC SOCIETY OF THE ENVIRONMENT PROTECTION
ŚRODKOWO-POMORSKIE TOWARZYSTWO NAUKOWE OCHRONY ŚRODOWISKA

Annual Set The Environment Protection
Rocznik Ochrona Środowiska

Volume/Tom 19. Year/Rok 2017 ISSN 1506-218X 745-759

Zastosowanie osadów potechnologicznych z uzdatniania wody do poprawy właściwości sedymentacyjnych osadu czynnego

Adam Masłoń, Ireneusz Opaliński
Politechnika Rzeszowska

1. Wstęp

Jednym z bardziej poważnych zaburzeń technologicznych biologicznego oczyszczania ścieków jest pęcznienie i pienienie osadu czynnego. Osad spęczniały, wywołany nadmiernym rozwojem organizmów nitkowatych, posiada niedostateczne właściwości sedymentacyjne. Prowadzą one do pogarszania efektywności usuwania zanieczyszczeń ze ścieków w systemach z osadem czynnym (Bezak-Mazur i in. 2016). Poprawę właściwości sedymentacyjnych osadu czynnego można uzyskać przez dawkowanie chemicznych reagentów – soli glinu, żelaza, ditlenku chloru, podchlorynu sodu (Budzińska i in. 2015), mononadsiarczanu potasu i nadsiarczanu sodu (Chłąd i in. 2015). Mankamentem metod chemicznych jest jednak negatywny wpływ na biocenozę osadu czynnego oraz wysokie koszty. Alternatywnie możliwe jest zatem dawkowanie mineralnych obciążników w postaci substancji pylistych, które zostają zintegrowane w matrycę kłaczka osadu czynnego. Efektem aplikacji mineralnych ziaren, jest poprawa struktury i gęstości osadu czynnego (Masłoń & Tomaszek 2012, Masłoń i in. 2013, Masłoń 2015, Masłoń 2016).

Procesy uzdatniania wody generują produkty odpadowe, m.in. osady potechnologiczne, do których zaliczyć można osady pokoagulacyjne z uzdatniania wód powierzchniowych (pozostałości z procesów koagulacji) oraz popłuczyny z uzdatniania wód podziemnych (wody zużyte powstające w wyniku płukania filtrów; wody popłuczne) (Piaskowski 2010). Unieszkodliwienie osadów potechnologicznych stanowi istot-

ny problem, bowiem ilość powstających osadów stanowi do 5% oczyszczanej wody i w znacznym stopniu zależy od zanieczyszczeń występujących w ujmowanej wodzie oraz dodawanych koagulantów (Juraszka & Sumara 2013, Szerzyna 2013). W zależności od układu technologicznego wśród osadów potechnologicznych wyróżnić można m.in. osady żelazowe lub glinowe. Aktualnie poszukuje się alternatywnych metod wykorzystania osadów z uzdatniania wody (Piaskowski 2010, Krajewski & Sozański 2010, Jaroszyński i in. 2011, Kyncl i in. 2012, Kida i in., 2015). W ostatnim czasie testowano osady potechnologiczne w procesie oczyszczania ścieków, np. do usuwania fosforanów ze ścieków (Totczyk i in. 2013), koagulacji (Nair i Ahammed 2015, Ahmad i in. 2016) i kondycjonowania osadów ściekowych (Li i in 2016). Ze względu na właściwości fizykochemiczne możliwe staje się wykorzystanie osadów potechnologicznych w technologii osadu czynnego, podobnie jak mineralnych substancji pylistych dawkowanych w postaci suchej.

Celem pracy są badania nad zastosowaniem osadów potechnologicznych z uzdatniania wody – osadów pokoagulacyjnych i popłuczyn, do poprawy właściwości sedymentacyjnych osadu czynnego.

2. Metodyka badań

Badania nad zastosowaniem osadów potechnologicznych z uzdatniania wody do poprawy właściwości sedymentacyjnych osadu czynnego przeprowadzono w warunkach laboratoryjnych na podstawie testu sedymentacji i obserwacji opadalności osadu czynnego z dodatkiem zróżnicowanych ilości popłuczyn i osadu pokoagulacyjnego. W odróżnieniu od klasycznych testów sedymentacyjnych prowadzonych w lejach Imhoffa, badania wykonano w cylindrach miarowych o pojemności 1 dm^3, w celu eliminacji zakłóceń opadania osadu czynnego oporem ściany leja sedymentacyjnego. W badaniach wykorzystano osad czynny, pobrany z komory nitryfikacji z oczyszczalni ścieków w Rzeszowie. Osad czynny charakteryzował się właściwościami osadu spęczniałego FI = 4-6 (*filamentous index*). Indeks objętościowy osadu kształtował się na poziomie od 174,6 do 202,8 cm^3/g s.m., a stężenie wynosiło 4,88-5,43 g s.m./dm^3.

W badaniach wykorzystano osad pokoagulacyjny z uzdatniania wody powierzchniowej (OP) oraz popłuczyny ze stacji uzdatniania wody podziemnej (PP).

Osad pokoagulacyjny pochodził z Zakładu Uzdatniania Wody w Rzeszowie o wydajności 84 000 m^3/d. Technologia uzdatniania wody wykorzystuje procesy ozonowania wstępnego, koagulacji za pomocą koagulantu PAX XL10, sedymentację, filtrację pospieszną na filtrach antracytowo-piaskowych, ozonowanie pośrednie, filtrację na węglu aktywnym oraz dezynfekcję związkami chloru. Ze względu na aplikację chlorku poliglinu w procesach oczyszczania wody osad pokoagulacyjny zawierał duże ilości glinu.

Popłuczyny zostały pobrane w Stacji Uzdatniania Wody w miejscowości Rozbórz o wydajności ok. 400 m^3/d. W ZUW w Rozborzu zastosowany jest jednostopniowy układ filtracji w filtrze piaskowo-brausztynowym. Płukanie filtrów odbywało się raz na trzy dni, a popłuczyny odprowadzane były do odstojnika wód popłucznych. Raz na cztery dni dokonywano zrzutu wód nadosadowych. Z kolei raz w roku odstojnik jest opróżniany. Stężenie żelaza ogólnego w popłuczynach kształtowało się na poziomie 280 mg Fe/dm^3.

Zawartość suchej masy osadów potechnologicznych wynosiła 2,75% (OP) oraz 7,62% (PP). Ich konsystencja była płynna. Charakterystykę uziarnienia osadu pokoagulacyjnego i popłuczyn wyznaczono przy pomocy analizatora Mastersizer 2000 firmy Malvern Instruments Ltd. Rozkład cząstek stałych popłuczyn i osadu pokoagulacyjnego przedstawiono na rysunku 1, a parametry uziarnienia podano w tabeli 1. Skład granulometryczny przedstawiano w postaci rozkładu udziałów objętościowych, wyznaczano m.in. parametry charakterystyczne rozkładu – średnicę d_{10}, d_{50} i d_{90} odpowiadające 10%, 50% i 90% objętości zbioru cząstek. Wymiar d_{50} przyjmowano jako średnią średnicę (medianę) zbioru cząstek. Analizowane osady potechnologiczne posiadały mikrocząstki o wielkości do ok. 200 μm. Otrzymane wyniki wskazują na znaczące różnice w wielkości cząstek pomiędzy osadem pokoagulacyjnym a popłuczynami. Zdecydowanie większy rozrzut wielkości cząstek posiadały popłuczyny aniżeli osad pokoagulacyjny. W osadzie pokoagulacyjnym dominowały ziarna o wielkości od 1,5 do 20,0 μm. Natomiast w popłuczynach gros ziaren stanowiły cząstki o wymiarze 4,0-40,0 μm. Materiały zawierały niewielką ilość ziaren o wielkości powyżej 100 μm, wobec czego materiały należy uznać za drobnopyliste. Maksymalne wielkości ziaren w materiałach osiągały wielkość 158 μm (OP) oraz 141 μm (PP).

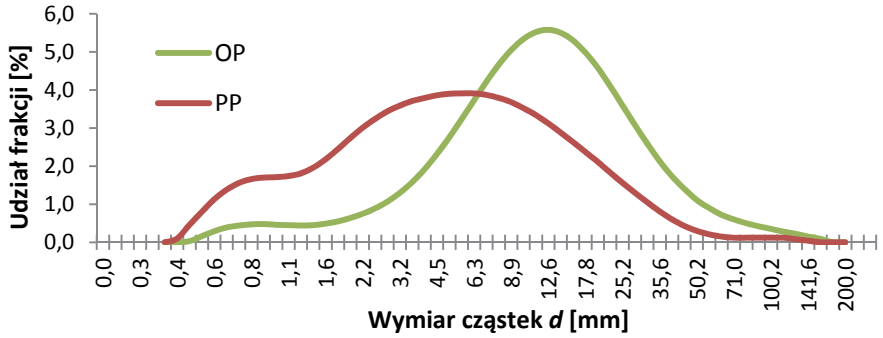

Rys. 1. Rozkład uziarnienia osadu pokoagulacyjnego (OP) oraz popłuczyn (PP)
Fig. 1. The particle-size distribution of post-coagulation sludge (OP) and bachwash water (PP)

Tabela 1. Parametry uziarnienia osadu pokoagulacyjnego i popłuczyn wykorzystanych w badaniach
Table 1. Parameters characterizing the particle-size distribution of OP and PP used in these studies

Parametr	OP	PP
Średnia średnica powierzchniowa (*Surface Mean Diameter*) [μm]	6,80	2,90
Średnia średnica objętosciowa (*Volume Mean Diameter*) [μm]	18,0	9,3
Średnica d_{10} [μm]	3,6	1,1
Średnica d_{50} [μm]	12,6	5,3
Średnica d_{90} [μm]	36,6	21,2
Rozpiętość [–]	2,62	3,77
Jednorodność [–]	0,882	1,26
Powierzchnia właściwa [m^2/g]	0,881	2,07
Wskaźnik jednorodności uziarnienia (C_U)	1,95	2,48
Wskaźnik krzywizny uziarnienia (C_C)	0,57	0,54

Zakres testów sedymentacyjnych zawierał, w zależności od aplikowanej ilości osadu potechnologicznego, analizę opadalności V_{30} i V_{60} (objętość osadu odpowiednio po 30 i 60 min. sedymentacji) z wyznaczeniem indeksu Mohlmanna (indeksu objętościowego osadu IO), indeksu Donaldsona (indeksu gęstości osadu IG) oraz prędkości sedymentacji v_s. Dodatkowo w celu weryfikacji poprawy opadalności z dodatkiem rea-

gentów wprowadzono wskaźnik opadalności W_o będący ilorazem V_{30}/V_{60}. Wskaźnik opadalności określa możliwości sedymentacji osadu względnie w dłuższym czasie w odniesieniu do powszechnie stosowanego indeksu objętościowego IO. W_o może mieć znaczenie podczas eksploatacji systemów z osadem czynnym np. sekwencyjnych reaktorów porcjowych, w których podczas fazy dekantacji ścieków oczyszczonych przebiega dalej sedymentacja osadu czynnego. Znajomość wskaźnika opadalności pozwala w takich przypadkach na regulację czasu uruchamiania dekantera lub skrócenie fazy sedymentacji w cyklogramie pracy reaktora SBR. Przebieg badań laboratoryjnych był następujący: 5 zlewek o objętości 2,0 dm^3 napełniano 1200 cm^3 osadu czynnego, przy czym do 4 z nich wprowadzono odpowiednie objętości osadów potechnologicznych w postaci płynnej (tabela 2).

Tabela 2. Dawki osadów potechnologicznych.
Table 2. Doses of post-technological sludges.

Materiał	**Jednostka**	**Nr próbki**				
		0	**1**	**2**	**3**	**4**
Osad pokoagulacyjny	cm^3/dm^3	0	7,5	15,0	30,0	45,0
	g/g s.m.	0	0,205	0,41	0,82	1,24
Popłuczyny	cm^3/dm^3	0	2,5	5,0	10,0	15,0
	g/g s.m.	0	0,19	0,38	0,76	1,14

W przypadku aplikacji osadu pokoagulacyjnego stosowano dawki na poziomie 7,5; 75,0, 30,0 i 45,0 cm^3/dm^3 osadu. W konsekwencji zawartość osadu pokoagulacyjnego w osadzie czynnym wynosiła odpowiednio 0,205 (1); 0,41 (2); 0,82 (3) oraz 1,24 (4) g/dm^3. Z kolei objętość dozowanych popłuczyn w zakresie 2,5; 5,0; 10,0 i 15,0 cm^3/dm^3 prowadziła do uzyskania stężenia mikrocząstek stałych w osadzie czynnym odpowiednio na poziomie 0,19; 0,38; 0,76 i 1,14 g/dm^3. Dawki osadów potechnologicznych zostały ustalone na podstawie poprzednich badań autora (Masłoń i in. 2013, Masłoń 2015, 2016). Poziom odniesienia (0) stanowiła próbka osadu czynnego bez dodatku reagentów. Zlewki umieszczono w mieszadle mechanicznym i przeprowadzono szybkie i wolne mieszanie. Oznaczono stężenie suchej masy osadu czynnego w próbce kontrolnej (0). Dla pozostałych próbek (1; 2; 3; 4) stężenie suchej masy osadu czynnego ustalono jako sumę osadu w próbce odniesie-

nia (0) i masy substancji pylistej wprowadzonej w postaci osadów potechnologicznych. Następnie uzupełniono cylindry miarowe badanymi próbkami osadu czynnego i przeprowadzono obserwację sedymentacji w okresie t = 60 min. Przeprowadzono 3 serie pomiarowe, z których wyliczono średnią arytmetyczną. Prędkość sedymentacji osadu czynnego v_s określono wg zależności (I) (van Loosdrecht i in. 2016).

$$v_s = 17.4 \cdot e^{-0.0113 \cdot IO} \ [m/h] \quad (I)$$

3. Wyniki badań i dyskusja

Uzyskane wyniki badań potwierdzają korzystny wpływ dawkowania osadów potechnologicznych z uzdatniania wody jako czynnik intensyfikujący proces sedymentacji osadu czynnego. Charakterystyka osadu czynnego poddawanego testom sedymentacyjnym z dodatkiem osadu pokogulacyjnego i popłuczyn miała decydujący wpływ na uzyskane wyniki. Przeprowadzone badania opadalności wykazały zróżnicowaną skuteczność poprawy właściwości osadu czynnego w zależności od rodzaju i dawki reagentów. Zawartość osadu pokoagulacyjnego w osadzie czynnym kształtowała się na poziomie od 0,035-0,037 g/g s.m. dla dawki 7,5 cm^3/dm^3; 0,07-0,077 g/g s.m. dla dawki 15,0 cm^3/dm^3; 0,131-0,144 g/g s.m. dla dawki 30,0 cm^3/dm^3; 0,186-0,203 g/g s.m. dla dawki 45,0 cm^3/dm^3, stanowiąc odpowiednio średnią zawartość procentową na poziomie: 3,7%; 7,4%; 13,7% i 19,5%. Z kolei zawartość popłuczyn w osadzie czynnym dla dawek 2,5; 5,0; 10,0 i 15,0 cm^3/dm^3 wyniosła odpowiednio 0,034-0,037 g/g s.m., 0,065-0,072 g/g s.m., 0,123-0,135 g/g s.m. i 0,174-0,189 g/g s.m., efektem czego średnia zawartość procentowa osiągnęła poziom: 3,6%; 6,9%; 12,9% i 18,2%.

Przebieg opadalności osadu czynnego w próbkach z poszczególnymi materiałami był inny, o czym przemawia kształt krzywych sedymentacyjnych (rys. 2). Obserwacja wizualna wolnego mieszania oraz procesu sedymentacji w cylindrach miarowych pozwala stwierdzić, że kłaczki osadu czynnego wspomaganego popłuczynami były większe aniżeli przy dawkowaniu osadu pokoagulacyjnego. Podczas wolnego mieszania aglomeracja osadu czynnego i popłuczyn była zdecydowanie bardziej intensywna w porównaniu do analogicznych testów z osadem pokoagulacyjnym. Na proces inkorporacji mikrocząstek pylistych w kłaczki osadu czynnego może mieć wpływ wielkość poszczególnych ziaren mi-

neralnych w aplikowanych osadach potechnologicznych. Popłuczyny charakteryzowały się bowiem mniejszymi ziarnami niż osad pokoagulacyjny (rys. 1). Zawiesiny zawarte w popłuczynach stanowią układy polidyspersyjne, tworzone przez cząstki o nieregularnej strukturze. Rozrzut wielkości cząstek popłuczyn również był bardzo duży, dzięki czemu następowała bardzo dobra ich agregacja w kłaczki osadu czynnego. Opaliński & Masłoń (2015) wykazali, że uziarnienie materiałów pylistych w istotny sposób wpływa na proces opadalności osadu czynnego. Wielkość kłaczków osadu czynnego wspomaganych ziarnami osadów potechnologicznych w dużej mierze przedłożyła się zatem na przebieg sedymentacji osadu czynnego. Kłaczki o niewielkich wymiarach i porach wykazywały słabą opadalność, natomiast duże i gęste kłaczki charakteryzują się zdecydowanie lepszą sedymentacją. Przy aplikacji osadu pokoagulacyjnego sedymentacja osadu czynnego była spokojna i zrównoważona, natomiast w przypadku dawkowania popłuczyn odnotowano w pierwszych minutach sedymentacji w miarę szybką i gwałtowną sedymentację dużych kłaczków osadu czynnego, a dalej spokojną sedymentację mniejszych kłaczków. Wraz ze wzrostem objętości osadów potechnologicznych skuteczność poprawy sedymentacji osadu czynnego ulegała zwiększaniu.

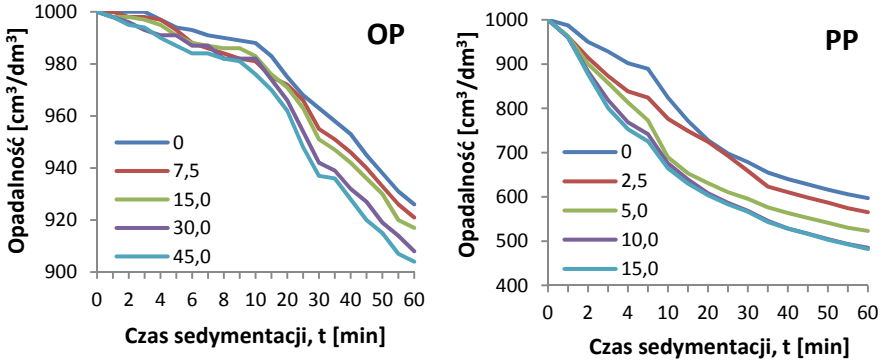

Rys. 2. Przebieg opadalności osadu czynnego z dodatkiem osadu pokoagulacyjnego (OP) oraz popłuczyn (PP)
Fig. 2. Course of settleability of activated sludge with post-coagulation sludge (OP) and backwash water (PP)

Mechanizm poprawy opadalności osadu czynnego z dodatkiem osadów potechnologicznych jest trudny do określenia bowiem, z jednej strony stanowią one zawiesinę, w której obecne są mikrocząstki mineralne będące obciążnikiem kłaczków osadu czynnego. Z drugiej jednak strony obecność żelaza w PP oraz jonów glinu w OP może wpływać na proces opadalności osadu czynnego w analogiczny sposób jak apliacja koagulantów chemicznych.

Zmniejszenie opadalności V_{30} i V_{60}, zmiana indeksu objętościowego ΔIO i wzrost indeksu gęstości ΔIG, jak również intensyfikacja prędkości osadu czynnego stanowią miarę efektywności stosowania pylistych obciążników (Masłoń i in. 2013, Masłoń 2015). Badania wykazały, że bardziej skutecznym materiałem w aspekcie poprawy opadalności osadu czynnego były popłuczyny z uzdatniania wód podziemnych. Przy porównywalnych dawkach ilościowych (tabela 2) uzyskano ponad 2-krotnie wyższą poprawę parametru V_{30} oraz ponad 3-krotnie wyższą poprawę V_{60} w obecności popłuczyn (rys. 3). Skutkiem aplikacji osadu pokoagulacyjnego oraz popłuczyn do analizowanego osadu czynnego było intensywne zmniejszenie wartości indeksu Mohlmanna. Dawkowanie osadu pokoagulacyjnego spowodowało zmniejszenie IO z 187,5 cm^3/g s.m. (próbka kontrolna) maksymalnie do poziomu 147,1 cm^3/g s.m przy dawce 45 cm^3/dm^3 (wartość średnia). Z kolei przy dozowaniu popłuczyn osiągnięto spadek IO z poziomu 189,6 cm^3/g s.m do wartości 140,1 cm^3/g s.m przy dawce 15,0 cm^3/dm^3 (rys. 4).

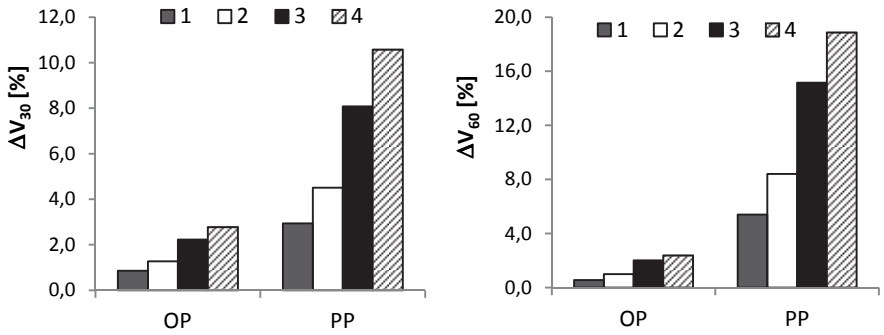

Rys. 3. Wpływ osadów potechnologicznych na poprawę opadalności analizowanego osadu czynnego; dawki (0), (1), (2), (3), (4) wg tabeli 2
Fig. 3. Impact of post-technological sludges on the improvement of activated sludge settleability; (0) (1), (2), (3), (4) doses according to table 2

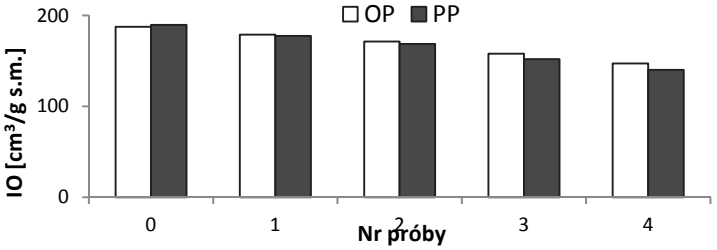

Rys. 4. Wpływ osadu pokoagulacyjnego (OP) i popłuczyn (PP) na zmniejszenie indeksu objętościowego
Fig. 4. Impact of post-coagulation sludge (OP) and backwash water (PP) on decrease of sludge volume index

Wraz ze wzrostem ilości stosowanego reagenta indeks osadu czynnego ulegał obniżeniu. Stwierdzono statystycznie istotne zależności pomiędzy zawartością osadów potechnologicznych w osadzie czynnym a zmianą indeksu objetościowego (rys. 5). Podobne zależności odnotowano w innych badaniach autora, przy czym dla najbardziej efektywnych materiałów pylistych (glina czerwona i mączka ceglana) stwierdzono związek statystyczny nieliniowy (Masłoń 2015).

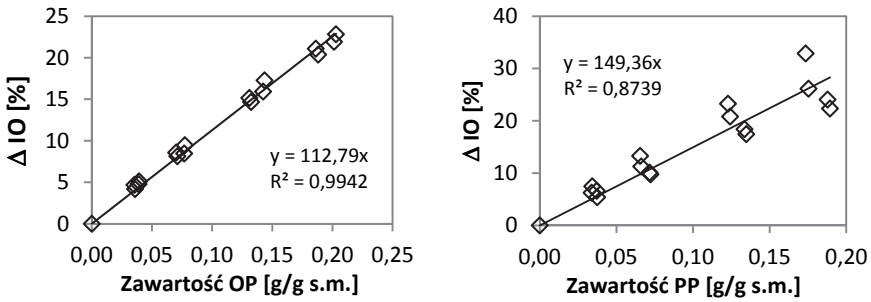

Rys. 5. Zależność pomiędzy zawartością osadu pokoagulacyjnego i popłuczyn w osadzie czynnym a zmianą wartości IO (Δ IO)
Fig. 5. The relationship between the content of post-coagulation sludge and backwash water in the activated sludge and the change in value of sludge volume index (Δ IO)

Odnotowano zróżnicowane procentowe zmniejszenie indeksu osadu czynnego oraz wzrost indeksu gęstości względem próbki kontrolnej (wyjściowej) (rys. 6). Osiągnięto maksymalnie 21,6% oraz

26,4% zmniejszenie IO odpowiednio przy dawkowaniu osadu pokoagulacyjnego i popłuczyn. Dla porównania, w innych badaniach odnotowano ponad 70% obniżenie wartości IO przy zastosowaniu pylistej gliny ceglanej przy dawce 0,5-1,0 g/dm^3 (Masłoń 2015). Równolegle zaobserwowano dość duże zmiany indeksu gęstości osadu czynnego, maksymalnie 27,5% (OP) oraz 37,0% (PP). Analiza wskaźnika opadalności wykazała, że sedymentacja osadu czynnego z dodatkiem osadu pokoagulacyjnego w okresie od 30 do 60 minut nie ulegała już większym zmianom. Natomiast w obecności popłuczyn osad czynny w analogicznym przedziale czasowym nadal sedymentował, a dalej zagęszczał się (rys. 7).

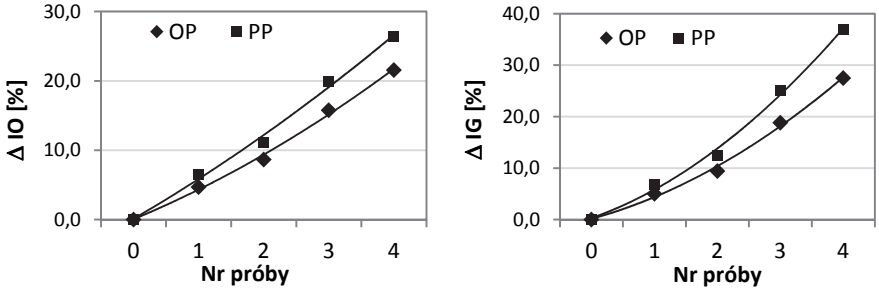

Rys. 6. Wpływ osadów potechnologicznych na zmianę wartości indeksu objętościowego (Δ IO) i indeksu gęstości osadu czynnego (Δ IG)
Fig. 6. Impact of post-technological sludges on change of sludge volume index (Δ IO) and sludge density index (Δ IG)

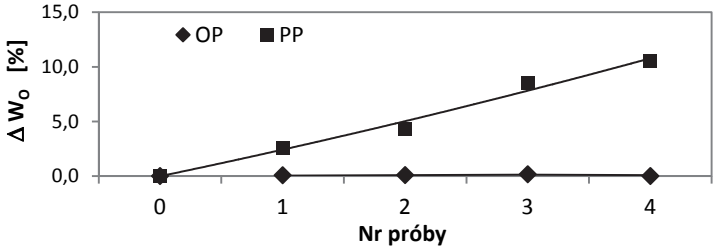

Rys. 7. Wpływ osadów potechnologicznych na zmianę wskaźnika opadalności (Δ W_O)
Fig. 7. Impact of post-technological sludges on change of sludge settleability ratio (Δ W_O)

Odzwierciedleniem poprawy właściwości sedymentacyjnych osadu czynnego jest również poprawa prędkości sedymentacji. Wzrost gęstości osadu czynnego prowadzi do uzyskania wyższych wartości v_s. W badaniach uzyskano różny poziom intensyfikacji prędkości sedymentacji osadu czynnego. Średnia prędkość v_s w poszczególnych próbkach z OP kształtowała się na poziomie: 2,11 m/h (0), 2,32 m/h (1), 2,53 m/h (2), 2,93 m/h (3), 3,31 m/h (4). Natomiast w testach z popłuczynami v_s w kolejnych próbkach wyniosła: 2,06 m/h (0), 2,37 m/h (1), 2,62 m/h (2), 3,17 m/h (3) i 3,64 m/h (4). Maksymalny wzrost prędkości sedymentacji uzyskano dla najwyższych dawek reagentów, odpowiednio 58,1% (OP) oraz 75,3% (PP) (rys. 8).

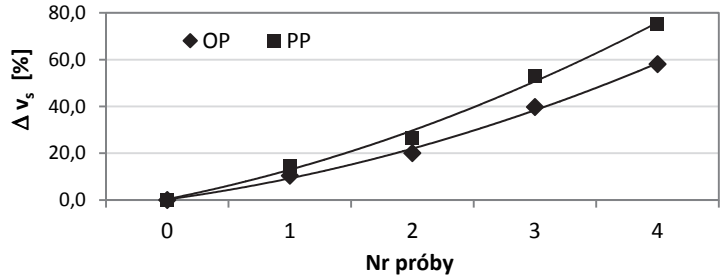

Rys. 8. Zmiana prędkości sedymentacji osadu czynnego (Δv_s) w zależności od dawki osadu pokoagulacyjnego (OP) i popłuczyn (PP).
Fig. 8. The change of velocity sedimentation of activated sludge depending on dose of post-coagulation sludge (OP) and backwash water (PP).

4. Wnioski

1. Przeprowadzone badania laboratoryjne wykazały przydatność zastosowania osadów potechnologicznych z uzdatniania wody do poprawy właściwości sedymentacyjnych osadu czynnego.
2. Odnotowano maksymalnie 21,6% oraz 26,4% zmniejszenie indeksu osadu czynnego odpowiednio przy dawkowaniu osadu pokoagulacyjnego i popłuczyn.
3. Maksymalny stopień poprawy wartości prędkości sedymentacji uzyskano dla najwyższych dawek osadów potechnologicznych, odpowiednio, 58,1% (OP) oraz 75,3% (PP).

4. Popłuczyny z uzdatniania wód podziemnych są bardziej efektywnym materiałem aniżeli osady pokoagulacyjne z uzdatniania wód powierzchniowych w aspekcie wspomagania sedymentacji osadu czynnego.
5. Mechanizm poprawy sedymentacji osadu czynnego z dodatkiem osadów potechnologicznych jest trudny do określenia, bowiem z jednej strony osad pokoagulacyjny i popłuczyny stanowią zawiesinę, w której obecne są cząstki mineralne o wielkości poniżej 200 μm będące obciążnikiem kłaczków osadu czynnego. Z drugiej jednak strony obecność żelaza w popłuczynach i glinu w osadach pokoagulacyjnych może mieć przebieg analogiczny jak procesy chemicznego stracania z wykorzystaniem koagulantów chemicznych PIX i PAX. Wobec tego złożony hybrydowy mechanizm wspomagania osadu czynnego z użyciem osadów potechnologicznych może wynikać z synergicznego efektu obecności jonów żelaza lub glinu oraz mineralnych mikroziaren.
6. Osady potechnologiczne z uzdatniania wody mogą być wykorzystane do poprawy właściwości sedymentacyjnych osadu czynnego.
7. W celu zweryfikowania uzyskanych efektów technologicznych konieczne staje się przeprowadzenie testów w pełnej skali w oczyszczalni ścieków.

Literatura

Ahmad, T., Ahmad, K., Ahad, A., Alam, M. (2016). Characterization of water treatment sludge and its reuse as coagulant. *Journal of Environmental Management, 182*, 606-611.

Bezak-Mazur, E., Stoińska, R., Szeląg, B. (2016). Ocena wpływu parametrów operacyjnych i występowania bakterii nitkowatych na objętościowy indeks osadu czynnego – studium przypadku. *Rocznik Ochrona Środowiska, 18(2),* 480-481.

Budzińska, K., Bochenek, M., Traczykowski, A., Szejniuk, B., Pasela, R., Jurek, A. (2015). Eliminacja bakterii nitkowatych w osadzie czynnym pod wpływem wybranych koagulantów i związków utleniających. *Rocznik Ochrona Środowiska, 17(2),* 1569-1586.

Chłąd, Z., Grübel, K., Wacławek, S., Przywara, L. (2015). Wpływ nadsiarczanu i mononadsiarczanu na właściwości fizykochemiczne osadu czynnego. *Proceedeings of ECOpole, 9(2),* 561-570.

Jaroszyński, T., Krajewski, P., Grześkowiak, K. (2011). Praktyczne wykorzystanie osadów żelazowych z procesów uzdatniania wody. *Technologia Wody*, *2*, 26-33.

Juraszka, B. & Sumara, A. (2013). Badania efektu odwadniania osadów pokoagulacyjnych w procesie sedymentacji odśrodkowej z zastosowaniem flokulantu kationowego Flopam DW 2160. *Rocznik Ochrona Środowiska, 15*, 1177-1190.

Kida, M., Masłoń, A., Tomaszek, J.A., Koszelnik, P. (2015). *The possibilities of limitation and elimination of activated sludge bulking*, 35-49. [in:] Tomaszek, J.A. & Koszelnik P., (eds) *Progress in Environmental Engineering*. London: CRC Press, Taylor&Francis Group.

Krajewski, P., Sozański, M.M. (2010). Możliwości i metody wykorzystania osadów z uzdatniania wody. *Technologia Wody, 5*, 30-36.

Kyncl, M., Číhalová, Š., Jurková, M., Langarová, S. (2012). Unieszkodliwianie i zagospodarowanie osadów z uzdatniania wody. *Journal of the Polish Mineral Engineering Society, 13(2),* 11-20.

Li, J., Liu, L., Liu, J., Ma, T., Yan, A., Ni, Y. (2016). Effect of adding alum sludge from water treatment plant on sewage sludge dewatering. *Journal of Environmental Chemical Engineering, 4*, 746-752.

Masłoń, A. (2015). *Rozwiązanie problemu małych oczyszczalni ścieków – ograniczenie pęcznienia i pienienia osadu czynnego w oczyszczalniach poprzez zastosowanie substancji pylistych.* XVIII Kongres Naukowo-Techniczny WOD-KAN-EKO 2015. Serock k. Warszawy, 17-18.09.2015 r.

Masłoń A. (2016). Suplementy dla osadu czynnego. Zapobieganie spienianiu i pęcznieniu. *Kierunek WOD-KAN, 1(630),* 46-51.

Masłoń, A. (2015). Wpływ materiałów pylistych na poprawę właściwości sedymentacyjnych osadu czynnego. *Instal, 4,* 51-55.

Masłoń, A. & Tomaszek J.A. (2012). Kierunki zastosowania mineralnych materiałów pylistych w technologii osadu czynnego – studium literatury. *Prace Naukowe Inżynieria Środowiska – Współczesne problemy inżynierii i ochrony środowiska, 59*, 5-23.

Masłoń, A., Tomaszek, J.A., Opaliński, I. (2013). Badania nad poprawą właściwości sedymentacyjnych osadu czynnego przy zastosowaniu mineralnych substancji pylistych. *Gaz, Woda i Technika Sanitarna, 12*, 490-495.

Nair, A.T., Ahammed, M.M. (2015). The reuse of water treatment sludge as a coagulant for post-treatment of UASB reactor treating urban wastewater. *Journal of Cleaner Production, 96*, 272-281.

Opaliński, I. & Masłoń, A. (2015). *Charakterystyka uziarnienia materiałów pylistych w aspekcie wspomagania technologii osadu czynnego.* 8. Kongres Technologii Chemicznej „Surowce – energia – materiały". Rzeszów, 30.08-4.09 2015 r.

Piaskowski, K. (2010). Popłuczyny z uzdatniania wody podziemnej – źródło żelaza odpadowego. *Technologia Wody, 3*, 26-33.

Szerzyna, S. (2013). Możliwości wykorzystania osadów powstających podczas oczyszczania wody. 609-617 [w:] Traczewska, T.M., (red.) Interdyscyplinarne zagadnienia w inżynierii i ochronie środowiska. Tom 3. Oficyna Wydawnicza Politechniki Wrocławskiej, Wrocław.

Totczyk, G., Klugiewicz, I., Pasela, R., Górski, Ł. (2015). Usuwanie fosforanów z wykorzystaniem osadów potechnologicznych pochodzących ze stacji uzdatniania wody. *Rocznik Ochrona Środowiska, 17(2),* 1660-1673.

van Loosdrecht, M.C.M., Nielsen, P.H., Lopez-Vazquez, C.M., Brdjanovic, D. (2016). *Experimental Methods in Wastewater Treatment*. London: IWA Publishing.

Use of Post-technological Sludge from Water Treatment to Improve Sedimentation Properties of Activated Sludge

Abstract

The aim of the paper is the evaluation of post-technological sludge from Water Treatment Plant on improvement of sedimentation properties of activated sludge. The post-coagulation sludge from surface water treatment (OP) and backwash water from groundwater treatment (PP) were used in this study. The studies were performed in the laboratory scale by observing the settleability of activated sludge with the addition of different volume of post-technological sludge. The activated sludge quality used in this study was characterised by a strong sludge bulking and a wide range of sludge volume index. For the evaluation of the efficiency of tested materials in activated sludge the settleability after 30 (V_{30}) and 60 (V_{60}) minutes, the sludge volume index SVI, the Donaldson index SDI (Sludge Density Index) and value settling velocity v_s were determined. Additionally, in order to verify of activated sludge settleability with the addition of post-technological sludge was appointed a sludge settling ratio (Wo) which is a quotient of V_{30} and V_{60}.

Studies showed the usefulness of the application of post-technological sludge from water treatment to improve of sedimentation properties of the activated sludge. Settling tests showed different efficiencies in the activated sludge settleability, depending on the type and amount of post-technological sludge. At a dosage of post-coagulation sludge and backwash water was observed up to 21.6% and 26.4% reduction of sludge volume index. The maximum level of improvement of settling velocity at the highest doses of post-technological sludge amounted to 58.1% (OP) and 75.3% (PP). Better effects of improvement of activated sludge sedimentation were obtained using backwash water than post-coagulation sludge.

The mechanism of improvement of sedimentation properties of the activated sludge containing post-technological sludge is difficult to determine. On

the one hand the post-coagulation sludge and backwash water are a suspension, wherein the mineral particles are present, which is a weight of activated sludge flocs. The incorporation of particles into flocs of activated sludge increases its relative density On the other hand, the presence of iron ions in backwash water and aluminum ions in post-coagulation sludge may affect the sedimentation activated sludge in the same manner as the chemical coagulant.

The backwash water or post-coagulation sludge may be a new effective reagent in activated sludge technology.

Streszczenie

Przedmiotem opracowania jest określenie wpływu osadów potechnologicznych z uzdatniania wody na właściwości sedymentacyjne osadu czynnego. Przetestowane zostały popłuczyny z uzdatniania wód podziemnych oraz osad pokoagulacyjny z uzdatniania wód powierzchniowych. Badania przeprowadzono w warunkach laboratoryjnych na podstawie obserwacji opadalności osadu czynnego z dodatkiem zróżnicowanych objętości materiałów. Do oceny efektywności zastosowanych osadów potechnologicznych określono opadalność V_{30} i V_{60} (objętość osadu odpowiednio po 30 i 60 min. sedymentacji), indeks osadu czynnego, indeksu Donaldsona (indeksu gęstości osadu) oraz prędkość sedymentacji vs. Dodatkowo w celu weryfikacji poprawy opadalności z dodatkiem reagentów wprowadzono wskaźnik opadalności Wo będący ilorazem V_{30}/V_{60}. Badania wykazały przydatność zastosowania osadów potechnologicznych z uzdatniania wody do poprawy właściwości sedymentacyjnych osadu czynnego. Popłuczyny z uzdatniania wód podziemnych osiągnęły najwyższe efekty wspomagania osadu czynnego. Odnotowano maksymalnie 21,6% oraz 26,4% zmniejszenie indeksu osadu czynnego odpowiednio przy dawkowaniu osadu pokoagulacyjnego i popłuczyn. Maksymalny stopień poprawy prędkości sedymentacji osiągnięto przy najwyższych dawkach osadów technologicznych, odpowiednio 58,1% (OP) oraz 75,3% (PP). Mechanizm poprawy sedymentacji osadu czynnego z dodatkiem osadów potechnologicznych jest trudny do określenia, bowiem z jednej strony osad pokoagulacyjny i popłuczyny stanowią zawiesinę, w której obecne są cząstki mineralne o wielkości poniżej 200 μm będące obciążnikiem kłaczków osadu czynnego. Z drugiej jednak strony obecność żelaza w popłuczynach i glinu w osadach pokoagulacyjnych może wpływać na proces opadalności w analogiczny sposób jak koagulanty chemiczne PIX i PAX.

Słowa kluczowe:
osad pokoagulacyjny, popłuczyny, osad czynny, osad spęczniały

Keywords:
post-coagulation sludge, backwash water, activated sludge, sludge bulking

MIDDLE POMERANIAN SCIENTIFIC SOCIETY OF THE ENVIRONMENT PROTECTION
ŚRODKOWO-POMORSKIE TOWARZYSTWO NAUKOWE OCHRONY ŚRODOWISKA

Annual Set The Environment Protection
Rocznik Ochrona Środowiska

Volume/Tom 19. Year/Rok 2017 ISSN 1506-218X 760-776

Analiza zmian udziału frakcji ChZT w procesie denitryfikacji z zewnętrznym źródłem węgla

Joanna Smyk[*]*, Katarzyna Ignatowicz*[*]*, Jacek Piekarski*[**]
[*]*Politechnika Białostocka,*
[**]*Politechnika Koszalińska*

1. Wstęp

Różnorodność jednostkowych procesów biochemicznych występujących w zintegrowanym usuwaniu zanieczyszczeń ze ścieków ma istotny wpływ na zastosowanie symulacji komputerowych przy projektowaniu poszczególnych etapów usuwania zanieczyszczeń z oczyszczanych ścieków. Projektowanie technologicznych układów oczyszczania ścieków w większości przypadków odnosi się do ilości materii organicznej charakteryzowanej BZT_5. Wskaźnik ten dostarcza tylko informacji o zanieczyszczeniach łatwo ulegających biodegradacji. Nie są jednak brane pod uwagę zanieczyszczenia nie ulegające biodegradacji, które to obniżają skuteczność biologicznego oczyszczania ścieków. Dość częstym problemem jest uzyskanie efektywnego usuwania związków azotu. Skuteczna denitryfikacja wymaga określonej ilości związków węgla łatwo ulegających rozkładowi w procesie obróbki biologicznej. Denitryfikacja zachodzi bez zakłóceń, jeżeli stosunek ChZT/N jest na poziomie od 5 do 10. Mniejsza jego wartość powoduje, że zachodzi konieczność wprowadzania do ścieków zewnętrznego źródła węgla (Elefsioris, Li 2006; Kulikowska i in. 2009; Płuciennik-Koropczuk i in. 2013; Przywara 2015; Sadecka, Płuciennik-Koropczuk 2011; Struk-Sokołowska 2014; Wu i in. 2014).

Frakcjonowanie ChZT pozwala na zidentyfikowanie łatwo i trudno rozkładalnych frakcji z podziałem na zawartość rozpuszczoną i nierozpuszczalną. Znajomość wielkości poszczególnych frakcji ChZT, jak również ich zmian po kolejnych etapach oczyszczania, może znacząco wypłynąć na poprawę efektywności usuwania związków węgla i azotu ze ścieków (Pasztor i in. 2009; Struk-Sokołowska 2014; Wu i in. 2014).

ChZT ścieków, z podziałem na frakcje, można obliczać według zależności (Płuciennik-Koropczuk 2009; Sadecka, Myszograj 2004; Zdebik, Głodniok 2010; Ignatowicz, Puchlik 2011):

$$ChZT = S_S + S_I + X_S + X_I$$

gdzie:
S_S – ChZT rozpuszczonych związków organicznych biologicznie łatwo rozkładalnych (COD soluble readily biodegradable substrates),
S_I – ChZT rozpuszczonych związków biologicznie nierozkładalnych (COD inert soluble organic material),
X_S – ChZT nierozpuszczalnych związków biologicznie wolno rozkładalnych (COD particulate slowly biodegradable substrates,),
X_I – ChZT nierozpuszczalnych organicznych biologicznie nierozkładalnych (COD inert particulate organic material).

2. Metodyka badań

2.1. Obiekt badań

Obiektem badań była oczyszczalnia ścieków w Białymstoku. Przyjmuje ona ścieki z ponad trzystutysięcznej aglomeracji, a jej średnia przepustowość wynosi około 70 000 m^3/d. Jest to mechaniczno-biologiczna oczyszczalnia, która pracuje wykorzystując technologię osadu czynnego.

W części biologicznej komora predenitryfikacji (denitryfikacji I stopnia) oraz defosfatacji pełniły pierwotnie funkcję osadników wstępnych. Do komory predenitryfikacji jest recyrkulowany osad z osadników wtórnych, gdzie ulega procesowi częściowej denitryfikacji. W komorze defosfatacji mikroorganizmy osadu czynnego pobierają łatwo przyswajalną materię organiczną jednocześnie uwalniając zakumulowane ortofosforany. W tym miejscu wraz z odciekami z przeróbki osadów dostarczane są lotne kwasy tłuszczowe wytworzone podczas zagęszczania osa-

dów wstępnych w zagęszczaczach grawitacyjnych. Pozwala to na zwiększenie efektywności procesu defosfatacji.

Komora osadu czynnego podzielona jest na dwa główne baseny. W jednym z nich napowietrzanie jest prowadzone za pomocą dyfuzorów, natomiast w drugim przez aeratory. Każdy z basenów składa się z czterech komór osadu czynnego. Z kolei każda komora podzielona jest na sześć stref. Elementem wspólnym dwóch głównych basenów jest kanał recyrkulacji gdzie dawkowane jest zewnętrzne źródło węgla.

Pierwszym elementem komory osadu czynnego jest strefa denitryfikacji II stopnia. Recyrkulacja wewnętrzna (z ostatniej strefy nitryfikacji do strefy denitryfikacji) wynosi tu od 300 do 700%. Kolejną komorą jest tzw. strefa przejściowa, gdzie prowadzony jest przemiennie proces nitryfikacji (przy włączonym aeratorze) prowadzony z procesem denitryfikacji poprzez wyłączenie napowietrzania.

Miejsce dawkowania zewnętrznego źródła węgla ustalono doświadczalnie i znajduje się w komorze osadu czynnego w odległości 40 m od przelewu do strefy anoksycznej. Wspomaganie procesu denitryfikacji zewnętrznym źródłem węgla prowadzone jest przez cały rok z wyłączeniem okresów, kiedy temperatura ścieków w komorach ulega obniżeniu poniżej wartości wynoszącej 12°C (Simson 2009, 2008).

2.2. Metodyka badań

Badania prowadzono w październiku 2015 roku. Próbki ścieków, oprócz ścieków surowych i oczyszczonych, (3 serie) były pobierane bezpośrednio z komór biologicznych. Każdorazowo pobierano manualnie około 2 dm^3 ścieków w oczyszczalni ścieków w następującej kolejności: ścieki surowe, z komory predenityfikacji (denitryfikacji I stopnia), komory defosfatacji, z komory denitryfikacji (denitryfikacji II stopnia) w miejscu dawkowania zewnętrznego źródła węgla - Brenntaplus VP1, z komory denitryfikacji w kilkumetrowej odległości od miejsca dawkowania zewnętrznego źródła węgla oraz ścieki oczyszczone.

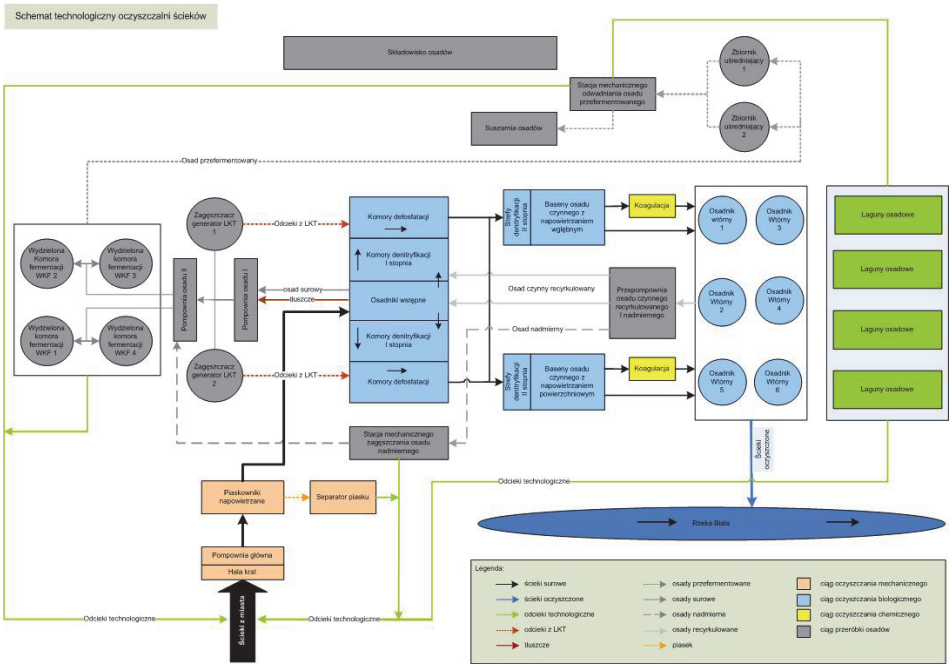

Rys. 1. Schemat oczyszczalni ścieków w Białymstoku; źródło: Wodociągi Białostockie
Fig. 1.

W pobranych próbkach ścieków oznaczano zgodnie z obowiązującą metodyką (Simson 2009; Ignatowicz, Kozłowski 2011):

- $ChZT_{Cr}$ – metodą dwuchromianową PN-74/C-04578.03,
- BZT_5 – metodą manometryczną systemem OxiTop Standard,
- $N\text{-}NH_4$ – metodą spektrofotometryczną wg: PN-ISO 7150-1:2002,
- $N\text{-}NO_3$ – metodą spektrofotometryczną wg: PN-82/C-04576/08,
- Nog – metodą spektrofotometryczną wg: PN-EN ISO 6878:2006,
- Pog – metodą spektrofotometryczną wg: PN-EN ISO 6878:2006.

W literaturze najczęściej spotykana jest metodologia wyznaczania poszczególnych frakcji ChZT na podstawie wytycznych ATW_A 131 (Sadecka, Myszograj 2004; Kulikowska i in. 2009; Sadecka, Płuciennik-Koropczuk 2011; Płuciennik-Koropczuk i in. 2013; Przywara 2015; Struk-Sokołowska 2014; Zdebik, Głodniok 2010; Wojciechowska 2014). Tak więc analogicznie z innymi autorami frakcje ChZT: S_S, S_I, X_S, X_I

wyznaczono na podstawie wytycznych ATV-A 131 (Wytyczne ATV-DVWK-A 131.2000):

- Stężenie rozpuszczonej materii organicznej określono w ściekach surowych, jako ChZT ścieków.
- W celu wyznaczenia frakcji rozpuszczonej biologicznie nierozkładalnej S_I (ChZT) próbkę ścieków oczyszczonych przesączono przez bibułowy sączek twardy o średnicy oczek 0,45 μm, a następnie oznaczono ChZT ścieków.
- Frakcję biologicznie łatwo rozkładalną S_S wyznaczono jako różnicę ogólnego stężenia rozpuszczonej materii organicznej i biologicznie nierozkładalnej materii organicznej S_I :

$$S_S = S_{ChZT} - S_I, [mg\ O_2/dm^3]$$

- W celu oznaczenia frakcji nierozpuszczalnych materii organicznej wolno rozkładalnych X_S, wyznaczono doświadczalnie BZT_5 ścieków surowych niesączonych, a następnie przyjmując stałą szybkości biochemicznego rozkładu k_1=0,6 obliczono wartość całkowitego BZT_C:

$$BZT_C = BZT_5 / 0,6, [mg\ O_2/dm^3$$

Mając określoną wartość BZT_C oraz wartość rozpuszczonej frakcji biologicznie łatwo rozkładalnej S_S, frakcję związków nierozpuszczalnych wolno rozkładalnych X_S wyznaczono z równania:

$$X_S = BZT_C - S_S, [mg\ O_2/dm^3]$$

- Całkowite stężenie materii organicznej nierozpuszczalnej określono korzystając z zależności podanej w normie ATV-131:

$$X_I = A \times X_{ChZT,} [mg\ O_2/dm^3]$$

Przy czym, w zależności od pochodzenia ścieków lub też od czasu ich zatrzymania w osadniku wstępnym, wartość współczynnika A może zmieniać się od 0,2 do 0,35. Dla ścieków bytowych przyjmuje się A=0,25. Podstawiając do równania :

$$X_{ChZT} = X_S + X_I \text{ zależność } X_I = 0,25 \times X_{ChZT,}$$

otrzymano:

$$X_{ChZT} = X_S/0,75, [mg\ O_2/dm^3]$$

- Frakcję związków nierozpuszczalnych biologicznie nierozkładalnych X_I określono z różnicy wartości X_{ChZT} i $X_{S,}$:

$$X_I = X_{ChZT} - X_{S,} [mg\ O_2/dm^3].$$

3. Wyniki i ich interpretacja

Wyniki przeprowadzonych badań umieszczono w tabeli 1.

Na początku części mechanicznej, przed częścią biologiczną proces oczyszczania powoduje zmniejszenie stężenia substratu materii organicznej potrzebnej mikroorganizmom do usuwania związków azotu. W komorze predenitryfikacji stężenie związków materii organicznej określonej ChZT w stosunku do ścieków surowych zostało obniżone o64,8%, natomiast BZT_5 o 75,0%. Zaobserwowano spadek stężenia azotu ogólnego o 76,3%, azotu amonowego o 86,9%, azotanów(V) o 42,3% oraz fosforu ogólnego o prawie 30,0%. W komorze defosfatacji nastąpił wzrost związków węgla określanych jako ChZT oraz BZT_5 z powodu dopływających odcieków z zagęszczaczy grawitacyjnych bogatych w lotne kwasy tłuszczowe. Również skutkiem tego procesu jest wzrost stężenia związków fosforu z 6,1 mg P/dm^3 do ponad 25,0 mg P/dm^3. Łatwo przyswajalne związki węgla są natychmiast pobierane przez mikroorganizmy biorące udział w procesie defosfatacji, jednocześnie uwalniając zakumulowane wcześniej ortofosforany. Między komorą defosfatacji a komorą denitryfikacji nastąpiło obniżenie stężenia fosforu do 1 mg P/dm^3 skutkując niskim stężeniem 0,7 mg P/dm^3 w odpływie, co świadczy o właściwym przebiegu procesu defosfatacji.

W komorze denitryfikacji w pobliżu miejsca dawkowania zewnętrznego źródła węgla zaobserwowano spadek stężenia materii organicznej charakteryzowanej za pomocą parametru ChZT o 12,8% między tą komorą a komorą defosfatacji. Również nastąpił ubytek materii organicznej określanej za pomocą parametru BZT_5 o 12,5%. Teoretycznie obniżenie ich wartości powinno być większe, jednakże zawartość związków węgla wyrażanych jako ChZT oraz BZT_5 jest uzupełniane poprzez dawkowanie zewnętrznego źródła węgla. W innej części komory oddalonej od źródła dawkowania widoczny jest wyraźny spadek ilości materii organicznej ChZT o 47,5% i BZT_5 o 28,3%.

Tabela 1. Wyniki pomiarów
Table 1. Results

Przepływ: ok. 53 500 m^3/d Dawka Brenntaplus VP1: ok. 90g/m^3							
Parametr / Miejsce poboru próbki	ChZT	BZT_5	$N\text{-}NO_3^-$	$N\text{-}NH_4^+$	Nog	Pog	pH
	mg O_2/ dm^3		mg N/dm^3			mg P/dm^3	
ścieki surowe	488,0	240,0	2,6	70,8	118,0	8,7	8,5
kom.predenitryfikacji	172,0	60,0	1,5	9,3	18,0	6,1	8,0
kom. defosfatacji	203,0	65,0	<1,0	23,8	32,0	25,0	7,9
kom. denitryfikacji + węgiel	177,0	35,0	3,9	2,7	14,0	1,0	7,9
kom. denitryfikacji	93,0	25,0	3,1	1,4	13,0	1,2	8,0
ścieki oczyszczone	87,0	10,0	4,6	0,0	9,4	0,7	7,9

Do komory denitryfikacji przepływają ścieki po procesie nitryfikacji stąd widoczny jest spadek stężenia azotu amonowego między ściekami surowymi (23,8 mg N/dm^3) a ściekami w komorze denitryfikacji (2,7 mg N/dm^3). Przemiany te powodują wzrost stężenia azotanów(V) w komorze denitryfikacji, ponieważ ścieki bogate w ten związek są recyrkulowane z komory nitryfikacji. W pewnej odległości od miejsca dawkowania węgla można zauważyć zachodzący proces denitryfikacji – obniżenie stężenia azotanów(V) o 0,8 mg N/dm^3.

W ściekach oczyszczonych odnotowano stężenie materii organicznej określanej jako ChZT na poziomie 87,0 mg O_2/dm^3 oraz BZT_5 10,0 mg O_2/dm^3. Jest to około o 82,0% obniżenie wartości ChZT oraz 96,0% BZT_5 w porównaniu do ścieków surowych. O skuteczności procesu usuwania azotu świadczą niskie stężenia w ściekach oczyszczonych. Zmniejszenie stężenia azotu amonowego do zera świadczy o efektywnym procesie nitryfikacji. Stężenie azotu ogólnego (9,4 mg N/dm^3) oraz fosforu ogólnego (0,7 mg P/dm^3) w ściekach oczyszczonych spełnia dopuszczalne stężeń podane w Rozporządzeniu Ministra Środowiska z dnia 18 listopada 2014 r. w sprawie warunków, jakie należy spełnić przy wprowadzaniu ścieków do wód lub do ziemi, oraz w sprawie substancji szczególnie szkodliwych dla środowiska wodnego. Niskie stężenie azotanów(V) w ściekach oczyszczonych (4,6 mg N/dm^3) jest efektem właściwie dobranych parametrów technicznych prowadzenia procesu denitryfikacji, jak również dzięki dawkowaniu zewnętrznego źródła węgla.

Obliczone wartości stężeń frakcji ChZT i ich udział podano w tabeli 2. oraz przedstawiono graficznie na rysunku 2.

Tabela 2. Stężenie oraz procentowy udział frakcji ChZT w ściekach
Table 2. Concentrations and partition in COD fraction in wastewater

Frakcje ChZT / Miejsce poboru próbki	S_I		X_I		S_S		X_S	
	mg O_2/l	%	mg O_2/l	%	mg O_2/l	%	mg O_2/l	%
ścieki surowe	51,0	10,3	44,0	8,9	268,0	54,1	132,0	26,7
kom.predenitryfikacji	51,0	29,8	20,3	11,9	39,0	22,8	61,0	35,6
kom. defosfatacji	51,0	39,7	10,9	8,5	34,0	26,5	32,7	25,4
kom. denitryfikacji + węgiel	51,0	40,9	15,4	12,4	12,0	9,6	46,3	37,1
kom. denitryfikacji	51,0	49,4	10,6	10,2	10,0	9,7	31,7	30,7
ścieki oczyszczone	51,0	69,7	5,6	7,6	0,0	0,0	16,7	22,8

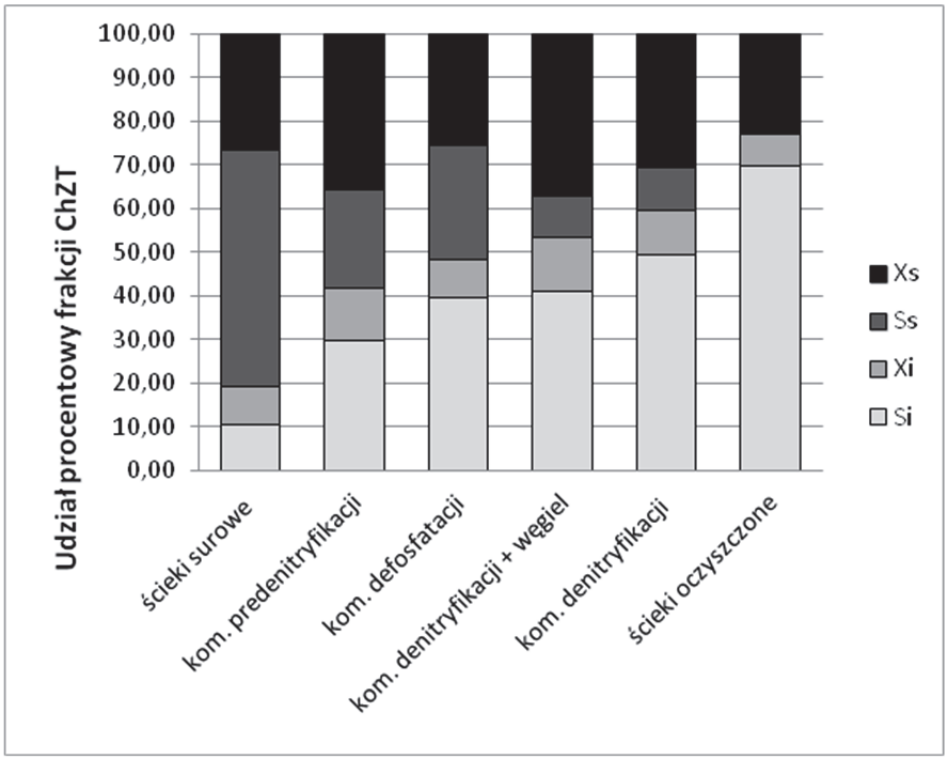

Rys. 2. Procentowy udział frakcji ChZT w kolejnych etapach oczyszczania
Fig. 2. Percentage of COD fraction after subsequent steps of treatment

Na podstawie obliczonych wartości stężeń frakcji ChZT stwierdzono, że ścieki surowe charakteryzują się zdecydowanym udziałem materii łatwo biodegradowalnej rozpuszczonej – 54,1% i trudno rozkładalnej nierozpuszczalnej – 26,7%. Najniższy udział miał miejsce w frakcji nierozkładalnej nierozpuszczalnej – 8,9%. W komorze predenitryfikacji udział poszczególnych frakcji ulega całkowitej zmianie. Najwyższą procentową zawartość ma frakcja X_S – 35,6%, natomiast frakcja S_I stanowi 29,8%. Frakcja rozpuszczona łatwo biodegradowalna stanowi tylko 22,8% całkowitego ChZT. W dalszym ciągu najniższy udział ma frakcja X_I – 11,9%. W komorze defosfatacji substancje ulegające biodegradacji są w dalszym ciągu pobierane przez mikroorganizmy, a ich zawartość procentowa wynosi 26,5% – S_s oraz do 25,4 – X_S. Najwyższy udział procentowy stwierdzono dla frakcji rozpuszczonej nierozkładalnej, która do

końca procesu oczyszczania ścieków będzie stanowiła większość całkowitego ChZT. W komorze denitryfikacji w miejscu dawkowania zewnętrznego źródła węgla można zaobserwować wyraźny spadek udziału frakcji S_S do 9,6%. Zwiększa się procentowa zawartość frakcji biodegradowalnej nierozpuszczalnej z 25,4% do 37,1%. Najwyższy procentowy udział ma frakcja S_I – 40,9%. Po wymieszaniu ścieków w komorze denitryfikacji stężenie frakcji S_S nie uległo zmianie. Nastąpiło natomiast obniżenie stężenia frakcji nierozuszczalnej X_S o ok. 7,0% oraz X_I w związku z czym udział procentowy frakcji S_I uległ zwiększeniu. Frakcja rozpuszczona łatwo rozkładalna została usunięta całkowicie ze ścieków oczyszczonych. Niewielki udział procentowy ma frakcja nierozpuszczalnych związków organicznych biologicznie nierozkładalnych – ok. 8,0%, natomiast frakcja X_s stanowi ok. 23,0% całkowitego ChZT w ściekach oczyszczonych. Zdecydowaną większość (prawie 70,0%) stanowiła frakcja S_I.

Na rysunku 3. przedstawiono zestawienie wielkości poszczególnych frakcji ChZT wraz ze stężeniem azotanów w procesie biologicznego oczyszczania ścieków. Materia organiczna we frakcji łatwo biodegradowalnej między komorą predenitryfikacji a defosfatacji uległy pobraniu przez mikroorganizmy i umożliwiły przemianę związków azotu. Jest to powodem obniżenia zawartość azotanów (V) w ściekach. Między komorą defosfatacji a komorą denitryfikacji w pobliżu miejsca dawkowania zewnętrznego źródła węgla nastąpił duży wzrost stężenia azotanów (V) spowodowanych recyrkulacją azotu amonowego z komory nitryfikacji. W komorze denitryfikacji nastąpiło intensywne przyswajanie materii organicznej we frakcji S_S dlatego stężenie azotanów (V) utrzymywało się na niskim poziomie. Prawdopodobnie bez dawkowania węgla stężenia byłyby wyższe.

Dodanie zewnętrznego źródła węgla do komory denitryfikacji spowodowało nagłe podwyższenie wartości stężeń związków organicznych nierozpuszczalnych biologicznie wolno rozkładalnych X_S o prawie 14 mg O_2/dm^3. Nastąpiło również uwolnienie przez kłaczki osadu niewielkiej ilości frakcji nierozkładalnej X_I co jest zjawiskiem korzystnym.

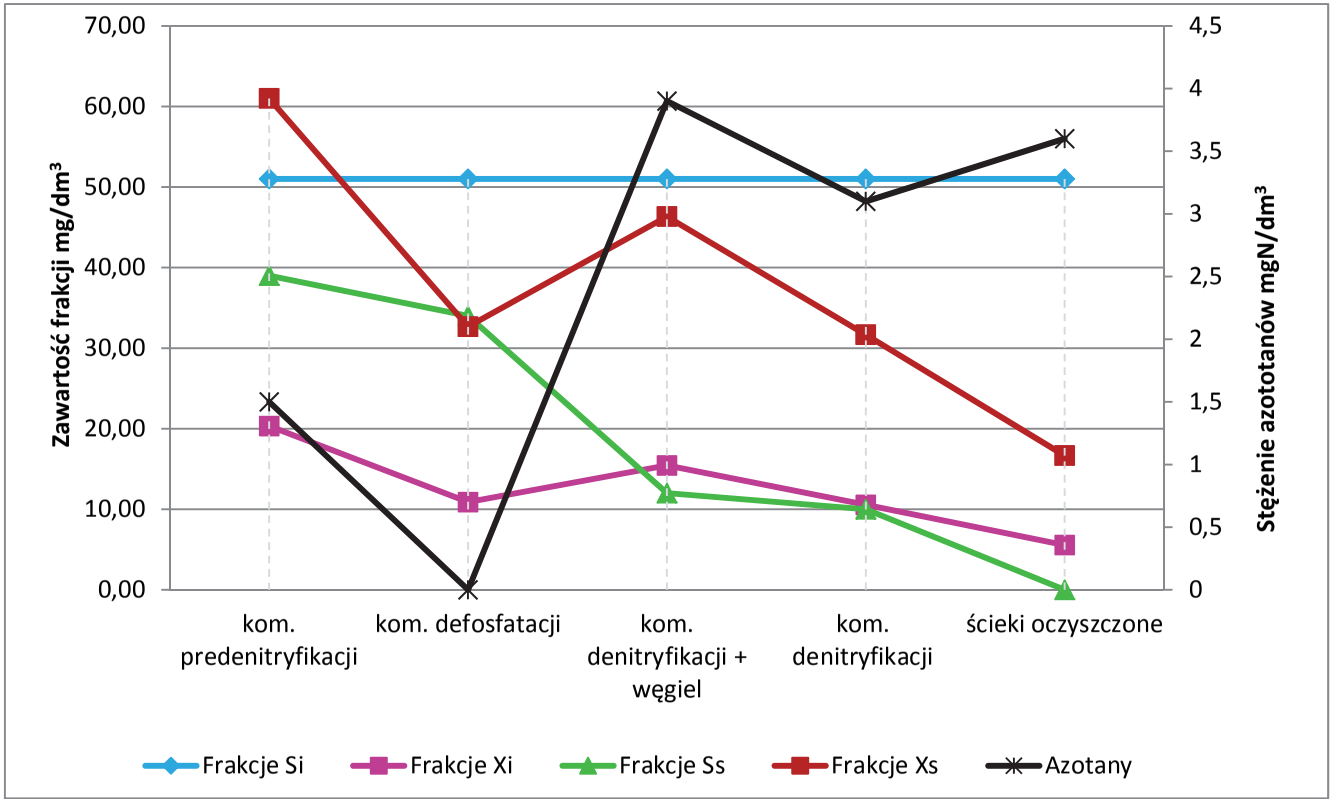

Rys. 3. Stężenie frakcji ChZT i azotanów (V) w procesie biologicznego oczyszczania ścieków
Fig. 3. The concentration of fraction of COD and nitrates (V) in the process of biological wastewater treatment

W pewnej odległości od miejsca dawkowania węgla stężenie frakcji X_S ulega ponownemu obniżeniu o prawie tyle samo ile nastąpił wzrost w okolicy miejsca dawkowania zewnętrznego źródła węgla. W dalszym ciągu następuje pobieranie frakcji rozpuszczonej łatwo przyswajalnej. W komorze denitryfikacji można zauważyć podobny spadek stężenia azotanów (V) o 0,8 mg N/dm^3 i frakcji S_S – o 2 mg N/dm^3. Niestety uprzednio uwolniona frakcja X_I ponownie zostaje wbudowana w kłaczki osadu.

Przepływ ścieków przez część biologiczną oczyszczalni spowodował obniżenie wszystkich frakcji ChZT z wyjątkiem frakcji S_I - frakcja ta pozostała bez zmian. Mała zawartość ilościowa frakcji ChZT nierozpuszczonej nierozkładalnej X_I w ściekach oczyszczonych świadczy o wbudowywaniu jej w kłaczki osadu czynnego, co jest zjawiskiem nie pożądanym ze względu na zwiększenie się masy osadu. W niewielkim stopniu wzrasta stężenie azotanów (V) w ściekach oczyszczonych, jednakże utrzymują się na niskim poziomie i nie ma potrzeby zwiększania dawki zewnętrznego źródła węgla ze względu na wysokie koszty.

4. Wnioski

Na podstawie przeprowadzonych analiz sformułowano następujące wnioski:

- W ściekach surowych doprowadzanych do oczyszczalni ścieków ponad 80% materii organicznej określanej jako ChZT stanowiły frakcje biologicznie rozkładalne X_S i S_S,
- Niskie stężenie udziału procentowego materii organicznej we frakcji S_S oraz X_S w ściekach oczyszczonych świadczy o przyswajaniu tych frakcji przez mikroorganizmy biorące udział w procesach usuwania związków azotu i fosforu,
- Niskie stężenie i procentowy udział materii organicznej we frakcji ChZT nierozpuszczalnej nierozkładalnej X_I w ściekach oczyszczonych świadczy o wbudowywaniu jej w kłaczki osadu czynnego,
- Układ technologiczny oczyszczania ścieków analizowanej oczyszczalni nie miał wpływu na zmianę stężenia rozpuszczonej frakcji biologicznie nierozkładalnej S_I w ściekach.
- Niskie stężenie azotanów (V) w ściekach oczyszczonych zostało uzyskane z powodu dawkowania zewnętrznego źródła węgla,

- Usuwanie zanieczyszczeń w oczyszczalni ścieków w Białymstoku przebiega prawidłowo i jest zgodne z polskimi regulacjami prawnymi.

Podziękowania

Praca powstała w ramach realizacji pracy statutowej S/WBIS/3/2014 oraz pracy MB/WBiIŚ/9/2016 w Katedrze Technologii w Inżynierii i Ochronie Środowiska Politechniki Białostockiej, a przede wszystkim dzięki życzliwości i pomocy Pana Grzegorza Simsona z Oczyszczalni Ścieków z Białegostoku.

Literatura

Elefsioris, P., D., Li, (2006). The effect of temperature and carbon source on denitrification using volatile fatty acids. *Biochemical Engineering Journal*, *28(2)*, 148-155.

Ignatowicz, K., Kozłowski, D. (2015). Intensyfikacja procesu denitryfikacji przy zastosowani preparatu Brenntaplus VP1 jako zewnętrznego źródła węgla. *Rocznik Ochrona Środowiska*, *17,* 25-50.

Ignatowicz, K., Puchlik, M. (2011). Złoża biologiczne jako alternatywa oczyszczania małych ilości ścieków. *Rocznik Ochrona Środowiska*. *13*, 1385-1404.

Ignatowicz, K. (2011). Metals content chosen for environmental component monitoring in graveyards. *Fresenius Environmental Bulletin, 20(1a),* 270-273.

Kogut P., Piekarski J., Ignatowicz K., (2014). Rozruch instalacji biogazowej z wykorzystaniem osadu zaszczepowego. *Rocznik Ochrona Środowiska, 16*, 534-545.

Kulikowska, D., Drzewnicki, A., Tomczykowska, M. (2009). Intensyfikacja procesu denitryfikacji ścieków na przykładzie oczyszczalni w Tyrowie. *Czasopismo Techniczne, z. 11. Środowisko z. 3-Ś*.

Pasztor, I., Thury, P., Pulai, J. (2009). Chemical oxygen demand fractions of municipal wastewater for modeling of wastewater treatment. International *Journal of Environmental Science and Technology*, *6(1)*, 51-56.

Płuciennik-Koropczuk, E., Sadecka, Z., Myszograj, S. (2013). COD fractions in raw and mechanically treated wastewater**.** *Civil And Environmental Engineering Reports, 11*.

Płuciennik-Koropczuk, E. (2009). Frakcje ChZT miarą skuteczności oczyszczania ścieków. *Gaz, Woda i Technika Sanitarna, VII-VIII*, 11-13.

Przywara, L. (2015). Analiza przemian materii organicznej podczas beztlenowego oczyszczania ścieków z produkcji tłuszczy jadalnych. *Inżynieria Ekologiczna, 41*, 142-147.

Sadecka, Z., Myszograj, S. (2004). Frakcje ChZT w procesach mechaniczno-biologicznego oczyszczania ścieków na przykładzie oczyszczalni ścieków w Sulechowie. *Rocznik Ochrona Środowiska, 6,* 233-244.

Sadecka, Z., Płuciennik-Koropczuk, E. (2011). Frakcje ChZT ścieków w mechaniczno-biologicznej oczyszczalni, *Rocznik Ochrona Środowiska, 13*, 1157-1172.

Simson, G. (2009). Intensyfikacja procesu denitryfikacji w Oczyszczalni ścieków w Białymstoku poprzez dozowanie preparatu Brenntaplus VP1 jako zewnętrznego źródła węgla organicznego – doświadczenia eksploatacyjne (część 2). *Forum Eksploatatora, 6,* 49-52.

Simson, G. (2008). Pierwsze doświadczenia – test technologiczny z zastosowaniem preparatu Brenntaplus VP1 jako zewnętrzne źródło węgla organicznego do intensyfikacji procesu denitryfikacji w Białostockiej Oczyszczalni Ścieków. *Forum Eksploatatora, 6*, 24-26.

Struk-Sokołowska, J. (2014). Specjacja materii organicznej za pomocą ChZT w ściekach na wybranym przykładzie. Materiały Eko-dok.

Wojciechowska, E. (2011). Analiza podatności na rozkład biologiczny odcieków składowiskowych oczyszczanych w wielostopniowym systemie hydrofilowym. *Inżynieria i Ochrona Środowiska, 17(4)*, 703-712.

Wu, J., Yan, G., Zhou, G., Xu, T. (2014). Wastewater COD biodegradability fractionated by simple physical-chemical analysis. *Chemical Engineering Journal 258*,450-459.

Wytyczne ATV-DVWK-A 131.2000. Wymiarowanie jednostopniowych oczyszczalni ścieków z osadem czynnym, Wydawnictwo Seidel- Przywecki.

Zdebik, D., Głodniok, M. (2010). Wyniki badań podatności ścieków na rozkład biologiczny - frakcje ChZT na przykładzie oczyszczalni ścieków w Rybniku, Prace Naukowe Gig. *Górnictwo I Środowisko, 4*.

Analysis of COD Fractions Changes During Denitrification Process with External Carbon Source

Abstract

The article presents results of analysis on concentration of COD fractions in mechanical-biological treatment plant with a size > 1000 000 RLM, located in Bialystok. Additionally determined BOD_5, ammonia nitrogen, nitrates (v), total nitrogen and total phosphorus.

The samples were tested: raw sewage, from the chamber predenitrification, from chamber of phosphorus removal, from the denitrification chamber in place of the dosage of external carbon source - Brenntaplus VP1, from the denitrification chamber at a distance from the place of dosing external

carbon source and samples of treated sewage. Methodology for determining the fraction of COD was developed based on the guidelines of ATV-131. During the studyidentified the followingfractions: S_S – COD of soluble organic easily biodegradable substances, S_I – COD of soluble organic non-biodegradable substances, X_S – COD of organic slowly biodegradable suspensions, X_I – COD of organic non-biodegradable suspensions.

Based on the study was formed the following conclusions that in raw wastewater, the dominating percent-age was recorded for fractions of biodegrad-able contaminants (S_S and X_S) reaching about 80% of the total COD of sewage. Low share content of organic matter in the fraction of S_S and X_S treated wastewater shows the absorption of these fractions by the microorganisms involved in processes for the removal of nitrogen and phosphorus. Low content of quantitative and percentage of organic compounds in the fraction of undissolved COD irreducible X_I in treated wastewater, testifies to its incorporation in activated sludge floc. The technological system of wastewater treatment plant does not change the concentration of the dissolved fraction in the wastewater biologically decomposable S_I. Low concentration of nitrates (V) in the treated wastewater was obtained by dosing an external source of carbon. Removal of pollutants in waste watertreatment plant in Bialystok is correct and is in line with the requirements of Polish law.

Streszczenie

W artykule przedstawiono wyniki badań dotyczące stężeń frakcji ChZT w mechaniczno-biologicznej oczyszczalni ścieków o wielkości >1000 000 RLM, zlokalizowanej w Białymstoku. Dodatkowo oznaczono BZT_5, azot amonowy, azotany (V), azot ogólny oraz fosfor ogólny.

Analizowanio próbki ścieków surowych, z komory predenityfikacji, komory defosfatacji, komory denitryfikacji w miejscu dawkowania zewnętrznego źródła węgla - Brenntaplus VP1, komory denitryfikacji w pewnej odległości od miejsca dawkowania zewnętrznego źródłem węgla oraz ścieki oczyszczone. Metodyka wyznaczania stężeń frakcji ChZT została opracowana na podstawie wytycznej ATV-131. Podczas wykonywania analizy określono następujące frakcje: nierozpuszczalnej materii organicznej, biologicznie wolno rozkładalnej (X_S), rozpuszczonej materii organicznej, biologicznie łatwo rozkładalnej, (S_S), nierozpuszczalnej materii organicznej, biologicznie trudno rozkładalnej (X_I) i rozpuszczonej materii organiczne, biologicznie nierozkładalnej (S_I).

Przeprowadzona analiza pokazała, że w ściekach surowych doprowadzanych do oczyszczalni ścieków ponad 80% materii organicznej określanej jako ChZT stanowiły frakcje biologicznie rozkładalne X_S i S_S. Niskie stężenie udziału procentowego materii organicznej we frakcji S_S oraz X_S w ściekach

oczyszczonych świadczy o przyswajaniu tych frakcji przez mikroorganizmy biorące udział w procesach usuwania związków azotu i fosforu. Niskie stężenie i procentowy udział materii organicznej we frakcji ChZT nierozpuszczalnej nierozkładalnej X_I w ściekach oczyszczonych świadczy o wbudowywaniu jej w kłaczki osadu czynnego. Układ technologiczny oczyszczania ścieków analizowanej oczyszczalni nie miał wpływu na zmianę stężenia rozpuszczonej frakcji biologicznie nierozkładalnej S_I w ściekach. Niskie stężenie azotanów (V) w ściekach oczyszczonych zostało uzyskane z powodu dawkowania zewnętrznego źródła węgla. Usuwanie zanieczyszczeń w oczyszczalni ścieków w Białymstoku przebiega prawidłowo i jest zgodne z polskimi regulacjami prawnymi.

Słowa kluczowe:
oczyszczanie ścieków, frakcje ChZT, zanieczyszczenia biodegradowalne i niebiodgradowalne, denitryfikacja, zewnętrze źródło węgla

Keywords:
wastewater treatment, COD fractions, pollution biodegradable and biodegradable, denitrification, the external carbon source

MIDDLE POMERANIAN SCIENTIFIC SOCIETY OF THE ENVIRONMENT PROTECTION
ŚRODKOWO-POMORSKIE TOWARZYSTWO NAUKOWE OCHRONY ŚRODOWISKA

Annual Set The Environment Protection
Rocznik Ochrona Środowiska

Volume/Tom 19. Year/Rok 2017 ISSN 1506-218X 777-794

Analiza możliwości pozyskiwania deficytowych surowców mineralnych w Polsce

Beata Witkowska-Kita, Katarzyna Biel,
Wiesław Blaschke, Anna Orlicka
Instytut Mechanizacji Budownictwa i Górnictwa Skalnego
Oddział Zamiejscowy, Katowice

1. Wprowadzenie

Zgodnie z definicją wprowadzoną w 2008 r. przez Komitet ds. Kopalin Krytycznych dla Gospodarki Stanów Zjednoczonych (Committee on Critical Mineral Impacts on the US Economy, 2008) oraz stosownie do Komunikatu Komisji Europejskiej do Parlamentu Europejskiego ws. Przeglądu wykazu surowców krytycznych dla UE (Komunikat COM(2014) 297final) surowce deficytowe to grupa kopalin/surowców posiadających istotne znaczenie ekonomiczne, ale w mniejszym stopniu stosowanych w rozwoju nowych technologii, a równocześnie mniej niż pozostałe zagrożonych ryzykiem niedoboru lub braku podaży. Zaliczono do nich m.in: baryt, diatomity, perlit, talk, gliny ceramiczne (wraz z kaolinem), surowce skaleniowe, bentonit, srebro, miedź, piaski kwarcowe, lit, tytan i wapienie, zwane surowcami deficytowymi (Biel, Blaschke, Orlicka i Witkowska-Kita, 2015; Biel, Blaschke, Orlicka i Witkowska-Kita, 2015a; Bolewski, 1993; Bolewski i Gruszczyk, 1982; Radwanek-Bąk, 2011).

W Unii Europejskiej pierwszy kompleksowy raport oraz lista 41 surowców krytycznych została opublikowana w czerwcu 2010 r. w dokumencie EU Commissision Enterprise and Industry: „Critical raw materials for the EU" (Report of the Ad-hoc Working Group on defining critical raw materials, 2010).

2. Źródła deficytowych surowców mineralnych w Polsce

Wobec szerokiego zastosowania surowców mineralnych ważne jest zapewnienie stałego dostępu do bazy surowcowej. Obecnie kraje Unii Europejskiej mają problemy z zapewnieniem stabilnych dostaw surowców, głównie surowców metalicznych. Wynika to z braku złóż wielu kopalin i uzupełnianiem podaży surowcowej tych kopalin importem z krajów spoza Unii Europejskiej. Deficyt surowców jest związany także z wyczerpaniem się złóż czy utrudnionym dostępem do złóż rozpoznanych, a także niezagospodarowaniem obszarów złożowych. Są to przyczyny naturalne, spowodowane budową geologiczną. Ponadto, jednym z powodów braku dostępnych surowców może być sytuacja polityczno-ekonomiczna danego kraju.

W Polsce nie występują złoża kopalin litu oraz kopalin litonośnych. Talk występuje w małych ilościach oraz brak jest perspektyw na odkrycie dużych złóż talku w Polsce. Nie występują także złoża perlitu oraz brak realnych szans na ich odkrycie. Surowce litu, tytanu, perlitu nie są produkowane w Polsce. Natomiast srebro występuje w niewielkich ilościach w rudach miedzi (okolice Lubina i Polkowic, w Miedziance koło Chęcin, w Kletnie koło Stronia Śląskiego oraz w śląsko-krakowskich złożach rud cynku i ołowiu). Obecnie znaczenie gospodarcze mają stratoidalne złoża rud miedziowo-srebrowych, które zlokalizowane są w utworach cechsztynu w niecce północnosudeckiej oraz monoklinie przedsudeckiej. Największe koncentracje tytanu występują w Ławicy Odrzańskiej i Słupskiej. Ich zasoby szacuje się na 12 tys. Mg TiO_2. Złoża tytanomagnetytów znajdują się w rejonie Suwałk, są rozpoznane, ale nie zagospodarowane. Zasoby te są oceniane na ok. 96,4 mln Mg TiO_2. W Polsce nie produkuje się surowców tytanu. Jedno z większych złóż barytu występuje w okolicach Boguszowa. W ww. złożu występuje: baryt z siarczkami (galeną, sfalerytem, chalkopirytem, pirytem), baryt z fluorytem oraz baryt z kwarcem. Obecnie kopalnie barytu zostały zamknięte, a krajowe zapotrzebowanie na baryt pokrywane jest importem. W Polsce diatomity występują w Leszczawce, Jawornicach, Kuźminie, Borku Nowym, Jaworniku. Piaski kwarcowe do produkcji cegły wapienno-piaskowej stanowią złoża czwartorzędowe. Piaski te występują na powierzchni, są też poławiane w nurtach rzek. Złoża tych piasków występują w północnej i środkowej Polsce. Piaski kwarcowe do produkcji

betonów komórkowych tworzą również złoża czwartorzędowe. Polska posiada liczne złoża skał wapiennych, głównie w regionie świętokrzyskim, Wyżynie Krakowsko-Częstochowskiej oraz w Karpatach i Sudetach oraz województwach zachodniopomorskim, pomorskim i warmińsko-mazurskim (wapienie jeziorne). W Polsce bentonitów jest niewiele, występują jako iły bentonitowe i montmorillonitowe (z 50-75% zawartością montmorillonitu i stosunkowo dużą ilością minerałów nieilastych). Występują one w południowej części kraju - na obszarze Zapadliska Przedkarpackiego i Karpat, a także na Kielecczyźnie. Bogata baza zasobowa iłów (glin) kamionkowych, wykorzystywanych w przemyśle ceramicznym występuje na północnym obrzeżu Gór Świętokrzyskich (tzw. glinki baranowskie wieku triasowego w rejonie Suchedniowa i glinki opoczyńskie wieku jurajskiego z okolic Opoczna-Przysucha) oraz na Dolnym Śląsku (tzw. glinki bolesławieckie wieku kredowego i trzeciorzędowego w rejonie Bolesławca oraz niektóre odmiany kamionkowych iłów poznańskich, np. w rejonie Gozdnicy w województwie lubuskim czy krańca koło Wrocławia). Iły barwnie wypalające się są także kopaliną towarzyszącą w eksploatowanych złożach węgla brunatnego Turów i Bełchatów. W 2013 r. bazę zasobową kopalin skaleniowych w Polsce tworzyło 10 złóż kopalin skaleniowo-kwarcowych i kwarcowo-skaleniowych, z których większość zlokalizowana jest na Dolnym Śląsku i jedno złoże w okolicach Krakowa (Komunikat COM (2014)297 final; Galos, Nieć, Radwanek-Bąk, Smakowski i Szamałek, 2012; Galos i Szamałek, 2011).

3. Gospodarka deficytowymi surowcami mineralnymi w Polsce

3.1. Surowce deficytowe metaliczne

Produkcja srebronośnych koncentratów rud miedzi w latach 2008-2013 wahała się w granicach 1150-1200 Mg, a produkcja **srebra** metalicznego, utrzymywała się na poziomie ok. 1200 Mg. Polska jest największym dostawcą i producentem srebra w Europie. W dużych ilościach eksportuje się srebro m.in. do Niemiec i Belgii, a w ostatnich latach obserwuje się zapotrzebowanie ze strony USA i Wielkiej Brytanii na srebro metaliczne wytwarzane w Polsce. W ostatnich latach eksport srebra kształtował się na poziomie 1100-1300 Mg. Import srebra rafinowanego

do Polski w tych latach był nieznaczny i wynosił 5-7 Mg/rok. Jedynie w 2009 r. osiągnął najwyższą wartość 47 Mg/rok. Rzeczywisty poziom zużycia srebra w Polsce jest trudny do określenia, ponieważ brak jest danych m.in. o wielkości odzysku srebra ze złomów, jak i poziomie zapasów u producentów (Smakowski, Galos i Lewocka, 2015).

W Polsce rudy **miedzi** wydobywane są w trzech oddziałach górniczych Legnicko-Głogowskiego Okręgu Miedziowego przez KGHM Polska Miedź S.A.: ZG Lubin (zdolność wydobywcza 7,8 mln Mg/rok), ZG Polkowice-Sieroszowice (zdolność wydobywcza 9,1 mln Mg/rok) i ZG Rudna (zdolność wydobywcza ponad 16,3 mln Mg/rok). W latach 2008-2012 wydobycie brutto rud miedzi utrzymywało się na poziomie 29-30 mln Mg/rok. Przeciętna zawartość miedzi w urobku uległa ograniczeniu z 1,68% w 2009 r. do 1,59% w 2012 r. W odniesieniu do koncentratów rud miedzi, w latach 2008-2013 produkcja utrzymywała się na poziomie 425-429 tys. Mg/rok. Średnia zawartość miedzi w koncentratach w ostatnich latach wynosiła około 23%. Koncentraty rud miedzi oraz surowce miedzionośne (tj. odpady, złomy) różnego pochodzenia przetwarzane są na miedź konwertorową, zawierającą 98,5-99,0% miedzi, która poddawana jest rafinacji ogniowej do miedzi anodowej w hutach KGHM „Polska Miedź" S.A. Produkcja miedzi konwertorowej, w latach 2008-2012, utrzymywała się na poziomie rzędu 540-550 tys. Mg/rok, przy obniżeniu w 2009 r. do poziomu 515 tys. Mg. W odniesieniu do produkcji miedzi anodowej występuje tendencja wzrostowa z 574 tys. Mg w 2009 r. do 656 tys. Mg w 2012 r. W latach 2008-2012 produkcja miedzi rafinowanej (elektrolitycznej) w KGHM mieściła się w granicach 502-571 tys. Mg/rok, osiągając najwyższy poziom w 2011 r. Należy zaznaczyć, iż Polska jest głównym dostawcą miedzi elektrolitycznej oraz jej półproduktów. W ostatnich latach eksport miedzi rafinowanej z Polski systematycznie się zwiększał, osiągając w 2012 r. poziom 333 tys. Mg. Głównymi odbiorcami miedzi rafinowanej były Niemcy i Chiny. Niewielkie ilości miedzi elektrolitycznej (7-27 tys. Mg/rok) były również do Polski importowane. W ostatnich latach głównymi jej dostawcami były Niemcy i Czechy. Natomiast zużycie miedzi elektrolitycznej w latach 2008-2012 kształtowało się na poziomie 203-260 tys. Mg/rok. W trakcie prowadzenia procesu wzbogacania rud miedzi powstają odpady flotacyjne w ilości 20-27 mln Mg/rok. Ich masa stanowi od 93 do 94% wydobytej kopaliny. Odpady te są gromadzone

w stawie osadowym Żelazny Most. Usytuowany on jest na wschód od Polkowic przy miejscowości Rudna, w Legnicko-Głogowskim Okręgu Miedziowym. Odpady są stosowane do nadbudowy zapór i uszczelniania czaszy stawu (Smakowski, Galos i Lewocka, 2015).

W Polsce nie występują złoża kopalin **litu** oraz nie produkuje się jego surowców. W związku z tym zapotrzebowanie na surowce litu pokrywane jest wyłącznie importem tlenku i wodorotlenku litu oraz węglanu litu. W latach 2008-2012 obrót surowcami litu był w Polsce prowadzony na niewielką skalę. Obecnie obserwuje się tendencję wzrostową importowanych tlenków i wodorotlenków litu oraz węglanu litu. W 2013 r. import tlenków i wodorotlenków litu wynosił łącznie 98 Mg, a import węglanu litu wynosił 173 Mg. Głównymi dostawcami tych surowców do Polski są: Chiny, Chile, Rosja i Szwajcaria (Smakowski, Galos i Lewocka, 2015).

W Polsce nie produkuje się surowców **tytanu**. Zapotrzebowanie na ww. surowce pokrywane jest importem. W latach 2008-2009 dostawy tytanu metalicznego i proszku tytanu wahały się w granicach 40 Mg/rok. W latach 2010-2012 odnotowano wzrost wielkości importu tytanu metalicznego do ilości ok. 55 tys. Mg w 2012 r. Natomiast w 2013 r. dostawy tego surowca znacznie się obniżyły i osiągnęły wartość tylko ok. 39 Mg. Głównymi dostawcami tytanu metalicznego i proszku tytanu były Niemcy, Holandia, Chiny, Belgia i Hiszpania. W latach 2008-2013 do Polski sprowadzany był także żelazotytan oraz żelazokrzemotytan głównie z Niemiec, Rosji, Wielkiej Brytanii i Holandii w ilościach 100-290 Mg/rok oraz importowano rudy koncentratu tytanu w ilościach 85-105 Mg/rok (w 2013 r. – 96,3 Mg). Koncentraty ilmenitu i rutylu przetwarzane są na biel tytanową w Zakładach Chemicznych „Police" S.A. metodą siarczanową. W ostatnich pięciu latach wielkość produkcji bieli tytanowej utrzymywała się na poziomie 36-42 tys. Mg/rok. Import bieli tytanowej, głównie z Niemiec, Włoch, Chin i Finlandii, wahał się w przedziale 700-1300 Mg/rok. Brak jest danych o strukturze zużycia tytanu metalicznego, jego stopów oraz wyrobów (Smakowski, Galos i Lewocka, 2015).

3.2. Surowce deficytowe niemetaliczne

Produkcja górnicza **barytu** w Polsce do 1997 r. pochodziła ze złóż Boguszów i Stanisławów, eksploatowanych przez Kopalnię Barytu „Boguszów" Sp. z o.o. Surowce były pozyskiwane ze zgromadzonych

przez kilkadziesiąt lat odpadów poflotacyjnych. W latach 1999-2006 produkcja wahała się w granicach 2-3 tys. Mg/rok, a w 2008 r. wyniosła tylko 324 Mg. Od 2009 r. produkcja barytu nie jest w Polsce prowadzona. Ze względu na niskie wydobycie barytu, zapotrzebowanie na ten surowiec było uzupełniane importem. W ostatnich latach, import stał się wyłącznym źródłem barytu w Polsce. Głównym dostawcą do 2010 r. była Słowacja, pozostałe ilości sprowadzano z Chin, Niemiec, Włoch, Hiszpanii, Wielkiej Brytanii oraz od pośredników holenderskich. Wraz ze wzrostem zapotrzebowania na mączki barytowe, dodatkowo większe ilości sprowadzono z Maroka i niewielkie z Turcji. Obecnie to właśnie z tych krajów pochodzi największa ilość importowanego barytu. W większości sprowadzane są mączki barytowe dla wiertnictwa naftowego, resztę stanowią wyższej jakości mączki dla przemysłu szklarskiego, farb i lakierów, gumowego czy chemicznego. Wielkość importu w latach 2008-2011 wynosiła ok. 10-13 tys. Mg/rok, w 2012 r. osiągnęła wartość 20,1 tys. Mg, a w 2013 r. – 9,7 tys. Mg. W ostatnich latach nastąpiło zwiększenie krajowego zapotrzebowania na baryt. Wynika to z rozwoju poszukiwań gazu ziemnego występującego w łupkach i wzrostu ilości wykonywanych wierceń głębokich, do których m.in. wykorzystywana jest mączka barytowa (Smakowski, Galos i Lewocka, 2015).

Jedynym krajowym producentem **surowców diatomitowych** w Polsce jest Specjalistyczne Przedsiębiorstwo Górnicze „Górtech" w Krakowie, prowadzące od 1992 r. eksploatację złoża Jawornik w kopalni Jawornik Ruski. W tym zakładzie przeróbczym urobek jest przerabiany na granulaty 0,2-2 i 2-5 mm służące jako sorbent, oraz pyły 0-0,5 i 0-1,0 mm do produkcji materiałów termoizolacyjnych. Ze względu na niską jakość materiału wyjściowego produkcja tych wyrobów jest niewielka, w ilości ok. 600 Mg w 2013 r. Z powodu małej ilości diatomitu wysokiej jakości, import tych surowców w latach 2008-2013 wynosił od 7 do 10 tys. Mg/rok. Największym importerem diatomitu do Polski są Stany Zjednoczone i Dania. Zwiększa się też wielkość importu z Niemiec oraz Meksyku. Natomiast eksport surowców diatomitowych kształtował się na poziomie 100-800 Mg/rok, za wyjątkiem znaczących wzrostów do 3 tys. Mg w 2012 r. i 5,4 tys. Mg w 2013 r. Poziom tego importu nie przekracza kilku Mg/rok. Dokładna struktura zużycia diatomitów w Polsce nie jest znana. Obecnie występuje niski poziom zapotrzebowania na surowce diatomitowe w Polsce (Smakowski, Galos i Lewocka, 2015).

W Polsce **perlit** surowy nie jest produkowany. Zapotrzebowanie jest pokrywane całkowicie importem perlitu. W 2013 r. łączny import tego surowca wzrósł do poziomu 22,4 tys. Mg. Największym importerem perlitu są Węgry, mniejszymi dostawcami są Słowacja i Niemcy. W związku z rozwojem produkcji perlitu ekspondowanego w zakładach krajowych, import perlitu systematycznie wzrasta. Ustalenie łącznego poziomu produkcji perlitu ekspandowanego nie jest możliwe, gdyż jest ewidencjonowany łącznie z wermikulitem porowatym, iłami porowatymi, żużlem spienionym i podobnymi porowatymi materiałami mineralnymi, włącznie z ich mieszaninami. Na podstawie danych od krajowych producentów szacuje się, że poziom produkcji perlitu może sięgać 350-450 tys. m^3/rok. Firma Perlipol S.C. w Bełchatowie jest największym krajowym dostawcą perlitu ekspandowanego, oferującym produkty do zastosowań budowlanych, filtracyjnych i rolniczych. Firma bazuje na surowcu sprowadzanym głównie z Węgier, ze Słowacji i Turcji. Posiada ona trzy linie technologiczne do produkcji ekspandowanego perlitu o wydajności 300 tys. m^3/rok. W związku ze wzrostem popytu na perlit do zastosowań budowlanych, który stanowi około 90% łącznej podaży spółki, produkcja systematycznie wzrasta, osiągając poziom 250-270 tys. m^3/rok w latach 2011-2013, i prawie w całości jest zbywana na rynku krajowym. Firma oferuje także agroperlit do zastosowań w ogrodnictwie i perlit filtracyjny do zastosowań w przemyśle spożywczym (cukrownie, browary, producenci soków). Drugim, co do wielkości producentem na rynku polskim, a jednocześnie pionierem produkcji perlitu ekspandowanego są Zakłady Górniczo-Metalowe „Zębiec" w Starachowicach, które w 1999 r. podjęły ekspandację perlitu surowego sprowadzanego z Węgier. Produkcja w latach 2011-2013 wahała się w granicach 66-75 tys. m^3/rok. Perlit produkowany w tych zakładach w 80 % znajduje zastosowanie w budownictwie, rolnictwie, ogrodnictwie (Smakowski, Galos i Lewocka, 2015).

W Polsce nie pozyskuje się **talku** ani surowców pokrewnych. Całkowite zapotrzebowanie na talk i surowce pokrewne (m.in. steatyt) zaspokajane jest importem, głównie z Finlandii i Austrii i wahał się między 26 a 28 tys. Mg/rok, a w 2013 r. wyniósł 34,2 tys. Mg. Do większych dostawców zaliczyć można również Włochy, Holandię, Belgię, Chiny i Francję. Niewielki eksport głównie talku, sproszkowanego kierowany jest na Ukrainę, a także na Białoruś, do Rumunii, Estonii, Czech, Litwy,

Węgier i Niemiec. W Polsce nie jest dokładnie znany poziom zużycia talku i surowców pokrewnych. Łączne zużycie pozorne talku i surowców pokrewnych wahało się w latach 2008-2013 w przedziale 25,1-33,4 tys. Mg/rok, z chwilowym ograniczeniem do 17,6 tys. Mg w 2009 r. (Smakowski, Galos i Lewocka, 2015).

W 2013 r. wydobycie **piasków** do produkcji wyrobów wapienno-piaskowych prowadzone było w 13 kopalniach w 8 województwach. Wielkość produkcji zależy od potrzeb rynków lokalnych i zwykle nie przekracza 50 tys. m^3/rok z pojedynczego złoża. Wydobycie piasków kwarcowych do produkcji betonów komórkowych w 2012 r. było prowadzone w 12 kopalniach w 8 województwach. Wielkość produkcji jest dość zmienna ze względu na zapotrzebowania rynku i nie przekracza z reguły 50 tys. m^3/rok. Łączne wydobycie piasków kwarcowych do produkcji betonów komórkowych kształtowało się w ostatnich latach w przedziale 340-414 tys. Mg/rok, niemniej do wytwarzania betonów komórkowych stosuje się również dobrej jakości surowce ze złóż piasków budowlanych, a także popioły lotne. W 2013 r. wydobycie piasków do produkcji wyrobów wapienno-piaskowych było prowadzone w 20 kopalniach w 12 województwach. Ponadto 7 złóż posiadało status eksploatowanych okresowo, jednak w ostatnim roku wydobycie z nich nie było wykazywane. Piaski do produkcji wyrobów wapienno-piaskowych są surowcami o znaczeniu lokalnym, użytkowanymi w przyległych zakładach. W 2013 r. odnotowano wydobycie na poziomie 519 tys. m^3. W latach 2008-2009 spadła produkcja wyrobów silikatowych (wapienno-piaskowych – cegły, pustaki, bloki, korytka) do poziomu 915-940 tys. m^3/rok, co było spowodowane kryzysem finansowo-gospodarczym. Jednak w kolejnych latach produkcja wzrosła do ponad 1,1 mln m^3 w roku 2013, przy czy w ostatnim okresie można zauważyć zmniejszenie udziału cegły wapienno-piaskowej w łącznej produkcji wyrobów silikatowych z 45% w 2011 r., 48% w 2012 r. do 50% w 2013 r. Wyroby silikatowe stanowią jedynie około 9% ściennych wyrobów budowlanych, zaś największy udział w rynku przypada wyrobom z betonu komórkowego (ponad 43% rynku) oraz z tzw. ceramiki czerwonej (34%) (Smakowski, Galos i Lewocka, 2015).

W Polsce **wapienie** były wydobywane w 2013 r. w 76 odkrywkach, w tym: w 16 kopalniach wapieni i margli dla przemysłu cementowego, 16 kopalniach wapieni dla przemysłu wapienniczego (z czego

dwie odkrywki: Górażdże i Bukowa były eksploatowane dla potrzeb przemysłu cementowego i wapienniczego równocześnie) oraz w 44 kopalniach użytkujących złoża wapieni lub marmurów. W latach 2008-2011 wzrosło znacząco wydobycie różnych gatunków wapieni, osiągając poziom ponad 69,6 mln Mg/rok w 2011 r. W 2012 r. poziom wydobycia wapieni zmniejszył się do poziomu 56,9 mln Mg, a w 2013 r. osiągnął poziom 52,7 mln Mg. Jest to spowodowane mniejszym wydobyciem w grupie kopalin dla potrzeb przemysłu wapienniczego oraz wapieni ze złóż kamieni budowlanych i drogowych, najmniejszy zaś w przypadku wapieni dla potrzeb przemysłu cementowego. Wapienie są wykorzystywane do produkcji kilku grup wyrobów: cementu, wyrobów wapienniczych, kruszyw wapiennych łamanych oraz elementów budowlanych i nawozów. Wyroby wypalane są obecnie produkowane w sześciu zakładach należących do dwóch międzynarodowych koncernów wapienniczych. Ich roczna produkcja wynosi 1500-1800 tys. Mg/rok Wyroby wapienne niewypalane produkowane są w bardzo szerokim asortymencie- kamień wapienny na zbyt, nawozy wapniowe i wapienne kruszywa łamane oraz sorbenty, mączka wapienna, pył wapienny, kreda itp. Kamień wapienny jest dostarczany w znacznych ilościach od dostawców z województwa świętokrzyskiego. Udział ich przekracza obecnie 40% łącznej podaży tego asortymentu wapienniczego. Łączne dostawy kamienia wapiennego kształtowały się na poziomie ok. 12,0 mln Mg/rok w latach 2008-2009, 2011 r. a wzrosły do 19,8 mln Mg, a w 2013 r. obniżyły się do poziomu 17,5 mln Mg. Odbiorcą kamienia jest głównie hutnictwo żelaza i metali nieżelaznych, a także branża cukrownicza i przemysł chemiczny.

Produkcja **wapna**, po wyraźnym spadku do nieco powyżej 1,7 mln Mg w 2009 r., zaczęła wzrastać w kolejnych latach, nieznacznie w 2010 r. i wyraźnie w 2011 r., osiągając poziom ponad 2,0 mln Mg, a w latach 2012-2013 osiągnęła poziom z 2009 r. Głównie produkuje się wapno palone, w mniejszym stopniu wapno hydratyzowane i wapno hydrauliczne. Nawozy wapniowe tlenkowe i węglanowe wytwarzane są z odpadów w zakładach wapienniczych i cementowo-wapienniczych oraz kruszywowych. Produkcja nawozów węglanowych pochodzi w większości ze złóż wapieni jeziornych pozyskiwanych przez lokalnych producentów w północnej części kraju. Ich wydobycie systematycznie maleje. Łączna produkcja nawozów wapniowych w Polsce kształtuje się na po-

ziomie ok. 500 tys. Mg tlenku wapnia/rok. Polska eksportuje przede wszystkim wapno palone. Łączny eksport wapna w latach 2010-2013 wzrósł znacząco i kształtował się na poziomie prawie 90 tys. Mg/rok. Najważniejszymi odbiorcami polskiego wapna są Litwa, Finlandia i Ukraina, natomiast głównymi dostawcami są Niemcy i Słowacja, a okazjonalnie Czechy i Białoruś. W imporcie przeważa wapno palone, stanowiące ostatnio 60-80% łącznych dostaw wapna. Import jest kilkakrotnie niższy od eksportu. Relacje między poziomem eksportu i importu kamienia wapiennego skutkują dodatnim saldem jego obrotów. (Smakowski, Galos i Lewocka, 2015).

Łączna produkcja **bentonitów**, ziem odbarwiających i bielących w Polsce po znacznym spadku w 2009 r., zaczęła stopniowo wzrastać uzyskując w 2011 r poziom 114 tys. Mg, a w 2012 r. i w 2013 r. – 102 tys. Mg. Jedynym z producentów górniczym surowców bentonitowych w Polsce jest obecnie Przedsiębiorstwo Górniczo-Produkcyjne „Bazalt" z Wilkowic. Pozyskuje ono zwietrzelinę smektytową ze złoża Krzeniów i sprzedaje ją w postaci surowej w ilościach 1-3 tys. Mg/rok, obecnie w całości Przedsiębiorstwu Techniczno-Przemysłowemu „Certech". Tradycyjnym dostawcą różnych gatunków bentonitu wzbogaconego na rynek krajowy są Zakłady Górniczo-Metalowe „Zębiec" S.A. koło Starachowic. Od kilkunastu lat ich produkcja bazuje na importowanych bentonitach surowych, pochodzących głównie ze Słowacji (złoże Stara Kremnicka-Jelsovy Potok) i Ukrainy. Kolejnym krajowym dostawcą produktów bentonitowych jest Przedsiębiorstwo Techniczno-Przemysłowe „Certech" z zakładem w Niedomicach k. Tarnowa. Dostawcą żwirków bentonitowych zoologicznych jest też przedsiębiorstwo Celpap Sp. z o.o. z siedzibą w Wieliczce. Wielkość jego produkcji nie jest znana. Dostawcą przetwarzającym bentonity importowane ze Słowacji (głównie ze złóż Brezina-Kuzmice) i Indii jest firma Hekobentonity Sp. z o.o. w Korzeniowie k. Dębicy, dostarczająca głównie produkty bentonitowe i bentonitowo-polimerowe dla wiertnictwa (60% sprzedaży), budownictwa hydrotechnicznego i konstrukcji inżynierskich. Ze względu na łączne traktowanie w statystykach handlu zagranicznego importowanych bentonitów surowych i wzbogaconych, krajowe zapotrzebowanie na surowce przetworzone można jedynie szacować. W ostatnich latach krajowe zużycie różnych gatunków bentonitów wzbogaconych (przetworzonych) w Polsce kształtowała się na poziomie 130-180 tys. Mg/rok.

Znaczne ilości bentonitów pochłania w Polsce przemysł odlewniczy, ceramiczny, spożywczy oraz budownictwo w pracach geoinżynierskich i hydroizolacyjnych (m.in. w budownictwie ziemnym, do uszczelniania podłoża wysypisk odpadów i obwałowań cieków wodnych). Ponadto bentonity znajdują zastosowanie w browarnictwie, winiarstwie i cukrownictwie (jako środek filtrujący do klarowania), a także w przemyśle papierniczym (jako absorbent), kosmetycznym i farmaceutycznym (jako środek żelujący). Krajowe zapotrzebowanie na bentonity surowe niemal w całości pokrywane jest importem. Od kilku lat obserwuje się systematyczny wzrost dostaw, za wyjątkiem 2009 r. w którym odnotowano ich znaczne ograniczenie do ok. 123 tys. Mg. W 2012 r. import wynosił 229,2 tys. Mg, a w 2013 r. – 208,8 tys. Mg. Największym dostawcą tych surowców jest Słowacja (ok. 50% importu). Od 2007 r. za sprawą wzrostu dostaw z Indii (ponad 40 tys. Mg), a od 2009 r. również z Turcji (ponad 30 tys. Mg), udział importu ze Słowacji obniżył się do 40-42%. Na znacznie mniejszą skalę prowadzony jest eksport bentonitów, które wysyłano przeważnie do Niemiec (w 2013 r. niemal 40% sprzedaży zagranicznej) i Rosji (20%). Sprzedaż eksportowa nieznacznie łagodzi ujemne saldo obrotów tymi surowcami. Łączny eksport bentonitów wahał się w granicach od 20,0 tys. Mg (w 2008 r.) do 24,4 tys. Mg (w 2011 r.), a w 2012 r. osiągając wartość 22,9 tys. Mg, a w 2013 r. – 37 tys. Mg przy równoczesnym ograniczeniu importu (Smakowski, Galos i Lewocka, 2015).

Głównymi producentami **iłów (glin)** biało wypalających się w Polsce jest Ekoceramika Sp. z o.o. w Suszkach koło Bolesławca (ich produkcja w ostatnich latach wynosiła 30-40 tys. Mg/rok) oraz Bolesławieckie Zakłady Materiałów Ogniotrwałych w nowym zakładzie przeróbczym w Czerwonej Wodzie koło Węglińca (wielkość ich produkcji w ostatnich latach nie przekraczała 10 tys. Mg/rok). Wydobycie i produkcja iłów (glin) ogniotrwałych do 2008 r. wrastało m.in. dzięki ponownemu rozwojowi zapotrzebowania ze strony przemysłu materiałów ogniotrwałych Całość krajowej produkcji iłów ogniotrwałych pochodzi obecnie ze złoża Rusko-Jaroszów eksploatowanego przez JARO S.A. w Jaroszowie. Począwszy od połowy lat 90-tych nastąpił silny wzrost importu iłów ceramicznych do Polski, który wynikał przede wszystkim z rozwoju zapotrzebowania producentów płytek ceramicznych i wyrobów sanitarnych na iły biało i jasno wypalające się. W latach 2008-2013 wielkość importu

iłów ceramicznych do Polski utrzymywała się na poziomie ok. 300-450 tys. Mg. Eksport iłów ceramicznych jest nieznaczny i w latach 2008-2013 nie przekroczył 56 tys. Mg. W latach 2008-2013 największy poziom produkcji odnotowano w przypadku iłów kamionkowych. Kształtowała się ona na poziomie 512-1291 tys. Mg z tendencją spadkową od 2011 r. Natomiast wielkość wydobycia iłów ceramiki budowlanej o cechach iłów kamionkowych wynosiła w 2013 r. 113 tys. m^3 i uległa zmniejszeniu o ok. 46% w stosunku do 2009 r.

Import iłów pochodził przede wszystkim z Niemiec (w 2013 r. – 134, 3 tys. Mg) i Ukrainy (w 2012 r. – 251,1 tys. Mg, w 2013 r. – 243,8 tys. Mg). W 2013 r. zarejestrowano eksport iłów ceramicznych m. in. do Niemiec na poziomie 12 tys. Mg (Smakowski, 2011; Smakowski, Galos i Lewocka, 2015).

Wydobycie **piasków kaolinitowych** ze złóż Maria III (pow. bolesławiecki) i Dunino (pow. legnicki) w 2013 r. wynosiło 267,0 tys. Mg. Produkcja kaolinu wzbogaconego w Polsce, po znacznym spadku do 125 tys. Mg w 2010 r., w 2011 r. wzrosła o 30%, osiągając poziom 164 tys. Mg. Natomiast w 2012 r. nastąpiło jej zmniejszenie o 13% do wartości 137,8 tys. Mg, głównie w związku z mniejszą ilością zamówień tego surowca przez wytwórców płytek ceramicznych. W 2013 r. wielkość produkcji surowców kaolinowych wyniosła 166 tys. Mg. Rodzima produkcja surowców kaolinowych pochodziła m.in. z następujących zakładów: Surmin-Kaolin S.A. w Nowogrodźcu – łącznie 70-87 tys. Mg/rok, Grudzeń Las Sp. z o.o. w Sławnie k. Opoczna – łącznie 42-65 tys. Mg/rok, Tomaszowskie Kopalnie Surowców Mineralnych Biała Góra Sp. z o.o. w Smardzewicach – łącznie 14-19 tys. Mg/rok.

W latach 2008-2013 odnotowano niewielki eksport kaolinu wzbogaconego głównie do Niemiec i Słowacji i kształtował się on na poziomie 8-13 tys. Mg/rok. Całkowity import kaolinu od 2010 r. systematycznie wzrastał, osiągając w 2013 r. poziom 131,1 tys. Mg. Główne kierunki importu to Niemcy (89,7 tys. Mg) i Czechy (28,1 tys. Mg) (Smakowski, Galos i Lewocka, 2015).

Produkcja **surowców skaleniowo-kwarcowych** w Polsce w 2008 r. osiągnęła najwyższą wartość 640 tys. Mg, natomiast w latach 2009-2013 kształtowała się na poziomie 480-540 tys. Mg.

Największym krajowym dostawcą tych surowców są Strzeblowskie Kopalnie Surowców Mineralnych Sp. z o.o. w Sobótce (ponad 80%

rodzimej podaży), użytkujące złoża granitoidów zlokalizowane w masywie Strzegom-Sobótka: Pagórki Wschodnie, Pagórki Zachodnie, Strzeblów I (od 2007 r.) i Stary Łom (od 2011 r.). Produkcja wynosiła ok. 500 tys. Mg/rok. W analizowanym okresie import surowców skaleniowych do Polski osiągnął maksymalny poziom 412 tys. Mg w 2011 r., a najniższą wartość w 2009 r. – 276 tys. Mg. Największymi dostawcami surowców skaleniowych, zwykle o charakterze sodowym, tj. z przewagą Na_2O nad K_2O w składzie chemicznym były Turcja (w 2012 r. – 133,0 tys. Mg, w 2013 r. – 137,7 tys. Mg) i Czechy (w 2012 r. – 132 tys. Mg, w 2013 r. – 136,4 tys. Mg). Import prowadzony był również z Francji. Wielkość eksportu surowców skaleniowym w 2012 r. wyniosła 8,6 tys. Mg, a w 2013 r. – 9,1 tys. Mg. Regularnymi odbiorcami były: Ukraina, Rosja i Węgry. W 2009 r. ich krajowe zużycie zmniejszyło się do 745 tys. Mg, tj. o 23% w stosunku do poprzedniego roku. W następnych latach nastąpił wzrost zużycia do poziomu 940 tys. Mg w 2011 r. Natomiast całkowite zużycie tych surowców w 2012 r. osiągnęło poziom 842,9 tys. Mg, a w 2013 r. – 878,4 tys. Mg (Smakowski, Galos i Lewocka, 2015).

4. Podsumowanie

4.1. Surowce deficytowe metaliczne

Na podstawie zebranych informacji można stwierdzić, że Polska, w zakresie surowców deficytowych metalicznych, jest:

- producentem miedzi (niecały 1 mln Mg/rok) oraz srebra (ok. 2,4 tys. Mg/rok),
- eksporterem miedzi głównie elektrolitycznej i rafinowanej (eksportuje 1/3 ilości miedzi wyprodukowanej m. in. do Niemiec, Chin, Czech) oraz srebra (Niemcy, Belgia, USA, Wielka Brytania),
- importerem: miedzi (Chile, Maroko) oraz litu i tytanu.

W Polsce nie występują złoża kopalin litu oraz nie produkuje się litu i surowców tytanu (z wyjątkiem bieli tytanowej w ilości 38,8 tys. Mg/rok). Zapotrzebowanie na lit w postaci tlenków i wodorotlenków litu oraz węglanu litu pokrywane jest importem z Chin, Chile, Rosji i Szwajcarii. Zapotrzebowanie na tytan jest pokrywane importem tytanu metalicznego i proszku tytanu z Niemiec, Holandii, Chin, Belgii i Hiszpanii.

W Polsce jest największe zużycie miedzi (ok. 660 tys. Mg/rok), lecz nie przewyższające jej produkcji. Zużycie tytanu wynosi ponad 120 tys. Mg/rok, czego ok. 70% pochodzi z importu. Najniższe jest zużycie srebra (ok. 1,2 tys. Mg/rok) i litu (ok. 0,2 tys. Mg/rok).

4.2. Surowce deficytowe niemetaliczne

Na podstawie informacji przedstawionych powyżej można stwierdzić, że Polska, w zakresie surowców deficytowych niemetalicznych, jest:

- dużym producentem i eksporterem wapieni i wapna (łącznie) na Litwę i Ukrainę oraz do Finlandii i Niemiec w postaci wapna palonego oraz kamienia wapiennego,
- importerem kaolinu - główne kierunki importu to m. in.: Niemcy, Czechy, Wielka Brytania oraz Ukraina,
- eksport kaolinu wzbogaconego odbywał się do Niemiec Czech i Wielkiej Brytanii Najbardziej regularnym odbiorcą tego surowca były Niemcy, a największym – Słowacja,
- importerem: barytu (głównie Słowacja oraz Chiny, Niemcy, Włochy, Hiszpania, Wielka Brytania, Maroko i Turcja), perlitu (głównie Węgry i Słowacja), talku (głównie Francja i Austria), których się nie produkuje bądź nie wydobywa się oraz wapieni i diatomitu,
- importerem iłów (glin) były Niemcy i Ukraina zarejestrowano także reeksport iłów ceramicznych m. in. do Niemiec na poziomie ok. 10 tys. Mg/rok,
- największymi dostawcami surowców skaleniowych były Turcja i Czechy. Import prowadzony był również z Norwegii, Niemiec i Francji,
- regularnymi eksporterami surowców skaleniowym były: Ukraina, Rosja i Węgry.

Wydobycie piasków i ich wyrobów wynosiło łącznie ok. 2,3 mln m^3 (3,8 mln Mg) w 2012 r., a w 2013 r. – ok. 1,95 mln m^3 (3,6 mln Mg).

Zapotrzebowanie (zużycia) surowców deficytowych niemetalicznych w Polsce było następujące:

surowce	zapotrzebowanie (zużycie) w 2013 r. [tys. Mg]
wapienie	34 984,0
piaski	3 600,0
wapno	1 678,8
skalenie	878,4
kaolin	287,1
bentonity*	180,0
iły (gliny ceramiczne)**	42,8
talk i steatyt	33,4
perlit	22,0
baryt	9,7
diatomity i surowce pokrewne	2,0

**w 2012 r., za 2013 r. – bd*
*** tylko iły ogniotrwałe*

W Polsce największym poziomem zużycia surowców deficytowych niemetalicznych charakteryzuje się grupa wapieni (34 mln Mg/rok). Zapotrzebowanie na piaski jest na poziomie 3,8 mln Mg/rok, a na wapno na poziomie 1,7 mln Mg/rok. Zapotrzebowanie krajowe na skalenie ok. 880 tys. Mg/rok, na kaolin jest na poziomie 290 tys. Mg/rok. Zużycie bentonitów szacuje się na ok. 180 tys. Mg/rok. Zużycie glin ceramicznych to poziom 42 tys. Mg/rok. Zużycia talku i steatytu wynosi 33,4 tys. Mg/rok, perlitu – 22 tys. Mg/rok, a barytu – niecałe 10 tys. Mg/rok. Natomiast diatomity i surowce pokrewne osiągają poziom zużycia ok. 2 tys. Mg/rok.

Podsumowując, można stwierdzić, że niewielkie zasoby krajowych złóż surowców niemetalicznych deficytowych lub ograniczone możliwości eksploatacji tych złóż, sprawiają, że zapotrzebowanie na te surowce pokrywane jest w dużej mierze importem, a rozwój technologii ich pozyskiwania i przeróbki jest znikomy.

Literatura

Biel, K., Blaschke, W., Orlicka, A., Witkowska-Kita, B. (2015). Studium pozyskiwania surowców deficytowych w Polsce. Proceedings International Conference „*The present and Future of the Mining*". Demanowska Dolina. Slivak Republik: Wydawnictwo Slovakian Mining Society, 37-51.

Biel, K., Blaschke, W., Orlicka, A., Witkowska-Kita, B. (2015a). Surowce deficytowe – studium pozyskiwania w Polsce. Monografia: *Innowacyjne i przyjazne dla środowiska techniki i technologie przeróbki surowców mineralnych*. Gliwice: Wydawnictwo ITG KOMAG, 158-170.

Bolewski, A. (red.). (1993). *Encyklopedia surowców mineralnych*. Kraków: Wydawnictwo CPPGSMiE PAN.

Bolewski, A., Gruszczyk, H. (1982). *Surowce mineralne. Źródła-Produkcja-Gospodarka-Informacja*. Surowce Mineralne Świata. Warszawa: Wydawnictwo Geologiczne.

Committee on Critical Mineral Impacts on the U.S. Economy – Minerals, Critical Minerals and the U.S. Economy–Committee on Earth Resources, National Research Council of the National Academies–Washington (D.C.) USA, 2008.

Critical raw materials for the EU – Report of the Ad-hoc Working Group on defining critical raw materials. EU Commission Enterprise and Industry, 2010.

Komunikat Komisji do Parlamentu Europejskiego, Rady Europejskiego Komitetu Ekonomiczno-Społecznego i Komitetu Regionów w sprawie przeglądu wykazu surowców krytycznych dla UE i wdrażania inicjatywy na rzecz surowców. Bruksela. COM (2014)297 final.

Galos, K., Nieć, M., Radwanek-Bąk, B., Smakowski, T., Szamałek, K. (2012). *Bezpieczeństwo surowcowe Polski w Unii Europejskiej i na świecie*. Biuletyn Państwowego Instytutu Geologicznego, (2011)452, 43-52.

Galos, K., Szamałek, K. (2011). *Ocena bezpieczeństwa surowcowego Polski w zakresie surowców nieenergetycznych.* Zeszyty Naukowe Instytutu Gospodarki Surowcami Mineralnymi i Energii Polskiej Akademii Nauk, *81*, 37-58.

Radwanek-Bąk, B. (2011). Zasoby kopalin Polski w aspekcie oceny surowców krytycznych Unii Europejskiej. *Gospodarka Surowcami Mineralnymi*, Kraków: Wydawnictwo Instytutu Gospodarki Surowcami Mineralnymi i Energii Polskiej Akademii Nauk, *27(1)*, 5-19.

Smakowski, T. (2011). *Surowce mineralne – krytyczne czy deficytowe dla gospodarki UE i Polski.* Zeszyty Naukowe Instytutu Gospodarki Surowcami Mineralnymi i Energii Polskiej Akademii Nauk, *81*, 59-68.

Smakowski, T., Galos, K., Lewocka, E. (red.) (2015) *Bilans gospodarki surowcami mineralnymi Polski i świata 2013.* Warszawa: Wydawnictwo Instytutu Gospodarki Surowcami Mineralnymi i Energii Polskiej Akademii Nauk.

Analysis of Obtainment Potential of Deficit Minerals in Poland

Streszczenie

W 2008 r. Komitet ds. Kopalin Krytycznych dla Gospodarki Stanów Zjednoczonych przedstawił definicję surowców strategicznych, która została również przyjęta przez kraje Unii Europejskiej

Grupę surowców strategicznych stanowi 14 surowców, tj.: baryt, diatomity, perlit, talk, gliny ceramiczne (wraz z kaolinem), surowce skaleniowe, surowce boru, bentonit, srebro, miedź, piaski kwarcowe, lit, tytan i wapienie. Mają one ważne znaczenie ekonomiczne i charakteryzują się wysokim ryzykiem niedoboru lub braku podaży. Sytuacja ta jest wynikiem ograniczonej ilości źródeł ich pozyskiwania. Niniejszy rozdział prezentuje podsumowanie pracy przeglądowej IMBiGS dotyczącej surowców deficytowych. Praca ta zawierała m. in. informacje o: kopalinach/surowcach krytycznych i ich właściwościach fizykochemicznych oraz ich występowaniu i wydobyciu w Polsce, stosowanych technologiach wzbogacania rud i przetwórstwie koncentratów w celu pozyskania surowców deficytowych a także gospodarce surowcami deficytowymi w Polsce oraz o obszarach ich zastosowania.

Kompleksowa ocena potencjału surowcowego krajów Unii Europejskiej oraz identyfikacja tzw. surowców krytycznych, niezbędnych dla jej harmonijnego i zrównoważonego rozwoju gospodarczego oraz postępu technologicznego, jest jednym z priorytetów polityki surowcowej UE.

Abstract

In 2008 Committee on Critical Mineral Impacts of the U.S. Economy, presented a definition of deficit raw materials, which was also adopted by the countries of the European Union.

A group of deficit raw materials includes 14 minerals/materials which have economic importance and have a high risk of deficiency or lack of supply. These are: barytes, diatomites, perlite, talc, clay ceramics (including kaolin), feldspar, raw material boron, bentonite, silver, copper, silica sands, lithium, titanium and limestone. Such situation is the result of a limited number of

sources of acquisition. This paper is a summary of the review work performed by IMBiGS for deficit raw materials. This work contains information on: fuels/raw materials and their physico-chemical properties, occurrence and production in Poland, enrichment of ores and processing concentrates, deficit raw materials management in Poland and the fields of application of these materials.

A comprehensive assessment of mineral potential of the European Union countries and the identification of the so-called deficit raw materials necessary for its harmonious and sustainable economic development and technological progress, is one of the priorities of the EU's raw materials policy.

Słowa kluczowe:
surowce deficytowe, raport Komitetu UE, technologie pozyskiwania, produkcja, zapotrzebowanie

Keywords:
deficit raw materials, the report of the Committee of the EU, technology acquisition, production, demand

MIDDLE POMERANIAN SCIENTIFIC SOCIETY OF THE ENVIRONMENT PROTECTION
ŚRODKOWO-POMORSKIE TOWARZYSTWO NAUKOWE OCHRONY ŚRODOWISKA

Annual Set The Environment Protection
Rocznik Ochrona Środowiska

Volume/Tom 19. Year/Rok 2017 ISSN 1506-218X 795-808

Probabilistic and Statistical Modelling of the Harmful Transport Impurities in the Atmosphere from Motor Vehicles

Waldemar Wojcik[*], *Saltanat Adikanova*[**], *Yerzhan Amangazinovich Malgazhdarov*[**], *Muratkan Nabenovich Madiyarov*[**], *Anar Bazarovna Myrzagaliyeva*[**], *Nurlan Muhanovich Temirbekov*[**], *Mukhtar Junisbekov*[**], *Lucjan Pawłowski*[*]

[*]*Lublin University of Technology, Poland*
[**]*East Kazakhstan State Technical University, Ust-Kamenogorsk, Kazakhstan,*

1. Introduction

Realization of the concept of sustainable development depends, among others, on preservation of the caring capacity of global environment. Transport contributes significantly to deterioration of the environment in two ways: rise of CO_2 emissions and thus accelerated climate change (Olejnik & Sobiecka 2017, Drastichowa 2017, Cel et al. 2016, Żukowska et al. 2016) and rising local concentration of particulate matter, mostly PM 2.5 and nitrogen oxides causing acid rain (Cao et al. 2016). Therefore, mitigation of the negative impact of the transport is of great importance.

One of the central problems of describing the transport of harmful impurities in the atmosphere is the mathematical modelling of the gas and aerosol composition variability in the atmosphere, as well as the assessment of the effect of atmospheric contaminants on the environment.

The atmosphere is a complex dynamic and turbulent system in which various dynamic and physicochemical processes occur.

For the turbulent flow of the atmosphere, chaotic random velocity pulsations are characteristic in all directions at all points of the flow, giving almost all stochastic processes to all the processes taking place. The consequence of chaotic pulsation motions is disorderly intensive mixing and specific turbulent diffusion, considerably exceeding the molecular, turbulent viscosity of the gas, more uniform than in laminar flow, the distribution of the averaged velocity and its sharp drop in the wall region, a sharp increase in friction losses.

2. Modelling

The instantaneous velocity of the atmosphere at any point of the flow in each direction can be represented as the sum of the averaged velocity and the velocity of pulsations:

$$u = \overline{u} + u', \quad v = \overline{v} + v', \quad u = \overline{w} + w' \tag{1}$$

The statement of these expressions in the Navier-Stokes equations of motion and averaging over time and space leads to the Reynolds equations of motion, which include additional tangential stresses,

Causing increased viscosity and hydraulic resistance. Statistical or semiempirical theories of turbulence are used to close the system of equations, an analogy between turbulent and molecular stresses is used, experimental data on the statistical relationships between pulsations in space and in time (Antonia & Luxton 1971, Betchov 1977, Riahi 2000). However, the use of the statistical theory requires preliminary information about the turbulent flow characteristics, therefore the statistical-phenomenological theories of turbulent transport that are characterized by the intensity and scale or kinetic energy of the pulsation motion and the rate of its dissipation have become most widespread (Tennekes & Lumley 1972, Simpson et al. 1990, Trunev 1996, Holt & Raman 1988). To describe the processes of turbulent transport, along with the equations of the averaged turbulent flow, the balance equations of the pulsating energy are applied, additional hypotheses are adopted for closing the system of equations (Hurley 1997, Hogstrom 1996).

It is usually assumed that the mutual influence of particles can be neglected and their stochastic motion is determined only by the turbu-

lence of the flow (Castillo 1997, Swinney & Gollub 1981). Due to the complicated turbulent structure of the flow, considerable simplifying assumptions are made in determining the diffusion behaviour and the turbulent diffusion coefficient of the particles, depending on the flow parameters and particle characteristics. In addition, it is often assumed that isotropic turbulence which is satisfactorily confirmed under normal conditions by experimental data.

The main drawback of all diffusion models is the assumption that the field of turbulent pulsations is homogeneous in all directions, in addition, as already noted, the nature of the motion of a dispersed phase in a turbulent flow is probably stochastic, and attempts to describe it by deterministic dependencies significantly reduce the possibilities for analyzing and making managerial decisions . The use of deterministic methods in most cases makes it possible to determine only the approximate or averaged values of the parameters and characteristics of the process, which often leads to errors, a decrease in the accuracy of calculations, or the need for introducing empirical coefficients. And the use of diffusion models leads, in addition, to the necessity of introducing very vague coefficients of longitudinal mixing or effective diffusion, which do not have a clear physical meaning (Edward 1993, Paladin & Vulpiani 1986).

In this paper, we consider the numerical implementation of the probably statistical model described in (Sugak 2003) for modelling the distribution of harmful impurities in the atmosphere from vehicles using the example of the city of Ust-Kamenogorsk.

In the atmosphere, a particle of an impurity can move together with air currents or under the influence of external forces, or through turbulent diffusion under the influence of turbulent pulsations of the atmosphere. Accordingly, the trajectory of motion of impurity particles can be considered as a total random path: any of its coordinates at any time can be represented as the sum of the deterministic and random components:

$$x(t) = \int_0^t u_x(t)dt + x'(t), \tag{2}$$

where $x(t)$ is the projection of the deterministic velocity, m/s and $x'(t)$ is Random process.

If we consider the motion of an impurity particle as a sequence of discontinuous displacements of length h in small intervals Δt in one of the six possible directions in an orthogonal coordinate system xyz, then the trajectory of motion will be a three-dimensional broken line, and the direction of motion at each instant of time will be determined by the corresponding probabilities: p_i: p_{+x}, p_{-x}, p_{+y}, p_{-y}, p_{+z}, p_{-z}.

It is obvious that at any time

$$p_{+x}(t)+p_{-x}(t)+p_{+y}(t)+p_{-y}(t)+p_{+z}(t)+p_{-z}(t)=1. \qquad (3)$$

In the absence of convective motion and the influence of external forces, with isotropic turbulence, when a particle of an impurity performs only random movements, all directions of motion are equally probable and the probabilities are the same:

$$p_{+x}(t)=p_{-x}(t)=p_{+y}(t)=p_{-y}(t)=p_{+z}(t)=p_{-z}(t)=\frac{1}{6}$$

Let us consider the transfer of a single impurity particle from a point source (for example, from a tube of industrial enterprise). Let the wind direction coincide with the axis Ox. Then we can proceed to a two-dimensional coordinate system xOz, and at each instant of time consider the motion of impurity particles in one of four possible directions. And the probabilities of each direction will be p_{+x}, p_{-x}, p_{-z} and $p_{-z}\left(p_{+x}(t)+p_{-x}(t)+p_{+z}(t)+p_{-z}(t)=1\right)$.

Obviously, in the absence of wind and isotropic turbulence $p_{+x} = p_{-x} = p_{+z}, = p_{-z} = 1/4$. And in the presence of wind, with a direction coinciding with the axis, its influence can be expressed in terms of the ratio of the corresponding probabilities of the directions of motion: with ascending currents and isotropic turbulence in a fixed coordinate system $p_{+x}(t) \succ p_{-x}(t)=p_{+z}(t)=p_{-z}(t)$.

Using the above described model, for known values of probabilities p_i and a random number generator, variants of possible trajectories of one and ten impurity particles in a turbulent flow are calculated (Fig. 1 and Fig. 2, respectively).

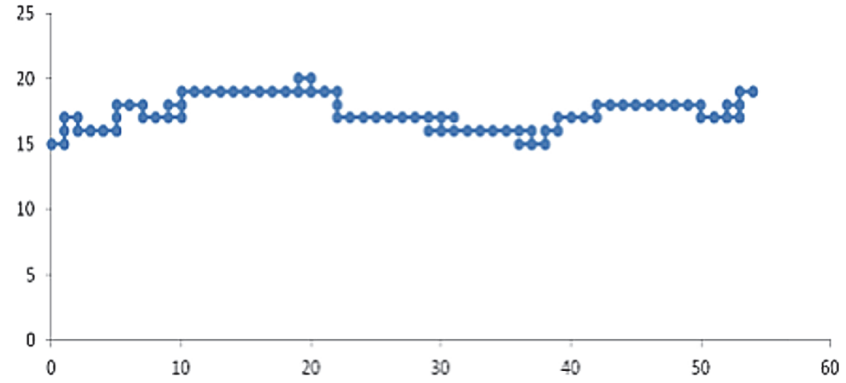

Fig. 1. One particle, $p_{+x} = 0.7$, $p_{-x} = p_{+y} = 0.1$ (100 steps)
Rys. 1. Jedna cząstka, $p_{+x} = 0{,}7$, $p_{-x} = p_{+y} = 0{,}1$ (100 kroków)

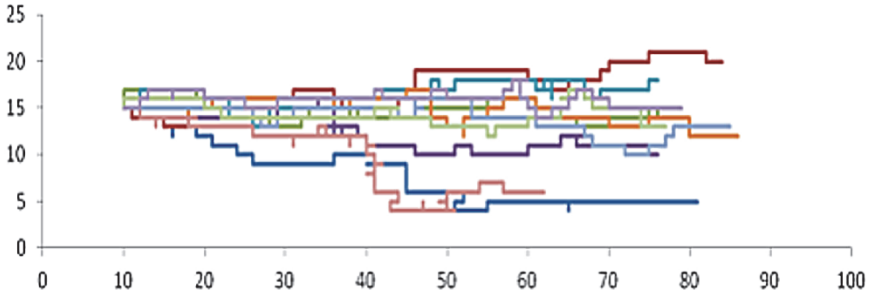

Fig. 2. 10 particles, $p_{+x} = 0.7$, $p_{-x} = p_{+y} = 0.1$ (10x100 steps)
Rys. 2. 10 cząstek, $p_{+x} = 0{,}7$, $p_{-x} = p_{+y} = 0{,}1$ (10 x 100 kroków)

But this approach makes it difficult to calculate when there are many sources and volumes of emissions of harmful substances. However, it can be noted that at any time, each particle can be in one of these grid nodes and each of these positions can be considered as a possible state of the particle at the time instant with a corresponding probability $P(i, j, t)$ where i, j are numbers of grid nodes).

Suppose that the probabilities of all positions of the particle are known at the time t, and we consider the change in the probability of finding the particle in position (i, j) through a small time interval Δt

At time $t + \Delta t$ the probability of a particle $P(i, j, t + \Delta t)$ can be determined by two cases: the first is when the position (i, j) flows in from neighbouring nodes $((i - 1), (i + 1, j), (i, j - 1)$ and $(i, j + 1))$; Second when flowing into neighbouring nodes $((i - 1, j), (i + 1, j), (i, j - 1)$ and

$(i, j + 1)$) (Figure 3). Presumably at each moment of time $t + \Delta t$, the position*(i, j)* is determined by the probable direction of the particle's transition $p_{l,i,j}^{n+1}, l = \{+z,-x,+z,-z\}$ and accordingly what is flowing in is added, but what is flowing is taken away. Thus, the equation for determining the probability of finding a particle at a position (i, j) at the time $t + \Delta t$ moment is as follows:

$$P_{i,j}^{n+1} = P_{i,j}^{n} + p_{+x,i,j}^{n+1} P_{i-1,j}^{n} + p_{-x,i,j}^{n+1} P_{i+1,j}^{n} + p_{+z,i,j}^{n+1} P_{i,j-1}^{n} + p_{-z,i,j}^{n+1} P_{i,j+1}^{n} + \\ + \left(p_{+x,i,j}^{n+1} + p_{-x,i,j}^{n+1} + p_{+z,i,j}^{n+1} + p_{+z,i,j}^{n+1}\right) P_{i,j}^{n} \tag{4}$$

where $P_{i,j}^{n+1}$ is the probability of finding a particle at the moment of time $t + \Delta t$ in position (i, j), $p_{+x,i,j}^{n+1}$ is the probability of transitions to (i, j), and from the position (i, j), at time $t + \Delta t$

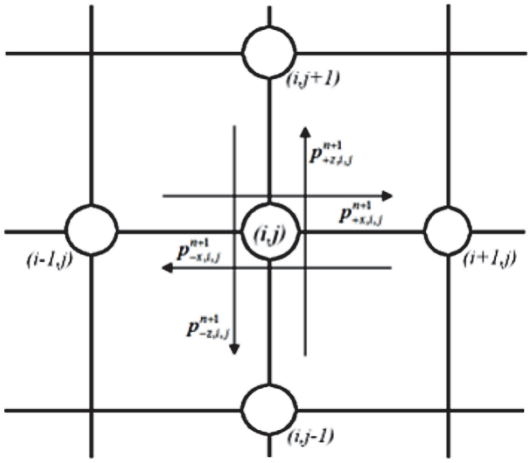

Fig. 3. Schemes of particle transitions
Rys. 3. Schematy przejścia cząstek

For a recurrent Poisson flow of events with $\mu_l(i, j)\Delta t << 1$:

$$p_{l,i,j}^{n+1} = 1 - \exp\left[-\mu_l(i, j)\Delta t\right] \approx 1 - \exp\left[-\mu_l(i, j)\Delta t\right] = \mu_l(i, j)\Delta t$$

where μ_l, $l = \{+z,-x,+z,-z\}$ is the intensity of the corresponding transitions, which in the turbulent flow are determined by the intensity of the turbulent pulsations c^{-1}.

Analogous approximations can also be written for all transitions denoting $\mu_{l,i,j}$. Then equation (4) takes the form

$$P_{i,j}^{n+1} = P_{i,j}^{n} + \mu_{+x,i,j}\Delta t P_{i-1,j}^{n} + \mu_{-x,i,j}\Delta t P_{i+1,j}^{n} + \mu_{+z,i,j}\Delta t P_{i,j-1}^{n} + \mu_{-z,i,j}\Delta t P_{i,j+1}^{n} - \\ -\left(\mu_{+x,i,j} + \mu_{-x,i,j} + \mu_{+z,i,j} + \mu_{-z,i,j}\right)P_{i,j}^{n}\Delta t \tag{5}$$

It is possible to obtain from expression (5)

$$\frac{P_{i,j}^{n+1} - P_{i,j}^{n}}{\Delta t} = \mu_{+x,i,j}P_{i-1,j}^{n} + \mu_{-x,i,j}P_{i+1,j}^{n} + \mu_{+z,i,j}P_{i,j-1}^{n} + \mu_{-z,i,j}P_{i,j+1}^{n} - \\ -\left(\mu_{+x,i,j} + \mu_{-x,i,j} + \mu_{+z,i,j} + \mu_{-z,i,j}\right)P_{i,j}^{n}$$

Passing to the limit for$\Delta t \to 0$, we obtain a differential equation with respect to the probability of finding the particle at the time t instant at the point (i, j):

$$\frac{\partial P}{\partial t} = \mu_{+x,i,j}P_{i-1,j}^{n} + \mu_{-x,i,j}P_{i+1,j}^{n} + \mu_{+z,i,j}P_{i,j-1}^{n} + \mu_{-z,i,j}P_{i,j+1}^{n} - \\ -\left(\mu_{+x,i,j} + \mu_{-x,i,j} + \mu_{+z,i,j} + \mu_{-z,i,j}\right)P_{i,j}^{n} \tag{6}$$

The probability of finding a single particle in any position $P_{i,j}^{n}$ in accordance with the law of large numbers simultaneously means the fraction of particles $N(i,j,t)/N$ from their total number in the system that are in an elementary volume $V(i,j)$ by the cross $h_x \times h_z$ section at time t, that is,

$$P_{i,j}^{n} = \frac{N(i,j,t)}{N} = \varphi_{i,j}^{n}\frac{V(i,j)}{N} \tag{7}$$

where $\varphi_{i,j}^{n}$ is the local numerical impurity concentration, m^{-3}.

Substituting expressions (7) into equations (6), we can obtain the following expression

$$\frac{V(i,j)}{N}\frac{\partial \varphi}{\partial t} = \mu_{+x,i,j}\frac{V(i,j)}{N}\left(\varphi_{i-1,j}^{n} - \varphi_{i,j}^{n}\right) + \mu_{-x,i,j}\frac{V(i,j)}{N}\left(\varphi_{i+1,j}^{n} - \varphi_{i,j}^{n}\right) + \\ + \mu_{+z,i,j}\frac{V(i,j)}{N}\left(\varphi_{i,j-1}^{n} - \varphi_{i,j}^{n}\right) + \mu_{-z,i,j}\frac{V(i,j)}{N}\left(\varphi_{i,j+1}^{n} - \varphi_{i,j}^{n}\right) \tag{8}$$

Taking into account that the total number of divisions and the elementary volume is constant and adding a function describing the sources of harmful emissions into equations (8), we obtain

$$\frac{\partial \varphi}{\partial t} = \mu_{+x,i,j}\left(\varphi^n_{i-1,j} - \varphi^n_{i,j}\right) + \mu_{-x,i,j}\left(\varphi^n_{i+1,j} - \varphi^n_{i,j}\right) + \\ + \mu_{+z,i,j}\left(\varphi^n_{i,j-1} - \varphi^n_{i,j}\right) + \mu_{-z,i,j}\left(\varphi^n_{i,j+1} - \varphi^n_{i,j}\right) + f \tag{9}$$

where f is the function describing the source of emission of harmful substances.

The system of differential equations (9) for given initial and boundary conditions makes it possible to determine the concentration of harmful impurities and its variation. We will consider two types of boundary conditions: a free boundary and a solid wall. In a free boundary, we exclude those terms that go beyond the boundary. For example, on the border $x = X$:

$$\left.\frac{\partial \varphi}{\partial t}\right|_{x=X} = \mu_{+x,n_1,j}\left(\varphi^n_{n_1-1,j} - \varphi^n_{n_1,j}\right) + \mu_{-x,n_1,j}\left(-\varphi^n_{n_1,j}\right) + \\ + \mu_{+z,i,j}\left(\varphi^n_{n_1,j-1} - \varphi^n_{n_1,j}\right) + \mu_{-z,i,j}\left(\varphi^n_{n_1,j+1} - \varphi^n_{n_1,j}\right) + f \tag{10}$$

This means that the admixture from the calculated region flows unhindered, but does not flow in. Thus, if necessary, it is possible to determine the volume of impurities derived from the calculated region, to determine the self-cleaning of the atmosphere by wind regimes.

If the boundary is a solid wall, for example, on the boundary $z = 0$:

$$\left.\frac{\partial \varphi}{\partial t}\right|_{z=0} = \mu_{+x,i,1}\left(\varphi^n_{i-1,1} - \varphi^n_{i,1}\right) + \mu_{-x,i,1}\left(\varphi^n_{i+1,1} - \varphi^n_{i,1}\right) + \\ + \mu_{+z,i,1}\left(-\varphi^n_{i,1}\right) + \mu_{-z,i,1}\left(\varphi^n_{n_1,2}\right) + f \tag{11}$$

In this case, the impurity does not flow in and out. Similarly, one can obtain boundary conditions for all boundaries of the region under consideration.

The intensities of the transitions $\mu_{+x,i,j}$, $\mu_{-x,i,j}$, $\mu_{+z,i,j}$ and $\mu_{-z,i,j}$ are determined by the determined velocities and intensities of the turbulent pulsations in the corresponding directions. The velocity of a particle of impurities in any direction is determined by the sum of the deterministic and random components

$$u = \overline{u} + u' \tag{12}$$

Then the total intensity of the transitions along any of the axes is determined by the sum of the averaged deterministic velocity and the turbulent pulsations.

$$\mu_{+x} = u + \mu_{+x}, \mu_{-x} = \left|-u\right| + \mu_{-x}, \mu_{+z} = w + \mu_{+z}, \mu_{-z} = \left|-w\right| + \mu_{-z}$$

where *u, w* are the components of wind speed. In the atmosphere in the absence of wind, the intensity of turbulent pulsations in all directions can be considered identical, i.e. $\mu_{+x} = \mu_{-x} = \mu_{+z} = \mu_{-z}$.

If we assume that the wind direction coincides with the direction of the axis *Ox*, then the intensity of the transitions will be determined as follows:

$$\mu_{+x} = \overline{u}_x + \mu_{+x}, \mu_{-x} = \mu_{+z} = \mu_{-z}$$

When the equations (9) are numerically realized from the intensity of the transitions $\mu_{+x,i,j}$, $\mu_{-x,i,j}$, $\mu_{+z,i,j}$ and $\mu_{-z,i,j}$ only one takes the value 1, and the remaining ones 0. This approach ensures that conditions (3) are satisfied. And which of them takes the value 1, is determined with the help of a random number generator.

Using the above-described probabilistic-stochastic model, methodical calculations of impurity transfer from point and linear sources have been carried out.

Figures 4 and 5 clearly show the effect of the wind speed regime. At a wind speed of 3 m/s, the impurity is carried away faster, without having time to succumb to diffusion processes. And with a wind speed of 1 m/s, the transfer process is slower.

And in Figures 6 and 7 the results of calculations of the transport of harmful impurities from linear sources on the horizontal section are presented. In Figure 5, the initial values of emissions on the main roads of the city used in (Danaev et al. 2014), and in Figure 6, the results of numerical calculations of the problem (9)-(11), which coincides with the results of (Danaev et al. 2014).

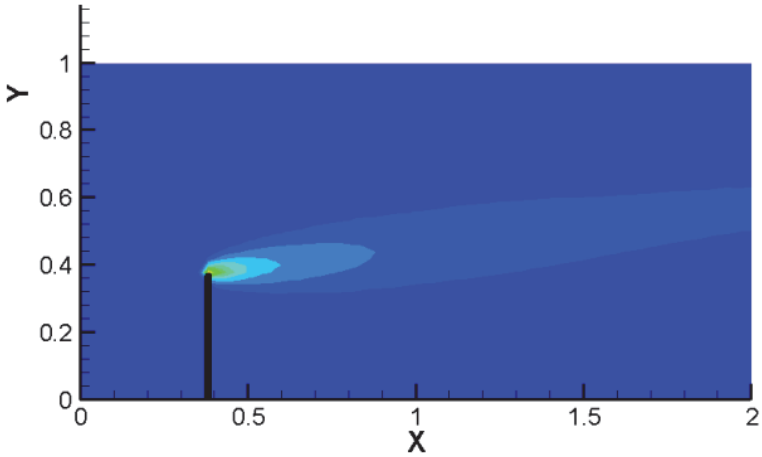

Fig. 4. Wind speed 3 m/s, point source
Rys. 4. Prędkość wiatru 3 m/s, źródło punktowe

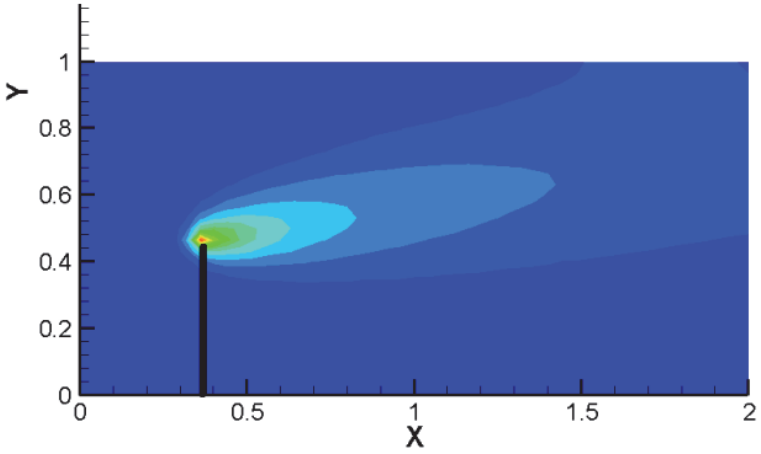

Fig. 5. Wind speed 1 m/s, point source
Rys. 5. Prędkość wiatru 1 m/s, źródło punktowe

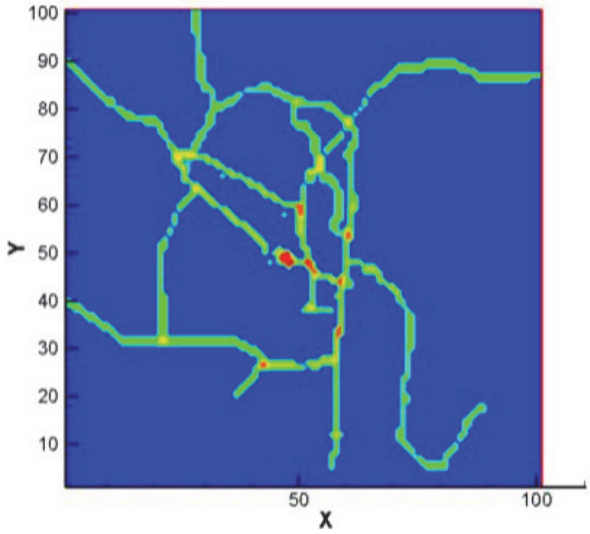

Fig. 6. Input from a linear source
Rys. 6. Napływ ze źródła liniowego

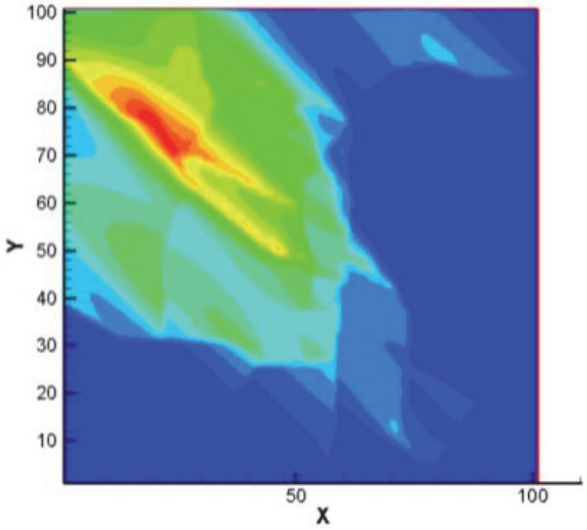

Fig. 6. Propagation from a linear source, wind speed 5 m/s, North-west direction
Rys. 6. Propagacja ze źródła liniowego, prędkość wiatru 5 m/s, kierunek północny-zachód

3. Conclusions

Using a simplified methodology of stochastic modelling, it is possible to construct effective numerical computational algorithms that significantly reduce the amount of computation without losing their accuracy.

From technical standpoint it is of great importance to control emissions from transport (Niewczas et al. 2002, Kordas et al. 2008, Droździel 2007).

References

Antonia, R.A. & Luxton, R.E. (1971) The Response of a Turbulent Boundary Layer to a Step Change in Surface Roughness, Pt. 1. Smooth to Rough. *J. Fluid Mech., 48*, 721-762.

Betchov, R. (1977) *Transition, Handbook of Turbulence, Vol. 1.* eds. W. Frost & T. H. Moulden, NY: Plenum Press.

Cao, Y., You, J., Shi, Y., Hu, W. (2016) Evaluation of automobile manufacturing enterprise competitiveness from social responsibility perspective. *Problemy Ekorozwoju/Problems of Sustainable Development, 11(2)*, 89-98.

Castillo, L. (1997) *Similarity analysis of turbulent boundary layers.* Ph. D. Thesis, The Graduate School of the State University of New York, Buffalo.

Cel, W., Czechowska-Kosacka, A., Zhang, T. (2016) Mitigation of greenhouse gases emissions. *Problemy Ekorozwoju/Problems of Sustainable Development, 11(1)*, 173-176.

Danaev, N.T., Temirbekov, A.N., Malgazhdarov, E.A. (2014) Modelling of Pollutants in the Atmosphere Based on Photochemical Reactions. *Eurasian Chemico-Technological Journal, 16(1)*, 61-71.

Drastichowa, M. (2017) Decomposition analysis of the greenhouse gas emissions in the European Union. *Problemy Ekorozwoju/Problems of Sustainable Development, 12(2)*, 27-35

Droździel, P. (2007) O rozruchu silnika o zapłonie samoczynnym. *Eksploatacja i Niezawodność, 2(34)*, 51-59.

Edward, O. (1993) *Chaos in Dynamic Systems.* Cambridge University Press.

Hogstrom, U. (1996) Review of Some Basic Characteristics of the Atmosphere Surface Layer. *Boundary-Layer Meteorol., 78*, 215-246.

Holt, T. & Raman, S. (1988) A Review and Comparative Evaluation of Multilevel Boundary Layer Parameterisations for First Order and Turbulent Kinetic Energy Closure Schemes. *Rev. Geophys. Space Phys., 26*, 761-780.

Hurley, P.J. (1997) An Evaluation of Several Turbulence Schemes for the Prediction of Mean and Turbulent Fields in Complex Terrain. *Boundary-Layer Meteorol., 83*, 43-73.

Kordas, P., Sarnowski, C., Droździel, P., (2008) Wpływ regulacji i stanu technicznego aparatury wtryskowej silnika wysokoprężnego na zadymienie spalin. *Zeszyty Naukowe Instytutu Pojazdów, 2(69),* 41-48.

Niewczas, A., Droździel, P., Kordos, P. (2002) Wpływ warunków rozruchu na zadymienie spalin silnika o zapłonie samoczynnym. *Ekotechnologie XXI wieku*, Polskie Towarzystwo Inżynierii Ekologicznej, 149-156.

Olejnik, T.P., Sobiecka, E. (2017) Utilitarian technological solutions to reduce CO_2 emission in the aspects of sustainable development. *Problemy Ekorozwoju/Problems of Sustainable Development, 12(2)*, 173-179.

Paladin, G. & Vulpiani, A. (1986) Fractal Models of 2D and 3D Turbulence. *Fractals in Physics*, eds. L. Pietronero & E. Tosatti, Elsevier Science Publishers, 624-631.

Riahi, D.N. (2000) *Flow Instability.* Southampton and Boston: WIT Press.

Simpson, R.L., Agarwal, N.K., Nagabushana, K.A., Olcmen, S., (1990) Spectral Characteristics and Other Features of Separated Turbulent Flows. *AIAA Journal, 3*, 446-452.

Sugak, E.V. (2003) Probabilistic-statistical modelling of turbulent gas-dispersed flows (in Russian). *Journal of Computational Technologies. 8, (4C),* 81-96.

Swinney, H.L. & Gollub J.P. (eds.) (1981) *Hydrodynamic Instabilities and the Transition to Turbulence. Topics in Applied Physics, Vol. 45.* NY: Springer-Verlag.

Tennekes, H., & Lumley, J.L. (1972) *A First Course in Turbulence.* Cambridge: MIT Press.

Trunev, A.P. (1996) Similarity theory for turbulent flow over natural rough surface in pressure and temperature gradients. *Air Pollution IV. Monitoring, Simulation and Control,* eds. B. Caussade, H. Power & C.A. Brebbia, Comp. Mech. Pub., Southampton, 275-286.

Żukowska, G., Myszura, M., Baran, S., Wesołowska, S., Pawłowska, M., Dobrowolski, Ł. (2016) Agriculture vs. alleviating the climate change. *Problemy Ekorozwoju/Problems of Sustainable Development, 11(2)*, 67-74.

Probabilistyczne i statystyczne modelowanie rozprzestrzeniania się w atmosferze szkodliwych zanieczyszczeń z pojazdów silnikowych

Streszczenie

Celem pracy jest stworzenie matematycznego modelu rozprzestrzeniania się zanieczyszczeń z pojazdów. W tym artykule zaproponowano zastosowanie podejścia probabilistycznego i statystycznego do modelowania rozprzestrzeniania się szkodliwych zanieczyszczeń w atmosferze z pojazdów na przykładzie miasta Ust-Kamenogorsk. Stosując uproszczoną metodologię modelowania stochastycznego, można konstruować skuteczne numeryczne algorytmy obliczeniowe, które znacznie redukują ilość obliczeń bez utraty dokładności.

Abstract

The aim of the work is to create a mathematical model for the distribution of emissions from vehicles. In this article, it was proposed to use the probabilistic and statistical approach for modelling the distribution of harmful impurities in the atmosphere from vehicles using the example of the Ust-Kamenogorsk city. Using a simplified methodology of stochastic modelling, it is possible to construct effective numerical computational algorithms that significantly reduce the amount of computation without losing their accuracy.

Słowa kluczowe:
pulsacje turbulentne, model statystyczny, pojazdy mechaniczne,
rozwiązanie numeryczne, źródło,
rozprzestrzenianie się szkodliwych zanieczyszczeń

Keywords:
turbulent pulsations, statistical model, motor vehicles, numerical solution,
source, distribution of harmful impurities.

MIDDLE POMERANIAN SCIENTIFIC SOCIETY OF THE ENVIRONMENT PROTECTION
ŚRODKOWO-POMORSKIE TOWARZYSTWO NAUKOWE OCHRONY ŚRODOWISKA

Annual Set The Environment Protection
Rocznik Ochrona Środowiska

Volume/Tom 19. Year/Rok 2017 ISSN 1506-218X 809-823

Comparison of Hard Structures for Age Estimation and Chemical Composition Analysis of Otoliths of Perch from Lake Trzesiecko under Reclamation

Magdalena Lampart-Kałużniacka, Tomasz Heese
Koszalin University of Technology

1. Introduction

The study was carried out on perch harvested from Lake Trzesiecko in 2009. The lake has been subject to reclamation measures since 2005, involving: aeration of the near-bottom zone by means of an aerator, application of chemical compounds, e.g. iron sulphate, aimed at the release of phosphates from water depths and their accumulation in the near-bottom layer in the form of insoluble salts, as well as biomanipulation measures involving controlling of the abundance of planktivorous fish by predatory fish (Heese et al. 2013). One of such predatory fish species is perch. It is a typical predator of European waters, and is commonly used in biomanipulation (Eklöv & Van Kooten 2001). All of the measures, both chemical and technical, are aimed to contribute to the improvement of the ecological state of the lake discussed.

Measures involving biomanipulation are always difficult to perform. It is important to continuously control the participating groups of specimens/organisms/populations. The accurate determination of their health condition or population features, including the age structure, is of key importance in the execution of such a task (Newman & Dunk 2002). This results in the necessity to seek a simple but reliable element permitting obtaining possibly accurate results. The objective of this paper was to find such an element among: the scale, rays of the dorsal and anal fins, and the otolith, for the purpose of precise age estimation, determination

of the readability of the aforementioned structures, and calculation of the growth rate for perch from Lake Trzesiecko. The chemical composition analysis of the otolith was also performed for the purpose of determining the ability of the applied iron sulphate to penetrate biological membranes and accumulate in its structure. Its presence suggests a certain threat resulting from human interference into the ecosystem of Lake Trzesiecko through the introduction of chemical agents to the waters.

2. Material and methods

The present study covered 35 individuals of perch harvested from Lake Trzesiecko on 8-9 October 2009. Each of the individuals was weighed by means of an Axix scale with an accuracy to 0.01g, and measured by means of a ruler. Both total length and body length were determined with an accuracy to 1 mm. A scale was then sampled from the left side, from the area of the body over the lateral line under the first dorsal fin. Mucus and other contaminants were removed from the place before sampling the scale. The sampled material was placed in previously labelled paper bags. Before the age analysis, each of the scales was rinsed in 5% ammonia solution. Several clean scales of the same fish were mounted on a microscope slide and covered with a cover slip. Otoliths and dorsal (D) and anal (A) fin rays were sampled during the anatomical study, also involving the identification of the sex of the individuals analysed. Fin rays were cut off together with their base immersed in muscles. The obtained fin rays were then labelled and dried at room temperature until residues of skin and muscle could be easily removed from the rays. The resulting material was submerged in binary synthetic resin. The obtained blocks were cut by means of a slow-speed circular saw Izomet by Buehler into slices with a thickness of 0.75 mm. This way, microscope slides were prepared. The otoliths were sampled from the head by performing a cut from the top of the head to the inner ear. Both of the sagitta were removed and placed in labelled paper bags. Before further analyses, the otoliths were submerged in water, and residues of membranes were removed. They were then rinsed in deionised water. They were weighed with an accuracy to 0.001 g. Further works were conducted under a stereoscopic microscope Olimpus SZX16. For all of the four structures, microscopic photographs were taken by means of a camera Olimpus CX50. With the application of the cellSens

Standard software, measurements and labelling were performed, permitting age estimation and calculation of growth rate. The works were conducted following the methodology proposed by Secor et al. (1991) and Gabriel et al. (2000). Chemical composition analysis of the otoliths was also performed by means of a scanning electron microscope by JEOL with an EDS analyser. Each of the otoliths was rinsed with deionised water prior to the analysis. The analysis was conducted in one plane from the right side of the otolith to the left one. Three places were selected for detailed chemical composition analysis (Pattanaik 2004).

3. Calculation

The age of the studied fish was estimated based on the scale, D and A fin rays, and the otolith (Fig. 4). When the age could not be estimated based on a given structure, an empty space was left in the table. When the estimated age varied between one year and another, years were recorded using a slash (Table 1). When different age was determined for the same fish based on the analysed structures, the result obtained for at least two of the structures was adopted.

The growth rate of the fish was calculated based on the scale, by means of the back-reading method, in accordance with the Fraser-Lee equation: $L_n = C+S_n/S_c \cdot (L_c-C)$, where L_n – length of fish at age n, C – length of fish at which a scale is formed in the case of perch 2.5 cm, S_n – length of scale radius corresponding to particular annual rings, S_c – total length of scale radius at the moment of harvesting of a given fish Heese (1992).

Basic statistic data, i.e. the mean and range, were also determined for total length, body length, body weight, gutted weight, length and weight of the otoliths, and for the chemical composition of the otoliths.

The significance and strength of correlation between the weight and length of otoliths was also verified with the application of the Statistica 10.0 PL software. The correlation scales were adopted following Stanisz (1998). The results of the chemical composition analysis were averaged for all of the three places analysed.

Table 1. Morphological characteristics of the perch individuals studied and comparison of age on the basis of hard structures and scales
Tabela 1. Charakterystyka morfologiczna okonia oraz porównanie struktur twardych do szacowania wieku

Lp.	Total length [cm]	Lenght body [cm]	Body mass [g]	Gutted weight [g]	Longest axis otolith [mm]	Otolith mass [g]
1	25.1	22.2	192.98	167.65	7.526	0.03
2	16.4	13.5	44.06	39.93	6.430	0.018
3	25.2	21.5	213.41	186.17	7.581	0.027
4	29.0	25.6	352.15	303.62	9.334	0.036
5	24.3	21.3	192.92	165.56	8.037	0.029
6	28.0	24.5	278.46	244.54	8.548	0.031
7	21.2	18.8	106.5	98.11	6.716	0.017
8	20.5	17.8	90.24	82.83	6.112	0.013
9	30.0	27.0	350.1	305.33	9.619	0.044
10	25.6	22.5	217.67	189.64	8.659	0.032
11	25.6	22.8	206.02	183.27	8.192	0.025
12	12.2	10.9	20.22	16.84	4.557	0.007
13	25.3	21.8	210.03	189.07	7.577	0.024
14	25.0	21.9	191.33	164.68	8.455	0.027
15	23.1	20.4	159.58	140	6.860	0.02
16	26.5	23.7	267.9	234.6	8.659	0.028
17	27.5	23.8	270.77	230.88	8.867	0.033
18	20.9	18.3	103.92	88.15	7.263	0.024
19	28.9	25.2	327.48	258.67	8.356	0.028
20	30.7	27.1	365.44	316.52	9.099	0.04
21	30.0	28.0	353.31	307.07	9.801	0.041
22	28.0	27.5	306.82	269.7	9.188	0.033
23	38.4	32.6	811.7	691.4	11.164	0.073
24	27.9	24.7	286.87	257.77	9.026	0.034
25	37.9	32.7	793	680.2	11.375	0.057
26	36.8	31.5	699.7	604.2	11.596	0.062
27	30.3	25.4	412.9	365.4	9.225	0.041
28	30.6	25.8	354.7	310.9	8.810	0.03
29	37.5	31.7	784.8	674.5	11.473	0.065
30	31.8	26.8	479.4	416.2	9.924	0.047
31	31.4	26.8	451.6	395	10.748	0.046
32	31.7	26.4	454.8	390.9	9.650	0.04
33	31.5	26.7	454.1	392.6	9.519	0.037
34	27.3	23.1	254.1	220.6	7.987	0.026
35	31.6	27.0	441.3	383.4	9.486	0.036
min	**12.2**	**10.9**	**20.22**	**16.84**	**4.56**	**0.01**
max	**38.4**	**32.7**	**811.7**	**691.40**	**11.60**	**0.07**
average	**27.82**	**24.21**	**328.58**	**284.74**	**8.73**	**0.03**

Table 1. cont.
Tabela 1. cd.

Lp.	Males or females	Age scale	Age dorsal spine	Age anual spine	Age otolith
1	F	5+	5+	5+	5+
2	M	2+	2+	-	-
3	F	4+/5+	5+	5+	5+
4	F	6+	6+	-	-
5	F	4+	4+	4+	4+
6	F	6+	6+	6+	6+
7	F	4+	4+	-	-
8	M	3+	3+	3+	3+
9	F	5+/6+	6+	-	5/6+
10	F	5+	5+/6+	5+/6+	5+
11	F	5+	5+	5+	5+
12	M	2+	2+	2+	2+
13	F	4+/5+	5+	-	5+
14	M	5+	5+	4+/5+	-
15	F	4+	4+	4+	-
16	F	5+	5+	5+	5+
17	F	6+	6+	4+/5+	5+
18	M	4+	5+	4+	-
19	F	6+	4+	5+	6+
20	F	6+	6+	5+	-
21	F	5+	5+	4+	5+/6+
22	F	6+	6+	6+	6+
23	F	7+/8+	8+	8+	8+
24	F	6+	6+	-	6+
25	F	8+	7+/8+	-	7+/8+
26	F	8+	8+	8+/7+	7+/8+
27	F	6+	6+	5+/6+	6+
28	F	6+	6+	6+	6+
29	F	8+	8+	8+	8+
30	F	7+	7+	6+	6+
31	F	6+/7+	7+	6+	7+
32	F	6+	6+	6+	6+
33	F	6+	6+	6+	6+
34	F	6+	6+	6+	6+
35	F	6+	6+	6+	6+
min	**M=5**				
max	**F=40**				

4. Results

The studied individuals had a total length from 12.2 to 38.4 cm. Their body length varied from 10.9 to 32.7 cm (Table 1). The smallest fishes turned out to be the youngest, with the estimated age of 2+. They also had the lowest weight (Table 1). The number of such young individuals in the study amounted to 2 individuals. The age of the remaining individuals varied from 3+ to 8+. The most numerous were fishes aged 6+ (15 individuals) and 5+ (8 individuals). The least numerous were individuals aged 3+ and 7+, represented by one and two fishes, respectively (Fig. 1). The obtained data concerning the total scale radius and partial radiuses in particular years of life of the fish were used to calculate the growth rate of the analysed perch (Fig. 2). It was determined to grow the fastest in the first year of life. Perch in the second and third year of life also had a quite fast growth rate. Somewhat slower growth was observed in older fishes (Fig. 3).

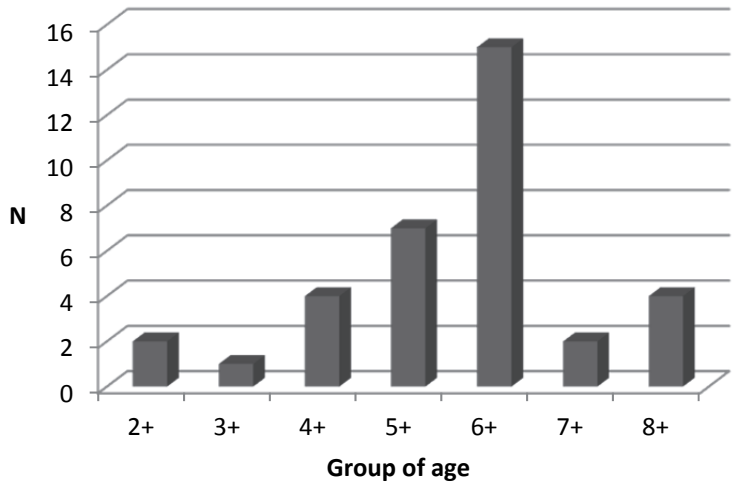

Fig. 1. Age of perch *Perca fluviatilis*
Fig. 1. Liczebność w grupach wiekowych okonia *Perca fluviatilis*

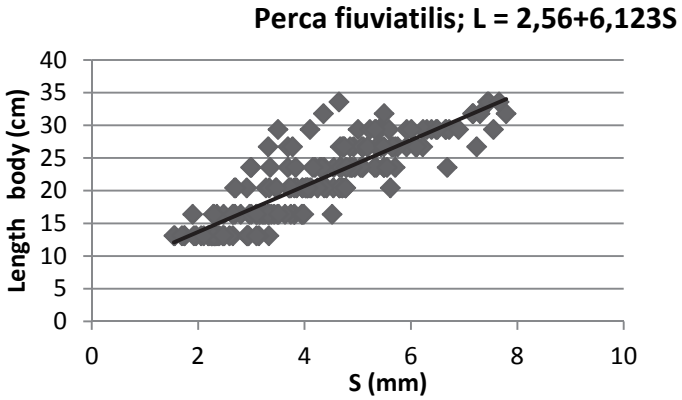

Fig. 2. Correlation between the scale radius (S) and body length of the perch analysed
Fig. 2. Zależność pomiędzy promieniem łuski (S) a długością ciała badanego okonia

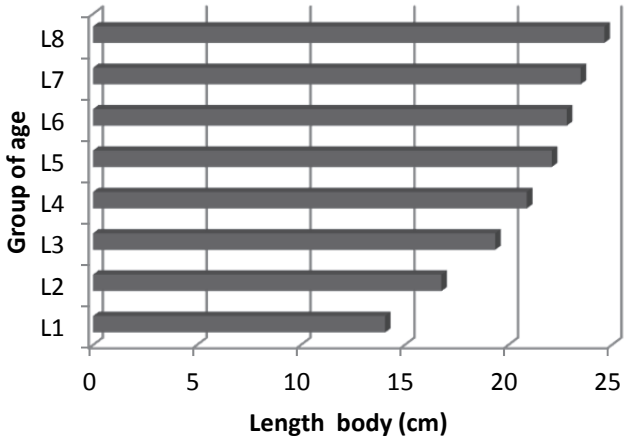

Fig. 3. Growth rate for particular age groups of the perch studied
Fig. 3. Tempo wzrostu dla poszczególnych grup wiekowych u badanego okonia

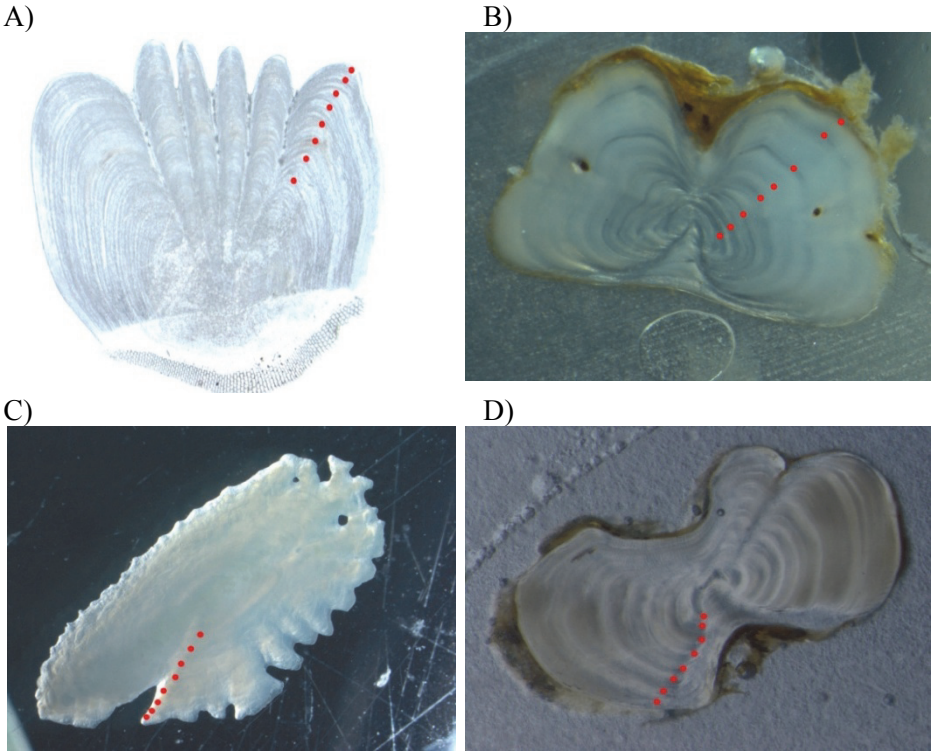

Fig. 4. Age of perch 8+ based on the analysed structures: a) scale, b) anal fin ray, c) otolith and d) dorsal fin ray
Fig. 4. Wiek okonia 8+ na podstawie analizowanych struktur: a) łuska, b) promień płetwy A, c) otolith i d) promień płetwy D

Table 2. Chemical composition of the perch specimens studied
Tabela 2. Skład chemiczny otolitów badanego okonia

Chemical element	Range weight %	Range atomic %
C	19.99-32.13	23.59-39.32
O	46.25-63.85	45.14-62.44
N	5.43-13.95	6.40-19.94
Ca	0.18-21.62	0.02-9.75
Al	0.02-10.27	0.01-5.26
Ba	0.0-1.43	0.00-1.88
Mg	0.02-4.27	0.01-1.74

Table 2. cont.
Tabela 2. cd.

Chemical element	Range weight %	Range atomic %
Na	0.01-0.34	0.02-0.24
P	0.01-0.29	0.00-0.17
Mn	0.01-0.46	0.00-0.16
Cr	0.01-0.38	0.00-0.12
Fe	0.01-0.26	0.03-0.07
Mo	0.02-0.21	0.01-0.03
Si	0.01-0.16	0.00-0.09
S	0.02-0.06	0.01-0.03

Chemical analyses provided data on the chemical composition of the otoliths. They showed very high percent weight and percent mass contribution of the following elements: carbon, calcium, oxygen, and nitrogen. Varied amounts of other elements were also recorded, including metals such as: aluminium, manganese, chromium, molybdenum, or iron (Table 2).

5. Discusion

accurate estimation of the age of particular individuals is a very important issue in studies on population structure. It requires the selection of a reliable structure based on which the reading can be performed. The reliability of the element is strictly related to its readability, i.e. facility of identification of annual marks (Lampart-Kałużniacka et al. 2013). Since the moment of discovery of annual growth marks on the scale, the assessment of those structures has been continuously discussed, and the most readable structure has been searched for. These may be opercula, fin rays, rings, or otoliths (Zymonas & McMahon 2009). Otoliths have gained a lot of recognition over the latest years. Their popularity is not only limited to the estimation of the age and growth rate, but also to the determination of the effect of the environment on the organism through their chemical composition analysis, the estimation of the duration of the larval stage of a given fish, or in the case of diadromous fish, the estimation of time spent in particular ecosystems (Campana 2005). It should be mentioned that each otolith located in the inner ear of a fish, in the number of 6, i.e. three pairs (Payan et al. 2004), is suitable for age estimation.

Sagitta is used for this purpose the most frequently, although for fish from family Cyprynidae, it is the lapillus (Bao-Shan et al. 2012). The size and readability of the otolith seem to be features determining its selection to the largest degree, but they are also mutually excluding features, because smaller fish have a smaller otolith which is more difficult to extract, but usually more readable. A larger otolith is less readable, but easier to identify. Readability is related to the biomineralisation process, i.e. the development of consecutive layers of calcium carbonate during the growth, i.e. aging of a fish (Melancon et al. 2005). It is assumed that otoliths "grow" in such a manner that the oldest part is located on the inside, around the nucleus, and the youngest on the edges (Radtke 1984). Annual growth marks are two zones, light and dark, around the nucleus (Panfili et al. 2002). Unfortunately, not every otolith is distinguished by such readability. Very often, it is difficult to determine particular annual marks, i.e. zones. It has been evidenced that their development is affected both by physiological and environmental factors (Clark& Friedland 2004; Checkley et al. 2004; Fukuda et al. 2009). Therefore, it is difficult to unequivocally determine the cause of low readability of otoliths. Similarly, in the present study, the readability of sagittas was dissatisfactory. In 11 out of 35 cases, no or an inaccurate reading was obtained (the age varied between one year and another). According to Panfili et al. (2002), much more readable otoliths could be obtained by means of cutting them into a microscope slide which could then be polished. Extracted otoliths of perch from Lake Trzesiecko, however, were distinguished by high brittleness. Attempts to cut slides on a slow-speed circular saw caused crumbling of the material. Such analyses were therefore given up. The causes of the "brittleness" of the studied otoliths might be numerous, but they are all related to the crystal structure of calcium carbonate (Gebauer et al. 2010). It can take the form of aragonite, vaterite, and calcite. It was determined that otoliths composed of aragonite are less brittle and more readable. They can be used for more accurate identification of annual marks, which cannot be done in vaterite or calcite structures (Melancon et al. 2005). Whether calcium carbonate in otoliths takes the form of aragonite, vaterite, or calcite determines not only their readability, but also other properties, e.g. brittleness, because a change in the crystal structure results in obtaining different, new, and not necessarily favoured properties (Pattanaik 2004). In the case of problems with the identifica-

tion of annual marks on the otolith as a structure recognised as very reliable, the analysis of its crystal structure should be conducted. A high contribution of vaterite and calcite crystals suggests that an otolith will not be very useful for age estimation, and the risk of error of over- or underestimation of age is much higher. Both cases will result in inaccurate conclusions affecting the calculation of the growth rate, and determination of the population's age structure, the protected length of fish, and sexual maturity of a given species.

The occurring difficulties in age estimation based on otoliths resulted in the lack of possibility to determine correlations between body length and otolith radius. This made the application of the back-reading method for the estimation of fish length in a given year of life impossible. Therefore, it is important that the estimation of age of a given fish is not only be based on one structure. In the present study, such estimation was also based on rays of the dorsal fin D and anal fin A, and the scale. Both the rays and the scale in the perch studied were distinguished by high readability. Particularly the dorsal fin ray can be recognised here as a readable structure distinguished by high facility of identification of annual marks. High variability of shapes of dorsal fin rays in the microscope section resulted in no possibility to retain the constant direction of the structure's ray, which made it impossible to apply the back-reading method for the determination of fish length. Therefore, in the case of perch from Lake Trzesiecko, only the scale turned out to be the structure for which the Fraser-Lee equation could be applied, permitting the determination of the growth rate for the perch studied. The obtained results suggest that in the first years of life, the perch grows the most intensively, although reaching 12 cm body length in the first year of life is improbable. Such body length probably covers two years of life, because following Heese (1992), perch from environments rich in food in the first year of life reaches a body length of approximately 7 cm. This is caused by the difficulty to identify the first mark on the scale in older fishes aged 5+ and older which are dominant in the study. Scales of such fish are often so non-transparent in the middle that the first years are identified only in their further sections. This may result from a certain allometry occurring during the scale's growth (Fig. 4A). Such an interpretation is supported by the fact that the same age for the same specimen was often obtained for different structures, e.g. for ray D. The obtained results for

scales, however, contributed to the overestimation of the body length of perch for group L1 in the present study.

The estimated age of the fish studied varied from 2+ to 8+, and was largely coherent for the structures analysed. Several cases were recorded, where the age varied for all of the structures, and could not be unequivocally determined. This can result from among others the period of harvesting of fish for analysis. Differences in the term of development of the annual mark for a given structure were determined. It is assumed that in autumn, the ring for the scale and otolith is formed (Heese 1992), and in summer, for rays (Zymonas & McMahon 2009). Considering this information, it can be observed that in the case of fins, particularly D, rings were already developed, and any doubts only existed in two cases. In the case of the remaining structures, problematic readings were more numerous, particularly for the scale which could be sampled before the full development of the annual ring.

Another objective of the present study was the analysis of the chemical composition of otoliths. Maximum percent mass and weight contributions were recorded for elements both composing the mineral part of the otolith ($CaCO_3$), and constituting its organic part (N) (Asenath-Smith 2012). Particular attention was paid to the presence of metals, and particularly iron, which due to the temporary application of $Fe_2(SO_4)_3$ can occur in excess in water, or be released from bottom sediments in anaerobic conditions (Kajak 1996). Therefore, it should be thoroughly assessed whether the application of chemical compounds has any negative effect on the biotope of Lake Trzesiecko. This requires more detailed analytical-toxicological studies showing not only the metabolical paths of the elements introduced to the ecosystem by man, but also showing potential threats for the organisms inhabiting the environment. It is also disturbing to record the presence of other elements in the otoliths, including heavy metals, suggesting other threats.

References

Asenath-Smith, E. Li. H., Keene, E.C., She, Z.W., Estroff, L. A. (2012). Crystal growth of calcium carbonate in hydrogels as a model of biomineralization. Adv. Funct. Mater. 22, 2891-2914.

Bao-Shan, M., Cong-Xin, X., Bin, H., Xue-Feng, Y., Shui-Son,g Ch. (2012). Reproductive Biology of *Schizothorax o'connori* (Cyprinidae: Schizothoracinae) in the Yarlung Zangbo River, Tibet. *Zoological Studies 51*, 7, 1066-1076.

Campana, S.E. (2005). Otolith science entering the 21st century. *Marine and Freshwater Research. 56*, 485-495.

Checkley, Jr. D. M., Dickson, A.G., Takahashi, M., Radich, A.J., Esienkolb N., Asch, R. (2009). Elevated CO_2 enhances otolith growth in young fish. *Science. 324*, 1683.

Clarke, L.M., Friedland, K. D. (2004). Influence of growth and temperatue on strontium deposition in the otoliths of Atlantic salmon. *Journal of Fish Biology. 65*, 744-759.

Eklöv, P., & Van Kooten, T. (2001). Facilitation among piscivorous predators: effects of prey habitat use. *Ecology 82*, 2486–2494.

Fukuda, N., Kuroki, M., Schinoda, A., Yamada, Y., Okamura, A., Aoyama, J., Tsukamoto, K. (2009). Influence of water temperature and feeding regime on otolith growth in *Anguilla japonica* Glass eels and elvers: does otolith cease at low temperatures? *Journal of Fish Biology. 74*, 1915-1933.

Gabriel, J., Lombarte, A., Morales-Nin, B. (2000). Variability of the sulcus acusticus in the sagittal otolith of the genus *Merluccius (Merlucciidae).* Special Issue: 2nd International Symposium On Fish Otolith Research & Application, Bergen, Norway, 20-25 June 1998. In: *Fisheries Research. 46*, 3, 5-13.

Gebauer, D., Gunawidjaja, P.N., Ko, Y.P, Bacsik, Z., Aziz, B., Liu, L., Hu, Y., Bergstrom, L., Tai, Ch., Sham, T., Eden, M., Hedin, N. (2010). Proto-Calcite and Proto-Vaterite in Amorphous Calcium Carbonates. Zuerst ersch. In: *Angewandte Chemie International Edition, 49*, 47, 8889-8891.

Heese, T. (1992). *Optymalizacja metod określania tempa wzrostu ryb za pomocą odczytów wstecznych* [Optimisation of methods of determination of growth rate of fish by means of the back-reading method]. WSI. Koszalin. (in Polish).Nr 42, 155.

Heese, T., Willk-Woźniak, E., Żurek, R., Kaczorkiewicz, M., Szmidt, R., Arciszewski, M., Pikuła, K., Wojcieszonek, A., Chrzczonowicz, H., Zakościelna, A. (2013). *Ocena efektu ekologicznego zabiegów rekultywacji prowadzonego w latach 2005-2012 na Jeziorze Trzesiecko* [Assessment of the ecological effect of reclamation measures conducted in the years 2005-2012 on Lake Trzesiecko]. In: Ryszard Wisniewski ed., Ochrona i rekultywacja jezior [Protection and reclamation of lakes], Toruń. 65-75 (in Polish).

Kajak, Z. (1938). *Hydrobiologia-limnologia* [Hydrobiology-limnology]. PWN Warszawa. 360 (in Polish).

Lampart-Kałużniacka, M., Pietraszewsk, D., Marszał, M., Heese, T., Przybylski, M. (2013). Age validation of spined loach (*Cobitis taenia*) and golden loach (*Sabanejewia aurata*) using some calcinated structures. *Rocznik Ochrona Środowiska. 15*, 25-50.

Melancon, S., Fryer, B.J., Ludsin, S.A. (2005). Effects of crystal structure on the uptake of metals by lake trout (Salvelinus namaycush) otoliths. *Canadian Journal of Fisheries and Aquatic Sciences. 62(11)*, 2609-2619.

Newman, S.J., Dunk, I.J. (2002). Growth, Age Validation, Mortality, and other Population Characteristics of the Red Emperor Snapper, *Lutjanus sebae* (Cuvier, 1828), off the Kimberley Coast of North-Western Australia. Estuarine. *Coastal and Shelf Science. 55(1)*, 67-80.

Panfili, J., de Pontual, H., Troadec, H., Wright, P.J. (2002). *Manual of fish sclerochronology* Ifemer, XLC Le Relecq Kerhuon, France. 463.

Pattanaik, S. (2004). X-ray diffraction, XAFS and scanning electron microscopy study of otolith of a crevalle jack fish (*Caranx hippos*). NIMB. 229(3-4), 367-374.

Payan, P., De Pontual, H., Gilles B., Mayer-Gostan, N. (2004). Endolymph chemistry and otolith growth in fish. *Comptes Rendus Palevol, 3(6)*, 535-547.

Radtke, R. L. (1984). Cod fish otoliths: information storage structures. *Fløde-vigen rapportser 1(273)*, 298.

Secor D.H., Dean, J.M., Laban, E.H. (1991). *Manual for otolith removal and preparation for microstructural examination*. Electric Power Research Institute and the Belle W. Baruch Institute for Marine Biology and Coastal Research. 1, 85.

Stanisz, A. (1992). *Przystępny kurs statystyki* [Intelligible course in statistics]. Kraków. StatSoft Polska. 351. (in Polish)

Zymonas, N.D., McMahon, T.E. (2009). Comparison of pelvic fin rays, scales and otoliths for estimating age and growth of bull trout, *Salvelinus confluentus*. *Fisheries Management and Ecology. 16*, 155-164.

Przydatności struktur do szacowania wieku i analiza składu chemicznego otolitów okonia *Perca fluviatilis* (L.) z Jeziora Trzesiecko, poddanego zabiegom w celu obniżenia trofii wód

Streszczenie

Prezentowany Porównanie przydatności struktur twardych do szacowania wieku i analiza składu chemicznego otolitów okonia *Perca fluviatilis* (L.) pochodzącego z rekultywowanego Jeziora Trzesiecko.

Prowadzone badania wskazały, że najbardziej czytelną strukturą do szacowania wieku u okonia pochodzącego z Jeziora Trzeskiecko był promień płetwy grzbietowej D. Otolity okazały się strukturami bardziej problematycznymi. Trudno było na ich podstawie szacować wiek, jednocześnie były bardzo „kruche", co uniemożliwiło wykonanie na ich podstawie preparatów mikroskopowych. Prawdopodobnie było to związane z ich budową krystaliczną. Tempo wzrostu można było obliczyć tylko na podstawie łuski. Stąd rozsądne wydaje się działanie w którym, szacowanie wieku i wyznaczanie tempa wzrostu prowadzi się w oparciu o kilka elementów. Opieranie badań tylko na jednej wybranym elemencie, skutkuje dużą zmiennością uzyskiwanych wyników. Świadczyć o tym może, chociażby brak zgodności danych, uzyskiwanych w czasie badań, prowadzonych przez różne osoby, które szacowały wiek dla ryb w oparciu o te same struktury twarde. Odnotowanie atomów żelaza w otolitach, może być efektem kumulacji tego metalu w organizmach żywych, a źródłem jego jest związek chemiczny, aplikowany do jeziora w celu poprawy jego stanu ekologicznego.

Abstract

The study revealed that the ray of the dorsal fin D was the most readable structure for age estimation in perch from Lake Trzesiecko. Otoliths turned out to be more problematic structures. Age estimation based on otoliths was difficult, and the structures were very brittle, which made it impossible to prepare microscope slides. This was probably related to their crystal structure. Growth rate could only be calculated based on the scale. In the case of older specimens aged 5+ and more, however, it was difficult to identify the mark related to the first year of life due to the low readability of the middle part of the scale. This results in inflated results obtained for group L1. Studies on age of fish should be conducted based on several structures due to the possibility of verification of the obtained results. Performing the analysis of only one selected element results in high variability of the obtained data, and therefore inaccurate conclusions. The recorded presence of iron atoms in the otoliths suggests the accumulation of the metal resulting from the application of chemical compounds by man in living organisms.

Słowa kluczowe:
Okoń *Perca fluviatilis*, otolity, łuski, promienie płetw, wiek,
skład chemiczny w otolitach

Keywords:
perch *Perca fluviatilis*, otolith, scales, rays fins, age,
chemical compositions of otolith

Editorial Committee

Section's Editors

Komitet Redakcyjny

Redaktorzy Działowi

Przewodniczący *prof. dr hab. inż. Tadeusz Piecuch*	Redaktor Naczelny Redaktor działu – technika wodno-ściekowa i utylizacja odpadów
Z-ca Przewodniczącego *prof. dr hab. inż. Wojciech Piotrowski*	Redaktor działu – rolnictwo ekologiczne
Z-ca Przewodniczącego *prof. dr hab. inż. Aleksander Szkarowski*	Redaktor działu – energetyka, sieci i instalacje
Prof. dr hab. *Włodzimierz Deluga*	Redaktor działu – ekonomika ochrony środowiska
Prof. dr hab. *Józef Domagała*	Redaktor działu – rezerwaty przyrody – ochrona życia i zdrowia zwierząt
dr inż. *Tomasz Dąbrowski*	Redaktor działu – współpraca z zagranicą
Prof. dr hab. inż. *Jan Hehlmann*	Redaktor działu – inżynieria i aparatura chemiczna
Prof. dr hab. inż. *Renata Krzyżyńska*	Redaktor działu – ochrona powietrza, neutralizacja i odpylanie gazów
Prof. dr hab. inż. *Hanna Obarska-Pempkowiak*	Redaktor działu – biotechnologia
Prof. dr hab. *Janusz Pempkowiak*	Redaktor działu – chemia i biochemia morza, jezior i rzek
Prof. dr hab. inż. *Czesława Rosik-Dulewska*	Redaktor działu – ochrona powierzchni ziemi
Prof. dr hab. *Kazimierz Szymański*	Redaktor działu – chemia

Redaktorzy techniczni

dr inż. Janusz Dąbrowski, dr inż. Tomasz Dąbrowski

Redaktor strony internetowej http://ros.edu.pl

dr hab. inż. Jacek Piekarski, prof. PK

The list of Institutions – Libraries where this publication has been forwarded

Thomson Reuters
500 Spring Garden Street, 4th Floor, Pa 19130, Philadelphia, USA

St. Petersburg State University of Architecture
and Civil Engineering
2-nd Krasnoarmeiskaia St. 4, 190005 St. Petersburg, Russia

Universitaetsbibliothek Hannover und
Technische Informationsbibliothek (UB/TIB)
East-European Department/Exchange
Welfengarten 1B
30167 Hannover

Polish National Library
Al. Niepodległości 213, 02-086 Warszawa

Library of Institute of Environmental Engineering
of the Polish Academy of Sciences
M. Curie Skłodowskiej 34, 41-819 Zabrze

Library of Bialystok University of Technology
Zwierzyniecka 16, 15-333 Białystok

Library of Czestochowa University of Technology
Aleja Armii Krajowej 36, 42-200 Częstochowa

Library of Gdańsk University of Technology
G. Narutowicza 11/12, 80-952 Gdańsk

Library of Koszalin University of Technology
Racławicka 15/17, 75-620 Koszalin

Library of Cracow University of Technology
Warszawska 24, 31-155 Kraków

Library of Lublin University of Technology
Nadbystrzycka 36A, 20-618 Lublin

Library of Łodz University of Technology
Wólczańska 223, 90-924 Łódź

Library of Poznan University of Technology
Piotrowo 2, 61-139 Poznań

Library of Szczecin University
Mickiewicza 16, 70-384 Szczecin

Library of West Pomeranian University of Technology
Ku Słońcu 140, 71-073 Szczecin

Library of Silesian University of Technology in Gliwice
Kaszubska 23, 44-100 Gliwice

Library of Silesian University of Technology branch in Katowice
Krasińskiego 8, 40-019 Katowice

Library of Warsaw University of Technology
Pl. Politechniki 1, 00-661 Warszawa

Library of Wrocław University of Technology
Wybrzeże S. Wyspiańskiego 27, 50-370 Wrocław

Wykaz Instytucji – Bibliotek, do których zawsze przekazywano wydawnictwo

Thomson Reuters
500 Spring Garden Street, 4th Floor, Pa 19130, Philadelphia, USA

St. Petersburg State University of Architecture
and Civil Engineering
2-nd Krasnoarmeiskaia St. 4, 190005 St. Petersburg, Russia

Universitaetsbibliothek Hannover und
Technische Informationsbibliothek (UB/TIB)
East-European Department/Exchange
Welfengarten 1B
30167 Hannover

Biblioteka Narodowa
Al. Niepodległości 213, 02-086 Warszawa

Biblioteka Instytutu Podstaw Inżynierii Środowiska Polskiej Akademii Nauk
ul. M. Curie Skłodowskiej 34, 41-819 Zabrze

Biblioteka Politechniki Białostockiej
ul. Zwierzyniecka 16, 15-333 Białystok

Biblioteka Politechniki Częstochowskiej
Aleja Armii Krajowej 36, 42-200 Częstochowa

Biblioteka Politechniki Gdańskiej
ul. G. Narutowicza 11/12, 80-952 Gdańsk

Biblioteka Politechniki Koszalińskiej
ul. Racławicka 15/17, 75-620 Koszalin

Biblioteka Politechniki Krakowskiej
ul. Warszawska 24, 31-155 Kraków

Biblioteka Politechniki Lubelskiej
ul. Nadbystrzycka 36A, 20-618 Lublin

Biblioteka Politechniki Łódzkiej
ul. Wólczańska 223, 90-924 Łódź

Biblioteka Politechniki Poznańskiej
ul. Piotrowo 2, 61-139 Poznań

Biblioteka Uniwersytetu Szczecińskiego
ul. Mickiewicza 16, 70-384 Szczecin

Biblioteka Zachodniopomorskiego Uniwersytetu Technologicznego
ul. Ku Słońcu 140, 71-073 Szczecin

Biblioteka Politechniki Śląskiej w Gliwicach
ul. Kaszubska 23, 44-100 Gliwice

Biblioteka Politechniki Śląskiej filia w Katowicach
ul. Krasińskiego 8, 40-019 Katowice

Biblioteka Politechniki Warszawskiej
Pl. Politechniki 1, 00-661 Warszawa

Biblioteka Politechniki Wrocławskiej
Wybrzeże S. Wyspiańskiego 27, 50-370 Wrocław